

CHAPTER 2

SITE CHARACTERISTICS

TABLE OF CONTENTS

<u>Section</u>	<u>Title</u>	<u>Page</u>
2.0	SITE CHARACTERISTICS	2.0-1
2.1	GEOGRAPHY AND DEMOGRAPHY	2.1-1
2.1.1	SITE LOCATION AND DESCRIPTION	2.1-1
2.1.1.1	Specification of Location	2.1-2
2.1.1.2	Site Area Map	2.1-3
2.1.1.2.1	Boundaries for Establishing Effluent Release Limits	2.1-4
2.1.2	EXCLUSION AREA AUTHORITY AND CONTROL	2.1-4
2.1.2.1	Authority	2.1-4
2.1.2.2	Control of Activities Unrelated to Plant Operation	2.1-5
2.1.2.3	Arrangements For Traffic Control	2.1-5
2.1.2.4	Abandonment or Relocation of Roads	2.1-5
2.1.3	POPULATION DISTRIBUTION	2.1-5
2.1.3.1	Population Within 10 Miles	2.1-6
2.1.3.2	Population Between 10 and 50 Miles	2.1-7
2.1.3.3	Transient Population	2.1-7
2.1.3.3.1	Transient Population Within 10 Miles	2.1-8
2.1.3.3.2	Transient Population Between 10 and 50 Miles	2.1-8
2.1.3.3.2.1	Recreational Transients	2.1-9
2.1.3.3.2.2	Seasonal Populations	2.1-9
2.1.3.3.2.3	Transient Workforce	2.1-10
2.1.3.3.2.4	Special Facilities (Schools, Hospitals, Nursing Homes, etc.)	2.1-10
2.1.3.3.3	Total Permanent and Transient Populations	2.1-10
2.1.3.3.4	Transient Populations Outside the 50-Mile Region	2.1-11
2.1.3.4	Low-Population Zone	2.1-11
2.1.3.5	Population Center	2.1-12
2.1.3.6	Population Density	2.1-12
2.1.4	COMBINED LICENSE INFORMATION FOR GEOGRAPHY AND DEMOGRAPHY	2.1-13
2.1.5	REFERENCES	2.1-13
2.2	NEARBY INDUSTRIAL, TRANSPORTATION, AND MILITARY FACILITIES	2.2-1
2.2.1	LOCATIONS AND ROUTES	2.2-1
2.2.2	DESCRIPTIONS	2.2-3
2.2.2.1	Description of Facilities	2.2-3
2.2.2.1.1	Ninety-Nine Islands Hydroelectric Dam	2.2-3
2.2.2.1.2	Herbie Famous Fireworks	2.2-3
2.2.2.1.3	Broad River Energy Center	2.2-4

TABLE OF CONTENTS (Continued)

<u>Section</u>	<u>Title</u>	<u>Page</u>
2.2.2.1.4	Electrical Generation Plants	2.2-4
2.2.2.1.5	Mining and Quarrying Activities	2.2-4
2.2.2.1.6	Military Facilities	2.2-4
2.2.2.1.7	DSE Systems, LLC	2.2-5
2.2.2.2	Description of Products and Materials	2.2-5
2.2.2.2.1	Ninety-Nine Islands Hydroelectric Dam	2.2-5
2.2.2.2.2	Herbie Famous Fireworks	2.2-5
2.2.2.2.3	Broad River Energy Center	2.2-5
2.2.2.2.4	Mining and Quarrying Activities	2.2-5
2.2.2.2.5	Military Facilities	2.2-6
2.2.2.2.6	Waterways	2.2-6
2.2.2.2.7	Highways	2.2-6
2.2.2.2.8	Railroads	2.2-6
2.2.2.2.9	DSE Systems, LLC (Description of Products)	2.2-6
2.2.2.3	Description of Pipelines	2.2-7
2.2.2.4	Description of Waterways	2.2-8
2.2.2.5	Description of Highways	2.2-9
2.2.2.6	Description of Railroads	2.2-9
2.2.2.7	Description of Airports	2.2-10
2.2.2.7.1	Airports	2.2-10
2.2.2.7.2	Airways	2.2-12
2.2.2.8	Projections of Industrial Growth	2.2-12
2.2.3	EVALUATION OF POTENTIAL ACCIDENTS	2.2-12
2.2.3.1	Determination of Design Basis Events	2.2-13
2.2.3.1.1	Explosions	2.2-13
2.2.3.1.1.1	Transportation Routes	2.2-13
2.2.3.1.1.2	Pipelines	2.2-14
2.2.3.1.1.3	Nearby Industrial Facilities	2.2-15
2.2.3.1.1.4	Onsite Chemicals	2.2-17
2.2.3.1.2	Flammable Vapor Clouds (Delayed Ignition)	2.2-18
2.2.3.1.3	Toxic Chemicals	2.2-21
2.2.3.1.3.1	Background	2.2-21
2.2.3.1.3.2	Sources of Potentially Dangerous Releases	2.2-22
2.2.3.1.3.2.1	Stationary Sources	2.2-22
2.2.3.1.3.2.2	Mobile Sources	2.2-22
2.2.3.1.3.3	Analysis of Hazardous Materials	2.2-23
2.2.3.1.4	Fires	2.2-24
2.2.3.1.5	Collisions with Intake Structure	2.2-25
2.2.3.1.6	Liquid Spills	2.2-25
2.2.3.2	Effects of Design Basis Events	2.2-25
2.2.4	COMBINED LICENSE INFORMATION	2.2-26
2.2.5	REFERENCES	2.2-26

TABLE OF CONTENTS (Continued)

<u>Section</u>	<u>Title</u>	<u>Page</u>
2.3	METEOROLOGY	2.3-1
2.3.1	REGIONAL CLIMATOLOGY	2.3-1
2.3.1.1	General Climate	2.3-1
2.3.1.2	Regional Meteorological Conditions for Design and Operating Bases	2.3-8
2.3.1.2.1	Hurricanes	2.3-9
2.3.1.2.2	Tornadoes	2.3-10
2.3.1.2.3	Thunderstorms	2.3-12
2.3.1.2.4	Lightning	2.3-12
2.3.1.2.5	Hail	2.3-12
2.3.1.2.6	Regional Air Quality	2.3-13
2.3.1.2.7	Severe Winter Storm Events	2.3-14
2.3.1.2.7.1	Estimated Weight of the 100-year Return Snowpack	2.3-15
2.3.1.2.7.2	Estimated Weight of the 48-hour Maximum Winter Precipitation	2.3-16
2.3.1.2.7.3	Weight of Snow and Ice on Safety-Related Structures	2.3-16
2.3.1.2.8	100-Year Return Period Fastest Mile of Wind	2.3-16
2.3.1.2.9	Probable Maximum Annual Frequency and Duration of Dust Storms	2.3-17
2.3.2	LOCAL METEOROLOGY	2.3-17
2.3.2.1	Winds	2.3-18
2.3.2.1.1	Greenville/Spartanburg Wind Distribution	2.3-18
2.3.2.1.2	Lee Nuclear Site Wind Distribution	2.3-18
2.3.2.1.3	Wind Direction Persistence	2.3-19
2.3.2.2	Air Temperature	2.3-19
2.3.2.3	Atmospheric Moisture	2.3-22
2.3.2.3.1	Precipitation	2.3-22
2.3.2.3.2	Snow	2.3-23
2.3.2.3.3	Fog	2.3-24
2.3.2.4	Atmospheric Stability	2.3-24
2.3.2.4.1	Mixing Heights	2.3-24
2.3.2.5	Potential Influence of the Plant and Its Facilities on Local Meteorology	2.3-25
2.3.2.5.1	Cooling Tower Plumes	2.3-26
2.3.2.6	Topographical Description of the Surrounding Area	2.3-29
2.3.2.7	Current and Projected Site Air Quality Conditions	2.3-29
2.3.3	ONSITE METEOROLOGICAL MEASUREMENT PROGRAMS	2.3-30
2.3.3.1	Onsite Meteorological Monitoring Program	2.3-30
2.3.3.2	Meteorological Data Processing	2.3-32

TABLE OF CONTENTS (Continued)

<u>Section</u>	<u>Title</u>	<u>Page</u>
2.3.3.2.1	Data Acquisition	2.3-32
2.3.3.2.2	Data Processing	2.3-33
2.3.3.2.3	Data Validation	2.3-33
2.3.3.3	Meteorological Instrumentation Inspection and Maintenance	2.3-34
2.3.4	SHORT-TERM DIFFUSION ESTIMATES	2.3-35
2.3.4.1	Calculation Methodology	2.3-35
2.3.4.2	Calculations and Results	2.3-37
2.3.4.3	Short-Term Atmospheric Dispersion Estimates for the Control Room Emergency Air Intake	2.3-39
2.3.4.4	Short-Term Atmospheric Dispersion Estimates for the Technical Support Center	2.3-40
2.3.5	LONG-TERM DIFFUSION ESTIMATES	2.3-41
2.3.5.1	Calculation Methodology and Assumptions	2.3-41
2.3.5.2	Results	2.3-43
2.3.6	COMBINED LICENSE INFORMATION	2.3-43
2.3.6.1	Regional Climatology	2.3-43
2.3.6.2	Local Meteorology	2.3-43
2.3.6.3	Onsite Meteorological Measurements Program	2.3-44
2.3.6.4	Short-Term Diffusion Estimates	2.3-44
2.3.6.5	Long-Term Diffusion Estimates	2.3-44
2.3.7	REFERENCES	2.3-44
2.4	HYDROLOGIC ENGINEERING	2.4-1
2.4.1	HYDROLOGIC DESCRIPTION	2.4-2
2.4.1.1	Site and Facilities	2.4-2
2.4.1.1.1	Previous Construction Activities	2.4-2
2.4.1.1.2	Plant Design	2.4-3
2.4.1.1.3	Safety-Related Structures	2.4-3
2.4.1.1.4	Plant Water Systems	2.4-3
2.4.1.2	Hydrosphere	2.4-5
2.4.1.2.1	Physiography and Topography	2.4-6
2.4.1.2.2	Upper Broad River Watershed	2.4-7
2.4.1.2.2.1	Local Watersheds	2.4-7
2.4.1.2.2.2	Broad River Description	2.4-8
2.4.1.2.2.3	Major Tributaries	2.4-12
2.4.1.2.2.4	Local Tributaries	2.4-13
2.4.1.2.2.5	Ninety-Nine Islands Reservoir	2.4-14
2.4.1.2.2.6	Surface Water Impoundments	2.4-16
2.4.1.2.2.7	Local Wetlands	2.4-19
2.4.1.2.3	Dams and Reservoirs	2.4-19
2.4.1.2.3.1	Upstream Dams and Reservoirs	2.4-20
2.4.1.2.3.2	Downstream Dams and Reservoirs	2.4-21
2.4.1.2.3.3	Water Management Changes	2.4-22

TABLE OF CONTENTS (Continued)

<u>Section</u>	<u>Title</u>	<u>Page</u>
2.4.1.2.4	Regional Hydrogeology	2.4-22
2.4.1.2.5	Water Use	2.4-23
2.4.1.2.5.1	Surface Water Use	2.4-23
2.4.1.2.5.2	Groundwater Use	2.4-24
2.4.2	FLOODS	2.4-25
2.4.2.1	Flood History	2.4-25
2.4.2.2	Flood Design Considerations	2.4-26
2.4.2.3	Effects of Local Intense Precipitation	2.4-27
2.4.3	PROBABLE MAXIMUM FLOOD ON STREAMS AND RIVERS	2.4-31
2.4.3.1	Probable Maximum Precipitation	2.4-32
2.4.3.2	Precipitation Losses	2.4-34
2.4.3.3	Runoff and Stream Course Models	2.4-36
2.4.3.4	Probable Maximum Flood Flow	2.4-44
2.4.3.5	Water Level Determinations	2.4-46
2.4.3.6	Coincident Wind Wave Activity	2.4-47
2.4.4	POTENTIAL DAM FAILURES	2.4-48
2.4.4.1	Dam Failure Permutations	2.4-49
2.4.4.2	Unsteady-Flow Analysis of Potential Dam Failures	2.4-54
2.4.4.3	Water Level at the Plant Site	2.4-55
2.4.5	PROBABLE MAXIMUM SURGE AND SEICHE FLOODING	2.4-57
2.4.6	PROBABLE MAXIMUM TSUNAMI	2.4-61
2.4.7	ICE EFFECTS	2.4-62
2.4.8	COOLING WATER CANALS AND RESERVOIRS	2.4-63
2.4.9	CHANNEL DIVERSIONS	2.4-63
2.4.10	FLOODING PROTECTION REQUIREMENTS	2.4-64
2.4.11	LOW WATER CONSIDERATIONS	2.4-64
2.4.11.1	Low Flow in Rivers and Streams	2.4-64
2.4.11.2	Low Water Resulting from Surges, Seiches, or Tsunami	2.4-65
2.4.11.3	Historical Low Water	2.4-65
2.4.11.4	Future Controls	2.4-67
2.4.11.5	Plant Requirements	2.4-69
2.4.11.6	Heat Sink Dependability Requirements	2.4-70
2.4.12	GROUNDWATER	2.4-71
2.4.12.1	Description and On-Site Use	2.4-71
2.4.12.1.1	Regional Aquifers, Formations, Sources, and Sinks	2.4-71
2.4.12.1.2	Local Aquifers, Formations, Sources, and Sinks	2.4-72
2.4.12.2	Sources	2.4-73
2.4.12.2.1	Regional and Local Groundwater Uses	2.4-73
2.4.12.2.2	Historical On-Site Conditions	2.4-74
2.4.12.2.3	On-Site Conditions in 2006 to 2007 and Projected Post-Construction On-Site Conditions	2.4-75
2.4.12.2.3.1	Maximum Post-Construction Groundwater Analysis	2.4-78

TABLE OF CONTENTS (Continued)

<u>Section</u>	<u>Title</u>	<u>Page</u>
2.4.12.2.4	Aquifer Characteristics.....	2.4-79
2.4.12.2.4.1	Porosity	2.4-79
2.4.12.2.4.2	Permeability	2.4-80
2.4.12.3	Groundwater Movement	2.4-82
2.4.12.3.1	Groundwater Pathways	2.4-82
2.4.12.3.2	Groundwater Velocity	2.4-83
2.4.12.3.3	Effects of Local Area Pumping	2.4-84
2.4.12.4	Monitoring or Safeguard Requirements.....	2.4-85
2.4.12.5	Site Characteristics for Subsurface Hydrostatic Loading.....	2.4-85
2.4.13	ACCIDENTAL RELEASES OF RADIOACTIVE LIQUID EFFLUENTS IN GROUND AND SURFACE WATERS	2.4-86
2.4.13.1	Groundwater	2.4-86
2.4.13.2	Accident Scenario	2.4-87
2.4.13.3	Source Term	2.4-89
2.4.13.4	Conceptual Model	2.4-90
2.4.13.5	Sensitive Parameters.....	2.4-91
2.4.13.6	Regulatory Compliance	2.4-92
2.4.14	TECHNICAL SPECIFICATIONS AND EMERGENCY OPERATION REQUIREMENTS.....	2.4-92
2.4.15	COMBINED LICENSE INFORMATION.....	2.4-93
2.4.15.1	Hydrological Description	2.4-93
2.4.15.2	Floods	2.4-93
2.4.15.3	Cooling Water Supply	2.4-93
2.4.15.4	Groundwater	2.4-94
2.4.15.5	Accidental Release of Liquid Effluents into Ground and Surface Water	2.4-94
2.4.15.6	Emergency Operation Requirement	2.4-94
2.4.16	REFERENCES	2.4-94
2.5	GEOLOGY, SEISMOLOGY, AND GEOTECHNICAL ENGINEERING	2.5-1
2.5.1	BASIC GEOLOGIC AND SEISMIC INFORMATION	2.5-2
2.5.1.1	Regional Geology	2.5-2
2.5.1.1.1	Regional Physiography, Geomorphology, and Stratigraphy	2.5-3
2.5.1.1.1.1	The Appalachian Plateau Physiographic Province	2.5-4
2.5.1.1.1.2	The Valley and Ridge Physiographic Province	2.5-4
2.5.1.1.1.3	The Blue Ridge Physiographic Province.....	2.5-4
2.5.1.1.1.4	The Piedmont Physiographic Province	2.5-6
2.5.1.1.1.5	The Atlantic Coastal Plain Physiographic Province	2.5-9
2.5.1.1.1.6	Mesozoic Rift Basins.....	2.5-9
2.5.1.1.2	Regional Tectonic Setting.....	2.5-10
2.5.1.1.2.1	Regional Geologic History	2.5-10
2.5.1.1.2.2	Tectonic Stress in the Mid-Continent Region.....	2.5-13

TABLE OF CONTENTS (Continued)

<u>Section</u>	<u>Title</u>	<u>Page</u>
2.5.1.1.2.3	Gravity and Magnetic Data of the Site Region and Site Vicinity	2.5-15
2.5.1.1.2.3.1	Gravity Data of the Site Region and Site Vicinity	2.5-15
2.5.1.1.2.3.2	Magnetic Data of the Site Region and Site Vicinity....	2.5-17
2.5.1.1.2.4	Principal Regional Tectonic Structures	2.5-21
2.5.1.1.2.4.1	Regional Geophysical Anomalies and Lineaments....	2.5-21
2.5.1.1.2.4.2	Regional Paleozoic Tectonic Structures	2.5-24
2.5.1.1.2.4.3	Regional Mesozoic Tectonic Structures.....	2.5-29
2.5.1.1.2.4.4	Regional Cenozoic Tectonic Structures	2.5-30
2.5.1.1.2.4.5	Regional Quaternary Tectonic Structures	2.5-32
2.5.1.1.3	Regional Seismicity and Paleoseismology	2.5-35
2.5.1.1.3.1	Central and Eastern U.S. Seismicity	2.5-35
2.5.1.1.3.2	Seismic Sources Defined by Regional Seismicity.....	2.5-36
2.5.1.1.3.2.1	Charleston Tectonic Features	2.5-36
2.5.1.1.3.2.2	Eastern Tennessee Seismic Zone	2.5-42
2.5.1.1.3.2.3	Giles County Seismic Zone.....	2.5-43
2.5.1.1.3.2.4	Selected Seismogenic and Capable Tectonic Sources Beyond the Site Region	2.5-44
2.5.1.2	Site Geology	2.5-46
2.5.1.2.1	Site Area Physiography and Geomorphology.....	2.5-47
2.5.1.2.2	Site Area Geologic Setting and History	2.5-48
2.5.1.2.3	Site Area Stratigraphy and Lithology	2.5-52
2.5.1.2.3.1	Battleground Formation	2.5-52
2.5.1.2.3.2	Site Pluton (Rock Mass Zto)	2.5-54
2.5.1.2.3.3	Other Lithologic and Stratigraphic Units within the Site Area	2.5-55
2.5.1.2.4	Site Area Structural Geology	2.5-55
2.5.1.2.4.1	Structures Within the Site Area.....	2.5-57
2.5.1.2.5	Site Geology	2.5-58
2.5.1.2.5.1	Site Physiography and Geomorphology	2.5-58
2.5.1.2.5.2	Site Geologic Setting and History	2.5-58
2.5.1.2.5.3	Site Stratigraphy and Lithology	2.5-59
2.5.1.2.5.4	Site Area Structure.....	2.5-59
2.5.1.2.5.5	Site Geologic Mapping.....	2.5-66
2.5.1.2.6	Site Area Engineering Geology	2.5-72
2.5.1.2.7	Site Area Seismicity and Paleoseismology.....	2.5-73
2.5.1.2.8	Site Groundwater Conditions.....	2.5-74
2.5.1.3	References	2.5-74
2.5.2	VIBRATORY GROUND MOTION.....	2.5-98
2.5.2.1	Seismicity.....	2.5-100
2.5.2.1.1	Seismicity Catalog Used for 2012 CEUS SSC Project	2.5-100
2.5.2.1.2	Recent and Historical Seismicity	2.5-101
2.5.2.1.3	Evaluation of the Potential for Reservoir-Induced Seismicity.....	2.5-101

TABLE OF CONTENTS (Continued)

<u>Section</u>	<u>Title</u>	<u>Page</u>
2.5.2.2	Geologic and Tectonic Characterizations of the Site and Region	2.5-106
2.5.2.2.1	Overview of CEUS SSC	2.5-106
2.5.2.2.1.1	CEUS SSC Methodology	2.5-107
2.5.2.2.1.2	CEUS SSC Earthquake Recurrence Rate	2.5-108
2.5.2.2.1.3	CEUS SSC Maximum Magnitude	2.5-108
2.5.2.2.2	CEUS SSC Mmax Zones Included in the Lee Nuclear Site PSHA.....	2.5-109
2.5.2.2.2.1	Mesozoic and Younger Extended Crust (MESE).....	2.5-110
2.5.2.2.2.2	Non-Mesozoic and Younger Extended Crust (NMESE).....	2.5-110
2.5.2.2.2.3	Study Region	2.5-111
2.5.2.2.3	CEUS SSC Seismotectonic Zones Included in the Lee Nuclear Site PSHA	2.5-111
2.5.2.2.3.1	Atlantic Highly Extended Crust (AHEX)	2.5-111
2.5.2.2.3.2	Extended Continental Crust-Atlantic Margin (ECC-AM)	2.5-112
2.5.2.2.3.3	Extended Continental Crust-Gulf Coast zone (ECC-GC)	2.5-113
2.5.2.2.3.4	Illinois Basin Extended Basement (IBEB)	2.5-113
2.5.2.2.3.5	Paleozoic Extended Crust (PEZ)	2.5-114
2.5.2.2.3.6	Midcontinent Craton (MidC) Seismotectonic Zones	2.5-115
2.5.2.2.3.7	Reelfoot Rift (RR)-Rough Creek Graben (RCG).....	2.5-115
2.5.2.2.4	CEUS SSC RLME Sources Included in the Lee Nuclear Site PSHA.....	2.5-116
2.5.2.2.4.1	Charleston.....	2.5-116
2.5.2.2.4.2	New Madrid Fault System.....	2.5-117
2.5.2.2.5	Post-CEUS SSC Studies	2.5-118
2.5.2.2.5.1	Geologic Investigations of the Eastern Tennessee Seismic Zone	2.5-118
2.5.2.2.5.2	Investigations of the 2011 Mineral, Virginia Earthquake.....	2.5-119
2.5.2.3	Correlation of Earthquake Activity with Seismic Sources	2.5-121
2.5.2.4	Probabilistic Seismic Hazard Analysis and Controlling Earthquake	2.5-125
2.5.2.4.1	New Ground Motion Models	2.5-126
2.5.2.4.2	Updated Probabilistic Seismic Hazard Analysis and Deaggregation	2.5-126
2.5.2.5	Seismic Wave Transmission Characteristics of the Site.....	2.5-128
2.5.2.6	Ground Motion Response Spectra (GMRS)	2.5-129
2.5.2.7	Development of FIRS for Units 1 and 2	2.5-130
2.5.2.7.1	Site Response Analysis	2.5-131
2.5.2.7.1.1	Implementation of Approach 3	2.5-133
2.5.2.7.1.1.1	Development of Transfer Functions	2.5-133

TABLE OF CONTENTS (Continued)

<u>Section</u>	<u>Title</u>	<u>Page</u>
2.5.2.7.2	Development of V/H Ratios	2.5-135
2.5.2.7.3	UHRs Interpolation and Extrapolation.....	2.5-138
2.5.2.7.4	Design Basis Response Spectra	2.5-139
2.5.2.8	References	2.5-139
2.5.3	SURFACE FAULTING.....	2.5-154
2.5.3.1	Geological, Seismological, and Geophysical Investigations.....	2.5-155
2.5.3.1.1	Previous Lee Nuclear Site Investigations	2.5-156
2.5.3.1.2	Published Geologic Mapping	2.5-156
2.5.3.1.3	Current Geologic Mapping.....	2.5-157
2.5.3.1.4	Previous Seismicity Data	2.5-159
2.5.3.1.5	Current Seismicity Data	2.5-160
2.5.3.1.6	Current Aerial and Field Reconnaissance	2.5-161
2.5.3.2	Geological Evidence, or Absence of Evidence, for Surface Deformation.....	2.5-162
2.5.3.3	Correlation of Earthquakes With Capable Tectonic Sources.....	2.5-164
2.5.3.4	Ages of Most Recent Deformations	2.5-164
2.5.3.5	Relationships of Tectonic Structures in the Site Area to Regional Tectonic Structures.....	2.5-164
2.5.3.6	Characterization of Capable Tectonic Sources	2.5-165
2.5.3.7	Designation of Zones of Quaternary Deformation in the Site Region	2.5-165
2.5.3.8	Potential for Surface Tectonic Deformation at the Site.....	2.5-165
2.5.3.9	References	2.5-166
2.5.4	STABILITY OF SUBSURFACE MATERIALS AND FOUNDATIONS	2.5-170
2.5.4.1	Geologic Features	2.5-171
2.5.4.1.1	Geologic History and Stress Conditions	2.5-172
2.5.4.1.2	Stratigraphy, Lithology, and Soil and Rock Characteristics	2.5-173
2.5.4.1.2.1	Site Area Stratigraphy and Lithology	2.5-174
2.5.4.1.2.2	Soil and Rock Characteristics	2.5-175
2.5.4.1.3	Groundwater	2.5-177
2.5.4.1.4	Effects of Human Activities	2.5-177
2.5.4.1.5	Summary of Geologic Hazards.....	2.5-177
2.5.4.2	Properties of Subsurface Materials.....	2.5-178
2.5.4.2.1	Site Explorations.....	2.5-179
2.5.4.2.1.1	Soil, Rock, and Concrete Borings	2.5-180
2.5.4.2.1.2	Groundwater Monitoring Wells.....	2.5-182
2.5.4.2.1.3	Surface Geophysical Testing	2.5-182
2.5.4.2.1.4	Cone Penetration Testing	2.5-182
2.5.4.2.1.5	Geotechnical Test Pits and Geologic Trenches	2.5-183

TABLE OF CONTENTS (Continued)

<u>Section</u>	<u>Title</u>	<u>Page</u>
2.5.4.2.1.6	In Situ Testing	2.5-183
2.5.4.2.1.6.1	Goodman Jack Testing	2.5-183
2.5.4.2.1.6.2	Borehole Pressuremeter Testing	2.5-184
2.5.4.2.1.6.3	Borehole Geophysical Testing	2.5-184
2.5.4.2.1.6.4	Packer Testing	2.5-184
2.5.4.2.1.7	Petrographic Testing	2.5-184
2.5.4.2.2	Soil and Rock Sampling.....	2.5-185
2.5.4.2.2.1	Standard Penetration Test Sampling	2.5-185
2.5.4.2.2.2	Coring	2.5-186
2.5.4.2.2.3	Undisturbed Sampling.....	2.5-186
2.5.4.2.2.4	Bulk Sampling (Test Pits).....	2.5-186
2.5.4.2.2.5	Sample Control and Preservation	2.5-187
2.5.4.2.3	Laboratory Testing.....	2.5-188
2.5.4.2.3.1	Particle Size Analysis, ASTM D 422-63 (2002) and ASTM D 6913-04	2.5-189
2.5.4.2.3.2	Chemical Analysis (pH, Resistivity), ASTM G 51-95 (2005), ASTM G 57-95a (2001)	2.5-190
2.5.4.2.3.3	Chemical Analysis (Chloride, Sulfate), EPA SW-846 9056/300.0, EPA SW-846 8056/300.0	2.5-190
2.5.4.2.3.4	Unit Weight of Soil, ASTM D 5084-03 (Sections 5.7 – 5.9, 8.1, 11.3.2).....	2.5-190
2.5.4.2.3.5	Deleted.....	2.5-191
2.5.4.2.3.6	Deleted.....	2.5-191
2.5.4.2.3.7	Consolidated – Undrained Triaxial Shear Testing, ASTM D 4767-04	2.5-191
2.5.4.2.3.8	Deleted.....	2.5-191
2.5.4.2.3.9	Deleted.....	2.5-191
2.5.4.2.3.10	Specimen Preparation – Rock Cores, ASTM D 4543-04	2.5-191
2.5.4.2.3.11	Compressive Strength and Elastic Moduli – Rock Cores, ASTM D 7012-04.....	2.5-192
2.5.4.2.3.12	Consolidation Tests, ASTM D 2435-04.....	2.5-192
2.5.4.2.3.13	Deleted.....	2.5-193
2.5.4.2.3.14	Deleted.....	2.5-193
2.5.4.2.4	Material Properties.....	2.5-193
2.5.4.2.4.1	Geotechnical Model	2.5-193
2.5.4.2.4.1.1	Pre-existing Engineered Fill Soils	2.5-193
2.5.4.2.4.1.2	Alluvial Soils	2.5-193
2.5.4.2.4.1.3	Residual Soils	2.5-193
2.5.4.2.4.1.4	Saprolite Soils	2.5-194
2.5.4.2.4.1.5	Partially Weathered Rock	2.5-194
2.5.4.2.4.1.6	Pre-existing Concrete	2.5-194
2.5.4.2.4.1.7	Rock.....	2.5-194
2.5.4.2.4.1.8	Granular Backfill.....	2.5-195
2.5.4.2.4.2	Static Properties of Geotechnical Materials	2.5-195

TABLE OF CONTENTS (Continued)

<u>Section</u>	<u>Title</u>	<u>Page</u>
2.5.4.3	Foundation Interfaces	2.5-196
2.5.4.3.1	Power Block Exploration	2.5-196
2.5.4.3.2	Surrounding and Adjacent Structures Exploration	2.5-197
2.5.4.3.3	Geotechnical Data Logs and Records	2.5-197
2.5.4.3.4	Borehole Summaries	2.5-198
2.5.4.3.5	Geotechnical Profiles	2.5-198
2.5.4.3.6	Extent of Granular Fill	2.5-199
2.5.4.4	Geophysical Surveys	2.5-200
2.5.4.4.1	Spectral Analysis of Surface Waves (SASW) Surveys	2.5-200
2.5.4.4.1.1	Survey Method	2.5-201
2.5.4.4.1.2	Survey Results	2.5-201
2.5.4.4.2	Seismic Cone Penetration Tests	2.5-201
2.5.4.4.2.1	Seismic CPT Methods	2.5-201
2.5.4.4.3	Suspension and Downhole Velocity Logging	2.5-202
2.5.4.4.3.1	P-S Velocity Logging Methods	2.5-202
2.5.4.4.3.2	Downhole Velocity Logging Methods	2.5-203
2.5.4.4.3.3	Velocity Logging Results	2.5-203
2.5.4.4.4	Acoustic and Optical Televiewer Logging	2.5-203
2.5.4.5	Excavations and Backfill	2.5-204
2.5.4.5.1	Sources and Quantities	2.5-204
2.5.4.5.2	Extent of Excavation	2.5-205
2.5.4.5.2.1	Unit 1 Excavation Conditions	2.5-206
2.5.4.5.2.2	Unit 2 Excavation Conditions	2.5-207
2.5.4.5.3	Specifications and Control	2.5-208
2.5.4.5.3.1	Nuclear Island Foundation Materials	2.5-208
2.5.4.5.3.2	Fill Concrete beneath the Nuclear Island Foundation Limits	2.5-209
2.5.4.5.3.3	Foundation Materials Outside the Nuclear Island	2.5-210
2.5.4.5.3.4	Fill Concrete Outside the Nuclear Island Foundation Limits	2.5-211
2.5.4.5.3.5	Granular Backfill Outside the Nuclear Island	2.5-211
2.5.4.5.4	Groundwater Control	2.5-213
2.5.4.6	Groundwater Conditions	2.5-214
2.5.4.6.1	Groundwater Occurrence	2.5-214
2.5.4.6.2	Permeability Testing	2.5-214
2.5.4.6.3	Construction Dewatering	2.5-215
2.5.4.6.4	Groundwater Impacts on Foundation Stability	2.5-215
2.5.4.7	Response of Soil, Granular Fill, and Rock to Dynamic Loading	2.5-216
2.5.4.7.1	Prior Earthquake Effects and Geologic Stability	2.5-217
2.5.4.7.2	Field Dynamic Measurements	2.5-217
2.5.4.7.3	Deleted	2.5-219

TABLE OF CONTENTS (Continued)

<u>Section</u>	<u>Title</u>	<u>Page</u>
2.5.4.7.4	Foundation Conditions and Uniformity.....	2.5-219
2.5.4.7.4.1	Lee Nuclear Station, Unit 1 Nuclear Island	2.5-219
2.5.4.7.4.2	Lee Nuclear Station, Unit 2 Nuclear Island	2.5-220
2.5.4.7.5	Dynamic Profiles	2.5-221
2.5.4.8	Liquefaction Potential	2.5-224
2.5.4.9	Earthquake Site Characteristics	2.5-226
2.5.4.10	Static Stability	2.5-227
2.5.4.10.1	Bearing Capacity	2.5-228
2.5.4.10.1.1	Bearing Capacity of Nuclear Islands	2.5-228
2.5.4.10.1.2	Bearing Capacity of Adjacent Structures	2.5-229
2.5.4.10.2	Settlement.....	2.5-232
2.5.4.10.2.1	Settlement of Nuclear Islands	2.5-232
2.5.4.10.2.2	Settlement of Adjacent Structures	2.5-233
2.5.4.10.3	Lateral Pressures.....	2.5-234
2.5.4.11	Design Criteria	2.5-236
2.5.4.12	Techniques to Improve Subsurface Conditions	2.5-236
2.5.4.13	References	2.5-238
2.5.5	STABILITY OF SLOPES	2.5-242
2.5.5.1	Slope Characteristics	2.5-243
2.5.5.1.1	General Discussion.....	2.5-243
2.5.5.1.2	Exploration Program	2.5-244
2.5.5.1.3	Groundwater and Seepage.....	2.5-244
2.5.5.1.4	Slope Materials and Properties.....	2.5-244
2.5.5.2	Design Criteria and Analyses	2.5-245
2.5.5.3	Logs of Borings	2.5-245
2.5.5.3.1	Soil Borings.....	2.5-246
2.5.5.3.2	Rock Borings	2.5-246
2.5.5.3.3	Test Pits and Trenches.....	2.5-246
2.5.5.4	Compacted Fill.....	2.5-246
2.5.5.5	References	2.5-246
2.5.6	COMBINED LICENSE INFORMATION.....	2.5-246
2.5.6.1	Basic Geologic and Seismic Information	2.5-246
2.5.6.2	Site Seismic and Tectonic Characteristics Information.....	2.5-246
2.5.6.3	Geoscience Parameters	2.5-247
2.5.6.4	Surface Faulting.....	2.5-247
2.5.6.5	Site and Structures	2.5-247
2.5.6.6	Properties of Underlying Materials.....	2.5-247
2.5.6.7	Excavation and Backfill	2.5-247
2.5.6.8	Groundwater Conditions	2.5-247
2.5.6.9	Liquefaction Potential	2.5-247
2.5.6.10	Bearing Capacity	2.5-247
2.5.6.11	Earth Pressures	2.5-248
2.5.6.12	Static and Dynamic Stability of Facilities	2.5-248
2.5.6.13	Subsurface Instrumentation.....	2.5-248
2.5.6.14	Stability of Slopes	2.5-248

TABLE OF CONTENTS (Continued)

<u>Section</u>	<u>Title</u>	<u>Page</u>
2.5.6.15	Embankments and Dams	2.5-248
2.5.6.16	Settlement of Nuclear Island.....	2.5-248
2.5.6.17	Waterproofing Systems	2.5-248
APP. 2AA	LEE NUCLEAR STATION FIELD EXPLORATION DATA	2AA-1
APP. 2BB	CHEROKEE NUCLEAR STATION GEOTECHNICAL BORING LOGS	2BB-1
APP. 2CC	EVALUATION OF METEOROLOGICAL DATA	2CC-1
APP. 2DD	COOLING TOWER PLUME ANALYSES	2DD-1

LIST OF TABLES

<u>Number</u>	<u>Title</u>
2.0-201	Comparison of AP1000 DCD Site Parameters and Lee Nuclear Station Units 1 & 2 Site Characteristics
2.0-202	Comparison of Control Room Atmospheric Dispersion Factors for Accident Analysis for AP1000 DCD and Lee Nuclear Station Units 1 & 2 (Reference Table 2.3-285)
2.1-201	Counties Entirely or Partially Located within the Lee Nuclear Station 50-Mi. Buffer
2.1-202	US Census Bureau Estimated Year 2000 Populations within a 10-Mi. Radius
2.1-203	The Projected Permanent Population for Each Sector 0- to 16-km (0 to 10–Mi.) for Years 2007, 2016, 2026, 2036, 2046, and 2056
2.1-204	The Projected Permanent Population for Each Sector 16-km (10-Mi.) – 80-km (50-Mi.) for Years 2007, 2016, 2026, 2036, 2046, and 2056
2.1-205	Major Contributors to Transient Population within 80-km (50-Mi.)
2.1-206	Daily and Annual Passenger Counts for Commercial Airports in the Lee Nuclear Station Region
2.1-207	Fishing, Hunting, and Wildlife Watching within the Lee Nuclear Station Region
2.1-208	The Projected Transient Population for Each Sector 0- to 80-km (50-Mi.) for Years 2007, 2016, 2026, 2036, 2046, and 2056
2.1-209	Population Distribution in the Low Population Zone
2.2-201	Registered Storage Tanks within a 5-Mi. Radius
2.2-202	Industrial Facilities Near the Lee Nuclear Station
2.2-203	Products Stored on Site at the Broad River Energy Center
2.2-204	Broad River Energy Center Site Specific OSHA Permissible Exposure Limits (PEL) Z-1 Table
2.2-205	Historical Air Traffic at Greenville-Spartanburg International Airport
2.2-206	Projected Air Traffic at Greenville-Spartanburg International Airport

LIST OF TABLES (Continued)

<u>Number</u>	<u>Title</u>
2.2-207	Historical Air Traffic at Charlotte Douglas International Airport
2.2-208	Projected Air Traffic at Charlotte Douglas International Airport
2.2-209	Parameters Used in the Analysis of an Off-Site Chemical Release
2.2-210	Leakage from Assumed Large Hole (4.5 m ²) from a Truck on Highway 29
2.2-211	Leakage from Assumed Large Hole (4.5 m ²) from a Railroad Tanker
2.3-201	Rainfall Frequency Distribution Greenville/Spartanburg, South Carolina Number of Hours Per Month, Average Year
2.3-202	Hurricanes in North Carolina and South Carolina 1899 – 2005
2.3-203	Frequency of Tropical Cyclones (by Month) for the States of South Carolina and North Carolina
2.3-204	Tornadoes in Cherokee, Spartanburg, Union, Chester, and York Counties, South Carolina and Cleveland, Gaston, Mecklenburg, Polk, and Rutherford Counties, North Carolina
2.3-205	Thunderstorms Greenville-Spartanburg, SC and Charlotte, NC
2.3-206	Hail Storm Events Cherokee, Spartanburg, Union, Chester, and York Counties, South Carolina and Cleveland, Gaston, and Mecklenburg Counties, North Carolina
2.3-207	Mean Ventilation Rate By Month Greensboro, NC
2.3-208	Ice Storms Cherokee, Spartanburg, Union, Chester, and York Counties, South Carolina and Cleveland, Gaston, and Mecklenburg Counties, North Carolina
2.3-209	Percentage Frequency of Wind Direction and Speed (mph) Greenville/Spartanburg, South Carolina January, 1997 – 2005
2.3-210	Percentage Frequency of Wind Direction and Speed (mph) Greenville/Spartanburg, South Carolina February, 1997 – 2005
2.3-211	Percentage Frequency of Wind Direction And Speed (mph) Greenville/Spartanburg, South Carolina March, 1997 – 2005

LIST OF TABLES (Continued)

<u>Number</u>	<u>Title</u>
2.3-212	Percentage Frequency of Wind Direction and Speed (mph) Greenville/Spartanburg, South Carolina April, 1997-2005
2.3-213	Percentage Frequency of Wind Direction and Speed (mph) Greenville/Spartanburg, South Carolina May, 1997-2005
2.3-214	Percentage Frequency of Wind Direction and Speed (mph) Greenville/Spartanburg, South Carolina June, 1997-2005
2.3-215	Percentage Frequency of Wind Direction and Speed (mph) Greenville/Spartanburg, South Carolina July, 1997-2005
2.3-216	Percentage Frequency of Wind Direction And Speed (mph) Greenville/Spartanburg, South Carolina August, 1997-2005
2.3-217	Percentage Frequency of Wind Direction and Speed (mph) Greenville/Spartanburg, South Carolina September, 1997-2005
2.3-218	Percentage Frequency of Wind Direction and Speed (mph) Greenville/Spartanburg, South Carolina October, 1997-2005
2.3-219	Percentage Frequency of Wind Direction and Speed (mph) Greenville/Spartanburg, South Carolina November, 1997-2005
2.3-220	Percentage Frequency of Wind Direction and Speed (mph) Greenville/Spartanburg, South Carolina December, 1997-2005
2.3-221	Percentage Frequency of Wind Direction And Speed (mph) Greenville/Spartanburg, South Carolina All Months, 1997-2005
2.3-222	Percentage Frequency of Wind Direction and Speed (mph) Lee Nuclear Station Site January
2.3-223	Percentage Frequency of Wind Direction and Speed (mph) Lee Nuclear Station Site February
2.3-224	Percentage Frequency of Wind Direction and Speed (mph) Lee Nuclear Station Site March
2.3-225	Percentage Frequency of Wind Direction and Speed (mph) Lee Nuclear Station Site April
2.3-226	Percentage Frequency of Wind Direction and Speed (mph) Lee Nuclear Station Site May

LIST OF TABLES (Continued)

<u>Number</u>	<u>Title</u>
2.3-227	Percentage Frequency of Wind Direction and Speed (mph) Lee Nuclear Station Site June
2.3-228	Percentage Frequency of Wind Direction and Speed (mph) Lee Nuclear Station Site July
2.3-229	Percentage Frequency of Wind Direction and Speed (mph) Lee Nuclear Station Site August
2.3-230	Percentage Frequency of Wind Direction and Speed (mph) Lee Nuclear Station Site September
2.3-231	Percentage Frequency of Wind Direction and Speed (mph) Lee Nuclear Station Site October
2.3-232	Percentage Frequency of Wind Direction and Speed (mph) Lee Nuclear Station Site November
2.3-233	Percentage Frequency of Wind Direction and Speed (mph) Lee Nuclear Station Site December
2.3-234	Percentage Frequency of Wind Direction And Speed (mph) Lee Nuclear Site All Months
2.3-235	Joint Frequency Distribution of Wind Speed and Direction by Atmospheric Stability Class Stability Class A
2.3-236	Joint Frequency Distribution of Wind Speed and Direction by Atmospheric Stability Class Stability Class B
2.3-237	Joint Frequency Distribution of Wind Speed and Direction by Atmospheric Stability Class Stability Class C
2.3-238	Joint Frequency Distribution of Wind Speed and Direction by Atmospheric Stability Class Stability Class D
2.3-239	Joint Frequency Distribution of Wind Speed and Direction by Atmospheric Stability Class Stability Class E
2.3-240	Joint Frequency Distribution of Wind Speed and Direction by Atmospheric Stability Class Stability Class F
2.3-241	Joint Frequency Distribution of Wind Speed and Direction by Atmospheric Stability Class Stability Class G

LIST OF TABLES (Continued)

<u>Number</u>	<u>Title</u>
2.3-242	Maximum Number of Consecutive Hours with Wind from a Single Sector Greenville/Spartanburg, South Carolina
2.3-243	Maximum Number of Consecutive Hours with Wind from Three Adjacent Sectors, Greenville/Spartanburg, South Carolina
2.3-244	Maximum Number of Consecutive Hours with Wind from Five Adjacent Sectors, Greenville/Spartanburg, South Carolina
2.3-245	Comparison of Maximum Wind Persistence at Lee Nuclear Station Site and Greenville/Spartanburg South Carolina
2.3-246	Ninety-Nine Islands Monthly Climate Summary NCDC 1971-2000 Monthly Normals
2.3-247	Deleted
2.3-248	Deleted
2.3-249	Deleted
2.3-250	Deleted
2.3-251	Deleted
2.3-252	Deleted
2.3-253	Relative Humidity Greenville/Spartanburg, South Carolina for 4 Time Periods Per Day 1997-2005
2.3-254	Ninety-Nine Islands Monthly Climate Summary Ninety-Nine Islands, South Carolina (386293) Period of Record: 8/1/1948 to 12/31/2005
2.3-255	Comparison of Relative Humidity Lee Nuclear Site (2005 – 2006) and Greenville/Spartanburg, South Carolina (1997 – 2005) for 4 Time Periods Per Day
2.3-256	Precipitation Data (Inches of Rain) Greenville/Spartanburg, South Carolina
2.3-257	Point Precipitation Frequency

LIST OF TABLES (Continued)

<u>Number</u>	<u>Title</u>
2.3-258	Percent of Total Observations (by Month) of Indicated Wind Directions and Precipitation Greenville/Spartanburg, South Carolina
2.3-259	Percent of Total Observations (by Month) of Precipitation and Wind Direction Lee Nuclear Site
2.3-260	Rainfall Frequency Distribution Lee Nuclear Station Site Number of Hours Per Month
2.3-261	Precipitation Data (Inches of Rain) Lee Nuclear Station Site
2.3-262	Ninety-Nine Islands, South Carolina Monthly Total Snowfall (Inches) 1947 - 2006
2.3-263	Average Hours of Fog And Haze At Greenville/Spartanburg, South Carolina
2.3-264	Inversion Heights and Strengths, Greensboro, North Carolina January, 1999 - 2005
2.3-265	Inversion Heights and Strengths, Greensboro, North Carolina February, 1999 - 2005
2.3-266	Inversion Heights and Strengths, Greensboro, North Carolina March, 1999 - 2005
2.3-267	Inversion Heights and Strengths, Greensboro, North Carolina April, 1999 - 2005
2.3-268	Inversion Heights and Strengths, Greensboro, North Carolina May, 1999 - 2005
2.3-269	Inversion Heights and Strengths, Greensboro, North Carolina June, 1999 - 2005
2.3-270	Inversion Heights and Strengths, Greensboro, North Carolina July, 1999 - 2005
2.3-271	Inversion Heights and Strengths, Greensboro, North Carolina August, 1999 - 2005
2.3-272	Inversion Heights and Strengths, Greensboro, North Carolina September, 1999 - 2005

LIST OF TABLES (Continued)

<u>Number</u>	<u>Title</u>
2.3-273	Inversion Heights and Strengths, Greensboro, North Carolina October, 1999 - 2005
2.3-274	Inversion Heights and Strengths, Greensboro, North Carolina November, 1999 – 2005
2.3-275	Inversion Heights and Strengths, Greensboro, North Carolina December, 1999 – 2005
2.3-276	Inversion Heights and Strengths, Greensboro, North Carolina Annual, 1999 – 2005
2.3-277	Mixing Heights at Greensboro, North Carolina
2.3-278	Visible Plume Frequency of Occurrence by Season (All wind directions)
2.3-279	Frequency of Plume Shadowing by Season (Average for all wind directions)
2.3-280	Maximum Salt Drift Deposition Rate (kg/km ² /mo)
2.3-281	Meteorological Tower Instrumentation for MET Towers 1 & 2 and the Permanent MET Tower
2.3-282	Minimum Exclusion Area Boundary (EAB) Distances and Site Boundary Distances [From Inner 448 Ft (137 M) Radius Circle Encompassing All Site Release Points]
2.3-283	Lee Nuclear Station Offsite Atmospheric Dispersion Short-term Diffusion Estimates for Accidental Releases
2.3-284	Lee Nuclear Station Control Room χ/Q Input Data
2.3-285	Control Room Atmospheric Dispersion Factors (χ/Q) for Accident Dose Analysis (s/m ³)
2.3-286	Lee Nuclear Site Offsite Receptor Locations
2.3-287	Annual Average χ/Q (sec/m ³) for Normal Releases No Decay, Undepleted (for Each 22.5° Sector at the Distances (Miles) Shown at the Top)

LIST OF TABLES (Continued)

<u>Number</u>	<u>Title</u>
2.3-288	Annual Average χ/Q (sec/m ³) for Normal Releases No Decay, Depleted (for Each 22.5° Sector at the Distances (Miles) Shown at the Top)
2.3-289	χ/Q and D/Q Values for Normal Releases
2.3-290	Annual Average χ/Q (sec/m ³) for Normal Releases 2.26 Day Decay, Undepleted (for Each 22.5° Sector at the Distances (Miles) Shown at the Top)
2.3-291	Annual Average χ/Q (sec/m ³) for Normal Releases 8.00 Day Decay, Depleted (for Each 22.5° Sector at the Distances (Miles) Shown at the Top)
2.3-292	D/Q (m ⁻²) at Each 22.5° Sector for Normal Releases (for Each Distance (Miles) Shown at the Top)
2.3-293	Lee Nuclear Station Design Temperatures
2.3-294	Lee Nuclear Station TSC HVAC Distances and Directions
2.3-295	TSC Atmospheric Dispersion Factors (χ/Q) for Accident Dose Analysis (s/m ³)
2.4.1-201	Site Features and Elevations
2.4.1-202	Description of Upper Broad River Watersheds
2.4.1-203	USGS Gauging Stations on the Broad River
2.4.1-204	Broad River Monthly Discharge and Temperature Variability
2.4.1-205	Major Reservoirs Located in the Upper Broad River Basin
2.4.1-206	SCDHEC 2005 Water Usage for Cherokee County, South Carolina
2.4.1-207	SCDHEC 2005 Water Usage for Cherokee, Chester, Greenville, Spartanburg, Union, and York Counties, South Carolina
2.4.1-208	2000 Water Use Totals by County in the Upper Broad River Watershed
2.4.1-209	Area Surface Water Intakes in and Downstream from the Upper Broad River Watershed

LIST OF TABLES (Continued)

<u>Number</u>	<u>Title</u>
2.4.1-210	Estimated Surface Water Withdrawal and Consumption for Lee Nuclear Station Operations
2.4.1-211	Estimated Discharge Volume From Station Operations
2.4.1-212	Historical Domestic Wells in Vicinity of Site
2.4.2-201	Peak Streamflow of the Broad River Near Gaffney, South Carolina (USGS Station 02153500) 1939-1990
2.4.2-202	Peak Gauge Height of the Broad River below Ninety-Nine Islands Reservoir, South Carolina (USGS Station 02153551) 1999-2005
2.4.2-203	Local Intense Probable Maximum Precipitation for the Lee Nuclear Site
2.4.2-204	Site Drainage Areas Details
2.4.3-201	Broad River Watershed PMP (in.) Depth-Area-Duration Relationship
2.4.3-202	Broad River Watershed 6-hr. Incremental PMP Estimates
2.4.3-203	Broad River Watershed Subbasin Hourly Incremental PMP Estimates
2.4.3-204	Broad River Watershed Subbasin Precipitation Losses
2.4.3-205	Broad River Watershed Subbasin Unit Hydrographs
2.4.3-206	Broad River Watershed Subbasin Input Parameters
2.4.3-207	Make-Up Pond C Subbasin Unit Hydrograph
2.4.3-208	Make-Up Pond B Subbasin Unit Hydrograph
2.4.3-209	Upper Arm Subbasin Unit Hydrograph
2.4.4-201	Peak Flows and Resulting Water Surface Elevations
2.4.7-201	Water Temperature Data for the Broad River Near Gaffney, South Carolina (USGS Station 02153500)

LIST OF TABLES (Continued)

<u>Number</u>	<u>Title</u>
2.4.11-201	Minimum Daily Streamflow Observed on the Broad River Below Ninety-Nine Islands Dam, South Carolina, (USGS Station 02153551) 1998-2006
2.4.11-202	Minimum Daily Streamflow Observed on the Broad River Near Gaffney, South Carolina, (USGS Station 02153500) 1938-1990
2.4.11-203	100-Yr. Return Period Low Flow Rates
2.4.12-201	Well Construction and Water Table Elevations (ft above msl)
2.4.12-202	Water Table Elevations
2.4.12-203	Deleted
2.4.12-204	Aquifer Characteristics
2.4.12-205	Maximum Historically-Recorded Rainfall Distribution (Tropical Storm Jerry)
2.4.13-201	Distribution Coefficients (K_d)
2.4.13-202	AP1000 Tanks Containing Radioactive Liquid
2.4.13-203	Listing of Lee Nuclear Station Data and Modeling Parameters Supporting the Effluent Holdup Tank Failure
2.4.13-204	Radionuclide Concentration at Nearest Drinking Water Source in an Unrestricted Area Due to Effluent Holdup Tank Failure
2.5.1-201	Definitions of Classes Used in the Compilation of Quaternary Faults, Liquefaction Features, and Deformation in the Central and Eastern United States
2.5.1-202	Radiometric Age Determinations from Undisturbed Site Rocks
2.5.1-203	Deformation Phases and Structural Elements in the Study Area
2.5.1-204	Deformation Events Recorded at the Site Location
2.5.2-201	Deleted
2.5.2-202	Deleted
2.5.2-203	Deleted

LIST OF TABLES (Continued)

<u>Number</u>	<u>Title</u>
2.5.2-204	Deleted
2.5.2-205	Deleted
2.5.2-206	Deleted
2.5.2-207	Deleted
2.5.2-208	Deleted
2.5.2-209	Deleted
2.5.2-210	Deleted
2.5.2-211	Deleted
2.5.2-212	Deleted
2.5.2-213	Deleted
2.5.2-214	Deleted
2.5.2-215	Deleted
2.5.2-216	Deleted
2.5.2-217	UHRs Amplitudes for 10^{-4} , 10^{-5} , and 10^{-6}
2.5.2-218	Controlling Earthquakes from Deaggregation
2.5.2-219	Horizontal UHRs and GMRS Amplitudes
2.5.2-220	Vertical UHRs and GMRS Amplitudes
2.5.2-221	Point Source Parameters
2.5.2-222	Weighting Scheme to Develop V/H Ratios
2.5.2-223	Moment Magnitude, Distance Ranges, and Weights For V/H Ratios
2.5.2-224	FIRS and UHRs for Profile A1
2.5.2-225	FIRS and UHRs for Profile A5
2.5.2-226	FIRS and UHRs for Profile C4

LIST OF TABLES (Continued)

<u>Number</u>	<u>Title</u>
2.5.2-227	Distributed Seismicity Sources
2.5.2-228	Alternative Mmax Zonation Models
2.5.2-229	Alternative Mmax Zonation Model Weights
2.5.2-230	Assessment of Default Characteristics of Future Earthquakes in the CEUS
2.5.2-231	Characteristics of Future Earthquakes for Individual Seismic Sources
2.5.2-232	Maximum Magnitude Distributions for Seismotectonic Distributed Seismicity Sources
2.5.2-233	Maximum Magnitude Distribution for Charleston RLME Source
2.5.2-234	Maximum Magnitude Distribution for NEW MADRID RLME Source
2.5.2-235	Mean Rock Hazard and % Differences Between LCI PSHA Software Calculations and CEUS Data for Chattanooga Test Site
2.5.3-201	Summary of Bedrock Faults Mapped Within the Site Vicinity
2.5.4-201	Petrographic Test Results
2.5.4-202	Summary of Lee Nuclear Station Geotechnical Exploration
2.5.4-203	Summary of Completed Exploration Borings and Field Tests
2.5.4-204	Summary of Geotechnical Borings for Completed Monitoring Wells
2.5.4-205	Summary of Completed Cone Penetrometer Test Soundings
2.5.4-206	Summary of Completed Geotechnical Test Pit and Geologic Trench Locations
2.5.4-207	Summary of Completed Surface Geophysical Test Locations
2.5.4-208	Summary of Goodman Jack Test Results
2.5.4-209	Summary of Pressuremeter Test Results
2.5.4-210	Laboratory Testing Quantities By Sample Type and Test Method

LIST OF TABLES (Continued)

<u>Number</u>	<u>Title</u>
2.5.4-211	Average Engineering Properties of Soil
2.5.4-212	Corrosion Testing of Soil Fill
2.5.4-213	Summary of Laboratory Test Results for Intact Rock Cores
2.5.4-214	Summary of SASW Velocity Survey
2.5.4-215	Summary of Seismic CPT Shear Wave (Vs) Velocity Results
2.5.4-216	Borehole Geophysical Test Locations – P-S Suspension, Downhole, and Televiewer Tests
2.5.4-217	Summary of Interpreted P-S Suspension Velocity Layer Models
2.5.4-218	Summary of Downhole Velocity Layer Models
2.5.4-219	Quality Control Recommendations for Nuclear Island Foundation Materials
2.5.4-220	Quality Control Recommendations for Nuclear Island Fill Concrete
2.5.4-221	Deleted
2.5.4-222	Quality Control Recommendations for Generic Engineered Granular Backfill
2.5.4-223	Assumed Material Properties for Concrete Materials
2.5.4-224	Deleted
2.5.4-224A	Best Estimate Layering, Velocities, Moduli, and Ranges of Granular Fill (GW or Macadam Base Course) For Yard El. 592 Ft
2.5.4-224B	Best Estimate Layering, Velocities, Moduli, and Ranges of Granular Fill (GP or Macadam Base Course) For Yard El. 592 Ft
2.5.4-224C	Best Estimate Layering, Velocities, Moduli, and Ranges of Granular Fill (SW) For Yard El. 592 Ft
2.5.4-224D	Modulus and Damping Ratio of Granular Fill (GW or Macadam Base Course)

LIST OF TABLES (Continued)

<u>Number</u>	<u>Title</u>
2.5.4-224E	Modulus and Damping Ratio of Granular Fill (GP or Macadam Base Course)
2.5.4-224F	Modulus and Damping Ratio of Granular Fill (SW or Macadam Base Course)
2.5.4-225	Deleted
2.5.4-225A	Active Earth Pressure from Granular Backfill
2.5.4-225B	At-Rest Earth Pressure from Granular Backfill
2.5.4-225C	Passive Earth Pressure from Granular Backfill
2.5.4-226	Deleted
2.5.4-226A	Compaction-Induced Earth Pressure from Granular Backfill Material
2.5.4-226B	Criteria for Soil Compactors Operated in Close Proximity of Nuclear Island Foundation Wall
2.5.4-227	Dynamic Earth Pressure from Granular Backfill Material
2.5.4-228	Allowable Bearing Pressure Based on Factor of Safety
2.5.4-229	Allowable Bearing Pressure Based on Limiting Settlement
2.5.4-230	Structure Sizes
2.5.5-201	Permanent Slopes within One-Quarter Mile of Unit 1 and 2 Nuclear Island Structures

LIST OF FIGURES

<u>Number</u>	<u>Title</u>
2.1-201	Site Plot Plan
2.1-202	Vicinity (6-Mi. Radius) Base Map
2.1-203	Regional (50-Mi. Radius) Base Map
2.1-204	USGS Topographic Map
2.1-205	16-Km (10-Mi.) to 80-Km (50-Mi.) Population Sector Map
2.1-206	0 to 16-Km (10-Mi.) Population Sector Map
2.1-207	10-Mi. Base Map
2.1-208	Low Population Zone Map
2.1-209	Deleted
2.1-209A	Distance to EAB Map for Unit 1
2.1-209B	Distance to EAB Map for Unit 2
2.1-210	Graphs of Total Population
2.2-201	Transportation Routes, Storage Tank Locations, and Industrial Facilities Near Lee Nuclear Station
2.2-202	Airways Near Lee Nuclear Station
2.3-201	South Carolina Average Annual Snowfall 1961-1990
2.3-202	Air Stagnation Trend
2.3-203	Lee Nuclear Wind Rose, Annual
2.3-204	Normal Sea Level Pressure Distribution Over North America and the North Atlantic Ocean
2.3-205	Greenville/Spartanburg Wind Rose, 1997-2005, January
2.3-206	Greenville/Spartanburg Wind Rose, 1997-2005, February
2.3-207	Greenville/Spartanburg Wind Rose, 1997-2005, March

LIST OF FIGURES (Continued)

<u>Number</u>	<u>Title</u>
2.3-208	Greenville/Spartanburg Wind Rose, 1997-2005, April
2.3-209	Greenville/Spartanburg Wind Rose, 1997-2005, May
2.3-210	Greenville/Spartanburg Wind Rose, 1997-2005, June
2.3-211	Greenville/Spartanburg Wind Rose, 1997-2005, July
2.3-212	Greenville/Spartanburg Wind Rose, 1997-2005, August
2.3-213	Greenville/Spartanburg Wind Rose, 1997-2005, September
2.3-214	Greenville/Spartanburg Wind Rose, 1997-2005, October
2.3-215	Greenville/Spartanburg Wind Rose, 1997-2005, November
2.3-216	Greenville/Spartanburg Wind Rose, 1997-2005, December
2.3-217	Greenville/Spartanburg Wind Rose, 1997-2005, Annual
2.3-218	Lee Nuclear Wind Rose, January
2.3-219	Lee Nuclear Wind Rose, February
2.3-220	Lee Nuclear Wind Rose, March
2.3-221	Lee Nuclear Wind Rose, April
2.3-222	Lee Nuclear Wind Rose, May
2.3-223	Lee Nuclear Wind Rose, June
2.3-224	Lee Nuclear Wind Rose, July
2.3-225	Lee Nuclear Wind Rose, August
2.3-226	Lee Nuclear Wind Rose, September
2.3-227	Lee Nuclear Wind Rose, October
2.3-228	Lee Nuclear Wind Rose, November

LIST OF FIGURES (Continued)

<u>Number</u>	<u>Title</u>
2.3-229	Lee Nuclear Wind Rose, December
2.3-230	Lee Nuclear Wind Rose, Winter
2.3-231	Lee Nuclear Wind Rose, Spring
2.3-232	Lee Nuclear Wind Rose, Summer
2.3-233	Lee Nuclear Wind Rose, Fall
2.3-234	January Average Maximum Temperature (1971-2000)
2.3-235	January Average Minimum Temperature (1971-2000)
2.3-236	July Average Maximum Temperature (1971-2000)
2.3-237	July Average Minimum Temperature (1971-2000)
2.3-238	Ninety-Nine Islands, South Carolina Monthly Mean Maximum Temperature 1971-2000 Temperature and Precipitation
2.3-239	Ninety-Nine Islands (Blacksburg, SC) Relative Humidity
2.3-240	Annual Precipitation Rose Greenville/Spartanburg, SC 2001-2005
2.3-241	Lee Nuclear Precipitation Rose, Annual Precipitation Intensity
2.3-242	Ninety-Nine Islands, South Carolina Precipitation by Month
2.3-243	Ninety-Nine Islands, South Carolina Daily Precipitation Average and Extreme
2.3-244	Ninety-Nine Islands Annual Snowfall (inches)
2.3-245	Topographic Maps
2.3-246	Terrain Elevation Profiles Within 50 miles of the Lee Nuclear Site
2.3-247	Location of Meteorological Towers and Plant Structures

LIST OF FIGURES (Continued)

<u>Number</u>	<u>Title</u>
2.3-248	January Precipitation Rose Greenville/Spartanburg, SC 2001-2005
2.3-249	February Precipitation Rose Greenville/Spartanburg, SC 2001-2005
2.3-250	March Precipitation Rose Greenville/Spartanburg, SC 2001-2005
2.3-251	April Precipitation Rose Greenville/Spartanburg, SC 2001-2005
2.3-252	May Precipitation Rose Greenville/Spartanburg, SC 2001-2005
2.3-253	June Precipitation Rose Greenville/Spartanburg, SC 2001-2005
2.3-254	July Precipitation Rose Greenville/Spartanburg, SC 2001-2005
2.3-255	August Precipitation Rose Greenville/Spartanburg, SC 2001-2005
2.3-256	September Precipitation Rose Greenville/Spartanburg, SC 2001-2005
2.3-257	October Precipitation Rose Greenville/Spartanburg, SC 2001-2005
2.3-258	November Precipitation Rose Greenville/Spartanburg, SC 2001-2005
2.3-259	December Precipitation Rose Greenville/Spartanburg, SC 2001-2005
2.3-260	Lee Nuclear Precipitation Rose, January
2.3-261	Lee Nuclear Precipitation Rose, February
2.3-262	Lee Nuclear Precipitation Rose, March
2.3-263	Lee Nuclear Precipitation Rose, April
2.3-264	Lee Nuclear Precipitation Rose, May

LIST OF FIGURES (Continued)

<u>Number</u>	<u>Title</u>
2.3-265	Lee Nuclear Precipitation Rose, June
2.3-266	Lee Nuclear Precipitation Rose, July
2.3-267	Lee Nuclear Precipitation Rose, August
2.3-268	Lee Nuclear Precipitation Rose, September
2.3-269	Lee Nuclear Precipitation Rose, October
2.3-270	Lee Nuclear Precipitation Rose, November
2.3-271	Lee Nuclear Precipitation Rose, December
2.3-272	Cyclones Within 75 miles of Greer, South Carolina, 1851 through 2006
2.3-273	South Carolina Geographic Regions
2.3-274	Visible Plume Length Frequency - Winter Cooling Tower
2.3-275	Visible Plume Radius Frequency - Winter Cooling Tower
2.3-276	Hours of Plume Shadowing by Downwind Distance - Winter Cooling Tower
2.3-277	Salt Deposition Rate (kg/km ² -month) - Summer Maximum at 200 meters Cooling Tower
2.3-278	Water Deposition Rate - Fall Cooling Tower
2.3-279	Deleted
2.4.1-201	Site Surface Water Features
2.4.1-202	Deleted
2.4.1-203	Physiographic and Hydrogeologic Provinces of South Carolina
2.4.1-204	The Broad River Within the Santee River Basin
2.4.1-205	Upper Broad River Basin and Subbasins

LIST OF FIGURES (Continued)

<u>Number</u>		<u>Title</u>
2.4.1-206		The Broad River and its Tributaries Above Ninety-Nine Islands Dam
2.4.1-207		Cherokee County Watershed: Select Facilities and Monitoring Stations
2.4.1-208		Broad River Width and Depth Data
2.4.1-209	Sheet 1	Bathymetry Map: Ninety-Nine Island Reservoir
2.4.1-209	Sheet 2	Bathymetric Map: Make-Up Pond B
2.4.1-209	Sheet 3	Bathymetric Map: Make-Up Pond A
2.4.1-209	Sheet 4	Bathymetric Map: Hold-Up Pond A
2.4.1-210		The Piedmont Aquifer System
2.4.1-211		Relevant Surface Water Intakes on the Broad River
2.4.1-212		Groundwater Supply Wells Surrounding the Lee Nuclear Site
2.4.1-213		Make-Up Pond C Location and Bathymetry
2.4.1-214		Pond B Conceptual Debris Barrier
2.4.2-201		Gauging Station Locations
2.4.2-202		Grading and Drainage Plan
2.4.2-203		Local Intense Probable Maximum Precipitation Depth-Duration Curve
2.4.2-204		Site Analysis Drainage Areas
2.4.3-201		Make-Up Pond A and Make-Up Pond B Watersheds
2.4.3-202		HMR-52 Standard Isohyetal Pattern
2.4.3-203		Broad River Watershed Subbasins
2.4.3-204		Local Intense Probable Maximum Precipitation 6-Hour Hyetograph

LIST OF FIGURES (Continued)

<u>Number</u>	<u>Title</u>
2.4.3-205	Local Intense Probable Maximum Precipitation 72-Hour Hyetograph
2.4.3-206	HEC-HMS Broad River Watershed Subbasin Schematic
2.4.3-207	Subbasin Unit Hydrographs: LS-1, LA-2, CC-16, KMR-13, BR-5, and BD3-6
2.4.3-208	Subbasin Unit Hydrographs: 2BR-7, BD2-8, SS-09, FB-10, GS-11, and BD1-12
2.4.3-209	Subbasin Unit Hydrographs: LL-4, BC-14, BR-15, GD-3, USS-18A, 2BR-19, and WLCHL
2.4.3-210	Discharge Rating Curve, Tuxedo Dam
2.4.3-211	Discharge Rating Curve, Turner Shoals Dam
2.4.3-212	Discharge Rating Curve, Gaston Shoals Dam
2.4.3-213	Discharge Rating Curve, Ninety-Nine Islands Dam
2.4.3-214	Discharge Rating Curve, Lake Lure Dam
2.4.3-215	Discharge Rating Curve, Kings Mountain Reservoir Dam
2.4.3-216	Discharge Rating Curve, Cherokee Falls Dam
2.4.3-217	Discharge Rating Curve, Lockhart Dam
2.4.3-218	Gaston Shoals Dam PMF Combined Inflow Hydrograph
2.4.3-219	Subbasin BD1-12 PMF Inflow Hydrograph
2.4.3-220	Subbasin BC-14 and Routed Subbasin KMR-13 PMF Combined Inflow Hydrograph
2.4.3-221	Subbasin BR-15 PMF Inflow Hydrograph
2.4.3-222	Discharge Rating Curve, Make-Up Pond B
2.4.3-223	Storage Capacity Curve, Make-Up Pond B

LIST OF FIGURES (Continued)

<u>Number</u>	<u>Title</u>
2.4.3-224	Discharge Rating Curve, Make-Up Pond A
2.4.3-225	Storage Capacity Curve, Make-Up Pond A
2.4.3-226	PMF Hydrograph, Broad River at Lee Nuclear Station
2.4.3-227	PMF Hydrograph Without Upper Arm Dam Failure, Make-Up Pond B
2.4.3-228	PMF Hydrograph Make-Up Pond A
2.4.3-229	PMF Elevation Hydrograph, Broad River at Lee Nuclear Station
2.4.3-230	Flood El. Hydrograph Make-Up Pond B Without Upper Arm Dam Failure, 6-hr. Local Intense Precipitation
2.4.3-231	Flood El. Hydrograph Make-Up Pond B Without Upper Arm Dam Failure, 72-hr. Local Intense Precipitation
2.4.3-232	Deleted
2.4.3-233	Flood Elevation Hydrograph Make-Up Pond A 6-Hour Local Intense Precipitation
2.4.3-234	Make-Up Pond B Coincident Wind Wave Fetch Length
2.4.3-235	Local Intense Probable Maximum Precipitation 6-Hour End Peaking Hyetograph
2.4.3-236	Local Intense Probable Maximum Precipitation 72-Hour End Peaking Hyetograph
2.4.3-237	Make-Up Pond B Unit Hydrographs
2.4.3-238	Discharge Rating Curve, Lake Whelchel
2.4.3-239	Make-Up Pond C Watershed
2.4.3-240	Make-Up Pond C Watershed 72-Hour End Peaking Hyetograph
2.4.3-241	Subbasin Unit Hydrographs: Make-Up Pond C (MUPC)
2.4.3-242	Discharge Rating Curve, Make-Up Pond C

LIST OF FIGURES (Continued)

<u>Number</u>	<u>Title</u>
2.4.3-243	Subbasin Make-Up Pond C (MUPC) PMF Inflow Hydrograph
2.4.3-244	Storage Capacity Curve, Make-Up Pond C
2.4.3-245	Subbasin Lake Wheelchel (WLCHL) PMF Inflow Hydrograph
2.4.3-246	Upper Arm Dam Unit Hydrographs
2.4.3-247	Discharge Rating Curve, Upper Arm Dam
2.4.3-248	Storage Capacity Rating Curve, Upper Arm Dam
2.4.3-249	Drainage Culvert Schematic, Upper Arm Dam
2.4.4-201	Broad River Coincident Wind Wave Fetch Length
2.4.4-202	Make-Up Pond A Coincident Wind Wave Fetch Length
2.4.4-203	PMF Hydrograph With Upper Arm Dam Failure, Make-Up Pond B
2.4.4-204	Deleted
2.4.4-205	Flood El. Hydrograph Make-Up Pond B With Upper Arm Dam Failure, 72-hr. Local Intense Precipitation
2.4.5-201	Make-Up Pond A Extreme Wind Speed Fetch Length
2.4.5-202	Make-Up Pond B Extreme Wind Speed Fetch Length
2.4.6-201	USACE Tsunami Zone Map and Wave Heights
2.4.7-201	USACE Ice Jam Flooding Map
2.4.12-201	1973 Water Table Map
2.4.12-202	Radius of Influence of Cherokee Nuclear Site Construction Dewatering
2.4.12-203	Hydrographs for Observation Wells

LIST OF FIGURES (Continued)

<u>Number</u>	<u>Title</u>
2.4.12-204	Sheet 1 Potentiometric Surface Map April 2006
2.4.12-204	Sheet 2 Potentiometric Surface Map May 2006
2.4.12-204	Sheet 3 Potentiometric Surface Map July 2006
2.4.12-204	Sheet 4 Potentiometric Surface Map September 2006
2.4.12-204	Sheet 5 Potentiometric Surface Map November 2006
2.4.12-204	Sheet 6 Potentiometric Surface Map January 2007
2.4.12-204	Sheet 7 Potentiometric Surface Map March 2007
2.4.12-204	Sheet 8 Potentiometric Surface Map Projected Post-Construction Water Table
2.4.12-205	Sheet 1 Cross Sections of Lee Nuclear Site: Index Map
2.4.12-205	Sheet 2 Cross Sections of Lee Nuclear Site: A - A'
2.4.12-205	Sheet 3 Cross Sections of Lee Nuclear Site: B - B'
2.4.12-205	Sheet 4 Cross Sections of Lee Nuclear Site: C - C'
2.4.12-206	Soil Map of the Lee Nuclear Site
2.4.12-207	Hydraulic Conductivities of Subsurface Materials
2.4.12-208	Groundwater Pathway Analysis
2.4.12-209	Post-Construction Surface Cover Treatment in Power Block and Immediate Surrounding Area
2.4.12-210	Maximum Post-Construction Groundwater Analysis, MODFLOW Model Domain
2.4.12-211	Maximum Post-Construction Groundwater Analysis, Results Hydrograph
2.4.13-201	Deleted

LIST OF FIGURES (Continued)

<u>Number</u>	<u>Title</u>
2.5.1-201	Map of Physiographic Provinces and Mesozoic Rift Basins
2.5.1-202a	Lithotectonic Map of the Site Region
2.5.1-202b	Explanation of Lithotectonic Map of the Site Region
2.5.1-203a	Site Region Geologic Map
2.5.1-203b	Explanation of Site Region Geologic Map
2.5.1-204a	Lithotectonic Map of the Appalachian Orogen
2.5.1-204b	Explanation of Lithotectonic Map of Appalachian Orogen
2.5.1-205	Regional Gravity Data
2.5.1-206	Regional Aeromagnetic Data
2.5.1-207	Regional Cross-Section E4
2.5.1-208	Site Vicinity Gravity and Magnetic Profiles
2.5.1-209	Site Region Tectonic Features
2.5.1-210	Tectonic Features and Seismicity Within 50 Miles of the Site
2.5.1-211	Major Eastern U.S. Aeromagnetic Anomalies
2.5.1-212	Crustal Ages from Johnston et al. (1994)
2.5.1-213	Potential Quaternary Features in the Site Region
2.5.1-214	Seismic Zones and Seismicity in CEUS
2.5.1-215	Regional Charleston Tectonic Features
2.5.1-216	Local Charleston Tectonic Features
2.5.1-217	Charleston Area Seismicity and Postulated Faults

LIST OF FIGURES (Continued)

<u>Number</u>	<u>Title</u>
2.5.1-218a	Site Vicinity Geologic Map
2.5.1-218b	Site Vicinity Geologic Map Explanation
2.5.1-219a	Site Area Geologic Map
2.5.1-219b	Site Area Geologic Map Explanation
2.5.1-220	Site Geologic Map
2.5.1-221	Site Area Relief Map
2.5.1-222	Site Topographic Map
2.5.1-223	Site Area Geochronology Chart
2.5.1-224	Schematic Diagram of Stratigraphic Relations in the Site Area (Prior to Earliest Deformation)
2.5.1-225	Lower Hemisphere Equal Area Projections of Fold Axes and Foliations in Site Area
2.5.1-226	Field Investigation Data Used to Constrain Western Pluton Boundary
2.5.1-227	Top of Rock Contour Map
2.5.1-228	Photographs of Existing Excavation
2.5.1-229	Surficial Geologic Map of Existing Excavation
2.5.1-230	Schematic Diagrams of Fracture Formation and Deformation
2.5.1-231	Stereonet Projection of Poles to Shear Planes - CNS Units 1 and 2 Selected Zone Mapping
2.5.1-232	January 1, 1913 E[M] 4.54 Union County Earthquake Ground Shaking Intensities (Rossi-Forel Scale)
2.5.1-233	Site Vicinity Magnetic Field
2.5.1-234	Site Area Magnetic Field

LIST OF FIGURES (Continued)

<u>Number</u>	<u>Title</u>
2.5.1-235	Correlations between Physiographic Provinces and Recent Lithotectonic Classifications
2.5.1-236	Late- to Post-Kinematic Mineralization Overgrown Ductile Fabric and Brittle Fabric
2.5.1-237	Photomicrographs of Example Low Birefringent Material K-feldspar in Veins Cross Cutting Structural Fabric
2.5.1-238	Thermodynamic Stability Fields for Laumontite (Lm) and Associated Reaction Products along with the Closure Intervals of Selected Mineral Phases
2.5.1-239	Pressure-Temperature Evolution for the Southeastern Piedmont Region
2.5.1-240	Stereonet Projection of Poles to Shear Planes - CNS Unit 1 Foundation
2.5.1-241	Stereonet Projection of Poles to Shear Planes - CNS Unit 2 Foundation
2.5.1-242	Stereonet Projection of Poles to Shear Planes - WLS COLA Mapping at CNS Unit 2 Foundation
2.5.1-243	Stereonet Projection of Poles to Shear Planes CNS Unit 2 and WLS COLA Mapping
2.5.1-244	Stereonet Projection of Poles to Shear Planes - All Foundation Mapping
2.5.1-245	Stress Measurements for the CEUS
2.5.1-246	Charleston RLME Source Zones
2.5.2-201	Deleted
2.5.2-202	Deleted
2.5.2-203	Deleted
2.5.2-204	Deleted
2.5.2-205	Deleted

LIST OF FIGURES (Continued)

<u>Number</u>	<u>Title</u>
2.5.2-206	Deleted
2.5.2-207	Deleted
2.5.2-208	Deleted
2.5.2-209	Deleted
2.5.2-210	Deleted
2.5.2-211	Deleted
2.5.2-212	Deleted
2.5.2-213	Deleted
2.5.2-214	Deleted
2.5.2-215	Deleted
2.5.2-216	Deleted
2.5.2-217	Deleted
2.5.2-218	Deleted
2.5.2-219	Deleted
2.5.2-220	Deleted
2.5.2-221	Deleted
2.5.2-222	Deleted
2.5.2-223	Mean and Fractile Rock Hazard for PGA
2.5.2-224	Mean and Fractile Rock Hazard for 25 Hz
2.5.2-225	Mean and Fractile Rock Hazard for 10 Hz
2.5.2-226	Mean and Fractile Rock Hazard for 5 Hz
2.5.2-227	Mean and Fractile Rock Hazard for 2.5 Hz
2.5.2-228	Mean and Fractile Rock Hazard for 1 Hz

LIST OF FIGURES (Continued)

<u>Number</u>	<u>Title</u>
2.5.2-229	Mean and Fractile Rock Hazard for 0.5 Hz
2.5.2-230	Deleted
2.5.2-231	Combined Deaggregation of Mean Rock Hazard for 10^{-4} M-R- ϵ deaggregation for 1 and 2.5 Hz
2.5.2-232	Combined Deaggregation of Mean Rock Hazard for 10^{-4} M-R- ϵ deaggregation for 5 and 10 Hz
2.5.2-233	Combined Deaggregation of Mean Rock Hazard for 10^{-5} M-R- ϵ deaggregation for 1 and 2.5 Hz
2.5.2-234	Combined Deaggregation of Mean Rock Hazard for 10^{-5} M-R- ϵ deaggregation for 5 and 10 Hz
2.5.2-235	Combined Deaggregation of Mean Rock Hazard for 10^{-6} M-R- ϵ deaggregation for 1 and 2.5 Hz
2.5.2-236	Combined Deaggregation of Mean Rock Hazard for 10^{-6} M-R- ϵ deaggregation for 5 and 10 Hz
2.5.2-237	Deleted
2.5.2-238	Deleted
2.5.2-239	Rock GMRS for Horizontal and Vertical Motion
2.5.2-240	Deleted
2.5.2-240a	Example of Median V/H Ratios Computed for M 5.1, Single-Corner Source Model, Unit 1 FIRS A1
2.5.2-240b	Example of Median V/H Ratios Computed for M 5.1, Single-Corner Source Model, Unit 1 FIRS A5
2.5.2-240c	Example of Median V/H Ratios Computed for M 5.1, Single-Corner Source Model, Unit 2 FIRS C4
2.5.2-241	Deleted
2.5.2-241a	Amplification Factors for M 5.1, Single-Corner Source Model, Unit 1 FIRS A1 Computed Using Spectral Shapes as Control Motions

LIST OF FIGURES (Continued)

<u>Number</u>	<u>Title</u>
2.5.2-241b	Amplification Factors for M 5.1, Single-Corner Source Model, Unit 1 FIRS A5 Computed Using Spectral Shapes as Control Motions
2.5.2-241c	Amplification Factors for M 5.1, Single-Corner Source Model, Unit 2 FIRS C4 Computed Using Spectral Shapes as Control Motions
2.5.2-242	Example of Median V/H Ratios Computed for M 5.1, Campbell and Bozorgnia (2003) Model Rock
2.5.2-243	Example of Median V/H Ratios Computed for M 8.0, Campbell and Bozorgnia (2003) Rock Model
2.5.2-244	Deleted
2.5.2-244a	Horizontal Component Unit 1 FIRS A1 Compared to the GMRS
2.5.2-244b	Horizontal Component Unit 1 FIRS A5 Compared to the GMRS
2.5.2-244c	Horizontal Component Unit 2 FIRS C4 Compared to the GMRS
2.5.2-245	Deleted
2.5.2-245a	Vertical Component Unit 1 FIRS A1 Compared to the GMRS
2.5.2-245b	Vertical Component Unit 1 FIRS A5 Compared to the GMRS
2.5.2-245c	Vertical Component Unit 2 FIRS C4 Compared to the GMRS
2.5.2-246	Deleted
2.5.2-246a	Comparison of Horizontal and Vertical FIRS A1
2.5.2-246b	Comparison of Horizontal and Vertical FIRS Computed for Profile A5
2.5.2-246c	Comparison of Horizontal and Vertical FIRS Computed for Profile C4

LIST OF FIGURES (Continued)

<u>Number</u>	<u>Title</u>
2.5.2-247	Deleted
2.5.2-247a	Unit 1 FIRS A1 Horizontal and Vertical Component UHRS at Annual Exceedence Probabilities 10^{-4} , 10^{-5} , and 10^{-6} yr ⁻¹
2.5.2-247b	Unit 1 FIRS A5 Horizontal and Vertical Component UHRS at Annual Exceedence Probabilities 10^{-4} , 10^{-5} , and 10^{-6} yr ⁻¹
2.5.2-247c	Unit 2 FIRS C4 Horizontal and Vertical Component UHRS at Annual Exceedence Probabilities 10^{-4} , 10^{-5} , and 10^{-6} yr ⁻¹
2.5.2-248	Distribution of Seismicity and Seismotectonic Source Zones
2.5.2-249	CEUS SSC Mmax Zones
2.5.2-250	Master Logic Tree for Conceptual Approach of the CEUS-SSC
2.5.2-251	CEUS SSC Logic Tree for Mmax Zones
2.5.2-252	CEUS SSC Seismotectonic Zones Models A and B
2.5.2-253	CEUS SSC Seismotectonic Zones Models C and D
2.5.2-254a	CEUS SSC Logic Tree for Seismotectonic Zones (Narrow)
2.5.2-254b	CEUS SSC Logic Tree for Seismotectonic Zones (Wide)
2.5.2-255	CEUS SSC RLME Sources
2.5.2-256	CEUS SSC Mmax Zones and RLMEs in the Site Region
2.5.2-257	CEUS SSC Seismotectonic Zones in Site Region
2.5.2-258	Bouguer Gravity and Magnetic Anomalies with Regional Seismotectonic Source Zones
2.5.2-259	Regional Seismicity and 2011 Mineral Earthquake

LIST OF FIGURES (Continued)

<u>Number</u>	<u>Title</u>
2.5.2-260	RLME Sources Contributing to Hazard at Duke Lee Site
2.5.2-261a	CEUS SSC Logic Tree for Charleston RLME
2.5.2-261b	CEUS SSC Logic Tree for Charleston RLME
2.5.2-261c	CEUS SSC Logic Tree for Charleston RLME Corrected on June 27, 2012
2.5.2-261d	CEUS SSC Logic Tree for Charleston RLME Corrected on June 27, 2012
2.5.2-262	New Madrid Fault System RLME
2.5.2-263a	CEUS SSC Logic Tree for New Madrid Fault System RLME
2.5.2-263b	CEUS SSC Logic Tree for New Madrid Fault System RLME Corrected on June 27, 2012
2.5.2-264	Mineral Earthquake Aftershock Pattern, August 23, 2011 through May 2, 2012
2.5.2-265	Comparison of seismicity between the Reelfoot Rift (RR) and Reelfoot Rift-Rough Creek Graben (RR-RCG)
2.5.2-266a	High and Low Frequency Mean Spectra for MAFEs of 10^{-4} , 10^{-5} and 10^{-6}
2.5.2-266b	Mean rock UHRS for MAFEs of 10^{-4} , 10^{-5} and 10^{-6}
2.5.4-201	Site Features of Lee Nuclear Station Units 1 and 2
2.5.4-202	Topographic Comparison - Representation of Net Topographic Change between 1971 and 2006
2.5.4-203	Hand Sample Photograph and Photomicrograph of Meta-quartz Diorite, Sample B-1004 at 33.2 - 33.3 feet
2.5.4-204	Hand Sample Photograph and Photomicrograph of Mica-schist, Sample B-1014 at 7.3 - 7.4 feet
2.5.4-205	Hand Sample Photograph and Photomicrograph of Meta-dacite Porphyry, Sample B-1007 at 22.8-22.9 feet

LIST OF FIGURES (Continued)

<u>Number</u>	<u>Title</u>
2.5.4-206	Hand Sample Photograph and Photomicrograph of Meta-basalt, Sample B-1018 at 39.8 - 39.9 feet
2.5.4-207	Site Exploration Map - Explanation
2.5.4-208	Site Exploration Map - Overview
2.5.4-209	Site Exploration Map - Power Block and Adjacent Areas
2.5.4-210	Groundwater Monitoring Well and Packer Test Locations
2.5.4-211	Surface Geophysical Test Locations
2.5.4-212	CPT Test Locations
2.5.4-213	Geotechnical Test Pit and Geologic Trench Locations
2.5.4-214	Borehole In-Situ Test Locations
2.5.4-215	Borehole Geophysical Test Locations
2.5.4-216	Petrographic Test Locations
2.5.4-217	Deleted
2.5.4-218	Boring Summary Sheet Explanation
2.5.4-219	Boring Summary Sheet, Boring B-1000
2.5.4-220	Boring Summary Sheet, Boring B-1002
2.5.4-221	Boring Summary Sheet, Boring B-1004
2.5.4-222	Boring Summary Sheet, Boring B-1011
2.5.4-223	Boring Summary Sheet, Boring B-1012
2.5.4-224	Boring Summary Sheet, Boring B-1015
2.5.4-225	Boring Summary Sheet, Boring B-1017
2.5.4-226	Boring Summary Sheet, Boring B-1024
2.5.4-227	Boring Summary Sheet, Boring B-1037A

LIST OF FIGURES (Continued)

<u>Number</u>	<u>Title</u>
2.5.4-228	Boring Summary Sheet, Boring B-1068
2.5.4-229	Boring Summary Sheet, Boring B-1070
2.5.4-230	Boring Summary Sheet, Boring B-1074
2.5.4-231	Boring Summary Sheet, Boring B-1074A
2.5.4-232	Boring Summary Sheet, Boring B-1075A
2.5.4-233	Deleted
2.5.4-233a	Boring Summary Sheet, B-2000
2.5.4-233b	Boring Summary Sheet, B-2001
2.5.4-233c	Boring Summary Sheet, B-2002
2.5.4-233d	Boring Summary Sheet, B-2003
2.5.4-233e	Boring Summary Sheet, B-2004
2.5.4-233f	Boring Summary Sheet, B-2005
2.5.4-233g	Boring Summary Sheet, B-2006
2.5.4-234	Geologic Cross Section BB-BB'
2.5.4-235	Geologic Cross Section CC-CC'
2.5.4-236	Geologic Cross Section EE-EE'
2.5.4-237	Geologic Cross Section F-F'
2.5.4-238	Geologic Cross Section FF-FF'
2.5.4-239	Geologic Cross Section UU-UU'
2.5.4-240	Geologic Cross Section ZZ-ZZ'
2.5.4-241	Top of Continuous Rock, Power Block and Adjacent Areas
2.5.4-242	Deleted

LIST OF FIGURES (Continued)

<u>Number</u>	<u>Title</u>
2.5.4-243	Planned Excavation Limits
2.5.4-244a	Cherokee Nuclear Station Foundation Drainage and Lee Nuclear Station Nuclear Island
2.5.4-244b	CNS Foundation with Drainage Channels at Bottom of Mat
2.5.4-244c	CNS Foundation with Drainage Channels within Fill Concrete
2.5.4-244d	Cherokee Nuclear Station Foundation Drainage and Lee Nuclear Station Nuclear Island-Detail 3
2.5.4-244e	CNS Foundation with Waterproofing Membrane in Local Pit – Detail 4
2.5.4-245	Planned Excavation Profile, Geologic Cross Section UU-UU'
2.5.4-246	Deleted
2.5.4-247	Locations of Dynamic Velocity Profiles, Associated Data Sources, and Cross Section Locations
2.5.4-248	Smoothed Velocity Profile A
2.5.4-249	Deleted
2.5.4-250	Smoothed Velocity Profile C
2.5.4-251	Deleted
2.5.4-251a	Best Estimate Layer Velocity Profile G, Generic Engineered Granular Fill Profile – GW
2.5.4-251b	Best Estimate Layer Velocity Profile G, Generic Engineered Granular Fill Profile – GP
2.5.4-251c	Best Estimate Layer Velocity Profile G, Generic Engineered Granular Fill Profile – SW
2.5.4-252	Deleted
2.5.4-252a	Dynamic Profile - Base Case A1

LIST OF FIGURES (Continued)

<u>Number</u>	<u>Title</u>
2.5.4-252b	Dynamic Profile - Base Case A5
2.5.4-252c	Dynamic Profile - Base Case C4
2.5.4-253	Deleted
2.5.4-253a	Best Estimate Shear Modulus and Damping Ratio Plots for Generic Engineered Granular Fill - GW
2.5.4-253b	Best Estimate Shear Modulus and Damping Ratio Plots for Generic Engineered Granular Fill - GP
2.5.4-253c	Best Estimate Shear Modulus and Damping Ratio Plots for Generic Engineered Granular Fill - SW
2.5.4-254	Deleted
2.5.4-255	Deleted
2.5.4-255a	Static Lateral Active Pressures on Nuclear Island
2.5.4-255b	Static Lateral At-Rest Pressures on Nuclear Island
2.5.4-255c	Passive Lateral Pressure on Nuclear Island
2.5.4-256	Deleted
2.5.4-256a	Compaction-Induced Earth Pressures on Nuclear Island
2.5.4-256b	Dynamic Earth Pressures on Nuclear Island
2.5.4-257	Treatment of Narrow Zone of Soil or Weathered Rock - Steeply Dipping
2.5.4-258	Treatment of Narrow Zone of Soil or Weathered Rock - Dipping Less than 60° and No Removal of Rock Overhang
2.5.4-259	Treatment of Narrow Zone of Soil or Weathered Rock - Dipping Less than 60° and Removal of Rock Overhang
2.5.4-260	Planned Excavation Profile Geologic Cross Section BB-BB'

LIST OF FIGURES (Continued)

<u>Number</u>	<u>Title</u>
2.5.4-261	Planned Excavation Profile Geologic Cross Section CC-CC'
2.5.4-262	Planned Excavation Profile Geologic Cross Section EE-EE'
2.5.4-263	Planned Excavation Profile Geologic Cross Section F-F'
2.5.4-264	Planned Excavation Profile, Geologic Cross Section FF-FF'
2.5.4-265	Planned Excavation Profile Geologic Cross Section ZZ-ZZ'
2.5.4-266	Cherokee Basemat and Lower Room Details
2.5.4-267	Fill Concrete Configuration along East Side of WLS Unit 2
2.5.5-201	Permanent Slopes within One-Quarter Mile of Units 1 and 2 Nuclear Island Structures

CHAPTER 2

SITE CHARACTERISTICS

The **introductory information** at the beginning of Chapter 2 of the referenced DCD is incorporated by reference with the following departures and/or supplements.

Insert the following subsection at the end of the introductory text of DCD Chapter 2, prior to DCD Section 2.1.

2.0 SITE CHARACTERISTICS

WLS SUP 2.0-1 Chapter 2 describes the characteristics and site-related design parameters of the Lee Nuclear Site (Lee). The site location, characteristics and parameters, as described in the following five sections are provided in sufficient detail to support a safety assessment:

- Geography and Demography (**Section 2.1**)
- Nearby Industrial, Transportation, and Military Facilities (**Section 2.2**)
- Meteorology (**Section 2.3**)
- Hydrology (**Section 2.4**)
- Geology and Seismology (**Section 2.5**)

In this chapter, the following definitions and figures are provided to assist the reader in understanding the scope of the discussion:

- Lee Nuclear Station site – the 1,900 acre (ac.) area identified by the site boundary (**Figure 2.1-201**).
- Lee Nuclear Site vicinity – the area within approximately the 6-mile (mi.) radius around the site (**Figure 2.1-202**).
- Lee Nuclear Site region – the area within approximately the 50-mi. radius around the site (**Figure 2.1-203**).

Table 2.0-201 provides a comparison of site-related design parameters for which the AP1000 plant is designed and site characteristics specific to Lee Nuclear Site in support of this safety assessment. The first two columns of **Table 2.0-201** are a compilation of the site parameters from **DCD Table 2-1** and **DCD Tier 1 Table 5.0-1**. The third column of **Table 2.0-201** is the corresponding site characteristic for the Lee Nuclear Site. The fourth column denotes the place within the Lee Nuclear Site FSAR that this data is presented.

The last column indicates whether or not the site characteristic falls within the AP1000 site parameters. Control room atmospheric dispersion factors (χ/Q) for accident dose analysis are presented in [Table 2.0-202](#). All of the control room χ/Q values fall within the AP1000 parameters.

WLS SUP 2.0-1

TABLE 2.0-201 (Sheet 1 of 8)
COMPARISON OF AP1000 DCD SITE PARAMETERS AND LEE NUCLEAR STATION UNITS 1 & 2 SITE
CHARACTERISTICS

	AP 1000 DCD Site Parameters	Lee Site Characteristic	Lee FSAR Reference	Lee Within Site Parameter
Air Temperature				
Maximum Safety	115°F dry bulb / 86.1°F coincident wet bulb ^{(a),(h)}	107°F dry bulb / 84°F coincident wet bulb (100-year maximum)	Table 2.3-293	Yes
	86.1°F wet bulb (noncoincident)	85°F (100-year maximum)	Table 2.3-293	Yes
Minimum Safety	-40°F ^(a)	-5°F (100-year minimum)	Table 2.3-293	Yes
Maximum Normal	101°F dry bulb / 80.1°F coincident wet bulb ^(b)	94°F dry bulb / 77°F coincident wet bulb (0.4% annual exceedance)	Table 2.3-293	Yes
	80.1°F wet bulb (noncoincident) ^(c)	77°F wet bulb (0.4% annual exceedance)	Table 2.3-293	Yes
Minimum Normal	-10°F ^(b)	20°F (99.6% annual exceedance)	Table 2.3-293	Yes
Wind Speed				
Operating Basis	145 mph (3 second gust); importance factor 1.15 (safety), 1.0 (nonsafety); exposure C; topographic factor 1.0	96 mph (3 second gust) (110 mph with 1.15 importance factor); exposure C; topographic factor 1.0	Subsection 2.3.1.2.8	Yes
Tornado	300 mph	230 mph	Subsection 2.3.1.2.2	Yes
	Maximum Pressure Differential of 2.0 lb/in ²	1.2 lb/in ²	Subsection 2.3.1.2.2	Yes

WLS SUP 2.0-1

TABLE 2.0-201 (Sheet 2 of 8)
COMPARISON OF AP1000 DCD SITE PARAMETERS AND LEE NUCLEAR STATION UNITS 1 & 2 SITE CHARACTERISTICS

		AP 1000 DCD Site Parameters	Lee Site Characteristic	Lee FSAR Reference	Lee Within Site Parameter
	Seismic				
WLS DEP 2.0-1	CSDRS	<p>CSDRS free field peak ground acceleration of 0.30 g with modified Regulatory Guide 1.60 response spectra (See Figures 5.0-1 and 5.0-2). The SSE is now referred to as CSDRS. Seismic input is defined at finished grade, except for sites where the nuclear island is founded on hard rock.^(d) If the site-specific spectra exceed the response spectra in Figures 5.0-1 and 5.0-2 at any frequency, or if soil conditions are outside the range evaluated for AP1000 design certification, a site-specific evaluation can be performed. This evaluation will consist of a site-specific dynamic analysis and generation of in-structure response spectra at key locations to be compared with the floor response spectra of the certified design at 5-percent damping. The site is acceptable if the floor response spectra from the site-specific evaluation do not exceed the AP1000 spectra for each of the locations or the exceedances are justified.</p> <p>The hard rock high frequency (HRHF) envelope response spectra are shown in Figure 5.0-3 and Figure 5.0-4 defined at the foundation level for 5% damping. The HRHF envelope response spectra provide an alternative set of spectra for evaluation of site specific GMRS. A site is acceptable if its site-specific GMRS fall within the AP1000 HRHF envelope response spectra.^(e) Evaluation of a site for application of the HRHF envelope response spectra includes consideration of the limitation on shear wave velocity identified for use of the HRHF envelope response spectra. This limitation is defined by a shear wave velocity at the bottom of the basemat equal to or higher than 7,500 fps, while maintaining a shear wave velocity equal to or above 8,000 fps at the lower depths.</p>	<p>GMRS PGA = 0.345g Unit 1 FIRS PGA = 0.352g GMRS and Unit 1 FIRS exceed the CSDRS and the hard rock high frequency spectra. A site-specific evaluation is performed and the site is demonstrated to be acceptable.</p>	<p>Subsection 2.5.2.6 Subsection 2.5.2.7 Subsection 3.7.1.1.1 Subsection 3.7.2.8.4 Figure 3.7-201 Figure 3.7-202 Figure 3.7-213a Figure 3.7-213b Figure 3.7-214a Figure 3.7-214b Appendix 3I Subsection 19.55.6.3</p>	No

WLS SUP 2.0-1

TABLE 2.0-201 (Sheet 3 of 8)
COMPARISON OF AP1000 DCD SITE PARAMETERS AND LEE NUCLEAR STATION UNITS 1 & 2 SITE CHARACTERISTICS

	AP 1000 DCD Site Parameters	Lee Site Characteristic	Lee FSAR Reference	Lee Within Site Parameter
Fault Displacement Potential	No potential fault displacement considered beneath the seismic Category I and seismic Category II structures and immediate surrounding area. The immediate surrounding area includes the effective soil supporting media associated with the seismic Category I and seismic Category II structures.	Negligible.	Subsection 2.5.3.8	Yes
Soil				
Average Allowable Static Bearing Capacity	The allowable bearing capacity, including a factor of safety appropriate for the design load combination, shall be greater than or equal to the average bearing demand of 8,900 lb/ft ² over the footprint of the nuclear island at its excavation depth.	190,000 to 242,000 lb/ft ²	Subsection 2.5.4.10.1	Yes
Dynamic Bearing Capacity for Normal Plus Safe Shutdown Earthquake (SSE)	The allowable bearing capacity, including a factor of safety appropriate for the design load combination, shall be greater than or equal to the maximum bearing demand of 35,000 lb/ft ² at the edge of the nuclear island at its excavation depth, or site-specific analyses demonstrate factor of safety appropriate for normal plus safe shutdown earthquake loads.	190,000 to 242,000 lb/ft ²	Subsection 2.5.4.10.1	Yes
Shear Wave Velocity	Greater than or equal to 1,000 ft/sec based on minimum low-strain soil properties over the footprint of the nuclear island at its excavation depth	9000 to 10,000 ft/sec	Subsection 2.5.4.7	Yes
Lateral Variability	Soils supporting the nuclear island should not have extreme variations in subgrade stiffness. This may be demonstrated by one of the following: 1. Soils supporting the nuclear island are uniform in accordance with Regulatory Guide 1.132 if the geologic and stratigraphic features at depths less than 120 feet below grade can be correlated from one boring or sounding location to the next with relatively smooth variations in thicknesses or properties of the geologic units, or	Category I structures are founded on hard rock; Case 1 applies	Subsection 2.5.1.2.6	N/A

WLS SUP 2.0-1

TABLE 2.0-201 (Sheet 4 of 8)
COMPARISON OF AP1000 DCD SITE PARAMETERS AND LEE NUCLEAR STATION UNITS 1 & 2 SITE CHARACTERISTICS

	AP 1000 DCD Site Parameters	Lee Site Characteristic	Lee FSAR Reference	Lee Within Site Parameter
	<p>2. Site-specific assessment of subsurface conditions demonstrates that the bearing pressures below the footprint of the nuclear island do not exceed 120% of those from the generic analyses of the nuclear island at a uniform site, or</p> <p>3. Site-specific analysis of the nuclear island basemat demonstrates that the site specific demand is within the capacity of the basemat.</p> <p>As an example of sites that are considered uniform, the variation of shear wave velocity in the material below the foundation to a depth of 120 feet below finished grade within the nuclear island footprint and 40 feet beyond the boundaries of the nuclear island footprint meets the criteria in the case outlined below.</p> <p>Case 1: For a layer with a low strain shear wave velocity greater than or equal to 2500 feet per second, the layer should have approximately uniform thickness, should have a dip not greater than 20 degrees, and should have less than 20 percent variation in the shear wave velocity from the average velocity in any layer.</p>	Case 1 applies. Non-dipping meta-plutonic rock displaying less than 20 percent variation in the shear wave velocity.	Subsection 2.5.4.7.4	Yes
Minimum Soil Angle of Internal Friction	<p>Minimum soil angle of internal friction is greater than or equal to 35 degrees below the footprint of nuclear island at its excavation depth.</p> <p>If the minimum soil angle of internal friction is below 35 degrees, a site specific analysis shall be performed using the site specific soil properties to demonstrate stability.</p>	Category I structures are founded on hard rock, which satisfies the criterion.	Not applicable	Yes

WLS SUP 2.0-1

TABLE 2.0-201 (Sheet 5 of 8)
COMPARISON OF AP1000 DCD SITE PARAMETERS AND LEE NUCLEAR STATION UNITS 1 & 2 SITE CHARACTERISTICS

	AP 1000 DCD Site Parameters	Lee Site Characteristic	Lee FSAR Reference	Lee Within Site Parameter
Liquefaction Potential	No liquefaction considered beneath the seismic Category I and seismic Category II structures and immediate surrounding area. The immediate surrounding area includes the effective soil supporting media associated with the seismic Category I and seismic Category II structures.	None. Category I structures are founded on hard rock. Foundations for adjacent structures have negligible liquefaction potential.	Subsection 2.5.4.8	Yes
Missiles				
Tornado	4000 - lb automobile at 105 mph horizontal, 74 mph vertical	4000 - lb automobile at 105 mph horizontal, 74 mph vertical	Subsection 3.5.1.5 ^(f)	Yes ^(f)
	275 - lb, 8 in. shell at 105 mph horizontal, 74 mph vertical	275 - lb, 8 in. shell at 105 mph horizontal, 74 mph vertical	Subsection 3.5.1.5 ^(f)	Yes ^(f)
	1 inch diameter steel ball at 105 mph in the most damaging direction	1 inch diameter steel ball at 105 mph in the most damaging direction	Subsection 3.5.1.5 ^(f)	Yes ^(f)
Flood Level	Less than plant elevation 100' (Lee Elevation 593' msl)	592.56 ft. msl ⁽ⁱ⁾	Subsection 2.4.2.3	Yes
Groundwater Level	Less than plant elevation 98' (Lee Elevation 591' msl)	Maximum groundwater elevation considering the most severe historically recorded natural phenomena has been estimated to be approximately 584 ft. msl, with AP1000 elevation 100 ft at 593 ft. msl. This allows for approximately 9 ft. of unsaturated interval below the plant elevation 593 ft.	Subsection 2.4.12.2.3.1	Yes

WLS SUP 2.0-1

TABLE 2.0-201 (Sheet 6 of 8)
COMPARISON OF AP1000 DCD SITE PARAMETERS AND LEE NUCLEAR STATION UNITS 1 & 2 SITE CHARACTERISTICS

	AP 1000 DCD Site Parameters	Lee Site Characteristic	Lee FSAR Reference	Lee Within Site Parameter
Plant Grade Elevation	Less than plant elevation 100' (Lee elevation 593' msl) except for portion at a higher elevation adjacent to the annex building	592 ft. msl	Subsection 2.4.1.1.3	Yes
Precipitation				
Rain	20.7 in./hr [1-hr 1-mi ² PMP]	18.9 in./hr. [1-hr 1-mi ² PMP]	Table 2.4.2-203	Yes
Snow / Ice	75 pounds per square foot on ground with exposure factor of 1.0 and importance factors of 1.2 (safety) and 1.0 (non-safety)	17.7 pounds per square foot	Subsection 2.3.1.2.7.3	Yes
Atmospheric Dispersion Values χ/Q				
Site Boundary (0-2 hr) ^(g)	$\leq 5.1 \times 10^{-4} \text{ sec/m}^3$	Unit 1: $3.32 \times 10^{-4} \text{ sec/m}^3$ Unit 2: $3.55 \times 10^{-4} \text{ sec/m}^3$	Table 2.3-283 Subsection 2.3.4.2	Yes
Site Boundary (Annual Average)	$\leq 2.0 \times 10^{-5} \text{ sec/m}^3$	$1.5 \times 10^{-5} \text{ sec/m}^3$	Table 2.3-289 (Site Boundary Unit 1 NW)	Yes
Low population zone boundary				
0-8 hr	$\leq 2.2 \times 10^{-4} \text{ sec/m}^3$	$8.05 \times 10^{-5} \text{ sec/m}^3$	Table 2.3-283	Yes
8-24 hr	$\leq 1.6 \times 10^{-4} \text{ sec/m}^3$	$5.52 \times 10^{-5} \text{ sec/m}^3$	Table 2.3-283	Yes
24-96 hr	$\leq 1.0 \times 10^{-4} \text{ sec/m}^3$	$2.43 \times 10^{-5} \text{ sec/m}^3$	Table 2.3-283	Yes
96-720 hr	$\leq 8.0 \times 10^{-5} \text{ sec/m}^3$	$7.52 \times 10^{-6} \text{ sec/m}^3$	Table 2.3-283	Yes
Control Room	Table 2.0-202	Table 2.0-202	Table 2.0-202	Yes

WLS SUP 2.0-1

TABLE 2.0-201 (Sheet 7 of 8)
COMPARISON OF AP1000 DCD SITE PARAMETERS AND LEE NUCLEAR STATION UNITS 1 & 2 SITE
CHARACTERISTICS

	AP 1000 DCD Site Parameters	Lee Site Characteristic	Lee FSAR Reference	Lee Within Site Parameter
Population Distribution				
Exclusion area (site)	0.5 mi	Unit 1: Minimum distance from the Effluent Release Boundary to the Exclusion Area Boundary is 3070 feet. The radius of the effluent release boundary is 448 feet. The total minimum distance from the Unit 1 center point to the EAB is 3518 feet (0.67 mi).	Subsection 2.1 Figure 2.1-209A	Yes ^(j)
		Unit 2: Minimum distance from the Effluent Release Boundary to the Exclusion Area Boundary is 2914 feet. The radius of the effluent release boundary is 448 feet. The total minimum distance from the Unit 2 center point to the EAB is 3362 feet (0.64 mi).	Subsection 2.1 Figure 2.1-209B	Yes ^(j)

WLS SUP 2.0-1

TABLE 2.0-201 (Sheet 8 of 8)
COMPARISON OF AP1000 DCD SITE PARAMETERS AND LEE NUCLEAR STATION UNITS 1 & 2 SITE
CHARACTERISTICS

AP 1000 DCD Site Parameters	Lee Site Characteristic	Lee FSAR Reference	Lee Within Site Parameter
<p>a) Maximum and minimum safety values are based on historical data and exclude peaks of less than 2 hours duration.</p> <p>b) The maximum normal value is the 1-percent seasonal exceedance temperature. The minimum normal value is the 99-percent seasonal exceedance temperature. The minimum temperature is for the months of December, January, and February in the northern hemisphere. The maximum temperature is for the months of June through September in the northern hemisphere. The 1-percent seasonal exceedance is approximately equivalent to the annual 0.4-percent exceedance. The 99-percent seasonal exceedance is approximately equivalent to the annual 99.6-percent exceedance.</p> <p>c) The noncoincident wet bulb temperature is applicable to the cooling tower only.</p> <p>d) With ground response spectra as given in DCD Figure 3.7.1-1 and DCD Figure 3.7.1-2. Seismic input is defined at finished grade except for sites where the nuclear island is founded on hard rock.</p> <p>e) Sites that fall within the hard rock high frequency envelope response spectra given in DCD Figures 3I.1-1 and 3I.1-2 and satisfy the limitation on shear wave velocity in DCD Subsection 2.5.2.1 are acceptable.</p> <p>f) Per APP-GW-GLR-020, the kinetic energies of the missiles discussed in DCD Section 3.5 are greater than the kinetic energies of the missiles discussed in Regulatory Guide 1.76 and results in a more conservative design.</p> <p>g) For AP1000, the term "site boundary" and "exclusion area boundary" are used interchangeably. Thus, the χ/Q specified for the site boundary applies whenever a discussion refers to the exclusion area boundary. At Lee Nuclear Station, the "site boundary" and the "exclusion area boundary" are <u>not</u> interchangeable. See Figures 2.1-209A and 2.1-209B.</p> <p>h) The containment pressure response analysis is based on a conservative set of dry-bulb and wet-bulb temperatures. These results envelop any conditions where the dry-bulb temperature is 115°F or less and wet-bulb temperature of less than or equal to 86.1°F.</p> <p>(i) The maximum flood level of 592.56 ft. msl is a result of local PMP event as described in Subsection 2.4.2.3. See Subsection 2.4.2.2 for discussion of design basis considerations.</p> <p>(j) Lee Nuclear Station Units 1 and 2 comply with 0.5 mi EAB site parameter specified in the AP1000 DCD (Table 2-1).</p>			

TABLE 2.0-202 (Sheet 1 of 4)
COMPARISON OF CONTROL ROOM ATMOSPHERIC DISPERSION FACTORS FOR ACCIDENT ANALYSIS
FOR AP1000 DCD AND LEE NUCLEAR STATION UNITS 1 & 2 (REFERENCE [TABLE 2.3-285](#))

WLS SUP 2.0-1

	χ/Q (s/m ³) at HVAC Intake for the Identified Release Points ^(a)			χ/Q (s/m ³) at Annex Building Door for the Identified Release Points ^(b)		
	Plant Vent or PCS Air Diffuser ^(c)			Plant Vent or PCS Air Diffuser ^(c)		
	Plant Vent	PCS Air Diffuser		Plant Vent	PCS Air Diffuser	
	DCD	FSAR	FSAR	DCD	FSAR	FSAR
0 – 2 hours	3.0E-03	2.01E-03	1.78E-03	1.0E-03	4.41E-04	4.83E-04
2 – 8 hours	2.5E-03	1.52E-03	1.45E-03	7.5E-04	3.47E-04	3.69E-04
8 – 24 hours	1.0E-03	5.84E-04	6.36E-04	3.5E-04	1.37E-04	1.61E-04
1 – 4 days	8.0E-04	4.76E-04	5.26E-04	2.8E-04	1.13E-04	1.32E-04
4 – 30 days	6.0E-04	3.56E-04	3.36E-04	2.5E-04	8.22E-05	9.13E-05

	χ/Q (s/m ³) at HVAC Intake for the Identified Release Points ^(a)				χ/Q (s/m ³) at Annex Building Door for the Identified Release Points ^(b)			
	Steam Line Break Releases	Steam Line Break Releases	Condenser Air Removal Stack ^(g)	Condenser Air Removal Stack	Steam Line Break Releases	Steam Line Break Releases	Condenser Air Removal Stack ^(g)	Condenser Air Removal Stack
	DCD	FSAR	DCD	FSAR	DCD	FSAR	DCD	FSAR
	DCD	FSAR	DCD	FSAR	DCD	FSAR	DCD	FSAR
0 – 2 hours	2.4E-02	1.25E-02	6.0E-3	1.59E-03	4.0E-03	8.50E-04	2.0E-2	3.40E-03
2 – 8 hours	2.0E-02	7.22E-03	4.0E-3	1.27E-03	3.2E-03	6.44E-04	1.8E-2	2.91E-03
8 – 24 hours	7.5E-03	2.95E-03	2.0E-3	5.10E-04	1.2E-03	2.84E-04	7.0E-3	1.31E-03
1 – 4 days	5.5E-03	2.40E-03	1.5E-3	3.86E-04	1.0E-03	1.93E-04	5.0E-3	9.21E-04
4 – 30 days	5.0E-03	1.79E-03	1.0E-3	2.82E-04	8.0E-04	1.39E-04	4.5E-3	6.40E-04

TABLE 2.0-202 (Sheet 2 of 4)
 COMPARISON OF CONTROL ROOM ATMOSPHERIC DISPERSION FACTORS FOR ACCIDENT ANALYSIS
 FOR AP1000 DCD AND LEE NUCLEAR STATION UNITS 1 & 2 (REFERENCE [TABLE 2.3-285](#))

	χ/Q (s/m ³) at HVAC Intake for the Identified Release Points ^(a)		χ/Q (s/m ³) at Annex Building Door for the Identified Release Points ^(b)	
	Ground Level Containment Release Points ^(d)		Ground Level Containment Release Points ^(d)	
	DCD	FSAR	DCD	FSAR
0 – 2 hours	6.0E-03	2.70E-03	1.0E-03	5.01E-04
2 – 8 hours	3.6E-03	1.79E-03	7.5E-04	3.98E-04
8 – 24 hours	1.4E-03	7.39E-04	3.5E-04	1.59E-04
1 – 4 days	1.8E-03	6.90E-04	2.8E-04	1.36E-04
4 – 30 days	1.5E-03	4.75E-04	2.5E-04	9.76E-05

	χ/Q (s/m ³) at HVAC Intake for the Identified Release Points ^(a)		χ/Q (s/m ³) at Annex Building Door for the Identified Release Points ^(b)	
	PORV and Safety Valve Releases ^(e)		PORV and Safety Valve Releases ^(e)	
	DCD	FSAR	DCD	FSAR
0 – 2 hours	2.0E-02	1.08E-02	4.0E-03	8.71E-04
2 – 8 hours	1.8E-02	5.62E-03	3.2E-03	6.83E-04
8 – 24 hours	7.0E-03	2.28E-03	1.2E-03	2.96E-04
1 – 4 days	5.0E-03	1.89E-03	1.0E-03	2.05E-04
4 – 30 days	4.5E-03	1.47E-03	8.0E-04	1.46E-04

TABLE 2.0-202 (Sheet 3 of 4)
COMPARISON OF CONTROL ROOM ATMOSPHERIC DISPERSION FACTORS FOR ACCIDENT ANALYSIS
FOR AP1000 DCD AND LEE NUCLEAR STATION UNITS 1 & 2 (REFERENCE TABLE 2.3-285)

	χ/Q (s/m ³) at HVAC Intake for the Identified Release Points ^(a)			χ/Q (s/m ³) at Annex Building Door for the Identified Release Points ^(b)		
	Fuel Handling Area ^(f)	Fuel Building Blowout Panel	Radwaste Building Truck Staging Area Door	Fuel Handling Area ^(f)	Fuel Building Blowout Panel	Radwaste Building Truck Staging Area Door
	DCD	FSAR	FSAR	DCD	FSAR	FSAR
0 – 2 hours	6.0E-03	1.64E-03	1.17E-03	6.0E-03	3.64E-04	3.46E-04
2 – 8 hours	4.0E-03	1.20E-03	8.98E-04	4.0E-03	2.65E-04	2.53E-04
8 – 24 hours	2.0E-03	4.25E-04	3.30E-04	2.0E-03	1.01E-04	9.78E-05
1 – 4 days	1.5E-03	4.09E-04	2.93E-04	1.5E-03	8.87E-05	8.71E-05
4 – 30 days	1.0E-03	3.69E-04	2.59E-04	1.0E-03	7.37E-05	7.57E-05

- a) These dispersion factors are to be used 1) for the time period preceding the isolation of the main control room and actuation of the emergency habitability system, 2) for the time after 72 hours when the compressed air supply in the emergency habitability system would be exhausted and outside air would be drawn into the main control room, and 3) for the determination of control room doses when the non-safety ventilation system is assumed to remain operable such that the emergency habitability system is not actuated.
- b) These dispersion factors are to be used when the emergency habitability system is in operation and the only path for outside air to enter the main control room is that due to ingress/egress.
- c) These dispersion factors are used for analysis of the doses due to a postulated small line break outside of containment. The plant vent and PCS air diffuser are potential release paths for other postulated events (loss-of-coolant accident, rod ejection accident, and fuel handling accident inside the containment); however, the values are bounded by the dispersion factors for ground level releases.
- d) The listed values represent modeling the containment shell as a diffuse area source, and are used for evaluating the doses in the main control room for a loss-of-coolant accident, for the containment leakage of activity following a rod ejection accident, and for a fuel handling accident occurring inside the containment.
- e) The listed values bound the dispersion factors for releases from the steam line safety and power-operated relief valves. These dispersion factors would be used for evaluating the doses in the main control room for a steam generator tube rupture, a main steam line break, a locked reactor coolant pump rotor, and for the secondary side release from a rod ejection accident.

TABLE 2.0-202 (Sheet 4 of 4)
COMPARISON OF CONTROL ROOM ATMOSPHERIC DISPERSION FACTORS FOR ACCIDENT ANALYSIS
FOR AP1000 DCD AND LEE NUCLEAR STATION UNITS 1 & 2 (REFERENCE [TABLE 2.3-285](#))

- f) The listed values bound the dispersion factors for releases from the fuel storage and handling area. The listed values also bound the dispersion factors for releases from the fuel storage area in the event that spent fuel boiling occurs and the fuel building relief panel opens on high temperature. These dispersion factors are used for the fuel handling accident occurring outside containment and for evaluating the impact of releases associated with spent fuel pool boiling.
- g) This release point is included for information only as a potential activity release point. None of the design basis accident radiological consequences analyses model release from this point.

2.1 GEOGRAPHY AND DEMOGRAPHY

This **section** of the referenced DCD is incorporated by reference with the following departures and/or supplements.

WLS COL 2.1-1 This section of the Safety Analysis Report provides information regarding site location and description including the distribution of infrastructure, natural features, and populations in the Lee Nuclear Station area. The discussion below addresses the expectations of NUREG-0800, "Standard Review Plan for the Review of Safety Analysis Reports for Nuclear Power Plants," and Regulatory Guide 1.206, "Combined License Applications for Nuclear Power Plants (LWR Edition)." Radius distances defined by the NUREG-1555 were used for the population analysis rather than the distances described in RG 1.206 as an alternate method. The alternative method was used for correlation of the population data between the SAR and ER. No other exceptions to the regulatory documents noted or alternative methods were applied in development of this section.

Subsection 2.1.1 of the DCD is renumbered as **Subsection 2.1.4** and moved to the end of **Section 2.1**. This is being done to accommodate the incorporation of Regulatory Guide 1.206 numbering conventions for **Section 2.1**.

STD DEP 1.1-1 2.1.1 SITE LOCATION AND DESCRIPTION

WLS COL 2.1-1 Duke Energy proposes to construct and operate two Westinghouse AP1000 reactors at their Lee Nuclear Station 1,900-acre site, located in rural Cherokee County, South Carolina. The two AP1000 reactors are referred to as Lee Nuclear Station Units 1 and 2. Units 1 and 2 and supporting infrastructure are sited in the area delineated in **Figure 2.1-201**. Prominent natural and man-made features, including rivers, lakes, state and county lines, and industrial, military, and transportation facilities, are illustrated in **Figures 2.1-201, 2.1-202, and 2.1-203**. **Figure 2.1-202** illustrates the features within the vicinity of the site.

The Lee Nuclear Site lies within the 7.5 minute Blacksburg South and Kings Creek Quadrangles. The Quadrangles that bracket the site area are Blacksburg North, Grover, Kings Mountain, Filbert, Sharon, Hickory Grove, Wilkinsville, Pacolet Mills, Gaffney, and Boiling Springs South. All quadrangles lie completely or partially within South Carolina (**References 210 and 212**).

The coordinates of the two new reactors are given below:

LONGITUDE AND LATITUDE (decimal degrees [NAD83])

UNIT 1:	35.036527 North	-81.512962 West
UNIT 2:	35.036995 North	-81.510351 West

UNIVERSAL TRANSVERSE MERCATOR NAD83 ZONE 17 (Meters)

	Northing	Easting
UNIT 1:	3877214.1	453211.9
UNIT 2:	3877264.7	453450.3

2.1.1.1 Specification of Location

Duke Energy owns the property on which the Lee Nuclear Station is located and directs land management activities at the site. Duke Energy is the named applicant and operator for the Lee Nuclear Station. The 1900-ac. site, the area within the site boundary, is bounded by the Broad River to the north and east, by McKowns Mountain Road to the south, and private properties to the south and west ([Figure 2.1-202](#)) ([References 207](#) and [208](#)). There are no public transportation routes that cross the Lee Nuclear Station site ([Reference 207](#)). Duke Energy owns the mineral rights on the Lee Nuclear Station site. There are no mineral resources, including oil and natural gas, within or adjacent to the site that are being exploited or of any known value ([Reference 204](#)).

The location for the Lee Nuclear Station is an industrial site that was evaluated and licensed for the construction of three nuclear units in the 1970s. Approximately 750 ac. of ground were disturbed by this early construction, which began in 1977 and was halted in 1982. These construction activities resulted in extensive alterations of the site. The site was purchased by Earl Owensby Studios in 1986 and used for the production of a movie and commercials. The site sat idle for a number of years and was acquired in 2005 by Cherokee Falls Development Company LLC (a subsidiary of Southern Company). Duke Energy purchased all outstanding ownership shares from Cherokee Falls Development Company in early 2007.

Previous construction activities on the site left in place a large excavated area, partially constructed power unit buildings (one partially completed power block and containment/shield building), and numerous other large and small on-site buildings that were used as warehouses, shops, construction support facilities, and a guard house. Concrete pads and remnant vehicle parking areas are present at various locations on the site. These constructed surface features are linked by a system of paved roads and a related system of unpaved roads that serve peripheral areas of the site. Buried utility pipelines, overhead electric power lines, and communications lines that once served the buildings and construction areas

are still present on the site. The electrical lines are suspended by wooden poles and metal towers. An abandoned railroad spur enters the site at a point on its northern boundary, extends across the north half of the site, and ends in a former construction area. The rails have been removed, so all that remains is the graded bed of the former spur. The site contains three major surface water impoundments that were established by previous construction activities on the site. These are the large Make-Up Pond B (formerly the Standby Nuclear Service Water Pond for the canceled Cherokee Plant) on the west side of the site, Make-Up Pond A on the east side of the site, and Hold-Up Pond A on the north end of the site. The majority of the site is surrounded by chain link fences with gates.

Units 1 and 2 are (upstream) approximately 1 mi. northwest of the Ninety-Nine Islands Hydroelectric Dam. The closest communities to Lee Nuclear Station are the city of Gaffney, South Carolina (8.2 mi. northwest), the city of East Gaffney, South Carolina (7.5 mi. northwest), and the town of Blacksburg, South Carolina (5.8 mi. north) (Reference 202). According to 2005 US Census Bureau population estimates, the city of Gaffney, South Carolina had a population of 12,934 and is the largest community within 10 mi. of the Lee Nuclear Station. The city of Blacksburg, South Carolina, the second largest community within 10 mi. of the Lee Nuclear Station, had a population of 1898 (Reference 206).

The nearest population center (as defined by 10 CFR 100.3) of the Lee Nuclear Station is Gastonia, North Carolina (References 202, 203, 206). Gastonia's urban border, as defined by the US Census Bureau, is situated 16 mi. to the northeast and was estimated in 2005 to have a population of 68,964 (References 203 and 206).

Interstate 85, passing through the northern side of Gaffney, South Carolina and connecting Greenville, South Carolina and Spartanburg, South Carolina with Charlotte, North Carolina, is located approximately 7 mi. north-northwest of the site (Reference 207). There are no military facilities located within the vicinity of the Lee Nuclear Site (Reference 233).

2.1.1.2 Site Area Map

Figure 2.1-203 illustrates the region surrounding the Nuclear Site within a radius of 50 mi. This map includes prominent geophysical and political features in the area. Table 2.1-201 lists the counties that are entirely or partially located within the 50-mi. region. Figure 2.1-202 shows greater detail of the Lee Nuclear Site out to a radius of 6 mi. The Lee Nuclear Station site boundary is boldly outlined. As shown in the figure, there are no industrial and transportation facilities, commercial, institutional, recreational, and residential structures within the site area.

Figure 2.1-204 is a USGS topographic map that shows prominent natural and manmade features. Figure 2.1-201 illustrates the site in greater detail. The reactor building, turbine building, and the cooling towers are labeled. The auxiliary buildings are shown in the background. Figures 2.1-209A and 2.1-209B illustrate the shortest distances from the Effluent Release Boundaries to the Exclusion Area Boundary (EAB) for both Units 1 and 2.

The total area contained by the site boundary is about 1,900 acres of land. There are no industrial, military, transportation facilities, commercial, institutional, recreational, or residential structures within the site area. The EAB generally follows the site boundary (but extends beyond it on the northern and eastern sides of the site). The Effluent Release Boundary is defined as an assumed 448 ft. radius circle around each reactor that encompasses all site release points.

Figures 2.1-209A and 2.1-209B show the location of the EAB and the shortest distances from the Effluent Release Boundaries associated with Units 1 and 2. The nearest segment of the EAB to the Effluent Release Boundary is 2914 feet.

2.1.1.2.1 Boundaries for Establishing Effluent Release Limits

There are no residents in the Exclusion Area. No areas within the site boundary are used for residential quarters or industrial, commercial, institutional, or recreational facilities not controlled by Duke Energy. Access within the site boundary is controlled as described in FSAR Section 2.1.2. FSAR Section 2.3 provides details on gaseous release points and their relation to the site boundary. The discussion of normal releases (gaseous and aqueous) are in FSAR Sections 11.2 and 11.3, and accidental releases are discussed in FSAR Chapter 15. All areas outside the exclusion area are unrestricted areas in the context of 10 CFR Part 20. For the Lee Nuclear Station, the Restricted Area is the same as the Protected Area. Figure 2.1-201 shows the Protected Area Boundary. For Lee Nuclear Station, the Protected Area is the fenced area surrounding the reactor buildings. It contains all of the buildings required for the operation of the reactor with the exception of the cooling towers (See Figure 2.1-201 for the site plot plan).

WLS COL 2.1-1 2.1.2 EXCLUSION AREA AUTHORITY AND CONTROL

The boundary on which limits for the release of radioactive effluents are based is the exclusion area boundary shown in Figures 2.1-209A and 2.1-209B. The site boundary is clearly posted with no trespassing signs, with the exception of a publicly accessible boat launch area located upstream of Ninety-Nine Islands Hydroelectric Dam. The no trespassing signs also include actions to be taken in the event of emergency conditions at the plant. The site's physical security plan contains information on actions to be taken by security force personnel in the event of unauthorized persons crossing the EAB during emergency operations.

2.1.2.1 Authority

All of the land inside the site boundary (Figure 2.1-201) is owned by Duke Energy. Duke Energy controls all activities within this area including exclusion and removal of personnel from the area during emergency operations. Duke Energy owns the mineral rights on the Lee Nuclear Site. There are no known easements that affect the Lee Nuclear Station. The Exclusion Area Boundary (EAB), shown in Figures 2.1-209A and 2.1-209B, extends beyond the site boundary to the north and east. Certain properties within the EAB that lay beyond the site boundary are currently not owned by Duke Energy. Negotiations regarding these properties have been initiated and Duke Energy ownership or control authority, including the mineral rights, will be obtained prior to start of construction.

2.1.2.2 Control of Activities Unrelated to Plant Operation

There are no residential quarters, and only limited recreational and commercial activities within the Exclusion Area. Commercial activities are limited to a sand dredging operation on the Broad River to the NNW of the site, and the Ninety-Nine Islands Hydroelectric Dam located on the Broad River east of the site. The recreational activities are limited to the Broad River, which crosses the EAB on the northern and eastern sides of the site. No public highways or active railroads traverse the exclusion area. There are four historical cemeteries within the site boundary. Access to these cemeteries is controlled by security personnel.

2.1.2.3 Arrangements For Traffic Control

Arrangements with Cherokee County for control of traffic in the event of an emergency is not required in that no publicly used transportation modes cross the EAB.

2.1.2.4 Abandonment or Relocation of Roads

There are no public roads presently within the Exclusion Area which, because of their location, have to be abandoned or relocated.

WLS COL 2.1-1 2.1.3 POPULATION DISTRIBUTION

To project total population for the Lee Nuclear Station Region, three Geographical Information System (GIS) mapping processes are used to produce a series of population tables. The first process converts US Census block data to sector data geography, the second process converts county level population projections to sector level data, and the third converts transient population data to sector level data. The data tables produced provide population values that correspond to the geographic area defined by radial distance from the Lee Nuclear Station site center point and 16 compass point directions. These tables correspond directly to the distances and directions displayed in [Figure 2.1-205](#) and [Figure 2.1-206](#).

A sector is defined as an area between two radial distances and two angular lines from a point. In the case of Lee Nuclear Station the radial distances are defined in NUREG-1555, the two angles form a wedge based on each of the 16 compass points and the center point is the designated site center point. Using NUREG-1555 as a guideline, GIS software produced shapefile, called a sector grid, is produced containing sectors in every direction. The population distribution is estimated in nine concentric radial bands at 0 to 2 km (1.24 mi.), 2 to 4 km (2.5 mi.), 4 to 6 km (3.7 mi.), 6 to 8 km (5 mi.), 8 to 10 km (6.2 mi.), 10 to 16 km (10 mi.), 16 to 40 km (25 mi.), 40 to 60 km (37 mi.), and 60 to 80 km (50 mi.) from the designated site center point between the two reactors. These bands are then subdivided into 16 directional sectors centered on the 16 compass points, with each direction consisting of 22.5 degrees as defined in NUREG-1555.

To display all sectors defined by the directions and distances, two maps were produced. Population sectors for 0 to 16 km (10 mi.) are shown in [Figure 2.1-206](#) and 16 to 80 km (50 mi.) in [Figure 2.1-205](#). To convert US Census Block data to

sector data, the sector grid shapefile is overlaid onto the census block shapefile, and the shapefiles are integrated. US Census blocks that have been bisected by the sector grid are area weighted. The values falling within each sector are summed. The resulting data has an unrounded population value for each sector for the year 2000. The population distribution surrounding the Lee Nuclear Site, up to an 80-km (50-mi.) radius, is estimated based upon the most recent US Census Bureau decennial census data ([Reference 218](#)).

Many states establish official population projections, and county projection information is available from a state's official on-line source. These population projections are used for economic development and planning purposes. Both North Carolina and South Carolina have population projection data available for specific years for every county in their respective state. North Carolina and South Carolina have projected county populations to 2030. The population projections for both states are derived from county estimates and based on the cohort-component method ([References 209](#) and [232](#)). The data set is reduced to the counties located within, or partially within the region. The plot of this data set illustrates a linear trend for all of the counties in the region. Due to this trend, a least squares linear regression is applied to the counties and an equation is produced for each county. These equations are then used to calculate population estimates for the years not projected by the state. The resulting values from the equations are used in conjunction with the 2000 census data to produce a growth ratio, or index, for each year and each county included in the region. The data is then joined to a county shapefile using GIS. The county indexes are area weighted by sector and summed for each sector, producing a population growth index by sector. For any county with a negative growth rate, a growth ratio of one is used to produce the most conservative results without overestimating. Using a growth ratio of one does not allow the county's population to decline.

The transient population data is collected by location. These locations are converted to points and areas, and using GIS, integrated into the sector polygon. Any area that is bisected by the sector grid is area weighted. The values falling within each sector are summed. The resulting data is the un-rounded transient sector population for the region.

The US Census based sector data (Block 2000) or the transient sector population is multiplied by these indices for each year of interest. Population tables are then generated for each sector and year of interest. Each sector is listed by compass direction and furthest radial distance. [Tables 2.1-203](#) and [2.1-204](#) correspond to [Figures 2.1-205](#) and [2.1-206](#) by compass direction and radial distance.

The commercial operation date was initially estimated to be 2016, but has been revised to approximately 2024. The FSAR evaluations are based on 2016; however, Duke Energy has evaluated the change and has determined that it is not significant.

2.1.3.1 Population Within 10 Miles

[Figure 2.1-207](#) shows a portion of the study area within 16 km (10 mi.) of the site center point. The map contains roads, railroads, nearby towns, and counties.

Based on the 2000 US Census Bureau estimates the populations of the towns within the 16-km (10-mi.) area are shown in [Table 2.1-202](#).

[Table 2.1-203](#) shows the projected permanent population for each sector and projections for 2007, 2016, 2026, 2036, 2046, and 2056. The distances defining the sectors are 0 to 2 km (1.24 mi.), 2 to 4 km (2.5 mi.), 4 to 6 km (3.7 mi.), 6 to 8 km (5 mi.), 8 to 10 km (6.2 mi.), and 10 to 16 km (10 mi.). These sectors can be seen in [Figure 2.1-206](#). The projections were carried out to 40 years past the initially estimated startup date of 2016. The population in the 16-km (10-mi.) area is shown in the “Cumulative Totals” field of [Table 2.1-203](#) for each projected year. The percent of the 16-km (10-mi.) permanent population within 8 km (5 mi.) is 12.1 percent for all years of projection.

2.1.3.2 Population Between 10 and 50 Miles

[Figure 2.1-205](#) illustrates a portion of the study area within 80 km (50 mi.) of the site center point. The map contains the sector grid, county boundaries, state boundaries and bodies of water. The distances defining the sectors are 16 km (10 mi.) to 40 km (25 mi.), 40 to 60 km (37 mi.), and 60 to 80 km (50 mi.). Charlotte, North Carolina is the largest city within the 80-km (50-mi.) area. Based on the 2005 US Census Bureau estimates, the population of Charlotte, North Carolina is 610,949. Smaller cities within the 80-km (50-mi.) area include Gastonia, North Carolina; Greenville, South Carolina; Hickory, North Carolina; Rock Hill, South Carolina; and Spartanburg, South Carolina. Based on the 2005 US Census Bureau estimates their populations are 68,964, 56,676, 40,232, 59,554, and 38,379 respectively. Many other small towns, cities, and urban areas with populations less than 25,000 are distributed within the 80-km (50-mi.) area. The cities of Concord, North Carolina and Monroe, North Carolina have very small portions inside the 80-km (50-mi.) area. Both of these cities have population in excess of 25,000 ([References 202](#) and [206](#)).

[Table 2.1-204](#) shows the projected permanent population for each sector and projections for 2007, 2016, 2026, 2036, 2046, and 2056. Again, the projections were carried out 40 years past the initially estimated startup date of 2016 for Unit 1. The number of people in the 16-km (10-mi.) to 80-km (50-mi.) area is shown in the “Cumulative Totals” field of the table for each projected year.

2.1.3.3 Transient Population

Transient population within the region of the Lee Nuclear Station is influenced by several factors. Shopping generates the most transients within 10 mi. of the Lee Nuclear Site. Natural attractions generate most of the remainder of visitors to the 50-mi. region, with the exception of Christmastown USA in McAdenville, North Carolina which gets over 600,000 visitors between December 1st and December 26th annually. McAdenville, North Carolina is approximately 30 mi. from the Lee Nuclear Station.

The city boundaries of Charlotte, North Carolina are enclosed by the Lee Nuclear Site regional boundary. Museums and science attractions make up the bulk of transients in that portion of the region.

Transient data were gathered through personal contact with businesses, companies, and local chambers of commerce within the region. This method for collecting transient data provides a more accurate accounting of people visiting the area and a much more precise location of transient contributors than using county estimates weighted over a sector area. Data out to 15 mi. were collected in accordance with regulation for the Emergency Planning Zone (EPZ). Major contributors to transient population are listed in [Table 2.1-205](#). Unless otherwise noted, all transient population data are from 2006.

To project the transient information, the transient data per sector were summed. The summed number was multiplied by the sector growth ratio derived from the county growth ratios described above for each year. Because the method for collecting transient data provides point locations, some sectors have a zero value. This is because there are no accountable transient contributors in the zero value sectors. [Table 2.1-208](#) illustrates the projected transient population for each sector and projections for 2007, 2016, 2026, 2036, 2046, and 2056 for the non-zero sectors ([References 209, 211, 230, 231, and 232](#)). The projections were carried out to 40 years past the initially estimated startup date of 2016. The sectors that have zero values are not illustrated in this table.

2.1.3.3.1 Transient Population Within 10 Miles

The Prime Outlets at Gaffney, South Carolina is the single largest tourist draw in the area of the Lee Nuclear Site, located approximately 11.7 mi. from the station center point. The Prime Outlets get a average of 7671 shoppers per day or over 2.8 million visitors per year. Forty-six percent of the shoppers are from South Carolina and 54 percent are from out-of-state ([Reference 211](#)).

The city of Gaffney, South Carolina is 8 mi. from the Lee Nuclear Site and hosts several events throughout the year ([Reference 202](#)). These include the South Carolina Peach Festival and Christmas on Limestone. Each of these events can host between 2,000 and 2,500 people per day during the event. The peach festival can last from five to ten days and the Christmas celebration is a one day event.

2.1.3.3.2 Transient Population Between 10 and 50 Miles

There are three commercial passenger airports within the region: Charlotte-Douglas International Airport (34 mi.) to the northeast, Greenville-Spartanburg International Airport (41 mi.) to the southwest, and Hickory Regional Airport (49 mi.) to the north. ([Reference 207](#)). The daily and annual passenger counts for these three airports are shown in [Table 2.1-206](#) ([References 213, 214, and 215](#)).

Amtrak has passenger train stations in Spartanburg, South Carolina, Charlotte, North Carolina, and Gastonia, North Carolina. Amtrak also has trackage rights on all rails within the region, meaning that there is a possibility that any rail section

can be used to move passengers from one station to another ([References 207 and 216](#)).

Charlotte's Thunder Road Marathon occurs every December and includes a marathon, half marathon, marathon relay, and a 5K race. Nearly 4,200 runners entered the 2006 events. This course winds through some of the city's most historic and eclectic neighborhoods before finishing in Uptown Charlotte ([Reference 205](#)).

Paramount's Carowinds Theme Park, located in Charlotte, North Carolina, had a 2002 annual attendance of 1.85 million visitors ([Reference 234](#)).

The Bank of America Stadium, home to the NFL's Carolina Panthers, has a capacity of 73,248 and a 2006 annual attendance of 587,700 people ([Reference 235](#)). The Bobcats Arena, home to the NBA's Charlotte Bobcats, has a capacity of 18,500 and a 2006-2007 season attendance of 637,520 people ([Reference 236](#)). Both of these facilities are located in Charlotte, North Carolina.

2.1.3.3.2.1 Recreational Transients

The nearest park to the proposed site is the Kings Mountain State Park, located approximately 8 mi. northeast of the Lee Nuclear Site center point. Other attractions near the Lee Nuclear Site are Cowpens National Battlefield, Kings Mountain National Military Park, and the Prime Outlets of Gaffney, South Carolina. The nearest of these are Cowpens National Battlefield and the Prime Outlets of Gaffney, South Carolina, both located in Gaffney, South Carolina. The Kings Mountain National Military Park immediately adjoins Kings Mountain State Park on its northwest border. A portion of the Francis Marion – Sumter National Forest falls within the region and accounts for an average of almost 3,000 visitors per day ([References 211, 217, 219, and 220](#)).

The U.S. National Whitewater Center in Charlotte, North Carolina is home to the world's largest manmade whitewater river and attracts approximately 500,000 visitors a year ([Reference 237](#)).

Fishing, hunting, and wildlife watching in the portions of North Carolina and South Carolina included in the region are an important recreational pastime, as shown in [Table 2.1-207](#). The combined wildlife related activities attract approximately 704,901 outdoor enthusiasts per year ([References 221 and 222](#)).

2.1.3.3.2.2 Seasonal Populations

Many of the attractions within the vicinity of the Lee Nuclear Site are based around outdoor activities. The peak times for these attractions, with the highest visitor numbers, occur from spring through mid-fall. The lowest levels occur during the winter months.

2.1.3.3.2.3 Transient Workforce

An estimated 4512 workers are required on site at the peak construction phase to complete the facility. In 2000, for the six counties surrounding the site, there was a total of just over 25,607 properties available, including homes for sale and rental properties^a. (References 223 and 224)

2.1.3.3.2.4 Special Facilities (Schools, Hospitals, Nursing Homes, etc.)

There are 33 2-year and 4-year colleges and universities within the region of the Lee Nuclear Site. Total enrollment for these schools is more than 98,145 students (References 225 and 226). The 2-year and 4-year colleges and universities in the region are typically near peak daily capacity for the majority of the year, excluding the summer months (mid-May through mid-August). Even with this educational reduction during the summer months, overall peak levels of transients are thought to still occur over that time period.

There are twenty-nine major hospitals and medical centers within 50 mi. of Lee Nuclear Site. These medical facilities have a combined capacity of 5,223 staffed beds and discharge more than 246,356 patients per year. The two closest major medical facilities to the Lee Nuclear Site are Upstate Carolina Medical Center in Gaffney, South Carolina and Kings Mountain Hospital in Kings Mountain, North Carolina. These two facilities account for 125 beds, 4442 annual discharges and 42 beds, 1949 annual discharges, respectively. The largest medical facility within the region is Carolinas Medical Center in Charlotte, North Carolina with 743 beds and more than 41,858 patient discharges annually (References 227 and 228).

The two nearest nursing home facilities to the Lee Nuclear Site are Brookview HealthCare Center and Cherokee County Long Term Care Facility. Brookview HealthCare Center is located in Gaffney, South Carolina and has a 132-bed capacity. Cherokee County Long Term Care Facility, also known as Peachtree Healthcare Center, also located in Gaffney, South Carolina, has a 145-bed capacity. The city of Spartanburg, South Carolina, has several nursing home facilities (Reference 229).

There are no federal prison facilities located within the Lee Nuclear Site Region (References 238 and 239). Eleven state correctional facilities are located within the Lee Nuclear Site region, three in South Carolina and eight in North Carolina (References 201 and 240).

2.1.3.3.3 Total Permanent and Transient Populations

The annual total of the special facilities and the transient populations within the region is approximately 10,316,432 people. The estimated 2007 summed transient population on any given day within the region is calculated to be

a. The six counties are Cherokee, Union, Spartanburg, and York in South Carolina and Cleveland and Gaston in North Carolina.

71,869^b (References 211, 219, 230, and 231). The estimated permanent population for 2007 for the region (the sum of entries in Tables 2.1-203 and 2.1-204) is 2,382,474 people (Reference 218). The estimated 2007 total population within the region at any one time is calculated to be approximately 2,454,343 people.

2.1.3.3.4 Transient Populations Outside the 50-Mile Region

There are two facilities located beyond the 50-mile radius, the Lowe's Motor Speedway and Concord Mills Mall. The Lowe's Motor Speedway is located approximately 51 mi. northeast of Lee Nuclear Site and attracts approximately 1.2 million people a year for events, tours, and driving schools. The peak months are May and October when the NASCAR NEXTEL Cup races occur. Concord Mills Mall is located approximately 51 mi. northeast of the site and reports over 17.6 million visitors a year. Their peak months are June and December.

2.1.3.4 Low-Population Zone

At Lee Nuclear Site, the Low Population Zone (LPZ) is defined as a two mile radius from the site center point. The center point is defined as the midway point between Unit 1 and Unit 2. Using this radius, there are only rural areas and the Lee Nuclear Station within the LPZ (See Figure 2.1-208).

According to the US Census Bureau 2000 data, there are 509 people living within the LPZ, distributed generally to the north and south of the site (see Table 2.1-209). There are no major contributors to the transient population in this area. This area is serviced by McKowns Mountain Road which is routed through the LPZ. No other major transportation features exist in the LPZ. There are no schools, hospitals, prisons, beaches, or parks in the LPZ. There are no facilities within 5 mi. that require special consideration such as hospitals, prisons, jails, or any other (trapped) populations.

The estimated Lee Nuclear Station workforce population is estimated at 957 people, causing the daily permanent population density within the LPZ to go from 41 people per square mile to 117 people per square mile.

At the projected end of Unit 1 reactor operation (2056), the expected permanent population of the LPZ is 880 giving a density value of 70 people per square mile. Combining this number with the estimated Lee Nuclear Station employee number, the total population is 1837 and the LPZ population density becomes 146 people per square mile.

-
- b. The daily total includes numbers from Christmastown USA that runs from December 1st through December 26th only. If this number is averaged out for the whole year the average number of transients per day drops to 41,780.

2.1.3.5 Population Center

The nearest population center, as defined by 10 CFR 100.3, is Gastonia, North Carolina. The distance to Gastonia's urban boundary, as defined by US Census Tiger files, is 16 mi. northeast from the center point between the two reactors (Reference 203). By using the county population projection ratios, the population of the city of Shelby, North Carolina may exceed 25,000 in approximately 2045. When this occurs, it is expected to be the nearest population center at a distance of 14.3 mi. north from the center point between the two reactors.

Incorporating transient population into the estimates and projecting the population for both transient and permanent population results in Gaffney, South Carolina having a total population number greater than 25,000 people. Gaffney's closest boundary, defined by the US Census Bureau, is 6 mi. northwest from the center point between the two reactors. All of these distances are greater than one and one third times the distance from the reactor center point to the boundary of the low population zone as required by NUREG-0800 and complies to the guidance provided by Regulatory Guide 4.7.

2.1.3.6 Population Density

The projected permanent population of the Lee Nuclear Station region was added to the projected transient population producing the total population. These values were plotted as a function of distance from the center point on Graphs 2.1-1, 2.1-2, 2.1-3 in Figure 2.1-210 for the initially estimated first year of operation (2016), about five years after the first year of operation, and the initially estimated projected final year of operation (2056), respectively. These dates used for projecting the population data were obtained from guidance current at the time of analysis. Recently the dates suggested in the guidance have changed. Since negative growth rates were held steady (see Subsection 2.1.3), the reported information is conservative. Plotted on Graph 2.1-1 and 2.1-2 in Figure 2.1-210 is the cumulative population that would result from a uniform population density of 500 people per square mile. Graph 2.1-3 of Figure 2.1-210 contains a similar plot except it contains a plot for a uniform population density of 1,000 people per square mile.

The projected permanent population for 2016 is 2,715,444 and the projected transient population for 2016 is 78,800. Transient population was projected using a ratio generated from transient sector population divided by the US Census Bureau 2000 population. The projected permanent population for years 2016, 2021, and 2056 were multiplied by this ratio to calculate the projected transient population. Thusly, the projected total population within an 80-km (50-mi.) radius for 2016 is 2,794,244 people. The total population density for the startup year is 360 people per square mile.

The projected total population within an 80-km (50-mi.) radius in 2021, about five years after the startup year for the plant, is 2,983,613. This includes the projected permanent population (2,899,824 people) and the projected transient population (83,789 people). The total population density is projected to be 384 people per mile.

The projected total population within an 80-km (50-mi.) radius in 2056, the projected Unit 1 end of licensing year for the plant, is 4,314,056. This includes the projected permanent population (4,195,335 people) and the projected transient population (118,721 people). The total population density in 2056 is projected to be 556 people per square mile.

The population density values in the region are within the values stated in NUREG-0800, Regulatory Guide 1.206, Regulatory Guide 1.70, and Regulatory Guide 4.7.

STD DEP 1.1-1	2.1.4	COMBINED LICENSE INFORMATION FOR GEOGRAPHY AND DEMOGRAPHY
---------------	-------	-----------------------------------------------------------

WLS COL 2.1-1	This COL item is addressed in Section 2.1 and Subsections 2.1.1, 2.1.2, and 2.1.3.
---------------	--------------------------------------------------------------------------------------------------

2.1.5 REFERENCES

201. North Carolina Department of Correction, North Carolina Prisons Listed by County, Website, <http://www.doc.state.nc.us/DOP/list/county.htm>, accessed December 12, 2006.
202. USGS Geographic Names Information System (GNIS), Website, http://geonames.usgs.gov/domestic/download_data.htm, accessed on August 8, 2006.
203. US Census Bureau 2000, "TIGER/Line Shapefiles for South Carolina and North Carolina," ESRI ArcData, Website, <http://www.census.gov/geo/www/tiger/>, accessed on August 8, 2006.
204. USGS "Active Mines and Mineral Processing Plants in the United States 2003," Website, <http://tin.er.usgs.gov/mineplant/>, accessed on August 10, 2006.
205. Thunder Road Marathon, "Race News", website, <http://www.runcharlotte.com/racenews.htm>, accessed on January 23, 2007.
206. US Census Bureau, "American FactFinder," Website http://factfinder.US Census.gov/servlet/SAFFPopulation?_submenuId=population_0&_sse=on, accessed on July 26, 2006.
207. US Department of Transportation, "National Transportation Atlas Databases (NTAD) 2005 Shapefile Format," CD-ROM.

208. National Hydrography Dataset (NHD), "Medium Resolution NHD Dataset," Website, <http://nhdgeo.usgs.gov/viewer.htm>, accessed on August 10, 2006.
209. South Carolina State Budget and Control Board, South Carolina Population Projections 2005-2030, Website <http://www.ors2.state.sc.us/population/proj2030.asp>, accessed June 19, 2006.
210. USGS, USGS Quad Blacksburg South, SC, North American Datum 1927.
211. Grubb & Ellis, The Furman Company, Restaurant & Big Box Retail Pad Sites at Prime Outlets Mall, Website, <http://www.furmanco-commercial.com/pdfs/FactoryShopsGaffney%20Site2360.pdf>, accessed October 15, 2006.
212. USGS, USGS Quad Kings Creek, SC, North American Datum 1927.
213. Bureau of Transportation Statistics, TranStats, Charlotte, North Carolina – Douglas Municipal, Airport Fact Sheet, Website, http://www.transtats.bts.gov/airports.asp?pn=1&Airport=CLT&Airport_Name=Charlotte, accessed October 3, 2006.
214. Bureau of Transportation Statistics, TranStats, Greenville/Spartanburg, South Carolina – Greenville-Spartanburg Airport, Airport Fact Sheet, Website, http://www.transtats.bts.gov/airports.asp?pn=1&Airport=GSP&Airport_Name=Greenville, accessed October 3, 2006.
215. Bureau of Transportation Statistics, TranStats, Hickory, NORTH CAROLINA – Hickory Municipal Airport, Airport Fact Sheet, Website, http://www.transtats.bts.gov/airports.asp?pn=1&Airport=HKY&Airport_Name=Hickory, accessed on October 3, 2006.
216. Amtrak, Rail Stations by Region – South, Website, http://www.amtrak.com/servlet/ContentServer?pagename=Amtrak/Page/Browse_Stations_Page&c=Page&cid=1081256321449&ssid=78, accessed October 10, 2006.
217. Kings Mountain National Military Park, Website, <http://www.nps.gov/kimo/home.htm>, accessed on August 24, 2006.
218. US Census Bureau, Census 2000 SF1 Data, Obtained from: <http://www.census.gov/Press-Release/www/2001/sumfile1.html>, accessed on September 15, 2006.
219. Kings Mountain State Park, Camping, Website, <http://www.southcarolinaparks.com/park-finder/state-park/945/camping.aspx>, accessed on September 25, 2006.

- 220. US Department of Agriculture, National Visitor Use Monitoring Results – Francis Marion & Sumter National Forests, USDA Forest Service Region 8.
- 221. US Fish and Wildlife Service, 2001 National Survey of Fishing, Hunting, and Wildlife-Associated Recreation – North Carolina, March 2003 (Revised).
- 222. US Fish and Wildlife Service, 2001 National Survey of Fishing, Hunting, and Wildlife-Associated Recreation – South Carolina, March 2003 (Revised).
- 223. US Census Bureau, 2000 Census of Population and Housing, Summary Population and Housing Characteristics, PHC-1-35, North Carolina, Washington, DC, 2002.
- 224. US Census Bureau, 2000 Census of Population and Housing, Summary Population and Housing Characteristics, PHC-1-42, South Carolina, Washington, DC, 2002.
- 225. College Toolkit: Colleges and Universities in North Carolina, Website, <http://www.collegetoolkit.com/Colleges/State/37.aspx>, accessed October 3, 2006.
- 226. College Toolkit: Colleges and Universities in South Carolina, Website, <http://www.collegetoolkit.com/Colleges/State/45.aspx>, accessed October 3, 2006.
- 227. American Hospital Directory, Individual Hospital Statistics for North Carolina, URL http://www.ahd.com/states/hospital_NC.html, accessed October 3, 2006.
- 228. American Hospital Directory, Individual Hospital Statistics for South Carolina, URL http://www.ahd.com/states/hospital_SC.html, accessed October 3, 2006.
- 229. NursinghomeINFO, Results near Gaffney, South Carolina, Website, <http://www.nursinghomeinfo.com/nw/temp/nw1010111915.htm>, accessed October 10, 2006.
- 230. North Carolina Department of Commerce, Top Attractions in North Carolina, website, <http://www.nccommerce.com/tourism/top/>, accessed on October 3, 2006.
- 231. South Carolina Department of Parks, Recreation and Tourism - State Parks Service, South Carolina Statistical Abstract - State Parks Visitation (Fiscal Year 2004-05, website, <http://www.ors2.state.sc.us/abstract/chapter15/recreation8.asp>, accessed on November 16, 2006.

232. North Carolina Office of State Budget and Management, Population Overview: 2000-2030, Website <http://demog.state.nc.us/demog/pop0030.html>, accessed June 20, 2006.
233. US Department of the Interior – National Park Service, "Military Bases in the Continental United States," Website, <http://www.cr.nps.gov/nagpra/DOCUMENTS/BasesMapIndex.htm>, accessed on May 19, 2006.
234. Charlotte Business Journal, "Carowinds coasts into new season with regional draw", May 23, 2003.
235. Ballparks.com, Bank of America Stadium, website, <http://football.ballparks.com/NFL/CarolinaPanthers/index.htm>, accessed September 20, 2007.
236. Ballparks.com, The Charlotte Bobcats Arena, website, <http://basketball.ballparks.com/NBA/CharlotteBobcats/index.htm>, accessed September 20, 2007.
237. Recreation Management, "Turn on the Tap - U.S. National Whitewater Center in Charlotte, N.C.", website, <http://www.recmanagement.com/200702fp01.php>, accessed September 20, 2007.
238. Federal Bureau of Prisons, Map of Facilities – Mid-Atlantic Region, Website, <http://bop.gov/locations/maps/MXR.jsp>, accessed December 12, 2006.
239. Federal Bureau of Prisons, Map of Facilities – Southeast Region, Website, <http://bop.gov/locations/maps/SER.jsp>, accessed December 12, 2006.
240. South Carolina Department of Corrections, SCDC Institutions, Website, <http://www.doc.sc.gov/InstitutionPages/Institutions.htm>, accessed December 12, 2006.

TABLE 2.1-201
COUNTIES ENTIRELY OR PARTIALLY LOCATED WITHIN THE
LEE NUCLEAR STATION 50-MI. BUFFER

North Carolina Counties		South Carolina Counties	
Burke	Lincoln	Cherokee	Laurens
Cabarrus	McDowell	Chester	Newberry
Catawba	Mecklenburg	Fairfield	Spartanburg
Cleveland	Polk	Greenville	Union
Gaston	Rutherford	Lancaster	York
Henderson	Union		
Iredell			

Reference 203

TABLE 2.1-202
US CENSUS BUREAU ESTIMATED YEAR 2000 POPULATIONS
WITHIN A 10-MI. RADIUS

Populated Places	Year 2000 Population
Gaffney, South Carolina	12,968
East Gaffney, South Carolina	3,349
Blacksburg, South Carolina	1,880
Smyrna, South Carolina	59
Hickory Grove, South Carolina	337
Grover, North Carolina	698

References 202 and 206

TABLE 2.1-203 (Sheet 1 of 6)
 THE PROJECTED PERMANENT POPULATION FOR EACH
 SECTOR 0- TO 16-KM (0 TO 10-MI.) FOR YEARS 2007, 2016,
 2026, 2036, 2046, AND 2056

Direction/Year	Sector						
	0-2 (km)	2-4 (km)	4-6 (km)	6-8 (km)	8-10 (km)	10-16 (km)	0-16 (km)
North							
2007	18	82	183	473	1,976	1,445	4,177
2016	20	90	201	517	2,160	1,569	4,557
2026	22	98	220	566	2,365	1,706	4,977
2036	24	107	239	616	2,570	1,844	5,400
2046	26	115	258	665	2,775	1,981	5,820
2056	28	124	277	714	2,980	2,119	6,242
NNE							
2007	16	67	131	162	247	1,500	2,123
2016	17	74	143	178	270	1,635	2,317
2026	19	81	157	194	295	1,786	2,532
2036	20	88	170	211	321	1,937	2,747
2046	22	95	184	228	346	2,089	2,964
2056	24	102	197	245	372	2,240	3,180
NE							
2007	15	50	67	99	335	466	1,032
2016	17	55	73	108	366	518	1,137
2026	18	60	80	118	401	576	1,253
2036	20	65	87	129	436	635	1,372
2046	21	71	94	139	471	693	1,489
2056	23	76	101	149	505	751	1,605

NOTE:

1. Based on 2000 Census data ([Reference 218](#))

TABLE 2.1-203 (Sheet 2 of 6)
 THE PROJECTED PERMANENT POPULATION FOR EACH
 SECTOR 0- TO 16-KM (0 TO 10-MI.) FOR YEARS 2007, 2016,
 2026, 2036, 2046, AND 2056

Direction/Year	Sector						
	0-2 (km)	2-4 (km)	4-6 (km)	6-8 (km)	8-10 (km)	10-16 (km)	0-16 (km)
ENE							
2007	12	21	24	163	299	854	1,373
2016	13	23	26	179	327	979	1,547
2026	14	25	29	196	359	1,119	1,742
2036	15	27	31	213	391	1,259	1,936
2046	17	29	34	230	423	1,399	2,132
2056	18	32	37	247	454	1,539	2,327
EAST							
2007	11	22	16	41	122	583	795
2016	12	25	18	47	140	671	913
2026	13	29	21	54	159	769	1,045
2036	15	32	23	61	179	867	1,177
2046	16	36	26	68	198	965	1,309
2056	17	39	29	74	218	1,063	1,440
ESE							
2007	4	21	37	80	70	464	676
2016	4	24	42	92	81	535	778
2026	4	28	48	105	93	613	891
2036	5	31	54	119	105	691	1,005
2046	5	34	61	132	116	769	1,117
2056	5	38	67	146	128	847	1,231

NOTE:

1. Based on 2000 Census data ([Reference 218](#))

TABLE 2.1-203 (Sheet 3 of 6)
 THE PROJECTED PERMANENT POPULATION FOR EACH
 SECTOR 0- TO 16-KM (0 TO 10-MI.) FOR YEARS 2007, 2016,
 2026, 2036, 2046, AND 2056

Direction/Year	Sector						
	0-2 (km)	2-4 (km)	4-6 (km)	6-8 (km)	8-10 (km)	10-16 (km)	0-16 (km)
SE							
2007	1	23	20	38	141	876	1,099
2016	1	26	23	44	163	1,009	1,266
2026	2	29	27	50	187	1,157	1,452
2036	2	32	30	57	210	1,304	1,635
2046	2	35	33	63	234	1,451	1,818
2056	2	37	37	70	258	1,599	2,003
SSE							
2007	7	44	13	18	31	177	290
2016	8	49	14	20	35	202	328
2026	9	53	16	23	40	231	372
2036	9	58	17	25	45	260	414
2046	10	62	18	27	50	288	455
2056	11	67	20	29	55	317	499
SOUTH							
2007	10	57	30	84	44	132	357
2016	11	62	32	91	48	144	388
2026	12	68	35	100	53	158	426
2036	13	74	39	109	58	172	465
2046	14	80	42	117	62	186	501
2056	15	86	45	126	67	200	539

NOTE:

1. Based on 2000 Census data ([Reference 218](#))

TABLE 2.1-203 (Sheet 4 of 6)
 THE PROJECTED PERMANENT POPULATION FOR EACH
 SECTOR 0- TO 16-KM (0 TO 10-MI.) FOR YEARS 2007, 2016,
 2026, 2036, 2046, AND 2056

Direction/Year	Sector						
	0-2 (km)	2-4 (km)	4-6 (km)	6-8 (km)	8-10 (km)	10-16 (km)	0-16 (km)
SSW							
2007	7	41	43	47	47	207	392
2016	8	44	47	52	51	226	428
2026	9	49	52	57	56	247	470
2036	10	53	56	62	61	269	511
2046	10	57	61	67	66	290	551
2056	11	61	65	72	71	312	592
SW							
2007	3	57	72	41	102	323	598
2016	3	62	79	44	111	353	652
2026	4	68	87	49	122	386	716
2036	4	74	94	53	132	420	777
2046	4	80	102	57	143	453	839
2056	5	86	109	61	153	487	901
WSW							
2007	0	65	74	89	173	1,583	1,984
2016	0	71	81	97	189	1,731	2,169
2026	0	78	88	107	207	1,895	2,375
2036	0	84	96	116	225	2,059	2,580
2046	0	91	104	125	242	2,224	2,786
2056	0	98	111	134	260	2,388	2,991

NOTE:

1. Based on 2000 Census data ([Reference 218](#))

TABLE 2.1-203 (Sheet 5 of 6)
 THE PROJECTED PERMANENT POPULATION FOR EACH
 SECTOR 0- TO 16-KM (0 TO 10-MI.) FOR YEARS 2007, 2016,
 2026, 2036, 2046, AND 2056

Direction/Year	Sector						
	0-2 (km)	2-4 (km)	4-6 (km)	6-8 (km)	8-10 (km)	10-16 (km)	0-16 (km)
WEST							
2007	1	67	169	445	365	4,596	5,643
2016	1	73	185	487	399	5,025	6,170
2026	1	80	202	533	437	5,501	6,754
2036	1	87	220	579	475	5,978	7,340
2046	1	94	237	625	513	6,455	7,925
2056	1	101	255	671	551	6,932	8,511
WNW							
2007	4	64	275	360	664	16,266	17,633
2016	4	70	301	394	726	17,785	19,280
2026	4	76	329	431	795	19,472	21,107
2036	5	83	358	469	864	21,160	22,939
2046	5	89	386	506	933	22,847	24,766
2056	5	96	415	544	1,002	24,535	26,597
NW							
2007	4	43	142	216	293	1,784	2,482
2016	4	47	155	236	321	1,951	2,714
2026	5	52	170	259	351	2,136	2,973
2036	5	56	185	281	381	2,321	3,229
2046	5	61	200	304	412	2,506	3,488
2056	6	65	214	326	442	2,691	3,744

NOTE:

1. Based on 2000 Census data ([Reference 218](#))

TABLE 2.1-203 (Sheet 6 of 6)
 THE PROJECTED PERMANENT POPULATION FOR EACH
 SECTOR 0- TO 16-KM (0 TO 10-MI.) FOR YEARS 2007, 2016,
 2026, 2036, 2046, AND 2056

Direction/Year	Sector						
	0-2 (km)	2-4 (km)	4-6 (km)	6-8 (km)	8-10 (km)	10-16 (km)	0-16 (km)
NNW							
2007	8	124	230	372	308	1,436	2,478
2016	9	135	251	407	336	1,568	2,706
2026	10	148	275	446	368	1,715	2,962
2036	11	161	299	484	400	1,863	3,218
2046	12	174	322	523	432	2,010	3,473
2056	13	187	346	561	464	2,157	3,728
Totals							
2007	121	848	1,526	2,728	5,217	32,692	43,132
2016	132	930	1,671	2,993	5,723	35,901	47,350
2026	146	1,022	1,836	3,288	6,288	39,467	52,047
2036	159	1,112	1,998	3,584	6,853	43,039	56,745
2046	170	1,203	2,162	3,876	7,416	46,606	61,433
2056	184	1,295	2,325	4,169	7,980	50,177	66,130
Sector							
Cumulative Totals	0-2 (km)	0-4 (km)	0-6 (km)	0-8 (km)	0-10 (km)	0-16 (km)	
2007	121	969	2,495	5,223	10,440	43,132	
2016	132	1,062	2,733	5,726	11,449	47,350	
2026	146	1,168	3,004	6,292	12,580	52,047	
2036	159	1,271	3,269	6,853	13,706	56,745	
2046	170	1,373	3,535	7,411	14,827	61,433	
2056	184	1,479	3,804	7,973	15,953	66,130	

NOTE:

1. Based on 2000 Census data ([Reference 218](#))

TABLE 2.1-204 (Sheet 1 of 6)
 THE PROJECTED PERMANENT POPULATION FOR EACH
 SECTOR 16-KM (10-MI.) – 80-KM (50-MI.) FOR YEARS 2007,
 2016, 2026, 2036, 2046, AND 2056

Direction/Years	Sector			
	16-40 (km)	40-60 (km)	60-80 (km)	16-80 (km)
North				
2007	38,714	16,194	57,871	112,779
2016	40,905	17,691	62,189	120,785
2026	43,339	19,354	66,986	129,679
2036	45,773	21,017	71,784	138,574
2046	48,207	22,680	76,581	147,468
2056	50,641	24,342	81,379	156,362
NNE				
2007	30,164	43,594	71,754	145,512
2016	31,669	49,078	80,489	161,236
2026	33,340	55,171	90,195	178,706
2036	35,011	61,264	99,901	196,176
2046	36,683	67,357	109,606	213,646
2056	38,354	73,450	119,312	231,116
NE				
2007	64,806	63,972	81,956	210,734
2016	68,160	67,825	96,044	232,029
2026	71,887	72,106	111,696	255,689
2036	75,614	76,387	127,349	279,350
2046	79,341	80,668	143,002	303,011
2056	83,068	84,949	158,654	326,671

NOTE:

1. Based on 2000 Census data ([Reference 218](#))

TABLE 2.1-204 (Sheet 2 of 6)
 THE PROJECTED PERMANENT POPULATION FOR EACH
 SECTOR 16-KM (10-MI.) – 80-KM (50-MI.) FOR YEARS 2007,
 2016, 2026, 2036, 2046, AND 2056

Direction/Years	Sector			
	16-40 (km)	40-60 (km)	60-80 (km)	16-80 (km)
ENE				
2007	33,928	123,495	444,073	601,496
2016	37,928	141,988	541,141	721,057
2026	42,374	162,536	648,994	853,904
2036	46,819	183,084	756,848	986,751
2046	51,264	203,632	864,701	1,119,597
2056	55,709	224,180	972,554	1,252,443
EAST				
2007	23,554	111,434	237,822	372,810
2016	27,121	129,708	301,029	457,858
2026	31,084	150,012	371,259	552,355
2036	35,047	170,316	441,489	646,852
2046	39,010	190,619	511,719	741,348
2056	42,973	210,923	581,949	835,845
ESE				
2007	17,869	66,163	39,213	123,245
2016	20,575	74,624	44,076	139,275
2026	23,582	84,025	49,480	157,087
2036	26,589	93,426	54,883	174,898
2046	29,595	102,827	60,287	192,709
2056	32,602	112,228	65,690	210,520

NOTE:

1. Based on 2000 Census data ([Reference 218](#))

TABLE 2.1-204 (Sheet 3 of 6)
 THE PROJECTED PERMANENT POPULATION FOR EACH
 SECTOR 16-KM (10-MI.) – 80-KM (50-MI.) FOR YEARS 2007,
 2016, 2026, 2036, 2046, AND 2056

Direction/Years	Sector			
	16-40 (km)	40-60 (km)	60-80 (km)	16-80 (km)
SE				
2007	3,922	18,411	9,178	31,511
2016	4,393	19,143	9,594	33,130
2026	4,917	19,956	10,057	34,930
2036	5,440	20,768	10,520	36,728
2046	5,964	21,581	10,983	38,528
2056	6,487	22,394	11,446	40,327
SSE				
2007	2,172	2,690	3,603	8,465
2016	2,338	2,802	3,799	8,939
2026	2,523	2,926	4,017	9,466
2036	2,708	3,050	4,235	9,993
2046	2,892	3,174	4,453	10,519
2056	3,077	3,298	4,671	11,046
SOUTH				
2007	3,691	3,433	6,144	13,268
2016	3,739	3,455	6,487	13,681
2026	3,792	3,480	6,868	14,140
2036	3,844	3,505	7,249	14,598
2046	3,897	3,529	7,630	15,056
2056	3,949	3,554	8,012	15,515

NOTE:

1. Based on 2000 Census data ([Reference 218](#))

TABLE 2.1-204 (Sheet 4 of 6)
 THE PROJECTED PERMANENT POPULATION FOR EACH
 SECTOR 16-KM (10-MI.) – 80-KM (50-MI.) FOR YEARS 2007,
 2016, 2026, 2036, 2046, AND 2056

Direction/Years	Sector			
	16-40 (km)	40-60 (km)	60-80 (km)	16-80 (km)
SSW				
2007	17,533	3,002	20,073	40,608
2016	17,675	3,057	21,828	42,560
2026	17,832	3,118	23,778	44,728
2036	17,989	3,179	25,728	46,896
2046	18,147	3,240	27,678	49,065
2056	18,304	3,302	29,628	51,234
SW				
2007	6,257	14,072	31,423	51,752
2016	6,510	15,173	34,451	56,134
2026	6,792	16,396	37,815	61,003
2036	7,074	17,619	41,180	65,873
2046	7,355	18,842	44,544	70,741
2056	7,637	20,065	47,909	75,611
WSW				
2007	44,615	69,520	156,415	270,550
2016	48,564	75,559	171,892	296,015
2026	52,951	82,270	189,088	324,309
2036	57,338	88,981	206,285	352,604
2046	61,725	95,691	223,482	380,898
2056	66,113	102,402	240,679	409,194

NOTE:

1. Based on 2000 Census data ([Reference 218](#))

TABLE 2.1-204 (Sheet 5 of 6)
 THE PROJECTED PERMANENT POPULATION FOR EACH
 SECTOR 16-KM (10-MI.) – 80-KM (50-MI.) FOR YEARS 2007,
 2016, 2026, 2036, 2046, AND 2056

Direction/Years	Sector			
	16-40 (km)	40-60 (km)	60-80 (km)	16-80 (km)
WEST				
2007	33,913	68,076	86,269	188,258
2016	36,930	73,990	94,905	205,825
2026	40,282	80,561	104,500	225,343
2036	43,634	87,132	114,095	244,861
2046	46,986	93,703	123,691	264,380
2056	50,338	100,275	133,286	283,899
WNW				
2007	17,054	12,829	21,303	51,186
2016	18,498	14,027	23,784	56,309
2026	20,103	15,358	26,541	62,002
2036	21,707	16,690	29,298	67,695
2046	23,312	18,022	32,055	73,389
2056	24,917	19,353	34,812	79,082
NW				
2007	14,322	38,107	11,067	63,496
2016	15,131	39,630	11,664	66,425
2026	16,029	41,322	12,327	69,678
2036	16,928	43,013	12,991	72,932
2046	17,827	44,705	13,654	76,186
2056	18,725	46,397	14,318	79,440

NOTE:

1. Based on 2000 Census data ([Reference 218](#))

TABLE 2.1-204 (Sheet 6 of 6)
 THE PROJECTED PERMANENT POPULATION FOR EACH
 SECTOR 16-KM (10-MI.) – 80-KM (50-MI.) FOR YEARS 2007,
 2016, 2026, 2036, 2046, AND 2056

Direction/Years	Sector			
	16-40 (km)	40-60 (km)	60-80 (km)	16-80 (km)
N-NW				
2007	18,177	7,787	27,708	53,672
2016	19,200	8,145	29,491	56,836
2026	20,337	8,542	31,473	60,352
2036	21,474	8,940	33,455	63,869
2046	22,611	9,338	35,437	67,386
2056	23,747	9,735	37,418	70,900
Totals				
2007	370,691	662,779	1,305,872	2,339,342
2016	399,336	735,895	1,532,863	2,668,094
2026	431,164	817,133	1,785,074	3,033,371
2036	462,989	898,371	2,037,290	3,398,650
2046	494,816	979,608	2,289,503	3,763,927
2056	526,641	1,060,847	2,541,717	4,129,205
Cumulative Totals				
	16-40 (km)	16-60 (km)	16-80 (km)	
2007	370,691	1,033,470	2,339,342	
2016	399,336	1,135,231	2,668,094	
2026	431,164	1,248,297	3,033,371	
2036	462,989	1,361,360	3,398,650	
2046	494,816	1,474,424	3,763,927	
2056	526,641	1,587,488	4,129,205	

NOTE:

1. Based on 2000 Census data ([Reference 218](#))

TABLE 2.1-205
MAJOR CONTRIBUTORS TO TRANSIENT POPULATION WITHIN
80-KM (50-MI.)

Name	Average Daily Transients ^{(a)(b)}	Peak Daily Transients
Christmastown USA	23,077	
Charlotte Knights Baseball Club		10,000
Prime Outlets at Gaffney	7671	
Sumter National Forest	7,268	
Daniel Stowe Botanical Garden	6,000	
South Carolina Peach Festival		2,500
Christmas on Limestone		2,000
Kings Mountain National Military Park	1,452	
Spartanburg Museum of Art	1,000	
Crowder's Mountain State Park	930	
Mint Museum of Art	750	
Chimney Rock Park	684	
Cowpens National Battlefield	573	
Kings Mountain State Park	548	
South Mountain State Park	527	
Roper Mountain Science Center	515	
Schiele Museum of Natural History	500	
Hollywild Animal Park	411	
Croft State Natural Area	345	
Hatcher Garden and Woodland Preserve	305	
Charlotte Museum of History	113	
Lansford Canal State Park	82	
Chester State Park	64	
Paris Mountain State Park	52	
Charlotte Steeplechase	41	
Gaffney Visitor's Center	35	
Musgrove Mill State Historic Site	28	
Spartanburg County Historical Museum	15	
Rose Hill Plantation State Historic Site	15	

a) Daily transients are peak numbers, when available. Otherwise a daily average derived from the yearly total is used.

b) Additional contributors to transient population are described in [Subsection 2.1.3.3.2](#).

TABLE 2.1-206
DAILY AND ANNUAL PASSENGER COUNTS FOR
COMMERCIAL AIRPORTS IN THE LEE NUCLEAR STATION
REGION

Airport Name	Daily Passenger Count	Annual Passenger Count
Charlotte-Douglas Int'l	72,132	26,328,000
Greenville-Spartanburg Int'l	4,422	1,614,000
Hickory Regional	49	18,000

References 213, 214, and 215

TABLE 2.1-207
FISHING, HUNTING, AND WILDLIFE WATCHING WITHIN THE
LEE NUCLEAR STATION REGION

Activity	SC Total Visitors	Region Visitors
Fishing	812,000	54,729
Hunting	265,000	17,861
Wildlife Watching	1,186,000	79,936
Total	2,263,000	152,526

Activity	NC Total Visitors	Region Visitors
Fishing	1,287,000	189,575
Hunting	295,000	43,454
Wildlife Watching	2,168,000	319,346
Total	3,750,000	552,375

References 221 and 222

TABLE 2.1-208
THE PROJECTED TRANSIENT POPULATION FOR EACH
SECTOR 0- TO 80-KM (50-MI.) FOR YEARS 2007, 2016, 2026,
2036, 2046, AND 2056

Distance	Direction	2007	2016	2026	2036	2046	2056
8	N	992	1,084	1,187	1,291	1,394	1,497
16	ENE	38	43	49	55	62	68
16	NE	935	1,040	1,156	1,274	1,391	1,507
16	WNW	4,838	5,290	5,792	6,294	6,795	7,297
40	ENE	200	224	250	277	303	329
40	NE	1,487	1,563	1,649	1,734	1,820	1,905
40	S	146	148	150	152	154	156
40	SSE	77	83	90	96	103	109
40	SW	74	77	81	84	87	91
40	WNW	10,809	11,724	12,741	13,758	14,775	15,792
40	WSW	1,379	1,501	1,637	1,772	1,908	2,044
60	E	11,483	13,366	15,458	17,550	19,642	21,734
60	ENE	32,650	37,539	42,972	48,404	53,837	59,269
60	N	17	19	20	22	24	26
60	NNW	5	5	6	6	6	6
60	S	730	735	740	746	751	756
60	SSE	140	146	153	159	165	172
60	SSW	485	494	503	513	523	533
60	W	441	479	521	564	606	649
60	WSW	327	355	387	418	450	482
80	E	52	65	81	96	111	126
80	ENE	1,026	1,251	1,500	1,749	1,998	2,248
80	ESE	91	102	114	127	139	152
80	N	335	360	387	415	443	471
80	NNW	191	203	217	230	244	258
80	NW	708	746	788	831	873	915
80	S	911	962	1,018	1,075	1,131	1,188
80	SSE	151	159	169	178	187	196
80	SSW	539	587	639	691	744	796
80	W	56	62	68	75	81	87
80	WSW	556	611	672	734	795	856

(References 209, 211, and 230)

TABLE 2.1-209
POPULATION DISTRIBUTION IN THE LOW POPULATION
ZONE

	0-1 (mi.)	1-2 (mi.)	0-2 (mi.) TOTAL
N	7	47	54
NNE	5	40	45
NE	5	38	43
ENE	3	27	30
E	2	23	25
ESE	0	17	17
SE	0	17	17
SSE	0	38	38
S	0	46	46
SSW	0	28	28
SW	0	37	37
WSW	0	22	22
W	0	15	15
WNW	1	14	15
NW	1	16	17
NNW	4	56	60
Total	28	481	509

2.2 NEARBY INDUSTRIAL, TRANSPORTATION, AND MILITARY FACILITIES

This **section** of the referenced DCD is incorporated by reference with the following departures and/or supplements.

WLS COL 2.2-1 The Lee Nuclear Station is located in Cherokee County, South Carolina. Cherokee County is bordered on the west by Spartanburg County, South Carolina, on the north by Rutherford, Cleveland, and Gaston counties, North Carolina, on the east by York County, South Carolina, and on the south by Union County, South Carolina, as seen in **Figure 2.1-203**.

The Lee Nuclear Station is accessible only by road. Interstate 85 (I-85) connects Gaffney, South Carolina (8.2 miles (mi.) northwest of the site) and Blacksburg, South Carolina (5.8 mi. north of the site) to Spartanburg, South Carolina, and Charlotte, North Carolina (**References 201** and **202**). Several state and federal highways pass within 5 mi. of the site and are discussed in more detail in **Subsections 2.2.2.2.7** and **2.2.2.5**. There is also an abandoned rail spur that runs from East Gaffney, South Carolina, to the Lee Nuclear Station (**Reference 201**).

This section provides information regarding the potential effects on the safe operation of the nuclear facility from industrial, transportation, mining, and military installations in the Lee Nuclear Station area.

STD DEP 1.1-1 Subsection 2.2.1 of the DCD is renumbered as Subsection 2.2.4 and moved to the end of Section 2.2. This is being done to accommodate the incorporation of Regulatory Guide 1.206 numbering conventions for Section 2.2.

2.2.1 LOCATIONS AND ROUTES

WLS COL 2.2-1 Within a 5-mi. radius of the Lee Nuclear Station, there are major industrial facilities, one railroad, four state highways, and one federal highway, all with commercial traffic (**Reference 201**). The following transportation routes and facilities are shown in **Figure 2.2-201**:

- Broad River Energy Center
- DSE Systems, LLC
- Herbie Famous Fireworks (South Carolina Distributors)
- Ninety-Nine Islands Hydroelectric Dam
- U.S. Highway 29 (U.S. 29)

***Withheld from Public Disclosure Under 10 CFR 2.390(d)(1)
(see COL Application **Part 9**)***

- South Carolina State Highway 5 (South Carolina 5)
- South Carolina State Highway 97 (South Carolina 97)
- South Carolina State Highway 105 (South Carolina 105)
- South Carolina State Highway 329 (South Carolina 329)
- Railroad spur line from Blacksburg to Kings Creek, South Carolina

Environmental Data Resources, Inc. (EDR) provided the results from a database search of storage tanks registered by the state of South Carolina. State regulations for tank registrations were reported to be compliant and consistent with federal regulations. According to the South Carolina Code of Regulations 61-92, an underground storage tank (UST) is defined as any one or combination of tanks (including underground pipes connected thereto) that is used to contain an accumulation of regulated substances, and the volume of which (including the volume of underground pipes connected thereto) is 10 percent or more beneath the surface of the ground. South Carolina requires that all underground storage tanks greater than 110 gal. capacity be registered. The registered tank database includes petroleum storage tanks used for bulk, retail, industrial, private, airport, and government purposes. Farm and residential tanks less than 1100 gal. capacity used for storing motor oil for noncommercial purposes, tanks used for storing heating oil for consumptive use on the premises where stored, and Septic tanks are not classified as USTs and do not fall under these regulations (**References 203 and 232**).

[

] ^{SRI}

In addition to the above storage facility, there are a total of four separate locations within the 5-mi. radius that have registered aboveground storage tanks (ASTs) or USTs. **Table 2.2-201** shows the contents and capacity of all registered storage tanks and **Figure 2.2-201** shows the location of all registered storage tanks within 5-mi. radius of the site (**Reference 203**).

Onsite storage of liquid hydrogen will be in accordance with the approved site plot plan and the AP1000 standard plant design, located in the Bulk Gas Storage Area near the Unit 1 mechanical draft cooling towers, at a safe distance from the nuclear island ([Figure 1.1-202](#)). Compressed gas storage will be in the yard adjacent to the Turbine Building. The AP1000 standard plant contains 500 standard cubic feet (scf) bottles of compressed hydrogen gas at 6000 pounds per square inch (psig) and 1500 gallons of liquid hydrogen at 150 psig. Three thousand gallons of liquid nitrogen and 6 tons of liquid carbon dioxide are also located in the Bulk Gas Storage Area to support plant operation. No propane or liquid oxygen is anticipated to be used at the Lee Nuclear Station.

Mining and quarrying operations, drilling operations, and wells are discussed in [Subsections 2.2.2.1.5](#) and [2.2.2.2.4](#). Oil and gas pipelines are discussed in [Subsection 2.2.2.3](#). Military bases and missile sites are discussed in [Subsection 2.2.2.1.6](#). None of these facilities were found in the 5-mi. radius of the site (military bases and missile sites). Evaluations of explosions postulated to occur on transportation routes near nuclear power plants are addressed in [Subsection 2.2.3](#).

2.2.2 DESCRIPTIONS

The industries within the immediate area of the Lee Nuclear Station are mostly located in Gaffney, East Gaffney, Cherokee Falls, and Blacksburg, South Carolina. All of these industries, with the exception of the Ninety-Nine Islands Hydroelectric Dam, the Broad River Energy Center, and Herbie Famous Fireworks, lie more than 5 mi. from the site. [Table 2.2-202](#) describes the primary function/major products and the number of persons employed at these industrial facilities ([References 202, 204, 205, and 206](#)). A brief description of several major industrial facilities is listed below. These industries are some of the largest employers in the area.

2.2.2.1 Description of Facilities

Four major industrial facilities are located within 5 mi. of the Lee Nuclear Site. Descriptions of these facilities are detailed in [Subsections 2.2.2.1.1 to 2.2.2.1.3](#), and [2.2.2.1.7](#). [Subsection 2.2.2.1.4](#) provides detailed information on electrical generation plants closest to the Lee Nuclear Site. [Subsection 2.2.2.1.5](#) details mining and quarrying activities in the area and [Subsection 2.2.2.1.6](#) details military facilities near the site.

2.2.2.1.1 Ninety-Nine Islands Hydroelectric Dam

The Ninety-Nine Islands Hydroelectric Dam is located on the Broad River adjacent to the Lee Nuclear Site boundary, approximately 1.1 mi. south of the Lee Nuclear Station centerpoint (see [Figure 2.1-201](#)).

2.2.2.1.2 Herbie Famous Fireworks

Herbie Famous Fireworks (South Carolina Distributors) is a 1.4G (Class C) consumer fireworks wholesale distribution company. Herbie Famous Fireworks

operates a warehouse facility located approximately 2.7 mi. north to northwest of the site (see [Figure 2.2-201](#)) ([Reference 202](#)).

2.2.2.1.3 Broad River Energy Center

The Broad River Energy Center is a natural gas-fired peaking electric generation plant located approximately 4.7 mi. northwest of the site (see [Figure 2.2-201](#)).

2.2.2.1.4 Electrical Generation Plants

The Mill Creek Combustion Turbine Station is located approximately 9.5 mi. northeast of the site, approximately 1 mi. south of the North Carolina state line. This is a natural gas-fired peaking electric generation plant that opened in 2003. Mill Creek Combustion Turbine Station is an eight-unit facility with a capacity of 640 megawatts. The plant uses natural gas as a primary fuel source and fuel oil as a secondary fuel source ([Reference 205](#)).

The Cliffside Steam Station is located approximately 19 mi. northwest of the Lee Nuclear Station. It is a five-unit coal-fired generating facility with a capacity of 760 megawatts. There are plans to expand this facility as early as 2010 by adding a new 800 megawatt, highly efficient, coal-fueled unit ([Reference 206](#)).

The Catawba Nuclear Station lies approximately 25 mi. east of the Lee Nuclear Station. The Catawba Nuclear Station, located in Clover, South Carolina on a 391 ac. peninsula, has two Westinghouse PWR reactors producing 1129 megawatts each. A license renewal application was submitted to the NRC on June 14, 2001 and was approved December 5, 2003. These two reactors are the largest in the state ([Reference 207](#)).

The McGuire Nuclear Station is located approximately 42 mi. northeast of the Lee Nuclear Station. The McGuire Nuclear Station, located in Cornelius, North Carolina, has two Westinghouse PWR reactors producing 1100 megawatts each. A license renewal application was submitted to the NRC on June 14, 2001 and was approved December 5, 2003 ([Reference 208](#)).

2.2.2.1.5 Mining and Quarrying Activities

There are three permitted mines operated by three separate entities located within 5 mi. of the Lee Nuclear Station ([Reference 209](#)).

2.2.2.1.6 Military Facilities

There are no military facilities within 5 mi. of the Lee Nuclear Station. The closest military facility is the Charlotte Douglas IAP Air Guard Station. This United States Air Force installation is located approximately 34 mi. to the northeast ([Reference 227](#)).

Withheld from Public Disclosure Under 10 CFR 2.390(d)(1)
(see COL Application Part 9)

2.2.2.1.7 DSE Systems, LLC

DSE Systems, LLC has acquired a vacant textile plant near Gaffney, South Carolina. The facility is located 4.6 miles to the northwest of the Lee Nuclear Site boundary on State Highway 329. It is just north of US Highway 29 and on the western bank of the Broad River. The company intends to use the facility for the assembly of ammunition for the US military.

2.2.2.2 Description of Products and Materials

2.2.2.2.1 Ninety-Nine Islands Hydroelectric Dam

The Ninety-Nine Islands Hydroelectric Dam is a six unit facility with an electrical output of 18-megawatts (MW) that was completed in 1909. The dam is about 88 feet (ft.) high (maximum) and 1567 ft. long that creates a reservoir with a surface area of 433 acres (ac.) at 100 percent capacity. There is a 94-ft. high, 197-ft. long concrete intake structure. This facility is currently operated as a peaking facility, primarily in the summer and winter.

2.2.2.2.2 Herbie Famous Fireworks

[
]SRI

2.2.2.2.3 Broad River Energy Center

The facility consists of five combustion turbines with a capacity of 847 megawatts (Reference 204). Information regarding the products stored on the Broad River Energy Center site is summarized in Table 2.2-203. The Occupational Safety and Health Administration (OSHA) permissible exposure limits for the reported toxic materials are in Table 2.2-204 (Reference 233).

2.2.2.2.4 Mining and Quarrying Activities

The closest permitted mine is operated by Thomas Sand Company and is located approximately 1 mi. north of the site. This mine, named Blacksburg Plant, is used to mine sand. Martin Mine, operated by Cunningham Brick Company, is the second closest permitted mine located 3.2 mi. north of the site. This mine is used to mine manganese schist (type of mica). Kings Creek Mine, operated by Industrial Minerals, Inc. is the third permitted mine within 5 mi. of the site. Kings Creek Mine, located approximately 4.9 mi. northeast of the site, is used to mine sericite (type of mica). None of the above mines use explosives (Reference 209).

2.2.2.2.5 Military Facilities

There are no military facilities within 5 mi. of the Lee Nuclear Station. The closest military facility is the Charlotte Douglas IAP Air Guard Station. This United States Air Force installation is located approximately 34 mi. to the northeast ([Reference 227](#)).

2.2.2.2.6 Waterways

The Lee Nuclear Station footprint is located approximately 4800 ft. west and approximately 2400 ft. south of the Broad River, and 1.1 mi. upstream (north) of the Ninety-Nine Islands Hydroelectric Dam (See [Figure 2.1-201](#)). The Broad River upstream of the Lee Nuclear Station is a shallow, unnavigable river; however, from the Ninety-Nine Islands Hydroelectric Station to the confluence with the Pacolet River, the Broad River is considered navigable waters under Regulation 19-450 of the South Carolina Code of Laws 1976, as amended.

2.2.2.2.7 Highways

The nearest highway with heavy commercial traffic is U.S. 29, passing approximately 4.6 mi. northwest from the site center point at its closest. In addition to U.S. 29, segments of South Carolina 5, 97, 105, and 329 are located within a 5-mi. radius of the site ([Reference 201](#)).

Any material registered with the federal government as a hazardous material is allowed to travel along any public road in the state of South Carolina provided it is properly packaged and transported, and the proper credentials are obtained by the carrier. The amount of explosives shipped along the public roads within 5 mi. of the facility is unknown, since no agencies are required by law to keep records of this information.

2.2.2.2.8 Railroads

Norfolk Southern Railroad Company (NSRC) owns and operates a small spur that passes within the 5-mi. radius ([Reference 211](#)). This line runs at its closest point approximately 4.7 mi. from the site centerpoint. Any material registered with the federal government as a hazardous material that is legally allowed to be transported via American railroads could potentially be transported at some point along the rails that are situated near the site. Items that may be legally transported on the rails near the site include many types of hazardous materials and other industrial chemicals. The amount of hazardous materials transported along the rails near the site is unknown due to the sensitive nature of this information and confidentiality agreements within NSRC.

2.2.2.2.9 DSE Systems, LLC (Description of Products)

The items intended to be manufactured by DSE Systems, LLC at the Gaffney, South Carolina site include the following:

*Withheld from Public Disclosure Under 10 CFR 2.390(d)(1)
(see COL Application **Part 9**)*

- [
-
-
-
-
-

]SRI

2.2.2.3 Description of Pipelines

Nine major pipelines operated by three separate entities are located within 5 mi. of the Lee Nuclear Station. The possibility that any pipeline near the site could carry product other than the one presently carried and whether the pipeline is used for gas storage at higher-than-normal pressure was not released by any pipeline operator in the 5-mi. area due to the sensitive nature of this information.

[

***Withheld from Public Disclosure Under 10 CFR 2.390(d)(1)
(see COL Application **Part 9**)***

}SRI

In addition to these major pipelines, there are numerous lines delivering natural gas to residential, commercial, and other industrial units. These lines are operated by Piedmont Natural Gas and vary in size and pressure from 6-inch-diameter 500 psi distribution mains to 1-inch-diameter lines connected to homes and businesses.

2.2.2.4 Description of Waterways

As stated in **Subsection 2.2.2.2.6**, the Lee Nuclear Station footprint is located approximately 4800 ft. west and approximately 2400 ft. south of the Broad River, and 1.1 mi. upstream (north) of the Ninety-Nine Islands Hydroelectric Dam (See **Figure 2.1-201**). The Broad River upstream of the Lee Nuclear Station is a shallow, unnavigable river; however, from the Ninety-Nine Islands Hydroelectric Station to the confluence with the Pacolet River, the Broad River is considered navigable waters under Regulation 19-450 of the South Carolina Code of Laws 1976, as amended. In 1991, this entire section was designated a State Scenic River (**Reference 214**). The Broad River is not classified as a National Wild and Scenic River by the federal government (**Reference 215**). There are no ports within 50 mi. of the Lee Nuclear Station site (**Reference 201**).

There are two public access points to the Scenic Corridor of the Broad River. The Ninety-Nine Islands Boat Landing is a public boat access area operated by Duke Energy. This landing is located in Cherokee County, South Carolina at the end of State Secondary Road 43, between the towns of Cherokee Falls in Cherokee County and Hickory Grove in York County, South Carolina. There is a large parking lot, concrete paved double boat ramp, and a wooden wildlife viewing/fishing dock. The Cherokee Landing is located across the river from the Ninety-Nine Islands Boat Landing at the end of State Secondary Road 13. This landing has a very small paved parking lot and the landing is very steep (**Reference 214**).

Figure 2.1-201 shows the proposed location of the intake structure in the Broad River for the Lee Nuclear Station. Water from the Broad River will be withdrawn at this location for use as cooling tower makeup, service water cooling system makeup, and other miscellaneous water uses. **Figure 2.1-201** shows the proposed location of the release point in the Broad River for the Lee Nuclear Station. Water from the plant is released back into the Broad River at this location when it is no longer needed by the plant.

2.2.2.5 Description of Highways

As stated in [Subsection 2.2.2.2.7](#), the nearest highway with heavy commercial traffic is U.S. 29, passing approximately 4.6 mi. northwest from the site center point at its closest. In addition to U.S. 29, segments of South Carolina 5, 97, 105, and 329 are located within a 5-mi. radius of the site ([Reference 201](#)). Interstate 85 could be used as an alternate route of U.S. 29; however it is located outside the 5-mi. radius.

Any material registered with the federal government as a hazardous material is allowed to travel along any public road in the state of South Carolina provided it is properly packaged and transported, and the proper credentials are obtained by the carrier. The amount of explosives shipped along the public roads within 5 mi. of the facility is unknown, since no agencies are required by law to keep records of this information.

Estimated Annual Average Daily Traffic (AADT) counts for 2005 indicate the following:

- 7000 vehicles travel on U.S. 29 between South Carolina 329 and South Carolina 5.
- 5600 vehicles travel on South Carolina 5 between U.S. 29 and South Carolina 55.
- 5000 vehicles also travel along South Carolina 105 between South Carolina 211 and South Carolina 18.
- 1600 vehicles travel on South Carolina 329 between South Carolina 105 and U.S. 29.
- 950 vehicles travel on Cherokee County Highway 13 (McKowns Mountain Road) between South Carolina 105 and the end of the road (near the Broad River).
- 425 vehicles travel on South Carolina 97 between South Carolina 5 and the York County line ([Reference 210](#)).

2.2.2.6 Description of Railroads

Norfolk Southern Railroad Company (NSRC) owns and operates a small spur that passes within the 5-mi. radius ([Reference 211](#)). This line runs at its closest point approximately 4.7 mi. from the site center point on the northeastern side and has an average of two trains per day (one round trip) on these tracks. The speed limit is 25 mph on the majority of this spur with a speed limit of 10 mph around many of the curves. This spur carries freight only; no passenger trains use this route ([Reference 212](#)).

A major rail line owned by NSRC runs at its closest point 5.5 mi. from the site. This line runs from Atlanta, Georgia to Charlotte, North Carolina, eventually on to the

New York City area on the northern end, and to the New Orleans area on the southern end. This line is the main line, or core route, in the northern South Carolina area, running through downtown Gaffney and Blacksburg (Reference 211). This main line averages 22 trains per day and has a speed limit of 50 mph. This line is primarily used for freight service, although one passenger train, the Amtrak Crescent, uses the line (References 211 and 212). The speed limit for passenger trains along this stretch of track is 79 mph, although they are unlikely to reach more than approximately 60 mph between Gaffney, South Carolina and Blacksburg, South Carolina due to curves in the tracks.

As stated in Subsection 2.2.2.2.8, any material registered with the federal government as a hazardous material that is legally allowed to be transported via American railroads could potentially be transported at some point along the rails that are situated near the site. Items that may be legally transported on the rails near the site include many types of hazardous materials and other industrial chemicals.

It is important to note that the proposed Southeast High-Speed Rail Corridor runs through this area. The proposed route is projected to follow the existing tracks that run from Atlanta, Georgia to Charlotte, North Carolina. Trains are expected to travel at a maximum speed of 110 mph along this corridor. The proposed date for implementation of service along this route is 2012 at the earliest and is projected to carry more than 1.6 million passengers annually by the year 2015 (Reference 210).

2.2.2.7 Description of Airports

2.2.2.7.1 Airports

There were no airports found within the Lee Nuclear Station 50- mi. region that meet or exceed the criteria defined in NUREG-0800 Subsection 3.5.1.6 and RG 1.206 Part III Subsections C.I.2.2.2.7 and C.I.3.5.1.6.

There are no airports located within 10 mi. of the Lee Nuclear Station; however, one heliport is located within 10 mi. of the plant (Reference 201). The Milliken & Co. heliport is located approximately 6 mi. to the north of the site and has a 25 ft. square concrete helipad (Reference 216).

York Airport is the closest airport that has reported numbers of operations to the Lee Nuclear Station (14.7 mi. to the east). It has a 2580 ft. turf runway. The airport is exclusively used by single-engine private aircraft with 12 single-engine aircraft based at the field. The average number of operations (landings and takeoffs are counted separately) is approximately 62 per week. General aviation accounts for 69 percent of operations while 31 percent are transient general aviation (Reference 217).

There are two large commercial airports within 50 mi. of the Lee Nuclear Station, Greenville-Spartanburg International Airport (GSP) and Charlotte Douglas International Airport (CLT). GSP is located 41.3 mi. west to southwest of the site and CLT is located 34.4 mi. northeast of the site (Reference 201).

GSP has one 11,001 ft. asphalt runway. Federal Aviation Administration (FAA) information, effective June 7, 2006, indicates that 23 aircraft are based on the field. Five of these are single-engine aircraft, 10 are multi-engine aircraft and eight are jet aircraft. The average number of operations is approximately 182 per day. Air taxi accounts for 69 percent of operations, 17 percent are transient general aviation, 11 percent are commercial, 2 percent are military, and 1 percent is local general aviation ([Reference 218](#)).

Fifty-one aviation accidents or incidents have occurred since 1965 in Greenville, South Carolina. Of the 51 accidents, eight have been fatal resulting in 18 deaths ([Reference 229](#)). Thirty-eight aviation accidents or incidents have occurred since 1964 in Spartanburg, South Carolina. Of the 38 accidents, four have been fatal resulting in five deaths ([Reference 230](#)).

CLT has three runways; the first is a 10,000 ft. concrete runway, the second is an 8674 ft. asphalt/concrete runway, and the third is a 7502 ft. asphalt/concrete runway. FAA information, effective June 7, 2006, indicates that 146 aircraft are based on the field. Twenty-five of these are single-engine aircraft, 22 are multi-engine aircraft, 87 are jet aircraft, 2 are helicopters, and 10 are military aircraft. The average number of operations is approximately 1372 per day. Commercial accounts for 47 percent of operations, 45 percent are air taxi, 7 percent are transient general aviation, and less than 1 percent are military ([Reference 219](#)).

One hundred forty-four aviation accidents or incidents have occurred since 1962 in Charlotte, North Carolina. Of the 144 accidents, 21 have been fatal resulting in 162 deaths ([Reference 231](#)).

Based on historical flight data recorded from 1963 to 2005 for GSP ([Table 2.2-205](#)), projections for air traffic up to fiscal year 2025 are given in [Table 2.2-206](#) for GSP ([Reference 220](#)). GSP recently performed a study to determine the projected needs of the airport. They developed a plan to accommodate the projected growth in passenger traffic. Plans are now in place to expand, if needed, the terminal building from the current 13 attached jet gates to as many as 43 attached jet gates and adding a new 8200 ft. runway. This plan is expected to allow them to accommodate the projected 5.3 million passengers the study calculated the airport would see by the year 2023 ([References 222](#) and [223](#)).

Based on historical flight data recorded from 2000 to 2005 for CLT ([Table 2.2-207](#)), projections for air traffic up to fiscal year 2025 are given in [Table 2.2-208](#) for CLT ([Reference 221](#)). CLT is currently in the middle of a multimillion dollar expansion to meet the needs of future passenger and cargo traffic. Construction has begun on a new 9000 ft. runway and a new 3000 space parking facility has recently been completed. This expansion and renovation is expected to meet the projected demands of the future by expanding many existing airport facilities ([Reference 224](#)).

Approach and departure paths at CLT and GSP are not aligned with the Lee Nuclear Station.

2.2.2.7.2 Airways

Two low altitude (below 18,000 ft.) federal air routes are located within 15 mi. of the Lee Nuclear Station - Airway V54 and V415. The centerline of Airway V54 is approximately 4 mi. north of the site and Airway V415 is approximately 10 mi. southwest of the site ([Figure 2.2-202](#)) ([Reference 225](#)). These routes, also known as Victor air routes, are primarily flown by general aviation aircraft. These routes generally have a width of eight nautical miles and occupy the airspace between 18,000 ft. and the floor of controlled airspace, which is 700 - 1200 ft. There are no Military Training Routes within 10 mi. of the site.

Two high altitude (18,000 ft. above MSL through 45,000 ft. pressure altitude) federal air routes are located within 15 mi. of the Lee Nuclear Station - Airway J208 and J14. The centerline of Airway J208 is located approximately 9 mi. southeast of the site and the centerline of Airway J14 is 12.5 mi. northwest of the site ([Figure 2.2-202](#)) ([Reference 226](#)). These airways are primarily used by commercial air carriers, the military and high performance general aviation aircraft. These routes also have a width of eight nautical miles and are flown from 18,000 ft. to the top of controlled airspace, 45,000 ft. All flights above 18,000 ft. are required to be IFR flights; hence, all altitudes and routes are assigned by air traffic controllers.

Due to the close proximity of airways to the Lee Nuclear Station, an evaluation of hazards from air traffic along all airways within 10 mi. of the Lee Nuclear Station is presented in [Subsection 3.5.1.6](#).

2.2.2.8 Projections of Industrial Growth

There are no industrial parks within 5 mi. of the Lee Nuclear Station ([Reference 228](#)). There are two industrial companies within the 5-mi. radius. The Broad River Energy Center and Herbie Famous Fireworks (South Carolina Distributors) as described in [Subsections 2.2.2.1.3](#) and [2.2.2.1.2](#), respectively ([References 202](#) and [204](#)). There is no planned industrial growth within the 5 mi. area ([Reference 228](#)).

2.2.3 EVALUATION OF POTENTIAL ACCIDENTS

- WLS COL 2.2-1 The consideration of a variety of potential accidents, and their effects on the plant or plant operation, is included in this section. Types of accidents considered include explosions, flammable vapor clouds, toxic chemicals, fires, collisions with intake structures, and liquid spills. General Design Criterion 4, "Environmental and Missile Design Basis," of Appendix A, "General Design Criteria for Nuclear Power Plants," to 10 CFR Part 50, "Licensing of Production and Utilization Facilities," requires that nuclear power plant structures, systems, and components important to safety be appropriately protected against dynamic effects resulting from equipment failures that may occur within the nuclear power plant as well as events and conditions that may occur outside the nuclear power plant.

2.2.3.1 Determination of Design Basis Events

Design basis events internal and external to the nuclear power plant are defined as those accidents that have a probability of occurrence on the order of about 10^{-7} per year or greater and potential consequences serious enough to affect the safety of the plant to the extent that the guidelines in 10 CFR Part 100 could be exceeded. The following categories are considered for the determination of design basis events: explosions, flammable vapor clouds with a delayed ignition, toxic chemicals, fires, collision with intake structures, and liquid spills.

2.2.3.1.1 Explosions

2.2.3.1.1.1 Transportation Routes

Accidents were postulated for the nearby highways and railroads. Accidents on the Broad River were not evaluated because this river is considered to be non-navigable. The nearest highway with heavy commercial traffic is US Highway 29, which passes approximately 4.24 miles northwest of the Lee Nuclear Site at its closest point to the site boundary. The accident of concern along US Highway 29 is one that results in the detonation of a highly explosive cargo carried by a truck. It is necessary to demonstrate that such an explosion on the highway does not result in a peak positive incident overpressure that exceeds 1psi at the critical structures on-site. The maximum probable hazardous cargo for a single highway truck is based on Regulatory Guide 1.91, Revision 1, in terms of equivalent trinitrotoluene (TNT). The TNT equivalency is based on (Reference 235):

$$W_E = \frac{H_{EXP}^d}{H_{TNT}^d} W_{EXP}, \text{ where } W_E \text{ is the effective charge weight, } H_{EXP}^d \text{ is the heat}$$

of detonation of the explosive in question, H_{TNT}^d is the heat of detonation of TNT, and W_{EXP} is the weight of the explosive in question.

The methodology presented in Regulatory Guide 1.91, Revision 1, established the safe distance beyond which no damage would be expected (i.e. a peak positive incident overpressure of less than 1 psi at the critical structures on the Lee Nuclear Site) from a truck explosion along U.S. Highway 29 at its closest point. An evaluation performed for materials with a TNT equivalency of 2.24 and using the maximum cargo for two trucks (50,000 lbs. per truck) determined the safe distance to be 0.52 miles, hence, there is considerable margin between the required safe distance and the actual distance. The effects of blast-generated missiles are less than those associated with the blast overpressure levels considered in Regulatory Guide 1.91, Revision 1. Because the overpressure criteria of the guide are not exceeded, the effects of blast-generated missiles are not considered.

The Norfolk Southern Railroad passes approximately 4.18 miles northeast of the site at its closest point. The maximum probable quantity of explosive material shipped by a single railroad boxcar in terms of equivalent pounds of TNT is based on Regulatory Guide 1.91, Revision 1. It is recognized that cargo shipments by

Withheld from Public Disclosure Under 10 CFR 2.390(d)(1)
(see COL Application Part 9)

railroad typically constitute the usage of more than one boxcar. For the purpose of qualifying the explosion hazard involved in this railroad analysis, thirty combined boxcar values for intended explosives are incorporated into the calculation. This corresponds to a TNT equivalency of 8,870,400 lbs (30 boxcars x 132,000 lbs/boxcar x 2.24). These values may be considered conservatively bounding because it is reasonable to assume the initial explosion would involve only one boxcar associated with initiating the explosion. Should additional boxcars become involved, related explosions would be subsequent in time and neither coincident with, nor additive to, the effects associated with those from the first boxcar explosion. The evaluation determined the required safe distance to be 1.76 miles, which is less than the distance of 4.18 miles from the railroad to the site at its closest point. Therefore the proximity to the railroad does not present an explosion hazard.

2.2.3.1.1.2 Pipelines

If the natural gas pipeline were to rupture resulting in natural gas released into the atmosphere, the vapor plume would not detonate in such a fashion to cause an overpressure event. Instead, it would burn with a relatively slow deflagration rate. A natural gas release would not explode if the release is into an unconfined space, therefore a free vapor cloud explosion of a release is into an unconfined space, and therefore a free vapor cloud explosion of a release from the natural gas pipeline is not credible.

The Colonial Pipeline and Plantation Pipeline contain refined petroleum products and are located 3.24 miles from the Lee Nuclear Site at the closest point. The 40-inch Colonial Pipeline was analyzed because it has the largest diameter of the refined petroleum pipelines. [

]^{SRI} Using Equation 1 from Regulatory Guide 1.91, Revision 1, the safe standoff distance is calculated as 14,948 ft or 2.83 miles.

The result for the unconfined vapor explosion safe standoff distance is less than the distance of the pipeline to the site boundary at its closest point of 3.24 miles. Therefore, the postulated pipeline explosion does not generate an overpressure above 1 psi at the site. Based on several factors, this is a conservative result, e.g., no consideration is taken for depressurization of the pipe, instantaneous evaporation of the leaked gasoline is assumed, and no credit is taken for the fact

***Withheld from Public Disclosure Under 10 CFR 2.390(d)(1)
(see COL Application **Part 9**)***

the pipe is buried three to four feet underground. Hence, it is concluded the refined petroleum pipelines are not an explosion hazard for the Lee Nuclear Site.

2.2.3.1.1.3 Nearby Industrial Facilities

Herbie Famous Fireworks is a 1.4G consumer fireworks wholesale distribution company located 2.31 miles from the Lee Nuclear Site boundary. The U.S. Department of Transportation labels Division 1.4G as explosives that present a minor explosion hazard. The explosive effects are largely confined to the package and no blast or projection of appreciable size or range is expected. [

] ^{SRI} Using Equation 1 from Regulatory Guide 1.91, Revision 1, the safe standoff distance is calculated as 2,522 ft or 0.48 miles. Since the safe standoff distance is less than the distance to Herbie Famous Fireworks, the postulated explosion at Herbie Famous Fireworks does not generate an overpressure above 1 psi at the site.

As shown in **Table 2.2-201**, the Broad River Energy Center has the largest capacity of registered storage tanks and has the only above ground tanks listed. The Broad River Energy Center is located 4.34 miles from the site boundary. [

] ^{SRI} Using Equation 1 from Regulatory Guide 1.91, Revision 1, the safe standoff distance for a confined vapor explosion is calculated as 7,588 ft (1.44 miles), and the safe standoff distance for an unconfined vapor explosion is calculated as 13,269 ft (2.51 miles). Since the safe standoff distances are less than the distance to the Broad River Energy Center, the postulated confined and unconfined vapor explosions do not generate an overpressure above 1 psi at the site.

[

*Withheld from Public Disclosure Under 10 CFR 2.390(d)(1)
(see COL Application **Part 9**)*

]SRI

The other potentially hazardous commodities stored at the DSE Systems location were examined for the potential to generate an overpressure above 1 psi at the site or adversely affect control room environment. Screening criteria based on the toxic release, confined, unconfined, and solid material explosion equations, as defined above in the Broad River Energy Center postulated explosion discussion, were developed to help identify potential explosion or toxic hazard threats. Only materials of NFPA 704 (**Reference 238**) health hazard, flammability, and reactivity Class 3 and Class 4 were considered for the screening, due to their unstable and volatile physical properties. This evaluation demonstrated that for a given mass, the hazard from a toxic material release would always be limiting when compared to a solid material explosion or confined or unconfined vapor explosion. [

]SRI A DSE Systems facility representative indicated that there are no chemicals stored at the site which would meet the developed screening criterion, and therefore there is no postulated explosion or toxic

chemical release hazards to the Lee Nuclear Site from other commodities stored at DSE Systems, LLC.

2.2.3.1.1.4 Onsite Chemicals

WLS COL 2.2-1 As discussed in **DCD Section 1.9**, the AP1000 uses small amounts of combustible
WLS COL 6.4-1 gases for normal plant operation. Most of these gases are used in limited quantities and are associated with plant functions or activities that do not jeopardize any safety-related equipment. These gases are found in areas of the plant that are removed from the nuclear island. The exception to this is the hydrogen supply line to the chemical and volume control system (CVS).

The CVS is the only system on the nuclear island that uses hydrogen gas. Hydrogen is supplied to the AP1000 CVS inside containment from a single hydrogen bottle. The release of the contents of an entire bottle of hydrogen in the most limiting building volumes, both inside containment and in the auxiliary building would not result a volume percent of hydrogen large enough to reach a detonable level.

DCD Subsection 3.5.1.1.2.2 states that the battery compartments are ventilated by a system that is designed to preclude the possibility of hydrogen accumulation. The DCD states further that the storage tank area for plant gases is located sufficiently far from the nuclear island that an explosion would not result in missiles more energetic than the tornado missiles for which the nuclear island is designed.

The plant gas system provides hydrogen, carbon dioxide, and nitrogen gases to the plant systems as required. The effects of the plant gas system on main control room habitability are addressed in **DCD Section 6.4** including explosive gases and burn conditions for those gases. For explosions, the plant gas system is designed for conformance with Regulatory Guide 1.91 (**DCD Subsection 9.3.2.3**).

Table 6.4-202, Part B, identifies additional site specific chemicals that are outside the scope of DCD evaluations. These site specific chemicals were screened for solid material explosion, confined and unconfined vapor explosion, flammability, and toxic gas release event hazards. These chemicals are not in solid state and are not flammable; therefore, solid material explosion hazard, confined and unconfined vapor explosion hazard, and flammability hazard evaluations are not required. Based on the screening guidance provided in Regulatory Guide 1.78, with two exceptions, none of the site-specific chemicals used were found to be a credible habitability threat to main control room occupants in case of a release. See **Section 6.4** for analysis of site specific chemicals requiring additional evaluation.

Table 6.4-202, Part A, provides specific information about the chemicals described in **DCD Table 6.4-1**. This includes chemical names or limiting types and quantities. Except as noted, these chemicals have been suggested by Westinghouse for use in the AP1000 and have been evaluated in conjunction with

***Withheld from Public Disclosure Under 10 CFR 2.390(d)(1)
(see COL Application **Part 9**)***

AP1000 standard design and found not to present a hazard to the control room operators or to safety-related systems, structures, or components. No further evaluation or analysis regarding impact to control room habitability for these chemicals is required.

2.2.3.1.2 Flammable Vapor Clouds (Delayed Ignition)

WLS COL 2.2-1 The potential for detonation in a plume resulting from release of the commodities from a transportation accident is evaluated, as well as a potential release from nearby facilities and pipelines. This evaluation assumes dispersion downwind toward the Lee Nuclear Station, with a delayed ignition. For each commodity of interest, the vapor dispersion is based on a wind speed of 1.8 mph, a Stability Class of D, and a 90°F ambient air temperature. These meteorological conditions are intended to maximize the vaporization rate of the commodity of interest while limiting the downwind dispersion. The ALOHA code (**Reference 236**) is used to evaluate the dispersion and detonation of the vapor clouds.

For the evaluation of the potential effects of accidents on US Highway 29, conservatively large tanker truck volumes (9,000 gallons) are assumed along with an assumed 48.4 square feet rupture size. The basis for a 48.4 square feet rupture size is that, for this scenario, this rupture size is the largest permissible by the ALOHA code. ALOHA's constraints do not have an impact on the analysis because all the chemicals from a tanker of this size are capable of being released within the allotted time duration, eliminating the need to postulate a larger rupture. Because almost any commodity can be transported along the highways, various commodities are assumed. Gasoline and propane are analyzed due to the fact that these are commonly transported commodities.

Other less popular commodities are analyzed that have a relatively low flash point and relatively high heats of combustion, hence have a potential to result in a high overpressure if the vapor cloud is ignited. The results are summarized in **Table 2.2-210**.

Similarly, for the Norfolk Southern Railroad, various commodities are analyzed with the ALOHA code, assuming conservatively large tanker sizes (40,000 gallons) and rupture sizes of 48.4 square feet. The results are summarized in **Table 2.2-211**.

For the evaluation of the vapor cloud resulting from ruptured pipelines, rupture sizes equivalent to pipe cross-sectional areas are assumed. The pipelines are assumed to leak for a duration of one hour. [

*Withheld from Public Disclosure Under 10 CFR 2.390(d)(1)
(see COL Application **Part 9**)*

***Withheld from Public Disclosure Under 10 CFR 2.390(d)(1)
(see COL Application **Part 9**)***

J^{SRI}

For the postulated accidents on U.S. Highway 29, the Norfolk Southern Railroad, and natural gas pipelines, the overpressure at the Lee Nuclear Station resulting from the delayed ignition of a vapor cloud is negligible. The only postulated accident that results in a slight overpressure at the Lee Nuclear Site is the postulated rupture of the refined petroleum pipeline, where a conservatively large release of gasoline is assumed. Even for this case, the overpressure is less than 1 psi at the Lee Nuclear Site.

In order to demonstrate that the atmospheric conditions assumed were conservative, a sensitivity study was performed for the situation that caused the largest overpressure at the site, which was a pipeline carrying gasoline, which produced a maximum overpressure of 0.459 psi for a release rate of 3,920 ft³/sec. The wind speed was increased from 1.55 knots (0.8 m/s) to 1 m/s, while at the same time the Stability Class was changed from "D" to "F". For this case the overpressure dropped to 0.455 psi. Increasing the wind speed would allow for the chemical to evaporate more quickly and travel at a quicker rate. However, the higher wind speed would disperse the vapor cloud at a quicker rate causing a less significant overpressure. The Stability Class is a measurement of how turbulent the atmosphere is from solar radiation and other contributing factors. By increasing the Stability Class from "D" to "F" the program is decreasing the amount of solar radiation included in the model, allowing for less dispersion to occur. Decreasing the solar radiation also decreases the amount of evaporation that occurs and therefore causes a decrease in overpressure. These results demonstrate that the assumptions of a wind speed of 1.55 knots and a Stability Class of "D" are conservative for this calculation.

Because the resulting overpressure from the delayed ignition of potential vapor clouds is much less than 1 psi, the Regulatory Guide 1.91, Revision 1, acceptance criteria, it is concluded that the delayed ignition of vapor clouds from nearby transportation routes and pipelines does not pose a hazard to the Lee Nuclear Station.

2.2.3.1.3 Toxic Chemicals

- WLS COL 2.2-1 As stated in [Subsection 2.2.3.1.1.4](#), analysis of site specific chemicals (stored onsite) requiring further evaluation is presented in [Section 6.4](#). Accidents involving
- WLS COL 6.4-1 the release of toxic chemicals from nearby mobile and stationary sources are addressed in this section and in [Subsection 6.4.4.2](#).

2.2.3.1.3.1 Background

A control room habitability analysis was performed in accordance with Regulatory Guide 1.78. The Regulatory Guide specifies that mobile and stationary sources of hazardous materials within a five mile radius of the plant be analyzed as a potential threat to plant operations.

[Subsections 2.2.1](#) and [2.2.2](#) provide sources of potentially airborne hazardous chemicals that may be in the area. These sources are in the form of stationary industrial facilities and transportation pathways in the form of a highway and a rail spur.

The nearby Broad River is not navigable by barges and does not transport commercial traffic, and hence is eliminated from further investigation.

[Figure 2.2-201](#) shows the potential rail, road, and stationary industrial sources within the proximity of Lee Nuclear Station.

The screening criteria for airborne hazardous chemicals is established in Regulatory Guide 1.78 based on the National Institute for Safety and Health (NIOSH) Immediately Dangerous to Life and Health (IDLH) limits for 30 minute exposures. The criteria of Regulatory Guide 1.78 was supplemented in the screening assessment by considering chemical properties and health hazard classifications established by the National Fire Protection Association or Hazardous Materials Identification System. Per Regulatory Guide 1.78, the NIOSH IDLH values were utilized to evaluate concentrations of hazardous chemicals to determine their effect on control room habitability. For those cases in which neither Regulatory Guide 1.78 nor NUREG/CR-6624 establish an IDLH value, an appropriate toxicity limit was applied consistent with current industry standards.

Regulatory Guide 1.78 specifies the use of HABIT software for evaluating control room habitability. The HABIT software consists of modules that evaluate radiological and toxic chemical transport and exposure. A hybrid modeling approach was developed using the ALOHA code, which incorporates a heavy gas

model, in conjunction with the HABIT code which utilizes a Gaussian dispersion model, to model toxic chemical transport and model chemical exposure to control room personnel using control room design parameters.

2.2.3.1.3.2 Sources of Potentially Dangerous Releases

2.2.3.1.3.2.1 Stationary Sources

There are no site-specific sources of airborne hazardous materials stored on the Lee Nuclear Station site in sufficient quantity to affect control room habitability.

Subsection 2.2.2.1 lists four major industrial facilities within a five mile radius of the site or at greater distances as appropriate based on their significance: Herbie Famous Fireworks, Ninety-Nine Islands Hydroelectric Station, the Broad River Energy Center, and DSE Systems, LLC. Herbie Famous Fireworks has indicated that they do not have potentially dangerous airborne toxic chemicals on site. Although the Broad River Energy Center stores chemicals on site per FSAR **Table 2.2-203**, there are no stored potentially poisonous gasses such as chlorine or anhydrous ammonia nor other recognizable hazardous chemicals that may affect control room habitability at the site. The exact quantities of the chemicals in **Table 2.2-203** are not known. However, an inquiry was sent to Broad River Energy Center to identify chemicals that are stored in quantities greater than 29,000 pounds or that have an Immediately Dangerous to Life or Health rating less than 30 mg/m³. Further analysis of the chemicals identified by Broad River Energy Center indicates that there are no toxic chemical release threats to the Lee Nuclear Site from the Broad River Energy Center. There are no toxic chemical release threats to the Lee Nuclear Site from DSE Systems, LLC, based on the discussion of chemical screening criteria in **Subsection 2.2.3.1.1.3**.

2.2.3.1.3.2.2 Mobile Sources

Preliminary statistical analysis evaluated the general risk from mobile sources of hazardous materials. This preliminary risk analysis indicates that although the accident risk is quite low, it is not less than the evaluation limit of 1E-6 per year for mobile sources set in Regulatory Guide 1.78. Therefore, a wholly risk-based approach was not considered.

2.2.3.1.3.2.2.1 Local Highways

As illustrated on **Figure 2.2-201**, the nearest highway with heavy commercial traffic is U.S. Highway 29, passing approximately 4.5 mi. northwest from the site at its closest point. In addition to U.S. Highway 29, segments of South Carolina State Highways 5, 97, 105, and 329 are located within a 5-mi. radius of the site.

Any material registered with the federal government as a hazardous material is allowed to travel along any public road in the state of South Carolina provided it is properly packaged and transported, and the proper credentials are obtained by the carrier.

Annual Average Daily Traffic (AADT) counts for 2005 indicate a moderate level of traffic on several roads within five miles of the Lee Nuclear Station. This information was used to estimate the total annual vehicle-miles traveled within a 5-mile radius. Calculations to estimate the probability of a hazardous road release were conducted based upon hazardous material risk information from the Federal Motor Carrier Safety Administration. The estimated total annual vehicle-miles were modified using the risk information for the percent of all vehicles that are trucks, percent of trucks that carry hazardous materials, hazardous material truck accident rate, and release rate per hazardous material accident, to ultimately arrive at an annual hazardous release probability for the roads within a 5-mi. radius of Lee Nuclear Station.

The results of a risk study indicate that general hazardous material incidents have a release probability of approximately $1\text{E-}2$ per year, while DOT Class 2.3 releases have a release probability of approximately $5\text{E-}5$ per year. Although the results of those calculations indicate that the probability of a road release within a 5-mi. radius of Lee Nuclear Station is very low, the risk of a release is higher than the Regulatory Guide 1.78 evaluation limit of $1\text{E-}6$ per year for mobile sources, therefore further analysis is required. This further analysis is discussed in [Subsection 2.2.3.1.3.3](#).

2.2.3.1.3.2.2.2 Local Rail Lines

A Norfolk Southern rail line is located approximately 4.5 miles northeast of the site. This rail line is a spur off of the main line running southeast of Blacksburg and terminating in Kings Creek. This rail line carries predominately Iron Ore, and is not expected to carry hazardous materials, and is thus not evaluated for hazardous materials.

2.2.3.1.3.3 Analysis of Hazardous Materials

An analysis of the surrounding area and of the materials that may be in the area reveals that the roadways pose the most significant toxic hazard to control room habitability.

Any chemical sanctioned to be legally transported by state and federal department of transportation guidelines may be transported on the roads, but due to the distance from the site it is determined that only the most toxic gaseous chemicals (DOT class 2.3) could reach the control room intake under ideal calm conditions.

An analysis of a tractor-trailer based chlorine release at the closest point of passage of Route 329 was performed. Chlorine was deemed to be the worst case release of a toxic gas as it is commonly transported, is highly toxic with an IDLH of 10 PPM, and is heavier than air so it can travel laterally without significant dispersion under stable, light wind conditions. The model utilizes AP1000 HVAC parameters, worst-case meteorological conditions, and physical characteristics of the modeled chemical.

To model the concentration of hazardous chemicals at the control room intake several site specific parameters are gathered. These parameters include release weight, in this case the complete tractor-trailer cargo weight, along with distance to the control room, HVAC intake height, and worst case meteorological conditions.

Meteorological data was analyzed to determine the worst meteorological conditions at the site. In the case of a released gaseous hazardous material cloud, the worst case condition is essentially a calm night. A wind speed of 1 m/s and Class G stability conditions were utilized in the model to represent these worst-case conditions.

Variable parameters utilized in this analysis are provided in [Table 2.2-209](#).

A hybrid modeling approach was developed to account for heavier-than-air chemical vapor transport using the ALOHA code. The HABIT code was then used to analyze the chemical spill at a reduced distance utilizing a Gaussian dispersion model. The distance that a heavier-than-air gas model is appropriate was first calculated using ALOHA based on a downwind distance required to reduce the chemical concentration to 10,000 ppm where the model transitions to a non-dense plume. The ALOHA analysis concluded the transition occurs at 615 meters from the spill. This distance is subtracted from the 5100 m minimum distance between a potential chemical release site and the control room intake. Only the remaining distance of 4485 meters was credited in the HABIT analysis.

The results of the analysis using this methodology indicate that under worst case meteorological conditions for the site, a pressurized liquid chlorine tractor-trailer burst type accident would elevate control room HVAC intake concentrations beyond IDLH values; however, the habitability analysis discussed in [Section 6.4.4.2](#) concluded that the concentration in the control room would be less than the chlorine IDLH value.

2.2.3.1.4 Fires

WLS COL 2.2-1 Fires originating from accidents at any of the facilities or transportation routes
WLS COL 6.4-1 discussed previously would not endanger the safe operation of the station because of the distances between potential accident locations and the location of the Lee Nuclear Station are at least 2.31 miles away.

The Nuclear Island is situated sufficiently clear of trees and brush. The distance exceeds the minimum fuel modification area requirements of thirty feet per NFPA 1144 ([Reference 234](#)). Therefore, there is no threat from brush or forest fires.

Fire and smoke from accidents at nearby homes, industrial facilities, transportation routes, or from area forest or brush fires, does not jeopardize the safe operation of the plant due to the separation distance of potential fires from the plant. The main control room HVAC system continuously monitors the outside air using smoke monitors located at the outside air intake plenum and monitors the return air for smoke upstream of the supply air handling units ([DCD](#)

Subsection 9.4.1.2.3.1). If a high concentration of smoke is detected in the outside air intake, an alarm is initiated in the main control room and the main control room/control support area HVAC subsystem is manually realigned to the recirculation mode by closing the outside air and toilet exhaust duct isolation valves. Therefore, any potential heavy smoke problems at the main control room air intakes would not affect the plant operators.

On-site fuel storage facilities are designed in accordance with applicable fire codes, and plant safety is not jeopardized by fires or smoke in these areas. A detailed description of the plant fire protection system is presented in **DCD Subsection 9.5.1.**

2.2.3.1.5 Collisions with Intake Structure

WLS COL 2.2-1 The raw water intake structure on the Broad River is used to pump raw water into Make-Up Pond A. A makeup intake structure located in Make-Up Pond A is used to pump makeup water to the plant water systems. During low-flow conditions in the Broad River, a makeup intake structure located on Make-Up Pond B is used to pump raw water to Make-Up Pond A to provide makeup water for plant water systems. The portion of the Broad River adjacent to the Lee Nuclear Station is considered to be not navigable, so collisions with the intake structure are not considered to be credible. Likewise, there are no credible events or concerns associated with collisions to intakes on Make-Up Pond A or Make-Up Pond B.

2.2.3.1.6 Liquid Spills

The accidental release of petroleum products or corrosive liquids upstream of the Broad River intake structure would not affect operation of the plant. Normal operation of the water intake structure pumps requires submergence. Liquids with a specific gravity less than unity, such as petroleum products, would float on the surface of the river and consequently are not likely to be drawn into the makeup water system. Liquids with a specific gravity greater than unity could be drawn into the intake pipes. However, such liquids would be diluted by the water in Make-Up Pond A before it is drawn into the makeup intake structure.

The raw water system is not a safety related system and is not designed to function during design basis accidents or following low-probability events such as seismic, fire, sabotage, passive failures or multiple active failures. Failure of components of the raw water system would not preclude essential functions of safety related systems.

2.2.3.2 Effects of Design Basis Events

Potential design basis events associated with accidents at nearby facilities and transportation routes have been analyzed in **Subsection 2.2.3.1.** The effects of

these events on the safety-related components of the plant are insignificant as discussed in [Subsection 2.2.3.1](#).

STD DEP 1.1-1 2.2.4 COMBINED LICENSE INFORMATION

WLS COL 2.2-1 This COL item is addressed in [Subsection 2.2.3](#).

2.2.5 REFERENCES

201. U.S. Department of Transportation, National Transportation Atlas Databases (NTAD) 2006 Shapefile Format, CD-ROM.
202. U.S. Geological Survey, Geographic Names Information System (GNIS), Website, http://geonames.usgs.gov/domestic/download_data.htm, accessed August 8, 2006.
203. Environmental Data Resources, Inc, *Cherokee – Cherokee, SC*, March 7, 2006.
204. Calpine, Calpine Power Plants – Broad River Energy Center, Website, <http://www.calpine.com/power/plant.asp?plant=96>, accessed June 26, 2006.
205. Duke Energy, Mill Creek Combustion Turbine Station, Website, http://www.duke-energy.com/about/plants/franchised/combustion/mill_creek/, accessed October 12, 2006.
206. Duke Energy, Cliffside Steam Station, Website, <http://www.duke-energy.com/about/plants/franchised/coal/cliffside/>, accessed June 26, 2006.
207. Energy Information Administration, Catawba Nuclear Power Plant, South Carolina, Website, http://www.eia.doe.gov/cneaf/nuclear/page/at_a_glance/reactors/catawba.html, accessed June 26, 2006.
208. Energy Information Administration, “U.S. Nuclear Plants – McGuire”, Website, http://www.eia.doe.gov/cneaf/nuclear/page/at_a_glance/reactors/mcguire.html, accessed June 26, 2006.
209. South Carolina Bureau of Land & Waste Management - Division of Mining and Solid Waste, *Search Mining Companies and Solid Waste Disposal Facilities*, Website, http://www.scdhec.gov/lwm/html/min_search.asp, accessed July 13, 2006.

210. South Carolina Department of Transportation, "Average Daily Traffic - June 22, 2006."
211. Norfolk Southern Corporation, "System Map 2006," Section N – 15.
212. Amtrak, "Routes serving the South," Website, http://www.amtrak.com/servlet/ContentServer?pagename=Amtrak/Page/Browse_Routes_Page&c=Page&cid=1081256321428&ssid=136, accessed November 6, 2006.
213. U.S. Department of Transportation Southeast High Speed Rail Corridor, "Southeast High Speed Rail Corridor – from Washington, DC to Charlotte, NC," Website, <http://www.sehsr.org/faq.html>, accessed June 16, 2006.
214. Broad Scenic River Advisory Council Report, "Broad Scenic River Management Plan 2003 Update – Report 32."
215. National Wild and Scenic Rivers System, "Wild and Scenic Rivers by State," Website, <http://www.nps.gov/rivers/wildriverslist.html>, accessed August 11, 2006.
216. AirNav.com, "SC84 – Milliken & Company Heliport," Website, <http://www.airnav.com/airport/SC84>, accessed June 7, 2006.
217. AirNav.com, "01SC – York Airport," Website, <http://www.airnav.com/airport/01SC>, accessed June 7, 2006.
218. AirNav.com, "KGSP – Greenville-Spartanburg International Airport," Website, <http://www.airnav.com/airport/KGSP>, accessed June 7, 2006.
219. AirNav.com, "KCLT – Charlotte Douglas International Airport," Website, <http://www.airnav.com/airport/KCLT>, accessed June 7, 2006.
220. GSP International Airport, "GSP Passenger Statistics," Website, http://www.gspairport.com/passenger_stats.shtml, accessed June 8, 2006.
221. Charlotte Douglas International Airport, "Aviation Activity for December 2000 – December 2005."
222. Greenville-Spartanburg International Airport, "Master Plan Update December 2003 – Section 3: Development Concept."
223. Greenville-Spartanburg International Airport, "Master Plan Update December 2003 – Section 4: Traffic Projections."
224. Charlotte Douglas International Airport, "Construction Update," Website, <http://www.charmeck.org/Departments/Airport/About+CLT/Construction+Update.htm>, accessed September 11, 2007.

225. U.S. Department of Transportation - Federal Aviation Administration, IFR Enroute Low Altitude – U.S.”, Panel L-20, effective February 16, 2006.
226. U.S. Department of Transportation - Federal Aviation Administration, “IFR Enroute High Altitude – U.S.”, Panel H-9, effective February 16, 2006.
227. U.S. Department of the Interior – National Park Service, “Military Bases in the Continental United States”, Website, <http://www.cr.nps.gov/nagpra/DOCUMENTS/BasesMapIndex.htm>, accessed May 19, 2006.
228. Cherokee County Chamber of Commerce, “2005-2006 Quality of Life.”
229. U.S. Department of Transportation - Federal Aviation Administration, “Aviation Accident Database and Synopsis – Greenville,” Website, <http://www.nts.gov/ntsb/query.asp>, accessed June 27, 2006.
230. U.S. Department of Transportation - Federal Aviation Administration, “Aviation Accident Database and Synopsis – Spartanburg,” Website, <http://www.nts.gov/ntsb/query.asp>, accessed June 27, 2006.
231. U.S. Department of Transportation - Federal Aviation Administration, “Aviation Accident Database and Synopsis – Charlotte,” Website, <http://www.nts.gov/ntsb/query.asp>, accessed June 27, 2006.
232. South Carolina Legislature, South Carolina Code of Regulations – Regulation 61-92 Underground Storage Tank Control Regulations, Website, <http://www.scstatehouse.net/coderegs/c061f.htm#61-92>, accessed April 6, 2007.
233. US Department of Labor - Occupational Safety & Health Administration, “Table Z-1,” Website, http://www.osha.gov/pls/oshaweb/owadisp.show_document?p_table=STANDARDS&p, accessed December 22, 2006.
234. Technical Committee on Forest and Rural Fire Protection. “Standard for Protection of Life and Property from Wildfire.” NFPA 1144. National Fire Protection Association, 2002.
235. U.S. Department of the Army, Structures to Resist the Effects of Accidental Explosions, Technical Manual TM 5-1300.
236. U.S. Environmental Protection Agency, ALOHA (Areal Location of Hazardous Atmospheres). Version 5.4 User Manual, February 2006.
237. Department of Defense, Contractor’s Safety Manual for Ammunition and Explosives, DoD 4145.26-M, March 13, 2008.
238. National Fire Protection Association. “NFPA 704: Standard System for the Identification of the Hazards of Materials for Emergency Response,” 2007.

*Withheld from Public Disclosure Under 10 CFR 2.390(d)(1)
(see COL Application **Part 9**)*

WLS COL 2.2-1

TABLE 2.2-201
REGISTERED STORAGE TANKS WITHIN A 5-MI. RADIUS

WLS COL 2.2-1

TABLE 2.2-202
INDUSTRIAL FACILITIES NEAR THE LEE NUCLEAR STATION

Name of Facility	Primary Function / Major Products	Persons Employed
Ninety-Nine Islands Hydroelectric Dam	Hydroelectric peaking electric generation plant	5
Herbie Famous Fireworks (South Carolina Distributors)	1.4G consumer fireworks warehouse facility	40
DSE Systems, LLC	US military ammunitions assembly facility	200
Broad River Energy Center	Natural gas-fired peaking electric generation plant	12
Mill Creek Combustion Turbine Station	Natural gas-fired peaking electric generation plant	5
Cliffside Steam Station	Coal-fired electric generation plant	104

(References 202, 204, 205, 206, and 207)

*Withheld from Public Disclosure Under 10 CFR 2.390(d)(1)
(see COL Application **Part 9**)*

WLS COL 2.2-1

TABLE 2.2-203 (Sheet 1 of 11)
PRODUCTS STORED ON SITE AT THE BROAD RIVER ENERGY CENTER

WLS COL 2.2-1

TABLE 2.2-203 (Sheet 2 of 11)
PRODUCTS STORED ON SITE AT THE BROAD RIVER ENERGY CENTER

*Withheld from Public Disclosure Under 10 CFR 2.390(d)(1)
(see COL Application **Part 9**)*

WLS COL 2.2-1

TABLE 2.2-203 (Sheet 3 of 11)
PRODUCTS STORED ON SITE AT THE BROAD RIVER ENERGY CENTER

*Withheld from Public Disclosure Under 10 CFR 2.390(d)(1)
(see COL Application **Part 9**)*

WLS COL 2.2-1

TABLE 2.2-203 (Sheet 4 of 11)
PRODUCTS STORED ON SITE AT THE BROAD RIVER ENERGY CENTER

WLS COL 2.2-1

TABLE 2.2-203 (Sheet 5 of 11)
PRODUCTS STORED ON SITE AT THE BROAD RIVER ENERGY CENTER

WLS COL 2.2-1

TABLE 2.2-203 (Sheet 6 of 11)
PRODUCTS STORED ON SITE AT THE BROAD RIVER ENERGY CENTER

WLS COL 2.2-1

TABLE 2.2-203 (Sheet 7 of 11)
PRODUCTS STORED ON SITE AT THE BROAD RIVER ENERGY CENTER

WLS COL 2.2-1

TABLE 2.2-203 (Sheet 8 of 11)
PRODUCTS STORED ON SITE AT THE BROAD RIVER ENERGY CENTER

**Withheld from Public Disclosure Under 10 CFR 2.390(d)(1)
(see COL Application **Part 9**)**

TABLE 2.2-203 (Sheet 9 of 11)

WLS COL 2.2-1

PRODUCTS STORED ON SITE AT THE BROAD RIVER ENERGY CENTER

**Withheld from Public Disclosure Under 10 CFR 2.390(d)(1)
(see COL Application **Part 9**)**

TABLE 2.2-203 (Sheet 10 of 11)

WLS COL 2.2-1

PRODUCTS STORED ON SITE AT THE BROAD RIVER ENERGY CENTER

*Withheld from Public Disclosure Under 10 CFR 2.390(d)(1)
(see COL Application **Part 9**)*

WLS COL 2.2-1

TABLE 2.2-203 (Sheet 11 of 11)
PRODUCTS STORED ON SITE AT THE BROAD RIVER ENERGY CENTER

Withheld from Public Disclosure Under 10 CFR 2.390(d)(1)
*(see COL Application **Part 9**)*

WLS COL 2.2-1

TABLE 2.2-204
BROAD RIVER ENERGY CENTER SITE SPECIFIC OSHA
PERMISSIBLE EXPOSURE LIMITS (PEL) Z-1 TABLE

WLS COL 2.2-1

TABLE 2.2-205 (Sheet 1 of 2)
 HISTORICAL AIR TRAFFIC AT GREENVILLE-SPARTANBURG
 INTERNATIONAL AIRPORT

Year	Total Passengers	Percent Change
1963	158,068	
1964	182,798	15.65
1965	195,893	7.16
1966	195,898	0.00
1967	256,885	31.13
1968	298,221	16.09
1969	332,090	11.36
1970	325,686	-1.93
1971	349,735	7.38
1972	411,683	17.71
1973	462,565	12.36
1974	496,019	7.23
1975	465,058	-6.24
1976	531,695	14.33
1977	569,246	7.06
1978	665,203	16.86
1979	690,904	3.86
1980	666,541	-3.53
1981	582,352	-12.63
1982	513,450	-11.83
1983	620,508	20.85
1984	735,961	18.61
1985	854,092	16.05
1986	937,863	9.81

WLS COL 2.2-1

TABLE 2.2-205 (Sheet 2 of 2)
 HISTORICAL AIR TRAFFIC AT GREENVILLE-SPARTANBURG
 INTERNATIONAL AIRPORT

Year	Total Passengers	Percent Change
1987	1,105,752	17.90
1988	1,139,640	3.06
1989	1,110,314	-2.57
1990	1,184,580	6.69
1991	1,055,823	-10.87
1992	1,097,287	3.93
1993	1,171,826	6.79
1994	1,560,042	33.13
1995	1,322,540	-15.22
1996	1,428,223	7.99
1997	1,450,174	1.54
1998	1,424,669	-1.76
1999	1,518,561	6.59
2000	1,590,786	4.76
2001	1,412,567	-11.20
2002	1,386,828	-1.82
2003	1,350,648	-2.61
2004	1,575,117	16.62
2005	1,792,597	13.81
	AVERAGE	6.53

(Reference 220)

WLS COL 2.2-1

TABLE 2.2-206
PROJECTED AIR TRAFFIC AT GREENVILLE-SPARTANBURG
INTERNATIONAL AIRPORT

Year	Total Passengers ^(a)
2006	1,909,654
2007	2,034,354
2008	2,167,197
2009	2,308,715
2010	2,459,474
2011	2,620,078
2012	2,791,169
2013	2,973,432
2014	3,167,598
2015	3,374,442
2016	3,594,793
2017	3,829,533
2018	4,079,601
2019	4,345,999
2020	4,629,793
2021	4,932,118
2022	5,254,186
2023	5,597,284
2024	5,962,787
2025	6,352,157

a) Projections based upon average of 6.53 percent annual increase in passengers as of 2005 (Reference [Table 2.2-205](#)).

([Reference 220](#))

WLS COL 2.2-1

TABLE 2.2-207
HISTORICAL AIR TRAFFIC AT CHARLOTTE DOUGLAS
INTERNATIONAL AIRPORT

Year	Total Passengers	Percent Change
2000	23,088,455	
2001	23,177,555	0.39
2002	23,597,926	1.81
2003	23,062,570	-2.27
2004	25,543,374	10.76
2005	28,206,052	10.42
	AVERAGE	4.22

(Reference 219)

WLS COL 2.2-1

TABLE 2.2-208
PROJECTED AIR TRAFFIC AT CHARLOTTE DOUGLAS
INTERNATIONAL AIRPORT

Year	Total Passengers ^(a)
2006	29,396,347
2007	30,636,873
2008	31,929,749
2009	33,277,185
2010	34,681,482
2011	36,145,040
2012	37,670,361
2013	39,260,050
2014	40,916,825
2015	42,643,515
2016	44,443,071
2017	46,318,568
2018	48,273,212
2019	50,310,342
2020	52,433,438
2021	54,646,129
2022	56,952,196
2023	59,355,578
2024	61,860,384
2025	64,470,892

a) Projections based upon average historical percent change in passengers

WLS COL 2.2-1

TABLE 2.2-209
PARAMETERS USED IN THE ANALYSIS OF AN OFF-SITE
CHEMICAL RELEASE

Parameter	Value	Unit
Initial mass	20000	(kg)
Release height	0	(m)
Storage temperature	25	(Celsius)
Distance to intake	5100	(m)
Intake height	17	(m)
Atmospheric pressure	760	(mm Hg)
Stability class	G & F ^(a)	(N/A)
Wind speed	1	(m/s)

a) The HABIT model utilizes a G stability class and the ALOHA model utilizes an F stability class.

TABLE 2.2-210
LEAKAGE FROM ASSUMED LARGE HOLE (4.5 m²) FROM A TRUCK ON HIGHWAY 29

Chemical	Truck Capacity (tons)	LEL (ppm)	Pool Diameter (yards)	Flammable Area of Vapor Cloud (yards)	Concentration at site (ppm)	Overpressure at site (psi)
Gasoline (n-heptane)	25.4	10,000	102	113	0.0	0.0
Propane	21.9	20,000	91	0	0.0	0.0
Acetylene	12.3	25,000	(a)	643	0.0	0.0
Ethylacetylene	24.0	16,000	(a)	874	0.0	0.0
Ethylene Oxide	32.2	30,000	(a)	836	0.0	0.0
Propylene Oxide	30.6	19,000	99	412	0.0	0.0
1,3 Propylene Oxide	33.2	28,000	101	252	0.0	0.0

a) Two-phase flow release.

TABLE 2.2-211
LEAKAGE FROM ASSUMED LARGE HOLE (4.5 m²) FROM A RAILROAD TANKER

Chemical	Tanker Capacity (tons)	LEL (ppm)	Pool Diameter (yards)	Flammable Area of Vapor Cloud (yards)	Concentration at site (ppm)	Overpressure at site (psi)
Gasoline (n-heptane)	113	10,000	214	303	0.0	0.0
Propane	97.3	20,000	191	20	0.0	0.0
Acetylene	54.4	25,000	(a)	902	0.0	0.0
Ethylacetylene	107	16,000	(a)	1,306	0.0	0.0
Ethylene Oxide	143	30,000	(a)	1,220	0.0	0.0
Propylene Oxide	136	19,000	204	846	0.0	0.0
1,3 Propylene Oxide	148	28,000	210	542	0.0	0.0

a) Two-phase flow release.

2.3 METEOROLOGY

This **section** of the referenced DCD is incorporated by reference with the following departures and/or supplements.

This section discusses regional and local meteorological conditions, the onsite meteorological measurement program, and short-term and long-term diffusion estimates.

2.3.1 REGIONAL CLIMATOLOGY

WLS COL 2.3-1 The description of the general climate of the region is based primarily on climatological records for Greenville/Spartanburg International Airport (GSP), located between Greenville and Spartanburg, South Carolina. This first order station was selected because the terrain and land-use in the surrounding area is similar to the area around the Lee Nuclear Site (i.e., rural). This description uses data from those records, as appropriate, and is augmented by recent data from the Lee Nuclear Station site meteorological tower (Tower 2). Meteorological data for the Lee Nuclear Site collected from 12/1/2005 through 11/30/2007 is presented and used in FSAR **Section 2.3** to calculate atmospheric dispersion values. FSAR **Appendix 2CC** provides an evaluation which concludes that one-year and two-year site data sets are consistent and representative of long-term conditions of the site.

Topographical considerations and examination of the records indicate that meteorological conditions at the Greenville/Spartanburg International Airport are representative of the general climate of the region that encompasses the site. Because the Ninety-Nine Islands cooperative observer station (Station No. 386293) in Blacksburg, South Carolina, is the closest National Weather Service (NWS) station (two miles southeast), the tables and figures included are based primarily on data from this location when the period of record and observational procedures are considered adequate. Climate data from the National Oceanic and Atmospheric Administration (NOAA) first order weather station at the Greenville/Spartanburg International Airport (GSP) in Greer, SC approximately 42 miles west are also presented. Data from the National Oceanic and Atmospheric Administration (NOAA) first order weather station in Charlotte, NC (CLT) approximately 35 miles ENE of the site is also used in the cooling tower plume analysis. In cases such as the reoccurrence rate of rare events based on decades of observation (e.g. climatology), the National Weather Service off-site data is preferable, due to the shorter period of meteorological data currently available on site.

2.3.1.1 General Climate

The most important factors controlling the local climate are the state's location in the northern mid-latitudes, its proximity to both the Atlantic Ocean and the

Appalachian Mountains, and local elevation. South Carolina's geographic regions are shown on [Figure 2.3-273](#). The Lee Nuclear Station site is located in the piedmont region of South Carolina. The Lee Nuclear Station is located in Cherokee County which is in South Carolina Climate Division 2. South Carolina's mid-latitude location allows for solar radiation to vary throughout the year, producing four distinct seasons. At the summer solstice, the sun is nearly overhead at solar noon with a maximum zenith angle of approximately $79\frac{1}{2}^{\circ}$; at winter solstice, the sun is low in the southern horizon at solar noon with a maximum zenith angle of approximately $23\frac{1}{2}^{\circ}$. This allows for a variance in length of day sufficient to produce ample daytime heating during summer and nighttime cooling during winter ([Reference 201](#)).

The state's position on the eastern coast of a continent is important because land and water heat and cool at different rates. This provides for cooling sea breezes during the summer and warms the immediate coast during the winter. Also, it influences the way pressure and wind systems affect the state. During the summer, South Carolina's weather is dominated by a maritime tropical air mass known as the Bermuda High. Airflow passing over the Gulf Stream, as it circulates around the Bermuda High brings warm, moist air inland from the ocean. As the air comes inland, it rises and forms localized thunderstorms, resulting in precipitation maxima ([Reference 201](#)).

The Appalachian Mountains also exert a major influence on the state's climate in three ways. First, they tend to block many of the cold air masses arriving from the northwest, thus making the winters somewhat milder. Second, the occurrence of downslope winds, which warm the air by compression, causes the areas leeward of the mountains to experience slightly higher temperatures than the surrounding areas. Hence, the proximity of the mountains to the state results in a more temperate climate than otherwise would be experienced. Lastly, the mountains cause a leeside rain shadow, an area of decreased precipitation across the Midlands and roughly parallel to the fall line where the upland region meets the coastal plain ([Reference 201](#)).

The climate of South Carolina is humid and subtropical with a short cold season and a relatively long warm season. Synoptic features during winter cause rather frequent alternation between mild and cool periods with occasional outbreaks of cold air. Such intrusions of cold air, however, are modified in the crossing and descent of the Appalachian Mountains. Summers, noted for their greater persistence in flow pattern, experience fairly constant trajectories from the south and southwest with advection of maritime tropical air. In this area of the Southeast, significant local circulation often results during periods of weak synoptic circulation. These effects, usually induced by the local terrain, are responsible for a redistribution of wind directions and speeds from those expected in the absence of the local terrain ([Reference 202](#)). General climatic assessments at the time of [Reference 202](#) remain valid.

The state's annual average temperature, in Fahrenheit, varies from the mid-50's in the Mountains to low 60's along the coast. During the winter, average temperatures range from the mid-30's in the Mountains to low 50's in the Low Country. During summer, average temperatures range from the upper 60's in the

Mountains to the mid-70's in the Low Country ([Reference 201](#)). Temperatures in the region indicate warm summers and mild winters.

Precipitation in South Carolina is ample and distributed with two maxima and two minima throughout the year. The maxima occur during March and August; the minima occur during April and November. There is no wet or dry season; only relatively heavy precipitation periods or light precipitation periods. No month averages less than two inches of precipitation anywhere in South Carolina. In northwestern South Carolina, winter precipitation is greater than summer precipitation; the reverse is true for the remainder of the state. During summer and early fall of most years, the state is affected by one or more tropical storms or hurricanes ([Reference 201](#)). Average annual precipitation is heaviest in northwestern South Carolina, and annual totals vary directly with elevation, soil type, and vegetation. In the Mountains, 70 to 80 inches of rainfall occur at the highest elevations with the highest annual total at Caesars Head, South Carolina (79.29 inches). Across the Foothills, average annual precipitation ranges from 60 to more than 70 inches. In the eastern and southern portions of the Piedmont, the average annual rainfall ranges from 45 to 50 inches. The driest portion of the state, on average, is the Midlands where annual totals are mostly between 42 and 47 inches ([Reference 201](#)).

The annual number of days of precipitation greater than or equal to one inch varies with elevation, varying from more than 24 days in the Upstate to less than 12 days in the Midlands. The annual number of days of precipitation greater than or equal to 0.1 inches varies from 95 in the Upstate to less than 70 in a portion of the Midlands. The annual number of days of precipitation greater than or equal to 0.5 inches varies from 48 in the Upstate to less than 30 in a portion of the Midlands ([Reference 201](#)). Yearly average precipitation at Greenville/Spartanburg International Airport based on 30 years of data is about 50 inches ([Table 2.3-256](#)).

Snow and sleet may occur separately, together, or mixed with rain during the winter months from November to March, although snow has occurred as late as May in the mountains. Measurable snowfall may occur from one to three times in a winter in all areas except the Low Country where snowfall occurs on average once every three years. Accumulations seldom remain very long on the ground except in the mountains ([Reference 201](#)). Typically, snowfall occurs when a mid-latitude cyclone moves northeastward along or just off the coast. Snow usually occurs about 150 to 200 miles inland from the center of the cyclone. The greatest snowfall in a 24-hour period was 24 inches at Rimini, South Carolina, in February 1973. During December 1989, Charleston, South Carolina, experienced its first white Christmas on record, and other coastal locations had more than six inches of snow on the ground for several days following it. The greatest snowfall for Ninety-Nine Islands was 13 inches on January 7, 1988. [Figure 2.3-201](#) shows the annual distribution of snow across the state ([Reference 201](#)).

Sleet and freezing rain vary from 3.75 events per year in Chesterfield County to less than 0.75 events per year in the Low Country. The highest frequency by month occurs in January with more than 1.5 events per year in the Charlotte area and Chesterfield County to less than 0.25 events per year in the Low Country. One of the most severe cases of ice accumulation from freezing rain took place

February 1969 in several Piedmont and Midlands counties. Timber losses were tremendous and power and telephone services were seriously disrupted over a large area (Reference 201). Another significant storm was the ice storm of December 2005. This was a damaging winter storm that produced extensive ice damage in a large portion of the Southern United States on December 14 - 16, 2005. It led to enormous and widespread power outages and at least 7 deaths. The ice storm left more than 700,000 people without power in and near the Appalachians, including 30,000 customers in Georgia, 358,000 in South Carolina, 328,000 in North Carolina and 13,000 in Virginia. An ice storm (also called glaze ice) is the accretion of generally clear and smooth ice formed on exposed objects by the freezing of a film of super-cooled water deposited by rain, drizzle, or possibly condensed from super-cooled water vapor. The weight of this ice is often sufficient to greatly damage telephone and electric power lines and poles. Most glaze is the result of freezing rain or drizzle falling on surfaces with temperatures between 25°F and 32°F (Reference 204). The glaze ice belt of the United States includes all of the area east of the Rocky Mountains. However, in the Southeast and Gulf Coast sections of the country, below freezing temperatures seldom last more than a few hours after glaze storms.

Hail occurs infrequently, falling most often during spring thunderstorms from March through May. The incidence of hail varies from 1 to 1.5 hail days per year in the Midlands, Piedmont, and Foothills to 0.5 day per year in the Low Country. Although hail can occur in every month during the year, May has the highest incidence with an average of more than five events per year. Typically, it occurs during the late afternoon and early evening between the hours of 3:00 p.m. and 8:00 p.m. (Reference 201). Severe weather occurs in South Carolina occasionally in the form of violent thunderstorms and tornadoes. Although less frequent than surrounding states, thunderstorms are common in the summer months. The more violent storms generally accompany squall lines and active cold fronts of late-winter or spring. Strong thunderstorms usually bring high winds, hail, considerable lightning, and rarely spawn a tornado (Reference 201).

In the 40-year period from 1950 through 1989, an average of 11 tornadoes occurred per year in South Carolina. Since a tornado is very small and affects a localized area, the probability of a tornado striking a specific point in a given year is low. The majority of tornadoes, 88 percent, occur from February through September. May and August are peak months. The May peak is primarily due to squall lines and cold fronts; the August peak is due to tropical cyclone activity. A secondary maxima, nine percent of all occurrences, happens in November and December (Reference 201). During spring, tornadoes result from active cold fronts, whereas during summer and early fall many are associated with the passage of tropical cyclones. During November and December, it is not uncommon to have active cold fronts and tornadic activity. Tornado frequency is at a minimum in October and January; only 3 percent of the total are experienced during these two months (Reference 201).

Tropical cyclones affect the South Carolina coast on an infrequent basis, but do provide significant influence annually through enhanced rainfall inland during the summer and fall months. Depending on the storm's intensity and proximity to the coast, tropical systems can be disastrous. The major coastal impacts from tropical

cyclones are storm surge, winds, precipitation, and tornadoes. Hurricanes are the most intense warm season coastal storms and are characterized by wind speeds exceeding 64 knots (74 miles per hour) and central pressure usually less than 980 millibars (mb) (28.94 inches of mercury). Less intense, but more frequent, are tropical storms (winds over 34 knots and under 64 knots: greater than 980 mb central pressure) and tropical depressions (winds under 34 knots).

(Reference 201) Tracks of tropical cyclones within 75 miles of Greer, South Carolina between 1851 and 2006 are shown on Figure 2.3-272.

Winds are usually the most destructive force associated with tropical cyclones, particularly inland. Strong winds, resulting from the low central pressure and forward movement, also combine to result in significant ocean rise and wave action. This resulting water rise, known as the storm surge, plagues coastal inlands and low-lying inland areas as these storms make landfall. Because of the low central pressure in a hurricane, a 100 mb drop in ocean surface pressure results in about a one meter increase of ocean elevation. (Reference 201).

The Mountains have a strong influence on the prevailing surface wind direction. On a monthly basis, prevailing winds tend to be either from the northeast or southwest. Winds from all directions occur throughout the state during the year, but the prevailing statewide directions by season are as follows: (Reference 201)

<u>Season</u>	<u>Direction</u>	<u>Degrees</u>
Spring	Southwest	210 to 240
Summer	South and Southwest	170 to 250
Autumn	Northeast	20 to 60
Winter	Northeast and Southwest	20 to 60 and 210 to 240

Average surface wind speeds across the state for all months range between six and 10 miles per hour. Winds at more than 1500 meters above msl are usually southwest to northwest in winter and spring, south to southwest in summer, and southwest to west in autumn. The mountains control wind direction during all seasons, but have a more pronounced effect in the winter, summer, and autumn (Reference 201). During winter, most cyclones that affect the state pass to the south of the Mountains. As these systems move around the Mountains, the winds are generally southwest. As the cyclone moves over the Atlantic Ocean, the winds shift to the northeast. During summer, air flows north from the Gulf of Mexico along the western edge of the Bermuda High. Quite often the Mountains form the western extent of the Bermuda High. During autumn, winds are northeast because the mountains form a western barrier to the northeast surface winds wrapping around the predominant continental high pressure centered over New England. This northeast flow wedges in cool air at the surface and moves southward along the eastern seaboard (Reference 201).

The Bermuda High also contributes to air stagnation, especially during the summer. During the period 1936-75, it was shown that the state experienced 20 stagnation days per year in the Coastal Plain, and more than 28 stagnation days per year occurred in the Central Savannah River area. The winds in stagnant air are very light and tend to be rather disorganized in direction ([Reference 201](#)).

Relative potential for air pollution can be demonstrated by the seasonal distribution of atmospheric stagnation cases that persist for at least four days. Data for the 50-year period (1948 to 1998), analyzed by Julian X. L. Wang and James K. Angell ([Reference 205](#)), show that, in South Carolina, air stagnation conditions exist between 10 and 20 days per year. The meteorological condition which is favorable to an air pollution episode is an air stagnation event. The air stagnation event identifies areas where air may be trapped by poor ventilation due to persistent light or calm winds, and by the presence of inversions. Most air stagnation events happen in an extended summer season from May to October. This is the result of the weaker pressure and temperature gradients, and therefore weaker wind circulation during this period. In the eastern U.S., there is a relative minimum of stagnation in July accompanied by relative maxima in May-June and August-October. This mid-summer decrease of air stagnation is due to the impact of the Bermuda High on the eastern United States. The Bermuda High is strongest in July; and hence, the meridional wind in the Gulf States is a maximum then due to the increased pressure gradient, resulting in a relative minimum of air stagnation. Therefore, the Bermuda High is an additional and unique controlling factor for air stagnation conditions over the eastern United States, besides the seasonal cycle of minimum wind in summer and maximum wind in winter.

Another unique feature of air stagnation in the eastern U.S. is its early onset in May, compared to the onset in June in the west and central U.S. This results in a prolonged but weaker air stagnation season in the eastern U.S. ([Reference 205](#)). For the eastern United States, their results show a regionally averaged mean annual cycle of six cases in the spring, 14 cases in the summer, and 11 cases in the fall for the region.

Just to the North of the Lee Nuclear Station site, is the border of North Carolina. The climate in this area is typical of the Piedmont area of North Carolina. The three principal physiographic divisions of the eastern United States are particularly well developed in North Carolina. From east to west, they are the Coastal Plain, the Piedmont, and the Mountains. The fall line is the dividing line between the Coastal Plain and the Piedmont. The Piedmont area, comprising about one-third of the State, rises gently from about 200 feet at the fall line to near 1,500 feet at the base of the Mountains.

The westernmost, or Mountain Division of North Carolina is the smallest of the three, comprising a little more than one-fifth of the total area of the State. Its range of elevation, however, is by far the greatest; it stretches upward from around 1,500 feet along the eastern boundary to 6,684 feet at the summit of Mount Mitchell. Some of the valleys drop to 1,000 feet above sea level while some 125 peaks exceed 5,000 feet and 43 tower above 6,000 feet.

Latitude accounts for some climatic variations, as do soils, plant cover, and inland bodies of water. The Gulf Stream has some direct effect on North Carolina temperatures, especially on the immediate coast. Though the Gulf Stream lies some 50 miles offshore, warm water eddies spin off from it and moderate the winter air temperatures along the Outer Banks. Coastal fronts are common during the winter months, and can push inland, bringing warmer than expected temperatures to coastal areas.

The most important single influence contributing to the variability of North Carolina climate is altitude. In all seasons of the year, the average temperature varies more than 20° Fahrenheit from the lower coast to the highest elevations. The average annual temperature at Southport on the lower coast is nearly as high as that of interior northern Florida, while the average on the summit of Mount Mitchell is lower than that of Buffalo, NY.

In winter, the greater part of North Carolina is partially protected by the mountain ranges from the frequent outbreaks of cold air which move southeastward across the central States. Such outbreaks often move southward all the way to the Gulf of Mexico without attaining sufficient strength and depth to traverse the heights of the Appalachian Range. When cold waves do break across, they are usually modified by the crossing and the descent on the eastern slopes. The temperature drops to 10° or 12° F about once during an average winter over central North Carolina, ranging some 10° F warmer along the coast and 10° F colder in the upper mountains. Temperatures as low as 0° F are rare outside the mountains, but have occurred throughout the western part of the State. The lowest temperature of record is minus 34° F recorded January 21, 1985, at Mount Mitchell. Winter temperatures in the eastern sections are modified by the Atlantic Ocean, which raises the average winter temperature and decreases the average day-to-night range. In spring, the storm systems that bring cold weather southward reach North Carolina less often and less forcefully, and temperatures begin to moderate. The rise in average temperatures is greater in May than in any other month. Occasional invasions of cool dry air from the north continue during the summer, but their effect on temperatures is slight and of short duration.

The increase in sunshine in the spring usually brings temperatures back up quickly. When the dryness of the air is sufficient to keep cloudiness at a minimum for several days, temperatures may occasionally reach 100° F or higher in the interior at elevations below 1,500 feet. Ordinarily, however, summer cloudiness develops to limit the sun's heating while temperatures are still in the 90-degree range. An entire summer sometimes passes without a high of 100° F being recorded in South Carolina. The average daily maximum reading in midsummer is below 90° F for most localities.

Autumn is the season of most rapidly changing temperature, the daily downward trend being greater than the corresponding rise in spring. The drop-off is greatest during October, and continues at a rapid pace in November, so that average daily temperatures by the end of that month are within about five degrees of the lowest point of the year.

While there are no distinct wet and dry seasons in North Carolina, average rainfall does vary around the year. Summer precipitation is normally the greatest, and July is the wettest month. Summer rainfall is also the most variable, occurring mostly in connection with showers and thunderstorms. Daily showers are not uncommon, nor are periods of one to two weeks without rain. Autumn is the driest season, and November the driest month. Precipitation during winter and spring occurs mostly in connection with migratory low pressure storms, which appear with greater regularity and in a more even distribution than summer showers. In southwestern North Carolina, where moist southerly winds are forced upward in passing over the mountain barrier, the annual average rainfall is more than 90 inches. This region is the rainiest in the eastern United States. Less than 50 miles to the north, in the valley of the French Broad River, sheltered by mountain ranges on all sides, is the driest point south of Virginia and east of the Mississippi River. Here the average annual precipitation is only 37 inches. East of the Mountains, average annual rainfall ranges mostly between 40 and 55 inches.

Winter-type precipitation usually occurs with southerly through easterly winds, and is seldom associated with very cold weather. Snow and sleet occur on an average once or twice a year near the coast, and not much more often over the southeastern half of the State. Such occurrences are nearly always connected with northeasterly winds, generated when a high pressure system over the interior, or northeastern United States, causes a southward flow of cold dry air down the coastline, while offshore a low pressure system brings in warmer, moist air from the North Atlantic. Farther inland, over the Mountains and western Piedmont, frozen precipitation sometimes occurs in connection with low pressure storms, and in the extreme west with cold front passages from the northwest. Average winter snowfall over North Carolina ranges from about an inch per year on the outer banks and along the lower coast to about 10 inches in the northern Piedmont and 16 inches in the southern Mountains. Some of the higher mountain peaks and upper slopes receive an average of nearly 50 inches a year.

The average relative humidity does not vary greatly from season to season but is generally the highest in winter and lowest in spring. The lowest relative humidity is found over the southern Piedmont, where the year around average is about 65 percent.

2.3.1.2 Regional Meteorological Conditions for Design and Operating Bases

This section describes severe weather phenomena that may require consideration in design of safety related structures, systems and components. Most recent data is taken from the NCDC storm event database that covers the period from 1950 through 2005 ([Reference 207](#)), but even longer data periods are used for some phenomena to try to capture the occurrence of rare events.

Severe synoptic-scale storms are relatively infrequent in the Lee Nuclear Station site area. The effects of such storms are generally restricted to local flooding from heavy rains. Damage from snow, freezing rain, or ice storms in mid-winter are uncommon.

The passive containment cooling system is the ultimate heat sink for the AP1000 and does not rely upon offsite or onsite AC power sources as described in DCD [Section 3.1.1](#). The AP1000 design parameters for the ultimate heat sink are given in [DCD Table 2-1](#). The regional meteorological conditions relevant to the design and operating bases for the Lee Nuclear Station site are discussed below. FSAR [Table 2.0-201](#) gives a comparison of the Lee Nuclear Station site characteristics with the AP1000 DCD design parameters.

General Design Criterion (GDC) 2 in Appendix A to 10 CFR Part 50 requires “consideration of the most severe of the natural phenomena that have been historically reported for the site and surrounding area, with sufficient margin for the limited accuracy, quantity, and period of time in which the historical data have been accumulated.”

Extreme weather calculations for Lee Nuclear Station were conducted over the maximum data span available. Certified climatological data obtained from the U.S. National Climatic Data Center (NCDC) was used for the severe weather phenomena evaluations. This data selection supports accurate severe weather phenomena projections for the area in the vicinity of the Lee Nuclear Station site. This extensive historic data record provides the historical climatic trends and severe natural phenomena to be included in the site characterization.

Dry-bulb, coincident wet-bulb, and non-coincident wet-bulb temperatures represent significant site characteristics because this data is used in demonstrating that the AP1000 DCD site parameters are bounding (i.e., more conservative) than the Lee Nuclear Station site characteristics. The Lee Nuclear Station site characteristic temperatures were developed by considering both 100-year return temperatures and 0% exceedance temperatures. These values were calculated using all available hourly data from a 45-year (1963-2007) sequential meteorological data set for Greenville-Spartanburg Airport, Greer, South Carolina, Station No. 03870, National Weather Service (NWS) station. The difference between the Lee Nuclear Station site characteristics and the DCD design parameters, as provided in FSAR [Table 2.0-201](#), provide additional margin to the selected Lee Nuclear Station site characteristic maximum safety temperatures. This margin accounts for any limitations to the accuracy, quantity, and period of time in which the historical data have been accumulated.

General predictions on global or U.S. climatic changes expected during the period of reactor operation are uncertain and are only applicable on a macroclimatic scale. Since the maximum data span available was used in the severe weather analysis, accurate severe weather phenomena have been provided based on best-available historic data. Projections of future severe weather conditions at the Lee Nuclear Station site are speculative at best, based on current understanding and modeling of global climate change.

2.3.1.2.1 Hurricanes

During the period 1899 to 2005 there were 50 documented tropical cyclones that affected either North Carolina (31 cyclones) or South Carolina (19 cyclones) ([Reference 209](#), [Reference 210](#), and [Reference 235](#)). See [Table 2.3-202](#). Of

these 50 cyclones, 20 (40 percent) were Category 1, 15 (30 percent) were Category 2, 11 (22 percent) were Category 3, and 4 (8 percent) were Category 4 hurricanes. The storm category cited is the category observed as the cyclone entered either North Carolina or South Carolina. [Table 2.3-203](#) presents a monthly breakdown of the 50 cyclones and provides a definition of the storm categories. Tropical cyclones, including hurricanes, lose strength as they move inland from the coast and the greatest concern for an inland site is possible flooding due to excessive rainfall. The maximum one day rainfall at Ninety-Nine Islands for the years 1949-2005 was 7.16 inches on 8/17/1985 resulting from hurricane Danny which was a tropical depression when it passed through this part of South Carolina ([Reference 203](#)).

2.3.1.2.2 Tornadoes

The probability that a tornado will occur at the Lee Nuclear Station site is low. Records show that in a 56-year period (1950-2005) there were 15 tornadoes reported in Cherokee County, the location of the site. The data reported by NOAA's National Environmental Satellite, Data, and Information Service (NESDIS) ([Reference 207](#)) is given in [Table 2.3-204](#). From this data, the total tornado area in Cherokee County, ignoring events with a zero path length (i.e., no path length or no path length reported), is approximately 3.6 square miles. Using the principle of geometric probability described by H. C. S. Thom ([Reference 211](#)), a mean tornado path area of 0.24 square miles and an average tornado frequency of 0.27 per year was calculated for the area of Cherokee County (392.7 mi²), the point probability of a tornado striking the Lee Nuclear Station is 1.64×10^{-4} /year $[(\text{total tornado area in Cherokee County})/(\text{area of Cherokee County})) \times (\text{number of tornadoes per year})]$. This corresponds to an estimated recurrence interval of 6108 years.

The tornadoes reported during the years 1950-2005 in the vicinity of Cherokee, Spartanburg, Union, Chester, and York Counties in South Carolina and Polk, Rutherford, Cleveland, Gaston, and Mecklenburg Counties in North Carolina are shown in [Table 2.3-204](#). During the period 1950 to 2005, a total of 125 tornadoes touched down in these counties, which have a combined total land area of 5,131.2 square miles ([Reference 212](#)). These local tornadoes have a mean path area of 0.459 square miles, excluding tornadoes without a length specified. The site recurrence frequency of tornadoes can be calculated using the point probability method as follows:

Total area of tornado sightings = 5,131.2 sq mi

Average annual frequency = 125 tornadoes/56 years = 2.23 tornadoes/year

Annual frequency of a tornado striking a particular point P = $[(0.459 \text{ mi}^2/\text{tornado}) (2.23 \text{ tornadoes/year})] / 5,131.2 \text{ sq. mi} = 0.0002 \text{ yr}^{-1}$

Mean recurrence interval = $1/P = 5000 \text{ years}$.

This result shows that the frequency of a tornado in the immediate vicinity of the site is slightly lower than the frequency in the surrounding counties. Another methodology for determining the tornado strike probability at the Lee Nuclear Station is given in NUREG/CR-4461 (Reference 213). Based on a 2° longitude and latitude box centered on the Lee Nuclear Station site, the number of tornadoes is 221 from data collected from 1950 through August 2003. The corresponding expected maximum tornado wind speed and upper limit (95th percentile) of the expected wind speed is given below with the associated probabilities.

Probability	Expected maximum tornado wind speed mph	Upper limit (95 percent) of the expected tornado wind speed mph
10^{-5}	142	153
10^{-6}	180	190
10^{-7}	215	226

The design basis tornado characteristics are specific to the site location and region of the country in which the site is located. However, rather than conducting site research on tornado characteristics, most sites in past licensing proceedings have relied on NRC-endorsed studies that set conservative values for key design basis tornado characteristics. These characteristics were then used in the design of the subject facility.

Regulatory Guide 1.76, Revision 1, provides design basis tornado characteristics, depending on the proposed site location in the country. Based on these criteria, the best estimated exceedance frequency is 10^{-7} per year. The design basis tornado characteristics defined for Lee Nuclear Station, which is in Region I, are based on the guidance in Regulatory Guide 1.76. The below listed characteristics are associated with a Region I site.

Region I Tornado Characteristics

Maximum wind speed, mph	230
Rotational speed, mph	184
Maximum Translational speed, mph	46
Radius of maximum rotational speed, ft	150
Pressure drop, psi	1.2
Rate of pressure drop, psi/sec	0.5

The above maximum tornado wind speed is bounded by the AP1000 DCD value of 300 mph (see FSAR [Table 2.0-201](#) for a comparison of the Lee Nuclear Station site characteristics with the DCD design parameters). In accordance with Regulatory Guide 1.76, the wind velocities and pressures are not assumed to vary with height. Tornado missiles (including the missile spectrum) are discussed in [Section 3.5](#). Waterspouts are common along the southeast U.S. coast, especially off southern Florida and the Keys and can happen over seas, bays, and lakes worldwide. However, they are not expected to occur at the Lee Nuclear Station site since the only nearby body of water is the Broad River.

2.3.1.2.3 Thunderstorms

Thunderstorms occur an average of approximately 41.6 days a year based on the National Climatic Data Center (NCDC) Local Climatic Data (LCD) when data from Greenville-Spartanburg (Greer), South Carolina (Station ID GSP) ([Reference 236](#)) and Charlotte, North Carolina (Station ID CLT) ([Reference 239](#)) are combined for the years 1963 through 2007 and 1948 through 2007, respectively. [Table 2.3-205](#) presents the thunderstorm data for Greer and Charlotte for the years 1963 through 2007 and 1948 through 2007, respectively. Approximately 57 percent of the thunderstorms in this area occur during the warm months (June-August), indicating that the majority are warm-air-mass thunderstorms. As shown in [Table 2.3-205](#), the highest occurrence of thunderstorm days is in July with an average of approximately 10 days per year.

2.3.1.2.4 Lightning

Data on lightning strike density is becoming more readily available due to the National Lightning Detection Network (NLDN), which has measured cloud-to-ground (CG) lightning for the contiguous United States since 1989. Prior to the availability of this data, isokeraunic maps of thunderstorm days were used to predict the relative incidence of lightning in a particular region. A general rule, based on a large amount of data from around the world, estimates the earth flash mean density to be 1-2 cloud to ground flashes per 10 thunderstorm days per square kilometer. ([Reference 214](#)). The annual mean number of thunderstorm days in the site area is estimated to be 50 based on interpolation from the isokeraunic map ([Reference 215](#)); therefore, it is estimated that the annual lightning strike density in the Lee Nuclear Station site area is 26 strikes per square mile per year. Other studies gave a ground flash density (GFD) in strikes/km²/yr, based on thunderstorm days per year (TSD) as $GFD = 0.04 (TSD)^{1.25} = 0.04 (50)^{1.25} = 5.3 \text{ strikes/km}^2/\text{yr}$ or 14 strikes/mi²/yr. ([Reference 216](#)). Recent studies based on data from the NLDN ([Reference 217](#)) indicate that the above strike densities are upper bounds for the Lee Nuclear Station site. Mean annual flash density for 1989-96 is 5 strikes/km²/yr or 13 strikes/mi²/yr in northern South Carolina.

2.3.1.2.5 Hail

From January 1, 1995 through May 31, 2006, 432 hailstorms occurred in the region with Cherokee County receiving approximately ten percent, as shown in

Table 2.3-206. For this table, each occurrence of hail was counted as an individual event, even if two counties recorded hail simultaneously. The most probable months of hail occurrence are May and June in Cherokee County. The average number of hailstorms in Cherokee County is approximately 3.5 per year. The maximum hail size reported was 2.75 inch diameter and the average size was slightly more than 1 inch diameter. Property damage occurs infrequently, with no recorded events in Cherokee County, South Carolina in this 12-year period ([Reference 207](#)).

2.3.1.2.6 Regional Air Quality

The Clean Air Act, which was last amended in 1990, requires the U.S. Environmental Protection Agency (EPA) to set National Air Quality Standards for pollutants considered harmful to the public health and the environment. The EPA Office of Air Quality Planning and Standards has set National Ambient Air Quality Standards for six principle pollutants, which are called "Criteria" pollutants. Units of measure for the standards are parts per million (ppm), milligrams per cubic meter (mg/m^3), and micrograms per cubic meter of air ($\mu\text{gm}/\text{m}^3$). Areas are either in attainment of the air quality standards or in non-attainment. Attainment means that the air quality is better than the standard.

The newly promulgated U.S. Environmental Protection Agency (EPA) 8-hour ozone standard (62FR 36, July 18, 1997) is 0.08 ppm in accordance with 40 CFR 50.10. Cherokee is in the Greenville-Spartanburg Intrastate Air Quality Control Region (South Carolina). Cherokee County is in attainment for all criteria pollutants (carbon monoxide, lead, nitrogen dioxide, particulate matter (PM_{10} , particulate matter less than 10 micron), particulate matter ($\text{PM}_{2.5}$, particulate matter less than 2.5 micron), ozone, and sulfur oxides. There are six areas in South Carolina that are in non-attainment with the 8-hour ozone standard ([Reference 218](#)). Currently designated (as of March 02, 2006) non-attainment areas in South Carolina for the criteria pollutants are as follows:

County	Pollutant	Area Name
Anderson Co	8-Hr Ozone	Greenville-Spartanburg-Anderson, SC
Greenville Co	8-Hr Ozone	Greenville-Spartanburg-Anderson, SC
Lexington Co	8-Hr Ozone	Columbia, SC
Richland Co	8-Hr Ozone	Columbia, SC
Spartanburg Co	8-Hr Ozone	Greenville-Spartanburg-Anderson, SC
York Co	8-Hr Ozone	Charlotte-Gastonia-Rock Hill, NC-SC

The bordering North Carolina counties are Cleveland, Gaston, and Mecklenburg. Both Gaston County and Mecklenburg County are in non-attainment for 8-hr ozone. Cleveland County is in attainment for all criteria pollutants.

The ventilation rate is a significant consideration in the dispersion of pollutants. Higher ventilation rates are better for dispersing pollution than lower ventilation rates. The atmospheric ventilation rate is numerically equal to the product of the mixing height and the wind speed within the mixing layer. A tabulation of daily mixing heights and mixing layer wind speeds for both morning and afternoon was obtained from the EPA's SCRAM Website for 1984-1987 and 1989-1991 at the Greensboro-High Point, North Carolina station (Reference 206). This data was used to generate the morning and afternoon ventilation rates in Table 2.3-207. Morning ventilation is less than 4000 m²/s throughout the year and is less than 2400 m²/s from June through October. Afternoon ventilation is higher than 9200 m²/s from March through June, but lower than 6500 m²/s from August through January. The highest daily air pollution potentials exist in the morning from June through October when ventilation rates are lower. Lowest air pollution potentials occur from December through March due to the relatively high morning mean ventilation rates.

Other data sources provide independent checks on this conclusion. According to Wang and Angell (Reference 205), the annual average air stagnation cases for South Carolina over a fifty-one year period (1948-1998) was four cases per year with a mean duration of five days. The annual mean days of air stagnation was given as 20 for South Carolina. This report also concluded that the highest number of air stagnation days occurred from July through October with the lowest air stagnation days from November through March. The number of air stagnation days in the South Carolina region exhibited a slightly increasing trend over the 50 years evaluated (see Figure 2.3-202). This almost imperceptible positive trend shown in Figure 2.3-202 in the number of air stagnation days has no impact on the Lee Nuclear Station Site.

2.3.1.2.7 Severe Winter Storm Events

The occurrences and durations of recorded ice storms and heavy snowstorms in the vicinity of the Lee Nuclear Station site for the thirteen-year period 1993-2005 is shown in Table 2.3-208. From these data, the frequency of winter storms is estimated to be 22 events per year in this regional area. For the region, each occurrence of a severe winter storm was counted as an individual event, even if two counties recorded a severe winter event simultaneously. For Cherokee County, the frequency is 3.6 events per year.

The equivalent ice thickness due to freezing rain with concurrent 3-second gust speeds for a 100-year mean recurrence interval is given in "Extreme Ice Thicknesses from Freezing Rain" (Reference 208) as 0.75 inch for the north central South Carolina area.

The 48-hour maximum recorded winter precipitation based on the data for the Greenville-Spartanburg NWS (GSP) at Greer, covering the time period of 1997-2005, is 3.54 inches (Reference 224).

In the Ninety-Nine Islands/Lee Nuclear Station site area, snow melts and/or evaporates quickly, usually within 48 hours and before additional snow is added.

Because the plant site is subjected to a subtropical climate with mild winters, prolonged snowfalls or large accumulations of snow or ice on the ground and structures are not anticipated.

2.3.1.2.7.1 Estimated Weight of the 100-year Return Snowpack

Snowpack, as used in this section, is defined as a layer of snow and/or ice on the ground surface and is usually reported daily in inches by the NWS at all first order weather stations.

The density of the snowpack varies with age and the conditions to which it has been subjected. Thus, the depth of the snowpack is not a true indication of the pressure the snowpack exerts on the surface it covers. Due to the variable density in snowpack, a more useful statistic for estimating the snowpack pressure is the water equivalent (in inches) of the snowpack.

South Carolina is not a heavy snow load region. ANSI/ASCE 7-05, "Minimum Design Loads for Buildings and Other Structures," identifies that the ground snowload for the Greenville-Spartanburg area is 7 lbf/ft² based on a 50-yr recurrence. This is converted to a 100-yr recurrence weight of 8.54 lbf/ft² (psf) using a factor of 1.22 (1 / 0.82) taken from ANSI/ASCE 7-05 Table C7-3. Local snow measurements support this ANSI/ASCE 7-05 (Reference 220) value.

To estimate the weight of the 100-year snowpack at the Lee Nuclear Station site, the maximum reported snow and/or ice depths at Ninety-Nine Islands, South Carolina, was determined. The current Southeast Regional Climate Office Database (Reference 203) indicates the greatest snow depth in the data period (8/1/1948 to 12/31/2005) occurred on January 7, 1988. The snow depth recorded on this date was 13 inches. The 100-year recurrence snow depth is 15.2 inches based on 57 years of data back to 1948. Based on NCDC Snow Climatology database, the highest observed maximum snowfall amount, maximum snow depth, and 100-year estimate of snowfall for Cherokee County, SC occurred at the Gaffney 6E observation station. The 100-year snowfall for Gaffney 6E, based on data from 1894 through 2006, was 16.3 inches, the maximum snow depth was 17.0 inches, and the observed maximum snowfall was 17.0 inches. The 100-year snow depth of 17.0 inches will be used in determining the snow load (Reference 237).

Freshly fallen snow has a snow density (the ratio of the volume of melted water to the original volume of snow) of 0.07 to 0.15, and glacial ice formed from compacted snow has a maximum density of 0.91 (Reference 221). In the Lee Nuclear Station site area, snow melts and/or evaporates quickly, usually within 48 hours, and before additional snow is added; thus, the water equivalent of the snowpack can be considered equal to the water equivalent of the falling snow as reported hourly during the snowfall. A conservative estimate of the water equivalent of snowpack in the Lee Nuclear Station site area would be 0.20 inches of water per inch of snowpack. Then, the water equivalent of the 100-year return snowpack would be 17.0 inches snowpack x 0.2 inches water equivalent/inch snowpack = 3.4 inches of water.

Because one cubic inch of water is approximately 0.0361 pounds in weight, a one inch water equivalent snowpack would exert a pressure of 5.20 pounds per square foot ($0.0361 \text{ lb/cu in/in} \times 144 \text{ sq in/sq ft}$).

For the 100-year return snowpack, the water equivalent would exert a pressure of 17.7 pounds per square foot ($5.2 \text{ lbm/sq ft/inch} \times 3.4 \text{ inches}$).

2.3.1.2.7.2 Estimated Weight of the 48-hour Maximum Winter Precipitation

The 48-hour probable maximum winter precipitation (PMWP) based on HMR 53 (Reference 234) is 30.5 inches. The rain load is considered separately from the snow and ice roof load. The roofs of the nuclear island have no lips around the edges, therefore, water and snow melt build up on the roofs of the Nuclear island are negligible. The Shield Building roof is sloped with no lips around the edge of the roof to allow water build up. The PCS tank is flat with no lip; however, there is the central hole that can allow water to drain down in between the Shield wall and the SCV, but not to accumulate on the roof area. The Auxiliary Building. has sloped roofs with three varying elevations (high points given); Area 1&2 155'-6", Area 3&4 163'-0", and Area 5&6 180'-9" (elevations are above plant grade). The south side (directions are relative to called North in the DCD) of the nuclear island wall 1 is above the Radwaste Building roof elevation 136'-4". The east side of the nuclear island, wall 1, is below the Annex Building roof elevation 183'-4.25", but the Auxiliary Building roof is sloped so that areas 3&4 drain on to areas 1&2 roof, which is sloped from east to west. There are no lips on the roof of the Auxiliary Bldg. that could prevent the flow of water. The North side of the nuclear island is also below the Turbine building roof elevation 246'-3", but again Areas 1&2 are sloped such that the run-off will flow off the west side. As a result of the nuclear island roof design there is no loading from the PMWP.

2.3.1.2.7.3 Weight of Snow and Ice on Safety-Related Structures

Based on the evaluations given in "Extreme Ice Thicknesses from Freezing Rain," Reference 208, the probability of freezing rain (glaze ice) with a thickness of 15 mm at the Lee Nuclear site in any year is 0.02. The probability of freezing rain with a thickness of 20 mm at the Lee Nuclear site in any year is 0.01 [Reference 208].

Because the plant site is subjected to a subtropical climate with mild winters, prolonged snowfalls or large accumulations of snow or ice on the ground and structures are not anticipated. The estimated depth of the 100-year return snowpack is 17.0 inches, or 3.4 inches of water equivalent, as discussed above. The safety-related structures at the Lee Nuclear Station would be designed to withstand 17.7 pounds per square foot snow load. No damage from snow or ice loading on structures is expected because the DCD design loading is 75 pounds per square foot (see Table 2.0-201).

2.3.1.2.8 100-Year Return Period Fastest Mile of Wind

The fastest mile of wind speed recorded in 56 years (1950-2006) in the NWS storm events database for Cherokee County is 80.6 mph. A Gumbel-Lieblein

extreme value analysis of this data gives an estimated value of 88 mph for the 100-year return period fastest mile of wind in Cherokee County.

The design basis wind velocity is based on the data from ASCE 7-95 (Reference 222). From Figure 6-1 of ASCE 7-95, the 50-year return 3-second gust wind speed at 33 feet above ground for the Lee Nuclear Station site is 90 mph. This gives a design basis 100-year return wind speed of 96 mph, based on Table C6-5 of ASCE 7-95. The Lee Nuclear Plant site characteristic 3-second gust wind speed of 96 mph is compared to the AP1000 design criteria in Table 2.0-201. The safety and non-safety importance factors, exposure category, and topographic factor are given in Section 3.3.

2.3.1.2.9 Probable Maximum Annual Frequency and Duration of Dust Storms

The occurrence of dust storms (i.e., blowing dust or blowing sand) is a rare phenomenon in the Lee Nuclear Station site area. Although there are categories for dust and sand in the NCDC meteorological database, no hours are identified under this category for Cherokee County in the period from 01/01/1950 to 05/31/2006.

WLS COL 2.3-2 2.3.2 LOCAL METEOROLOGY

This section discusses the local meteorological conditions at the Lee Nuclear Station site. Local site meteorological conditions reflect the synoptic-scale atmospheric processes and are consistent with the regional meteorology. There are two exceptions caused by local effects from the Broad River. First, there is higher humidity directly adjacent to the river. Second, there is a possibility of channeling of low-level winds along the river valley. Channeling of flow from the NW is indicated in the site's wind rose in Figure 2.3-203. This figure shows that the predominant wind direction is from the Northwest, which aligns with the river valley.

The Lee Nuclear Station site is located in a temperate latitude in northern South Carolina about 250 miles northwest of the Atlantic coast and is in a region strongly influenced for much of the year by the Azores-Bermuda anticyclonic circulation (Reference 223). This behavior is shown in Figure 2.3-204 which gives the Atlantic subtropical anticyclone seasonality. In late summer and fall, the position of the subtropical high is such that the region experiences extended periods of fair weather and light wind conditions. In winter and early spring, the frequency of eastward moving migratory highs or low-pressure systems increases, alternately bringing cold and warm air masses into the Lee Nuclear Station site area. Frequent and prolonged incursions of warm moist air from the Atlantic Ocean and the Gulf of Mexico are experienced from late spring through summer.

The general direction of airflow across the region is from the northerly sectors during much of the year, although the prevailing direction may be from one of the southerly sectors during some months. The monthly wind joint frequency distributions for the Greenville/Spartanburg International Airport are shown in [Tables 2.3-209](#) through [2.3-221](#).

Long-term temperature and precipitation records from Ninety-Nine Islands were compared to records from Greenville/Spartanburg. This comparison indicates that, for these parameters, data from Greenville/Spartanburg reasonably represent meteorological conditions in the vicinity of the site. Presumably, this is indicative of the similarity in controlling synoptic influences throughout the region. Other meteorological parameters are assumed to be subject to the same synoptic controls.

2.3.2.1 Winds

2.3.2.1.1 Greenville/Spartanburg Wind Distribution

[Tables 2.3-209](#) through [2.3-221](#) provide monthly percent joint frequency distributions for wind directions and speeds, based on a 9-year period of record from 1997 through 2005 for Greenville/Spartanburg. [Table 2.3-221](#) provides an annual summary of the data. On an annual basis, Greenville/Spartanburg wind data collected in the 9 years from 1997 through 2005 show that northeastern wind direction is the most frequent (11 percent). Wind from the ESE was the least likely with a frequency of approximately one percent. At the Greenville/Spartanburg NWS station, winds average 7.1 mph from January through June, and 5.6 mph from July through December. Mean annual wind speed is 6.4 mph ([Tables 2.3-209](#) through [2.3-221](#)).

The Greenville/Spartanburg meteorological station winds are presented graphically in [Figures 2.3-205](#) through [2.3-217](#). These wind roses cover the period from 1997 through 2005 and represent the frequency of winds from a particular direction by the length of the line in that direction. Greenville/Spartanburg data shows a usual pattern of winds coming from the northeast or southwest. During the fall, winds from the northeast are more common. At Greenville/Spartanburg, winds from the northwest or southeast occur infrequently.

2.3.2.1.2 Lee Nuclear Site Wind Distribution

For the Lee Nuclear site, the annual wind direction frequency is fairly uniform with the NW direction slightly more frequent at approximately 15 percent. Wind from the West was the least frequent at about 3 percent. At the Lee Nuclear site, winds average 5.3 mph from January through June, and 4.5 mph from July through December. Mean annual wind speed is 5.0 mph ([Tables 2.3-222](#) through [2.3-234](#)).

Monthly wind roses for the Lee Nuclear site are given in [Figures 2.3-218](#) through [2.3-229](#) and seasonal wind roses are given in [Figures 2.3-230](#) through [2.3-233](#). On a seasonal basis, the prevailing wind direction is from the northwest. This is also shown on the annual wind rose given in [Figure 2.3-203](#). Joint frequency distributions of wind speed and direction by atmospheric stability class are

provided in [Tables 2.3-235](#) through [2.3-241](#). Stability classes are as defined in Regulatory Guide 1.23 (see [Subsection 2.3.4.2](#)).

2.3.2.1.3 Wind Direction Persistence

Hourly weather observation records from the NWS at Greenville/Spartanburg, South Carolina, for the years 1997 through 2005 were examined for wind direction persistence. The longest persistence periods from a single sector (22.5 degrees), three adjoining sectors (67.5 degrees), and five adjoining sectors (112.5 degrees) were determined from each sector during each year. The results are shown in [Tables 2.3-242](#) through [2.3-244](#). During the period, the single sector maximum persistence was greatest (23 hours) for the NE direction. The average maximum persistence (14.0 hours) was greatest for the NE direction. For the persistence in three adjoining sectors, the NE sector had the longest period of persistence (82 hours). The largest average maximum persistence (57.8 hours) was also for the NE sector, as shown in [Table 2.3-243](#). The longest persistence period (150 hours) from five adjoining sectors occurred in the NE sector ([Table 2.3-244](#)). The NE sector also showed the greatest average maximum persistence (91.0 hours).

For the Lee Nuclear Station site, the single sector maximum persistence was greatest (15 hours) for the NW direction. For the persistence in three adjoining sectors, the NW sector had the longest period of persistence (45 hours). The longest persistence period (71 hours) from five adjoining sectors occurred in the NNE sector ([Table 2.3-245](#)).

2.3.2.2 Air Temperature

In the Lee Nuclear site area, January average maximum temperatures are between 50 and 55°F with average minimums between 25 and 30°F (see [Figures 2.3-234](#) and [2.3-235](#)). In July, average minimum temperatures are in the vicinity of 65 to 70°F, while the average maximum is between 85 and 90°F, (see [Figures 2.3-236](#) and [2.3-237](#)). The maximum and minimum mean temperatures at the Ninety-Nine Islands weather station in Blacksburg, South Carolina are given in the monthly climate summary [Table 2.3-246](#). The daily maximum, minimum, and average temperatures from the Ninety-Nine Islands weather station, spanning the years 1971 - 2000, are given in [Figure 2.3-238](#).

The annual average maximum monthly temperature at the Ninety-Nine Islands weather station from 8/1/1948 to 12/31/2005 was 71.5°F, and the annual average minimum monthly temperature was 45.6°F. The average maximum monthly temperature was 89.0°F in July, and the average minimum monthly temperature was 26.7°F in January.

Data from the Southeast Regional Climate Center indicates that temperature extremes for Ninety-Nine Islands, South Carolina, for the years 1971 through 2000 have ranged from the highest mean temperature of 94.4°F (July 1993) to the lowest mean minimum temperature of 17.2°F (January 1977) ([Reference 203](#)). [Table 2.3-246](#) presents the temperature means and extremes for Ninety-Nine Islands collected over a 30-year period.

The maximum temperature at the Lee Nuclear Station site during the 2005-2006 data collection period was 96°F and the minimum was 20°F which is within the bounds of the historic record for Ninety-Nine Islands, South Carolina (see [Figure 2.3-238](#)). The temperature range at the Lee Nuclear Station site is consistent with the temperature ranges for Ninety-Nine Islands and the Greenville/Spartanburg areas. For the Lee Nuclear Station site, the 0% exceedance dry bulb temperature was determined in accordance with the definition provided by Westinghouse AP1000 DCD, Tier 2 [Table 2-1](#) and FSAR [Table 2.0-201](#). The maximum coincident dry bulb/wet bulb temperature limit is based on the maximum dry bulb temperature that has existed for 2 hours or more combined with the maximum wet bulb temperature that exists in that population of dry bulb temperatures. Consequently, the term “coincident wet bulb temperature” is not defined in the same way as used in ASHRAE “Climatic Design Information” (i.e., the Mean Coincident Wet Bulb, MCWB), [Reference 238](#).

The DCD specifies that “[t]he Combined License applicant must provide information to demonstrate that the site parameters are within the limits specified for the standard design.” Consistent with the Westinghouse methodology described above, the highest dry bulb temperature that persists for at least 2 hours has been determined to be 103°F from a 45-year (1963-2007) sequential hourly meteorological data set for the NWS station at Greer Greenville/Spartanburg Airport, South Carolina (see [Table 2.3-293](#)). The highest of the coincident wet bulb temperatures has been determined to be 78°F.

Similar to the approach described above for determining the maximum safety dry bulb temperature, the highest (non-coincident) wet bulb temperature that persists for at least 2 hours has been determined to be 81°F from the 45-year sequential hourly meteorological data set for the Greer Greenville/Spartanburg Airport NWS station. The minimum safety dry bulb temperature persisting for at least 2 hours was also determined, using the approach discussed above, to be -1°F.

1% Seasonal Exceedance Dry Bulb and Wet Bulb Temperature

As described in [DCD Table 2-1](#), the 1% seasonal exceedance is approximately equivalent to the 0.4% annual exceedance. The maximum normal limits represent the maximum normal range of operation for power generation systems. The maximum coincident normal temperature limit is based on a 1% seasonal exceedance dry bulb temperature that persists for two hours or more in historical meteorological data. The complementary coincident wet bulb temperature is not selected based on a median or a maximum value from the 0.4% annual exceedance coincident data set. Since a slightly lower dry bulb temperature with its complementary coincident wet bulb temperature may be more limiting, the 0.4% annual exceedance wet bulb value, disregarding any hourly persistence limitation, was selected as the coincident wet bulb temperature. This methodology specified by Westinghouse is considered a conservative approach to the selection of the maximum normal coincident condition. Based on the 45-year sequential hourly meteorological data set for the Greer Greenville/Spartanburg Airport NWS station, the 0.4% annual exceedance dry bulb temperature was 94°F and the coincident 0.4% annual exceedance wet bulb temperature was 77°F.

The maximum normal non-coincident wet bulb temperature limit is the 0.4% annual exceedance wet bulb temperature that has existed at the site for 2 hours or more based on historical meteorological data. From the 45-year sequential hourly meteorological data set for the Greer Greenville/Spartanburg Airport NWS station, the maximum normal non-coincident wet bulb temperature was determined to be 77°F.

100-Year Return Period Dry Bulb and Wet Bulb Temperature

Because reliable, sequential hourly meteorological data sets do not exist for durations of 100 years, the maximum 100-year return period dry bulb temperature value must be extrapolated. The maximum 100-year return period dry bulb temperature was calculated using the 45-year sequential hourly meteorological data set for the Greer Greenville/Spartanburg Airport NWS station, and was based on methodology provided in ASHRAE Fundamentals Handbook 2001, Chapter 27 – Climatic Design Information ([Reference 238](#)). See Equations 1 and 2 below:

$$T_n = M + IFs \quad \text{Equation 1}$$

where:

T_n = n -year return period value of extreme dry bulb temperature to be estimated, years

M = mean of the annual extreme maximum or minimum dry bulb temperatures, °F

s = standard deviation of the annual extreme maximum or minimum dry bulb temperatures, °F

$I = 1$, if maximum dry bulb temperatures are being considered

$I = -1$, if minimum dry bulb temperatures are being considered

$$F = -\frac{\sqrt{6}}{\pi} \left\{ 0.5772 + \ln \left[\ln \left(\frac{n}{n-1} \right) \right] \right\} \quad \text{Equation 2}$$

The resultant maximum 100-year return period dry bulb temperature was 107°F.

Since the maximum 100-year return period dry bulb temperature value was extrapolated, there are no occurrences of maximum dry bulb temperatures to pair with concurrent wet bulb temperature values to determine a coincident wet bulb temperature. In order to calculate a 100-year return period coincident wet bulb temperature, the 45-year sequential hourly meteorological data set for the Greer Greenville/Spartanburg Airport NWS station was used to develop a dry bulb to coincident wet bulb correlation curve. The 100-year return period coincident wet-bulb temperature methodology was determined using a dry-bulb to coincident

wet-bulb correlation curve reflective of the entire meteorological data set. The resultant 100-year return period coincident wet bulb temperature was 84°F.

Similar to the approach described above for determining the maximum 100-year return period dry bulb temperature, the maximum 100-year return period wet bulb temperature (non-coincident) was calculated to be 85°F using the 45-year sequential hourly meteorological data set for the Greer Greenville/Spartanburg Airport NWS station. Likewise, the minimum 100-year return period dry bulb temperature was calculated to be -5°F.

2.3.2.3 Atmospheric Moisture

All of South Carolina experiences moderately high humidity during much of the year. At Greenville/Spartanburg, during the years 1997-2005, humidities of 50 percent or higher have occurred at any hour of the day. Mean relative humidities for four time periods per day at Greenville/Spartanburg are shown in [Table 2.3-255](#). The highest humidity is most frequent in the early morning hours with an annual average of 81 percent. At times in the summer, a combination of high temperatures and high humidities develops; this usually builds up progressively for several days and becomes oppressive for one or more days. Lower humidities on the order of 50 percent occur on some days each month, usually in the early afternoon hours. ([Reference 224](#)).

Relative humidity in Blacksburg, South Carolina, averages near 70 percent for the year ([Figure 2.3-239](#)). Climatic records of humidity in Greenville/Spartanburg are shown in [Table 2.3-253](#). These data show that relative humidity in the region is high throughout the year. Nighttime relative humidities are highest in summer and lowest in the winter. Daytime humidities are highest in the summer. Seasonal variations are in the vicinity of 5 to 15 percent. Highest relative humidities occur in the early morning hours (00:00 - 6:00 a.m.), averaging greater than 81 percent during all months. Lowest relative humidities occur during the afternoon with averages below 60 percent for all months. The temperature regime of the region can be described by the data shown in [Table 2.3-254](#).

Similar relative humidity data for the Lee Nuclear Station site is presented in [Table 2.3-255](#). As shown, the site humidity follows the same pattern as the Greenville/Spartanburg data with the highest humidity in the early morning hours with an annual average of 86 percent. The afternoon average relative humidity is 50 percent at the Lee Nuclear Station site.

2.3.2.3.1 Precipitation

Precipitation averages 48.37 inches annually at the Ninety-Nine Islands meteorological station and is generally well distributed throughout the year ([Table 2.3-246](#)). The annual precipitation during the fall months (September - November) is slightly less than 12 inches (11.6 inches), and the other seasons have an annual precipitation of more than 12 inches. April is the driest month with an average precipitation of approximately 3 inches (see [Table 2.3-246](#)). Precipitation data from the 2005-2006 data period at the Lee Nuclear site is in general agreement with the longer-term data record from Ninety-Nine Islands with

a total rainfall of 39.72 inches. This total is below the long-term mean of 47.34 inches for Ninety-Nine Islands but is above the long-term low of 32.27 inches.

For Greenville/Spartanburg, the maximum normal mean monthly precipitation is in March (5.31 inches) based on 30 years of data from the NCDC ([Reference 240](#)), and the minimum monthly mean (3.54 inches) occurs in April. Based on 45 years of data from the NCDC ([Reference 240](#)), the maximum monthly precipitation in Greenville/Spartanburg is 17.37 inches, which occurred in August 1995 from tropical storm Jerry ([Table 2.3-256](#)). [Table 2.3-256](#) provides the monthly frequency distribution of rainfall rates at the Greenville/Spartanburg meteorological station. [Table 2.3-201](#) gives the monthly rainfall intensity frequency distribution for the Greenville/Spartanburg meteorological station.

The maximum short period precipitation frequency for this region is given in [Table 2.3-257](#) ([Reference 225](#)). [Figure 2.3-240](#) shows the annual precipitation wind rose for Greenville/Spartanburg, South Carolina, based on data from the years 1997 through 2005 and [Figure 2.3-241](#) gives the annual precipitation wind rose for the Lee Nuclear Station site. [Table 2.3-258](#) provides the monthly precipitation by direction at Greenville/Spartanburg. This data shows that the highest rainfall frequency at Greenville/Spartanburg occurs most often in the months of November through April, and the most common directions are N through ENE. Winds speeds during precipitation average 7.1 mph annually.

[Figure 2.3-242](#) gives the average total monthly precipitation for Ninety-Nine Islands, South Carolina for the period of 1948 through 2005. The daily precipitation average and extreme is given in [Figure 2.3-243](#) for the same time period. Similar data for the Lee Nuclear Station site is provided in [Table 2.3-259](#). This data shows that the highest rainfall frequency is during the months of October through January and the highest frequency directions are N through NE. The Lee Nuclear Station site monthly rainfall frequency distribution is given in [Table 2.3-260](#) and the maximum 24-hour rainfall is given in [Table 2.3-261](#). Monthly precipitation wind roses for Greenville/Spartanburg are given in [Figures 2.3-248](#) through [2.3-259](#). Similar figures for the Lee Nuclear Site are given in [Figures 2.3-260](#) through [2.3-271](#).

2.3.2.3.2 Snow

Snowfall is not a rare event in north central South Carolina. During the 59 years from 1947-48 through 2005-06, measurable snow fell on Ninety-Nine Islands in 24 years. As [Table 2.3-262](#) shows, during these 59 years, snow or sleet fell in January in 11 years and February in 12 years ([Reference 203](#)). Average winter snowfall at the Ninety-Nine Islands meteorological station is three inches ([Table 2.3-262](#)).

Annual average snowfall in the area of the Lee Nuclear Station site is estimated to be approximately 3.0 inches. This estimate is based on 59 years of record (1948-2005) at Ninety-Nine Islands ([Reference 203](#)). The monthly and annual snowfall at Ninety-Nine Islands is given in [Table 2.3-262](#). [Figure 2.3-244](#) provides the daily snowfall average and extreme for Ninety-Nine Islands between 1948 and 2005.

The maximum monthly snowfall at Ninety-Nine Islands was 14 inches in February 1978-79 ([Reference 203](#)).

The Southeast Regional Climate Center snowfall records for Ninety-Nine Islands (8/1/1948 through 12/31/2005) give a maximum 24-hour snowfall of 13.0 inches ([Reference 203](#)).

2.3.2.3.3 Fog

Fog is an aggregate of minute water droplets suspended in the atmosphere near the surface of the earth. According to international definition, fog reduces visibility to less than 0.62 miles. [Table 2.3-263](#) indicates that, over the period 1997 to 2005, Greenville/Spartanburg has averaged approximately 38 hours/year of fog with November, December, and January having the greatest frequency of fog.

2.3.2.4 Atmospheric Stability

The frequency and strength of inversion layers are evaluated using seven years of weather balloon data collected at the Greensboro radiosonde station ([Reference 226](#)). Weather balloons are released twice daily at 0:00 GMT (7:00 p.m. EST) and 12:00 GMT (7:00 a.m. EST) to obtain vertical profiles of temperature, wind, and dewpoint temperature. The monthly data are provided in [Tables 2.3-264](#) through [2.3-275](#) in terms of number of mornings and afternoons containing inversions, average inversion layer elevation, and the average strength of the inversions. [Table 2.3-276](#) provides annual average data for the period. An inversion is defined as any three readings on a sounding that show temperatures increasing with elevation (below 3000 meters). The inversion layer height is the point (found by interpolation between readings) at which temperature again starts to decrease with elevation. The maximum inversion strength is the maximum temperature rise divided by elevation difference within the inversion layer.

2.3.2.4.1 Mixing Heights

Mixing heights for Greensboro, North Carolina, are shown in [Table 2.3-277](#). These were obtained from the EPA Support Center for Regulatory Atmospheric Modeling (SCRAM) Mixing Height Data collection for the period 1984-1987 and 1990-1991 ([Reference 206](#)). The average mixing heights in the mornings are lowest during the fall, and the average mixing heights in the afternoon are lowest in the winter.

Based on the EPA's SCRAM mixing height data for Greensboro, North Carolina ([Reference 206](#)), the mean morning mixing height for the area is approximately 470 meters in the winter, 475 meters in the spring, 470 meters in the summer, 380 meters in the fall, and 450 meters annually. The mean afternoon mixing height for the area is about 860 meters in the winter, 1540 meters in the spring, 1610 meters in the summer, 1140 meters in the fall, and 1290 meters annually (see [Table 2.3-277](#)).

The ventilation rate is a measure of the dispersion of pollutants. Higher ventilation rates are better for dispersing pollution than lower ventilation rates. Mean ventilation rates by month for Greensboro, North Carolina, are given in

Table 2.3-207. This data was obtained from EPA SCRAM mixing height data (Reference 206) for the years 1984-1987 and 1989-1991.

Morning ventilation is less than 4000 m²/s throughout the year and is less than 2700 m²/s from May through October. Afternoon ventilation is higher than 7000 m²/s from February through July but lower than 6300 m²/s from August through January. Based on this and the tendency of pollutants to increase in the surface layer during the course of a day, the highest daily air pollution potentials exist during the afternoon from August through January when ventilation rates are lower. Lowest air pollution potentials occur in the spring due to the relatively high mean ventilation rates.

2.3.2.5 Potential Influence of the Plant and Its Facilities on Local Meteorology

The potential for the operation of Units 1 and 2 at the Lee Nuclear site to influence the local climatology is discussed in this section. It is concluded that impacts will be negligible.

The only aspects of the Lee Nuclear Station site that could be categorized as contributing to a unique micro-climate are the presence of the Ninety-Nine Islands Reservoir and the Broad River. The proximity of the river increases the local humidity. There is also a slight tendency for lower level winds to be channeled along the river valley.

New construction at the site is not expected to impact this climatic situation significantly. Although there will be some ground leveling, there are no significant climate-shaping topographic features to be changed. The site is already a relatively flat area with more significant hills to the northwest and southwest that will not be impacted by construction (refer to **Figure 2.3-245** for a depiction of topography around the site). There may be some tree removal, but the trees within the construction area are small in number compared to the surrounding forested land. There are no significant changes anticipated or proposed in terms of local hydrologic features. There are no changes to local roadways anticipated in support of the proposed new facility which would impact the local climate. The impacts of more structures, facilities, or activities in this relatively remote, rural area are not expected to be noticeable in terms of local meteorology. The topography of the regional areas within 50-miles and 5-miles of the Lee Nuclear Site are shown in **Figure 2.3-245**.

Operation of power generation units can affect the local environment in three ways, additional generation of particulates (increased fog or haze), temperature effects on local water sources, and cooling tower plume effects. Since the proposed unit is nuclear, any increase in particulate emissions during operation would be due to a modest increase in automobile traffic and the infrequent operation of diesel generators. Therefore it can be concluded that the net increase in particulates will be negligible and will not cause any noticeable environmental effects.

Lee Nuclear Station Units 1 and 2 utilize cooling towers, so that the vast majority of rejected heat would go to the atmosphere. The amount of heat input to the flow of the Broad River would be relatively small, with little impact on local meteorology.

The remainder of this section discusses the cooling tower plume effects. From the wind rose of [Figure 2.3-203](#), it can be seen that the prevailing winds are from the northwest. This means that the cooling tower plumes will usually extend out over the Lee Nuclear Station site itself. Therefore, it can be concluded that most of the local climatological effects such as increased moisture and shading will be limited to the Lee Nuclear Station site.

2.3.2.5.1 Cooling Tower Plumes

The following discussion focuses on an evaluation of cooling tower plume effects. An assessment of the contribution of moisture to the ambient environment from cooling tower blowdown waste heat discharge is included. Finally, a qualitative evaluation of the effects of the cooling system on daily variations of several meteorological parameters is presented.

The operation of two circular mechanical draft cooling towers (CMDCTs) for each unit at the site will result in the emission of small water droplets entrained in the tower air flow (i.e., drift). The droplets contain the dissolved solids found in the circulating water (e.g., salts) that may eventually deposit on the ground as well as on structures and vegetation. The drift droplet emissions are controlled by the use of drift eliminators that rely on inertial separation caused by exhaust flow direction changes. State-of-the-art drift eliminators installed in the CMDCTs are capable of reducing the emissions to approximately 0.0005 percent of the circulating water flow. In addition to drift emissions, there is another potential impact of the cooling towers to the environment. The warm saturated air leaving the towers is cooled by the ambient air such that the water vapor condenses into a visible plume that may persist for some distance downwind depending on meteorological conditions (e.g., wind speed, relative humidity). These visible plume occurrences may pose some aesthetic and ground shadowing impacts. Under relatively high wind speeds and humid conditions, the aerodynamic wake turbulence caused by air flowing around the tower housing may result in the visible plume touching down causing ground level fogging and, under freezing conditions, icing.

An analysis of the potential environmental impacts caused by the operation of CMDCTs was conducted using the Electric Power Research Institute (EPRI) sponsored Seasonal/Annual Cooling Tower Impact (SACTI) Program. This model is considered a state-of-the-art cooling tower impact model by EPRI and the nuclear industry. It was developed by Argonne National Laboratory (ANL) using the knowledge obtained from extensive research conducted on cooling tower environmental effects. The SACTI model provides salt drift deposition pattern (i.e., kg/km^2 per month) as a function of distance and direction from the cooling towers as well as the frequency of occurrence of visible plumes, hours of plume shadowing, and ground level fogging and icing occurrences by season resulting from the operation of the cooling towers. The most recent 5-year database (i.e.,

2001-2005) from the National Weather Service (NWS) site in Charlotte, North Carolina, was used in the SACTI analysis. Additionally, the seasonal mixing height values for Greensboro, North Carolina ([Reference 219](#)), are used in the SACTI model. Appendix 2DD provides justification for use of this five-year meteorological dataset as reasonably representative of the conditions expected at the Lee Nuclear Station site.

The SACTI results, as presented in [Table 2.3-278](#), indicate that the majority (i.e. >50 percent) of the visible plumes do not reach 1000 meters downwind and 300 meters in height. The longest and largest visible plumes occur in the winter with smaller plumes occurring in the spring and fall seasons due to the cold air in winter causing condensation of the moist plumes more readily than in the warmer seasons (i.e., cold air has a much smaller capacity of holding water vapor). The summer visible plumes are noticeably smaller since warmer ambient air results in less condensation of the moist plumes due to its ability to accommodate higher water vapor concentrations. On an annual basis, 40 percent of the plumes reach 500 meters downwind and 230 meters in height. The winter visible plume length frequency as a function of direction is shown on [Figure 2.3-274](#). The winter visible plume radius frequency as a function of direction is shown on [Figure 2.3-275](#).

The largest visible plumes shown in [Table 2.3-278](#) reach a distance of 9900 meters (6.15 miles) downwind of the towers and a height of approximately 1600 meters and occur approximately one percent of the time. It should be noted that the longest plumes occur during conditions of high ambient relative humidity that are conducive to natural fog formation and poor visibility conditions. Under these conditions, the atmosphere is already at, or close to, saturation. Therefore, the largest plumes may not be discernable from the ambient fogging conditions.

[Table 2.3-279](#) provides the downwind distances at which plume shadowing effects are felt for a range of hours of occurrence by season. Consistent with the visible plume frequency results, most shadowing occurs in the winter season with lesser amounts in the spring and fall and the least amounts in the summer. The hours of plume shadowing during the winter season are given in [Figure 2.3-276](#). Annually, plume shadowing effects reach 1200 meters downwind 1 percent of the time with the farthest impact reaching approximately 4000 meters downwind for 0.5 percent of the time. The SACTI output also shows that there are no occurrences of ground level fogging. More importantly, no occurrences of ground level icing are predicted.

The salt deposition pattern shown in [Table 2.3-280](#) indicates that there is negligible salt deposition with the highest amount being approximately $1.03 \text{ kg/km}^2/\text{month}$ occurring 200 meters north of the towers in the summer. All other salt deposition amounts are below $1 \text{ kg/km}^2/\text{month}$. On an annual basis, the largest amount of deposition is $0.71 \text{ kg/m}^2/\text{month}$ occurring 200 meters north of the towers. The summer salt deposition rate as a function of downwind sector is shown on [Figure 2.3-277](#). The maximum salt deposition amount can be compared with a value of $400 \text{ kg/km}^2/\text{month}$ below which damage to vegetation is not expected to occur according to a study of the environmental effects of cooling towers. In addition, according to NUREG-1555, general guidelines for predicting

effects of drift deposition on plants suggest that many species have thresholds for visible leaf damage in the range of 10 to 20 kg/ha/mo of NaCl deposited on leaves during the growing season. This range of deposition corresponds to 1000 to 2000 kg/km²/month. Therefore, no impacts on vegetation are expected.

While salt deposition from evaporative cooling towers has the potential to build up on bushings of electrical equipment such as transformers, switchyard equipment, and transmission lines, IEEE C57.19.100-1995 "IEEE Guide for Application of Power Apparatus Bushings" (Reference 241), Section 9 and Table 1, indicates that environments of less than 0.03 mg/cm² are below the typical measured equivalent salt deposition threshold to be designated the lowest level of contamination.

Assuming the worst case seasonal potential salt deposition rate of 1.03 kg/km²/month (0.000103 mg/cm²/month), based on 5 years of CLT meteorological data and no washing/cleaning from rain/wind at the Lee Nuclear Station site for an entire month, the result would be a monthly accumulation of only 0.34 percent (0.34%) of the 0.03 mg/cm², or 300 kg/km² threshold amount for contamination designation by IEEE C57.19.100-1995. If it was assumed that no washing occurred over an entire year, the annual accumulation rate of 0.000071 mg/cm²/month would result in only 2.8 percent (2.8%) of the threshold amount. Using the annual salt deposition rate of 0.000071 mg/cm²/month and no washing/cleaning of electrical equipment and insulators from rain/wind, it would take 422 months (35+ years) before the buildup would equal the minimum buildup level classified as contaminated environment by IEEE C57.19.100-1995.

Due to natural wash off from local precipitation, total deposits are not expected to ever reach a level requiring attention. Therefore, none of the outdoor electrical equipment in the transformer yard or the switchyard requires special consideration for application in the environment at the Lee Nuclear Station site, and cooling tower plume generated salt deposits are not expected to adversely affect any electrical equipment at the Lee Nuclear Station site.

Plant heating, ventilation and air conditioning (HVAC) intakes and equipment are located at distances ranging approximately 200 to 800 meters from the centerline of either group of Unit 1 or Unit 2 cooling towers. Due to the spatially distributed nature of the cooling towers and plant equipment, cooling tower plumes from a wide range of plume directions could potentially impact plant equipment. Plume trajectories moving downwind from Unit 1 cooling towers toward sectors ranging from NE to ESE could potentially result in exposure of HVAC intakes and plant equipment to salt deposition from Unit 1 cooling tower plumes, while plume trajectories from Unit 2 cooling towers toward sectors ranging from WSW to NW could potentially result in salt deposition from Unit 2 cooling tower plumes.

Table 2.3-280 shows that the maximum salt deposition rate anticipated at the distance range and directions where HVAC intakes and equipment are located is less than 0.00004 mg/cm²/month. Based on guidance provided by IEEE C57.19.100-1995, it would take more than 750 months (62.5 years) of buildup without washing/cleaning from rain/wind before the threshold for low level

contamination would be reached. Therefore, impacts from cooling tower plume salt deposition on HVAC intakes or equipment are negligible.

The maximum predicted water deposition rate, occurring during the fall season, is 740 kg/km²/month at a downwind distance of 900 meters SE of the cooling towers. The water deposition rate during the fall is shown in [Figure 2.3-278](#). This deposition rate is the rainfall equivalent of 0.00003 inch per month based on the density of water (i.e., 1000 kg/m³), which is a trivial amount. The NWS considers precipitation of less than 0.01 inch as a trace amount.

The drift deposition results are indicative of the performance of the state-of-the-art drift eliminators, minimizing the size of the drift droplets. Small drift droplet sizes tend to evaporate and remain suspended in air. The entrained salt particles would then separate from the vapor and would either deposit out or remain suspended in the air. The trivial drift deposition that does occur is most likely the result of meteorological conditions conducive to reduced plume rise (i.e., stronger wind speeds). The use of fresh water as make-up minimizes the total dissolved solids content of the circulating water.

2.3.2.6 Topographical Description of the Surrounding Area

The Lee Nuclear site is located approximately 1000 yards west of the Broad River with mountain ridges of 1000 to 2500 feet above msl to the northwest, north, and northeast. The elevation range over most of the site is approximately 500 to 660 feet above msl.

The terrain surrounding the Lee Nuclear Station site is dominated by Silver Mine Ridge 2.8 miles across the Broad River to the northwest. This ridge runs in a north-east to south-west direction and is 800 feet above mean sea level (MSL) through this area. To the north and west, the terrain is flatter and wooded. The only significant feature in this direction is Draytonville Mountain (see [Figure 2.5.1-221](#)), located 4.7 miles west, which has an elevation of approximately 1000 feet above mean sea level. The terrain in the immediate vicinity of the Lee Nuclear Station site can be described as gently rolling hills. The only notable terrain feature in the immediate vicinity of the site is McKowns Mountain to the SSW with an elevation of approximately 800 feet (approximately 200 feet above the site grade elevation). [Figure 2.3-246](#) presents the terrain elevation profiles within 50 miles of the Lee Nuclear Station site. ([Reference 227](#)). Topographic maps of the areas within 50 miles and 5 miles of the Lee Nuclear Site are shown on [Figure 2.3-245](#).

2.3.2.7 Current and Projected Site Air Quality Conditions

Attainment areas are areas where the ambient air quality levels are better than the EPA-designated (national) ambient air quality standards. The Lee Nuclear Station site is located within the Greenville-Spartanburg Intrastate Air Quality Control Region (AQCR). This region is designated as being in non-attainment for 8-Hr Ozone ([Reference 228](#)). Currently, Cherokee County is designated as attainment for all criteria pollutants. Criteria pollutants are those for which National Ambient

Air Quality Standards (NAAQS) have been established (i.e., sulfur dioxide (SO₂), fine particulate matter (PM₁₀), carbon monoxide (CO), nitrogen dioxide (NO₂), ozone (O₃), and lead (Pb)) (National Ambient Air Quality Standards, 40 CFR Part 50).

South Carolina is also subject to the revised 8-hour O₃ standard and the new standard for PM_{2.5} (fine particulate matter with an aerodynamic diameter of less than or equal to 2.5 microns), both promulgated by the EPA in July 1997 in accordance with 62 CFR Part 38711.

These air quality characteristics are not expected to be a significant factor in the design and operating bases of Units 1 and 2. The new nuclear steam supply system and other related radiological systems are not sources of criteria pollutants or other air toxics. The addition of supporting auxiliary boilers, emergency diesel generators, and station blackout generators (and other non-radiological emission sources) are not expected to be significant sources of criteria pollutant emissions because these units operate on an intermittent test and/or emergency basis.

2.3.3 ONSITE METEOROLOGICAL MEASUREMENT PROGRAMS

WLS COL 2.3-3 The meteorological monitoring program is described in this section. This program will provide continuous monitoring from the preapplication through the operational phases. The meteorological monitoring program for the construction and operational phases will entail relocation of the meteorological tower to a permanent site outside the influence of the permanent plant structures.

2.3.3.1 Onsite Meteorological Monitoring Program

The meteorological monitoring for the pre-construction phase utilized the meteorological tower (Tower 2), located east of the planned Nuclear Island. Either prior to or during the construction phase, Tower 2 is expected to be terminated. The Permanent Meteorological (MET) Tower is installed and located for use during the construction and operational phases. The Permanent MET Tower was formerly named Tower 3.

Calculations to determine diffusion estimates for both short- and long-term conditions are provided in [Subsections 2.3.4](#) and [2.3.5](#), respectively. These analyses were completed using data from the meteorological Tower 2. The short-term and long-term χ/Q modeling is based on the 24-month period from December 1, 2005 to November 30, 2007.

The locations of meteorological Towers 1 and 2 relative to other preapplication structures are shown on [Figure 2.3-247](#). The local topography for the Lee Nuclear Site is shown on [Figure 2.3-245](#). These figures illustrate that the location of

meteorological Tower 2 is sufficiently removed from any existing structures or significant topographic features. This ensures that the system provides adequate data to represent onsite meteorological conditions and to describe the local and regional atmospheric transport and diffusion characteristics prior to construction.

The Permanent MET Tower is located relative to permanent plant structures as shown in [Figure 1.1-202](#). This figure illustrates that the location of the Permanent MET Tower is sufficiently removed from permanent plant structures and topographical features, meeting the “10L” guidance of Regulatory Guide 1.23, Revision 1. This ensures that the system provides adequate data to represent onsite meteorological conditions and to describe the local and regional atmospheric transport and diffusion characteristics during the operational phase.

The Tower 1 meteorological installation encompassed an original 55-meter (m) tower and a 10-m tower from the original Cherokee Nuclear site. Tower 1 was located at 588 ft. msl roughly 5 ft. lower than the future final grade of the Lee Nuclear Station containment structures. Because of its large size (e.g., transmission style tower), Tower 1 did not meet the structural requirements of Regulatory Guide 1.23, Revision 1, “Meteorological Monitoring Programs for Nuclear Power Plants.” Consequently, Tower 1 data was not used for the Lee Nuclear Station COLA analyses and are not discussed further. Tower 1 was decommissioned in May 2011.

Tower 2 is a 60-m meteorological tower, located on the east side of the power block. This tower is representative of both the wider site area and regional weather conditions. The base elevation for Tower 2 is approximately 611 ft., or approximately 18 ft. above the 593 ft. plant elevation. Data collection from this meteorological tower began on December 1, 2005.

The Permanent MET Tower to be utilized during the operational phase of the plant is a 60-meter tower located north and west of Tower 2 as shown on [Figure 1.1-202](#). The Permanent MET Tower is located at a base elevation of 595.5 ft. The tree line and vegetation around the Permanent MET Tower are periodically maintained to ensure an open exposure meeting the “10 obstruction heights” criterion.

Instrument Description

All instrumentation and measurements associated with Tower 2 and the Permanent MET Tower meet the guidance provided in Regulatory Guide 1.23, Revision 1 (March 2007). The specifications for the meteorological tower instrumentation are provided in [Table 2.3-281](#).

Tower 2 serves as the representative meteorological tower at Lee Nuclear site for the preapplication phase. Tower 2 and the Permanent MET Tower are instrumented at two levels, 10 m and 60 m, and measure temperature, wind speed, wind direction, and vertical temperature gradient. Dewpoint is also measured at the 10-meter level. Station pressure and temperature are measured at the 2-meter level in addition to ground-level precipitation. See [Table 2.3-281](#) for a complete listing of the instrumentation provided. Note that some parameters are

optional. A system of lightning and surge protection circuitry with proper grounding is included in the facility design. Replacement sensors, which may be of a different manufacturer or model, satisfy the requirements of Regulatory Guide 1.23, Revision 1.

Trees and vegetation were cleared around Tower 2 and the Permanent MET Tower to ensure an open exposure, meeting the "10 obstruction heights" criterion. Instrument booms are oriented in the northwest direction (298 degrees relative to true north for Tower 2 and 300 degrees for the Permanent MET Tower) on the tower, with a boom length of 8 ft.

Data recovery from the Tower 2 instrumentation, based on evaluation of data from December 2005 to November 2006, was 96.5 percent for wind direction, wind speed, and delta temperature after screening the data using flagging criteria based on NUREG-0917, "Nuclear Regulatory Commission Staff Computer Programs for Use with Meteorological Data." Prior to this additional flagging, the data recovery for the Tower 2 meteorological quality-assured data was 99.2 percent for the same period. Data recovery for the second year of data (from December 2006 through November 2007) for the Tower 2 instrumentation was 95.7 percent for wind direction, wind speed, and delta temperature after screening the data using flagging criteria based on NUREG-0917. Prior to this additional flagging, the joint recovery for wind direction, wind speed, and delta temperature for the quality-assured data was 98.0 percent for the second year of data. Data recovery for the two-year combined data set was 96.1 percent for wind direction, wind speed, and delta temperature.

2.3.3.2 Meteorological Data Processing

The data management process for Lee Nuclear Station Site meteorological data involves three basic steps:

- Data acquisition ([Subsection 2.3.3.2.1](#))
- Data processing ([Subsection 2.3.3.2.2](#))
- Data validation ([Subsection 2.3.3.2.3](#))

This subsection includes a summary of the data collection methods and description of the processing and evaluation of the data.

2.3.3.2.1 Data Acquisition

The meteorological data collection system is designed and replacement components are chosen to meet or exceed specifications for accuracy identified in Regulatory Guide 1.23, Revision 1.

All wind speeds are recorded in miles per hour. Wind directions are measured on a 0-540 analog scale and recorded on a digital 0-360 degrees scale. Temperatures are recorded in degrees Celsius (°C). The precipitation measurement is a digital step trace, each step representing 0.01 inches.

One-minute data traces can be generated electronically, eliminating the need for stripcharts.

Electronic signals from individual instrument sensors on the tower, or otherwise placed at the meteorological sites, are sent to the signal conditioning equipment in the co-located instrument shelter/building, and from there to the datalogger. The on-site meteorological data are recorded in digital form in the archive. Some additional processing is performed by the datalogger, resulting in the final meteorological measurements.

The measured data are stored by the datalogger and available for remote access. The amount of datalogger storage is affected by the number of parameters and averaging intervals. Typical storage is 4 days or longer. The data are downloaded from the datalogger by a dedicated computer (i.e. "central PC") at the Duke Energy Environmental Center (Huntersville, NC) for validation, reporting, and archiving. The data are remotely polled and downloaded from the on-site datalogger at each tower, via modem, over data lines installed on-site.

Data quality assurance and archiving of final data occur via the designated, "central PC" located in the Environmental Center. The on-site meteorological data are recorded in digital form.

2.3.3.2.2 Data Processing

The equipment processors and datalogger control data acquisition at each tower location. The output of each meteorological sensor is scanned periodically, scaled, and the data values are stored as one-minute averages and one-hour averages, or totals. For precipitation, the total accumulation for the minute and hour is recorded. The datalogger does not store one-minute data for the calculated parameters (i.e., delta-T and sigma-theta). Digital data compiled as 15-minute averages, as detailed in Regulatory Guide 1.23, are provided for real-time display in the appropriate emergency response facilities (e.g., control room, technical support center, and emergency operations facility).

Datalogger channels are sampled at a minimum of every second; sampling for measured parameters may be more frequent. For the measured data points, one-minute and one-hour averages are calculated and recorded. The quality of the samples is reflected in the quality of the averages. The time the average was calculated is recorded with each value. Software data processing routines within the dataloggers accumulate output and perform data calculations to generate the data sampling averages and totals.

The datalogger checks each piece of data to assure it is between the datalogger analog input limits and assigns a quality flag as needed. This quality indication and the time are recorded with each value.

2.3.3.2.3 Data Validation

The Duke Ambient Monitoring Group reviews the daily data, received from the meteorological systems, to detect system problems and perform preliminary data

verifications. On-site system checks are performed by the field staff at least monthly to verify proper operation of the systems. After the system checks are completed, site technicians complete a thorough review of all meteorological data collected for the previous month. Data are also reviewed by the ambient monitoring team lead and an in-house meteorologist. Data edits are performed on the central computer database following the data reviews. Both raw (unedited) and QA'd (edited) data files are maintained on the central computer. Backup copies of the data files are maintained.

2.3.3.3 Meteorological Instrumentation Inspection and Maintenance

The meteorological equipment is kept in proper operating condition by staff that are trained and qualified for the necessary tasks. Meteorological instruments are inspected and serviced at a frequency that assures at least a 90 percent data recovery (Regulatory Guide 1.23, Revision 1) and that minimizes extended periods of instrument outage.

Equipment is calibrated or replaced at least after every 6 months of service. The methods for maintaining a calibrated status for the components of the meteorological data collection system (sensors, recorders, electronics, datalogger, etc.) include field checks, field calibration, and/or replacement by a laboratory-calibrated component. More frequent calibration and/or replacement intervals for individual components may be conducted on the basis of the operational history of the component type. Administrative controls such as appropriate maintenance processes procedures, work order/work request documents, etc. are used to calibrate and maintain meteorological and station equipment.

The operational phase of the meteorological program includes those procedures and responsibilities related to activities beginning with the initial fuel loading and continuing through the life of the plant. The meteorological data collection program is continuous without major interruptions during the operational phase. The meteorological program has been developed to be consistent with the guidance given in Regulatory Guide 1.23, Revision 1. The basic objective is to maintain data collection performance to assure at least 90 percent joint recoverability and availability of data needed for assessing the relative concentrations and doses resulting from accidental or routine releases in accordance with Regulatory Guide 1.23, Revision 1.

The restoration of the data collection capability of the meteorological facility in the event of equipment failure or malfunction is accomplished by replacement or repair of affected equipment. A stock of spare parts and equipment is maintained to minimize and shorten the periods of outages. Equipment malfunctions or outages are detected by personnel during routine or special checks. When an outage of one or more of the critical data items occurs, the appropriate maintenance personnel are notified. Records documenting results of calibrations,

major causes of instrument outages or drift from calibration, and corrective action taken are maintained.

2.3.4 SHORT-TERM DIFFUSION ESTIMATES

WLS COL 2.3-4 The consequences of a design basis accident in terms of human exposure are a function of the atmospheric dispersion conditions at the site of the potential release. Atmospheric dispersion consists of two components: 1) atmospheric transport due to organized or mean airflow within the atmosphere and 2) atmospheric diffusion due to disorganized or random air motions. Atmospheric diffusion conditions are represented by relative air concentration (χ/Q) values. This section describes the development of the short-term diffusion estimates for the EAB, low population zone (LPZ), and the control room.

2.3.4.1 Calculation Methodology

The efficiency of diffusion is primarily dependent on winds (speed and direction) and atmospheric stability characteristics. Dispersion is rapid during periods of stability classes A through D and much slower during periods of stability classes E through G. (Regulatory Guide 1.145 and NUREG/CR-2858).

Relative concentrations of released gases, χ/Q values, as a function of direction for various time periods at the EAB and the outer boundary of the LPZ, were determined by the use of the computer code PAVAN, NUREG/CR-2858 (Reference 233). This code implements the guidance provided in Regulatory Guide 1.145. The χ/Q calculations are based on the theory that material released to the atmosphere will be normally distributed (Gaussian) about the plume centerline. A straight-line trajectory is assumed between the point of release and all distances for which χ/Q values are calculated in accordance with NUREG/CR-2858 and Regulatory Guide 1.145. NUREG/CR-2858 refers to Regulatory Guide 1.111 for discussion of the effects of spatial and temporal variations in airflow in the region of a site. These effects are not described by the constant mean wind direction model. Consequently, the effects of hill and valley topography on airflow characteristics near the Lee Nuclear Station site were examined to identify any variation of atmospheric transport and diffusion conditions.

As stated in Subsection 2.3.2.6, the terrain in the immediate vicinity of the Lee Nuclear Station site can be described as gently rolling hills. The only notable terrain feature in the immediate vicinity of the site is McKowns Mountain, approximately one mile to the SSW with a peak elevation of approximately 800 feet (approximately 200 feet above the site grade elevation). Given the distance and minimal elevation rise from Lee Nuclear Station to the peak of McKowns Mountain (see Figures 2.1-204, 2.3-245, and 2.4.2-202), it can be concluded that McKowns Mountain would not have a significant effect on short term diffusion estimates.

The wind characteristics of the site were compared with the same parameters at the Greenville-Spartanburg airport (see [Subsection 2.3.2.1](#)). The representativeness of the regional climatology (within 2 miles) was also assessed (see [Subsection 2.3.1](#)). Although the Lee Nuclear Station 10 meter meteorological data shows a locally induced NW flow field at low wind speeds within the valley of the Broad River, this trend would not bias short term diffusion estimates. Therefore, no adjustments to represent non-straight line trajectories were applied.

Using joint frequency distributions of wind direction and wind speed by atmospheric stability, PAVAN provides the χ/Q values as functions of direction for various time periods at the EAB and the LPZ. The meteorological data needed for this calculation includes wind speed, wind direction, and atmospheric stability. The meteorological data used for this analysis was obtained from the onsite meteorological Tower 2 data from December 1, 2005 through November 30, 2007. The joint frequency distribution for this period is reported in [Table 2.3-235](#) through [Table 2.3-241](#). Other plant specific data included tower height at which wind speed was measured (10.0 m) and distances to the EAB and LPZ. The Exclusion Area Boundary (EAB) for Lee Nuclear Station is shown in FSAR [Figures 2.1-209A](#) and [2.1-209B](#). The minimum EAB distances are reported in [Table 2.3-282](#). In this table, the distances are measured from a 448-foot radius effluent release boundary (from each Unit's containment building) to the EAB. The LPZ is defined as a circle with a 2-mile radius centered on the midpoint between the Unit 1 and 2 containment buildings.

Within the ground release category, two sets of meteorological conditions are treated differently. During neutral (D) or stable (E, F, or G) atmospheric stability conditions when the wind speed at the 10-meter level is less than 6 meters per second (m/s), horizontal plume meander is considered. The χ/Q values are determined through the selective use of the following set of equations for ground-level relative concentrations at the plume centerline:

$$\chi/Q = \frac{1}{\bar{U}_{10}(\pi\sigma_y\sigma_z + A/2)} \quad \text{Equation 1}$$

$$\chi/Q = \frac{1}{\bar{U}_{10}(3\pi\sigma_y\sigma_z)} \quad \text{Equation 2}$$

$$\chi/Q = \frac{1}{\bar{U}_{10}\pi\Sigma_y\sigma_z} \quad \text{Equation 3}$$

where:

χ/Q is relative concentration, in sec/m³,

\bar{U}_{10} is wind speed at 10 meters above plant grade, in m/sec

σ_y is lateral plume spread, in meters, a function of atmospheric stability and distance

σ_z is vertical plume spread, in meters, a function of atmospheric stability and distance

Σ_y is lateral plume spread with meander and building wake effects, in meters, a function of atmospheric stability, wind speed, and distance

A is the smallest vertical-plane cross-sectional area of the reactor building, in m²

For wind speeds less than 6 m/sec and neutral or stable stability classes (D through G), PAVAN calculates χ/Q values using Equations 1, 2, and 3. The values from Equations 1 and 2 are compared and the higher value is selected. This value is then compared with the value from Equation 3, and the lower value of these two is selected as the appropriate χ/Q value.

During all other meteorological conditions, unstable (A, B, or C) atmospheric stability and/or 10-meter level wind speeds of 6 m/s or more, plume meander is not considered. The higher value calculated from Equation 1 or 2 is used as the appropriate χ/Q value.

From here, PAVAN constructs a cumulative probability distribution of χ/Q values for each of the 16 directional sectors. This distribution is the probability of the given χ/Q values being exceeded in that sector during the total time. The sector χ/Q values and the maximum sector χ/Q value are determined by effectively "plotting" the χ/Q versus probability of being exceeded and selecting the χ/Q value that is exceeded 0.5 percent of the total time. This same method is used to determine the 5 percent overall site χ/Q value.

The χ/Q value for the EAB or LPZ boundary evaluations will be the maximum sector χ/Q or the 5 percent overall site χ/Q , whichever is greater in accordance with Regulatory Guide 1.145. All direction-dependent sector values are also calculated.

2.3.4.2 Calculations and Results

The methodology described in Regulatory Guide 1.145 divides release configurations into two modes, ground release and stack release. A stack or elevated release includes all release points that are effectively greater than two and one-half times the height of the adjacent solid structures. Since the AP1000 release points do not meet this criterion, releases are considered to be ground level releases. The analysis also assumed a 448 ft radius circle, centered on each Unit's containment, which encompasses all release points (sources) when calculating distances to the receptors.

PAVAN requires the meteorological data in the form of joint frequency distributions of wind direction and wind speed by atmospheric stability class. These analyses

were completed using data from the Tower 2 meteorological instrumentation during the 24-month period of December 2005 to November 2007.

The stability classes were based on the classification system given in Table 2 of U.S. Nuclear Regulatory Commission Regulatory Guide 1.23, as follows:

Classification of Atmospheric Stability
(Reference, Regulatory Guide 1.23)

Stability Classification	Pasquill Categories	Temperature change with height (°C/100m)
Extremely unstable	A	$\Delta T \leq -1.9$
Moderately unstable	B	$-1.9 < \Delta T \leq -1.7$
Slightly unstable	C	$-1.7 < \Delta T \leq -1.5$
Neutral	D	$-1.5 < \Delta T \leq -0.5$
Slightly stable	E	$-0.5 < \Delta T \leq 1.5$
Moderately stable	F	$1.5 < \Delta T \leq 4.0$
Extremely stable	G	$\Delta T > 4.0$

Joint frequency distribution tables were developed from the meteorological data with the assumption that if data required as input to the PAVAN program (i.e., lower level wind direction, lower wind speed, and temperature differential) was missing from the hourly data record, all data for that hour was discarded. Also, the data in the joint frequency distribution tables was rounded for input into the PAVAN code.

Building cross-sectional area is defined as the smallest vertical-plane area of the reactor building, in square meters. The area of the reactor building to be used in the determination of building-wake effects will be conservatively estimated as the above grade, cross-sectional area of the shield building. This area was determined to be 2843 m². Building height is the height above plant grade of the containment structure used in the building-wake term for the annual-average calculations. The Passive Containment Cooling System (PCS) tank roof is at Elevation 329 ft. The DCD design grade elevation for the AP1000 is 100 ft; therefore, the height above plant grade of the containment structure or building height is 229 ft.

As described in Regulatory Guide 1.145, a ground release includes all release points that are effectively lower than two and one-half times the height of adjacent solid structures. Therefore, as stated above, a ground release was assumed.

The tower height is the height at which the wind speed was measured. Based on the ground level release assumption, the lower measurement level (i.e., 10-meter level) on the tower height was used.

Table 2.3-283 gives the direction-dependent sector and the direction independent χ/Q values at the EAB and LPZ along with the 5 percent maximum χ/Q values for both Units 1 and 2. As shown, the 0.5 percent direction dependent maximum sector relative dispersion exceeds the 5 percent direction independent overall site dispersion at the EAB. Since a higher relative dispersion coefficient is conservative, the 0.5 percent maximum sector (SE at 1410 m for Unit 1 and SE at 1309 m for Unit 2) relative dispersion is limiting for the EAB. For the LPZ, the comparison also resulted in the conclusion that the 0.5 percent direction dependent relative dispersion was limiting. A summary of these results is provided below.

Short Term Accident χ/Q VALUES for Unit 1 (sec/m³)
(Based on December 2005-November 2007 Meteorological Data)

	0-2 Hrs	0-8 Hrs	8-24 Hrs	24-96 Hrs	96-720 Hrs
EAB (1410 m, SE sector)	3.32E-04	N/A	N/A	N/A	N/A
LPZ (3219 m, SE sector)	N/A	8.05E-05	5.52E-05	2.43E-05	7.52E-06

Short Term Accident χ/Q VALUES for Unit 2 (sec/m³)
(Based on December 2005-November 2007 Meteorological Data)

	0-2 Hrs	0-8 Hrs	8-24 Hrs	24-96 Hrs	96-720 Hrs
EAB (1309 m, SE sector)	3.55E-04	N/A	N/A	N/A	N/A
LPZ (3219 m, SE sector)	N/A	8.05E-05	5.52E-05	2.43E-05	7.52E-06

As seen from the above tables, the atmospheric dispersion values for Unit 2 are limiting. The above Lee Nuclear Station site characteristics are compared to the AP1000 design criteria in Table 2.0-201.

2.3.4.3 Short-Term Atmospheric Dispersion Estimates for the Control Room Emergency Air Intake

The atmospheric dispersion estimates for the Lee Nuclear Control Room were calculated based on the guidance provided in Regulatory Guide 1.194. The Control Room χ/Q s were calculated for all probable release points to the Control Room HVAC Intake and the Annex Building Entrance using the ARCON96 computer code (Reference 230) based on the hourly meteorological data. The directions relative to True North from the Control Room HVAC Intake and Annex Building Entrance (receptors) to the assumed release points (sources) are provided in Table 2.3-284. In all cases, the intervening structures between the release points (sources) and the receptors were ignored for calculational

simplicity, thereby underestimating the true distance from the release points. This conservatism results in overestimating the Control Room χ/Q values.

Atmospheric stability was determined by the vertical temperature difference (ΔT) measured over the difference in measurement height and the stability classes given in Regulatory Guide 1.23. All releases were assumed to be point sources and ground level releases. For each of the source-to-receptor combinations, the χ/Q value that is not exceeded more than 5.0 percent of the total hours in the meteorological data set (e.g., 95-percentile χ/Q) was determined. The χ/Q values for source-receptor pairs are shown in [Table 2.3-285](#). Atmospheric dispersion used for Control Room habitability is discussed in [FSAR Section 6.4](#).

2.3.4.4 Short-Term Atmospheric Dispersion Estimates for the Technical Support Center

The atmospheric dispersion estimates (χ/Q s) for the Lee Nuclear Technical Support Center (TSC) were calculated based on the guidance provided in Regulatory Guide 1.194. The TSC χ/Q s were calculated for the limiting design basis release point to the nearest point on the maintenance support building using the ARCON96 computer code ([Reference 230](#)). The nearest point on the maintenance support building was conservatively selected to bound the distance to the final TSC air intake location. The atmospheric dispersion calculation used hourly meteorological data from December 1, 2005 through November 30, 2007.

Because the limiting TSC radiological consequences are associated with the design basis LOCA and the containment shell is the most probable LOCA release location (see [DCD Subsection 15.6.5.3.3](#), Release Pathways), a release from the containment shell was assumed. Intervening structures between the release point and the surrogate TSC air intake location were ignored for calculational simplicity, thereby underestimating the true distance from the release point to the surrogate TSC air intakes. This conservatism, in addition to using the conservative surrogate TSC air intake location, resulted in overestimating the TSC χ/Q values. A straight-line path from the source to receptor was conservatively assumed to minimize distances. Distances and directions were taken between the release point (center of the containment wall) to the closest point on the maintenance support building for each unit, as listed in [Table 2.3-294](#). The surrogate TSC intake locations were assumed to be 1.5 m above grade.

Atmospheric stability was determined by the vertical temperature difference (ΔT), measured between the 60-meter and 10-meter instrumentation levels, and the stability classes given in Regulatory Guide 1.23. The containment shell was modeled as a diffuse area source with the elevation of the assumed release equal to the vertical center of the projected plane of the containment shell above the Auxiliary Building and below the conical roof (i.e., 35.4 m above grade). The building area used for building wake corrections is the above grade containment shell area which was conservatively calculated to be 2843 m². The initial diffusion estimates (i.e., sigma-y and sigma-z) were based on the Regulatory Guide 1.194 methodology, using a source width of 145 ft, and a source height 110.5 ft with the area of the conical roof and PCS air diffuser conservatively neglected. The

χ/Q values that are not exceeded more than 5.0 percent of the total hours in the meteorological data set (e.g., 95-percentile χ/Q) were determined. The χ/Q values for Units 1 and 2 LOCA releases to the nearest corner of the Maintenance Support Building are shown in [Table 2.3-295](#).

2.3.5 LONG-TERM DIFFUSION ESTIMATES

WLS COL 2.3-5 For a routine gaseous effluent release, the concentration of radioactive material in the surrounding region depends on the amount of effluent released, the height of the release, the momentum and buoyancy of the emitted plume, the wind speed, atmospheric stability, airflow patterns of the site, and various effluent removal mechanisms. Annual average relative concentration, χ/Q , and annual average relative deposition, D/Q , for gaseous effluent routine releases were calculated.

2.3.5.1 Calculation Methodology and Assumptions

The XOQDOQ Computer Program NUREG/CR-2919 ([Reference 231](#)) which implements the assumptions outlined in Regulatory Guide 1.111 was used to generate the annual average relative concentration, χ/Q , and annual average relative deposition, D/Q . Values of χ/Q and D/Q were determined at points of maximum potential concentration outside the site boundary, at points of maximum individual exposure and at points within a radial grid of sixteen 22-1/2° sectors and extending to a distance of 50 miles. Radioactive decay and dry deposition were considered.

The gridded receptor locations were determined from the locations obtained from the 2007 and 2008 land use information. Hourly meteorological data was used in the development of joint frequency distributions, in hours, of wind direction and wind speed by atmospheric stability class. The wind speed categories used were consistent with the Lee Nuclear short-term (accident) diffusion χ/Q calculation discussed above. Calms (wind speeds below the anemometer starting speed of 1 mph) were distributed into the first wind speed class with the same proportion and direction as the direction frequency of the 2nd wind-speed class.

Joint frequency distribution tables were developed from the hourly meteorological data with the assumption that if data required as input to the XOQDOQ program (i.e., lower level wind direction and wind speed, and temperature differential as opposed to upper level wind direction and wind speed) was missing from the hourly data record, all data for that hour would be discarded. This assumption maximizes the data being included in the calculation of the χ/Q and D/Q values since hourly data is not discarded if only upper data is missing. The joint frequency distribution tables generated using the methodology and data described above are given in [Tables 2.3-235 through 2.3-241](#).

For receptors located at the site boundary, the analysis assumed a ground level point source located at the Effluent Release Boundary closest to the receptor. For

other offsite receptors such as cows and gardens, the analysis assumed a ground level point source located at the center of the facility midpoint between the Unit 1 and 2 containment buildings. At ground level locations beyond several miles from the plant, the annual average concentration of effluents are essentially independent of release mode; however, for ground level concentrations within a few miles, the release mode is important. Gaseous effluents released from tall stacks generally produce peak ground-level air concentrations near or beyond the site boundary. Near ground level releases usually produce concentrations that decrease from the release point to all locations downwind. Guidance for selection of the release mode is provided in Regulatory Guide 1.111. In general, in order for an elevated release to be assumed, either the release height must be at least twice the height of adjacent buildings or detailed information must be known about the wind speed at the height of the release. For this analysis, the routine releases were conservatively modeled as ground level releases.

The building cross-sectional area and building height are used in calculation of building wake effects. Regulatory Guide 1.111 identifies the tallest adjacent building, in many cases, the reactor building, as appropriate for use. The AP1000 plant arrangement is comprised of five principal building structures; the nuclear island, the turbine building, the annex building, the diesel generator building, and the radwaste building. The nuclear island consists of a free-standing steel containment building, a concrete shield building, and an auxiliary building. As the shield building is the tallest building in the AP1000 arrangement, the shield building cross-sectional area and building height will be used in calculation of building wake effects. The use of the shield building area, as opposed to the area of the nuclear island, is a conservative assumption since use of a smaller area minimizes wake effects resulting in higher calculated relative offsite concentrations.

Consistent with Regulatory Guide 1.111 guidance regarding radiological impact evaluations, radioactive decay and deposition were considered. For conservative estimates of radioactive decay, an overall half-life of 2.26 days is acceptable for short-lived noble gases and a half-life of 8 days for all iodines released to the atmosphere. At sites where there is not a well-defined rainy season associated with a local grazing season such as the region around the Lee Nuclear Site, wet deposition does not have a significant impact. In addition, the dry deposition rate of noble gases is so slow that the depletion is negligible within 50 miles. Therefore, in this analysis only the effects of dry deposition of iodines were considered. The calculation results, with and without consideration of dry deposition, are identified in the output as "depleted" and "undepleted".

As described in [Subsection 2.3.4.1](#), the gently rolling terrain in the vicinity of the Lee Nuclear Station site would not have a significant effect on atmospheric dispersion estimates. The shallow river valley in which the Lee Nuclear Station site is located does not create a significant topographic barrier to air dispersion. In addition, the wind characteristics of the site are representative of the vicinity. Therefore, terrain recirculation adjustments as described in Regulatory Guide 1.111 were not applied for the Lee Nuclear Station site.

2.3.5.2 Results

Receptor locations for the long-term atmospheric dispersion at the Lee Nuclear Station site were also evaluated. χ/Q and/or D/Q at points of potential maximum concentration outside the site boundary, at points of maximum individual exposure, and at points within a radial grid of sixteen 22½ degree sectors (centered on true north, north-northeast, northeast, etc.) and extending to a distance of 50 miles from the station were determined. Receptor locations included in the evaluation are given in [Table 2.3-286](#). A set of data points were located within each sector at increments of 0.25 mile to a distance of 1 mile from the plant, at increments of 0.5 mile from a distance of 1 mile to 5 mile, at increments of 2.5 mile from a distance of 5 mile to 10 mile, and at increments of 5 miles thereafter to a distance of 50 miles. Estimates of χ/Q (undecayed and undepleted; depleted for radioiodines) and D/Q radioiodines and particulates is provided at each of these grid points.

The results of the analysis, based on two years of data collected on site, are presented in [Tables 2.3-287](#) through [2.3-292](#). The limiting atmospheric dispersion factor (χ/Q) at the site boundary, $1.5 \times 10^{-5} \text{ sec/m}^3$, is in the NW direction from Unit 1 at 427 meters (approximately 0.27 mi.) from the effluent release boundary. The limiting atmospheric dispersion at the nearest residence, $4.60 \times 10^{-6} \text{ sec/m}^3$, is in the SE direction at 1588 meters. Atmospheric dispersion factors for other receptors are given in [Table 2.3-289](#). Long term atmospheric dispersion factors are not given in the AP1000 DCD except at the EAB. The DCD site boundary annual average χ/Q is $2.0 \times 10^{-5} \text{ sec/m}^3$. This bounds the Lee Nuclear Station annual average routine release site boundary χ/Q value of $1.5 \times 10^{-5} \text{ sec/m}^3$. [Table 2.0-201](#) provides a comparison of the Lee Nuclear Station site characteristics with the DCD design parameters.

2.3.6 COMBINED LICENSE INFORMATION

2.3.6.1 Regional Climatology

WLS COL 2.3-1 This COL item is addressed in [Subsection 2.3.1](#)

2.3.6.2 Local Meteorology

WLS COL 2.3-2 This COL item is addressed in [Subsection 2.3.2](#)

2.3.6.3 Onsite Meteorological Measurements Program

WLS COL 2.3-3 This COL item is addressed in **Subsection 2.3.3**

2.3.6.4 Short-Term Diffusion Estimates

WLS COL 2.3-4 This COL item is addressed in **Subsection 2.3.4**

2.3.6.5 Long-Term Diffusion Estimates

WLS COL 2.3-5 This COL item is addressed in **Subsection 2.3.5**

2.3.7 REFERENCES

201. South Carolina State Climate Office, South Carolina Department of Natural Resources, Columbia, SC, <http://www.dnr.sc.gov/climate/sco/>, accessed 8/21/2006.
202. Duke Power Company, Cherokee Nuclear Station - Environmental Report, Amendment 4, October 1975.
203. Southeast Regional Climate Center, South Carolina Department of Natural Resources, Columbia South Carolina, NINETY NINE ISLANDS, SOUTH CAROLINA, Period of Record Daily Climate Summary, Daily Records for station 386293 NINETY NINE ISLANDS. <http://cirrus.dnr.state.sc.us/cgi-bin/sercc/cliMAIN.pl?sc6293>, accessed 8/15/2006 through 8/31/2006.
204. Ice Storms: Hazardous Beauty, Keith C Heidorn, December 2001, <http://www.islandnet.com/~see/weather/elements/icestorm.htm>, accessed 6/19/2006.
205. Air Stagnation Climatology for the United States (1948-1998), NOAA/Air Resources Laboratory ATLAS No. 1, Julian X.L. Wang and James K. Angell, April 1999.

206. Environmental Protection Agency (EPA) Research Triangle Park, North Carolina, SCRAM Mixing Height Data for Greensboro, NC for 1984 through 1987, 1990 and 1991.
<http://www.epa.gov/scram001/mixingheightdata.htm>, accessed 4/22/2007.
207. NCDC Storm Event Database, National Climate Data Center (NCDC) Storm Event Data Base, January 1, 1950 through May 31, 2006.
<http://www4.ncdc.noaa.gov/cgi-win/wwwcgi.dll?wwEvent~Storms>, accessed 8/31/2006, 9/1/2006.
208. Extreme Ice Thicknesses from Freezing Rain, September 2004, American Lifelines Alliance, Kathleen F. Jones, Project Manager, Neal Lott, and Ronald Thorkildson, <http://www.americanlifelinesalliance.org/>, accessed 4/22/2007.
209. Atlantic Tropical Storms and Hurricanes Affecting the United States: 1899-1999, NOAA Technical Memorandum NWS SR-206, Donovan Landreneau, National Weather Service Office, Lake Charles, Louisiana.
210. Atlantic Tropical Storms And Hurricanes Affecting The United States: 1899-2002, NOAA Technical Memorandum NWS SR-206, Donovan Landreneau, National Weather Service Office, Lake Charles, Louisiana, (Updated Through 2002).
211. Thom, H. C. S., Tornado Probabilities, Monthly Weather Review, Vol. 91, October-December 1963, pp 730-736.
212. U.S. Census Bureau: State and County QuickFacts, Data derived from Population Estimates, 2000 Census of Population and Housing, <http://quickfacts.census.gov/qfd/states>, accessed 8/16/2006.
213. NUREG/CR-4461, Rev. 2, Tornado Climatology of the Contiguous United States, Pacific Northwest National Laboratory, February 2007.
214. IAEA Safety Standards Series No. NS-G-3.4, "Meteorological Events in Site Evaluation for Nuclear Power Plants", Vienna: International Atomic Energy Agency, 2003, ISBN 92-0-102103-8.
215. Isokeraunic map contained in Hubbell Power Systems, Lightning: The Most Common Source of Overvoltage, Bulletin EU 1422-H, 2001.
216. A Statistical Analysis of Strike Data From Real Installations Which Demonstrates Effective Protection of Structures Against Lightning, F. D'Alessandro, ERICO Lightning Technologies, Hobart, Australia.
217. American Meteorological Society 1999, "Lightning Ground Flash Density and Thunderstorm Duration in the Continental United States: 1989-96", Gary R. Huffines and Richard E. Orville, Cooperative Institute for Applied Meteorological Studies, Department of Meteorology, Texas A&M University, College Station, Texas.

218. EPA 8-Hour Ozone Non-Attainment State/Area/County Report, 2006.
219. George C. Holzworth, "Mixing Heights, Wind Speeds, and Potential for Urban Air Pollution Throughout the Contiguous United States", Environmental Protection Agency, Office of Air Programs, January 1972.
220. American Society of Civil Engineers, ANSI/ASCE 7-05, Minimum Design Loads for Buildings and Other Structures.
221. Huschke, Ralph E., Ed., Glossary of Meteorology, American Meteorological Society, Boston, Massachusetts, 1959.
222. American Society of Civil Engineers, ASCE 7-95, "Minimum Design Loads for Buildings and Other Structures," June 6, 1996.
223. The North Atlantic Subtropical Anticyclone, Robert E. Davis, Bruce P. Hayden, David A. Gay, William L. Phillips, and Gregory V. Jones, Department of Environmental Sciences, University of Virginia, Charlottesville, Virginia, Journal of Climate: Vol. 10, No. 4, pp. 728-744, August 22, 1996.
224. Local Climatological Data, NCDC Local Climatological Data-Unedited, Online Individual Station, Hourly Surface Data, Greenville/Spartanburg, South Carolina, 1997 to 2005. Quality Controlled online data, Order No. W15119.
225. "'Precipitation-Frequency Atlas of the United States" NOAA Atlas 14, Volume 2, Version 3, G.M. Bonnin, D. Martin, B. Lin, T. Parzybok, M. Yekta, and D. Riley, NOAA, National Weather Service, Silver Spring, Maryland, 2004, Extracted: Thu Aug 24 2006. Location: South Carolina 35.024 N 81.524 W 777 feet. http://hdsc.nws.noaa.gov/hdsc/pfds/orb/sc_pfds.html.
226. Forecast Systems Laboratory (now the Global Systems Division [GSD]) of the Earth System Research Laboratory (ESRL), FSL/NCDC Radiosonde Data Archive, Radiosonde Database Access, <http://raob.fsl.noaa.gov/>, accessed 6/7-8/2006.
227. DeLorme, Two DeLorme Drive, P.O. Box 298, Yarmouth, ME 04096 USA, Latitude 43°48.491' North, Longitude 70°09.844' West, Topo USA 6.0.
228. EPA - Green Book - Currently Designated Non-Attainment Areas for All Criteria Pollutants, <http://www.epa.gov/oar/oaqps/greenbk/ancl.html>, assessed 10/2/2006.
229. NUREG-0917, "Nuclear Regulatory Commission Staff Computer Programs for Use with Meteorological Data", July 1982
230. NUREG/CR-6331, Revision 1, May 1997, "Atmospheric Relative Concentrations in Building Wakes".

231. NUREG/CR-2919, XOQDOQ: Computer Program for the Meteorological Evaluation of Routine Effluent Releases at Nuclear Power Stations, September 1982.
232. Blacksburg South Carolina - Climate, Thomson Gale, 2005, <http://www.city-data.com/city/Blacksburg-South-Carolina.html>, accessed 4/22/2007.
233. PNL-4413, PAVAN: An Atmospheric Dispersion Program for Evaluating Design Basis Accidental Releases of Radioactive Materials from Nuclear Power Stations, November 1982.
234. NUREG/CR-1486, Hydrometeorological Report 53, April 1980, "Seasonal Variation of 10-square-mile Maximum Precipitation Estimates, United States East of the 105th Meridian."
235. National Oceanic and Atmospheric Administration (NOAA) Coastal Service Center, Hurricane data for years 1899 - 2005.
236. National Climatic Data Center (NCDC) Local Climatic Data Annual Summary with Comparative Data for Greenville-Spartanburg (Greer), South Carolina (Station ID GSP), 2007.
237. National Climatic Data Center (NCDC), "Extreme Snowfall Amount Corresponding to 4 Return Periods (plus Observed Extreme)," Gaffney 6 E, South Carolina, last updated 2007.
238. ASHRAE Fundamentals Handbook 2001, Chapter 27 - Climatic Design Information.
239. National Climatic Data Center (NCDC) Local Climatic Data Annual Summary with Comparative Data, for Charlotte, North Carolina (Station ID CLT), 2007.
240. National Climatic Data Center (NCDC) Local Climatic Data (LCD), Data for Greenville-Spartanburg (Greer), South Carolina (Station ID GSP), 2007.
241. IEEE Standard C57.19.100-1995, Guide for Application of Power Apparatus Bushings.

WLS COL 2.3-1

TABLE 2.3-201
 RAINFALL FREQUENCY DISTRIBUTION
 GREENVILLE/SPARTANBURG, SOUTH CAROLINA
 NUMBER OF HOURS PER MONTH, AVERAGE YEAR

Rainfall (inch/hr)	Jan	Feb	Mar	Apr	May	Jun	Jul	Aug	Sep	Oct	Nov	Dec	Average Annual Hours
0.01-0.019	18.2	17.0	19.4	17.1	15.4	14.3	14.2	9.6	12.2	13.6	15.6	17.2	15.3
0.02-.099	33.2	34.0	30.6	26.0	17.9	19.6	14.8	9.2	20.4	17.1	30.2	26.6	23.3
0.10-0.249	8.3	10.8	12.3	9.4	7.3	7.2	5.3	3.6	9.4	5.9	6.9	13.1	8.3
0.25-0.499	1.3	0.6	2.4	2.7	2.0	3.4	3.2	1.3	2.7	2.3	1.4	1.4	2.1
0.50-0.99	0.2	0.1	0.4	0.2	0.9	1.7	1.6	1.6	1.0	0.8	0.4	0.2	0.8
1.00-1.99	0.0	0.0	0.0	0.2	0.0	0.1	0.8	0.3	0.3	0.1	0.0	0.0	0.2
2.0 & over	0.0	0.0	0.0	0.0	0.0	0.0	0.2	0.1	0.0	0.0	0.0	0.0	0.0
Total	61.2	62.5	65.1	55.6	43.5	46.3	40.1	25.7	46.0	39.8	54.5	58.5	49.9

NOTES:

1. Data from NCDC, 1997-2005.

WLS COL 2.3-1

TABLE 2.3-202 (Sheet 1 of 2)
HURRICANES IN NORTH CAROLINA AND SOUTH CAROLINA
1899 – 2005

North Carolina

Year	Month	Name	Category
1899	AUG	-	3
1899	OCT	-	2
1901	JUL	-	1
1904	SEP	-	1
1906	SEP	-	3
1908	JUL	-	1
1913	SEP	-	1
1918	AUG	-	1
1933	AUG	-	2
1933	SEP	-	3
1944	AUG	-	1
1944	SEP	-	3
1953	AUG	Barbara	2
1954	AUG	Carol	2
1954	OCT	Hazel	4
1955	AUG	Connie	3
1955	AUG	Diane	1
1955	SEP	Ione	3
1960	SEP	Donna	3
1964	OCT	Isbell	1
1971	SEP	Ginger	1
1984	SEP	Diana	3
1985	SEP	Gloria	3
1986	AUG	Charley	1
1989	SEP	Hugo	2
1996	JUL	Bertha	2
1996	SEP	Fran	3
1998	AUG	Bonnie	2
1999	SEP	Floyd	2
2003	SEP	Isabel	2
2004	AUG	Charley	1

WLS COL 2.3-1

TABLE 2.3-202 (Sheet 2 of 2)
HURRICANES IN NORTH CAROLINA AND SOUTH CAROLINA
1899 – 2005

South Carolina

Year	Month	Name	Category
1899	OCT	-	2
1904	SEP	-	1
1906	SEP	-	3
1911	AUG	-	2
1913	OCT	-	1
1916	JUL	-	2
1928	SEP	-	1
1940	AUG	-	2
1947	OCT	-	2
1952	AUG	Able	1
1954	OCT	Hazel	4
1959	JUL	Cindy	1
1959	SEP	Gracie	4
1979	SEP	David	2
1985	JUL	Bob	1
1985	NOV	Kate	1
1989	SEP	Hugo	4
2004	AUG	Gaston	1
2004	AUG	Charley	1

NOTES:

1. Data is from "Atlantic Tropical Storms And Hurricanes Affecting The United States:1899-2002," NOAA Technical Memorandum NWS SR-206 (Updated through 2002).
2. Additional data from National Oceanic and Atmospheric Administration (NOAA) Coastal Service Center, years 1899 - 2005.

WLS COL 2.3-1

TABLE 2.3-203 (Sheet 1 of 2)
 FREQUENCY OF TROPICAL CYCLONES (BY MONTH) FOR THE STATES OF
 SOUTH CAROLINA AND NORTH CAROLINA

	Category of Storm 1899 – 2005 (Saffir-Simpson Scale)					Monthly Total (No.)	Annual Frequency (yr ⁻¹)	% of Total
	1 (No.)	2 (No.)	3 (No.)	4 (No.)	5 (No.)			
Jun	0	0	0	0	0	0	0.00	0%
Jul	4	2	0	0	0	6	0.06	12%
Aug	8	6	2	0	0	16	0.15	32%
Sep	5	4	9	2	0	20	0.19	40%
Oct	2	3	0	2	0	7	0.07	14%
Nov	1	0	0	0	0	1	0.01	2%
Total	20	15	11	4	0	50	0.47	100%

Note: Storm Category is the category of the storm entering either North Carolina or South Carolina.

TABLE 2.3-203 (Sheet 2 of 2)
 FREQUENCY OF TROPICAL CYCLONES (BY MONTH) FOR THE STATES OF
 SOUTH CAROLINA AND NORTH CAROLINA

Area	Number of Hurricanes: 1899 – 2005 Saffir/Simpson Category Number					Annual Frequency (yr ⁻¹)	Return Period (years)
	1	2	3	4	5		
North Carolina (NC)	11	9	10	1	0	31	0.29
South Carolina (SC)	9	6	1	3	0	19	0.18

Where the definition of Storm Category is as follows:

Storm Category (Saffir-Simpson Scale)	Wind Speed (mph)	Storm Surge (ft. above normal)
1	74 to 95	4 to 5
2	96 to 110	6 to 8
3	111 to 130	9 to 12
4	131 to 155	13 to 18
5	Greater than 155	Greater than 18

NOTES:

1. Data is from "Atlantic Tropical Storms And Hurricanes Affecting The United States:1899-2002," NOAA Technical Memorandum NWS SR-206 (Updated through 2002), and NOAA Technical Memorandum NWS TPC-4 for data through 2004.
2. Additional data from National Oceanic and Atmospheric Administration (NOAA) Coastal Services Center, years 1899 - 2005.

WLS COL 2.3-1

TABLE 2.3-204 (Sheet 1 of 9)
TORNADOES IN CHEROKEE, SPARTANBURG, UNION, CHESTER, AND YORK COUNTIES,
SOUTH CAROLINA AND CLEVELAND, GASTON, MECKLENBURG, POLK, AND RUTHERFORD COUNTIES,
NORTH CAROLINA

Location or County	Date	Time	Magnitude Fujita Scale	Length (mi.)	Width (yards)	Area (mi ²)
Cherokee County, SC						
1 CHEROKEE	2/16/1954	1902	F1	1	33	0.02
2 CHEROKEE	5/22/1963	1715	F1	1	100	0.06
3 CHEROKEE	7/15/1964	1530	F0	1	100	0.06
4 CHEROKEE	4/18/1969	1430	F2	1	83	0.05
5 CHEROKEE	5/27/1973	1820	F3	20	100	1.14
6 CHEROKEE	12/5/1977	1342	F1	0	17	
7 CHEROKEE	4/4/1989	1645	F1	8	50	0.23
8 CHEROKEE	5/5/1989	1633	F4	3	700	1.19
9 CHEROKEE	2/10/1990	0742	F1	3	50	0.09
10 CHEROKEE	4/28/1990	1655	F1	5	40	0.11
11 Cowpens	8/16/1994	1656	F1	3	75	0.13
12 Blacksburg To	8/16/1994	1736	F2	4	100	0.23
13 Gaffney To	5/1/1995	2025	F0	9	50	0.26
14 Blacksburg	5/29/1996	1610	F0	0	30	
15 Gaffney	9/27/2004	2115	F1	1	50	0.03

WLS COL 2.3-1

TABLE 2.3-204 (Sheet 2 of 9)
 TORNADOES IN CHEROKEE, SPARTANBURG, UNION, CHESTER, AND YORK COUNTIES,
 SOUTH CAROLINA AND CLEVELAND, GASTON, MECKLENBURG, POLK, AND RUTHERFORD COUNTIES,
 NORTH CAROLINA

Location or County	Date	Time	Magnitude Fujita Scale	Length (mi.)	Width (yards)	Area (mi ²)
Spartanburg County, SC						
1 SPARTANBURG	5/10/1952	1415	F3	16	83	0.75
2 SPARTANBURG	4/7/1964	1208	F1	0	100	
3 SPARTANBURG	4/28/1964	1730	F0	0	0	
4 SPARTANBURG	4/28/1964	1830	F0	0	0	
5 SPARTANBURG	3/22/1968	1730	F1	1	13	0.01
6 SPARTANBURG	5/18/1969	2100	F1	0	50	
7 SPARTANBURG	5/27/1973	1730	F3	11	150	0.94
8 SPARTANBURG	6/19/1976	1630	F1	0	50	
9 SPARTANBURG	9/7/1977	1400	F1	0	77	
10 SPARTANBURG	12/5/1977	1335	F1	0	20	
11 SPARTANBURG	5/23/1980	1910	F2	3	100	0.17
12 SPARTANBURG	8/17/1985	1050	F2	9	100	0.51
13 SPARTANBURG	4/4/1989	1618	F2	2	73	0.08
14 SPARTANBURG	5/5/1989	1620	F4	6	700	2.39
15 SPARTANBURG	2/10/1990	0738	F1	2	50	0.06
16 SPARTANBURG	4/28/1990	1610	F0	2	30	0.03

WLS COL 2.3-1

TABLE 2.3-204 (Sheet 3 of 9)
 TORNADOES IN CHEROKEE, SPARTANBURG, UNION, CHESTER, AND YORK COUNTIES,
 SOUTH CAROLINA AND CLEVELAND, GASTON, MECKLENBURG, POLK, AND RUTHERFORD COUNTIES,
 NORTH CAROLINA

Location or County	Date	Time	Magnitude Fujita Scale	Length (mi.)	Width (yards)	Area (mi ²)
17 SPARTANBURG	4/28/1990	1620	F1	6	50	0.17
18 Inman	3/27/1994	1655	F2	25	75	1.07
19 Lyman To Blackburg	3/27/1994	1730	F1	33	100	1.88
20 Cross Anchor	10/22/1994	1810	F0	2	75	0.09
21 Walnut Grove	7/26/1996	1555	F1	0	10	
22 Roebuck	2/21/1997	1633	F2	1	75	0.04
23 Pacolet Mills	6/6/1998	1600	F0	1	10	0.01
24 Cherokee Spgs	3/11/2000	1500	F0	0	20	
25 Chesnee	7/7/2005	0951	F0	0	50	
Union County, SC						
1 UNION	4/8/1957	1500	F2	15	100	0.85
2 UNION	8/17/1985	1315	F0	3	30	0.05
3 UNION	6/4/1992	1050	F0	0	40	
4 UNION	6/4/1992	1115	F0	0	23	
5 Southside To	4/15/1993	1626	F2	6	600	2.05
6 Union	7/26/1996	1625	F0	0	10	
7 Carlisle	6/6/1998	1610	F1	2	50	0.06

WLS COL 2.3-1

TABLE 2.3-204 (Sheet 4 of 9)
 TORNADOES IN CHEROKEE, SPARTANBURG, UNION, CHESTER, AND YORK COUNTIES,
 SOUTH CAROLINA AND CLEVELAND, GASTON, MECKLENBURG, POLK, AND RUTHERFORD COUNTIES,
 NORTH CAROLINA

Location or County	Date	Time	Magnitude Fujita Scale	Length (mi.)	Width (yards)	Area (mi ²)
8 Adamsburg	5/25/2000	1900	F1	1	20	0.01
9 Carlisle	6/9/2001	1415	F0	1	0	
10 Union	9/7/2004	2300	F1	4	225	0.51
11 Santuc	11/24/2004	1425	F0	1	50	0.03
Chester County, SC						
1 CHESTER	4/6/1955	1230	F1	2	100	0.11
2 CHESTER	5/15/1975	1200	F1	0	3	
3 CHESTER	4/19/1981	1845	F1	2	33	0.04
4 Lowrys	4/16/1994	0111	F2	3	75	0.13
5 Chester	8/16/1994	1755	F1	0	75	
6 Chester	5/1/1995	2305	F0	0	20	
7 Richburg	5/29/1996	1700	F1	1	100	0.06
8 Ft Lawn	7/24/1997	1200	F1	0	25	
9 Chester	6/4/1998	1730	F0	0	50	
10 Chester	9/7/2004	1915	F1	1	50	0.03

WLS COL 2.3-1

TABLE 2.3-204 (Sheet 5 of 9)
 TORNADOES IN CHEROKEE, SPARTANBURG, UNION, CHESTER, AND YORK COUNTIES,
 SOUTH CAROLINA AND CLEVELAND, GASTON, MECKLENBURG, POLK, AND RUTHERFORD COUNTIES,
 NORTH CAROLINA

Location or County	Date	Time	Magnitude Fujita Scale	Length (mi.)	Width (yards)	Area (mi ²)
York County, SC						
1 YORK	7/16/1961	1400	F0	0	7	
2 YORK	6/22/1964	1820	F1	2	53	0.06
3 YORK	5/24/1973	1520	F2	2	67	0.08
4 YORK	5/28/1973	1630	F2	2	100	0.11
5 YORK	3/24/1975	1115	F1	9	100	0.51
6 YORK	12/5/1977	1640	F1	2	100	0.11
7 YORK	5/3/1984	1525	F1	6	10	0.03
8 YORK	8/17/1985	1255	F1	3	30	0.05
9 YORK	8/17/1985	1300	F0	1	30	0.02
10 YORK	3/6/1989	1230	F0	1	10	0.01
11 Clover	3/27/1994	1843	F1	1	30	0.02
12 York	8/16/1994	1650	F0	0	50	
13 YORK	5/1/1995	2103	F0	1	50	0.03
14 Clover	2/21/1997	1720	F0	2	100	0.11
15 Clover	4/19/1998	1430	F0	0	20	
16 Rock Hill	4/19/1998	1508	F0	0	10	

WLS COL 2.3-1

TABLE 2.3-204 (Sheet 6 of 9)
 TORNADOES IN CHEROKEE, SPARTANBURG, UNION, CHESTER, AND YORK COUNTIES,
 SOUTH CAROLINA AND CLEVELAND, GASTON, MECKLENBURG, POLK, AND RUTHERFORD COUNTIES,
 NORTH CAROLINA

Location or County	Date	Time	Magnitude Fujita Scale	Length (mi.)	Width (yards)	Area (mi ²)
17 Rock Hill	2/22/2003	1005	F0	0	25	
18 Rock Hill	9/7/2004	1043	F1	1	100	0.06
Cleveland County, NC						
1 CLEVELAND	5/27/1973	1900	F3	13	100	0.74
2 CLEVELAND	5/15/1975	1430	F1	0	0	
3 CLEVELAND	6/24/1979	0030	F1	1	300	0.17
4 CLEVELAND	5/5/1989	1654	F4	5	800	2.27
5 CLEVELAND	2/10/1990	0800	F2	0	50	
6 CLEVELAND	4/10/1990	1950	F0	0	30	
7 CLEVELAND	6/4/1992	1602	F0	0	200	
8 CLEVELAND	11/22/1992	2115	F1	5	500	1.42
9 Earl	8/16/1994	1730	F1	2	200	0.23
10 Shelby	9/16/1996	1735	F0	0	180	
11 Polkville	7/12/2003	1925	F1	6	200	0.68
12 Waco	9/17/2004	0505	F0	1	40	0.02
13 Patterson Spgs	9/27/2004	2200	F1	2	30	0.03

WLS COL 2.3-1

TABLE 2.3-204 (Sheet 7 of 9)
 TORNADOES IN CHEROKEE, SPARTANBURG, UNION, CHESTER, AND YORK COUNTIES,
 SOUTH CAROLINA AND CLEVELAND, GASTON, MECKLENBURG, POLK, AND RUTHERFORD COUNTIES,
 NORTH CAROLINA

Location or County	Date	Time	Magnitude Fujita Scale	Length (mi.)	Width (yards)	Area (mi ²)
Gaston County, NC						
1 GASTON	4/6/1956	1300	F1	56	100	3.18
2 GASTON	5/28/1973	1800	F0	0	0	
3 GASTON	4/2/1974	0153	F1	10	100	0.57
4 GASTON	5/15/1975	1530	F1	0	0	
5 Crowders	2/21/1997	1722	F1	15	200	1.70
6 Cherryville	7/12/2003	2000	F1	18	200	2.05
7 Gastonia	3/8/2005	0715	F0	0	50	
Mecklenburg County, NC						
1 MECKLENBURG	2/18/1960	1245	F1	24	33	0.45
2 MECKLENBURG	4/12/1961	1710	F1	1	200	0.11
3 MECKLENBURG	8/10/1964	1645	F1	0	0	
4 MECKLENBURG	9/12/1965	1930	F2	0	70	
5 MECKLENBURG	6/7/1968	1430	F2	17	200	1.93
6 MECKLENBURG	5/28/1973	0500	F2	10	100	0.57
7 MECKLENBURG	5/28/1973	1700	F1	0	0	
8 MECKLENBURG	10/8/1975	1425	F1	0	50	

WLS COL 2.3-1

TABLE 2.3-204 (Sheet 8 of 9)
 TORNADOES IN CHEROKEE, SPARTANBURG, UNION, CHESTER, AND YORK COUNTIES,
 SOUTH CAROLINA AND CLEVELAND, GASTON, MECKLENBURG, POLK, AND RUTHERFORD COUNTIES,
 NORTH CAROLINA

Location or County	Date	Time	Magnitude Fujita Scale	Length (mi.)	Width (yards)	Area (mi ²)
9 MECKLENBURG	9/16/1977	1330	F1	0	7	
10 MECKLENBURG	8/14/1978	1145	F0	0	0	
11 MECKLENBURG	5/3/1984	1545	F1	14	100	0.80
12 MECKLENBURG	6/6/1985	1620	F0	1	267	0.15
13 MECKLENBURG	11/28/1990	1940	F1	0	20	
14 MECKLENBURG	3/10/1992	2107	F2	3	180	0.31
15 Mint Hill	3/20/1998	1442	F0	0	25	
16 Cornelius	5/7/1998	1845	F0	6	50	0.17
17 Pineville	8/1/1999	1935	F0	0	10	
18 Charlotte	9/7/2004	1045	F2	2	200	0.23
19 Charlotte	3/8/2005	0740	F1	3	50	0.09
Polk County, NC						
1 Polk	8/17/1977	1136	F1	6	33	0.11
Rutherford County, NC						
1 Rutherford	5/27/1973	1915	F0	0	0	
2 Rutherford	5/18/1975	100	F2	0	0	
3 Rutherford	5/18/1989	1630	F1	0	0	

WLS COL 2.3-1

TABLE 2.3-204 (Sheet 9 of 9)
TORNADOES IN CHEROKEE, SPARTANBURG, UNION, CHESTER, AND YORK COUNTIES,
SOUTH CAROLINA AND CLEVELAND, GASTON, MECKLENBURG, POLK, AND RUTHERFORD COUNTIES,
NORTH CAROLINA

Location or County	Date	Time	Magnitude Fujita Scale	Length (mi.)	Width (yards)	Area (mi ²)
4 Rutherford	5/5/1989	1635	F4	6	400	1.36
5 Rutherford	5/24/2000	1720	F0	2	30	0.03
6 Forest City	7/7/2005	952	F1	1	50	0.03

NOTES:

1. Tornado data from all years were used to calculate the annual frequencies given in text.
2. Tornadoes with a zero (or missing) reported area, path length, or width do not represent valid data for statistical purposes.
3. Data recorded in the NOAA's National Environmental Satellite, Data, and Information Service (NEDSIS) - NCDC Storm Event database, 1950-2005, <http://www4.ncdc.noaa.gov/cgi-win/wwcgi.dll?wwevent~storms>

WLS COL 2.3-1

TABLE 2.3-205
THUNDERSTORMS
GREENVILLE-SPARTANBURG, SC AND CHARLOTTE, NC

Number of Days with Thunderstorms													
Station	JAN	FEB	MAR	APR	MAY	JUN	JUL	AUG	SEP	OCT	NOV	DEC	YEAR
GSP ⁽¹⁾	0.8	0.9	2.4	3.2	6.1	7.4	9.8	6.9	3.3	0.8	0.8	0.6	43.0
CLT ⁽²⁾	0.6	1.0	2.1	3.4	5.3	7.1	9.1	6.9	2.5	1.1	0.7	0.4	40.2
Average	0.7	1.0	2.3	3.3	5.7	7.3	9.5	6.9	2.9	1.0	0.8	0.5	41.6

NOTES:

1. 2007 Local Climatological Data Annual Summary with Comparative Data for Greenville-Spartanburg (Greer), South Carolina (Station ID GSP), data for years 1963 through 2007, National Climatic Data Center (NCDC). (Reference 236)
2. 2007 Local Climatological Data Annual Summary with Comparative Data for Charlotte, North Carolina (Station ID CLT), data for years 1948 through 2007, National Climatic Data Center (NCDC). (Reference 239)

WLS COL 2.3-1

TABLE 2.3-206
HAIL STORM EVENTS
CHEROKEE, SPARTANBURG, UNION, CHESTER, AND YORK COUNTIES, SOUTH CAROLINA AND
CLEVELAND, GASTON, AND MECKLENBURG COUNTIES, NORTH CAROLINA

County	Number of Events	Percentage	Events with Property Damage
Cherokee, SC	42	10%	0
Spartanburg, SC	91	21%	5
Union, SC	42	10%	0
Chester, SC	28	6%	0
York, SC	53	12%	2
Cleveland, NC	55	13%	0
Gaston, NC	49	11%	1
Mecklenburg, NC	72	17%	1
Total	432	100%	9

Number per year = 36

NOTES:

1. Data from NOAA's Satellite & Information System - NCDC Storm Events Database, January 1, 1995 through May 31, 2006, <http://www4.ncdc.noaa.gov/cgi-win/wwcgi.dll?wwevent~storms>
2. For this table, each occurrence of hail was counted as an individual event, even if two counties recorded hail simultaneously.

WLS COL 2.3-1

TABLE 2.3-207
MEAN VENTILATION RATE BY MONTH
GREENSBORO, NC

	Morning Ventilation Rate (m ² /s)	Afternoon Ventilation Rate (m ² /s)	Mean Ventilation Rate (m ² /s)
Jan	3914	6289	5101
Feb	3937	7379	5658
Mar	3979	9203	6591
Apr	3490	12736	8113
May	2631	9404	6017
Jun	2373	9469	5921
July	2338	7779	5059
Aug	2129	6096	4113
Sep	2172	6228	4200
Oct	2025	6262	4143
Nov	2882	5743	4312
Dec	3719	5904	4811

NOTES:

1. Source of data is EPA SCRAM data for 1984-1987, 1989-1991 for Greensboro, High Point, NC, Station 13723 (Lat 36.083, Long 79.950), <http://www.epa.gov/scram001/mixingheightdata.htm>
2. Atmospheric ventilation rate is numerically equal to the product of the mixing height and the average wind speed within the mixing layer.

WLS COL 2.3-1

TABLE 2.3-208 (Sheet 1 of 19)
 ICE STORMS
 CHEROKEE, SPARTANBURG, UNION, CHESTER, AND YORK COUNTIES, SOUTH CAROLINA AND
 CLEVELAND, GASTON, AND MECKLENBURG COUNTIES, NORTH CAROLINA

Date	Time	Type	Deaths	Injuries	Property Damage	Crop Damage
Cherokee County, SC						
3/13/1993	0200	Winter Storm	0	0	0	0
12/22/1993	2100	Snow	0	0	0	0
2/10/1994	1800	Freezing Rain/sleet	0	0	0	0
2/11/1994	1110	Ice Storm	0	0	5.0M	0
1/6/1995	1400	Freezing Rain	0	0	100K	0
1/23/1995	1400	Snow	0	0	0	0
2/7/1995	1800	Snow	0	0	0	0
2/10/1995	0500	Snow Freezing Rain	0	0	0	0
1/6/1996	1800	Winter Storm	0	0	50K	0
1/6/1996	0800	Winter Storm	0	0	0	0
1/7/1996	0000	Winter Storm	0	0	50K	0
1/11/1996	2000	Winter Storm	0	0	0	0
2/2/1996	0100	Freezing Rain	0	0	0	0
2/2/1996	1630	Ice Storm	0	0	0	0
2/2/1996	0500	Ice Storm	0	0	0	0

WLS COL 2.3-1

TABLE 2.3-208 (Sheet 2 of 19)
ICE STORMS
CHEROKEE, SPARTANBURG, UNION, CHESTER, AND YORK COUNTIES, SOUTH CAROLINA AND
CLEVELAND, GASTON, AND MECKLENBURG COUNTIES, NORTH CAROLINA

Date	Time	Type	Deaths	Injuries	Property Damage	Crop Damage
2/16/1996	0600	Snow	0	0	0	0
1/9/1997	0000	Ice Storm	0	0	200K	0
2/13/1997	1200	Ice Storm	0	0	0	0
12/29/1997	0530	Snow	0	0	0	0
1/19/1998	0600	Snow	0	0	0	0
12/23/1998	0900	Freezing Rain/sleet	0	0	0	0
12/24/1998	0500	Ice Storm	0	0	0	0
1/2/1999	1800	Ice Storm	0	0	20.0M	0
1/31/1999	1200	Snow And Sleet	0	0	0	0
2/1/1999	0000	Freezing Rain	0	0	0	0
2/19/1999	1200	Snow	0	0	0	0
1/22/2000	1800	Heavy Snow	0	0	0	0
1/24/2000	1000	Heavy Snow	0	0	0	0
1/29/2000	2100	Ice Storm	0	0	0	0
11/19/2000	0600	Snow	0	0	0	0
12/3/2000	0200	Snow	0	0	0	0

WLS COL 2.3-1

TABLE 2.3-208 (Sheet 3 of 19)
ICE STORMS
CHEROKEE, SPARTANBURG, UNION, CHESTER, AND YORK COUNTIES, SOUTH CAROLINA AND
CLEVELAND, GASTON, AND MECKLENBURG COUNTIES, NORTH CAROLINA

Date	Time	Type	Deaths	Injuries	Property Damage	Crop Damage
12/13/2000	1300	Freezing Rain	0	0	0	0
12/19/2000	0200	Snow	0	0	0	0
12/21/2000	1400	Freezing Rain	0	0	0	0
4/17/2001	0700	Snow Showers	0	0	0	0
1/3/2002	0000	Heavy Snow	0	0	0	0
12/4/2002	1500	Ice Storm	0	0	100.0M	0
1/16/2003	1800	Winter Weather/mix	0	0	0	0
1/23/2003	0600	Heavy Snow	0	0	0	0
12/4/2003	0600	Winter Weather/mix	0	0	0	0
1/27/2004	0000	Winter Weather/mix	0	0	0	0
2/26/2004	1000	Heavy Snow	0	0	1.9M	0
1/29/2005	1300	Winter Storm	0	0	0	0
1/29/2005	0400	Winter Weather/mix	0	0	0	0
12/8/2005	1600	Winter Weather	0	0	0	0
12/15/2005	0600	Ice Storm	0	0	900K	0
12/15/2005	0000	Winter Weather	0	0	0	0

WLS COL 2.3-1

TABLE 2.3-208 (Sheet 4 of 19)
ICE STORMS
CHEROKEE, SPARTANBURG, UNION, CHESTER, AND YORK COUNTIES, SOUTH CAROLINA AND
CLEVELAND, GASTON, AND MECKLENBURG COUNTIES, NORTH CAROLINA

Date	Time	Type	Deaths	Injuries	Property Damage	Crop Damage
Spartanburg County, SC						
1/11/1994	0300	Freezing Rain	0	0	0	0
2/10/1994	1800	Freezing Rain/sleet	0	0	0	0
2/11/1994	1110	Ice Storm	0	0	5.0M	0
1/6/1995	1400	Freezing Rain	0	0	100K	0
2/7/1995	1800	Snow	0	0	0	0
2/10/1995	0500	Snow Freezing Rain	0	0	0	0
1/6/1996	1800	Winter Storm	0	0	50K	0
1/6/1996	0800	Winter Storm	0	0	0	0
1/7/1996	0000	Winter Storm	0	0	50K	0
1/11/1996	2000	Winter Storm	0	0	0	0
2/2/1996	0100	Freezing Rain	0	0	0	0
2/2/1996	1630	Ice Storm	0	0	0	0
2/16/1996	0600	Snow	0	0	0	0
12/18/1996	1800	Heavy Snow	0	0	0	0
1/9/1997	0000	Ice Storm	0	0	200K	0

WLS COL 2.3-1

TABLE 2.3-208 (Sheet 5 of 19)
ICE STORMS
CHEROKEE, SPARTANBURG, UNION, CHESTER, AND YORK COUNTIES, SOUTH CAROLINA AND
CLEVELAND, GASTON, AND MECKLENBURG COUNTIES, NORTH CAROLINA

Date	Time	Type	Deaths	Injuries	Property Damage	Crop Damage
2/13/1997	1200	Ice Storm	0	0	0	0
12/29/1997	0530	Heavy Snow	0	0	0	0
1/19/1998	0600	Snow	0	0	0	0
12/23/1998	0900	Freezing Rain/sleet	0	0	0	0
12/24/1998	0500	Ice Storm	0	0	0	0
1/2/1999	1800	Ice Storm	0	0	20.0M	0
1/31/1999	1200	Snow And Sleet	0	0	0	0
2/1/1999	0000	Freezing Rain	0	0	0	0
2/24/1999	0000	Snow	0	0	0	0
3/9/1999	0400	Winter Storm	0	0	0	0
1/22/2000	1800	Heavy Snow	0	0	0	0
1/23/2000	0300	Ice Storm	0	0	0	0
1/24/2000	1000	Heavy Snow	0	0	0	0
1/29/2000	2100	Ice Storm	0	0	0	0
11/19/2000	0600	Snow	0	0	0	0
12/3/2000	0200	Snow	0	0	0	0

WLS COL 2.3-1

TABLE 2.3-208 (Sheet 6 of 19)
ICE STORMS
CHEROKEE, SPARTANBURG, UNION, CHESTER, AND YORK COUNTIES, SOUTH CAROLINA AND
CLEVELAND, GASTON, AND MECKLENBURG COUNTIES, NORTH CAROLINA

Date	Time	Type	Deaths	Injuries	Property Damage	Crop Damage
12/13/2000	1300	Freezing Rain	0	0	0	0
12/19/2000	0200	Snow	0	0	0	0
12/21/2000	1400	Freezing Rain	0	0	0	0
3/20/2001	0700	Heavy Snow	0	0	0	0
4/17/2001	0700	Snow Showers	0	0	0	0
1/3/2002	0000	Heavy Snow	0	0	0	0
12/4/2002	1500	Ice Storm	0	0	100.0M	0
1/16/2003	1800	Winter Weather/mix	0	0	0	0
1/23/2003	0600	Heavy Snow	0	0	0	0
2/16/2003	1400	Winter Storm	0	0	0	0
12/4/2003	0600	Winter Weather/mix	0	0	0	0
1/27/2004	0000	Winter Weather/mix	0	0	0	0
2/2/2004	1800	Winter Weather/mix	0	0	0	0
2/26/2004	1000	Heavy Snow	0	0	1.9M	0
1/29/2005	1300	Winter Storm	0	0	0	0
1/29/2005	0400	Winter Weather/mix	0	0	0	0

WLS COL 2.3-1

TABLE 2.3-208 (Sheet 7 of 19)
ICE STORMS
CHEROKEE, SPARTANBURG, UNION, CHESTER, AND YORK COUNTIES, SOUTH CAROLINA AND
CLEVELAND, GASTON, AND MECKLENBURG COUNTIES, NORTH CAROLINA

Date	Time	Type	Deaths	Injuries	Property Damage	Crop Damage
12/8/2005	1600	Winter Weather	0	0	0	0
12/15/2005	0600	Ice Storm	0	0	900K	0
12/15/2005	0000	Winter Weather	0	0	0	0
Union County, SC						
12/22/1993	2100	Snow	0	0	0	0
2/10/1994	1800	Freezing Rain/sleet	0	0	0	0
2/11/1994	1110	Ice Storm	0	0	5.0M	0
1/6/1995	1400	Freezing Rain	0	0	100K	0
1/7/1996	0300	Winter Storm	0	0	0	0
2/3/1996	0200	Freezing Rain	0	0	0	0
2/16/1996	0600	Snow	0	0	0	0
12/29/1997	0530	Snow	0	0	0	0
1/19/1998	0600	Snow	0	0	0	0
1/2/1999	1800	Ice Storm	0	0	20.0M	0
1/22/2000	1800	Heavy Snow	0	0	0	0
1/23/2000	0300	Ice Storm	0	0	0	0

WLS COL 2.3-1

TABLE 2.3-208 (Sheet 8 of 19)
ICE STORMS
CHEROKEE, SPARTANBURG, UNION, CHESTER, AND YORK COUNTIES, SOUTH CAROLINA AND
CLEVELAND, GASTON, AND MECKLENBURG COUNTIES, NORTH CAROLINA

Date	Time	Type	Deaths	Injuries	Property Damage	Crop Damage
1/24/2000	1000	Heavy Snow	0	0	0	0
1/29/2000	2100	Ice Storm	0	0	0	0
11/19/2000	0600	Snow	0	0	0	0
4/17/2001	0700	Snow Showers	0	0	0	0
1/3/2002	0000	Heavy Snow	0	0	0	0
12/4/2002	1500	Ice Storm	0	0	100.0M	0
1/23/2003	0600	Heavy Snow	0	0	0	0
2/16/2003	1400	Winter Storm	0	0	0	0
1/27/2004	0000	Winter Weather/mix	0	0	0	0
2/26/2004	1000	Heavy Snow	0	0	1.9M	0
1/29/2005	0400	Winter Weather/mix	0	0	0	0
12/15/2005	0700	Ice Storm	0	0	250K	0
12/15/2005	0000	Winter Weather	0	0	0	0
Chester County, SC						
2/10/1994	1800	Freezing Rain/sleet	0	0	0	0
2/11/1994	1110	Ice Storm	0	0	5.0M	0

WLS COL 2.3-1

TABLE 2.3-208 (Sheet 9 of 19)
ICE STORMS
CHEROKEE, SPARTANBURG, UNION, CHESTER, AND YORK COUNTIES, SOUTH CAROLINA AND
CLEVELAND, GASTON, AND MECKLENBURG COUNTIES, NORTH CAROLINA

Date	Time	Type	Deaths	Injuries	Property Damage	Crop Damage
1/6/1996	1200	Ice Storm	0	0	0	0
1/7/1996	0300	Winter Storm	0	0	0	0
1/7/1996	0600	Ice Storm	0	0	0	0
1/11/1996	2200	Ice Storm	0	0	0	0
2/3/1996	0200	Freezing Rain	0	0	0	0
12/29/1997	0530	Snow	0	0	0	0
1/19/1998	0600	Snow	0	0	0	0
1/23/2000	0300	Ice Storm	0	0	0	0
1/24/2000	1000	Heavy Snow	0	0	0	0
1/29/2000	2100	Ice Storm	0	0	0	0
11/19/2000	0600	Snow	0	0	0	0
12/3/2000	0200	Snow	0	0	0	0
1/2/2002	2000	Heavy Snow	0	0	0	0
1/2/2002	2120	Winter Storm	0	0	0	0
12/4/2002	1500	Ice Storm	0	0	100.0M	0
12/4/2002	0755	Ice Storm	0	0	0	0

WLS COL 2.3-1

TABLE 2.3-208 (Sheet 10 of 19)
ICE STORMS
CHEROKEE, SPARTANBURG, UNION, CHESTER, AND YORK COUNTIES, SOUTH CAROLINA AND
CLEVELAND, GASTON, AND MECKLENBURG COUNTIES, NORTH CAROLINA

Date	Time	Type	Deaths	Injuries	Property Damage	Crop Damage
1/23/2003	0600	Heavy Snow	0	0	0	0
1/23/2003	0600	Winter Storm	0	0	0	0
2/16/2003	1400	Winter Storm	0	0	0	0
2/16/2003	2206	Ice Storm	0	22	0	0
1/25/2004	1500	Winter Storm	0	0	0	0
1/27/2004	0000	Winter Weather/mix	0	0	0	0
2/26/2004	0722	Winter Storm	0	0	0	0
2/26/2004	1000	Heavy Snow	0	0	1.9M	0
12/26/2004	0415	Ice Storm	0	0	0	0
12/26/2004	0600	Winter Weather/mix	0	0	0	0
1/29/2005	0400	Winter Weather/mix	0	0	0	0
1/29/2005	1220	Ice Storm	0	0	0	0
12/15/2005	0300	Winter Weather	0	0	0	0
York County, SC						
2/10/1994	1800	Freezing Rain/sleet	0	0	0	0
2/11/1994	1110	Ice Storm	0	0	5.0M	0

WLS COL 2.3-1

TABLE 2.3-208 (Sheet 11 of 19)
 ICE STORMS
 CHEROKEE, SPARTANBURG, UNION, CHESTER, AND YORK COUNTIES, SOUTH CAROLINA AND
 CLEVELAND, GASTON, AND MECKLENBURG COUNTIES, NORTH CAROLINA

Date	Time	Type	Deaths	Injuries	Property Damage	Crop Damage
1/6/1996	1800	Winter Storm	0	0	50K	0
1/6/1996	0800	Winter Storm	0	0	0	0
1/7/1996	0600	Ice Storm	0	0	0	0
1/7/1996	0000	Winter Storm	0	0	50K	0
1/11/1996	2000	Winter Storm	0	0	0	0
2/2/1996	1630	Ice Storm	0	0	0	0
2/16/1996	0600	Snow	0	0	0	0
2/13/1997	1200	Ice Storm	0	0	0	0
12/29/1997	0530	Snow	0	0	0	0
1/19/1998	0600	Snow	0	0	0	0
12/23/1998	0900	Freezing Rain/sleet	0	0	0	0
12/24/1998	0500	Ice Storm	0	0	0	0
2/19/1999	1200	Snow	0	0	0	0
1/22/2000	1800	Snow	0	0	0	0
1/23/2000	0300	Ice Storm	0	0	0	0
1/24/2000	1000	Heavy Snow	0	0	0	0

WLS COL 2.3-1

TABLE 2.3-208 (Sheet 12 of 19)
 ICE STORMS
 CHEROKEE, SPARTANBURG, UNION, CHESTER, AND YORK COUNTIES, SOUTH CAROLINA AND
 CLEVELAND, GASTON, AND MECKLENBURG COUNTIES, NORTH CAROLINA

Date	Time	Type	Deaths	Injuries	Property Damage	Crop Damage
1/29/2000	2100	Ice Storm	0	0	0	0
11/19/2000	0600	Snow	0	0	0	0
12/21/2000	1400	Freezing Rain	0	0	0	0
4/17/2001	0700	Snow Showers	0	0	0	0
1/2/2002	2000	Heavy Snow	0	0	0	0
12/4/2002	1500	Ice Storm	0	0	100.0M	0
1/23/2003	0600	Heavy Snow	0	0	0	0
1/27/2004	0000	Winter Weather/mix	0	0	0	0
2/26/2004	1000	Heavy Snow	0	0	1.9M	0
1/29/2005	1300	Winter Storm	0	0	0	0
1/29/2005	0400	Winter Weather/mix	0	0	0	0
12/15/2005	0300	Winter Weather	0	0	0	0
Cleveland County, NC						
2/10/1994	1000	Ice Storm	0	0	0	0
1/11/1996	1800	Winter Storm	0	0	0	0
2/2/1996	0600	Ice Storm	0	0	10.0M	0

WLS COL 2.3-1

TABLE 2.3-208 (Sheet 13 of 19)
 ICE STORMS
 CHEROKEE, SPARTANBURG, UNION, CHESTER, AND YORK COUNTIES, SOUTH CAROLINA AND
 CLEVELAND, GASTON, AND MECKLENBURG COUNTIES, NORTH CAROLINA

Date	Time	Type	Deaths	Injuries	Property Damage	Crop Damage
2/3/1996	1800	Snow	0	0	0	0
2/16/1996	0200	Snow	0	0	0	0
2/13/1997	1500	Ice Storm	0	0	0	0
2/13/1997	1000	Winter Storm	0	0	0	0
12/29/1997	0530	Snow	0	0	0	0
12/23/1998	0900	Freezing Rain/sleet	0	0	0	0
1/2/1999	1800	Ice Storm	0	0	0	0
2/1/1999	0000	Freezing Rain	0	0	0	0
2/19/1999	1200	Snow	0	0	0	0
3/9/1999	0300	Snow And Sleet	0	0	0	0
1/18/2000	0400	Snow	0	0	0	0
1/22/2000	1500	Heavy Snow	0	0	0	0
1/24/2000	1300	Heavy Snow	0	0	0	0
1/29/2000	2100	Freezing Rain	0	0	0	0
11/19/2000	0600	Snow	0	0	0	0
12/3/2000	0300	Snow	0	0	0	0

WLS COL 2.3-1

TABLE 2.3-208 (Sheet 14 of 19)
ICE STORMS
CHEROKEE, SPARTANBURG, UNION, CHESTER, AND YORK COUNTIES, SOUTH CAROLINA AND
CLEVELAND, GASTON, AND MECKLENBURG COUNTIES, NORTH CAROLINA

Date	Time	Type	Deaths	Injuries	Property Damage	Crop Damage
12/13/2000	1700	Freezing Rain	0	0	0	0
2/22/2001	0300	Snow/sleet	0	0	0	0
3/20/2001	0800	Heavy Snow	0	0	0	0
4/17/2001	0700	Snow Showers	0	0	0	0
1/3/2002	0000	Heavy Snow	0	0	0	0
12/4/2002	1500	Ice Storm	0	0	99.0M	0
1/16/2003	1800	Winter Weather/mix	0	0	0	0
1/23/2003	0400	Heavy Snow	0	0	0	0
2/27/2003	0000	Winter Weather/mix	0	0	0	0
12/4/2003	0600	Winter Weather/mix	0	0	0	0
12/14/2003	0800	Ice Storm	0	0	3K	0
1/27/2004	0000	Winter Weather/mix	0	0	0	0
2/26/2004	1000	Heavy Snow	0	0	3.1M	0
1/29/2005	1300	Winter Storm	0	0	0	0
1/29/2005	0400	Winter Weather/mix	0	0	0	0
3/17/2005	0200	Winter Weather/mix	0	0	0	0

WLS COL 2.3-1

TABLE 2.3-208 (Sheet 15 of 19)
 ICE STORMS
 CHEROKEE, SPARTANBURG, UNION, CHESTER, AND YORK COUNTIES, SOUTH CAROLINA AND
 CLEVELAND, GASTON, AND MECKLENBURG COUNTIES, NORTH CAROLINA

Date	Time	Type	Deaths	Injuries	Property Damage	Crop Damage
12/8/2005	1600	Winter Weather	0	0	0	0
12/15/2005	0600	Ice Storm	0	0	450K	0
12/15/2005	0000	Winter Weather	0	0	0	0
3/20/2006	1200	Winter Weather	0	0	0	0
Gaston County, NC						
2/10/1994	1000	Ice Storm	0	0	0	0
1/6/1996	1800	Winter Storm	0	0	0	0
1/11/1996	1800	Winter Storm	0	0	0	0
2/2/1996	0600	Ice Storm	0	0	10.0M	0
2/3/1996	1800	Snow	0	0	0	0
2/16/1996	0200	Snow	0	0	0	0
2/13/1997	1500	Ice Storm	0	0	0	0
2/13/1997	1000	Winter Storm	0	0	0	0
12/29/1997	0530	Snow	0	0	0	0
1/19/1998	0600	Snow	0	0	0	0
12/23/1998	0900	Freezing Rain/sleet	0	0	0	0

WLS COL 2.3-1

TABLE 2.3-208 (Sheet 16 of 19)
 ICE STORMS
 CHEROKEE, SPARTANBURG, UNION, CHESTER, AND YORK COUNTIES, SOUTH CAROLINA AND
 CLEVELAND, GASTON, AND MECKLENBURG COUNTIES, NORTH CAROLINA

Date	Time	Type	Deaths	Injuries	Property Damage	Crop Damage
12/24/1998	0500	Ice Storm	0	0	0	0
1/2/1999	1800	Ice Storm	0	0	0	0
2/1/1999	0000	Freezing Rain	0	0	0	0
2/19/1999	1200	Snow	0	0	0	0
3/9/1999	0300	Snow And Sleet	0	0	0	0
1/18/2000	0400	Snow	0	0	0	0
1/22/2000	1500	Heavy Snow	0	0	0	0
1/24/2000	1300	Heavy Snow	0	0	0	0
1/29/2000	2100	Ice Storm	0	0	0	0
11/19/2000	0600	Snow	0	0	0	0
4/17/2001	0700	Snow Showers	0	0	0	0
1/3/2002	0000	Heavy Snow	0	0	0	0
12/4/2002	1500	Ice Storm	0	0	99.0M	0
1/16/2003	1800	Winter Weather/mix	0	0	0	0
1/23/2003	0600	Heavy Snow	0	0	0	0
2/27/2003	0000	Winter Weather/mix	0	0	0	0

WLS COL 2.3-1

TABLE 2.3-208 (Sheet 17 of 19)
ICE STORMS
CHEROKEE, SPARTANBURG, UNION, CHESTER, AND YORK COUNTIES, SOUTH CAROLINA AND
CLEVELAND, GASTON, AND MECKLENBURG COUNTIES, NORTH CAROLINA

Date	Time	Type	Deaths	Injuries	Property Damage	Crop Damage
1/27/2004	0000	Winter Weather/mix	0	0	0	0
2/26/2004	1000	Heavy Snow	0	0	3.1M	0
1/29/2005	1300	Winter Storm	0	0	0	0
1/29/2005	0400	Winter Weather/mix	0	0	0	0
12/15/2005	0600	Ice Storm	0	0	450K	0
12/15/2005	0000	Winter Weather	0	0	0	0
Mecklenburg County, NC						
2/10/1994	1000	Ice Storm	0	0	0	0
1/6/1996	1800	Winter Storm	0	0	0	0
1/11/1996	1800	Winter Storm	0	0	0	0
2/2/1996	0600	Ice Storm	0	0	10.0M	0
2/3/1996	1800	Snow	0	0	0	0
2/16/1996	0200	Snow	0	0	0	0
2/13/1997	1500	Ice Storm	0	0	0	0
12/29/1997	0530	Snow	0	0	0	0
1/19/1998	0600	Snow	0	0	0	0

WLS COL 2.3-1

TABLE 2.3-208 (Sheet 18 of 19)
ICE STORMS
CHEROKEE, SPARTANBURG, UNION, CHESTER, AND YORK COUNTIES, SOUTH CAROLINA AND
CLEVELAND, GASTON, AND MECKLENBURG COUNTIES, NORTH CAROLINA

Date	Time	Type	Deaths	Injuries	Property Damage	Crop Damage
12/23/1998	0900	Freezing Rain/sleet	0	0	0	0
12/24/1998	0500	Ice Storm	0	0	0	0
2/19/1999	1200	Snow	0	0	0	0
1/18/2000	0400	Snow	0	0	0	0
1/22/2000	1500	Heavy Snow	0	0	0	0
1/24/2000	1300	Heavy Snow	0	0	0	0
1/29/2000	2100	Ice Storm	0	0	0	0
11/19/2000	0600	Snow	0	0	0	0
1/2/2002	2000	Heavy Snow	0	0	0	0
12/4/2002	1500	Ice Storm	0	0	99.0M	0
1/16/2003	1800	Winter Weather/mix	0	0	0	0
1/23/2003	0600	Heavy Snow	0	0	0	0
2/27/2003	0000	Winter Weather/mix	0	0	0	0
12/4/2003	0600	Winter Weather/mix	0	0	0	0
1/27/2004	0000	Winter Weather/mix	0	0	0	0
2/26/2004	1000	Heavy Snow	0	0	3.1M	0

WLS COL 2.3-1

TABLE 2.3-208 (Sheet 19 of 19)
ICE STORMS
CHEROKEE, SPARTANBURG, UNION, CHESTER, AND YORK COUNTIES, SOUTH CAROLINA AND
CLEVELAND, GASTON, AND MECKLENBURG COUNTIES, NORTH CAROLINA

Date	Time	Type	Deaths	Injuries	Property Damage	Crop Damage
1/29/2005	1300	Winter Storm	0	0	0	0
1/29/2005	0400	Winter Weather/mix	0	0	0	0
12/15/2005	1100	Ice Storm	1	0	300K	0

NOTES:

1. Lee Nuclear Station site is in Cherokee County. The other counties are surrounding Cherokee County.
2. Data recorded in the NOAA Storm Events Database, 01/01/1950 - 12/31/2005 <http://www4.ncdc.noaa.gov/cgi-win/wwcgi.dll?wwevent~storms>.

WLS COL 2.3-1

TABLE 2.3-209 (Sheet 1 of 2)
 PERCENTAGE FREQUENCY OF WIND DIRECTION AND SPEED (MPH)
 GREENVILLE/SPARTANBURG, SOUTH CAROLINA
 JANUARY, 1997 – 2005

January	Wind Speed (mph)							Total (%)	Avg. Speed
	0-3	4-7	8-12	13-17	18-22	23-27	≥28		
Direction From	Frequency of Occurrence (%)								
N	0.70%	2.36%	3.18%	0.96%	0.33%	0.03%	0.00%	7.56%	9.19
NNE	0.90%	2.76%	2.23%	0.40%	0.15%	0.01%	0.00%	6.45%	7.72
NE	1.00%	3.51%	3.57%	0.90%	0.09%	0.04%	0.00%	9.11%	8.24
ENE	0.55%	2.51%	2.20%	0.64%	0.12%	0.00%	0.00%	6.02%	8.34
E	0.60%	1.43%	1.06%	0.13%	0.04%	0.00%	0.00%	3.27%	7.30
ESE	0.25%	0.63%	0.07%	0.01%	0.00%	0.00%	0.00%	0.97%	5.32
SE	0.27%	0.51%	0.13%	0.00%	0.00%	0.00%	0.00%	0.91%	5.21
SSE	0.33%	0.76%	0.25%	0.00%	0.00%	0.00%	0.00%	1.34%	5.65
S	0.99%	2.24%	0.97%	0.25%	0.00%	0.00%	0.00%	4.45%	6.61
SSW	0.87%	2.17%	2.06%	0.42%	0.04%	0.01%	0.00%	5.57%	7.59
SW	0.76%	2.91%	5.59%	2.24%	0.45%	0.04%	0.01%	12.01%	9.97
WSW	0.42%	2.99%	5.36%	2.26%	0.61%	0.06%	0.00%	11.69%	10.43
W	0.66%	1.99%	2.30%	0.55%	0.09%	0.04%	0.00%	5.63%	8.35

WLS COL 2.3-1

TABLE 2.3-209 (Sheet 2 of 2)
 PERCENTAGE FREQUENCY OF WIND DIRECTION AND SPEED (MPH)
 GREENVILLE/SPARTANBURG, SOUTH CAROLINA
 JANUARY, 1997 – 2005

January	Wind Speed (mph)							Total (%)	Avg. Speed
	0-3	4-7	8-12	13-17	18-22	23-27	≥28		
Direction From	Frequency of Occurrence (%)								
WNW	0.24%	0.75%	0.31%	0.10%	0.01%	0.00%	0.00%	1.42%	6.74
NW	0.25%	0.76%	0.55%	0.12%	0.00%	0.00%	0.00%	1.69%	7.41
NNW	0.37%	1.02%	1.51%	0.51%	0.18%	0.04%	0.00%	3.63%	9.62
CALM	14.22%	0.00%	0.00%	0.00%	0.00%	0.00%	0.00%	14.22%	
MISSING	4.06%							4.06%	
Total	27.43%	29.29%	31.35%	9.50%	2.12%	0.30%	0.01%	100.00%	7.73

NOTES:

1. Calm is classified as a wind speed less than 2.3 mph (anemometer start speed) or a variable wind direction, or no wind direction provided.
2. Missing data is data with missing wind speed, missing wind direction, or denoted as "variable" wind direction.
3. Data from Unedited Local Climatological Data, National Oceanic and Atmospheric Administration, U. S. Department of Commerce, Asheville, NC, Greenville/Spartanburg International Airport, Station No. 03870.
4. Period of Record - 9 years (1997 - 2005).

WLS COL 2.3-1

TABLE 2.3-210 (Sheet 1 of 2)
 PERCENTAGE FREQUENCY OF WIND DIRECTION AND SPEED (MPH)
 GREENVILLE/SPARTANBURG, SOUTH CAROLINA
 FEBRUARY, 1997 – 2005

February	Wind Speed (mph)							Total (%)	Avg. Speed
	0-3	4-7	8-12	13-17	18-22	23-27	≥28		
Direction From	Frequency of Occurrence (%)								
N	0.95%	2.44%	2.40%	0.80%	0.15%	0.00%	0.00%	6.74%	8.28
NNE	0.64%	2.87%	2.82%	0.66%	0.07%	0.02%	0.00%	7.07%	8.02
NE	1.02%	4.18%	5.00%	1.38%	0.51%	0.20%	0.00%	12.29%	9.18
ENE	0.80%	2.46%	2.77%	0.80%	0.33%	0.20%	0.00%	7.37%	9.12
E	0.43%	1.67%	1.35%	0.07%	0.00%	0.02%	0.00%	3.53%	7.17
ESE	0.28%	0.71%	0.23%	0.00%	0.00%	0.00%	0.00%	1.21%	5.71
SE	0.28%	0.74%	0.18%	0.00%	0.00%	0.00%	0.00%	1.20%	5.60
SSE	0.34%	1.28%	0.23%	0.00%	0.00%	0.00%	0.00%	1.85%	5.60
S	0.72%	2.30%	0.95%	0.07%	0.02%	0.00%	0.00%	4.05%	6.41
SSW	0.80%	2.07%	1.62%	0.38%	0.15%	0.05%	0.00%	5.07%	7.96
SW	0.59%	2.72%	3.64%	1.30%	0.43%	0.05%	0.02%	8.74%	9.56
WSW	0.75%	2.23%	3.89%	1.59%	0.43%	0.11%	0.03%	9.04%	10.04
W	0.46%	1.79%	2.13%	0.69%	0.26%	0.05%	0.00%	5.38%	9.25

WLS COL 2.3-1

TABLE 2.3-210 (Sheet 2 of 2)
 PERCENTAGE FREQUENCY OF WIND DIRECTION AND SPEED (MPH)
 GREENVILLE/SPARTANBURG, SOUTH CAROLINA
 FEBRUARY, 1997 – 2005

February	Wind Speed (mph)							Total (%)	Avg. Speed
	0-3	4-7	8-12	13-17	18-22	23-27	≥28		
Direction From	Frequency of Occurrence (%)							Total (%)	Avg. Speed
WNW	0.31%	0.59%	0.51%	0.23%	0.08%	0.02%	0.00%	1.74%	8.56
NW	0.33%	0.62%	0.31%	0.20%	0.00%	0.00%	0.00%	1.46%	7.15
NNW	0.25%	0.89%	0.80%	0.34%	0.15%	0.00%	0.00%	2.43%	8.88
CALM	15.76%	0.00%	0.00%	0.00%	0.00%	0.00%	0.00%	15.76%	
MISSING	5.07%							5.07%	
Total	29.79%	29.56%	28.84%	8.50%	2.56%	0.71%	0.05%	100.00%	7.90

NOTES:

1. Calm is classified as a wind speed less than 2.3 mph (anemometer start speed) or a variable wind direction.
2. Missing data is data with missing wind speed, missing wind direction, or denoted as "variable" wind direction.
3. Data from Unedited Local Climatological Data, National Oceanic and Atmospheric Administration, U. S. Department of Commerce, Asheville, NC, Greenville/Spartanburg International Airport, Station No. 03870.
4. Period of Record - 9 years (1997 - 2005).

WLS COL 2.3-1

TABLE 2.3-211 (Sheet 1 of 2)
 PERCENTAGE FREQUENCY OF WIND DIRECTION AND SPEED (MPH)
 GREENVILLE/SPARTANBURG, SOUTH CAROLINA
 MARCH, 1997 – 2005

March	Wind Speed (mph)							Total (%)	Avg. Speed
	0-3	4-7	8-12	13-17	18-22	23-27	≥28		
Direction From	Frequency of Occurrence (%)								
N	0.54%	1.88%	2.70%	1.24%	0.37%	0.00%	0.01%	6.75%	9.66
NNE	0.48%	2.72%	3.24%	0.64%	0.18%	0.00%	0.00%	7.26%	8.60
NE	0.72%	3.23%	5.12%	1.34%	0.30%	0.07%	0.00%	10.78%	9.25
ENE	0.51%	2.33%	3.54%	1.11%	0.09%	0.01%	0.00%	7.59%	8.92
E	0.33%	1.45%	1.52%	0.19%	0.00%	0.00%	0.00%	3.49%	7.57
ESE	0.27%	0.63%	0.28%	0.01%	0.00%	0.00%	0.00%	1.19%	6.07
SE	0.18%	0.75%	0.33%	0.00%	0.00%	0.00%	0.00%	1.25%	6.07
SSE	0.27%	1.31%	0.34%	0.00%	0.00%	0.00%	0.00%	1.93%	6.00
S	0.72%	2.37%	1.57%	0.10%	0.01%	0.00%	0.00%	4.78%	7.03
SSW	0.54%	2.12%	2.27%	0.70%	0.15%	0.01%	0.00%	5.79%	8.69
SW	0.52%	2.09%	3.67%	1.70%	0.51%	0.13%	0.01%	8.65%	10.44
WSW	0.45%	2.08%	3.99%	1.94%	0.76%	0.33%	0.03%	9.57%	11.26
W	0.45%	1.94%	2.42%	1.00%	0.37%	0.16%	0.03%	6.38%	10.03

WLS COL 2.3-1

TABLE 2.3-211 (Sheet 2 of 2)
 PERCENTAGE FREQUENCY OF WIND DIRECTION AND SPEED (MPH)
 GREENVILLE/SPARTANBURG, SOUTH CAROLINA
 MARCH, 1997 – 2005

March	Wind Speed (mph)							Total (%)	Avg. Speed
	0-3	4-7	8-12	13-17	18-22	23-27	≥28		
Direction From	Frequency of Occurrence (%)								
WNW	0.27%	0.66%	0.61%	0.24%	0.06%	0.07%	0.00%	1.91%	9.21
NW	0.16%	0.73%	0.70%	0.12%	0.04%	0.01%	0.00%	1.78%	8.00
NNW	0.30%	0.94%	1.16%	0.51%	0.18%	0.04%	0.00%	3.14%	9.72
CALM	11.66%	0.00%	0.00%	0.00%	0.00%	0.00%	0.00%	11.66%	
MISSING	6.09%							6.09%	
Total	24.45%	27.23%	33.48%	10.86%	3.03%	0.87%	0.09%	100.00%	8.53

NOTES:

1. Calm is classified as a wind speed less than 2.3 mph (anemometer start speed) or a variable wind direction.
2. Missing data is data with missing wind speed, missing wind direction, or denoted as "variable" wind direction.
3. Data from Unedited Local Climatological Data, National Oceanic and Atmospheric Administration, U. S. Department of Commerce, Asheville, NC, Greenville/Spartanburg International Airport, Station No. 03870.
4. Period of Record - 9 years (1997 - 2005).

WLS COL 2.3-1

TABLE 2.3-212 (Sheet 1 of 2)
 PERCENTAGE FREQUENCY OF WIND DIRECTION AND SPEED (MPH)
 GREENVILLE/SPARTANBURG, SOUTH CAROLINA
 APRIL, 1997-2005

Direction From	Wind Speed (mph)							Total (%)	Avg. Speed
	0-3	4-7	8-12	13-17	18-22	23-27	≥28		
Frequency of Occurrence (%)									
N	0.82%	1.71%	2.48%	0.76%	0.29%	0.06%	0.00%	6.13%	9.13
NNE	0.56%	1.84%	2.07%	0.68%	0.02%	0.03%	0.02%	5.20%	8.52
NE	0.51%	2.47%	3.43%	1.54%	0.23%	0.03%	0.00%	8.21%	9.62
ENE	0.66%	1.84%	2.05%	0.71%	0.32%	0.00%	0.00%	5.59%	8.85
E	0.42%	1.05%	1.19%	0.11%	0.00%	0.00%	0.00%	2.76%	7.37
ESE	0.03%	0.42%	0.37%	0.02%	0.00%	0.00%	0.00%	0.83%	7.26
SE	0.17%	0.66%	0.46%	0.03%	0.00%	0.00%	0.00%	1.33%	6.74
SSE	0.17%	1.20%	0.80%	0.09%	0.00%	0.00%	0.00%	2.27%	6.86
S	0.82%	2.92%	2.33%	0.40%	0.06%	0.00%	0.00%	6.53%	7.54
SSW	0.62%	2.76%	3.58%	1.02%	0.20%	0.00%	0.00%	8.18%	8.93
SW	0.48%	3.43%	5.54%	2.11%	0.59%	0.11%	0.02%	12.27%	10.11
WSW	0.54%	2.90%	4.20%	2.07%	0.80%	0.29%	0.02%	10.82%	10.46
W	0.43%	2.21%	2.31%	1.02%	0.45%	0.19%	0.06%	6.67%	10.31

WLS COL 2.3-1

TABLE 2.3-212 (Sheet 2 of 2)
 PERCENTAGE FREQUENCY OF WIND DIRECTION AND SPEED (MPH)
 GREENVILLE/SPARTANBURG, SOUTH CAROLINA
 APRIL, 1997-2005

Direction From	Wind Speed (mph)							Total (%)	Avg. Speed
	0-3	4-7	8-12	13-17	18-22	23-27	≥28		
Frequency of Occurrence (%)									
WNW	0.17%	0.63%	0.66%	0.25%	0.11%	0.08%	0.00%	1.90%	9.75
NW	0.29%	0.69%	0.54%	0.15%	0.06%	0.00%	0.00%	1.74%	7.89
NNW	0.28%	0.65%	0.97%	0.42%	0.12%	0.00%	0.00%	2.44%	9.25
CALM	11.62%	0.00%	0.00%	0.00%	0.00%	0.00%	0.00%	11.62%	
MISSING	5.52%							5.52%	
Total	24.10%	27.38%	32.99%	11.37%	3.26%	0.79%	0.11%	100.00%	8.66

NOTES:

1. Calm is classified as a wind speed less than 2.3 mph (anemometer start speed) or a variable wind direction.
2. Missing data is data with missing wind speed, missing wind direction, or denoted as "variable" wind direction.
3. Data from Unedited Local Climatological Data, National Oceanic and Atmospheric Administration, U. S. Department of Commerce, Asheville, NC, Greenville/Spartanburg International Airport, Station No. 03870.
4. Period of Record - 9 years (1997 - 2005).

WLS COL 2.3-1

TABLE 2.3-213 (Sheet 1 of 2)
 PERCENTAGE FREQUENCY OF WIND DIRECTION AND SPEED (MPH)
 GREENVILLE/SPARTANBURG, SOUTH CAROLINA
 MAY, 1997-2005

Direction From	Wind Speed (mph)							Total (%)	Avg. Speed
	0-3	4-7	8-12	13-17	18-22	23-27	≥28		
May	Frequency of Occurrence (%)								
N	0.85%	1.96%	1.51%	0.22%	0.06%	0.01%	0.00%	4.61%	7.36
NNE	0.76%	2.99%	2.43%	0.30%	0.03%	0.00%	0.00%	6.51%	7.39
NE	0.55%	2.97%	3.39%	0.90%	0.04%	0.00%	0.00%	7.86%	8.58
ENE	0.45%	1.48%	2.08%	0.48%	0.12%	0.00%	0.00%	4.60%	8.65
E	0.34%	1.14%	1.08%	0.12%	0.03%	0.00%	0.00%	2.70%	7.55
ESE	0.21%	0.49%	0.34%	0.00%	0.00%	0.00%	0.00%	1.05%	6.54
SE	0.21%	0.57%	0.46%	0.00%	0.00%	0.00%	0.00%	1.24%	6.56
SSE	0.27%	1.48%	0.42%	0.01%	0.00%	0.00%	0.00%	2.18%	6.10
S	0.75%	2.70%	1.58%	0.07%	0.00%	0.00%	0.00%	5.11%	6.67
SSW	0.69%	2.39%	2.72%	0.67%	0.12%	0.00%	0.00%	6.59%	8.38
SW	0.57%	3.00%	5.63%	1.87%	0.43%	0.15%	0.01%	11.66%	9.99
WSW	0.55%	3.54%	5.03%	1.85%	0.40%	0.01%	0.00%	11.39%	9.51
W	0.45%	2.49%	2.69%	0.90%	0.21%	0.01%	0.00%	6.75%	8.75

WLS COL 2.3-1

TABLE 2.3-213 (Sheet 2 of 2)
 PERCENTAGE FREQUENCY OF WIND DIRECTION AND SPEED (MPH)
 GREENVILLE/SPARTANBURG, SOUTH CAROLINA
 MAY, 1997-2005

Direction From	May	Wind Speed (mph)						Total (%)	Avg. Speed
	0-3	4-7	8-12	13-17	18-22	23-27	≥28		
Frequency of Occurrence (%)									
WNW	0.16%	0.67%	0.57%	0.19%	0.03%	0.01%	0.00%	1.64%	8.20
NW	0.19%	0.51%	0.36%	0.04%	0.01%	0.00%	0.00%	1.12%	7.32
NNW	0.39%	0.64%	0.39%	0.07%	0.01%	0.00%	0.00%	1.51%	6.70
CALM	16.58%	0.00%	0.00%	0.00%	0.00%	0.00%	0.00%	23.48%	
missing	6.90%							6.90%	
Total	30.87%	29.02%	30.68%	7.71%	1.51%	0.21%	0.01%	100.00%	7.77

NOTES:

1. Calm is classified as a wind speed less than 2.3 mph (anemometer start speed) or a variable wind direction.
2. Missing data is data with missing wind speed, missing wind direction, or denoted as "variable" wind direction.
3. Data from Unedited Local Climatological Data, National Oceanic and Atmospheric Administration, U. S. Department of Commerce, Asheville, NC, Greenville/Spartanburg International Airport, Station No. 03870.
4. Period of Record - 9 years (1997 - 2005).

WLS COL 2.3-1

TABLE 2.3-214 (Sheet 1 of 2)
 PERCENTAGE FREQUENCY OF WIND DIRECTION AND SPEED (MPH)
 GREENVILLE/SPARTANBURG, SOUTH CAROLINA
 JUNE, 1997-2005

Direction From	June	Wind Speed (mph)						Total (%)	Avg. Speed
	0-3	4-7	8-12	13-17	18-22	23-27	≥28		
Frequency of Occurrence (%)									
N	0.82%	2.01%	1.22%	0.23%	0.02%	0.00%	0.00%	4.29%	7.00
NNE	0.88%	3.07%	2.24%	0.35%	0.02%	0.00%	0.00%	6.56%	7.26
NE	0.77%	4.06%	3.33%	0.71%	0.06%	0.00%	0.00%	8.94%	7.89
ENE	0.59%	2.19%	2.58%	0.56%	0.03%	0.00%	0.00%	5.94%	8.19
E	0.62%	1.74%	2.07%	0.34%	0.00%	0.02%	0.00%	4.78%	7.92
ESE	0.26%	0.85%	0.48%	0.02%	0.00%	0.00%	0.00%	1.60%	6.33
SE	0.31%	0.69%	0.45%	0.06%	0.00%	0.00%	0.00%	1.51%	6.54
SSE	0.34%	1.37%	0.74%	0.03%	0.00%	0.00%	0.00%	2.48%	6.34
S	0.88%	2.15%	1.62%	0.26%	0.06%	0.02%	0.00%	4.98%	7.25
SSW	0.43%	1.74%	1.90%	0.23%	0.02%	0.02%	0.00%	4.34%	8.04
SW	0.65%	3.64%	3.83%	0.96%	0.05%	0.00%	0.00%	9.12%	8.28
WSW	0.71%	3.16%	4.65%	0.96%	0.17%	0.05%	0.00%	9.69%	8.80
W	0.62%	2.61%	2.82%	0.42%	0.11%	0.02%	0.00%	6.59%	7.83

WLS COL 2.3-1

TABLE 2.3-214 (Sheet 2 of 2)
 PERCENTAGE FREQUENCY OF WIND DIRECTION AND SPEED (MPH)
 GREENVILLE/SPARTANBURG, SOUTH CAROLINA
 JUNE, 1997-2005

June	Wind Speed (mph)							Total (%)	Avg. Speed
	0-3	4-7	8-12	13-17	18-22	23-27	≥28		
Direction From	Frequency of Occurrence (%)								
WNW	0.39%	1.03%	0.49%	0.08%	0.02%	0.00%	0.00%	2.01%	6.53
NW	0.35%	0.71%	0.26%	0.03%	0.00%	0.00%	0.00%	1.36%	5.99
NNW	0.43%	0.65%	0.45%	0.05%	0.00%	0.00%	0.00%	1.57%	6.33
CALM	17.87%	0.00%	0.00%	0.00%	0.00%	0.00%	0.00%	17.87%	
MISSING	6.36%							6.36%	
Total	33.27%	31.68%	29.12%	5.28%	0.54%	0.11%	0.00%	100.00%	7.28

NOTES:

1. Calm is classified as a wind speed less than 2.3 mph (anemometer start speed) or a variable wind direction.
2. Missing data is data with missing wind speed, missing wind direction, or denoted as "variable" wind direction.
3. Data from Unedited Local Climatological Data, National Oceanic and Atmospheric Administration, U. S. Department of Commerce, Asheville, NC, Greenville/Spartanburg International Airport, Station No. 03870.
4. Period of Record - 9 years (1997 - 2005).

WLS COL 2.3-1

TABLE 2.3-215 (Sheet 1 of 2)
 PERCENTAGE FREQUENCY OF WIND DIRECTION AND SPEED (MPH)
 GREENVILLE/SPARTANBURG, SOUTH CAROLINA
 JULY, 1997-2005

Direction From	Wind Speed (mph)							Total (%)	Avg. Speed
	0-3	4-7	8-12	13-17	18-22	23-27	≥28		
N	1.28%	2.42%	0.97%	0.06%	0.00%	0.00%	0.00%	4.73%	5.84
NNE	1.02%	3.70%	1.51%	0.13%	0.01%	0.00%	0.00%	6.38%	6.45
NE	0.97%	3.79%	2.97%	0.54%	0.03%	0.01%	0.00%	8.32%	7.37
ENE	0.43%	1.88%	1.76%	0.12%	0.00%	0.00%	0.00%	4.20%	7.18
E	0.36%	1.84%	1.15%	0.12%	0.00%	0.01%	0.00%	3.48%	7.06
ESE	0.30%	0.81%	0.45%	0.03%	0.00%	0.00%	0.00%	1.58%	6.45
SE	0.46%	1.08%	0.36%	0.06%	0.00%	0.00%	0.00%	1.96%	6.19
SSE	0.39%	1.36%	0.63%	0.04%	0.01%	0.00%	0.00%	2.43%	6.46
S	0.79%	2.06%	1.08%	0.13%	0.03%	0.00%	0.00%	4.09%	6.73
SSW	0.69%	1.85%	1.67%	0.30%	0.06%	0.00%	0.00%	4.57%	7.53
SW	0.73%	3.14%	3.81%	0.64%	0.06%	0.00%	0.00%	8.38%	8.16
WSW	0.84%	3.49%	2.84%	0.42%	0.03%	0.00%	0.00%	7.62%	7.56
W	1.06%	3.21%	2.12%	0.16%	0.01%	0.00%	0.00%	6.57%	6.77

WLS COL 2.3-1

TABLE 2.3-215 (Sheet 2 of 2)
 PERCENTAGE FREQUENCY OF WIND DIRECTION AND SPEED (MPH)
 GREENVILLE/SPARTANBURG, SOUTH CAROLINA
 JULY, 1997-2005

Direction From	Wind Speed (mph)							Total (%)	Avg. Speed
	0-3	4-7	8-12	13-17	18-22	23-27	≥28		
WNW	0.63%	1.21%	0.49%	0.04%	0.01%	0.00%	0.00%	2.39%	6.08
NW	0.75%	0.94%	0.43%	0.00%	0.00%	0.00%	0.00%	2.12%	5.65
NNW	0.48%	0.81%	0.49%	0.06%	0.00%	0.00%	0.00%	1.84%	6.15
CALM	21.64%	0.00%	0.00%	0.00%	0.00%	0.00%	0.00%	21.64%	
MISSING	7.71%							7.71%	
Total	40.52%	33.59%	22.73%	2.87%	0.27%	0.03%	0.00%	100.00%	6.73

NOTES:

1. Calm is classified as a wind speed less than 2.3 mph (anemometer start speed) or a variable wind direction.
2. Missing data is data with missing wind speed, missing wind direction, or denoted as "variable" wind direction.
3. Data from Unedited Local Climatological Data, National Oceanic and Atmospheric Administration, U. S. Department of Commerce, Asheville, NC, Greenville/Spartanburg International Airport, Station No. 03870.
4. Period of Record - 9 years (1997 - 2005).

WLS COL 2.3-1

TABLE 2.3-216 (Sheet 1 of 2)
 PERCENTAGE FREQUENCY OF WIND DIRECTION AND SPEED (MPH)
 GREENVILLE/SPARTANBURG, SOUTH CAROLINA
 AUGUST, 1997-2005

Direction From	August	Wind Speed (mph)						Total (%)	Avg. Speed
	0-3	4-7	8-12	13-17	18-22	23-27	≥28		
Frequency of Occurrence (%)									
N	1.45%	2.03%	0.93%	0.09%	0.00%	0.00%	0.00%	4.50%	5.87
NNE	1.43%	4.05%	2.33%	0.18%	0.01%	0.00%	0.00%	8.00%	6.59
NE	1.34%	5.68%	4.21%	0.25%	0.00%	0.00%	0.00%	11.48%	7.06
ENE	0.82%	2.97%	2.30%	0.25%	0.00%	0.00%	0.00%	6.35%	7.11
E	0.64%	1.96%	1.93%	0.19%	0.01%	0.00%	0.00%	4.73%	7.24
ESE	0.24%	0.94%	0.54%	0.01%	0.00%	0.00%	0.00%	1.73%	6.60
SE	0.31%	0.99%	0.42%	0.04%	0.01%	0.00%	0.00%	1.78%	6.39
SSE	0.42%	1.39%	0.61%	0.04%	0.00%	0.00%	0.00%	2.46%	6.26
S	0.76%	2.30%	1.05%	0.06%	0.07%	0.01%	0.00%	4.26%	6.69
SSW	0.51%	2.20%	1.42%	0.15%	0.00%	0.01%	0.00%	4.29%	7.09
SW	0.66%	3.15%	2.43%	0.25%	0.04%	0.00%	0.00%	6.54%	7.40
WSW	0.81%	2.64%	1.94%	0.33%	0.00%	0.00%	0.00%	5.72%	7.12
W	0.75%	1.93%	1.31%	0.07%	0.00%	0.00%	0.00%	4.06%	6.22

WLS COL 2.3-1

TABLE 2.3-216 (Sheet 2 of 2)
 PERCENTAGE FREQUENCY OF WIND DIRECTION AND SPEED (MPH)
 GREENVILLE/SPARTANBURG, SOUTH CAROLINA
 AUGUST, 1997-2005

August	Wind Speed (mph)							Total (%)	Avg. Speed
	0-3	4-7	8-12	13-17	18-22	23-27	≥28		
Direction From	Frequency of Occurrence (%)								
WNW	0.30%	0.60%	0.31%	0.01%	0.00%	0.00%	0.00%	1.22%	5.90
NW	0.27%	0.48%	0.21%	0.00%	0.00%	0.00%	0.00%	0.96%	5.72
NNW	0.33%	0.57%	0.21%	0.03%	0.00%	0.01%	0.00%	1.15%	6.13
CALM	23.72%	0.00%	0.00%	0.00%	0.00%	0.00%	0.00%	23.72%	
MISSING	7.05%							7.05%	
Total	41.80%	33.86%	22.15%	1.99%	0.16%	0.04%	0.00%	100.00%	6.59

NOTES:

1. Calm is classified as a wind speed less than 2.3 mph (anemometer start speed) or a variable wind direction.
2. Missing data is data with missing wind speed, missing wind direction, or denoted as "variable" wind direction.
3. Data from Unedited Local Climatological Data, National Oceanic and Atmospheric Administration, U. S. Department of Commerce, Asheville, NC, Greenville/Spartanburg International Airport, Station No. 03870.
4. Period of Record - 9 years (1997 - 2005).

WLS COL 2.3-1

TABLE 2.3-217 (Sheet 1 of 2)
 PERCENTAGE FREQUENCY OF WIND DIRECTION AND SPEED (MPH)
 GREENVILLE/SPARTANBURG, SOUTH CAROLINA
 SEPTEMBER, 1997-2005

Direction From	Wind Speed (mph)							Total (%)	Avg. Speed
	0-3	4-7	8-12	13-17	18-22	23-27	≥28		
	Frequency of Occurrence (%)								
N	1.45%	2.61%	1.45%	0.42%	0.02%	0.02%	0.00%	5.96%	6.81
NNE	1.77%	6.76%	4.20%	1.11%	0.12%	0.00%	0.00%	13.97%	7.42
NE	1.65%	5.82%	6.30%	1.73%	0.23%	0.08%	0.00%	15.80%	8.44
ENE	0.76%	2.65%	3.77%	0.76%	0.17%	0.00%	0.00%	8.10%	8.63
E	0.54%	1.94%	1.87%	0.17%	0.09%	0.00%	0.00%	4.61%	7.76
ESE	0.40%	1.03%	0.39%	0.03%	0.03%	0.00%	0.00%	1.88%	6.50
SE	0.31%	1.19%	0.43%	0.06%	0.02%	0.03%	0.00%	2.04%	6.64
SSE	0.32%	1.33%	0.43%	0.03%	0.02%	0.00%	0.00%	2.13%	6.18
S	0.39%	2.08%	1.05%	0.26%	0.02%	0.00%	0.00%	3.80%	7.36
SSW	0.46%	0.94%	0.62%	0.17%	0.03%	0.00%	0.00%	2.22%	7.42
SW	0.28%	1.25%	1.33%	0.15%	0.02%	0.00%	0.00%	3.02%	7.96
WSW	0.42%	1.22%	1.44%	0.19%	0.00%	0.00%	0.00%	3.26%	7.62
W	0.37%	1.22%	1.13%	0.09%	0.02%	0.00%	0.00%	2.82%	7.53

WLS COL 2.3-1

TABLE 2.3-217 (Sheet 2 of 2)
 PERCENTAGE FREQUENCY OF WIND DIRECTION AND SPEED (MPH)
 GREENVILLE/SPARTANBURG, SOUTH CAROLINA
 SEPTEMBER, 1997-2005

September	Wind Speed (mph)							Total (%)	Avg. Speed
	0-3	4-7	8-12	13-17	18-22	23-27	≥28		
Direction From	Frequency of Occurrence (%)								
WNW	0.22%	0.59%	0.32%	0.03%	0.02%	0.00%	0.00%	1.17%	6.97
NW	0.20%	0.39%	0.32%	0.03%	0.02%	0.00%	0.00%	0.96%	7.13
NNW	0.19%	0.51%	0.48%	0.06%	0.05%	0.00%	0.00%	1.28%	7.82
CALM	21.40%	0.00%	0.00%	0.00%	0.00%	0.00%	0.00%	21.40%	
MISSING	5.57%							5.57%	
Total	36.70%	31.53%	25.51%	5.29%	0.85%	0.12%	0.00%	100.00%	7.39

NOTES:

1. Calm is classified as a wind speed less than 2.3 mph (anemometer start speed) or a variable wind direction.
2. Missing data is data with missing wind speed, missing wind direction, or denoted as "variable" wind direction.
3. Data from Unedited Local Climatological Data, National Oceanic and Atmospheric Administration, U. S. Department of Commerce, Asheville, NC, Greenville/Spartanburg International Airport, Station No. 03870.
4. Period of Record - 9 years (1997 - 2005).

WLS COL 2.3-1

TABLE 2.3-218 (Sheet 1 of 2)
 PERCENTAGE FREQUENCY OF WIND DIRECTION AND SPEED (MPH)
 GREENVILLE/SPARTANBURG, SOUTH CAROLINA
 OCTOBER, 1997-2005

October	Wind Speed (mph)							Total (%)	Avg. Speed
	0-3	4-7	8-12	13-17	18-22	23-27	≥28		
Direction From	Frequency of Occurrence (%)								
N	1.19%	1.76%	2.49%	0.46%	0.07%	0.00%	0.00%	5.99%	7.77
NNE	1.16%	4.79%	3.84%	0.40%	0.00%	0.00%	0.00%	10.20%	7.13
NE	1.75%	5.48%	5.70%	0.78%	0.04%	0.00%	0.00%	13.75%	7.68
ENE	0.90%	3.09%	2.84%	0.39%	0.00%	0.00%	0.00%	7.21%	7.52
E	0.60%	1.96%	0.88%	0.07%	0.01%	0.00%	0.00%	3.52%	6.45
ESE	0.16%	0.69%	0.13%	0.00%	0.00%	0.00%	0.00%	0.99%	5.56
SE	0.30%	0.91%	0.15%	0.00%	0.00%	0.00%	0.00%	1.36%	5.43
SSE	0.37%	1.25%	0.30%	0.03%	0.01%	0.00%	0.00%	1.97%	5.82
S	0.72%	2.12%	0.60%	0.03%	0.01%	0.00%	0.00%	3.48%	5.89
SSW	0.67%	1.88%	1.06%	0.15%	0.00%	0.00%	0.00%	3.76%	6.66
SW	0.72%	2.45%	2.31%	0.57%	0.04%	0.00%	0.00%	6.09%	7.90
WSW	0.64%	1.81%	2.05%	0.37%	0.07%	0.00%	0.00%	4.94%	8.01
W	0.49%	1.34%	1.08%	0.19%	0.04%	0.03%	0.00%	3.18%	7.62

WLS COL 2.3-1

TABLE 2.3-218 (Sheet 2 of 2)
 PERCENTAGE FREQUENCY OF WIND DIRECTION AND SPEED (MPH)
 GREENVILLE/SPARTANBURG, SOUTH CAROLINA
 OCTOBER, 1997-2005

Direction From	October	Wind Speed (mph)						Total (%)	Avg. Speed
	0-3	4-7	8-12	13-17	18-22	23-27	≥28		
Frequency of Occurrence (%)									
WNW	0.24%	0.42%	0.12%	0.06%	0.03%	0.00%	0.00%	0.87%	6.50
NW	0.27%	0.61%	0.33%	0.06%	0.00%	0.00%	0.00%	1.27%	6.77
NNW	0.25%	0.64%	0.84%	0.19%	0.01%	0.01%	0.00%	1.96%	8.61
CALM	24.16%	0.00%	0.00%	0.00%	0.00%	0.00%	0.00%	24.16%	
MISSING	5.29%							5.29%	
Total	39.89%	31.21%	24.72%	3.76%	0.37%	0.04%	0.00%	100.00%	6.96

NOTES:

1. Calm is classified as a wind speed less than 2.3 mph (anemometer start speed) or a variable wind direction.
2. Missing data is data with missing wind speed, missing wind direction, or denoted as "variable" wind direction.
3. Data from Unedited Local Climatological Data, National Oceanic and Atmospheric Administration, U. S. Department of Commerce, Asheville, NC, Greenville/Spartanburg International Airport, Station No. 03870.
4. Period of Record - 9 years (1997 - 2005).

WLS COL 2.3-1

TABLE 2.3-219 (Sheet 1 of 2)
 PERCENTAGE FREQUENCY OF WIND DIRECTION AND SPEED (MPH)
 GREENVILLE/SPARTANBURG, SOUTH CAROLINA
 NOVEMBER, 1997-2005

November	Wind Speed (mph)							Total (%)	Avg. Speed
	0-3	4-7	8-12	13-17	18-22	23-27	≥28		
Direction From	Frequency of Occurrence (%)								
N	1.36%	2.58%	1.96%	0.51%	0.14%	0.03%	0.00%	6.57%	7.63
NNE	1.45%	3.56%	1.94%	0.35%	0.03%	0.02%	0.00%	7.36%	6.76
NE	1.42%	4.18%	3.13%	0.57%	0.03%	0.00%	0.00%	9.34%	7.28
ENE	0.57%	2.61%	1.94%	0.22%	0.09%	0.00%	0.00%	5.43%	7.52
E	0.52%	1.28%	0.94%	0.03%	0.00%	0.00%	0.00%	2.78%	6.58
ESE	0.23%	0.59%	0.20%	0.02%	0.00%	0.00%	0.00%	1.03%	5.85
SE	0.28%	0.40%	0.17%	0.02%	0.00%	0.00%	0.00%	0.86%	5.81
SSE	0.31%	0.71%	0.39%	0.06%	0.02%	0.00%	0.00%	1.48%	6.91
S	1.00%	2.08%	1.11%	0.46%	0.09%	0.00%	0.00%	4.75%	7.19
SSW	0.91%	2.41%	2.21%	0.49%	0.19%	0.02%	0.00%	6.22%	7.74
SW	0.83%	3.56%	3.86%	1.19%	0.11%	0.02%	0.00%	9.57%	8.52
WSW	0.66%	2.87%	2.98%	1.13%	0.32%	0.05%	0.00%	8.01%	9.14
W	0.57%	1.71%	1.45%	0.31%	0.02%	0.02%	0.00%	4.07%	8.04

WLS COL 2.3-1

TABLE 2.3-219 (Sheet 2 of 2)
 PERCENTAGE FREQUENCY OF WIND DIRECTION AND SPEED (MPH)
 GREENVILLE/SPARTANBURG, SOUTH CAROLINA
 NOVEMBER, 1997-2005

November	Wind Speed (mph)							Total (%)	Avg. Speed
	0-3	4-7	8-12	13-17	18-22	23-27	≥28		
Direction From	Frequency of Occurrence (%)								
WNW	0.31%	0.79%	0.25%	0.05%	0.00%	0.02%	0.00%	1.40%	6.46
NW	0.25%	0.74%	0.48%	0.09%	0.00%	0.00%	0.00%	1.56%	7.04
NNW	0.32%	0.97%	1.37%	0.25%	0.12%	0.00%	0.00%	3.04%	8.68
CALM	22.82%	0.00%	0.00%	0.00%	0.00%	0.00%	0.00%	22.82%	
MISSING	3.69%							3.69%	
Total	37.52%	31.05%	24.38%	5.74%	1.16%	0.15%	0.00%	100.00%	7.32

NOTES:

1. Calm is classified as a wind speed less than 2.3 mph (anemometer start speed) or a variable wind direction.
2. Missing data is data with missing wind speed, missing wind direction, or denoted as "variable" wind direction.
3. Data from Unedited Local Climatological Data, National Oceanic and Atmospheric Administration, U. S. Department of Commerce, Asheville, NC, Greenville/Spartanburg International Airport, Station No. 03870.
4. Period of Record - 9 years (1997 - 2005).

WLS COL 2.3-1

TABLE 2.3-220 (Sheet 1 of 2)
 PERCENTAGE FREQUENCY OF WIND DIRECTION AND SPEED (MPH)
 GREENVILLE/SPARTANBURG, SOUTH CAROLINA
 DECEMBER, 1997-2005

December	Wind Speed (mph)							Total (%)	Avg. Speed
	0-3	4-7	8-12	13-17	18-22	23-27	≥28		
Direction From	Frequency of Occurrence (%)								
N	1.11%	2.06%	1.91%	0.52%	0.06%	0.00%	0.00%	5.66%	7.86
NNE	0.81%	3.24%	2.06%	0.36%	0.00%	0.00%	0.00%	6.47%	7.22
NE	1.14%	4.08%	5.56%	1.08%	0.01%	0.01%	0.00%	11.87%	8.41
ENE	0.73%	2.76%	2.97%	0.46%	0.03%	0.00%	0.00%	6.96%	7.80
E	0.52%	1.21%	0.78%	0.00%	0.00%	0.00%	0.00%	2.51%	5.98
ESE	0.22%	0.39%	0.07%	0.00%	0.00%	0.00%	0.00%	0.69%	5.28
SE	0.24%	0.42%	0.04%	0.00%	0.00%	0.00%	0.00%	0.70%	4.89
SSE	0.36%	0.79%	0.07%	0.01%	0.00%	0.00%	0.00%	1.24%	5.14
S	0.75%	1.66%	0.66%	0.07%	0.01%	0.01%	0.00%	3.17%	5.91
SSW	0.81%	2.49%	1.57%	0.18%	0.10%	0.00%	0.00%	5.15%	7.03
SW	1.00%	3.30%	4.21%	1.14%	0.30%	0.00%	0.00%	9.95%	8.66
WSW	0.82%	3.12%	4.96%	1.69%	0.43%	0.06%	0.00%	11.08%	9.50
W	0.63%	2.66%	2.37%	0.55%	0.21%	0.01%	0.00%	6.44%	8.34

WLS COL 2.3-1

TABLE 2.3-220 (Sheet 2 of 2)
 PERCENTAGE FREQUENCY OF WIND DIRECTION AND SPEED (MPH)
 GREENVILLE/SPARTANBURG, SOUTH CAROLINA
 DECEMBER, 1997-2005

December	Wind Speed (mph)							Total (%)	Avg. Speed
	0-3	4-7	8-12	13-17	18-22	23-27	≥28		
Direction From	Frequency of Occurrence (%)								
WNW	0.31%	0.67%	0.39%	0.18%	0.01%	0.00%	0.00%	1.57%	7.51
NW	0.28%	0.85%	0.69%	0.13%	0.00%	0.00%	0.00%	1.96%	7.18
NNW	0.43%	0.97%	1.46%	0.19%	0.06%	0.00%	0.00%	3.12%	8.28
CALM	18.32%	0.00%	0.00%	0.00%	0.00%	0.00%	0.00%	18.32%	
MISSING	3.32%							3.32%	
Total	31.63%	30.68%	29.78%	6.57%	1.24%	0.10%	0.00%	100.00%	7.19

NOTES:

1. Calm is classified as a wind speed less than 2.3 mph (anemometer start speed) or a variable wind direction.
2. Missing data is data with missing wind speed, missing wind direction, or denoted as "variable" wind direction.
3. Data from Unedited Local Climatological Data, National Oceanic and Atmospheric Administration, U. S. Department of Commerce, Asheville, NC, Greenville/Spartanburg International Airport, Station No. 03870.
4. Period of Record - 9 years (1997 - 2005).

WLS COL 2.3-1

TABLE 2.3-221 (Sheet 1 of 2)
 PERCENTAGE FREQUENCY OF WIND DIRECTION AND SPEED (MPH)
 GREENVILLE/SPARTANBURG, SOUTH CAROLINA
 ALL MONTHS, 1997-2005

All Months	Wind Speed (mph)							Total (%)	Avg. Speed
	0-3	4-7	8-12	13-17	18-22	23-27	≥28		
Direction From	Frequency of Occurrence (%)								
N	1.04%	2.15%	1.93%	0.52%	0.13%	0.01%	0.00%	5.78%	7.86
NNE	0.99%	3.53%	2.57%	0.46%	0.05%	0.01%	0.00%	7.62%	7.40
NE	1.07%	4.12%	4.31%	0.97%	0.13%	0.04%	0.00%	10.63%	8.25
ENE	0.65%	2.40%	2.56%	0.54%	0.11%	0.02%	0.00%	6.27%	8.21
E	0.49%	1.56%	1.31%	0.13%	0.02%	0.00%	0.00%	3.51%	7.25
ESE	0.24%	0.68%	0.30%	0.01%	0.00%	0.00%	0.00%	1.23%	6.22
SE	0.28%	0.74%	0.30%	0.02%	0.00%	0.00%	0.00%	1.34%	6.13
SSE	0.32%	1.19%	0.43%	0.03%	0.01%	0.00%	0.00%	1.98%	6.19
S	0.77%	2.25%	1.21%	0.18%	0.03%	0.00%	0.00%	4.45%	6.83
SSW	0.67%	2.09%	1.89%	0.40%	0.09%	0.01%	0.00%	5.15%	7.90
SW	0.65%	2.89%	3.82%	1.18%	0.25%	0.04%	0.01%	8.84%	9.14
WSW	0.63%	2.68%	3.61%	1.23%	0.34%	0.08%	0.01%	8.57%	9.44
W	0.58%	2.10%	2.01%	0.50%	0.15%	0.04%	0.01%	5.38%	8.37

WLS COL 2.3-1

TABLE 2.3-221 (Sheet 2 of 2)
 PERCENTAGE FREQUENCY OF WIND DIRECTION AND SPEED (MPH)
 GREENVILLE/SPARTANBURG, SOUTH CAROLINA
 ALL MONTHS, 1997-2005

All Months	Wind Speed (mph)							Total (%)	Avg. Speed
	0-3	4-7	8-12	13-17	18-22	23-27	≥28		
Direction From	Frequency of Occurrence (%)								
WNW	0.30%	0.72%	0.42%	0.12%	0.03%	0.02%	0.00%	1.60%	7.48
NW	0.30%	0.67%	0.43%	0.08%	0.01%	0.00%	0.00%	1.50%	7.01
NNW	0.34%	0.77%	0.85%	0.22%	0.07%	0.01%	0.00%	2.26%	8.38
CALM	18.33%	0.00%	0.00%	0.00%	0.00%	0.00%	0.00%	18.33%	
MISSING	5.56%							5.56%	
Total	30.51%	27.97%	27.97%	6.60%	1.41%	0.29%	0.02%	100.00%	7.63

NOTES:

1. Calm is classified as a wind speed less than 2.3 mph (anemometer start speed) or a variable wind direction.
2. Missing data is data with missing wind speed, missing wind direction, or denoted as "variable" wind direction.
3. Data from Unedited Local Climatological Data, National Oceanic and Atmospheric Administration, U. S. Department of Commerce, Asheville, NC, Greenville/Spartanburg International Airport, Station No. 03870.
4. Period of Record - 9 years (1997 - 2005).

WLS COL 2.3-2

TABLE 2.3-222 (Sheet 1 of 2)
 PERCENTAGE FREQUENCY OF WIND DIRECTION AND SPEED (MPH)
 LEE NUCLEAR STATION SITE
 JANUARY

January	Wind Speed (mph)							Total (%)	Avg. Speed
	0-3	4-7	8-12	13-17	18-22	23-27	≥28		
Direction From	Frequency of Occurrence (%)								
N	2.33%	1.51%	0.55%	0.00%	0.00%	0.00%	0.00%	4.38%	4.52
NNE	2.88%	2.19%	0.41%	0.00%	0.00%	0.00%	0.00%	5.48%	4.32
NE	1.37%	0.82%	0.68%	0.00%	0.00%	0.00%	0.00%	2.88%	4.68
ENE	2.74%	0.27%	0.14%	0.00%	0.00%	0.00%	0.00%	3.15%	2.58
E	2.05%	0.00%	0.00%	0.00%	0.00%	0.00%	0.00%	2.05%	2.02
ESE	4.11%	0.27%	0.00%	0.00%	0.00%	0.00%	0.00%	4.38%	2.44
SE	5.07%	1.37%	0.27%	0.00%	0.00%	0.00%	0.00%	6.71%	3.51
SSE	4.79%	1.78%	0.68%	0.82%	0.27%	0.00%	0.00%	8.36%	5.90
S	2.19%	6.44%	1.51%	0.27%	0.14%	0.00%	0.00%	10.55%	6.28
SSW	0.96%	3.42%	5.48%	0.14%	0.00%	0.00%	0.00%	10.00%	8.00
SW	0.41%	1.78%	4.25%	0.82%	0.27%	0.00%	0.00%	7.53%	9.60
WSW	1.51%	1.10%	0.96%	0.14%	0.00%	0.00%	0.00%	3.70%	5.93
W	1.78%	1.23%	0.14%	0.00%	0.00%	0.00%	0.00%	3.15%	4.30

WLS COL 2.3-2

TABLE 2.3-222 (Sheet 2 of 2)
 PERCENTAGE FREQUENCY OF WIND DIRECTION AND SPEED (MPH)
 LEE NUCLEAR STATION SITE
 JANUARY

January	Wind Speed (mph)							Total (%)	Avg. Speed
	0-3	4-7	8-12	13-17	18-22	23-27	≥28		
Direction From	Frequency of Occurrence (%)								
WNW	3.29%	3.29%	1.37%	1.37%	0.41%	0.00%	0.00%	9.73%	7.00
NW	6.44%	2.47%	0.55%	0.82%	0.14%	0.00%	0.00%	10.41%	4.89
NNW	2.60%	2.05%	0.68%	0.55%	0.55%	0.00%	0.00%	6.44%	6.93
Calm	1.10%	0.00%	0.00%	0.00%	0.00%	0.00%	0.00%	1.10%	0.00
Total	44.52%	30.00%	17.67%	4.93%	1.78%	0.00%	0.00%	100.00%	5.71

NOTES:

1. Calm is classified as a wind speed less than or equal to 1.0 mph.
2. Lee Nuclear Station site Data, 12/1/2005 - 11/30/2006.

WLS COL 2.3-2

TABLE 2.3-223 (Sheet 1 of 2)
 PERCENTAGE FREQUENCY OF WIND DIRECTION AND SPEED (MPH)
 LEE NUCLEAR STATION SITE
 FEBRUARY

February	Wind Speed (mph)							Total (%)	Avg. Speed
	0-3	4-7	8-12	13-17	18-22	23-27	≥28		
Direction From	Frequency of Occurrence (%)								
N	1.49%	2.24%	1.19%	0.60%	0.00%	0.00%	0.00%	5.52%	6.69
NNE	1.64%	2.09%	0.45%	0.00%	0.00%	0.00%	0.00%	4.18%	5.41
NE	0.90%	1.79%	0.00%	0.00%	0.00%	0.00%	0.00%	2.69%	4.77
ENE	2.39%	0.45%	0.00%	0.00%	0.00%	0.00%	0.00%	2.84%	2.98
E	2.54%	0.15%	0.00%	0.00%	0.00%	0.00%	0.00%	2.69%	2.81
ESE	3.88%	0.15%	0.00%	0.00%	0.00%	0.00%	0.00%	4.03%	2.60
SE	2.54%	1.34%	0.00%	0.00%	0.00%	0.00%	0.00%	3.88%	3.22
SSE	2.69%	1.94%	0.15%	0.00%	0.00%	0.00%	0.00%	4.78%	4.18
S	2.39%	4.78%	1.49%	0.15%	0.00%	0.00%	0.00%	8.81%	5.64
SSW	1.49%	5.97%	3.88%	0.15%	0.00%	0.00%	0.00%	11.49%	7.35
SW	1.19%	3.13%	3.43%	0.90%	0.30%	0.00%	0.00%	8.96%	8.72
WSW	1.19%	2.84%	3.28%	0.60%	0.15%	0.00%	0.00%	8.06%	8.01
W	0.75%	2.54%	0.90%	0.30%	0.00%	0.00%	0.00%	4.48%	6.75

WLS COL 2.3-2

TABLE 2.3-223 (Sheet 2 of 2)
 PERCENTAGE FREQUENCY OF WIND DIRECTION AND SPEED (MPH)
 LEE NUCLEAR STATION SITE
 FEBRUARY

February	Wind Speed (mph)							Total (%)	Avg. Speed
	0-3	4-7	8-12	13-17	18-22	23-27	≥28		
Direction From	Frequency of Occurrence (%)							Total (%)	Avg. Speed
WNW	3.28%	3.58%	1.64%	0.30%	0.30%	0.00%	0.00%	9.10%	6.00
NW	7.76%	2.99%	1.04%	0.15%	0.00%	0.00%	0.00%	11.94%	4.39
NNW	2.39%	2.24%	0.45%	0.00%	0.00%	0.00%	0.00%	5.07%	4.38
Calm	1.49%	0.00%	0.00%	0.00%	0.00%	0.00%	0.00%	1.49%	0.00
Total	38.51%	38.21%	17.91%	3.13%	0.75%	0.00%	0.00%	100.00%	5.69

NOTES:

1. Calm is classified as a wind speed less than or equal to 1.0 mph.
2. Lee Nuclear Station site Data, 12/1/2005 - 11/30/2006.

WLS COL 2.3-2

TABLE 2.3-224 (Sheet 1 of 2)
 PERCENTAGE FREQUENCY OF WIND DIRECTION AND SPEED (MPH)
 LEE NUCLEAR STATION SITE
 MARCH

March	Wind Speed (mph)							Total (%)	Avg. Speed
	0-3	4-7	8-12	13-17	18-22	23-27	≥28		
Direction From	Frequency of Occurrence (%)								
N	2.44%	2.84%	2.71%	0.14%	0.00%	0.00%	0.00%	8.12%	6.62
NNE	1.35%	2.98%	0.27%	0.00%	0.00%	0.00%	0.00%	4.60%	5.06
NE	1.76%	1.62%	0.27%	0.00%	0.00%	0.00%	0.00%	3.65%	4.83
ENE	2.03%	0.68%	0.00%	0.00%	0.00%	0.00%	0.00%	2.71%	3.32
E	2.98%	0.68%	0.00%	0.00%	0.00%	0.00%	0.00%	3.65%	2.96
ESE	2.03%	0.41%	0.00%	0.00%	0.00%	0.00%	0.00%	2.44%	3.00
SE	3.79%	0.95%	0.00%	0.00%	0.00%	0.00%	0.00%	4.74%	3.35
SSE	1.76%	3.25%	0.27%	0.27%	0.00%	0.00%	0.00%	5.55%	5.43
S	1.08%	5.82%	0.95%	0.41%	0.00%	0.00%	0.00%	8.25%	6.22
SSW	0.41%	4.06%	4.74%	1.49%	0.27%	0.00%	0.00%	10.96%	9.38
SW	0.54%	1.22%	2.71%	2.30%	0.41%	0.00%	0.00%	7.17%	11.40
WSW	0.54%	1.35%	0.41%	0.14%	0.00%	0.00%	0.00%	2.44%	6.51
W	0.54%	0.81%	0.41%	0.00%	0.00%	0.00%	0.00%	1.76%	5.32

WLS COL 2.3-2

TABLE 2.3-224 (Sheet 2 of 2)
 PERCENTAGE FREQUENCY OF WIND DIRECTION AND SPEED (MPH)
 LEE NUCLEAR STATION SITE
 MARCH

March	Wind Speed (mph)							Total (%)	Avg. Speed
	0-3	4-7	8-12	13-17	18-22	23-27	≥28		
Direction From	Frequency of Occurrence (%)								
WNW	2.57%	4.74%	2.44%	1.22%	0.27%	0.00%	0.00%	11.23%	7.36
NW	4.47%	5.28%	2.71%	0.68%	0.41%	0.00%	0.00%	13.53%	6.46
NNW	3.38%	3.79%	1.62%	0.00%	0.00%	0.00%	0.00%	8.80%	5.38
Calm	0.41%	0.00%	0.00%	0.00%	0.00%	0.00%	0.00%	0.41%	0.00
Total	31.66%	40.46%	19.49%	6.63%	1.35%	0.00%	0.00%	100.00%	6.47

NOTES:

1. Calm is classified as a wind speed less than or equal to 1.0 mph.
2. Lee Nuclear Station site Data, 12/1/2005 - 11/30/2006.

WLS COL 2.3-2

TABLE 2.3-225 (Sheet 1 of 2)
 PERCENTAGE FREQUENCY OF WIND DIRECTION AND SPEED (MPH)
 LEE NUCLEAR STATION SITE
 APRIL

Direction From	Wind Speed (mph)							Total (%)	Avg. Speed
	0-3	4-7	8-12	13-17	18-22	23-27	≥28		
N	1.39%	2.50%	0.70%	0.00%	0.00%	0.00%	0.00%	4.59%	5.48
NNE	1.53%	1.25%	1.53%	0.00%	0.00%	0.00%	0.00%	4.31%	5.83
NE	2.36%	4.17%	0.42%	0.00%	0.00%	0.00%	0.00%	6.95%	4.87
ENE	1.67%	2.09%	0.83%	0.00%	0.00%	0.00%	0.00%	4.59%	5.13
E	2.92%	1.11%	0.00%	0.00%	0.00%	0.00%	0.00%	4.03%	3.38
ESE	3.06%	0.56%	0.00%	0.00%	0.00%	0.00%	0.00%	3.62%	2.70
SE	4.31%	1.95%	0.00%	0.00%	0.00%	0.00%	0.00%	6.26%	3.48
SSE	2.23%	3.48%	0.00%	0.00%	0.00%	0.00%	0.00%	5.70%	4.29
S	1.25%	4.03%	0.83%	0.14%	0.00%	0.00%	0.00%	6.26%	5.72
SSW	0.56%	2.36%	4.31%	0.83%	0.28%	0.00%	0.00%	8.34%	9.27
SW	0.97%	3.62%	4.87%	1.11%	0.14%	0.00%	0.00%	10.71%	9.01
WSW	1.25%	2.92%	4.31%	0.56%	0.42%	0.00%	0.00%	9.46%	8.63
W	0.70%	0.70%	0.97%	0.14%	0.00%	0.00%	0.00%	2.50%	6.59

WLS COL 2.3-2

TABLE 2.3-225 (Sheet 2 of 2)
 PERCENTAGE FREQUENCY OF WIND DIRECTION AND SPEED (MPH)
 LEE NUCLEAR STATION SITE
 APRIL

Direction From	Wind Speed (mph)							Total (%)	Avg. Speed
	0-3	4-7	8-12	13-17	18-22	23-27	≥28		
Frequency of Occurrence (%)									
WNW	3.06%	1.81%	1.39%	0.00%	0.14%	0.00%	0.00%	6.40%	5.55
NW	5.84%	3.06%	0.70%	0.14%	0.14%	0.00%	0.00%	9.87%	4.54
NNW	3.34%	1.11%	0.00%	0.00%	0.00%	0.00%	0.00%	4.45%	3.04
Calm	1.95%	0.00%	0.00%	0.00%	0.00%	0.00%	0.00%	1.95%	0.00
Total	36.44%	36.72%	20.86%	2.92%	1.11%	0.00%	0.00%	100.00%	5.81

NOTES:

1. Calm is classified as a wind speed less than or equal to 1.0 mph.
2. Lee Nuclear Station site Data, 12/1/2005 - 11/30/2006.

WLS COL 2.3-2

TABLE 2.3-226 (Sheet 1 of 2)
 PERCENTAGE FREQUENCY OF WIND DIRECTION AND SPEED (MPH)
 LEE NUCLEAR STATION SITE
 MAY

May	Wind Speed (mph)							Total (%)	Avg. Speed
	0-3	4-7	8-12	13-17	18-22	23-27	≥28		
Direction From	Frequency of Occurrence (%)								
N	2.30%	2.17%	0.27%	0.00%	0.00%	0.00%	0.00%	4.74%	4.59
NNE	1.90%	3.12%	0.00%	0.00%	0.00%	0.00%	0.00%	5.01%	4.76
NE	4.20%	2.71%	0.27%	0.00%	0.00%	0.00%	0.00%	7.18%	4.08
ENE	3.39%	2.44%	0.14%	0.00%	0.00%	0.00%	0.00%	5.96%	3.96
E	2.71%	1.63%	0.00%	0.00%	0.00%	0.00%	0.00%	4.34%	3.43
ESE	3.66%	0.41%	0.00%	0.00%	0.00%	0.00%	0.00%	4.07%	2.64
SE	4.07%	0.68%	0.00%	0.00%	0.00%	0.00%	0.00%	4.74%	3.03
SSE	2.71%	1.63%	0.00%	0.00%	0.00%	0.00%	0.00%	4.34%	3.61
S	1.36%	1.76%	0.00%	0.00%	0.00%	0.00%	0.00%	3.12%	4.77
SSW	1.36%	2.71%	1.90%	0.00%	0.00%	0.00%	0.00%	5.96%	6.66
SW	1.49%	2.17%	5.01%	1.90%	0.14%	0.00%	0.00%	10.70%	9.57
WSW	1.36%	3.25%	1.90%	0.95%	0.14%	0.00%	0.00%	7.59%	8.18
W	1.90%	1.08%	1.22%	0.14%	0.00%	0.00%	0.00%	4.34%	5.71

WLS COL 2.3-2

TABLE 2.3-226 (Sheet 2 of 2)
 PERCENTAGE FREQUENCY OF WIND DIRECTION AND SPEED (MPH)
 LEE NUCLEAR STATION SITE
 MAY

Direction From	May	Wind Speed (mph)						Total (%)	Avg. Speed
	0-3	4-7	8-12	13-17	18-22	23-27	≥28		
Frequency of Occurrence (%)									
WNW	4.47%	2.17%	0.27%	0.14%	0.00%	0.00%	0.00%	7.05%	4.25
NW	9.76%	2.71%	1.08%	0.41%	0.00%	0.00%	0.00%	13.96%	4.44
NNW	5.01%	1.49%	0.14%	0.00%	0.00%	0.00%	0.00%	6.64%	3.32
Calm	0.27%	0.00%	0.00%	0.00%	0.00%	0.00%	0.00%	0.27%	0.00
Total	51.63%	32.11%	12.20%	3.52%	0.27%	0.00%	0.00%	100.00%	5.12

NOTES:

1. Calm is classified as a wind speed less than or equal to 1.0 mph.
2. Lee Nuclear Station site Data, 12/1/2005 - 11/30/2006.

WLS COL 2.3-2

TABLE 2.3-227 (Sheet 1 of 2)
 PERCENTAGE FREQUENCY OF WIND DIRECTION AND SPEED (MPH)
 LEE NUCLEAR STATION SITE
 JUNE

June	Wind Speed (mph)							Total (%)	Avg. Speed
	0-3	4-7	8-12	13-17	18-22	23-27	≥28		
Direction From	Frequency of Occurrence (%)								
N	2.23%	1.25%	2.37%	0.00%	0.00%	0.00%	0.00%	5.85%	6.30
NNE	2.65%	2.65%	1.11%	0.00%	0.00%	0.00%	0.00%	6.41%	5.03
NE	2.23%	2.23%	0.00%	0.00%	0.00%	0.00%	0.00%	4.46%	4.10
ENE	3.06%	1.67%	0.42%	0.00%	0.00%	0.00%	0.00%	5.15%	4.03
E	5.15%	1.39%	0.00%	0.00%	0.00%	0.00%	0.00%	6.55%	3.08
ESE	4.46%	2.09%	0.28%	0.00%	0.00%	0.00%	0.00%	6.82%	3.54
SE	4.74%	3.76%	0.00%	0.00%	0.00%	0.00%	0.00%	8.50%	3.74
SSE	2.51%	4.46%	0.70%	0.00%	0.00%	0.00%	0.00%	7.66%	5.20
S	1.67%	3.62%	0.14%	0.00%	0.00%	0.00%	0.00%	5.43%	5.15
SSW	1.53%	1.53%	0.42%	0.00%	0.00%	0.00%	0.00%	3.48%	4.76
SW	0.70%	3.20%	1.95%	0.14%	0.00%	0.00%	0.00%	5.99%	7.10
WSW	0.97%	2.37%	0.28%	0.00%	0.00%	0.00%	0.00%	3.62%	5.14
W	0.56%	2.37%	0.56%	0.00%	0.00%	0.00%	0.00%	3.48%	6.08

WLS COL 2.3-2

TABLE 2.3-227 (Sheet 2 of 2)
 PERCENTAGE FREQUENCY OF WIND DIRECTION AND SPEED (MPH)
 LEE NUCLEAR STATION SITE
 JUNE

June	Wind Speed (mph)							Total (%)	Avg. Speed
	0-3	4-7	8-12	13-17	18-22	23-27	≥28		
Direction From	Frequency of Occurrence (%)								
WNW	4.74%	1.81%	0.14%	0.00%	0.00%	0.00%	0.00%	6.69%	3.66
NW	9.19%	2.51%	0.56%	0.00%	0.14%	0.00%	0.00%	12.40%	3.88
NNW	4.74%	2.23%	0.56%	0.00%	0.00%	0.00%	0.00%	7.52%	4.12
Calm	0.00%	0.00%	0.00%	0.00%	0.00%	0.00%	0.00%	0.00%	0.00
Total	51.11%	39.14%	9.47%	0.14%	0.14%	0.00%	0.00%	100.00%	4.55

NOTES:

1. Calm is classified as a wind speed less than or equal to 1.0.
2. Lee Nuclear Station site Data, 12/1/2005 - 11/30/2006.

WLS COL 2.3-2

TABLE 2.3-228 (Sheet 1 of 2)
 PERCENTAGE FREQUENCY OF WIND DIRECTION AND SPEED (MPH)
 LEE NUCLEAR STATION SITE
 JULY

Direction From	Wind Speed (mph)							Total (%)	Avg. Speed
	0-3	4-7	8-12	13-17	18-22	23-27	≥28		
Frequency of Occurrence (%)									
N	4.17%	0.81%	0.00%	0.00%	0.00%	0.00%	0.00%	4.97%	2.76
NNE	2.28%	1.48%	0.00%	0.00%	0.00%	0.00%	0.00%	3.76%	3.37
NE	4.17%	2.28%	0.27%	0.00%	0.00%	0.00%	0.00%	6.72%	3.79
ENE	4.03%	2.42%	0.13%	0.00%	0.00%	0.00%	0.00%	6.59%	3.81
E	4.57%	0.94%	0.00%	0.00%	0.00%	0.00%	0.00%	5.51%	2.88
ESE	4.30%	1.34%	0.13%	0.00%	0.00%	0.00%	0.00%	5.78%	3.37
SE	4.17%	1.48%	0.00%	0.00%	0.00%	0.00%	0.00%	5.65%	3.12
SSE	4.57%	3.36%	0.27%	0.00%	0.00%	0.00%	0.00%	8.20%	4.11
S	4.17%	4.30%	0.27%	0.13%	0.00%	0.00%	0.00%	8.87%	4.53
SSW	2.69%	5.11%	1.34%	0.00%	0.00%	0.00%	0.00%	9.14%	5.60
SW	0.94%	4.84%	1.88%	0.13%	0.00%	0.00%	0.00%	7.80%	6.69
WSW	1.75%	2.96%	1.08%	0.00%	0.00%	0.00%	0.00%	5.78%	5.56
W	0.67%	1.34%	0.40%	0.00%	0.00%	0.00%	0.00%	2.42%	5.68

WLS COL 2.3-2

TABLE 2.3-228 (Sheet 2 of 2)
 PERCENTAGE FREQUENCY OF WIND DIRECTION AND SPEED (MPH)
 LEE NUCLEAR STATION SITE
 JULY

Direction From	Wind Speed (mph)							Total (%)	Avg. Speed
	0-3	4-7	8-12	13-17	18-22	23-27	≥28		
Frequency of Occurrence (%)									
WNW	2.02%	1.21%	0.54%	0.13%	0.00%	0.00%	0.00%	3.90%	4.76
NW	7.66%	1.48%	0.00%	0.00%	0.00%	0.00%	0.00%	9.14%	3.12
NNW	4.84%	0.67%	0.00%	0.00%	0.00%	0.00%	0.00%	5.51%	2.66
Calm	0.27%	0.00%	0.00%	0.00%	0.00%	0.00%	0.00%	0.27%	0.00
Total	56.99%	36.02%	6.32%	0.40%	0.00%	0.00%	0.00%	100.00%	4.15

NOTES:

1. Calm is classified as a wind speed less than or equal to 1.0 mph.
2. Lee Nuclear Station site Data, 12/1/2005 - 11/30/2006.

WLS COL 2.3-2

TABLE 2.3-229 (Sheet 1 of 2)
 PERCENTAGE FREQUENCY OF WIND DIRECTION AND SPEED (MPH)
 LEE NUCLEAR STATION SITE
 AUGUST

August	Wind Speed (mph)							Total (%)	Avg. Speed
	0-3	4-7	8-12	13-17	18-22	23-27	≥28		
Direction From	Frequency of Occurrence (%)								
N	5.53%	0.81%	0.13%	0.00%	0.00%	0.00%	0.00%	6.47%	2.81
NNE	4.72%	2.56%	0.00%	0.00%	0.00%	0.00%	0.00%	7.28%	3.61
NE	4.58%	4.45%	0.94%	0.00%	0.00%	0.00%	0.00%	9.97%	4.78
ENE	4.04%	3.91%	0.54%	0.00%	0.00%	0.00%	0.00%	8.49%	4.68
E	4.72%	2.96%	0.54%	0.00%	0.00%	0.00%	0.00%	8.22%	3.99
ESE	3.77%	1.35%	0.00%	0.00%	0.00%	0.00%	0.00%	5.12%	3.13
SE	4.45%	2.16%	0.00%	0.00%	0.00%	0.00%	0.00%	6.60%	3.52
SSE	4.04%	2.43%	0.00%	0.00%	0.00%	0.00%	0.00%	6.47%	3.84
S	3.10%	2.43%	0.13%	0.00%	0.00%	0.00%	0.00%	5.66%	4.00
SSW	1.75%	2.83%	0.40%	0.00%	0.00%	0.00%	0.00%	4.99%	5.09
SW	1.89%	2.43%	0.40%	0.00%	0.00%	0.00%	0.00%	4.72%	4.89
WSW	1.08%	1.75%	0.00%	0.00%	0.00%	0.00%	0.00%	2.83%	4.78
W	1.21%	0.94%	0.13%	0.00%	0.00%	0.00%	0.00%	2.29%	4.44

WLS COL 2.3-2

TABLE 2.3-229 (Sheet 2 of 2)
 PERCENTAGE FREQUENCY OF WIND DIRECTION AND SPEED (MPH)
 LEE NUCLEAR STATION SITE
 AUGUST

August	Wind Speed (mph)							Total (%)	Avg. Speed
	0-3	4-7	8-12	13-17	18-22	23-27	≥28		
Direction From	Frequency of Occurrence (%)								
WNW	2.29%	2.02%	0.13%	0.00%	0.00%	0.00%	0.00%	4.45%	4.00
NW	6.87%	3.50%	0.00%	0.00%	0.00%	0.00%	0.00%	10.38%	3.49
NNW	4.58%	1.08%	0.00%	0.13%	0.00%	0.00%	0.00%	5.80%	3.22
Calm	0.27%	0.00%	0.00%	0.00%	0.00%	0.00%	0.00%	0.27%	0.00
Total	58.63%	37.60%	3.37%	0.13%	0.00%	0.00%	0.00%	100.00%	3.97

NOTES:

1. Calm is classified as a wind speed less than or equal to 1.0 mph.
2. Lee Nuclear Station site Data, 12/1/2005 - 11/30/2006.

WLS COL 2.3-2

TABLE 2.3-230 (Sheet 1 of 2)
 PERCENTAGE FREQUENCY OF WIND DIRECTION AND SPEED (MPH)
 LEE NUCLEAR STATION SITE
 SEPTEMBER

September	Wind Speed (mph)							Total (%)	Avg. Speed
	0-3	4-7	8-12	13-17	18-22	23-27	≥28		
Direction From	Frequency of Occurrence (%)								
N	5.28%	3.47%	0.42%	0.00%	0.00%	0.00%	0.00%	9.17%	3.94
NNE	4.72%	2.92%	0.14%	0.00%	0.00%	0.00%	0.00%	7.78%	3.78
NE	4.86%	2.36%	0.00%	0.00%	0.00%	0.00%	0.00%	7.22%	3.39
ENE	3.75%	2.36%	0.00%	0.00%	0.00%	0.00%	0.00%	6.11%	3.68
E	3.75%	2.08%	0.14%	0.00%	0.00%	0.00%	0.00%	5.97%	3.61
ESE	3.61%	1.81%	0.00%	0.00%	0.00%	0.00%	0.00%	5.42%	3.45
SE	2.50%	1.11%	0.00%	0.00%	0.00%	0.00%	0.00%	3.61%	3.54
SSE	2.50%	1.39%	0.28%	0.00%	0.00%	0.00%	0.00%	4.17%	4.12
S	2.36%	2.08%	0.00%	0.00%	0.00%	0.00%	0.00%	4.44%	4.19
SSW	0.28%	3.75%	1.67%	0.00%	0.00%	0.00%	0.00%	5.69%	7.14
SW	1.11%	1.67%	2.36%	0.56%	0.00%	0.00%	0.00%	5.69%	8.06
WSW	0.28%	0.83%	0.69%	0.00%	0.00%	0.00%	0.00%	1.81%	7.23
W	0.00%	0.69%	0.00%	0.00%	0.00%	0.00%	0.00%	0.69%	6.12

WLS COL 2.3-2

TABLE 2.3-230 (Sheet 2 of 2)
 PERCENTAGE FREQUENCY OF WIND DIRECTION AND SPEED (MPH)
 LEE NUCLEAR STATION SITE
 SEPTEMBER

September	Wind Speed (mph)							Total (%)	Avg. Speed
	0-3	4-7	8-12	13-17	18-22	23-27	≥28		
Direction From	Frequency of Occurrence (%)								
WNW	2.22%	2.22%	0.00%	0.00%	0.00%	0.00%	0.00%	4.44%	4.17
NW	14.03%	4.58%	0.14%	0.00%	0.00%	0.00%	0.00%	18.75%	3.53
NNW	6.11%	2.64%	0.14%	0.00%	0.00%	0.00%	0.00%	8.89%	3.39
Calm	0.14%	0.00%	0.00%	0.00%	0.00%	0.00%	0.00%	0.14%	0.00
Total	57.36%	35.97%	5.97%	0.56%	0.00%	0.00%	0.00%	100.00%	4.20

NOTES:

1. Calm is classified as a wind speed less than or equal to 1.0 mph.
2. Lee Nuclear Station site Data, 12/1/2005 - 11/30/2006.

WLS COL 2.3-2

TABLE 2.3-231 (Sheet 1 of 2)
 PERCENTAGE FREQUENCY OF WIND DIRECTION AND SPEED (MPH)
 LEE NUCLEAR STATION SITE
 OCTOBER

October	Wind Speed (mph)							Total (%)	Avg. Speed
	0-3	4-7	8-12	13-17	18-22	23-27	≥28		
Direction From	Frequency of Occurrence (%)								
N	3.10%	2.70%	0.27%	0.00%	0.00%	0.00%	0.00%	6.06%	4.12
NNE	2.29%	3.91%	0.94%	0.00%	0.00%	0.00%	0.00%	7.14%	5.73
NE	3.50%	1.89%	2.43%	0.13%	0.00%	0.00%	0.00%	7.95%	5.71
ENE	3.50%	2.02%	0.00%	0.00%	0.00%	0.00%	0.00%	5.53%	3.36
E	4.58%	0.54%	0.13%	0.00%	0.00%	0.00%	0.00%	5.26%	2.61
ESE	2.83%	0.27%	0.00%	0.00%	0.00%	0.00%	0.00%	3.10%	2.75
SE	3.10%	0.27%	0.00%	0.00%	0.00%	0.00%	0.00%	3.37%	2.88
SSE	2.16%	1.08%	0.54%	0.00%	0.00%	0.00%	0.00%	3.77%	4.55
S	1.62%	2.56%	0.13%	0.00%	0.00%	0.00%	0.00%	4.31%	4.66
SSW	0.67%	2.70%	1.08%	0.00%	0.00%	0.00%	0.00%	4.45%	6.32
SW	0.67%	2.02%	1.35%	0.00%	0.00%	0.00%	0.00%	4.04%	6.94
WSW	1.21%	2.02%	1.48%	0.00%	0.00%	0.00%	0.00%	4.72%	6.41
W	1.08%	0.94%	1.08%	0.13%	0.00%	0.00%	0.00%	3.23%	6.02

WLS COL 2.3-2

TABLE 2.3-231 (Sheet 2 of 2)
 PERCENTAGE FREQUENCY OF WIND DIRECTION AND SPEED (MPH)
 LEE NUCLEAR STATION SITE
 OCTOBER

October	Wind Speed (mph)							Total (%)	Avg. Speed
	0-3	4-7	8-12	13-17	18-22	23-27	≥28		
Direction From	Frequency of Occurrence (%)								
WNW	4.31%	2.02%	1.35%	0.67%	0.13%	0.00%	0.00%	8.49%	5.82
NW	12.26%	5.39%	2.29%	0.54%	0.00%	0.00%	0.00%	20.49%	4.78
NNW	5.66%	1.62%	0.67%	0.00%	0.00%	0.00%	0.00%	7.95%	3.79
Calm	0.13%	0.00%	0.00%	0.00%	0.00%	0.00%	0.00%	0.13%	0.00
Total	52.56%	31.94%	13.75%	1.48%	0.13%	0.00%	0.00%	100.00%	4.82

NOTES:

1. Calm is classified as a wind speed less than or equal to 1.0 mph.
2. Lee Nuclear Station site Data, 12/1/2005 - 11/30/2006.

WLS COL 2.3-2

TABLE 2.3-232 (Sheet 1 of 2)
 PERCENTAGE FREQUENCY OF WIND DIRECTION AND SPEED (MPH)
 LEE NUCLEAR STATION SITE
 NOVEMBER

November	Wind Speed (mph)							Total (%)	Avg. Speed
	0-3	4-7	8-12	13-17	18-22	23-27	≥28		
Direction From	Frequency of Occurrence (%)								
N	3.36%	2.24%	1.12%	0.56%	0.00%	0.00%	0.00%	7.28%	5.56
NNE	0.98%	3.50%	4.20%	0.70%	0.00%	0.00%	0.00%	9.38%	8.25
NE	1.54%	1.54%	0.56%	0.28%	0.00%	0.00%	0.00%	3.92%	5.58
ENE	1.96%	1.40%	0.00%	0.00%	0.00%	0.00%	0.00%	3.36%	3.73
E	2.38%	0.56%	0.00%	0.00%	0.00%	0.00%	0.00%	2.94%	2.65
ESE	2.66%	0.14%	0.00%	0.00%	0.00%	0.00%	0.00%	2.80%	2.42
SE	3.78%	1.40%	0.56%	0.00%	0.00%	0.00%	0.00%	5.74%	3.82
SSE	1.68%	0.98%	1.12%	0.00%	0.00%	0.00%	0.00%	3.78%	5.31
S	3.08%	1.54%	0.98%	0.14%	0.00%	0.00%	0.00%	5.74%	5.13
SSW	0.84%	1.12%	0.70%	0.00%	0.00%	0.00%	0.00%	2.66%	6.00
SW	0.56%	1.40%	0.42%	1.12%	0.28%	0.00%	0.00%	3.78%	9.77
WSW	0.84%	0.84%	0.42%	0.28%	0.00%	0.00%	0.00%	2.38%	6.34
W	0.98%	0.98%	0.14%	0.00%	0.00%	0.00%	0.00%	2.10%	4.75

WLS COL 2.3-2

TABLE 2.3-232 (Sheet 2 of 2)
 PERCENTAGE FREQUENCY OF WIND DIRECTION AND SPEED (MPH)
 LEE NUCLEAR STATION SITE
 NOVEMBER

November	Wind Speed (mph)							Total (%)	Avg. Speed
	0-3	4-7	8-12	13-17	18-22	23-27	≥28		
Direction From	Frequency of Occurrence (%)								
WNW	2.52%	2.10%	0.42%	0.00%	0.00%	0.00%	0.00%	5.04%	4.26
NW	9.38%	14.29%	0.98%	0.56%	0.00%	0.00%	0.00%	25.21%	4.69
NNW	4.34%	3.50%	2.80%	0.42%	0.00%	0.00%	0.00%	11.06%	6.18
Calm	2.80%	0.00%	0.00%	0.00%	0.00%	0.00%	0.00%	2.80%	0.00
Total	40.90%	37.54%	14.43%	4.06%	0.28%	0.00%	0.00%	100.00%	5.26

NOTES:

1. Calm is classified as a wind speed less than or equal to 1.0 mph.
2. Lee Nuclear Station site Data, 12/1/2005 - 11/30/2006.

WLS COL 2.3-2

TABLE 2.3-233 (Sheet 1 of 2)
 PERCENTAGE FREQUENCY OF WIND DIRECTION AND SPEED (MPH)
 LEE NUCLEAR STATION SITE
 DECEMBER

December	Wind Speed (mph)							Total (%)	Avg. Speed
	0-3	4-7	8-12	13-17	18-22	23-27	≥28		
Direction From	Frequency of Occurrence (%)								
N	3.35%	1.54%	0.28%	0.00%	0.00%	0.00%	0.00%	5.17%	3.67
NNE	1.68%	2.23%	0.98%	0.00%	0.00%	0.00%	0.00%	4.89%	5.14
NE	1.54%	5.31%	0.28%	0.00%	0.00%	0.00%	0.00%	7.12%	5.36
ENE	3.07%	1.96%	0.42%	0.00%	0.00%	0.00%	0.00%	5.45%	3.83
E	2.09%	0.70%	0.00%	0.00%	0.00%	0.00%	0.00%	2.79%	2.96
ESE	3.63%	0.00%	0.00%	0.00%	0.00%	0.00%	0.00%	3.63%	2.56
SE	4.05%	0.56%	0.00%	0.00%	0.00%	0.00%	0.00%	4.61%	2.66
SSE	3.63%	0.98%	0.00%	0.00%	0.00%	0.00%	0.00%	4.61%	3.28
S	1.54%	3.21%	0.28%	0.00%	0.00%	0.00%	0.00%	5.03%	4.85
SSW	1.12%	3.07%	0.98%	0.00%	0.00%	0.00%	0.00%	5.17%	6.16
SW	1.54%	2.37%	2.65%	0.00%	0.00%	0.00%	0.00%	6.56%	6.83
WSW	1.54%	2.65%	2.09%	0.28%	0.00%	0.00%	0.00%	6.56%	6.77
W	1.26%	1.12%	0.70%	0.14%	0.00%	0.00%	0.00%	3.21%	5.68

WLS COL 2.3-2

TABLE 2.3-233 (Sheet 2 of 2)
 PERCENTAGE FREQUENCY OF WIND DIRECTION AND SPEED (MPH)
 LEE NUCLEAR STATION SITE
 DECEMBER

December	Wind Speed (mph)							Total (%)	Avg. Speed
	0-3	4-7	8-12	13-17	18-22	23-27	≥28		
Direction From	Frequency of Occurrence (%)								
WNW	3.91%	2.79%	1.68%	0.70%	0.00%	0.00%	0.00%	9.08%	5.93
NW	10.34%	6.98%	1.54%	0.14%	0.00%	0.00%	0.00%	18.99%	4.38
NNW	4.33%	0.84%	0.56%	0.00%	0.00%	0.00%	0.00%	5.73%	3.71
Calm	1.40%	0.00%	0.00%	0.00%	0.00%	0.00%	0.00%	1.40%	0.00
Total	48.60%	36.31%	12.43%	1.26%	0.00%	0.00%	0.00%	100.00%	4.70

NOTES:

1. Calm is classified as a wind speed less than or equal to 1.0 mph.
2. Lee Nuclear Station site Data, 12/1/2005 - 11/30/2006.

WLS COL 2.3-2

TABLE 2.3-234 (Sheet 1 of 2)
 PERCENTAGE FREQUENCY OF WIND DIRECTION AND SPEED (mph)
 LEE NUCLEAR SITE
 ALL MONTHS

Direction From	Wind Speed							Total	Avg. Speed
	0-3	4-7	8-12	13-17	18-22	23-27	>=28		
N	3.09%	2.00%	0.83%	0.10%	0.00%	0.00%	0.00%	6.03%	4.78
NNE	2.39%	2.58%	0.83%	0.06%	0.00%	0.00%	0.00%	5.86%	5.15
NE	2.77%	2.60%	0.52%	0.03%	0.00%	0.00%	0.00%	5.92%	4.64
ENE	2.98%	1.82%	0.22%	0.00%	0.00%	0.00%	0.00%	5.02%	3.89
E	3.38%	1.07%	0.07%	0.00%	0.00%	0.00%	0.00%	4.52%	3.17
ESE	3.50%	0.74%	0.03%	0.00%	0.00%	0.00%	0.00%	4.27%	2.97
SE	3.89%	1.42%	0.07%	0.00%	0.00%	0.00%	0.00%	5.37%	3.38
SSE	2.95%	2.23%	0.33%	0.09%	0.02%	0.00%	0.00%	5.63%	4.56
S	2.15%	3.54%	0.55%	0.10%	0.01%	0.00%	0.00%	6.36%	5.24
SSW	1.14%	3.21%	2.23%	0.22%	0.05%	0.00%	0.00%	6.85%	7.21
SW	1.00%	2.49%	2.60%	0.75%	0.13%	0.00%	0.00%	6.96%	8.42
WSW	1.13%	2.07%	1.39%	0.24%	0.06%	0.00%	0.00%	4.89%	6.99
W	0.95%	1.22%	0.55%	0.07%	0.00%	0.00%	0.00%	2.80%	5.67
WNW	3.22%	2.47%	0.94%	0.38%	0.10%	0.00%	0.00%	7.12%	5.55

WLS COL 2.3-2

TABLE 2.3-234 (Sheet 2 of 2)
 PERCENTAGE FREQUENCY OF WIND DIRECTION AND SPEED (mph)
 LEE NUCLEAR SITE
 ALL MONTHS

Direction From	Wind Speed							Total	Avg. Speed
	0-3	4-7	8-12	13-17	18-22	23-27	>=28		
NW	8.66%	4.59%	0.97%	0.29%	0.07%	0.00%	0.00%	14.58%	4.44
NNW	4.29%	1.93%	0.63%	0.09%	0.05%	0.00%	0.00%	6.99%	4.34
Calm	0.84%	0.00%	0.00%	0.00%	0.00%	0.00%	0.00%	0.84%	0.00
Total	47.50%	35.98%	12.77%	2.43%	0.48%	0.00%	0.00%	100.00%	5.03

NOTES:

1. Calm is classified as a wind speed less than or equal to 1.0 mph.
2. Lee Nuclear Site Data, 12/1/2005 - 11/30/2006.

WLS COL 2.3-2

TABLE 2.3-235 (Sheet 1 of 2)
 JOINT FREQUENCY DISTRIBUTION OF WIND SPEED AND DIRECTION BY
 ATMOSPHERIC STABILITY CLASS
 STABILITY CLASS A

STABILITY CLASS A		HOURS AT EACH WIND SPEED AND DIRECTION												Average Wind Speed (m/sec)	
		Wind Speed (m/sec)											Total		
DIR		U≤0.5	0.5<U ≤0.75	0.75<U ≤1.0	1.0<U ≤1.25	1.25<U ≤1.5	1.5<U ≤2.0	2.0<U ≤3.0	3.0<U ≤4.0	4.0<U ≤5.0	5.0<U ≤6.0	6.0<U ≤8.0			U>8
N		0	0	0	0	2	5	10	8	11	4	2	0	42	3.5
NNE		0	0	0	0	0	8	13	21	5	3	2	0	52	3.2
NE		0	0	0	0	0	13	33	31	4	1	0	0	82	2.9
ENE		0	0	0	1	3	9	27	30	8	1	0	0	79	2.9
E		0	0	0	1	1	8	25	6	0	0	0	0	41	2.4
ESE		0	0	0	1	3	15	17	1	0	0	0	0	37	2.0
SE		0	1	0	2	1	14	35	13	0	0	0	0	66	2.4
SSE		0	0	0	1	4	19	40	21	2	0	2	0	89	2.7
S		0	1	0	0	2	13	35	26	5	3	1	0	86	2.9
SSW		0	0	0	0	3	9	32	62	40	18	9	2	175	3.9
SW		0	0	0	0	1	1	23	55	37	33	27	4	181	4.5
WSW		0	0	0	0	2	3	14	37	28	11	17	3	115	4.4
W		0	0	0	1	0	3	9	8	17	3	1	0	42	3.7

WLS COL 2.3-2

TABLE 2.3-235 (Sheet 2 of 2)
 JOINT FREQUENCY DISTRIBUTION OF WIND SPEED AND DIRECTION BY
 ATMOSPHERIC STABILITY CLASS
 STABILITY CLASS A

STABILITY CLASS A

HOURS AT EACH WIND SPEED AND DIRECTION

DIR	Wind Speed (m/sec)												Total	Average Wind Speed (m/sec)
	U≤0.5	0.5<U ≤0.75	0.75<U ≤1.0	1.0<U ≤1.25	1.25<U ≤1.5	1.5<U ≤2.0	2.0<U ≤3.0	3.0<U ≤4.0	4.0<U ≤5.0	5.0<U ≤6.0	6.0<U ≤8.0	U>8		
WNW	0	0	1	0	4	2	13	18	17	16	15	6	92	4.6
NW	0	0	0	1	1	3	12	14	16	15	15	5	82	4.8
NNW	0	0	0	0	0	4	7	11	2	6	0	0	30	3.5
CALM	0													
TOTAL	0	2	1	8	27	129	345	362	192	114	91	20	1291	

NOTES:

1. Data from Lee Nuclear Station site Data, 12/1/2005 - 11/30/2007.
2. Stability class is determined by the upper temperature gradient between 60m and 10m.
3. Wind direction data is from the 10 m level.
4. Calms are wind speeds below 1 mph (0.45 m/sec).

WLS COL 2.3-2

TABLE 2.3-236 (Sheet 1 of 2)
 JOINT FREQUENCY DISTRIBUTION OF WIND SPEED AND DIRECTION BY
 ATMOSPHERIC STABILITY CLASS
 STABILITY CLASS B

STABILITY CLASS B		HOURS AT EACH WIND SPEED AND DIRECTION												Average Wind Speed (m/sec)
DIR	Wind Speed (m/sec)												Total	
	U≤0.5	0.5<U ≤0.75	0.75<U ≤1.0	1.0<U ≤1.25	1.25<U ≤1.5	1.5<U ≤2.0	2.0<U ≤3.0	3.0<U ≤4.0	4.0<U ≤5.0	5.0<U ≤6.0	6.0<U ≤8.0	U>8		
N	0	0	0	1	1	6	8	16	16	4	0	0	52	3.5
NNE	0	0	0	0	0	10	19	16	10	8	1	0	64	3.4
NE	0	0	0	1	3	15	20	28	8	3	0	0	78	2.9
ENE	0	0	0	2	7	5	23	32	4	1	1	0	75	2.9
E	0	0	0	2	0	8	24	6	2	0	0	0	42	2.5
ESE	0	0	0	0	2	7	17	1	0	0	0	0	27	2.2
SE	0	0	1	1	1	11	22	1	0	0	0	0	37	2.2
SSE	0	0	0	2	4	14	33	2	0	0	1	0	56	2.2
S	0	0	0	1	4	11	46	11	2	2	0	0	77	2.5
SSW	0	0	0	0	0	4	39	39	25	12	6	2	127	3.7
SW	0	0	0	0	0	5	32	32	37	25	18	3	152	4.3

WLS COL 2.3-2

TABLE 2.3-236 (Sheet 2 of 2)
 JOINT FREQUENCY DISTRIBUTION OF WIND SPEED AND DIRECTION BY
 ATMOSPHERIC STABILITY CLASS
 STABILITY CLASS B

STABILITY CLASS B

HOURS AT EACH WIND SPEED AND DIRECTION

DIR	Wind Speed (m/sec)												Total	Average Wind Speed (m/sec)
	U≤0.5	0.5<U ≤0.75	0.75<U ≤1.0	1.0<U ≤1.25	1.25<U ≤1.5	1.5<U ≤2.0	2.0<U ≤3.0	3.0<U ≤4.0	4.0<U ≤5.0	5.0<U ≤6.0	6.0<U ≤8.0	U>8		
WSW	0	0	0	0	0	7	27	39	16	12	10	1	112	3.9
W	0	0	0	0	1	1	19	14	12	8	2	0	57	3.7
WNW	0	0	0	0	1	6	18	13	7	10	8	8	71	4.4
NW	0	0	0	0	2	10	30	15	10	10	7	4	88	3.8
NNW	0	0	1	1	1	0	7	8	8	3	0	1	30	3.6
CALM	0													
TOTAL	0	0	2	11	27	120	384	273	157	98	54	19	1145	

NOTES:

1. Data from Lee Nuclear Station site Data, 12/1/2005 - 11/30/2007.
2. Calms are wind speeds below 1 mph (0.45 m/sec).

WLS COL 2.3-2

TABLE 2.3-237 (Sheet 1 of 2)
 JOINT FREQUENCY DISTRIBUTION OF WIND SPEED AND DIRECTION BY
 ATMOSPHERIC STABILITY CLASS
 STABILITY CLASS C

STABILITY CLASS C

HOURS AT EACH WIND SPEED AND DIRECTION

														Average Wind Speed (m/sec)
DIR	Wind Speed (m/sec)												Total	
	U≤0.5	0.5<U ≤0.75	0.75<U ≤1.0	1.0<U ≤1.25	1.25<U ≤1.5	1.5<U ≤2.0	2.0<U ≤3.0	3.0<U ≤4.0	4.0<U ≤5.0	5.0<U ≤6.0	6.0<U ≤8.0	U>8		
N	0	0	1	3	3	10	16	9	5	1	1	0	49	2.7
NNE	0	0	0	0	3	5	24	21	15	4	0	0	72	3.3
NE	0	0	0	2	5	16	47	23	10	3	0	0	106	2.8
ENE	0	0	0	2	4	14	32	21	5	0	1	0	79	2.7
E	0	0	0	0	2	21	22	4	1	0	0	0	50	2.2
ESE	0	0	0	0	3	12	12	1	0	0	0	0	28	2.0
SE	0	0	0	3	8	29	35	0	0	0	0	0	75	1.9
SSE	0	0	0	4	8	31	49	6	0	1	0	0	99	2.2
S	0	0	1	2	2	13	53	9	3	3	0	0	86	2.5
SSW	0	0	0	0	2	9	44	33	22	10	10	2	132	3.6
SW	0	0	1	1	2	8	41	27	21	11	29	8	149	4.3

WLS COL 2.3-2

TABLE 2.3-237 (Sheet 2 of 2)
 JOINT FREQUENCY DISTRIBUTION OF WIND SPEED AND DIRECTION BY
 ATMOSPHERIC STABILITY CLASS
 STABILITY CLASS C

STABILITY CLASS C

HOURS AT EACH WIND SPEED AND DIRECTION

DIR	Wind Speed (m/sec)												Total	Average Wind Speed (m/sec)
	U≤0.5	0.5<U ≤0.75	0.75<U ≤1.0	1.0<U ≤1.25	1.25<U ≤1.5	1.5<U ≤2.0	2.0<U ≤3.0	3.0<U ≤4.0	4.0<U ≤5.0	5.0<U ≤6.0	6.0<U ≤8.0	U>8		
WSW	0	0	0	1	5	11	48	23	13	7	4	5	117	3.4
W	0	0	1	2	3	8	24	11	4	2	2	0	57	2.8
WNW	0	0	0	3	1	13	18	12	6	3	5	3	64	3.5
NW	0	0	0	0	1	13	25	10	9	7	13	6	84	4.1
NNW	0	0	0	1	0	5	16	8	2	5	0	1	38	3.1
CALM	0													
TOTAL	0	0	4	24	52	218	506	218	116	57	65	25	1285	

NOTES:

1. Data from Lee Nuclear Station site Data, 12/1/2005 - 11/30/2007.
2. Calms are wind speeds below 1 mph (0.45 m/sec)

WLS COL 2.3-2

TABLE 2.3-238 (Sheet 1 of 2)
 JOINT FREQUENCY DISTRIBUTION OF WIND SPEED AND DIRECTION BY
 ATMOSPHERIC STABILITY CLASS
 STABILITY CLASS D

STABILITY CLASS D

HOURS AT EACH WIND SPEED AND DIRECTION

														Average Wind Speed (m/sec)
DIR	Wind Speed (m/sec)												Total	
	U≤0.5	0.5<U ≤0.75	0.75<U ≤1.0	1.0<U ≤1.25	1.25<U ≤1.5	1.5<U ≤2.0	2.0<U ≤3.0	3.0<U ≤4.0	4.0<U ≤5.0	5.0<U ≤6.0	6.0<U ≤8.0	U>8		
N	0	0	13	17	32	60	113	38	39	15	5	0	332	2.6
NNE	0	1	11	18	28	84	151	78	41	11	2	0	425	2.6
NE	0	1	10	14	25	62	143	64	26	11	1	0	357	2.6
ENE	0	1	14	25	30	58	105	47	10	5	0	0	295	2.3
E	0	4	19	17	30	39	46	11	3	0	0	0	169	1.8
ESE	0	1	15	14	28	50	35	7	0	1	0	0	151	1.8
SE	0	3	5	19	48	78	71	10	9	2	0	0	245	2.0
SSE	1	1	8	15	35	82	92	12	10	4	6	3	269	2.3
S	1	1	8	8	36	83	113	48	21	5	7	1	332	2.5
SSW	0	0	9	5	16	48	143	93	65	28	4	3	414	3.1
SW	0	1	8	10	17	36	83	71	62	53	27	1	369	3.6

WLS COL 2.3-2

TABLE 2.3-238 (Sheet 2 of 2)
JOINT FREQUENCY DISTRIBUTION OF WIND SPEED AND DIRECTION BY
ATMOSPHERIC STABILITY CLASS
STABILITY CLASS D

STABILITY CLASS D

HOURS AT EACH WIND SPEED AND DIRECTION

DIR	Wind Speed (m/sec)												Total	Average Wind Speed (m/sec)
	U≤0.5	0.5<U ≤0.75	0.75<U ≤1.0	1.0<U ≤1.25	1.25<U ≤1.5	1.5<U ≤2.0	2.0<U ≤3.0	3.0<U ≤4.0	4.0<U ≤5.0	5.0<U ≤6.0	6.0<U ≤8.0	U>8		
WSW	0	0	5	13	10	28	56	44	30	15	13	5	219	3.3
W	0	1	8	9	7	25	43	23	11	7	2	0	136	2.6
WNW	0	3	8	10	16	23	40	22	23	17	13	8	183	3.3
NW	0	2	14	18	26	58	62	30	36	27	29	13	315	3.3
NNW	0	3	16	20	33	41	57	43	27	20	7	4	271	2.8
CALM	5													
TOTAL	7	23	171	232	417	855	1353	641	413	221	116	38	4487	

NOTES:

1. Data from Lee Nuclear Station site Data, 12/1/2005 - 11/30/2007.
2. Calms are wind speeds below 1 mph (0.45 m/sec)

WLS COL 2.3-2

TABLE 2.3-239 (Sheet 1 of 2)
 JOINT FREQUENCY DISTRIBUTION OF WIND SPEED AND DIRECTION BY
 ATMOSPHERIC STABILITY CLASS
 STABILITY CLASS E

STABILITY CLASS E

HOURS AT EACH WIND SPEED AND DIRECTION

DIR	Wind Speed (m/sec)												Total	Average Wind Speed (m/sec)
	U≤0.5	0.5<U ≤0.75	0.75<U ≤1.0	1.0<U ≤1.25	1.25<U ≤1.5	1.5<U ≤2.0	2.0<U ≤3.0	3.0<U ≤4.0	4.0<U ≤5.0	5.0<U ≤6.0	6.0<U ≤8.0	U>8		
N	0	8	34	31	34	46	43	17	3	4	1	0	221	1.8
NNE	1	9	25	23	35	39	49	28	2	0	0	0	211	1.9
NE	1	8	32	27	36	36	41	18	3	0	0	0	202	1.7
ENE	1	13	25	17	27	30	36	3	1	0	0	0	153	1.6
E	0	11	40	37	30	32	18	1	0	0	0	0	169	1.3
ESE	0	8	33	42	30	28	13	1	0	0	0	0	155	1.3
SE	0	3	31	36	44	48	23	3	1	0	0	0	189	1.5
SSE	1	1	20	37	45	70	41	12	5	2	1	0	235	1.8
S	0	4	12	24	38	82	132	38	2	0	2	0	334	2.1
SSW	0	4	8	21	20	29	105	56	26	9	0	0	278	2.6
SW	0	3	7	10	10	31	52	51	45	13	3	0	225	3.0

WLS COL 2.3-2

TABLE 2.3-239 (Sheet 2 of 2)
 JOINT FREQUENCY DISTRIBUTION OF WIND SPEED AND DIRECTION BY
 ATMOSPHERIC STABILITY CLASS
 STABILITY CLASS E

STABILITY CLASS E

HOURS AT EACH WIND SPEED AND DIRECTION

DIR	Wind Speed (m/sec)												Total	Average Wind Speed (m/sec)
	U≤0.5	0.5<U ≤0.75	0.75<U ≤1.0	1.0<U ≤1.25	1.25<U ≤1.5	1.5<U ≤2.0	2.0<U ≤3.0	3.0<U ≤4.0	4.0<U ≤5.0	5.0<U ≤6.0	6.0<U ≤8.0	U>8		
WSW	0	1	7	12	9	26	33	27	14	4	0	0	133	2.6
W	0	4	11	4	9	21	37	20	3	0	0	0	109	2.2
WNW	0	0	15	23	27	45	58	24	11	6	0	0	209	2.2
NW	1	6	28	58	63	74	69	39	7	0	2	0	347	1.9
NNW	1	8	29	30	47	55	53	32	9	2	1	0	267	1.9
CALM	12													
TOTAL	18	91	357	432	504	692	803	370	132	40	10	0	3449	

NOTES:

1. Data from Lee Nuclear Station site Data, 12/1/2005 - 11/30/2007.
2. Calms are wind speeds below 1 mph (0.45 m/sec).

WLS COL 2.3-2

TABLE 2.3-240 (Sheet 1 of 2)
 JOINT FREQUENCY DISTRIBUTION OF WIND SPEED AND DIRECTION BY
 ATMOSPHERIC STABILITY CLASS
 STABILITY CLASS F

STABILITY CLASS F			HOURS AT EACH WIND SPEED AND DIRECTION												
														Average Wind Speed (m/sec)	
Wind Speed (m/sec)															
DIR	U≤0.5	0.5<U ≤0.75	0.75<U ≤1.0	1.0<U ≤1.25	1.25<U ≤1.5	1.5<U ≤2.0	2.0<U ≤3.0	3.0<U ≤4.0	4.0<U ≤5.0	5.0<U ≤6.0	6.0<U ≤8.0	U>8	Total		
N	3	15	30	19	11	11	7	0	0	0	0	0	96	1.1	
NNE	1	18	28	14	17	10	4	0	0	0	0	0	92	1.1	
NE	1	19	28	13	11	14	2	1	0	0	0	0	89	1.1	
ENE	2	17	34	20	8	2	2	0	0	0	0	0	85	1.0	
E	0	20	55	24	8	3	0	0	0	0	0	0	110	0.9	
ESE	2	17	42	38	11	5	1	0	0	0	0	0	116	1.0	
SE	0	7	30	29	35	20	6	1	0	0	0	0	128	1.2	
SSE	0	6	15	30	26	24	11	0	2	0	0	0	114	1.4	
S	1	2	12	9	17	22	31	5	0	0	0	0	99	1.8	
SSW	0	0	9	6	9	7	22	5	0	1	0	0	59	2.0	
SW	0	1	3	6	9	10	3	0	0	0	0	0	32	1.5	

WLS COL 2.3-2

TABLE 2.3-240 (Sheet 2 of 2)
 JOINT FREQUENCY DISTRIBUTION OF WIND SPEED AND DIRECTION BY
 ATMOSPHERIC STABILITY CLASS
 STABILITY CLASS F

STABILITY CLASS F

HOURS AT EACH WIND SPEED AND DIRECTION

DIR	Wind Speed (m/sec)												Total	Average Wind Speed (m/sec)
	U≤0.5	0.5<U ≤0.75	0.75<U ≤1.0	1.0<U ≤1.25	1.25<U ≤1.5	1.5<U ≤2.0	2.0<U ≤3.0	3.0<U ≤4.0	4.0<U ≤5.0	5.0<U ≤6.0	6.0<U ≤8.0	U>8		
WSW	0	3	9	10	1	7	7	2	0	0	0	0	39	1.5
W	0	4	12	6	11	12	10	2	1	0	0	0	58	1.6
WNW	0	7	31	23	28	48	34	3	2	0	0	0	176	1.6
NW	1	15	44	49	82	102	65	4	0	0	1	0	363	1.6
NNW	0	18	46	31	31	22	20	4	0	0	0	0	172	1.3
CALM	33													
TOTAL	44	169	428	327	315	319	225	27	5	1	1	0	1861	

NOTES:

1. Data from Lee Nuclear Station site Data, 12/1/2005 - 11/30/2007.
2. Calms are wind speeds below 1 mph (0.45 m/sec).

WLS COL 2.3-2

TABLE 2.3-241 (Sheet 1 of 2)
 JOINT FREQUENCY DISTRIBUTION OF WIND SPEED AND DIRECTION BY
 ATMOSPHERIC STABILITY CLASS
 STABILITY CLASS G

STABILITY CLASS G

HOURS AT EACH WIND SPEED AND DIRECTION

DIR	Wind Speed (m/sec)											U>8	Total	Average Wind Speed (m/sec)
	U≤0.5	0.5<U ≤0.75	0.75<U ≤1.0	1.0<U ≤1.25	1.25<U ≤1.5	1.5<U ≤2.0	2.0<U ≤3.0	3.0<U ≤4.0	4.0<U ≤5.0	5.0<U ≤6.0	6.0<U ≤8.0			
N	7	49	65	27	8	3	1	0	0	0	0	0	160	0.9
NNE	7	56	36	14	6	5	1	0	0	0	0	0	125	0.8
NE	3	44	40	7	8	2	1	0	0	0	0	0	105	0.8
ENE	8	41	57	12	3	1	0	0	0	0	0	0	122	0.8
E	6	40	81	24	22	3	1	0	0	0	0	0	177	0.9
ESE	5	45	73	41	18	3	0	0	0	0	0	0	185	0.9
SE	2	40	71	33	21	11	3	0	0	0	0	0	181	1.0
SSE	2	17	24	17	13	8	3	0	0	0	0	0	84	1.1
S	0	15	5	4	2	2	4	0	0	0	0	0	32	1.0
SSW	1	2	3	1	3	4	1	0	0	0	0	0	15	1.2
SW	0	4	5	3	3	1	0	0	0	0	0	0	16	1.0

WLS COL 2.3-2

TABLE 2.3-241 (Sheet 2 of 2)
 JOINT FREQUENCY DISTRIBUTION OF WIND SPEED AND DIRECTION BY
 ATMOSPHERIC STABILITY CLASS
 STABILITY CLASS G

STABILITY CLASS G

HOURS AT EACH WIND SPEED AND DIRECTION

DIR	Wind Speed (m/sec)												Total	Average Wind Speed (m/sec)
	U≤0.5	0.5<U ≤0.75	0.75<U ≤1.0	1.0<U ≤1.25	1.25<U ≤1.5	1.5<U ≤2.0	2.0<U ≤3.0	3.0<U ≤4.0	4.0<U ≤5.0	5.0<U ≤6.0	6.0<U ≤8.0	U>8		
WSW	0	6	9	3	2	0	0	0	0	0	0	0	20	0.9
W	1	7	17	12	6	7	6	0	0	0	0	0	56	1.2
WNW	7	25	36	39	46	80	60	1	0	0	0	0	294	1.5
NW	7	48	108	165	246	412	226	0	0	0	0	0	1212	1.6
NNW	5	61	114	90	57	19	5	2	0	0	0	0	353	1.0
CALM	180													
TOTAL	241	500	744	492	464	561	312	3	0	0	0	0	3317	

NOTES:

1. Data from Lee Nuclear Station site Data, 12/1/2005 - 11/30/2007.
2. Calms are wind speeds below 1 mph (0.45 m/sec).

WLS COL 2.3-1

TABLE 2.3-242 (Sheet 1 of 2)
 MAXIMUM NUMBER OF CONSECUTIVE HOURS WITH WIND FROM A SINGLE SECTOR
 GREENVILLE/SPARTANBURG, SOUTH CAROLINA

Sector	1997	1998	1999	2000	2001	2002	2003	2004	2005	Maximum	Average
N	8	13	12	10	8	7	10	10	9	13	9.8
NNE	7	5	4	11	13	12	15	10	12	15	9.6
NE	11	13	14	15	13	12	23	11	14	23	14.0
ENE	15	17	13	11	5	6	8	8	6	17	10.4
E	5	9	7	7	7	7	7	8	7	9	7.1
ESE	5	3	5	5	3	6	3	3	3	6	4.1
SE	3	4	4	3	4	7	5	6	5	7	4.5
SSE	4	4	5	4	6	6	5	4	7	6	4.8
S	7	13	6	10	10	10	9	8	12	13	9.1
SSW	5	8	5	8	8	8	9	6	9	9	7.1
SW	5	10	7	10	10	9	12	11	11	12	9.3
WSW	16	19	12	14	9	8	7	11	10	19	12.0
W	8	12	7	8	7	7	6	7	9	12	7.8
WNW	4	4	6	3	4	5	5	3	3	6	4.3

WLS COL 2.3-1

TABLE 2.3-242 (Sheet 2 of 2)
MAXIMUM NUMBER OF CONSECUTIVE HOURS WITH WIND FROM A SINGLE SECTOR
GREENVILLE/SPARTANBURG, SOUTH CAROLINA

Sector	1997	1998	1999	2000	2001	2002	2003	2004	2005	Maximum	Average
NW	3	3	2	6	4	5	4	4	4	6	3.9
NNW	6	6	8	7	7	7	5	5	7	8	6.4

NOTES:

1. Wind values which were either not provided, had a zero speed value, or a VRB wind direction were not included, and assumed to break any consecutive wind direction count.
2. Data from Unedited Local Climatological Data, National Oceanic and Atmospheric Administration, U. S. Department of Commerce, Asheville, NC, Greenville/Spartanburg International Airport, Station No. 03870.
3. Period of Record - 9 years (1997 - 2005).

WLS COL 2.3-1

TABLE 2.3-243 (Sheet 1 of 2)
 MAXIMUM NUMBER OF CONSECUTIVE HOURS WITH WIND FROM THREE ADJACENT
 SECTORS, GREENVILLE/SPARTANBURG, SOUTH CAROLINA

Sector	1997	1998	1999	2000	2001	2002	2003	2004	2005	Maximum	Average
N	17	32	23	28	21	19	25	29	20	32	24.3
NNE	20	17	26	46	24	54	45	32	48	54	33.0
NE	37	60	61	82	32	78	65	47	66	82	57.8
ENE	41	70	66	62	30	16	37	35	23	70	44.6
E	18	22	36	21	11	10	16	19	13	36	19.1
ESE	8	14	9	10	14	10	12	20	13	20	12.1
SE	8	8	9	8	20	12	14	13	14	20	11.5
SSE	8	14	17	11	25	15	11	12	21	25	14.1
S	12	14	16	15	16	27	17	18	26	27	16.9
SSW	16	21	14	18	40	29	21	34	27	40	24.1
SW	24	38	37	26	49	36	49	36	32	49	36.9
WSW	35	53	46	48	43	31	38	45	31	53	42.4
W	33	48	34	28	18	18	25	21	18	48	28.1
WNW	13	16	18	14	18	8	18	10	19	18	14.4
NW	7	7	14	11	16	12	10	8	12	16	10.6

WLS COL 2.3-1

TABLE 2.3-243 (Sheet 2 of 2)
MAXIMUM NUMBER OF CONSECUTIVE HOURS WITH WIND FROM THREE ADJACENT
SECTORS, GREENVILLE/SPARTANBURG, SOUTH CAROLINA

Sector	1997	1998	1999	2000	2001	2002	2003	2004	2005	Maximum	Average
NNW	24	27	20	29	41	22	32	19	23	41	26.8

NOTES:

1. Wind values which were either not provided, had a zero speed value, or a VRB wind direction were not included, and assumed to break any consecutive wind direction count.
2. Data from Unedited Local Climatological Data, National Oceanic and Atmospheric Administration, U. S. Department of Commerce, Asheville, NC, Greenville/Spartanburg International Airport, Station No. 03870.
3. Period of Record - 9 years (1997 - 2005).

WLS COL 2.3-1

TABLE 2.3-244 (Sheet 1 of 2)
 MAXIMUM NUMBER OF CONSECUTIVE HOURS WITH WIND FROM FIVE ADJACENT
 SECTORS, GREENVILLE/SPARTANBURG, SOUTH CAROLINA

Sector	1997	1998	1999	2000	2001	2002	2003	2004	2005	Maximum	Average
N	29	44	32	48	43	54	45	41	48	54	42.0
NNE	38	69	64	82	44	96	75	69	114	96	67.1
NE	54	70	107	82	88	150	80	97	146	150	91.0
ENE	61	70	111	82	53	128	66	79	110	128	81.3
E	43	70	76	62	30	18	37	35	38	76	46.4
ESE	18	22	36	24	20	12	17	30	20	36	22.4
SE	10	19	22	13	26	23	18	22	27	26	19.1
SSE	12	14	22	15	26	27	18	22	33	27	19.5
S	16	21	30	18	42	36	24	34	35	42	27.6
SSW	26	49	38	49	54	61	77	65	38	77	52.4
SW	49	114	68	66	81	60	93	76	49	114	75.9
WSW	42	57	67	56	77	70	99	49	83	99	64.6
W	35	55	49	48	43	38	41	45	38	55	44.3
WNW	33	48	45	28	18	19	29	21	24	48	30.1

WLS COL 2.3-1

TABLE 2.3-244 (Sheet 2 of 2)
MAXIMUM NUMBER OF CONSECUTIVE HOURS WITH WIND FROM FIVE ADJACENT
SECTORS, GREENVILLE/SPARTANBURG, SOUTH CAROLINA

Sector	1997	1998	1999	2000	2001	2002	2003	2004	2005	Maximum	Average
NW	24	27	20	29	41	22	35	25	34	41	27.9
NNW	28	36	23	47	41	23	33	29	26	47	32.5

NOTES:

1. Wind values which were either not provided, had a zero speed value, or a VRB wind direction were not included, and assumed to break any consecutive wind direction count.
2. Data from Unedited Local Climatological Data, National Oceanic and Atmospheric Administration, U. S. Department of Commerce, Asheville, NC, Greenville/Spartanburg International Airport, Station No. 03870.
3. Period of Record - 9 years (1997 - 2005).

WLS COL 2.3-1

TABLE 2.3-245 (Sheet 1 of 2)
 COMPARISON OF MAXIMUM WIND PERSISTENCE
 AT LEE NUCLEAR STATION SITE AND GREENVILLE/SPARTANBURG
 SOUTH CAROLINA

Sector	Wind Persistence (hrs)								
	Single Sector			Three Adjacent Sectors			Five Adjacent Sectors		
	Lee	GSP ⁵	GSP ⁴	Lee	GSP ⁵	GSP ⁴	Lee	GSP ⁵	GSP ⁴
N	9	15	13	34	32	32	55	76	54
NNE	12	6	15	36	50	54	71	68	96
NE	12	13	23	31	43	82	66	56	150
ENE	6	4	17	20	31	70	34	43	128
E	4	6	9	23	11	36	25	31	76
ESE	5	5	6	19	11	20	26	11	36
SE	6	3	7	15	8	20	26	20	26
SSE	11	5	6	20	19	25	25	19	27
S	7	12	13	22	19	27	40	26	42
SSW	9	7	9	30	23	40	42	70	77
SW	10	11	12	41	33	49	62	88	114
WSW	7	10	19	31	44	53	53	88	99

WLS COL 2.3-1

TABLE 2.3-245 (Sheet 2 of 2)
COMPARISON OF MAXIMUM WIND PERSISTENCE
AT LEE NUCLEAR STATION SITE AND GREENVILLE/SPARTANBURG
SOUTH CAROLINA

Sector	Wind Persistence (hrs)								
	Single Sector			Three Adjacent Sectors			Five Adjacent Sectors		
	Lee	GSP ⁵	GSP ⁴	Lee	GSP ⁵	GSP ⁴	Lee	GSP ⁵	GSP ⁴
W	8	8	12	21	20	48	45	44	55
WNW	6	3	6	30	9	18	48	20	48
NW	15	4	6	45	8	16	47	31	41
NNW	14	8	8	27	31	41	62	36	47
Max	15	15	23	45	50	82	71	88	150
Average	8.8	7.5	11.3	27.8	24.5	39.4	45.4	45.4	69.8

NOTES:

1. Wind values which were either not provided, had a zero speed value, or a VRB wind direction were not included, and assumed to break any consecutive wind direction count.
2. Wind persistence values above are the maximum persistence durations for the period of record.
3. Period of record at Lee Nuclear Station site, 12/1/2005 through 11/30/2006, Tower 2 at 10 meter level.
4. Period of record at Greenville/Spartanburg, 1997 - 2005.
5. Period of record at Greenville/Spartanburg, 12/1/2005 through 11/30/2006.

WLS COL 2.3-1

TABLE 2.3-246 (Sheet 1 of 2)
 NINETY-NINE ISLANDS MONTHLY CLIMATE SUMMARY
 NCDC 1971-2000 MONTHLY NORMALS

	Jan	Feb	Mar	Apr	May	Jun	Jul	Aug	Sep	Oct	Nov	Dec	Annual
Mean Max. Temperature (°F)	50.5	55.1	62.9	71.3	77.7	83.9	87.5	86	80.4	71.7	62	53.2	70.2
Highest Mean Max. Temperature (°F)	59.3	64.3	68.6	76.4	82.9	89.2	94.4	91.8	84.5	77.9	68.4	62.1	94.4
Year Highest Occurred	1974	1976	2000	1986	2000	1986	1993	1999	1973	1984	1999	1984	1993
Lowest Mean Max. Temperature (°F)	39.7	46.1	56.9	66	73.2	77.9	83	81.9	77	66.2	54.4	45.1	39.7
Year Lowest Occurred	1977	1978	1971	1984	1997	1997	1979	1992	1974	1976	1996	2000	1977
Mean Temperature (°F)	39	42.3	49.6	57.1	65.2	72.6	76.8	75.7	69.5	58.5	49	41.4	58.1
Highest Mean Temperature (°F)	50	48.6	54.1	61.4	70.3	76.9	81.2	79.4	73.1	65.8	57	49.6	81.2
Year Highest Occurred	1974	1990	2000	1999	1991	1986	1993	1999	1973	1984	1985	1971	1993
Lowest Mean Temperature (°F)	28.5	34	44.1	52.5	60.7	68.2	73.7	72.9	66.8	52.2	42	34.1	28.5
Year Lowest Occurred	1977	1978	1971	1983	1997	1972	1979	1997	1984	1987	1976	2000	1977
Mean Min. Temperature (°F)	27.4	29.5	36.2	42.9	52.7	61.3	66.1	65.3	58.5	45.2	35.9	29.5	45.9
Highest Mean Min. Temperature (°F)	40.7	36.4	42.7	49.2	60.6	65.6	69	69.1	62.2	53.9	48	38.8	69.1
Year Highest Occurred	1974	1998	1973	1991	1991	1994	1991	1995	1980	1971	1985	1971	1995
Lowest Mean Min. Temperature (°F)	17.2	21.5	30.5	37.7	47.9	55.5	62.9	61.1	53.5	35.7	28.4	23	17.2
Year Lowest Occurred	1977	1977	1981	1971	1981	1972	1976	1997	1999	1987	1976	2000	1977

WLS COL 2.3-1

TABLE 2.3-246 (Sheet 2 of 2)
 NINETY-NINE ISLANDS MONTHLY CLIMATE SUMMARY
 NCDC 1971-2000 MONTHLY NORMALS

	Jan	Feb	Mar	Apr	May	Jun	Jul	Aug	Sep	Oct	Nov	Dec	Annual
Mean Precipitation (in.)	4.53	4.07	4.93	3.05	4.15	3.76	3.78	4.83	4.08	3.85	3.67	3.67	48.37
Highest Precipitation (in.)	8.25	6.6	9.54	6.65	10.5	10.5	10.9	11.9	9.73	14.9	8.83	8.75	14.93
Year Highest Occurred	1978	1997	1980	1998	1975	1995	1971	1994	1987	1990	1985	1983	1990
Lowest Precipitation (in.)	0.3	0.64	1.15	0.39	1.13	0.17	0.85	0.88	0.59	0	0.88	0.83	0
Year Lowest Occurred	1981	1978	1985	1976	1988	1986	1977	1999	1985	2000	1973	1980	2000
Heating Degree Days (°F)	807	637	480	243	88	8	0	0	21	236	483	734	3737
Cooling Degree Days (°F)	0	0	0	7	94	236	366	330	155	33	2	0	1223

NOTES:

1. Ninety-Nine Islands, South Carolina (Station No. 386293), Monthly Climate Summary, Period of Record: 1971 to 2000.
2. Reference: Southeast Regional Climate Center, <http://cirrus.dnr.state.sc.us/cgi-bin/sercc/cliMAIN.pl?sc6293>

TABLE 2.3-247
DELETED

TABLE 2.3-248
DELETED

TABLE 2.3-249
DELETED

TABLE 2.3-250
DELETED

TABLE 2.3-251
DELETED

TABLE 2.3-252
DELETED

WLS COL 2.3-1

TABLE 2.3-253
RELATIVE HUMIDITY
GREENVILLE/SPARTANBURG, SOUTH CAROLINA
FOR 4 TIME PERIODS PER DAY
1997-2005^{(a)(b)}

Time	00:00 - 06:00	06:00-12:00	12:00-18:00	18:00-24:00
Jan	75%	69%	53%	67%
Feb	76%	69%	52%	66%
Mar	73%	65%	49%	63%
Apr	78%	65%	50%	66%
May	84%	68%	53%	71%
Jun	87%	71%	58%	76%
Jul	89%	72%	59%	79%
Aug	87%	72%	56%	77%
Sep	85%	71%	56%	77%
Oct	86%	72%	57%	78%
Nov	81%	71%	56%	74%
Dec	77%	70%	54%	69%
Annual	81%	69%	54%	72%

a) Data from Unedited Local Climatological Data, National Oceanic and Atmospheric Administration, U.S. Department of Commerce, Asheville, NC, Greenville/Spartanburg International Airport, Station No. 03870.

b) Data from Unedited Local Climatological Data, National Oceanic and Atmospheric Administration, U. S. Department of Commerce, Asheville, NC, Greenville/Spartanburg International Airport, Station No. 03870.

TABLE 2.3-254
 NINETY-NINE ISLANDS MONTHLY CLIMATE SUMMARY
 NINETY-NINE ISLANDS, SOUTH CAROLINA (386293)
 PERIOD OF RECORD: 8/1/1948 TO 12/31/2005

	Jan	Feb	Mar	Apr	May	Jun	Jul	Aug	Sep	Oct	Nov	Dec	Annual
Average Max. Temperature (F)	51.5	55.6	63.8	72.6	79.4	85.4	89.0	87.6	82.1	73.2	63.7	54.0	71.5
Average Min. Temperature (F)	26.7	29.1	35.7	43.3	52.7	61.3	65.9	65.1	58.2	45.1	35.6	28.4	45.6
Average Total Precipitation (in.)	4.10	4.06	4.99	3.40	3.94	3.89	4.12	4.69	3.89	3.32	3.30	3.81	47.52
Average Total Snowfall (in.)	1.1	1.1	0.5	0	0	0	0	0	0	0	0	0.4	3.1
Average Snow Depth (in.)	0	0	0	0	0	0	0	0	0	0	0	0	0

Percent of possible observations for period of record.

Max. Temp.: 76.3% Min. Temp.: 76.3% Precipitation: 99.6%: Snowfall: 84.1% Snow Depth: 84.2%.

NOTES:

1. Data from: Southeast Regional Climate Center, <http://cirrus.dnr.state.sc.us/cgi-bin/sercc/cliMAIN.pl?sc6293>

WLS COL 2.3-2

TABLE 2.3-255
COMPARISON OF RELATIVE HUMIDITY FOR LEE NUCLEAR SITE (2005 – 2006^(a)) AND
GREENVILLE/SPARTANBURG, SOUTH CAROLINA (1997 – 2005^(b))
FOR 4 TIME PERIODS PER DAY

	00:00 - 06:00		06:00 - 12:00		12:00 - 18:00		18:00 - 24:00	
Time	Lee	GSP	Lee	GSP	Lee	GSP	Lee	GSP
Jan	78%	75%	69%	69%	53%	53%	67%	67%
Feb	76%	76%	68%	69%	44%	52%	58%	66%
Mar	73%	73%	63%	65%	41%	49%	54%	63%
Apr	78%	78%	75%	65%	43%	50%	55%	66%
May	88%	84%	77%	68%	50%	53%	67%	71%
Jun	92%	87%	80%	71%	51%	58%	72%	76%
Jul	94%	89%	83%	72%	55%	59%	75%	79%
Aug	94%	87%	86%	72%	60%	56%	78%	77%
Sep	93%	85%	86%	71%	59%	56%	82%	77%
Oct	90%	86%	83%	72%	52%	57%	74%	78%
Nov	85%	81%	74%	71%	46%	56%	74%	74%
Dec	86%	77%	78%	70%	49%	54%	71%	69%
Annual	86%	81%	77%	69%	50%	54%	69%	72%

a) Lee Nuclear Station site Data, 12/1/2005 - 11/30/2006.

b) Data from Unedited Local Climatological Data, National Oceanic and Atmospheric Administration, U.S. Department of Commerce, Asheville, NC, Greenville/Spartanburg International Airport, Station No. 03870.

WLS COL 2.3-1

TABLE 2.3-256
PRECIPITATION DATA (INCHES OF RAIN)
GREENVILLE/SPARTANBURG, SOUTH CAROLINA

GSP Precipitation	Period of Record	Jan	Feb	Mar	Apr	May	Jun	Jul	Aug	Sep	Oct	Nov	Dec	Year
Normal (in)	30	4.41	4.24	5.31	3.54	4.59	3.92	4.65	4.08	3.97	3.88	3.79	3.86	50.24
Maximum Monthly (in)	45	7.19	7.43	11.37	11.30	8.89	10.12	13.57	17.37	11.65	10.24	7.85	8.45	17.37
Year of Occurrence		1993	1971	1980	1964	1972	1994	1984	1995	1975	1964	1992	1983	AUG 1995
Minimum Monthly (in)	45	0.29	0.53	1.13	0.69	1.09	0.17	0.75	0.79	0.16	0.00	0.89	0.37	0.00
Year of Occurrence		1981	1978	1985	1976	1965	1993	1993	1999	2005	2000	2007	1965	OCT 2000
Maximum In 24 Hours (in)	45	3.30	3.57	4.45	3.76	3.79	4.80	4.68	12.32	6.21	4.93	2.83	3.54	12.32
Year of Occurrence		1982	1984	1963	1963	1996	1980	2005	1995	1973	1990	1964	2004	AUG 1995
Normal No. Days With:														
Precipitation >= 0.01	30	11.3	9.3	11.0	8.7	10.6	10.2	11.8	10.2	9.1	7.1	9.4	10.3	119.0
Precipitation >= 1.00	30	1.1	1.1	1.7	1.0	1.4	1.0	1.4	1.0	1.2	1.0	1.2	1.1	14.2

NOTES:

1. National Climatic Data Center (NCDC) Local Climatic Data (LCD), data for Greenville-Spartanburg (Greer), South Carolina (Station ID GSP), 2007. (Reference 240).

WLS COL 2.3-1

TABLE 2.3-257
POINT PRECIPITATION FREQUENCY

Duration	Recurrence Intervals (Years)						
	1	2	5	10	25	50	100
5 minutes	0.4	0.5	0.6	0.6	0.7	0.8	0.8
10 minutes	0.7	0.8	0.9	1.0	1.1	1.2	1.3
15 minutes	0.8	1.0	1.2	1.3	1.4	1.5	1.7
30 minutes	1.1	1.4	1.6	1.9	2.1	2.3	2.5
1 hour	1.4	1.7	2.1	2.4	2.8	3.2	3.5
2 hours	1.6	2.0	2.4	2.8	3.4	3.8	4.2
3 hours	1.7	2.1	2.6	3.0	3.6	4.1	4.7
6 hours	2.1	2.6	3.2	3.7	4.5	5.1	5.8
12 hours	2.6	3.1	3.9	4.5	5.4	6.2	7.1
24 hours	3.1	3.7	4.6	5.4	6.4	7.3	8.1
2 days	3.6	4.4	5.4	6.3	7.5	8.4	9.4
4 days	4.1	4.9	6.0	6.9	8.2	9.2	10.2
7 days	4.7	5.7	6.9	7.9	9.2	10.3	11.5
10 days	5.4	6.4	7.7	8.7	10.1	11.2	12.3

NOTES:

1. From "Precipitation-Frequency Atlas of the United States" NOAA Atlas 14, Volume 2, Version 3, G. M. Bonnin, D. Martin, B. Lin, T. Parzybok, M. Yekta, and D. Riley, NOAA, National Weather Service, Silver Spring, Maryland, 2004, Extracted: Aug 24 2006. Location: South Carolina 35.024 N 81.524 W 777 feet. http://hdsc.nws.noaa.gov/hdsc/pfds/orb/sc_pfds.html

WLS COL 2.3-1

TABLE 2.3-258
PERCENT OF TOTAL OBSERVATIONS (BY MONTH) OF INDICATED WIND DIRECTIONS AND
PRECIPITATION
GREENVILLE/SPARTANBURG, SOUTH CAROLINA

Sector	January	February	March	April	May	June	July	August	September	October	November	December	Total
N	1.55	1.39	1.27	1.25	1.25	1.25	1.13	1.09	1.49	0.94	1.35	1.76	15.71
NNE	1.30	0.92	1.60	0.97	0.89	0.73	0.57	0.45	1.00	1.42	1.02	1.20	12.06
NE	2.21	2.57	2.99	2.00	1.03	1.06	1.13	0.65	1.09	1.46	1.25	2.77	20.21
ENE	1.65	1.59	1.78	1.36	0.36	0.43	0.61	0.34	0.59	0.78	0.73	1.42	11.64
E	0.57	0.43	0.39	0.32	0.18	0.41	0.46	0.29	0.31	0.24	0.33	0.39	4.33
ESE	0.15	0.09	0.11	0.13	0.17	0.34	0.20	0.13	0.15	0.04	0.13	0.04	1.68
SE	0.10	0.04	0.05	0.27	0.09	0.17	0.19	0.13	0.17	0.06	0.15	0.03	1.44
SSE	0.10	0.09	0.13	0.29	0.11	0.22	0.29	0.22	0.31	0.11	0.24	0.13	2.24
S	0.69	0.31	0.36	0.65	0.42	0.69	0.29	0.33	0.55	0.20	0.65	0.24	5.37
SSW	0.48	0.38	0.41	0.74	0.50	0.46	0.41	0.15	0.20	0.18	0.66	0.25	4.82
SW	0.93	0.66	0.57	0.60	0.69	0.59	0.60	0.33	0.28	0.28	0.88	0.59	6.98
WSW	0.45	0.65	0.46	0.48	0.62	0.62	0.38	0.43	0.27	0.24	0.59	0.47	5.66
W	0.33	0.37	0.33	0.34	0.39	0.42	0.34	0.22	0.20	0.14	0.31	0.32	3.71
WNW	0.09	0.01	0.11	0.10	0.19	0.24	0.11	0.13	0.06	0.08	0.05	0.04	1.22
NW	0.11	0.08	0.25	0.14	0.15	0.22	0.15	0.06	0.09	0.08	0.10	0.09	1.53
NNW	0.20	0.08	0.13	0.15	0.09	0.14	0.14	0.09	0.06	0.04	0.10	0.18	1.40
Total	10.93	9.64	10.95	9.78	7.12	7.96	7.02	5.04	6.82	6.30	8.52	9.91	100

NOTES:

1. Instances of "trace" precipitation were counted as precipitation.
2. Data from Unedited Local Climatological Data, National Oceanic and Atmospheric Administration, U. S. Department of Commerce, Asheville, NC, Greenville/Spartanburg International Airport, Station No. 03870.
3. Period of Record - 9 years (1997 - 2005).

WLS COL 2.3-2

TABLE 2.3-259 (Sheet 1 of 2)
 PERCENT OF TOTAL OBSERVATIONS (BY MONTH) OF PRECIPITATION AND WIND DIRECTION
 LEE NUCLEAR SITE

Sector	January	February	March	April	May	June	July	August	September	October	November	December	Total
N	1.38	1.58	0.59	0.40	0.79	0.79	0.20	0.59	0.99	0.59	1.38	1.98	11.26
NNE	1.58	0.59	1.19	0.40	0.59	1.38	0.00	0.79	0.98	0.99	3.56	2.37	14.43
NE	0.00	0.40	0.00	0.79	0.40	0.99	0.00	0.40	1.58	0.99	0.79	2.17	8.50
ENE	0.59	0.40	0.40	0.00	0.40	1.19	0.59	1.38	0.40	0.79	0.40	0.40	6.92
E	0.00	0.00	0.79	0.20	0.20	0.99	0.59	1.78	0.00	0.00	0.00	0.59	5.14
ESE	0.40	0.00	0.00	0.00	0.40	0.99	0.20	0.40	0.00	0.40	0.20	0.40	3.36
SE	1.19	0.20	0.00	0.40	0.20	0.40	0.20	0.00	0.00	0.20	0.99	0.99	4.74
SSE	1.19	0.20	0.00	0.59	0.00	0.40	0.59	0.59	0.00	1.58	0.20	0.20	5.53
S	3.56	1.19	0.20	0.99	0.20	0.20	0.40	0.40	0.20	0.20	0.00	0.40	7.91
SSW	0.79	0.79	0.20	0.99	0.20	0.00	0.40	0.40	0.00	0.20	0.20	0.00	4.15
SW	0.40	0.79	0.40	0.00	0.40	0.40	0.20	0.20	0.00	0.00	0.20	0.99	3.95
WSW	0.00	0.20	0.00	0.40	0.20	0.00	0.59	0.20	0.00	0.20	0.20	0.40	2.37
W	0.40	0.20	0.00	0.20	0.20	0.59	0.59	0.59	0.40	0.00	0.20	0.20	3.56
WNW	0.40	0.00	0.00	0.00	0.59	0.40	0.40	0.40	0.00	1.19	0.20	0.20	3.75
NW	1.19	0.00	0.20	0.59	0.40	0.59	0.59	0.00	0.40	1.98	0.99	0.59	7.51
NNW	0.59	0.79	0.20	0.40	0.00	0.79	0.20	0.59	0.59	0.79	0.99	0.99	6.92

WLS COL 2.3-2

TABLE 2.3-259 (Sheet 2 of 2)
PERCENT OF TOTAL OBSERVATIONS (BY MONTH) OF PRECIPITATION AND WIND DIRECTION
LEE NUCLEAR SITE

Sector	January	February	March	April	May	June	July	August	September	October	November	December	Total
Total	13.64	7.31	4.15	6.32	5.14	10.08	5.73	8.70	5.53	10.08	10.47	12.85	100

NOTES:

1. Instances of "trace" precipitation were counted as precipitation.
2. Data from Lee Nuclear Site Data, 12/1/2005 - 11/30/2006.
3. Hours of missing wind direction or missing precipitation were not included in the frequency calculation.
4. Calm values classified by precipitation occurrences under variable wind direction conditions.

WLS COL 2.3-2

TABLE 2.3-260
 RAINFALL FREQUENCY DISTRIBUTION
 LEE NUCLEAR STATION SITE
 NUMBER OF HOURS PER MONTH

Rainfall (inch/hr)	Jan	Feb	Mar	Apr	May	Jun	Jul	Aug	Sep	Oct	Nov	Dec
0.01-0.019	23	16	8	8	7	15	7	14	8	16	8	10
0.02-.099	37	19	10	15	10	19	13	21	9	22	27	37
0.10-0.249	6	2	4	7	9	13	6	4	7	11	16	19
0.25-0.499	2	0	0	2	3	2	2	3	3	2	1	1
0.50-0.99	1	0	0	0	0	2	0	2	1	0	1	0
1.00-1.99	0	0	0	0	0	0	1	0	0	0	0	0
2.0 & over	0	0	0	0	0	0	0	0	0	0	0	0
Total	69.0	37.0	22.0	32.0	29.0	51.0	29.0	44.0	28.0	51.0	53.0	67.0

NOTES:

1. Lee Nuclear Station site data, 12/1/2005 - 11/30/2006.

WLS COL 2.3-2

TABLE 2.3-261
PRECIPITATION DATA (INCHES OF RAIN)
LEE NUCLEAR STATION SITE

Month	Monthly Hours	Max 24 hour Rain (in)	Number of days with rainfall >0 in
Jan	69	1.35	15
Feb	37	0.29	10
Mar	22	0.97	8
Apr	32	0.92	11
May	29	1.14	9
Jun	51	1.38	13
Jul	29	2.55	9
Aug	44	1.38	11
Sep	28	2.68	10
Oct	51	1.80	13
Nov	53	1.87	7
Dec	67	1.75	8
Annual	512	2.68	124

NOTES:

1. Lee Nuclear Station site data, 12/1/2005 - 11/30/2006.

TABLE 2.3-262 (Sheet 1 of 4)
 NINETY-NINE ISLANDS, SOUTH CAROLINA
 MONTHLY TOTAL SNOWFALL (INCHES)
 1947 - 2006

YEAR(S)	JUL	AUG	SEP	OCT	NOV	DEC	JAN	FEB	MAR	APR	MAY	JUN	Annual
1947-48	0.00z	0.00z	0.00z	0.00z	0.00z	0.00z	0.00z	0.00z	0.00z	0.00z	0.00z	0.00z	0.00
1948-49	0.00z	0.00	0.00	0.00	0.00	0.00	0.00	0.00	0.00	0.00	0.00	0.00	0.00
1949-50	0.00	0.00	0.00	0.00	0.00	0.00	0.00	0.00	0.00	0.00	0.00	0.00	0.00
1950-51	0.00	0.00	0.00	0.00	0.00	0.00z	0.00	0.00	0.00z	0.00z	0.00	0.00	0.00
1951-52	0.00	0.00	0.00	0.00	0.00z	0.00z	0.00	0.00z	0.00z	0.00z	0.00z	0.00z	0.00
1952-53	0.00z	0.00z	0.00z	0.00z	0.00z	0.00z	0.00z	0.00z	0.00z	0.00z	0.00z	0.00z	0.00
1953-54	0.00z	0.00z	0.00z	0.00z	0.00z	0.00z	0.00z	0.00z	0.00z	0.00z	0.00z	0.00z	0.00
1954-55	0.00z	0.00z	0.00z	0.00z	0.00z	0.00z	0.00z	0.00z	0.00z	0.00z	0.00z	0.00z	0.00
1955-56	0.00z	0.00z	0.00z	0.00z	0.00z	0.00z	0.00z	0.00z	0.00z	0.00z	0.00z	0.00z	0.00
1956-57	0.00z	0.00z	0.00z	0.00	0.00z	0.00	0.00z	0.00z	0.00z	0.00z	0.00z	0.00	0.00
1957-58	0.00	0.00z	0.00z	0.00z	0.00z	0.00z	0.00z	0.00z	0.00z	0.00z	0.00z	0.00z	0.00
1958-59	0.00z	0.00	0.00	0.00	0.00	0.00z	0.00	0.00z	0.00z	0.00z	0.00	0.00z	0.00
1959-60	0.00z	0.00	0.00	0.00	0.00	0.00	0.00z	0.00z	0.00z	0.00z	0.00z	0.00z	0.00
1960-61	0.00z	0.00z	0.00z	0.00	0.00	0.00	1.00	0.50	0.00	0.00	0.00	0.00	1.50
1961-62	0.00	0.00	0.00	0.00	0.00	0.00	0.00z	0.00a	1.00	0.00	0.00	0.00	1.00
1962-63	0.00	0.00	0.00	0.00	0.00	0.00	0.00	0.00z	0.00	0.00a	0.00	0.00	0.00
1963-64	0.00	0.00a	0.00	0.00	0.00	2.50	1.50	0.00	0.00	0.00	0.00	0.00	4.00
1964-65	0.00	0.00	0.00	0.00	0.00	0.00z	8.50	2.00	0.00	0.00	0.00	0.00	10.50
1965-66	0.00	0.00	0.00	0.00	0.00	0.00	9.00	1.00	0.00	0.00	0.00	0.00	10.00
1966-67	0.00	0.00	0.00	0.00	0.00	0.00	0.00	2.00	0.00	0.00	0.00	0.00	2.00

TABLE 2.3-262 (Sheet 2 of 4)
 NINETY-NINE ISLANDS, SOUTH CAROLINA
 MONTHLY TOTAL SNOWFALL (INCHES)
 1947 - 2006

YEAR(S)	JUL	AUG	SEP	OCT	NOV	DEC	JAN	FEB	MAR	APR	MAY	JUN	Annual
1967-68	0.00	0.00	0.00	0.00	0.00	0.00	3.00	2.00	0.00	0.00	0.00	0.00	5.00
1968-69	0.00	0.00	0.00	0.00	0.00c	0.00	0.00	12.30	5.00	0.00	0.00z	0.00	17.30
1969-70	0.00	0.00	0.00	0.00	0.00	0.00	1.70	0.00	0.00	0.00	0.00	0.00	1.70
1970-71	0.00	0.00	0.00	0.00	0.00	3.00	0.00	0.00a	6.30	0.00	0.00	0.00	9.30
1971-72	0.00	0.00	0.00	0.00	0.00	12.00	0.00	1.00	2.00	0.00	0.00	0.00	15.00
1972-73	0.00	0.00	0.00	0.00	0.00	0.00	3.80	2.00	0.00	0.00	0.00	0.00	5.80
1973-74	0.00	0.00	0.00	0.00	0.00	0.00a	0.00	0.00	0.00	0.00	0.00	0.00	0.00
1974-75	0.00	0.00	0.00	0.00	0.00	0.00	0.00	0.00	0.00	0.00	0.00	0.00	0.00
1975-76	0.00	0.00	0.00	0.00	0.00	0.00	0.00	0.00	0.00	0.00	0.00	0.00	0.00
1976-77	0.00	0.00	0.00	0.00	0.00	0.00	5.50	0.00	0.00	0.00	0.00	0.00	5.50
1977-78	0.00	0.00	0.00	0.00	0.00	0.00	0.00	0.00	2.50	0.00	0.00	0.00	2.50
1978-79	0.00	0.00	0.00	0.00	0.00	0.00	0.00	14.00	0.00	0.00	0.00	0.00	14.00
1979-80	0.00	0.00	0.00	0.00	0.00	0.00	0.00	0.00b	0.00b	0.00	0.00	0.00	0.00
1980-81	0.00	0.00	0.00	0.00	0.00	0.00	0.00a	0.00	0.00	0.00	0.00	0.00	0.00
1981-82	0.00	0.00	0.00	0.00	0.00	0.00	5.20	0.00a	0.00	0.00	0.00	0.00	5.20
1982-83	0.00	0.00	0.00	0.00	0.00	0.00	0.00a	0.00a	6.00	0.00	0.00	0.00	6.00
1983-84	0.00	0.00	0.00	0.00	0.00	0.00	0.00	4.00	0.00	0.00	0.00	0.00	4.00
1984-85	0.00	0.00	0.00	0.00	0.00	0.00	0.00z	0.00	0.00	0.00	0.00	0.00	0.00
1985-86	0.00	0.00	0.00	0.00	0.00	0.00	0.00	0.00a	0.00	0.00	0.00	0.00	0.00
1986-87	0.00	0.00	0.00	0.00	0.00	0.00	0.00d	0.00	0.00	0.00	0.00	0.00	0.00

TABLE 2.3-262 (Sheet 3 of 4)
 NINETY-NINE ISLANDS, SOUTH CAROLINA
 MONTHLY TOTAL SNOWFALL (INCHES)
 1947 - 2006

YEAR(S)	JUL	AUG	SEP	OCT	NOV	DEC	JAN	FEB	MAR	APR	MAY	JUN	Annual
1987-88	0.00	0.00	0.00	0.00	0.00	0.00	13.00	0.00	0.00	0.00	0.00	0.00	13.00
1988-89	0.00	0.00	0.00	0.00	0.00	0.00	0.00	2.10	0.00	0.00	0.00	0.00	2.10
1989-90	0.00	0.00	0.00	0.00	0.00	0.00	0.00	0.00	0.00	0.00	0.00	0.00	0.00
1990-91	0.00	0.00	0.00	0.00	0.00	0.00	0.00	0.00	0.00	0.00	0.00	0.00	0.00
1991-92	0.00	0.00	0.00	0.00	0.00	0.00	0.00	0.00	0.00	0.00	0.00	0.00	0.00
1992-93	0.00	0.00	0.00	0.00	0.00	0.00	0.00	0.00b	2.00	0.00	0.00	0.00	2.00
1993-94	0.00	0.00	0.00	0.00	0.00	1.00	0.00a	0.00	0.00	0.00	0.00	0.00	1.00
1994-95	0.00	0.00	0.00	0.00	0.00	0.00	0.00	0.00	0.00	0.00	0.00	0.00	0.00
1995-96	0.00	0.00	0.00	0.00	0.00	0.00	0.00a	0.00	0.00	0.00	0.00	0.00	0.00
1996-97	0.00	0.00	0.00	0.00	0.00	0.00	0.00a	0.00a	0.00	0.00	0.00	0.00	0.00
1997-98	0.00	0.00	0.00	0.00	0.00	0.00	0.00	0.00	0.00	0.00	0.00	0.00	0.00
1998-99	0.00	0.00	0.00	0.00	0.00	0.00	0.00	0.00	0.00	0.00	0.00	0.00	0.00
1999-00	0.00	0.00	0.00	0.00	0.00	0.00	0.00	0.00	0.00	0.00	0.00	0.00	0.00
2000-01	0.00	0.00	0.00	0.00	0.00	0.00	0.00	0.00	0.00	0.00	0.00	0.00	0.00
2001-02	0.00	0.00	0.00	0.00	0.00	0.00	2.00	0.00	0.00	0.00	0.00	0.00	2.00
2002-03	0.00	0.00	0.00a	0.00	0.00	0.00	0.00	0.00a	0.00b	0.00a	0.00a	0.00	0.00
2003-04	0.00	0.00	0.00	0.00	0.00	0.00	0.00	8.00a	0.00	0.00	0.00	0.00	8.00
2004-05	0.00	0.00	0.00	0.00	0.00b	0.00	0.00a	0.00	0.00	0.00	0.00	0.00	0.00
2005-06	0.00	0.00	0.00	0.00	0.00	0.00	0.00	0.00	0.00	0.00	0.00	0.00	0.00

TABLE 2.3-262 (Sheet 4 of 4)
 NINETY-NINE ISLANDS, SOUTH CAROLINA
 MONTHLY TOTAL SNOWFALL (INCHES)
 1947 - 2006

YEAR(S)	JUL	AUG	SEP	OCT	NOV	DEC	JAN	FEB	MAR	APR	MAY	JUN	Annual
MEAN	0.00	0.00	0.00	0.00	0.00	0.38	1.11	1.06	0.52	0.00	0.00	0.00	2.88
S.D.	0.00	0.00	0.00	0.00	0.00	1.79	2.71	2.90	1.48	0.00	0.00	0.00	4.22
SKEW	0.00	0.00	0.00	0.00	0.00	5.89	2.86	3.44	3.02	0.00	0.00	0.00	1.53
MAX	0.00	0.00	0.00	0.00	0.00	12.00	13.00	14.00	6.30	0.00	0.00	0.00	15.00
MIN	0.00	0.00	0.00	0.00	0.00	0.00	0.00	0.00	0.00	0.00	0.00	0.00	0.00
NO YRS	49	51	51	53	51	49	49	48	48	48	49	50	41

*** Note *** Provisional Data *** After Year/Month 2006/03

a = 1 day missing, b = 2 days missing, c = 3 days missing, etc.,

z = 26 or more days missing, A = Accumulations present

NOTES:

1. Long-term means based on columns; thus, the monthly row may not sum (or average) to the long-term annual value.
2. Maximum allowable number of missing days: 5
3. Individual months not used for annual or monthly statistics if more than 5 days are missing. Individual years not used for annual statistics if any month in that year has more than 5 days missing.
4. Data from Southeast Regional Climate Center, <http://cirrus.dnr.state.sc.us/cgi-bin/sercc/cliMAIN.pl?sc629>

WLS COL 2.3-1

TABLE 2.3-263
AVERAGE HOURS OF FOG AND HAZE AT GREENVILLE/SPARTANBURG, SOUTH CAROLINA

Month	Fog (hours/month)			Haze (hours/month)		
	Average	Maximum	Minimum	Average	Maximum	Minimum
Jan	6.8	21.2	0.3	0.3	2.0	0.0
Feb	4.5	10.5	0.0	0.9	2.7	0.0
Mar	2.4	5.3	0.0	0.8	2.8	0.0
Apr	2.5	5.2	0.0	0.4	0.9	0.0
May	0.9	4.9	0.0	2.9	8.0	0.0
Jun	0.9	2.2	0.0	5.8	14.5	1.4
Jul	1.2	2.4	0.1	10.1	20.1	0.9
Aug	1.3	3.7	0.0	7.5	24.4	2.1
Sep	2.1	5.7	0.0	4.2	14.6	0.0
Oct	2.5	6.1	0.0	3.0	13.4	0.0
Nov	6.7	11.6	1.4	1.0	3.9	0.0
Dec	6.3	10.8	2.2	0.1	0.8	0.0
Annual (hours/yr)	38.1	46.5	29.4	37.0	61.6	24.3

NOTES:

1. Data from Unedited Local Climatological Data, National Oceanic and Atmospheric Administration, U. S. Department of Commerce, Asheville, NC, Greenville/Spartanburg International Airport, Station No. 03870.
2. Period of Record - 9 years (1997 - 2005).

WLS COL 2.3-1

TABLE 2.3-264
INVERSION HEIGHTS AND STRENGTHS, GREENSBORO, NORTH CAROLINA
JANUARY, 1999 - 2005

January	Mornings with Inversions ¹	Average Morning Height ² (m)	Average Morning Strength ³ (0.1°C/m)	Afternoons with Inversions ¹	Average Afternoon Height ² (m)	Average Afternoon Strength ³ (0.1°C/m)
1999	7	632	0.435	9	899	0.301
2000	15	1069	0.181	7	1108	0.334
2001	10	774	0.349	3	938	0.101
2002	12	949	0.256	9	983	0.250
2003	10	961	0.299	4	1131	0.085
2004	12	654	0.443	9	1251	0.263
2005	1	820	0.467	3	1582	0.164
Total	67	864	0.315	44	1092	0.245

NOTES:

1. Inversion is defined as three or more NOAA weather balloon elevation readings showing consecutive increases in temperature with height below 3000 m.
2. Balloons were released each day at 0:00 Greenwich Mean Time (GMT) and 12:00 GMT. Height is defined as elevation in meters where temperature first increases and is averaged only over those days with inversions.
3. Strength is the maximum temperature gradient in tenths of a degree centigrade per meter within the inversion layer.
4. Data from: FSL/NCDC Radiosonde Data Archive, <http://raob.fsl.noaa.gov/>

WLS COL 2.3-1

TABLE 2.3-265
INVERSION HEIGHTS AND STRENGTHS, GREENSBORO, NORTH CAROLINA
FEBRUARY, 1999 - 2005

February	Mornings with Inversions ¹	Average Morning Height ² (m)	Average Morning Strength ³ (0.1°C/m)	Afternoons with Inversions ¹	Average Afternoon Height ² (m)	Average Afternoon Strength ³ (0.1°C/m)
1999	9	664	0.704	4	933	0.344
2000	8	955	0.228	7	1217	0.155
2001	7	1107	0.188	6	1787	0.390
2002	7	938	0.523	6	1529	0.225
2003	11	933	0.229	11	874	0.265
2004	14	1035	0.244	13	1146	0.252
2005	0			2	429	0.629
Total	56	941	0.341	49	1174	0.277

NOTES:

1. Inversion is defined as three or more NOAA weather balloon elevation readings showing consecutive increases in temperature with height below 3000 m.
2. Balloons were released each day at 0:00 Greenwich Mean Time (GMT) and 12:00 GMT. Height is defined as elevation in meters where temperature first increases and is averaged only over those days with inversions.
3. Strength is the maximum temperature gradient in tenths of a degree centigrade per meter within the inversion layer.
4. Data from: FSL/NCDC Radiosonde Data Archive, <http://raob.fsl.noaa.gov/>

WLS COL 2.3-1

TABLE 2.3-266
INVERSION HEIGHTS AND STRENGTHS, GREENSBORO, NORTH CAROLINA
MARCH, 1999 - 2005

March	Mornings with Inversions ¹	Average Morning Height ² (m)	Average Morning Strength ³ (0.1°C/m)	Afternoons with Inversions ¹	Average Afternoon Height ² (m)	Average Afternoon Strength ³ (0.1°C/m)
1999	5	943	0.290	3	1463	0.277
2000	7	883	0.245	2	1770	0.323
2001	2	1702	0.217	3	2019	0.234
2002	12	842	0.267	6	1281	0.146
2003	3	680	0.338	3	552	0.236
2004	11	1125	0.389	3	2324	0.299
2005	0			1	2891	1.636
Total	40	970	0.303	21	1580	0.300

NOTES:

1. Inversion is defined as three or more NOAA weather balloon elevation readings showing consecutive increases in temperature with height below 3000 m.
2. Balloons were released each day at 0:00 Greenwich Mean Time (GMT) and 12:00 GMT. Height is defined as elevation in meters where temperature first increases and is averaged only over those days with inversions.
3. Strength is the maximum temperature gradient in tenths of a degree centigrade per meter within the inversion layer.
4. Data from: FSL/NCDC Radiosonde Data Archive, <http://raob.fsl.noaa.gov/>

WLS COL 2.3-1

TABLE 2.3-267
INVERSION HEIGHTS AND STRENGTHS, GREENSBORO, NORTH CAROLINA
APRIL, 1999 - 2005

April	Mornings with Inversions ¹	Average Morning Height ² (m)	Average Morning Strength ³ (0.1°C/m)	Afternoons with Inversions ¹	Average Afternoon Height ² (m)	Average Afternoon Strength ³ (0.1°C/m)
1999	5	1299	0.321	0		
2000	7	568	0.398	0		
2001	2	1712	0.444	1	2372	0.103
2002	7	956	0.182	0		
2003	8	751	0.294	2	1300	0.302
2004	10	614	0.379	2	647	0.179
2005	1	760	0.162	0		
Total	40	837	0.322	5	1253	0.213

NOTES:

1. Inversion is defined as three or more NOAA weather balloon elevation readings showing consecutive increases in temperature with height below 3000 m.
2. Balloons were released each day at 0:00 Greenwich Mean Time (GMT) and 12:00 GMT. Height is defined as elevation in meters where temperature first increases and is averaged only over those days with inversions.
3. Strength is the maximum temperature gradient in tenths of a degree centigrade per meter within the inversion layer.
4. Data from: FSL/NCDC Radiosonde Data Archive, <http://raob.fsl.noaa.gov/>

WLS COL 2.3-1

TABLE 2.3-268
INVERSION HEIGHTS AND STRENGTHS, GREENSBORO, NORTH CAROLINA
MAY, 1999 – 2005

May	Mornings with Inversions ¹	Average Morning Height ² (m)	Average Morning Strength ³ (0.1°C/m)	Afternoons with Inversions ¹	Average Afternoon Height ² (m)	Average Afternoon Strength ³ (0.1°C/m)
1999	5	513	0.401	0		
2000	4	950	0.225	0		
2001	4	1290	0.175	0		
2002	3	627	0.196	2	1187	0.090
2003	1	1576	0.099	2	1248	0.175
2004	1	389	0.104	0		
2005	2	631	0.268	0		
Total	20	832	0.247	4	1217	0.132

1. Inversion is defined as three or more NOAA weather balloon elevation readings showing consecutive increases in temperature with height below 3000 m.
2. Balloons were released each day at 0:00 GTM and 12:00 GMT. Height is defined as elevation in meters where temperature first increases and is averaged only over those days with inversions.
3. Strength is the maximum temperature gradient in tenths of a degree centigrade per meter within the inversion layer.
4. Data from: FSL/NCDC Radiosonde Data Archive, <http://raob.fsl.noaa.gov/>

WLS COL 2.3-1

TABLE 2.3-269
INVERSION HEIGHTS AND STRENGTHS, GREENSBORO, NORTH CAROLINA
JUNE, 1999 – 2005

June	Mornings with Inversions ¹	Average Morning Height ² (m)	Average Morning Strength ³ (0.1°C/m)	Afternoons with Inversions ¹	Average Afternoon Height ² (m)	Average Afternoon Strength ³ (0.1°C/m)
1999	4	1479	0.284	0		
2000	1	277	0.667	0		
2001	2	2153	0.255	1	2403	0.667
2002	5	1008	0.456	0		
2003	2	1693	0.436	1	2038	0.211
2004	0			0		
2005	0			1	2548	0.277
Total	14	1352	0.390	3	2330	0.385

1. Inversion is defined as three or more NOAA weather balloon elevation readings showing consecutive increases in temperature with height below 3000 m.
2. Balloons were released each day at 0:00 GMT and 12:00 GMT. Height is defined as elevation in meters where temperature first increases and is averaged only over those days with inversions.
3. Strength is the maximum temperature gradient in tenths of a degree centigrade per meter within the inversion layer.
4. Data from: FSL/NCDC Radiosonde Data Archive, <http://raob.fsl.noaa.gov/>

WLS COL 2.3-1

TABLE 2.3-270
INVERSION HEIGHTS AND STRENGTHS, GREENSBORO, NORTH CAROLINA
JULY, 1999 - 2005

July	Mornings with Inversions ¹	Average Morning Height ² (m)	Average Morning Strength ³ (0.1°C/m)	Afternoons with Inversions ¹	Average Afternoon Height ² (m)	Average Afternoon Strength ³ (0.1°C/m)
1999	1	640	0.079	0		
2000	0			0		
2001	1	277	0.101	1	1896	0.238
2002	0			0		
2003	0			0		
2004	0			0		
2005	0			0		
Total	2	459	0.090	1	1896	0.238

1. Inversion is defined as three or more NOAA weather balloon elevation readings showing consecutive increases in temperature with height below 3000 m.
2. Balloons were released each day at 0:00 GMT and 12:00 GMT. Height is defined as elevation in meters where temperature first increases and is averaged only over those days with inversions.
3. Strength is the maximum temperature gradient in tenths of a degree centigrade per meter within the inversion layer.
4. Data from: FSL/NCDC Radiosonde Data Archive, <http://raob.fsl.noaa.gov/>

WLS COL 2.3-1

TABLE 2.3-271
INVERSION HEIGHTS AND STRENGTHS, GREENSBORO, NORTH CAROLINA
AUGUST, 1999 - 2005

August	Mornings with Inversions ¹	Average Morning Height ² (m)	Average Morning Strength ³ (0.1°C/m)	Afternoons with Inversions ¹	Average Afternoon Height ² (m)	Average Afternoon Strength ³ (0.1°C/m)
1999	3	661	0.371	0		
2000	3	829	0.461	2	2287	0.306
2001	2	1285	0.515	0		
2002	2	1340	0.188	0		
2003	1	277	0.329	0		
2004	2	1309	0.258	3	2420	0.303
2005	2	1429	0.630	1	1941	0.476
Total	15	1031	0.400	6	2296	0.333

1. Inversion is defined as three or more NOAA weather balloon elevation readings showing consecutive increases in temperature with height below 3000 m.
2. Balloons were released each day at 0:00 GMT and 12:00 GMT. Height is defined as elevation in meters where temperature first increases and is averaged only over those days with inversions.
3. Strength is the maximum temperature gradient in tenths of a degree centigrade per meter within the inversion layer.
4. Data from: FSL/NCDC Radiosonde Data Archive, <http://raob.fsl.noaa.gov/>

WLS COL 2.3-1

TABLE 2.3-272
INVERSION HEIGHTS AND STRENGTHS, GREENSBORO, NORTH CAROLINA
SEPTEMBER, 1999 - 2005

September	Mornings with Inversions ¹	Average Morning Height ² (m)	Average Morning Strength ³ (0.1°C/m)	Afternoons with Inversions ¹	Average Afternoon Height ² (m)	Average Afternoon Strength ³ (0.1°C/m)
1999	5	1022	0.427	4	2064	0.232
2000	8	1364	0.233	7	1569	0.279
2001	7	1877	0.318	4	1935	0.425
2002	3	1583	0.223	2	1586	0.105
2003	3	1631	0.217	1	2001	0.118
2004	13	1440	0.248	5	1414	0.272
2005	10	1469	0.387	6	2227	0.331
Total	49	1474	0.299	29	1813	0.285

1. Inversion is defined as three or more NOAA weather balloon elevation readings showing consecutive increases in temperature with height below 3000 m.
2. Balloons were released each day at 0:00 GMT and 12:00 GMT. Height is defined as elevation in meters where temperature first increases and is averaged only over those days with inversions.
3. Strength is the maximum temperature gradient in tenths of a degree centigrade per meter within the inversion layer.
4. Data from: FSL/NCDC Radiosonde Data Archive, <http://raob.fsl.noaa.gov/>

WLS COL 2.3-1

TABLE 2.3-273
INVERSION HEIGHTS AND STRENGTHS, GREENSBORO, NORTH CAROLINA
OCTOBER, 1999 - 2005

October	Mornings with Inversions ¹	Average Morning Height ² (m)	Average Morning Strength ³ (0.1°C/m)	Afternoons with Inversions ¹	Average Afternoon Height ² (m)	Average Afternoon Strength ³ (0.1°C/m)
1999	13	1122	0.364	9	1690	0.331
2000	4	596	0.696	1	2089	0.200
2001	9	1890	0.254	3	1925	0.319
2002	7	727	0.291	4	1654	0.215
2003	4	1500	0.338	4	1901	0.365
2004	3	1395	0.263	4	1202	0.311
2005	8	1248	0.358	5	1629	0.360
Total	48	1234	0.351	30	1675	0.317

1. Inversion is defined as three or more NOAA weather balloon elevation readings showing consecutive increases in temperature with height below 3000 m.
2. Balloons were released each day at 0:00 GMT and 12:00 GMT. Height is defined as elevation in meters where temperature first increases and is averaged only over those days with inversions.
3. Strength is the maximum temperature gradient in tenths of a degree centigrade per meter within the inversion layer.
4. Data from: FSL/NCDC Radiosonde Data Archive, <http://raob.fsl.noaa.gov/>

WLS COL 2.3-1

TABLE 2.3-274
INVERSION HEIGHTS AND STRENGTHS, GREENSBORO, NORTH CAROLINA
NOVEMBER, 1999 – 2005

November	Mornings with Inversions ¹	Average Morning Height ² (m)	Average Morning Strength ³ (0.1°C/m)	Afternoons with Inversions ¹	Average Afternoon Height ² (m)	Average Afternoon Strength ³ (0.1°C/m)
1999	5	1235	0.464	2	1109	0.177
2000	4	690	0.279	4	1287	0.300
2001	12	941	0.397	5	1987	0.228
2002	9	990	0.525	2	1320	0.198
2003	12	767	0.346	5	1211	0.409
2004	6	907	0.169	3	1185	0.501
2005	14	662	0.593	5	964	0.293
Total	62	856	0.426	26	1322	0.312

1. Inversion is defined as three or more NOAA weather balloon elevation readings showing consecutive increases in temperature with height below 3000 m.
2. Balloons were released each day at 0:00 GMT and 12:00 GMT. Height is defined as elevation in meters where temperature first increases and is averaged only over those days with inversions.
3. Strength is the maximum temperature gradient in tenths of a degree centigrade per meter within the inversion layer.
4. Data from: FSL/NCDC Radiosonde Data Archive, <http://raob.fsl.noaa.gov/>

WLS COL 2.3-1

TABLE 2.3-275
INVERSION HEIGHTS AND STRENGTHS, GREENSBORO, NORTH CAROLINA
DECEMBER, 1999 – 2005

December	Mornings with Inversions ¹	Average Morning Height ² (m)	Average Morning Strength ³ (0.1°C/m)	Afternoons with Inversions ¹	Average Afternoon Height ² (m)	Average Afternoon Strength ³ (0.1°C/m)
1999	18	748	0.723	6	1561	0.347
2000	15	873	0.272	14	1026	0.229
2001	11	1398	0.340	7	1035	0.225
2002	18	776	0.333	16	1030	0.273
2003	14	762	0.339	10	1354	0.278
2004	11	840	0.519	9	1566	0.318
2005	12	900	0.294	9	1099	0.233
Total	99	875	0.412	71	1197	0.267

1. Inversion is defined as three or more NOAA weather balloon elevation readings showing consecutive increases in temperature with height below 3000 m.
2. Balloons were released each day at 0:00 GMT and 12:00 GMT. Height is defined as elevation in meters where temperature first increases and is averaged only over those days with inversions.
3. Strength is the maximum temperature gradient in tenths of a degree centigrade per meter within the inversion layer.
4. Data from: FSL/NCDC Radiosonde Data Archive, <http://raob.fsl.noaa.gov/>

WLS COL 2.3-1

TABLE 2.3-276
INVERSION HEIGHTS AND STRENGTHS, GREENSBORO, NORTH CAROLINA
ANNUAL, 1999 – 2005

Annual	Mornings with Inversions ¹	Average Morning Height ² (m)	Average Morning Strength ³ (0.1°C/m)	Afternoons with Inversions ¹	Average Afternoon Height ² (m)	Average Afternoon Strength ³ (0.1°C/m)
1999	80	901	0.487	37	1386	0.304
2000	76	915	0.287	44	1295	0.255
2001	69	1325	0.311	34	1675	0.286
2002	85	907	0.328	47	1212	0.223
2003	69	926	0.305	43	1212	0.268
2004	83	981	0.339	51	1396	0.290
2005	50	1009	0.420	33	1491	0.348
Total	512	988	0.352	289	1366	0.279

1. Inversion is defined as three or more NOAA weather balloon elevation readings showing consecutive increases in temperature with height below 3000 m.
2. Balloons were released each day at 0:00 GMT and 12:00 GMT. Height is defined as elevation in meters where temperature first increases and is averaged only over those days with inversions.
3. Strength is the maximum temperature gradient in tenths of a degree centigrade per meter within the inversion layer.
4. Data from: FSL/NCDC Radiosonde Data Archive, <http://raob.fsl.noaa.gov/>

WLS COL 2.3-1

TABLE 2.3-277
MIXING HEIGHTS AT GREENSBORO, NORTH CAROLINA

Month	Morning (m)	Afternoon (m)
January	480	825
February	477	982
March	502	1310
April	489	1735
May	431	1578
June	445	1764
July	473	1629
August	495	1435
September	394	1384
October	342	1187
November	402	853
December	450	781
Annual	448	1289

NOTES:

1. Data is from the NCDC SCRAM Mixing Height Data collection for the period of 1984-1987 and 1990-1991 <http://www.epa.gov/scram001/surfacemetdata.htm#tn>

WLS COL 2.3-2

TABLE 2.3-278
 VISIBLE PLUME FREQUENCY OF OCCURRENCE BY SEASON
 (ALL WIND DIRECTIONS)

	Percent Frequency of Occurrence					
	100	80	60	40	20	1
Winter:						
length (m)	100	300	500	3,300	5,900	9,900
height (m)	60	160	200	1,200	1,400	1,600
radius (m)	30	50	65	320	540	1,200
Spring:						
length (m)	100	200	300	500	5,100	9,900
height (m)	60	150	170	200	1,400	1,600
radius (m)	30	45	50	65	470	900
Summer:						
length (m)	100	200	250	300	700	9,800
height (m)	60	150	170	190	350	1,600
radius (m)	30	40	45	50	85	880
Fall:						
length (m)	100	250	300	500	4,900	9,900
height (m)	60	150	170	220	1,400	1,600
radius (m)	30	45	50	70	420	1,200
Annual:						
length (m)	100	200	300	500	4,900	9,900
height (m)	60	150	180	230	1,400	1,600
radius (m)	30	45	50	70	435	1,200

Notes:

1. SACTI results based on: U. S. Department of Commerce, National Oceanic and Atmospheric Administration National Climatic Data Center (NCDC), "Integrated Surface Hourly", 2001-2005, Charlotte, NC.
2. Mixing height from George C. Holzworth, "Mixing Heights, Wind Speeds, and Potential for Urban Air Pollution Throughout the Contiguous United States", [Reference 219](#).

WLS COL 2.3-2

TABLE 2.3-279
 FREQUENCY OF PLUME SHADOWING BY SEASON
 (AVERAGE FOR ALL WIND DIRECTIONS)

	Percent Frequency of Occurrence				
	10%	5%	2%	1%	0.5%
Winter:					
downwind distance (m)	200	400	800	2,000	6,000
Spring:					
downwind distance (m)	200	400	600	1,400	5,400
Summer:					
downwind distance (m)	200	300	500	800	1,600
Fall:					
downwind distance (m)	200	300	500	1,000	2,400
Annual:					
downwind distance (m)	200	300	600	1,200	4,000

Notes:

1. SACTI results based on: U. S. Department of Commerce, National Oceanic and Atmospheric Administration National Climatic Data Center (NCDC), "Integrated Surface Hourly", 2001-2005, Charlotte, NC.
2. Mixing height from George C. Holzworth, "Mixing Heights, Wind Speeds, and Potential for Urban Air Pollution Throughout the Contiguous United States", [Reference 219](#).

WLS COL 2.3-2

TABLE 2.3-280 (Sheet 1 of 4)
 MAXIMUM SALT DRIFT DEPOSITION RATE (KG/KM²/MO)

Downwind Distance (m)	Summer Plume Headed																Avg.
	S	SSW	SW	WSW	W	WNW	NW	NNW	N	NNE	NE	ENE	E	ESE	SE	SSE	
100.	.00	.00	.00	.00	.00	.00	.00	.00	.00	.00	.00	.00	.00	.00	.00	.00	.00
200.	.33	.07	.10	.13	.16	.03	.12	.16	1.03	.58	.39	.13	.23	.29	.31	.20	.27
300.	.09	.02	.03	.05	.04	.01	.04	.06	.30	.21	.14	.05	.07	.11	.11	.07	.09
400.	.01	.00	.00	.00	.00	.00	.00	.01	.06	.01	.01	.01	.00	.02	.03	.01	.01
500.	.01	.00	.00	.00	.00	.00	.00	.01	.06	.01	.01	.01	.00	.02	.03	.01	.01
600.	.01	.00	.00	.00	.00	.00	.00	.01	.06	.02	.01	.01	.00	.02	.03	.01	.01
700.	.01	.00	.01	.01	.00	.00	.00	.01	.06	.02	.01	.01	.00	.02	.03	.01	.01
800.	.03	.00	.01	.01	.00	.01	.00	.02	.14	.03	.02	.01	.00	.05	.06	.01	.02
900.	.03	.00	.02	.01	.00	.01	.00	.03	.16	.04	.03	.01	.00	.07	.08	.01	.03
1000.	.03	.01	.02	.01	.01	.01	.00	.02	.14	.04	.03	.01	.00	.06	.08	.01	.03
1100.	.02	.01	.01	.01	.01	.00	.00	.01	.06	.03	.02	.00	.00	.03	.04	.00	.02
1200.	.02	.01	.01	.01	.01	.00	.00	.01	.06	.02	.02	.00	.00	.02	.03	.00	.01
1300.	.02	.01	.01	.01	.01	.00	.00	.01	.06	.03	.02	.00	.00	.02	.03	.00	.01
1400.	.02	.01	.01	.01	.01	.00	.00	.01	.06	.03	.02	.00	.00	.02	.03	.00	.01
1500.	.02	.01	.01	.01	.01	.00	.00	.01	.06	.03	.02	.00	.00	.02	.03	.00	.01
1600.	.01	.01	.01	.01	.00	.00	.00	.01	.05	.02	.01	.00	.00	.02	.03	.00	.01
1700.	.00	.01	.01	.01	.00	.00	.00	.00	.01	.01	.01	.00	.00	.01	.01	.00	.00
1800.	.00	.01	.01	.01	.00	.00	.00	.00	.01	.01	.01	.00	.00	.00	.00	.00	.00
1900.	.00	.01	.01	.01	.00	.00	.00	.00	.01	.01	.01	.00	.00	.00	.00	.00	.00
2000.	.00	.01	.01	.01	.00	.00	.00	.00	.01	.01	.01	.00	.00	.00	.00	.00	.00

WLS COL 2.3-2

TABLE 2.3-280 (Sheet 2 of 4)
 MAXIMUM SALT DRIFT DEPOSITION RATE (kg/km²/mo)

Downwind Distance (m)	Fall Plume Headed																Avg.
	S	SSW	SW	WSW	W	WNW	NW	NNW	N	NNE	NE	ENE	E	ESE	SE	SSE	
100.	.00	.00	.00	.00	.00	.00	.00	.00	.00	.00	.00	.00	.00	.00	.00	.00	.00
200.	.48	.11	.13	.13	.23	.15	.08	.27	.55	.46	.25	.04	.16	.25	.39	.23	.24
300.	.14	.04	.05	.05	.07	.06	.03	.10	.18	.18	.10	.01	.05	.10	.15	.09	.09
400.	.03	.00	.00	.01	.01	.01	.01	.04	.06	.03	.01	.01	.00	.05	.08	.04	.02
500.	.03	.00	.00	.01	.01	.01	.01	.04	.06	.03	.01	.01	.00	.06	.08	.04	.03
600.	.03	.00	.00	.01	.01	.01	.01	.04	.06	.03	.01	.01	.00	.06	.08	.04	.03
700.	.03	.01	.01	.01	.01	.01	.01	.04	.07	.03	.01	.01	.00	.06	.08	.04	.03
800.	.06	.01	.01	.01	.02	.01	.03	.09	.15	.04	.01	.02	.01	.13	.18	.10	.05
900.	.07	.01	.01	.01	.02	.02	.04	.14	.18	.06	.01	.03	.01	.19	.26	.14	.07
1000.	.05	.01	.01	.01	.01	.01	.04	.13	.15	.04	.00	.03	.01	.18	.24	.13	.07
1100.	.03	.02	.01	.01	.01	.01	.02	.06	.06	.02	.00	.01	.00	.09	.12	.06	.03
1200.	.03	.02	.01	.01	.01	.00	.02	.05	.06	.02	.01	.01	.00	.07	.09	.05	.03
1300.	.03	.02	.01	.01	.01	.00	.02	.05	.06	.02	.01	.01	.00	.07	.09	.05	.03
1400.	.03	.02	.01	.01	.01	.00	.02	.05	.06	.02	.01	.01	.00	.07	.09	.05	.03
1500.	.03	.02	.01	.01	.01	.00	.02	.05	.06	.02	.01	.01	.00	.07	.09	.05	.03
1600.	.02	.01	.01	.01	.01	.00	.02	.05	.06	.02	.00	.01	.00	.07	.09	.05	.03
1700.	.01	.01	.01	.01	.00	.00	.00	.02	.01	.01	.00	.00	.00	.02	.03	.02	.01
1800.	.01	.01	.01	.01	.00	.00	.00	.00	.01	.01	.00	.00	.00	.00	.00	.00	.00
1900.	.01	.01	.01	.01	.00	.00	.00	.00	.01	.01	.00	.00	.00	.00	.00	.00	.00
2000.	.01	.01	.01	.01	.00	.00	.00	.00	.01	.01	.00	.00	.00	.00	.00	.00	.00

WLS COL 2.3-2

TABLE 2.3-280 (Sheet 3 of 4)
 MAXIMUM SALT DRIFT DEPOSITION RATE (kg/km²/mo)

Downwind Distance	Winter Plume Headed																Avg.
	S	SSW	SW	WSW	W	WNW	NW	NNW	N	NNE	NE	ENE	E	ESE	SE	SSE	
100.	.00	.00	.00	.00	.00	.00	.00	.00	.00	.00	.00	.00	.00	.00	.00	.00	.00
200.	.22	.07	.03	.04	.06	.08	.13	.29	.45	.46	.10	.08	.12	.23	.23	.13	.17
300.	.07	.03	.01	.02	.02	.03	.05	.11	.14	.17	.04	.03	.03	.08	.08	.05	.06
400.	.02	.01	.00	.00	.00	.00	.01	.02	.06	.03	.01	.01	.02	.02	.02	.03	.02
500.	.02	.01	.00	.00	.00	.00	.01	.02	.06	.03	.01	.01	.02	.02	.03	.03	.02
600.	.02	.01	.00	.00	.00	.00	.01	.02	.05	.03	.01	.01	.02	.02	.03	.03	.02
700.	.02	.01	.00	.00	.00	.00	.01	.02	.06	.03	.01	.01	.02	.02	.03	.03	.02
800.	.04	.01	.00	.00	.01	.00	.01	.04	.13	.05	.02	.03	.05	.05	.06	.06	.04
900.	.04	.02	.01	.01	.01	.00	.01	.06	.16	.08	.03	.05	.06	.08	.09	.09	.05
1000.	.03	.02	.01	.01	.01	.00	.01	.05	.13	.07	.04	.05	.06	.07	.09	.08	.05
1100.	.01	.01	.01	.01	.01	.00	.00	.03	.06	.05	.02	.03	.02	.04	.04	.04	.02
1200.	.01	.02	.01	.01	.01	.00	.00	.02	.06	.05	.02	.02	.03	.03	.03	.03	.02
1300.	.02	.02	.01	.01	.01	.00	.00	.02	.06	.05	.02	.02	.03	.03	.03	.03	.02
1400.	.02	.02	.01	.01	.01	.00	.00	.02	.06	.05	.02	.02	.03	.03	.03	.03	.02
1500.	.02	.02	.01	.01	.01	.00	.00	.02	.06	.05	.02	.02	.03	.03	.04	.03	.02
1600.	.02	.02	.01	.01	.01	.00	.00	.02	.05	.05	.02	.02	.02	.03	.04	.03	.02
1700.	.01	.01	.01	.01	.00	.00	.00	.01	.01	.03	.01	.01	.00	.01	.01	.01	.01
1800.	.01	.01	.01	.01	.00	.00	.00	.00	.01	.02	.01	.01	.00	.00	.00	.00	.01
1900.	.01	.01	.01	.01	.00	.00	.00	.00	.01	.02	.01	.01	.00	.00	.00	.00	.01
2000.	.01	.01	.01	.01	.00	.00	.00	.00	.01	.02	.01	.01	.00	.00	.00	.00	.01

WLS COL 2.3-2

TABLE 2.3-280 (Sheet 4 of 4)
 MAXIMUM SALT DRIFT DEPOSITION RATE (kg/km²/mo)

Downwind Distance (m)	Spring Plume Headed																Avg.
	S	SSW	SW	WSW	W	WNW	NW	NNW	N	NNE	NE	ENE	E	ESE	SE	SSE	
100.	.00	.00	.00	.00	.00	.00	.00	.00	.00	.00	.00	.00	.00	.00	.00	.00	.00
200.	.15	.06	.07	.06	.09	.05	.06	.22	.79	.46	.13	.06	.11	.25	.12	.16	.18
300.	.04	.02	.02	.02	.03	.02	.02	.08	.23	.17	.05	.02	.03	.09	.04	.06	.06
400.	.03	.00	.01	.01	.00	.00	.00	.01	.04	.01	.01	.00	.00	.02	.01	.01	.01
500.	.03	.00	.01	.01	.00	.00	.00	.01	.03	.01	.01	.00	.00	.02	.01	.01	.01
600.	.03	.00	.01	.01	.00	.00	.00	.01	.03	.01	.01	.00	.00	.02	.01	.01	.01
700.	.03	.01	.01	.01	.00	.00	.00	.01	.04	.02	.01	.00	.00	.02	.01	.01	.01
800.	.08	.01	.02	.01	.01	.00	.00	.01	.08	.03	.02	.01	.00	.03	.01	.02	.02
900.	.10	.01	.03	.02	.01	.00	.00	.02	.09	.04	.02	.01	.00	.04	.02	.03	.03
1000.	.09	.01	.03	.02	.01	.00	.00	.02	.07	.04	.02	.01	.00	.04	.02	.03	.02
1100.	.04	.01	.02	.01	.00	.00	.00	.01	.03	.03	.01	.01	.00	.02	.01	.01	.01
1200.	.04	.01	.02	.01	.01	.00	.00	.01	.04	.03	.01	.01	.00	.01	.01	.01	.01
1300.	.04	.01	.02	.01	.01	.00	.00	.01	.04	.03	.02	.01	.00	.01	.01	.01	.01
1400.	.04	.01	.02	.01	.01	.00	.00	.01	.04	.03	.02	.01	.00	.01	.01	.01	.01
1500.	.04	.01	.02	.01	.01	.00	.00	.01	.04	.03	.02	.01	.00	.01	.01	.01	.01
1600.	.03	.01	.02	.01	.00	.00	.00	.01	.03	.02	.01	.01	.00	.01	.01	.01	.01
1700.	.00	.01	.01	.01	.00	.00	.00	.00	.01	.02	.01	.00	.00	.01	.00	.00	.01
1800.	.00	.01	.01	.01	.00	.00	.00	.00	.01	.01	.01	.00	.00	.00	.00	.00	.00
1900.	.00	.01	.01	.01	.00	.00	.00	.00	.01	.01	.01	.00	.00	.00	.00	.00	.00
2000.	.00	.01	.01	.01	.00	.00	.00	.00	.01	.01	.01	.00	.00	.00	.00	.00	.00

Notes:

1. Shaded Values indicate on-site locations
2. SACTI modeling based on surface meteorological data from CLT, U. S. Department of Commerce, National Oceanic and Atmospheric Administration National Climatic Data Center (NCDC), "Integrated Surface Hourly", 2001-2005, Charlotte, NC.
3. Mixing height from George C. Holzworth, "Mixing Heights, Wind Speeds, and Potential for Urban Air Pollution Throughout the Contiguous United States", [Reference 219](#).

WLS COL 2.3-3

TABLE 2.3-281 (Sheet 1 of 3)
 METEOROLOGICAL TOWER INSTRUMENTATION
 FOR MET TOWERS 1 & 2 AND THE PERMANENT MET TOWER

Meteorological Variable	Range	Units	Accuracy	Resolution	Basis	Sensor Description	Sensor Height (meters)
Wind Speed, scalar (10 & 60m)	0 to 60	mph	± 0.5 or 5% of observed wind speed; starting threshold < 1 mph	0.1	NRC Regulatory Guide 1.23	Cup Anemometer	10 & 60 ^{(a)(b)} 10 & 55 ^(c)
Wind Direction, scalar (10 & 60m)	0 to 360	(degrees from True North)	± 5	1	NRC Regulatory Guide 1.23	Vane (resolver phase displacement)	10 & 60 ^{(a)(b)} 10 & 55 ^(c)
Sigma-Theta	0 to 100	(degrees from True North)	± 5	1	ANSI/ANS 3.11-2005	Vane (resolver phase displacement)	10 & 60 ^{(a)(b)} 10 & 55 ^(c)
Dry Bulb Temperature ^(d) (10 & 60m)	-20 to +40	Celsius	± 0.5	0.1	NRC Regulatory Guide 1.23	Platinum Wire Resistance Detector (RTD) with aspirated radiation shield	10 & 60 ^{(a)(b)} 10 & 55 ^(c)
Delta-T ^(d) (60m - 10m)	Calculated ^(d)	Celsius	± 0.1	0.01	NRC Regulatory Guide 1.23	Platinum Wire Resistance Detector (RTD) with aspirated radiation shield	10 & 60 ^{(a)(b)} 10 & 55 ^(c)

WLS COL 2.3-3

TABLE 2.3-281 (Sheet 2 of 3)
 METEOROLOGICAL TOWER INSTRUMENTATION
 FOR MET TOWERS 1 & 2 AND THE PERMANENT MET TOWER

Meteorological Variable	Range	Units	Accuracy	Resolution	Basis	Sensor Description	Sensor Height (meters)
Surface Temperature ^(e) (2m)	-20 to +40	Celsius	± 0.5	0.1	NRC Regulatory Guide 1.23	Platinum Wire Resistance Detector (RTD) with aspirated radiation shield	2
Dewpoint Temperature (10m)	-50 to +50	Celsius	± 1.5	0.1	NRC Regulatory Guide 1.23	Chilled Mirror with imbedded RTD in aspirated assembly	10
Precipitation, total	---	Inches	± 10%	0.01	NRC Regulatory Guide 1.23	Tipping bucket rain gauge	1
Station Pressure ^(e)	880 to 1085	millibars	± 3 or 0.25%	0.1	ANSI/ANS 3.11-2005	Static Inlet Point	2
Incoming Solar Radiation (shortwave), total ^(e)	0 to 1400	watts/m ²	± 10 or 5%	1	ANSI/ANS 3.11-2005	Black and White Pyranometer	1
Outgoing Longwave Radiation (upwelling from ground), total ^(e)	0 to 700	watts/m ²	± 10 or 5%	1	ANSI/ANS 3.11-2005	Precision Infrared Radiometer	1

WLS COL 2.3-3

TABLE 2.3-281 (Sheet 3 of 3)
 METEOROLOGICAL TOWER INSTRUMENTATION
 FOR MET TOWERS 1 & 2 AND THE PERMANENT MET TOWER

Meteorological Variable	Range	Units	Accuracy	Resolution	Basis	Sensor Description	Sensor Height (meters)
Time ^(f)	0000 to 2359	minutes	± 5	1	NRC Regulatory Guide 1.23	---	---
Datalogger Sampling Rate	---	---	At least 5 seconds	---	NRC Regulatory Guide 1.23	---	---

- a) This value applies to Tower 2. Tower 2 data has been used for air dispersion modeling and site characterization in the ER and FSAR, and most representative of the site. The equipment was operational on December 1, 2005.
- b) This value applies to the Permanent MET Tower.
- c) This value applies to Tower 1 only. This tower was decommissioned in May 2011.
- d) Delta temperature between the 60m and 10m levels is used in stability class determination. Delta-T is calculated by datalogger from upper and lower temperature sensor output (i.e., $T_{\text{upper}} - T_{\text{lower}}$). Although the range of measureable vertical temperature difference is constrained only by temperature sensor range limitations, a range of -4 to +8 degree Celsius is applied in calibration procedure bases for demonstrating compliance with the ± 0.1 °C accuracy requirement for Delta-T.
- e) Optional measurement variable only.
- f) The 1-minute readings are averaged into 1-hour averages on Tower 2 during the pre-construction/pre-operational phase. During the operational phase, the 1-minute readings will be compiled into 15-minute averages and 1-hour averages for real-time display in emergency response facilities from the Permanent MET Tower. Hourly averaged data is verified and archived.

WLS COL 2.3-4

TABLE 2.3-282 (Sheet 1 of 2)
 MINIMUM EXCLUSION AREA BOUNDARY (EAB) DISTANCES
 AND SITE BOUNDARY DISTANCES
 [FROM INNER 448 FT (137 M) RADIUS CIRCLE
 ENCOMPASSING ALL SITE RELEASE POINTS]

Direction	EAB Distance (ft)	EAB Distance (m)	Site Boundary Distance (ft)	Site Boundary Distance (m)
UNIT 1				
S	4593	1400	4593	1400
SSW	4593	1400	4593	1400
SW	5147	1569	5145	1568
WSW	5361	1634	5361	1634
W	3814	1163	3816	1163
WNW	3814	1163	3266	995
NW	3973	1211	1401	427
NNW	3070	936	1401	427
N	3070	936	1647	502
NNE	3190	972	2012	613
NE	3385	1032	2076	633
ENE	4153	1266	2645	806
E	5171	1576	2747	837
ESE	5084	1550	2973	906
SE	4625	1410	4352	1326
SSE	4625	1410	4626	1410

WLS COL 2.3-4

TABLE 2.3-282 (Sheet 2 of 2)
 MINIMUM EXCLUSION AREA BOUNDARY (EAB) DISTANCES
 AND SITE BOUNDARY DISTANCES
 [FROM INNER 448 FT (137 M) RADIUS CIRCLE
 ENCOMPASSING ALL SITE RELEASE POINTS]

Direction	EAB Distance (ft)	EAB Distance (m)	Site Boundary Distance (ft)	Site Boundary Distance (m)
UNIT 2				
S	4847	1477	4847	1477
SSW	4847	1477	4847	1477
SW	5201	1585	5203	1586
WSW	5876	1791	5876	1791
W	4497	1371	4499	1371
WNW	4497	1371	1752	534
NW	3135	956	1752	534
NNW	3130	954	1729	527
N	2914	888	1723	525
NNE	2914	888	1723	525
NE	3159	963	1956	596
ENE	3668	1118	1948	594
E	4379	1335	1948	594
ESE	5116	1559	2095	639
SE	4295	1309	3104	946
SSE	4295	1309	4295	1309

NOTE:

1. Exclusion Area Boundary (EAB) and Site Boundary for Lee Nuclear Station are shown in FSAR [Figures 2.1-209A](#) and [2.1-209B](#).
2. In accordance with Regulatory Guide 1.145, the distance to the EAB or Site Boundary is the closest distance within a 45-degree section centered on the compass direction of interest.
3. Site Boundary and EAB are co-located in the S, SSE, SSW, SW, WSW, and W directions.

WLS COL 2.3-4

TABLE 2.3-283 (Sheet 1 of 2)
LEE NUCLEAR STATION OFFSITE ATMOSPHERIC
DISPERSION
SHORT-TERM DIFFUSION ESTIMATES FOR ACCIDENTAL
RELEASES

Unit 1 Exclusion Area Boundary χ/Q Values (sec/m^3)^(a)

Time Period	Direction Dependent χ/Q		Direction Independent χ/Q
	0.5% Max Sector χ/Q ^(b)	Sector/Distance	5% Overall Site Limit
0-2 Hrs	3.32E-04	SE / 1410 m	2.64E-04

Unit 1 Low Population Zone χ/Q Values (sec/m^3)^(a)

Time Period	Direction Dependent χ/Q		Direction Independent χ/Q
	0.5% Max χ/Q ^(b)	Sector	5% Site Limit
0-8 Hrs	8.05E-05	SE	6.28E-05
8-24 Hrs	5.52E-05	SE	4.41E-05
1-4 Days	2.43E-05	SE	2.05E-05
4-30 Days	7.52E-06	SE	6.84E-06

Limiting Relative Dispersion Values^(a)
Lee Nuclear Station Unit 1 0.5% Maximum χ/Q Values (sec/m^3)

	0 – 2 Hrs	0 – 8 Hrs	8 – 24 Hrs	24 – 96 Hrs	96 – 720 Hrs
EAB (SE, 1410 m) ^(b)	3.32E-04	N/A	N/A	N/A	N/A
LPZ (SE, 3219 m) ^(b)	N/A	8.05E-05	5.52E-05	2.43E-05	7.52E-06

WLS COL 2.3-4

TABLE 2.3-283 (Sheet 2 of 2)
LEE NUCLEAR STATION OFFSITE ATMOSPHERIC
DISPERSION
SHORT-TERM DIFFUSION ESTIMATES FOR ACCIDENTAL
RELEASES

Unit 2 Exclusion Area Boundary χ/Q Values (sec/m^3)^(a)

Time Period	Direction Dependent χ/Q		Direction Independent χ/Q
	0.5% Max Sector χ/Q ^(b)	Sector/Distance	5% Overall Site Limit
0-2 Hrs	3.55E-04	SE / 1309 m	2.80E-04

Unit 2 Low Population Zone χ/Q Values (sec/m^3)^(a)

Time Period	Direction Dependent χ/Q		Direction Independent χ/Q
	0.5% Max χ/Q ^(b)	Sector	5% Site Limit
0-8 Hrs	8.05E-05	SE	6.28E-05
8-24 Hrs	5.52E-05	SE	4.41E-05
1-4 Days	2.43E-05	SE	2.05E-05
4-30 Days	7.52E-06	SE	6.84E-06

Limiting Relative Dispersion Values^(a)
Lee Nuclear Station Unit 2 0.5% Maximum χ/Q Values (sec/m^3)

	0 – 2 Hrs	0 – 8 Hrs	8 – 24 Hrs	24 – 96 Hrs	96 – 720 Hrs
EAB (SE, 1309 m) ^(b)	3.55E-04	N/A	N/A	N/A	N/A
LPZ (SE, 3219 m) ^(b)	N/A	8.05E-05	5.52E-05	2.43E-05	7.52E-06

a) Based on Lee Nuclear Station meteorological data for December 2005 - November 2007.

b) 0.5% χ/Q values represent the maximum for all sector-dependent values.

WLS COL 2.3-4

TABLE 2.3-284
LEE NUCLEAR STATION CONTROL ROOM χ/Q INPUT DATA

Control Room HVAC Intake (El. 19.9 m) Directions

Release Point	Direction to Source (degrees)
Plant Vent	2
PCS Air Diffuser	33
Fuel Building Blowout Panel	347
Radwaste Building Truck Staging Area Door	337
Steam Line Break Releases	75
PORV/Safety Valves	85
Condenser Air Removal Stack	175
Containment Shell	24

Annex Building Access (El. 1.5 m) Directions

Release Point	Direction to Source (degrees)
Plant Vent	6
PCS Air Diffuser	17
Fuel Building Blowout Panel	358
Radwaste Building Truck Staging Area Door	353
Steam Line Break Releases	21
PORV/Safety Valves	23
Condenser Air Removal Stack	57
Containment Shell	11

Notes:

- Directions are relative to True North at the Lee Nuclear Station site.

WLS COL 2.3-4

TABLE 2.3-285 (Sheet 1 of 2)
 CONTROL ROOM ATMOSPHERIC DISPERSION FACTORS (χ/Q)
 FOR ACCIDENT DOSE ANALYSIS (S/M³)

Control Room χ/Q at HVAC Intake^(a)

Time Interval	Plant Vent	PCS Air Diffuser	Fuel Bldg. Blowout Panel	Radwaste Bldg. Truck Staging Area Door
0 -2 hours	2.01E-03	1.78E-03	1.64E-03	1.17E-03
2 – 8 hours	1.52E-03	1.45E-03	1.20E-03	8.98E-04
8 – 24 hours	5.84E-04	6.36E-04	4.25E-04	3.30E-04
1 – 4 days	4.76E-04	5.26E-04	4.09E-04	2.93E-04
4 – 30 days	3.56E-04	3.36E-04	3.69E-04	2.59E-04
	Steam Line Break Releases	PORV & Safety Valves	Condenser Air Removal Stack	Containment Shell
0 -2 hours	1.25E-02	1.08E-02	1.59E-03	2.70E-03
2 – 8 hours	7.22E-03	5.62E-03	1.27E-03	1.79E-03
8 – 24 hours	2.95E-03	2.28E-03	5.10E-04	7.39E-04
1 – 4 days	2.40E-03	1.89E-03	3.86E-04	6.90E-04
4 – 30 days	1.79E-03	1.47E-03	2.82E-04	4.75E-04

WLS COL 2.3-4

TABLE 2.3-285 (Sheet 2 of 2)
 CONTROL ROOM ATMOSPHERIC DISPERSION FACTORS (χ/Q)
 FOR ACCIDENT DOSE ANALYSIS (S/M³)

Control Room χ/Q at Annex Building Access Door^(a)

Time Interval	Plant Vent	PCS Air Diffuser	Fuel Bldg. Blowout Panel	Radwaste Bldg. Truck Staging Area Door
0 - 2 hours	4.41E-04	4.83E-04	3.64E-04	3.46E-04
2 – 8 hours	3.47E-04	3.69E-04	2.65E-04	2.53E-04
8 – 24 hours	1.37E-04	1.61E-04	1.01E-04	9.78E-05
1 – 4 days	1.13E-04	1.32E-04	8.87E-05	8.71E-05
4 – 30 days	8.22E-05	9.13E-05	7.37E-05	7.57E-05

	Steam Line Break Releases	PORV & Safety Valves	Condenser Air Removal Stack	Containment Shell
0 - 2 hours	8.50E-04	8.71E-04	3.40E-03	5.01E-04
2 – 8 hours	6.44E-04	6.83E-04	2.91E-03	3.98E-04
8 – 24 hours	2.84E-04	2.96E-04	1.31E-03	1.59E-04
1 – 4 days	1.93E-04	2.05E-04	9.21E-04	1.36E-04
4 – 30 days	1.39E-04	1.46E-04	6.40E-04	9.76E-05

a) Based on Lee Nuclear Station meteorological data for December 2005 - November 2007.

WLS COL 2.3-5

TABLE 2.3-286
LEE NUCLEAR SITE OFFSITE RECEPTOR LOCATIONS

Sector	Garden	Cow (Milk/Meat)	House	Goat (Milk)
S	1592	5204	1597	-
SSW	1917	2091	1761	1690
SW	2011	1950	2011	-
WSW	3961	4497	3954	-
W	3543	3857	2887	4192
WNW	4110	4033	3553	6230
NW	3279	6163	3311	6163
NNW	2452	4722	2263	7013
N	2263	3648	1705	5506
NNE	2216	5464	2268	-
NE	1802	2364	1838	7886
ENE	1563	1956	1833	-
E	4460	4914	1985	-
ESE	4339	5002	3877	-
SE	6570	2650	1588	-
SSE	1606	1728	1752	2275

NOTES:

1. Distances, in meters, from the midpoint between Units 1 and 2 to the nearest receptor, of each type, for a given 22.5 degree sector.
2. 2007 and 2008 survey results.

WLS COL 2.3-5

TABLE 2.3-287 (Sheet 1 of 3)
 ANNUAL AVERAGE χ/Q (SEC/M³) FOR NORMAL RELEASES NO DECAY, UNDEPLETED
 (FOR EACH 22.5° SECTOR AT THE DISTANCES (MILES) SHOWN AT THE TOP)

Sector	0.250	0.500	.750	1.000	1.500	2.000	2.500	3.000	3.500	4.000	4.500
S	1.95E-05	5.77E-06	2.88E-06	1.82E-06	1.01E-06	6.71E-07	4.94E-07	3.93E-07	3.24E-07	2.74E-07	2.37E-07
SSW	1.78E-05	5.30E-06	2.67E-06	1.69E-06	9.35E-07	6.20E-07	4.55E-07	3.61E-07	2.97E-07	2.51E-07	2.16E-07
SW	1.45E-05	4.32E-06	2.19E-06	1.39E-06	7.72E-07	5.13E-07	3.76E-07	2.97E-07	2.44E-07	2.05E-07	1.76E-07
WSW	1.79E-05	5.29E-06	2.64E-06	1.67E-06	9.19E-07	6.10E-07	4.49E-07	3.57E-07	2.94E-07	2.49E-07	2.15E-07
W	1.84E-05	5.40E-06	2.68E-06	1.70E-06	9.37E-07	6.23E-07	4.58E-07	3.65E-07	3.02E-07	2.56E-07	2.21E-07
WNW	1.84E-05	5.40E-06	2.68E-06	1.69E-06	9.37E-07	6.25E-07	4.61E-07	3.68E-07	3.04E-07	2.58E-07	2.23E-07
NW	1.61E-05	4.78E-06	2.40E-06	1.52E-06	8.40E-07	5.58E-07	4.10E-07	3.25E-07	2.68E-07	2.26E-07	1.95E-07
NNW	1.18E-05	3.54E-06	1.82E-06	1.16E-06	6.47E-07	4.30E-07	3.15E-07	2.48E-07	2.02E-07	1.70E-07	1.45E-07
N	8.81E-06	2.69E-06	1.42E-06	9.22E-07	5.19E-07	3.45E-07	2.52E-07	1.96E-07	1.59E-07	1.32E-07	1.12E-07
NNE	6.57E-06	2.01E-06	1.07E-06	6.93E-07	3.85E-07	2.54E-07	1.85E-07	1.43E-07	1.15E-07	9.56E-08	8.11E-08
NE	5.02E-06	1.55E-06	8.22E-07	5.32E-07	2.94E-07	1.93E-07	1.40E-07	1.08E-07	8.64E-08	7.15E-08	6.05E-08
ENE	4.41E-06	1.34E-06	6.99E-07	4.48E-07	2.48E-07	1.63E-07	1.18E-07	9.19E-08	7.43E-08	6.17E-08	5.25E-08
E	5.86E-06	1.75E-06	8.86E-07	5.63E-07	3.12E-07	2.07E-07	1.52E-07	1.20E-07	9.80E-08	8.24E-08	7.08E-08
ESE	1.93E-05	5.65E-06	2.78E-06	1.75E-06	9.64E-07	6.41E-07	4.72E-07	3.78E-07	3.13E-07	2.66E-07	2.30E-07
SE	5.07E-05	1.48E-05	7.21E-06	4.52E-06	2.48E-06	1.65E-06	1.21E-06	9.75E-07	8.10E-07	6.90E-07	5.98E-07
SSE	2.59E-05	7.58E-06	3.75E-06	2.37E-06	1.31E-06	8.67E-07	6.39E-07	5.11E-07	4.23E-07	3.59E-07	3.10E-07

WLS COL 2.3-5

TABLE 2.3-287 (Sheet 2 of 3)
 ANNUAL AVERAGE χ/Q (SEC/M³) FOR NORMAL RELEASES NO DECAY, UNDEPLETED
 (FOR EACH 22.5° SECTOR AT THE DISTANCES (MILES) SHOWN AT THE TOP)

SECTOR	5.000	7.500	10.000	15.000	20.000	25.000	30.000	35.000	40.000	45.000	50.000
S	2.07E-07	1.25E-07	8.78E-08	5.33E-08	3.75E-08	2.86E-08	2.29E-08	1.90E-08	1.62E-08	1.41E-08	1.24E-08
SSW	1.89E-07	1.14E-07	7.94E-08	4.81E-08	3.37E-08	2.57E-08	2.06E-08	1.71E-08	1.45E-08	1.26E-08	1.11E-08
SW	1.54E-07	9.18E-08	6.38E-08	3.84E-08	2.68E-08	2.04E-08	1.63E-08	1.35E-08	1.14E-08	9.89E-09	8.70E-09
WSW	1.88E-07	1.14E-07	7.95E-08	4.83E-08	3.40E-08	2.59E-08	2.08E-08	1.73E-08	1.47E-08	1.28E-08	1.13E-08
W	1.94E-07	1.18E-07	8.26E-08	5.03E-08	3.55E-08	2.71E-08	2.18E-08	1.81E-08	1.54E-08	1.34E-08	1.18E-08
WNW	1.96E-07	1.19E-07	8.35E-08	5.09E-08	3.59E-08	2.74E-08	2.20E-08	1.83E-08	1.56E-08	1.36E-08	1.20E-08
NW	1.71E-07	1.03E-07	7.18E-08	4.35E-08	3.05E-08	2.33E-08	1.86E-08	1.55E-08	1.32E-08	1.14E-08	1.01E-08
NNW	1.27E-07	7.48E-08	5.16E-08	3.07E-08	2.14E-08	1.61E-08	1.29E-08	1.06E-08	8.98E-09	7.76E-09	6.81E-09
N	9.74E-08	5.62E-08	3.82E-08	2.22E-08	1.52E-08	1.13E-08	8.93E-09	7.31E-09	6.15E-09	5.28E-09	4.61E-09
NNE	7.01E-08	4.02E-08	2.71E-08	1.57E-08	1.07E-08	7.98E-09	6.28E-09	5.13E-09	4.31E-09	3.70E-09	3.23E-09
NE	5.22E-08	2.97E-08	2.00E-08	1.15E-08	7.84E-09	5.83E-09	4.58E-09	3.74E-09	3.14E-09	2.69E-09	2.35E-09
ENE	4.55E-08	2.63E-08	1.79E-08	1.04E-08	7.18E-09	5.39E-09	4.26E-09	3.50E-09	2.95E-09	2.54E-09	2.22E-09
E	6.18E-08	3.68E-08	2.55E-08	1.53E-08	1.07E-08	8.12E-09	6.49E-09	5.37E-09	4.56E-09	3.95E-09	3.47E-09
ESE	2.02E-07	1.23E-07	8.70E-08	5.33E-08	3.78E-08	2.89E-08	2.33E-08	1.94E-08	1.65E-08	1.44E-08	1.27E-08
SE	5.27E-07	3.24E-07	2.30E-07	1.42E-07	1.01E-07	7.73E-08	6.23E-08	5.20E-08	4.44E-08	3.87E-08	3.42E-08
SSE	2.73E-07	1.66E-07	1.17E-07	7.16E-08	5.06E-08	3.87E-08	3.11E-08	2.59E-08	2.21E-08	1.92E-08	1.70E-08

WLS COL 2.3-5

TABLE 2.3-287 (Sheet 3 of 3)
 ANNUAL AVERAGE χ/Q (SEC/M³) FOR NORMAL RELEASES NO DECAY, UNDEPLETED
 (FOR EACH 22.5° SECTOR AT THE DISTANCES (MILES) SHOWN AT THE TOP)

SECTOR	.5-1	1-2	2-3	3-4	4-5	5-10	10-20	20-30	30-40	40-50
S	3.05E-06	1.04E-06	5.01E-07	3.25E-07	2.37E-07	1.27E-07	5.40E-08	2.87E-08	1.91E-08	1.41E-08
SSW	2.82E-06	9.63E-07	4.61E-07	2.98E-07	2.16E-07	1.15E-07	4.87E-08	2.58E-08	1.71E-08	1.26E-08
SW	2.31E-06	7.94E-07	3.81E-07	2.44E-07	1.77E-07	9.32E-08	3.89E-08	2.04E-08	1.35E-08	9.90E-09
WSW	2.79E-06	9.48E-07	4.55E-07	2.95E-07	2.15E-07	1.15E-07	4.89E-08	2.60E-08	1.73E-08	1.28E-08
W	2.85E-06	9.65E-07	4.65E-07	3.02E-07	2.21E-07	1.19E-07	5.09E-08	2.72E-08	1.81E-08	1.34E-08
WNW	2.84E-06	9.65E-07	4.67E-07	3.05E-07	2.23E-07	1.20E-07	5.15E-08	2.75E-08	1.83E-08	1.36E-08
NW	2.54E-06	8.65E-07	4.15E-07	2.68E-07	1.95E-07	1.04E-07	4.40E-08	2.34E-08	1.55E-08	1.14E-08
NNW	1.91E-06	6.65E-07	3.19E-07	2.03E-07	1.46E-07	7.60E-08	3.12E-08	1.62E-08	1.06E-08	7.77E-09
N	1.48E-06	5.31E-07	2.55E-07	1.59E-07	1.13E-07	5.73E-08	2.26E-08	1.14E-08	7.33E-09	5.29E-09
NNE	1.11E-06	3.96E-07	1.87E-07	1.16E-07	8.13E-08	4.10E-08	1.60E-08	8.03E-09	5.15E-09	3.71E-09
NE	8.53E-07	3.02E-07	1.41E-07	8.68E-08	6.07E-08	3.04E-08	1.18E-08	5.86E-09	3.75E-09	2.70E-09
ENE	7.30E-07	2.54E-07	1.20E-07	7.45E-08	5.26E-08	2.68E-08	1.06E-08	5.42E-09	3.51E-09	2.55E-09
E	9.34E-07	3.21E-07	1.54E-07	9.83E-08	7.09E-08	3.74E-08	1.55E-08	8.16E-09	5.38E-09	3.95E-09
ESE	2.96E-06	9.95E-07	4.79E-07	3.13E-07	2.30E-07	1.25E-07	5.39E-08	2.90E-08	1.94E-08	1.44E-08
SE	7.69E-06	2.56E-06	1.23E-06	8.11E-07	5.99E-07	3.27E-07	1.43E-07	7.75E-08	5.20E-08	3.87E-08
SSE	3.99E-06	1.35E-06	6.48E-07	4.23E-07	3.11E-07	1.68E-07	7.24E-08	3.89E-08	2.60E-08	1.92E-08

WLS COL 2.3-5

TABLE 2.3-288 (Sheet 1 of 3)
 ANNUAL AVERAGE χ/Q (SEC/M³) FOR NORMAL RELEASES NO DECAY, DEPLETED
 (FOR EACH 22.5° SECTOR AT THE DISTANCES (MILES) SHOWN AT THE TOP)

Sector	0.250	0.500	.750	1.000	1.500	2.000	2.500	3.000	3.500	4.000	4.500
S	1.85E-05	5.27E-06	2.57E-06	1.60E-06	8.57E-07	5.56E-07	4.00E-07	3.12E-07	2.53E-07	2.10E-07	1.79E-07
SSW	1.69E-05	4.84E-06	2.38E-06	1.48E-06	7.94E-07	5.13E-07	3.69E-07	2.87E-07	2.32E-07	1.93E-07	1.63E-07
SW	1.37E-05	3.94E-06	1.95E-06	1.22E-06	6.56E-07	4.24E-07	3.05E-07	2.36E-07	1.90E-07	1.57E-07	1.33E-07
WSW	1.69E-05	4.83E-06	2.35E-06	1.46E-06	7.81E-07	5.05E-07	3.63E-07	2.83E-07	2.29E-07	1.91E-07	1.62E-07
W	1.74E-05	4.93E-06	2.39E-06	1.48E-06	7.95E-07	5.16E-07	3.71E-07	2.90E-07	2.36E-07	1.96E-07	1.67E-07
WNW	1.74E-05	4.93E-06	2.39E-06	1.48E-06	7.96E-07	5.17E-07	3.73E-07	2.92E-07	2.37E-07	1.98E-07	1.69E-07
NW	1.53E-05	4.36E-06	2.14E-06	1.33E-06	7.13E-07	4.62E-07	3.32E-07	2.58E-07	2.09E-07	1.74E-07	1.47E-07
NNW	1.12E-05	3.23E-06	1.62E-06	1.02E-06	5.50E-07	3.56E-07	2.55E-07	1.97E-07	1.58E-07	1.30E-07	1.10E-07
N	8.34E-06	2.45E-06	1.27E-06	8.07E-07	4.40E-07	2.86E-07	2.04E-07	1.56E-07	1.24E-07	1.01E-07	8.50E-08
NNE	6.22E-06	1.84E-06	9.53E-07	6.07E-07	3.27E-07	2.11E-07	1.50E-07	1.14E-07	8.99E-08	7.34E-08	6.13E-08
NE	4.75E-06	1.41E-06	7.32E-07	4.65E-07	2.49E-07	1.60E-07	1.13E-07	8.54E-08	6.74E-08	5.49E-08	4.58E-08
ENE	4.17E-06	1.23E-06	6.23E-07	3.92E-07	2.10E-07	1.35E-07	9.59E-08	7.30E-08	5.79E-08	4.74E-08	3.97E-08
E	5.54E-06	1.60E-06	7.89E-07	4.93E-07	2.65E-07	1.71E-07	1.23E-07	9.51E-08	7.65E-08	6.33E-08	5.35E-08
ESE	1.83E-05	5.16E-06	2.48E-06	1.53E-06	8.19E-07	5.31E-07	3.83E-07	3.00E-07	2.44E-07	2.04E-07	1.74E-07
SE	4.80E-05	1.35E-05	6.43E-06	3.96E-06	2.11E-06	1.36E-06	9.83E-07	7.74E-07	6.32E-07	5.29E-07	4.53E-07
SSE	2.45E-05	6.92E-06	3.34E-06	2.07E-06	1.11E-06	7.18E-07	5.17E-07	4.06E-07	3.30E-07	2.75E-07	2.35E-07

WLS COL 2.3-5

TABLE 2.3-288 (Sheet 2 of 3)
 ANNUAL AVERAGE χ/Q (SEC/M³) FOR NORMAL RELEASES NO DECAY, DEPLETED
 (FOR EACH 22.5° SECTOR AT THE DISTANCES (MILES) SHOWN AT THE TOP)

SECTOR	5.000	7.500	10.000	15.000	20.000	25.000	30.000	35.000	40.000	45.000	50.000
S	1.55E-07	8.83E-08	5.90E-08	3.32E-08	2.19E-08	1.58E-08	1.21E-08	9.61E-09	7.86E-09	6.57E-09	5.59E-09
SSW	1.41E-07	8.02E-08	5.34E-08	2.99E-08	1.97E-08	1.42E-08	1.08E-08	8.61E-09	7.03E-09	5.87E-09	4.99E-09
SW	1.15E-07	6.47E-08	4.29E-08	2.39E-08	1.57E-08	1.13E-08	8.57E-09	6.79E-09	5.54E-09	4.62E-09	3.92E-09
WSW	1.40E-07	8.00E-08	5.34E-08	3.00E-08	1.99E-08	1.44E-08	1.10E-08	8.72E-09	7.13E-09	5.96E-09	5.07E-09
W	1.45E-07	8.29E-08	5.55E-08	3.13E-08	2.07E-08	1.50E-08	1.15E-08	9.14E-09	7.48E-09	6.26E-09	5.32E-09
WNW	1.46E-07	8.37E-08	5.61E-08	3.17E-08	2.10E-08	1.52E-08	1.16E-08	9.24E-09	7.56E-09	6.33E-09	5.38E-09
NW	1.27E-07	7.24E-08	4.82E-08	2.70E-08	1.78E-08	1.29E-08	9.83E-09	7.81E-09	6.38E-09	5.33E-09	4.53E-09
NNW	9.44E-08	5.27E-08	3.47E-08	1.91E-08	1.25E-08	8.93E-09	6.78E-09	5.35E-09	4.35E-09	3.62E-09	3.07E-09
N	7.26E-08	3.96E-08	2.56E-08	1.38E-08	8.87E-09	6.27E-09	4.71E-09	3.69E-09	2.98E-09	2.47E-09	2.08E-09
NNE	5.23E-08	2.83E-08	1.82E-08	9.76E-09	6.26E-09	4.42E-09	3.31E-09	2.59E-09	2.09E-09	1.73E-09	1.46E-09
NE	3.89E-08	2.10E-08	1.34E-08	7.16E-09	4.58E-09	3.22E-09	2.42E-09	1.89E-09	1.52E-09	1.26E-09	1.06E-09
ENE	3.39E-08	1.85E-08	1.20E-08	6.49E-09	4.20E-09	2.98E-09	2.25E-09	1.77E-09	1.43E-09	1.19E-09	1.00E-09
E	4.61E-08	2.60E-08	1.72E-08	9.53E-09	6.26E-09	4.50E-09	3.42E-09	2.71E-09	2.21E-09	1.84E-09	1.56E-09
ESE	1.51E-07	8.70E-08	5.85E-08	3.32E-08	2.21E-08	1.60E-08	1.23E-08	9.77E-09	8.01E-09	6.71E-09	5.72E-09
SE	3.93E-07	2.29E-07	1.54E-07	8.81E-08	5.88E-08	4.28E-08	3.29E-08	2.62E-08	2.15E-08	1.81E-08	1.54E-08
SSE	2.03E-07	1.17E-07	7.86E-08	4.45E-08	2.96E-08	2.14E-08	1.64E-08	1.31E-08	1.07E-08	8.97E-09	7.64E-09

WLS COL 2.3-5

TABLE 2.3-288 (Sheet 3 of 3)
 ANNUAL AVERAGE χ/Q (SEC/M³) FOR NORMAL RELEASES NO DECAY, DEPLETED
 (FOR EACH 22.5° SECTOR AT THE DISTANCES (MILES) SHOWN AT THE TOP)

SECTOR	.5-1	1-2	2-3	3-4	4-5	5-10	10-20	20-30	30-40	40-50
S	2.74E-06	8.87E-07	4.06E-07	2.54E-07	1.79E-07	9.00E-08	3.39E-08	1.60E-08	9.66E-09	6.59E-09
SSW	2.53E-06	8.22E-07	3.74E-07	2.32E-07	1.64E-07	8.18E-08	3.06E-08	1.43E-08	8.65E-09	5.89E-09
SW	2.07E-06	6.78E-07	3.09E-07	1.91E-07	1.34E-07	6.61E-08	2.44E-08	1.14E-08	6.82E-09	4.63E-09
WSW	2.50E-06	8.09E-07	3.69E-07	2.30E-07	1.63E-07	8.16E-08	3.07E-08	1.45E-08	8.76E-09	5.98E-09
W	2.55E-06	8.24E-07	3.77E-07	2.36E-07	1.67E-07	8.44E-08	3.20E-08	1.51E-08	9.18E-09	6.27E-09
WNW	2.55E-06	8.24E-07	3.79E-07	2.38E-07	1.69E-07	8.53E-08	3.23E-08	1.53E-08	9.28E-09	6.35E-09
NW	2.27E-06	7.38E-07	3.37E-07	2.10E-07	1.48E-07	7.38E-08	2.77E-08	1.30E-08	7.84E-09	5.35E-09
NNW	1.71E-06	5.68E-07	2.59E-07	1.58E-07	1.10E-07	5.39E-08	1.96E-08	9.01E-09	5.38E-09	3.64E-09
N	1.33E-06	4.53E-07	2.07E-07	1.24E-07	8.53E-08	4.07E-08	1.42E-08	6.34E-09	3.71E-09	2.47E-09
NNE	9.96E-07	3.38E-07	1.51E-07	9.04E-08	6.16E-08	2.92E-08	1.01E-08	4.47E-09	2.61E-09	1.74E-09
NE	7.64E-07	2.58E-07	1.14E-07	6.78E-08	4.59E-08	2.16E-08	7.40E-09	3.26E-09	1.90E-09	1.26E-09
ENE	6.54E-07	2.17E-07	9.72E-08	5.82E-08	3.98E-08	1.90E-08	6.69E-09	3.01E-09	1.78E-09	1.19E-09
E	8.37E-07	2.74E-07	1.25E-07	7.68E-08	5.37E-08	2.65E-08	9.77E-09	4.54E-09	2.72E-09	1.85E-09
ESE	2.65E-06	8.49E-07	3.89E-07	2.45E-07	1.74E-07	8.85E-08	3.38E-08	1.61E-08	9.81E-09	6.73E-09
SE	6.90E-06	2.19E-06	1.00E-06	6.33E-07	4.53E-07	2.32E-07	8.98E-08	4.31E-08	2.63E-08	1.81E-08
SSE	3.57E-06	1.15E-06	5.26E-07	3.31E-07	2.35E-07	1.19E-07	4.55E-08	2.16E-08	1.31E-08	8.99E-09

WLS COL 2.3-5

TABLE 2.3-289 (Sheet 1 of 6)
 χ/Q AND D/Q VALUES FOR NORMAL RELEASES

Type of Location	Sector	Distance		χ/Q (sec/m ³)	χ/Q (sec/m ³)	χ/Q (sec/m ³)	χ/Q (sec/m ³)	D/Q
				No Decay	No Decay	2.26 Day Decay	8.00 Day Decay	
		(miles)	(meters)	Undepleted	Depleted	Undepleted	Depleted	(m ⁻²)
SITE BOUNDARY (U1)	S	0.87	1400	2.30E-06	2.00E-06	2.20E-06	2.00E-06	4.60E-09
SITE BOUNDARY (U1)	SSW	0.87	1400	2.10E-06	1.90E-06	2.10E-06	1.90E-06	5.00E-09
SITE BOUNDARY (U1)	SW	0.97	1568	1.40E-06	1.30E-06	1.40E-06	1.30E-06	4.00E-09
SITE BOUNDARY (U1)	WSW	1.02	1634	1.60E-06	1.40E-06	1.60E-06	1.40E-06	3.30E-09
SITE BOUNDARY (U1)	W	0.72	1163	2.90E-06	2.50E-06	2.80E-06	2.50E-06	4.90E-09
SITE BOUNDARY (U1)	WNW	0.62	995	3.70E-06	3.40E-06	3.70E-06	3.40E-06	5.90E-09
SITE BOUNDARY (U1)	NW	0.27	427	1.50E-05	1.30E-05	1.40E-05	1.30E-05	2.90E-08
SITE BOUNDARY (U1)	NNW	0.27	427	1.10E-05	9.90E-06	1.10E-05	9.90E-06	3.00E-08
SITE BOUNDARY (U1)	N	0.31	502	5.90E-06	5.50E-06	5.90E-06	5.50E-06	2.60E-08
SITE BOUNDARY (U1)	NNE	0.38	613	3.20E-06	2.90E-06	3.10E-06	2.90E-06	2.20E-08
SITE BOUNDARY (U1)	NE	0.39	633	2.30E-06	2.10E-06	2.30E-06	2.10E-06	1.90E-08
SITE BOUNDARY (U1)	ENE	0.50	806	1.30E-06	1.20E-06	1.30E-06	1.20E-06	8.80E-09
SITE BOUNDARY (U1)	E	0.52	837	1.60E-06	1.50E-06	1.60E-06	1.50E-06	5.70E-09
SITE BOUNDARY (U1)	ESE	0.56	906	4.60E-06	4.20E-06	4.60E-06	4.10E-06	1.10E-08
SITE BOUNDARY (U1)	SE	0.82	1326	6.20E-06	5.50E-06	6.10E-06	5.50E-06	1.30E-08
SITE BOUNDARY (U1)	SSE	0.88	1410	2.90E-06	2.60E-06	2.90E-06	2.60E-06	5.40E-09

WLS COL 2.3-5

TABLE 2.3-289 (Sheet 2 of 6)
 χ/Q AND D/Q VALUES FOR NORMAL RELEASES

Type of Location	Sector	Distance		χ/Q (sec/m ³)	χ/Q (sec/m ³)	χ/Q (sec/m ³)	χ/Q (sec/m ³)	D/Q (m ⁻²)
				No Decay	No Decay	2.26 Day Decay	8.00 Day Decay	
		(miles)	(meters)	Undepleted	Depleted	Undepleted	Depleted	
SITE BOUNDARY (U2)	S	0.92	1477	2.10E-06	1.80E-06	2.10E-06	1.80E-06	4.20E-09
SITE BOUNDARY (U2)	SSW	0.92	1477	1.90E-06	1.70E-06	1.90E-06	1.70E-06	4.50E-09
SITE BOUNDARY (U2)	SW	0.99	1586	1.40E-06	1.20E-06	1.40E-06	1.20E-06	3.90E-09
SITE BOUNDARY (U2)	WSW	1.11	1791	1.40E-06	1.20E-06	1.40E-06	1.20E-06	2.80E-09
SITE BOUNDARY (U2)	W	0.85	1371	2.20E-06	1.90E-06	2.20E-06	1.90E-06	3.70E-09
SITE BOUNDARY (U2)	WNW	0.33	534	1.10E-05	1.00E-05	1.10E-05	1.00E-05	1.60E-08
SITE BOUNDARY (U2)	NW	0.33	534	9.70E-06	9.00E-06	9.70E-06	9.00E-06	2.10E-08
SITE BOUNDARY (U2)	NNW	0.33	527	7.30E-06	6.70E-06	7.30E-06	6.70E-06	2.20E-08
SITE BOUNDARY (U2)	N	0.33	525	5.50E-06	5.10E-06	5.50E-06	5.10E-06	2.40E-08
SITE BOUNDARY (U2)	NNE	0.33	525	4.10E-06	3.80E-06	4.10E-06	3.80E-06	2.80E-08
SITE BOUNDARY (U2)	NE	0.37	596	2.50E-06	2.30E-06	2.50E-06	2.30E-06	2.10E-08
SITE BOUNDARY (U2)	ENE	0.37	594	2.20E-06	2.10E-06	2.20E-06	2.10E-06	1.40E-08
SITE BOUNDARY (U2)	E	0.37	594	2.90E-06	2.70E-06	2.90E-06	2.70E-06	9.80E-09
SITE BOUNDARY (U2)	ESE	0.40	639	8.50E-06	7.80E-06	8.50E-06	7.80E-06	1.90E-08
SITE BOUNDARY (U2)	SE	0.59	946	1.10E-05	1.00E-05	1.10E-05	1.00E-05	2.20E-08
SITE BOUNDARY (U2)	SSE	0.81	1309	3.30E-06	2.90E-06	3.30E-06	2.90E-06	6.10E-09

WLS COL 2.3-5

TABLE 2.3-289 (Sheet 3 of 6)
 χ/Q AND D/Q VALUES FOR NORMAL RELEASES

Type of Location	Sector	Distance		χ/Q (sec/m ³)	χ/Q (sec/m ³)	χ/Q (sec/m ³)	χ/Q (sec/m ³)	D/Q (m ⁻²)
				No Decay	No Decay	2.26 Day Decay	8.00 Day Decay	
		(miles)	(meters)	Undepleted	Depleted	Undepleted	Depleted	
NEAREST HOUSE	S	0.99	1597	1.80E-06	1.60E-06	1.80E-06	1.60E-06	3.60E-09
NEAREST HOUSE	SSW	1.09	1761	1.50E-06	1.30E-06	1.50E-06	1.30E-06	3.40E-09
NEAREST HOUSE	SW	1.25	2011	1.00E-06	8.70E-07	9.90E-07	8.60E-07	2.60E-09
NEAREST HOUSE	WSW	2.46	3954	4.60E-07	3.70E-07	4.50E-07	3.70E-07	7.10E-10
NEAREST HOUSE	W	1.79	2887	7.30E-07	6.10E-07	7.10E-07	6.00E-07	1.00E-09
NEAREST HOUSE	WNW	2.21	3553	5.40E-07	4.50E-07	5.30E-07	4.40E-07	6.70E-10
NEAREST HOUSE	NW	2.06	3311	5.40E-07	4.40E-07	5.30E-07	4.40E-07	9.80E-10
NEAREST HOUSE	NNW	1.41	2263	7.10E-07	6.10E-07	7.00E-07	6.00E-07	2.00E-09
NEAREST HOUSE	N	1.06	1705	8.50E-07	7.40E-07	8.40E-07	7.40E-07	3.50E-09
NEAREST HOUSE	NNE	1.41	2268	4.20E-07	3.60E-07	4.20E-07	3.60E-07	2.40E-09
NEAREST HOUSE	NE	1.14	1838	4.40E-07	3.80E-07	4.40E-07	3.80E-07	3.30E-09
NEAREST HOUSE	ENE	1.14	1833	3.7E-07	3.20E-07	3.70E-07	3.20E-07	2.2E-09
NEAREST HOUSE	E	1.23	1985	4.10E-07	3.60E-07	4.10E-07	3.60E-07	1.30E-09
NEAREST HOUSE	ESE	2.41	3877	4.90E-07	4.00E-07	4.80E-07	4.00E-07	8.90E-10
NEAREST HOUSE	SE	0.99	1588	4.60E-06	4.00E-06	4.60E-06	4.00E-06	9.40E-09
NEAREST HOUSE	SSE	1.09	1752	2.10E-06	1.80E-06	2.10E-06	1.80E-06	3.70E-09

WLS COL 2.3-5

TABLE 2.3-289 (Sheet 4 of 6)
 χ/Q AND D/Q VALUES FOR NORMAL RELEASES

Type of Location	Sector	Distance		χ/Q (sec/m ³)	χ/Q (sec/m ³)	χ/Q (sec/m ³)	χ/Q (sec/m ³)	D/Q (m ⁻²)
				No Decay	No Decay	2.26 Day Decay	8.00 Day Decay	
		(miles)	(meters)	Undepleted	Depleted	Undepleted	Depleted	
NEAREST GARDEN	S	0.99	1592	1.90E-06	1.60E-06	1.80E-06	1.60E-06	3.70E-09
NEAREST GARDEN	SSW	1.19	1917	1.30E-06	1.10E-06	1.30E-06	1.10E-06	2.90E-09
NEAREST GARDEN	SW	1.25	2011	1.00E-06	8.70E-07	9.90E-07	8.60E-07	2.60E-09
NEAREST GARDEN	WSW	2.46	3961	4.60E-07	3.70E-07	4.40E-07	3.70E-07	7.10E-10
NEAREST GARDEN	W	2.20	3543	5.40E-07	4.50E-07	5.30E-07	4.40E-07	7.30E-10
NEAREST GARDEN	WNW	2.55	4110	4.50E-07	3.60E-07	4.40E-07	3.60E-07	5.20E-10
NEAREST GARDEN	NW	2.04	3279	5.40E-07	4.50E-07	5.40E-07	4.50E-07	9.90E-10
NEAREST GARDEN	NNW	1.52	2452	6.30E-07	5.40E-07	6.30E-07	5.40E-07	1.70E-09
NEAREST GARDEN	N	1.41	2263	5.70E-07	4.90E-07	5.60E-07	4.80E-07	2.10E-09
NEAREST GARDEN	NNE	1.38	2216	4.40E-07	3.70E-07	4.30E-07	3.70E-07	2.50E-09
NEAREST GARDEN	NE	1.12	1802	4.50E-07	3.90E-07	4.50E-07	3.90E-07	3.40E-09
NEAREST GARDEN	ENE	0.97	1563	4.70E-07	4.10E-07	4.70E-07	4.10E-07	2.90E-09
NEAREST GARDEN	E	2.77	4460	1.30E-07	1.10E-07	1.30E-07	1.10E-07	3.20E-10
NEAREST GARDEN	ESE	2.70	4339	4.30E-07	3.50E-07	4.20E-07	3.40E-07	7.30E-10
NEAREST GARDEN	SE	4.08	6570	6.70E-07	5.20E-07	6.60E-07	5.10E-07	7.90E-10
NEAREST GARDEN	SSE	1.00	1606	2.40E-06	2.10E-06	2.40E-06	2.10E-06	4.30E-09

WLS COL 2.3-5

TABLE 2.3-289 (Sheet 5 of 6)
 χ/Q AND D/Q VALUES FOR NORMAL RELEASES

Type of Location	Sector	Distance		χ/Q (sec/m ³)	χ/Q (sec/m ³)	χ/Q (sec/m ³)	χ/Q (sec/m ³)	D/Q (m ⁻²)
		(miles)	(meters)	No Decay	No Decay	2.26 Day Decay	8.00 Day Decay	
				Undepleted	Depleted	Undepleted	Depleted	
COW	S	3.23	5204	3.60E-07	2.80E-07	3.50E-07	2.80E-07	4.70E-10
COW	SSW	1.30	2091	1.20E-06	9.90E-07	1.10E-06	9.90E-07	2.50E-09
COW	SW	1.21	1950	1.10E-06	9.10E-07	1.00E-06	9.00E-07	2.70E-09
COW	WSW	2.79	4497	3.90E-07	3.10E-07	3.80E-07	3.10E-07	5.70E-10
COW	W	2.40	3857	4.80E-07	3.90E-07	4.70E-07	3.90E-07	6.30E-10
COW	WNW	2.51	4033	4.60E-07	3.70E-07	4.50E-07	3.70E-07	5.40E-10
COW	NW	3.83	6163	2.40E-07	1.80E-07	2.30E-07	1.80E-07	3.30E-10
COW	NNW	2.93	4722	2.50E-07	2.00E-07	2.50E-07	2.00E-07	5.40E-10
COW	N	2.27	3648	2.90E-07	2.40E-07	2.90E-07	2.40E-07	9.40E-10
COW	NNE	3.40	5464	1.20E-07	9.40E-08	1.20E-07	9.40E-08	5.20E-10
COW	NE	1.47	2364	3.00E-07	2.60E-07	3.00E-07	2.60E-07	2.10E-09
COW	ENE	1.22	1956	3.40E-07	2.90E-07	3.30E-07	2.90E-07	2.00E-09
COW	E	3.05	4914	1.20E-07	9.30E-08	1.10E-07	9.20E-08	2.70E-10
COW	ESE	3.11	5002	3.60E-07	2.90E-07	3.50E-07	2.80E-07	5.70E-10
COW	SE	1.65	2650	2.20E-06	1.80E-06	2.10E-06	1.80E-06	3.90E-09
COW	SSE	1.07	1728	2.10E-06	1.90E-06	2.10E-06	1.80E-06	3.80E-09

WLS COL 2.3-5

TABLE 2.3-289 (Sheet 6 of 6)
 χ/Q AND D/Q VALUES FOR NORMAL RELEASES

Type of Location	Sector	Distance		χ/Q (sec/m ³)	χ/Q (sec/m ³)	χ/Q (sec/m ³)	χ/Q (sec/m ³)	D/Q (m ⁻²)
				No Decay	No Decay	2.26 Day Decay	8.00 Day Decay	
		(miles)	(meters)	Undepleted	Depleted	Undepleted	Depleted	
GOAT	S	-	-	-	-	-	-	-
GOAT	SSW	1.05	1690	1.60E-06	1.40E-06	1.60E-06	1.40E-06	3.60E-09
GOAT	SW	-	-	-	-	-	-	-
GOAT	WSW	-	-	-	-	-	-	-
GOAT	W	2.60	4192	4.40E-07	3.50E-07	4.30E-07	3.50E-07	5.40E-10
GOAT	WNW	3.87	6230	2.70E-07	2.10E-07	2.60E-07	2.00E-07	2.50E-10
GOAT	NW	3.83	6163	2.40E-07	1.80E-07	2.30E-07	1.80E-07	3.30E-10
GOAT	NNW	4.36	7013	1.50E-07	1.20E-07	1.50E-07	1.10E-07	2.70E-10
GOAT	N	3.42	5506	1.60E-07	1.30E-07	1.60E-07	1.30E-07	4.50E-10
GOAT	NNE	-	-	-	-	-	-	-
GOAT	NE	4.90	7886	5.40E-08	4.00E-08	5.30E-08	4.00E-08	2.50E-10
GOAT	ENE	-	-	-	-	-	-	-
GOAT	E	-	-	-	-	-	-	-
GOAT	ESE	-	-	-	-	-	-	-
GOAT	SE	-	-	-	-	-	-	-
GOAT	SSE	1.41	2275	1.40E-06	1.20E-06	1.40E-06	1.20E-06	2.40E-09

WLS COL 2.3-5

TABLE 2.3-290 (Sheet 1 of 3)
 ANNUAL AVERAGE χ/Q (SEC/M³) FOR NORMAL RELEASES
 2.26 DAY DECAY, UNDEPLETED
 (FOR EACH 22.5° SECTOR AT THE DISTANCES (MILES) SHOWN AT THE TOP)

SECTOR	0.25	0.5	0.75	1	1.5	2	2.5	3	3.5	4	4.5
S	1.95E-05	5.74E-06	2.86E-06	1.81E-06	9.94E-07	6.57E-07	4.81E-07	3.81E-07	3.12E-07	2.63E-07	2.26E-07
SSW	1.78E-05	5.28E-06	2.65E-06	1.68E-06	9.21E-07	6.07E-07	4.44E-07	3.50E-07	2.86E-07	2.41E-07	2.06E-07
SW	1.45E-05	4.30E-06	2.17E-06	1.38E-06	7.62E-07	5.04E-07	3.68E-07	2.90E-07	2.36E-07	1.98E-07	1.69E-07
WSW	1.78E-05	5.26E-06	2.61E-06	1.65E-06	9.04E-07	5.97E-07	4.36E-07	3.45E-07	2.82E-07	2.37E-07	2.04E-07
W	1.83E-05	5.37E-06	2.66E-06	1.68E-06	9.24E-07	6.11E-07	4.48E-07	3.55E-07	2.92E-07	2.46E-07	2.12E-07
WNW	1.84E-05	5.38E-06	2.66E-06	1.67E-06	9.24E-07	6.13E-07	4.50E-07	3.57E-07	2.94E-07	2.48E-07	2.13E-07
NW	1.61E-05	4.76E-06	2.38E-06	1.51E-06	8.31E-07	5.50E-07	4.03E-07	3.19E-07	2.61E-07	2.20E-07	1.89E-07
NNW	1.18E-05	3.53E-06	1.81E-06	1.15E-06	6.41E-07	4.24E-07	3.09E-07	2.42E-07	1.97E-07	1.65E-07	1.41E-07
N	8.80E-06	2.68E-06	1.42E-06	9.17E-07	5.15E-07	3.41E-07	2.49E-07	1.93E-07	1.56E-07	1.29E-07	1.10E-07
NNE	6.56E-06	2.01E-06	1.07E-06	6.90E-07	3.83E-07	2.52E-07	1.82E-07	1.41E-07	1.13E-07	9.37E-08	7.93E-08
NE	5.01E-06	1.54E-06	8.19E-07	5.30E-07	2.92E-07	1.92E-07	1.38E-07	1.06E-07	8.53E-08	7.04E-08	5.95E-08
ENE	4.40E-06	1.34E-06	6.96E-07	4.46E-07	2.46E-07	1.62E-07	1.17E-07	9.07E-08	7.31E-08	6.06E-08	5.14E-08
E	5.84E-06	1.74E-06	8.81E-07	5.59E-07	3.09E-07	2.04E-07	1.49E-07	1.17E-07	9.57E-08	8.03E-08	6.87E-08
ESE	1.93E-05	5.63E-06	2.76E-06	1.73E-06	9.52E-07	6.30E-07	4.62E-07	3.68E-07	3.04E-07	2.57E-07	2.21E-07
SE	5.06E-05	1.47E-05	7.18E-06	4.49E-06	2.46E-06	1.63E-06	1.20E-06	9.56E-07	7.92E-07	6.72E-07	5.82E-07
SSE	2.58E-05	7.55E-06	3.73E-06	2.35E-06	1.29E-06	8.54E-07	6.26E-07	4.99E-07	4.11E-07	3.48E-07	3.00E-07

WLS COL 2.3-5

TABLE 2.3-290 (Sheet 2 of 3)
 ANNUAL AVERAGE χ/Q (SEC/M³) FOR NORMAL RELEASES
 2.26 DAY DECAY, UNDEPLETED
 (FOR EACH 22.5° SECTOR AT THE DISTANCES (MILES) SHOWN AT THE TOP)

SECTOR	5	7.5	10	15	20	25	30	35	40	45	50
S	1.97E-07	1.16E-07	7.88E-08	4.54E-08	3.03E-08	2.19E-08	1.67E-08	1.32E-08	1.07E-08	8.88E-09	7.48E-09
SSW	1.80E-07	1.05E-07	7.14E-08	4.09E-08	2.72E-08	1.97E-08	1.50E-08	1.18E-08	9.57E-09	7.92E-09	6.66E-09
SW	1.47E-07	8.59E-08	5.83E-08	3.35E-08	2.24E-08	1.63E-08	1.25E-08	9.88E-09	8.05E-09	6.69E-09	5.65E-09
WSW	1.77E-07	1.04E-07	7.07E-08	4.05E-08	2.69E-08	1.94E-08	1.47E-08	1.16E-08	9.37E-09	7.73E-09	6.48E-09
W	1.85E-07	1.10E-07	7.50E-08	4.36E-08	2.93E-08	2.14E-08	1.64E-08	1.30E-08	1.06E-08	8.85E-09	7.48E-09
WNW	1.86E-07	1.10E-07	7.57E-08	4.40E-08	2.96E-08	2.16E-08	1.66E-08	1.32E-08	1.08E-08	8.95E-09	7.57E-09
NW	1.65E-07	9.74E-08	6.68E-08	3.90E-08	2.65E-08	1.95E-08	1.51E-08	1.21E-08	9.92E-09	8.32E-09	7.09E-09
NNW	1.22E-07	7.08E-08	4.79E-08	2.75E-08	1.84E-08	1.34E-08	1.03E-08	8.24E-09	6.75E-09	5.64E-09	4.79E-09
N	9.47E-08	5.39E-08	3.61E-08	2.04E-08	1.36E-08	9.87E-09	7.57E-09	6.04E-09	4.95E-09	4.14E-09	3.52E-09
NNE	6.83E-08	3.86E-08	2.57E-08	1.45E-08	9.60E-09	6.95E-09	5.33E-09	4.24E-09	3.47E-09	2.91E-09	2.48E-09
NE	5.12E-08	2.89E-08	1.92E-08	1.09E-08	7.25E-09	5.28E-09	4.07E-09	3.26E-09	2.68E-09	2.26E-09	1.93E-09
ENE	4.44E-08	2.54E-08	1.70E-08	9.72E-09	6.52E-09	4.77E-09	3.68E-09	2.95E-09	2.43E-09	2.04E-09	1.74E-09
E	5.98E-08	3.50E-08	2.38E-08	1.38E-08	9.31E-09	6.83E-09	5.27E-09	4.22E-09	3.47E-09	2.91E-09	2.48E-09
ESE	1.94E-07	1.16E-07	7.98E-08	4.69E-08	3.18E-08	2.34E-08	1.81E-08	1.45E-08	1.19E-08	1.00E-08	8.54E-09
SE	5.11E-07	3.09E-07	2.16E-07	1.29E-07	8.90E-08	6.64E-08	5.21E-08	4.22E-08	3.51E-08	2.98E-08	2.56E-08
SSE	2.62E-07	1.57E-07	1.08E-07	6.36E-08	4.32E-08	3.18E-08	2.46E-08	1.98E-08	1.62E-08	1.36E-08	1.16E-08

WLS COL 2.3-5

TABLE 2.3-290 (Sheet 3 of 3)
 ANNUAL AVERAGE χ/Q (SEC/M³) FOR NORMAL RELEASES
 2.26 DAY DECAY, UNDEPLETED
 (FOR EACH 22.5° SECTOR AT THE DISTANCES (MILES) SHOWN AT THE TOP)

SECTOR	.5-1	1-2	2-3	3-4	4-5	5-10	10-20	20-30	30-40	40-50
S	3.03E-06	1.02E-06	4.88E-07	3.13E-07	2.26E-07	1.17E-07	4.61E-08	2.21E-08	1.33E-08	8.91E-09
SSW	2.80E-06	9.49E-07	4.50E-07	2.87E-07	2.07E-07	1.07E-07	4.16E-08	1.98E-08	1.19E-08	7.94E-09
SW	2.29E-06	7.85E-07	3.73E-07	2.37E-07	1.70E-07	8.73E-08	3.41E-08	1.64E-08	9.92E-09	6.71E-09
WSW	2.77E-06	9.32E-07	4.42E-07	2.83E-07	2.04E-07	1.06E-07	4.12E-08	1.95E-08	1.16E-08	7.75E-09
W	2.83E-06	9.53E-07	4.54E-07	2.93E-07	2.12E-07	1.11E-07	4.42E-08	2.15E-08	1.31E-08	8.87E-09
WNW	2.82E-06	9.52E-07	4.56E-07	2.95E-07	2.14E-07	1.12E-07	4.47E-08	2.17E-08	1.32E-08	8.97E-09
NW	2.52E-06	8.57E-07	4.08E-07	2.62E-07	1.89E-07	9.88E-08	3.96E-08	1.96E-08	1.21E-08	8.34E-09
NNW	1.90E-06	6.58E-07	3.13E-07	1.98E-07	1.41E-07	7.20E-08	2.80E-08	1.35E-08	8.27E-09	5.65E-09
N	1.48E-06	5.27E-07	2.51E-07	1.56E-07	1.10E-07	5.51E-08	2.09E-08	9.94E-09	6.06E-09	4.15E-09
NNE	1.11E-06	3.93E-07	1.84E-07	1.14E-07	7.95E-08	3.95E-08	1.48E-08	7.01E-09	4.26E-09	2.92E-09
NE	8.51E-07	3.00E-07	1.40E-07	8.57E-08	5.97E-08	2.96E-08	1.11E-08	5.32E-09	3.27E-09	2.26E-09
ENE	7.28E-07	2.53E-07	1.18E-07	7.34E-08	5.16E-08	2.59E-08	9.92E-09	4.80E-09	2.96E-09	2.05E-09
E	9.29E-07	3.18E-07	1.51E-07	9.60E-08	6.88E-08	3.55E-08	1.40E-08	6.87E-09	4.23E-09	2.91E-09
ESE	2.94E-06	9.83E-07	4.69E-07	3.04E-07	2.22E-07	1.17E-07	4.75E-08	2.35E-08	1.46E-08	1.00E-08
SE	7.66E-06	2.54E-06	1.21E-06	7.93E-07	5.82E-07	3.13E-07	1.31E-07	6.67E-08	4.23E-08	2.98E-08
SSE	3.97E-06	1.33E-06	6.36E-07	4.12E-07	3.00E-07	1.59E-07	6.44E-08	3.20E-08	1.98E-08	1.37E-08

WLS COL 2.3-5

TABLE 2.3-291 (Sheet 1 of 3)
 ANNUAL AVERAGE χ/Q (SEC/M³) FOR NORMAL RELEASES 8.00 DAY DECAY, DEPLETED
 (FOR EACH 22.5° SECTOR AT THE DISTANCES (MILES) SHOWN AT THE TOP)

SECTOR	0.25	0.5	0.75	1	1.5	2	2.5	3	3.5	4	4.5
S	1.85E-05	5.26E-06	2.56E-06	1.59E-06	8.54E-07	5.52E-07	3.97E-07	3.09E-07	2.50E-07	2.08E-07	1.76E-07
SSW	1.69E-05	4.84E-06	2.37E-06	1.48E-06	7.91E-07	5.10E-07	3.66E-07	2.84E-07	2.29E-07	1.90E-07	1.61E-07
SW	1.37E-05	3.94E-06	1.95E-06	1.22E-06	6.53E-07	4.22E-07	3.03E-07	2.34E-07	1.88E-07	1.56E-07	1.32E-07
WSW	1.69E-05	4.82E-06	2.34E-06	1.45E-06	7.77E-07	5.02E-07	3.60E-07	2.81E-07	2.27E-07	1.88E-07	1.60E-07
W	1.74E-05	4.92E-06	2.39E-06	1.48E-06	7.92E-07	5.13E-07	3.69E-07	2.88E-07	2.33E-07	1.94E-07	1.65E-07
WNW	1.74E-05	4.93E-06	2.38E-06	1.47E-06	7.93E-07	5.14E-07	3.71E-07	2.90E-07	2.35E-07	1.96E-07	1.66E-07
NW	1.53E-05	4.36E-06	2.13E-06	1.33E-06	7.11E-07	4.60E-07	3.30E-07	2.57E-07	2.07E-07	1.72E-07	1.46E-07
NNW	1.12E-05	3.23E-06	1.62E-06	1.02E-06	5.48E-07	3.55E-07	2.54E-07	1.95E-07	1.57E-07	1.29E-07	1.09E-07
N	8.33E-06	2.45E-06	1.27E-06	8.06E-07	4.39E-07	2.85E-07	2.03E-07	1.55E-07	1.23E-07	1.01E-07	8.44E-08
NNE	6.22E-06	1.84E-06	9.52E-07	6.06E-07	3.27E-07	2.10E-07	1.49E-07	1.13E-07	8.95E-08	7.30E-08	6.09E-08
NE	4.75E-06	1.41E-06	7.32E-07	4.65E-07	2.49E-07	1.59E-07	1.13E-07	8.52E-08	6.72E-08	5.47E-08	4.55E-08
ENE	4.17E-06	1.23E-06	6.22E-07	3.91E-07	2.10E-07	1.35E-07	9.56E-08	7.27E-08	5.77E-08	4.72E-08	3.95E-08
E	5.54E-06	1.59E-06	7.88E-07	4.92E-07	2.64E-07	1.71E-07	1.22E-07	9.45E-08	7.60E-08	6.28E-08	5.31E-08
ESE	1.83E-05	5.15E-06	2.47E-06	1.53E-06	8.16E-07	5.28E-07	3.80E-07	2.98E-07	2.42E-07	2.02E-07	1.72E-07
SE	4.80E-05	1.35E-05	6.42E-06	3.95E-06	2.10E-06	1.36E-06	9.79E-07	7.70E-07	6.28E-07	5.26E-07	4.49E-07
SSE	2.45E-05	6.92E-06	3.34E-06	2.07E-06	1.11E-06	7.15E-07	5.15E-07	4.03E-07	3.27E-07	2.73E-07	2.32E-07

WLS COL 2.3-5

TABLE 2.3-291 (Sheet 2 of 3)
 ANNUAL AVERAGE χ/Q (SEC/M³) FOR NORMAL RELEASES 8.00 DAY DECAY, DEPLETED
 (FOR EACH 22.5° SECTOR AT THE DISTANCES (MILES) SHOWN AT THE TOP)

SECTOR	5	7.5	10	15	20	25	30	35	40	45	50
S	1.52E-07	8.63E-08	5.72E-08	3.16E-08	2.06E-08	1.46E-08	1.10E-08	8.60E-09	6.93E-09	5.70E-09	4.77E-09
SSW	1.39E-07	7.84E-08	5.17E-08	2.85E-08	1.85E-08	1.31E-08	9.86E-09	7.70E-09	6.19E-09	5.09E-09	4.26E-09
SW	1.13E-07	6.35E-08	4.18E-08	2.29E-08	1.49E-08	1.05E-08	7.92E-09	6.19E-09	4.98E-09	4.10E-09	3.43E-09
WSW	1.38E-07	7.80E-08	5.17E-08	2.85E-08	1.85E-08	1.32E-08	9.89E-09	7.73E-09	6.21E-09	5.11E-09	4.27E-09
W	1.43E-07	8.12E-08	5.40E-08	3.00E-08	1.96E-08	1.40E-08	1.06E-08	8.28E-09	6.68E-09	5.51E-09	4.63E-09
WNW	1.44E-07	8.20E-08	5.45E-08	3.04E-08	1.98E-08	1.41E-08	1.07E-08	8.37E-09	6.76E-09	5.57E-09	4.68E-09
NW	1.26E-07	7.13E-08	4.72E-08	2.62E-08	1.71E-08	1.22E-08	9.23E-09	7.26E-09	5.87E-09	4.85E-09	4.08E-09
NNW	9.34E-08	5.19E-08	3.39E-08	1.85E-08	1.20E-08	8.46E-09	6.35E-09	4.96E-09	3.99E-09	3.29E-09	2.75E-09
N	7.20E-08	3.92E-08	2.52E-08	1.35E-08	8.59E-09	6.02E-09	4.49E-09	3.49E-09	2.79E-09	2.29E-09	1.91E-09
NNE	5.19E-08	2.80E-08	1.79E-08	9.53E-09	6.06E-09	4.24E-09	3.15E-09	2.44E-09	1.96E-09	1.60E-09	1.34E-09
NE	3.87E-08	2.08E-08	1.33E-08	7.04E-09	4.48E-09	3.14E-09	2.34E-09	1.82E-09	1.46E-09	1.19E-09	9.99E-10
ENE	3.37E-08	1.83E-08	1.18E-08	6.36E-09	4.08E-09	2.88E-09	2.16E-09	1.68E-09	1.35E-09	1.11E-09	9.34E-10
E	4.56E-08	2.56E-08	1.68E-08	9.24E-09	6.00E-09	4.27E-09	3.22E-09	2.52E-09	2.03E-09	1.68E-09	1.41E-09
ESE	1.49E-07	8.54E-08	5.70E-08	3.19E-08	2.10E-08	1.50E-08	1.14E-08	8.94E-09	7.24E-09	5.99E-09	5.04E-09
SE	3.90E-07	2.25E-07	1.52E-07	8.57E-08	5.67E-08	4.09E-08	3.12E-08	2.47E-08	2.01E-08	1.67E-08	1.41E-08
SSE	2.01E-07	1.15E-07	7.69E-08	4.30E-08	2.82E-08	2.02E-08	1.53E-08	1.21E-08	9.77E-09	8.09E-09	6.81E-09

WLS COL 2.3-5

TABLE 2.3-291 (Sheet 3 of 3)
 ANNUAL AVERAGE χ/Q (SEC/M³) FOR NORMAL RELEASES 8.00 DAY DECAY, DEPLETED
 (FOR EACH 22.5° SECTOR AT THE DISTANCES (MILES) SHOWN AT THE TOP)

SECTOR	.5-1	1-2	2-3	3-4	4-5	5-10	10-20	20-30	30-40	40-50
S	2.73E-06	8.84E-07	4.03E-07	2.51E-07	1.77E-07	8.80E-08	3.24E-08	1.48E-08	8.65E-09	5.72E-09
SSW	2.52E-06	8.19E-07	3.72E-07	2.30E-07	1.62E-07	8.00E-08	2.92E-08	1.33E-08	7.74E-09	5.11E-09
SW	2.06E-06	6.76E-07	3.07E-07	1.89E-07	1.32E-07	6.49E-08	2.35E-08	1.06E-08	6.22E-09	4.12E-09
WSW	2.50E-06	8.05E-07	3.66E-07	2.27E-07	1.60E-07	7.96E-08	2.92E-08	1.33E-08	7.77E-09	5.12E-09
W	2.55E-06	8.21E-07	3.75E-07	2.34E-07	1.65E-07	8.28E-08	3.07E-08	1.41E-08	8.32E-09	5.53E-09
WNW	2.54E-06	8.20E-07	3.77E-07	2.36E-07	1.67E-07	8.35E-08	3.11E-08	1.43E-08	8.41E-09	5.59E-09
NW	2.27E-06	7.36E-07	3.36E-07	2.08E-07	1.46E-07	7.28E-08	2.68E-08	1.23E-08	7.29E-09	4.87E-09
NNW	1.71E-06	5.66E-07	2.57E-07	1.57E-07	1.09E-07	5.31E-08	1.90E-08	8.54E-09	4.99E-09	3.30E-09
N	1.33E-06	4.52E-07	2.06E-07	1.24E-07	8.47E-08	4.03E-08	1.39E-08	6.09E-09	3.51E-09	2.30E-09
NNE	9.95E-07	3.37E-07	1.51E-07	8.99E-08	6.12E-08	2.88E-08	9.86E-09	4.29E-09	2.46E-09	1.61E-09
NE	7.64E-07	2.57E-07	1.14E-07	6.75E-08	4.57E-08	2.14E-08	7.29E-09	3.17E-09	1.83E-09	1.20E-09
ENE	6.53E-07	2.17E-07	9.69E-08	5.80E-08	3.96E-08	1.89E-08	6.56E-09	2.91E-09	1.69E-09	1.12E-09
E	8.36E-07	2.73E-07	1.24E-07	7.63E-08	5.32E-08	2.61E-08	9.49E-09	4.31E-09	2.53E-09	1.69E-09
ESE	2.65E-06	8.46E-07	3.87E-07	2.43E-07	1.72E-07	8.69E-08	3.26E-08	1.51E-08	8.99E-09	6.01E-09
SE	6.89E-06	2.18E-06	9.96E-07	6.30E-07	4.50E-07	2.29E-07	8.75E-08	4.12E-08	2.48E-08	1.67E-08
SSE	3.57E-06	1.15E-06	5.23E-07	3.28E-07	2.33E-07	1.17E-07	4.40E-08	2.04E-08	1.21E-08	8.11E-09

WLS COL 2.3-5

TABLE 2.3-292 (Sheet 1 of 3)
D/Q (M⁻²) AT EACH 22.5° SECTOR FOR NORMAL RELEASES
(FOR EACH DISTANCE (MILES) SHOWN AT THE TOP)

SECTOR	0.25	0.5	0.75	1	1.5	2	2.5	3	3.5	4	4.5
S	3.38E-08	1.14E-08	5.86E-09	3.60E-09	1.80E-09	1.09E-09	7.36E-10	5.33E-10	4.06E-10	3.19E-10	2.59E-10
SSW	3.67E-08	1.24E-08	6.37E-09	3.91E-09	1.95E-09	1.18E-09	8.00E-10	5.79E-10	4.41E-10	3.47E-10	2.81E-10
SW	3.55E-08	1.20E-08	6.17E-09	3.79E-09	1.89E-09	1.15E-09	7.74E-10	5.61E-10	4.27E-10	3.36E-10	2.72E-10
WSW	3.16E-08	1.07E-08	5.49E-09	3.37E-09	1.68E-09	1.02E-09	6.89E-10	5.00E-10	3.80E-10	2.99E-10	2.42E-10
W	2.67E-08	9.02E-09	4.63E-09	2.84E-09	1.42E-09	8.60E-10	5.82E-10	4.21E-10	3.20E-10	2.52E-10	2.04E-10
WNW	2.48E-08	8.37E-09	4.30E-09	2.64E-09	1.32E-09	7.98E-10	5.40E-10	3.91E-10	2.97E-10	2.34E-10	1.90E-10
NW	3.19E-08	1.08E-08	5.54E-09	3.40E-09	1.69E-09	1.03E-09	6.95E-10	5.04E-10	3.83E-10	3.02E-10	2.44E-10
NNW	3.29E-08	1.11E-08	5.71E-09	3.51E-09	1.75E-09	1.06E-09	7.17E-10	5.20E-10	3.95E-10	3.11E-10	2.52E-10
N	3.62E-08	1.22E-08	6.28E-09	3.86E-09	1.92E-09	1.17E-09	7.88E-10	5.71E-10	4.34E-10	3.42E-10	2.77E-10
NNE	4.14E-08	1.40E-08	7.18E-09	4.41E-09	2.20E-09	1.33E-09	9.02E-10	6.53E-10	4.97E-10	3.91E-10	3.17E-10
NE	3.87E-08	1.31E-08	6.71E-09	4.12E-09	2.06E-09	1.25E-09	8.43E-10	6.11E-10	4.64E-10	3.66E-10	2.96E-10
ENE	2.60E-08	8.78E-09	4.51E-09	2.77E-09	1.38E-09	8.37E-10	5.66E-10	4.10E-10	3.12E-10	2.46E-10	1.99E-10
E	1.78E-08	6.02E-09	3.09E-09	1.90E-09	9.47E-10	5.74E-10	3.88E-10	2.81E-10	2.14E-10	1.69E-10	1.36E-10
ESE	3.82E-08	1.29E-08	6.63E-09	4.07E-09	2.03E-09	1.23E-09	8.32E-10	6.03E-10	4.58E-10	3.61E-10	2.92E-10
SE	8.66E-08	2.93E-08	1.50E-08	9.23E-09	4.60E-09	2.79E-09	1.89E-09	1.37E-09	1.04E-09	8.19E-10	6.63E-10
SSE	4.05E-08	1.37E-08	7.03E-09	4.32E-09	2.15E-09	1.31E-09	8.83E-10	6.40E-10	4.87E-10	3.83E-10	3.10E-10

WLS COL 2.3-5

TABLE 2.3-292 (Sheet 2 of 3)
D/Q (M⁻²) AT EACH 22.5° SECTOR FOR NORMAL RELEASES
(FOR EACH DISTANCE (MILES) SHOWN AT THE TOP)

SECTOR	5	7.5	10	15	20	25	30	35	40	45	50
S	2.14E-10	1.05E-10	6.58E-11	3.33E-11	2.01E-11	1.35E-11	9.67E-12	7.26E-12	5.64E-12	4.51E-12	3.68E-12
SSW	2.32E-10	1.14E-10	7.15E-11	3.61E-11	2.19E-11	1.47E-11	1.05E-11	7.89E-12	6.13E-12	4.90E-12	4.00E-12
SW	2.25E-10	1.10E-10	6.92E-11	3.50E-11	2.12E-11	1.42E-11	1.02E-11	7.64E-12	5.94E-12	4.74E-12	3.87E-12
WSW	2.00E-10	9.82E-11	6.16E-11	3.11E-11	1.89E-11	1.26E-11	9.06E-12	6.80E-12	5.29E-12	4.22E-12	3.45E-12
W	1.69E-10	8.28E-11	5.20E-11	2.63E-11	1.59E-11	1.07E-11	7.64E-12	5.74E-12	4.46E-12	3.56E-12	2.91E-12
WNW	1.57E-10	7.69E-11	4.82E-11	2.44E-11	1.48E-11	9.89E-12	7.09E-12	5.32E-12	4.14E-12	3.31E-12	2.70E-12
NW	2.02E-10	9.90E-11	6.21E-11	3.14E-11	1.90E-11	1.27E-11	9.13E-12	6.85E-12	5.33E-12	4.26E-12	3.48E-12
NNW	2.08E-10	1.02E-10	6.41E-11	3.24E-11	1.96E-11	1.31E-11	9.42E-12	7.07E-12	5.50E-12	4.39E-12	3.59E-12
N	2.29E-10	1.12E-10	7.05E-11	3.56E-11	2.16E-11	1.45E-11	1.04E-11	7.78E-12	6.05E-12	4.83E-12	3.94E-12
NNE	2.62E-10	1.29E-10	8.06E-11	4.07E-11	2.47E-11	1.65E-11	1.19E-11	8.90E-12	6.92E-12	5.53E-12	4.51E-12
NE	2.45E-10	1.20E-10	7.53E-11	3.81E-11	2.30E-11	1.55E-11	1.11E-11	8.31E-12	6.46E-12	5.16E-12	4.21E-12
ENE	1.65E-10	8.06E-11	5.06E-11	2.56E-11	1.55E-11	1.04E-11	7.44E-12	5.58E-12	4.34E-12	3.47E-12	2.83E-12
E	1.13E-10	5.53E-11	3.47E-11	1.75E-11	1.06E-11	7.12E-12	5.10E-12	3.83E-12	2.98E-12	2.38E-12	1.94E-12
ESE	2.42E-10	1.19E-10	7.44E-11	3.76E-11	2.28E-11	1.53E-11	1.09E-11	8.21E-12	6.38E-12	5.10E-12	4.16E-12
SE	5.48E-10	2.69E-10	1.69E-10	8.52E-11	5.16E-11	3.46E-11	2.48E-11	1.86E-11	1.45E-11	1.16E-11	9.43E-12
SSE	2.57E-10	1.26E-10	7.89E-11	3.99E-11	2.41E-11	1.62E-11	1.16E-11	8.71E-12	6.77E-12	5.41E-12	4.42E-12

WLS COL 2.3-5

TABLE 2.3-292 (Sheet 3 of 3)
D/Q (M⁻²) AT EACH 22.5° SECTOR FOR NORMAL RELEASES
(FOR EACH DISTANCE (MILES) SHOWN AT THE TOP)

SECTOR	.5-1	1-2	2-3	3-4	4-5	5-10	10-20	20-30	30-40	40-50
S	6.09E-09	1.88E-09	7.49E-10	4.09E-10	2.60E-10	1.12E-10	3.46E-11	1.37E-11	7.33E-12	4.54E-12
SSW	6.62E-09	2.05E-09	8.14E-10	4.45E-10	2.83E-10	1.21E-10	3.76E-11	1.49E-11	7.97E-12	4.93E-12
SW	6.41E-09	1.98E-09	7.88E-10	4.31E-10	2.74E-10	1.18E-10	3.65E-11	1.45E-11	7.71E-12	4.78E-12
WSW	5.71E-09	1.76E-09	7.02E-10	3.83E-10	2.44E-10	1.05E-10	3.25E-11	1.29E-11	6.87E-12	4.25E-12
W	4.81E-09	1.49E-09	5.92E-10	3.23E-10	2.06E-10	8.83E-11	2.74E-11	1.09E-11	5.79E-12	3.59E-12
WNW	4.47E-09	1.38E-09	5.49E-10	3.00E-10	1.91E-10	8.19E-11	2.54E-11	1.01E-11	5.38E-12	3.33E-12
NW	5.75E-09	1.78E-09	7.07E-10	3.86E-10	2.46E-10	1.06E-10	3.27E-11	1.30E-11	6.92E-12	4.29E-12
NNW	5.93E-09	1.83E-09	7.30E-10	3.99E-10	2.53E-10	1.09E-10	3.38E-11	1.34E-11	7.14E-12	4.42E-12
N	6.52E-09	2.02E-09	8.02E-10	4.38E-10	2.79E-10	1.20E-10	3.71E-11	1.47E-11	7.85E-12	4.86E-12
NNE	7.46E-09	2.31E-09	9.18E-10	5.01E-10	3.19E-10	1.37E-10	4.25E-11	1.68E-11	8.99E-12	5.56E-12
NE	6.97E-09	2.16E-09	8.57E-10	4.69E-10	2.98E-10	1.28E-10	3.97E-11	1.57E-11	8.40E-12	5.20E-12
ENE	4.69E-09	1.45E-09	5.76E-10	3.15E-10	2.00E-10	8.59E-11	2.66E-11	1.06E-11	5.64E-12	3.49E-12
E	3.21E-09	9.93E-10	3.95E-10	2.16E-10	1.37E-10	5.89E-11	1.83E-11	7.24E-12	3.87E-12	2.39E-12
ESE	6.89E-09	2.13E-09	8.46E-10	4.63E-10	2.94E-10	1.26E-10	3.92E-11	1.55E-11	8.29E-12	5.13E-12
SE	1.56E-08	4.82E-09	1.92E-09	1.05E-09	6.67E-10	2.86E-10	8.88E-11	3.52E-11	1.88E-11	1.16E-11
SSE	7.31E-09	2.26E-09	8.98E-10	4.91E-10	3.12E-10	1.34E-10	4.16E-11	1.65E-11	8.80E-12	5.45E-12

TABLE 2.3-293
LEE NUCLEAR STATION DESIGN TEMPERATURES

	Frequency of Occurrence		
	0%	100-year	0.4 %
Cooling dry-bulb temperature, °F	103	107	94
Coincident wet-bulb temperature, °F	78	84	77
Evaporation wet-bulb (noncoincident), °F	81	85	77

	Dry Bulb Temperature °F	
	Maximum	Minimum
0.4 percent annual exceedance	94	20
0 percent exceedance	103	-1
100-year return	107	-5

Notes:

1. Based on 45 years (1963-2007) of meteorological data measured at the NWS station at Greenville-Spartanburg Airport (GSP).

TABLE 2.3-294
LEE NUCLEAR STATION TSC HVAC DISTANCES AND
DIRECTIONS

WLS COL 2.3-4	Release Point	Distance (m)	Direction to Source
			from receptor (°)
	Unit 1 Containment Shell	214.6	341
	Unit 2 Containment Shell	249.6	18

Notes:

1. Distances and directions based on the nearest point on the Maintenance Support Building from each unit's containment shell.
2. Directions are relative to true North.

TABLE 2.3-295
TSC ATMOSPHERIC DISPERSION FACTORS (χ/Q) FOR
ACCIDENT DOSE ANALYSIS (S/M³)

WLS COL 2.3-4	Time Interval	Unit 1 Containment Shell Release	Unit 2 Containment Shell Release
	0 – 2 hours	1.31E-04	1.07E-04
	2 – 8 hours	9.58E-05	8.89E-05
	8 – 24 hours	3.44E-05	3.77E-05
	1 – 4 days	2.78E-05	3.16E-05
	4 – 30 days	2.13E-05	2.16E-05

2.4 HYDROLOGIC ENGINEERING

This **section** of the referenced DCD is incorporated by reference with the following departures and/or supplements

Section 2.4 describes the hydrological characteristics of the Lee Nuclear Site. The site location and description are provided in **Section 2.1** of this report in sufficient detail to support the safety analysis. This section discusses characteristics and natural phenomena that have the potential to affect the design basis for the Westinghouse AP1000 reactor (AP1000) units. The section is divided into the following 14 subsections:

- **2.4.1** Hydrologic Description.
 - **2.4.2** Floods.
 - **2.4.3** Probable Maximum Flood on Streams and Rivers.
 - **2.4.4** Potential Dam Failures.
 - **2.4.5** Probable Maximum Surge and Seiche Flooding.
 - **2.4.6** Probable Maximum Tsunami Flooding.
 - **2.4.7** Ice Effects.
 - **2.4.8** Cooling Water Canals and Reservoirs.
 - **2.4.9** Channel Diversions.
 - **2.4.10** Flood Protection Requirements.
 - **2.4.11** Low Water Considerations.
 - **2.4.12** Groundwater.
 - **2.4.13** Accidental Releases of Liquid Effluents in Ground and Surface Waters.
 - **2.4.14** Technical Specifications and Emergency Operation Requirements.
-

Subsection 2.4.1 of the DCD is renumbered as Subsection 2.4.15. This is being done to accommodate the incorporation of Regulatory Guide 1.206 numbering conventions for Section 2.4.

WLS COL 2.4-1
STD DEP 1.1-1

2.4.1 HYDROLOGIC DESCRIPTION

Information provided in this subsection includes descriptions of the site and its features, hydrosphere, hydrologic characteristics, drainage, dams and reservoirs, water management changes, and surface water uses.

2.4.1.1 Site and Facilities

The 1900-acre (ac.) Lee Nuclear Site is located south and west of the Broad River in eastern Cherokee County, South Carolina (Figure 2.2-201). The nuclear island for the Lee Nuclear Station is located south and west of the Ninety-Nine Islands Reservoir portion of the Broad River, approximately 1 mile (mi.) due northwest of the Ninety-Nine Islands Dam. In addition to the Broad River and several tributaries, the Ninety-Nine Islands Reservoir, Make-Up Pond B, Make-Up Pond A, and Hold-Up Pond A (Figure 2.4.1-201) make up the majority of the surface water features in the vicinity of the site. Make-Up Pond C is an off-site facility, located on a tributary of the Broad River, west of the Lee Nuclear Station (Figure 2.4.1-213).

2.4.1.1.1 Previous Construction Activities

The Lee Nuclear Site, formerly known as Cherokee Nuclear Station, was evaluated for and received a construction permit from the U.S. Nuclear Regulatory Commission to construct three Combustion Engineering System 80+ nuclear units. Approximately 750 ac. of ground were disturbed during the 1977-1982 construction activities, which resulted in extensive alteration of the site. This alteration included vegetation clearing; establishment of on-site construction roads; establishment of a railroad spur to the site; extensive excavation and grading with heavy equipment; building of on-site warehouses, shops, and construction support facilities; and construction of power unit buildings (portion of one power block building and about half of its associated cylindrical reactor containment/shield building). About 25 ac. were excavated into underlying bedrock for construction of the reactor units.

The site currently consists of open, partially-developed industrial land with low groundcover vegetation and scattered areas of sparse tree growth. However, the terrestrial environment surrounding the site consists primarily of deciduous hardwood forest and farms. The aquatic environs are dominated by the Broad River and the Ninety-Nine Islands Reservoir.

The Lee Nuclear Station is planned within the large, open, contiguous area of land that was cleared for previous construction activities on the site. The partially built reactor containment building is to be razed prior to new construction. The base mat slab and several warehouses will be kept. Construction of the intake structure

is planned on the Broad River, and the blowdown discharge sparger is planned on upstream side of Ninety-Nine Islands Dam.

2.4.1.1.2 Plant Design

Duke Energy selected the AP1000 certified plant design for the Lee Nuclear Station combined operating license application. The AP1000 units (Units 1 and 2) are planned to be in the vicinity of the previously proposed Cherokee Units 1 and 3. The AP1000 is rated at 3400 megawatts thermal (MWt) with a minimum electrical output of 1000 megawatts electrical (MWe). Each unit uses two mechanical draft towers for circulating water system cooling with the intake system providing all raw water requirements. During normal flow conditions raw water is pumped from Broad River raw water intake structure to Make-Up Pond A through the raw water discharge structure. During low-flow conditions raw water from Make-Up Pond B is pumped from the Make-Up Pond B intake structure to Make-Up Pond A through the raw water discharge structure. If Make-Up Pond B usable storage is not sufficient to meet plant needs, Make-Up Pond C is then used to supply supplemental water. Water is pumped from the Make-Up Pond C intake structure to a discharge structure in Make-Up Pond B and then is pumped from Make-Up Pond B to Make-Up Pond A, as previously described. The ultimate heat sink for the Lee Nuclear Station is the atmosphere.

2.4.1.1.3 Safety-Related Structures

The plant arrangement is comprised of five principal structures (as described in [DCD Section 1.2.1.6](#)): nuclear island, turbine building, annex building, diesel generator building, and radioactive waste building. Of the five principal structures, only the nuclear island is designed to Category I seismic requirements, and it contains all safety-related equipment for accident mitigation. The nuclear island consists of a free-standing steel containment building, a concrete shield building, and an auxiliary building. The foundation for the nuclear island is an integral basemat that supports these buildings.

The DCD reference floor elevation of 100 ft. corresponds to the nuclear island finished floor elevation set at 593 ft. above msl. Therefore, the nuclear island basemat elevation is 553.5 ft. above msl. Yard grade elevation is 592 ft. above msl, which keeps water from pooling in areas of safety related structures ([Subsection 2.4.2.3](#)). An extensive site stormwater drainage system is planned and is slated for implementation before the construction commences on Units 1 and 2. The elevations of safety-related components are presented on [Table 2.4.1-201](#).

2.4.1.1.4 Plant Water Systems

Plant water consumption and water treatment for the Lee Nuclear Station are determined from the AP1000 Design Control Document, site characteristics, and engineering evaluations. The raw water system supplies water to Make-Up Pond A for plant use, including make-up to the circulating water system (CWS) cooling towers, to makeup for water consumed as a result of evaporation, drift and blowdown. The raw water intake structure is located on the west bank of the

Broad River, north-northeast of Unit 2 (Figure 2.4.1-201). The raw water discharge structure is located at the north end of Make-Up Pond A near the Unit 2 cooling towers. Water withdrawn from the Broad River is pumped into Make-Up Pond A and from there enters the make-up water intake structure. Raw water is also processed through the clarifier and used in plant water systems including the service water system, the demineralized water treatment system and the fire protection system. Effluent from the Lee Nuclear Station is to be diffused into the river at the upstream face of the Ninety-Nine Islands Dam near the intakes for the hydroelectric station (Reference 256), avoiding recirculation of the plant effluent to the intake structure located approximately 1.25 river miles upstream (Figure 2.4.1-201).

Intake System

The intake system provides all raw water requirements for the plant. During normal flow conditions, raw water is pumped from the Broad River raw water intake structure to Make-Up Pond A through the raw water discharge structure. During low flow conditions, raw water from Make-Up Pond B is pumped from the Make-Up Pond B intake structure to Make-Up Pond A through the raw water discharge structure. If Make-Up Pond B usable storage is not sufficient to meet plant needs, Make-Up Pond C is then used to supply supplemental water. Water is pumped from the Make-Up Pond C intake structure to a discharge structure in Make-Up Pond B and then is pumped from Make-Up Pond B to Make-Up Pond A, as previously described.

After low flow conditions have ceased, Make-Up Pond B is replenished using water from the Broad River which is pumped into Make-Up Pond A and subsequently into Make-Up Pond B. Raw water is pumped from the Make-Up Pond A intake structure to Make-Up Pond B using the same piping to supply Make-Up Pond A with water from Make-Up Pond B. Water is discharged into Make-Up Pond B using the Make-Up Pond B intake structure. An alternative refill path is to use the refill pumps on the river intake structure that pump directly to Make-Up Pond B.

Make-Up Pond C is normally refilled directly from the river using the same refill pumps on the river intake structure that pump directly to Make-Up Pond B. The section of pipe between Make-Up Pond B and Make-Up Pond C is used to both supply Make-Up Pond B from Make-Up Pond C and to refill Make-Up Pond C from the river. Water is discharged into Make-Up Pond C using the Make-Up Pond C intake structure. An alternative refill path for Make-Up Pond C is to pump from the Broad River into Make-Up Pond A, then pump from Make-Up Pond A to Make-Up Pond B, and then pump from Make-Up Pond B to Make-Up Pond C using a dedicated line only for refilling Make-Up Pond C. The intake, discharge, and pump structures for Make-Up Ponds A and B are shown in Figure 2.4.1-201. Make-Up Pond C is an off-site facility, located west of the Lee Nuclear Station, as shown in Figure 2.4.1-213.

The river intake structure serves as a platform to support trash racks, traveling screens, pumps, motors, and other equipment. Intake water taken from the Broad River passes through bar screens and traveling screens designed to minimize

uptake of aquatic biota and debris. Each traveling screen has fish collection and return capability. Return of impinged fish is to a location downstream of the intake. Debris collected by the trash racks and traveling screens is collected and disposed of as solid waste (Reference 256).

The raw water requirements vary depending on the operating mode, therefore the flow rates and intake velocities also vary. During the first four modes of operation, which include power operation, startup, hot standby, and safe shutdown, both the CWS and the service water system (SWS) require makeup water. The raw water system (RWS) supplies an average of 35,030 gallons per minute (gpm) (60,001 gpm maximum) raw water flow as makeup to the CWS, the SWS, and the demineralized water treatment system for the two units. Flow to the fire protection system (FPS) and the waste water system (WWS) is intermittent. The screens are sized so that the average through-screen velocity is in accordance with the Section 316 (b) of the Clean Water Act. The intake velocity is less than 0.5 fps. For the remaining two modes of operation, cold shutdown and refueling, the flow rate and the intake velocity is less as only the SWS requires makeup water from the raw water intake. For these final two modes of operation, the flow rate is 650 gpm per unit and the intake velocity is negligible.

Discharge System

The primary purpose of the discharge system is to disperse cooling tower blowdown into the Broad River along with other wastewater streams to limit the concentration of dissolved solids in the heat rejection system. Any additives in the discharge are as approved by the U.S. Environmental Protection Agency (EPA) as safe for humans and the environment. The volume and concentration of the constituents discharged to the environment will meet the requirements established in the South Carolina Department of Health and Environmental Control (SCDHEC) administered National Pollution Discharge Elimination System (NPDES) permit.

Effluent from the Lee Nuclear Station is to be diffused into the river at the upstream face of the Ninety-Nine Islands Dam near the intakes for the hydroelectric generating units. This discharge includes non-radioactive process waste (including cooling tower blowdown) and low level liquid radioactive waste (at an average rate of 4 gpm within regulatory limits).

The discharge structure consists of a submerged pipe that is perforated for the last portion of its length, diffusing the effluent into the hydroelectric station intakes. The effluent discharge rate to the Broad River during normal operations is approximately 8216 gpm with a maximum plant water discharge rate of 28,778 gpm (for two units).

2.4.1.2 Hydrosphere

The location of the Lee Nuclear Station, as described in Subsection 2.4.1.1, falls within the Broad River basin. The Broad River and Ninety-Nine Islands Reservoir are the main hydrologic features that may affect or be affected by construction activities in the immediate vicinity of the Lee Nuclear Site. Ninety-Nine Islands

Reservoir is the nearest major body of surface water to the Lee Nuclear Site. This reservoir is an impoundment of the Broad River by Ninety-Nine Islands Dam. The Lee Nuclear Site is located adjacent to the reservoir, which surrounds the site to the north and east. Land along the south boundary of the site is private property. Current surface water features at the site include Make-Up Pond B, Make-Up Pond A, and Hold-Up Pond A. Make-Up Pond C is an off-site facility, located on a tributary of the Broad River, west of the Lee Nuclear Station. A brief description of local groundwater conditions is also provided in this subsection.

2.4.1.2.1 Physiography and Topography

The Lee Nuclear Site is located within the Piedmont physiographic province, a southwest to northeast-oriented province of the Appalachian Mountain System (Figure 2.4.1-203). The Piedmont province is 80 – 120 mi. wide, and it is situated between the Blue Ridge province, a mountainous region to the northwest, and the Atlantic Coastal Plain province to the southeast. The province is a seaward-sloping plateau, dominated by a monotonous topography of low rounded ridges with gentle slopes and ravines largely underlain by saprolite developed on crystalline rock.

The principal drainageway in the region of the Lee Nuclear Site is the Broad River. Near the larger streams, tributaries cut through deep and steep valleys that (when traced headward) become wide, shallow, and of gentle gradient. The regional southeastward drainage of the Broad River basin is reflected in the trend of the Broad River (Reference 220). The Piedmont region of the Broad River basin is a plateau of forested, rolling hills with tight, dissected river valleys that generally contain small floodplains. The tributaries of the Broad River generally follow a dendritic pattern before draining to the Broad River and eventually the Atlantic Ocean.

Construction activities at the former Cherokee Nuclear Site altered local topography to cut and fill the site to a yard-grade elevation of 588 ft. above msl. Following excavation in the power block area, site topography changed from hills and valleys to a relatively flat upland setting punctuated by a massive excavation to competent rock, which over time filled with water from both groundwater seepage and precipitation. Subsection 2.4.12.2.3 describes the dewatering of this excavation in support of exploration activities for the Lee Nuclear Station. Numerous springs and seeps identified during the 1973 investigation (Reference 214) were disturbed during the 1975 – 1982 construction activities for the Cherokee Nuclear Station. Those springs and seeps were located within valley draws and natural drainage ways. Surface conditions around these springs appear to have been altered so that no flow-through discharge occurs. The undisturbed topography remaining at the Lee Nuclear Site is generally characterized by rounded hilltops and narrow valleys with elevations ranging from 511 ft. at the Broad River to around 810 ft. along the ridgeline of McKowns Mountain, located west of the power block area and south of Make-Up Pond B.

2.4.1.2.2 Upper Broad River Watershed

The Broad River basin region, the Broad River, and the majority of its tributaries originate in the Blue Ridge Mountains of North Carolina and extend toward the foothills before entering the Piedmont ecoregion, all within the larger Santee River basin, U.S. Geological Survey (USGS) (six-digit Hydrological Unit Code [HUC] 030501) (Figure 2.4.1-204) (Reference 290).

The USGS divides the Broad River basin into the Upper Broad (HUC 03050105) and Lower Broad (HUC 03050106) River basins with the Lee Nuclear Site positioned within the Upper Broad River basin (Figure 2.4.1-204). The Upper Broad River basin is located in both North and South Carolina. The Broad River drainage basin above Ninety-Nine Islands Dam is located within the Upper Broad River basin and includes the Green River, First Broad River, Second Broad River, and Buffalo Creek as major tributaries (Figure 2.4.1-205) (Reference 231). The drainage area of the Upper Broad River basin is approximately 2500 sq. mi. (Table 2.4.1-202) and is situated over the North Carolina-South Carolina state border. The drainage area of the Upper Broad River basin to Ninety-Nine Islands Dam (one-half river mile downstream from the site) is approximately 1550 sq. mi. (Reference 216).

Watershed elevations range from about 1200 ft. above msl at the headwaters of the First Broad River in the mountains of North Carolina to 620 ft. above msl when the Broad River crosses the North Carolina/South Carolina border. Watershed elevations along the Broad River continue to decrease southward to 511 ft. above msl upstream of Ninety-Nine Islands Dam, and 440 ft. below Ninety-Nine Islands Dam. At the confluence of the Broad River with the Saluda River in Columbia, South Carolina the elevation is 140 ft. above msl. The slope percentage of the Broad River is 0.55, and it has a gradient of 28.9 ft/mi (Reference 290).

The Broad River starts in Buncombe County, flows through Henderson, Rutherford and Cleveland counties in North Carolina and then into Cherokee County, South Carolina. In North Carolina, the basin encompasses most of Cleveland, Polk, and Rutherford counties and small portions of Buncombe, Henderson, Lincoln, Gaston, Burke and McDowell counties (Figure 2.4.1-206). Larger municipalities within the basin include the towns of Forest City, Kings Mountain, Lake Lure, Rutherfordton, Shelby, and Spindale. Approximately one-half of the basin is covered in forest; however, agriculture is still widespread (Reference 231).

2.4.1.2.2.1 Local Watersheds

The Broad River accepts drainage from Ross Creek (Sarratt Creek), Mikes Creek, Bowens River (Wylies Creek), the Buffalo Creek watershed, and the Cherokee watershed (Figure 2.4.1-207). Further downstream, Peoples Creek (Furnace Creek, Toms Branch) drains into the Broad River near the city of Gaffney. Doolittle Creek enters the river near the town of Blacksburg, followed by London Creek (which feeds Lake Cherokee and Make-Up Pond C, and has the Little London Creek as a tributary), Bear Creek, McKowns Creek (which feeds Make-Up Pond B at the site), Dry Branch, the Kings watershed, and Quinton Branch. Mud Creek

enters the Broad River next, downstream from Mud Islands, followed by Guyonmbore Creek, Mountain Branch, Abington Creek (Wolf Branch, Service Branch, and Jenkins Branch), the Thicketty Creek watershed, Beaverdam Creek (McDaniel Branch), the Bullock Creek watershed, and Dry Creek (Nelson Creek). There are numerous ponds and lakes located off-site (totaling 246 ac., not including the approximately 620 ac. Make-Up Pond C) in this watershed (03050105-090) and all 133 stream mi. are classified as fresh water (Reference 268).

The Lee Nuclear Site is located in USGS Hydrologic Unit 03050105-090 of Cherokee and York counties, South Carolina, and this unit consists primarily of the Broad River and its tributaries from the North Carolina border to the Pacolet River (Figure 2.4.1-205). Land use/land cover in the watershed includes: 67.8 percent forested, 18.8 percent agriculture land, 5 percent scrub/shrub land, 4.5 percent urban land, 2.8 percent water, and 1.1 percent barren (Reference 268).

2.4.1.2.2.2 Broad River Description

The Broad River has a length of about 185 river mi. The drainage area of the Upper Broad River basin is approximately 2500 sq. mi. (North Carolina and South Carolina). The drainage area of the Upper Broad River basin to Ninety-Nine Islands Dam, one-half river mile downstream from the site, is approximately 1550 sq. mi. The Broad River drainage basin above Ninety-Nine Islands Dam includes these major tributaries: Green River, First Broad River, Second Broad River, and Buffalo Creek (Reference 232).

The Broad River originates upstream of Lake Lure. Lake Lure Dam is located on the east side of Lake Lure, and the majority of the lake water is provided by the Broad River (also known as the Rocky Broad River).

The middle and lower portions of the Broad River in North Carolina cover about 40 river mi. from Lake Lure to the confluence of the Second Broad River near the Cleveland-Rutherford county line. Major tributaries in this section include the Green and Second Broad Rivers. The headwaters of these tributaries begin in the Mountains and then flow into the Piedmont ecoregion. Smaller tributary catchments of the Broad River include Mountain and Cleghorn creeks (Reference 232). The headwater reaches of the Green River are located in Henderson County, North Carolina.

Discharge Characteristics

The nature of flow in the Broad River was characterized by USGS gauging stations described in Table 2.4.1-203. The 2005 annual mean flows are also provided in Table 2.4.1-203 to illustrate the Broad River's gaining stream characteristics. USGS gauging stations are shown on Figure 2.4.1-205.

Broad River discharge recorded at the USGS Station No. 02153551 located just below Ninety-Nine Islands Dam ranged from 138 cubic feet per second (cfs) on September 14, 2002, to over 60,000 cfs in September 2004. Additionally, the

Gaffney USGS Station (No. 02133500) located approximately 8 mi. north of the Lee Nuclear Site and having about 60 sq. mi. less drainage area than Ninety-Nine Islands Reservoir, detected the highest recorded flow on record of 119,100 cfs, recorded on August 14, 1940 ([Reference 214](#)).

Based on an 83-year period of record (1926 – 2008) for the Broad River at the Gaffney Station, an average annual flow of the Broad River was determined to be approximately 2500 cfs. The 83-year period of record was derived using three USGS stream gauges located on the Broad River. The Broad River gauge near Gaffney, SC (USGS 02153500) is located just upstream of the Lee Nuclear Site and has available data from 1938-1971 and 1986-1990. The Gaffney gauge data was used without correction for drainage area size and applied to the site.

The Broad River gauge near Blacksburg, SC (USGS 02153200) is located upstream from the Gaffney gauge and has available data from 1997-2008. The Blacksburg gauge data was corrected by a ratio of drainage areas for the Gaffney gauge to the Blacksburg gauge and then applied to the site. The Broad River gauge near Boiling Springs, NC (USGS 02151500) is located upstream from the Blacksburg gauge and has available data from 1926-2008. Only data from the absent years of the Gaffney and Blacksburg gauges were corrected by a ratio of drainage areas for the Gaffney gauge to the Boiling Springs gauge and then applied to the site. The overlapping data from the Boiling Springs gauge were not utilized.

Low-flow conditions on the Broad River are a function of natural flow in the rivers and streams, available storage capacity of upstream reservoirs, and regulated discharge flow from upstream dams. Low-flow conditions are generally defined as the lowest consecutive 7-day stream flow that is likely to occur every 10 years (7Q10). The 7Q10 was calculated with the same database described above to be 439 cfs using Log-Pearson Type III distribution ([Subsection 2.4.11.5](#)).

The South Carolina climate is subject to periodic droughts. Since 1900, severe droughts have occurred statewide in 1925, 1933, 1954, 1977, 1983, 1986, 1990, 1993, 1998, 2002, 2007, and 2008. The drought that officially began in June 1998 abated in the late summer of 2002 with the onset of the hurricane season. The effects of these droughts are reflected in the Broad River discharge characteristics. Low-flow conditions are further discussed in [Subsection 2.4.11](#).

In September 2006, during a bathymetry study ([Reference 298](#)), water velocities were characterized in the vicinity of the intake structure. Station No. 02153551 (located below the Ninety-Nine Islands Dam) measured Broad River discharge ranging from 1960–3090 cfs at the time of this assessment. Bathymetry at the intake structure shows a narrow linear feature (i.e., scour hole) aligned along the direction of flow and appears to be approximately 30-ft. deep (elevation 480 ft. msl). This linear feature is located in a section of the Broad River channel that is approximately 240 ft. across. Water velocities were measured at seven stations along a transect crossing the Broad River perpendicular to the intake at channel depths of 1, 5, 10, and 15 ft. Water velocity around the intake structure had an average flow rate of 0.32 feet per second (fps) with a standard deviation of 0.04 fps. No water velocity measurements were obtained near the dam and the proposed

plant discharge location due to access restrictions and safety considerations related to hydroelectric operations.

To supplement characterization of the Broad River as a heat sink for the discharge of cooling water blowdown, temperature data from USGS Station No. 02156500 (located near Carlisle, South Carolina, in Union County) were compiled and are presented in [Table 2.4.1-204](#). For the period 1996 to 2006, the monthly water temperatures ranged from 40.8°F to 85.3°F (4.9°C to 29.6°C).

Generally, the Broad River flow conditions and discharge characteristics are consistent with those observed in the 1970's. As such, the bedforms and sediment transport observations presented in the Cherokee Nuclear Station Construction Permit Environmental Report (ER) are relevant today and are discussed below.

Bedforms

The bottom of the Broad River is influenced by the formation of bedforms. Bedforms are likely to be (1) scoured in bedrock, (2) formed from sand resulting in migrating dunes, (3) created from alluvial bed material of mixed sizes forming pools and riffles, or (4) produced by a combination of the above. Pools and riffles are the most common bedforms. At low flow, riffles are essentially flow-resistant dams forming each upstream pool. Water velocity over the riffles at low flow is considerably greater than that in adjacent pools. Therefore, fine sediment such as sand or silt is found on riffles.

At high flow, the stepped water surface characteristic of pools and riffles at low flow tends to disappear, and bedform conditions may be greatly altered from that found at low flow. At high flow, pools become areas of greater scour and thus may have similar water velocity as that found in the adjacent riffle areas. Although pools are quiet environments similar to impoundments during low flow, they generally have a high water velocity at the center of the river and the outside bends of the river. During high river flows the riparian vegetation and inside bends of the river provide the low velocity regions typically provided by the pools at low flow. The boundary between a pool and the adjacent riffles is primarily a function of discharge. The basic morphology of these forms does not change through exposure to a variety of flow levels. The most distinct break is between a riffle and an upstream pool; the deepest part of the pool is likely to be fairly close to the adjacent downstream riffle ([Reference 214](#)).

Bedform surveys for areas on the Broad River upstream and downstream of the Lee Nuclear Station were conducted in the 1970s. Between the Gaston Shoals impoundment and U.S. Highway 29 (U.S. 29), the Broad River channel was characterized by pools and riffles. The riffles were bedrock ridges cut into felsic schist. The bed material in pools and moving through riffles was entirely composed of uniform sand. Between U.S. 29 and Cherokee Falls, a resistant outcrop of felsic gneiss formed a long, continuous area of shallow riffles in which no pools had developed. From Cherokee Falls to Ninety-Nine Islands Reservoir, the stream was again characterized by bedrock highs (riffles) formed from schist, alternating with deeper pools in which the substrate material was nearly all sand. Below the reservoir another resistant gneiss bedrock outcrop created a long,

continuous shallow riffle area that gave way downstream to more pools and riffles. Below the Irene Bridge, the pools became larger and much longer while the riffles became smaller and less conspicuous. This dominance of pools was accompanied by steeper river banks, a diminution of sand beds, and the introduction of silt and mud substrates in the pools (Reference 214).

In summary, alternating pools and riffles cut in bedrock are the dominant bedforms of the Broad River above and below the Lee Nuclear Station. Where bands of resistant gneiss cross the course of the river, they create anomalous shallow riffles. The bedload is mostly coarse sand, making scoured rock outcrops and sand beds the two common substrate types (Reference 214).

Sediment Transport

The Broad River is generally wide and fairly shallow (Figure 2.4.1-208), and it normally carries a high bedload composed mainly of sands with some coarse gravels and cobbles. Water samples were collected in the early 1970s to estimate the suspended sediment load in the river for the Cherokee Nuclear Station Construction Permit Environmental Report (ER). Samples were collected from October 1973 through September 1974.

Sample results from Station 8, located just above the proposed site (Figure 2.4.1-206), ranged from 20 to 282 mg/L and an average sediment concentration of 73.9 mg/L, with a standard deviation of 63.3 mg/L (Reference 214). In a study conducted in 1989 – 1990 for the Ninety-Nine Islands Dam license renewal, the Broad River exhibited a mean TSS of 41 mg/L, ranging from 6 to 243 mg/L (Reference 216). Suspended solids concentrations can vary widely as a function of stream flow.

Analytical results from samples collected quarterly in 2006 show a mean TSS concentration of 11.5 mg/L. TSS concentrations ranged from 1 to 62 mg/L with a standard deviation of 12.4 mg/L. The waters within the main channel of the Broad River near the intake structure exhibited a mean TSS concentration of 10.2 mg/L. Additional sampling of the Ninety-Nine Islands Reservoir, conducted in 2007, reported a TSS range of less than 4 to 204 mg/L. Particle size analyses of suspended solids revealed a range from 0.00035 (clay) to 0.35355 millimeters (mm) (medium grade sand). From the five water samples collected and analyzed, the average of their median particle sizes was 0.0171 mm (medium silt) with a settling velocity calculated to be 0.0001 feet per second (fps).

The values used for the design basis are an average TSS concentration of 20 mg/L and a maximum TSS concentration of 300 mg/L, based on current Broad River data from Duke's surrounding power plants.

Modeling studies conducted for the water intake structure of the former Cherokee Nuclear Station demonstrated that local flows near the intake are expected to deter significant sediment accumulation in the local scour hole near the intake structure. However, this same study noted some bedload sediment deposits in the intake structure as a result of pump operations and high-flow events, which will require

annual maintenance dredging. Dredging would usually be limited to approximately 150 cubic yards (cu. yd.) annually.

2.4.1.2.2.3 Major Tributaries

The four major tributaries of the Broad River above the Lee Nuclear Site include the First Broad River, Second Broad River, Green River, and Buffalo Creek (Figure 2.4.1-206) (Reference 233).

First Broad River

The First Broad River originates in Rutherford County and flows into the Broad River in Cleveland County, North Carolina, just above the South Carolina border (Figure 2.4.1-205). The entire First Broad River and its tributaries are located in USGS Hydrologic Subbasin 030804. Tributaries of the First Broad River include Brier Creek and North Fork First Broad Creek, Brushy, Hinton, Knob, and Wards creeks (Reference 231, Figure 2.4.1-206).

Approximately two-thirds of the 426 sq mi. (Table 2.4.1-202) of the First Broad River subbasin are forested and one-third is in pasture. The largest urbanized areas in this subbasin are the towns of Shelby and Boiling Springs. These municipalities are restricted to the southern third of the subbasin and are concentrated along the U.S. 74 corridor. There are 11 permitted dischargers in the subbasin, including the towns of Shelby and Boiling Springs, wastewater treatment plants, and PPG Industries (Reference 232). The First Broad River has a slope of 0.33 percent and a gradient of 17.4 ft./mi., based on analysis of a USGS topographic map (Reference 290).

Second Broad River

The Second Broad River originates in McDowell County and flows into the Broad River near the Rutherford and Cleveland counties border (Figures 2.4.1-205 and 2.4.1-206). The Second Broad River and its tributaries lie within USGS Hydrologic Subbasin 030802; it has a drainage area of approximately 513 sq mi. (Table 2.4.1-202). Tributaries of the Second Broad River include Catheys, Hollands, and Roberson creeks (Figure 2.4.1-206). The largest urbanized areas are the towns of Spindale and Forest City. There are three permitted dischargers in this subbasin that release greater than 0.5 million gallons per day (Mgd) of effluent to the Second Broad River watershed. These are the wastewater plants for the towns of Spindale, Forest City, and Cone Denim LLC (Reference 232). The Second Broad River has a slope of 0.37 percent and a gradient of 19.7 ft./mi. (Reference 289).

Green River

The Green River has been impounded at two locations to form Lake Summit and Lake Adger (Figure 2.4.1-205). Both reservoirs are used to produce hydroelectric power. The Green River and its tributaries lie within USGS Hydrologic Subbasins 030802 and 030803 (Figures 2.4.1-205 and 2.4.1-206) and comprise a drainage area of approximately 137 sq. mi. (Table 2.4.1-202). This drainage area

is mostly undeveloped with more than 90 percent of the surface area forested. Tributaries of the Green River include the Hungry River and Brights Creek (Figure 2.4.1-206). R.J.G. Inc.'s Six Oaks Complex has the only permit to discharge on the Green River (above Summit Dam). The Bright's Creek Golf Club development has a temporary construction discharge permit; however, once the facility is operational, it is expected to have a nondischarge permit (Reference 232). The Green River has a slope of 0.69 percent and a gradient of 36.5 ft./mi. (Reference 289).

Buffalo Creek

Buffalo Creek drains eastern Cleveland, southwestern Lincoln, and northwestern Gaston counties in North Carolina (Figure 2.4.1-206), and this creek and its tributaries flow south through USGS Hydrologic Subbasins 030805 and 100 (Figure 2.4.1-206). The Buffalo Creek drainage area is approximately 181 sq. mi. (Table 2.4.1-202) in North Carolina and 16 sq. mi. in South Carolina. Approximately 40 percent of the surface area is pasture land, and almost 50 percent continues to be forested. Tributaries of Buffalo Creek include Muddy Fork and Beason Creek (Figure 2.4.1-206). Buffalo Creek is impounded approximately 16 river mi. northeast of the Lee Nuclear Site to form Kings Mountain Reservoir in North Carolina. The creek discharges into the Broad River approximately 7 river mi. north of Ninety-Nine Islands Dam (Reference 232). Buffalo Creek has a slope percentage of 0.29 and a gradient of 15.1 ft/mi (Reference 289).

2.4.1.2.2.4 Local Tributaries

In addition to the Broad River and its major tributaries, there are several smaller streams in the vicinity of the Lee Nuclear Site (above Ninety-Nine Islands Dam), including Cherokee Creek, Doolittle Creek, London Creek, and McKowns Creek. In addition, an intermittent stream flows into Make-Up Pond A (Figure 2.4.1-206).

The most significant of these features is McKowns Creek, which is dammed at the Lee Nuclear Site to form Make-Up Pond B (see Subsection 2.4.1.2.2.6). McKowns Creek's drainage area is estimated to be 1633 ac., including a small impoundment feeding the creek. The small impoundment has a drainage area of approximately 181 ac. (Reference 254). The intermittent stream mentioned in the previous paragraph features a drainage area of approximately 385 ac.

There are a number of other creeks and impoundments within a 6-mi. radius of the Lee Nuclear Site. Most of these features are hydraulically insignificant (i.e., small storage, low hazard structures, or outside drainage) with the exception of Make-Up Pond C. The largest of these features within this radius is Make-Up Pond C located on London Creek, as shown in Figure 2.4.1-213, which has a maximum storage of approximately 22,000 acre-feet (ac.-ft.). Details of Make-Up Pond C are provided in Subsection 2.4.1.2.3.1. Lake Cherokee (also known as Wildlife Dam and Reservoir) is located on London Creek just upstream of Make-Up Pond C. Lake Cherokee has a maximum storage of 720 ac.-ft. and is hydraulically insignificant.

2.4.1.2.2.5 Ninety-Nine Islands Reservoir

Ninety-Nine Islands Dam is located on the Broad River approximately 1 linear mi. southeast of the Lee Nuclear Station. The reservoir backs up to Cherokee Falls Dam, approximately 3 mi. to the north. The Ninety-Nine Islands Dam and associated hydroelectric plant were constructed in 1910, and the dam structure is a concrete gravity dam 62 ft. in height and 1568 ft. in length ([References 216 and 217](#)).

The Federal Energy Regulatory Commission (FERC) operating license for Ninety-Nine Islands Hydroelectric Station limits reservoir drawdown to 1 ft. below full pond (511 ft. above msl) from March through May and 2 ft. below full pond elevation from June through February. In addition, the minimum flows to be maintained below the dam are: 966 cfs January through April; 725 cfs May, June, and December; and 483 cfs July through November ([Reference 216](#)). When river flow drops below 483 CFS and the elevations drop to the maximum drawdown limit, the Ninety-Nine Islands Hydroelectric Station must discharge accumulated inflow on an hourly basis.

Reservoir Characteristics

Ninety-Nine Islands Dam impounds a 433-ac. mainstem “run-of-the-river” reservoir^a with a normal water level at 511 ft. above msl and a shoreline of approximately 14 mi. ([Reference 216](#)). Flow through Ninety-Nine Islands Reservoir is dominated by the flow of the river channel, which divides the reservoir into two backwater regions. The two backwater regions exhibit very little circulation during nonflood periods. Therefore, the average transit time through the reservoir is conservatively estimated from the volume of the reservoir along the main channel excluding the backwater areas. Based on a storage volume of 570 ac-ft along the main channel to a point about 0.7 river mi. upstream from the dam and an average annual flow of the Broad River of approximately 2500 cfs, the average transit time for water flow through the reservoir is approximately 3 hours. During low flow conditions the transit time slows to around 14 hours ([Subsection 2.4.11](#)).

From October 1998 to 2006, the USGS recorded a minimum pool elevation in the Ninety-Nine Islands Reservoir of 508.20 ft. on February 14, 2005 ([Reference 293](#)). Duke Power data from 1964 to 1973 indicate that the minimum pool elevation was 505.6 ft. during May 1965 ([Reference 214](#)). Low water considerations are discussed in [Subsection 2.4.11](#). The maximum water surface elevation for the Broad River at the site is discussed in [Subsections 2.4.2, 2.4.3 and 2.4.4](#). Based on the flood frequency curve generated from analysis of the USGS Gaffney gauge, the projected 100-yr flow is 97,900 cfs and the projected

-
- a. The mainstem refers to the main channel of the river in a river basin, as opposed to the streams and smaller rivers that feed into it. A “run-of-the-river” dam is a dam without a large reservoir and, therefore, with only a limited capacity for water storage.

500-year flow is 127,000 cfs. The corresponding elevations based on interpolation of the rating curve for Ninety-Nine Islands Dam and assuming flashboard failure are 520.95 ft. and 522.63 ft. for the 100-year and 500-year events, respectively.

Because the Ninety-Nine Islands Reservoir is a “run-of-the-river” reservoir, evaporation and seepage have little effect on the water budget of the reservoir. The aspects of annual yield and dependability as they relate to the construction or operation of Lee Nuclear Station are discussed above in terms of discharge and low-flow characteristics of the Broad River.

Morphology

Ninety-Nine Islands Reservoir is characterized by three hydrographic areas, the main river channel and two backwater areas, that have developed because of sedimentation patterns since impoundment of the reservoir. The reservoir is a dynamic system that is constantly changing, due to the effects of floods, low flow, sedimentation, and scouring. In its present state the reservoir is a combination of two large backwater areas separated by the river channel and its associated sediment bars, spits, banks, and coves. A bathymetry study of the reservoir was conducted in the fall of 1973 by Duke Power Company ([Reference 214](#)). In the fall of 2006, additional bathymetry of the reservoir and the Broad River was conducted. This impoundment exhibited a maximum depth of 35.2 ft. ([Figure 2.4.1-209](#), Sheet 1) and a mean depth of 9.2 ft. The impoundment is relatively shallow and relatively minor fluctuations in reservoir levels can result in significant changes in surface area. The estimated volume of storage is 1691 ac.-ft. based on the limited 233-ac. survey area. The U.S. Army Corps of Engineers (USACE) National Inventory of Dams (NID) reports the storage volume as 2300 ac.-ft. Deltaic sedimentation associated with creeks was evident in the backwater areas and limited the aerial extent of the survey.

The backwater areas can be divided into two hydrographic sections: one paralleling the river-influenced channel areas (being separated from them by an area of sediment deposition) and the other located at the lower end of each backwater area perpendicular to the main stream flow. Shallow backwater sections parallel to the main channel areas contain large deposits of river-borne sediments deposited during flooding conditions. The areas of backwater perpendicular to the river flow are less influenced by the main channel sediment transport. These sections exhibit relatively deeper waters with shoreline and bathymetric profiles more reflective of local topography and original reservoir characteristics ([Reference 214](#)).

The main channel area is characterized by a shallow sand and gravel bed extending through the center of the reservoir area and between the two major backwater areas. Unlike the previously described backwater areas, the main channel portion of the reservoir has a strong current when the hydroelectric station is operating and has relatively homogeneous physiochemical characteristics.

River-borne sedimentation has greatly altered the reservoir from its original condition. Dredging in the dam area has been performed periodically to ensure

efficient hydroelectric generating operations. Dredging activities include keeping the hydroelectric intakes clear of sediment, which is a routine maintenance issue for most hydroelectric projects in this area. Large areas of the stream bed in the original reservoir have been filled completely and stabilized by heavy vegetation growth. During the 1973 study, backwater areas that were not already completely filled, exhibited changes in some water depths in the first 6-month sampling period, thus illustrating the influence of heavy sedimentation (Reference 214).

Circulation and Mixing

Ninety-Nine Islands Reservoir circulation and mixing characteristics are influenced primarily by discharge. The central channel is almost completely dominated by river discharge and accounts for the primary circulation pattern of the reservoir during nonflood periods. Currents through the Ninety-Nine Islands Reservoir are much stronger than expected for an impoundment, although less than currents in the upstream and downstream river. Based on data from the 1975 Cherokee Nuclear Station Construction Permit ER, temperature and chemical constituents were homogeneous at all depths due to thorough turbulent mixing. Sampling performed in 2006 confirms the thorough mixing (Reference 214).

Backwater areas exhibit a very different flow regime because of the lack of circulation in these waters, especially during nonflood periods. Stagnation is common during low-flow periods. The backwater areas are influenced by temperature and tend to slightly stratify during periods of warm weather.

Wind apparently has little effect upon circulation in these backwater areas because they are protected by topographic relief and heavy vegetation, especially in the limited floodplain areas. Lower than normal dissolved oxygen concentrations result from decomposition of organic materials and poor circulation.

Flooding conditions greatly alter the normal hydrologic setting. Washover from the river channel portion of the reservoir during high flow tends to flush waters from the upper backwaters toward the lower portion of the reservoir. During these periods, extremely turbid conditions prevail throughout the impoundment due to the import of river-borne sediments and the resuspension of lake sediments (Reference 214).

2.4.1.2.2.6 Surface Water Impoundments

The Lee Nuclear Site has three manmade impoundments: (1) Make-Up Pond B, including the Upper Arm feature, (2) Make-Up Pond A, and (3) Hold-Up Pond A. These features, along with the constructed earthen dams and site structures, are shown in Figure 2.4.1-201. New retention ponds are constructed or existing ponds are used, if necessary, to accommodate surface water runoff and allow sediment-laden water from dewatering activities to pass through the impoundments prior to discharge at a NPDES permitted outfall. Make-Up Pond C is an off-site facility, located on a tributary of the Broad River, west of the Lee Nuclear Station. Details of Make-Up Pond C are provided in Subsection 2.4.1.2.3.1.

Make-Up Pond B

Make-Up Pond B was formed by constructing an earthen dam that impounds McKowns Creek west of Lee Nuclear Station. This reservoir was constructed in the 1970s in the initial construction phase of the Cherokee Nuclear Station. A cofferdam within Make-Up Pond B was utilized to support the original construction of the Make-Up Pond B dam. Upon filling of the pond, the cofferdam was submerged creating a bathymetric division of the pond. Very little to no sediment accumulation is observed within this impoundment.

The cofferdam is apparent on the bathymetric map, [Figure 2.4.1-209](#) (Sheet 2 of 4), as two approximately parallel 540 ft. contours midway between McKowns Mountain and the Make-Up Pond B dam. This cofferdam will be breached to allow full communication between the two bathymetric divisions within Make-Up Pond B.

Make-Up Pond B dam crest elevation is 590 ft. Make-Up Pond B has a normal full pond elevation of 570 ft. above msl (spillway elevation) and occupies approximately 11 percent of the total drainage area of McKowns Creek. Bathymetry exhibited a maximum depth of 59.3 ft., a mean depth of 31.4 ft., total storage capacity of approximately 4000 ac.-ft. and the surface area at full pond is approximately 150 ac. ([Figure 2.4.1-209](#), Sheet 2). The useable storage is approximately 3200 ac.-ft.

During 2006 – 2007, water levels in Make-Up Pond B varied 0.49 ft., representing approximately 73 ac-ft or approximately 1.8 percent of the total storage volume. It should be noted that Make-Up Pond B was receiving waters from dewatering activities, thus affecting the water balance. These activities were conducted to remove water from the original excavation for Cherokee Nuclear Station which was full of water prior to site characterization activities in 2006. All of this water was pumped to Make-Up Pond B. Inflow from rainfall and runoff contribute approximately 1271 gpm to the impoundment. Site observations and aerial photographs indicate that Make-Up Pond B retains water to near full pond level under natural conditions.

Make-Up Pond B includes an adequately sized outlet structure and is not located on a sizeable river or stream. Therefore, the potential for significant debris to be picked up by a rise in the water level and then transported to the outlet structure where it could collect as an obstruction is minimal which eliminates the need for clear cutting around the perimeter of the pond. Floating debris has not been a problem historically and no clogging of the overflow spillway has been recorded.

To ensure no debris blockage of the spillway, a shoreline management program is established along the banks of Make-Up Pond B. The shoreline management program consists of annually inspecting the shoreline around Make-Up Pond B and removing any trees that show distress of falling into the pond and removing any trees that may be down on the ground. In addition, Duke Energy will inspect the spillway after any rain event greater than 3 inches per hour to ensure that the spillway remains clear of any debris.

Even though the shoreline management program is considered to be adequate for preventing debris blockage of the spillway, as a secondary measure a debris barrier system will be installed approximately 350 feet away from the spillway as shown on [Figure 2.4.1-214](#). The debris barrier is designed to rise and fall with fluctuations in the pond water level. The debris barrier system is considered non-safety related.

The maximum flood level of surface water features at the Lee Nuclear Station is elevation 589.10 ft. msl. This elevation would result from a Probable Maximum Flood (PMF) event on Make-Up Pond B watershed with the added effects of coincident wind wave activity as described in [Subsection 2.4.4](#). The Lee Nuclear Station safety-related structures have a grade elevation of 593 ft. msl.

An access road spanning across the Upper Arm Dam embankment was constructed in the late 1970's during Cherokee Nuclear Station construction. The result of this construction created a separate impoundment of Make-Up Pond B that takes surface water runoff from the east slope of McKowns Mountain, and from the west slope of ridge to east of Upper Arm. A 54 in. culvert pipe was placed to allow for positive drainage between the Upper Arm and Make-Up Pond B. The location of this dam is shown on [Figure 2.4.1-209](#), Sheet 2.

The Upper Arm Dam has a design crest elevation of 590 ft. located at the access road. The normal pool elevation of the Upper Arm is 575 ft and the Upper Arm Pond surface area at full pond conditions is approximately 5 percent of the total drainage area of the Upper Arm watershed. Bathymetry exhibited a maximum depth of 32.2 ft., a mean depth of 31.4 ft., total storage capacity of approximately 101 ac.-ft. and the surface area at full pond is approximately 9.1 ac. ([Figure 2.4.1-209](#), Sheet 2).

Make-Up Pond A

Make-Up Pond A was also constructed in the 1970s during the initial construction phase of the Cherokee Nuclear Station. The basin is situated east of the proposed Lee Nuclear Station reactor locations and was formed by constructing an earthen dam across a backwater arm of Ninety-Nine Islands Reservoir. Very little to no sediment accumulation is observed within this impoundment.

Make-Up Pond A crest elevation varies from 557.5 ft. to a low point of 555 ft. above msl ([Reference 254](#)). At the time of the survey, the impoundment elevation was approximately 546.1 ft. above msl with full pond elevation at 547 ft. This is a relatively small surface water impoundment with a full pond surface area of approximately 62 ac. Bathymetry exhibited a maximum depth of 59.6 ft., a mean depth of 26.1 ft., and an estimated volume storage of 1425 ac.-ft. ([Figure 2.4.1-209](#), Sheet 3). The useable storage is approximately 1200 ac.-ft.

During 2006 – 2007, water levels in Make-Up Pond A varied 0.89 ft., representing approximately 53 ac-ft or 3.7 percent of the total storage volume. Rainfall and runoff contribute on average 396 gpm to the impoundment. Based on site observations and review of available historical aerial photographs, Make-Up Pond A retains water to near full pond level under natural conditions.

Hold-Up Pond A

Hold-Up Pond A is a small impoundment located north of the proposed reactor locations ([Figure 2.4.1-209](#), Sheet 4). Two dams were built in the 1970s to form this impoundment. The crest elevation of the dam is approximately 539.7 ft. above msl, and it has a current normal pond elevation of approximately 536 ft. above msl ([Reference 254](#)). Very little to no sediment accumulation was observed in this impoundment. The surface area at full pond is 4.4 ac. and the total storage volume at full pond is 56.4 ac-ft. Rainfall and runoff contribute on average 18 gpm to the pond. Based on site observation and review of available historical aerial photographs, Hold-Up Pond A retains water to near full pond level under natural conditions.

2.4.1.2.2.7 Local Wetlands

Wetlands are areas that are inundated or saturated by surface water or groundwater at a frequency and duration sufficient to support, and that under normal circumstances do support, a prevalence of vegetation typically adapted for life in saturated soil conditions. At the Lee Nuclear Site, wetlands occupy a total of 46.4 ac. or 2.4 percent of the site. They are currently represented by Alluvial Wetlands, Non-alluvial Wetlands, and Non-jurisdictional Wetlands that total 3.2 ac. (0.2 percent), 10.8 ac. (0.6 percent), and 32.4 ac. (1.7 percent) of the total site area, respectively. No appreciable seasonal variations of wetland settings were documented during 2006.

2.4.1.2.3 Dams and Reservoirs

There have been dams in the Upper Broad River drainage basin since the construction of Cherokee Falls Dam in 1826. The primary functions of the larger storage reservoirs are water supply and hydroelectric power. [Table 2.4.1-205](#) presents information for the six major reservoirs in the Upper Broad River Basin including drainage areas, elevation-storage relationships, and short term (maximum storage) and long term (normal storage) storage allocations. Ninety-Nine Islands Dam, Cherokee Falls Dam, and Gaston Shoals Dam are in the vicinity of the Lee Nuclear Site, and all are used for hydroelectric power. Most of the dams within the Upper Broad River basin were not constructed for flood control.

There are approximately 132 dams (five recreational dams are listed as breached) upstream from the Lee Nuclear Site ([Reference 276](#)). Six large dams (see [Subsection 2.4.1.2.3.1](#) below) are upstream from the site and represent approximately 88 percent of the total storage capacity for the Broad River basin. There are two additional smaller dams (Cherokee Falls and Gaston Shoals) immediately upstream of the site on the Broad River; however, they possess less than 2 percent of the total storage capacity for the basin. Both of these dams are essentially run-of-river structures used for hydroelectric power and not flood control. Currently, Cherokee Falls Dam is not operating and is a low-head structure without much volume/storage.

In addition, according to the *Federal Register* (Reference 224), USACE and the Cleveland County Sanitary District are proposing to construct an upstream dam and reservoir on the First Broad River (a tributary of the Broad River) approximately 1 mi. north of Lawndale, North Carolina (about 22 mi. north of the Lee Nuclear Site). Additional information on this dam is presented in Subsection 2.4.1.2.3.3.

2.4.1.2.3.1 Upstream Dams and Reservoirs

Make-Up Pond C, shown in Figure 2.4.1-213, is located approximately 2 mi. west of the Lee Nuclear Station on London Creek in Cherokee County, South Carolina. Make-Up Pond C is formed by construction of an earthen dam and saddle dikes that impound London Creek just upstream of the confluence with Little London Creek. The Make-Up Pond C dam crest elevation is 660 ft. above msl. A labyrinth spillway sets the normal pool elevation at 650 ft. above msl. Make-Up Pond C has a drainage area of 2479 ac. At normal pool elevation, bathymetry exhibits a maximum depth of 116 ft., a total storage capacity of approximately 22,000 ac.-ft., and a surface area of approximately 620 ac. Make-Up Pond C water is used to supplement the Lee Nuclear Station during low flow conditions. The useable storage is approximately 17,500 ac.-ft.

Lake Whelchel is located approximately 8 mi. northwest of the Lee Nuclear Site on Cherokee Creek in Cherokee County, South Carolina. This Lake Whelchel dam is an earthen design that was constructed in 1964 and modified in 1989. The dam height is 61 ft. and the length is 2100 ft. The dam creates a reservoir that is owned by and used as a water supply source for Gaffney, South Carolina. The dam and associated reservoir are owned and operated by the city of Gaffney. The normal pool elevation of the reservoir is 670 ft. above msl (Table 2.4.1-205). The reservoir has a surface area of approximately 177 ac. and a normal storage of approximately 2438 ac.-ft. The maximum storage of Lake Whelchel at the dam crest elevation of 685 ft. is approximately 5698 ac.-ft. No hydroelectric power plant is associated with this dam.

Kings Mountain Reservoir (Moss Lake Dam) is located in Cleveland County, North Carolina, approximately 16 mi. northeast of the Lee Nuclear Site. Discharge waters from this dam are released to Buffalo Creek. The dam was constructed in 1973 and created Kings Mountain Reservoir, which is owned by the city of Kings Mountain and used as a water supply source for the city of Shelby, North Carolina, as well as several smaller communities. In addition, the reservoir is used for recreational activities such as boating and fishing. Moss Lake Dam is an earthen structure that is 840 ft. long and 99 ft. in height. The normal pool elevation of Kings Mountain Reservoir is 736 ft. above msl (Table 2.4.1-205). The reservoir has a surface area of approximately 1329 ac. and a normal storage of 44,400 ac.-ft. and a maximum storage capacity of 53,280 ac.-ft. No hydroelectric power plant is associated with this dam.

Lake Adger (also Turner Shoals) is located on the Green River approximately 44 mi. northwest of the Lee Nuclear Site in Polk County, North Carolina. The Lake Adger dam and associated hydroelectric plant were constructed in 1925 and are owned and operated by Hydro LLC. In addition, the reservoir (Lake Adger) is used

for recreational activities such as boating and fishing. Lake Adger Dam is a concrete multiple-arch design that is 689 ft. in length and 90 ft. in height. The normal pool elevation of Lake Adger is 912 ft. above msl (Table 2.4.1-205). The lake has a surface area of approximately 460 ac. and an estimated normal storage of 11,700 ac.-ft. The maximum storage is 16,760 ac.-ft.

Lake Lure is located on the Broad River in Rutherford County, North Carolina, approximately 46 mi. northwest of the Lee Nuclear Site. The Lake Lure dam and associated hydroelectric plant were constructed in 1927 and are owned and operated by the town of Lake Lure. In addition, the reservoir is used for recreational activities such as boating and fishing. Lake Lure Dam is a concrete multiple-arch design that is 480 ft. in length and 124 ft. in height. The normal pool elevation of Lake Lure is 991 ft. above msl (Table 2.4.1-205). The lake has a surface area of approximately 740 ac., a normal storage of 32,295 ac.-ft. and a maximum capacity of 44,914 ac.-ft.

Lake Summit Dam is located on the Green River in Henderson County, North Carolina, approximately 52 mi. northwest of the Lee Nuclear Site. The dam and associated hydroelectric plant were constructed in 1920 and are owned and operated by Duke Energy. In addition, the reservoir is used for recreational activities such as boating and fishing. Lake Summit Dam is a single-concrete-arch design with a concrete buttress structure that is 254 ft. in length and 130 ft. in height. The normal pool elevation of Lake Summit is 2012.6 ft. above msl (Table 2.4.1-205). The lake has a surface area of approximately 276 ac. and a normal storage of 9300 ac.-ft. and maximum storage of 15,840 ac.-ft. The maximum drawdown is 20 ft., yielding a useable storage of 4134 ac.-ft.

2.4.1.2.3.2 Downstream Dams and Reservoirs

There are two significant reservoirs located downstream from the Lee Nuclear Site: Ninety-Nine Islands Reservoir and the Lockhart Reservoir. Similar to the Cherokee Falls and Gaston Shoals dams, Ninety-Nine Islands and Lockhart dams are run-of-river structures and are not used for flood control. Dams located further downstream include Neal Shoals Dam (approximately 50 mi.) and Parr Shoals Dam (approximately 52 mi.).

As shown on Figure 2.4.1-205, Lockhart Dam is located in Union County, South Carolina, on the Broad River, 3 mi. south of the confluence with the Pacolet River and approximately 19 mi. south to southeast of the Lee Nuclear Site. The normal pool elevation of the Lockhart Reservoir is around 395 ft. above msl with a surface area of approximately 300 ac. and a normal storage of 2400 ac.-ft. The Lockhart Dam and its associated hydroelectric power plant were constructed in 1921 and are currently owned and operated by Lockhart Power Company of Lockhart, South Carolina.

Completed in 1905, the Neal Shoals Dam is located in Chester and Union Counties. The normal pool elevation of Neal Shoals reservoir is around 325 ft. above msl. with a surface area of approximately 550 ac. and a normal storage of 1350 ac.-ft.

2.4.1.2.3.3 Water Management Changes

As mentioned in [Subsection 2.4.1.2.3](#), USACE and the Cleveland County Sanitary District (CCSD) are proposing to construct a dam on the First Broad River (upstream and hydraulically connected to the Broad River) approximately 1 mi. north of Lawndale, North Carolina. This is about 26 mi. north of the Lee Nuclear Site. The USACE permit application (Section 404 of the Clean Water Act) states that the dam affects approximately 24 mi. of river and stream habitat and approximately 1 ac. of wetlands. Initial feasibility estimates state that an earth-filled dam across the First Broad River may be approximately 83 ft. high and 1245 ft. wide at the base. The associated emergency spillway, located south of the dam, is approximately 1000 ft. wide. The dam creates a reservoir with a surface area of approximately 2245 ac., impounding those areas below 860 ft. above msl. A 100-ft. buffer zone would likely surround the reservoir ([Reference 224](#)).

The CCSD is proposing this dam to increase the water supply for the region. Based on current rates of growth, CCSD projects that water needs for its customers would double by 2050 ([Reference 224](#)). The reservoir is also projected to lessen the occurrence of water shortages during drought conditions.

2.4.1.2.4 Regional Hydrogeology

The Piedmont aquifer system is basically a two-layered slope-aquifer system. The shallow water table aquifer is comprised of the saprolite and residual soil, which is typically low-yielding. The underlying bedrock aquifer consists of weathered and unweathered crystalline igneous and metamorphic rocks that store and transmit water through fractures. The shallow aquifer is unconfined, meaning that the upper surface of the saturated zone is not effectively separated from the ground surface by a low-permeability clay layer. The bedrock fracture system is a network of discontinuities that increases in prevalence upward through the crystalline rock as it transitions into saprolite ([Figure 2.4.1-210](#)). Because of the permeability of the transition zone, the bedrock aquifer is also considered unconfined and not effectively isolated. Thus, the saprolite and bedrock zones function as one interconnected aquifer system ([Reference 266](#)).

Groundwater occurs almost everywhere throughout the Piedmont region; however, it is not in a single, widespread aquifer. It occurs in various local aquifer systems and compartments that have similar characteristics and are hydraulically connected. Groundwater recharge in this area is derived entirely from infiltration by local precipitation. Groundwater flow within this combined system can be complex. The fractures, relic rock textures, and directional differences in permeability or ease of groundwater movement may significantly affect the local groundwater flow direction. Recharging of the groundwater in the Piedmont occurs by the addition of rainwater, first to the shallow saprolite aquifer and then to the uppermost fracture zone. Recharge occurs mostly on upland topographic highs or at least above the slopes of stream valleys.

The average annual rainfall in the region is about 50 inches. The annual pan evaporation rate is 51.8 inches for the region. Pan evaporation rates are higher

than actual lake evaporation due to radiation and heat exchange effects. The pan coefficients range from 0.64 and 0.81, with an average of 0.7 used for the United States. Therefore, the annual evaporation rate is 36.26 inches. Groundwater is contained in the pores that occur in the weathered material (residual soil, saprolite) above the relatively unweathered rock and within the fractures in the igneous and metamorphic rock. The depth to the water table depends on climate, topography, rock type, and rock weathering. The water table varies from ground surface elevation in valleys to more than 100 ft. below the surface on sharply rising hills. Although the precipitation in the Piedmont is relatively evenly distributed throughout the year, the water table fluctuates noticeably, typically declining during the late spring and summer due to evapotranspiration and rising in the late fall and winter when the evaporation potential is reduced (Reference 297).

A detailed discussion of regional and local groundwater characteristics is presented in Subsection 2.4.12. A detailed discussion of regional and local geology and soil properties is presented in Section 2.5.

2.4.1.2.5 Water Use

This subsection describes surface water and groundwater in the vicinity of the Lee Nuclear Site that could affect or be affected by the construction and operation of two AP1000 units. The information provided in this subsection includes descriptions of surface water and groundwater uses that could affect or be affected by construction or operation of the Lee Nuclear Station, including transmission corridors and off-site facilities. In addition, a detailed assessment of water use within the vicinity of the facility, types of consumptive and nonconsumptive water uses, identification of their locations, and qualification of water withdrawals and returns are discussed in this subsection.

2.4.1.2.5.1 Surface Water Use

The Lee Nuclear Site is located on the west bank of the Broad River approximately 3 mi. south-southeast (downstream) of Cherokee Falls and 1 mi. north-northwest (upstream) of the Ninety-Nine Islands Dam and Hydroelectric Station. Surface water in the vicinity of the Lee Nuclear Site consists of the Broad River, three on-site man-made impoundments, and one off-site man-made impoundment. These features are discussed in detail in Subsections 2.4.1.2.2.6 and 2.4.1.2.3.1.

According to available SCDHEC information on water use for 2005 (Reference 267), total water usage in Cherokee County was 8.4 Mgd. This information is presented in Table 2.4.1-206. Total 2005 water withdrawals from Cherokee, Chester, Greenville, Spartanburg, Union, and York counties, South Carolina, are presented in Table 2.4.1-207 (Reference 267).

No surface water usage in Cherokee County was reported for domestic self-supplied systems, aquaculture, golf courses, irrigation, livestock, mining, or thermoelectric power uses. According to SCDHEC, water use for hydroelectric power was 1116 Mgd in 2005 for Cherokee County (Reference 267). The USGS

2000 data did not reference hydroelectric power water use; however, these data were included in the 1995 data set. According to the U.S. Army Corps of Engineers National Inventory of Dams, there have been no hydroelectric dams constructed in the watershed since 1995. Therefore, the USGS 1995 data remains unchanged. According to the USGS, there were 2037.1 Mgd of instream water use for hydroelectric power in 1995 for Cherokee County. Surface water-use details for the Broad River watershed within 60 mi. of the Lee Nuclear Site are presented in [Tables 2.4.1-207](#) and [2.4.1-208](#).

Nineteen permitted surface water intakes at sixteen separate facilities are located in the Upper Broad River basin upstream from the Lee Nuclear Site ([Table 2.4.1-209](#), [Figure 2.4.1-211](#)). The closest surface water intake is the Gaffney Board of Public Works intake about 8 mi. upstream on the Broad River. In addition to the existing intakes, Duke Energy anticipates modernizing and expanding the Cliffside Steam Station (located 19 mi. upstream from the site in Cleveland County, North Carolina), which will use the existing surface water intake from the Broad River. Cliffside Steam Station expansion is discussed in [Subsections 2.2.2.1.4](#) and [2.4.11.4](#).

Three permitted surface water intakes for public water supply are located downstream from the Lee Nuclear Site ([Figure 2.4.1-211](#)). The closest of these is the city of Union, which withdraws water from the Broad River about 21 mi. downstream from the site and has a maximum withdrawal rate of 23.8 Mgd. The second and third are the Carlisle Cone Mills (approximately 30 miles downstream; maximum capacity 8.1 Mgd) and the V.C. Summer Nuclear Station (approximately 52 miles downstream; maximum capacity 3.1 Mgd) ([Table 2.4.1-209](#)). Two additional AP1000 units are planned for the V.C. Summer Nuclear Station. Details are not currently available. Additional surface water uses not included in the table are located within 20 – 50 mi. of the site. These additional intakes are relatively insignificant because they are located outside the watershed or on tributaries that join the Broad River downstream from the site.

The plant water use is discussed in [Subsection 2.4.1.1.4](#). [Table 2.4.1-210](#) and [Table 2.4.1-211](#) present raw water use and effluent discharge as a percentage of Broad River flow rates. The maximum consumption rate of Broad River water, predominantly resulting from evaporation during plant operations, is expected to be 63 cfs, approximately 3 percent of the average annual mean discharge of the Broad River (approximately 2500 cfs).

2.4.1.2.5.2 Groundwater Use

Groundwater produced for water supply in counties located in the Piedmont aquifer system is reported to be approximately 79 Mgd (122.5 cfs). This can be compared to some Upper Coastal Plain counties that withdraw up to several thousand Mgd of groundwater ([Reference 293](#)).

A reported 1.02 million gal. of groundwater were used for thermoelectric power generation in Cherokee County ([Reference 267](#)). No groundwater usage in Cherokee County for domestic self-supplied systems, aquaculture, golf courses, irrigation, livestock, mining, or thermoelectric power was reported in the 2005

***Withheld from Public Disclosure Under 10 CFR 2.390(a)(9)
(see COL Application **Part 9**)***

SCDHEC data ([Reference 267](#)). According to a private well report from SCDHEC, based on data from January 1985 to June 2006, the number of reported private wells in Cherokee County was 1076 ([Reference 261](#)). The USGS and state water-use data were reviewed, and groundwater withdrawals are presented in [Tables 2.4.1-207](#) and [2.4.1-208](#). Groundwater withdrawals for Cherokee and surrounding counties in South Carolina ([Table 2.4.1-207](#)) only account for 4.7 Mgd, and the majority (85 percent) of that volume is pumped from Spartanburg County, approximately 25 mi. west of the Lee Nuclear Site.

[

}^{SRI}

The Lee Nuclear Site is not expected to use groundwater as a source of water for any purpose. Water for temporary fire protection, concrete batching, and other construction uses will be obtained from the Draytonville Water District. Groundwater is not used as a safety-related source of water or as a primary water supply resource for any purpose. Further discussion regarding groundwater characteristics and use is provided in [Subsection 2.4.12](#).

WLS COL 2.4-2 2.4.2 FLOODS

2.4.2.1 Flood History

Floods on the Broad River occur primarily as a result of precipitation runoff over the watershed. There have been dams in the Upper Broad River drainage basin since the construction of Cherokee Falls Dam in 1826. However, the majority are not flood control dams. The primary function of the larger storage reservoirs are water supply and hydroelectric power. Ninety-Nine Islands Dam, Cherokee Falls Dam, and Gaston Shoals Dam, in the vicinity of the Lee Units 1 and 2, are all used

for hydroelectric power ([Reference 276](#)). The hydroelectric facility at Cherokee Falls Dam is not currently operating. Although these structures affect the low flow conditions of the Broad River, peak flow conditions at Lee Units 1 and 2 are generally not affected by regulation. The limited flood control dams in the basin are small storage structures and would have limited effect on peak flows.

The Gaffney stream gauge station (USGS No. 02153500) is located about 5 river miles upstream of Lee Units 1 and 2 between Gaston Shoals Dam and Cherokee Falls Dam. [Figure 2.4.2-201](#) shows the location of area gauges. The Gaffney gauge has a drainage area of 1490 sq. mi., about 96 percent of the drainage area at the site. The drainage area of the Broad River at the Lee Nuclear Station is about 1550 sq. mi. [Table 2.4.2-201](#) summarizes peak flow for the broken period of record from 1939 to 1990 ([Reference 290](#)). The flood of record for the Gaffney gauge, 119,000 cfs on August 14, 1940, corresponds to a Ninety-Nine Islands reservoir elevation of about 522.5 ft. at Lee Nuclear Station.

The Ninety-Nine Islands reservoir elevation is maintained by Duke Energy and recorded on a daily basis from 1999 to 2005 by USGS gauge No. 02153550. The USGS gauge record high is 107.29 ft. on September 8, 2004 for a reservoir elevation of 518.75 ft. ([Reference 208](#)). The gauge datum is 411.46 ft. above the National Geodetic Vertical Datum of 1929 (NGVD 1929). Earlier reservoir records from 1964 to 1973 indicate that the highest elevation was about 513.6 ft. during May 1972.

The stream gauge station below Ninety-Nine Islands Dam (USGS No. 02153551, listed in [Table 2.4.1-203](#) as Broad River below Cherokee Falls, SC) is located in the tailrace and has a drainage area of 1550 sq. mi. Peak flow records are limited for this station and the gauge is not calibrated for large flows. [Table 2.4.2-202](#) summarizes peak flow and gauge height for the period of record from 1999 to 2005 ([Reference 290](#)).

No historical data exists regarding flooding due to surges, seiches, tsunamis, dam failures, or landslides. Surge and seiches are discussed in [Subsection 2.4.5](#). Tsunamis are discussed in [Subsection 2.4.6](#). Dam failures are discussed in [Subsection 2.4.4](#). Channel diversions are discussed in [Subsection 2.4.9](#). Historical information related to icing and ice jams is provided in [Subsection 2.4.7](#).

2.4.2.2 Flood Design Considerations

The Lee Nuclear Station conforms to Regulatory Position 1 of Regulatory Guide 1.59. There are no safety-related structures that could be affected by floods and flood waves.

The type of events evaluated to determine the worst potential flood include (1) probable maximum precipitation (PMP) on the total watershed and critical sub-watersheds including seasonal variations and potential consequent dam failures, as discussed in [Subsection 2.4.3](#), (2) dam failures, as discussed in [Subsection 2.4.4](#), including in a postulated safe shutdown earthquake with a coincident 25-year flood or operating basis earthquake with a coincident one-half probable maximum flood (PMF), (3) local intense precipitation, and (4) two year

coincident wind waves as discussed in [Subsection 2.4.3](#). Local intense precipitation is discussed below. Both static and dynamic assumed hypothetical conditions to determine the design flood protection level are evaluated in [Subsections 2.4.3](#) and [2.4.4](#).

Specific analysis of Broad River flood levels resulting from ocean front surges, seiches, and tsunamis is not required because of the inland location and elevation characteristics of the Lee Nuclear Station. Additional details are provided in [Subsection 2.4.5](#) and [Subsection 2.4.6](#). Snowmelt and ice effect considerations are unnecessary because of the temperate zone location of the Lee Nuclear Station. Additional details are provided in [Subsection 2.4.7](#). Flood waves from landslides into upstream reservoirs required no specific analysis, in part because of the absence of major elevation relief. In addition, elevation characteristics of the vicinity relative to the Broad River, combined with the limited storage volume availability of nearby upstream reservoirs, prohibit significant landslide induced flood waves. Additional details are provided in [Subsection 2.4.9](#).

The maximum flood level at the Lee Nuclear Station is established as the maximum of calculated results from flooding events analyzed in [Section 2.4](#). That maximum flood level is elevation 592.56 ft. msl. This elevation would result from a PMP event on the Lee Nuclear Station site (local intense precipitation) as described in [Subsection 2.4.2.3](#). The Lee Nuclear Station safety-related plant elevation is 593 ft. msl. This maximum flood level is identified as a site characteristic in [Table 2.0-201](#).

2.4.2.3 Effects of Local Intense Precipitation

The Lee Nuclear Station drainage system was evaluated for a storm producing the PMP on the local area. For the purpose of the evaluation all subsurface drainage features (i.e., culverts, inlets, etc.) including the vehicle barrier system trench are assumed non-functional and all precipitation is assumed to be transformed to runoff.

The site is generally defined by wide flat areas. However, the site is graded such that runoff will drain away from safety-related structures either to Make-Up Pond B, Make-Up Pond A, or directly to the Broad River. Runoff from a specific power block area flows through four graded channels per unit as described in the discussion below and then flows across the site to the receiving water body. Computed water surface elevations in the vicinity of safety-related structures are below plant elevation 593 ft. The site grading and drainage plan is shown in [Figure 2.4.2-202](#).

The site is graded to drain runoff away from the power blocks. The finished floor elevation of the safety related structures for each unit is 593 ft. The areas immediately adjacent to the power blocks range in elevation from 592 ft. to 590 ft. The adjacent area is generally bounded by a roadway surrounding the power blocks. The power block area bounded by the roadway is either paved or gravel surfaced. Areas beyond the roadway are generally maintained grass surfaces. Further from the power blocks, the site is flat from the roadway to the plant side of the vehicle barrier system at elevation 590 ft. The opposite bank of the vehicle

barrier system is at elevation 588 ft. Beyond the vehicle barrier system, the site is generally flat at elevation 588 ft. before encountering the steeper slopes into the adjacent, downstream water bodies.

The effects of local intense precipitation are analyzed using a series of models, each establishing boundary conditions for additional modeling. The overall site, generally described by the flat areas at elevation 588 ft., is idealized as a dry reservoir and modeled using level-pool storage routing with U.S. Army Corps of Engineers HEC-HMS 3.5 computer software (Reference 302) for the site drainage area shown in Figure 2.4.2-202. The area of the site upstream of the vehicle barrier system, generally described by the flat areas at elevation 590 ft. are also idealized as a dry reservoir and modeled using level-pool storage routing with HEC-HMS 3.5 computer software.

The idealized reservoir for the overall site is defined by an elevation-discharge-storage relationship. Storage is based on an elevation-area relationship and is developed using the available storage areas across the site within the drainage area. Storage routing does not incorporate the entire area of the power block bounded by the vehicle barrier system and a sloped area that transitions from elevation 590 ft. to 588 ft., located north of Unit 2. In addition, all other site structures and the switchyard area are assumed to provide no storage.

The discharge relationship for this idealized reservoir is determined using broad crested weir flow. The 588 ft. contour along the banks of the steeper slopes into adjacent, downstream water bodies is used to develop the length of the weir. The total length was reduced to account for ineffective areas where adjacent slopes may not be as steep as areas where structures could obstruct flow discharging from the site. The downstream water bodies are used to establish boundary conditions and determine any tailwater effects. Although tailwater effects are not determined to affect weir flow, a conservative estimate of 2.0 is used for the weir flow coefficient.

The local intense PMP is defined by Hydrometeorological Report (HMR) Nos. 51 and 52. PMP values for durations from 6-hr. to 72-hr. are determined using the procedures as described in HMR No. 51 for areas of 10-sq. mi. (Reference 255). Using the Lee Nuclear Station location, the rainfall depth is read from the HMR No. 51 PMP charts for each duration.

The 1-sq. mi. PMP values for durations of 1-hour and less are determined using the procedures as described in HMR No. 52 (Reference 225). Using the Lee Nuclear Station location, the rainfall depth is read from the HMR No. 52 PMP charts for each duration. A smooth curve is fitted to the points. The derived PMP curve is detailed in Table 2.4.2-203. The corresponding PMP depth duration curve is shown in Figure 2.4.2-203.

HMR 52 guidance indicates that PMP rates for 10-sq. mi. areas are the same as point rainfall. Also indicated in HMR 52, the 1-sq. mi. PMP rates may also be considered the point rainfall for areas less than 1-sq. mi. Therefore, intensities for any drainage areas with durations longer than 1-hr. are derived from the PMP

rates for 10-sq. mi. areas. Intensities for drainage areas with durations equal to or less than 1-hr. are derived from the PMP rates for 1-sq. mi. areas.

The AP1000 plant design is based on a PMP of 20.7 in/hr as provided in [DCD Table 2-1](#). As shown in [Figure 2.4.2-203](#), the site is within the plant design limits for PMP. The PMP is identified as a precipitation site characteristic in [Table 2.0-201](#). Roofs are sloped to preclude ponding of water.

Two storms are modeled on the basis of the PMP curve detailed in [Table 2.4.2-203](#) and [Figure 2.4.2-203](#). A 72-hr. duration storm with a 1-hr. precipitation interval is examined along with a 6-hr. duration storm with a 5-min. precipitation interval to capture the effect of the short-term, high intensity on the peak flow. The local intense PMP is converted to runoff at each increment by multiplying the drainage area by the intensity of each increment and converting the units to cubic feet per second. This approach is essentially equivalent to the Rational Method ([Reference 201](#)) using a runoff coefficient of one. Therefore, all rainfall is converted to runoff instantaneously and no runoff losses are included.

Runoff is applied to the site reservoir model in HEC-HMS and level-pool storage routing is used to determine the resulting water surface elevation. Several time distributions are examined for both modeled storm events. For the 72-hr. duration storm, several temporal distributions produce the highest water surface elevation for the site. For reference, the tail end peaking hyetograph is provided in [Figure 2.4.3-236](#).

As a conservative approach, the results from the 72-hr. duration storm are used to establish the starting elevation for the 6-hr. duration storm. For the 6-hr. duration storm, a tail end peaking storm event is found to result in the highest water surface elevation for the site. The corresponding hyetograph is provided in [Figure 2.4.3-235](#). Based on a combination of the two storms the maximum water surface elevation determined using HEC-HMS is 588.82 ft. This elevation is applied to the overall site and used as the downstream boundary condition for the analysis of the area upstream of the vehicle barrier system.

Similar to the previous discussion, the idealized reservoir for the area upstream of the vehicle barrier system is defined by an elevation-discharge-storage relationship. Storage is based on an elevation-area relationship and is developed using the available storage areas within the drainage area. Storage routing does not incorporate the entire area of the power block bounded by the elevation 590 ft. contour adjacent to the road looping around the power block. In addition, all other structures in the area are assumed to provide no storage.

The discharge relationship for this idealized reservoir is determined using broad crested weir flow. The upstream, higher side of the vehicle barrier system 590 ft. contour is used to develop the length of the weir. The total length does not include the sloped transition area north of Unit 2 and was reduced to account for ineffective areas where structures could obstruct flow discharging from the area. The result for the downstream area is less than the bank elevation of 590 ft. Therefore, there are no tailwater effects. As a conservative estimate, a weir flow coefficient of 2.0 is used.

Two storms are modeled as previously identified for the downstream area. The local intense PMP is converted to runoff instantaneously and no runoff losses are included. Runoff is applied to the idealized reservoir model in HEC-HMS and level-pool storage routing is used to determine the resulting water surface elevation. Several time distributions are examined for both modeled storm events. For the 72-hr. duration storm, all temporal distributions produce the same water surface elevation for the area.

As a conservative approach, the results from the 72-hr. duration storm are used to establish the starting elevation for the 6-hr. duration storm. For the 6-hr. duration storm, several temporal distributions produce the highest water surface elevation for the area. Based on a combination of the two storms the maximum water surface elevation determined using HEC-HMS is 590.56 ft. This elevation is applied to the area upstream of the vehicle barrier system and used as the downstream boundary condition for the analysis of the power block area.

As shown in [Figure 2.4.2-204](#), runoff is directed away from the power block units to lower lying areas via four discharge channels. Under the assumption that all subsurface drainage features are non-functional, runoff would flow over roadways or other topographical features as the flow exits the areas immediately adjacent to the power block units.

For each power block area shown in [Figure 2.4.2-204](#), the peak runoff is determined using the maximum PMP intensity of 6.2 in/5 min from [Table 2.4.2-203](#). The peak runoff is determined by multiplying the drainage area by the intensity and converting the units to cubic feet per second. This approach is essentially equivalent to the Rational Method using a runoff coefficient of one. Therefore, all rainfall is converted to runoff instantaneously and no runoff losses are included.

The power block drainage areas, shown in [Figure 2.4.2-204](#), are evaluated using the maximum water surface elevation for the idealized reservoir as the downstream boundary condition. Therefore, the HEC-HMS modeling for the idealized reservoir becomes the downstream boundary condition for the power block areas' channel flow evaluation. The four discharge channels for the Unit 1 power block area and the four discharge channels for the Unit 2 power block area are evaluated by steady state, open channel flow, backwater analysis, modeled using HEC-RAS version 4.1.0 software.

Cross sections for each of the four discharge channels (A1, B1, C1, and D1), which discharge from the Unit 1 power block area, are determined based on the grading and drainage plan. Cross sections for each of the four Unit 2 related discharge channels (A2, B2, C2, and D2), are determined in the same manner. Site structures are modeled to obstruct flow and are assumed to provide no storage. A Manning's roughness coefficient of $n = 0.026$ is used for all of the power block cross sections, which bounds the ground cover used for site conditions (i.e., gravel lined channels). HEC-RAS modeling was performed using steady state analysis to establish a maximum water surface elevation at the upstream cross section.

The resulting water surface elevations are provided in [Table 2.4.2-204](#). The maximum water surface elevation determined is 592.56 ft. and occurs at drainage area B1 of the Unit 1 power block area and at drainage area B2 of the Unit 2 power block area. These drainage areas, B1 and B2, are located on the west side of each, respective, power block area between the Annex Building, north storage tanks and ramp, and the Transformer Area. All Lee Nuclear Station safety-related structures are located above the effects of local intense precipitation at plant elevation 593 ft.

Due to the temperate climate and relatively light snowfall, significant icing is not expected. Based on the site layout and grading, any potential ice accumulation on site facilities is not expected to affect flooding conditions or damage safety-related facilities. Ice effects are discussed in [Subsection 2.4.7](#).

2.4.3 PROBABLE MAXIMUM FLOOD ON STREAMS AND RIVERS

WLS COL 2.4-2 The guidance in Appendix A of U.S. Nuclear Regulatory Commission (NRC) Regulatory Guide 1.59 was followed in determining the Probable Maximum Flood (PMF) by applying the guidance of ANSI/ANS-2.8-1992 ([Reference 202](#)). ANSI/ANS-2.8-1992 was issued to supersede ANSI N170-1976, which is referred to by Regulatory Guide 1.59. Although ANSI/ANS-2.8-1992 has been withdrawn, there has been no replacement standard issued. The NRC NUREG-0800 retains both Regulatory Guide 1.59 and ANSI/ANS-2.8-1992 as historical technical references.

Broad River

The PMF for the Broad River above the Lee Nuclear Station is determined from the probable maximum precipitation (PMP) for the watershed of Ninety-Nine Islands Dam. Lee Nuclear Station is located about 1 mi. upstream from the dam and adjacent to the Broad River. The 1550-sq. mi. Broad River drainage basin at Ninety-Nine Islands Dam is shown in [Figure 2.4.1-205](#).

McKowns Creek/Make-Up Pond B

The PMF for McKowns Creek and Make-Up Pond B is determined from the PMP for the 2.190-sq. mi. drainage basin of Make-Up Pond B and the 0.294 sq. mi. drainage basin of the Upper Arm. The Make-Up Pond B drainage basin, including the Upper Arm, is shown in [Figure 2.4.3-201](#).

Intermittent Stream/Make-Up Pond A

The PMF for the intermittent stream and Make-Up Pond A are determined from the PMP for the 0.619-sq. mi. drainage basin of Make-Up Pond A. Make-Up Pond A drainage basin is shown in [Figure 2.4.3-201](#).

London Creek/Make-Up Pond C

The Make-Up Pond C reservoir is located on a tributary of the Broad River, west of the Lee Nuclear Station, as shown in [Figure 2.4.1-213](#), but is not adjacent to the Lee Nuclear Station. However, the PMF for London Creek and Make-Up Pond C is determined for combination with dam failure permutations as discussed in [Subsection 2.4.4.1](#). The PMF is determined from the PMP for the 3.87-sq. mi. drainage basin of Make-Up Pond C. The Make-Up Pond C drainage basin is shown in [Figure 2.4.3-239](#).

2.4.3.1 Probable Maximum Precipitation

Broad River

The PMP for the watershed above the Lee Nuclear Station is defined by Hydrometeorological Report (HMR) Nos. 51 and 52 ([References 255 and 225](#)). The PMP is based on an existing study for Ninety-Nine Islands Dam ([Reference 217](#)) and modified to include antecedent storm conditions, as specified by Appendix A of Regulatory Guide 1.59.

Using the location of the drainage basin, HMR-51 PMP charts are used to determine generalized estimates of the all-season PMP for drainage areas from 10 to 20,000 sq. mi. for durations from 6 to 72 hrs. The resulting depth-area-duration (DAD) values are shown in [Table 2.4.3-201](#).

HMR-52 is used to determine spatial and temporal distribution of PMP estimates derived from HMR-51. The recommended elliptical isohyetal pattern from HMR-52, shown in [Figure 2.4.3-202](#), is used for the watershed. The watershed model contains 20 subbasins and is shown in [Figure 2.4.3-203](#). The Lake Whelchel and Make-Up Pond C subbasins were not included in the existing study for Ninety-Nine Islands Dam. Both the Lake Whelchel and Make-Up Pond C watersheds are contained within the original subbasin labeled BR-15. Therefore, appropriate modifications were made to subbasin BR-15 to accommodate subbasins for Lake Whelchel and Make-Up Pond C.

HMR-52 computer software ([Reference 271](#)), developed by the U.S. Army Corps of Engineers (USACE), is used to determine the optimum storm size and orientation to produce the greatest PMP over the entire basin using the HMR-51 derived DAD table. The HMR-52 recommended temporal distribution is also used and provided by the HMR-52 computer software. Several storm centers were examined and the critical storm center was found to be near the centroid of the watershed for Gaston Shoals Dam, located upstream of Ninety-Nine Islands Dam based on the runoff model discussed in [Subsection 2.4.3.3](#). The critical storm area was found to be 1000 sq. mi., corresponding to isohyet I in [Figure 2.4.3-202](#). The critical storm orientation was found to be 270 degrees. Refer to [Figure 2.4.1-205](#) for structure locations and watershed.

The critical 72-hr. storm PMP rainfall total is 25.48 in. for the entire watershed. The corresponding temporal arrangement of 6-hr. precipitation increments is

provided in [Table 2.4.3-202](#). The hourly temporal distribution of the 72-hr. PMP rainfall of each of the 20 subbasins is provided in [Table 2.4.3-203](#).

In accordance with Appendix A of NRC Regulatory Guide 1.59, the 72-hr. PMP storm is combined with an antecedent storm equal to 40 percent of the PMP. Therefore, the complete sequential storm considered includes a 3-day, 40 percent PMP event followed by a 3-day dry period, which is followed by the 3-day full PMP event.

The PMP estimates are associated with the summer months. HMR 53 ([Reference 260](#)) provides estimates for maximum seasonal precipitation. Although HMR 53 applies to 10 sq. mi. drainage areas, it is used as a basis for the larger Broad River watershed. HMR 53 winter precipitation estimates for December through February are less than 57 percent of the all-season PMP estimates identified in [Table 2.4.3-201](#) for the 10 sq. mi. drainage area. The 57 percent ratio is applied to the all-season PMP for the Broad River watershed identified in [Table 2.4.3-202](#) to determine the maximum winter precipitation estimates.

According to guidance ([Reference 202](#)) the winter precipitation is evaluated coincident with the 100-yr. snowpack. The water equivalent of the 100-yr. snowpack identified in [Subsection 2.3.1.2.7.1](#) is approximately 13 percent of the 72-hr. PMP for the Broad River watershed identified in [Table 2.4.3-202](#). It is assumed that the 100-yr. snowpack is distributed across the entire watershed and completely melts during a winter precipitation event. The combined result of winter precipitation and 100-yr. snowpack is approximately 70 percent of the PMP. Therefore, snowmelt is not considered to be a factor in modeling the PMF event.

McKowns Creek /Make-Up Pond B

The PMP for McKowns Creek, Make-Up Pond B, and the Upper Arm, is defined in [Subsection 2.4.2.3](#). Two storms were modeled on the basis of the PMP curve detailed in [Table 2.4.2-203](#) and [Figure 2.4.2-203](#). The total PMP depth of the 72-hr. duration storm is 46.8 in. A 6-hr. storm with a 5-min. precipitation interval was examined to capture the effect of the short-term, high intensity on the peak flow. In addition, a 72-hr. storm with a 1-hr. precipitation interval was examined to identify the total runoff volume of a PMP event.

Several time distributions were examined for both modeled events. For Make-Up Pond B, for a 72-hr. storm, a tail end peaking storm event was found to provide the greatest runoff and the peak water surface elevation. For the 6-hr. storm, a two-thirds peaking storm event was found to provide the greatest runoff and peak water surface elevation for the short term event.

For the Upper Arm to Make-Up Pond B, for a 72-hr. storm, a tail end peaking storm event was found to provide the greatest runoff and the peak water surface elevation. For the 6-hr. storm, the one-third, two-thirds and center peaking storms were found to provide the greatest runoff. However, the tail-end peaking storm provides the peak water surface elevation. The 6-hr and 72-hr. storm events are discussed in [Subsection 2.4.3.5](#). Hyetographs are provided in [Figure 2.4.3-204](#)

and [Figure 2.4.3-205](#) for the two-thirds peaking storm events. Hyetographs are provided in [Figure 2.4.3-235](#) and [Figure 2.4.3-236](#) for the tail end peaking storm events.

Intermittent Stream/Make-Up Pond A

The PMP for the intermittent stream and Make-Up Pond A is defined in [Subsection 2.4.2.3](#). Two storms were modeled on the basis of the PMP curve detailed in [Table 2.4.2-203](#) and [Figure 2.4.2-203](#). The total PMP depth of the 72-hr. duration storm is 46.8 in. A 6-hr. storm with a 5-min. precipitation interval was examined to capture the effect of the short-term, high intensity on the peak flow. In addition, a 72-hr. storm with a 1-hr. precipitation interval was examined to identify the total runoff volume of a PMP event.

Several time distributions were examined for both modeled events. For the 72-hr. storm, a tail end peaking storm event was found to provide the greatest runoff and peak water surface elevation. The corresponding hyetograph is provided in [Figure 2.4.3-236](#). For the 6-hr. storm, multiple peaking distributions, including the two-thirds peaking distribution provided the maximum runoff and peak water surface elevation. For reference, the two-thirds peaking hyetograph is provided in [Figure 2.4.3-204](#).

London Creek/Make-Up Pond C

The PMP for London Creek and Make-Up Pond C is defined in [Subsection 2.4.2.3](#). The storm is modeled on the basis of the 72-hr. PMP curve detailed in [Table 2.4.2-203](#) and [Figure 2.4.2-203](#). The total PMP depth of the 72-hr. duration storm is 46.8 in.

The 72-hr. PMP storm is combined with an antecedent storm equal to 40 percent of the PMP. Therefore, the complete sequential storm considered includes a 3-day, 40 percent PMP event followed by a 3-day dry period, which is followed by the 3-day full PMP event.

Several time distributions were examined for the PMP event using a 1-hr. precipitation interval. A tail end peaking storm event was found to provide the greatest discharge and water surface elevation at Make-Up Pond C. The hyetograph is provided in [Figure 2.4.3-240](#).

2.4.3.2 Precipitation Losses

Broad River

Precipitation losses are based on an existing study ([Reference 217](#)) using the U.S. Department of Agriculture (USDA), Soil Conservation Service (SCS) (now the Natural Resources Conservation Service [NRCS]) curve number method. The initial study used geographic information systems (GIS) and the NRCS state soil geographic database (STATSGO) to determine hydrologic soil group values. The GIS and U.S. Geological Survey (USGS) information were also used to determine

land-use and impervious cover. An average antecedent moisture condition (AMC II) was then used to compute a weighted curve number for each subbasin.

The SCS Curve Number method was also used to determine precipitation losses for the Lake Whelchel subbasin and the Make-Up Pond C subbasin. The NRCS Web Soil Survey ([Reference 300](#) and [Reference 301](#)) was used to determine hydrologic soil group values. Aerials and USGS information were used to determine land-use and impervious cover. An average antecedent moisture condition (AMC II) was also used to compute a weighted curve number for the subbasin.

Precipitation losses are incorporated into the USACE HEC-HMS model discussed in [Subsection 2.4.3.3](#). Initial losses of the SCS Curve Number loss model are developed using the initial abstraction formula.

$$I_a = 0.2 * S$$

where I_a = initial abstraction (in.)

S = maximum potential storage of the watershed (in.)

where $S = 1000 / CN - 10$ and CN = average curve number for the watershed

Initial losses for each subbasin are provided in [Table 2.4.3-204](#).

The SCS Curve Number loss model collectively includes interception, infiltration, storage, evaporation, and transpiration. Precipitation losses are derived from the equation for precipitation excess.

$$P_e = (P - I_a)^2 / (P - I_a + S)$$

where P_e = accumulated precipitation excess at time t (in.)

P = accumulated rainfall depth at time t (in.)

I_a = initial abstraction (in.)

S = maximum potential storage of the watershed (in.)

where $S = 1000 / CN - 10$ and CN = average curve number for the watershed

The precipitation loss rate is variable and decreases as cumulative rainfall increases during the storm. The total precipitation depth, losses, and excess for each subbasin are provided in [Table 2.4.3-204](#). Antecedent precipitation is 40 percent of the PMP, preceding the main storm for 3 days, with a 3 day dry period between. During the antecedent storm, precipitation losses account for between 37 and 74 percent of the total rainfall with an average of 53 percent.

During the main storm, precipitation losses only account for between 3 to 22 percent with an average of 9 percent.

As discussed in [Subsection 2.4.3.3](#), the existing study used three significant storm events occurring in October 1964, June 1972, and October 1976 to verify the subbasin unit hydrographs. As part of the verification process, loss rates were verified by comparison with back calculated curve numbers from the three historical extreme storm events.

McKowns Creek/Make-Up Pond B

No precipitation losses were assumed for evaluation of Make-Up Pond B watershed. All rainfall was assumed to be transformed to runoff.

Intermittent Stream/Make-Up Pond A

No precipitation losses were assumed for evaluation of Make-Up Pond A watershed. All rainfall was assumed to be transformed to runoff.

London Creek/Make-Up Pond C

Precipitation losses are incorporated into the USACE HEC-HMS model, as discussed in [Subsection 2.4.3.3](#), using the SCS Curve Number method as previously described for the Broad River. The NRCS Web Soil Survey ([Reference 300](#)) was used to determine hydrologic soil group values. Aerials and USGS information were used to determine land-use and impervious cover. An average antecedent moisture condition (AMC II) was then used to compute a weighted curve number for the watershed.

The SCS Curve Number loss model collectively includes interception, infiltration, storage, evaporation, and transpiration. Initial losses and precipitation losses are derived as previously described for the Broad River. The precipitation loss rate is variable and decreases as cumulative rainfall increases during the storm. Most losses occur during the antecedent precipitation as identified in the hyetograph, [Figure 2.4.3-240](#). The total precipitation depth is 65.52 in., including the antecedent storm. Precipitation losses account for 4.57 in. resulting in 60.95 in. of precipitation converted to runoff.

2.4.3.3 Runoff and Stream Course Models

Broad River

The Broad River runoff and stream course model is based on an existing HEC-1 study ([Reference 217](#)) and modified to include the antecedent rainfall conditions. The watershed in [Figure 2.4.1-205](#) was divided into 20 subbasins as shown in [Figure 2.4.3-203](#). The watershed is predominately identified as Piedmont, as discussed in [Subsection 2.4.1.2.1](#). Referencing [Figure 2.4.3-203](#), subbasins labeled LS-1, LA-2, LL-4, CC-16, 2BR-19, and USS-18A correspond to mountainous areas and foothills of the Blue Ridge Mountains. Topographic characteristics of the Broad River watershed are also discussed in

Subsection 2.4.1.2.2. The USACE HEC-HMS, Version 3.0.1 ([Reference 272](#)), modeling software was used for rainfall runoff and routing calculations. [Figure 2.4.3-206](#) shows the HEC-HMS model watershed routing layout.

Unit hydrographs for all subbasins except Make-Up Pond C were derived from the techniques described in the regional unit hydrograph study for South Carolina, which was performed by the USGS ([Reference 203](#)). The USGS study uses a multiple regression analysis to describe regional unit hydrographs with an adjusted lag time, based on each region of the study. For the HEC-1 study, the unit hydrographs were subsequently converted to 1-hr. durations.

Methods adopted to account for nonlinear basin response at high rainfall rates include increasing the peak of each unit hydrograph by 20 percent and reducing the time to peak by approximately 33 percent. The remaining ordinates of the modified unit hydrographs were adjusted to maintain smooth unit hydrographs with the standard characteristic of 1 in. of runoff. To accommodate the Lake Whelchel subbasin and the Make-Up Pond C subbasin, the BR-15 subbasin unit hydrograph was also modified based on the decrease in drainage area. The resulting unit hydrographs for 19 of the subbasins except Make-Up Pond C are presented in [Figure 2.4.3-207](#), [Figure 2.4.3-208](#), and [Figure 2.4.3-209](#) and tabulated in [Table 2.4.3-205](#).

For the Make-Up Pond C subbasin, the SCS unit hydrograph method was used as a basis for a modified unit hydrograph to transform rainfall to runoff and account for nonlinear basin response. An equivalent SCS unit hydrograph was first determined using the equations and ratios of the SCS dimensionless unit hydrograph. The equivalent SCS unit hydrograph was then modified by increasing the peak of the unit hydrograph by 20 percent and reducing the time to peak by approximately 33 percent. The remaining ordinates of the modified unit hydrograph were adjusted to maintain a smooth unit hydrograph with the standard characteristic of 1 in. of runoff.

The best calibration of the modified SCS unit hydrograph with the initial SCS unit hydrograph was found using a 10-min. computational time step in the HEC-HMS modeling software. Therefore, the time step used to define the ordinates of the modified SCS unit hydrograph is also 10 min. The Make-Up Pond C subbasin has a lag time of 77 min. The initial SCS unit hydrograph and modified unit hydrograph to account for the effects of nonlinear basin response are provided in [Figure 2.4.3-241](#). The modified SCS unit hydrograph is tabulated in [Table 2.4.3-207](#).

The Muskingum-Cunge 8-point cross section method was used for the river routing reaches, except for the Green River reach between Lake Summit and Lake Adger. Because of the Lake Adger backwater effects on the reach, the Modified Puls storage routing method was used. Channel slope, length, and cross section data were developed using USGS quadrangles. Cross sections were field-verified as part of the existing study and modified as necessary. Manning's roughness coefficients were estimated on the basis of accepted published tables by Chow ([Reference 206](#)).

The existing study ([Reference 217](#)) contained discharge rating curves for the Tuxedo, Turner Shoals, Gaston Shoals and Ninety-Nine Islands dams. These curves were developed from Duke Power Company project file data. The rating curves for Lake Lure, Kings Mountain Reservoir, Cherokee Falls, and Lockhart dams were estimated in the existing study by using drawings obtained from the dam owners and the North Carolina State Dam Safety Engineer's office. Reservoirs were modeled using full-pond starting elevations and no turbine discharges were assumed. The flashboards at Gaston Shoals and Ninety-Nine Islands dams were assumed to fail due to overtopping and were incorporated into the rating curves. Additionally, the gates at Lake Lure were assumed to be closed. Reservoir rating curves are presented in [Figure 2.4.3-210](#), [Figure 2.4.3-211](#), [Figure 2.4.3-212](#), [Figure 2.4.3-213](#), [Figure 2.4.3-214](#), [Figure 2.4.3-215](#), [Figure 2.4.3-216](#), and [Figure 2.4.3-217](#).

The Lake Whelchel discharge rating curve is based on a riser with outlet pipe and spillway configuration. The riser maintains the normal pool elevation of 670 ft. The outlet pipe through the dam is a 48 in. concrete pipe. The spillway elevation varies from 680 ft. to 683 ft. The Lake Whelchel rating curve is presented in [Figure 2.4.3-238](#). Lake Whelchel was modeled using a full-pond starting elevation.

The Make-Up Pond C discharge rating curve is based on the designed 4-cycle labyrinth spillway rating curve. Each cycle has a lateral width of 20 ft. The spillway crest elevation is 650 ft. Sensitivity analyses were performed based on a 10 percent increase and decrease of the designed labyrinth spillway rating curve. The Make-Up Pond C rating curve is presented in [Figure 2.4.3-242](#). Make-Up Pond C was modeled using a full-pond starting elevation.

The entire watershed and individual subbasin unit hydrographs of the existing HEC-1 study were verified using three significant storm events occurring in October 1964, June 1972, and October 1976. Base-flow separation was estimated by evaluating semilog plots of each storm event and confirmed with historical daily mean flows at USGS gauging locations. Several USGS gauges are located throughout the watershed. Subbasin input parameters, including the modified BR-15 subbasin, Lake Whelchel subbasin, and Make-Up Pond C subbasin, are listed in [Table 2.4.3-206](#). The exponential recession method is used to model baseflow. The Lake Whelchel subbasin and the Make-Up Pond C subbasin use the same baseflow characteristics as the BR-15 subbasin with an adjusted recession threshold based on the ratio of drainage areas for the two subbasins. Snowmelt is not considered to be a factor in modeling the PMF event, as described in [Subsection 2.4.3.1](#).

To assure HEC-HMS model calibration with the existing study, the HEC-HMS model was first examined using the existing HEC-1 model inputs without antecedent conditions or the modifications for the addition of the Lake Whelchel subbasin and the Make-Up Pond C subbasin. The results were satisfactorily comparable. The HEC-HMS model was then examined using the modifications for the addition of the Lake Whelchel subbasin and the Make-Up Pond C subbasin and the PMP with antecedent rainfall conditions.

Because of large magnitude flows and backwater effects at Gaston Shoals, Cherokee Falls, and Ninety-Nine Islands dams, a standard step method, unsteady-flow hydraulic analysis was performed to more accurately determine the water surface elevation at the Lee Nuclear Station. The USACE HEC-RAS, Version 3.1.3 (Reference 273), modeling software was used to route hydrographs from above Gaston Shoals Dam to Lockhart Dam.

Cross sections were estimated using the existing study, USGS quadrangles, and the USACE NID database. Cross section interpolations were done as necessary to provide a stabilized HEC-RAS model. Manning's roughness coefficients range from 0.03 to 0.08. Contraction and expansion coefficients are based on gradual transitions. Reservoir cross sections were created to approximate the volumes associated with each reservoir. Rating curves were approximated using modeled inline structures. The HEC-RAS model uses a 5-min. computation interval.

The HEC-RAS model is based on the existing study's NWS DAMBRK model. To assure HEC-RAS model calibration, the HEC-RAS model was examined using the DAMBRK input and without antecedent conditions. The results were satisfactorily comparable. Hydrographs from the HEC-HMS analysis, including antecedent rainfall and accounting for nonlinear basin response, were then used as inflow to the HEC-RAS model. Lateral inflows representing local flow between Gaston Shoals Dam and Ninety-Nine Islands Dam were also included in the model. Input hydrographs are shown in Figure 2.4.3-218, Figure 2.4.3-219, Figure 2.4.3-220, Figure 2.4.3-221, Figure 2.4.3-243, and Figure 2.4.3-245.

McKowns Creek/Make-Up Pond B

For McKowns Creek and Make-Up Pond B and the Upper Arm, HEC-HMS modeling software was used for rainfall runoff and storage routing calculations. The watershed is shown in Figure 2.4.3-201. Methods adopted to account for nonlinear basin response at high rainfall rates include increasing the peak of the unit hydrograph by 20 percent and reducing the time to peak by approximately 33 percent. Topographic characteristics of the site and watershed are described in Subsection 2.4.1.2.1.

The Soil Conservation Service (SCS) unit hydrograph method was used as a basis for a modified unit hydrograph to transform rainfall to runoff. An equivalent SCS unit hydrograph was first determined using the equations and ratios of the SCS dimensionless unit hydrograph. The equivalent SCS unit hydrograph was then modified by increasing the peak of the unit hydrograph by 20 percent and reducing the time to peak by approximately 33 percent. The remaining ordinates of the modified unit hydrograph were adjusted to maintain a smooth unit hydrograph with the standard characteristic of 1 in. of runoff.

The best calibration of the modified SCS unit hydrograph with the initial SCS unit hydrograph was found using a 10-min. computational time step in Make-Up Pond B in the HEC-HMS modeling software. Therefore, the time step used to define the ordinates of the modified SCS unit hydrograph is also 10 min. The Make-Up Pond B subbasin has a lag time of 76.8 min. The initial SCS unit hydrograph and modified unit hydrograph to account for the effects of nonlinear

basin response are provided in [Figure 2.4.3-237](#). The modified SCS unit hydrograph is tabulated in [Table 2.4.3-208](#).

The best calibration of the modified SCS unit hydrograph with the initial SCS unit hydrograph was found using a 2-min. computational time step in the Upper Arm watershed in the HEC-HMS modeling software. Therefore, the time step used to define the ordinates of the modified SCS unit hydrograph is also 2 min. The Upper Arm subbasin has a lag time of 16.2 min. The initial SCS unit hydrograph and modified unit hydrograph to account for the effects of nonlinear basin response are provided in [Figure 2.4.3-246](#). The modified SCS unit hydrograph is tabulated in [Table 2.4.3-209](#).

The drainage area, length of watercourse, and average slope of the Make-Up Pond B and Upper Arm watershed was determined from aerial topography created for the area. The lag time was determined using the standard SCS curve number regression equation:

$$T_{lag} = (L^{0.8} * (S+1)^{0.7}) / (1900 * Y^{0.5})$$

where

T_{lag} = lag time (hr.)

L = hydraulic length of the watershed (ft.)

S = maximum potential storage of the watershed (in.);

where $S = 1000/CN - 10$ and CN = average curve number for the watershed

Y = average watershed land slope (percent)

The resulting characteristic parameters for the Make-Up Pond B watershed are as follows:

Drainage Area (sq. mi.)	L (ft.)	CN	S (in.)	Y (%)	T_{lag} (hr.)
2.190	10,320	87	1.49	1.60	1.28

The resulting characteristic parameters for the Upper Arm watershed are as follows:

Drainage Area (sq. mi.)	L (ft.)	CN	S (in.)	Y (%)	T_{lag} (hr.)
0.294	3194	86	1.63	6.03	0.27

The curve number is used to determine the lag time only. During rainfall routing, the model does not use the curve number loss method, under the conservative

assumption that precipitation losses do not occur. The curve number was developed using the NRCS Web Soil Survey ([Reference 278](#)) to determine the soil types in the watershed. About 95 percent of the soil belongs to Hydrologic Soil Group B, and the remaining 5 percent to Hydrologic Soil Group C. The land use is predominately wooded. Make-Up Pond B and the Upper Arm watersheds are modeled as impervious cover. Wet antecedent moisture conditions (AMC III) were also assumed.

Base flow was determined using the minimum average monthly flow of the Gaffney and Ninety-Nine Island gauges (USGS No. 02153500 and 02153551). The flow was then corrected on the basis of a ratio of drainage basin areas. Base flow was estimated to be 1.77 cfs for the Make-Up Pond B watershed and 0.24 cfs for the Upper Arm watershed. Baseflow is applied to the model as a constant rate.

Make-Up Pond B outflow structure rating curve was developed using standard weir and orifice flow equations with coefficients of 3.5 and 0.8 respectively. The structure is a 35 ft. wide concrete ogee spillway with a crest elevation of 570 ft. The road along Make-Up Pond B crest restricts the opening of the structure to a height of 13.5 ft. The outlet empties into backwaters of the Broad River. The Make-Up Pond B rating curve is provided in [Figure 2.4.3-222](#). Available storage was determined based on aerial topography. [Figure 2.4.3-223](#) provides the storage capacity curve. Full pond elevation of 570 ft. was assumed for antecedent conditions.

The Upper Arm Dam outlet structures consist of a 54 in. steel pipe with headwalls at both the upstream and downstream inverts. The upstream invert within the Upper Arm Dam is placed at an elevation of 575.0 ft., which is the normal full pond elevation. The downstream invert emptying into Make-Up Pond B is placed at an elevation of 570.0 ft. [Figure 2.4.3-249](#) shows a schematic of the Upper Arm culvert structure. The Upper Arm culvert is evaluated considering full flow capacity and also no flow.

The access road separating the Upper Arm Dam from Make-Up Pond B is at elevation 590.0 ft. and acts as a broad-crested weir with a crest length of 390 ft. with a crest breadth of 8 ft. The maximum height of the dam is 15 ft. from the normal full pond elevation of 575 ft. up to the crest embankment. Water volume below 575 ft. is not considered due to nearly equivalent hydrostatic forces on both sides of the dam embankment during the PMF event. Overtopping of the Upper Arm dam crest is evaluated using the standard weir flow equation with a coefficient of 2.6. The Upper Arm Dam overtopping discharge rating curve is provided in [Figure 2.4.3-247](#). Available storage was determined based on aerial topography. [Figure 2.4.3-248](#) provides the storage capacity curve. Antecedent conditions for the normal full pond elevation were assumed to be 575 ft. based on historical observation.

Intermittent Stream/Make-Up Pond A

For the intermittent stream and Make-Up Pond A, HEC-HMS modeling software was used for rainfall runoff calculations. The watershed is shown in [Figure 2.4.3-201](#). The following analysis for Make-Up Pond A does not account for

nonlinear basin response at high rainfall rates. During severe flooding events, Make-Up Pond A is inundated by backwaters of the Broad River. Broad River flooding coincident with dam failures, as discussed in [Subsection 2.4.4](#), exceeds the maximum flooding elevation for Make-Up Pond A. Therefore, coincident wind wave activity for Make-Up Pond A is based on flooding from the Broad River. By incorporating the Broad River analysis to determine the maximum water surface elevation, the Make-Up Pond A coincident wind wave evaluation accounts for nonlinear basin response at high rainfall rates as discussed above. Topographic characteristics of the site and watershed are described in [Subsection 2.4.1.2.1](#).

The SCS unit hydrograph method was used to transform rainfall to runoff. The drainage area, length of watercourse, and average slope of the watershed were determined from aerial topography created for the area. The lag time was determined using the standard SCS curve number regression equation:

$$T_{lag} = (L^{0.8} * (S+1)^{0.7}) / (1900 * Y^{0.5})$$

where

T_{lag} = lag time (hr.)

L = hydraulic length of the watershed (ft.)

S = maximum potential storage of the watershed (in.);

where $S = 1000/CN - 10$ and CN = average curve number for the watershed

Y = average watershed land slope (percent)

The resulting characteristic parameters for the watershed are as follows:

Drainage Area (sq. mi.)	L (ft.)	CN	S (in.)	Y (%)	T_{lag} (hr.)
0.619	3340	92	0.87	3.48	0.29

The curve number is used to determine the lag time only. During rainfall routing, the model does not use the curve number loss method, under the conservative assumption that precipitation losses do not occur. The curve number was developed using the NRCS Web Soil Survey ([Reference 278](#)) to determine the soil types in the watershed. About 95 percent of the soil belongs to Hydrologic Soil Group B, and the remaining 5 percent to Hydrologic Soil Group C. The land use is predominately industrial. Make-Up Pond A is modeled as impervious cover. Wet antecedent moisture conditions (AMC III) were also assumed.

Base flow was determined using the minimum average monthly flow of the Gaffney and Ninety-Nine Island gauges (USGS No. 02153500 and 02153551). The flow was then corrected on the basis of a ratio of drainage basin areas. Base flow was estimated to be 0.50 cfs and applied to the model as a constant rate.

Although the full pond elevation is 547 ft., the crest elevation low point of 555.1 ft. was assumed for water surface elevation antecedent conditions. Make-Up Pond A overtopping flows empty into backwaters of the Broad River. The outflow rating curve was developed using the standard weir flow equation with a 2.6 discharge coefficient. The embankment crest is approximately 1500 ft. long and has an irregular shape. The rating curve is provided in [Figure 2.4.3-224](#). Available storage was determined based on aerial topography. [Figure 2.4.3-225](#) provides the storage capacity curve.

London Creek/Make-Up Pond C

For London Creek and Make-Up Pond C, HEC-HMS modeling software was used for rainfall runoff calculations. The watershed is shown in [Figure 2.4.3-239](#). The SCS unit hydrograph method was used as a basis for a modified unit hydrograph to transform rainfall to runoff and account for nonlinear basin response. As discussed above for the Make-Up Pond C subbasin in the Broad River watershed, an equivalent SCS unit hydrograph was first determined using the equations and ratios of the SCS dimensionless unit hydrograph. The equivalent SCS unit hydrograph was then modified by increasing the peak of the unit hydrograph by 20 percent and reducing the time to peak by approximately 33 percent. The remaining ordinates of the modified unit hydrograph were adjusted to maintain a smooth unit hydrograph with the standard characteristic of 1 in. of runoff.

The best calibration of the modified SCS unit hydrograph with the initial SCS unit hydrograph was found using a 10-min. computational time step in the HEC-HMS modeling software. Therefore, the time step used to define the ordinates of the modified SCS unit hydrograph is also 10 min. The initial SCS unit hydrograph and modified unit hydrograph to account for the effects of nonlinear basin response are provided in [Figure 2.4.3-241](#). The modified SCS unit hydrograph is tabulated in [Table 2.4.3-207](#).

The drainage area, length of watercourse, and average slope of the watershed were determined from aerial topography created for the area. The lag time was determined using the standard SCS curve number regression equation:

$$T_{lag} = (L^{0.8} * (S+1)^{0.7}) / (1900 * Y^{0.5})$$

Where:

T_{lag} = lag time (hr.)

L = hydraulic length of the watershed (ft.)

S = maximum potential storage of the watershed (in.);

where $S = 1000/CN - 10$ and CN = average curve number for the watershed

Y = average watershed land slope (percent)

The resulting characteristic parameters for the watershed are as follows:

Drainage Area (sq. mi.)	L (ft.)	CN	S (in.)	Y (%)	T _{lag} (min.)
3.87	5393	63.9	5.65	2.23	77

The curve number was developed using the NRCS Web Soil Survey ([Reference 300](#)) to determine the soil types in the watershed. About 87.4 percent of the soil belongs to Hydrologic Soil Group B, 10.4 percent belonging to Hydrologic Soil Group C, and the remaining 2.2 percent to Hydrologic Soil Group C/D and D. The land use is predominately wooded, grassland, and large lot residential. The watershed contains approximately 27.8 percent impervious cover, including Make-Up Pond C and Lake Cherokee. Average antecedent moisture conditions (AMC II) were used, along with the 40 percent PMP antecedent rainfall.

Base flow was determined based on the Broad River watershed BR-15 subbasin. The recession baseflow method was used with an initial discharge per area of 1.63 cfs/sq. mi. and a recession constant of 0.4919. The recession threshold was calculated to be 23 cfs based on a ratio of the Make-Up Pond C and BR-15 subbasin drainage areas.

The Make-Up Pond C discharge rating curve is based on the designed 4-cycle labyrinth spillway rating curve. Each cycle has a lateral width of 20 ft. The spillway crest elevation is 650 ft. Sensitivity analyses were performed based on a 10 percent increase and decrease of the designed labyrinth spillway rating curve. The Make-Up Pond C rating curve is presented in [Figure 2.4.3-242](#). Available storage was determined based on aerial topography. [Figure 2.4.3-244](#) provides the storage capacity curve. A full pond elevation of 650 ft. msl was assumed for antecedent conditions.

2.4.3.4 Probable Maximum Flood Flow

Broad River

Applying the precipitation, described in [Subsection 2.4.3.1](#), and the precipitation losses, described in [Subsection 2.4.3.2](#), to the runoff model, described in [Subsection 2.4.3.3](#), the peak PMF discharge at the Lee Nuclear Station was determined to be 823,212 cfs resulting from the 1000-sq. mi. storm centered near the centroid of the Gaston Shoals Dam drainage basin. The resulting flow hydrograph at the Lee Nuclear Station is shown in [Figure 2.4.3-226](#). Temporal distribution of the PMP and storm location is discussed in [Subsection 2.4.3.1](#). Inclusion of upstream and downstream river structures is discussed in [Subsection 2.4.3.3](#). Dam failures are discussed in [Subsection 2.4.4](#). No credit is taken for the lowering of flood levels at the site due to downstream dam failure.

McKowns Creek/Make-Up Pond B

The precipitation, described in [Subsection 2.4.3.1](#), with no precipitation losses, described in [Subsection 2.4.3.2](#) is applied to the runoff model, described in [Subsection 2.4.3.3](#). Assuming the Upper Arm Dam culvert is not functional produces the maximum conditions. The McKowns Creek and Make-Up Pond B peak PMF runoff was determined to be 20,039 cfs resulting from the 6-hr. two-thirds peaking storm event. The routed peak discharge is 6471 cfs.

However, the 72-hr. tail end peaking storm event resulting in a peak PMF runoff of 18,937 cfs and a routed discharge of 8386 cfs provided the controlling water surface elevation. The peak runoff in the Upper Arm Dam during the 72-hr. tail end peaking storm event will be 3577 cfs with a peak discharge of 3549 cfs. The resulting Make-Up Pond B flow hydrograph for the 72-hr. tail end peaking storm event is shown in [Figure 2.4.3-227](#). Temporal distribution of the PMP is discussed in [Subsection 2.4.3.1](#).

Because the Make-Up Pond B and Upper Arm Dam watersheds are small, the position of the PMP is considered point rainfall affecting the entire watershed equally. With the exception of the Upper Arm Dam, there are no upstream structures. Failure of the Upper Arm Dam is discussed in [Subsection 2.4.4](#). No credit is taken for the lowering of flood levels at the site due to downstream dam failure.

Intermittent Stream/Make-Up Pond A

Applying the precipitation, described in [Subsection 2.4.3.1](#), with no precipitation losses, described in [Subsection 2.4.3.2](#), to the runoff model, described in [Subsection 2.4.3.3](#), the intermittent stream and Make-Up Pond A peak PMF runoff was determined to be 11,644 cfs resulting from the 6-hr. storm event. The routed peak discharge is 9847 cfs. The resulting flow hydrograph is shown in [Figure 2.4.3-228](#). Temporal distribution of the PMP is discussed in [Subsection 2.4.3.1](#). Because the watershed is small, the position of the PMP is considered point rainfall affecting the entire watershed equally. There are no upstream structures. No credit is taken for the lowering of flood levels at the site due to downstream dam failure.

London Creek/Make-Up Pond C

Applying the precipitation, described in [Subsection 2.4.3.1](#), and the precipitation losses, described in [Subsection 2.4.3.2](#), to the runoff model, described in [Subsection 2.4.3.3](#), the London Creek and Make-Up Pond C peak PMF runoff providing the highest water surface elevation from the 72-hr. tail end peaking storm event was determined to be 29,167 cfs. The routed peak discharge is 10,577 cfs. Temporal distribution of the PMP is discussed in [Subsection 2.4.3.1](#). Because the watershed is small, the position of the PMP is considered point rainfall affecting the entire watershed equally. The upstream Lake Cherokee watershed was incorporated into the Make-Up Pond C watershed. Therefore, Lake Cherokee was assumed to pass runoff flow without any detention. No credit

is taken for the lowering of flood levels at the Lee Nuclear Station due to downstream dam failure.

2.4.3.5 Water Level Determinations

Broad River

Subsection 2.4.4.3 addresses coincident wind wave activity for the Broad River. The maximum Lee Nuclear Station flood elevation is 551.49 ft. resulting from the 1000-sq. mi. storm centered near the centroid of the Gaston Shoals Dam drainage basin. **Subsection 2.4.3.3** describes the models used to translate the PMP discharge to the elevation hydrograph. The resulting elevation hydrograph at the Lee Nuclear Station is shown in **Figure 2.4.3-229**. The maximum flood elevation is well below the station's safety-related plant elevation of 593 ft.

McKowns Creek/Make-Up Pond B

Subsection 2.4.4.3 addresses coincident wind wave activity for Make-Up Pond B. The maximum water surface elevation of Make-Up Pond B without considering Upper Arm Dam failure, resulting from the 6-hr. two-thirds peaking storm event modeled with a 1-min. time step, was found to be 583.29 ft. The elevation hydrograph is provided in **Figure 2.4.3-230**. The maximum water surface elevation of Make-Up Pond B resulting from the 72-hr. tail end peaking storm event modeled with a 1-min. time step was found to be 584.40 ft. The maximum is produced by the condition that the Upper Arm Dam culvert is not functional, but does include overtopping flows. The peak water surface elevation in the Upper Arm Dam for the 72-hr. tail end, peaking storm will be 592.28 ft. The ridge on the east side of the Upper Arm Dam separates the Upper Arm and the site, as illustrated in **Figure 2.4.3-201**. At elevations above 590.0 ft., discharge across the dam embankment flows directly into Make-Up Pond B. Nevertheless, peak water surface elevations for the Upper Arm are below the station's safety-related plant elevation of 593 ft. The elevation hydrograph for Make-Up Pond B is provided in **Figure 2.4.3-231**.

Make-Up Pond B includes an adequately sized outlet structure and is not located on a sizeable river or stream. Therefore, the potential for significant debris to be picked up by a rise in the water level and then transported to the outlet structure where it could collect as an obstruction is minimal. Blockage of the outlet structure was not considered in the analysis and debris blockage of the outlet structure is not considered to be a credible event due to Duke Energy's shoreline management program and debris barrier system discussed in **Subsection 2.4.1.2.2.6**.

Intermittent Stream/Make-Up Pond A

Subsection 2.4.4.3 addresses coincident wind wave activity for Make-Up Pond A. The maximum water surface elevation of Make-Up Pond A, resulting from the 6-hr. storm, two-thirds peaking distribution, modeled with a 1-min. time step, was found to be 558.15 ft. The elevation hydrograph is provided in **Figure 2.4.3-233**.

Subsection 2.4.3.3 describes the models used to translate the PMP discharge to elevation.

London Creek/Make-Up Pond C

The Make-Up Pond C reservoir is located on a tributary of the Broad River, west of the Lee Nuclear Station, as shown in **Figure 2.4.1-213**, but is not adjacent to the Lee Nuclear Station. However, the PMF for London Creek and Make-Up Pond C is determined for the purpose of combination with dam failure permutations as discussed in **Subsection 2.4.4.1**. Because the PMF discharge flow from Make-Up Pond C is bounded by the Broad River watershed PMF, spillover from Make-Up Pond C during a PMF event is not a limiting event for flooding at the Lee Nuclear Station when taken as an isolated event. For reference to the dam failure permutations, the maximum water surface elevation of Make-Up Pond C, resulting from the 72-hr storm modeled with a 10 min. time step, was found to be 656.68 ft. **Subsection 2.4.3.3** describes the models used to translate the PMP discharge to elevation.

2.4.3.6 Coincident Wind Wave Activity

Coincident wind wave activity is evaluated for the Broad River, Make-Up Pond A and Make-Up Pond B. Fetch lengths are determined using the longest straight line fetch based on U.S. Geological Survey quadrangles and the site grading and drainage plan. Wave height, setup, and runup are estimated using U.S. Army Corps of Engineers guidance (**Reference 295**). A coincident 2-year annual extreme mile wind speed of 50 mph is estimated based on ANSI/ANS-2.8-1992 (**Reference 202**). Wind setup is estimated using additional U.S. Army Corps of Engineers guidance (**Reference 269**).

Broad River

Coincident wind wave activity for the Broad River is addressed in **Subsection 2.4.4.3**.

Intermittent Stream/Make-Up Pond A

Coincident wind wave activity for Make-Up Pond A is addressed in **Subsection 2.4.4.3**.

McKowns Creek/Make-Up Pond B

Coincident wind wave activity for Make-Up Pond B is addressed in **Subsection 2.4.4.3**.

London Creek/Make-Up Pond C

The Make-Up Pond C reservoir is located on a tributary of the Broad River, west of the Lee Nuclear Station, as shown in **Figure 2.4.1-213**, such that wind wave activity has no consequence to the Lee Nuclear Station. However, a postulated failure of the Make-Up Pond C dam would release water to the Broad River prior

to reaching the Lee Nuclear Station. A failure of the Make-Up Pond C dam coincident with the PMF is discussed in [Subsection 2.4.4.1](#), and flooding effects as a result of wind wave activity are bounded by that discussion.

2.4.4 POTENTIAL DAM FAILURES

WLS COL 2.4-2 The guidance in Appendix A of NRC Regulatory Guide 1.59, Rev. 2, *Design Basis Floods for Nuclear Power Plants*, was followed in evaluating potential dam failures, by applying the guidance of American National Standards Institute/American Nuclear Society-2.8-1992, *Determining Design Basis Flooding at Power Reactor Sites* ([Reference 202](#)).

The Upper Broad River drainage basin upstream of Ninety-Nine Islands Dam derives water from several tributaries that contain a considerable number of dams. According to the U.S. Army Corps of Engineers (USACE), National Inventory of Dams, there are approximately 131 upstream dams, not including Make-Up Pond C, and five of those have been breached ([Reference 276](#)). Most of the dams in the drainage basin have small to insignificant storage capacity. The six largest reservoirs in the basin represent about 88 percent of the total storage capacity for the basin. Two additional dams, Cherokee Falls and Gaston Shoals, located immediately upstream from the Lee Nuclear Station, possess less than 2 percent of the total storage capacity for the basin.

Make-Up Pond B and Make-Up Pond A are located at elevations much lower than the Lee Nuclear Station's safety-related facilities. Failure of these water features would result in a discharge to smaller ponds and then directly to the Broad River. The respective volumes are small compared to the available capacity of the Broad River and the freeboard available at the site. Failure of the on-site reservoirs would not affect the safety-related facilities.

The Upper Arm Dam is located upstream of Make-Up Pond B southwest of the nuclear island. Failure of this dam would result in discharges directly to Make-Up Pond B. The resulting rapid increase of water volume would increase the peak water surface levels and discharge rates in Make-Up Pond B. The volume of discharge from the Upper Arm Dam is small compared to the volume of Make-Up Pond B. Failure of this reservoir will not affect the safety-related facilities.

Make-Up Pond C is located on a tributary of the Broad River, west of the Lee Nuclear Station. As described below, the critical dam failure evaluation coincident with the PMF for the Broad River watershed includes the assumed overtopping failure of Make-Up Pond C. Assumed overtopping dam failure coincident with the PMF for the Make-Up Pond C watershed has also been evaluated, but does not exceed the maximum flood elevation associated with the Broad River critical dam failure event and, thus, is bounded by the critical dam failure event. Therefore, there are no safety-related structures that could be affected by flooding due to a Make-Up Pond C dam failure.

The described studies have been made solely to ensure the safety-related facilities of the Lee Nuclear Station are protected against floods caused by the assumed failure of dams. The postulated dam failure events do not infer or concede that the dams are unsafe.

The critical dam failure event is the assumed overtopping failures of Lake Lure Dam, Tuxedo Dam, Turner Shoals Dam, Lake Welchel Dam, Kings Mountain Reservoir Dam, and Make-Up Pond C Dam, including the dam at Lake Cherokee, coincident with the probable maximum flood (PMF). The resulting flow rate and water surface elevation at the station is provided in the discussion below. There are no safety-related structures that could be affected by flooding due to dam failure. All elevations provided in this subsection are above mean sea level.

2.4.4.1 Dam Failure Permutations

According to guidance ([Reference 202](#)), seismic dam failure is to be examined using the safe shutdown earthquake coincident with the peak of the 25-year flood and operating basis earthquake coincident with the peak of one-half PMF or the 500-year flood. Dam failure permutations were first examined assuming hydrologic failure of dams coincident with the PMF. Many of the upstream structures are designed to withstand overtopping. However, structural analysis of each structure has not been performed. The PMF is a more extreme event than the listed hydrologic events coincident with seismic dam failure. Seismic dam failure coincident with lesser flooding would result in lower flood elevations and has not been examined. Therefore, the evaluations described below comply with Regulatory Guide 1.59.

Broad River

The considered upstream structures are described below. Reservoirs were modeled using normal water surface elevations with no turbine discharges. Additionally, the gates at Lake Lure were assumed to be closed. Antecedent conditions are discussed in [Subsection 2.4.3](#).

Failure of the downstream structure, Ninety-Nine Islands Dam, would result in lowering the water surface elevation at the Lee Nuclear Station to some degree. Conservatively, Ninety-Nine Islands Dam has not been considered to fail during any of the dam failure scenarios. However, failure of the flashboards has been incorporated into the rating curve.

Cherokee Falls and Gaston Shoals

Cherokee Falls Dam is approximately 4.5 river mi. upstream of Ninety-Nine Islands Dam on the Broad River in Cherokee County, South Carolina. The dam, built in 1826, is a concrete gravity structure approximately 1700 ft. long and 16 ft. high. It has an ogee spillway elevation of 531.5 ft. with 4-ft. flashboards raising the operating pond level to 535.5 ft. The impounded reservoir has an estimated storage capacity of 200 ac.-ft. at normal water surface elevation. Flashboard failure is incorporated into the discharge rating curve used for the structure.

Gaston Shoals Dam is approximately 11.5 river mi. upstream of Ninety-Nine Islands Dam on the Broad River in Cherokee County, South Carolina. The dam, built in 1908, is a series of three gravity structures. The upper masonry gravity spillway is about 707 ft. long with an overflow spillway crest elevation of 599.40 ft. and 6-ft. flashboards that raise the operating pond level to 605.4 ft. The middle concrete gravity section was built in 1917 and is about 381 ft. long. The overflow spillway crest elevation is 601.2 ft. with 4-ft. flashboards up to 605.2 ft. The masonry gravity bulkhead section is about 472 ft. long with a crest elevation of 613.4 ft. The impounded reservoir has an estimated storage capacity of 2500 ac.-ft. at normal water surface elevation. Flashboard failure is incorporated into the discharge rating curve used for the structure.

Both dams are significantly overtopped for a lengthy duration during PMF conditions. Dam failure has been conservatively assumed to occur coincident with the PMF peak flood wave in order to maximize water surface elevations. The breach characteristics for Cherokee Falls assume complete failure of the full height and length of the structure to occur in 0.5 hours (hr.). The breach characteristics for Gaston Shoals assume failure of the full height and length of the middle spillway structure to occur in 0.5 hr., along with failure of the embankment abutments separating the three structures.

An overtopping breach of Gaston Shoals, coincident with the PMF, results in a flow of 824,000 cfs and a water surface elevation of 551.52 ft. at the Lee Nuclear Station. Overtopping breaches of both Gaston Shoals and Cherokee Falls, coincident with the PMF, result in the same flow and water surface elevation. Because of the small reservoir volumes and large PMF discharge, the dam failures have little effect on the resulting flow and water surface elevations.

Major Upstream Structures

Lake Lure is about 47 mi. northwest of the Lee Nuclear Station on the Broad River in Rutherford County, North Carolina. The dam, built in 1927, is a concrete, multiple-arch structure approximately 480 ft. long and 124 ft. high, with a full pond elevation at 991 ft. There are gated spillways and the arches are set at various elevations, providing additional discharge capacity. The discharge rating curve, used for modeling purposes, conservatively assumes the gates are in the closed position. The impounded reservoir has an estimated storage capacity of about 32,295 ac.-ft. at normal water surface elevation.

Tuxedo Dam, impounding Lake Summit, is about 52 mi. northwest of the Lee Nuclear Station on the Green River in Henderson County, North Carolina. The dam, built in 1920, is a concrete-arch structure approximately 254 ft. long and 130 ft. high, with a full pond elevation at 2012.6 ft. The impounded reservoir has an estimated storage capacity of about 9300 ac.-ft. at normal water surface elevation.

Turner Shoals Dam, impounding Lake Adger, is about 43 mi. northwest of the Lee Nuclear Station, downstream of Tuxedo Dam on the Green River in Polk County, North Carolina. The dam, built in 1925, is a concrete, multiple-arch structure approximately 689 ft. long and 90 ft. high, with a full pond elevation at 911.6 ft. The

impounded reservoir has an estimated storage capacity of about 11,700 ac.-ft. at normal water surface elevation.

Kings Mountain Reservoir Dam, also referred to as Moss Lake Dam, is about 17 mi. northeast of the Lee Nuclear Station on Buffalo Creek in Cleveland County, North Carolina. The dam, built in 1973, is a compacted earth-fill structure approximately 840 ft. long and 99 ft. high. The top of the dam is at an elevation of 750 ft. The spillway is located at the right abutment and consists of a 350 ft. long concrete ogee section with a crest elevation of 736 ft. The impounded reservoir has an estimated storage capacity of 44,400 ac.-ft. at normal water surface elevation.

Lake Whelchel is located approximately 8 mi. northwest of the Lee Nuclear Station on Cherokee Creek in Cherokee County, South Carolina. The dam at Lake Whelchel, built in 1964, is a compacted earth-fill structure approximately 2100 ft. long and 61 ft. high. The dam crest elevation is 685 ft. A riser and 48 in. concrete pipe outlet works sets the normal pool elevation at 670 ft. The spillway is 565 ft. long and varies in elevation from 680 ft. to 683 ft. Lake Whelchel has an estimated storage capacity of approximately 2438 ac.-ft. at normal water surface elevation.

Make-Up Pond C is located approximately 2 mi. west of the Lee Nuclear Station on London Creek in Cherokee County, South Carolina. Make-Up Pond C is formed by construction of an earthen dam and saddle dikes that impound London Creek just upstream of the confluence with Little London Creek. The Make-Up Pond C dam crest elevation is 660 ft. A labyrinth spillway sets the normal pool elevation at 650 ft. The designed 4-cycle labyrinth spillway has a lateral width of 20 ft. per cycle. The dam is 132 ft. high. The impounded reservoir has an estimated storage capacity of approximately 22,000 ac.-ft. at normal water surface elevation.

Lake Lure Dam, Tuxedo Dam, and Turner Shoals Dam are designed to withstand overtopping. However, the structural integrity of the dams and foundations has not been examined. The degree and duration of overtopping each dam is capable of withstanding is not considered in this evaluation. Therefore, overtopping dam failure has been calibrated to occur coincident with the PMF peak flood wave in order to maximize water surface elevations for Lake Lure Dam and Tuxedo Dam. Lake Summit and Lake Adger are located in series on the Green River. Overtopping failure of the Turner Shoals Dam was calibrated to coincide with the resulting peak flood wave of the Tuxedo Dam failure. Breach parameters assume failure of the complete structures to occur in 0.1 hr.

Kings Mountain Reservoir Dam, the Lake Whelchel Dam, and the Make-Up Pond C Dam are not expected to be overtopped based on the PMF analysis with antecedent storm conditions. However, overtopping failure is postulated for this analysis, and dam failures have been calibrated to occur coincident with the PMF peak flood wave in order to maximize water surface elevations.

Lake Cherokee is located just upstream of Make-Up Pond C on a tributary of London Creek in Cherokee County, South Carolina. The dam is a compacted earth-fill structure approximately 940 ft. long, 40 ft. high and has an estimated

maximum storage capacity of 720 ac.-ft. The dam at Lake Cherokee is assumed to fail by overtopping based on the full height of the structure. The peak failure flow is derived using the HEC-HMS dam failure equation identified below. No tailwater elevation was assumed, maximizing the head difference and breach outflow. The peak outflow is added to the PMF peak flood wave for the Make-Up Pond C watershed to maximize the Make-Up Pond C dam failure.

$$Q_{\max} = 3.09 * W_b * h^{1.5} + 2.48 * S * h^{2.5}$$

Where:

- Q_{\max} = peak outflow (cfs)
- W_b = width of breach (ft.)
- h = smaller of the head difference between the reservoir interior water surface elevation and the tailwater surface elevation, or head difference between the reservoir interior water surface elevation and the breach bottom invert elevation (ft.)
- S = side slope of the breach

Embankment breach characteristics are based on the USACE RD-13 (Reference 250). Failure development time for embankment sections is estimated to occur from 0.5 to 4 hr. Breach width for embankment sections is estimated to be from 0.5 to 3 times the dam height. Side slopes for an embankment breach are estimated to be from 0:1 to 1:1 (horizontal:vertical). To maximize the peak outflow, a breach width of 3 times the dam height was used along with 1:1 side slopes and the shortest failure development time of 0.5 hr.

Sensitivity was also performed based on the time of failure for the various structures. Additionally, several failure times were examined based on the peak outflow time at Ninety-Nine Islands Dam. Using the same breach parameters as discussed above, all structures were assumed to fail simultaneously, rather than individually based on the peak flood wave at each dam. It was determined that the critical dam failure scenario occurred when all dams failed simultaneously with a failure time near to the peak PMF outflow at Ninety-Nine Islands Dam.

The multiple failures due to overtopping, coincident with the PMF, result in a peak flow of approximately 1,850,000 cfs. The peak flow is determined using the HEC-HMS model discussed in Subsection 2.4.4.2.

McKowns Creek/Make-Up Pond B

As described earlier in Subsection 2.4.4, the failure of the Upper Arm Dam would directly impact Make-Up Pond B. The dam crest is at 590 ft. Simulation of dam failure was performed in HEC-HMS. Embankment breach parameters were selected based on the USACE RD-13 (Reference 250) document. Failure development time for embankment sections is estimated to occur at 0.5 hr. from the onset of dam breach. Breach width for embankment sections is estimated to be 3 times the height of the Upper Arm Dam as described in Subsection 2.4.3.3.

Side slopes for the embankment breach facing the Make-Up Pond B are set at 1:1. Dam breach parameters were selected to maximize the peak outflow.

The maximum peak PMF runoff from Make-Up Pond B, considering Upper Arm Dam failure, resulting from the 6-hr. tail end peaking storm event modeled with a 1-minute time step, was found to be 23,726 cfs. However, the controlling water surface elevation resulted from the 72-hr. tail end peaking storm event modeled with a 1-minute time step. The peak elevation is produced by the condition that the Upper Arm Dam culvert is not functional. The peak PMF runoff from the 72-hr. tail end peaking storm into Make-Up Pond B was found to be 23,515 cfs. The peak runoff hydrograph is provided in [Figure 2.4.4-203](#). The peak runoff in the Upper Arm Dam resulting from the 72-hr. tail end peaking storm is 3577 cfs with a dam failure peak discharge of 6785 cfs.

Make-Up Pond C Dam

Assumed overtopping dam failure of the Make-Up Pond C Dam has also been evaluated coincident with a more intense PMF confined to the smaller Make-Up Pond C watershed as described in [Subsection 2.4.3](#). As previously discussed, failure of the dam at Lake Cherokee was also included to maximize the peak dam failure outflow from Make-Up Pond C.

The Make-Up Pond C peak dam failure outflow was combined with the maximum historical flow recorded on the Broad River at Gaffney, identified in [Table 2.4.2-201](#), to account for any coincidental flow in the Broad River. However, the resulting combined peak outflow of 1,336,000 cfs does not exceed the critical dam failure event for the Broad River watershed previously described. Therefore, even if routed to the Lee Nuclear Station without attenuation, the resulting water surface elevation would not exceed the elevation determined from the critical multiple dam failure scenario coincident with the Broad River watershed PMF.

Cleveland County Sanitary District

According to the Federal Register ([Reference 226](#)), a notice of intent was filed on July 11, 2006, for a Draft Environmental Impact Statement (DEIS) to be prepared for a proposed reservoir on the First Broad River in Cleveland County, North Carolina. The Cleveland County Sanitary District applied for a permit to construct a water supply reservoir about 1 mi. north of Lawndale, North Carolina. The DEIS is currently in preparation. Lawndale is about 26 mi. northeast of the Lee Nuclear Station.

The proposed embankment dam may be about 83 ft. high and 1245 ft. long, impounding a surface area of 2245 ac. and inundating areas lower than 860 ft. Using USGS quadrangle contours, volume calculations estimate the storage to be about 47,500 ac.-ft. The embankment is approximately the same size as Kings Mountain Reservoir. The reservoir contains approximately the same storage with twice the surface area of the Kings Mountain Reservoir. It is assumed that the dam is designed to prevent failure during a PMF event. Based on the distance from the Lee Nuclear Station and available freeboard, it is also assumed that any failure effects due to seismic activity coincident with lesser flood events would be

no worse than those estimated for the Kings Mountain Reservoir. The above evaluation includes failure of the Kings Mountain Reservoir Dam during the PMF. Therefore, any failure effects from the proposed embankment dam would be less than those provided.

Other Considerations

There are no safety-related facilities that could be affected by loss of water supply due to dam failure. This is addressed further in [Subsection 2.4.11](#). Additionally, there are no safety-related facilities that could be affected by water supply blockages due to sediment deposition or erosion during dam failure induced flooding. There are no onsite water control or storage structures located above site grade that may induce flooding. As discussed in [Subsection 2.4.4.3](#), the Lee Nuclear Station's safety-related facilities are located above the resulting water surface elevation. Therefore, no safety-related structures could be affected by waterborne missiles.

2.4.4.2 Unsteady-Flow Analysis of Potential Dam Failures

The failures for the dams immediately upstream of the Lee Nuclear Station, Cherokee Falls and Gaston Shoals, were examined using the same HEC-RAS unsteady flow model from the PMF calculation described in [Subsection 2.4.3](#). The model was modified by including the HEC-RAS breach feature and adjusting the computation interval to 30 sec. Unsteady state flow is computer solved using the principles of the continuity and momentum equations.

The failures of the additional dams upstream of the Lee Nuclear Station, were first examined using the same HEC-HMS quasi-unsteady flow model from the PMF calculation described in [Subsection 2.4.3](#). The dam breach feature in the HEC-HMS model was used to determine the resulting flow of the Broad River at Ninety-Nine Islands Dam. HEC-HMS employs finite difference methods approximating the continuity and momentum equations.

The HEC-HMS peak flow determined at Ninety-Nine Islands Dam was then used as input to the HEC-RAS model from the PMF calculation described in [Subsection 2.4.3](#). Steady state analysis was performed to determine the water surface elevation at the Lee Nuclear Station. Steady state flow is computer solved using the principles of the continuity and energy equations.

Verification of the models is discussed in [Subsection 2.4.3](#). However, verifying the models with actual data approaching the magnitude of the PMF is not possible. The resulting extreme flows determined using HEC-HMS, HEC-RAS unsteady state flow, and HEC-RAS steady state flow are discussed below. The comparative results indicate the models are appropriate for artificially large floods.

The HEC-RAS models are used to route the flood flow through downstream Ninety-Nine Islands Dam and Lockhart Dam. Coefficients, antecedent conditions, and coincident flow are discussed above and in [Subsection 2.4.3](#). Domino-type failure is discussed above. As discussed in [Subsection 2.4.4.3](#), the Lee Nuclear Station's safety-related facilities are located above the resulting water surface

elevation. Therefore, no safety-related structures could be affected by flood waves.

2.4.4.3 Water Level at the Plant Site

The methods and models used to determine the resulting water surface elevation are described above and in [Subsection 2.4.3](#). Model verification and reliability is also discussed above and in [Subsection 2.4.3](#). The HEC-RAS model, as described above, was used to model a resulting steady state flow of 1,850,000 cfs to determine the water surface elevation at the station.

The resulting water surface elevation at the Lee Nuclear Station is 576.50 ft. The maximum flood elevation is well below the station's safety-related plant elevation of 593 ft. The resulting water surface elevation of the dam failure analysis using HEC-HMS and HEC-RAS was compared with the resulting water surface elevations of the PMF analysis using HEC-HMS and HEC-RAS. The comparison is provided in [Table 2.4.4-201](#). Given the significant freeboard remaining at the site, a full unsteady-flow analysis to determine dam breach flows and resulting water surface elevations with greater precision was determined to be unnecessary.

McKowns Creek/Make-Up Pond B

Using the HEC-HMS model, the maximum water surface elevation of Make-Up Pond B, considering Upper Arm Dam failure, resulting from the 72-hr. tail end peaking storm event modeled with a 1-min. time step was found to be 585.06 ft. The maximum is produced by the condition that the Upper Arm Dam culvert is not functional. The elevation hydrograph is provided in [Figure 2.4.4-205](#). The peak water surface in the Upper Arm Dam resulting from the 72-hr. tail end peaking storm is 592.28 ft. The ridge on the east side of the Upper Arm separates the Upper Arm and the site, as illustrated in [Figure 2.4.3-201](#). At elevations above 590.0 ft., discharge across the dam embankment flows directly into Make-Up Pond B. Nevertheless, peak water surface elevations for the Upper Arm are below the station's safety-related plant elevation of 593 ft.

Coincident Wind Wave Activity

Coincident wind wave activity is evaluated for the Broad River, Make-Up Pond A and Make-Up Pond B. Fetch lengths are estimated using the longest straight line fetch based on U.S. Geological Survey quadrangles and the site grading and drainage plan. Wave height, setup, and runup are estimated using U.S. Army Corps of Engineers guidance ([Reference 295](#)). A coincident 2-year annual extreme mile wind speed of 50 mph is estimated based on ANSI/ANS-2.8-1992 ([Reference 202](#)). Wind setup is estimated using additional U.S. Army Corps of Engineers guidance ([Reference 269](#)).

Broad River

Wind wave activity on the Broad River is evaluated coincident with the maximum water surface elevation of the PMF including the effects of dam failures as

discussed above. The determined fetch length of 2.77 mi., shown in [Figure 2.4.4-201](#), has a runup slope of 40 percent. The PMF including effects of dam failures and the coincident wind wave activity results in a flood elevation of 584.79 ft. msl. The Lee Nuclear Station safety-related plant elevation is 593 ft. msl and is unaffected by flood conditions and coincident wind wave activity. A more critical wind wave activity result was determined considering a fetch length through Make-Up Pond A, which becomes inundated by backwaters of the Broad River during severe flooding events. Therefore, the critical wind wave activity for the Broad River is equal to the wind wave activity for Make-Up Pond A, as discussed below.

Intermittent Stream/Make-Up Pond A

During severe flooding events, Make-Up Pond A is inundated by backwaters of flooding of the Broad River. Therefore, wind wave activity on Make-Up Pond A is evaluated coincident with the maximum water surface elevation of the PMF on the Broad River including the effects of dam failures as discussed above. The determined critical fetch length of 2.69 mi. is shown in [Figure 2.4.4-202](#). The 2-year annual extreme mile wind speed is adjusted based on the factors of fetch length, level overland or over water, critical duration, and stability. The critical duration is approximately 53 min. The adjusted wind speed is 49.9 mph.

Significant wave height (average height of the maximum 33-1/3 percent of waves) is estimated to be 2.76 ft., crest to trough. The maximum wave height (average height of the maximum 1 percent of waves) is estimated to be 4.59 ft., crest to trough. The corresponding wave period is 2.6 sec.

The 47 percent slopes along the banks of Make-Up Pond A adjacent to the site are used to determine the wave setup and runup. The maximum runup, including wave setup, is estimated to be 8.79 ft. The maximum wind setup is estimated to be 0.07 ft. Therefore, the total wind wave activity is estimated to be 8.86 ft. The PMF including effects of dam failures and the coincident wind wave activity results in a flood elevation of 585.36 ft. msl for Make-Up Pond A and the Broad River. The Lee Nuclear Station safety-related plant elevation is 593 ft. msl and is unaffected by flood conditions and coincident wind wave activity.

McKowns Creek/Make-Up Pond B

Wind wave activity on Make-Up Pond B is evaluated coincident with the maximum water surface elevation of the PMF including the effects of dam failure, as discussed above. The determined critical fetch length of 1.39 mi. is shown in [Figure 2.4.3-234](#). The 2-year annual extreme mile wind speed is adjusted based on the factors of fetch length, level overland or over water, critical duration, and stability. The critical duration is approximately 35 min. The adjusted wind speed is 50.33 mph.

Significant wave height (average height of the maximum one-third of waves) is estimated to be 2.00 ft., crest to trough. The maximum wave height (average height of the maximum 1 percent of waves) is estimated to be 3.35 ft., crest to trough. The corresponding wave period is 2.1 sec.

The slopes approaching the units are not constant. The slopes above the PMF elevation are steep up to elevation 588 ft., then level out to a flat area. To represent a conservative approach, runup is calculated assuming the runup slope continues above elevation 588 ft. A conservative estimate of 25 percent is determined for the runup slope based on finished grade contours. The maximum runup, including wave setup, is estimated to be 3.97 ft. The maximum wind setup is estimated to be 0.07 ft. Therefore, the total wind wave activity is estimated to be 4.04 ft. The PMF and the coincident wind wave activity results in a flood elevation of 589.10 ft. msl. The Lee Nuclear Station safety-related plant elevation is 593 ft. msl and is unaffected by flood conditions and coincident wind wave activity.

London Creek/Make-Up Pond C

The Make-Up Pond C reservoir is located on a tributary of the Broad River, west of the Lee Nuclear Station, as shown in [Figure 2.4.1-213](#), such that a postulated failure of the Make-Up Pond C dam would release water to the Broad River prior to reaching the Lee Nuclear Station. Failure of the Make-Up Pond C dam coincident with the PMF for the Make-Up Pond C watershed is discussed in [Subsection 2.4.4.1](#). Flooding effects as a result of dam failure due to wind wave activity are bounded by that discussion.

Other Smaller Upstream Dams

Numerous other ponds and small lakes with dam structures are located in the Ninety-Nine Islands watershed. However, these numerous features have negligible storage capacity. A breach would have no measurable effect on the water surface elevations determined by the PMF analysis.

2.4.5 PROBABLE MAXIMUM SURGE AND SEICHE FLOODING

WLS COL 2.4-2 Regulatory guidance prescribed by Regulatory Guide 1.59 describes the probable maximum surge and seiche flooding based on a probable maximum hurricane (PMH), probable maximum windstorm, or moving squall line. The region of occurrence for a PMH is along U.S. coastline areas ([Reference 202](#)). The probable maximum windstorm region of occurrence is along coastline areas and large bodies of water such as the Great Lakes. A moving squall line is considered for the Great Lakes region.

The U.S. Army Corps of Engineers guideline procedures for geologic hazard evaluations consider seiche waves greater than 7 ft. to be rare ([Reference 281](#)). According to U.S. Army Corps of Engineers guidance, the seiche hazard can be screened out for sites located more than 7 ft. above the adjacent water body.

Regulatory guidance prescribed by Regulatory Guide 1.59 indicates consideration of a PMH for areas within 200 miles of coastal areas. The Lee Nuclear Station is located approximately 175 miles inland from the Atlantic Coast. The safety-related

plant elevation is 593 ft. The normal maximum water surface elevation of the Broad River is 511.1 ft., the spillway flashboard elevation at Ninety-Nine Islands Dam ([Reference 217](#)).

The Broad River is a tributary of the Santee River which flows to the Atlantic Ocean. The mouth of the Santee River is about 45 mi. northeast of Charleston, South Carolina. The Santee River is also diverted by a series of lakes, Lake Marion and Lake Moultrie, to the Cooper River. The Cooper River flows into the Atlantic Ocean at Charleston, South Carolina.

According to Regulatory Guide 1.59, the probable maximum surge estimate for Folly Island, located at Charleston, South Carolina, is 28.2 ft. above mean low water. The surge estimate includes wind setup of 17.15 ft., pressure setup of 3.23 ft., initial water level of 1.0 ft., and 10 percent exceedance high tide of 6.80 ft. Mean sea level is 2.7 ft. higher than mean low water at Charleston, South Carolina ([Reference 202](#)). The maximum surge estimate is 25.5 ft. above mean sea level. A sea level anomaly of 1.0 ft. has been known to occur for the predicted astronomical tides at Charleston, South Carolina ([Reference 202](#)). Therefore, the probable maximum surge estimate is 26.5 ft. above mean sea level.

Regulatory Guide 1.59 only contains surge data up to 1975. The maximum storm surge along the Atlantic Coast after 1975 occurred as a result of hurricane Hugo. Storm surge from hurricane Hugo inundated the South Carolina coast from Charleston to Myrtle Beach in 1989. Maximum storm tides of 20 ft. were observed. Although the site is within 200 miles of the coastline, surge due to a PMH event would not cause flooding at the site. Transposition of the probable maximum surge, without any type of reduction for distance or instream structures, is nearly three times less than the 81.9-ft. difference in elevation between the station and the adjacent river.

There are no known documented surge or seiche occurrences on the Broad River near the Lee Nuclear Station. Seismically induced seiche are discussed in [Subsection 2.4.6](#). Based on data provided above, and site location and elevation characteristics, the station's safety-related facilities are not considered at risk from surge and seiche flooding. Resonance wave phenomena including oscillations of waves at natural periodicity, lake reflection, and harbor resonance are traditionally characteristics of harbors, estuaries, and large lakes and not associated with river settings. Any effects on the Broad River produced by similar phenomena would not affect the Lee Nuclear site. Coincident wind-generated wave activity is discussed in [Subsection 2.4.3.6](#). Additionally, there are no safety-related facilities that could be affected by water supply blockages due to sediment deposition or erosion during storm surge or seiching.

Surge flooding is evaluated for Make-Up Pond A and Make-Up Pond B using the maximum wind speed identified in [Subsection 2.3.1.2.8](#). This is consistent with the maximum wind speeds identified in U.S. Army Corps of Engineers guidance ([Reference 295](#)). Fetch lengths are estimated using the longest straight line fetch directed toward the site for each water body. Wave height, setup, and runup are estimated using U.S. Army Corps of Engineers guidance ([Reference 295](#)). Wind

setup is estimated using additional U.S. Army Corps of Engineers guidance (Reference 269).

Estimates for surge flooding are made coincident with 100-yr. flood levels of Make-Up Pond A and Make-Up Pond B. Resulting 100-yr. runoff rates for the watersheds are determined using USGS regression equations for small watersheds in South Carolina (Reference 296). The overflow rating curves for the respective ponds, discussed in Subsection 2.4.3.3, are used to determine the resulting coincident water surface elevations.

Make-Up Pond A

Make-Up Pond A surge flooding is evaluated coincident with the 100-yr. water surface elevation of 556.08 ft. The critical fetch length is 0.39 mi. as shown in Figure 2.4.5-201. The wind speed is adjusted based on the factors of fetch length, level overland or over water, critical duration, and stability using U.S. Army Corps of Engineers guidance (Reference 295). The critical duration is 11 min. The adjusted wind speed is 92.7 mph.

Significant wave height (average height of the maximum 33-1/3 percent of waves) is estimated to be 2.30 ft., crest to trough. The maximum wave height (average height of the maximum 1 percent of waves) is estimated to be 3.84 ft., crest to trough. The corresponding wave period is 1.8 sec.

The slopes along the banks of Make-Up Pond A adjacent to the site area are approximately 42 percent at most and are used to determine the wave setup and runup. The maximum runup, including wave setup, is estimated to be 5.48 ft. The maximum wind setup is estimated to be 0.12 ft. Therefore, the total water surface elevation increase due to high speed wind wave activity is estimated to be 5.60 ft. The resulting flood elevation is 561.68 ft. The Lee Nuclear Station safety-related plant elevation is 593 ft. and is unaffected by high speed wind wave activity flooding conditions.

Make-Up Pond B

Make-Up Pond B surge flooding is evaluated coincident with the 100-yr. water surface elevation of 576.18 ft. The critical fetch length is 1.38 mi. as shown in Figure 2.4.5-202. The wind speed is adjusted based on the factors of fetch length, level overland or over water, critical duration, and stability using U.S. Army Corps of Engineers guidance (Reference 295). The critical duration is 28 min. The adjusted wind speed is 89.9 mph.

Significant wave height (average height of the maximum 33-1/3 percent of waves) is estimated to be 4.10 ft., crest to trough. The maximum wave height (average height of the maximum 1 percent of waves) is estimated to be 6.86 ft., crest to trough. The corresponding wave period is 2.7 sec.

The slopes along the banks of Make-Up Pond B adjacent to the site area are approximately 25 percent and are used to determine the wave setup and runup. The maximum runup, including wave setup, is estimated to be 7.48 ft. The

maximum wind setup is estimated to be 0.28 ft. Therefore, the total water surface elevation increase due to high speed wind wave activity is estimated to be 7.76 ft. The resulting flood elevation is 583.94 ft. The Lee Nuclear Station safety-related plant elevation is 593 ft. and is unaffected by high speed wind wave flooding conditions.

Seiche evaluation is based on the natural fundamental period for Make-Up Pond A and Make-Up Pond B. The natural fundamental period of both water bodies is determined using Merian's formula ([Reference 295](#)).

$$T = 2 * L / (g * h)^{0.5}$$

where;

T = natural oscillation period at the fundamental mode (sec.)

L = fetch length (ft.)

g = gravitational acceleration (ft/sec²)

h = depth of water (ft.)

Based on bathymetry mapping, an average depth of 20.10 ft. is determined for Make-Up Pond A and used as the depth of water. The resulting natural fundamental period is 2.7 min. The Make-Up Pond B average depth is 28.59 ft. The resulting natural fundamental period is 8.0 min. The wave periods determined above (1.8 sec. and 2.7 sec.) are much shorter than the natural fundamental period for both water bodies (2.7 min. and 8.0 min.). Furthermore, natural fundamental periods are significantly shorter than meteorologically induced wave periods (e.g., synoptic storm pattern frequency and dramatic reversals in steady wind direction necessary for wind setup). Since the natural periods of Make-Up Pond A and Make-Up Pond B are significantly different than the period of the excitations, they are not susceptible to meteorologically induced seiche waves. Seismically induced waves are discussed in [Subsection 2.4.6](#).

Make-Up Pond C

The Make-Up Pond C reservoir is located on a tributary of the Broad River, west of the Lee Nuclear Station, as shown in [Figure 2.4.1-213](#), such that a postulated failure of the Make-Up Pond C dam would release water to the Broad River prior to reaching the Lee Nuclear Station. Failure of the Make-Up Pond C dam coincident with the PMF for the Make-Up Pond C watershed is discussed in [Subsection 2.4.4.1](#). Flooding effects as a result of dam failure due to surge and seiche are bounded by that discussion.

WLS COL 2.4-2 2.4.6 PROBABLE MAXIMUM TSUNAMI

Tsunamis affecting the Atlantic Coast have not been extensively studied due to the lack of significant trigger mechanisms. No specific tsunami hazard maps are available for the East Coast of the United States. The U.S. Army Corps of Engineers has developed a general tsunami risk map (Figure 2.4.6-201) (Reference 281). The East Coast is located in Zone 1, which corresponds to a wave height of 5 ft.

According to the National Oceanic & Atmospheric Administration (NOAA) tsunami database (Reference 228), the maximum recorded tsunami wave height along the East Coast is about 20 ft. This was recorded at Daytona Beach, Florida, on July 3, 1992. The database notes that the wave was probably meteorologically induced.

The Lee Nuclear Station is located approximately 175 mi. inland from the Atlantic Coast. The safety-related plant elevation is 593 ft. Based on data provided above, and site location and elevation characteristics, the station's safety-related facilities are not considered at risk from tsunami flooding.

Significant landslide generated waves triggered by hill slope failure are not plausible for the on-site Ponds A and B. No irregular weathering conditions or natural landslide hazards are noted in field investigations, as discussed in Subsection 2.5.1.1. There is no documented evidence that landslides of sufficient magnitude (e.g., size and velocity) at the site or adjacent to the ponds would occur. Potential slope failures that could occur would be of limited size and characterized as shallow soil or fill 'popouts'. Landslides of this type are considered minor, contain an insufficient volume of material, and are of low velocity so that potential landslide-induced waves would be insignificant.

Slopes surrounding Make-up Ponds A and B are either natural slopes that have existed for a long period of time (through most or all of the Holocene; natural slopes), or cut and fill slopes developed as part of the Cherokee Nuclear Station construction in the early 1980's. These slopes exhibit acceptable stability without visual evidence of groundwater seepage, past failure, incipient movement, or major creep, as discussed in Subsection 2.5.5.1.

Seismic induced waves resulting from surface fault rupture in the site vicinity are also not plausible. As discussed in Subsection 2.5.3, there are no capable tectonic sources within the Lee Nuclear Site vicinity (25 mi. radius), and there is negligible potential for tectonic fault rupture at the site and within the site vicinity. The only identified occurrence of a seismic induced seiche on the Broad River was measured approximately 64 miles downstream of the Lee Nuclear Station. A 0.08 ft. seiche was induced by the Alaska earthquake of 1964. Any seismic event that could occur would generate potential waves that would be insignificant compared to the available freeboard of the on-site make-up ponds or the Broad River.

As shown in Figure 2.4.1-209, Make-Up Pond A and Make-Up Pond B have normal pool elevations of 547 ft. msl and 570 ft. msl, respectively. Safety-related facilities are located at an elevation of 593 ft. Therefore, Make-Up Pond A has an

available freeboard of 46 ft. and Make-Up Pond B has an available freeboard 23 ft. The geology and seismology and geotechnical engineering characteristics of the Lee Nuclear Station are presented in [Section 2.5](#).

Make-Up Pond C

The Make-Up Pond C reservoir is located on a tributary of the Broad River, west of the Lee Nuclear Station, as shown in [Figure 2.4.1-213](#), such that a postulated failure of the Make-Up Pond C dam would release water to the Broad River prior to reaching the Lee Nuclear Station. Failure of the Make-Up Pond C dam coincident with the PMF for the Make-Up Pond C watershed is discussed in [Subsection 2.4.4.1](#). Flooding effects as a result of dam failure due to seismic- or landslide-induced waves are bounded by that discussion.

2.4.7 ICE EFFECTS

WLS COL 2.4-2 There are 10 U.S. Geological Survey (USGS) gauging stations, located upstream of the Lee Nuclear Site on the Broad River and its tributaries, that recorded water temperatures for different periods between 1962 and 1981 ([Reference 290](#)). [Figure 2.4.2-201](#) identifies the location of area gauges. The lowest recorded water temperatures during winter periods range from 32°F to 48.2°F. The lowest was recorded on the Broad River near Earl, North Carolina (USGS No. 02152622), located about 14 river mi. upstream of the site. The lowest was also recorded on Buffalo Creek near Grover, North Carolina (USGS No. 02153456), located about 14 river mi. upstream of the site.

The USGS gauging station on the Broad River east of Gaffney (USGS No. 02153500), located about 5 river mi. upstream of the site at the U.S. Highway 29 bridge crossing, is most representative of water temperatures near the site. The gauge recorded water temperatures from 1969 to 1973. The lowest recorded water temperature was 41.9°F. The recordings are summarized in [Table 2.4.7-201](#). The longest record from a gauge near the site is located about 40 river mi. downstream of the site on the Broad River near Carlisle, South Carolina (USGS No. 02156500). The gauge recorded water temperatures from 1962 to 1975. The lowest recorded water temperature near Carlisle was 38.3°F.

According to the EPA STORET database ([Reference 284](#)), four stations located on the Broad River near the site recorded water temperatures between 1959 and 2004. The lowest water temperature recorded was 35.6°F near Gaffney, South Carolina (Station B-042). This gauge is located about 8 river mi. upstream of the site. A second station also recorded a water temperature of 35.6°F (Station B-044). This station is located about 9 river mi. downstream from the site.

The North Carolina Department of Environmental and Natural Resources collected temperature data from 1995 to 2000 at nine gauging stations in North Carolina on the Broad River and its tributaries ([Reference 231](#)). Minimum temperatures vary from 33.8°F to 39.2°F. The nine gauging stations are in the vicinity of 10 USGS gauging stations discussed above. The resulting minimum

temperatures are also within the range measured by USGS gauges. Historical and more recent measurements consistently indicate that Broad River water temperatures remain above freezing.

According to the U.S. Army Corps of Engineers ([Reference 275](#)), ice jams occur in 36 states, primarily in the northern tier of the United States ([Figure 2.4.7-201](#)). Neither South Carolina nor North Carolina is included in this coverage. The U.S. Army Corps of Engineers Cold Regions Research and Engineering Laboratory historical ice jam database was consulted for the Broad River ([Reference 274](#)). There are no recorded ice jams for the Broad River. A query for ice jams in South Carolina also yielded no historical occurrence of an ice jam. However, one ice jam was recorded in North Carolina on the Neuse River at Kinston from January 26 to January 29, 1940. The maximum stage of the Neuse River resulting from the ice jam was well below flood stage. Kinston is located about 220 mi. east of the site. There are no known documented ice sheet or ice ridge occurrences on the Broad River.

The Lee Nuclear Station's safety-related plant elevation is 593 ft. The normal maximum water surface elevation for the Broad River adjacent to the Lee Nuclear Station is 511.1 ft., due to operation of the Ninety-Nine Islands Dam and hydropower plant ([Reference 217](#)). The maximum water surface elevation during a probable maximum flood event is more than 40 ft. below the site ([Subsection 2.4.3](#)). The possibility of inundating the site due to an ice jam is remote.

According to the U.S. Army Corps of Engineers, frazil ice forms in supercooled, turbulent water in rivers and lakes ([Reference 275](#)). Anchor ice is defined as frazil ice attached to the river bottom, irrespective of the nature of its formation. Although the potential for freezing (i.e., frazil or anchor ice) and subsequent ice jams on the Broad River is remote, the numerous pond and lake features adjacent to the site may be susceptible to some degree of freezing. However, there are no safety-related water storage bodies. Additionally, sustained periods of subfreezing water temperatures are not characteristic of the region. The climate and operation of Ninety-Nine Islands Reservoir prevent any significant icing on the Broad River. There are no safety-related facilities that could be affected by ice-induced low flow of the Broad River or reduction in capacity of water storage facilities.

2.4.8 COOLING WATER CANALS AND RESERVOIRS

- WLS COL 2.4-3 There are no current or proposed safety-related cooling water canals or reservoirs required for the Lee Nuclear Station. The atmosphere provides the ultimate heat sink (UHS) with the containment vessel and passive containment cooling system (PCS) providing the heat transfer mechanism. Additional details are provided in [Subsection 2.4.11](#).

2.4.9 CHANNEL DIVERSIONS

- WLS COL 2.4-3 There is no evidence to suggest historical diversions or realignments of the Broad River. Several shoals are located in the Broad River near the Lee Nuclear Site. However, these features are confined within the natural banks of the river. The

topography does not suggest potential diversions or landslides. The streams and rivers in the region are characterized by traditional shaped valleys with no steep, unstable side slopes that could contribute to landslide cutoffs or diversions. There is no evidence of ice-induced channel diversion.

Several instream dams are located upstream and downstream of the Lee Nuclear Station ([References 217](#) and [276](#)). Cherokee Falls Dam was completed in 1826. Gaston Shoals Dam was completed in 1908. Both are located immediately upstream of the site and are run-of-river hydroelectric power plants. Ninety-Nine Islands Dam, completed in 1910, is located immediately downstream and is also a run-of-river hydroelectric power plant.

The greatest potential for geothermal energy exists in areas of above average heat flow, generally the result of recent volcanic activity or active tectonics. The eastern United States has below average to average geothermal heat flow and is characterized as low temperature ([Reference 251](#)). The eastern United States is relatively tectonically stable ([Reference 252](#)). No thermal anomalies in the eastern United States are attributed to young-to-contemporary volcanic or other igneous activity ([Reference 291](#)). Therefore, channel diversion because of geothermal activity is not expected.

The atmosphere provides the UHS with the containment vessel and PCS providing the heat transfer mechanism. The UHS does not directly rely on the Broad River intake. Therefore, channel diversion cannot adversely affect safety-related structures or systems. Additional details are provided in [Subsection 2.4.11](#). Geologic and seismic characteristics of the region are discussed in [Section 2.5](#).

2.4.10 FLOODING PROTECTION REQUIREMENTS

WLS COL 2.4-2

All safety-related facilities are located at an elevation above the maximum flood levels resulting from all types of flooding as described in [Subsection 2.4.2](#). The critical flooding event is identified and discussed in detail in [Subsection 2.4.2](#). Based on the design information provided above, flood protection measures and emergency procedures to address flood protection are not required.

2.4.11 LOW WATER CONSIDERATIONS

2.4.11.1 Low Flow in Rivers and Streams

WLS SUP 2.4.11-1 The headwaters of the Broad River and its major tributaries originate in the higher elevations of the Appalachian Mountains of North Carolina before descending into the foothills and Piedmont region of North Carolina ([Reference 231](#)). The Broad River continues its course through the gently rolling hills and narrow stream valleys of the Piedmont region in South Carolina ([Reference 259](#)). The Lee Nuclear Station is located on this section of the river, just upstream of Ninety-Nine Islands Dam.

The Upper Broad River drainage basin above the Ninety-Nine Islands Dam derives water from several smaller tributaries that contain a considerable number of dams. According to the U.S. Army Corps of Engineers National Inventory of Dams, there are approximately 132 upstream dams of which five dams have been breached ([Reference 276](#)). Therefore, the water volume available during low-flow conditions on the Broad River is a function of natural flow in contributing rivers and streams, available storage capacity of upstream reservoirs, and regulated discharge flow from upstream dams.

Dam failure could affect normal operation during low-flow conditions. Failure of Ninety-Nine Islands Dam would drain the associated reservoir. In this portion of the Broad River, flow would resemble a function of natural flow. However, there are no safety-related facilities that could be affected by low-flow or drought conditions, since the passive cooling system does not rely on the Broad River as a source of water. If necessary, the make-up ponds can be used to supplement natural flow to support continued operations for additional periods of time. Non-safety related water supply during drought is addressed in [Subsection 2.4.11.5](#).

2.4.11.2 Low Water Resulting from Surges, Seiches, or Tsunami

There are no safety-related facilities that could be affected by low water. The site is not at risk to low water resulting from surge, seiche, or tsunami effects, due to the inland location on a run-of-river reservoir with limited storage capacity. See [Subsection 2.4.5](#) and [2.4.6](#) for additional details.

Flooding due to ice jams has not been recorded at the site. It is unlikely that an ice jam would occur based on the historical water temperatures of the Broad River. Therefore, low flow due to or exaggerated by ice effects is not expected to occur at the site. See [Subsection 2.4.7](#) for additional details.

2.4.11.3 Historical Low Water

Low-flow conditions at the site were analyzed based on stream flow records at USGS gauging stations on the Broad River ([Reference 290](#)). Low-flow conditions typically exist during the months of July through November. The six largest reservoirs in the basin, Lake Lure, Lake Summit, Lake Adger, Kings Mountain Reservoir, Lake Whelchel, and Make-Up Pond C represent about 88 percent of the total storage capacity for the basin. Two additional dams, Cherokee Falls and Gaston Shoals, immediately upstream from the Lee Nuclear Site, possess less than 2 percent of the total storage capacity for the basin.

The Gaston Shoals Dam has affected the drainage basin upstream of the site since 1908. Ninety-Nine Islands Dam downstream of the site was completed in 1910. Cherokee Falls Dam, located upstream of the site between Gaston Shoals Dam and Ninety-Nine Islands Dam, was completed in 1826.

Gaston Shoals Dam is part of a hydropower facility owned and operated by Duke Energy. The facility is regulated by the Federal Energy Regulatory Commission (FERC). During the months of July through November, license requirements maintain a release of at least 434 cfs or the natural flow in the Broad River,

whichever is less. Should natural flow in the Broad River become less than 434 cfs, the FERC license provides measures for flow to be stored and released on an hourly basis ([Reference 222](#)).

Cherokee Falls Dam is part of a hydropower facility owned and operated by the Broad River Electric Cooperative. However, the hydroelectric facility at Cherokee Falls Dam is not currently operating. The dam is essentially a run-of-river facility with spillway flow at high-flow conditions and low-level outlets to provide constant flow under low-flow conditions ([Reference 204](#)).

The Ninety-Nine Islands Dam is part of a hydropower facility owned and operated by Duke Energy. The facility is regulated by the FERC. During the months of July through November, license requirements maintain a release of at least 483 cfs or the natural flow in the Broad River, whichever is less. Should natural flow in the Broad River become less than 483 cfs, the FERC license provides measures for the reservoir to be drawn down, at most 2 ft. below the full pool elevation of 511.1 ft., depending on the time of year. Release of accumulated flow is then made on an hourly basis ([Reference 223](#)).

There is a USGS gauging station (USGS No. 02153551) located about 2 river mi. downstream from the site in the tailrace below Ninety-Nine Islands Dam. The drainage area associated with this gauge is 1550 sq. mi. This is essentially the same drainage basin for the Broad River adjacent to the site. The annual minimum daily flows for the period of record (1998 to 2006) are presented in [Table 2.4.11-201](#). The minimum flow observed during the period of record is 138 cfs on September 14, 2002. While these data are insufficient to determine the frequency of low-flow occurrences or to determine the lowest recorded flow, they are instructive in that this flow occurred during a period of severe drought. The flow gauge is located downstream of the Ninety-Nine Islands dam and does not measure the flow passing in front of the plant intake, although it is representative of river conditions.

The USGS gauging station (USGS No. 02153500), located about 5 river mi. upstream from the site on the Broad River near Gaffney, South Carolina, has a drainage area of 1490 sq. mi. This gauge is located downstream from Gaston Shoals Dam and upstream from Cherokee Falls Dam. The annual minimum daily flows for the period of record (1938 to 1990) are presented in [Table 2.4.11-202](#). The gauge was discontinued in 1990 by the USGS. The minimum flow observed during the period of record is 224 cfs on October 24, 1954.

Low-flow frequency analysis was performed in accordance with USGS Bulletin 17B using the Log-Pearson Type III distribution method ([Reference 253](#), [Reference 270](#), and [Reference 287](#)). Due to the importance of the more recent drought years, not included in the period of record for the Gaffney gauge, the Ninety-Nine Islands gauge data were combined with the Gaffney gauge data to determine low-flow frequencies. The results provide more conservative flow estimates than if only the Gaffney gauge had been used in the analysis.

[Table 2.4.11-203](#) provides 100-yr. drought flow rates at different durations. The 30-day 100-yr. drought flow rate is 346 cfs. A 100-yr. return period is defined as a

1 percent chance the event will occur during any one year. Therefore, the 30-day 100-yr. drought flow rate has a 1 percent chance each year that the flow rate or less will occur for at least 30 consecutive days.

Historical flow data at Gaffney, South Carolina (USGS No. 02153500) indicate that 30-day 100-yr. drought flow rates or less have been achieved on 12 days from 1938 to 1990. Historical flow data from the gauging station just below Ninety-Nine Islands Dam (USGS No. 02153551) indicate that 30-day 100-yr. drought flow rates or less have been achieved 79 days from 1998 to 2002. During this time, there were 26 consecutive days with less than 30-day 100-yr. drought flow rates. Additionally, there were 54 days of 30-day 100-yr. drought flows concentrated over a 61-day period.

Since 1900, according to the South Carolina Department of Health and Environmental Control, severe droughts have occurred statewide in 1925, 1933, 1954, 1977, 1983, 1986, 1990, 1993, and 1998 (Reference 267). USGS reports indicate more recent droughts occurred from 1998 to 2002 in areas of North Carolina belonging to the headwaters of the Broad River and in South Carolina (Reference 294). Most of the drainage area for the Broad River adjacent to the site is in North Carolina. The Gaffney gauge period of record includes the 1954, 1977, 1983, 1986 and 1990 drought years, while the gauge at Ninety-Nine Islands Dam includes the more recent years. Mid-to-late 2007 weather patterns indicate a potential for Broad River flows to drop to levels characteristic of drought conditions. While 2007 data are continuing to be collected, an analysis of these data was not available in time to be included with the application. An analysis will be conducted upon termination of current drought conditions and provided to the NRC.

The normal full pool elevation of the Ninety-Nine Islands reservoir is 511.1 ft. (Reference 217). Provisions are made to draw the reservoir down by at most 2 ft. below normal full pool during periods of low flow. Due to maintenance operations, the pool has dropped below the 2 ft. drawdown limit for short periods. The following historical lows were due to maintenance. According to USGS water year reports, the historical minimum pool elevation was 508.2 ft. on February 14, 2005 (Reference 208). The water year reports have a period of record from October 1998 to the present. Additional historical data from 1964 to 1973 indicate the minimum pool elevation was about 505.7 ft. during May 1965.

The U.S. Army Corps of Engineers historical database of ice jams on the Broad River was reviewed (Reference 274). See Subsection 2.4.7 for additional discussion. Ice effects are not a concern for low water considerations, due to the climate and reservoir operations.

2.4.11.4 Future Controls

The majority of the Broad River drainage basin upstream of the site is in North Carolina. According to the North Carolina State Water Supply Plan, public supply water use in the Broad River watershed is projected to increase by about 56 percent from 2000 to 2020 (Reference 233). This includes both surface water

and groundwater use. Available supply is noted as the withdrawal capacity in [Table 2.4.1-209](#).

According to the North Carolina Local Water Supply Plans, none of the upstream surface water public supply systems require more than 80 percent of their maximum use rate before 2030. Of the five surface water public supply systems, only the Cleveland County Sanitary District indicated exceeding 80 percent of their maximum use rate before 2050. Demand is expected to increase 238 percent by 2050, for a total demand of 28.6 million gpd.

According to the Federal Register, a Notice of Intent was filed on July 11, 2006 for a Draft Environmental Impact Statement (DEIS) to be prepared for a proposed reservoir on the First Broad River in Cleveland County, North Carolina ([Reference 226](#)). The Cleveland County Sanitary District applied for a permit to construct a water supply reservoir with a surface area of approximately 2245 ac., about 1 mi. north of Lawndale, North Carolina. The DEIS is currently in preparation. Lawndale is about 26 miles north of the Lee Nuclear site.

The USGS maintained a gauge (USGS No. 02152500) about 2.5 mi. southeast of Lawndale on the First Broad River from 1940 to 1971. During this period, the average monthly flow at Lawndale represented about 11 percent of the flow in the Broad River at Gaffney. The drainage area at the Lawndale gauge is 200 sq. mi., or roughly 13 percent of the drainage area at the USGS gauge near Gaffney.

Duke Energy is planning to expand the Cliffside Steam Station by as early as 2010. The incremental additional consumptive use withdrawal from the Broad River upstream from the station is estimated to be 17 cfs. However, four of the five existing units at Cliffside will be retired. Additional intake sources not represented by the USGS stream gauges include an expansion of the Shelby, North Carolina, water system. Shelby has constructed an intake on the Broad River, and it may withdraw up to 10 million gpd on a temporary emergency basis ([Reference 207](#)).

The North Carolina General Statutes require registration for interbasin transfers of 100,000 gpd or more ([Reference 249](#)). The North Carolina Division of Water Resources does not require a transfer certificate unless the transfer is 2 million gpd or more. Total known interbasin transfers include about 1.47 million gpd out of the basin and about 0.15 million gpd into the basin ([Reference 230](#)). North Carolina also requires registration of withdrawals of 100,000 gpd or more.

State regulations for South Carolina currently require registration of withdrawals of surface water in excess of 3,000,000 gallons per month ([Reference 258](#)). This is essentially 100,000 gpd. The construction of the embayment and intake structure requires coordination with the U.S. Army Corps of Engineers. The design and placement of the embayment and intake structure are done in accordance with the appropriate federal and state regulations. There are no safety-related facilities that could be adversely affected by any increase in water use or drought conditions.

2.4.11.5 Plant Requirements

Raw water needs, including makeup to the normal heat sink cooling towers, are supplied by the intake as described in [Subsection 2.4.1.1.4](#). The intake structure includes necessary intake screens, pumps, etc. to convey the river water to Make-Up Pond A. Use of raw water from Make-Up Pond A is described in [Subsection 2.4.1.1.4](#). Intake screen locations consider the Broad River minimum level. There are no safety-related plant requirements provided by the Broad River.

WLS SUP 2.4.11-2 The normal river intake flow rate for the station is approximately 35,000 gpm. The maximum expected river intake flow is approximately 60,000 gpm. Institutional restraints on water use are imposed by Federal and State agencies as discussed. Title 40 Code of Federal Regulations Part 125 Section 84 requires that for cooling water intake structures located in a freshwater river or stream, the total design intake flow must be no greater than five percent of the source water annual mean flow. Water use and annual mean flow are discussed in [Subsection 2.4.1.2.5.1](#) and [Subsection 2.4.1.2.2.2](#). The South Carolina Code of Laws Title 49 Chapter 23 Part 40 identifies that during a drought declaration, the use of water from a managed watershed impoundment shall not be restricted as long as minimum streamflow or flow equal to the 7Q10 is maintained, whichever is less. Make-Up Pond B and Make-Up Pond C are expected to be used to supplement flow during periods of low flow.

The 7Q10 for the Gaffney gauge was determined to be 439 cfs using the USGS recommended Log-Pearson Type III distribution. However, because the 7Q10 is less than the Ninety-Nine Islands Dam FERC license minimum flow requirement of 483 cfs for July through November ([Subsection 2.4.11.3](#)), the FERC license minimum flow was used as a constraint in evaluating operation during low flow conditions. Furthermore, FERC license minimum flow requirements are more restrictive than the 100-year drought flow rates described in [Subsection 2.4.11.3](#) and [Table 2.4.11-203](#). Therefore, the following low flow analysis applies to the discussion of nonsafety related water supply during a 100-year drought.

A low flow analysis was performed based on the FERC licensed 483 cfs minimum flow requirements at Ninety-Nine Islands Dam and the Lee Nuclear Station consumptive use requirements. Consumptive use is estimated to be approximately 55 cfs. When flows in the Broad River drop below 538 cfs, combined FERC licensed 483 cfs minimum flow plus 55 cfs consumptive use, makeup water to the station is supplemented by on-site water storage, Make-Up Pond B and off-site Make-Up Pond C. When flows in the Broad River drop below 483 cfs, the station relies only on Make-Up Pond B and Make-Up Pond C storage for consumptive uses of the station.

Detailed bathymetry mapping of the on-site Make-Up Pond B ([Figure 2.4.1-209 Sheet 2](#)) and Make-Up Pond A ([Figure 2.4.1-209 Sheet 3](#)) was performed in September 2006. Make-Up Pond A is designed for a normal full pond elevation of

547 ft. Based on current topography Make-Up Pond A retains a volume of 1425 ac.-ft. The usable storage is approximately 1200 ac.-ft.

Make-Up Pond B is designed for a normal full pond elevation of 570 ft. Based on current topography, Make-Up Pond B retains a volume of approximately 4000 ac.-ft. The usable storage is approximately 3200 ac.-ft.

Make-Up Pond C is designed for a normal full pond elevation of 650 ft. Based on the bathymetry shown in [Figure 2.4.1-213](#), Make-Up Pond C retains a volume of approximately 22,000 ac.-ft. The usable off-site storage capacity is approximately 17,500 ac.-ft. The total usable storage capacity of Make-Up Pond B and Make-Up Pond C is approximately 20,700 ac.-ft. Make-Up Pond C has sufficient capacity to support full power operation for approximately 160 days. Make-Up Pond B has sufficient capacity to support full power operations for approximately 30 days.

There are no safety-related water requirements for normal plant shutdown associated with the AP1000. Make-Up Pond A nominally provides for approximately 1200 ac.-ft. of usable water storage. Make-Up Pond A has sufficient capacity to conduct a normal plant shutdown and to maintain shutdown conditions for both units. Make-Up Pond A can be replenished with water from the Broad River, from Make-Up Pond B, and from Make-Up Pond C via Make-Up Pond B.

The circulating water system for the station is a closed-cycle type system coupled with mechanical draft, wet cooling towers. For each unit the circulating water system flow rate is estimated at 600,000 gpm ([Subsection 10.4.5](#)). [Figure 10.4-201](#) presents the circulating water system. Make-Up Ponds B and C are used to supplement flow during periods of low flow. Emergency cooling is discussed in [Subsection 2.4.11.6](#).

Effluent from the new facility discharges into the river at the upstream face of the Ninety-Nine Islands Dam near the intakes for the hydroelectric generating units. This configuration ensures no recirculation to the embayment area and intake screens of the new facility.

2.4.11.6 Heat Sink Dependability Requirements

The atmosphere is the UHS. A continuous natural circulation flow of air removes heat from the containment vessel. The steel containment vessel and PCS provides the heat transfer mechanism, as described in [Section 6.2](#). A separate gravity-drained, passive containment cooling water storage tank provides containment wetting. The PCS is not reliant on the source of water from the river intake. Makeup to the passive containment cooling water storage tank is provided by demineralized water from the passive containment cooling ancillary water storage tank. Therefore, no warning of impending low flow from the river water makeup system is required. Low river water conditions would not affect the ability of the emergency cooling water systems and the UHS to provide the required cooling for emergency conditions.

The passive containment cooling water storage tank has a volume capacity for 72 hours of containment wetting. The passive containment cooling ancillary water storage tank has a volume capacity to maintain containment wetting for an additional 4 days. Makeup for long-term containment wetting can be supplied to the PCS by Make-Up Pond A or alternate external resources, through multiple system paths. Site-related events and natural phenomena would not affect the atmosphere functioning as the UHS. As described in [Subsection 2.4.3](#), the station is capable of withstanding the PMF. Seismic design is addressed in [Section 3.7](#).

2.4.12 GROUNDWATER

WLS COL 2.4-4 2.4.12.1 Description and On-Site Use

2.4.12.1.1 Regional Aquifers, Formations, Sources, and Sinks

The Lee Nuclear Site is located within the Piedmont physiographic province, a southwest-northeast-oriented province of the Appalachian Mountain System ([Figure 2.4.1-203](#)). The Piedmont province is 80 – 120 mile (mi.) wide and situated between the Blue Ridge province, a mountainous region to the northwest, and the Atlantic Coastal Plain province to the southeast. The majority of rocks in the Piedmont are medium-to high-grade metamorphic rocks. These rocks are generally stratified and compositionally layered with distinct foliation. In addition, lineaments and fault systems are common in the region, and several major thrust sheets are present in the basin. Numerous granitic plutons and stocks have intruded older metamorphic rocks, and are often marked by areas of higher topography; a result of the massive, resistant nature of these intrusive rocks. The Lee Nuclear Site is located within the Kings Mountain Belt of the Piedmont province, which contains a complex series of deformed rocks consisting of felsic and mafic schists and gneisses, quartzites, conglomerates, and marble, generally considered to be of Precambrian and early Paleozoic age ([Subsection 2.5.1](#)).

Throughout the Piedmont region, bedrock is overlain by a mantle of unconsolidated material known as regolith. The regolith includes, where present, the soil zone, a zone of weathered and decomposed bedrock known as saprolite, and alluvium. Saprolite, the product of chemical and mechanical weathering of underlying bedrock, is typically composed of clay and coarser granular material that may reflect the texture of the rock from which it was formed. Typically, the formation of soils is attributed to the in-place weathering of the underlying rock and the deposition of material transported by water and laid down as clay, silt, sand, or large rock fragments ([Reference 285](#)). Crystalline rocks are commonly weathered in the Piedmont region because of the warm, humid conditions. Iron oxide-stained kaolinite and other aluminosilicate clay minerals are the dominant constituents of upland soils in many areas. Modern fluvial sediments generally occupy only the active beds and small floodplains of local streams and rivers.

The Piedmont aquifer system is basically a two layered slope-aquifer system ([Figure 2.4.1-210](#)). The shallow water table aquifer is composed of the saprolite and residual soil, which is typically low yielding. The shallow water table aquifer is

unconfined, meaning that the upper surface of the saturated zone is not effectively separated from the ground surface by a low-permeability clay layer. The underlying bedrock aquifer consists of weathered and unweathered crystalline igneous and metamorphic rocks that store and transmit water through fractures. The fracture system in the bedrock is a network of discontinuities that increase in prevalence upward through the crystalline rock as it transitions into saprolite. Because of the permeability of the transition zone, the bedrock aquifer is also considered unconfined and not effectively isolated. Thus, the saprolite and bedrock zones function as one interconnected aquifer system (Reference 266). While confined settings can occur in fracture bedrock, none were indicated in this study. The rocks typically yield small amounts of water to domestic users, small cities, and low-water-demanding industries.

Groundwater occurs almost everywhere throughout the Piedmont province; however, it is not a single, widespread aquifer. Groundwater occurs in various local aquifer systems and compartments that have similar characteristics and are hydraulically connected. Groundwater recharge in this area is derived from infiltration by local precipitation or infiltration from nearby surface water. Additionally, with the construction of the on-site impoundments, recharge also occurs from these surface waters.

The on-site impoundments consist of Make-Up Pond B, Make-Up Pond A, and Hold-Up Pond A. Details of these impoundments are discussed in Subsection 2.4.1.2.2.6. Surface water in these impoundments is in direct communication with groundwater and the water levels represent the water table.

The water table varies from ground surface elevation in valleys to more than 100 ft. below the surface on sharply rising hills. The groundwater levels in the Piedmont typically decline during the late spring and summer due to evapotranspiration and rise in the late fall and winter when the evaporation potential is reduced (Reference 297).

The fractures, relic rock textures, and directional differences in permeability or ease of groundwater movement may significantly affect the direction of local groundwater flow. Recharging of the groundwater in the Piedmont is by the addition of precipitation water, first to the shallow soil/saprolite aquifer (referred to as the water table aquifer in the regional discussion) and then to the uppermost fracture zone (transition zone). Recharge mostly occurs on upland topographic highs or at least above the slopes of stream valleys. Water does not generally move to great depths, but it is directed almost laterally by reduced permeabilities of crystalline rock with lower fracture density.

Cross-sections of the Lee Nuclear Site are presented in Figure 2.4.12-205, Sheets 1 to 4, and depict the relationship between groundwater beneath the site and the surface water bodies surrounding the site.

2.4.12.1.2 Local Aquifers, Formations, Sources, and Sinks

The Lee Nuclear Site overlies rocks of the Battleground Formation with the exception of later diabase dikes (Figures 2.5.1-218a, 2.5.1-219a, and 2.5.1-220).

The Battleground Formation comprises rocks primarily felsic to intermediate in composition (dacite to andesite protoliths), volcanoclastic sequences with intrusions of similar composition (meta granodiorite to metatonalite, metadiorite, and meta gabbro), and interfingering, marine-influenced metasedimentary sequences. Petrographic examination of thin sections obtained from the Lee Nuclear Station site revealed the following rock types: Mica Schist, Meta Quartz Diorite, Meta Dacite Porphyry, and Meta Basalt (Section 2.5). Geologic maps show the distribution of rock types, which tend to have locally erratic outcrop and subsurface distribution patterns, but regionally trend northeast to southwest.

Subsurface investigations performed at the Lee Nuclear Site in 1973 for the former Cherokee Nuclear Station and in March 2006 reveal that geologic and hydrologic conditions at the Lee Nuclear Site are similar to the regional conditions described above in Subsection 2.4.12.1.1. The first occurrence of groundwater beneath the Lee Nuclear Site is within the surficial hydrogeologic unit. The groundwater flows under unconfined conditions in the surficial hydrogeologic unit, which is generally composed of three different media beneath the site: (1) fill material placed in valley lows during site grading using on-site borrow materials, (2) the soil and saprolite zone that overlies the bedrock, and (3) partially weathered rock. The shallow groundwater beneath the site is mostly affected by the excavated area and the current dewatering activities (effects of the dewatering are discussed in Subsection 2.4.12.2).

WLS COL 2.4-4 2.4.12.2 Sources

The AP1000 reactor design has no safety-related heat sink that relies on groundwater supplies. The Lee Nuclear Site is not expected to use groundwater as a source of water for any purpose. Additional information related to local and on-site groundwater use is presented in Subsection 2.4.1.2.5.2.

2.4.12.2.1 Regional and Local Groundwater Uses

Groundwater supplies in the Piedmont physiographic province of South Carolina occur in three types of hydrogeologic environments. These are the unweathered and fractured crystalline rocks, overlying saprolite and residuum, and to a lesser extent, alluvial valley-fill deposits. Most public water supply wells are completed in fractured igneous and metamorphic rocks, often referred to as “crystalline bedrock,” while some private wells are simply dug or bored into the overlying saprolite. Yields of 4 – 170 gpm have been recorded from 30 South Carolina ambient groundwater quality network wells in the Piedmont bedrock (Reference 257). Regional groundwater studies consulted during the Cherokee Nuclear Station site investigation indicated that most domestic wells are not drilled to develop maximum yield, are generally less than 150 ft. deep, and have flow rates ranging from 3 to 150 gpm with a median flow rate of 7 gpm (Reference 214).

According to South Carolina Department of Health and Environmental Control (SCDHEC) water-use data for 2005, 1.02 million gallons (gal.) of groundwater were used for thermoelectric power generation in Cherokee County. No groundwater use in Cherokee County for domestic self-supplied systems,

aquaculture, golf courses, industry, irrigation, livestock, mining, or hydroelectric power was reported in the 2005 SCDHEC data (Reference 267). According to a private well report from SCDHEC, based on data from January 1985 to June 2006, the number of domestic wells completed in Cherokee County was 1076 (Reference 261). The USGS and state water-use data were reviewed, and groundwater withdrawals for counties located in the Upper Broad River watershed are presented in Table 2.4.1-208. Groundwater withdrawals for Cherokee and surrounding counties in South Carolina (Table 2.4.1-207) account for only 4.7 million gal. per day (Mgd), and the majority (85 percent) of that volume is pumped from Spartanburg County, outside the watershed for the Lee Nuclear Site.

Local groundwater use in the vicinity of Lee Nuclear Station is predominantly from domestic wells, and is described in Subsection 2.4.1.2.5.2.

2.4.12.2.2 Historical On-Site Conditions

Site hydrologic data were gathered prior to construction activities (through the early 1970s) and during the construction activities (late 1970s to the early 1980s). Surface and groundwater conditions at the Lee Nuclear Site have changed because of the excavation and site grading conducted as part of the construction activities for the former Cherokee Nuclear Station. No significant changes to the Lee Nuclear site have occurred since those construction activities.

Prior to the construction activities for the Cherokee Nuclear Station, a subsurface investigation was conducted, and water level measurements were obtained to develop an understanding of the groundwater setting. A groundwater table elevation map was developed to represent site conditions at that time and is presented in Figure 2.4.12-201. Initial potentiometric surface data collected from July, August, and September 1973 indicated site-specific groundwater flow directions were primarily toward the north and east from the reactor area, which generally mimicked the preconstruction site topography. A north-south-trending groundwater divide was apparent west of the reactor area and east of the Nuclear Service Water Reservoir, now known as Make-Up Pond B.

According to the former Cherokee Nuclear site groundwater investigation, measured depths to groundwater beneath ridges ranged from about 40 to 80 ft. below ground surface. The groundwater table was reportedly at or near the surface in valleys and draws, as was evidenced by observed springs. Near the proposed locations of the reactor buildings, the groundwater table varied between depths of 10 – 60 ft. below ground surface with potentiometric surface elevations ranging from 570 to around 605 ft. above msl (Reference 220).

Construction activities for the Cherokee Nuclear Station began in the late 1970s, resulting in significant alterations to on-site topography. Because of the relationship between topography and depth to water, changes to the potentiometric surface were monitored with a network of observation wells across the site. A review of historical data identified groundwater levels in observation wells prior to and during the construction. Based on water level data, construction dewatering from the site excavation was indicated around January 1977. Between

***Withheld from Public Disclosure Under 10 CFR 2.390(a)(9)
(see COL Application **Part 9**)***

November 1977 and March 1978, approximately 5.74 million gal. of water were reportedly pumped from the water table aquifer through dewatering wells over the 5-month period. These wells were pumped at average rates ranging from 38 to 65 gpm with well depths from 200 to 280 ft. below ground surface. The effect of construction dewatering was assessed on the basis of historical groundwater measurements collected across the site and in the nearest residential well during construction dewatering activities. The apparent drawdown in the observation wells, caused by the cumulative dewatering activities, is shown on **Figure 2.4.12-202**. The dewatering activities did not affect observation wells outside the area shown. In addition, the nearest residential well, the []^{SRI} well, was not affected by construction dewatering activities (**References 215 and 218**). The []^{SRI} well is completed in the Piedmont Aquifer and is located approximately 5000 ft. south of the center of the excavation on the north side of McKowns Mountain Road. Several wells located adjacent to the excavation, around the site, and at a nearby residence (the []^{SRI} well) were gauged on a monthly basis between 1976 and 1985, providing limited-term historical water level data. Only observation wells nearest the excavation, as shown in **Figure 2.4.12-202**, appeared to be affected by the Cherokee site dewatering activities.

2.4.12.2.3 On-Site Conditions in 2006 to 2007 and Projected Post-Construction On-Site Conditions

In March 2006, a groundwater investigation was initiated as part of the subsurface study to evaluate hydrogeologic conditions for the Lee Nuclear Site. The dewatering of the existing excavation preceded the subsurface investigation, thus returning the site to hydrogeologic conditions similar to those of the previous construction phase. Approximately 740 million gal. of water were removed from the excavation from December 19, 2005, through September 7, 2006. Following the initial dewatering, an apparent 5-foot thick interval of staining was observed on the existing Cherokee concrete structures, the top of which was surveyed at an elevation of 578.72 ft. msl. The staining observed between elevations 574 and 579 ft. msl is indicative of the range that water level fluctuated in the open excavation since termination of Cherokee era construction activities. A comparison of the apparent water levels in this impoundment, as shown on the February 1994 and February 2005 aerial photographs, with the topographic survey conducted in 2006 indicated a similar range of water levels in the excavation area (574 ft. msl in 1994 to 579 ft. msl in 2005). Precipitation data for the period preceding these observations indicated near normal conditions, confirming the aerial images captured typical impoundment water levels. Ongoing maintenance dewatering activities are expected to end following construction activities.

As part of the 2006-2007 groundwater investigation, fifteen borings were drilled into the crystalline bedrock, and monitoring wells were installed in partially weathered rock intervals. In July 2006, nine additional monitoring wells were

installed to evaluate shallow groundwater conditions across the site. Details regarding well construction are presented in [Table 2.4.12-201](#).

WLS COL 2.4-5 Following well development, water levels were measured monthly from April 2006 to April 2007 ([Table 2.4.12-202](#)) to characterize seasonal trends in groundwater levels and to identify flow pathways surrounding the Lee Nuclear Site. The hydrograph for this groundwater data is presented on [Figure 2.4.12-203](#). Surface waters at four locations were also gauged as part of the monitoring program. These locations included Make-Up Pond B, a water retention impoundment below Make-Up Pond B, Make-Up Pond A, and Hold-Up Pond A. Based on this year of study, groundwater levels were observed to fluctuate, with the highest groundwater elevations observed between January and April 2007 and the lowest groundwater elevations between September and November 2006. This trend correlates with both the river flow and rainfall patterns and confirms that both groundwater levels and river flow are governed by local precipitation ([Section 2.3](#)).

Potentiometric surface maps developed from water level data showed that during the 2006 construction dewatering and site investigation, groundwater was drawn toward the excavation ([Figure 2.4.12-204](#), Sheets 1 - 7). During the dewatering activities, continuous decline of water levels in areas downgradient of the excavation was observed, as recharge entering the power block area from the south was intercepted by the excavation, pumped and discharged to Make-Up Pond B. Following the completion of construction dewatering, the potentiometric surface beneath the reactor buildings is expected to rebound to equilibrium conditions.

Under natural conditions the topography of the water table within the Piedmont mimics the topography of the land surface, but has less relief. Cross-sections of the Lee Nuclear Site are presented in [Figure 2.4.12-205](#), Sheets 1 - 4. These figures depict the relationship between groundwater beneath the site and the surface water bodies surrounding the site. Groundwater flow in the Piedmont province is typically restricted to the topographic area underlying the slope that extends from a divide to an adjacent stream.

Both regionally and locally, surface topography plays a dominant role in groundwater occurrence. Post-Cherokee plant construction topography was observed to affect groundwater conditions such that cuts in topography induce a lowered water table and fill induces a raised water table. Field evidence for this is based on comparison between the Cherokee water table map ([Figure 2.4.12-201](#)) and the maps developed from the Lee Nuclear Site investigation ([Figure 2.4.12-204](#), Sheets 1-7). For example, MW-1204, located on the Unit 2 Cooling Tower Pad, is where construction fill was placed during Cherokee construction, resulting in a significantly higher land surface elevation (approximately 610 ft. msl compared to its pre-grading elevation of around 560 ft. msl). Consequently, the water table elevation is higher in MW-1204: groundwater elevation of approximately 570 ft. msl compared with the former groundwater elevation of less than 550 ft. msl. Another example includes MW-1200, located west-northwest of Unit 1, where construction cuts resulted in a significantly lower land surface elevation (approximately 590 ft. msl compared to its pre-grading elevation of approximately 670 ft. msl). Consequently, the water table elevation

has lowered (groundwater elevation of 565 ft. msl compared with the former groundwater elevation of more than 585 ft. msl).

Following construction of the Lee Nuclear Station and return to equilibrium conditions, the water table is expected to mimic land surface elevation contours, consistent with slope-aquifer conditions of the Piedmont physiographic province. The potentiometric surface elevation near Lee Units 1 and 2 is expected to rebound between 574 and 579 ft. msl, consistent with concrete stain observations discussed previously. Allowing for moderate frequency short-term fluctuations in water table level above this range that may not be evident in concrete stain observations, groundwater level near Lee Units 1 and 2 may occur between 574 ft. and 584 ft. msl.

The projected post-dewatering water table conditions following the construction of the Lee Nuclear Station are illustrated in [Figure 2.4.12-204](#), Sheet 8. The potentiometric conditions shown in [Figure 2.4.12-204](#), Sheet 8 affect the directions of groundwater flow surrounding the Lee Nuclear Station. Each of the ponds serves as a constant head flow boundary. Ultimately, groundwater flow discharges to the Broad River, which is the groundwater sink for the site and the surrounding area.

Based on site observations, a network of storm drains and buried piping was partially installed during the Cherokee project to manage surface water runoff. While no as-built drawings for the existing storm drain system for the former Cherokee Nuclear Station exist, a review of stormwater plans was conducted to assess the drain system's potential effect on groundwater movement. Storm drains located more than 500 ft. upgradient (south) of the power block could potentially intercept the water table and allow shallow groundwater movement towards Make-Up Pond A; these drains do not affect groundwater movement in the power block area. Other storm drains appear to be above the water table and would not affect the movement of groundwater. One exception is a storm drain originally designed to transfer stormwater from the Cherokee power block area to Hold-Up Pond A. The depth of this storm drain pipe appears to be below the projected water table. Therefore, if left in place, this conduit could potentially cause a preferential groundwater pathway from the power block area downgradient to Hold-Up Pond A once groundwater recovers from the construction dewatering activities. The existing storm drain and bedding materials will be removed by overexcavation. The remaining void will then be plugged with low-permeability backfill material, and compacted to density sufficient to assure no short-circuiting can occur.

Stormwater controls at the Lee Nuclear Station include a combination of surface grading to facilitate surface water flow, construction of a storm drain system (DRS), and construction of a roof drain and collection system. The Lee Nuclear Station DRS is designed to facilitate and control the runoff of precipitation along surface water flow paths, diverting surface runoff away from the power block area and reducing the potential for flooding. The site grading and drainage plan is shown in [Figure 2.4.2-202](#). As discussed in [Subsection 2.4.2.3](#), portions of the site are relatively flat; however, the site is graded such that overall runoff will drain away from safety-related structures to Make-Up Pond B, Make-Up Pond A, or

directly to the Broad River. Precipitation falling on buildings is captured by a roof drain and collection system, channeled through drainage downspouts, and directed to the DRS. The DRS is not expected to directly affect groundwater flow system of the limiting groundwater flow pathway.

2.4.12.2.3.1 Maximum Post-Construction Groundwater Analysis

An analysis of maximum post-construction groundwater elevation in the area of the Units 1 and 2 power block areas was performed. The analysis utilized MODFLOW numerical method model ([Reference 306](#)). The following summarizes the analysis approach.

- The analysis considered planned post-construction surface cover treatment, as illustrated in [Figure 2.4.12-209](#).
- The model domain covered a 3,000 ft. by 3,000 ft. area that includes both Unit 1 and Unit 2 power block areas and extends to include much of the area encompassed by the vehicle barrier system. However, no credit was taken in this analysis for vehicle barrier system drainage capacity. MODFLOW observation points were defined and located to provide estimated groundwater elevations over the duration of the simulation run. The model domain and location of observation points, relative to the power block areas, are shown in [Figure 2.4.12-210](#). [Figure 2.4.12-211](#) provides a hydrograph of groundwater elevations at each observation point over the duration of the modeled storm event.
- The model reflects the fill, soil/saprolite, and PWR uppermost aquifer unit of the Lee site. Placement of granular fill and general fill was also included in the model construction. Hydraulic conductivity and specific yield values were derived from site investigations and expected properties of granular fill materials to be used during plant construction.
- Starting groundwater elevations for the analysis were based on hydraulic heads from the projected potentiometric surface map in [Figure 2.4.12-204](#), Sheet 8.
- Precipitation input was developed from the 1995 Tropical Storm Jerry which exhibited the maximum monthly precipitation and maximum 24-hr precipitation at the regional Greenville/Spartanburg station near Greer, South Carolina. This storm is considered the most severe historically recorded precipitation event for the site and surrounding area. The storm duration, based on gage data from the Greer station is presented in [Table 2.4.12-205](#). To maximize saturation of soils and associated groundwater mounding, the storm event definition included an antecedent storm (40% of the [Table 2.4.12-205](#) distribution values), a 72-hr dry-out period, and followed by the full 100% precipitation, using the [Table 2.4.12-205](#) distribution.
- Infiltration is assumed to occur instantaneously (with no time lag as water travels through the vadose zone). Infiltration occurs at a constant rate

determined by the runoff coefficient of the surface material and does not consider a decrease in actual soil absorption capacity during the precipitation event.

- Modeled surface runoff from impervious surfaces is considered as additional water directed onto grass covered areas. This additional water is added to precipitation that falls directly on the down-slope grass surface.

The analysis concluded that the maximum post-construction groundwater elevation remained below 584 ft. msl; therefore, satisfying the DCD site parameter for maximum groundwater elevation of less than 591 ft. msl ([Table 2.0-201](#)).

WLS COL 2.4-5 2.4.12.2.4 Aquifer Characteristics

2.4.12.2.4.1 Porosity

Site-specific subsurface materials in the area surrounding the power block include fill, residual soil, saprolite, and partially weathered rock (PWR). Based on the results of the geotechnical investigation, representative engineering properties of the soils were determined according to methods described in [Subsection 2.5.4.2](#). Characterization of porosity and effective porosity were made using the data provided in [Table 2.5.4-211](#).

Fill materials are located in former drainageways, which were built up to existing elevations during Cherokee construction. Based on the specific gravity (particle density, 2.71 grams per cubic centimeter, g/cc) and dry unit weight (101 pounds per cubic foot, pcf) provided for fill material, a mean total porosity of 40 percent was determined. The effective porosity is assumed to be equivalent to specific yield, and was estimated using grain size distribution described within Water Supply Paper 1662-D ([Reference 299](#)). This technique indicates effective porosity was estimated to be 9 percent. Fill materials have been cut from other areas of the site, and they are typically comprised of undifferentiated materials (residual soils, saprolite, and/or PWR) similar to native materials.

The residual soils have undergone relatively complete weathering and lack the relict features found in the saprolite zone. Saprolite is the isovolumetrically weathered zone which does not reflect the characteristics of surficial soil development processes, but does reflect some of the physical properties of the underlying parent rock from which it was formed. According to the U.S. Department of Agriculture (USDA) Natural Resources Conservation Service (NRCS), surficial soils in the vicinity of the power block area consisted predominantly of Tatum silty clay loam and Tatum very fine sandy loam with variable slope and erosion ([Figure 2.4.12-206](#)). Tatum soils are well-drained (not seasonally saturated) and are typically derived from sericite schist, phyllite, and/or other related metamorphic rocks of the Piedmont. Tatum soils are typically composed of a surficial 0 - 8 in. silty clay loam or very fine sandy loam (CL, CL-ML, ML). These soil horizons grade subsoils of clay, silty clay, and/or silty clay loam (CH, MH). Clay content in the subsoil stratum of Tatum soils ranges from

12 to 60 percent. Tatum soils transition at depths of 45-60 inches to saprolite materials reflecting the characteristics of the underlying parent rock. The saturated hydraulic conductivity of Tatum soils is reported by the NRCS to be moderately permeable: 4 to 14 micrometers per second ($\mu\text{m/s}$) (4 to 14 x 10^{-4} centimeters per second [cm/s]). Tatum soils are not prone to flooding and exhibit erosion factors (K_f) that range from 0.32 to 0.43. The soils are highly corrosive to both concrete and steel ([Reference 278](#)). Based on geotechnical analyses of both the residual soil and saprolite, a mean total porosity of 45 percent was estimated for these materials. The effective porosity was estimated to be approximately 20 percent. The native soils in the immediate area of the power block were essentially completely removed or mixed with deeper saprolite materials to become site fill materials during Cherokee-era activities. Regardless, knowledge of the natural properties of these surface soil materials is useful in understanding characteristics of site soils, and conditions in the undisturbed portions of the site.

PWR is a transitional weathering zone between the saprolite and the hard, competent, underlying bedrock. The PWR materials are similar to the overlying saprolite zone, but include more fragments of less weathered and less porous rock. PWR was conservatively estimated to have an effective porosity of 8 percent. This value is based on the free drainage (specific yield) represented by the difference between saturated unit weight (140 pcf) and the wet unit weight (135 pcf). The total porosity of PWR, based on saturated unit weight, is estimated to be 27 percent.

2.4.12.2.4.2 Permeability

The permeability of a material is a measure of its ability to transmit water. Generally within the Piedmont region, the soil/saprolite zone has a low permeability. Also, fractures within the competent bedrock become sparse and poorly connected at increasing depths, thus limiting crystalline bedrock permeability. Fracture permeability consistently occurs in the transition zone, including the uppermost part of bedrock; therefore, this zone often exhibits the highest consistent permeability.

During the Cherokee investigation in the 1970's, 135 field and laboratory tests were conducted to characterize soil and rock permeability. Fifty-five packer tests were conducted in soil and rock intervals in 17 soil borings across the site. An additional 42 field and 38 laboratory tests were performed to evaluate soil permeability. The recent investigation supplements the above investigation with the performance of an additional 11 packer tests in bedrock materials, 16 slug-out tests across the site, and one multi-well aquifer pump test performed within the limiting groundwater flow path (i.e., the flow path with the shortest time-of-travel) from the nuclear island area toward the Broad River to the north.

Based on results from the Cherokee investigation, packer tests, multiwell pumping tests, geotechnical laboratory analyses, and field tests (combined with the results of the 2006 slug tests, packer tests, and multiwell pumping tests), the following conclusions are made regarding aquifer permeability at the Lee Nuclear Site,

noting that maintenance dewatering is ongoing and may have affected the recent aquifer test results:

- Reported vertical soil hydraulic conductivities (K_v) of soil and saprolite ranges from 2.45×10^{-8} cm/s to a maximum value of 2.55×10^{-4} cm/s with a median of 2.10×10^{-6} cm/s. For samples exceeding the median hydraulic conductivity of the data set, the geometric mean (4.4×10^{-5} cm/s) represents a conservative vertical hydraulic conductivity value for the residuum. For the purpose of permeability analysis, a conservative value is one that increases the rate of water movement. Vertical hydraulic conductivity generally increases with depth.
- Reported horizontal hydraulic conductivities (K_h) of soil and saprolite ranges from 9.67×10^{-7} cm/s (i.e., the lower limit of the test range) to a maximum value of 2.26×10^{-3} cm/s with a median of 1.14×10^{-4} cm/s. For samples exceeding the median hydraulic conductivity of the data set, the geometric mean (4.5×10^{-4} cm/s) represents a conservative hydraulic conductivity value for the residuum.
- Reported hydraulic conductivities measured in the partially weathered rock (PWR), or transition zone, range from approximately 9.67×10^{-7} cm/s to a maximum value of 9.89×10^{-3} cm/s with a median of 1.53×10^{-4} cm/s. For samples exceeding the median hydraulic conductivity of the data set, the geometric mean (1.0×10^{-3} cm/s) represents a conservative hydraulic conductivity value for the PWR transition zone across the site. Based on its thorough review of the properties of the PWR zone, Duke asserts that a value of 1.4×10^{-3} cm/s is a scientifically-sound, conservative, and representative hydraulic conductivity value for PWR materials at the Lee site. This is the value obtained from an aquifer test in 2006 for an area believed to best represent the limiting groundwater flow path, and is used as the representative value of hydraulic conductivity for PWR. **Figure 2.4.12-207** includes three PWR samples that were subsequently excavated in the area of the reactors.
- Values of hydraulic conductivity reported in the Cherokee-era studies represent the upper 100 ft. of the saturated interval. This undifferentiated aquifer zone is comprised of residual soil, saprolite, and partially weathered rock. The resultant hydraulic conductivity values range from 2.21×10^{-4} cm/s to 3.90×10^{-3} cm/s. These results are consistent with and support the recent findings of the Lee-era site investigation. These more recent studies determined the hydraulic conductivity of PWR, the most hydraulically conductive aquifer material, to be 1.4×10^{-3} cm/s.
- Fill materials placed in former valleys during site grading are currently groundwater aquifer materials in some areas. Slug tests conducted in 2006 and 2007 characterized these materials to have hydraulic conductivities ranging from 1.81×10^{-5} cm/s to 7.44×10^{-5} cm/s. The

median hydraulic conductivity for the fill material is 5.39×10^{-5} cm/s. For samples equal to and greater than the median hydraulic conductivity of the data set, the geometric mean (7.0×10^{-5} cm/s) represents a conservative hydraulic conductivity value for the fill materials.

A summary of the various test results is presented in [Table 2.4.12-204](#). [Figure 2.4.12-207](#) depicts the distribution of hydraulic conductivities with depth. This figure shows the wide variability of hydraulic conductivities observed across the site during both the Cherokee and Lee site investigations. Hydraulic conductivities generally decrease with depth as partially weathered rock transitions to continuous rock. [Figure 2.4.12-207](#) includes the results for partially weathered rock samples that were subsequently removed during excavation for the Cherokee Nuclear Station reactor buildings.

WLS COL 2.4-5 2.4.12.3 Groundwater Movement

2.4.12.3.1 Groundwater Pathways

The nature and depth of groundwater circulation in the Piedmont is predictably variable. This variability is a function of the singular aquifer system being comprised of weathered saprolite, partially weathered rock, and fractured bedrock, and the degree of interconnection of pores and fractures between these materials. Typical of the Piedmont, groundwater flow is from topographic positions (recharge areas) to the regional drainage features (discharge areas). Groundwater flow at this site likewise generally mirrors the surface topography, with strong gradients and flow paths from the power block area, northward to the Broad River.

The projected groundwater movement in the vicinity of the Lee Nuclear Station power block was assessed to evaluate contaminant migration for the postulated release scenario ([Subsection 2.4.13](#)). For the release scenario, radwaste contaminant sources include the Units 1 and 2 radwaste storage tanks, located below plant grade at elevation 559.5 ft. msl. This elevation is 32.5 ft. below plant grade. For the assessment of alternative pathways, four locations were assumed to be plausible points of exposure (i.e., locations at which groundwater would be discharged to the surface to allow human contact or to facilitate transport). The pathways evaluated are:

- Pathway 1: Unit 2 to Hold-Up Pond A
- Pathway 2: Unit 2 to the Broad River
- Pathway 3: Unit 2 to Make-Up Pond A
- Pathway 4: Unit 1 to Make-Up Pond B

The impacts of construction and operation of Make-Pond Up C within the London Creek watershed were evaluated and determined not to affect groundwater conditions beyond Little London Creek drainage way. Consequently, Make-Up Pond C does not affect the groundwater flow regime at the Lee Nuclear Station, including the evaluation of hydrostatic loading (Subsection 2.4.12.5) or analyses of accidental releases of radioactive liquid effluents (Subsection 2.4.13).

2.4.12.3.2 Groundwater Velocity

The rate of flow (i.e., the velocity) of groundwater depends on (1) the permeability and effective porosity of the medium through which it is moving and (2) the hydraulic gradient. Average interstitial groundwater flow velocity within the water table aquifer was determined using a form of the Darcy equation as follows:

$$V = K (dh/dl)/n_e$$

Where: V = average groundwater velocity (ft/yr)

K = hydraulic conductivity (cm/s converted to ft/yr)

dh/dl = groundwater gradient (ft/ft)

n_e = effective porosity (%)

After construction dewatering and the return to static conditions, the potentiometric surface in the area of the reactor buildings is expected to rebound to a maximum elevation of approximately 584 ft. msl. These conditions reflect the maximum anticipated groundwater level during operations.

Travel distances for contaminants from postulated release points at the reactors to downgradient receptors were estimated from site information for each of four possible flow paths. Although the aquifer is comprised principally of saprolite and PWR, the more conservative PWR values for hydraulic conductivity and effective porosity were used in the analysis of groundwater velocities. Estimated travel times for the four groundwater flow paths are as follows:

- Pathway 1: Groundwater travels from Unit 2 to Hold-Up Pond A in approximately 1.6 years.
- Pathway 2: From Unit 2 to the Broad River in approximately 2.6 years.
- Pathway 3: From Unit 2 to Make-Up Pond A in approximately 4.0 years.
- Pathway 4: From Unit 1 to Make-Up Pond B in approximately 5.5 years.

These flow paths are represented on Figure 2.4.12-208. This analysis indicates the limiting flow path for the evaluated postulated release to be from the Unit 2 radwaste storage tank to Hold-Up Pond A (Pathway 1, Figure 2.4.12-205, Sheet 3).

Soil distribution characteristics for radiological isotopes (i.e., Co-60, Cs-137, Fe-55, I-129, Ni-63, Pu-242, Tc-99, U-235) were determined from soil and water samples collected along the preferred groundwater flow path. This data is presented in [Subsection 2.4.13](#) to assist in the development of calculations for fate and transport analyses in the event of accidental releases of effluents to groundwater.

2.4.12.3.3 Effects of Local Area Pumping

While the groundwater is not intended to be used at the Lee Nuclear Site, consideration is given to the movement of groundwater beneath the site in response to potential pumping associated with dewatering or domestic well use. Based on permeability characteristics beneath the site and an understanding of typical wells in the vicinity, a radius of influence can be estimated. For unconfined aquifers, such as those encountered in the Piedmont province, the radius of influence can be determined using the following equation provided by the Departments of the Army, the Navy, and the Air Force in Publication TM5-818-5:

$$R = 3\Delta H (K \times 10^4)^{1/2}$$

Where: R = the radius of influence of a pumping well (ft.)

ΔH = the drawdown within the well (ft.)

K = the hydraulic conductivity of the aquifer (cm/s)

Most domestic wells in the vicinity of the Lee Nuclear Site are completed as either shallow bored wells, or deeper drilled wells. Shallow bored wells are usually completed in the saprolite zone, typically no deeper than 75 ft. Deeper drilled wells are installed in the PWR and fractured bedrock zones. Both types of wells generally have yields of 5-10 gpm, or less. Using these conditions provides a conservative estimate of the potential reach of a typical domestic well producing at full capacity. Assuming the hydraulic conductivities are consistent with partially weathered rock, as listed in [Table 2.4.12-204](#), the radius of influence is approximately 1700 ft. (0.32 mi.) from these wells. The lateral area of influence of the dewatered excavation is approximately 500 ft. (0.095 mi.).

Based on site reconnaissance of the area, the closest domestic water supply well is located approximately 5000 ft. (0.95 mi.) south of the nuclear island. The influence of the surrounding impoundments (i.e., Make-Up Pond B and Make-Up Pond A) would further buffer the potential draw created from off-site pumping or on-site pumping, if needed. No off-site wells are considered capable of reversing groundwater flow beneath the site, or vice versa, based on the geographic positions of these wells (i.e., the distance of the domestic wells) and the character of these wells (i.e., the typical low-flow rates and the relatively shallow completion depths).

The Cherokee Nuclear Station Construction Permit ER identified 50 domestic water wells and provided construction details for these wells, including well

diameter, well depth, and depth to water (see [Table 2.4.1-212](#) and [Figure 2.4.1-212](#)). Only three of these 50 wells have total depths of 150 ft. or greater. Since 1985, 19 wells have been installed within a 1-mi. radius of the Lee Nuclear Site property boundary and to a depth greater than 150 ft. ([Reference 261](#)). However, according to information provided by the Draytonville Water District, public water supply lines were installed in the late 1990s and continue to be added in the area surrounding the Lee Nuclear Site. As of 2007, since public water supply lines were installed in the area, approximately 55 percent of residents within a 2-mi. radius of the reactor buildings have converted from self-supplied groundwater systems to public water supplies. Furthermore, with the addition of water-supply lines planned for completion in 2009, the public water is expected to be available to approximately 83 percent of those residents within the 2-mi. radius of the plant. The projected use of self-supplied groundwater systems is expected to decline as public water supply lines are built into rural areas and residents increase their dependence on the public water supply.

2.4.12.4 Monitoring or Safeguard Requirements

WLS COL 2.4-5 There are two potential sources for radiological impacts to groundwater: (1) leaks from radioactive waste tanks and (2) leaks from the spent fuel pool. To minimize the potential for contact of radioactive material with groundwater, the Lee Nuclear Site is equipped with a water barrier around the building foundation up to 1 ft. above grade. The water barrier is installed to prevent water from seeping into the auxiliary building that holds the liquid radioactive waste tanks. In addition, groundwater monitoring will be conducted at the Lee Nuclear Site. The groundwater monitoring program will be consistent with the guidance in "Generic FSAR Template Guidance for Life Cycle Minimization of Contamination" (NEI 08-08). The groundwater monitoring program will include a network of wells for early detection (near-field wells) and for verification of no off-site migration (far-field wells). Wells will be installed in proximity to plant systems that may be a source of radiological releases, and/or in nearby plausible down-gradient flow direction from such sources. Both shallow and deep wells will be utilized as needed to monitor the location closest to the potential release area. The laboratory analyses of groundwater samples will include gamma isotopes and tritium.

The groundwater monitoring program is described in [Subsection 12AA.5.4.14](#). Accident effects are discussed in [Subsection 2.4.13](#). Additionally, analysis of the relationship of the Lee Nuclear Site groundwater to seismicity and the potential for related soil liquefaction and the potential for undermining of safety-related structures is discussed in [Section 2.5](#).

2.4.12.5 Site Characteristics for Subsurface Hydrostatic Loading

WLS COL 2.4-4 According to the AP1000 Design Control Document (DCD), the design maximum groundwater elevation is 2 ft. below plant elevation. The Lee Nuclear Station plant elevation is 593 ft. above msl and the yard grade is 592 ft. above msl; therefore, the design maximum groundwater elevation for the Lee Site is 591 ft. above msl. A maximum groundwater elevation, considering the most severe historically

recorded natural phenomena for the Lee site is estimated to be approximately 584 ft. msl, as discussed in [Subsection 2.4.12.2.3.1](#). The hydrostatic loading is not expected to exceed design criteria. An unsaturated zone of at least 8 ft. below plant grade elevation will be maintained during operations. The installation and operation of a permanent dewatering system is not a facility design requirement.

WLS COL 2.4-5	2.4.13	ACCIDENTAL RELEASES OF RADIOACTIVE LIQUID EFFLUENTS IN GROUND AND SURFACE WATERS
WLS COL 15.7-1		

2.4.13.1 Groundwater

This section provides a conservative analysis of a postulated accidental liquid effluent release to the environment at the Lee Nuclear Site. The following sections describe the scenario and conceptual model used to evaluate the transport pathways to the nearest potable water supply in an unrestricted area. RESRAD-OFFSITE Version 2.0 is used to model the transport and provide resulting radionuclide concentration values in the potable water receptor body.

Acceptable results are those that are less than the effluent concentrations listed in 10 CFR 20 Appendix B, Table 2, Column 2. Individual radionuclide concentration results and the sum of fractions value are compared against these limits. The sum of fractions (i.e., unity value) is a comparison of the ratio of known radionuclides to their limit. This unity value may not exceed "1". As applied through Branch Technical Position 11-6, these criteria apply to the nearest potable water supply in an unrestricted area.

Historical and projected groundwater flow paths were evaluated in [Subsection 2.4.12](#) to characterize groundwater movement from the nuclear island area to a point of exposure. Groundwater at the Lee Site exists as a single, undifferentiated aquifer, comprised of soil, saprolite, partially weathered rock (PWR), competent bedrock, and, to a limited extent, fill soils. Although the projected groundwater flow paths travel through zones with saprolite, fill, and PWR, the more conservative hydrogeologic characteristics of PWR were used in both the determination of the limiting groundwater flow path and as inputs, where appropriate, into the RESRAD-OFFSITE model. Using the PWR characteristics for hydraulic conductivity, bulk density, and effective porosity, the flow path from the Unit 2 effluent hold-up tank to Hold-Up Pond A is assumed to be the limiting pathway of radionuclide migration, with the shortest (i.e., most rapid) travel time to a surface water body. For purposes of this analysis, because the spillway and dam of Hold-Up Pond A are proximal to the Broad River, entry concentrations at Hold-Up Pond A are assumed to be entry concentrations at the Broad River. This direct conveyance to the Broad River thus provides for no additional retardation, hold-up, or restrictions to transport between Hold-Up Pond A and the Broad River. [Figures 2.4.12-204](#), Sheet 8 and [2.4.12-205](#), Sheet 3 depict subsurface conditions that control the movement of groundwater beneath the Lee Nuclear Station.

While groundwater functions as the transport media for fugitive radionuclides, interaction of individual radionuclides with the soil matrix can potentially delay their movement. The solid/liquid distribution coefficient, K_d , is, by definition, an equilibrium constant that describes the process wherein a species (e.g., a radionuclide) is partitioned between a solid phase (soil, by adsorption or precipitation) and a liquid phase (groundwater, by dissolution). Soil properties affecting the distribution coefficient include the texture of soils (sand, loam, clay, or organic soils), the organic matter content of the soils, pH values, the soil solution ratio, the solution or pore water concentration, and the presence of competing cations and complexing agents. Because of its dependence on many soil properties, the value of the distribution coefficient for a specific radionuclide in soils can range over several orders of magnitude under different conditions. The measurement of distribution coefficients of radionuclides within the limiting groundwater pathway allows further characterization of the rate of movement of fugitive radionuclides in groundwater.

Soil and groundwater samples were collected from Monitoring Wells MW-1208 and MW-1210 located on the north and south sides of the nuclear island (Figure 2.4.12-205, Sheet 1). Three soil samples were collected from the saturated zone at depths ranging from 45 to 73 ft. below ground level. The samples were submitted for laboratory analysis of soil distribution characteristics for specific radiological isotopes (Co-60, Cs-137, Fe-55, I-129, Ni-63, Pu-242, Sr-90, Tc-99, U-235). Results of these analyses are presented in Table 2.4.13-201, along with default K_d values found in literature, for comparison. For conservatism, those radionuclides which had been evaluated for site-specific distribution coefficients used the lowest measured K_d values in the evaluation, regardless of the media from which the samples were collected. The values are adjusted to the low limit of their reporting range (e.g., for a reported Cs-137 value of $1156 \pm 163 \text{ cm}^3/\text{g}$, a value of $993 \text{ cm}^3/\text{g}$ was used in the analysis). All other radionuclides use the most conservative K_d value of 0.

2.4.13.2 Accident Scenario

The limiting postulated failure of a Unit 2 effluent holdup tank, located in the Unit 2 auxiliary building, is analyzed to estimate the resulting concentration of radioactive contaminants entering Hold-Up Pond A via groundwater flow. Contaminant concentrations at this point are then assumed to represent entry concentrations to the surface water receptor, the Broad River, which is located proximal to Hold-Up Pond A.

The event is defined as an unexpected and uncontrolled release of radioactive water produced by plant operations from a tank rupture. The AP1000 tanks which normally contain radioactive liquid are listed in Table 2.4.13-202. The contents from the effluent holdup tank are conservatively assumed to enter the environment instantaneously, allowing radionuclides to be transported in the direction of groundwater flow. The flow path from Unit 2 to Hold-Up Pond A is determined to be the limiting pathway based on travel time.

It is noted that no outdoor tanks contain radioactivity. In particular, the AP1000 does not require boron changes for load follow and so does not recycle boric acid or water; therefore, the boric acid tank is not radioactive.

The spent resin tanks are excluded from consideration, because most of their activity is bound to the spent resins; they have minimal free water that would be capable of migrating from the tank in the event of a tank failure. Tanks inside the containment building were not considered because the containment building, a seismic Category I structure, is a freestanding cylindrical steel containment vessel (DCD Subsection 1.2.4.1). Credit is taken for the steel liner to mitigate the effect of a postulated tank failure.

The Liquid Radwaste System (WLS) monitor tanks located in the radwaste building extension are considered because of their location in a non-seismic building. These tanks have a maximum capacity of 15,000 gallons each. They receive fluid that has been processed and must be monitored prior to discharge. The radwaste building has a well sealed, contiguous basemat with integral curbing that can hold the maximum liquid inventory of any tank. Floor drains in the area lead to the liquid radwaste system. The foundation for the entire building is a reinforced concrete mat on grade. Liquid spilled due to failure of any one of these tanks would be contained within the building, and would involve low activity liquids being held for discharge. Any release to the environment would be leakage through cracks in the concrete. The radiological consequences of such leakage are bounded by the analysis for the effluent holdup tanks. Therefore, these monitor tanks are not the limiting fault.

The remaining four tank applications were considered - the effluent holdup tanks, waste holdup tanks, monitor tanks (located in the auxiliary building), and chemical waste tank. Of these tanks, the effluent holdup tanks have both the highest potential radioactive isotope concentrations and the largest volume. The effluent holdup tanks are also located on the lowest level of the auxiliary building, which is a limiting location relative to an uncontrolled release from the auxiliary building via the groundwater pathway. Therefore, an effluent holdup tank is limiting for the purpose of calculating the effects of the failure of a radioactive liquid-containing tank.

The effluent holdup tanks are located in an unlined room on the lowest level of the auxiliary building. This level is 32 feet 6 inches below the existing surface grade elevation of the plant. Each unit has two effluent holdup tanks, one of which is postulated to fail.

The analysis considers the tank liquid level, decay of the tank contents, potential paths of spilled liquid to the environment, and other pertinent factors.

The total volume of each effluent holdup tank is 28,000 gallons. Since credit can not be taken for liquid retention by unlined building foundations; a conservative analysis assumes that the tank content (80 percent of capacity, or 22,400 gallons) is immediately released through cracks in the auxiliary building walls and floor into the surrounding sub-surface soil. These assumptions follow the position in Branch Technical Position 11-6, March 2007.

2.4.13.3 Source Term

The radioactive source term is:

- Tritium source term concentration is 1.0 microcuries per gram taken from [DCD Table 11.1-8](#);
- Corrosion product source terms Cr-51, Mn-54, Mn-56, Fe-55, Fe-59, Co-58, and Co-60 taken from [DCD Table 11.1-2](#);
- Other isotope source terms taken from [DCD Table 11.1-2](#) multiplied by 0.12/0.25 to adjust the radionuclide concentrations to the required 0.12 percent failed fuel fraction outlined in Branch Technical Position 11-6, March, 2007; and
- Gaseous state nuclides and nuclides with short half-lives not included in the RESRAD default library are removed from consideration as they have no impact on the evaluation. These radionuclides include:

Ba-137m	Br-83	Br-85	I-131
I-133	Kr-83m	Kr-85	Kr-85m
Kr-87	Kr-88	Kr-89	Rh-106
Te-131	Te-131m	Xe-131m	Xe-133
Xe-133m	Xe-135	Xe-137	Xe-138

WLS COL 2.4-5 Analysis of failure of the effluent holdup tank of Unit 2 rather than Unit 1 is conservative in that the pathway from the Unit 2 effluent holdup tank to Hold-Up Pond A has the shortest (i.e., most rapid) travel duration, assuming conservative PWR characteristics along the entire flow path.

The impacts of construction and operation of Make-Up Pond C within the London Creek watershed were evaluated and determined not to affect groundwater conditions beyond Little London Creek drainage way. Consequently, Make-Up Pond C does not affect the groundwater flow regime at the Lee Nuclear Station and therefore has no impact on the transport paths and accidental release analyses discussed in this subsection.

As discussed in [Subsection 2.4.12](#), dewatering activities are currently occurring at the site. After construction is complete, dewatering activities will end.

The conceptual model of radionuclide transport through groundwater, from Unit 2 to Hold-Up Pond A, is shown in [Figure 2.4.12-205](#) (Sheet 3). As stated in [Subsection 2.4.13.1](#), a direct conveyance between Hold-Up Pond A and the Broad River is assumed. With the failure of the effluent holdup tank and subsequent liquid release to the environment, radionuclides enter the subgrade soils at an elevation of 32 feet 6 inches below the surrounding grade. The contaminated zone is, therefore, a volume of contaminated soil for which the effective porosity is saturated with contaminated water released from the liquid

effluent holdup tank. The contaminated zone soil is assumed to exhibit PWR characteristics. Because RESRAD-OFFSITE considers soil at the source of the contamination, the liquid initial source term concentrations were converted to an equivalent concentration on a soil mass basis.

Currently, the overburden soils continually receive the average annual onsite precipitation. In general, the precipitation that does not run off or is not lost to evapotranspiration infiltrates the overlying unsaturated zone and contributes to groundwater as recharge. However, as an additional conservative measure in the model, runoff was assumed to be zero, and precipitation not lost to evapotranspiration was treated by RESRAD-OFFSITE as recharge.

2.4.13.4 Conceptual Model

The conceptual model assumes that one of the liquid effluent tanks, located at the lowest level of the auxiliary building, ruptures while containing 80 percent of its total capacity. The liquid is assumed to be released in accordance with Branch Technical Position 11-6 of NUREG-0800. The liquid from the ruptured tank would flood the tank room and proceed to the auxiliary building radiologically controlled area sump by way of the floor drains. The sump pumps are assumed to be inoperable to create a bounding case. The liquid then enters the environment outside the auxiliary building. The consequence is a release of 22,400 gallons of contaminated liquid into the soil. The liquid is transported via groundwater flow to the surface water receptor, the Broad River. Because Hold-Up Pond A is the surface water body with the shortest (i.e., most rapid) groundwater transport time, assuming PWR characteristics, the model calculates radionuclide concentrations in a hypothetical well at the edge of this pond. The dam and spillway of Hold-Up Pond A are proximal to the Broad River. This model then assumes that concentrations in Hold-Up Pond A are immediately conveyed to the Broad River, without any additional intermediate retardation, hold up, or transport restrictions between Hold-Up Pond A and the Broad River. The conceptual model then assumes the liquid is diluted in the Broad River reservoir upstream of the Ninety-Nine Islands Dam. This is conservative because the nearest potable water supply using the Broad River surface water is located approximately 21 miles downstream from the postulated release point, at the City of Union public water supply. Concentrations are modeled for an evaluation period of 1,000 years.

The conceptual model is conservative because it provides for the shortest (i.e., most rapid) travel time to a surface water body, even though that surface water body is not the receptor body, and it also includes faulting the limiting tank. The analysis uses conservative estimates for parameters that are not developed from site-specific data. In addition, site-specific inputs to the model are also conservative, including the use of the lowest K_d values and the assumption that all groundwater pathways traveled through geo-media with the porosity and conductivity properties of PWR. Values used as inputs in the model are shown in [Table 2.4.13-203](#). The straight-line flow path is used, which is also conservative as actual groundwater pathways are more tortuous, have longer transport times, and lower hydraulic conductivities for the fractures and joints.

Radionuclide concentrations in the hypothetical well at the edge of Hold-Up Pond A and in the Broad River at the Ninety-Nine Islands Dam are modeled using RESRAD-OFFSITE (Reference 212). The model considers the effects of different transport rates for radionuclides and progeny nuclides, while allowing radioactive decay during the transport process. The concentration of each radionuclide transmitted to the Broad River is determined by the transport through the groundwater system, dilution by groundwater and infiltrating surface water from the overburden soils, adsorption, and radioactive decay.

Radionuclide decay during transport by groundwater occurs and is considered in the analysis. Radionuclide transport by groundwater is assumed to be affected by adsorption by the surrounding soils. As discussed in Subsection 2.4.12, the soils surrounding the auxiliary building at the elevation of the liquid release are modeled as having the porosity and hydraulic conductivity characteristics of PWR.

The saturated zone dispersion values are set to mimic infusion, rather than injection, of the contaminated liquid into the groundwater flow by assigning a value to the longitudinal dispersivity equal to one-hundredth of the length of the transport distance (contaminated zone). The horizontal dispersivity is one tenth of the longitudinal dispersivity and the vertical dispersivity is one hundredth of the longitudinal dispersivity distance. FSAR Table 2.4.13-203 indicates the values used in the analysis for these parameters. These settings allow the contamination to move with the natural groundwater flow rather than be pushed through the groundwater and arrive over a longer time frame in a more dilute state.

2.4.13.5 Sensitive Parameters

Sensitivity analyses were performed on a number of input parameters to evaluate the sensitivity of the RESRAD-OFFSITE model to a range of values for specific input factors. A parameter is considered sensitive if the resulting effect on the evaluated radionuclide concentration varied by more than 10 percent. Input parameters evaluated in the sensitivity analyses include:

- Hydraulic gradient of the saturated zone (varied by a factor of 2);
- Well pump intake depth (varied by a factor of 2);
- Volume of the surface water receptor (varied by a factor of 2); and
- K_d values in the saturated zone for site-specific (non-zero) radionuclides (varied by a factor of 10).

Overall, the sensitivity analyses indicate that variations in the single parameters analyzed have no significant impact on the resulting concentrations; in no case do the resulting concentrations exceed 10 CFR 20 Appendix B, Table 2, Column 2 limits or a sum of fractions calculation. Of particular note:

- When the surface water volume is reduced by a factor of 2, concentrations doubled, but the sum of fractions remained in the E-05 range. This

expected outcome confirmed that even with a significant reduction in available volume, the sum of fractions remained below the unity value of one.

- Even with a relatively high hydraulic gradient (0.06 ft/ft considered not plausible for this site), increases in radionuclide concentrations varied by less than 10 percent, and the sum of fractions remained below 10 CFR 20 Appendix B, Table 2, Column 2 limits and unity standard.

2.4.13.6 Regulatory Compliance

WLS COL 2.4-5 10 CFR 20 Appendix B states, "The columns in Table 2 of this appendix captioned "Effluents," "Air," and "Water," are applicable to the assessment and control of dose to the public, particularly in the implementation of the provisions of §20.1302. The concentration values given in Columns 1 and 2 of Table 2 are equivalent to the radionuclide concentrations which, if inhaled or ingested continuously over the course of a year, would produce a total effective dose equivalent of 0.05 rem (50 millirem or 0.5 millisieverts)." Thus, meeting the concentration limits of 10 CFR 20 Appendix B, Table 2 Column 2 results in a dose of less than 0.05 rem and therefore demonstrates that the requirements of 10 CFR 20.1301 and 10 CFR 20.1302 are met.

The radiological consequence of a postulated failure of the Unit 2 effluent holdup tank as the limiting fault is evaluated and determined not to exceed 10 CFR 20 Appendix B, Table 2, Column 2 limits at the nearest waters adjoining the Lee site (Broad River). The analysis demonstrates that radionuclide concentrations in both the hypothetical well located at the edge of Hold-Up Pond A and in the Broad River at the Ninety-Nine Islands Dam are below 10 CFR 20 Appendix B, Table 2, Column 2 limits. Further, the nearest potable water supply located in an unrestricted area using the Broad River surface water is the City of Union public water supply located approximately 21 miles downstream of the Ninety-Nine Islands Dam.

The maximum radionuclide concentration for each isotope sum of fractions of 10 CFR 20 Appendix B, Table 2, Column 2 limits calculated for both the hypothetical well at the edge of Hold-Up Pond A and in the receptor body, the Broad River, during the 1,000-year period, is below a value of 1. [Table 2.4.13-204](#) provides the fraction of effluent concentration for the significant radionuclide.

2.4.14 TECHNICAL SPECIFICATIONS AND EMERGENCY OPERATION REQUIREMENTS

WLS COL 2.4-6 The maximum flood level at the Lee Nuclear Station is established as the maximum of calculated results from flooding events analyzed in [Section 2.4](#). That

maximum flood level is elevation 592.56 ft. msl. This elevation would result from a PMP event on the Lee Nuclear Station site (local intense precipitation) as described in [Subsection 2.4.2.3](#). The Lee Nuclear Station safety-related structures have a plant elevation of 593 ft. msl. This maximum flood level is identified as a site characteristic in [Table 2.0-201](#). Also, [Subsection 2.4.12.5](#) describes plant elevation relative to the maximum anticipated groundwater level. The hydrostatic loading is not expected to exceed design criteria.

There are no safety-related facilities that could be affected by low-flow or drought conditions of the Broad River. At low flow conditions, water is drawn from Make-Up Ponds B and C ([Subsection 2.4.11.5](#)). Full power plant operations could be sustained for approximately 190 days with water from Make-Up Ponds B and C, with sufficient water remaining in Make-Up Pond A to shutdown the plant and maintain safe shutdown conditions.

Based on site-specific conditions of the Lee Nuclear Station, there are no emergency protective measures designed to minimize the impact of adverse hydrology-related events on safety-related facilities.

STD DEP 1.1-1 2.4.15 COMBINED LICENSE INFORMATION

2.4.15.1 Hydrological Description

WLS COL 2.4-1 This COL item is addressed in [Subsection 2.4.1](#).

2.4.15.2 Floods

WLS COL 2.4-2 This COL item is addressed in [Subsections 2.4.2, 2.4.3, 2.4.4, 2.4.5, 2.4.6, 2.4.7, and 2.4.10](#).

2.4.15.3 Cooling Water Supply

WLS COL 2.4-3 This COL item is addressed in [Subsections 2.4.8, 2.4.9, and 2.4.11.5](#).

2.4.15.4 Groundwater

WLS COL 2.4-4 This COL item is addressed in Subsections 2.4.12.1, 2.4.12.2, 2.4.12.3, and 2.4.12.5.

2.4.15.5 Accidental Release of Liquid Effluents into Ground and Surface Water

WLS COL 2.4-5 This COL item is addressed in Subsections 2.4.12.2.3, 2.4.12.2.4, 2.4.12.3, 2.4.12.4, and 2.4.13.

2.4.15.6 Emergency Operation Requirement

WLS COL 2.4-6 This COL item is addressed in Subsection 2.4.14.

2.4.16 REFERENCES

201. American Iron and Steel Institute, "Modern Sewer Design," AISC, Washington, D.C., Fourth Edition 1999.
202. American Nuclear Society, "American National Standard for Determining Design Basis Flooding at Power Reactor Sites," ANSI/ANS-2.8-1992, American Nuclear Society, La Grange Park, Illinois, July 28, 1992.
203. Bohman, L.R., "Determination of Flood Hydrographs for Streams in South Carolina: Volume 1. Simulation of Flood Hydrographs for Rural Watersheds in South Carolina" U.S. Geological Survey, Water-Resources Investigations Report 89-4087, Columbia, South Carolina, 1990.
204. Broad River Electric Cooperative, Inc., Written Communication from Douglas E. Wilson to Gerald Gotzmer regarding the Cherokee Falls Hydro Minimum Flow, July 15, 2002.
205. Calpine, Website, Website, www.calpine.com/power/plant.asp?plant=96, accessed April 3, 2007.
206. Chow, V.T., "Open Channel Hydraulics," McGraw-Hill, New York, 1959.

207. City of Shelby, "2003 Annual Water Quality Report," Website, <http://www.cityofshelby.com/econdev/water.htm>, accessed March 2006.
208. Cooney, T.W, P.A Drewes, S.W. Ellisor, T.H. Lanier, and F. Melendez, "Water Resources Data, South Carolina, Water Year 2005," U.S. Geological Survey Water-Data Report SC-05-1, 2006.
209. C. Yu, C. Loureiro, J.-J. Cheng, L.G. Jones, Y.Y. Wang, Y.P. Chia, and E. Faillace, Environmental Assessment and Information Sciences Division, Argonne National Laboratory, *Data Collection Handbook to Support Modeling Impacts of Radioactive Material in Soil*, 1993.
210. C. Yu, A.J. Zielen, J.-J. Cheng, D.J., LePoire, E. Gnanapragasam, S. Kamboj, J. Arnish, A. Wallo III,* W.A. Williams,* and H. Peterson*, Environmental Assessment Division, Argonne National Laboratory, *User's Manual for RESRAD Version 6*, Appendix E, pg. E9-E13, 2001.
211. Devine, Tarbell & Associates Inc, Cherokee Hydrology Summary Report, 2005.
212. U.S. Department of Energy, "User's Manual for RESRAD-Offsite Version 2," ANL/EVS/TM/07-1, DOE/HS-0005, NUREG/CR-6937, Argonne National Laboratory, Environmental Science Division, Argonne, Illinois, June 2007.
213. Removed
214. Duke Power Company, Cherokee Nuclear Station – Environmental Report, Sections 2.2, 2.4 and 2.5, revised 1975.
215. Duke Power Company, Groundwater Levels Notebook, Site Groundwater Monitoring Field Observations 1976 -1985, Project 81 Cherokee Nuclear Station, Cherokee County, SC.
216. Duke Power Company, Ninety-Nine Islands Dam Project License Renewal, Environmental Report, 1996.
217. Duke Power Company, "Ninety-Nine Islands Hydro Project, FERC Project No. 2331, Determination of the Probable Maximum Flood," Duke Engineering Services, Charlotte, North Carolina, November 7, 1997.
218. Duke Power Company, Powerhouse Groundwater Control, 1977-1978, Cherokee Nuclear Project Manual, Cherokee Nuclear Station.
219. Duke Energy, "Preliminary Application for Certificate of Public Convenience and Necessity Cleveland County & Rutherford County Cliffside Project," May 11, 2005.
220. Duke Power Company, *Preliminary Safety Analysis Report, Project 81 – Cherokee Nuclear Station, Cherokee County, SC*, 1974.

-
221. Environmental Data Resources, Environmental Database and Geotcheck® search, date extracted March 2006.
222. Federal Energy Regulatory Commission, "Order Issuing New License to Duke Power Company, Project No. P-2332-003," June 12, 1996.
223. Federal Energy Regulatory Commission, "Order Issuing New License to Duke Power Company, Project No. P-2331-002," June 17, 1996.
224. Federal Register Vol. 71, No. 133, Pages 39308-39309 (July 12, 2006).
225. Hansen, E.M., L.C. Schreiner, and J.F. Miller, "Application of Probable Maximum Precipitation Estimates - United States East of the 105th Meridian," Hydrometeorological Report No. 52, U.S. Department of Commerce, National Oceanic and Atmospheric Administration, National Weather Service, Washington, D.C., August 1982.
226. National Archives and Records Administration, Federal Register Document 06-6139, Vol. 71, No. 133, July 12, 2006.
227. Removed
228. National Oceanic & Atmospheric Administration, National Geophysical Data Center Tsunami Database, Website, http://www.ngdc.noaa.gov/seg/hazard/tsu_db.shtml, accessed July 2006.
229. National Weather Services Greenville-Spartanburg Station historical records, Website, www.erh.noaa.gov/gsg/climate/climatology/climatology.htm, April 10, 2007.
230. North Carolina Department of Environment and Natural Resources, "Broad River Basinwide Water Quality Plan," March 2003.
231. North Carolina Department of Environmental and Natural Resources, Division of Water Quality, "Basinwide Assessment Report, Broad River Basin," December, 2001.
232. North Carolina Department of Environmental and Natural Resources, Basinwide Assessment Report, Broad River Basin, 2006.
233. North Carolina Department of Environment and Natural Resources, "North Carolina State Water Supply Plan," January 2001.
234. North Carolina Division of Water Resources, 2002 Local Water Supply Plan for Broad River Water Authority, Website, http://www.ncwater.org/Water_Supply_Planning/Local_Water_Supply_Plan/, accessed March 2007.

235. North Carolina Division of Water Resources, 2002 Local Water Supply Plan for Cleveland County Sanitary District, Website, http://www.ncwater.org/Water_Supply_Planning/Local_Water_Supply_Plan/, accessed March 2007.
236. North Carolina Division of Water Resources, 2002 Local Water Supply Plan for Forest City, Website, http://www.ncwater.org/Water_Supply_Planning/Local_Water_Supply_Plan/, accessed March 2007.
237. North Carolina Division of Water Resources, 2002 Local Water Supply Plan for Kings Mountain, Website, http://www.ncwater.org/Water_Supply_Planning/Local_Water_Supply_Plan/, accessed March 2007.
238. North Carolina Division of Water Resources, 2002 Local Water Supply Plan for Shelby, Website, http://www.ncwater.org/Water_Supply_Planning/Local_Water_Supply_Plan/, accessed March 2007.
239. North Carolina Division of Water Resources, 1999 Water Withdrawal Registration 0028-0002 J.C. Cowan Plant, Website, <http://dwr.ehnr.state.nc.us/cgi-bin/foxweb.exe/c:/foxweb/reg99a>, accessed June 2006.
240. North Carolina Division of Water Resources, 1999 Water Withdrawal Registration 0057-0002 Cliffside Steam Station, Website, <http://dwr.ehnr.state.nc.us/cgi-bin/foxweb.exe/c:/foxweb/reg99a>, accessed June 2006.
241. North Carolina Division of Water Resources, 1999 Water Withdrawal Registration 0057-0007 Tuxedo Hydro-Electric Facility, Website, <http://dwr.ehnr.state.nc.us/cgi-bin/foxweb.exe/c:/foxweb/reg99a>, accessed June 2006.
242. North Carolina Division of Water Resources, 1999 Water Withdrawal Registration 0219-0028 Kings Mountain Quarry, Website, <http://dwr.ehnr.state.nc.us/cgi-bin/foxweb.exe/c:/foxweb/reg99a>, accessed June 2006.
243. North Carolina Division of Water Resources, 1999 Water Withdrawal Registration 0351-0001 Kenmure Golf Course, Website, <http://dwr.ehnr.state.nc.us/cgi-bin/foxweb.exe/c:/foxweb/reg99a>, accessed June 2006.
244. North Carolina Division of Water Resources, 1999 Water Withdrawal Registration 0354-0001 Cleveland Country Club Golf Course, Website, <http://dwr.ehnr.state.nc.us/cgi-bin/foxweb.exe/c:/foxweb/reg99a>, accessed June 2006.

245. North Carolina Division of Water Resources, 1999 Water Withdrawal Registration 0359-0001 Ticona-Shelby Facility, Website, <http://dwr.ehnr.state.nc.us/cgi-bin/foxweb.exe/c:/foxweb/reg99a>, accessed June 2006.
246. North Carolina Division of Water Resources, 1999 Water Withdrawal Registration 0360-0001 Cleveland-Caroknit, Website, <http://dwr.ehnr.state.nc.us/cgi-bin/foxweb.exe/c:/foxweb/reg99a>, accessed June 2006.
247. North Carolina Division of Water Resources, 1999 Water Withdrawal Registration 0361-0002 Turner Shoals Hydroelectric Plant, Website, <http://dwr.ehnr.state.nc.us/cgi-bin/foxweb.exe/c:/foxweb/reg99a>, accessed June 2006.
248. North Carolina Division of Water Resources, 1999 Water Withdrawal Registration 0361-0003 Stice Shoals Hydroelectric Plant (misabeled as Spencer Mountain Hydroelectric Project), Website, <http://dwr.ehnr.state.nc.us/cgi-bin/foxweb.exe/c:/foxweb/reg99a>, accessed June 2006.
249. North Carolina General Statutes, Chapter 143-215.22H, 2005.
250. Owen, J.H., "Flood Emergency Plans, Guidelines for Corps Dams," U.S. Army Corps of Engineers, RD-13, June 1980.
251. Reed, M.J., "Assessment of Low-Temperature Geothermal Resources of the United States - 1982," U.S. Geological Survey Circular 892, 1982.
252. Renner, J.L. and T.L. Vaught, "Geothermal Resources of the Eastern United States," U.S. Department of Energy DOE/ET/28373-T2, Gruy Federal Inc., Arlington, Virginia, December 1979.
253. Riggs, H.C., "Techniques of Water-Resources Investigations of the United States Geological Survey," Book 4, Chapter B1, "Low-Flow Investigations," United States Government Printing Office, Washington, D.C., 1972.
254. Sanborn LLC, Ground Control Surveying Report of Duke-Cherokee County, South Carolina Site, 2006.
255. Schreiner, L.C., and J.T., Riedel, "Probable Maximum Precipitation Estimates, United States East of the 105th Meridian," Hydrometeorological Report No. 51, U.S. Department of Commerce, National Oceanic and Atmospheric Administration, National Weather Service, Washington, D.C., June 1978.
256. Shaw Stone & Webster Inc., WS. Lee Units 1 and 2 COLA Conceptual Design Package (CDP) for the Raw Water System (RWS), August 2007.

257. South Carolina Ambient Groundwater Quality Monitoring Network Annual Report, Summary, revised 2004, Website, [http://www.scdhec.gov/water/pubs/amb2004.pdf#search=22Technical20Report3A22Technical 20Report3A20005-0620South20Carolina20Ambient20South20 Carolina20Ambient22](http://www.scdhec.gov/water/pubs/amb2004.pdf#search=22Technical20Report3A22Technical20Report3A20005-0620South20Carolina20Ambient20South20Carolina20Ambient22), accessed April 9, 2007.
258. South Carolina Code of Laws, Title 49, Chapter 4, Section 49-4-20, 2005.
259. South Carolina Department of Health and Environmental Control, "Broad River Water Quality Assessment," 2001.
260. Ho, F.P., and J.T. Riedel, "Seasonal Variation of 10-Square Mile Probable Maximum Precipitation Estimates, United States East of the 105th Meridian," Hydrometeorological Report No. 53, U.S. Department of Commerce, National Oceanic and Atmospheric Administration, National Weather Service, Washington D.C., April 1980.
261. South Carolina Department of Health and Environmental Control, "LASTREP2 - Private Well Report for Cherokee County for dates 01/01/1985 to 06/22/2006" (text file), revised 2006.
262. South Carolina Department of Health and Environmental Control, "Source Water Assessment Carlisle Cone Mills System No 4430003," April 29, 2003.
263. South Carolina Department of Health and Environmental Control, "Source Water Assessment City of Union System No 4410001," April 29, 2003.
264. South Carolina Department of Health and Environmental Control, "Source Water Assessment Gaffney BPW System No 1110001," April 29, 2003.
265. South Carolina Department of Health and Environmental Control, "Source Water Assessment VC Summer Nuclear Station System No 2030004," April 29, 2003.
266. South Carolina Department of Health and Environmental Control, South Carolina Source Water Assessment and Protection Program, revised 1999, Website, <http://www.scdhec.net/water/pubs/swpplan.pdf>, accessed April 9, 2007.
267. South Carolina Department of Health and Environmental Control, South Carolina Water Use Report 2005 Summary, Technical Document Number: 006-06, 2006.
268. South Carolina Department of Health and Environmental Control, Watershed Water Quality Assessment – Broad River Basin, Technical Report No. 001-01, 2001.

-
269. U.S. Army Corps of Engineers, "Engineering and Design Hydrologic Engineering Requirements for Reservoirs." EM 1110-2-1420, October 31, 1997.
270. U.S. Army Corps of Engineers, "Engineering and Design Hydrologic Frequency Analysis," EM 1110-2-1415, March 5, 1993.
271. U.S. Army Corps of Engineers, Hydrologic Engineering Center, Generalized Computer Program, HMR52, Probable Maximum Storm, Revised April 1991.
272. U.S. Army Corps of Engineers, Hydrologic Engineering Center, Hydrologic Modeling System, HEC-HMS computer software, version 3.0.1.
273. U.S. Army Corps of Engineers, Hydrologic Engineering Center, River Analysis System, HEC-RAS computer software, version 3.1.3.
274. U.S. Army Corps of Engineers, Ice Jam Database, Website, <http://www.crrel.usace.army.mil/ierd/ijdb/>, data extracted April, 2006.
275. U.S. Army Corps of Engineers, "Ice Jam Flooding: Causes and Possible Solutions," EP 1110-2-11, November 30, 1994.
276. U.S. Army Corps of Engineers, National Inventory of Dams, Website, <http://crunch.tec.army.mil/nid/webpages/nid.cfm>, accessed June 2006.
277. Removed
278. U.S. Department of Agriculture, Natural Resources Conservation Service, Web Soil Survey, Website, <http://websoilsurvey.nrcs.usda.gov/app/>, accessed January 2007.
279. Removed
280. United States Department of Agriculture, Soil Conservation, Cherokee County, South Carolina Soil Survey, 1977.
281. U.S. Department of Defense, "Unified Facilities Criteria, Design: Seismic Design for Buildings," UFC 3-310-03A, March 1, 2005.
282. Removed
283. Removed
284. U.S. Environmental Protection Agency, STORET, Website, <http://www.epa.gov/storet/>, accessed May 2006.

285. LeGrand, Harry E. Sr., A Master Conceptual Model for Hydrogeological Site Characterization in the Piedmont and Mountain Region of North Carolina, Website, http://h2o.enr.state.nc.us/aps/gpu/documents/legrand_04.pdf#search=%2A%20Master%20Conceptual%20Model%20for%20Hydrogeological%20Site%20Characterization%20in%20the%20Piedmont%20and%20Mountain%20%22A%20Master%20Conceptual%20Model%20for%20Hydrogeological%20Site%20Characterization%20in%20the%20Piedmont%20and%20Mountain%20%22, November 11, 2006.
286. U.S. Geological Survey, "Estimated Use of Water in the United States, County-Level Data for 2000," Website, <http://water.usgs.gov/watuse/data/2000/index.html>, accessed April 11, 2007.
287. U.S. Geological Survey, "Guidelines for Determining Flood Flow Frequency, Bulletin #17B of the Hydrology Subcommittee," March 1982.
288. U.S. Geological Survey, Horton, Jr., Wright and Dicken, C., "Preliminary Digital Geologic Map of the Appalachian Piedmont and Blue Ridge, South Carolina Segment," U.S. Geological Survey Open-File Report 01-298, revised 2004, Website, <http://pubs.usgs.gov/of/2001/of01-298/>, accessed on November 5, 2006.
289. U.S. Geological Survey, Igage Mapping Corp., USGS topographic map using All Topo Maps V7, The Carolina's, 2004.
290. U.S. Geological Survey, National Water Information System: Web Interface, USGS Surface-Water Data for the Nation, Website, <http://waterdata.usgs.gov/usa/nwis/sw>, accessed July 2006.
291. U.S. Geological Survey, "Potential of Hot-Dry-Rock Geothermal Energy in the Eastern United States," Open-File Report 93-377, November 1993.
292. Removed
293. U.S. Geological Survey, Water Resources Data, South Carolina Water Year 2005, 2006.
294. Weaver, J.C., "The Drought of 1998 - 2002 in North Carolina, Precipitation and Hydrologic Conditions," U.S. Geological Survey Scientific Investigations Report 2005-5053, Reston, Virginia, 2005.
295. U.S. Army Corps of Engineers, "Engineering and Design, Coastal Engineering Manual," EM 1110-2-1100, Change 2: June 1, 2006.
296. U.S. Geological Survey, Estimating the Magnitude of Peak Discharges for Selected Flood Frequencies on Small Streams in South Carolina [1975], Open File Report 82-337, 1975.

297. LeGrand, Harry E. Sr., *A Master Conceptual Model for Hydrogeological Site Characterization in the Piedmont and Mountain Region of North Carolina*, North Carolina Department of Environment and Natural Resources, Division of Water Quality, Groundwater Section, 2004.
298. Enercon Services, Inc., *Bathymetry Study for the COL Application*, June 2008.
299. U.S. Department of Interior, Johnson, A.I., "Specific Yield – Compilation of Specific Yields for Various Materials," Geological Survey Water Supply Paper 1662-D, prepared in accordance with California Department of Water Resources, 1967, Table 1.
300. U.S. Department of Agriculture, Natural Resources Conservation Service, Web Soil Survey, Website, <http://websoilsurvey.nrcs.usda.gov/app/HomePage.htm>, accessed November 2008.
301. U.S. Department of Agriculture, Natural Resources Conservation Service, Web Soil Survey, Website, <http://websoilsurvey.nrcs.usda.gov/app/HomePage.htm>, accessed August 2009.
302. U.S. Army Corps of Engineers, Hydrologic Engineering Center, Hydrologic Modeling System, HEC-HMS computer software, version 3.5.
303. Removed
304. Federal Highway Administration, "Hydraulic Design of Highway Culverts," Hydraulic Design Series No. 5, Second Edition, FHWA-NHI-01-020, May 2005.
305. National Oceanic & Atmospheric Administration Website, National Climatic Data Center, Local Climatic Data, Greenville-Spartanburg Station (Greer, SC), Station ID, GSP, Accessed at <http://www7.ncdc.noaa.gov/CDO/dataproduct> on October 4, 2011.
306. Harbaugh et. al., 2000, MODFLOW-2000, The U.S. Geological Survey Modular Ground-Water Model – User Guide to Modularization Concepts and the Ground-Water Flow Process, U.S. Geological Survey, Reston, Virginia.

WLS COL 2.4-1

TABLE 2.4.1-201 (Sheet 1 of 2)
SITE FEATURES AND ELEVATIONS

Site Feature	Elevation (ft. msl)
<u>Nuclear Island</u>	593
Railcar Bay/Filter Storage Area door	593
Bottom of Basemat (Units 1 and 2)	553.5
<u>Annex Building</u>	593
Temporary Electric Power Supply Room door	593
Door to SO3 Stairs	593
Door to SO4 Stairs	593
Men's Change Room door	593
Corridor 40321 door	593
Corridor door 40311	593
Access Area 40300 doors	593
Containment Access Corridor Hatch and Door	600.1
<u>Diesel Generator Building</u>	593
Diesel Generator Room A doors	593
Diesel Generator Room B doors	593
Combustion Air Cleaner Area A plenum	593
Combustion Air Cleaner Area B plenum	593
<u>Radwaste Building</u>	593
Mobile Systems Facility doors	593
HVAC Equipment Room door	593
Electrical/Mechanical Equipment Room door	593
<u>Turbine Building</u>	593
Mobile Systems Facility doors	593
Door to SO2 Stairs	593
Aux Boiler Room door	593
Motor Driven Fire Pump Room door	593
Door to SO1 Stairs	593
Turbine Building Grade Deck Room 20300	593

Source: Westinghouse AP1000 DCD Rev 19; Tier 2, Chapter 1.2.

WLS COL 2.4-1

TABLE 2.4.1-201 (Sheet 2 of 2)
SITE FEATURES AND ELEVATIONS

Site Feature	Elevation (ft. msl)
<u>Other Features</u>	
Heavy Haul Road	590
Raw Water Intake Pumping Station (base)	497.3
Raw Water Intake Pumping Station (entry)	508
Heavy Lift Derrick - Crane	589.5
Low Level Waste Storage Area	588
Wastewater Treatment Area	588
Ninety-Nine Islands Dam Crest	511
Broad River above Ninety-Nine Islands Dam	511
Broad River below Ninety-Nine Islands Dam	440
Make-Up Pond A	547
Make-Up Pond B	570
Hold-Up Pond A	536
Make-Up Pond C	650
Cooling Tower	588

ft. - feet

msl - mean sea level

WLS COL 2.4-1

TABLE 2.4.1-202 (Sheet 1 of 2)
DESCRIPTION OF UPPER BROAD RIVER WATERSHEDS

Watershed Name	Basin	Subbasin	Drainage Area (sq. mi.)	Drainage Area Above Ninety-Nine Islands Dam (sq. mi.)
Upper Broad River Basin (03050105) of North Carolina				
Upper Broad River and Lake Lure	03050105	030801	184	184
Second Broad River and tributaries	03050105	030802	513	513
Green River	03050105	030803	137	137
First Broad River	03050105	030804	426	426
Buffalo Creek	03050105	030805	181	163
North Palocet	03050105	030806	73	0
Upper Broad River Basin (03050105) of South Carolina				
Broad River	03050105	050	26	26
Broad River	03050105	090	129	65
Buffalo Creek	03050105	100	16	16
Cherokee Creek	03050105	110	23	23
Kings Creek	03050105	120	52	0
Thicketty Creek	03050105	130	157	0
Bullock Creek	03050105	140	118	0
North Pacolet River	03050105	150	49	0

WLS COL 2.4-1

TABLE 2.4.1-202 (Sheet 2 of 2)
DESCRIPTION OF UPPER BROAD RIVER WATERSHEDS

Watershed Name	Basin	Subbasin	Drainage Area (sq. mi.)	Drainage Area Above Ninety-Nine Islands Dam (sq. mi.)
South Pacolet River	03050105	160	91	0
Pacolet River	03050105	170	115	0
Lawsons Fork Creek	03050105	180	85	0
Pacolet River	03050105	190	102	0
Totals			2477	1553

Source (SC): [Reference 268](#)Source (NC): [Reference 230](#)

sq. mi. - square miles

WLS COL 2.4-1

TABLE 2.4.1-203 (Sheet 1 of 2)
USGS GAUGING STATIONS ON THE BROAD RIVER

Station Name	Station Number	Location	Drainage Area (sq. mi.)	2005 Water Year Annual Mean Flow (cfs)
Broad River near Boiling Springs, NC	02151500	Lat. 35°12'39", Long. 81°41'51", on right bank half mi. upstream from Sandy Creek, 3 mi. downstream from Second Broad River, and 3½ mi. SW of Boiling Springs, Cleveland County.	864	NIA
Broad River near Blacksburg, SC	02153200	Lat 35°07'26", Long 81°35'17", at upstream side of bridge on SC Highway 18, 1.2 mi upstream of Buffalo Creek, 1.2 mi downstream of Gaston Shoals Reservoir, 3.2 mi west of Blacksburg, and at mile 275.2.	1290	1802
Broad River near Gaffney, SC	02153500	Water-stage recorder, Lat. 35°05'20", Long. 81°34'20", at a bridge on US Hwy. 29, 0.3 mi. upstream from Cherokee Creek, 4.4 mi. downstream from Gaston Shoals Dam, and 4.5 mi. ENE of Gaffney, Cherokee County.	1490	NIA
Broad River below Cherokee Falls, SC	02153551	Water-stage recorder, Lat. 35°01'52", Long. 81°29'34", at left bank of tailrace below Ninety-Nine Islands Reservoir, 3.1 mi. downstream of Cherokee Falls, and 0.3 mi. upstream of Kings Creek.	1550	2532

WLS COL 2.4-1

TABLE 2.4.1-203 (Sheet 2 of 2)
USGS GAUGING STATIONS ON THE BROAD RIVER

Station Name	Station Number	Location	Drainage Area (sq. mi.)	2005 Water Year Annual Mean Flow (cfs)
Broad River near Carlisle, SC	02156500	Water-stage recorder, Lat. 34°35'46", Long. 81°25'20", on right bank at downstream side of bridge on State Highway 72, 1.3 mi upstream from Sandy River, 2.0 mi downstream from Seaboard Coast Line Railroad bridge, 2.5 mi east of Carlisle, 5.0 mi downstream from Neal Shoals Dam, and at mile 226.0., Union County.	2790	3892

Source: References 214, 290, and 293.

mi. - miles

See Figure 2.4.1-205

sq. mi. - square miles

NIA = No Information Available

WLS COL 2.4-1

TABLE 2.4.1-204 (Sheet 1 of 2)
BROAD RIVER MONTHLY DISCHARGE AND TEMPERATURE
VARIABILITY

DISCHARGE VARIABILITY

Monthly Mean Stream Flow Recorded in Cubic Feet Per Second (cfs)												
Year	Jan	Feb	Mar	Apr	May	Jun	Jul	Aug	Sep	Oct	Nov	Dec
1998											1098	1253
1999	2021	2040	1812	1851	1422	964	796	517	538	925	1137	1338
2000	1619	1840	2142	1997	1301	713	591	518	678	669	1129	890
2001	865	985	1727	1318	793	801	1020	589	764	574	630	843
2002	1336	1139	1473	1104	835	560	377	242	505	865	1592	3312
2003	1441	2747	6686	8733	7433	5608	5051	4983	1838	1619	2094	2727
2004	1744	3100	1637	2104	1439	2626	1503	1219	8764	2219	3541	4710
2005	2615	2229	3930	3162	1926	2489	5418	1998	1356	2658	997	2031
2006	2659	1773	1516	1382	1100	1394	982	1254	2054	1245	1828	2143
Mean of Monthly Discharge	1852	2102	2779	2935	2202	2085	2194	1583	2285	1493	1655	2323
Max:	2659	3100	6686	8733	7433	5608	5418	4983	8764	2658	3541	4710
Min:	865	985	1473	1104	793	560	377	242	393	574	630	843

Notes:

Average annual flow: Approximately 2500 cfs (1926-2008)
 Maximum monthly flow: 8764 cfs (1926-2006)
 Minimum monthly flow: 242 cfs (1998-2006)
 cfs - cubic feet per second
 Source:
 USGS 02153551 Broad River Below Ninety Nine Islands Reservoir, SC
 (1998 to 2006)

Cherokee County, South Carolina
 Hydrologic Unit Code 03050105
 Latitude 35°01'52", Longitude 81°29'34" NAD27
 Drainage area 1550 square miles
 Gauge datum 412.20 feet above sea level NGVD29
 Missing data - No information available from USGS

Maximum and Minimum Monthly Average Flows
1998 - 2006

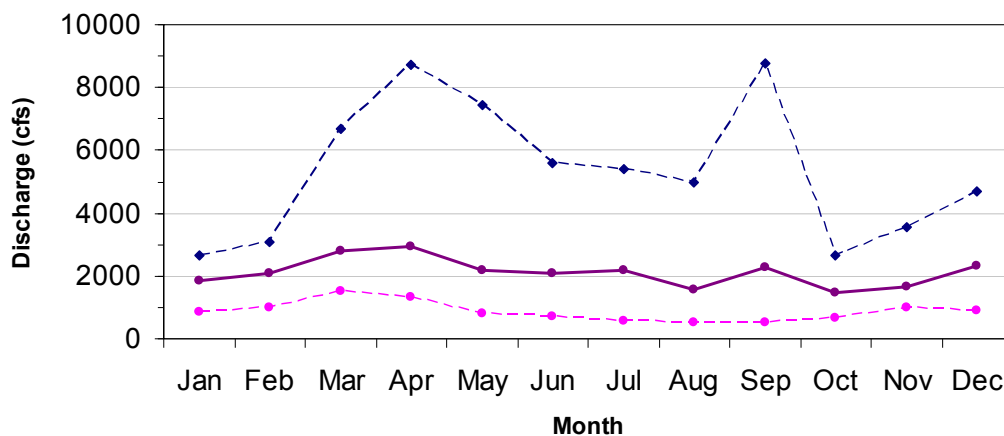


TABLE 2.4.1-204 (Sheet 2 of 2)
BROAD RIVER MONTHLY DISCHARGE AND TEMPERATURE VARIABILITY

TEMPERATURE VARIABILITY												
Monthly Mean Water Temperature (deg. C)												
YEAR	Jan	Feb	Mar	Apr	May	Jun	Jul	Aug	Sep	Oct	Nov	Dec
1996										16.9	11.3	7.55
1997	7.89	9.30	14.2	15.8	19.5	22.5	27.2	26.6	23.6	18.0	9.77	6.60
1998	7.40	8.77	11.3					27.2	25.4	19.1	13.4	9.81
1999	7.29	9.38	11.1	18.6	21.3	25.3	28.3	29.1	24.3	18.1	13.3	8.42
2000	6.87	8.33	14.0	16.5	23.7			27.9	23.6	18.4	11.9	
2001	4.92	9.86	11.7	18.3	23.3	26.4	27.0	28.3	23.6	17.3	12.7	10.6
2002	6.07	9.57	12.8	20.9	22.8	28.1	29.6	28.3	25.5	20.0		
2003		8.02	13.1	15.5	19.6	23.5	25.9	25.5		18.1	14.8	7.37
2004	6.83	6.83	13.4	17.5	24.4	26.0		26.4			14.0	7.54
2005	8.05	8.33	11.1	16.6	21.0				25.7	19.6	12.4	6.67
2006	8.42	8.51	13.0	19.8	22.2			28.5	24.3			
Mean of Monthly Temp.	7.10	8.70	12.6	17.7	22.0	25.4	27.7	27.5	24.5	18.4	12.6	8.10
Max:	8.4	9.9	14.2	20.9	24.4	28.1	29.6	29.1	25.7	20.0	14.8	10.6
Min:	4.9	6.8	11.1	15.5	19.5	22.5	25.9	25.5	23.6	16.9	9.8	6.6

Notes:

Average monthly temperature: 17.7°C

Average monthly maximum temperature: 19.6°C

Average monthly minimum temperature: 15.7°C

Maximum monthly temperature: 29.6°C

Minimum monthly temperature: 4.9°C

Degree Celsius - °C

Source:

USGS 02156500 Broad River Near Carlisle, SC (1996 to 2006)

No incomplete Data is used for Statistical Calculation

Union County, South Carolina

Hydrologic Unit Code 03050106

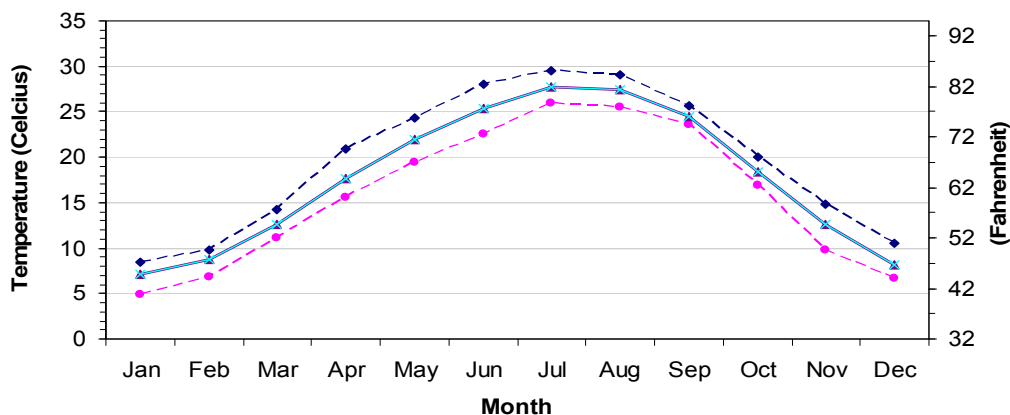
Latitude 34°35'46", Longitude 81°25'20" NAD27

Drainage area 2790 square miles

Gauge datum 290.79 feet above sea level NGVD29

Missing data - No information available

Maximum and Minimum Monthly Temperatures 1996 - 2006



WLS COL 2.4-1

TABLE 2.4.1-205
MAJOR RESERVOIRS LOCATED IN THE UPPER BROAD RIVER BASIN

Name	In Service Date	Owner	Type	Drainage Area (sq. mi.)	Water Surface Area (ac.)	Dam Height (ft.)	Dam Length (ft.)	Spillway Width (ft.)	Normal Storage (ac.-ft.)	Flood Storage ^(a) (ac.-ft.)	Normal Pool Elevation (ft. msl)
Ninety-Nine Islands	1910	DPC	CNPG	1550	433	62	1568	891 ⁽²⁾	2300	2300	511 ⁽²⁾
King Mountain Reservoir (Moss Lake)	1973	City of King Mtn.	RE	68 ⁽¹⁾	1329	99	840	(b)	44,400	53,280	736 ⁽²⁾
Lake Lure	1927	Town of Lake Lure	CNVA	95	740	124	480	(b)	32,295	44,914	991 ⁽²⁾
Lake Adger (Turner Shoals)	1925	Hydro, LLC	CNVA	138 ⁽¹⁾	460 ⁽¹⁾	90	689	(b)	11,700 ⁽¹⁾	16,760	912 ⁽²⁾
Lake Summit	1920 ⁽²⁾	Duke Energy	CNSA	43 ⁽¹⁾	276	130 ⁽²⁾	254 ⁽²⁾	(b)	9300	15,840	2012.6 ⁽²⁾
Lake Whelchel	1964	City of Gaffney	RE	14.7	177	61	2100	565	2438	5698	670 ⁽⁴⁾
Make-Up Pond C	(c)	Duke Energy	RE	3.87	620	132	2370	80	22,000	28,764	650

ac. - acre

ac.-ft. - acre-foot

sq. mi. - square miles

ft. - feet

msl - mean sea level

DPC - Duke Power Company

RE – earth filled

CN – concrete

CNPG – concrete gravity arch

CNVA - Concrete mult-arch

CNSA - Concrete single-arch

- a) Dams and reservoirs on the Broad River and its major tributaries are utilized for thermoelectric power, water supply, and recreation and not for significant flood control.
b) No seismic design or spillway design criteria available for review.
c) Under development.

Sources:

- 1) [Reference 230](#); North Carolina Department of Environmental and Natural Resources, "Broad River Basinwide Water Quality Plan", March 2003.
2) [Reference 217](#); Duke Power Company, "Ninety-Nine Islands Hydro Project, FERC Project No. 2331, Determination of Probable Maximum Flood", Duke Engineering Services, Charlotte, North Carolina, November 7, 1997."
3) [Reference 276](#); U.S. Army Corps of Engineers, "National Inventory of Dams, Website, <http://crunch/tec.army.mil/nid/webpages/nid.cfm>, accessed June 2006
4) USGS Quadrangle, Blacksburg South, South Carolina

WLS COL 2.4-1

TABLE 2.4.1-206
SCDHEC 2005 WATER USAGE FOR CHEROKEE COUNTY, SOUTH CAROLINA

Usage	Quantity		
	Million Gallons	Mgd ⁽¹⁾	cfs
Public Supply	2561.1	7.02	10.9
Industrial	504.13	1.38	2.14
TOTAL	3065.23	8.4	13.02

Source: [Reference 267](#)

Mgd - Million gallons per day

cfs - cubic feet per second

SCDHEC - South Carolina Department of Health and Environmental Control

(1) Quantity reported by SCDHEC in Million Gallons. Mgd was estimated by dividing SCDHEC's reported 2005 water use by 365 days.

WLS COL 2.4-1

TABLE 2.4.1-207
SCDHEC 2005 WATER USAGE FOR CHEROKEE, CHESTER,
GREENVILLE, SPARTANBURG, UNION, AND YORK COUNTIES, SOUTH CAROLINA

County Name	Total Withdrawals					
	Groundwater		Surface Water		Total	
	Mgd	cfs	Mgd	cfs	Mgd	cfs
Cherokee, SC	0.003	0.005	8.39	13.0	8.40	13.0
Chester, SC	0.07	0.11	3.55	5.50	3.62	5.61
Greenville, SC	0.34	0.53	66.6	103	67.0	104
Spartanburg, SC	4.01	6.22	41.6	64.5	45.6	70.7
Union, SC	0.008	0.012	4.88	7.56	4.89	7.58
York, SC	0.27	0.42	93.1	144	93.4	145

Note: Withdrawal totals excluded hydroelectric power usage

Source: [Reference 267](#)

Mgd - Million gallons per day

cfs - cubic feet per second

WLS SUP 2.4-1

TABLE 2.4.1-208
2000 WATER USE TOTALS BY COUNTY IN THE UPPER BROAD
RIVER WATERSHED

County Name	Total Withdrawals					
	Groundwater		Surface Water		Total	
	Mgd	cfs	Mgd	cfs	Mgd	cfs
Cherokee, SC	0.44	0.68	15.4	23.9	15.9	24.6
Chester, SC	1.80	2.79	4.6	7.1	6.4	9.9
Greenville, SC	3.03	4.70	53.3	82.6	56.3	87.1
Spartanburg, SC	4.01	6.22	57.0	88.3	61.0	94.4
Union, SC	0.25	0.39	8.2	12.7	8.5	13.2
York, SC	8.52	13.2	209	324	217	335.7
Buncombe, NC	8.77	13.6	33.7	52.3	42.5	65.8
Burke, NC	3.09	4.79	21.0	32.5	24.1	37.3
Catawba, NC	6.18	9.58	1182	1832	1188	1838
Cleveland, NC	2.51	3.89	189	293	192	297
Gaston, NC	7.67	11.9	965	1495	972	1504
Henderson, NC	3.7	5.74	13.4	20.8	17.1	26.5
Lincoln, NC	3.77	5.84	6.15	9.53	9.9	15.3
McDowell, NC	4.39	6.80	4.09	6.34	8.5	13.2
Polk, NC	1.24	1.92	1.48	2.29	2.7	4.2
Transylvania, NC	1.88	2.91	22.1	34.2	23.9	36.9

NOTES:

1. Greenville, Union, and York Counties within the Broad River Watershed are not part of the drainage basin for the Broad River adjacent to the site.
2. Cherokee, Cleveland, Polk, and Rutherford Counties compose the majority of the area in the Broad River Watershed above the site.
3. Total withdrawals for aquaculture and mining were 0 Mgd for all counties.
4. Hydroelectric water use not included.

Mgd - Million gallons per day

cfs - cubic feet per day

Source: [Reference 286](#)

WLS COL 2.4-1

TABLE 2.4.1-209 (Sheet 1 of 3)
 AREA SURFACE WATER INTAKES IN AND DOWNSTREAM FROM THE UPPER BROAD
 RIVER WATERSHED

Facility	County, State	Distance		Source	Withdrawal Capacity		Consumptive Use(f)		Use Type
		mi. ^(a)	Direction		Mgd	cfs	Mgd	cfs	
Gaffney BPW	Cherokee, SC	8	Upstream	Lake Whelchel	12	18.6	NIA	NIA	Public Supply
Gaffney BPW	Cherokee, SC	9	Upstream	Broad River	(b)	(b)	NIA	NIA	Public Supply
CNA Holdings, Inc. – Ticona-Shelby	Cleveland, NC	12	Upstream	Buffalo Creek	1.15	1.78	0.290	0.45	Industrial
Shelby	Cleveland, NC	13	Upstream	Broad River	10 ^(c)	15.5	0	0	Public Supply
Northbrook Carolina Hydro, LLC – Stice Shoals Plant	Cleveland, NC	14	Upstream	First Broad River	(e)	(e)	(e)	(e)	Instream Hydro
Martin Marietta Materials, Inc (Kings Mountain Quarry)	Cleveland, NC	16	Upstream	Storm Water Quarry	0.23	0.36	0	0	Industrial
Kings Mountain	Cleveland, NC	17	Upstream	Moss Lake	37.6	58.3	1.611	2.50	Public Supply
Cleveland County Country Club	Cleveland, NC	18	Upstream	Lake/Pond	1.15	1.79	0.047	0.07	Golf Course
Shelby	Cleveland, NC	19	Upstream	First Broad River	18	28	2.424	4	Public Supply
Duke Energy Corp. – Cliffside Steam Station	Cleveland, NC	19	Upstream	Broad River	288	446	75	116	Industrial
Duke Energy Corp. – Cliffside Steam Station (planned) ^(d)	Cleveland, NC	19	Upstream	Broad River	32	50	20.645	32	Industrial
Cleveland-Caroknit	Cleveland, NC	25	Upstream	First Broad River	1	1.55	0.017	0.03	Industrial

WLS COL 2.4-1

TABLE 2.4.1-209 (Sheet 2 of 3)
 AREA SURFACE WATER INTAKES IN AND DOWNSTREAM FROM THE UPPER BROAD
 RIVER WATERSHED

Facility	County, State	Distance		Source	Withdrawal Capacity		Consumptive Use(f)		Use Type
		mi. ^(a)	Direction		Mgd	cfs	Mgd	cfs	
Mako Marine International (formerly ITG/Burlington Industries – J.C. Cowan Plant)	Rutherford, NC	26	Upstream	Second Broad River	3	4.65	0.07	0.11	Industrial
Cleveland County Sanitary District	Cleveland, NC	27	Upstream	First Broad River	6	9.3	3.364	5.21	Public Supply
Cleveland County Sanitary District (planned)	Cleveland, NC	27	Upstream	Knob Creek	6	9.3	3.445	5.3	Public Supply
Forest City	Rutherford, NC	31	Upstream	Second Broad River	12	18.60	1.483	2.30	Public Supply
Broad River Water Authority (formerly Rutherfordton- Spindale)	Rutherford, NC	33	Upstream	Broad River	13	20.15	4.733	7.34	Public Supply
Northbrook Carolina Hydro, LLC – Turner Shoals Plant	Polk, NC	43	Upstream	Green River	(e)	(e)	(e)	(e)	Instream Hydro
Duke Energy Corp. – Tuxedo Hydro	Henderson, NC	52	Upstream	Lake Summit	(e)	(e)	(e)	(e)	Instream Hydro
Kenmure Country Club	Henderson, NC	54	Upstream	King Creek	0.82	1.26	0.97	1.50	Golf Course
City of Union	Union, SC	21	Downstream	Broad River	23.80	36.89	NIA	NIA	Public Supply
Carlisle Cone Mills	Union, SC	30	Downstream	Broad River	8.10	12.56	NIA	NIA	Public Supply
V.C. Summer Nuclear Station	Fairfield, SC	52	Downstream	Lake Monticello	3.1	4.81	NIA	NIA	Industrial

WLS COL 2.4-1

TABLE 2.4.1-209 (Sheet 3 of 3)
 AREA SURFACE WATER INTAKES IN AND DOWNSTREAM FROM THE UPPER BROAD
 RIVER WATERSHED

Facility	County, State	Distance		Source	Withdrawal Capacity		Consumptive Use(f)		Use Type
		mi.(a)	Direction		Mgd	cfs	Mgd	cfs	
V.C. Summer Nuclear Station (planned)	Fairfield, SC	52	Downstream	Lake Monticello	NIA	NIA	NIA	NIA	Industrial

Notes:

a) Distance provided is a linear distance and not river miles.

b) The Gaffney BPW (Board of Public Works) system is authorized 18 Mgd and uses Lake Whelchel for storage.

c) The Shelby Broad River intake is used as a temporary emergency supply intake.

d) Additional Cliffside Steam Plant use rate is based on anticipated expansion of 1 unit. "Planned" figures include the consumption of the existing Cliffside Unit 5 (15 cfs), and the planned expansion unit (17 cfs)

e) Instream hydro facilities maximum use rate not reported. Instream water use indicates water is returned directly to source. Additional hydro facilities are present within watershed, but no withdrawal permits exist.

f) Consumptive Use based on reported withdrawals and returns from 1999 registration and 2002 LWSP reports.

Source: Reference 268, References 234 - 248, References 262 - 265.

See Figure 2.4.1-211

NIA - No Information Available

Mgd - Million gallons per day

cfs - cubic feet per second

WLS COL 2.4-1

TABLE 2.4.1-210
ESTIMATED SURFACE WATER WITHDRAWAL AND CONSUMPTION FOR LEE NUCLEAR STATION
OPERATIONS

Broad River Flow Rates ^(a)		Average Withdrawal		Maximum Withdrawal	
cfs	gpm	gpm	cfs	gpm	cfs
Mean Annual Flow Approximately 2500 cfs (1926-2008)	1,122,000	35,030	78	60,001	134
Regulatory Low Flow ^(b) (FERC) 483 cfs	216,867	35,030	78	NA	NA

Broad River Flow Rates ^(a)		Average Consumption		Maximum Consumption	
cfs	gpm	gpm	cfs	gpm	cfs
Mean Annual Flow Approximately 2500 cfs (1926-2008)	1,122,000	24,813	55	28,274	63
Regulatory Low Flow ^(b) (FERC) 483 cfs	216,867	24,813	55	NA	NA

gpm - gallons per minute

cfs - cubic feet per second

NA - not applicable

Notes:

- a) Broad River flow rates were compiled from USGS measurements recorded at the Gaffney Gauge (USGS Gauge #02153500), the Blacksburg Gauge (#02153200) and Boiling Springs Gauge (#02151500) for average annual flow.
- b) The 7Q10 for the Gaffney gauge was determined to be 439 cfs using the USGS recommended Log-Pearson Type III distribution. However, because the 7Q10 is less than the Ninety-Nine Islands Dam FERC license minimum flow requirement of 483 cfs for July through November, the FERC license minimum flow was used as a constraint in evaluating operation during low flow conditions.

WLS COL 2.4-1

TABLE 2.4.1-211
ESTIMATED DISCHARGE VOLUME FROM STATION OPERATIONS

BroadRiverFlowRates ^(a)		Average Discharge		Maximum Discharge	
cfs	gpm	gpm	cfs	gpm	cfs
MeanAnnualFlow					
Approximately 2500 cfs (1926-2008)	1,122,000	8,216	18	28,778	64
Regulatory Low Flow ^(b) (FERC)					
483 cfs	216,867	8,216	18	28,778	64

Notes:

- a) Broad River flow rates were compiled from USGS measurements recorded at the Gaffney Gauge (USGS Gauge #02153500), the Blacksburg Gauge (#02153200) and Boiling Springs Gauge (#02151500) for average annual flow.
- b) The 7Q10 for the Gaffney gauge was determined to be 439 cfs using the USGS recommended Log-Pearson Type III distribution. However, because the 7Q10 is less than the Ninety-Nine Islands Dam FERC license minimum flow requirement of 483 cfs for July through November, the FERC license minimum flow was used as a constraint in evaluating operation during low flow conditions.

*Withheld from Public Disclosure Under 10 CFR 2.390(a)(6) & (a)(9)
(see COL Application **Part 9**)*

WLS COL 2.4-4

TABLE 2.4.1-212 (Sheet 1 of 3)
HISTORICAL DOMESTIC WELLS IN VICINITY OF SITE

*Withheld from Public Disclosure Under 10 CFR 2.390(a)(6) & (a)(9)
(see COL Application **Part 9**)*

WLS COL 2.4-4

TABLE 2.4.1-212 (Sheet 2 of 3)
HISTORICAL DOMESTIC WELLS IN VICINITY OF SITE

*Withheld from Public Disclosure Under 10 CFR 2.390(a)(6) & (a)(9)
(see COL Application **Part 9**)*

WLS COL 2.4-4

TABLE 2.4.1-212 (Sheet 3 of 3)
HISTORICAL DOMESTIC WELLS IN VICINITY OF SITE

TABLE 2.4.2-201 (Sheet 1 of 2)
 PEAK STREAMFLOW OF THE BROAD RIVER NEAR
 GAFFNEY, SOUTH CAROLINA
 (USGS STATION 02153500) 1939-1990

WLS COL 2.4-2

Water Year ^(a)	Date	Discharge (cfs)
1939	8/18/1939	21,000
1940	8/14/1940	119,000
1941	7/17/1941	26,000
1942	2/17/1942	21,800
1943	1/28/1943	38,400
1944	3/20/1944	21,700
1945	9/18/1945	61,600
1946	1/7/1946	43,400
1947	6/15/1947	27,800
1948	8/4/1948	25,600
1949	11/29/1948	35,700
1950	10/7/1949	31,000
1951	12/8/1950	23,900
1952	3/4/1952	44,200
1953	2/21/1953	21,900
1954	1/23/1954	41,000
1955	2/7/1955	14,700
1956	4/16/1956	22,400
1957	4/6/1957	23,400
1958	4/28/1958	37,900
1959	9/30/1959	38,600
1960	2/6/1960	37,200
1961	6/22/1961	26,600
1962	12/13/1961	28,400
1963	3/13/1963	41,800
1964	4/8/1964	31,100
1965	10/6/1964	67,100
1966	3/4/1966	32,600

WLS COL 2.4-2

TABLE 2.4.2-201 (Sheet 2 of 2)
 PEAK STREAMFLOW OF THE BROAD RIVER NEAR
 GAFFNEY, SOUTH CAROLINA
 (USGS STATION 02153500) 1939-1990

Water Year ^(a)	Date	Discharge (cfs)
1967	8/24/1967	33,800
1968	3/13/1968	25,900
1969	4/19/1969	25,400
1970	8/10/1970	47,500
1971	10/31/1970	14,300
1972	10/16/1971	46,900
1973	3/17/1973	42,900
1974	4/5/1974	34,400
1975	3/15/1975	55,300
1976	10/18/1975	32,100
1977	10/10/1976	84,900
1978	11/7/1977	38,100
1980	7/21/1980	37,600
1981	10/1/1980	10,500
1982	1/4/1982	33,900
1983	2/3/1983	21,900
1984	2/14/1984	39,900
1985	8/18/1985	26,600
1986	8/18/1986	10,900
1987	3/1/1987	65,800
1988	1/20/1988	8,700
1989	2/28/1989	12,500
1990	10/2/1989	38,800

a) Water Year = October 1 to September 30

Note: Peak streamflow for water year 1979 not available.

(Reference 290)

TABLE 2.4.2-202
PEAK GAUGE HEIGHT OF THE BROAD RIVER BELOW
NINETY-NINE ISLANDS RESERVOIR, SOUTH CAROLINA
(USGS STATION 02153551) 1999-2005

WLS COL 2.4-2	Water Year ^(a)	Date	Gauge Height ^(b) (feet)	Discharge (cfs)
	1999	4/2/1999	30.77	4,350
	2000	3/21/2000	32.91	(c)
	2001	3/30/2001	31.37	(c)
	2002	1/24/2002	30.01	4,490
	2003	3/20/2003	38.22	(c)
	2004	9/9/2004	40.43	(c)
	2005	12/10/2004	35.19	(c)

a) Water Year = October 1 to September 30

b) Datum = 412.2 feet above NGVD29

c) not recorded

(Reference 290)

TABLE 2.4.2-203
LOCAL INTENSE PROBABLE MAXIMUM PRECIPITATION FOR
THE LEE NUCLEAR SITE

WLS COL 2.4-2

	Duration								
	5-min.	15-min.	30-min.	1-hr.	6-hr.	12-hr.	24-hr.	48-hr.	72-hr.
PMP(in.)	6.2	9.7	14	18.9	29.9	35.5	40.4	44.3	46.8

Note: Durations from 5-min. to 1-hr. derived from HMR No. 52, 1-sq. mi. point rainfall. Durations from 6-hr. to 72-hr. derived from HMR No. 51, 10-sq. mi. point rainfall.

TABLE 2.4.2-204
SITE DRAINAGE AREAS DETAILS

WLS COL 2.4-2	Drainage Area	Area Acres (ac)	Flow Rate (cfs)	Maximum Velocity (fps)	Maximum Depth of Flow (ft.)	Maximum Water Surface Elevation (ft.)
	A1	1.62	121	3.51	0.43	592.43
	B1	5.19	389	3.44	0.76	592.56
	C1	2.01	151	1.39	0.53	592.03
	D1	7.93	595	2.05	0.35	592.35
	A2	1.62	121	3.51	0.43	592.43
	B2	5.19	389	3.44	0.76	592.56
	C2	2.01	151	1.39	0.53	592.03
	D2	7.44	558	1.97	0.32	592.32

TABLE 2.4.3-201
BROAD RIVER WATERSHED PMP (IN.)
DEPTH-AREA-DURATION RELATIONSHIP

	Area (sq. mi.)	Duration (hr.)				
		6	12	24	48	72
WLS COL 2.4-2	10	29.7	35.3	40	43.5	46
	200	21.5	25.8	30.1	33.5	36
	1000	15.9	20.7	24.8	28.2	30.1
	5000	9.3	13.1	16.9	20.9	23
	10,000	7.1	10.4	13.9	17.7	19.7
	20,000	5.1	8.4	11.2	14.8	16.8

Note: Values derived from the all-season PMP charts published in HMR-51
([Reference 255](#)).

TABLE 2.4.3-202
BROAD RIVER WATERSHED 6-HR.
INCREMENTAL PMP ESTIMATES

	Duration (hr.)	Incremental PMP (in.)
WLS COL 2.4-2	6	0.38
	12	0.46
	18	0.59
	24	0.83
	30	1.38
	36	4.30
	42	12.80
	48	2.09
	54	1.03
	60	0.69
	66	0.52
	72	0.41
	Total	25.48

Note: Values derived from HMR-51 ([Reference 255](#)), HMR-52 ([Reference 225](#)) and the use of the USACE HMR-52 computer software ([Reference 271](#)). Critical storm was determined to be 1000 sq. mi. with a 270 degree orientation centered near the centroid of the watershed for Gaston Shoals Dam.

WLS COL 2.4-2

TABLE 2.4.3-203 (Sheet 1 of 7)
BROAD RIVER WATERSHED SUBBASIN HOURLY INCREMENTAL PMP ESTIMATES

	Subbasin Hourly Incremental PMP (in.)									
Time (hr.)	LS-1	LA-2	GD-3	LL-4	BR-5	BD3-6	2BR-7	BD2-8	SS-09	WLCHL
Day 1	0.045	0.067	0.069	0.064	0.069	0.066	0.069	0.064	0.067	0.039
0100										
0200	0.045	0.067	0.069	0.064	0.069	0.066	0.069	0.064	0.067	0.039
0300	0.045	0.067	0.069	0.064	0.069	0.066	0.069	0.064	0.067	0.039
0400	0.045	0.067	0.069	0.064	0.069	0.066	0.069	0.064	0.067	0.039
0500	0.045	0.067	0.069	0.064	0.069	0.066	0.069	0.064	0.067	0.039
0600	0.045	0.067	0.069	0.064	0.069	0.066	0.069	0.064	0.067	0.039
0700	0.055	0.082	0.084	0.078	0.084	0.080	0.084	0.078	0.082	0.047
0800	0.055	0.082	0.084	0.078	0.084	0.080	0.084	0.078	0.082	0.047
0900	0.055	0.082	0.084	0.078	0.084	0.080	0.084	0.078	0.082	0.047
1000	0.055	0.082	0.084	0.078	0.084	0.080	0.084	0.078	0.082	0.047
1100	0.055	0.082	0.084	0.078	0.084	0.080	0.084	0.078	0.082	0.047
1200	0.055	0.082	0.084	0.078	0.084	0.080	0.084	0.078	0.082	0.047
1300	0.070	0.106	0.108	0.100	0.108	0.103	0.108	0.101	0.105	0.061
1400	0.070	0.106	0.108	0.100	0.108	0.103	0.108	0.101	0.105	0.061
1500	0.070	0.106	0.108	0.100	0.108	0.103	0.108	0.101	0.105	0.061
1600	0.070	0.106	0.108	0.100	0.108	0.103	0.108	0.101	0.105	0.061
1700	0.070	0.106	0.108	0.100	0.108	0.103	0.108	0.101	0.105	0.061
1800	0.070	0.106	0.108	0.100	0.108	0.103	0.108	0.101	0.105	0.061
1900	0.098	0.148	0.151	0.140	0.151	0.144	0.151	0.141	0.147	0.085
2000	0.098	0.148	0.151	0.140	0.151	0.144	0.151	0.141	0.147	0.085
2100	0.098	0.148	0.151	0.140	0.151	0.144	0.151	0.141	0.147	0.085
2200	0.098	0.148	0.151	0.140	0.151	0.144	0.151	0.141	0.147	0.085
2300	0.098	0.148	0.151	0.140	0.151	0.144	0.151	0.141	0.147	0.085
2400	0.098	0.148	0.151	0.140	0.151	0.144	0.151	0.141	0.147	0.085

WLS COL 2.4-2

TABLE 2.4.3-203 (Sheet 2 of 7)
BROAD RIVER WATERSHED SUBBASIN HOURLY INCREMENTAL PMP ESTIMATES

Time (hr.)	Subbasin Hourly Incremental PMP (in.)									
	LS-1	LA-2	GD-3	LL-4	BR-5	BD3-6	2BR-7	BD2-8	SS-09	WLCHL
Day 2	0.143	0.215	0.220	0.204	0.220	0.210	0.220	0.205	0.215	0.124
0100										
0200	0.149	0.225	0.230	0.213	0.229	0.219	0.229	0.214	0.224	0.129
0300	0.157	0.237	0.242	0.224	0.242	0.231	0.242	0.225	0.236	0.136
0400	0.167	0.251	0.257	0.238	0.256	0.244	0.256	0.239	0.250	0.144
0500	0.178	0.267	0.274	0.253	0.274	0.261	0.274	0.255	0.266	0.154
0600	0.190	0.286	0.293	0.271	0.294	0.279	0.294	0.273	0.285	0.165
0700	0.357	0.542	0.563	0.511	0.576	0.530	0.574	0.520	0.541	0.311
0800	0.411	0.628	0.655	0.591	0.674	0.614	0.670	0.602	0.628	0.361
0900	0.465	0.715	0.750	0.672	0.778	0.700	0.773	0.687	0.715	0.407
1000	0.517	0.803	0.849	0.753	0.889	0.788	0.881	0.775	0.804	0.450
1100	0.567	0.891	0.950	0.834	1.007	0.878	0.995	0.865	0.894	0.489
1200	0.616	0.980	1.054	0.916	1.131	0.971	1.115	0.958	0.985	0.526
1300	0.774	1.272	1.415	1.185	1.594	1.281	1.551	1.275	1.288	0.641
1400	1.040	1.804	2.067	1.667	2.418	1.837	2.332	1.839	1.836	0.838
1500	1.261	2.429	2.821	2.211	3.324	2.462	3.202	2.459	2.473	1.002
1600	1.309	3.994	4.838	3.430	5.757	3.954	5.539	3.908	4.069	1.040
1700	1.182	2.167	2.512	1.987	2.970	2.208	2.858	2.210	2.209	0.942
1800	0.964	1.637	1.865	1.518	2.170	1.665	2.095	1.666	1.665	0.782
1900	0.311	0.471	0.487	0.445	0.497	0.461	0.495	0.452	0.470	0.269
2000	0.279	0.419	0.432	0.397	0.439	0.410	0.438	0.402	0.418	0.242
2100	0.252	0.377	0.387	0.357	0.391	0.368	0.391	0.361	0.376	0.218
2200	0.230	0.343	0.351	0.325	0.354	0.335	0.354	0.328	0.342	0.199
2300	0.213	0.318	0.325	0.302	0.327	0.311	0.327	0.304	0.317	0.185
2400	0.201	0.302	0.309	0.286	0.310	0.295	0.310	0.288	0.301	0.174

WLS COL 2.4-2

TABLE 2.4.3-203 (Sheet 3 of 7)
BROAD RIVER WATERSHED SUBBASIN HOURLY INCREMENTAL PMP ESTIMATES

Time (hr.)	Subbasin Hourly Incremental PMP (in.)									
	LS-1	LA-2	GD-3	LL-4	BR-5	BD3-6	2BR-7	BD2-8	SS-09	WLCHL
Day 3	0.123	0.185	0.189	0.175	0.189	0.180	0.189	0.176	0.184	0.106
0100										
0200	0.123	0.185	0.189	0.175	0.189	0.180	0.189	0.176	0.184	0.106
0300	0.123	0.185	0.189	0.175	0.189	0.180	0.189	0.176	0.184	0.106
0400	0.123	0.185	0.189	0.175	0.189	0.180	0.189	0.176	0.184	0.106
0500	0.123	0.185	0.189	0.175	0.189	0.180	0.189	0.176	0.184	0.106
0600	0.123	0.185	0.189	0.175	0.189	0.180	0.189	0.176	0.184	0.106
0700	0.082	0.123	0.126	0.117	0.126	0.120	0.126	0.117	0.123	0.071
0800	0.082	0.123	0.126	0.117	0.126	0.120	0.126	0.117	0.123	0.071
0900	0.082	0.123	0.126	0.117	0.126	0.120	0.126	0.117	0.123	0.071
1000	0.082	0.123	0.126	0.117	0.126	0.120	0.126	0.117	0.123	0.071
1100	0.082	0.123	0.126	0.117	0.126	0.120	0.126	0.117	0.123	0.071
1200	0.082	0.123	0.126	0.117	0.126	0.120	0.126	0.117	0.123	0.071
1300	0.061	0.092	0.095	0.088	0.095	0.090	0.095	0.088	0.092	0.053
1400	0.061	0.092	0.095	0.088	0.095	0.090	0.095	0.088	0.092	0.053
1500	0.061	0.092	0.095	0.088	0.095	0.090	0.095	0.088	0.092	0.053
1600	0.061	0.092	0.095	0.088	0.095	0.090	0.095	0.088	0.092	0.053
1700	0.061	0.092	0.095	0.088	0.095	0.090	0.095	0.088	0.092	0.053
1800	0.061	0.092	0.095	0.088	0.095	0.090	0.095	0.088	0.092	0.053
1900	0.049	0.074	0.076	0.070	0.076	0.072	0.076	0.071	0.074	0.043
2000	0.049	0.074	0.076	0.070	0.076	0.072	0.076	0.071	0.074	0.043
2100	0.049	0.074	0.076	0.070	0.076	0.072	0.076	0.071	0.074	0.043
2200	0.049	0.074	0.076	0.070	0.076	0.072	0.076	0.071	0.074	0.043
2300	0.049	0.074	0.076	0.070	0.076	0.072	0.076	0.071	0.074	0.043
2400	0.049	0.074	0.076	0.070	0.076	0.072	0.076	0.071	0.074	0.043
Total	15.44	26.84	29.54	24.79	32.51	26.64	31.81	26.33	27.05	12.96

WLS COL 2.4-2

TABLE 2.4.3-203 (Sheet 4 of 7)
BROAD RIVER WATERSHED SUBBASIN HOURLY INCREMENTAL PMP ESTIMATES

Time (hr.)	Subbasin Hourly Incremental PMP (in.)									
	FB-10	GS-11	BD1-12	KMR-13	BC-14	BR-15	CC-16	USS-18A	2BR-19	MUPC
Day 1	0.064	0.046	0.045	0.065	0.052	0.031	0.064	0.064	0.065	0.024
0100										
0200	0.064	0.046	0.045	0.065	0.052	0.031	0.064	0.064	0.065	0.024
0300	0.064	0.046	0.045	0.065	0.052	0.031	0.064	0.064	0.065	0.024
0400	0.064	0.046	0.045	0.065	0.052	0.031	0.064	0.064	0.065	0.024
0500	0.064	0.046	0.045	0.065	0.052	0.031	0.064	0.064	0.065	0.024
0600	0.064	0.046	0.045	0.065	0.052	0.031	0.064	0.064	0.065	0.024
0700	0.078	0.057	0.055	0.079	0.063	0.038	0.078	0.078	0.080	0.029
0800	0.078	0.057	0.055	0.079	0.063	0.038	0.078	0.078	0.080	0.029
0900	0.078	0.057	0.055	0.079	0.063	0.038	0.078	0.078	0.080	0.029
1000	0.078	0.057	0.055	0.079	0.063	0.038	0.078	0.078	0.080	0.029
1100	0.078	0.057	0.055	0.079	0.063	0.038	0.078	0.078	0.080	0.029
1200	0.078	0.057	0.055	0.079	0.063	0.038	0.078	0.078	0.080	0.029
1300	0.100	0.073	0.070	0.102	0.081	0.049	0.101	0.100	0.102	0.038
1400	0.100	0.073	0.070	0.102	0.081	0.049	0.101	0.100	0.102	0.038
1500	0.100	0.073	0.070	0.102	0.081	0.049	0.101	0.100	0.102	0.038
1600	0.100	0.073	0.070	0.102	0.081	0.049	0.101	0.100	0.102	0.038
1700	0.100	0.073	0.070	0.102	0.081	0.049	0.101	0.100	0.102	0.038
1800	0.100	0.073	0.070	0.102	0.081	0.049	0.101	0.100	0.102	0.038
1900	0.140	0.102	0.098	0.142	0.114	0.069	0.141	0.140	0.143	0.053
2000	0.140	0.102	0.098	0.142	0.114	0.069	0.141	0.140	0.143	0.053
2100	0.140	0.102	0.098	0.142	0.114	0.069	0.141	0.140	0.143	0.053
2200	0.140	0.102	0.098	0.142	0.114	0.069	0.141	0.140	0.143	0.053
2300	0.140	0.102	0.098	0.142	0.114	0.069	0.141	0.140	0.143	0.053
2400	0.140	0.102	0.098	0.142	0.114	0.069	0.141	0.140	0.143	0.053

WLS COL 2.4-2

TABLE 2.4.3-203 (Sheet 5 of 7)
BROAD RIVER WATERSHED SUBBASIN HOURLY INCREMENTAL PMP ESTIMATES

Time (hr.)	Subbasin Hourly Incremental PMP (in.)									
	FB-10	GS-11	BD1-12	KMR-13	BC-14	BR-15	CC-16	USS-18A	2BR-19	MUPC
Day 2	0.204	0.148	0.143	0.207	0.165	0.100	0.206	0.204	0.208	0.077
0100										
0200	0.213	0.155	0.149	0.216	0.173	0.105	0.215	0.213	0.217	0.080
0300	0.224	0.163	0.157	0.228	0.182	0.110	0.226	0.224	0.229	0.085
0400	0.238	0.173	0.166	0.241	0.193	0.117	0.239	0.238	0.243	0.090
0500	0.254	0.184	0.178	0.257	0.205	0.124	0.255	0.253	0.259	0.096
0600	0.271	0.198	0.190	0.276	0.220	0.133	0.273	0.271	0.277	0.103
0700	0.511	0.370	0.357	0.516	0.410	0.247	0.514	0.510	0.527	0.181
0800	0.590	0.426	0.411	0.596	0.471	0.285	0.595	0.590	0.611	0.205
0900	0.670	0.481	0.465	0.676	0.533	0.319	0.675	0.670	0.697	0.225
1000	0.750	0.536	0.517	0.756	0.594	0.349	0.757	0.750	0.785	0.243
1100	0.831	0.589	0.567	0.835	0.656	0.376	0.839	0.832	0.876	0.258
1200	0.913	0.641	0.616	0.914	0.718	0.398	0.923	0.913	0.968	0.271
1300	1.180	0.811	0.774	1.171	0.918	0.468	1.196	1.182	1.282	0.309
1400	1.657	1.097	1.040	1.632	1.261	0.589	1.686	1.663	1.843	0.373
1500	2.191	1.335	1.261	2.159	1.572	0.690	2.233	2.198	2.470	0.429
1600	3.354	1.386	1.309	3.310	1.829	0.717	3.439	3.358	3.967	0.445
1700	1.972	1.251	1.182	1.939	1.456	0.652	2.009	1.979	2.216	0.407
1800	1.510	1.017	0.964	1.488	1.162	0.554	1.534	1.515	1.670	0.355
1900	0.445	0.323	0.311	0.450	0.359	0.216	0.448	0.445	0.458	0.162
2000	0.397	0.289	0.279	0.402	0.322	0.195	0.400	0.397	0.408	0.149
2100	0.357	0.261	0.252	0.363	0.291	0.177	0.360	0.357	0.366	0.137
2200	0.326	0.238	0.230	0.331	0.266	0.162	0.328	0.326	0.333	0.126
2300	0.302	0.221	0.213	0.307	0.246	0.150	0.304	0.302	0.308	0.117
2400	0.286	0.209	0.201	0.291	0.233	0.142	0.288	0.286	0.293	0.110

WLS COL 2.4-2

TABLE 2.4.3-203 (Sheet 6 of 7)
BROAD RIVER WATERSHED SUBBASIN HOURLY INCREMENTAL PMP ESTIMATES

Time (hr.)	Subbasin Hourly Incremental PMP (in.)									
	FB-10	GS-11	BD1-12	KMR-13	BC-14	BR-15	CC-16	USS-18A	2BR-19	MUPC
Day 3	0.175	0.127	0.123	0.178	0.142	0.086	0.176	0.175	0.179	0.066
0100										
0200	0.175	0.127	0.123	0.178	0.142	0.086	0.176	0.175	0.179	0.066
0300	0.175	0.127	0.123	0.178	0.142	0.086	0.176	0.175	0.179	0.066
0400	0.175	0.127	0.123	0.178	0.142	0.086	0.176	0.175	0.179	0.066
0500	0.175	0.127	0.123	0.178	0.142	0.086	0.176	0.175	0.179	0.066
0600	0.175	0.127	0.123	0.178	0.142	0.086	0.176	0.175	0.179	0.066
0700	0.117	0.085	0.082	0.119	0.095	0.057	0.118	0.117	0.119	0.044
0800	0.117	0.085	0.082	0.119	0.095	0.057	0.118	0.117	0.119	0.044
0900	0.117	0.085	0.082	0.119	0.095	0.057	0.118	0.117	0.119	0.044
1000	0.117	0.085	0.082	0.119	0.095	0.057	0.118	0.117	0.119	0.044
1100	0.117	0.085	0.082	0.119	0.095	0.057	0.118	0.117	0.119	0.044
1200	0.117	0.085	0.082	0.119	0.095	0.057	0.118	0.117	0.119	0.044
1300	0.088	0.064	0.061	0.089	0.071	0.043	0.088	0.088	0.089	0.033
1400	0.088	0.064	0.061	0.089	0.071	0.043	0.088	0.088	0.089	0.033
1500	0.088	0.064	0.061	0.089	0.071	0.043	0.088	0.088	0.089	0.033
1600	0.088	0.064	0.061	0.089	0.071	0.043	0.088	0.088	0.089	0.033
1700	0.088	0.064	0.061	0.089	0.071	0.043	0.088	0.088	0.089	0.033
1800	0.088	0.064	0.061	0.089	0.071	0.043	0.088	0.088	0.089	0.033
1900	0.070	0.051	0.049	0.071	0.057	0.034	0.071	0.070	0.072	0.026
2000	0.070	0.051	0.049	0.071	0.057	0.034	0.071	0.070	0.072	0.026
2100	0.070	0.051	0.049	0.071	0.057	0.034	0.071	0.070	0.072	0.026
2200	0.070	0.051	0.049	0.071	0.057	0.034	0.071	0.070	0.072	0.026
2300	0.070	0.051	0.049	0.071	0.057	0.034	0.071	0.070	0.072	0.026
2400	0.070	0.051	0.049	0.071	0.057	0.034	0.071	0.070	0.072	0.026
Total	24.64	16.14	15.44	24.63	18.48	9.82	24.96	24.67	26.60	6.91

WLS COL 2.4-2

TABLE 2.4.3-203 (Sheet 7 of 7)
BROAD RIVER WATERSHED SUBBASIN HOURLY INCREMENTAL PMP ESTIMATES

	Subbasin Hourly Incremental PMP (in.)
Notes:	
Reference Figure 2.4.3-203 for subbasin locations	
LS-1, Lake Summit/Tuxedo Hydro	
LA-2, Lake Adger/Turner Shoals	
GD-3, Green River (Turner Shoals to Broad R.)	
LL-4, Lake Lure/hydro	
BR-5, Broad River (Lake Lure to Green R.)	
BD3-6, Broad River (Green R. to Second Broad R.)	
2BR-7, Second Broad River	
BD2-8, Broad River (Second Broad R. to First Broad R.)	
SS-09, Stice Shoals	
FB-10, First Broad River (Stice Shoals to Broad R.)	
GS-11, Broad River (First Broad to Gaston Shoals)	
BD1-12, Broad River (Gaston Shoals to Buffalo Creek)	
KMR-13, Kings Mountain Reservoir (Buffalo Cr.)	
BC-14, Buffalo Creek (Kings Mountain Reservoir to Broad R.)	
BR-15, Broad River (Buffalo Cr. to Ninety-Nine Islands)	
CC-16, Cove Creek (Broad R. near Lake Lure)	
USS-18A, Upper First Broad River	
2BR-19, Upper Second Broad River	
MUPC, Make-Up Pond C	
WLCHL, Lake Wheelchel	

TABLE 2.4.3-204 (Sheet 1 of 2)
BROAD RIVER WATERSHED SUBBASIN PRECIPITATION LOSSES

WLS COL 2.4-2	Subbasin	CN	Initial Losses (in.)	Antecedent Precipitation			PMP Precipitation		
				Depth (in.)	Losses (in.)	Excess (in.)	Depth (in.)	Losses (in.)	Excess (in.)
	LS-1	55	1.64	6.18	4.51	1.66	15.44	2.86	12.57
	LA-2	56	1.57	10.73	5.76	4.97	26.84	2.21	24.63
	GD-3	60	1.33	11.81	5.41	6.40	29.54	1.64	27.89
	LL-4	56	1.57	9.92	5.55	4.37	24.79	2.28	22.50
	BR-5	58	1.45	13.01	5.90	7.11	32.51	1.77	30.74
	BD3-6	64	1.13	10.66	4.67	5.99	16.64	1.33	25.31
	2BR-7	60	1.33	12.72	5.54	7.18	31.81	1.57	30.23
	BD2-8	66	1.03	10.53	4.35	6.17	26.33	1.16	25.16
	SS-09	68	0.94	10.82	4.13	6.69	27.05	0.99	26.06
	FB-10	71	0.82	9.86	3.63	6.23	24.64	0.83	23.81
	GS-11	65	1.08	6.46	3.70	2.76	16.14	1.58	14.54
	BD1-12	67	0.99	6.18	3.45	2.73	15.44	1.42	14.01
	KMR-13	68	0.94	9.85	3.95	5.90	24.63	1.03	23.60
	BC-14	67	0.99	7.39	3.70	3.69	18.48	1.30	17.18
	BR-15	65	1.08	3.93	2.89	1.03	9.82	1.88	7.93
	CC-16	56	1.57	9.99	5.63	4.35	24.96	2.30	22.67
	USS-18A	56	1.57	9.87	5.61	4.26	24.67	2.31	22.36
	2BR-19	56	1.57	10.64	5.78	4.86	26.60	2.23	24.37
	MUPC	63.9	1.13	2.76	1.74	1.03	6.91	1.54	5.37
	WLCHL	63.7	1.14	5.18	3.42	1.77	12.96	1.86	11.10

TABLE 2.4.3-204 (Sheet 2 of 2)
BROAD RIVER WATERSHED SUBBASIN PRECIPITATION LOSSES

Notes:

Reference [Figure 2.4.3-203](#) for subbasin locations

LS-1, Lake Summit/Tuxedo Hydro

LA-2, Lake Adger/Turner Shoals

GD-3, Green River (Turner Shoals to Broad R.)

LL-4, Lake Lure/hydro

BR-5, Broad River (Lake Lure to Green R.)

BD3-6, Broad River (Green R. to Second Broad R.)

2BR-7, Second Broad River

BD2-8, Broad River (Second Broad R. to First Broad R.)

SS-09, Stice Shoals

FB-10, First Broad River (Stice Shoals to Broad R.)

GS-11, Broad River (First Broad to Gaston Shoals)

BD1-12, Broad River (Gaston Shoals to Buffalo Creek)

KMR-13, Kings Mountain Reservoir (Buffalo Cr.)

BC-14, Buffalo Creek (Kings Mountain Reservoir to Broad R.)

BR-15, Broad River (Buffalo Cr. to Ninety-Nine Islands)

CC-16, Cove Creek (Broad R. near Lake Lure)

USS-18A, Upper First Broad River

2BR-19, Upper Second Broad River

MUPC, Make-Up Pond C

WLCHL, Lake Whelchel

WLS COL 2.4-2

TABLE 2.4.3-205 (Sheet 1 of 7)
BROAD RIVER WATERSHED SUBBASIN UNIT HYDROGRAPHS

Time (hr.)	Subbasin Unit Hydrograph Discharge (cfs)								
	LS-1	LA-2	GD-3	LL-4	BR-5	BD3-6	2BR-7	BD2-8	SS-09
1	389	377	2	402	2	1	1	1	1
2	1597	2058	33	2055	33	22	24	32	12
3	2660	3601	144	3596	144	134	108	140	56
4	2883	4806	353	4799	352	380	270	364	156
5	2700	5306	660	5296	660	768	581	719	329
6	2400	4940	1051	5000	1050	1217	943	1140	589
7	2126	4490	1501	4500	1500	1729	1374	1712	941
8	1881	4138	1982	4086	1981	2272	1852	2254	1304
9	1652	3795	2470	3745	2469	2818	2354	2800	1705
10	1453	3437	2940	3390	2939	3163	2860	3147	2130
11	1271	3092	3276	3084	3275	3295	3350	3314	2565
12	1096	2805	3364	2798	3366	3200	3598	3250	3000
13	934	2515	3300	2508	3300	3080	3693	3110	3422
14	788	2232	3200	2225	3200	2950	3610	2950	3822
15	659	1964	3080	1958	3080	2800	3500	2825	4193
16	547	1715	2930	1709	2930	2670	3350	2700	4282
17	451	1488	2780	1483	2780	2560	3200	2600	4200
18	370	1283	2640	1279	2650	2439	3050	2457	4090
19	302	1101	2504	1097	2506	2327	2920	2349	3960
20	245	941	2379	937	2353	2197	2800	2220	3830
21	198	800	2238	797	2213	2079	2693	2105	3700
22	159	678	2087	675	2089	1976	2567	2003	3560
23	128	573	1954	570	1981	1864	2455	1893	3440
24	102	482	1816	480	1866	1747	2332	1777	3330
25	82	405	1700	403	1747	1627	2201	1657	3196
26	65	339	1603	337	1626	1507	2091	1537	3093
27	52	283	1504	282	1506	1389	1977	1438	2976
28	41	236	1404	235	1407	1291	1884	1338	2849
29	32	196	1306	195	1308	1194	1788	1240	2747
30	26	163	1209	162	1211	1101	1690	1145	2638
31	20	135	1116	134	1118	1011	1591	1053	2523

WLS COL 2.4-2

TABLE 2.4.3-205 (Sheet 2 of 7)
BROAD RIVER WATERSHED SUBBASIN UNIT HYDROGRAPHS

Time (hr.)	Subbasin Unit Hydrograph Discharge (cfs)								
	LS-1	LA-2	GD-3	LL-4	BR-5	BD3-6	2BR-7	BD2-8	SS-09
32	16	112	1026	111	1028	925	1493	965	2404
33	12	92	940	92	942	843	1396	881	2312
34	10	76	859	76	860	766	1301	802	2217
35	8	63	782	62	784	695	1209	728	2119
36	6	52	710	51	712	628	1121	659	2020
37	5	42	643	42	645	566	1036	595	1921
38	4	35	581	35	575	509	956	536	1822
39	3	28	524	28	519	457	880	482	1724
40	2	23	472	23	467	409	807	432	1627
41	2	19	423	19	419	365	740	387	1533
42	1	16	379	15	375	326	676	345	1442
43	1	13	339	13	336	290	617	308	1353
44	1	10	303	10	300	258	562	274	1268
45	1	8	270	8	267	228	511	243	1185
46	0	7	240	7	238	202	464	216	1107
47	0	6	213	6	211	179	421	191	1032
48	0	5	189	5	187	158	381	169	960
49	0	4	167	4	166	139	344	149	892
50	0	3	148	3	147	122	311	131	828
51	0	2	131	2	130	108	280	116	768
52	0	2	115	2	114	94	252	102	711
53	0	2	102	2	101	83	227	89	657
54	0	1	89	1	89	72	203	78	607
55	0	1	79	1	78	63	182	68	560
56	0	1	69	1	68	55	163	60	516
57	0	1	60	1	60	48	146	52	475
58	0	1	53	1	53	42	131	46	436
59	0	0	46	0	46	37	117	40	401
60	0	0	41	0	40	32	104	35	368
61	0	0	35	0	35	28	93	30	337
62	0	0	31	0	31	24	83	26	309

WLS COL 2.4-2

TABLE 2.4.3-205 (Sheet 3 of 7)
BROAD RIVER WATERSHED SUBBASIN UNIT HYDROGRAPHS

Time (hr.)	Subbasin Unit Hydrograph Discharge (cfs)								
	LS-1	LA-2	GD-3	LL-4	BR-5	BD3-6	2BR-7	BD2-8	SS-09
63	0	0	27	0	27	21	74	23	283
64	0	0	23	0	23	18	65	20	258
65	0	0	20	0	20	16	58	17	236
66	0	0	18	0	18	14	52	15	216
67	0	0	15	0	15	12	46	13	197
68	0	0	13	0	13	10	41	11	179
69	0	0	12	0	12	9	36	10	163
70	0	0	10	0	10	8	32	8	149
71	0	0	9	0	9	7	28	7	135
72	0	0	8	0	8	6	25	6	123
73	0	0	7	0	7	5	22	5	112
74	0	0	6	0	6	4	19	5	101
75	0	0	5	0	5	4	17	4	92
76	0	0	4	0	4	3	15	3	83
77	0	0	4	0	4	3	13	3	76
78	0	0	3	0	3	2	12	3	68
79	0	0	3	0	3	2	10	2	62
80	0	0	2	0	2	2	9	2	56
81	0	0	2	0	2	1	8	2	51
82	0	0	2	0	2	1	7	1	46
83	0	0	2	0	1	1	6	1	41
84	0	0	1	0	1	1	5	1	37
85	0	0	1	0	1	1	5	1	34
86	0	0	1	0	1	1	4	1	30
87	0	0	1	0	1	1	4	1	27
88	0	0	1	0	1	1	3	1	25
89	0	0	1	0	1	0	3	0	22
90	0	0	0	0	0	0	0	0	0

WLS COL 2.4-2

TABLE 2.4.3-205 (Sheet 4 of 7)
BROAD RIVER WATERSHED SUBBASIN UNIT HYDROGRAPHS

Time (hr.)	Subbasin Unit Hydrograph Discharge (cfs)									
	FB- 10	GS- 11	BD1- 12	KMR -13	BC- 14	BR- 15	CC-16	USS- 18A	2BR- 19	WLCHL
1	5	12	18	2	2	7	339	392	358	55
2	103	154	224	45	34	94	1754	1862	1723	566
3	366	521	701	203	142	346	3273	3826	3509	1125
4	772	1041	1290	536	347	800	4323	5139	4670	1366
5	1243	1679	1481	1008	651	1409	4625	5785	5112	1230
6	1814	1823	1400	1606	1037	2104	4360	5530	4840	1050
7	2070	1695	1220	2175	1483	2270	3950	5080	4430	886
8	1970	1540	1039	2581	2021	2170	3568	4684	4059	736
9	1810	1390	852	2747	2522	2020	3203	4237	3715	606
10	1640	1248	698	2710	3008	1870	2870	3865	3321	482
11	1496	1108	549	2580	3301	1730	2554	3500	2979	376
12	1366	965	430	2420	3392	1595	2292	3159	2634	284
13	1245	829	338	2260	3320	1489	2034	2851	2354	213
14	1123	707	261	2110	3180	1359	1786	2547	2084	156
15	996	600	197	1974	3020	1249	1555	2255	1828	112
16	879	501	147	1838	2870	1129	1344	1982	1592	80
17	766	412	108	1705	2730	1007	1153	1731	1377	56
18	660	336	78	1581	2580	899	984	1503	1185	38
19	562	270	56	1469	2444	794	836	1298	1014	26
20	474	215	40	1351	2324	695	707	1116	863	18
21	396	170	28	1232	2214	603	595	956	732	12
22	329	134	20	1129	2092	519	499	815	619	8
23	271	104	14	1028	1987	443	417	693	521	5
24	222	80	9	930	1875	376	347	587	438	3
25	181	62	6	836	1781	318	288	496	366	2
26	146	47	4	747	1682	267	239	418	306	1
27	118	36	3	665	1581	223	198	352	255	1
28	94	27	2	589	1479	185	163	295	212	1
29	75	21	1	519	1378	153	134	247	176	0
30	60	15	1	456	1278	126	110	206	145	0
31	47	12	1	399	1181	104	90	172	120	0

WLS COL 2.4-2

TABLE 2.4.3-205 (Sheet 5 of 7)
BROAD RIVER WATERSHED SUBBASIN UNIT HYDROGRAPHS

Time (hr.)	Subbasin Unit Hydrograph Discharge (cfs)									
	FB- 10	GS- 11	BD1- 12	KMR -13	BC- 14	BR- 15	CC-16	USS- 18A	2BR- 19	WLCHL
32	37	9	0	347	1088	85	74	143	99	0
33	29	6	0	302	999	69	60	119	82	0
34	23	5	0	261	914	56	49	99	67	0
35	18	4	0	226	834	46	40	82	55	0
36	14	3	0	194	759	37	33	68	45	0
37	11	2	0	167	689	30	27	56	37	0
38	8	1	0	143	623	24	22	46	30	0
39	7	1	0	122	563	19	17	38	25	0
40	5	1	0	104	507	15	14	31	20	0
41	4	1	0	89	456	12	11	26	16	0
42	3	0	0	75	410	10	9	21	13	0
43	2	0	0	64	367	8	7	18	11	0
44	2	0	0	54	328	6	6	14	9	0
45	1	0	0	46	293	5	5	12	7	0
46	1	0	0	39	261	4	4	10	6	0
47	1	0	0	33	232	3	3	8	5	0
48	1	0	0	27	206	2	3	6	4	0
49	0	0	0	23	183	2	2	5	3	0
50	0	0	0	19	162	2	2	4	3	0
51	0	0	0	16	143	1	1	4	2	0
52	0	0	0	13	127	1	1	3	2	0
53	0	0	0	11	112	1	1	2	1	0
54	0	0	0	9	99	1	1	2	1	0
55	0	0	0	8	87	0	1	2	1	0
56	0	0	0	7	76	0	0	1	1	0
57	0	0	0	5	67	0	0	1	1	0
58	0	0	0	4	59	0	0	1	0	0
59	0	0	0	4	52	0	0	1	0	0
60	0	0	0	3	45	0	0	1	0	0
61	0	0	0	3	40	0	0	0	0	0
62	0	0	0	2	35	0	0	0	0	0

WLS COL 2.4-2

TABLE 2.4.3-205 (Sheet 6 of 7)
BROAD RIVER WATERSHED SUBBASIN UNIT HYDROGRAPHS

Time (hr.)	Subbasin Unit Hydrograph Discharge (cfs)									
	FB- 10	GS- 11	BD1- 12	KMR -13	BC- 14	BR- 15	CC-16	USS- 18A	2BR- 19	WLCHL
63	0	0	0	2	30	0	0	0	0	0
64	0	0	0	1	26	0	0	0	0	0
65	0	0	0	1	23	0	0	0	0	0
66	0	0	0	1	20	0	0	0	0	0
67	0	0	0	1	17	0	0	0	0	0
68	0	0	0	1	15	0	0	0	0	0
69	0	0	0	1	13	0	0	0	0	0
70	0	0	0	0	11	0	0	0	0	0
71	0	0	0	0	10	0	0	0	0	0
72	0	0	0	0	9	0	0	0	0	0
73	0	0	0	0	7	0	0	0	0	0
74	0	0	0	0	6	0	0	0	0	0
75	0	0	0	0	6	0	0	0	0	0
76	0	0	0	0	5	0	0	0	0	0
77	0	0	0	0	4	0	0	0	0	0
78	0	0	0	0	4	0	0	0	0	0
79	0	0	0	0	3	0	0	0	0	0
80	0	0	0	0	3	0	0	0	0	0
81	0	0	0	0	2	0	0	0	0	0
82	0	<u>e</u>	0	0	2	0	0	0	0	0
83	0	0	0	0	2	0	0	0	0	0
84	0	0	0	0	2	0	0	0	0	0
85	0	0	0	0	1	0	0	0	0	0
86	0	0	0	0	1	0	0	0	0	0
87	0	0	0	0	1	0	0	0	<u>e</u>	0
88	0	0	0	0	1	0	0	0	0	0
89	0	0	0	0	1	0	0	0	0	0
90	0	0	0	0	0	0	0	0	0	0

TABLE 2.4.3-205 (Sheet 7 of 7)
WLS COL 2.4-2 BROAD RIVER WATERSHED SUBBASIN UNIT HYDROGRAPHS

Notes:

Reference [Figure 2.4.3-203](#) for subbasin locations

LS-1, Lake Summit/Tuxedo Hydro

LA-2, Lake Adger/Turner Shoals

GD-3, Green River (Turner Shoals to Broad R.)

LL-4, Lake Lure/hydro

BR-5, Broad River (Lake Lure to Green R.)

BD3-6, Broad River (Green R. to Second Broad R.)

2BR-7, Second Broad River

BD2-8, Broad River (Second Broad R. to First Broad R.)

SS-09, Stice Shoals

FB-10, First Broad River (Stice Shoals to Broad R.)

GS-11, Broad River (First Broad to Gaston Shoals)

BD1-12, Broad River (Gaston Shoals to Buffalo Creek)

KMR-13, Kings Mountain Reservoir (Buffalo Cr.)

BC-14, Buffalo Creek (Kings Mountain Reservoir to Broad R.)

BR-15, Broad River (Buffalo Cr. to Ninety-Nine Islands)

CC-16, Cove Creek (Broad R. near Lake Lure)

USS-18A, Upper First Broad River

2BR-19, Upper Second Broad River

WLCHL, Lake Wheelchel

TABLE 2.4.3-206 (Sheet 1 of 2)
BROAD RIVER WATERSHED SUBBASIN INPUT PARAMETERS

	Subbasin	Area (sq. mi.)	Base Flow (Recession Method), Recession Constant, k = 0.4919		Loss Rates (SCS Method)	
			Initial Discharge per Area (cfs / sq. mi.)	Recession Threshold (cfs)	Curve Number CN	% Impervious Area
WLS COL 2.4-2	LS-1	42.4	1.62	254	55	0.91
	LA-2	94.5	1.64	567	56	0.63
	GD-3	106.6	1.64	640	60	0.01
	LL-4	94.3	1.64	566	56	1.18
	BR-5	106.7	1.64	640	58	0
	BD3-6	101.8	1.64	611	64	0
	2BR-7	131	1.65	786	60	0
	BD2-8	103.3	1.64	620	66	0.45
	SS-09	182	1.66	1092	68	0
	FB-10	36.4	1.61	218	71	0
	GS-11	27.6	1.61	166	65	1.7
	BD1-12	17.38	1.59	102	67	1.7
	KMR-13	67.97	1.63	408	68	1.7
	BC-14	108.44	1.64	648	67	1.7
	BR-15	44.61	1.63	378	65	1.7
	CC-16	79	1.64	474	56	0
	USS-18A	106	1.64	636	56	0
	2BR-19	90	1.64	540	56	0
	MUPC	3.87	1.63	23	63.9	27.8
	WLCHL	14.71	1.63	88	63.7	2.5

TABLE 2.4.3-206 (Sheet 2 of 2)
BROAD RIVER WATERSHED SUBBASIN INPUT PARAMETERS

Notes:

Reference **Figure 2.4.3-203** for subbasin locations

LS-1, Lake Summit/Tuxedo Hydro

LA-2, Lake Adger/Turner Shoals

GD-3, Green River (Turner Shoals to Broad R.)

LL-4, Lake Lure/hydro

BR-5, Broad River (Lake Lure to Green R.)

BD3-6, Broad River (Green R. to Second Broad R.)

2BR-7, Second Broad River

BD2-8, Broad River (Second Broad R. to First Broad R.)

SS-09, Stice Shoals

FB-10, First Broad River (Stice Shoals to Broad R.)

GS-11, Broad River (First Broad to Gaston Shoals)

BD1-12, Broad River (Gaston Shoals to Buffalo Creek)

KMR-13, Kings Mountain Reservoir (Buffalo Cr.)

BC-14, Buffalo Creek (Kings Mountain Reservoir to Broad R.)

BR-15, Broad River (Buffalo Cr. to Ninety-Nine Islands)

CC-16, Cove Creek (Broad R. near Lake Lure)

USS-18A, Upper First Broad River

2BR-19, Upper Second Broad River

MUPC, Make-Up Pond C

WLCHL, Lake Whelchel

TABLE 2.4.3-207
MAKE-UP POND C SUBBASIN UNIT HYDROGRAPH

Time (min.)	Discharge (cfs)	Time (min.)	Discharge (cfs)	Time (min.)	Discharge (cfs)
10	124	150	333	290	21
20	380	160	273	300	17
30	843	170	227	310	14
40	1472	180	187	320	12
50	1641	190	154	330	10
60	1590	200	125	340	8
70	1410	210	103	350	7
80	1240	220	85	360	6
90	1083	230	69	370	4
100	942	240	57	380	3
110	794	250	46	390	2
120	660	260	38	400	1
130	533	270	31	410	0
140	419	280	26	420	0

Notes:

Reference [Figure 2.4.3-203](#) for subbasin locations
MUPC, Make-Up Pond C

TABLE 2.4.3-208
MAKE-UP POND B SUBBASIN UNIT HYDROGRAPH

Time (min.)	Discharge (cfs)	Time (min.)	Discharge (cfs)	Time (min.)	Discharge (cfs)
10	71.40	150	185.95	290	10.68
20	219.10	160	151.78	300	8.75
30	486.11	170	126.44	310	7.03
40	814.45	180	103.97	320	5.88
50	935.26	190	85.35	330	4.90
60	915.00	200	69.31	340	4.21
70	820.00	210	56.89	350	3.52
80	715.00	220	46.90	360	2.36
90	616.17	230	37.97	370	1.82
100	533.18	240	31.14	380	1.34
110	448.23	250	23.48	390	0.86
120	370.44	260	19.19	400	0.38
130	296.71	270	15.91	410	0.00
140	234.48	280	12.97		

TABLE 2.4.3-209
UPPER ARM SUBBASIN UNIT HYDROGRAPH

Time (min.)	Discharge (cfs)	Time (min.)	Discharge (cfs)	Time (min.)	Discharge (cfs)
2	36.65	32	120.53	62	7.39
4	115.29	34	99.59	64	6.13
6	221.30	36	83.78	66	5.00
8	368.06	38	69.99	68	4.22
10	555.70	40	58.29	70	3.52
12	588.82	42	47.42	72	3.08
14	570.00	44	39.87	74	2.62
16	520.00	46	33.02	76	2.16
18	456.33	48	27.36	78	1.71
20	395.86	50	22.66	80	1.32
22	334.32	52	18.49	82	0.94
24	277.50	54	15.53	84	0.57
26	228.85	56	12.82	86	0.19
28	183.74	58	10.74	88	0.00
30	147.85	60	8.90		

TABLE 2.4.4-201
PEAK FLOWS AND RESULTING WATER SURFACE ELEVATIONS

WLS COL 2.4-2

Event	Model	Peak Flow (cfs)	Lee Nuclear Station	Ninety-Nine Islands Dam
			Water Surface Elevation (ft.)	
PMF (no breach)	HEC-HMS	802,000	(a)	542.78
PMF (no breach)	HEC-RAS (unsteady state)	823,000	551.49	546.06
PMF (no breach)	HEC-RAS (steady state)	823,000	552.61	546.06
Gaston Shoals Dam failure coincident with the PMF	HEC-RAS (unsteady state)	824,000	551.52	546.09
Gaston Shoals Dam and Cherokee Falls Dam failures coincident with the PMF	HEC-RAS (unsteady state)	824,000	551.52	546.09
Major upstream structures failures coincident with the PMF ^(b)	HEC-HMS	1,850,000	(a)	560.10
Major upstream structures failures coincident with the PMF ^(b)	HEC-RAS (steady state)	1,850,000	576.50	564.93

a) Not calculated. Resulting hydrographs or peak flow used as input to the HEC-RAS model to determine the water surface elevations at the Lee Nuclear Station.

b) Upstream failures include overtopping failure of Lake Lure Dam, Tuxedo Dam, Turner Shoals Dam, Kings Mountain Reservoir Dam, Lake Whelchel, Lake Cherokee, and Make-Up Pond C. All failures occur simultaneously with a failure time near to the peak PMF outflow at Ninety-Nine Islands Dam.

WLS SUP 2.4.7-1

TABLE 2.4.7-201 (Sheet 1 of 2)
WATER TEMPERATURE DATA FOR THE BROAD RIVER NEAR
GAFFNEY, SOUTH CAROLINA
(USGS STATION 02153500)

SAMPLE DATE	°F
8/26/1969	75.0
9/24/1969	68.7
10/22/1969	65.8
11/17/1969	44.6
12/15/1969	44.1
1/11/1970	43.7
1/20/1970	42.6
2/19/1970	52.2
3/20/1970	53.4
4/27/1970	65.1
5/21/1970	76.1
6/16/1970	77.4
7/7/1970	83.1
8/18/1970	78.4
9/15/1970	80.6
10/15/1970	73.0
11/20/1970	52.7
12/21/1970	48.2
1/11/1971	43.7
2/22/1971	54.5
3/23/1971	53.6
4/19/1971	66.2
5/10/1971	69.8
6/14/1971	77.9
7/8/1971	76.1
8/24/1971	78.8
9/13/1971	76.1
10/4/1971	75.2

WLS SUP 2.4.7-1 TABLE 2.4.7-201 (Sheet 2 of 2)
WATER TEMPERATURE DATA FOR THE BROAD RIVER NEAR
GAFFNEY, SOUTH CAROLINA
(USGS STATION 02153500)

SAMPLE DATE	°F
11/22/1971	45.5
12/9/1971	49.1
1/19/1972	42.8
2/9/1972	41.9
3/24/1972	50
4/20/1972	68.9
5/22/1972	67.1
6/13/1972	72.5
7/25/1972	83.3
8/24/1972	79.7
10/2/1972	64.4
10/25/1972	62.6
11/16/1972	51.8
12/29/1972	46.4
1/23/1973	50.9
2/8/1973	48.2
3/20/1973	53.6
4/25/1973	64.4
5/30/1973	69.8
6/21/1973	71.6
Min T, 2/9/1972	41.9
Max T, 7/25/1972	83.3

(Reference 290)

WLS SUP 2.4.11-1

TABLE 2.4.11-201
 MINIMUM DAILY STREAMFLOW OBSERVED ON THE BROAD
 RIVER BELOW NINETY-NINE ISLANDS DAM,
 SOUTH CAROLINA, (USGS STATION 02153551)
 1998-2006

Climatic Year ^(a)	Date	Minimum Flow, cfs
1998 ^(b)	11/2/1998	805
1999	9/18/1999	233
2000	9/16/2000	342
2001	9/14/2001	224
2002	9/14/2002	138
2003	9/21/2003	1,230
2004	8/18/2004	605
2005	11/7/2005	851
2006 ^(b)	7/12/2006	534

a) Climatic Year – April 1 to March 31

b) Year 1998 incomplete, available data 10/30/1998 – 3/31/1999
 Year 2006 incomplete, available data 4/1/2006 – 9/30/2006

(Reference 290)

WLS SUP 2.4.11-1

TABLE 2.4.11-202 (Sheet 1 of 2)
 MINIMUM DAILY STREAMFLOW OBSERVED ON THE BROAD
 RIVER NEAR GAFFNEY, SOUTH CAROLINA,
 (USGS STATION 02153500) 1938-1990

Climatic Year ^(a)	Date	Minimum Flow, cfs
1938 ^(b)	12/24/1938	985
1939	10/22/1939	586
1940	7/2/1940	443
1941	10/14/1941	466
1942	7/21/1942	659
1943	9/27/1943	699
1944	9/10/1944	730
1945	9/3/1945	743
1946	10/7/1946	811
1947	9/22/1947	657
1948	7/6/1948	845
1949	7/5/1949	1,260
1950	10/16/1950	991
1951	10/21/1951	598
1952	7/29/1952	746
1953	8/30/1953	466
1954	10/24/1954	224
1955	9/20/1955	444
1956	9/3/1956	300
1957	9/8/1957	381
1958	12/7/1958	867
1959	8/24/1959	986
1960	9/26/1960	1,050
1961	10/10/1961	908
1962	9/3/1962	947
1963	8/19/1963	651
1964	9/28/1964	942
1965	9/19/1965	916

WLS SUP 2.4.11-1

TABLE 2.4.11-202 (Sheet 2 of 2)
 MINIMUM DAILY STREAMFLOW OBSERVED ON THE BROAD
 RIVER NEAR GAFFNEY, SOUTH CAROLINA,
 (USGS STATION 02153500) 1938-1990

Climatic Year ^(a)	Date	Minimum Flow, cfs
1966	9/11/1966	682
1967	8/20/1967	874
1968	9/4/1968	468
1969	7/21/1969	1,140
1970	7/21/1970	836
1971 ^(b)	7/19/1971 & 9/16/1971	1,270
1986 ^(b)	7/15/1986	261
1987	10/11/1987	560
1988	7/29/1988	300
1989	8/11/1989	656
1990 ^(b)	9/28/1990	1,030

a) Climatic Year – April 1 to March 31

b) Year 1938 incomplete, available data 12/1/1938 - 3/31/1939

Year 1971 incomplete, available data 4/1/1971 - 9/30/1971

No data available from 9/30/1971 - 6/9/1986

Year 1986 incomplete, available data 6/9/1986 - 3/31/1987

Year 1990 incomplete, available data 4/1/1990 - 9/30/1990

(Reference 290)

TABLE 2.4.11-203
100-YR. RETURN PERIOD LOW FLOW RATES^(a)

		Duration, days		
		1	7	30
WLS SUP 2.4.11-1	Flow Rate, cfs	172	269	346

- a) Low flow based on statistical analysis of combined data for USGS gauges on the Broad River near Gaffney, South Carolina (USGS No. 02153500 climatic years from 1938 to 1990) and below Ninety-Nine Islands Dam (USGS No. 02153551 climatic years from 1998 to 2002).

WLS COL 2.4-4

TABLE 2.4.12-201 (Sheet 1 of 4)
WELL CONSTRUCTION AND WATER TABLE ELEVATIONS (FT ABOVE MSL)

Well I.D.	Reference Elevations		Well Construction Depths						Material	Additional Info	
	GL Elev	TOC Elev	Boring Depth	TD from TOC	B/Screen	T/Screen	T/Sand	T/Seal		DTW WD	Date Plugged
MW-1200	591.93	593.99	41	41.93	40	25	23	20	2-inch PVC Sch40	23.0	NA
MW-1201	589.91	592.12	102.5	103.81	101.5	86.5	84.5	82.5	2-inch PVC Sch40	37.0	NA
MW-1201A	590.07	592.11	48	49.78	47	37	36	34	2-inch PVC Sch40	37.0	NA
MW-1202	587.47	589.68	78.5	79.82	77.5	62.5	58	55	2-inch PVC Sch40	20.6	NA
MW-1203	589.51	591.87	77	77.67	75	60	58	55	2-inch PVC Sch40	22.5	NA
MW-1204	609.92	612.42	115	116.59	114	99	97	95	2-inch PVC Sch40	37.1	NA
MW-1204A	609.93	612.42	50	51.82	49	39	37	35	2-inch PVC Sch40	37.1	NA
MW-1205	609.99	612.59	124	125.33	123	108	106	104	2-inch PVC Sch40	43.9	NA
MW-1206	589.66	591.51	68.5	69.89	67.5	52.5	50	47.5	2-inch PVC Sch40	31.7	NA
MW-1206A	589.75	591.43	43	44.09	42	32	31	29	2-inch PVC Sch40	31.7	NA
MW-1207	589.03	591.39	108	110.02	107	92	90	88	2-inch PVC Sch40	29.2	NA
MW-1207A	588.91	591.05	43	44.68	42	32	31	29	2-inch PVC Sch40	29.2	NA
MW-1208	587.77	590.00	79	78.92	76.5	61.5	59	56	2-inch PVC Sch40	47.0	NA
MW-1209	586.91	588.91	106	106.28	104	89	87	84.6	2-inch PVC Sch40	16.3	NA
MW-1209A	586.93	589.03	28	29.45	27	17	16	14	2-inch PVC Sch40	16.3	NA
MW-1210	589.78	592.27	101.5	103.10	101.5	86.5	84.5	82.5	2-inch PVC Sch40	16.5	NA
MW-1210A	589.42	591.66	30	32.06	29	19	18	16	2-inch PVC Sch40	16.5	NA
MW-1211	589.88	591.63	39	39.94	37.5	22.5	20.5	18	2-inch PVC Sch40	21.5	NA
MW-1212	610.24	612.29	47.5	48.88	46.5	31.5	29.5	26.5	2-inch PVC Sch40	31.0	NA
MW-1213	NA	NA	78.30	NA	NA	NA	NA	NA	NA	18.0	4/11/06
MW-1214	605.00	606.51	44.5	44.74	43	28	26	23	2-inch PVC Sch40	14.0	NA

WLS COL 2.4-4

TABLE 2.4.12-201 (Sheet 2 of 4)
WELL CONSTRUCTION AND WATER TABLE ELEVATIONS (FT ABOVE MSL)

Well I.D.	Reference Elevations		Well Construction Depths							Additional Info	
	GL Elev	TOC Elev	Boring Depth	TD from TOC	B/Screen	T/Screen	T/Sand	T/Seal	Material	DTW WD	Date Plugged
MW-1215	590.22	592.13	101.5	101.20	100	40	38	35.5	6-inch PVC	35.0	NA
MW-1216	588.01	590.69	29.0	31.31	28.0	18	17	15	2-inch PVC Sch40	18.0	NA
MW-1217	587.64	590.10	24.0	24.85	22.3	12	11	9	2-inch PVC Sch40	10.5	NA
MW-1218	588.12	590.18	16.0	18.31	15.0	5	4	2	2-inch PVC Sch40	17.5	NA
DW2	588.94	589.67	NIA	~150	NIA	NIA	NIA	NIA	6-inch Metal	NIA	NA
DW3	590.56	591.34	NIA	~107.5	NIA	NIA	NIA	NIA	6-inch PVC	NIA	NA
DW4	591.22	591.51	NIA	~130	NIA	NIA	NIA	NIA	6-inch PVC	NIA	NA
DW5	587.73	589.20	NIA	>201	NIA	NIA	NIA	NIA	6-inch Metal	NIA	NA

WLS COL 2.4-4

TABLE 2.4.12-201 (Sheet 3 of 4)
WELL CONSTRUCTION AND WATER TABLE ELEVATIONS (FT ABOVE MSL)

Well I.D.	Location Information				Reference Elevations		Well Construction Elevations			Boring Depth Elev.	Date Completed
	Latitude	Longitude	Northing	Easting	GL Elev	TOC Elev	T/Sand Elev.	T/Screen Elev.	B/Screen Elev.		
MW-1200	35.03776	-81.51582	1166348.442	1845571.069	591.93	593.99	568.93	566.93	551.93	550.93	4/10/06
MW-1201	35.03872	-81.51247	1166689.304	1846578.824	589.91	592.12	505.41	503.41	488.41	487.41	4/14/06
MW-1201A	NM	NM	1166693.529	1846576.539	590.07	592.11	554.07	553.07	543.07	542.07	7/18/06
MW-1202	35.03962	-81.50948	1167018.978	1847472.030	587.47	589.68	529.47	524.97	509.97	508.97	4/14/06
MW-1203	35.03874	-81.50824	1166702.120	1847838.422	589.51	591.87	531.51	529.51	514.51	512.51	4/11/06
MW-1204	35.03719	-81.50761	1166141.154	1848033.400	609.92	612.42	512.92	510.92	495.92	494.92	4/14/06
MW-1204A	NM	NM	1166133.724	1848034.258	609.93	612.42	572.93	570.93	560.93	559.93	7/17/06
MW-1205	35.03582	-81.50665	1165631.431	1848304.849	609.99	612.59	503.99	501.99	486.99	485.99	4/15/06
MW-1206	35.03862	-81.50948	1166655.908	1846689.086	589.66	591.51	539.66	537.16	522.16	521.16	4/18/06
MW-1206A	NM	-81.50948	1166656.288	1846693.299	589.75	591.43	558.75	557.75	547.75	546.75	7/17/06
MW-1207	35.03912	-81.51216	1166849.173	1846668.764	589.03	591.39	499.03	497.03	482.03	481.03	4/24/06
MW-1207A	NM	NM	1166846.232	1846673.410	588.91	591.05	557.91	556.91	546.91	545.91	7/18/06
MW-1208	35.04006	-81.51243	1167188.532	1846583.513	587.77	590.00	528.77	526.27	511.27	508.77	4/13/06
MW-1209	35.03431	-81.50742	1165084.761	1848071.547	586.91	588.91	499.91	497.91	482.91	480.91	4/18/06
MW-1209A	NM	NM	1165076.658	1848072.885	586.93	589.03	570.93	569.93	559.93	558.93	7/17/06
MW-1210	35.03496	-81.50956	1165321.305	1847439.208	589.78	592.27	505.28	503.28	488.28	488.28	4/16/06
MW-1210A	NM	NM	1165312.832	1847436.803	589.42	591.66	571.42	570.42	560.42	559.42	7/17/06
MW-1211	35.03460	-81.51307	1165197.583	1846406.261	589.88	591.63	569.38	567.38	552.38	550.88	4/11/06
MW-1212	35.03508	-81.51621	1165365.927	1845452.195	610.24	612.29	580.74	578.74	563.74	562.74	4/10/06
MW-1213	35.03876	-81.51229	NM	NM	NA	NA	NA	NA	NA	NA	NA
MW-1214	35.03181	-81.51050	1164177.882	1847153.830	605.00	606.51	579.00	577.00	562.00	560.50	4/11/06

WLS COL 2.4-4

TABLE 2.4.12-201 (Sheet 4 of 4)
WELL CONSTRUCTION AND WATER TABLE ELEVATIONS (FT ABOVE MSL)

Well I.D.	Location Information				Reference Elevations		Well Construction Elevations			Boring Depth Elev.	Date Completed
	Latitude	Longitude	Northing	Easting	GL Elev	TOC Elev	T/Sand Elev.	T/Screen Elev.	B/Screen Elev.		
MW-1215	35.03876	-81.51230	1166710.545	1846624.819	590.22	592.13	552.22	550.22	490.22	488.72	4/17/06
MW-1216	35.03452	-81.51129	1165171.882	1846927.273	588.01	590.69	571.01	570.01	560.01	559.01	7/19/06
MW-1217	35.03419	-81.51109	1165042.463	1846983.878	587.64	590.10	574.64	573.64	563.64	563.64	7/19/06
MW-1218	35.03368	-81.51059	1164859.672	1847139.635	588.12	590.18	584.12	583.12	573.12	572.12	7/18/06
DW2	35.03489	-81.51162	1165319.974	1846821.466	588.94	589.67	NIA	NIA	NIA	NIA	~1977
DW3	35.03521	-81.51028	1165408.943	1847234.503	590.56	591.34	NIA	NIA	NIA	NIA	~1977
DW4	35.03412	-81.51358	1165035.485	1846277.086	591.22	591.51	NIA	NIA	NIA	NIA	~1977
DW5	NM	NM	1167933.393	1847896.940	587.73	589.20	NIA	NIA	NIA	NIA	~1977

TOC Elev. = top of casing elevations obtained from professional surveyors (McKim & Creed)

GL Elev. = ground level elevations obtained from professional surveyors (McKim & Creed)

Latitude, Longitude: Obtained using hand-held Garmin Rino 120 GPS unit

Northing/Easting: Obtained from professional surveyors (McKim & Creed)

Wells designated "A" wells are the shallow cluster wells located around 5 feet from the cluster twin well.

Location 1213 was completed as a boring only. MW-1215 is the aquifer test pumping well.

Units are ft.

DTW WD = Depth to water while drilling

NIA = No Information Available

NA = Not Applicable

NM = Not Measured

DW Wells completed during Cherokee activities, records not available, possibly used for dewatering

WLS COL 2.4-4

TABLE 2.4.12-202 (Sheet 1 of 8)
WATER TABLE ELEVATIONS

Location	Reference Elev.		4/18/2006		5/14/2006		5/23/2006		5/29/2006		6/6/2006	
	TOC	GL	DTW	WT Elev	DTW	WT Elev	DTW	WT Elev	DTW	WT Elev	DTW	WT Elev
MW-1200	593.99	591.93	31.80	562.19	32.51	561.48	32.77	561.2	32.90	561.1	33.13	560.9
MW-1201	592.12	589.91			34.69	557.43	35.17	557.0	35.35	556.8	35.60	556.5
MW-1201A	592.11	590.07										
MW-1202	589.68	587.47	23.90	565.78	24.49	565.19	24.76	564.9	24.86	564.8	24.99	564.7
MW-1203	591.87	589.51	20.60	571.27	21.05	570.82	21.40	570.5	21.51	570.4	21.65	570.2
MW-1204	612.42	609.92	39.80	572.62	39.87	572.55	40.25	572.2	40.33	572.1	40.36	572.1
MW-1204A	612.42	609.93										
MW-1205	612.59	609.99	46.90	565.69	46.89	565.70	47.28	565.3	47.33	565.3	47.20	565.4
MW-1206	591.51	589.66			32.98	558.53	33.43	558.1	33.63	557.9	33.89	557.6
MW-1206A	591.43	589.75										
MW-1207	591.39	589.03			33.31	558.08	33.74	557.6	33.93	557.5	34.17	557.2
MW-1207A	591.05	588.91										
MW-1208	590.00	587.77	41.30	548.70	41.84	548.16	42.25	547.8	42.37	547.6	42.46	547.5
MW-1209	588.91	586.91			19.21	569.70	19.55	569.4	19.62	569.3	19.57	569.3
MW-1209A	589.03	586.93										
MW-1210	592.27	589.78	19.50	572.77	20.08	572.19	20.17	572.1	20.51	571.8	20.64	571.6
MW-1210A	591.66	589.42										
MW-1211	591.63	589.88	27.50	564.13	27.93	563.70	27.99	563.6	28.11	563.5	28.21	563.4
MW-1212	612.29	610.24	35.45	576.84	36.26	576.03	36.62	575.7	36.81	575.5	37.17	575.1
MW-1214	606.51	605.00	16.80	589.71	17.60	588.91	18.01	588.5	18.25	588.3	18.61	587.9
MW-1215	592.13	590.22			34.65	557.48	35.14	557.0	35.34	556.8	35.56	556.6
MW-1216	590.69	588.01										

WLS COL 2.4-4

TABLE 2.4.12-202 (Sheet 2 of 8)
WATER TABLE ELEVATIONS

Location	Reference Elev.		4/18/2006		5/14/2006		5/23/2006		5/29/2006		6/6/2006	
	TOC	GL	DTW	WT Elev	DTW	WT Elev	DTW	WT Elev	DTW	WT Elev	DTW	WT Elev
MW-1217	590.10	587.64										
MW-1218	590.18	588.12										
DW2	589.67	588.94	33.80	555.87	37.11	552.56	37.11	552.56	37.56	552.11	37.75	551.92
DW3	591.34	590.56	22.50	568.84	23.59	567.75	23.59	567.75	24.65	566.69	24.63	566.71
DW4	591.51	591.22										
DW5	589.20	587.73										
SG-1		568.23			0.98	569.21						
SG-2		547.81			1.40	546.41						
SG-3		536.09			2.40	533.69						
SG-4		525.64			1.40	524.24						

WLS COL 2.4-4

TABLE 2.4.12-202 (Sheet 3 of 8)
WATER TABLE ELEVATIONS

Location	Reference Elev.		6/12/2006		7/15/2006		7/21/2006		8/15/2006		9/11/2006	
	TOC	GL	DTW	WT Elev	DTW	WT Elev	DTW	WT Elev	DTW	WT Elev	DTW	WT Elev
MW-1200	593.99	591.93	33.29	560.7	34.13	559.9	34.31	559.68	34.95	559.0	36.64	557.3
MW-1201	592.12	589.91	35.80	556.3	36.80	555.3	36.97	555.15	37.55	554.6	38.19	553.9
MW-1201A	592.11	590.07					38.60	553.51	36.69	555.4	37.10	555.0
MW-1202	589.68	587.47	25.10	564.6	25.73	563.9	25.82	563.86	26.28	563.4	26.81	562.9
MW-1203	591.87	589.51	21.78	570.1	22.51	569.4	22.65	569.22	23.14	568.7	24.70	567.2
MW-1204	612.42	609.92	40.45	572.0	41.06	571.4	41.17	571.25	41.58	570.8	42.14	570.3
MW-1204A	612.42	609.93					33.54	578.88	33.06	579.4	33.44	579.0
MW-1205	612.59	609.99	47.25	565.3	47.66	564.9	47.75	564.84	47.98	564.6	48.50	564.1
MW-1206	591.51	589.66	34.10	557.4	35.10	556.4	35.29	556.22	35.89	555.6	36.51	555.0
MW-1206A	591.43	589.75					35.31	556.12	35.92	555.5	36.54	554.9
MW-1207	591.39	589.03	34.39	557.0	35.39	556.0	35.54	555.85	36.21	555.2	36.84	554.5
MW-1207A	591.05	588.91					34.77	556.28	35.39	555.7	36.03	555.0
MW-1208	590.00	587.77	42.62	547.4	43.18	546.8	43.38	546.62	43.69	546.3	44.20	545.8
MW-1209	588.91	586.91	19.62	569.3	20.10	568.8	20.20	568.71	20.51	568.4		
MW-1209A	589.03	586.93					17.72	571.31	17.78	571.3	18.27	570.8
MW-1210	592.27	589.78	20.95	571.3	21.67	570.6	21.91	570.36	22.26	570.0	22.61	569.7
MW-1210A	591.66	589.42					20.42	571.24	20.81	570.8	21.25	570.4
MW-1211	591.63	589.88	28.33	563.3	28.62	563.0	28.80	562.83	28.85	562.8	28.73	562.9
MW-1212	612.29	610.24	37.42	574.9	38.69	573.6	38.90	573.39	39.62	572.7	40.14	572.2
MW-1214	606.51	605.00	18.91	587.6	20.31	586.2	20.62	585.89	21.38	585.1	22.04	584.5
MW-1215	592.13	590.22	35.75	556.4	36.73	555.4	36.91	555.22	37.50	554.6	38.15	554.0
MW-1216	590.69	588.01					25.00	565.69	25.96	564.7	26.92	563.8
MW-1217	590.10	587.64					22.19	567.91	23.33	566.8	24.41	565.7

WLS COL 2.4-4

TABLE 2.4.12-202 (Sheet 4 of 8)
WATER TABLE ELEVATIONS

Location	Reference Elev.		6/12/2006		7/15/2006		7/21/2006		8/15/2006		9/11/2006	
	TOC	GL	DTW	WT Elev	DTW	WT Elev	DTW	WT Elev	DTW	WT Elev	DTW	WT Elev
MW-1218	590.18	588.12					16.63	573.55	17.22	573.0	17.77	572.4
DW2	589.67	588.94	37.73	551.94	38.90	550.77	39.41	550.26	40.03	549.64	40.42	549.25
DW3	591.34	590.56	25.24	566.10	26.24	565.10	26.88	564.46	26.90	564.44	27.33	564.01
DW4	591.51	591.22			23.82	567.69	23.91	567.60	23.94	567.57		
DW5	589.20	587.73							58.35	530.85	58.72	
SG-1		568.23			0.84	569.07					1.02	569.25
SG-2		547.81			1.70	546.11					1.6	546.21
SG-3		536.09			2.48	533.61					1.7	534.39
SG-4		525.64			1.20	524.44					1.38	524.26

WLS COL 2.4-4

TABLE 2.4.12-202 (Sheet 5 of 8)
WATER TABLE ELEVATIONS

Location	Reference Elev.		9/14/2006		10/10/2006		11/14/2006		12/20/2006		1/17/2006	
	TOC	GL	DTW	WT Elev	DTW	WT Elev	DTW	WT Elev	DTW	WT Elev	DTW	WT Elev
MW-1200	593.99	591.93	35.67	558.3	35.99	558.00	36.44	557.55	35.03	558.96	32.20	561.79
MW-1201	592.12	589.91			38.88	553.24	39.44	552.68	40.35	551.77	40.74	551.38
MW-1201A	592.11	590.07			38.12	553.99	37.90	554.21	39.04	553.07	39.64	552.47
MW-1202	589.68	587.47	26.82	562.9	27.19	562.49	27.67	562.01	28.02	561.66	28.06	561.62
MW-1203	591.87	589.51	23.64	568.2	23.93	567.94	24.17	567.70	23.97	567.90	23.59	568.28
MW-1204	612.42	609.92	41.95	570.5	42.37	570.05	42.68	569.74	42.95	569.47	42.81	569.61
MW-1204A	612.42	609.93	33.17	579.2	33.58	578.84	33.71	578.71	34.75	577.67	35.16	577.26
MW-1205	612.59	609.99	48.23	564.4	48.61	563.98	48.76	563.83	49.20	563.39	49.22	563.37
MW-1206	591.51	589.66			37.27	554.24	37.83	553.68	38.60	552.91	38.96	552.55
MW-1206A	591.43	589.75			37.31	554.12	37.85	553.58	38.62	552.81	38.98	552.45
MW-1207	591.39	589.03			36.88	554.51	38.16	553.23	38.90	552.49	39.25	552.14
MW-1207A	591.05	588.91			37.64	553.41	37.38	553.67	38.10	552.95	38.44	552.61
MW-1208	590.00	587.77			44.73	545.27	45.02	544.98	45.73	544.27	45.89	544.11
MW-1209	588.91	586.91	20.85	568.1	21.22	567.69	21.44	567.47	21.75	567.16	21.67	567.24
MW-1209A	589.03	586.93	18.01	571.0	18.46	570.57	18.80	570.23	20.02	569.01	20.21	568.82
MW-1210	592.27	589.78	22.18	570.1	23.06	569.21	22.54	569.73	22.67	569.60	21.66	570.61
MW-1210A	591.66	589.42	21.11	570.5	21.64	570.02	21.49	570.17	21.55	570.11	20.74	570.92
MW-1211	591.63	589.88	28.12	563.5	28.70	562.93	28.21	563.42	27.86	563.77	26.83	564.80
MW-1212	612.29	610.24	40.15	572.1	40.25	572.04	40.03	572.26	37.78	574.51	33.44	578.85
MW-1214	606.51	605.00	22.02	584.5	22.40	584.11	22.35	584.16	21.05	585.46	20.01	586.50
MW-1215	592.13	590.22			38.89	553.24	39.43	552.70	40.28	551.85	40.65	551.48
MW-1216	590.69	588.01	26.91	563.8	27.49	563.20	27.89	562.80	26.92	563.77	25.75	564.94
MW-1217	590.10	587.64	24.33	565.8	24.47	565.63	24.49	565.61	24.14	565.96	22.47	567.63

WLS COL 2.4-4

TABLE 2.4.12-202 (Sheet 6 of 8)
WATER TABLE ELEVATIONS

Location	Reference Elev.		9/14/2006		10/10/2006		11/14/2006		12/20/2006		1/17/2006	
	TOC	GL	DTW	WT Elev	DTW	WT Elev	DTW	WT Elev	DTW	WT Elev	DTW	WT Elev
MW-1218	590.18	588.12	8.60	581.6	17.88	572.30	17.77	572.41	16.63	573.55	15.10	575.08
DW2	589.67	588.94	40.12	549.55	40.64	549.03	40.44	549.23	40.11	549.56	38.99	550.68
DW3	591.34	590.56	25.92	565.42	27.88	563.46	26.50	564.84	26.54	564.80	24.57	566.77
DW4	591.51	591.22	23.32	568.19	23.88	567.63	23.51	568.00	23.05	568.46	21.93	569.58
DW5	589.20	587.73	58.62	530.58	58.84	530.36	58.92	530.28	59.12	530.08	59.08	530.12
SG-1		568.23			0.68	568.91	0.97	569.20	0.95	569.18	1.00	569.23
SG-2		547.81			1.95	545.86	1.87	545.94	1.47	546.34	1.25	546.56
SG-3		536.09			2.34	533.75	1.74	534.35	1.37	534.73	1.78	534.31
SG-4		525.64			1.47	524.17	1.38	524.26	0.00	525.64	1.38	524.27

WLS COL 2.4-4

TABLE 2.4.12-202 (Sheet 7 of 8)
WATER TABLE ELEVATIONS

Location	Reference Elev.		2/19/07		3/13/07		4/19/07	
	TOC	GL	DTW	WT Elev	DTW	WT Elev	DTW	WT Elev
MW-1200	593.99	591.93	32.00	561.99	28.88	565.11	31.26	562.73
MW-1201	592.12	589.91	40.91	551.21	41.14	550.98	41.46	550.66
MW-1201A	592.11	590.07	39.69	552.42	40.04	552.07	40.36	551.75
MW-1202	589.68	587.47	27.82	561.86	27.80	561.88	28.00	561.68
MW-1203	591.87	589.51	23.00	568.87	22.79	569.08	23.20	568.67
MW-1204	612.42	609.92	42.14	570.28	41.85	570.57	41.96	570.46
MW-1204A	612.42	609.93	34.71	577.71	35.06	577.36	35.00	577.42
MW-1205	612.59	609.99	48.59	564.00	48.56	564.03	48.39	564.20
MW-1206	591.51	589.66	39.22	552.29	39.46	552.05	39.82	551.69
MW-1206A	591.43	589.75	39.25	552.18	39.50	551.93	39.85	551.58
MW-1207	591.39	589.03	39.50	551.89	39.72	551.67	40.08	551.31
MW-1207A	591.05	588.91	38.71	552.34	38.92	552.13	39.29	551.76
MW-1208	590.00	587.77	45.77	544.23	45.89	544.11	45.92	544.08
MW-1209	588.91	586.91	20.92	567.99	20.79	568.12	20.61	568.30
MW-1209A	589.03	586.93	18.72	570.31	18.70	570.33	18.15	570.88
MW-1210	592.27	589.78	21.33	570.94	20.85	571.42	20.94	571.33
MW-1210A	591.66	589.42	20.24	571.42	19.83	571.83	19.93	571.73
MW-1211	591.63	589.88	27.06	564.57	26.53	565.10	26.83	564.80
MW-1212	612.29	610.24	34.08	578.21	31.21	581.08	33.91	578.38
MW-1214	606.51	605.00	18.68	587.83	17.72	588.79	17.32	589.19
MW-1215	592.13	590.22	40.84	551.29	41.06	551.07	41.40	550.73
MW-1216	590.69	588.01	24.66	566.03	23.91	566.78	24.24	566.45
MW-1217	590.10	587.64	21.46	568.64	20.33	569.77	20.97	569.13
MW-1218	590.18	588.12	14.76	575.42	13.69	576.49	14.19	575.99

WLS COL 2.4-4

TABLE 2.4.12-202 (Sheet 8 of 8)
WATER TABLE ELEVATIONS

Location	Reference Elev.		2/19/07		3/13/07		4/19/07	
	TOC	GL	DTW	WT Elev	DTW	WT Elev	DTW	WT Elev
DW2	589.67	588.94	38.94	550.73	37.62	552.05	38.17	551.50
DW3	591.34	590.56	24.77	566.57	23.14	568.20	23.26	568.08
DW4	591.51	591.22	22.66	568.85	21.72	569.79	18.19	573.32
DW5	589.20	587.73	58.95	530.25	58.65	530.55	58.49	530.71
SG-1		568.23	0.98	569.21	1.00	569.23	1.17	569.40
SG-2		547.81	1.23	546.58	1.23	546.58	1.06	546.75
SG-3		536.09	1.86	534.23	1.81	534.28	1.70	534.39
SG-4		525.64	1.38	524.27	1.50	524.14	1.34	524.30

TOC = top of casing elevation

DTW = depth to water

GL = ground level elevation

WT Elev = water table elevation

SG-1 = DTW value is height above reference elevation

BLANK - no data

All values expressed as feet above msl, except DTW, expressed in feet.

TABLE 2.4.12-203
DELETED

WLS COL 2.4-4

TABLE 2.4.12-204
AQUIFER CHARACTERISTICS

Material	Hydraulic Conductivity (K)				Source
	Minimum	Median	Conservative Estimate	Maximum	
Saprolite/Soil K_v	2.45×10^{-8}	2.10×10^{-6}	4.4×10^{-5}	2.55×10^{-4}	1973 investigation laboratory analyses.
Saprolite/Soil K_h	9.67×10^{-7}	1.14×10^{-4}	4.5×10^{-4}	2.26×10^{-3}	1973 investigation field tests and 2006 slug tests.
Bedrock - PWR K_h	9.67×10^{-7}	1.53×10^{-4}	1.4×10^{-3}	9.89×10^{-3}	1973 investigation packer tests and 2006 slug, aquifer pumping, and packer tests.
Undifferentiated Material	2.21×10^{-4}	4.0×10^{-4}	1.5×10^{-3}	3.90×10^{-3}	1977 aquifer pumping tests.
Fill Material	1.81×10^{-5}	5.39×10^{-5}	7.0×10^{-5}	7.44×10^{-5}	2006 slug tests.

Units are in centimeters per second (cm/sec).

PWR - Partially weathered rock.

K_v - Vertical hydraulic conductivity.

K_h - Horizontal hydraulic conductivity.

Conservative Estimate - The geometric mean of samples exceeding the median (applicable to Saprolite/Soil K_v , K_h and Fill Material).

Conservative Estimate for Bedrock K_h was obtained from results of 2006 pumping test and was used to calculate the groundwater velocity. The Bedrock K_h of 1.4×10^{-3} cm/s bounded the geometric mean of samples exceeding the median (i.e., 1×10^{-3} cm/s).

Undifferentiated Material - Identification used for 1977 data where well screens bracketed the entire saturated zone, and did not differentiate between the fill material, soil, saprolite, or partially weathered rock. Conservative estimate of Undifferentiated Material K_h is presented for comparison purposes only and is based on an average of results from 1977 pumping tests.

TABLE 2.4.12-205 (Sheet 1 of 3)
 MAXIMUM HISTORICALLY-RECORDED RAINFALL
 DISTRIBUTION (TROPICAL STORM JERRY)

Date	Time of Day (hr. : min.)	Rainfall (in.)	Cumulative Rainfall Duration (hr.)
25-Aug-95	1:00	0.00	
	2:00	0.00	
	3:00	0.00	
	4:00	0.00	
	5:00	0.00	
	6:00	0.00	
	7:00	0.00	
	8:00	0.00	
	9:00	0.00	
	10:00	0.00	
	11:00	0.00	
	12:00	0.00	
	13:00	0.00	
	14:00	0.00	
	15:00	0.00	
	16:00	0.00	
	17:00	0.30	1
	18:00	0.10	2
	19:00	0.00	3
	20:00	0.00	4
	21:00	0.00	5
	22:00	0.00	6
	23:00	0.00	7
	0:00	0.00	8

TABLE 2.4.12-205 (Sheet 2 of 3)
 MAXIMUM HISTORICALLY-RECORDED RAINFALL
 DISTRIBUTION (TROPICAL STORM JERRY)

Date	Time of Day (hr. : min.)	Rainfall (in.)	Cumulative Rainfall Duration (hr.)
26-Aug-95	1:00	0.00	9
	2:00	0.01	10
	3:00	0.32	11
	4:00	0.10	12
	5:00	0.11	13
	6:00	0.10	14
	7:00	0.14	15
	8:00	0.14	16
	9:00	0.11	17
	10:00	0.11	18
	11:00	0.14	19
	12:00	0.11	20
	13:00	0.26	21
	14:00	0.10 ^(a)	22
	15:00	0.30 ^(a)	23
	16:00	0.11 ^(a)	24
	17:00	0.33 ^(a)	25
	18:00	0.23 ^(a)	26
	19:00	0.70 ^(a)	27
	20:00	0.81 ^(a)	28
	21:00	0.54 ^(a)	29
	22:00	0.42 ^(a)	30
	23:00	1.51 ^(a)	31
	0:00	2.62 ^(a)	32

TABLE 2.4.12-205 (Sheet 3 of 3)
 MAXIMUM HISTORICALLY-RECORDED RAINFALL
 DISTRIBUTION (TROPICAL STORM JERRY)

Date	Time of Day (hr. : min.)	Rainfall (in.)	Cumulative Rainfall Duration (hr.)
27-Aug-95	1:00	1.74 ^(a)	33
	2:00	1.20 ^(a)	34
	3:00	0.17 ^(a)	35
	4:00	0.04 ^(a)	36
	5:00	0.06 ^(a)	37
	6:00	0.06 ^(a)	38
	7:00	0.03 ^(a)	39
	8:00	0.02 ^(a)	40
	9:00	0.01 ^(a)	41
	10:00	0.10 ^(a)	42
	11:00	0.18 ^(a)	43
	12:00	0.57 ^(a)	44
	13:00	0.47 ^(a)	45
	14:00	0.07	46
	15:00	0.03	47
	16:00	0.00	
	17:00	0.00	
	18:00	0.00	
	19:00	0.00	
	20:00	0.00	
	21:00	0.00	
	22:00	0.00	
	23:00	0.00	
	0:00	0.00	
	Maximum 24-hr Rainfall (in.)	12.32	
	Total 47-hr Storm Rainfall (in.)	14.47	

Note:

Data collected at Greenville-Spartanburg Airport, Greer, South Carolina
 GSP Station, Gage ID No. 383747 ([Reference 305](#))

a) Rainfall measurements during the 24-hour maximum period.

WLS COL 2.4-5

TABLE 2.4.13-201
DISTRIBUTION COEFFICIENTS (K_d)

	K_d Analytical Results per Argonne National Laboratory			Default K_d Values Used by RESRAD and Values From Other Sources ^(a)			
Sample Loc.	MW-1208	MW-1208	MW-1210	Sheppard & Thibault	IAEA	NUREG/ CR-5512 Kennedy & Streng (1992)	RESRAD (v. 5.62 & later)
Sample Depth ft bgs ^(b)	45-46	58.5-59	69-73				
Sample Zone	Soil/Saprolite	Soil/Saprolite	Soil/Saprolite				
Soil Sample Texture	Sand, silty (SM)	Sand, silty (SM)	Silt, sandy (ML)	Loam	Loam	Sand	NIA ^(c)
Element	cm ³ /g	cm ³ /g	cm ³ /g	cm ³ /g	cm ³ /g	cm ³ /g	cm ³ /g
Co	1103 ± 118	1971 ± 214	>7714	1300	1300	60	1000
Cs	3704 ± 524	2117 ± 299	1156 ± 163	4600	4400	270	1000
Fe	1689 ± 239	5478 ± 775	3628 ± 513	800	810	160	1000
I	1.4 ± 0.2	0.07 ± 0.01	2.5 ± 0.4	5	5	1	0.1
Ni	269 ± 38	167 ± 24	152 ± 22	300	300	400	1000
Pu-242	89 ± 13	>1921	987 ± 140	1200	1200	550	2000
Sr	739 ± 82	262 ± 33	73 ± 9	20	810	-	30
Tc-99	0.28 ± 0.04	0.04 ± 0.01	0.42 ± 0.06	0.1	-	0.1	0
U-235	>3159	1702 ± 241	>3636	15	-	15	50

a) References 209 and 210

b) Below ground surface

c) No information available

WLS COL 2.4-5

TABLE 2.4.13-202 (Sheet 1 of 2)
AP1000 TANKS CONTAINING RADIOACTIVE LIQUID

Tank	Location ^(a)	Nominal Tank Volume	Radioisotope Contents	Considerations/Features to Mitigate Release
PXS Tanks (IRWST and CMT's)	Inside Containment	NA	NA	Inside Containment; release need not be considered.
Spent Fuel Pool	Auxiliary Building	NA	NA	Not a tank, per se. Fully lined and safety related. Located entirely inside Auxiliary Building; does not have any potential for foundation cracks to allow leakage directly to environment. Leakage would be to another room of Auxiliary Building.
WLS Reactor coolant drain tank	Inside Containment	NA	NA	Inside containment; release need not be considered.
WLS Containment sump	Inside Containment	NA	NA	Inside containment; release need not be Considered.
WLS Effluent Holdup Tanks	Auxiliary building El. 66'-6"	28,000 gal	Essentially reactor coolant	Located in unlined room at lowest portion of Auxiliary Building
WLS Waste Holdup Tanks	Auxiliary Building El. 66'-6"	15,000 gal	Less than reactor coolant	Located in unlined room at lowest portion of Auxiliary Building
WLS Monitor Tanks A, B, C	Auxiliary Building El. 66'-6", 92'-6" and 107'- 2"	15,000 gal	Effluent prepared for environmental discharge - much less than reactor coolant	Located in unlined room at lowest portion of Auxiliary Building

WLS COL 2.4-5

TABLE 2.4.13-202 (Sheet 2 of 2)
AP1000 TANKS CONTAINING RADIOACTIVE LIQUID

Tank	Location ^(a)	Nominal Tank Volume	Radioisotope Contents	Considerations/Features to Mitigate Release
WLS Monitor Tanks D, E, F	Radwaste Building	15,000 gal	Effluent prepared for environmental discharge - much less than reactor coolant	Located in unlined room at grade level in curbed, non-seismic building
WLS Chemical Waste Tank	Auxiliary Building El. 66'-6"	8,900 gal	Less than reactor coolant	Located in unlined room at lowest portion of Auxiliary Building
WSS Spent Resin Storage Tanks	Auxiliary Building El. 100' ^(a)	300 ft ³ (liquid volume will be much less)	Approx. reactor coolant	Located entirely inside Auxiliary Building; does not have any potential for foundation cracks to allow leakage directly to environment. Leakage would be to another room of aux. building.

a) Floor elevations are based on design plant grade of 100 ft. as provided in the DCD.

WLS COL 2.4-5

TABLE 2.4.13-203 (Sheet 1 of 6)
LISTING OF LEE NUCLEAR STATION DATA AND MODELING PARAMETERS SUPPORTING THE
EFFLUENT HOLDUP TANK FAILURE

Soil Parameter	Parameter Description	Parameter Value ^(a) ^(b)	Parameter Justification
Silver Transport K_d Coefficient (cm^3/g) ^(b)	Radionuclide-specific retardation coefficient	0	A value of 0 assumes no retardation.
Barium Transport K_d Coefficient (cm^3/g)	Radionuclide-specific retardation coefficient	0	A value of 0 assumes no retardation.
Bromine Transport K_d Coefficient (cm^3/g)	Radionuclide-specific retardation coefficient	0	A value of 0 assumes no retardation.
Cerium Transport K_d Coefficient (cm^3/g)	Radionuclide-specific retardation coefficient	0	A value of 0 assumes no retardation.
Cobalt Transport K_d Coefficient (cm^3/g)	Radionuclide-specific retardation coefficient	985	Radionuclide-specific K_d values are measured by Argonne National Laboratory using Lee soil. Lowest value of the laboratory reporting range is used.
Chromium Transport K_d Coefficient (cm^3/g)	Radionuclide-specific retardation coefficient	0	A value of 0 assumes no retardation.
Cesium Transport K_d Coefficient (cm^3/g)	Radionuclide-specific retardation coefficient	993	Radionuclide-specific K_d values are measured by Argonne National Laboratory using Lee soil. Lowest value of the laboratory reporting range is used.
Iron Transport K_d Coefficient (cm^3/g)	Radionuclide-specific retardation coefficient	1,450	Radionuclide-specific K_d values are measured by Argonne National Laboratory using Lee soil. Lowest value of the laboratory reporting range is used.
Tritium Transport K_d Coefficient (cm^3/g)	Radionuclide-specific retardation coefficient	0	A value of 0 assumes no retardation.
Iodine Transport K_d Coefficient (cm^3/g)	Radionuclide-specific retardation coefficient	0.06	Radionuclide-specific K_d values are measured by Argonne National Laboratory using Lee soil. Lowest value of the laboratory reporting range is used.
Lanthanum Transport K_d Coefficient (cm^3/g)	Radionuclide-specific retardation coefficient	0	A value of 0 assumes no retardation.

WLS COL 2.4-5

TABLE 2.4.13-203 (Sheet 2 of 6)
LISTING OF LEE NUCLEAR STATION DATA AND MODELING PARAMETERS SUPPORTING THE
EFFLUENT HOLDUP TANK FAILURE

Soil Parameter	Parameter Description	Parameter Value ^(a) ^(b)	Parameter Justification
Manganese Transport K_d Coefficient (cm ³ /g)	Radionuclide-specific retardation coefficient	0	A value of 0 assumes no retardation.
Molybdenum Transport K_d Coefficient (cm ³ /g)	Radionuclide-specific retardation coefficient	0	A value of 0 assumes no retardation.
Niobium Transport K_d Coefficient (cm ³ /g)	Radionuclide-specific retardation coefficient	0	A value of 0 assumes no retardation.
Promethium Transport K_d Coefficient (cm ³ /g)	Radionuclide-specific retardation coefficient	0	A value of 0 assumes no retardation.
Rubidium Transport K_d Coefficient (cm ³ /g)	Radionuclide-specific retardation coefficient	0	A value of 0 assumes no retardation.
Rhodium Transport K_d Coefficient (cm ³ /g)	Radionuclide-specific retardation coefficient	0	A value of 0 assumes no retardation.
Ruthenium Transport K_d Coefficient (cm ³ /g)	Radionuclide-specific retardation coefficient	0	A value of 0 assumes no retardation.
Strontium Transport K_d Coefficient (cm ³ /g)	Radionuclide-specific retardation coefficient	64	Radionuclide-specific K_d values are measured by Argonne National Laboratory using Lee soil. Lowest value of the laboratory reporting range is used.
Technetium Transport K_d Coefficient (cm ³ /g)	Radionuclide-specific retardation coefficient	0.03	Radionuclide-specific K_d values are measured by Argonne National Laboratory using Lee soil. Lowest value of the laboratory reporting range is used.
Tellurium Transport K_d Coefficient (cm ³ /g)	Radionuclide-specific retardation coefficient	0	A value of 0 assumes no retardation.
Yttrium Transport K_d Coefficient (cm ³ /g)	Radionuclide-specific retardation coefficient	0	A value of 0 assumes no retardation.

WLS COL 2.4-5

TABLE 2.4.13-203 (Sheet 3 of 6)
LISTING OF LEE NUCLEAR STATION DATA AND MODELING PARAMETERS SUPPORTING THE
EFFLUENT HOLDUP TANK FAILURE

Soil Parameter	Parameter Description	Parameter Value ^(a) ^(b)	Parameter Justification
Zirconium Transport K_d Coefficient (cm ³ /g)	Radionuclide-specific retardation coefficient	0	A value of 0 assumes no retardation.
Precipitation (meters per year)	Average quantity of precipitation annually	1.27	Based on the 50 inches per year typical annual precipitation for Cherokee County.
Area of contaminated zone (square meters)	Area containing liquids released by the tank failure	~104	This is the area of a cube required to contain 80% of the effluent tank total capacity, distributed into that portion of the soil voids represented by the effective porosity (for PWR).
Thickness of contaminated zone (meters)	Describes the thickness of the area considered to be the contaminated zone	~10.2	The volume is assumed to be a cube. The area required to contain a volume with 80% of the liquid effluent tank (22,400 gallons), accounting for effective porosity of the contaminated zone.
Length of Primary Contamination in X direction (meters)	Describes the X-axis length of the primary contamination	~10.2	The width of the area of soil saturated with water from the effluent tank failure. The shape is assumed to be a cube.
Length of Primary Contamination in Y direction (meters)	Describes the Y-axis length of the primary contamination	~10.2	The length of the area of soil saturated with water from the effluent tank failure. The shape is assumed to be a cube.
Evapotranspiration coefficient	Describes the fraction of precipitation and irrigation water penetrating the topsoil that is lost to evaporation and by transpiration by vegetation	0.64	This is a parameter used by RESRAD-OFFSITE to determine the amount of available water obtained from either precipitation or irrigation that infiltrates to the saturated zone. The value, when used in conjunction with precipitation and runoff, creates a recharge rate of ~18 inches/yr. This value is suggested by a study of regional data and is conservative when considering conditions likely present following construction.
Runoff coefficient (unitless)	Coefficient (fraction) of precipitation that runs off the surface and does not infiltrate into the soil	0	This is a parameter used by RESRAD-OFFSITE to determine the amount of available water obtained from either precipitation or irrigation that infiltrates to the saturated zone. The value, when used in conjunction with precipitation and evapotranspiration, creates a recharge rate of ~18 inches/yr. This value is suggested by a study of regional data and is conservative when considering conditions likely present following construction.

WLS COL 2.4-5

TABLE 2.4.13-203 (Sheet 4 of 6)
 LISTING OF LEE NUCLEAR STATION DATA AND MODELING PARAMETERS SUPPORTING THE
 EFFLUENT HOLDUP TANK FAILURE

Soil Parameter	Parameter Description	Parameter Value ^(a) ^(b)	Parameter Justification
Contaminated zone total porosity (unitless)	Total porosity of the contaminated sample, which is the ratio of the soil pore volume to the total volume	2.7E-01	On-site data collected at Lee. A value representative of partially weathered rock is used for conservatism.
Density of contaminated zone (g/cm ³)	Density of the contaminated soil impacted by the liquid tank failure	1.8E+00	On-site data collected at Lee. A value representative of partially weathered rock is used for conservatism.
Contaminated zone hydraulic conductivity (meters per year)	Flow velocity of groundwater through the contaminated zone under a hydraulic gradient	~4.42E+02	The hydraulic conductivity was calculated from on-site data collected at Lee. Based on a value representative of 1.40E-03 cm/s for partially weathered rock is used for conservatism, converted to m/y.
Density of saturated zone (g/cm ³)	Density of the saturated zone soil that transmits groundwater	1.98E+00	On-site data was collected at Lee. A value representative of partially weathered rock is used for conservatism.
Saturated zone total porosity (unitless)	Total porosity of the saturated zone soil, which is the ratio of the pore volume to the total volume	2.7E-01	On-site data was collected at Lee. A value representative of partially weathered rock is used for conservatism.
Saturated zone effective porosity (unitless)	Ratio of the part of the pore volume where water can circulate to the total volume of a representative sample	8.0E-02	On-site data was collected at Lee. A value representative of partially weathered rock is used for conservatism.
Saturated zone hydraulic gradient to surface water body (unitless)	Change in groundwater elevation per unit of distance in the direction of groundwater flow to a surface water body	4.7E-02	The site-specific hydraulic gradient, representative of partially weathered rock, for the pathway having shortest (i.e., most rapid) travel time to the nearest off-site surface water body. Assumed to be nearest on-site surface water body (Hold-Up Pond A) for conservatism.

WLS COL 2.4-5

TABLE 2.4.13-203 (Sheet 5 of 6)
LISTING OF LEE NUCLEAR STATION DATA AND MODELING PARAMETERS SUPPORTING THE
EFFLUENT HOLDUP TANK FAILURE

Soil Parameter	Parameter Description	Parameter Value ^(a) ^(b)	Parameter Justification
Longitudinal dispersivity to surface water body (meters)	Describes the ratio between the longitudinal dispersion coefficient and the pore water velocity. The parameter depends on the length of the saturated zone	3.77E+00	Follows recommendations in the RESRAD-OFFSITE User Manual.
Lateral (horizontal) dispersivity to surface water body (meters)	Describes the ratio between the horizontal lateral dispersion coefficient and the pore water velocity	3.77E-01	Follows recommendations in the RESRAD-OFFSITE User Manual.
Lateral (vertical) dispersivity to the surface water body (meters)	Describes the vertical dispersion. The user may either model (a) vertical dispersion in the saturated zone and ignore the effects of clean infiltration along the length of the saturated zone or (b) ignore vertical dispersion in the saturated and model the effects of clean infiltration along the length of the saturated zone.	3.77E-02	Follows recommendations in the RESRAD-OFFSITE User Manual.
Distance to the nearest surface water body (meters)	Distance to the nearest off-site surface water body that contributes to a potable drinking water source	376.9	Site-specific value corresponding to the distance from the Unit 2 auxiliary building to the "hypothetical" well location, i.e., the nearest edge of Hold-Up Pond A minus the length of the contaminated zone.
Volume of the surface water body (m ³)	Describes the size of the surface water body	856,036	Site-specific value corresponding to the volume of the Broad River reservoir from the postulated release point downstream to the Ninety-Nine Islands Dam.

WLS COL 2.4-5

TABLE 2.4.13-203 (Sheet 6 of 6)
LISTING OF LEE NUCLEAR STATION DATA AND MODELING PARAMETERS SUPPORTING THE
EFFLUENT HOLDUP TANK FAILURE

Soil Parameter	Parameter Description	Parameter Value ^(a) ^(b)	Parameter Justification
Residence time (yrs)	The average time that water spends in the surface water body	0.00397	Site-specific value obtained by dividing the volume of the surface water body by the volume of water that is extracted annually from it.

a) Parameter values are provided in metric units as used with RESRAD-OFFSITE.

b) K_d values reported in the laboratory analysis for nickel, plutonium, and uranium are not included in the liquid effluent source term and, therefore, are not listed in this RESRAD-OFFSITE input table.

WLS COL 2.4-5

TABLE 2.4.13-204
RADIONUCLIDE CONCENTRATION AT NEAREST DRINKING
WATER SOURCE IN AN UNRESTRICTED AREA DUE TO
EFFLUENT HOLDUP TANK FAILURE

Detected Radionuclide	Radionuclide Concentration microcuries/ml	10 CFR 20 Appendix B Table 2 Column 2 microcuries/ml	Sum of Fractions Contribution ^(a)
H-3	3.47E-08	1.00E-03	3.47E-05
			Sum of Fractions ^(b)
			3.50E-05

a) Those radionuclides with Sum of Fractions Contribution less than 1.0E-5 are negligible and not included in the table.

b) Total for all detected radionuclides.

2.5 GEOLOGY, SEISMOLOGY, AND GEOTECHNICAL ENGINEERING

This **section** of the referenced DCD is incorporated by reference with the following departures and/or supplements:

STD DEP 1.1-1 Section 2.5 is renumbered to follow Regulatory Guide 1.206. The COL information items in DCD Subsections 2.5.1 through 2.5.6 and addressed in **Subsection 2.5.6**.

WLS COL 2.5-2 This section presents information on the geological, seismological, and geotechnical engineering properties of the Lee Nuclear Station and complies with Regulatory Guide (RG) 1.206. **Subsection 2.5.1** describes basic geological and seismologic data. **Subsection 2.5.2** describes the vibratory ground motion at the site, including an updated seismicity catalog, description of seismic sources, and development of the Ground Motion Response Spectra (GMRS) and Foundation Input Response Spectra (FIRS) for the Lee Nuclear Site. **Subsection 2.5.3** describes the potential for surface faulting in the site area. **Subsection 2.5.4**, describes the stability of subsurface materials and foundations. Lastly, **Subsection 2.5.5** describes the stability of slopes.

RG 1.208 provides guidance for the level of investigation recommended at different distances from a proposed site for a nuclear facility.

The following four terms for site map areas are designated by RG 1.208:

- Site region - area within 200 mi (320 km) of the site location.
- Site vicinity - area within 25 mi (40 km) of the site location.
- Site area - area within 5 mi (8 km) of the site location.
- Site - area within 0.6 mi (1 km) of the proposed Lee Nuclear Station Unit 1 and 2 locations.

These terms are used in **Subsections 2.5.1** through **2.5.5** to describe these specific areas of investigation. These terms are not applicable to other sections of this COL application.

Extensive field investigations and research of relevant geologic literature indicate that no geologic hazards have the potential to affect the Lee Nuclear Site with exception of vibratory ground motion. Seismic hazard at the Lee Nuclear Station is discussed in greater technical detail in **Subsection 2.5.2**.

2.5.1 BASIC GEOLOGIC AND SEISMIC INFORMATION

WLS COL 2.5-1 **Subsection 2.5.1** presents information on the geological and seismological characteristics of the Lee Nuclear Site region and site area. The information is divided in two parts. **Subsection 2.5.1.1** describes the geologic and tectonic setting of the site region (200 mi.), and **Subsection 2.5.1.2** describes the geology and structural geology of the site vicinity (25 mi.), site area (5 mi.), and site (0.6 mi.). The geological and seismological information was developed in accordance with the guidance presented in RG 1.206 and RG 1.208 and satisfies the requirements of 10 CFR 100.23(c). The geological and seismological information presented in this section is used as a basis for evaluating the detailed geologic, seismic, and man-made hazards at the site.

Subsection 2.5.2 describes the methodology used to develop the ground motion GMRS and FIRS for the Lee Nuclear Site. This section provides a description of the geological, seismological, and geophysical database for the Lee Nuclear Site, in the context of the 2012 Central and Eastern United States Seismic Source Characterization for Nuclear Facilities (CEUS SSC) project (**Reference 441**).

Subsection 2.5.1 presents geological and seismological information developed from a review of previous reports prepared for the Lee Nuclear Site, published geologic literature, interviews with experts in the geology and seismotectonics of the site region, and geologic field work performed as part of this study (including new boreholes drilled at the site of the Lee Nuclear Station Units, and geologic field reconnaissance). A review of published geologic literature supplements and updates the previous geological and seismological information.

2.5.1.1 Regional Geology

Subsection 2.5.1.1 describes the regional geology within a 200 mi. radius of the Lee Nuclear Site. The regional physiography, geomorphology, stratigraphy, and tectonic setting are discussed below. The information provided is a brief summary of the region, with an extensive and current bibliography. This regional information provides the basis for evaluating the geologic and seismologic hazards discussed in the succeeding sections.

Rocks within the site area are igneous and metamorphic crystalline rocks that are neither susceptible to karst-type dissolution collapse nor to subsidence due to fluid withdrawal. No irregular weathering conditions or natural landslide hazards are noted in field investigations. The stability of natural and manmade slopes for which failure could adversely impact safety-related structures is discussed in **Subsection 2.5.5**.

According to the 1997 Mineral Resource Map of South Carolina (**Reference 402**) there are neither areas of significant subsurface mineral extraction nor hydrocarbon extraction within the site area. This map shows one area of sand dredging within the site area. Additionally, this map shows one area of common clay extraction about five miles northwest of the site and one area of sericite schist

extraction about five miles east-northeast of the site. This map shows no other areas of mineral extraction within the site area.

2.5.1.1.1 Regional Physiography, Geomorphology, and Stratigraphy

The Lee Nuclear Site is located in the Piedmont physiographic province (Figure 2.5.1-201). From northwest to southeast, the Lee Nuclear Site region includes portions of five physiographic provinces: the Appalachian Plateau (the “Cumberland Plateau” at the latitude of the site region), Valley and Ridge, Blue Ridge, Piedmont, and Coastal Plain. Portions of major lithotectonic divisions of the Appalachian orogen (mountain belt) are found within a 200 mi. radius of the site. The structures and stratigraphic sequences within these divisions represent a complex geologic evolution that ends in the modern day passive margin of the Atlantic continental margin.

Each of these five physiographic provinces is described below, from northwest to southeast, in terms of their physiography, geomorphology, and stratigraphy. A more detailed discussion is provided for the Piedmont Physiographic Province, the province in which the Lee Nuclear Site is located. Although they do not technically constitute a physiographic province, Mesozoic rift basins are also discussed in this section because they contain a distinct assemblage of non-metamorphosed sedimentary rocks and are distributed across both the Piedmont and Coastal Plain provinces.

Depending on the focus of a given study, the Appalachian orogenic belt has been subdivided in a variety of ways by various researchers. These subdivisions, in the past, included provinces, belts, and terranes. More recent syntheses have been organized around lithotectonic associations based on common tectonic or depositional origins, mainly relative to the Iapetus ocean and its marginal continental masses, Laurentia and Gondwana (Hibbard et al. (2002) (Reference 204); Hibbard et al. (2006) (Reference 260); Hibbard et al. (2007) (Reference 428); Hatcher et al. (2007) (Reference 404)). Physiographic provinces are defined based on both physiography (landforms) and geology. However, with the modern emphasis on lithotectonic association, the influence of physiography has become subordinate and the “belt” concept has been abandoned.

Figure 2.5.1-235 diagrams how the modern lithotectonic classification schemata of Hibbard et al. (2006) (Reference 260) and Hibbard et al. (2007) (Reference 428) relate and compare to Hatcher et al. (2007) (Reference 404) and to the nomenclature for the physiographic provinces. Note for instance that the Tugaloo terrane of Hatcher et al. (2007) (Reference 404) falls on both sides of the Brevard Fault Zone, which roughly coincides with the boundary of the Blue Ridge and Piedmont Physiographic provinces. Similarly, this same fundamental physiographic boundary also transects the Hibbard et al. (2006) (Reference 260) Piedmont Domain. Also, note that the Piedmont physiographic province, in the schema of Hibbard et al. (2006) (Reference 260), is divided by the Central Piedmont shear zone into the Piedmont Domain to the west and Carolina (i.e., the “Carolina Zone” in Hibbard et al. (2002) (Reference 204)) to the east. These examples serve to illustrate the decreased role of physiography in modern lithotectonic classifications.

2.5.1.1.1.1 The Appalachian Plateau Physiographic Province

The Appalachian Plateau physiographic province includes the western part of the Appalachian Mountains, stretching from New York State to Alabama. The Appalachian Plateau is bounded on the west by the Interior Low Plateaus and on the east by the Valley and Ridge Province. The Appalachian Plateau surface slopes gently to the northwest and merges imperceptibly into the Interior Low Plateaus.

The Appalachian Plateau physiographic province overlies unmetamorphosed sedimentary rocks of Permian to Cambrian age. These strata are generally subhorizontal to gently folded and exhibit relatively little deformation.

2.5.1.1.1.2 The Valley and Ridge Physiographic Province

The Valley and Ridge physiographic province extends from the Hudson Valley in New York State through Pennsylvania, Maryland, and Virginia, and is about 50 mi. wide from southern Virginia southward to Alabama. The Valley and Ridge Province is bounded on the west by the Appalachian Plateau and on the east by the Blue Ridge. A topographic escarpment known as the Alleghany front in Pennsylvania and the Cumberland escarpment in Tennessee and Virginia marks the northwestern boundary of the Valley and Ridge Province. This physiographic province is underlain by a folded and faulted sequence of Paleozoic sedimentary rocks. The characteristic linear valleys and ridges of this province are the result of differential weathering and erosion of different rock types.

The eastern boundary of the Valley and Ridge province marks a change from folded, lesser-deformed Paleozoic sedimentary rocks to more penetratively deformed Precambrian rocks in the Blue Ridge.

2.5.1.1.1.3 The Blue Ridge Physiographic Province

The Blue Ridge physiographic province is located west of and adjacent to the Piedmont province. The Blue Ridge province extends from Pennsylvania to northern Georgia and varies from about 30 to 75 mi. wide. Elevations are highest in North Carolina and Georgia, with several peaks in North Carolina exceeding 5,900 ft. above mean sea level (msl), including Mount Mitchell, North Carolina, the highest point (6,684 ft. msl) in the Appalachian Mountains. The east-facing Blue Ridge escarpment, which is about 300 mi. in length and averages 1000 to 1650 ft. msl elevation, separates the highlands of the Blue Ridge from the lower relief Piedmont province in the southern Appalachians ([Reference 205](#)).

The Blue Ridge province is bounded on the northwest by the Valley and Ridge physiographic province and to the southeast by the Piedmont physiographic province delineated by the Brevard fault zone ([References 206 and 207](#)) ([Figures 2.5.1-201 and 202b](#)). The province is a complexly folded, faulted, penetratively deformed, and intruded metamorphosed basement/cover sequence. These rocks record multiple, late Proterozoic to late Paleozoic deformation events (extension and compression) associated with the formation of the Iapetus Ocean and the Appalachian orogen ([References 206, 208, 209, 210, and 211](#)). The Blue

Ridge province consists of a series of westward-vergent thrust sheets, each with different tectonic histories and lithologies, including gneisses, plutons, and metavolcanic and metasedimentary rift sequences, as well as continental and platform deposits (see [References 203](#) and [206](#) for an expanded bibliography). The Blue Ridge–Piedmont fault system thrusts the entire Blue Ridge province northwest over Paleozoic sedimentary rock of the Valley and Ridge province during the Alleghanian orogeny ([References 212, 213, 214, and 215](#)). The Blue Ridge province reaches its greatest width in the southern Appalachians.

The Blue Ridge is divided into western and eastern portions. The western Blue Ridge consists of an assemblage of Middle Proterozoic crystalline continental (Grenville) basement rock nonconformably overlain by Late Proterozoic to Early Paleozoic rift-facies sedimentary rock ([Reference 203](#)). The basement consists of various types of gneisses, amphibolite, gabbroic and volcanic rock, and metasedimentary rock. Grenville basement rock is metamorphosed to granulite or uppermost amphibolite facies ([Reference 203](#)). The calculated radiometric ages of these rocks generally range from 1,000 to 1,200 million years old (Ma) (e.g., [References 216, 217, and 218](#)). The rifting event during the Late Proterozoic through Early Paleozoic that formed the Iapetus Ocean is recorded in the terrigenous, clastic, rift-drift sedimentary sequence of the Ocoee Supergroup and Chillhowie Group (e.g., [References 219, 220, 221, 222, 223](#)). Taconic and possibly Acadian deformation and metamorphism later affected these rocks, along with the basement and sedimentary cover. The entire composite thrust sheet was transported west as an intact package during the Alleghanian collision event on the Blue Ridge–Piedmont thrust.

The eastern Blue Ridge comprises metasedimentary rocks originally deposited on a continental slope and rise and ocean floor metasedimentary rocks in association with oceanic or transitional to oceanic crust (for expanded bibliography see [References 203 and 224](#)). This is in contrast to the western Blue Ridge that contains metasedimentary rocks, thereby suggesting continental rift-drift facies of a paleomargin setting. The eastern Blue Ridge is structurally complex, with several major thrust faults, multiple fold generations, and two high-grade metamorphic episodes ([Reference 203](#)). Metamorphism occurred during the Taconic and possibly Acadian orogenies. The stratigraphy within the eastern Blue Ridge includes rare Grenville (Precambrian) gneisses, metasedimentary rocks of the Tallulah Falls Formation and the Coweeta Group, metamorphosed Paleozoic granitoids, and mafic and ultramafic complexes and rocks of the Dahlonga Gold Belt. The Paleozoic granitoids are part of a suite of similar granites found in the western Inner Piedmont, suggesting a common intrusive history. Metasedimentary rock sequences in the eastern Blue Ridge are correlated along strike as well as across some thrust fault boundaries, also suggesting a commonality in the original depositional history. Based on geochemical data, the mafic and ultramafic complexes found in particular thrust sheets in the eastern Blue Ridge have oceanic as well as continental affinities. However, their exact tectonic origin is not clear because the contacts with the host metasedimentary rock are obscure. The Brevard fault zone forms the southeastern boundary of the Blue Ridge with the Inner Piedmont.

2.5.1.1.1.4 The Piedmont Physiographic Province

The Lee Nuclear Site is located in the Piedmont physiographic province. The Piedmont physiographic province extends southwest from New York State to Alabama and lies west of and adjacent to the Atlantic section of the Coastal Plain. It is the easternmost physiographic province of the Appalachian Mountains. The Piedmont is a seaward-sloping plateau varying in width from about 10 mi. in southeastern New York State to almost 125 mi. in South Carolina; it is the least rugged of the Appalachian provinces. Elevation of the inland boundary ranges from about 200 ft. msl in New Jersey to over 1,800 ft. msl in South Carolina.

Within the Lee Nuclear Site region, the area of the Piedmont physiographic province is also divided on the basis of its geologic history and lithology into different lithotectonic associations, which include the Carolina Zone and the Piedmont Zone.

The Carolina Zone is also referred to in more recent literature as "Carolinia" (Hibbard et al. (2006 and 2007) (References 260 and 428)) or as the "Carolina Superterrane" (Hatcher et al. (2007) (Reference 404)). The terranes that compose the Carolina Zone are all considered to be of peri-Gondwanan association and are representative of volcanic arcs resulting from subduction in the Gondwanan realm of Iapetus (Hibbard et al. (2006) (Reference 260); Hibbard et al. (2007) (Reference 428); Hatcher et al. (2007) (Reference 404)). In detail, there is disagreement in the assignment of some terranes into this division. For instance, Hibbard et al. (2002) (Reference 204) consider the Gaffney terrane (i.e., the Kings Mountain terrane of Hatcher et al. (2007) (Reference 404)) to be exclusively of peri-Gondwanan association. However, Hatcher et al. (2007) (Reference 404) consider the Kings Mountain terrane to have both Laurentian and peri-Gondwanan associations. Recent detrital zircon work has shown that portions of the Kings Mountain terrane are as young as late Middle Cambrian, younger than previously thought (Reference 438).

These two lithotectonic elements, the Piedmont and Carolina zones, are separated by a series of faults collectively referred to as the Central Piedmont Shear Zone.

West of the Central Piedmont Shear Zone, the Piedmont Zone contains the Inner Piedmont block, the Smith River allochthon of Virginia and North Carolina, and the Sauratown Mountains anticlinorium in north central North Carolina (Reference 226) (Figure 2.5.1-202a). The province is a composite stack of thrust sheets containing a variety of gneisses, schists, amphibolite, sparse ultramafic bodies, and intrusive granitoids (References 227 and 228). The protoliths are immature quartzo-feldspathic sandstone, pelitic sediments, and mafic lavas.

The Inner Piedmont block is a fault-bounded, composite thrust sheet with metamorphic complexes of different tectonic affinities (Reference 226). Rocks within the Inner Piedmont block include gneisses, schists, amphibolites, sparse ultramafic bodies, and intrusive granitoids (References 227 and 228). There is some continental basement within the block (Reference 228) and scattered mafic and ultramafic bodies and complexes (Reference 229), suggesting the presence

of oceanic crustal material ([Reference 226](#)). The remainder of the block contains a coherent, though poorly understood, sequence of metasedimentary rock, metavolcanic gneisses, and schists ([Reference 226](#)).

The Smith River allochthon is a completely fault-bounded terrane that contains two predominantly metasedimentary units and a suite of plutonic rocks ([Figure 2.5.1-202b](#)). The Sauratown Mountains anticlinorium is a complex structural window of four stacked thrust sheets exposed in eroded structural domes ([Figure 2.5.1-202b](#)). Each sheet contains Precambrian basement with an overlying sequence of younger Precambrian to Cambrian metasedimentary and metaigneous rocks ([Reference 226](#)).

The stratigraphic and structural geologic data in the Western Piedmont reflect complex tectonic history from the Precambrian Grenville through Late Paleozoic Alleghanian orogenies. Metamorphism affected the basement rocks of the Sauratown Mountains anticlinorium at least twice: during the Precambrian Grenville orogen and later during the Paleozoic. A metamorphic event in the Paleozoic affected the metasedimentary cover sequence, the Smith River allochthon, and the Inner Piedmont block ([Reference 226](#)). The Alleghanian continental collision is reflected in the thrust and dextral strike slip fault systems such as the Brevard and Bowens Creek fault zones. A few late Paleozoic granites were emplaced in the Inner Piedmont block; however, the majority lies further east in the Carolina Zone. Early Mesozoic extension resulted in the formation of rift basins (Dan River and Davie County basins).

The Central Piedmont shear zone ([Reference 225](#)) ([Figure 2.5.1-202a](#)) includes the Ocmulgee, Middleton-Lowndesville, Cross Anchor, Kings Mountain, Eufola, and Hyco fault zones (Hibbard et al. (2006) ([Reference 260](#)) and Hatcher et al. (2007) ([Reference 404](#))). Since the Central Piedmont Shear Zone marks the boundary between rocks on both sides of Iapetus, it is associated with a "suture," (Hatcher et al. (2007) ([Reference 404](#))) although the polarity and timing of the subduction and suturing event are under debate, (Hibbard et al. (2007) ([Reference 428](#)); (Hatcher et al. (2007) ([Reference 404](#))). The detailed relationship of the Central Piedmont Shear Zone to the original structure associated with the suture is obscured by the fact that the original structure has been tectonically modified and overprinted by the final orogenic effects of the interactions of the Gondwanan and Laurentian continents during the Carboniferous (late Alleghanian orogeny). Hibbard et al. (2002) ([Reference 204](#)) and Hibbard et al. (2007) ([Reference 428](#)) consider the Central Piedmont Shear Zone to be a Late Alleghanian thrust that cut the original suture off in the subsurface and that the portion of the hanging wall containing the cut off suture has been eroded away (Hibbard et al. (1998) ([Reference 417](#))). Hatcher et al. (1989) ([Reference 429](#)) also consider that the Central Piedmont Shear Zone has been tectonically modified in the late Alleghanian orogeny, in large part by folding. This allows infolding of rocks with Laurentian affinities and rocks of peri-Gondwanan affinities to explain terranes considered to have mixed associations such as the Kings Mountain Terrane (Hatcher et al. (2007) ([Reference 404](#))).

The Lee Nuclear Site is located east of the Central Piedmont shear zone in the Carolina Zone (Hibbard et al. (2007) ([Reference 428](#)); (Carolina Superterrane of

Hatcher et al. (2007) (Reference 404)). The Carolina Zone represents an amalgamation of metaigneous-dominated terranes along the eastern flank of the southern Appalachians. The Carolina Zone and the terranes within the zone are intended to replace the archaic ‘belt’ terminology of the southern Appalachians (Reference 204). The Carolina terrane extends for more than 300 mi. from central Virginia to eastern Georgia and is characterized by generally low-grade metaigneous and metasedimentary rocks. The original definition of the Carolina terrane (Secor et al. 1983) (Reference 231) includes higher-grade metamorphic rocks along its western margin, but more recent classification (Reference 204) includes these rocks in the Charlotte terrane to the west.

The Lee Nuclear Site lies within the Charlotte terrane, the westernmost terrane of the Carolina Zone (Figure 2.5.1-202a). Neoproterozoic to Early Paleozoic plutonic rocks that intrude a suite of mainly metaigneous rocks dominate the Charlotte terrane (Reference 204). The rocks of the Carolina Zone are unconformably overlain by sediments of the Carolina Coastal Plain southeast of the Fall Line (Figure 2.5.1-202a).

The Carolina Zone is part of a late Precambrian–Cambrian composite arc terrane, exotic to North America (References 231 and 238), and accreted either during the Ordovician to Silurian (Hibbard et al. (2002) (Reference 204)) or during the Middle Devonian to Early Mississippian (Hatcher et al. (2007) (Reference 404)) sometime during the Ordovician to Devonian Period (Reference 239); (Reference 240). It comprises felsic to mafic metaigneous and metasedimentary rock. Middle Cambrian fossil fauna indicate a European or African affinity for the Carolina Zone (Reference 231).

Hibbard et al. (2002) (Reference 204) propose updated nomenclature for the Carolina Zone (“Carolinia” in Hibbard et al. (2006)) (Reference 260) based on the tectonothermal overprint of units. Suprastructural terranes (i.e., the upper structural layer in an orogenic belt subjected to relatively shallow or near-surface processes) comprise rocks of lower-grade metamorphism where original rock fabric is preserved. Infrastructural terranes (produced at relatively deep crustal levels at elevated temperature and pressure, located beneath suprastructural terranes) comprise higher-grade metamorphic units where original rock fabric has been completely destroyed.

The western part of the Carolina Zone in central Georgia, South Carolina, and North Carolina consists of the infrastructural Charlotte terrane and, to a lesser extent, the Savannah River terrane. The easternmost portion of the Carolina Zone in South Carolina and portions in North Carolina contains the Suprastructural Albemarle and South Carolina Sequence (Figure 2.5.1-202a). Metamorphic grade increases to the northwest from lower greenschist facies to upper amphibolite facies. Rocks include amphibolite, biotite gneiss, hornblende gneiss, and schist, and likely derived from volcanic, volcanoclastic, or sedimentary protoliths. Structures of Pre-Alleghanian age are predominantly northeast-trending, regional-scale folds with steeply dipping axial surfaces. The country rock of the Charlotte terrane was penetratively deformed during the Late Proterozoic to Early Cambrian (Hibbard et al. (2002) (Reference 204)), thereby producing axial plane cleavage

and foliation ([Reference 203](#)). The Charlotte terrane also contains numerous granitic and gabbroic intrusions dating to about 300 Ma.

2.5.1.1.1.5 The Atlantic Coastal Plain Physiographic Province

The Atlantic section of the Coastal Plain physiographic province extends southeastward from the Fall Line to the coastline, and southwestward from Cape Cod, Massachusetts to south-central Georgia where it merges with the Gulf section of the Coastal Plain. The Atlantic section of the Coastal Plain is a low-lying, gently rolling terrain developed on a seaward-dipping section of Cretaceous and younger semi-consolidated sedimentary rocks. Coastal Plain sediments generally thicken coastward. Sediment thickness at the New Jersey coastline is about 4,000 ft., increasing southward to as much as 8,000 ft. along the coast of Maryland and about 10,000 ft. along the coast of North Carolina. At the latitude of the Lee Nuclear Site, sediment thickness increases from zero at the Fall Line to about 4,000 ft. at the South Carolina coastline. Topographic relief is generally less than a few hundred feet, and the topographic gradient is usually less than about 5 ft/mi.

2.5.1.1.1.6 Mesozoic Rift Basins

Mesozoic-age rift basins are found along the entire eastern continental margin of North America from Nova Scotia to the Gulf Coast. The basins formed in response to the continental rifting that broke up the supercontinent Pangea and led to the formation of the Atlantic Ocean basin. Rift basins are locally exposed in the Piedmont province, generally buried beneath Coastal Plain sediments, and some basins are located offshore. Structurally, the basins are grabens or half-grabens generally elongated in a northeast direction and bounded by normal faults on one or both sides ([Reference 242](#)). Some basins are localized along reactivated Paleozoic fault zones ([References 243, 244, 245, 246, and 247](#)).

The basins are located in extended or rifted continental crust. The western boundary of this zone of extended crust is defined by the western-most edge of Triassic–Jurassic onshore rift basins or the boundaries of the structural blocks in which they occur ([References 248 and 249](#)). The eastern boundary of the zone of extended crust is the continental shelf ([Reference 250](#)).

The rift basins generally are filled with sedimentary and igneous rocks. Sedimentary strata consist mainly of non-marine sandstone, conglomerate, siltstone, and shale. Carbonate rocks and coal are found locally in several basins. Igneous rocks of basaltic composition occur as flows, sills, and stocks within the basins and as extensive dike swarms within and outside the basins ([Reference 251](#)). Basin fill strata are named the Newark Supergroup and can be divided into three sections ([References 252 and 253](#)):

- The lowest section is characteristically fluvial ([References 254 and 255](#)) and contains reddish-brown, arkosic, coarse-grained sandstone and conglomerate.

- The middle section mainly includes sediments of lacustrine origin (Reference 254). These sediments include gray-black, fossiliferous siltstone, carbonaceous shale, and thin coal beds (Reference 253).
- The uppermost section is a complex of deltaic, fluvial, and lacustrine sediments (References 256 and 257). These sediments include red-brown siltstone, arkosic sandstone, pebble sandstone, red and gray mudstone, and conglomerate (Reference 253).

A number of Mesozoic rift basins are located within the Lee Nuclear Site region. These include the Florence, Dunbarton, South Georgia, Riddleville, Jedburg, Deep River, Dan River, and Crowburg basins, as well as additional unnamed basins.

2.5.1.1.2 Regional Tectonic Setting

The regional tectonic setting of the Lee Nuclear Site is presented below. This section includes discussions of regional tectonic stresses, regional gravity and magnetic data, geophysical anomalies and lineaments, principal regional tectonic structures, and regional seismicity.

2.5.1.1.2.1 Regional Geologic History

Numerous researchers have mapped the geology of the Lee Nuclear Site region. Figures 2.5.1-203a and 203b present geologic mapping by King and Beikman (1974) (Reference 258) [as digitized by Schruben et al. (1994) (Reference 259)]. A more recent compilation of Appalachian lithotectonic mapping compiled by Hibbard et al. (2006) (Reference 260) covers much of the Lee Nuclear Site region (Figures 2.5.1-204a and 204b).

The Lee Nuclear Site lies within the southern part of the northeast-southwest-trending Appalachian orogenic belt, which extends nearly the entire length of the eastern United States from southern New York State to Alabama. The Appalachian orogenic belt formed during the Paleozoic Era and records multiple orogenic events related to the opening and closing of the proto-Atlantic along the eastern margin of ancestral North America.

Prior to the Appalachian orogenies, the continental mass ancestral to North America (i.e., Laurentia) was locally deformed and metamorphosed. This deformational event is called Grenville orogeny and occurred about 1.1 billion years ago. Portions of Grenvillian crust are exposed as external massifs in crystalline thrust sheets of the Blue Ridge geologic province and also as an internal massif in the Sauratown Mountains window (Reference 261). Beginning about 750 to 700 Ma, continental rifting of Laurentia led to the opening of the Iapetus Ocean, which formed a new eastern margin of ancestral North America.

Subsequent closing of the Iapetus and other proto-Atlantic ocean basins resulted in the accretion of exotic terranes to the eastern margin of Laurentia. These accreted terranes were of different sizes and represented fragments of oceanic crust, volcanic island arcs, and other continental masses, each with its own

geologic history. This long period of ocean closing and continental accretion during the Paleozoic was punctuated by four episodes of compression (collision) and associated metamorphism and magmatism (Reference 261). These four episodes occurred in the Late Cambrian to Early Ordovician (Penobscottian orogeny), Ordovician (Taconic orogeny), Devonian (Acadian orogeny), and Pennsylvanian to Permian (Alleghanian orogeny).

The Grenville Front is the leading edge of a northeast-southwest-trending Precambrian collisional orogen that involved rocks of the pre-Appalachian basement of Laurentia. The following discussion is summarized from White et al. (2000) (Reference 264). Like the younger Appalachian orogen, the Grenville orogen may have formed in part from exotic terranes that were assembled prior to 1,160 Ma, then deformed and thrust westward over the pre-Grenville Laurentian margin between 1,120 and 980 Ma. The Grenville orogen and Grenville front are exposed primarily in southeastern Canada, and can be traced in outcrop southwest to the latitude of Lake Ontario. Grenville-age rocks and structures continue on trend to the southeast into the United States, but are depositionally and structurally overlain by younger rocks, including terranes of the Appalachian orogen (References 262 and 263). Seismic reflection profiles indicate that the Grenville front and other prominent reflectors generally dip toward the east and extend to lower crustal depths (Reference 264). Bollinger and Wheeler (1988) (Reference 265) note that lapetan normal faults that formed as a result of lapetan extension likely decrease in size, abundance, and slip northwestward from the Grenville front.

The Penobscottian event is the earliest major orogeny recognized in the Appalachian belt and primarily is expressed in the northern Appalachians. Horton et al. (1989) (Reference 201) states that evidence for the Penobscottian orogeny has not been observed south of Virginia, where the orogeny is bracketed in age between Late Cambrian metavolcanic rocks and an Early Ordovician pluton.

The earliest Paleozoic deformation along or adjacent to the ancestral North American margin at the latitude of the Lee Nuclear Site region occurred in the Middle Ordovician and is known as the Taconian event or orogeny. The onset of the Taconian event is marked regionally throughout much of the Appalachian belt by an unconformity in the passive-margin sequence and deposition of clastic sediments derived from an uplifted source area or areas to the east. Horton et al. (1989) (Reference 201) and Hatcher et al. (1994) (Reference 203) interpret the Taconic event at the latitude of the Lee Nuclear Site region as the result of the collision of one or more terranes with North America. Rocks of the eastern Blue Ridge and Inner Piedmont are interpreted to have originated east of the Laurentian passive margin in Middle Ordovician time and, thus, are candidates for Taconic collision(s).

Horton et al. (1989) (Reference 201) includes the eastern Blue Ridge at the latitude of the site in the Jefferson terrane, a large body of sandstones, shales, basalt, and ultramafic rocks interpreted to be a metamorphosed accretionary wedge that accumulated above a subduction zone. Hatcher et al. (1994) (Reference 203) suggests that the Hayesville thrust, which forms the western structural boundary of the eastern Blue Ridge and dips eastward beneath it, may

be the “up-dip leading edge of an early Paleozoic subduction zone.” If this interpretation is correct, then the Hayesville thrust fault may be a Taconic suture. Horton et al. (1989) (Reference 201) and Hatcher et al. (1994) (Reference 203) interpret the Carolina-Avalon terrane as accreted during the Taconic orogeny. If this is correct, then the Towaliga fault between the Inner Piedmont and Carolina-Avalon terranes may be a Taconic structure.

According to Horton et al. (1989) (Reference 201), evidence for the middle Paleozoic Acadian orogeny is “neither pervasive nor widespread” south of New England. The Acadian event primarily is expressed at the latitude of the study region by unconformities in foreland stratigraphic succession, plutonism, and activity of several major faults (Hatcher et al. 1994) (Reference 203), and possibly ductile folding elsewhere in the southern Appalachians (Reference 201). To date, there is no compelling evidence for a major accretion event at the latitude of the Lee Nuclear Site region during the Acadian orogeny (References 201 and 203).

The final and most significant collisional event in the formation of the Appalachian belt is the late Paleozoic Alleghanian orogeny, during which Gondwana collided with Laurentia, closing the intervening Paleozoic ocean basin. At the latitude of the Lee Nuclear Site region, the Alleghanian collision telescoped the previously accreted Taconic terranes and drove them westward up and across the Laurentian basement, folding the passive margin sequence before them and creating the Valley and Ridge fold-and-thrust belt. The collisional process also thrust a fragment from the underlying Laurentian basement eastward over the passive margin sequence, forming the western Blue Ridge. Significant strike-slip faulting and lateral transport of terranes are interpreted to have occurred during the Alleghanian orogeny (Reference 203). According to Horton and Zullo (1991) (Reference 261), the evident effects of the Alleghanian orogeny in the Carolinas include:

- Numerous granitoid plutons southeast of the Brevard fault zone.
- Amphibolite-facies regional metamorphism and deformation in the Kiokee and Raleigh metamorphic belts of the eastern Piedmont.
- Strike-slip movement, along major faults from the Brevard fault zone southeastward to the eastern Piedmont fault system.
- Westward transport of a composite stack of crystalline thrust sheets which now constitutes the western Piedmont and Blue Ridge.
- Imbricate thrusting and folding in the Valley and Ridge province occurred during this orogeny.

Despite uncertainties regarding the precise origin, emplacement, and boundaries of belts and terranes, there is good agreement among tectonic models regarding first-order structural features of the southern Appalachian orogenic belt. At the latitude of the Lee Nuclear Site region, the ancestral North American basement of the Paleozoic passive margin underlies the Valley and Ridge, Blue Ridge, and Inner Piedmont provinces at depths of less than 6 to 9 mi., and possibly as

shallow 3 mi. or less beneath the Valley and Ridge. A basal decollement along the top of the North American basement is the root zone for Paleozoic thrust faults in the Valley and Ridge, Blue Ridge, and Inner Piedmont provinces. Although potential seismogenic sources may be present within the North American basement below the decollement ([References 265 and 267](#)), the locations, dimensions, and geometries of these deeper potential sources are not necessarily expressed in the exposed fold-thrust structures above the detachment. More recent geomorphic analyses of fluvial systems in the southern Appalachians of western Tennessee suggest that topographic relief associated with the Blue Ridge escarpment may be responding to mantle forcing ([Reference 439](#)).

The modern continental margin includes Mesozoic rift basins that record the beginning of extension and continental rifting during the early to middle Mesozoic leading to the formation of the current Atlantic Ocean. During the later stage of rifting (early Jurassic), the focus of extension shifted eastward to the major marginal, proto-Atlantic ocean basins. Eventually, rifting of continental crust ceased as sea floor spreading began in the Atlantic spreading center sometime around 175 Ma ([Reference 248](#)). The oldest ocean crust in contact with the eastern continental margin is late middle Jurassic ([Reference 266](#)). The significance of the age of transition from rifting to sea floor spreading is that the tectonic regime of rifting is no longer acting on the continental crust along the Eastern Atlantic margin.

Wheeler (1995) ([Reference 267](#)) suggests that many earthquakes in the eastern part of the Piedmont province and beneath the Coastal Plain province may be associated spatially with buried normal faults related to rifting that occurred during the Mesozoic Era. Normal faults in this region that bound Triassic basins may be listric into the Paleozoic detachment faults ([Reference 268](#)) or may penetrate through the crust as high-angle faults. No definitive correlation of seismicity with Mesozoic normal faults has been conclusively demonstrated. However, the CEUS SSC model ([Reference 441](#)) characterized these areas as two seismotectonic zones as discussed in [Subsection 2.5.1.1.3](#).

After the continental extension and rifting ended, a prograding shelf-slope began to form over the passive continental margin. The offshore Jurassic–Cretaceous clastic-carbonate bank sequence covered by younger Cretaceous and Tertiary marine sediments, and onshore Cenozoic sediments, represents a prograding shelf-slope and the final evolution to a passive margin ([Reference 203](#)). Cretaceous and Cenozoic sediments thicken from near zero at the Fall Line to about 4,000 ft. at the South Carolina coast. The fluvial-to-marine sedimentary wedge consists of alternating sand and clay with tidal and shelf carbonates common in the downdip Tertiary section.

2.5.1.1.2.2 Tectonic Stress in the Mid-Continent Region

Since the 1980's, researchers have assessed and compiled available stress data for the central and eastern United States, including well-bore breakouts, results of hydraulic fracturing studies, in situ stress measurements and earthquake focal mechanisms ([References 270, 271, 272, 440](#)). The most recent compilations as part of the CEUS SSC project confirm previous work that indicates the prevailing

stress field in the midcontinent is east-northeast to northeast maximum horizontal stress direction, with no strong evidence for stress subprovinces (Reference 441). This is consistent with the theoretical trend of compressive forces acting on the North American plate from the mid-Atlantic Ridge (Reference 272). As shown in Figure 2.5.1-245, data are ranked in terms of quality (A being the highest quality and C the being the lowest quality) and tectonic regime is characterized as normal, thrust, strike-slip or unknown (Reference 441).

In addition to better documenting the orientation of stress, research addresses quantitatively the relative contributions of various forces that may be acting on the North American plate to the total stress within the plate. Richardson and Reding (1991) (Reference 273) describe the results of numerical modeling of stress in the continental U.S. interior and consider the contribution to total tectonic stress to be from three classes of forces:

- Horizontal stresses that arise from gravitational body forces acting on lateral variations in lithospheric density. These forces commonly are called buoyancy forces. Richardson and Reding (1991) (Reference 273) emphasize that what is commonly called ridge-push force is an example of this class of force. Rather than a line-force that acts outwardly from the axis of a spreading ridge, ridge-push arises from the pressure exerted by positively buoyant, young oceanic lithosphere near the ridge against older, cooler, denser, less buoyant lithosphere in the deeper ocean basins (Reference 274). The force is an integrated effect over oceanic lithosphere ranging in age from about 0 to 100 Ma (Reference 275). The ridge-push force transmits as stress to the interior of continents by the elastic strength of the lithosphere.
- Shear and compressive stresses transmit across major plate boundaries (strike-slip faults and subduction zones).
- Shear tractions acting on the base of the lithosphere from relative flow of the underlying asthenospheric mantle.

Richardson and Reding (1991) (Reference 273) concludes that the observed northeast-southwest trend of principal stress in the CEUS dominantly reflects ridge-push forces. They estimate the magnitude of these forces to be about 2 to 3×10^{12} Newtons per meter (i.e., the total vertically integrated force acting on a column of lithosphere 3.28 ft [1 m] wide), which corresponds to average equivalent stresses of about 40 to 60 megapascals (MPa) distributed across a 30-mi.-thick elastic plate. Richardson and Reding (1991) (Reference 273) find that the fit of the model stress trajectories to data is improved by adding compressive stress (about 5 to 10 MPa) acting on the San Andreas fault and Caribbean plate boundary structures. The fit of the model stresses to data further indicates that shear stresses acting on these plate boundary structures must also be in the range of 5 to 10 MPa.

Richardson and Reding (1991) (Reference 273) note that numerical models that assume horizontal shear tractions acting on the base of the North American plate

reproduce the general northeast-southwest orientation of principal stress in the CEUS. Richardson and Reding (1991) (Reference 273) do not favor this as a significant contributor to total stress in the mid-continent region because their model would require an order-of-magnitude increase in the horizontal compressive stress from the eastern seaboard to the Great Plains.

2.5.1.1.2.3 Gravity and Magnetic Data of the Site Region and Site Vicinity

In 1987, the Geological Society of America published regional maps of the gravity and magnetic fields in North America as part of the Society's Decade of North American Geology (DNAG) project. These maps include the Committee for the Gravity Anomaly Map of North America (Reference 276) and the Committee for the Magnetic Anomaly Map of North America (Reference 277). The maps present the potential field data at 1:5,000,000-scale and are useful for identifying and assessing regional gravity and magnetic anomalies with wavelengths on the order of about 6 mi. or greater. Published maps of the gravity and aeromagnetic fields for the state of South Carolina (Reference 278) and the digital data from these maps are the basis of the gravity and magnetic maps in Figures 2.5.1-205 and 2.5.1-206, respectively as these data provide higher resolution than the regional datasets. Gravity and magnetic data were incorporated in the DNAG E-4 crustal transect, which traverses the Appalachian orogen to the northeast of the Lee Nuclear Site (Figure 2.5.1-207). The DNAG E-4 transect extends from central Kentucky to the Carolina trough in the offshore Atlantic basin, just north of the South Carolina-North Carolina state line (Reference 282) and passes a few miles to the northeast of the Lee Nuclear Site. Figure 2.5.1-207 presents geologic and potential field data from the DNAG E-4 transect. As part of the CEUS SSC database development, regional gravity and magnetic data were reprocessed and published as part of the CEUS SSC database (Reference 441). Because the 1987 data were incorporated in the DNAG E-4 transect and provide a useful reference to regional crustal structures and lithology, the CEUS SSC gravity and magnetic field data were overlain on the DNAG E-4 transect as shown on Figure 2.5.1-207.

2.5.1.1.2.3.1 Gravity Data of the Site Region and Site Vicinity

The gravity profile along the DNAG E-4 (Reference 276) crustal transect (Figure 2.5.1-207), documents a long-wavelength anomaly east of the Brevard fault zone. The Brevard fault zone marks the tectonic boundary between the Blue Ridge province to the west and the Piedmont province to the east (Figure 2.5.1-201). Bouguer gravity values increase by about 80 to 120 milliGals (mGal) across an approximately 125 to 155 mi. reach of the Piedmont east of the Blue Ridge (Figure 2.5.1-207). As shown on Figure 2.5.1-207, this gradient is present across the Piedmont physiographic province along much of the length of the Appalachian belt.

Previous workers refer to this long-wavelength feature in the gravity field as the "Piedmont gradient" (References 279 and 280). At the latitude of Virginia, north of the Lee Nuclear Site region, Harris et al. (1982) (Reference 279) interpret the Piedmont gradient to reflect the eastward thinning of the North American continental crust and associate positive relief on the Moho with proximity to the

Atlantic margin. Gravity models by Iverson and Smithson (1983) (Reference 281) along the southern Appalachian COCORP (Consortium for Continental Reflection Profiling) seismic reflection profile, and by Dainty and Frazier (1984) (Reference 280) in northeastern Georgia, suggest that the gradient likely arises from both eastward thinning of continental crust and the obduction of the Inner Piedmont and Carolina-Avalon terranes. These terranes have higher average densities than the underlying Precambrian basement of North America. The Lee Nuclear Site is located just northwest of the location where the gradient starts to flatten out as it passes into the Carolina – Avalon terrane to the east (Figure 2.5.1-207).

Superimposed on the long-wavelength Piedmont gradient are numerous high and low gravity anomalies that have wavelengths of about 6 to 12 mi., and are elliptical to irregular in plan view. These anomalies are especially well expressed in the Carolina-Avalon terrane (per Reference 203) to the south of the Lee Nuclear Site between the Central Piedmont shear zone and the Modoc shear zone (Figure 2.5.1-205). Based on comparison of the gravity maps with geologic maps, many of these anomalies are spatially associated with Paleozoic igneous intrusions and plutons. The basement of the Carolina-Avalon terrane at this latitude is interpreted as the crust of an oceanic island arc terrane or terranes that was accreted to the Appalachian orogen during the Taconic orogeny (References 201 and 203). The composition of this crust generally is intermediate between felsic and mafic (Reference 282). The intrusions and plutons in the Carolina-Avalon terrane with associated gravity anomalies fall more toward the extremes in felsic and mafic compositional ranges for igneous rocks. This gives rise to density contrasts with the country rock they intrude. In general, gravity highs are associated with mafic intrusions and mafic basement rocks, and gravity lows are associated with granitic plutons. Detailed gravity modeling by Cumbest et al. (1992) (Reference 283) in the vicinity of the Savannah River Site supports the general association of 6- to 12-mi.-high and -low anomalies in the Piedmont gravity field with mafic and felsic intrusions, respectively.

The origin of the high and low gravity anomalies beneath the Coastal Plain southeast of the Lee Nuclear Site (Figure 2.5.1-205) is uncertain due to lack of data on basement rock composition. Several high gravity anomalies appear to be associated with Triassic basin structures approximately 60 to 90 mi. southeast of the Lee Nuclear Site. A possible analogue for interpreting these anomalies is the well-studied Triassic Dunbarton basin beneath the Savannah River Site south of the Lee Nuclear Site. As shown on Figure 2.5.1-205, there is a pronounced gravity high along the southern margin of the Dunbarton basin. From a synthesis of borehole data and gravity modeling, Cumbest et al. (1992) (Reference 283) demonstrate that the extremes in the local gravity field at the Savannah River Site are highs associated with Triassic-Jurassic mafic intrusive complexes southeast of the Dunbarton basin, and lows associated with granitic plutons mapped to the north-northeast and east-northeast of the basin. Cumbest et al. (1992) (Reference 283) show that the predicted anomaly associated with the Mesozoic Dunbarton basin fill is a subordinate feature of the gravity field compared to the anomalies associated with the plutons and mafic intrusions. If similar geologic relations apply for the Triassic basins southeast of the Lee Nuclear Site, then it is likely that the high gravity anomalies are associated with Triassic mafic intrusions.

Gravity lows associated with the basin fill strata may be obscured by the relatively high amplitude of the anomalies associated with the mafic rocks.

Gravity data for the Lee Nuclear Site vicinity are coarse (spacing approximately 4 mi.), with consequent low-resolution information available for the gravity field (Figure 2.5.1-208). The site is located on a long wavelength gravity gradient of about 2 mGal/mi. that marks the transition from the relative gravity lows of the Inner Piedmont to the high field elliptical anomalies that represent the denser crustal components contained in the Carolina Zone. Across the site area the regional field ranges from about -42 mGal in the west to -30 mGal in the east (Figure 2.5.1-208). The regional gravity field is marked by approximately 25 mi. wavelength undulations, of about 5-mGal amplitude, as the regional gradient flattens and steepens slightly. The site occurs in the trough of one of these features. Correlation of the detailed response of the gravity field to specific features in the site area is unresolved due to the poor data density.

To summarize, gravity data published since the mid-1980s including the data reprocessed as part of the CEUS SSC database development, document that long-wavelength anomalies in the vicinity of the Lee Nuclear Site are characteristic of large parts of the Appalachian belt (References 276 and 441). Furthermore, these data reflect first-order features of the various provinces and accreted Paleozoic terranes, as well as west-to-east thinning of the ancestral North American continental crust. The dominant short-wavelength characteristics of the gravity field in the vicinity of the Lee Nuclear Site are gravity highs and lows associated with mafic and granitic intrusions, respectively.

In general, there is better spatial correlation in the Lee Nuclear Site study region among gravity anomalies and igneous intrusions than faults. The exceptions are the Paleozoic Modoc shear zone and the Brevard zone. The Modoc shear zone appears to separate higher density rocks to the northwest from lower density rocks to the southeast. The Brevard zone marks the western boundary of the Piedmont gravity gradient. The juxtaposition of basement terranes with varying densities across these faults occurred during the Paleozoic Alleghanian orogeny (Reference 203), and therefore does not reflect Cenozoic activity. The mapped trace of the southern segment of the East Coast fault system (ECFS) is not expressed in the gravity field and cuts across anomalies with wavelengths on the order of tens of miles without noticeable perturbation. This implies that the southern segment of the ECFS, if present, has not accumulated sufficient displacement to systematically juxtapose rocks of differing density, and thus produce an observable gravity anomaly at the scale of Figure 2.5.1-205.

2.5.1.1.2.3.2 Magnetic Data of the Site Region and Site Vicinity

In contrast to the gravity data, the magnetic field does not exhibit a long-wavelength anomaly east of the Brevard fault zone coincident with the accreted Taconic terranes of the Piedmont. As shown on the magnetic profile for the DNAG E-4 transect (Figure 2.5.1-207), the magnetic field across the Piedmont generally is characterized by high and low anomalies with wavelengths on the order of about 3 to 6 mi. Key features of the regional magnetic field include the following:

- The western Piedmont between the Brevard fault zone and Central Piedmont shear zone is characterized by a relatively uniform to smoothly varying magnetic field about a background value of approximately –500 nanotesla (nT) (Figures 2.5.1-206 and 2.5.1-207).
- The Carolina-Avalon terrane east of the Central Piedmont shear zone is characterized by numerous circular, elliptical, and irregular anomalies with plan dimensions on the order of about 3 to 12 mi. The change in character between the magnetic field of the Inner Piedmont and Carolina-Avalon terrane is very distinct across the Central Piedmont shear zone. Comparison of the magnetic data to geologic mapping indicates that the majority of these anomalies are associated with mafic and felsic intrusions or with zones of hydrothermal alteration resulting in magnetite mineralization associated with stratiform ores.
- The Modoc shear zone is clearly associated with elongate, east-northeast trending high and low magnetic anomalies. This is also characteristic of several other nearby Paleozoic faults that can be clearly traced under the Coastal Plain cover (i.e., faults of the Eastern Piedmont fault system.) The very short wavelengths and linear trends of the anomalies are characteristic of those produced by a susceptibility contrast across a dipping structural contact (Reference 283).
- Regionally extensive magnetic anomalies occur beneath the Coastal Plain east of the Modoc shear zone. The magnetic anomalies are relatively high, indicating the presence of rocks with higher magnetic susceptibility at depth, and they are paired with high gravity anomalies (Figures 2.5.1-205 and 2.5.1-206), indicating that the rocks are also relatively dense. Detailed modeling of magnetic data from the Savannah River Site on the South Carolina-Georgia border south of the Lee Nuclear Site indicates that these anomalies may be associated with mafic intrusions (Reference 283). Felsic plutons in this region are inferred to exist from borehole data and gravity modeling. These felsic plutons have modest susceptibility contrasts with the country rock they intrude and thus do not generate high-amplitude magnetic anomalies (Reference 283). Similarly, Mesozoic basin sediments are inferred to have relatively low susceptibility contrasts with the pre-intrusive basement rock. Modeling by Cumbest et al. (1992) (Reference 283) suggests that the anomaly associated with the sediments and margins of the Dunbarton basin is a second-order feature of the magnetic field relative to the amplitudes of the anomalies produced by the intrusive mafic rocks.

Several of the characteristics of the regional magnetic field and its relation to geology are illustrated in the magnetic field for the site vicinity (Figure 2.5.1-233) and on a northwest-southeast-trending profile that passes through the Lee Nuclear Site (Figure 2.5.1-208). The magnetic field for the site vicinity is modeled on a 1,312 ft. (400 m) grid that is based on flight lines spaced one mile apart, flown at 500 ft. above the ground surface, in an east-west orientation. The magnetic intensities northwest of the Central Piedmont Shear Zone are relatively

low compared to the magnetic field characterized by intense northeast trending magnetic highs and lows to the southeast. This expression in the magnetic field results from the exposures of mafic to intermediate composition metavolcanic basement rocks of the Charlotte terrane to the southeast and the relative lack of intense magnetic sources in the Inner Piedmont terrane to the northwest. In the site vicinity, the difference in the response of the magnetic field does not occur abruptly at the boundary between the Charlotte terrane and the Inner Piedmont (Central Piedmont Shear Zone), but is transitional over about a mile east of the Central Piedmont Shear Zone. This behavior has been attributed to a Central Piedmont Shear Zone that dips relatively shallowly to the east so that the rocks of the Charlotte terrane form a thin, easterly thickening upper plate over the Inner Piedmont (Milton (1981) (Reference 408); (Hatcher et al. (2007) (Reference 404)).

In the Charlotte terrane, southeast of the Central Piedmont Shear Zone, the northeast-trending fabric in the magnetic field defined by the intense magnetic highs and lows is interrupted by several elliptical shaped areas defined by a subdued magnetic response. Based on comparison with geologic maps, these subdued areas in the magnetic field correspond to late Paleozoic intrusions such as the Bald Rock, York and Clover plutons, and several related smaller intrusive bodies, which are felsic in composition and relatively nonmagnetic. In addition, other plutonic masses such as the Lowery's Pluton and the Greensboro Plutonic suite also correspond with subdued magnetic field response. Lowery's Pluton is part of the Silurian Concord suite (McSween et al. (1991) (Reference 409)). Although the Concord suite consists of mafic lithologies, Lowery's Pluton does not give rise to the intense magnetization present in the surrounding metavolcanic country rock. The faults within the Charlotte terrane such as the Tinsley Bridge fault and the Boogertown shear zone parallel the regional northeasterly trending magnetic fabric, and their magnetic signature and effects on the magnetic field are not readily apparent.

In a discussion of the Central Piedmont Suture, Hatcher et al. (2007) (Reference 404) noted a gravity and magnetic linear anomaly that they identified as possibly representing the trace of the subsurface northeastern extension of the Central Piedmont suture. This feature passed through the southeastern portions of the site vicinity approximately 12 miles southeast of the site (Figure 2.5.1-233).

The data within the site area reveal several elongate to elliptical dipole anomalies that are characterized by magnetic highs of various amplitudes, with associated magnetic lows to the northwest. The elongation direction and alignment of the magnetic highs form prominent northeast to north-northeasterly striking linear features throughout the site area (Figure 2.5.1-206). One of the most prominent linear anomalies trends northeast–southwest and is formed by several individual, elongate magnetic highs in the northern portion of the site area. The most salient anomaly of this group (Shown as A on Figure 2.5.1-234) that comprises this feature has amplitude of about 300 nT and is located about 3.5 mi. northwest of the site (near the town of Cherokee Falls, South Carolina). This anomaly is accompanied to the northeast by two anomalous highs (about 180 nT) and to the southwest by a 50 nT high. The linear alignment generally follows the regional geologic trend and the southeastern flank of the Cherokee Falls synform (discussed in Subsection 2.5.1.2.4.1). This coincides with the location of stratiform

iron deposits of massive and disseminated magnetite and other metallic sulphides (References 284 and 285).

Adjacent to and just southeast of the anomaly that marks the northeastern termination of the linear feature discussed above, an elongate magnetic high of about 230 nT (Shown as B on Figure 2.5.1-234) is oriented in a more northerly direction at a relatively high angle to the regional geologic trend. This location is closely associated with a zone of alteration as shown by Howard (2004) (Reference 286). The anomaly is parallel to a reentrant of the zone of alteration into the crystal metatuff unit to the south. Several small outcrops of diabase also occur in this area. The relatively high amplitude of the anomaly and the presence of the alteration zone suggest that concentrations of magnetite due to hydrothermal alteration are present and account for a significant amount of the magnetic response. However, the alignment of diabase outcrops in this area may exert some control on the orientation of this feature.

A 70 nT circular magnetic high is located about 3 mi. northeast of the site (Shown as C on Figure 2.5.1-234). This feature is accompanied by a more elongate north-northeasterly trending magnetic high to the south that shows amplitude of approximately 60 nT. These locations both correspond to diabase outcrops and are likely the magnetic response of these mafic lithologies. In contrast, the metagabbro unit just southwest of these anomalies only produces a slight bending of the magnetic contours. This is a consistent magnetic response compared to that of the mafic units of Lowery's Pluton, as discuss above. However, the association of the metagabbro with the Concord Suite is not demonstrated.

An elongate magnetic high (amplitude about 120 nT) is located about 2.5 mi. south of the site (Shown as D on Figure 2.5.1-234). This anomaly trends northeasterly, concordant with the regional geologic trend, and coincident with quartzite outcrops. The magnetic signature of this feature is likely the result of magnetite and other metallic sulphides associated with hydrothermal alteration.

To summarize, magnetic data published since the mid-1980s, including reprocessed data for the CEUS SSC database (Reference 441), provide additional characterization of the magnetic field in the Lee Nuclear Site region (Reference 277). The first-order magnetic anomalies are associated primarily with northeast-southwest-trending Paleozoic terranes of the Paleozoic Appalachian orogen. Superimposed on this regional magnetic field are anomalies with wavelengths on the order of 3 to 12 mi. that are associated with intrusive bodies or stratiform ore bodies resulting from hydrothermal alteration. The anomalous response of concentrations of magnetite associated with stratiform metallogenic deposits typically produce anomaly amplitudes of 100 to 300 nT, and are typically aligned with the regional geologic trend. Diabase dikes and other small outcrops produce secondary anomalous effects with amplitudes of about 50 nT. The metagabbro unit located about one mile east of the Lee Nuclear Site produces minimal effects on the magnetic field, and this response is consistent with the magnetic signature of Lowery's Pluton further to the southeast in the site vicinity.

The magnetic data generally are not of sufficient resolution to identify or map discrete faults such as border faults along the Triassic basins. In particular, the

southern segment of the ECFS has no expression in the magnetic field and cuts across anomalies with wavelengths on the order of tens of miles without noticeably perturbing or affecting them. If the ECFS exists as mapped, then it has not accumulated sufficient displacement to juxtapose rocks of varying magnetic susceptibility, and thus does not produce an observable magnetic anomaly at the scale of [Figure 2.5.1-206](#).

2.5.1.1.2.4 Principal Regional Tectonic Structures

Principal tectonic structures and features in the southeastern U.S. and within the 200 mi. Lee Nuclear Site region can be divided into four categories based on their age of formation or reactivation as shown in [Figures 2.5.1-209](#) and [210](#). These categories include structures that were most active during Paleozoic, Mesozoic, Cenozoic, or Quaternary time. Most of the Paleozoic and Mesozoic structures are regional in scale, and are geologically and geophysically recognizable. The Mesozoic rift basins and bounding faults show a high degree of parallelism with the structural grain of the Paleozoic Appalachian orogenic belt, which generally reflects reactivation of pre-existing Paleozoic structures. Tertiary and Quaternary structures are generally more localized and may be related to reactivation of portions of older bedrock structures.

2.5.1.1.2.4.1 Regional Geophysical Anomalies and Lineaments

A number of regional geophysical anomalies are located within 200 mi. of the Lee Nuclear Site ([Figures 2.5.1-209](#), [210](#) and [211](#)). From southeast to northwest these include the East Coast Magnetic Anomaly, the southeast boundary of Iapetan normal faulting, Clingman lineament, Ocoee lineament, New York-Alabama lineaments, the Appalachian gravity gradient, the northwest boundary of Iapetan normal faulting, Appalachian thrust front, and the Grenville Front. These features are described below, with more detail provided for those features within the 200-mi site region.

East Coast Magnetic Anomaly. The East Coast Magnetic Anomaly (ECMA) is a broad, 200 to 300 nT magnetic high that is located approximately 30 to 120 mi. off the coast of North America, and is continuously expressed for about 1,200 mi. from the latitude of Georgia to Nova Scotia ([References 248](#) and [289](#)) ([Figure 2.5.1-211](#)). The ECMA is subparallel to the Atlantic coastline, and is spatially associated with the eastern limit of North American continental crust ([Reference 248](#)). The ECMA has been variously interpreted to be a discrete, relatively magnetic body such as a dike or ridge, or an “edge effect” due to the juxtaposition of continental crust on the west with oceanic crust (higher magnetic susceptibility) on the east (in [Reference 287](#)). In the vicinity of the ECMA, deep seismic reflection profiling in the Atlantic basin has imaged packages of east-dipping reflectors that underlie the sequence of Mesozoic-Tertiary passive-margin marine strata ([Reference 288](#)). The rocks associated with the east-dipping reflectors are interpreted to be an eastward-thickening wedge of volcanic and volcanoclastic rocks that were deposited during the transition between rifting of the continental crust and opening of the Atlantic basin during the Mesozoic ([Reference 289](#)). Models of the magnetic data show that the presence of this

volcanic “wedge” can account for the wavelength and amplitude of the ECMA (Reference 248).

To summarize, the ECMA is a relict of the Mesozoic opening of the Atlantic basin, and likely arises from the presence of a west-tapering wedge of relatively magnetic volcanic rocks deposited along the eastern margin of the continental crust as the Atlantic basin was opening, rather than juxtaposition of rocks with differing magnetic susceptibilities across a fault. The ECMA is not directly associated with a fault or tectonic feature, and thus is not a potential seismic source.

Appalachian Gravity Gradient. This regional gravity gradient extends the length of the Appalachian orogen (Figure 2.5.1-209) and exhibits a southeastward rise in Bouguer gravity values as much as 50 to 80 mGal (References 265 and 295). The Appalachian gravity gradient represents the southeastern thinning of relatively intact Precambrian continental crust, and the early opening of the Iapetus Ocean (Reference 265).

Southeast and Northwest Boundaries of Iapetus Normal Faults. The southeast and northwest boundaries of Iapetus normal faults shown in Figure 2.5.1-209 define the extent of the Iapetus margin of the craton containing normal faults that accommodated extension during the late Proterozoic to early Paleozoic rifting that formed the Iapetus Ocean basin. Wheeler (1996) (Reference 295) defines the southeast boundary as the southeastern limit of the intact Iapetus margin, which is nearly coincident with the Appalachian gravity gradient in the southeastern United States. The Iapetus normal faults are concealed beneath Appalachian thrust sheets that overrode the margin of the craton during the Paleozoic. A few of these Iapetus faults are thought to be reactivated and responsible for producing earthquakes in areas such as eastern Tennessee; Giles County, Virginia; and Charlevoix, Quebec (References 265 and 295).

The southeast margin of the Iapetus normal faults shown on Figure 2.5.1-209 does not represent a potential seismic source since it does not represent a discrete crustal discontinuity or tectonic structure. The linear feature shown in the figure represents the southeastern extent of the intact Iapetus margin (with a location uncertainty of about 20 mi.), and therefore, the southeastern limit of potentially seismogenic Iapetus faults (Reference 295).

The New York-Alabama, Clingman, and Ocoee Lineaments. King and Zietz (1978) (Reference 290) identify a 1,000-mi.-long lineament in aeromagnetic maps of the eastern U.S. that they name the “New York-Alabama lineament” (NYAL) (Figure 2.5.1-209). The NYAL primarily is defined by a series of northeast-southwest-trending linear magnetic gradients in the Valley and Ridge province of the Appalachian fold belt that systematically intersect and truncate other magnetic anomalies. The NYAL also is present as complementary but less-well-defined lineament on regional gravity maps (Reference 290).

The Clingman lineament is an approximately 750-mi.-long, northeast-trending aeromagnetic lineament that passes through parts of the Blue Ridge and eastern Valley and Ridge provinces from Alabama to Pennsylvania (Reference 291). The

Ocoee lineament splays southwest from the Clingman lineament at about latitude 36°N (Reference 292). The Clingman-Ocoee lineaments are sub-parallel to and located about 30 to 60 mi. east of the NYAL.

King and Zietz (1978) (Reference 290) interpret the NYAL to be a major strike-slip fault in the Precambrian basement beneath the thin-skinned fold-and-thrust structures of the Valley and Ridge, and suggest that it may separate rocks on the northwest that acted as a mechanical buttress from the intensely deformed Appalachian fold belt to the southeast. Shumaker (2000) (Reference 293) interpret the NYAL to be a right-lateral strike-slip fault that formed during an initial phase of late Proterozoic continental rifting that eventually led to the opening of the Iapetus Ocean. The Clingman lineament also is interpreted to arise from a source or sources in the Precambrian basement beneath the accreted and transported Appalachian terranes (Reference 291).

Johnston et al. (1985) (Reference 292) observe that the “preponderance of southern Appalachian seismicity” occurs within the “Ocoee block”, a Precambrian basement block bounded by the NYAL and Clingman-Ocoee lineaments [the Ocoee block was previously defined by Johnston and Reinhold 1985 (Reference 294)]. Based on the orientations of nodal planes from focal mechanisms of small earthquakes, Johnston et al. (1985) (Reference 292) note that most events within the Ocoee block occurred by strike-slip displacement on north-south and east-west striking faults, and thus these researchers do not favor the interpretation of seismicity occurring on a single, through-going northeast-southwest-trending structure parallel to the Ocoee block boundaries.

The Ocoee block lies within a zone that Wheeler (1995 [Reference 267], 1996 [Reference 295]) defines as the cratonward limit of normal faulting along the ancestral rifted margin of North America that occurred during the opening of the Iapetus Ocean in late Precambrian to Cambrian time. Synthesizing geologic and geophysical data, Wheeler (1995, 1996) (References 267 and 295) maps the northwest extent of the Iapetus faults in the subsurface below the Appalachian detachment, and proposes that earthquakes within the Ocoee block may be the result of reactivation of Iapetus normal faults as reverse or strike-slip faults in the modern tectonic setting.

Appalachian Thrust Front. The northwestern limit of allochthonous crystalline Appalachian crust was termed the Appalachian thrust front by Seeber and Armbruster (1988) (Reference 399) (Figure 2.5.1-209). This front is a sharply defined boundary interpreted as a major splay of the master Appalachian detachment.

Grenville Front. The Grenville front (Figure 2.5.1-209) is defined by geophysical, seismic reflection, and scattered drill hole data in the southeastern U.S. This feature lies within the continental basement and is interpreted to separate the relatively undeformed eastern granite-rhyolite province on the northwest from the more highly deformed rocks of the Grenville province on the southeast (Reference 400).

2.5.1.1.2.4.2 Regional Paleozoic Tectonic Structures

The Lee Nuclear Site region encompasses portions of the Coastal Plain, Piedmont, Blue Ridge, Valley and Ridge, and Appalachian Plateau physiographic provinces (Figure 2.5.1-201). Rocks and structures within these provinces are often associated with thrust sheets that formed during convergent Appalachian orogenic events of the Paleozoic Era. Tectonic structures of this affinity also exist beneath the sedimentary cover of the Coastal Plain province. These types of structures are shown on Figure 2.5.1-209 and Figure 2.5.1-210, and include the following:

- Sutures juxtaposing allochthonous (tectonically transported) rocks with autochthonous (non-transported North American crust) rocks.
- Regionally extensive Appalachian thrust faults and oblique-slip shear zones.
- Numerous smaller structures that accommodated Paleozoic deformation within individual belts or terranes.

The majority of these structures dip eastward, initially at a steep angle that becomes shallower as they approach the basal Appalachian decollement (Figure 2.5.1-207). The Appalachian orogenic crust is relatively thin across the Valley and Ridge province, Blue Ridge province, and western part of the Piedmont province, and thickens eastward beneath the eastern part of the Piedmont province and the Coastal Plain province. Below the decollement are rocks that form the North American basement complex. These basement rocks contain northeast-striking, Late Precambrian to Cambrian normal faults that formed during the lapetan rifting that preceded the deposition of Paleozoic sediments.

Researchers observe that much of the sparse seismicity in eastern North America occurs within the North American basement below the basal decollement. Therefore, seismicity within the Appalachians may be unrelated to the abundant, shallow thrust sheets mapped at the surface (Reference 267). For example, seismicity in the Giles County, Virginia seismic zone (GCVSZ), located in the Valley and Ridge province, is occurring at depths ranging from 3 to 16 mi. (see Subsection 2.5.1.1.3.2.3) (References 265 and 371), which is generally below the Appalachian thrust sheets and basal decollement (Reference 265).

Paleozoic faults within 200 mi. of the Lee Nuclear Site are shown on Figure 2.5.1-209 and those within 25 mi. and 50 mi. are shown on Figure 2.5.1-210. The faults that are considered most important, either because of their regional tectonic significance or their proximity to the site, are discussed below. Not every fault depicted in Figures 2.5.1-209 and 2.5.1-210 is discussed explicitly.

Kings Mountain Shear Zone (Central Piedmont Shear Zone). The northeast-striking Kings Mountain shear zone is a zone of mylonitic deformation that separates the Inner Piedmont terrane from the Carolina terrane, and is considered part of the larger Central Piedmont shear zone (References 236, 296, and 297).

The Kings Mountain shear zone comprises smaller, localized shear zones, including the Blacksburg and Kings Creek shear zones. At its nearest point, the Kings Mountain shear zone is located 5 mi. north of the Lee Nuclear Site (Figure 2.5.1-210). The sense of motion on the Kings Mountain shear zone is unclear, but structural data suggest that the zone is a steeply northwest-dipping reverse fault (Reference 236). Mylonitic deformation in the Kings Mountain shear zone is overprinted by semi-brittle cleavage. Pegmatitic dikes in North Carolina intruded parallel to the semi-brittle cleavage and some have been ductilely deformed. Hence, the dikes are interpreted as syn- to post-kinematic and their Rb/Sr whole rock isochron age of 340 ± 5 Ma indicates that the late-stage semi-brittle deformation occurred in the Mississippian (Horton (1981) (Reference 421)).

Cross Anchor Fault. The greater than 60-mi.-long Cross Anchor fault is mapped by Hibbard et al. (2006) (Reference 260) as a thrust fault of variable strike. At its nearest point, the Cross Anchor fault is located approximately 10 mi. west of the Lee Nuclear Site (Figure 2.5.1-210). West (1998) (Reference 297) interprets the Cross Anchor fault as the Carolina-Inner Piedmont terrane boundary. Dennis and Wright (1995) (Reference 422) interpreted an unnamed granite, dated at 326 ± 3 Ma, to cut and post-date the Central Piedmont shear zone. However, West (1998) (Reference 297) interpreted the same pluton as syn- to pre-kinematic to deformation on the fault and interpreted movement on the fault to be approximately 325 Ma.

Hycos Shear Zone. In northern North Carolina and southern Virginia, the Hycos shear zone dips shallow to steeply to the southeast and juxtaposes the Carolina terrane rocks over the Milton terrane, rocks correlated with the Inner Piedmont or Piedmont zone (Hibbard et al. (1998) (Reference 417)) (FSAR Figure 2.5.1-209). Hence, it is interpreted as part of the Central Piedmont shear zone (Hibbard et al. (2002) (Reference 204)). Ages on granitoids interpreted as syn-kinematic to deformation on this structure range from about 320 Ma to about 335 Ma, and indicate a Mississippian age for deformation (Wortman et al. (1998) (Reference 418)).

Brindle Creek Thrust Fault. The Brindle Creek thrust was recognized in North Carolina as a low-angle fault with an extensive mylonite zone, but authors have indicated that the mapping of this structure in South Carolina is speculative (Bream (2002), Reference 403). According to Hatcher et al., 2007 (Reference 404), the following lines of evidence are used to map the Brindle Creek fault:

- The fault separates areas with different stratigraphy,
- The fault separates areas with different detrital zircon age distributions,
- The fault separates areas with different mafic and ultramafic rocks, and
- The fault separates areas with different age and character of plutons.

The fault is interpreted as an early Paleozoic unconformity that was activated as a mylonitic fault in the late Paleozoic during the Alleghanian orogeny (Dennis, 2007;

[Reference 405](#)) or as a Neocadian (early Mississippian) thrust (Hatcher et al., 2007; [Reference 404](#)). In North Carolina, a granite exposed only in the hanging-wall of the Brindle Creek fault has zircons with a weighted $^{206}\text{Pb}/^{238}\text{U}$ ion microprobe age of 366 ± 3 Ma (Giorgis et al. (2002) ([Reference 415](#))). This field relationship was interpreted to indicate that the Brindle Creek fault was active after the intrusion of the granite, or is Devonian or younger in age. Also in North Carolina, migmatitic, high-temperature deformation is spatially associated with the Brindle Creek fault (Giorgis et al. (2002) ([Reference 415](#))). Metamorphic rims in migmatitic rocks in the immediate footwall of the Brindle Creek fault yield ion-microprobe U-Pb ages of ca. 350 Ma, probably correlative with emplacement of the Brindle Creek hanging-wall (Merschhat and Kalbas (2002) ([Reference 416](#))). Recent mapping has extended the Brindle Creek fault, and thus the Cat Square terrane, into central Georgia ([Reference 442](#)).

Tinsley Bridge Fault. The Tinsley Bridge fault is a less than 20-mi.-long zone of retrograde mylonite with apparent down-to-the-northwest sense of slip (Dennis (1995) ([Reference 298](#))). At its nearest point, the Tinsley Bridge fault is located 5 mi. southwest of the Lee Nuclear Site ([Figure 2.5.1-210](#)). Based on the observations that mylonitic deformation occurred after peak metamorphic conditions (early Cambrian) and that the fault is cut by the undeformed Pacolet granite (whole-rock Rb/Sr age of 383 ± 5 Ma) the fault was active in the early Paleozoic ([Reference 298](#)).

Southwest Extension of the Boogertown Shear Zone. The northeast-striking Boogertown shear zone marks the boundary between the Kings Mountain belt and the Charlotte belt ([Reference 236](#)). At its nearest point, this shear zone is located 8 mi. east of the Lee Nuclear Site ([Figure 2.5.1-210](#)). The northeastern end of the Boogertown shear zone is truncated by an unsheared granitic pluton (Milton (1981) ([Reference 408](#))). This pluton is undated, but the youngest plutons within the Carolina Zone are 300-265 Ma (Hatcher et al. (2007) ([Reference 404](#))).

Reedy River Thrust Fault. The Reedy River thrust fault is a northeast-striking structure in the Inner Piedmont ([References 260, 299, and 300](#)). At its nearest point, the Reedy River thrust fault is located 18 mi. west-northwest of the Lee Nuclear Site ([Figure 2.5.1-210](#)).

Gold Hill-Silver Hill Shear Zone. The Gold Hill-Silver Hill shear zone (GSHSZ) is a dextral strike-slip shear zone located approximately 30 mi. south of the Lee Nuclear Site ([Figure 2.5.1-210](#)). Based upon cross-cutting relationships with intrusive igneous bodies and the Cross Anchor fault, West (1998) ([Reference 297](#)) constrains motion on this shear zone to between approximately 400 and 325 Ma. Work along the GSHSZ to the northeast has variably indicated deformation events of earliest Cambrian dextral-reverse faulting (Allen et al. (2007) ([Reference 427](#))), Late Ordovician sinistral deformation (Hibbard et al. (2007) ([Reference 425](#))), and Devonian to Mississippian remobilization (Hibbard et al. (2007) ([Reference 425](#)); Hibbard et al. (2008) ([Reference 426](#))). The best evidence for the latest movement on the GSHSZ, however, is based on its cross-cutting relationship with the Cross Anchor fault that indicates latest motion was sometime prior to 325 Ma (West (1998) ([Reference 297](#))).

Middleton-Lowndesville Shear Zone. The Lowndesville shear zone is located approximately 40 mi. south of the Lee Nuclear Site (Figure 2.5.1-210), and is a zone of predominantly mylonitic gneisses, along with local muscovite phyllonites and silicified breccias, with a subvertical, N65°E-striking foliation, bearing subhorizontal stretching lineations (West (1998) (Reference 297)). It coincides with the sharply defined southeastern boundary of the Piedmont zone (or Inner Piedmont terrane), characterized by amphibolites-facies to migmatitic rocks (Griffin (1981) (Reference 423)), and is interpreted as part of the Central Piedmont shear zone (West (1998) (Reference 297)). Where it extends south into Georgia, it is described as a cataclastic zone, striking northeast, where it is mapped in geophysical data (Rozen (1981) (Reference 235)). The ductile and brittle deformation features associated with this structure all occurred at a minimum of greenschist-facies conditions and the brittle features are interpreted to have formed near the brittle-ductile transition (Nelson (1981) (Reference 424)). In South Carolina the Lowndesville shear zone is mapped as being truncated by the Cross Anchor fault, and hence was active older than approximately 325 Ma (West (1998) (Reference 297)).

Beaver Creek Shear Zone. The Beaver Creek shear zone is a 4 km wide zone of mylonitic paragneiss, amphibolites and paragneiss (West (1998) (Reference 297)). The N80°E, subvertically dipping fabric bears dextral shear sense indicators and is cut by the Newberry granite, which is 415 ± 9 Ma in age (West (1998) (Reference 297)). The shear zone is also truncated by the Cross Anchor fault (West (1998) (Reference 297)).

Modoc Shear Zone. The Modoc shear zone is a region of high ductile strain separating the Carolina terrane (Carolina Slate and Charlotte belts) from amphibolite facies migmatitic and gneissic rocks (Reference 301). The northeast-trending Modoc zone dips steeply to the northwest and is traced through the Piedmont from central Georgia to central South Carolina based on geological and geophysical data. The Modoc shear zone appears to continue northeastward to North Carolina beneath the Coastal Plain, as demonstrated by geologic mapping and aeromagnetic data (Figure 2.5.1-206). At its nearest point, the Modoc shear zone is about 75 mi. south of the Lee Nuclear Site. The Modoc shear zone contains fabrics characterized by brittle and ductile deformation produced by ductile shear during an early phase of the Alleghanian orogeny (References 302, 303, 304, and 305). Geochronologic data from Dallmeyer et al. (1986) (Reference 410) indicate movement occurred between 315 and 290 Ma. Howard et al. (2005) (Reference 411) and McCarney et al. (2005) (Reference 412) describe the Modoc fault zone as exposed by construction of Saluda Dam on Lake Murray, west of Columbia, South Carolina. They interpret brittle features in the Saluda Dam spillway as the result of readjustment from different loading and unloading, as well as tectonic movement associated with latest Alleghanian deformation and initial Triassic rifting.

Hatcher et al. (1977) (Reference 306) suggest that the Modoc shear zone, the Irmo shear zone, and the Augusta fault are part of the proposed Eastern Piedmont fault system, an extensive series of faults and splays extending from Alabama to Virginia. Aeromagnetic, gravity, and seismic reflection data indicate that the

Augusta fault zone continues northeastward in the crystalline basement beneath the Coastal Plain province sediments.

Brevard Fault Zone. The northeast-trending Brevard fault zone extends for over 400 mi. from Alabama to Virginia (References 260 and 307). At its nearest point, the Brevard fault zone is located approximately 55 mi. northwest of the Lee Nuclear Site (Figure 2.5.1-210). The Brevard fault zone separates the Blue Ridge province to the west from the Piedmont province to the east. Diabase dikes preclude post Jurassic slip on the Brevard fault and cooling age histories indicate that no slip has occurred on the Brevard fault since the late Paleozoic (Reference 226).

Chappells Shear Zone. Horton and Dicken (2001) (Reference 308) and Hibbard et al. (2006) (Reference 260) map the 60-mi.-long Chappells shear zone as an approximately northeasterly-trending, 2-mi.-wide zone of ductile deformation. At its nearest point, the Chappells shear zone is located approximately 57 mi. south of the Lee Nuclear Site (Figure 2.5.1-210). Post-Paleozoic slip on the Chappells shear zone is precluded by cross-cutting relationships with the late Paleozoic (309 Ma; Reference 309) Winnsboro pluton.

Other Paleozoic Faults. Other Paleozoic faults are present in the site region, most are located northwest of the site and are oriented parallel to the regional structural grain (Figure 2.5.1-209). These include, but are not limited to, the Eufola and Tumblebug Creek faults shown on FSAR Figure 2.5.1-210, and the Pine Mountain, Bowens Creek, and Fries faults shown on Figure 2.5.1-209. While definitive timing evidence does not exist for many of the faults within the site region, any combination of many factors may have prompted workers to assess them as Paleozoic including:

- Mapping that indicates that these faults only deform rocks of Paleozoic or older age,
- Geometries and kinematics similar to other faults with established Paleozoic ages (e.g., west-directed thrusts), and/or
- Textural fabrics or mineral assemblages consistent with deformation at ductile high-temperature metamorphic conditions, the latest of which generally occurred during the late Paleozoic collision with Gondwana (e.g., Hatcher et al. (2007) (Reference 404)). For example, the Tumblebug Creek fault was active during upper amphibolites, sillimanite-grade metamorphism (Davis (1993) (Reference 419)).

Furthermore, no seismicity is attributed to the Paleozoic faults in the site region, and published literature does not indicate that any of these faults offset late Cenozoic deposits or exhibit a geomorphic expression indicative of Quaternary deformation. In addition, Crone and Wheeler (2000) (Reference 310) and Wheeler (2005) (Reference 311) do not show any of these faults to be potentially active Quaternary faults. Therefore, these Paleozoic structures in the site region are not considered to be capable tectonic sources.

2.5.1.1.2.4.3 Regional Mesozoic Tectonic Structures

Tectonic features in the site region of known or postulated Mesozoic age include faults and extensional rift basins. These features, which are described below, are shown and labeled on [Figure 2.5.1-210](#). The features also are shown on [Figure 2.5.1-209](#), but not all features are labeled due to the scale limitations of the figure.

Wateree Creek fault. Secor et al. (1982) ([Reference 312](#)) map the greater than 8-mi.-long Wateree Creek fault as an approximately north-striking, unsilicified fault zone. At its nearest point, the Wateree Creek fault is located approximately 55 mi. south of the Lee Nuclear Site. Based upon cross-cutting relationships with Triassic or Jurassic diabase dikes, Secor et al. (1982) ([Reference 312](#)) estimate a minimum age of Triassic for the Wateree Creek fault. More recent maps of the site area by Maher et al. (1991) ([Reference 314](#)) reinterpret the northernmost portion of the fault as striking northeast. The central and southern portion of the fault is well located due to roadcut and trench exposures ([Reference 313](#)). Detailed magnetometer surveys and trench studies of the central and southern portions of the Wateree Creek fault demonstrate the continuity of an unfaulted diabase dike of probable Triassic age across the fault, thereby constraining most-recent activity on the Wateree Creek fault to the Mesozoic or pre-Mesozoic ([References 312 and 313](#)).

Summers Branch fault. The approximately 8-mi.-long Summers Branch fault is mapped by Secor et al. (1982) ([Reference 312](#)) as an approximately north-striking, unsilicified fault zone. At its nearest point, the Summers Branch fault is located approximately 55 mi. south of the Lee Nuclear Site. By association with the Wateree Creek fault, Secor et al. (1982) ([Reference 312](#)) estimate a minimum age of Triassic for the Summers Branch fault. More recent maps of the site area have omitted the speculative Summers Branch fault ([Reference 314](#)). Despite questions regarding its existence, the Summers Branch fault is shown on [Figures 2.5.1-209 and 2.5.1-210](#).

Ridgeway Fault. Secor et al. (1998) ([Reference 315](#)) map the greater than 9-mi.-long Ridgeway fault as an approximately north-striking, unsilicified fault zone located approximately 60 mi. southeast of the Lee Nuclear Site. By association with both the Wateree Creek and Summers Branch faults, Secor et al. (1998) ([Reference 315](#)) estimate a minimum age of Triassic for the Ridgeway fault.

Longtown Fault. The Longtown fault strikes west-northwest in the Ridgeway-Camden area, about 60 mi. southeast of the Lee Nuclear Site. As mapped by Secor et al. (1998) ([Reference 315](#)), the Longtown fault terminates eastward against the Camden fault. The Longtown fault is associated with fracturing and brecciation of crystalline rocks, and fragments of silicified breccia are found along its trace ([Reference 315](#)). Total slip on the Longtown fault is uncertain, although Secor et al. (1998) ([Reference 315](#)) suggest total displacement on the order of hundreds to thousands of feet is likely in order to explain the apparent disruption of crystalline rocks across the fault. Secor et al. (1998) ([Reference 315](#)) suggest possible Cenozoic (pre-Oligocene) slip on the Longtown fault. However, more recent mapping by Barker and Secor (2005) ([Reference 316](#)) shows four diabase

dikes of probable Triassic age that cross, but are not offset by, the Longtown fault. Based on these cross-cutting relationships, a minimum age of Triassic is established for the Longtown fault.

Mulberry Creek Fault. The Mulberry Creek fault is located approximately 55 mi. southwest of the Lee Nuclear Site. This subvertical fault contains silicified breccia, microbreccia, and cataclasite (Reference 297). Evidence for the timing of slip on the Mulberry Creek fault is indirect. By association with other similar silicified breccias in North and South Carolina, West (1998) (Reference 297) suggests a Late Triassic to Early Jurassic age for the Mulberry Creek fault.

Mesozoic Rift Basins. A broad zone of fault-bounded, elongate, depositional basins associated with crustal extension and rifting formed during the opening of the Atlantic Ocean in early Mesozoic time. These rift basins are common features along the eastern coast of North America from Florida to Newfoundland (Figures 2.5.1-201 and 210). Wheeler (1995) (Reference 267) suggests that many earthquakes in the eastern part of the Piedmont province and beneath the Coastal Plain province may be associated spatially with buried normal faults related to rifting that occurred during the Mesozoic Era. However, definitive correlation of seismicity with Mesozoic normal faults is not conclusively demonstrated. Figure 2.5.1-210 shows the lack of spatial correlation between Mesozoic basins and seismicity within 50 miles of the site. As of March 2009, there was no positive correlation between earthquakes in the site region and Mesozoic basins. Normal faults in this region that bound Triassic basins may be listric into the Paleozoic detachment faults (Reference 268) or may penetrate through the crust as high-angle faults. Within regions of stable continental cratons, areas of extended crust potentially contain the largest earthquakes (Reference 317) (Figure 2.5.1-212). Mesozoic basins have long been considered potential sources for earthquakes along the eastern seaboard (Reference 318).

No seismicity is attributed to these Mesozoic features, and published literature does not indicate that any of these faults offset late Cenozoic deposits or exhibit a geomorphic expression indicative of Quaternary deformation. In addition, Crone and Wheeler (2000) (Reference 310) and Wheeler (2005) (Reference 311) do not show any of these faults to be potentially active Quaternary faults. Therefore, these Mesozoic structures in the site region are not considered to be capable tectonic sources; however, they are considered within the seismotectonic zone of Mesozoic extended crust (Extended Continental Crust-Atlantic Margin (ECC-AM)) in the CEUS SSC (Reference 441).

2.5.1.1.2.4.4 Regional Cenozoic Tectonic Structures

Within 200 mi. of the Lee Nuclear Site, only a few tectonic features, including faults, arches, domes, and embayments, demonstrate Cenozoic activity. These features are shown on Figures 2.5.1-209 and 2.5.1-210, and are described below.

Camden Fault. The northeast-striking Camden fault is located in the eastern part of the Ridgeway-Camden area, about 70 mi. southeast of the Lee Nuclear Site. Along much of its length, the Camden fault juxtaposes crystalline rocks of the Carolina terrane on the northwest against crystalline rocks interpreted to be part of

the Alleghanian Modoc shear zone on the southeast (Reference 315). Total slip on the Camden fault is uncertain, although Secor et al. (1998) (Reference 315) suggest total displacement on the order of miles is likely in order to explain the apparent disruption of crystalline rocks across the fault.

Up-to-the-north vertical separation of the basal Late Cretaceous unconformity of about 50 to 80 ft. suggests Late Mesozoic and possibly Cenozoic (pre-Oligocene) reactivation of the Camden fault (References 315 and 319). Map relationships in the northeastern Rabon Crossroads Quadrangle suggest a northwest-side up vertical separation of the unconformity at the base of the sand unit of about 82 ft., and map relationships at the southeastern corner of the Longtown Quadrangle suggest a northwest-side-up vertical separation of the unconformity of about 55 ft. (Reference 315).

Knapp et al. (2001) (Reference 320) describe seismic reflection and gravity data they interpret as suggesting an 80 to 100 ft. offset of the base of the Coastal Plain section. Knapp et al. (2001) (Reference 320) suggest that deposits of the Tertiary Upland formation cover the Camden fault, providing a potential upper age limit on the Cenozoic movement of the fault.

Prowell (1983) Faults. As part of the U.S. Geological Survey's Reactor Hazards Program, Prowell (1983) (Reference 321) compiled and mapped information regarding possible Cretaceous and younger faults in the eastern U.S. Three of these postulated faults are located within 50 mi. of the Lee Nuclear Site. Prowell's (1983) (Reference 321) faults numbered 63, 64, and 65 are located about 50 mi. northwest of the Lee Nuclear Site near Saluda, North Carolina (Figure 2.5.1-210). As noted by Prowell (1983) (Reference 321), faults numbered 63 and 64 are spatially associated with a slump block, and fault numbered 65 is a probable gravity slide plane. These features are likely the result of gravity-induced mass wasting processes and not the result of tectonic processes.

Arches and Embayments. The basement surface on which Coastal Plain sediments were deposited is not a simple planar platform. Instead, it is characterized by broad structural upwarps (arches) that separate depositional basins (embayments) (Horton and Zullo (1991) (Reference 261)). The hinge lines of these upwarps are aligned roughly perpendicular to the coastline. Two of these upwarps, the Cape Fear and Yamacraw arches, are located within the site region. The Cape Fear Arch is located near the South Carolina-North Carolina border and the Yamacraw Arch is located near the South Carolina-Georgia border (Figure 2.5.1-209).

Evidence constraining the timing of most-recent movement on the Cape Fear and Yamacraw arches is limited. Gohn (1998) (Reference 413) indicates that the Cape Fear Arch has affected the thickness and distribution of Late Cretaceous to late Tertiary strata. Prowell and Obermeier (1991) (Reference 414) suggest that upwarping on the Cape Fear Arch may have continued through the Pleistocene Epoch. Data constraining the timing of most-recent movement on the Yamacraw Arch are unavailable. However, since the tectonic history of the Yamacraw Arch likely is analogous to that of the Cape Fear Arch, the timing of most-recent movement on these two arches is assessed to be similar. Crone and Wheeler

(2000) ([Reference 310](#)) classify the Cape Fear Arch as a Class C feature based on lack of evidence for Quaternary faulting and do not include the Yamacraw Arch in their assessment.

2.5.1.1.2.4.5 Regional Quaternary Tectonic Structures

In an effort to provide a comprehensive database of Quaternary tectonic features, Crone and Wheeler (2000) ([Reference 310](#)) and Wheeler (2005) ([Reference 311](#)) compiled geological information on Quaternary faults, liquefaction features, and possible tectonic features in the CEUS. They evaluate and classified these features into one of four categories (Classes A, B, C, and D; see [Table 2.5.1-201](#) for definitions) based on strength of evidence for Quaternary activity. Charleston area liquefaction features are the only features identified by Crone and Wheeler (2000) ([Reference 310](#)) and Wheeler (2005) ([Reference 311](#)) with demonstrated Quaternary deformation (Class A) within the site region.

Within a 200 mi. radius of the Lee Nuclear Site, Crone and Wheeler (2000) ([Reference 310](#)) and Wheeler (2005) ([Reference 311](#)) identify 15 potential Quaternary features ([Table 2.5.1-201](#) and [Figure 2.5.1-213](#)). These include:

- Fall Lines of Weems (1998) ([Reference 322](#)) (Class C).
- Belair fault (Class C).
- Pen Branch fault (Class C).
- Cooke fault (Charleston feature, Class C).
- East Coast fault system (Charleston feature, Class C).
- Charleston liquefaction features (Charleston feature, Class A).
- Bluffton liquefaction features (Charleston feature, Class A).
- Georgetown liquefaction features (Charleston feature, Class A).
- Giles County seismic zone (Class C).
- Eastern Tennessee seismic zone (Class C).
- Cape Fear arch (Class C).
- Hares Crossroads fault (Class C).
- Lindside fault zone (Class C).
- Stanleytown-Villa Heights faults (Class C).
- Pembroke faults (Class B).

Each of these 15 potential features is discussed in detail. The Charleston features (including the East Coast fault system; the Cooke fault; and the Charleston, Georgetown, and Bluffton paleoliquefaction features) are discussed in [Subsection 2.5.1.1.3.2.1](#). The Eastern Tennessee and Giles County seismic zones are discussed in [Subsections 2.5.1.1.3.2.2](#) and [2.5.1.1.3.2.3](#). The remaining eight potential Quaternary features (namely, the Fall Lines of Weems (1998), the Belair fault zone, the Pen Branch fault, the Cape Fear arch, the Hares Crossroads fault, the Linside fault zone, the Stanleytown-Villa Heights faults, and the Pembroke faults) are discussed in detail below:

Fall Lines of Weems (1998). The Fall Lines of Weems (1998) ([Reference 322](#)) are alignments of rapids or anomalously steep sections of rivers draining the Piedmont and Blue Ridge Provinces of North Carolina and Virginia. The Weems (1998) ([Reference 322](#)) delineation of these fall zones is crude, but, as presented in his Figure 8, the Western Piedmont Fall Line appears to be located as close as 5 mi. from the Lee Nuclear Site at its nearest point ([Figure 2.5.1-213](#)). Wheeler (2005) ([Reference 311](#)) classifies the Fall Lines of Weems (1998) ([Reference 322](#)) as a Class C feature ([Table 2.5.1-201](#)) because: (1) identification of the fall zones is subjective and the criteria for recognizing them are not stated clearly enough to make the results reproducible; and (2) a tectonic faulting origin has not yet been demonstrated for the fall zones. Based on review of published literature, field reconnaissance, and work performed as part of the North Anna ESP application ([Reference 398](#)), the Fall Lines of Weems (1998) ([Reference 322](#)) are interpreted to be erosional features related to contrasting erosional resistances of adjacent rock types, and are not tectonic in origin.

Belair Fault zone. The Belair fault zone is mapped for at least 15 mi. as a series of northeast-striking, southeast-dipping, oblique-slip faults located 125 mi. south of the Lee Nuclear Site near Augusta, Georgia ([Figure 2.5.1-213](#)). The Belair fault juxtaposes Paleozoic phyllite over Late Cretaceous sands of the Coastal Plain province ([References 323](#) and [324](#)). Mapping and structural analysis by Bramlett et al. (1982) ([Reference 301](#)) indicate that the Belair fault likely is a tear fault or lateral ramp associated with the Augusta fault when displacement on these faults initiated during the Paleozoic Alleghanian orogeny. While simultaneous post-Paleozoic reactivation of the Belair and Augusta faults cannot be precluded by available data, it is not well established that these two faults share a common slip history and sense of displacement. Powell et al. ([Reference 324](#)) and Powell and O'Connor ([Reference 323](#)) document Cenozoic brittle reverse slip on the Belair fault. The latest well-constrained movement on the Augusta fault, as demonstrated by brittle overprinting of ductile fabrics, exhibits a normal sense-of-slip. Brittle slip occurred late in the Alleghanian during the transition from ductile to brittle conditions ([References 320](#) and [321](#)), with possible minor localized reactivation under Mesozoic hydrothermal conditions ([Reference 320](#)). No geomorphic expression of the fault has been reported ([Reference 310](#)).

Shallow trenches excavated across the Belair fault near Fort Gordon in Augusta, Georgia, were initially interpreted as revealing evidence for Holocene movement ([Reference 324](#)). However, the apparent youthfulness of movement is postulated as the result of contaminated radiocarbon samples. Powell and O'Connor (1978) ([Reference 323](#)) demonstrate that the Belair fault cuts beds of Late Cretaceous

and Eocene age. Overlying, undeformed strata provide a minimum constraint on the last episode of faulting, which is constrained to sometime between post-late Eocene and pre-26,000 years ago.

There is no evidence of historic or recent seismicity associated with the Belair fault. Crone and Wheeler (2000) (Reference 310) classify the Belair fault zone as a Class C feature because the most recent faulting is not demonstrably of Quaternary age. Quaternary slip on the Belair fault zone is permitted, but not demonstrated, by the available data.

Pen Branch fault. The more than 20-mi.-long Pen Branch fault is located about 150 mi. south of the Lee Nuclear Site. The northeast-striking Pen Branch fault bounds the northwest side of the Mesozoic Dunbarton Basin. The Pen Branch fault traverses the central portion of the Savannah River Site, and strikes southwestward into Georgia (References 325 and 326). The Pen Branch fault is not exposed or expressed at the surface (References 326, 327, and 328). Borehole and seismic reflection data collected from the Savannah River Site show no evidence for post-Eocene slip on the Pen Branch fault (Reference 328). Savannah River Site studies and work performed as part of the Vogtle ESP application specifically designed to assess the youngest deformed strata overlying the fault through shallow, high-resolution reflection profiles, drilling of boreholes, and geomorphic analyses consistently concludes that the youngest strata deformed are late Eocene in age. Crone and Wheeler (2000) (Reference 310) classify the Pen Branch fault zone as a Class C feature based on lack of evidence for Quaternary faulting.

Cape Fear Arch. The Cape Fear Arch is discussed previously in Subsection 2.5.1.1.2.4.4. Crone and Wheeler (2000) (Reference 310) classify the Cape Fear Arch as a Class C feature based on lack of evidence for Quaternary faulting.

Hares Crossroads fault. The postulated Hares Crossroads fault (identified by Prowell [1983] (Reference 321) as fault numbered 46) in east-central North Carolina is a single reverse fault that offsets the base of the Coastal Plain section, approximately 200 mi. east-northeast of the Lee Nuclear Site. This fault is recognized in a roadcut exposure. The fault is not recognized beyond this exposure, and geomorphic expression is negligible. This fault is likely the result of landsliding and is therefore likely non-tectonic in origin. Crone and Wheeler (2000) (Reference 310) classify the Hares Crossroads fault as a class C feature based on lack of evidence for Quaternary faulting.

Lindside fault zone. The northeast-striking, normal-slip Lindside fault is located in southern West Virginia, about 170 mi. north of the Lee Nuclear Site (Reference 310). The Lindside fault is mapped for a length of greater than 30 mi., with variable width up to about 1 mi. Dennison and Stewart (1998) (Reference 329) suggest that the Lindside fault zone accommodated latest Paleozoic gravitational collapse of Appalachian crust. The Lindside fault zone is poorly oriented for reactivation in the current stress field, and no evidence of Quaternary slip is reported for the zone. Crone and Wheeler (2000)

(Reference 310) classify the Linside fault zone as a class C feature based on lack of evidence for Quaternary faulting.

Stanleytown-Villa Heights faults. The postulated Stanleytown-Villa Heights faults are located in the Piedmont of southern Virginia, approximately 150 mi. northeast of the Lee Nuclear Site. These approximately 655-ft.-long faults juxtapose Quaternary alluvium against rocks of Cambrian age. The Stanleytown-Villa Heights faults are both short in mapped length, drop their east sides down in the downhill direction, and no other faults are mapped nearby (Reference 310). Evidence suggests these faults are likely the result of landsliding and are therefore likely non-tectonic in origin. Crone and Wheeler (2000) (Reference 310) classify the Stanleytown-Villa Heights faults as a Class C feature based on lack of evidence for Quaternary faulting.

Pembroke faults. The postulated Pembroke faults of western Virginia are located within alluvial deposits of probable Quaternary age (Reference 310), approximately 150 mi. north of the Lee Nuclear Site. The Pembroke faults are identified by geologic mapping, seismic profiles, gravity and magnetics, and ground-penetrating radar. The Pembroke faults are not expressed geomorphically, and it is unclear if these faults are of tectonic origin or the result of dissolution collapse. Crone and Wheeler (2000) (Reference 310) classify the Pembroke faults as a Class B feature based on evidence suggesting possible Quaternary faulting.

Crone and Wheeler (2000) (Reference 310) and Wheeler (2005) (Reference 311) identify potential Quaternary tectonic features in the CEUS. Work performed as part of this study, including literature review, interviews with experts, and geologic reconnaissance, did not identify any additional potential Quaternary tectonic features within the Lee Nuclear Site region.

2.5.1.1.3 Regional Seismicity and Paleoseismology

Subsection 2.5.1.1.3 includes descriptions of instrumental and historic earthquake activity in the Lee Nuclear Site region and beyond. Special emphasis is placed on the Charleston seismic zone because it one of the largest earthquakes in eastern U.S. history and it is located within 200 mi of the Lee Nuclear Site.

2.5.1.1.3.1 Central and Eastern U.S. Seismicity

Seismicity in the CEUS is in general broadly distributed, but areas of concentrated earthquake activity are shown in Figure 2.5.1-214. Areas of concentrated seismicity are described in this section. Although these areas have elevated seismicity rates, they do not all have well-defined evidence for being a source of Repeated Large Magnitude Earthquakes (RLMEs) as defined by the CEUS SSC project, that is having 2 or more earthquakes with $M > 6.5$ (Reference 441). Only Charleston and the New Madrid Fault System are RLMEs discussed as part of this application. The CEUS SSC project used smoothing of seismicity rates within larger sesimotectonic zones to account for the higher earthquake rates in areas that lack evidence for being a source of RLMEs, such as the Eastern Tennessee seismic zone (ETSZ), the Central Virginia seismic zone, and the Giles County, Virginia seismic zone (GCVSZ).

A discussion of the above seismic sources or areas of concentrated seismicity respective to the CEUS SSC model and application to the Probabilistic Seismic Hazard Analysis (PSHA) is provided in [Subsection 2.5.2](#).

2.5.1.1.3.2 Seismic Sources Defined by Regional Seismicity

Within 200 mi. of the Lee Nuclear Site, there are five principal areas of concentrated seismicity ([Figure 2.5.1-214](#)). Three of these (the Middleton-Place Summerville, Bowman, and Adams Run seismic zones) are located within 50 mi. of Charleston, South Carolina. [Subsection 2.5.1.1.3.2.1](#) presents discussion of these three areas of concentrated seismicity near Charleston. The ETSZ and GCVSZ are discussed in [Subsections 2.5.1.1.3.2.2](#) and [2.5.1.1.3.2.3](#), respectively. Two additional areas of concentrated seismicity beyond the site region (i.e., the New Madrid Fault Zone and Central Virginia seismic zone) are discussed in [Subsection 2.5.1.1.3.2.4](#).

2.5.1.1.3.2.1 Charleston Tectonic Features

The August 31, 1886, E[M] 6.90 Charleston, South Carolina, earthquake is the largest historical earthquake in the eastern United States ([Reference 441](#)). The event produced Modified Mercalli Intensity (MMI) X shaking in the epicentral area and was felt strongly as far away as Chicago ([Reference 330](#)). Strong ground shaking during the 1886 Charleston earthquake resulted in extensive liquefaction, primarily expressed as sand-blow craters at the ground surface ([Reference 355](#)). Because no primary tectonic surface rupture has been identified as the causative structure for the 1886 earthquake and the relatively high risk in the Charleston area, government agencies funded numerous investigations to identify the source of the earthquake and recurrence history of large magnitude events in the region. In spite of this effort, the source of the 1886 earthquake is not definitively attributed to any particular fault shown in [Figure 2.5.1-215](#). A combination of geologic, geophysical, geomorphic, and instrumental seismicity data have been used by multiple investigators to suggest several different faults as the potential source for Charleston-area seismicity (e.g., [References 342, 331, 343, 345, 338, 346, 443, 444, 445, 446, 448, 454](#)) (see discussion below).

Work has revealed that pre-1886 paleoliquefaction features occur throughout coastal South Carolina, indicating prior strong ground motions during prehistoric large earthquakes in the region (e.g., [References 447, 448, 335, 336, 357, 449](#)). The paleoliquefaction studies conducted in coastal South Carolina since the 1980s provide evidence that the Charleston seismic source exhibits RLME and that these earthquakes appear to be located only in the Charleston area. Because of this field evidence for liquefaction and paleoliquefaction features, the Charleston seismic zone was characterized as an RLME source by the EPRI CEUS project ([Reference 441](#)). Again, neither the 1886 nor the prehistoric (i.e. pre-1886) earthquakes preserved in the liquefaction record in the Charleston area can be definitively attributed to any specific fault or fault zone at the present time. Hence, the CEUS SSC project developed three alternative geometries for the Charleston source, Charleston Local, Charleston Narrow, and Charleston Regional ([Figure 2.5.1-246](#)).

The 1886 Charleston earthquake produced no identifiable primary tectonic surface deformation; therefore, the source of the earthquake is inferred based on the geology, geomorphology, and instrumental seismicity of the region (Figures 2.5.1-215, 2.5.1-216, and 2.5.1-217). Talwani (1982) (Reference 331) suggests that the inferred north-northeast-striking Woodstock fault produced the 1886 earthquake near its intersection with the northwest-striking Ashley River fault. Both the postulated Woodstock and Ashley River faults are inferred on the basis of seismicity (Reference 331). More recently, Marple and Talwani (1993, 2000) (References 337 and 338) suggest that a northeast-trending zone of river anomalies, referred to as the ECFS, represents the causative fault for the 1886 Charleston event. The southern segment of the ECFS coincides with a linear zone of micro-seismicity that defines the northeast-trending Woodstock fault of Talwani (1982) (Reference 331) and the isoseismal zone from the 1886 earthquake.

Potential Charleston Source Faults. Over the last several decades, a number of faults have been identified or described in the literature as possible sources related to the 1886 Charleston earthquake. These include paleoliquefaction features and numerous faults localized in the Charleston meizoseismal area.

There is evidence, in the form of paleoliquefaction features in the South Carolina Coastal Plain, that the source of the 1886 Charleston earthquake has repeatedly generated vibratory ground motion. Paleoliquefaction evidence is lacking for prehistoric earthquakes elsewhere along much of the eastern seaboard (e.g., References 334, 335, and 336). While the 1886 Charleston earthquake was likely produced by a capable tectonic source, the causative tectonic structure has yet to be identified. Various studies propose potential candidate faults for the 1886 event; however, a positive linkage between a discrete structure and the Charleston earthquake has yet to be determined.

These potential causative features are shown in Figures 2.5.1-215, 2.5.1-216, and 2.5.1-217 and are described below:

- *East Coast Fault System.* The inferred ECFS, the southern section of which is also known as the “zone of river anomalies” (ZRA) based on the alignment of river bends, is a northeast-trending, approximately 370-mi-long fault system extending from west of Charleston, South Carolina, to southeastern Virginia (Reference 338). The ECFS comprises three approximately 125-mi.-long, right-stepping sections (southern, central, and northern). Evidence for the southern section is strongest, with evidence becoming successively weaker northward (Reference 311). Even within the southern segment of the ECFS, Dura-Gomez and Talwani indicate that evidence for the existence and activity of the ECFS is greatest in the south and decreases northeastward (References 443 and 444). Marple and Talwani (1993) (Reference 337) identify a series of geomorphic anomalies (i.e., ZRA) located along and northeast of the Woodstock fault and attribute these to a buried fault much longer than the Woodstock fault. Marple and Talwani (References 337 and 338) suggest that this structure, the ECFS, may have been the source of the 1886 Charleston earthquake. Marple and Talwani (2000) (Reference 338) provide additional evidence for the existence of the southern section of the ECFS, including seismic

reflection data, linear aeromagnetic anomalies, exposed Plio-Pleistocene faults, local breccias, and upwarped strata. Because most of the geomorphic anomalies associated with the southern section of the ECFS are in late Pleistocene sediments, Marple and Talwani (2000) speculate that the fault has been active in the past 130 to 10 ka, and perhaps remains active. Wildermuth and Talwani (2001) (Reference 339) use gravity and topographic data to postulate the existence of a pull-apart basin between the southern and central sections of the ECFS, implying a component of right-lateral slip on the fault. Wheeler (2005) (Reference 311) classifies the ECFS as a Class C feature based on the lack of demonstrable evidence that the ECFS has or can generate strong ground motion and the lack of any demonstrable evidence for any sudden uplift anywhere along the proposed fault.

- *Adams Run Fault.* Weems and Lewis (2002) (Reference 340) postulate the existence of the Adams Run fault on the basis of microseismicity and borehole data. Their interpretation of borehole data suggests the presence of areas of uplift and subsidence separated by the inferred fault. However, review of these data shows that the pattern of uplift and subsidence does not appear to persist through time (i.e., successive stratigraphic layers) in the same locations and that the intervening structural lows between the proposed uplifts are highly suggestive of erosion along ancient river channels. In addition, there is no geomorphic evidence for the existence of the Adams Run fault, and analysis of microseismicity in the vicinity of the proposed Adams Run fault does not clearly define a discrete structure (Figure 2.5.1-217). Marple and Miller (Reference 450) call into question the existence of the Adams Run fault.
- *Ashley River Fault.* Talwani (1982) (Reference 331) identifies the Ashley River fault on the basis of a northwest-oriented, linear zone of seismicity located about 6 mi. west of Woodstock, South Carolina, in the meizoseismal area of the 1886 Charleston earthquake. The postulated Ashley River fault, a southwest-side-up reverse fault, is thought to offset the north-northeast-striking Woodstock fault about 3 to 4 mi. to the northwest near Summerville (References 331, 332, and 340), although revised depictions indicate that it is an aseismic structure extending only southeastward from the northern end of the southern segment of the Woodstock fault (References 443 and 444) (Figure 2.5.1-217).
- *Charleston Fault.* Lennon (1986) (Reference 341) proposes the Charleston fault on the basis of geologic map relations and subsurface borehole data. Weems and Lewis (2002) (Reference 340) suggest that the Charleston fault is a major, high-angle reverse fault that has been active at least intermittently in Holocene to modern times. The Charleston fault has no clear geomorphic expression, nor is it clearly defined by microseismicity (Figure 2.5.1-217). Note that Dura-Gomez and Talwani (References 443 and 444) also give the name "Charleston fault" to a different structure located in a stepover zone between segments of the Woodstock Fault (Figure 2.5.1-217).

- *Cooke Fault.* Behrendt et al. (1981) (Reference 342) and Hamilton et al. (1983) (Reference 343) identify the Cooke fault based on seismic reflection profiles in the meizoseismal area of the 1886 Charleston earthquake. This east-northeast-striking, steeply northwest-dipping fault has a total length of about 6 mi. (References 342 and 343). Marple and Talwani (References 337 and 338) reinterpret these data to suggest that the Cooke fault may be part of a longer, more northerly striking fault (i.e., the ZRA of Marple and Talwani [1993] [Reference 337] and the ECFS of Marple and Talwani [2000] [Reference 338]). Crone and Wheeler (2000) (Reference 310) classify the Cooke fault as a Class C feature based on lack of evidence for faulting younger than Eocene.
- *Helena Banks Fault Zone.* Seismic reflection lines offshore of South Carolina clearly image the Helena Banks fault zone (References 344 and 345). Relevant sources of information regarding the Helena Banks fault zone include:
 - In 2002, two magnitude m_b 3.5 earthquakes (m_b 3.5 and 4.4) occurred offshore of South Carolina in the vicinity of the Helena Banks fault zone in an area previously devoid of seismicity.
 - Bakun and Hopper (2004) (Reference 333) reinterpret intensity data from the 1886 Charleston earthquake and show that the calculated intensity center is located about 100 mi. offshore from Charleston (although they ultimately conclude that the epicentral location most likely lies onshore in the cluster of seismicity in the Middleton Place–Summerville area).
 - Crone and Wheeler (2000) (Reference 310) describe the Helena Banks fault zone as a potential Quaternary tectonic feature (although it is classified as a Class C feature that lacks sufficient evidence to demonstrate Quaternary activity). The occurrence of the 2002 earthquakes and the location of the Bakun and Hopper (2004) (Reference 333) intensity center offshore suggest, at a low probability, that the fault zone could be considered a potentially active fault. If the Helena Banks fault zone is an active source, its length and orientation may explain the distribution of paleoliquefaction features along the South Carolina coast.

The Helena Banks fault zone is included in the Charleston Regional seismic source configuration.

- *Sawmill Branch Fault.* Talwani and Katuna (2004) (Reference 346) postulate the existence of the Sawmill Branch fault on the basis of microseismicity and further speculate that this feature experienced surface rupture in the 1886 earthquake. According to Talwani and Katuna (2004) (Reference 346), this approximately 3-mi.-long, northwest-trending fault, a segment of the larger Ashley River fault, offsets the Woodstock fault in a left-lateral sense. Talwani and Katuna (2004) (Reference 346) use

earthquake damage to infer that surface rupture occurred in 1886. Field review of these localities, however, indicates that they are unlikely the direct result of earthquake surface rupture. Features along the banks of the Ashley River (small, discontinuous cracks in a tomb that dates to 1671 AD and displacements [less than 4 in] in the walls of colonial Fort Dorchester) are almost certainly the product of shaking effects as opposed to fault rupture. Moreover, assessment of microseismicity in the vicinity of the proposed Sawmill Branch fault does not clearly define a discrete structure distinct or separate from the larger Ashley River fault (Figure 2.5.1-217). Dura-Gomez and Talwani (References 443 and 444) refine the mapping of the Sawmill Branch fault.

- *Dorchester Fault.* Bartholomew and Rich (2007) (Reference 451) hypothesized the existence of this northwest-striking fault based upon cracking the walls of colonial Fort Dorchester and seismicity. As stated above, the cracking at Fort Dorchester is most likely due to shaking rather than fault rupture.
- *Summerville Fault.* Weems et al. (1997) (Reference 347) postulate the existence of the Summerville fault near Summerville, South Carolina, on the basis of previously located microseismicity. However, there is no geomorphic or borehole evidence for the existence of the Summerville fault. Analysis of microseismicity in the vicinity of the proposed Summerville fault does not clearly define a discrete structure (Figure 2.5.1-217).
- *Woodstock Fault.* Talwani (1982) (Reference 331) identifies the Woodstock fault, a postulated north-northeast-trending, dextral strike-slip fault, on the basis of a linear zone of seismicity located approximately 6 mi. west of Woodstock, South Carolina, in the meizoseismal area of the 1886 Charleston earthquake. Madabhushi and Talwani (References 348 and 349) use a revised velocity model to relocate Middleton Place–Summerville seismic zone earthquakes. The results of this analysis are used to further refine the location of the postulated Woodstock fault. Talwani (References 332 and 350) subdivides the Woodstock fault into two segments that are offset in a left-lateral sense across the northwest-trending Ashley River fault, and later maps the Charleston, Lincolnville, and Sawmill Branch faults in this contractional stepover (References 443 and 444) (Figure 2.5.1-217). However, others feel a bend in the Woodstock fault is a more likely geometry than an offset (Reference 443). Marple and Talwani include the Woodstock fault as part of their larger ZRA (Reference 337) and ECFS (Reference 338).

Charleston Area Seismic Zones. Three zones of increased seismic activity have been identified in the greater Charleston area. These include the Middleton Place–Summerville, Bowman, and Adams Run seismic zones. Each of these features is described in detail below, and the specifics of the seismicity catalog are discussed in Subsections 2.5.2.2.4.1 and 2.5.2.3.

- *Middleton Place–Summerville Seismic Zone.* The Middleton Place–Summerville seismic zone is an area of elevated microseismic activity located about 12 mi. northwest of Charleston (References 346, 349, 351, and 352) (Figure 2.5.1-216). Between 1980 and 1991, 58 events with M_d 0.8 to 3.3 were recorded in a 7- by 9-mi. area, with hypocentral depths ranging from about 1 to 7 mi. (Reference 349). The elevated seismic activity of the Middleton Place–Summerville seismic zone has been attributed to stress concentrations associated with the intersection of the Ashley River and Woodstock faults (References 331, 346, 349, and 353). Persistent foreshock activity was reported in the Middleton Place–Summerville seismic zone area (Reference 355), and it is speculated that the 1886 Charleston earthquake occurred within this zone (e.g., References 331, 333, and 351).
- *Bowman Seismic Zone.* The Bowman seismic zone is located about 50 mi. northwest of Charleston, South Carolina, outside of the meizoseismal area of the 1886 Charleston earthquake (Figure 2.5.1-216). The Bowman seismic zone is identified on the basis of a series of local Magnitude (M_L) $3 < M_L < 4$ earthquakes that occurred between 1971 and 1974 (References 352 and 354).
- *Adams Run Seismic Zone.* The Adams Run seismic zone, located within the meizoseismal area of the 1886 Charleston earthquake, is identified on the basis of four $M < 2.5$ earthquakes, three of which occurred in a 2-day period in December 1977 (Reference 351). Bollinger et al. (1991) (Reference 352) downplay the significance of the Adams Run seismic zone, noting that, in spite of increased instrumentation, no additional events were detected after October 1979. Magnitudes of the earthquakes in the Adams Run seismic zone (coda magnitudes [M_c] < 2.3) are too small to appear in the CEUS SSC earthquake catalog.

Charleston Area Seismically Induced Liquefaction Features. The presence of liquefaction features in the geologic record may be indicative of past earthquake activity in a region. Liquefaction features are recognized throughout coastal South Carolina and are attributed to both the 1886 Charleston and earlier moderate to large earthquakes in the region.

- *1886 Charleston Earthquake Liquefaction Features.* Liquefaction features produced by the 1886 Charleston earthquake are most heavily concentrated in the meizoseismal area (References 334, 355, and 356), but are reported as far away as Columbia, Allendale, Georgetown (Reference 356) and Bluffton, South Carolina (Reference 357) (Figures 2.5.1-215 and 2.5.1-216).
- *Paleoliquefaction Features in Coastal South Carolina.* Liquefaction features predating the 1886 Charleston earthquake are found throughout coastal South Carolina (Figures 2.5.1-215 and 2.5.1-216). The spatial distribution and ages of paleoliquefaction features in coastal South Carolina constrain possible locations and recurrence rates for large

earthquakes (References 334, 335, 336, 358, and 359). The CEUS SSC project developed a list of 3 to 5 possible prehistoric events, going back up to 5500 years BP identified by various authors (Reference 441). Geotechnical studies in the Charleston, South Carolina area suggest that magnitudes of prehistorical large earthquakes were in the high-5 to high-7 range (e.g., References 452, 453, 454, and 455).

2.5.1.1.3.2.2 Eastern Tennessee Seismic Zone

The Eastern Tennessee Seismic Zone (ETSZ) is one of the most active seismic zones in eastern North America in terms of the rate of small (i.e., $M < 5$) earthquakes. The ETSZ is located in the Valley and Ridge province of eastern Tennessee, approximately 150 mi. west-northwest of the Lee Nuclear Site (Figure 2.5.1-214). The ETSZ is about 185 mi. long and 60 mi. wide and has not produced a damaging earthquake in historical time (Reference 362).

Earthquakes in the ETSZ are occurring at depths from 3 to 16 mi. within Precambrian crystalline basement rocks buried beneath the exposed thrust sheets of Paleozoic rocks. The mean focal depth within the seismic zone is 9 mi., well below the Appalachian basal decollement's maximum depth of 3 mi. (Reference 362). The lack of seismicity in the shallow Appalachian thrust sheets implies that the seismogenic structures in the ETSZ are unrelated to the surface geology of the Appalachian orogen (Reference 292). The majority of earthquake focal mechanisms show right-lateral slip on northerly-striking planes or left-lateral slip on easterly-striking planes (Reference 364). A smaller number of focal plane solutions show right-lateral motion on northeasterly trending planes that parallel the overall trend of seismicity (Reference 363). Statistical analyses of focal mechanisms and epicenter locations suggest that seismicity is occurring on a series of northeast-striking en-echelon basement faults intersected by several east-west-striking faults (Reference 364). Potential structures most likely responsible for the seismicity in Eastern Tennessee are reactivated Cambrian or Precambrian normal faults formed during the rifting that formed the Iapetus Ocean and presently located beneath the Appalachian thrust sheets (Reference 267).

Earthquakes within the ETSZ cannot be attributed to known surface faults (Reference 362), and no capable tectonic sources are identified within the seismic zone. However, the seismicity is spatially associated with major geophysical lineaments or anomalies (References 290, 362, 352, 363). The western margin of the ETSZ is sharply defined and is coincident with the prominent gradient in the magnetic field defined by the New York-Alabama magnetic lineament (Reference 363). Powell et al. (Reference 362) proposed that the ETSZ is an evolving seismic zone in which slip on north- and east-striking surfaces coalesces into a larger strike-slip zone located near the northwestern boundary of the relatively weak Ocoee block in eastern Tennessee. Powell et al (Reference 362) also noted that the densest seismicity and the largest of the instrumentally located epicenters in the ETSZ generally lie close to and east of the New York-Alabama lineament between latitudes 34.3 °N and 36.5°N.

In spite of the observations of small to moderate earthquakes in the ETSZ, recent studies had found no geological evidence, such as paleoliquefaction, that

demonstrated the occurrence of prehistoric earthquakes larger than any historical shocks within the seismic zone (References 311, 363, and 456). As a result, Wheeler (2005) (Reference 311) classifies the ETSZ as a Class C feature for lack of geological evidence of large earthquakes. The CEUS SSC project did not delineate the ETSZ as a RLME source and relied upon the spatial smoothing of a- and b-values to account for elevated seismicity (Reference 441). The ETSZ is located within the Paleozoic Extended Crust (PEZ) seismotectonic zone, which was separated on the basis of Mmax and future earthquake characteristics.

However, very recent work has suggested that there may be a pre-historical record of larger earthquakes on the ETSZ. Hatcher et al. (2012) investigated the ETSZ and possible paleoliquefaction features (Reference 457). In this study, French Broad River terraces were inspected along Douglas Reservoir near Dandridge Tennessee. The soils and terraces exposed range from more than 200 ka (T_4) to as young as 10 ka (T_1) and bear a variety of small-displacement faults, fractures, and possible seismogenic features such as clastic dikes, fluidized alluvium and sand boils. Cross-cutting relationships indicate that at least two seismogenic events may have been responsible for the deformation observed along the shores of Douglas Reservoir. However, because of poor age limits on soils cut by fractures, the ages of the structures observed remain poorly defined and no recurrence intervals could be estimated (Reference 457). Nonetheless, Hatcher et al (Reference 457) conclude that one or more **M** 6.5 earthquakes could be associated with the ETSZ within the last 73 to approximately 200 ka.

While these recent studies strengthen the argument that the ETSZ has experienced at least one moderate-sized earthquake in the late Quaternary, they do not quantify parameters (e.g., recurrence interval, magnitude) necessary to demonstrate that the ETSZ produces repeating large-magnitude events. As such, the ETSZ is modeled within the Mesozoic-and-younger extended crust (MESE) Mmax zone and the PEZ seismotectonic zone using smooth seismicity. No RLME source is defined for the eastern Tennessee seismic zone in the CEUS SSC.

2.5.1.1.3.2.3 Giles County Seismic Zone

The GCVSZ is located in Giles County, southwestern Virginia, near the border with West Virginia, approximately 160 mi. from the Lee Nuclear Site (Figure 2.5.1-214). The largest known earthquake to occur in Virginia and the second largest earthquake in the entire southeastern United States is the 1897 **M** 5.9 (Reference 370) Giles County event. This event likely produced MMI VIII shaking intensities in the epicentral area.

Earthquakes in the GCVSZ occur within Precambrian crystalline basement rocks beneath the Appalachian thrust sheets at depths from 3 to 16 mi. (Reference 265). Earthquake foci define a 25-mi.-long, northeasterly striking, tabular zone that dips steeply to the southeast beneath the Valley and Ridge thrust sheets (References 265 and 371). The lack of seismicity in the shallow Appalachian thrust sheets, estimated to be about 2 to 3.5 mi. thick, implies that the seismogenic structures in the GCVSZ, similar to those inferred for the ETSZ, are unrelated to the surface geology of the Appalachian orogen (Reference 265).

The spatial distribution of earthquake hypocenters, together with considerations of the regional tectonic evolution of eastern North America, suggest that the earthquake activity is related to contractional reactivation of late Precambrian or Cambrian normal faults that initially formed during rifting associated with opening of the Iapetus Ocean ([References 265 and 352](#)).

No capable tectonic sources are identified within the GCVSZ, nor does the seismic zone have recognizable geomorphic expression ([Reference 311](#)). Thus, in spite of the occurrence of small to moderate earthquakes, no geological evidence demonstrates the occurrence of prehistoric earthquakes larger than any historical shocks within the zone ([Reference 311](#)). As a result, Wheeler (2005) ([Reference 311](#)) classifies the GCVSZ as a Class C feature for lack of geological evidence of large earthquakes.

Crone and Wheeler (2000) ([Reference 310](#)) identify a zone of small, Late Pleistocene faults within the GCVSZ near Pembroke, Virginia. The Pembroke faults are a set of extensional faults exposed in terrace deposits overlying limestone bedrock along the New River. Crone and Wheeler (2000) ([Reference 310](#)) rate these faults as Class B features because it has not yet been determined whether these faults are tectonic or the result of solution collapse in underlying limestone units. The shallow Pembroke faults do not appear to be related to the GCVSZ. Seismicity in the GCVSZ is located at depth beneath the Appalachian basal decollement in the North American basement.

Because the seismicity associated with the GCVSZ is located at depth beneath the Appalachian detachment surface, it, like the ETZS, is located in the Paleozoic Extended Crust sesimotectonic zone in the CEUS SSC model ([Reference 441](#)).

2.5.1.1.3.2.4 Selected Seismogenic and Capable Tectonic Sources Beyond the Site Region

In addition to the areas of concentrated seismicity within the site region, [Subsection 2.5.1.1.3.2.4](#) describes two additional areas of concentrated seismicity beyond the site region (i.e., the New Madrid and Central Virginia seismic zones):

New Madrid Seismic Zone. The New Madrid seismic zone extends from southeastern Missouri to southwestern Tennessee and is located more than 450 mi. west of the Lee Nuclear Site ([Figure 2.5.1-214](#)). The New Madrid seismic zone lies within the Reelfoot rift and is defined by post-Eocene to Quaternary faulting and historical seismicity.

The New Madrid seismic zone is approximately 125 mi. long and 25 mi. wide. Research conducted since 1986 identifies three distinct fault segments embedded within the seismic zone. These three fault segments include a southern northeast-trending dextral slip fault, a middle northwest-trending reverse fault, and a northern northeast-trending dextral strike-slip fault ([Reference 373](#)) referred to as the New Madrid fault system in the CEUS SSC. In the current east-northeast to west-southwest directed CEUS regional stress field, Precambrian and Late

Cretaceous age extensional structures of the Reelfoot rift appear to be reactivated as right-lateral strike-slip and reverse faults.

The New Madrid seismic zone produced three historical, large-magnitude earthquakes between December 1811 and February 1812 (Reference 374). The December 16, 1811, earthquake is associated with strike-slip faulting along the southern portion of the New Madrid seismic zone. Johnston (1996) (Reference 330) estimates a magnitude of $M 8.1 \pm 0.31$ for the December 16, 1811, event. However, Hough et al. (2000) (Reference 374) re-evaluate the isoseismal data for the region and concluded that the December 16 event had a magnitude of $M 7.2$ to 7.3 . Bakun and Hopper (2004) (Reference 333) similarly conclude this event had a magnitude of $M 7.2$.

The February 7, 1812, New Madrid earthquake is associated with reverse fault displacement along the middle part of the New Madrid seismic zone (Reference 375). This earthquake most likely occurred along the northwest-trending Reelfoot fault that extends approximately 43 mi. from northwestern Tennessee to southeastern Missouri. The Reelfoot fault is a northwest-striking, southwest-vergent reverse fault. The Reelfoot fault forms a topographic scarp developed as a result of fault-propagation folding (References 376, 377, and 378). Johnston (1996) (Reference 330) estimates a magnitude of $M 8.0 \pm 0.33$ for the February 7, 1812, event. However, Hough et al. (2000) (Reference 374) re-evaluate the isoseismal data for the region and conclude that the February 7, 1812 event had a magnitude of $M 7.4$ to 7.5 . More recently, Bakun and Hopper (2004) (Reference 333) estimate a similar magnitude of $M 7.4$.

The January 23, 1812, earthquake is associated with strike-slip fault displacement on the East Prairie fault along the northern portion of the New Madrid seismic zone. Johnston (1996) (Reference 330) estimates a magnitude of $M 7.8 \pm 0.33$ for the January 23, 1812, event. Hough et al. (2000) (Reference 374), however, re-evaluate the isoseismal data for the region and conclude that the January 23, 1812 event had a magnitude of $M 7.1$. More recently, Bakun and Hopper (2004) (Reference 333) estimate a similar magnitude of $M 7.1$.

Because there is very little surface expression of faults within the New Madrid seismic zone, earthquake recurrence estimates are based largely on dates of paleoliquefaction and offset geological features. The most recent summaries of paleoseismologic data (References 379, 380, 381, and 458) suggest a mean recurrence time of 500 years, which was used in the 2002 USGS model (Reference 360). Paleoseismic studies have suggested the seismic activity of the New Madrid Fault System source since the Holocene may not be indicative of the long-term recurrence rate (CEUS SSC) (Reference 441) and (Holbrook et al 2006) (Reference 458). Models of temporal clustering used to account for this uncertainty and other uncertainties associated with the paleoliquefaction record and recurrence are also accounted for in the New Madrid source characterization presented in Subsection 2.5.2.

Central Virginia Seismic Zone. CVSZ is an area of persistent, low-level seismicity in the Piedmont province, located more than 250 mi. from the Lee Nuclear Site (Figure 2.5.1-214). The zone extends about 75 mi. in a north-south direction and

about 90 mi. in an east-west direction from Richmond to Lynchburg, Virginia (Reference 382). The largest historical earthquake that has occurred in the CVSZ is the magnitude (M_w) 5.8 event on August 23, 2011 near the town of Mineral, in Louisa County, Virginia (Reference 462).

The Mineral earthquake may prove to be illuminating about the seismicity in this area, but current research on this earthquake is somewhat preliminary and only now beginning to be published in peer-reviewed journals (e.g., References 459, 460, 461). The most recent information indicates that the Mineral event occurred on a plane striking N28-30°E and dipping 45-51°SE, but not associated with a previously mapped fault (Reference 459).

Seismicity in the CVSZ ranges in depth from about 2 to 8 mi. (Reference 383) with a mean depth at 5 mi. (Reference 352). Coruh et al. (1988) (Reference 384) suggest that seismicity in the central and western parts of the zone may be associated with west-dipping reflectors that form the roof of a detached antiform, while seismicity in the eastern part of the zone near Richmond may be related to a near-vertical diabase dike swarm of Mesozoic age. However, given the depth distribution of 2 to 8 mi. (Reference 383) and broad spatial distribution, it is difficult to uniquely attribute the seismicity to any known geologic structure. The relatively shallow depth of seismicity compared to the basal Appalachian detachment (References 384 and 352), indicates that the CVSZ seismicity occurs on the Paleozoic and Mesozoic faults that lie above the Precambrian basement (Reference 441).

No capable faults or structures are identified within the CVSZ. Two paleoliquefaction sites are identified within the seismic zone (References 310 and 385), but the relative paucity of paleoliquefaction features along the coastlines and riverways of Virginia make it unlikely that the CVSZ has produced a $M > 7$ earthquake in the last 5,000 years (Reference 385). The seismicity of the CVSZ is encompassed in the ECC-AM sesimotectonic zone (Reference 441).

2.5.1.2 Site Geology

Subsection 2.5.1.2 presents descriptions of the geologic conditions present in the Lee Nuclear Site vicinity (25 mi. radius), Lee Nuclear Site area (5 mi. radius) and at the Lee Nuclear Site (0.6 mi. radius). Subsections detailing the physiography and geomorphology, geologic history, stratigraphy, structural geology, engineering geology, seismicity and paleoseismology, and groundwater of the site area are included.

The geology of the site and surrounding area is extensively studied (Figures 2.5.1-218a, 218b, 219a, 219b, and 220), and typical of the region. The Duke Power Co. Project 81 Preliminary Safety Analysis Report presents previous investigations of the Lee Nuclear Site (Reference 401). More recently-published literature and mapping, as well as field reconnaissance and detailed studies conducted in 2006 and 2007 as part of this project, supplement these data.

2.5.1.2.1 Site Area Physiography and Geomorphology

The site is located within the Piedmont physiographic province of central South Carolina (Figure 2.5.1-201). The Piedmont Physiographic Province is bounded on the southeast and northwest by the Coastal Plain and Blue Ridge physiographic provinces, respectively. The site lies approximately 8.5 mi. southeast of Gaffney, South Carolina on the western bank of the Broad River (Figure 2.5.1-218a and 218b). The site topography is characteristic of the region, with gently to moderately rolling hills and generally well-drained mature valleys. Within the 5 mi. site area, topography ranges from about 400 to 1,000 ft. msl (Figure 2.5.1-221). Elevations at the Lee Nuclear Site range from about 500 to 700 ft. msl (Figure 2.5.1-222).

The primary drainage in the site area is the Broad River. Typical of most first order Piedmont streams, the Broad River flows southeast normal to trend of most geologic contacts and structures. The streambed is at about 500 ft. msl and has incised into the Piedmont surface about 200 ft. below the drainage divides. The Broad River lacks a well-developed flood plain in the Lee Nuclear Site area.

The local tributaries drain into the Broad River. The local drainage pattern is generally dendritic, the result of lithologic control and rock jointing. In the vicinity of the Broad River, these tributaries occupy steep valleys that shallow headward. Drainage divides generally range in elevation from 630 to 750 ft. msl.

Surficial geologic materials consist predominantly of residual soils and saprolite that mantle igneous and metamorphic bedrock. Relatively few natural bedrock outcrops are present within the site area, characteristic of the long weathering history of the Piedmont. The long history of weathering and erosion has created a relatively flat, rolling plain with local relief generally the result of variations in the weathering resistance of bedrock and/or stream incision. In the site area, the most erosion-resistant rock types contain large amounts of quartz (typically metaconglomerate or chert deposits), and often support linear ridges (Figures 2.5.1-219a, 219b and 2.5.1-220). The highest point in the Lee Nuclear Site area is Draytonville Mountain at about 1,010 ft. msl. Draytonville Mountain is an elongated, east-west-trending ridge located 4 mi. west-northwest of the site and underlain by quartzite pebble-cobble metaconglomerate (References 386 and 387). Other ridges in the site area include McKowns Mountain, Silver Mine Ridge, and unnamed ridges near Cherokee Falls, South Carolina. The site area ridges are associated with erosion-resistant quartzite rocks.

The Preliminary Safety Analysis Report (PSAR) Project 81 prepared for the former Duke Cherokee nuclear site identifies five lineaments within the site vicinity based on 1:500,000- and 1:250,000-scale aerial photographs (Reference 401). These lineaments are interpreted to be the result of drainage patterns, variations in bedrock resistance to weathering, and/or land use. These lineaments are not attributed to differential surface movement from capable tectonic features. Field reconnaissance and review of aerial photography and digital topography of the site vicinity performed as part of this project confirm the findings of the earlier lineament study.

One of the lineaments identified by PSAR Project 81 (Lineament No. 1) (Figures 2.5.1-219a and 2.5.1-221) is of particular interest for two reasons: (1) its orientation parallel to the predominant regional structural grain, and (2) its proximity to the site (Reference 401). This 4- to 5-mi.-long linear feature is located approximately 2 mi. northwest of the Lee Nuclear Site, and strikes approximately N55°E, and is a relatively steep northwest-facing slope. London Creek flows northeastward along much of the length of the northwestern base of the slope, before joining with the Broad River near the southernmost tip of Ninety-Nine Islands. The lineament, most easily recognizable on the 1:40,000-scale USGS photography, terminates northeastward at the Broad River and is not expressed in the topography northeast of the river. Field reconnaissance performed for this project and geologic mapping by Nystrom (2004) (Reference 391) reveal that resistant, northeast-striking quartzite layers outcrop along the top of the slope. The linear topographic expression of this slope or ridge is the result of erosion by London Creek (and the erosion resistance of the quartzite layers) and is assessed to be non-tectonic in origin.

In summary, Lee Nuclear Site area topography records no expression of differential surface movement but is strongly controlled by variations in bedrock resistance to weathering. The most resistant rock types in the site area are mainly quartz-rich rocks such as metaconglomerate and chert.

2.5.1.2.2 Site Area Geologic Setting and History

The site area is underlain by a complexly deformed and metamorphosed plutonic–volcanic sequence and associated sediments. Under the “older” belt nomenclature these rocks are considered part of the “Kings Mountain Belt” (Reference 207). More recent classification of Hibbard et al. (2002) (Reference 204) associates these rocks with other Neoproterozoic – Early Paleozoic metagneous terranes that were formed in volcanic arc systems. The subduction associated with these systems occurred distant from Laurentia, and based on fossil evidence was in the Gondwana realm. This schema groups these diverse terranes into the Carolina Zone, which in more recent publications is called “Carolinia” (References 425 and 428) and is given “Domain” status. Carolinia forms the exposed eastern margin of the Appalachian system.

Hatcher et al. (2007) (Reference 404) use “Carolina Superterrane” to describe the amalgamated peri-Gondwanan volcanic arcs, but they consider the Kings Mountain Belt to have both Laurentian and peri-Gondwanan components. They consider the volcanic arc protoliths of the Battleground Formation to be of peri-Gondwanan origin, but consider the sedimentary protoliths of the Blacksburg Formation to have Laurentian affinities. However, they place the surface expression of the Carolina terrane suture to the west of the Battleground Formation.

Hibbard et al. (2002) (Reference 204) assign both the metasediments of the Blacksburg Formation and the metavolcanic rocks of the Battleground Formation to the Charlotte terrane of Carolinia. Their rationale for this association is the occurrence of similar rock types in both units, including protolithic felsic volcanics, quartzites that probably represent siliceous exhalatives related to hydrothermal

activity associated with felsic volcanism, and similar styles of gold mineralization. Hibbard et al. (2002) (Reference 204) consider the metasediments of the Blacksburg Formation to represent the late stage clastic and carbonate sedimentary cap to the volcanic arc comprising the Battleground Formation, and therefore assign all the formations of the Kings Mountain Belt to have peri-Gondwanan associations. The following geologic scenarios and discussion are based on the detailed discussion of the characteristics of the Charlotte terrane in Hibbard et al. (2002) (Reference 204).

The site area is located in the western portion of the Charlotte terrane. This terrane represents an “infrastructural” element of the Carolina Zone, characterized by lack of primary features due to regionally penetrative tectonothermal processes in Hibbard et al. (2002) (Reference 204). The Charlotte terrane contains elements from a long and complex geologic history (Figures 2.5.1-202a and 202b) that began with arc related magmatic activity in the Neoproterozoic, and extends through the rift related Triassic extension and magmatism associated with the opening of the modern Atlantic Ocean basin. Figure 2.5.1-223 is based on PSAR (1974) (FSAR Reference 401), Schaeffer (1981) (Reference 392), Hibbard et al. (2002) (Reference 204), and Hatcher et al. (2007) (Reference 404), and summarizes the geologic history of the site area.

The protoliths for the lithologies in the western portion of the Charlotte terrane are the result of magmatic activity (Stage II of Hibbard et al. (2002)) associated with subduction and arc rifting that straddled the Neoproterozoic–Cambrian boundary. An early stage of magmatism and deposition at about 570 Ma resulted in both felsic and mafic volcanism and shallow intrusion of tonalite and granodiorite plutonic bodies into the volcanic accumulation itself. Deposition of volcanic material was accompanied in later stages with deposition of both clastic and carbonate sediments that produced a volcanoclastic sequence with interfingered marine sediments. Locally, intense hydrothermal activity from the interaction of seawater with hot volcanic centers has significantly modified the bulk chemistry of these units. This modification occurred by severe leaching, transport, and redeposition of certain chemical components.

Subsequently, in the 549 to 535 Ma interval, the volcanic pile and its sedimentary units were intensely deformed and metamorphosed to upper greenschist to amphibolite facies, probably resulting from the complex thermal and tectonic interactions occurring in the subduction-magmatic environment (i.e., the Virgilina Event) (Reference 204). This event is associated with at least two deformational episodes (D1 and D2) and produced most of the more noticeable foliation, structures, and map patterns of geologic units in the site area. The ages of structures and fabrics associated with D1 and D2 are constrained to pre-535 Ma by crosscutting relationships with post-tectonic and post-metamorphic diorite in Hibbard et al. (2002) (Reference 204). At least three scenarios are proposed in the literature for the cause(s) of this tectonothermal activity. These three scenarios include: (1) back arc rifting and closure, (2) subduction of a block of isotopically different material into the subduction zone, and (3) assembly of the composite Charlotte and Carolina terranes. Other locations of the Charlotte terrane contain rock types resulting from a later stage of magmatism that occurred around 540 to 530 Ma (Stage III; Figure 2.5.1-223) resulting in intrusion of large mafic–ultramafic

complexes and granitic material. In the site area, these do not appear to occur (Reference 204) unless they are possibly represented by late gabbro intrusions (Figures 2.5.1-219a and 219b).

The Charlotte terrane also shows tectonic and thermal evidence from later events in the Silurian, Devonian, and Carboniferous-Permian (i.e., the Alleghanian event; Subsection 2.5.1.1.2.1). However, the record for pre-Carboniferous tectonic activity is obscure in the Charlotte terrane in Hibbard et al. (2002) (Reference 204) probably due to thermal and structural overprinting by Alleghanian tectonic processes (Hatcher et al. 2007) (Reference 404). Hibbard et al. (2002) (Reference 204) and subsequent publications (References 428 and 430) argue for Late Ordovician - Silurian subduction of Carolina and consequently the Charlotte terrane beneath Laurentia based on evidence from other portions of Carolina and the Silurian thermal activity in the Charlotte terrane.

Amphibole $^{40}\text{Ar}/^{39}\text{Ar}$ cooling ages (425 - 430 Ma) in North Carolina record the time when the thermal environment in that location cooled through the temperature at which radiogenic argon would be lost from the amphibole (about $500 \pm 50^\circ\text{C}$; Reference 388). Hibbard et al. (2002) (Reference 204) interpret this to indicate cooling following the elevated thermal conditions associated with the subduction of Carolina beneath Laurentia.

Based on detrital zircon ages in the Cat Square Terrane of the Inner Piedmont, Hatcher et al. (2007) (Reference 404) argue against Late Ordovician - Silurian subduction of Carolina beneath Laurentia and for Neoacadian to early Alleghanian (post ~405 Ma) subduction of Laurentia beneath the Carolina Subterrane. Hatcher et al. (2007) (Reference 404) also cite the existence of the Concord suite, which represents Devonian mafic plutonism that resulted from this subduction event. In any case, in addition to the Concord suite plutons, the record for Devonian tectonothermal activity in the Charlotte terrane is confined to the GHSHSZ. This indicates that Devonian effects may have been highly localized (Reference 204).

Alleghanian (Carboniferous-Permian) tectonothermal activity is heterogeneously distributed in the Charlotte terrane (Reference 204). Deformation occurs mainly in discrete shear zones within the terrane and at the Central Piedmont shear zone, which in the site vicinity comprises the Cross Anchor fault and the Kings Mountain shear zone. Metamorphism associated with Alleghanian orogenesis ranges from greenschist to amphibolite facies in the Charlotte terrane. Late Alleghanian tectonic activity is attributed to the thrusting of the Charlotte terrane onto the Inner Piedmont terrane in the site vicinity (References 204 and 404). However, proposed accretion of Carolina to Laurentia in either the Late Ordovician - Silurian (Reference 204) or in the Neoacadian - Early Alleghanian (Reference 404) means that the suture between Carolina and Laurentia is an older structure and the Alleghanian activity on the Central Piedmont shear zone must represent a later event. One explanation for this relationship is that the present surface expression of the Central Piedmont shear zone represents the head of the suture that was decapitated in the subsurface during the late Alleghanian collision of Laurentia and Gondwana (References 204 and 404).

Hatcher et al. (2007) ([Reference 404](#)) map the surface trace of the subsurface suture throughout the Carolina Superterrane based on geophysical evidence.

Although the Charlotte terrane experienced accretion either during the Late Ordovician - Silurian or during the Neocadian - early Alleghanian, the thermal and structural record is limited or obscure as discussed above. This has no doubt contributed to the controversy surrounding the timing and nature of the event. One K-Ar age for the site yields an age of 290 ± 7 Ma for hornblende ([Table 2.5.1-202](#)), and therefore it is uncertain if the site and site area experienced pre-late Alleghanian thermal elevation and therefore the extent of Late Ordovician or Neocadian - early Alleghanian tectonogenesis.

Undeformed potassium feldspar from the site gives a K-Ar age of 219 ± 1 Ma (closure to argon loss at about 250°C) shows that the rate of cooling decreased and that the site area and site passed below about 250°C around 219 Ma. These data suggest that the site has not experienced thermal conditions that could be associated with greenschist grade metamorphism since at least 219 Ma, and likely since around 300 Ma as described in [Subsection 2.5.1.2.5.4](#).

Based on the relatively limited record in the Charlotte terrane for Late Ordovician - Silurian and Devonian tectonics, the activity associated with Alleghanian tectonics is likely the cause of the last three deformational phases (D3 - Q5) at the site and site area. However, any or all of these structures could have resulted from earlier accretion events and could have been overprinted by the thermal elevation associated with the late Alleghanian interaction of Gondwana with Laurentia.

Mesozoic extensional tectonics associated with opening of the Atlantic Ocean almost certainly affected the area, at least to a limited extent, with the development of joints and fractures with associated quartz and zeolite mineralization. Mesozoic extension-related fracturing and brittle faulting associated with development of cataclasites, silicification, and zeolite mineralization are widespread features throughout the Piedmont in the site region and site vicinity ([Reference 420](#)). These features also are associated with late kinematic open to healed fractures lined with crystalline quartz and syntaxial extension veins filled with anhedral quartz. Garahan et al. (1993) ([Reference 420](#)) report brittle faulting associated with Mesozoic reactivation of the Kings Mountain shear zone, northwest of the site. Murphy and Butler (1981) ([Reference 389](#)) report limited displacement (less than 10 cm), small scale brittle faulting in the site area. Schaeffer (1981) ([Reference 392](#)) reports laumontite - calcite mineralization associated with S5 kink planes. Undeformed Triassic diabase dikes are the only documented evidence of Mesozoic activity in the site area. Subsequent to this rifting, broad flexure occurred as a result of erosional unloading and the onset of drift margin sedimentation.

In summary, the majority of rock types, metamorphism, and deformation in the site area can be attributed to Neoproterozoic–Early Cambrian subduction zone-related magmatic and tectonic activity. However, the site area may have experienced thermal environments and stresses associated with Silurian and/or Devonian orogenic events. Based on regional considerations, any effects resulting from these events are to be limited in the site area. In contrast,

Alleghanian tectonic activity likely produced folding and shearing localized in discrete zones under greenschist to amphibolite grade conditions as recorded in the mineral cooling ages. Alleghanian emplacement of the Charlotte terrane upon the Inner Piedmont was followed by rapid cooling that resulted from rapid unroofing and cooling. Extensional tectonics associated with the opening of the modern Atlantic Ocean probably caused some jointing and fracturing in the Lee Nuclear Site area. In addition, magmatism associated with this extension is evident in the site area as a set of undeformed diabase dikes.

2.5.1.2.3 Site Area Stratigraphy and Lithology

Rock units in the site area generally belong to the Battleground Formation (References 308, 391, 286, and 260). There is disagreement, however, as to whether the rock mass mapped at the site (map unit "Zto" on Figures 2.5.1-218a through 2.5.1-220) belongs to the Battleground Formation. Murphy and Butler (1981) (Reference 389) suggest that these rocks belong to the Battleground Formation, whereas more recent publications by Horton and Dicken (2001) (Reference 308) and Nystrom (2004) (Reference 391) indicate that rock mass Zto comprises plutonic rocks that intruded into the Battleground Formation. For the purposes of this COL application, rock mass Zto is assessed to be separate from, and younger than (or possibly coeval with), the Battleground Formation. Other rocks in the site area include Mesozoic diabase dikes (References 236 and 389) and Quaternary alluvial deposits (References 286 and 391).

Subsection 2.5.1.2.3.1 describes the Battleground Formation.

Subsection 2.5.1.2.3.2 describes intrusive rock mass Zto. Subsection 2.5.1.2.3.3 describes the Mesozoic diabase dikes and Quaternary alluvial deposits within the site area.

Figure 2.5.1-219a presents geologic mapping of the site area performed at two different scales by three different researchers (References 308, 286, and 391). As such, unit contacts do not match perfectly across adjacent source map boundaries.

2.5.1.2.3.1 Battleground Formation

The Battleground Formation primarily comprises metavolcanic and metasedimentary rocks of Neoproterozoic age (Reference 308) (Figures 2.5.1-219a and 219b). The occurrence of metasedimentary carbonate rocks is indicative of a marine depositional environment. The Battleground Formation includes felsic metavolcanic rocks, intermediate to mafic metavolcanic rocks, and quartz-rich metasedimentary rocks. Major units within the Battleground Formation are described below, with additional detail provided in Figures 2.5.1-219a and 219b.

Mafic to intermediate metavolcanic rocks (map unit Zbvm). Nystrom (2004) (Reference 391) maps mafic to intermediate metavolcanic rocks west and south of the site. These rocks are described as medium gray, dark gray, and green hornblende phyllite, hornblende gneiss, and amphibolite. Nystrom (2004) (Reference 391) maps the contact separating Zbvm from the western edge of

plutonic rock mass Zto as nearly linear ([Figure 2.5.1-219a](#)). [Subsection 2.5.3.1.3](#) describes evidence indicating the irregular and intrusive nature of this contact, as shown in [Figures 2.5.1-220](#) and [2.5.1-229](#).

Felsic metavolcanic rocks (map unit Zbv). Nystrom (2004) ([Reference 391](#)) maps assorted felsic metavolcanic rocks in the southeast corner of the Blacksburg South quadrangle. These rocks are described as medium gray, dark gray, and green in color.

Interlayered mafic and felsic gneiss (map unit Ztrs). Howard (2004) ([Reference 286](#)) maps interlayered mafic and felsic gneiss in the southwest corner of the Kings Creek quadrangle. Based on general unit descriptions and mapped location, units Ztrs and Zbv are assessed to be roughly equivalent across the quadrangle boundary. However, Nystrom (2004) ([Reference 391](#)) indicates that Zbv is part of the Battleground Formation, whereas Howard (2004) ([Reference 286](#)) suggests that Ztrs is not part of the Battleground Formation. For the purposes of this COL application, rock masses Zbv and Ztrs are assessed to be equivalent and part of the Battleground Formation.

Plagioclase crystal metatuff (map unit Zbct). Nystrom (2004) ([Reference 391](#)) describes unit Zbct as gray, generally well foliated, assorted metavolcanics of mainly felsic to intermediate composition with crystal and less abundant lithic metatuffs. This unit is assessed to be the equivalent of Howard's (2004) ([Reference 286](#)) crystal metatuff (Zbct).

Phyllitic metatuff (map unit Zbmp). Nystrom (2004) ([Reference 391](#)) describes unit Zbmp as gray to dark gray varied metavolcanics including crystal and lithic metatuffs. This unit is assessed to be equivalent to Howard's (2004) ([Reference 286](#)) mottled phyllite (lapilli metatuff) (map unit Zbmp). Howard (2004) ([Reference 286](#)) maps a siliceous alteration zone within unit Zbmp (shown as Zbmp-a on [Figure 2.5.1-219a](#)) that does not appear on Nystrom's (2004) ([Reference 391](#)) map.

Quartzite and metaconglomerate (map units Zbq, Zbkq, Zbdc, Zbc). Nystrom (2004) ([Reference 391](#)) maps various north- and northeast-striking quartzite and quartz metaconglomerate units within the site area. These long and thin "stringers" are described as white to gray, fine- to medium-grained quartzite and medium- to coarse-grained, schistose metaconglomerate. As described in [Subsection 2.5.1.2.1](#), some of these quartzite and metaconglomerate units are mapped atop ridges in the site area, including McKowns Mountain.

Due to intense deformation, few primary features survive with which to determine stratigraphic order within the Battleground Formation. However, inferred relationships ([References 236](#), [389](#), and [390](#)) suggest the proposed northeast-striking South Fork antiform forms a homocline such that units within the Battleground decrease in age to the northwest ([Reference 236](#)) ([Figure 2.5.1-219a](#)). If these inferred relationships are correct, then the oldest rocks would occur in the antiform's core and rocks farther from the core to the northwest would be younger. This inference is supported by the occurrence of the metasedimentary component primarily to the northwest, the expected

stratigraphic relationships for deposition of marine-dominated clastic and chemical precipitate rocks at the later stages of the volcanic pile accumulation (Reference 308). Figure 2.5.1-224 schematically shows the stratigraphic relationships of the various units in the site area.

2.5.1.2.3.2 Site Pluton (Rock Mass Zto)

The site is underlain by a metamorphosed plutonic rock mass, shown on Figures 2.5.1-218a through 2.5.1-220, 2.5.1-224, and 2.5.1-229 as rock mass Zto. Goldsmith et al. (1988) (Reference 228) report a discordant $^{207}\text{Pb}/^{206}\text{Pb}$ age of approximately 590 Ma for rock mass Zto. This rock mass has been mapped at various scales by various geologists and, consequently, has been described differently, as indicated below.

Murphy and Butler (1981) (Reference 389) note the similarity between the compositions of volcanoclastic units of the Battleground Formation and the plutonic units that intrude them (Zto). Based on this observation, they suggest that these metavolcanics were intruded by their own parent magmas, and assign both to the Battleground Formation. However, more recent mapping separates these plutonic rocks (Zto) from the Battleground Formation host units. For the purposes of this COL application, rock mass Zto not considered to be part of the Battleground Formation. This distinction largely is semantic, however, since the Battleground Formation and rock mass Zto likely formed at approximately the same time in the Neoproterozoic (Reference 389).

Horton and Dicken's (2001) (Reference 308) 1:500,000-scale mapping describes rock mass Zto at the site as Neoproterozoic metatonalite (Figures 2.5.1-218a and 218b), comprising metamorphosed biotite tonalite and lesser amounts of hornblende tonalite, trondhjemite, and granodiorite. Rock mass Zto locally contains angular xenoliths of Battleground Formation metavolcanic and metasedimentary rocks (Reference 308).

Nystrom's (2004) (Reference 391) 1:24,000-scale mapping of the Blacksburg South quadrangle describes rock mass Zto at the site as metatonalite (Figures 2.5.1-219a and 219b). This metatonalite is described as light to medium gray, coarse-grained, with large potassium feldspar and quartz grains (Reference 391).

Howard's (2004) (Reference 286) 1:24,000-scale mapping of the adjacent Kings Creek quadrangle describes rock mass Zto as metatonalite and volcanoclastic rocks (Figures 2.5.1-219a and 219b). These felsic rocks are of mixed origin, comprising intrusive tonalite, dacitic flows, and epiclastic byproducts of both (Reference 286). Howard (2004) (Reference 286) maps Zto approximately 3 miles east of the site (Figure 2.5.1-219a).

Whereas rock mass Zto generally is metatonalite, its composition varies spatially (Reference 286). Subsection 2.5.3.1 indicates that meta-granodiorite is the most abundant rock type present within map unit Zto exposed by the excavation at the site, based on petrographic analyses (Reference 401). As such, Figure 2.5.1-229

and discussions throughout [Subsection 2.5.3](#), describe rock mass Zto within the site excavation as meta-granodiorite.

2.5.1.2.3.3 Other Lithologic and Stratigraphic Units within the Site Area

In addition to the rocks described above, Mesozoic diabase dikes and Quaternary alluvial deposits are mapped within the site area. The diabase dikes primarily are of plagioclase, pyroxene, and olivine composition. These dikes crosscut, and therefore post-date, the units described above. These diabase dikes are undeformed and unmetamorphosed rocks of Jurassic-Triassic age ([References 236 and 389](#)).

Quaternary alluvial deposits are mapped in active river and stream channels in the site area. These deposits primarily are modern channel deposits and bars that are actively transported by the Broad River and its tributaries comprising gravels, sands, and silts.

2.5.1.2.4 Site Area Structural Geology

Previous geologic investigations include specific studies conducted for the Lee Nuclear Site and geologic mapping of the surrounding area. Schaeffer (1981) ([Reference 392](#)), Butler (1981) ([Reference 285](#)), and Murphy and Butler (1981) ([Reference 389](#)) present structural analyses for the site area. Schaeffer (1981) ([Reference 392](#)) incorporates much of the structural data obtained as part of the PSAR Project 81 ([Reference 401](#)). According to Schaeffer (1981) ([Reference 392](#)), the site area has experienced five deformational episodes (D_1 through D_5), which are expressed as associated cleavage development (S_1 through S_5), folding (F_1 through F_5), and lineations (L_1 through L_5) ([Table 2.5.1-203](#)). In addition to these penetrative fabrics, discrete zones of both ductile and brittle deformation are present, mainly concentrated in sheared-out fold limbs ([Table 2.5.1-203](#)). The map pattern of surface geology is mainly controlled by the planar S_1 and S_2 foliations, and by the axial surfaces of F_2 folds. Because the S_2 foliation is the best developed, these features are the most commonly seen. Both the D_1 and D_2 deformations are closely related and formed during the same greenschist- to amphibolite-grade metamorphic event. This metamorphism and deformation has been shown to have occurred near the Neoproterozoic-Cambrian boundary (549 to 535 Ma) in Hibbard et al. (2002) ([Reference 204](#)). In addition to the structures described above, Schaeffer (1981) ([Reference 392](#)) also notes probable effects resulting from Mesozoic extension.

The D_1 deformation phase resulted in a foliation (S_1) axial planar to small scale (0.4 to 1.2 in. wavelength) isoclinal upright folds (F_1). Schaeffer (1981) ([Reference 392](#)) reports that S_1 is probably parallel to S_0 (where S_0 is the primary bedding expressed as compositional layering). In some locations, the early foliation (S_1) can only be found in the hinge areas of the larger scale F_2 folds. In most locations, the limbs of F_1 folds are sheared out. Schaeffer (1981) ([Reference 392](#)) demonstrates that, in the hinge area of the Cherokee Falls synform, F_1 fold axes were rotated into the plane defined by S_2 ([Figure 2.5.1-225](#)).

The D_1 deformation event formed an intersection lineation of S_0 and S_1 . The rotation of the F_1 fold axes and the sub-parallel orientation of S_1 and S_2 indicate the transposition of D_1 structures during the D_2 event.

D_2 deformation caused isoclinal to closed upright folding (F_2) associated with a well-developed axial planar cleavage (S_2). The nature of the F_2 folding shows some lithologic control with isoclinal folding developing in more tightly foliated rocks (schist and phyllite) and close to tight folding in more massive units (quartzite, metaconglomerate, and gneiss). This resulted in a lineation defined by the intersection of S_1 and S_2 . In addition, the alignment of stretched bodies of biotite schist and quartzite form a lineation perpendicular to the F_2 axes. Rheologically less competent material (marble) shows stretching both parallel and perpendicular to F_2 fold axes to form pillow like structures.

The D_3 deformation event folded the S_2 foliation into asymmetric, flexural-slip folds with longer limbs to the southeast. These F_3 fold axes plunge at moderate angles to the northeast, with axial planes that dip steeply to the northwest, and display a well-developed axial planar cleavage (Figure 2.5.1-225). In places F_3 folds are observed to fold F_2 folds. An intersection lineation associated with D_3 is defined by the intersection of S_2 and S_3 . The D_3 phase also caused reactivation of D_2 shear zones with a later brittle overprint. Both the ductile and cataclastic fabrics record post kinematic overgrowths and veins with a lower greenschist assemblage consisting of quartz, epidote, muscovite, biotite, chlorite and potassium feldspar.

A fourth deformational event (D_4) produced open to tight flexural slip folds with poorly developed axial planar cleavage with axes that plunge gently to the northeast (Figure 2.5.1-225). The axial planar cleavage (S_4) is almost horizontal and dips gently both northeast and northwest. The intersection of S_4 and S_2 define the L_4 lineation.

The final deformation episode recognized in the site area resulted in kink folding and gentle to open warping of S_2 . The plunge of the fold axes is variable but primarily confined to the southeastern quadrant. Some of the kink folds occur in conjugate sets with sub-vertical axial and kink planes that strike northeast and northwest. The intersection lineation of S_5 and S_2 plunges steeply down dip on S_2 .

Based on the limited amount of evidence for Silurian and Devonian fabric development, D_3 , D_4 , and D_5 structures are likely Carboniferous (Alleghanian) in age. The youngest possible age of D_3 , D_4 , and D_5 structures is constrained by the post-kinematic greenschist overgrowth (pre-296 Ma), based on radiometric dating discussed in Subsection 2.5.1.2.2.

2.5.1.2.4.1 Structures Within the Site Area

Subsection 2.5.1.2.4.1 describes relevant geologic structures located within 5 mi. of the Lee Nuclear Site.

Cherokee Falls Synform. Mapping by Murphy and Butler (1981) (Reference 389) shows the axial trace of the Cherokee Falls synform about 4.5 mi. northwest of the Lee Nuclear Site (Figures 2.5.1-219a and 219b). Murphy and Butler (1981) (Reference 389) interpret this structure as an overturned synform, with a shallowly northeast-plunging fold axis and an axial surface that dips steeply to the southeast, characteristic of F_2 structures. The core of the synform contains metatrandjemite complex lithologies while mafic schist and sericite schist wrap around the nose and form the outer limbs of the synform. This structural relationship is modified by subsidiary folding that results in protrusions of mafic schist into the core parallel to the fold axis. The northwest limb is apparently sheared off as the map units are truncated. As noted previously, F_1 fold axes are rotated into the surface defined by the axial planar cleavage (S_2). Also, folding of S_1 is observed in the hinge area. This is an F_2 structure resulting from the D_2 phase of deformation. More recent mapping by Nystrom (2004) (Reference 391) does not include the Cherokee Falls synform.

Draytonville Synform. The Draytonville synform is located about 4.5 mi. northwest of the Lee Nuclear Site where a prominent metaconglomerate (the Draytonville metaconglomerate) is folded into an overturned syncline (Reference 389) (Figures 2.5.1-219a and 219b). The fold axis plunges shallowly to the northeast and the axial surface dips steeply southeast. Based on the fact that only compositional layering and one other surface is observed to be folded (Reference 389) and the similarity in fold geometry to the Cherokee Falls synform, the Draytonville synform is also considered an F_2 generation fold (Reference 387). More recent mapping by Nystrom (2004) (Reference 391) does not include the Draytonville synform.

Minor Striated Surfaces. Field reconnaissance for PSAR Project 81 (Reference 401) identifies several surfaces with mineralization and slickenside development within the Lee Nuclear Site area. These are not traceable beyond a single exposure, thereby indicating that they are small-displacement features and are not associated with any through-going fault. These features are characteristic of the Piedmont regionally, and are described below:

- PSAR Project 81 (Reference 401) maps a series of en echelon, epidote-covered slickensided surfaces at Cherokee Falls, South Carolina, about 3 mi. northwest of the site. These surfaces dip 45° east, with west-stepping en echelon geometry. These features are not traceable beyond Cherokee Falls. Detailed examination reveals that epidote crystals grew across the surfaces in addition to defining the slickenside lineation (Reference 401). This demonstrates that some epidote formed after movement on the surfaces had ceased. The stability field for epidote therefore precludes movement on these surfaces in a near-surface regime.

- PSAR Project 81 (Reference 401) maps another set of slickensides in a schistose zone in the Draytonville, South Carolina area about 4 mi. west of the site. This zone has a moderate southeasterly dip. These slickensides could not be traced beyond this single exposure.
- PSAR Project 81 (Reference 401) maps a minor offset with vertical dip and northwest strike about 4 mi. north of the site. Murphy and Butler (1981) (Reference 389) note a small amount of lateral offset, no measurable offset could be obtained.
- PSAR Project 81 (Reference 401) maps two offsets about 6 mi. northwest of the sites; however, the poor condition of the exposure prevented resolution of the fault orientation. One of the offsets indicated normal movement while the other indicates reverse movement.

The PSAR (Reference 401) does not describe precise locations of these minor features, and fieldwork performed for this project did not locate the minor features described above. As described in the PSAR, these minor features were not traced beyond a single exposure, and are not expressed geomorphically. These minor, localized features are similar to those found throughout the Piedmont, and are not evidence for recent movement.

2.5.1.2.5 Site Geology

Subsection 2.5.1.2.5 presents a detailed description of the site (0.6 mile radius) geology.

2.5.1.2.5.1 Site Physiography and Geomorphology

The physiographic and geomorphologic characteristics of the site are typical of those described for the site area. Elevations at the site range from 510 to 820 ft. msl (Figure 2.5.1-222). Site relief is largely the result of tributary drainage incision. McKowns Mountain, the linear, north-trending ridge west of the site, is the result of erosion-resistant quartzite.

The variation in bedrock resistance to weathering locally control drainage directions, and is also discussed in Subsection 2.5.1.2.1. Topography controlled by differential erosion is particularly evident in the orientations of McKowns Creek and a smaller creek that occurs between McKowns Mountain and a smaller quartzite ridge to the east. The smaller creek is essentially sub-parallel to the quartzite ridges and McKowns Creek and the confluence of the smaller creek can be seen to bend around the nose of McKowns Mountain.

2.5.1.2.5.2 Site Geologic Setting and History

The site geologic history is congruent with the scenario outlined above for the site area. However, whereas five deformational events are documented within the site area (Reference 392), at least two are recognized in rocks at the site. The reasons why all five events are not recorded in site rocks are: (1) the emplacement of the site plutonic rocks in Neoproterozoic time (FSAR

(Reference 308) post-dates some of the older deformational events recorded in site vicinity country rocks; and (2) the contrasting rheological properties between the site plutonic rocks and the surrounding metavolcanic country rocks makes correlation of deformational events problematic. These contrasting rheological properties make correlation of deformational events recorded in the pluton and the country rocks difficult because the plutonic mass probably developed different structures in response to stress relative to the surrounding country rock. The site is underlain by a pluton of granodiorite to tonalite composition that has intruded into mafic to felsic volcanoclastic country rock. Lee Nuclear Site rocks have undergone at least two deformational events and metamorphism to upper greenschist to amphibolite facies. These deformation events produced two foliations, and the second deformation event produced tight to isoclinal folding. These deformation events occurred in Neoproterozoic and Early Cambrian time in association with island arc subduction, probably located proximal to Gondwana (Reference 204).

2.5.1.2.5.3 Site Stratigraphy and Lithology

The eastern portion of the site, including the area for the facility foundations, is underlain by a meta-granodiorite to meta-diorite intrusive body (Figure 2.5.1-220). Western portions of the site are underlain by mafic to intermediate metavolcanic rocks that consist primarily of hornblende phyllite, hornblende gneiss, and amphibolite. The metavolcanic rocks locally contain quartzite bodies that form geomorphically prominent linear ridges.

Deep weathering has produced a mantle of saprolite at the site up to 100 ft. thick (typically 40 to 80 ft. thick). This weathering profile grades downward to partially weathered and unweathered rock. The saprolite varies from micaceous sandy silt to silty sand, and preserves relict rock textures and structure. The upper 2 to 8 ft. of saprolite has weathered to form a soil B-horizon consisting of clayey silty sand with no relict texture or structure.

Quaternary alluvial deposits are mapped in active stream channels at the site and include gravels, sands, and silts (Figure 2.5.1-220). These deposits primarily are modern channel deposits and bars that are actively transported by the Broad River and its tributaries.

2.5.1.2.5.4 Site Area Structure

As in the site vicinity, the major control on geologic trends in the country rock and map patterns are foliations and folding due to the D_2 deformation. However, the intrusive metagranodiorite-diorite pluton is massive in nature and locally contains discrete zones expressed as joints, fractures and shear/breccia zones. These features are discussed in detail below.

The relatively massive nature of the pluton compared to the surrounding country rock which is composed of volcanoclastic protoliths, probably indicates that there has been a significant difference in rheological properties between these two lithologies, both in strength and anisotropy. That this is the case, is indicated by

the fact that the volcanoclastic country rock carries a well developed, penetrative foliation compared to the pluton in which strain is expressed in more discrete zones. This rheological difference makes correlation of deformational events between the pluton and country rock problematic in that the strain from a single deformational event may be expressed as different structures in the country rock verses the pluton (i.e., folding in the foliated country rock verses discrete shearing in the pluton). For this reason the deformational events associated with the structures in the pluton will be annotated with lower case (i.e., d_1) as opposed to the deformational events in the site area (i.e., country rock) which are expressed as upper case (i.e., D_1) (Table 2.5.1-204).

McKowns Creek Antiform. Mapping by Butler (1981) (Reference 285) indicates that the metagranodiorite - diorite body that serves as the foundation for the Lee Nuclear Site structures is located in the nose of McKowns Creek antiform. This antiform is shown at the map scale by metatonalite-dacite-complex lithologies that are folded about a core of metaandesite (Figures 2.5.1-219a and 219b). Two prominent north-south oriented quartzite ridges are located in the western portion of the site on the eastern flank of the structure (Figures 2.5.1-219a and 219b). The dominant axial planar foliation is S_2 , which occurs at an angle to the lithologic contacts and an earlier foliation (S_1), is folded in the nose of the structure, Schaeffer (1981) (Reference 392). Based on these observations and the orientation of the fold axes and axial surface, Schaeffer (1981) (Reference 392) assigns this structure to F_2 . Therefore, this structure results from D_2 deformation and is Neoproterozoic to Early Cambrian in age. More recent mapping by Nystrom (2004) (Reference 391) does not include the McKowns Creek antiform.

Shear and Breccia Zones. Several “shear-breccia” zones were investigated during field studies performed for the Project 81 PSAR (Reference 401) and in subsequent foundation excavation mapping. These zones were mapped and studied in great detail including borings and detailed petrographic descriptions of the structural fabric.

Detailed mapping shows that these zones comprise smaller-scale anastomosing zones that are preferentially developed in the smaller dikes or along the margins of the larger dikes of the more mafic lithologies. The structural fabric in these zones contains an early ductile (foliated) component (d_1) with a late-stage brittle overprint (d_2). The orientation data for these zones are shown plotted on a stereonet in Figure 2.5.1-231. The most well developed zones strike a few degrees east of north and dip steeply east. A second, less well-developed set strikes northwest and dips moderately southwest.

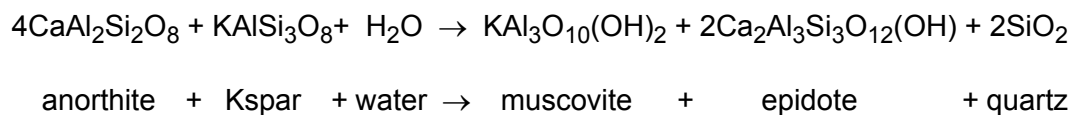
The early ductile fabric is composed primarily of elongated “polygonalized” polycrystalline quartz aggregates indicative of dynamic recrystallization and annealing recovery mechanisms (Reference 432). These quartz aggregates occur in a foliated matrix of white mica and sometimes biotite. Potassium feldspar and plagioclase porphyroclasts are reported and this fabric is described as mylonitic. The feldspar fraction is highly altered to white mica and epidote. Iron staining of the shear planes is ubiquitous. Biotite in the protolith is reported to be “olive

green” in color. In contrast, biotite reported in association with the shear zones is almost always reported to be “brown.”

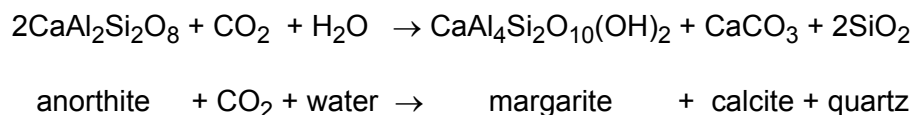
The early ductile fabric is overprinted by a brittle fabric that contains fractured and broken plagioclase, quartz and quartz aggregates in a finer grained matrix of smaller clasts and fine-grained material. This fine-grained matrix is overgrown by relatively undeformed white mica (Figure 2.5.1-236). This white mica occasionally stitches the boundary between larger clasts and the fine-grained matrix. In addition, the matrix contains randomly oriented chlorite plates and masses, along with epidote, calcite and pyrite.

Veins containing quartz, calcite, epidote, white mica, chlorite, pyrite and what is reported to be a low birefringent material identified as K-feldspar (probably adularia; Reference 433) cut the ductile and brittle fabrics (Figure 2.5.1-237). Veins also occur that contain various mixtures of these minerals and potassium feldspar. These veins are in various states of deformation ranging from undeformed, to slightly deformed, to folded and bent. In addition, stringers of the vein material are reported sub-parallel to the dominant foliation (Figure 2.5.1-230). This indicates that these veins are both syn- and post-kinematic with respect to both the ductile and brittle phases of deformation.

The relationships described above indicate that fluid-dominated metamorphic processes accompanied the ductile and brittle strain. This metamorphism resulted in a granodiorite to tonalite mineralogy consisting mainly of plagioclase (andesine–oligoclase), quartz, potassium feldspar, biotite, and amphibole transformed into more hydrous and carbon-rich phases. The presence of calcite and potassium feldspar in the metamorphic assemblage indicates that the fluid contained significant amounts of CO₂, and water. In addition to hydration of the mineralogy, this metamorphism is characterized by the release of significant amounts of calcium from the plagioclase due to removal of the anorthic component as the stable phase becomes albite in the presence of both H₂O and CO₂ (Reference 393):



in the presence of water and potassium feldspar (Reference 394), or:



These reactions are characteristic of greenschist-grade metamorphism (Reference 394). Additional potassium would be added to this system as a result of the breakdown of biotite and amphibole to chlorite.

The kinematic history of the shear-breccia zones began with a ductile event (d_1). The dynamic recrystallization and recovery features recorded in quartz indicate that this occurred at mid- to upper-greenschist facies conditions in the presence of a fluid with an aqueous component. During this initial stage, in association with mechanical processing of the other mineralogy, protolith plagioclase and potassium feldspar were metamorphosed to produce a foliated assemblage of dynamically recrystallized quartz, albite, white mica and possibly biotite. Subsequently, either due to reduced temperature, increased strain rate, or both, brittle deformation produced a cataclastic fabric (d_2) that contains clasts of the earlier fabric and probably protolith material. The metamorphic reactions discussed above and the breakdown of biotite and amphibole to chlorite produced white mica, calcite, quartz, epidote and chlorite.

Coeval with the ductile and brittle shearing, extensional fractures were generated and filled with metamorphic fluids that resulted in the crystallization of reaction products in the fracture void. Fractures initially formed parallel to the maximum compression direction (Figure 2.5.1-230), which occurred at some angle to the shear zone boundaries. As the shear strain increased, fractures rotated into the field of compression and were folded. Further shear continued to rotate the fractures out of the field of compression into the field of extension. The extensional strain deformed fractures and strung out into the structural fabric.

The persistence of elevated thermal conditions after the brittle deformation is indicated by the occurrence of extensional fractures with infilling of the metamorphic products that are undeformed and that crosscut the foliation that defines the structural fabric. This also resulted in the overgrowth of undeformed metamorphic products on the matrix material.

The geochronologic database for Duke Cherokee Nuclear Station consists primarily of K-Ar ages with a few Rb-Sr ages (Reference 401). K-Ar ages in slowly cooled settings (regional metamorphic) are typically interpreted in the context of closure temperature intervals; that is, the temperature intervals for which minerals become closed systems to argon volume diffusion (Reference 434 (Hodges, 1991); Reference 388 (McDougall and Harrison, 1999)). There are several potassium-containing minerals in which the closure temperature interval is well characterized either experimentally or empirically (Reference 434 (Hodges, 1991); Reference 388 (McDougall and Harrison, 1999)), including hornblende, muscovite, biotite, and K-feldspar (Figure 2.5.1-238, modified after Thompson, 1971 (Reference 436)). There are two important corollaries to the interpretation of K-Ar ages in the context of closure temperature intervals. One is that the K-Ar age records the time (date) at which a mineral passed through the closure interval as it cooled and therefore dates a temperature. The second is that the K-Ar age is the minimum age for the mineral to have crystallized. In order to have confidence in the validity of these corollaries, it is necessary that the K-Ar age is from a monomineralogic sample for which the K-Ar thermal systematics are well known (Figure 2.5.1-238). These criteria exclude whole rock samples in slowly cooled settings and minerals with little or no potassium in their composition. This also precludes the use of minerals whose structural state is unknown such as highly

deformed, weathered, or altered samples or minerals that may have incorporated significant amounts of non-radiogenic ^{40}Ar from the environment.

The geochronologic database for the Duke Cherokee Nuclear Station contains several samples that meet the above criteria (Reference 433). Sample B-28 is 106 ft. with a K-Ar age of 290 ± 9 Ma on undeformed hornblende (closure to argon loss of about 500°C ; Figure 2.5.1-238). Sample BP-7 is 59 ft. with a K-Ar age of 296 ± 7 Ma on undeformed biotite (closure to argon loss at about 300°C ; Figure 2.5.1-238). These ages are essentially the same and would indicate relatively rapid cooling of the terrane following emplacement of Late Paleozoic late- to post-kinematic granitic intrusions nearby (i.e., Bald Rock, York, and Clover plutons). Also, the K-Ar age reported for potassium feldspar from an undeformed vein in a dilatational feature that cross-cuts one of the shear zones is an important constraint on the minimum age possible for the shear-breccia zones. This sample gives a mineral age of 219 ± 1 Ma (sample GTP-7). This result is significant in two respects: (1) because the feldspar is undeformed and cross-cuts the shear zone, and the feldspar is older than 219 Ma, the timing of deformation related to shear zone formation is constrained to be older than 219 Ma and (2) the temperature for closure to argon loss for potassium feldspar is about 250°C (but has an interval as large as $\pm 100^\circ\text{C}$ (Reference 434)). These data indicate that the thermal environment at the site has probably not been sufficient to produce greenschist facies metamorphic effects (muscovite and biotite growth) since at least 219 Ma (Reference 433). However, the overgrowths of muscovite and biotite on both the ductile and brittle fabric components indicate that the fabric elements are significantly older since muscovite and biotite require thermal conditions above most of the closure interval of K-feldspar to grow. The K-Ar biotite age discussed above (i.e., Sample BP-7) indicates that these structural fabrics are 300 Ma or older. This conclusion is supported by the Rb-Sr age on biotite from sample B-51, 76 ft. of 291 ± 10 Ma, representing a minimum age constraint on biotite using an independent geochronologic dating technique. These data indicate the site has not experienced tectonic deformation since the Mesozoic, and possibly not since 219 Ma to 300 Ma (Reference 433).

The K-Ar geochronologic data indicate that the Cherokee site cooled through the closure intervals for both hornblende and biotite (500°C and 300°C , respectively) following regional heating, probably from the intrusion of nearby Late Paleozoic granitic plutons at about 300 Ma. The similar ages for both hornblende and biotite indicate that cooling through this temperature interval was relatively rapid. The K-Ar age for the K-feldspar of 219 Ma indicates that the Cherokee site cooled through about 250°C in the Triassic and provides a minimum age constraint on the shear-breccia zones although, based on overprinting biotite and muscovite, these zones are older. The Cherokee site age dates are consistent with those documented regionally in other studies, refer to Figure 2.5.1-239 (Reference 435).

The heavy line on Figure 2.5.1-239 shows the regional cooling and depressuration path for the southeastern Piedmont as established by Evans and Bartholomew (2010) (Reference 435) based on geochronology and fluid inclusion data. The cooling path shows cooling following intrusion of Late Paleozoic plutons through the closure interval of hornblende at 295 ± 3 Ma which is within error of

the hornblende ages obtained for the Cherokee site. The large grey rectangle represents intrusion of Late Paleozoic late- to post-kinematic granites at 286-309 Ma. The small grey rectangles represent closure to argon diffusion of hornblende (HBL) and muscovite (MUS). The muscovite closure interval on [Figure 2.5.1-239](#) is dated at 275 ± 3 Ma, which is younger than the 297 ± 6 Ma age for biotite from the Cherokee site. This muscovite is from the Augusta, Georgia area and may reflect slightly slower regional cooling at this location, the Kiokee terrane, relative to the Charlotte terrane.

Following regional cooling in the Late Paleozoic, the path shows a large negative pressure gradient in the Triassic at or slightly before 220 Ma based on K-feldspar alteration ([Figure 2.5.1-239](#)). This depressurization event resulted from Triassic crustal extension and unroofing during the formation of the Atlantic Ocean basin. The age of this event is identical to the K-feldspar age of 219 ± 1 Ma obtained at the Cherokee site. This indicates that the K-feldspar K-Ar ages at the Cherokee site also reflect cooling following regional unroofing related to Triassic crustal extension.

While the Late Paleozoic cooling rates may have differed for different geologic terranes in the southeastern United States, the general pressure-temperature history for the southeastern Piedmont (the rapid cooling following crustal extension and rifting in the Triassic) is applicable to the Cherokee site. These data indicate that the thermal environment at the site has not been sufficient to produce greenschist facies metamorphic effects since at least 219 Ma.

Although feldspar geochronology constrains the formation of the shear-breccia zones to be pre-219 Ma, the K-Ar biotite mineral age indicates cooling from greenschist grade thermal conditions at 296 ± 7 Ma. This cooling was probably associated with unroofing following thrusting of the Charlotte terrane over the Inner Piedmont along the nearby Kings Mountain shear zone. Schaeffer (1981) ([Reference 392](#)) assigns the development of ductile fabric in these zones to D_2 and the later brittle overprint to D_3 similar to features seen in sheared out F_2 fold limbs in the site area. The D_2 event is associated with upper greenschist to amphibolite grade metamorphism which would be consistent with the features observed in the ductile fabric elements. If this association is correct, then the ductile fabric in the shear - breccia zones would be Late Proterozoic to Early Cambrian in age. However, because of the probability that the pluton may have seen elevated thermal conditions and stresses in the Late Ordovician - Silurian, Hibbard et al. (2002) ([Reference 204](#)), or Devonian to late Mississippian, Hatcher et al. (2007) ([Reference 404](#)) or late Alleghanian, Hibbard et al. (2002) ([Reference 204](#)), Hatcher et al. (2007) ([Reference 404](#)) the ductile fabric (d_1) and subsequent cataclasis (d_2) in the shear-breccia zones could have resulted from, or been reactivated by stresses associated with any of these events. The only constraints are that the ductile fabric (d_1) is older than the cataclasis (d_2) and that the cataclasis is older than approximately 300 Ma based on the radiometric ages of the post-kinematic greenschist facies assemblage. It should be noted that ductile fabrics with brittle overprint are commonly reported with late stage Alleghanian tectonism. Therefore it is also possible that these shear breccia zones are related to, or have been reactivated by localized deformation of the

pluton in response to stresses associated with this thrusting event and may be Alleghanian in age.

Dilation Fractures. Dilation fractures (d_3) less than or equal to 4 in. thick and partially filled with undeformed quartz, potassium feldspar and minor amounts of calcite, pyrite and fluorite cut across the shear-breccia zones with no apparent effect except for the dilatational separation. The open spaces have euhedral crystals indicating growth from a hydrothermal fluid. These are straight breaks similar to joints and in locations where they change direction they become wider.

Based on the occurrence of similar mineralogy in the fracture filling, these dilational features were probably produced during the metamorphic event described above for the shear - breccia zones. In any event, the potassium feldspar that constrains the age of the shear-breccia zones cross cuts one of these features and places the same constraints on the age.

Joints. Joints are common at the site and in the surrounding area (Figure 2.5.1-225). Most of these features are steeply dipping (60° to 90°) and exhibit a range of strike directions, including slightly east of north, northeast, and east-west. The joint spacing ranges from one inch to several feet. Comparison of the orientations of the joint surfaces with Mesozoic structures in the site vicinity, Garahan et al. (1993) (Reference 420), indicates that at least one population of the joint sets may be related to Mesozoic extension (d_5).

Slickensides on Joint Surfaces. In some cases slickensides are mapped on joint surfaces and contacts between rock types. Study of these features in the geologic test pits indicate that they may extend from 2 to 20 ft. These surfaces cut across both the shear-breccia zones and the dilation fractures. These striated surfaces show various stages of development ranging from poorly developed with incipient chlorite films and striations to chlorite-calcite films up to 0.04 in. thick with well-developed striations. Chlorite is the most common phase on these surfaces but traces of calcite are commonly found. Microscopic study of these features shows that most of the movement has occurred in the chlorite, and that calcite is rarely deformed.

The displacement on the slickensided surfaces ranges from 0 to 1 in. in unweathered rock. One example in partially weathered rock measured 4 in., and a similar feature in saprolite recorded a 2 ft. displacement. These features apparently post-date both the dilatational fractures and the shear breccia zones, but the close association of chlorite with the movement on these surfaces indicates that they were also associated with the pre-219 Ma greenschist facies event (d_4).

Slickensides in Weathered Rock and Saprolite. Partially weathered rock and saprolite show slickensides (d_6) on surfaces coated with white clay and a black secondary material. The black material consists of gelatinous iron and manganese hydroxides of varying proportions. This material also contains clay (7 angstrom), which results from weathering of biotite and has a high iron content.

2.5.1.2.5.5 Site Geologic Mapping

Geologic mapping of the site in 2006 consisted of mapping available outcrops and exposures (Figure 2.5.1-220), including open exposures in the former Duke CNS Units 2 and 3 excavations (Figures 2.5.1-228 and 2.5.1-229). Previous excavation mapping completed as part of the construction of the Cherokee Nuclear Station was used to provide geologic information beneath the former Duke CNS Unit 1 foundation. The site geologic mapping relies on detailed evaluations of CNS and WLS mapping. Detailed evaluations performed by Fugro Consultants, Inc. (Reference 433) document site geologic mapping techniques and procedures used and conditions of the site at the time of mapping.

Elements evaluated as part of Fugro Consultants, Inc. 2011 mapping comparison include:

- Foundation Lithology – Rock classifications, infilled joint descriptions, petrographic analyses, and borehole data
- Distribution of Geologic Features – Assessment of mafic intrusions recorded on geologic maps
- Structural Orientation Measurements – Shear plane orientations.

Evaluation of the CNS era geologic records consists mainly of a comparison between CNS (PSAR and construction observations) and WLS (COLA) field studies. Direct comparison and evaluation of lithologic and structural features were performed as a means to corroborate geologic map records and interpretations performed as part of CNS construction (Reference 433).

Principal objectives of the WLS COLA excavation mapping program include the following:

- Confirm previous mapping accomplished as part of the construction activities (see discussion on Previous Rock Mapping).
- Document the age and structural relationship between rock masses.
- Investigate and document any evidence of tectonic movement or ground deformation.
- Identify and delineate the western pluton boundary.
- Delineate the thickness and character of the weathering profile as exposed around the perimeter of the excavation.
- Identify areas of groundwater seepage within the excavation.

The following discussion of previous rock mapping, its confirmation, and synthesis with local mapping data summarizes the results of previous and current mapping and the suitability of foundation bedrock (Subsection 2.5.1.2.6)

Previous Rock Mapping Program

An extensive mapping program was conducted during the initial construction phase at the former Duke CNS. The program included mapping excavations opened during construction. Two primary maps for each of the 3 units were developed. First, a top-of-rock map was produced after overburden was stripped, and completed prior to blasting operations. After blasting operations were completed and the rock debris removed, top-of-foundation (also referred to as final foundation) maps were produced. By the time mapping was started, blasting operations were underway for the former Duke CNS Unit 1, and top-of-rock mapping was completed for the former Duke CNS Units 2 and 3 locations. Top-of-foundation mapping was subsequently completed for the former Duke CNS Unit 1 while only a portion of former Duke CNS Unit 2 was completed before construction activities were halted.

At the time of CNS project cancelation, mapping of Unit 1 was complete with the concrete foundation in place, and excavation foundation level mapping of CNS Unit 2 was in progress. CNS Unit 2 mapping was nearly complete with all of the northern portion and parts of the southern portion mapped (Figure 2, [Reference 433](#)). As a result, a small area in the northern excavation for former Duke CNS Unit 2 was available to confirm the geologic mapping previously completed for the top-of-foundation. This approximately 119,000 square foot area is in the northernmost portion of the CNS Unit 2 power block area ([Reference 433](#), Appendix F, Sheet 4) of the compiled final foundation geologic map. Comparisons of CNS Unit 1 and Service Building foundation level geology are obscured by their concrete foundations.

This was important to confirm the geologic mapping completed for the top of foundation beneath the former Duke CNS Unit 1.

Confirmation of Previous Mapping

The CNS as-built final foundation geologic map record was not completed before that project's cancelation in 1983. The CNS final foundation geologic field maps were qualified for use as inputs using a project-specific record qualification and mapping procedures. The procedures and methodologies used to transform the CNS foundation level geologic field map records including comparisons to WLS field studies are described in the report titled "Cherokee Nuclear Station (CNS) Final Foundation Geologic Map Record Report," prepared by Fugro Consultants, Inc., 2011 ([Reference 433](#)). The CNS foundation level geologic maps were qualified for use as inputs using a project-specific qualification procedure in accordance with procedures described in American Society of Mechanical Engineers (ASME), 2004, NQA-1 Part III, Subpart 3.3, Nonmandatory Appendix 3.1, "Guidance on Qualification of Existing Data" ([Reference 437](#)). This report documents the results of CNS final foundation geologic mapping, comparisons of CNS and WLS foundation level geologic mapping, and also evaluates microstructural kinematic and geochronological constraints documented during CNS PSAR and construction activities.

As part of this process, the CNS foundation level geologic maps were reproduced digitally and were then compared to WLS geologic mapping which includes comparisons to evaluations of the microstructural kinematic and geochronologic constraints documented during CNS PSAR and construction activities. Using corroboration and comparison methods (Reference 437), CNS construction-derived geologic data and interpretations are independently confirmed using WLS COLA-derived subsurface explorations and surface mapping, geologic data, and interpretations (Reference 433).

Direct comparison and evaluations of lithologic and structural features were performed as a means to corroborate geologic map records and interpretations performed as part of CNS construction.

Both CNS and WLS mapping efforts used project-specific Geologic Mapping Procedures. Although these procedures differed in scale of mapping, density of recorded structural measurements, and efforts to provide clean visible surfaces, both methods provided geologists with adequate instructions and ability to perform geologic investigations at their respective level of detail (Reference 433).

Foundation Level Geology

Illustrated in both CNS and WLS geologic maps is a large plutonic body with several mafic intrusions. Subsection 2.5.1.2.5.4 summarized this leucocratic pluton as having intruded at a fairly high level in the crust, which cooled rapidly and ranged in composition from granodiorite to tonalite (quartz diorite). The pluton, composed of mostly light colored minerals, was later intruded by darker colored intermediate and more mafic magmas (dikes). Complex ductile deformation occurred both pre- and post-dike injection resulting in mineralogical alteration, or metamorphism of the pluton.

Independent methods of corroboration and comparison are used to confirm that the CNS final foundation geologic maps are acceptable for use in documenting the CNS foundation level geology. Comparison of CNS mapped geology to WLS borehole lithology is performed for WLS boreholes completed within CNS Unit 1 structures. For CNS Unit 2, the distribution of lithologic features is compared to WLS COLA-derived geologic mapping in the defined “area of comparison” located in the northern portion of CNS Unit 2. The comparison findings for CNS Unit 1 and Unit 2 are summarized below.

One means of verifying the validity of CNS excavation mapping against WLS lithologic interpretations is comparing CNS geologic maps to the WLS borehole log data. The locations of 13 WLS borings in the Unit 1 area, which is obscured by its concrete foundation, were plotted on CNS final foundation geologic maps. The lithology of the first rock encountered in the borings was compared to the lithologies presented on the CNS maps (Reference 433, Figure 14).

Except for boring B-1010, the CNS lithologies agree with the WLS bedrock nomenclature. The first rock observed in boring B-1010 is identified as metagranodiorite (felsic gneiss), whereas the foundation map identifies the rock as mafic gneiss. Two possible explanations for this difference include:

(1) following CNS foundation mapping, it is possible that subsequent excavations removed additional rock characterized as mafic gneiss, or (2) the bedrock was intermediate between mafic and felsic lithologies and could be interpreted as either rock type. Physical inspection of the recovered core in B-1010 indicates that the rock is intermediate and thus can be characterized as either felsic gneiss or mafic gneiss. A nearby outcrop exposure of similar intermediate rock is considered mafic gneiss. The difference in rock classification of this intermediate rock is not significant. Both CNS and WLS rock classifications describe the foundation level rock types as felsic plutonic rocks and mafic intrusive rocks, which have undergone deformation and metamorphism. Differences in rock nomenclature are attributed to different mapping schemes between CNS excavation mapping and WLS COLA mapping. Comparison of petrographic analyses, as well as CNS map and WLS boring log lithologies, correlates the CNS felsic gneiss and mafic gneiss to WLS meta-granodiorite/meta-quartz diorite, and meta-diorite/amphibolite, respectively.

A second alternative method was used to compare the two principal geologic units mapped during CNS and WLS activities. As previously described, the primary foundation rock type is composed of mostly felsic crystalline assemblages (felsic gneiss, meta-granodiorite/meta-quartz diorite) that is intruded by mafic dikes (mafic gneiss, metadiorite/amphibolite). These mafic dikes are distinct lithologic bodies, and therefore serve as the basis of comparison for distribution of geologic features. In general, the position and lateral thickness of mafic dikes agree well between both CNS and WLS geologic maps, particularly in the northern portion of the area of comparison. Survey points, located along the margins of the mafic dikes, confirm the similarity of these features ([Reference 433](#), Figure 15). In the northern portion of the mapped area, mafic dike positions are nearly coincident, with differences of up to 5 to 10 feet observed along mafic contacts along the southern boundary of the comparison ([Reference 433](#), Figure 16, Feature A).

Dissimilar features between CNS and WLS geologic maps are attributed to differences in mapping techniques and site conditions at the time of mapping. As such, differences of this type are insignificant with respect to quality of mapping and interpretation of features. Portions of two mafic dikes mapped on the CNS geologic map are absent from the WLS map ([Reference 433](#), Feature B). These dikes are located at northeastern and southwestern limits of the WLS geologic map coverage. In both cases there are gaps, reflecting areas not mapped, adjacent to the absent feature. The absent mafic units are the result of lack of clear visible mapping surface. These unmapped features are interpreted to be the result of an obscured rock surface during WLS COLA mapping as portions of the CNS Unit 2 area were obscured by water, minor accumulations of sediment, crushed rock, or construction/exploration equipment. The absence of these features on the WLS COLA maps is considered insignificant with respect to the mapping comparisons and interpretations.

Shear Plane Measurements

The bedrock exposed during CNS and WLS investigations contains numerous shears. The structural orientation of many of these shears was measured and

recorded during CNS and WLS geologic mapping activities. These shear plane results were compared to confirm the mapping of shear planes (Reference 433).

Structural attitude orientations of exposed shear planes collected during CNS-era final foundation mapping activities within the CNS excavation were digitized from final foundation map panels (Reference 433, Map Sheets 1 through 6). These shear measurement data were used to develop lower-hemisphere equal area stereonet plots of the poles to the shear planes illustrated in Figures 2.5.1-240 and 241. The orientation data cluster in three broad groups. The first zone includes a grouping of poles in the northwest quadrant of the stereonet, indicating shallowly to steeply dipping northeast-oriented shear planes that dip towards the southeast. The second grouping is clustered in the southeast quadrant of the stereonet and indicates a series of northeast-oriented, northwest-dipping shear planes. The last grouping is located in the northeast quadrant; these show a set of northwest-oriented shear planes that dip moderately towards the southwest. Concentration plots of the data show that the majority of the shear planes are oriented northeast-southwest and dip either towards the northwest or southeast (Figures 2.5.1-240 and 241).

Several shear-breccia zones were investigated during field studies performed during CNS-era investigation and construction activities. These are documented in a series of geologic zone reports (Reference 433, Appendices E and H). These reports included detailed mapping and collecting additional structural orientation data from exposed shear-breccia zones. Shear orientation data from Geologic Zone Reports 6 and 11 through 16 (Reference 433, Appendices E and H) were compiled and are plotted in Figure 2.5.1-235. The clustering of points in the northwest and southwest quadrants of the stereonet indicates a set of steeply dipping northwest- to northeast-oriented shear planes. A second cluster, located in the northeast quadrant of the stereonet, is indicative of a set of shear planes that are northwest oriented and dip moderately towards the southwest.

During geologic mapping of the WLS site in 2006 of open exposures in the former CNS Unit 2 and 3 excavations, additional shear plane orientation data were collected. The 30 data points are plotted on a lower-hemisphere equal area stereonet in Figure 2.5.1-242. The primary trend of the data collected during WLS mapping indicates a set of northeast-trending shear planes that dip moderately to steeply towards the southeast. There are three measurements located in the northeast quadrant of the plot that suggest northwest-trending shear planes that dip moderately towards the southwest.

Comparing shear orientation measurements obtained during CNS-era mapping with those obtained during WLS mapping reveals good agreement between the datasets. The following discussion summarizes both localized structural data (CNS Unit 2 area) and nonlocalized data (CNS Units 1, 2, and 3).

Figure 2.5.1-243 presents data collected from CNS Unit 2 area final foundation mapping with WLS data collected from the same area. From this figure, we can observe that:

- The WLS pole-to-plane data compare very well with the CNS data in the northwest quadrant of the stereonet. Both datasets indicate northeast-striking, southeast-dipping shear planes.
- The WLS pole-to-plane data fall within and correspond to the cluster of CNS data located in the northeast quadrant, indicating northwest-striking, southwest-dipping shear planes.

Figure 2.5.1-244 presents all data from both CNS and WLS mapping plotted together. From this figure, it is observed that:

- For any of the three pole-to-plane datasets, the highest concentration of poles is in the northwest quadrant of the stereonet, indicating a higher percentage of northeast-striking, southeast-dipping shear planes.
- The zone reports (Zones 6 and 11 through 16, Reference 433) and WLS mapping pole-to-plane data fall within the bounds of the data collected during final foundation mapping.

CNS Fault Features

During CNS construction activities, a fault zone (designated as Zone 6) was discovered within the excavation for the Unit 1 Reactor and Auxiliary Buildings. This fault constitutes the largest fault evaluated during CNS construction and was designated as a possible “nonsimilar” feature based on three important field observations: (1) feature orientation consisting of northwest strike with low southwest dip, (2) the occurrence of possible gouge infilled with low birefringent material within portions of the zone, and (3) initial thin section study of the zone which could not establish specific textural relationships of the zone to low birefringent minerals. Subsection 2.5.1.2.5.4 describes detailed CNS thin section studies that confirmed the low birefringent mineral as potassium feldspar (likely adularia(?)) mineralization that formed after the latest phase of deformation (Reference 433).

Comprehensive geologic evaluations performed at Zone 6 included detailed mapping at 1" = 20' and 1" = 5', thin section preparation and study, excavation of a test pit, and advancing two angle borings. The main trace of the fault zone is approximately 415 feet long. Along the main trace, the strike of the fault is highly variable, ranging from nearly east-west to nearly north. Broadly, the feature strikes towards the northwest and portions of the zone have low dips. Brittle and ductile deformation is observed both at a macroscopic and a microscopic level. Macroscopically, the fault is seen to offset fractures and mafic bodies, especially within the southern portion, but the northern exposure of the zone shows mafic rocks that have been stretched out and deformed along the shear planes (Reference 433, Appendix G, Map Sheets 1, 2, 5, and 6). Thin section samples prepared from the sheared material reveal schistose textures with quartz and feldspar augens, older biotite with brittle kinks, and younger, undeformed white mica as described in Figure 2.5.1-236.

Based primarily on the microscopic evidence observed in thin sections, the CNS geologic Zone Report 6 concluded that the latest deformation on this fault occurred during the later stages of greenschist metamorphism or hydrothermal activity. This report further states that the pressure and temperature conditions needed for the formation of these mineral assemblages must have existed prior to 170 Ma (i.e., middle Mesozoic) and that the fault cannot be considered to be a "capable fault" as defined by 10 CFR Part 100.

WLS investigation of this feature included analysis of the CNS-era maps and reexamination of CNS thin sections and age dates to confirm the geochronologic history of this fault zone. WLS investigations concur with CNS interpretations. WLS evaluations are described in Appendix I of Fugro Consultants, Inc., 2011 (Reference 433).

The WLS mapping comparison confirms the CNS final foundation geology documented during CNS construction, including rock types and orientations of fractures and shear zones. Evaluation of CNS and WLS geologic mapping reveals identical geologic interpretations. The site geochronology developed as part of detailed CNS PSAR and construction evaluations was confirmed as part of WLS COLA investigations by using closure temperature-age relationships of undeformed minerals. These data indicate the site has not experienced tectonic deformation since early Mesozoic, and possibly not since 219 Ma to 300 Ma (i.e., early Mesozoic to late Paleozoic) (Reference 433).

Synthesis of Local Mapping Data. Subsection 2.5.4.2 presents a detailed discussion of the boring, test pit, and trenching program. Boring data, test pits, trenches, existing exposures, and outcrops were used to map the distribution and geometry of the granitoid pluton within the site area (Figure 2.5.1-226). Top-of-rock maps and final foundation maps developed during construction of the Cherokee Nuclear Station and exposures in the existing excavation show the top of the rock generally dips to the northeast resulting in a thicker section of residuum and saprolite (Figure 2.5.1-227).

The western margin of the pluton was mapped using lithologic descriptions from borings, limited outcrops and test pits. As shown on Figure 2.5.1-226, borings located along the western edge of the site were used to constrain the alignment of the pluton. Test pits were used to confirm the contact zone between the granodiorite and metavolcanic country rock.

2.5.1.2.6 Site Area Engineering Geology

From an engineering geology perspective, the Lee Nuclear Site provides favorable geologic conditions for the construction of Lee Nuclear Station Units 1 and 2. The site and surrounding area is underlain by hard, crystalline rock of the Battleground Formation. In situ measurements of shear wave velocities (V_s) demonstrate that the unweathered or fresh rock underlying the site exhibits average V_s values in excess of 9,200 ft/sec, which classifies the site as a hard rock site, for the purposes of computing the GMRS.

Subsection 2.5.4 presents detailed description of V_s and other static and dynamic properties of foundation materials. Subsection 2.5.4 also presents a discussion of engineering soil properties, including index properties, static and dynamic strength, and compressibility. Variability and distribution of properties for the foundation-bearing layer will be evaluated and mapped as the excavation is completed. Settlement monitoring for the Lee Nuclear Station Units 1 and 2 nuclear island is not required because settlement is calculated to be 1/15 of an inch or less (Subsection 2.5.4.10.2).

The foundation-bearing unit is a felsic and mafic granitoid complex. Some minor zones of weathering along contacts between the felsic and mafic units are mapped. The widths of these weathering zones, however, do not exceed one foot, and vertical exposures along these contacts indicate that weathering is limited to the near surface. No evidence of weathered contact zones between rock units is noted in the rock core collected as part of the foundation investigation. Excavation will likely expose desiccation features, weathered zones, joints, and fractures. Removal and treatment of weathered rock is described in Subsection 2.5.4.12.

No deformational zones related to post plutonic activity are noted. The excavation mapping procedures used for verification and quality control of the nuclear island foundation materials are described in Subsection 2.5.4.5.3.

No mining operations (other than aggregate mines), excessive extraction or injection of groundwater, or impoundment of water are located within the site area that could affect geologic conditions. The crystalline and metamorphic bedrock at the site is not susceptible to subsidence due to groundwater withdrawal.

2.5.1.2.7 Site Area Seismicity and Paleoseismology

The largest earthquake within 25 mi. of the Lee Nuclear Site included in the updated CEUS SSC seismicity catalog is an E[M] 4.13 event that occurred in 1886.

The highest recorded shaking intensities estimated for the Lee Nuclear Site resulted from earthquakes located outside of the site area. The August 31, 1886, Charleston, South Carolina, earthquake is one of the largest historical earthquakes in the eastern United States. The event produced Modified Mercalli Intensity (MMI) X shaking in the epicentral area (Reference 395). Maximum MMI shaking intensity at the Lee Nuclear Site is estimated at approximately VI (Figure 2.5.1-215). The Charleston earthquake is discussed in greater detail in Subsections 2.5.1.1.3.2.1 and 2.5.2.3.

The January 1, 1913 E[M] 4.54 Union County, South Carolina earthquake (Reference 441) was felt over an area of approximately 43,000 square mi., with an estimated Rossi-Forel shaking intensity VIII (Reference 396, as reported in Reference 397). Rossi-Forel shaking intensity at the Lee Nuclear Site is estimated at approximately VI (Reference 396, as reported in Reference 397) (Figure 2.5.1-232). The epicenter of the Union County earthquake is poorly located and the fault on which this earthquake occurred has not been identified.

There are no published reports of paleoseismologic studies within the site area. Extensive studies of outcrops performed as part of this project have not indicated any evidence for post-Miocene earthquake activity within the site area.

The potential for reservoir-induced seismicity (RIS) is considered low and it is unlikely the induced magnitudes would exceed $M > 4$, a value well below the short-period controlling earthquake as described in [Subsection 2.5.2.1.3](#).

2.5.1.2.8 Site Groundwater Conditions

[Subsection 2.4.12](#) provides a detailed discussion of groundwater conditions.

2.5.1.3 References

201. Horton, J.W., Drake, A.A., and Rankin, D.W., *Tectonostratigraphic Terranes and Their Paleozoic Boundaries in the Central and Southern Appalachians*, Geological Society of America, Special Paper 230:213-245, 1989.
202. Horton, J.W., Drake, A.A., Rankin, D.W., and Dallmeyer, R.D., *Preliminary Tectonostratigraphic Terrane Map of the Central and Southern Appalachians*, U.S. Geological Survey, Miscellaneous Investigations Series Map I-2163, 1991.
203. Hatcher R.D. Jr., Colquhoun, D.J., Secor D.T. Jr., Cook, F.A., Dillon, W.P., Klitgord, K., Popenoe, P., Merschat, C.E., Wiener, L.E., Milici, R.C., Nelson, A.E., Sheridan, R.E., and Snoke, A.W., *Continent-Ocean Transect E5- Cumberland Plateau (North American Craton) to Blake Plateau Basin*, Geological Society of America, 2 plates, with 55p. accompanying text, 1994.
204. Hibbard, J.P., Stoddard, E.F., Secor, D.T., and Dennis, A.J., "The Carolina Zone: Overview of Neoproterozoic to Early Paleozoic Peri-Gondwanan Terranes Along the Eastern Flank of the Southern Appalachians," *Earth Science Reviews* (57):299-339, 2002.
205. Spotila, J.A., Bank, G.C., Reiners, P.W., Naeser, C.W., Naeser, N.D., and Henika, B.S., "Origin of the Blue Ridge Escarpment Along the Passive Margin of Eastern North America," *Basin Research* (16):41-63, 2004.
206. Hatcher, R.D. Jr. and Goldberg, S.A., "The Blue Ridge Geologic Province," in *The Geology of the Carolinas – Carolina Geological Society 50th Anniversary Volume*, University of Tennessee Press, 1991.
207. King, P.B., "A Geologic Cross Section Across the Southern Appalachians, An Outline of the Geology in the Segment in Tennessee, North Carolina, and South Carolina," in *Guides to Southeastern Geology*, Geological Society of America Annual Meeting, 1955.

208. Hopson, J.L., Hatcher, R.D. Jr., and Stieve, A.L., "Geology of The Eastern Blue Ridge of Northeast Georgia and the Adjacent Carolinas," in *Georgia Geological Society Guidebook* (9):1-38, 1989.
209. Hatcher, R.D. Jr., Costello, J.O., Edelman, S.H., "The Smokies Foothills Duplex and Possible Significance of the Guess Creek Fault: A Corollary to the Mapping of King and Neuman," *Geological Society of America Abstracts with Programs* (18):226, 1986.
210. Nelson, K.D., Arrow, J.A., McBride, J.H., Willemin, J.H., Huang, J., Zheng, L., Oliver, J.E., Brown, L.D., and Kaufman, S., "New COCORP Profiling in the Southeastern United States. Part I: Late Paleozoic Suture and Mesozoic Rift Basin," *Geology* (13):714-718, 1985.
211. Hatcher, R.D. Jr., "Tectonics of the Western Piedmont and Blue Ridge, Southern Appalachians: Review and Speculation," *American Journal of Science* (278):276-304, 1978.
212. Hatcher, R.D. Jr., "Stratigraphic, Petrologic, and Structural Evidence Favoring a Thrust Solution to the Brevard Problem," *American Journal of Science* 270 (9):177-202, 1971.
213. Hatcher, R.D. Jr., "Developmental Model for the Southern Appalachians," *Geological Society of America Bulletin* 83 (9):2,735-2,760, 1972.
214. Cook, F.A., Albaugh, D.S., Brown, L.D., Kaufman, S., Oliver, J.A., and Hatcher R.D. Jr., "Thin-Skinned Tectonics in the Crystalline Southern Appalachians; COCORP Seismic-Reflection Profiling of the Blue Ridge and Piedmont," *Geology* 7 (12): 563-567, 1979.
215. Coruh, C., Costain, J.K., Hatcher, R.D. Jr., Pratt, T.L., Williams, R.T., Phinney R.A., "Results from Regional Vibroseis Profiling: Appalachian Ultradeep Core Hole Site Study," *Geophysical Journal of the Royal Astronomical Society* 89 (1): 147-156, 1987.
216. Fullagar, P.D., Hatcher, R.D. Jr., and Merschat, C.E., "1,200-m.y.-old gneisses in the Blue Ridge Province of North and South Carolina," *Southeastern Geology* (20):69-78, 1979.
217. Fullagar, P.D. and Bartholomew, M.J., "Rubidium-Strontium Ages of the Watauga River, Cranberry, and Crossing Knob Gneisses, Northwestern North Carolina," in *Geological Investigations in the Blue Ridge of Northwestern North Carolina - 1983 Guidebook for the Carolina Geological Society*, North Carolina Division of Land Resources, 1983.
218. Fullagar, P.D. and Odom, A.L., "Geochronology of Precambrian Gneisses in the Blue Ridge Province of Northwestern North Carolina and Adjacent Parts of Virginia and Tennessee," *Geological Society of America Bulletin* 84 (9):3,065-3,080, 1973.

-
219. Wehr, F. and Glover, L. III, "Stratigraphy and Tectonics of the Virginia-North Carolina Blue Ridge - Evolution of a Late Proterozoic-Early Paleozoic Hinge Zone," *Geological Society of America Bulletin* (96):285-295, 1985.
220. Rast, N. and Kohles, K.M., "The Origin of the Ocoee Supergroup," *American Journal of Science* (286):593-616, 1986.
221. King, P.B., Neuman, R.B., and Hadley, J.B., *Geology of the Great Smoky Mountains National Park, Tennessee and North Carolina*, U.S. Geological Survey Professional Paper 587, 1968.
222. Neuman, R.B. and Nelson, W.H., *Geology of the Western Great Smoky Mountains, Tennessee*, U.S. Geological Survey Professional Paper 349-D, 1:62,500-scale, 1965.
223. King, P.B., *Geology of the Central Great Smoky Mountains, Tennessee*, U.S. Geological Survey Professional Paper 340-C, 1964.
224. Hopson, J.L., "Structure, Stratigraphy, and Petrogenesis of the Lake Burton Mafic-Ultramafic Complex," *Georgia Geological Society Guidebook* (9):93-100, 1989.
225. Hatcher, R.D. Jr., "Tectonics of the Southern and Central Appalachian Internides," *Annual Review of Earth and Planetary Sciences* (15):337-362, 1987.
226. Horton, J.W. Jr., and McConnell, K.I., "The Western Piedmont," in *The Geology of the Carolinas - Carolina Geological Society 50th Anniversary Volume*, ed. J.W. Horton, Jr. and V.A. Zullo, University of Tennessee Press, 1991.
227. Nelson, A.E., Horton, J.W. Jr., and Clarke, J.W., *Generalized Tectonic Map of the Greenville 1° x 2° Quadrangle, Georgia, South Carolina, and North Carolina*, U.S. Geological Survey Miscellaneous Field Studies Map MF-1898, scale 1:25,000, 1987.
228. Goldsmith, R., Milton, D.J. and Horton, J.W. Jr., *Geologic Map of the Charlotte 1° x 2° Quadrangle, North Carolina and South Carolina*, U.S. Geological Survey Miscellaneous Investigations Series Map I-1251-E, 1:250,000 scale, 1988.
229. Mittwee, S.K., Odegard, M., and Sharp, W.E., "Major Chemical Characteristics of the Hammett Grove Meta-Igneous Suite, Northwestern South Carolina," *Southeastern Geology* 28 (1):49-63, 1987.
230. Hatcher, R.D. Jr., Hopson, J.L., Edelman, S.H., Liu, A., McClellan, E.A., Stieve, A.L., "Detailed Geologic Map of the Appalachian Ultradeep Core Hole (ADCOH) Region: New Constraints on the Structure of the Southern Appalachian Internides," *Geological Society of America Abstracts with Programs* (18):631, 1986.

-
231. Secor, D.T. Jr., Samson, S.L., Snoke, A.W., and Palmer, A.R., "Confirmation of Carolina Slate Belt as an Exotic Terrane," *Science* (221):649-651, 1983.
232. Hatcher R.D. Jr., Odom, A.L., Engelder, T., Dunn, D.E., Wise, D.U., Geiser, P.A., Schamel, S., and Kish, S.A., "Characterization of Appalachian faults," *Geology* (16):178-181, 1988.
233. Hooper, R.J. and Hatcher, R.D. Jr., "Pine Mountain Terrane, a Complex Window in the Georgia and Alabama Piedmont; Evidence from the Eastern Termination," *Geology* (16):307-310, 1988.
234. Steltenpohl, M.G., "Kinematics of the Towaliga, Bartletts Ferry, and Goat Rock Fault Zones, Alabama: The Late Paleozoic Dextral Shear System in the Southernmost Appalachians," *Geology* (16):852-855, 1988.
235. Rozen, R.W., "The Middleton-Lowdensville Cataclastic Zone in the Elberton East Quadrangle, Georgia," in *Geological Investigations of the Kings Mountain Belt and Adjacent Areas in the Carolinas*, Carolina Geological Society Guidebook, 1981.
236. Horton, J.W. Jr., "Geologic Map of the Kings Mountain Belt Between Gaffney, South Carolina and Lincolnton, North Carolina," in *Geological Investigations of the Kings Mountain Belt and Adjacent Areas in the Carolinas*, Carolina Geological Society Field Trip Guidebook, 1981.
237. McConnell, K.I., "Geology of the Sauratown Mountains Anticlinorium: Vienna and Pinnacle 7.5-Minute Quadrangles," in *Structure of the Sauratown Mountains Window, North Carolina*, Carolina Geological Society Guidebook, 1988.
238. Samson, S., Palmer, A.R., Robinson, R.A., and Secor, D.T. Jr., "Biogeographical Significance of Cambrian Trilobites from the Carolina Slate Belts," *Geological Society of America Bulletin* 102 (11):1,459-1,470, 1990.
239. Vick, H.K., Channell, J.E.T., and Opdyke, N.D., "Ordovician Docking of the Carolina Slate Belt - Paleomagnetic Data," *Tectonics* (6):573-583, 1987.
240. Noel, J.R., Spariosu, D.J., and Dallmeyer, R.D., "Paleomagnetism and $^{40}\text{Ar}/^{39}\text{Ar}$ Ages from the Carolina Slate Belt, Albemarle, North Carolina - Implications for Terrane Amalgamation," *Geology* (16):64-68, 1988.
241. Butler, J.R., "The Carolina Slate Belt in North Carolina and Northeastern South Carolina - a Review," *Geological Society of America Abstracts with Programs* (11):172, 1979.
242. Manspeizer, W., Puffer, J.H., and Cousminer, H.L., "Separation of Morocco and Eastern North America: a Triassic-Liassic Stratigraphic Record," *Geological Society of America Bulletin* 89 (6):901-920, 1978.

243. Petersen, T.A., Brown, L.D., Cook, F.A., Kaufman, S., and Oliver, J.E., "Structure of the Riddleville Basin from COCORP Seismic Data and Implications for Reactivation Tectonics," *Journal of Geology*, 1984.
244. Hutchinson, D.R. and Klitgord, K.D., "Evolution of Rift Basins on the Continental Margin off Southern New England, in *Triassic-Jurassic Rifting; Continental Breakup and the Origin of the Atlantic Ocean and Passive Margins - Developments in Geophysics* 22 (AB):81-98, 1988.
245. Ratcliffe, N.M., "The Ramapo Fault System in New York and Adjacent Northern New Jersey: A Case of Tectonic Heredity," *Geological Society of America Bulletin* 82 (1):125-142, 1971.
246. Lindholm, R.C., "Triassic-Jurassic Faulting in Eastern North America - a Model Based on pre-Triassic Structures," *Geology* 6 (6):365-368, 1978.
247. Glover, L., III, Poland, F.B., Tucker, R.D. and Bourland, W.C., "Diachronous Paleozoic Mylonites and Structural Heredity of Triassic-Jurassic Basins in Virginia," *Geological Society of America Abstracts with Programs* 12, 1980.
248. Klitgord, K.D., Hutchinson, D.R., Schouten, H., "U.S. Atlantic Continental Margin: Structural and Tectonic Framework," in *The Geology of North America, The Atlantic Continental Margin: U.S.*, Decade of North American Geology Publication I-2, Geological Society of America, 1988.
249. Kanter, L.R., "Tectonic Interpretation of Stable Continental Crust," in *The Earthquakes of Stable Continental Regions*, prepared for Electric Power Research Institute, 1994.
250. Grow, J.A., Klitgord, K.D., and Schlee, J.S., "Structure and Evolution of Baltimore Canyon Trough," in *The Atlantic Continental Margin: U.S.*, Decade of North American Geology Publication I-2, Geological Society of America, 1988.
251. King, P.B., *Systematic Pattern of Triassic Dikes in the Appalachian Region - Second report*, U.S. Geological Survey Professional Paper 750-D, 1971.
252. Froelich, A.J. and Olsen, P.E., *Newark Supergroup, a Revision of the Newark Group in Eastern North America*, U.S. Geological Survey Bulletin 1537A, 1984.
253. Olsen, P.E., Froelich, A.J., Daniels, D.L., Smoot, J.P., and Gore, P.J.W., "Rift Basins of Early Mesozoic Age," in *The Geology of the Carolinas*, ed. J.W. Horton, Jr. and V.A. Zullo, University of Tennessee Press, 1991.

254. Smoot, J.P., "The Closed-Basin Hypothesis and its Use in Facies Analysis of the Newark Supergroup," in *Proceedings of the second U.S. Geological Survey Workshop on the Early Mesozoic Basins of the Eastern U.S.*, U.S. Geological Survey Circular 946, 1985.
255. Gore, P.J.W., "Depositional Framework of a Triassic Rift Basin - the Durham and Sanford Sub-Basins of the Deep River Basin, North Carolina," in *Society of Economic Paleontologists and Mineralogists Field Guidebook*, 1986.
256. Olsen, P.E. and Schlische, R.W., "Unraveling the Rules of Rift Basins," *Geological Society of America Abstracts with Programs* 20:A123, 1988.
257. Schlische, R.W. and Olsen, P.E., "Quantitative Filling Model for Continental Extensional Basins with Application to the Early Mesozoic Rifts of Eastern North America," *Journal of Geology* 98:135-155, 1990.
258. King, P.B. and Beikman H.M., *Geologic Map of the United States (Exclusive of Alaska and Hawaii)*, U.S. Geological Survey, 3 sheets, 1:250,000 scale, 1974.
259. Schruben, P.G., Arndt, R.E., Bawiec, W.J., King, P.B., and Beikman, H.M., *Geology of the Conterminous United States at 1:2,500,000 Scale - a Digital Representation of the 1974 P.B. King and H.M. Beikman Map*, U.S. Geological Survey Digital Data Series DDS-11, 1994.
260. Hibbard, J.P., van Staal, C.R., Rankin, D.W., Williams, H., *Lithotectonic Map of the Appalachian Orogen, Canada - United States of America*, Geological Society of Canada, map 2096A, 1:1,500,000 scale, 2006.
261. Horton, J.W. Jr. and Zullo, V.A., eds., *The Geology of the Carolinas - Carolina Geological Survey 50th Anniversary Volume*, University of Tennessee Press, 1991.
262. Bickford, M.E., Van Schmus, W.R., and Zietz, I., "Proterozoic History of the Midcontinent Region of North America," *Geology* 14 (6):492-496, 1986.
263. Hauser, E.C., "Grenville Foreland Thrust Belt Hidden Beneath the Eastern U.S. Mid-Continent," *Geology* 21(1):61-64, 1993.
264. White, T.S., Witzke, B.J., and Ludvigson, G.A., "Evidence for an Albian Hudson Arm Connection Between the Cretaceous Western Interior Seaway of North American and the Labrador Sea," *Bulletin of the Geological Society of America* 112 (9):1,342-1,355, 2000.
265. Bollinger, G.A. and Wheeler, R.L., *The Giles County, Virginia, Seismic Zone- Seismological Results and Geological Interpretations*, U.S. Geological Survey Professional Paper 1355, 1988.

266. Klitgord, K.D., Hutchinson, D.R., and Schouten, H.S. *Atlantic Continental Margin; Structural and Tectonic Framework*, in *The Geology of North America*, v. I-2: *The Atlantic Continental Margin: U.S.*, Decade of North American Geology Publication, Geological Society of America, 1988.
267. Wheeler, R.L., "Earthquakes and the Cratonward Limit of Iapetan Faulting in Eastern North America," *Geology* 23:105-108, 1995.
268. Dennis, A.J., Shervais, J.W., Mauldin, J., Maher, H.D., Jr., and Wright, J.E., "Petrology and Geochemistry of Neoproterozoic Volcanic Arc Terranes Beneath the Atlantic Coastal Plain, Savannah River Site, South Carolina," *Geological Society of America Bulletin* 116 (5-6):572-593, 2004.
269. Removed
270. Zoback, M.L. and Zoback, M.D., "Tectonic Stress Field of the Continental United States," in *Geophysical Framework of the Continental United States*, Geological Society of America Memoir 172:523-539, 1989.
271. Zoback, M.L., Zoback, M.D., Adams, J., Assumpcao, M., Bell, S., Bergman, E.A., Bluemling, P., Brereton, N.R., Denham, D., Ding, J., Fuchs, K., Gay, N., Gregersen, S., Gupta, H.K., Gvishiani, A., Jacob, K., Klein, R., Knoll, P., Magee, M., Mercier, J.L., Mueller, B.C., Paquin, C., Rajendran, K., Stephansson, O., Suarez, G., Suter, M., Udias, A., Xu, Z.H., and Zhizin, M., "Global Patterns of Tectonic Stress," *Nature* 341 (6240):291-298, 1989.
272. Zoback, M.L., "Stress Field Constraints on Intraplate Seismicity in Eastern North America," *Journal of Geophysical Research* 97 (B8):11,761-11,782, 1992.
273. Richardson, R.M., and Reding, L.M., "North American Plate Dynamics," *Journal of Geophysical Research* 96 (B7):12,201-212,223, 1991.
274. Turcotte, D.L. and Schubert, G., *Geodynamics*, Cambridge University Press, 2002.
275. Dahlen, F.A., "Isostasy and the Ambient State of Stress in the Oceanic Lithosphere," *Journal of Geophysical Research* 86 (B9):7,801-7,807, 1981.
276. Committee for the Gravity Anomaly Map of North America, *Gravity Anomaly Map of North America*, Geological Society of America, Continent-Scale Map-002, scale 1:5,000,000, 1987.
277. Committee for the Magnetic Anomaly Map of North America, *Magnetic Anomaly Map of North America*, Geological Society of America, Continent-Scale Map-003, scale 1:5,000,000, 1987.

-
278. Daniels, D.L., South Carolina Aeromagnetic and Gravity Maps and Data: a Website for Distribution of Data, U.S. Geological Survey Open-File Report 2005-1022, Website, <http://pubs.usgs.gov/of/2005/1022/>, accessed August 17, 2006.
279. Harris, L.D., de Witt, W. Jr., and Bayer, K.C., *Interpretive Seismic Profile Along Interstate I-64 from the Valley and Ridge to the Coastal Plain in Central Virginia*, U.S. Geological Survey, Oil and Gas Investigations Chart OC-123, 1982.
280. Dainty, A.M. and Frazier, J.E., "Bouguer Gravity in Northeastern Georgia - a Buried Suture, a Surface Suture, and Granites," *Geological Society of America Bulletin* 95:1,168-1,175, 1984.
281. Iverson, W.P. and Smithson, S.B., "Reprocessing and Reinterpretation of COCORP Southern Appalachian Profiles," *Earth and Planetary Science Letters* 62:75-90, 1983.
282. Rankin, D.W., Dillon, W.P., Black, D.F., Boyer, S.E., Daniels, D.L., Goldsmith, R., Grow, J.A., Horton, J.W., Jr., Hutchinson, D.R., Klitgord, K.D., McDowell, R.C., Milton, D.J., Owens, J.P., and Phillips, J.D., "Continent-Ocean Transect E-4, Central Kentucky to Carolina Trough," in *Publication of Decade of North American Geology*, Geological Society of America, 1991.
283. Cumbest, R.J., Price, V. and Anderson, E.E., "Gravity and Magnetic Modeling of the Dunbarton Triassic Basin, South Carolina," *Southeastern Geology* 33 (1):37-51, 1992.
284. Posey, H.H., "A Model for the Origin of Metallic Mineral Deposits in the Kings Mountain Belt," in *Geological Investigations of the Kings Mountain Belt and Adjacent Areas in the Carolinas*, Carolina Geological Society Field Trip Guidebook, 1981.
285. Butler, J.R., "Geology of the Blacksburg South Quadrangle, South Carolina," in *Geological Investigations of the Kings Mountain Belt and Adjacent Areas in the Carolinas*, Carolina Geological Society Field Trip Guidebook, 1981.
286. Howard S., *Geologic Map of the Kings Creek 7.5-Minute Quadrangle, Cherokee County, South Carolina*, South Carolina Department of Natural Resources Geological Survey, 1:24,000-scale, 2004.
287. Austin, J.A., Stoffa, P.L., Phillips, J.D., Oh, J., Sawyer, D.S., Purdy, G.M., Reiter, E., and Makris, J., "Crustal Structure of the Southeast Georgia Embayment-Carolina Trough: Preliminary Results of a Composite Seismic Image of a Continental Suture (?) and a Volcanic Passive Margin," *Geology* 18:1,023-1,027, 1990.

288. Sheridan, R.E., Musser, D.L., Glover III, L., Talwani, M., Ewing, J.L., Holbrook, W.S., Purdy, G.M., Hawman, R., and Smithson, S., "Deep Seismic Reflection Data of EDGE U.S. Mid-Atlantic Continental-Margin Experiment – Implications for Appalachian Sutures and Mesozoic Rifting and Magmatic Underplating," *Geology* 21: 563-567, 1993.
289. Withjack, M.O., Schlische, R.W., and Olsen, P.E., "Diachronous Rifting, Drifting, and Inversion on the Passive Margin of Central Eastern North America: An Analog for Other Passive Margins," *American Association of Petroleum Geologists Bulletin* 82 (5A):817-835, 1998.
290. King, E.R. and Zietz, I., "The New York-Alabama Lineament: Geophysical Evidence for a Major Crustal Break in the Basement Beneath the Appalachian Basin," *Geology* 6:312-318, 1978.
291. Nelson, A.E. and Zietz, I., "The Clingman Lineament: Aeromagnetic Evidence for a Major Discontinuity in the North American Basement," *Geological Society of America Abstracts with Programs* 13(1):31, 1981.
292. Johnston, A.C., Reinbold, D.J., and Brewer, S.I., "Seismotectonics of the Southern Appalachians," *Bulletin of the Seismological Society of America* 75(1): 291-312, 1985.
293. Shumaker, R.C., "The New York-Alabama Lineament; An Early Iapetan Wrench Fault?," *American Association of Petroleum Geologists Bulletin* 84 (9): 1393, September 2000.
294. Johnston, A.C. and Reinbold, D.J., "A Basement Block Model for Southern Appalachian Seismicity," *Geological Society of America Abstracts with Programs* 17 (2):97, 1985.
295. Wheeler, R.L., "Earthquakes and the Southeastern Boundary of the Intact Iapetan Margin in Eastern North America," *Seismological Research Letters* 67:77-83, 1996.
296. Dennis, A.J., 1991, "Is the Central Piedmont Suture a Low-Angle Normal Fault?," *Geology* 19:1,081–1,084, 1991
297. West Jr., T.E., "Structural Analysis of the Carolina-Inner Piedmont Terrane Boundary: Implications for the Age and Kinematics of the Central Piedmont Suture, a Terrane Boundary that Records Paleozoic Laurentia-Gondwana Interactions," *Tectonics* 17 (3):379-394, 1998.
298. Dennis, A.J., *Rocks of the Carolina Terrane in the Spartanburg 30- x 60-degree Quadrangle*, prepared for the 1995 Carolina Geological Survey annual meeting, 1:100,000 scale, 1995.

299. Nystrom, P.G. Jr., "Structure and Stratigraphy Across the Reedy River Thrust Fault, Inner Piedmont of South Carolina," *Geological Society of America Abstracts with Programs*, Southeastern 50th annual meeting, 2001.
300. Maybin, A.H. and Nystrom, P.G., *Geology of the Reedy River Thrust in the Vicinity of Southwest Spartanburg, South Carolina*, South Carolina Geological Survey Open-File Report 143, 2002.
301. Bramlett, K.W., Secor, D.T., and Prowell, D.C., "The Belair Fault: A Cenozoic Reactivation Structure in the Eastern Piedmont," *Geological Society of America Bulletin* 93:1,109-1,117, 1982.
302. Maher, H.D., Dallmeyer, R.D., Secor Jr., D.T., and Sacks, P.E., "40-Ar/39-Ar Constraints on Chronology of Augusta Fault Zone Movement and Late Alleghanian Extension, Southern Appalachian Piedmont, South Carolina and Georgia," *American Journal of Science* 294:428-448, 1994.
303. Secor, D.T. Jr., Snoke, A.W., Bramlett, K.W., Costello, O.P., and Kimbrell, O.P., "Character of the Alleghanian Orogeny in the Southern Appalachians Part I. – Alleghanian Deformation in the Eastern Piedmont of South Carolina," *Geological Society of America Bulletin* 97:1,319-1,328, 1986.
304. Secor Jr., D.T., Snoke, A.W., and Dallmeyer, R.D., "Character of the Alleghanian Orogeny in the Southern Appalachians: Part III Regional Tectonic Relations," *Geological Society of America Bulletin* 97:1,345-1,353, 1986.
305. Sacks, P.E., and Dennis, A.J., "The Modoc Zone-D2 (Early Alleghanian in the Eastern Appalachian Piedmont, South Carolina and Georgia: Anatomy of the Alleghanian Orogeny as Seen from the Piedmont of South Carolina and Georgia," in *South Carolina Geological Survey/Carolina Geological Society Field Trip Guidebook*, 1987.
306. Hatcher, R.D., Jr., Howell, D.E., and Talwani, P., "Eastern Piedmont Fault System: Speculations on its Extent," *Geology* 5:36-640, 1977.
307. Vauchez, A., "Brevard Fault Zone, Southern Appalachians a Medium-Angle, Dextral, Alleghanian Shear Zone," *Geology* 15:669-672, 1987.
308. Horton, J.W. Jr. and Dicken, C.L., *Preliminary Digital Geologic Map of the Appalachian Piedmont and Blue Ridge, South Carolina Segment*, U.S. Geological Survey Open-File Report 01-298, 1:500,000 scale, 2001.
309. Halpin, M.A. and Barker, C A., "Geological Investigation of the Carolina Terrane and Charlotte Terrane Boundary in North-Central South Carolina," *Geological Society of America Abstracts with Programs*, South-Central Section 38th annual meeting, 2004.

310. Crone, A.J. and Wheeler, R.L., *Data for Quaternary Faults, Liquefaction Features, and Possible Tectonic Features in the Central and Eastern United States, East of the Rocky Mountain Front*, U.S. Geological Survey Open-File Report 00-260, 2000.
311. Wheeler, R.L., *Known or Suggested Quaternary Tectonic Faulting, Central and Eastern United States - New and Updated Assessments for 2005*, U.S. Geological Survey Open-File Report 2005-1336, 2005.
312. Secor, D.T. Jr., Peck, L.S., Pitcher, D.M., Prowell, D.C., Simpson, D.H., Smith, W.A., and Snoke, A.W., "Geology of the Area of Induced Seismic Activity at Monticello Reservoir, South Carolina," *Journal of Geophysical Research* 87 (B8):6,945-6,957, 1982.
313. Simpson, D.H., *The Wateree Creek Fault Zone*, unpublished M.S. thesis, University of South Carolina, 1981.
314. Maher Jr., H.D., Sacks, P.E., and Secor Jr., D. T., "The Eastern Piedmont of South Carolina," in *The Geology of the Carolinas – Carolina Geological Society 50th Anniversary Volume*, ed. J.W. Horton, Jr. and V.A. Zullo, University of Tennessee Press, 1991.
315. Secor, D.T. Jr., Barker, C.A., Gillon, K.A., Mitchell, T.L., Bartholomew, M.H., Hatcher, R.D., and Balinsky, M.G., *A Field Guide to the Geology of the Ridgeway-Camden Area, South Carolina Piedmont*, Carolina Geological Society Field Trip Guidebook, 1998.
316. Barker, C.A. and Secor Jr. D.T., *Geologic Map of the Longtown and Ridgeway 7.5-minute Quadrangles, Fairfield, Kershaw, and Richland Counties, South Carolina*, South Carolina Department of Natural Resources, GQM-32, 1:24,000-scale, 2005.
317. Johnston, A.C., Coppersmith, K.J., Kanter, L.R., and Cornell, C.A., *The Earthquakes of Stable Continental Regions, Volume I: Assessment of Large Earthquake Potential*, Final Report TR-102261-V1, prepared for Electric Power Research Institute, 1994.
318. Wentworth, C.M., and Mergner-Keefer, M., "Regenerate Faults of Small Cenozoic Offset – Probable Earthquake Sources in the Southeastern United States," in *Studies Related to the Charleston, South Carolina Earthquake of 1886 Tectonics and Seismicity*, U.S. Geological Survey Professional Paper 1313:S1-S20, 1983.
319. Balinsky, M.G., *Field Evidence for Late Mesozoic and/or Cenozoic Reactivation Faulting Along the Fall Line Near Camden, South Carolina*, unpublished M.S. thesis, University of South Carolina, 1994.

320. Knapp, J.H., Domoracki, W.J., Secor, D.T., Waddell, M.G., Diaconescu, C.C., Peavy, S.T., Ackerman, S., Baldwin, W., Gangopadhyay, A., Kastner, T., Kepple, K., Luc, M., Morrison, K., Shehane, G., and Varga, M., "Shallow Seismic Profiling of the Camden Fault, South Carolina Coastal Plain," *Geological Society of America Abstracts with Programs*, Southeastern Section 50th annual meeting, 2001.
321. Prowell, D.C., *Index of Faults of Cretaceous and Cenozoic Age in the Eastern United States*, U.S. Geological Survey miscellaneous field studies map MF-1269, 2 sheets, 1:2,500,000 scale, 1983.
322. Weems, R.E., *Newly Recognized En Echelon Fall Lines in the Piedmont and Blue Ridge Provinces of North Carolina and Virginia, With a Discussion of Their Possible Ages and Origins*, U.S. Geological Survey Open-File Report 98-0374, 1998.
323. Prowell, D.C. and O'Connor, B.J., "Belair Fault Zone: Evidence of Tertiary Fault Displacement in Eastern Georgia," *Geology* 6:681-684, 1978.
324. Prowell, D.C., O'Connor, B.J., and Rubin, M., *Preliminary Evidence for Holocene Movement Along the Belair Fault Zone Near Augusta, Georgia*, U.S. Geological Survey Open-File Report 75-680, 15p., 1975.
325. Snipes, D.S., Fallaw, W.C., and Price Jr., V., *The Pen Branch Fault: Documentation of Late Cretaceous and Tertiary Faulting in the Coastal Plain of South Carolina (DRAFT)*, Westinghouse Savannah River Company draft report, January 8, 1989.
326. Snipes, D.S., W.C. Fallaw, V. Price, Jr., and R.J. Cumbest, "The Pen Branch Fault: Documentation of Late Cretaceous-Tertiary Faulting in the Coastal Plain of South Carolina," *Southeastern Geology* 33 (4):195-218, 1993.
327. Stieve, A. and Stephenson, D.E., "Geophysical Evidence for Post Late Cretaceous Reactivation of Basement Structures in the Central Savannah River Area," *Southeastern Geology* 35(1):1-20, 1995.
328. Cumbest, R.J., Wyatt, D.E., Stephenson, D.E., and Maryak, M., *Comparison of Cenozoic Faulting at the Savannah River Site to Fault Characteristics of the Atlantic Coast Fault Province: Implications for Fault Capability*, Westinghouse Savannah River Company, Technical Report 2000-00310, 2000.
329. Dennison, J.M. and Stewart, K.G., *Geologic Field Guide to Extensional Structures Along the Alleghany Front in Virginia and West Virginia Near the Giles County Seismic Zone*, Geological Society of America Southeastern Section Fieldtrip Guidebook, 1998.

-
330. Johnston, A.C., "Seismic Moment Assessment of Earthquake in Stable Continental Regions - III. New Madrid 1811-1812, Charleston 1886 and Lisbon 1755," *Geophysical Journal International* 126:314-344, 1996.
331. Talwani, P., "An Internally Consistent Pattern of Seismicity Near Charleston, South Carolina," *Geology* 10(12):654-658, 1982.
332. Talwani, P., "The Charleston Earthquake Cycle," *Seismological Research Letters* 71 (1):121, 2000.
333. Bakun, W.H. and Hopper, M.G., "Magnitudes and Locations of the 1811-1812 New Madrid, Missouri and the 1886 Charleston, South Carolina Earthquakes," *Bulletin of the Seismological Society of America* 94(1):64-75, 2004.
334. Amick, D.C., "A Reinterpretation of the Meizoseismal Area of the 1886 Charleston Earthquake," *Eos, Transactions of the American Geophysical Union* 61 (17): 289, 1980.
335. Amick, D., Gelinas, R., Maurath, G., Cannon, R., Moore, D., Billington, E., and Kempainen, H., *Paleoliquefaction Features Along the Atlantic Seaboard*, U.S. Nuclear Regulatory Commission Report, NUREG/CR-5613, 1990.
336. Amick, D., Maurath, G., and Gelinas, R., "Characteristics of Seismically Induced Liquefaction Sites and Features Located in the Vicinity of the 1886 Charleston, South Carolina Earthquake," *Seismological Research Letters* 61 (2):117-130, 1990.
337. Marple, R.T. and Talwani, P., "Evidence for possible tectonic upwarping along the South Carolina coastal plain from an examination of river morphology and elevation data," *Geology* 21:651-654, 1993.
338. Marple, R.T. and Talwani, P., "Evidence for a Buried Fault System in the Coastal Plain of the Carolinas and Virginia - Implications for Neotectonics in the Southeastern United States," *Geological Society of America Bulletin* 112 (2):200-220, 2000.
339. Wildermuth, E. and Talwani, P., "A Detailed Gravity Survey of a Pull-Apart Basin in Northeast South Carolina," *Geological Society of America Abstracts with Programs* 33 (6):240, 2001.
340. Weems, R.E. and Lewis, W.C., "Structural and Tectonic Setting of the Charleston, South Carolina, Region: Evidence From the Tertiary Stratigraphic Record," *Geological Society of America Bulletin* 114 (1):24-42, 2002.
341. Lennon, G., *Identification of a Northwest Trending Seismogenic Graben Near Charleston, South Carolina*, U.S. Nuclear Regulatory Commission Report, NUREG/CR-4075, 1986.

-
342. Behrendt, J.C., Hamilton, R.M., Ackermann, H.D., and Henry, V.J., "Cenozoic Faulting in the Vicinity of the Charleston, South Carolina, 1886 Earthquake," *Geology* 9 (3):117-122, 1981.
343. Hamilton, R.H., Behrendt, J.C., and Ackermann, H.D., "Land Multichannel Seismic-Reflection Evidence for Tectonic Features Near Charleston, South Carolina," in *Studies Related to the Charleston, South Carolina Earthquake of 1886 - Tectonics and Seismicity*, U.S. Geological Survey Professional Paper 1313-I:11-118, 1983.
344. Behrendt, J.C., Hamilton, R.M., Ackermann, H.D., Henry, V.H., and Bayer, K.C., "Marine Multichannel Seismic-Reflection Evidence for Cenozoic Faulting and Deep Crustal Structure Near Charleston, South Carolina," in *Studies Related to the Charleston, South Carolina, Earthquake of 1886 - Tectonics and Seismicity*, U.S. Geological Survey Professional Paper 1313-J:J1-J29, 1983.
345. Behrendt, J.C. and Yuan, A., "The Helena Banks Strike-Slip (?) Fault Zone in the Charleston, South Carolina Earthquake Area: Results from a Marine, High-Resolution, Multichannel, Seismic-Reflection survey," *Geological Society of America Bulletin* 98:591-601, 1987.
346. Talwani, P. and Katuna, M., *Macroseismic effects of the 1886 Charleston earthquake*, Carolina Geological Society Field Trip Guidebook, 2004.
347. Weems, R.E., Lemon, E.M. Jr., and Nelson, M.S., *Geology of the Pringletown, Ridgeville, Summerville, and Summerville Northwest 7.5-Minute Quadrangles, Berkeley, Charleston, and Dorchester Counties, South Carolina*, U.S. Geological Survey Miscellaneous Investigations Map 2502, 1:24,000 scale, 1997.
348. Madabhushi, S. and Talwani, P., "Composite Fault Plane Solutions of Recent Charleston, South Carolina, Earthquakes," *Seismological Research Letters* 61 (3-4):156, 1990.
349. Madabhushi, S. and Talwani, P., "Fault Plane Solutions and Relocations of Recent Earthquakes in Middleton Place-Summerville Seismic Zone Near Charleston, South Carolina," *Bulletin of the Seismological Society of America* 83 (5):1,442-1,466, 1993.
350. Talwani, P., "Fault Geometry and Earthquakes in Continental Interiors," *Tectonophysics* 305:371-379, 1999.
351. Tarr, A.C. and Rhea, B.S., "Seismicity Near Charleston, South Carolina, March 1973 to December 1979," in *Studies Related to the Charleston, South Carolina Earthquake of 1886 Tectonics and Seismicity*, U.S. Geological Survey Professional Paper 1313-R1-R17, 1983.

-
352. Bollinger, G.A., Johnston, A.C., Talwani, P., Long, L.T., Shedlock, K.M., Sibol, M.S., and Chapman, M.C., "Seismicity of the Southeastern United States; 1698-1986," in *Neotectonics of North America: Decade map volume to accompany the neotectonic maps*, Geological Society of America, Boulder, CO, 1991.
353. Gangopadhyay, A. and Talwani, P., "Fault Intersections and Intraplate Seismicity in Charleston, South Carolina: Insights from a 2-D Numerical Model," *Current Science* 88 (10), 2005.
354. Tarr, A.C., Talwani, P., Rhea, B.S., Carver, D., and Amick, D., "Results of Recent South Carolina Seismological Studies," *Bulletin of the Seismological Society of America* 71 (6):1,883-1,902, 1981.
355. Dutton, C.E., *The Charleston Earthquake of August 31, 1886*, U.S. Geological Survey ninth annual report 1887-88, 1889.
356. Seeber, L. and Armbruster, J.G., "The 1886 Charleston, South Carolina Earthquake and the Appalachian Detachment," *American Geophysical Research* 86 (B9):7,874-7,894, 1981.
357. Talwani, P. and Schaeffer, W.T., "Recurrence Rates of Large Earthquakes in the South Carolina Coastal Plain Based on Paleoliquefaction Data," *Journal of Geophysical Research* 106 (B4):6,621-6,642, 2001.
358. Obermeier, S.F., Gohn, G.S., Weems, R.E., Gelinas, R.L., and Rubin, M., "Geologic Evidence for Recurrent Moderate to Large Earthquakes Near Charleston, South Carolina," *Science* 227 (4685):408-411, 1985.
359. Obermeier, S.F., Jacobson, R.B., Smoot, J.P., Weems, R.E., Gohn, G.S., Monroe, J.E., and Powars, D.S., *Earthquake-Induced Liquefaction Features in the Coastal Setting of South Carolina and in the Fluvial Setting of the New Madrid Seismic Zone*, U.S. Geological Survey professional paper 1504, 1990.
360. Frankel, A.D., Petersen, M.D., Mueller, C.S., Haller, K.M., Wheeler, R.L., Leyendecker, E.V., Wesson, R.L., Harmsen, S.C., Cramer, C.H., Perkins, D.M., and Rukstales, K.S., *Documentation for the 2002 Update of the National Seismic Hazard Maps*, U.S. Geological Survey Open-File Report 02-420, 2002.
361. Removed
362. Powell, C.A., Bollinger, G.A., Chapman, M.C., Sibol, M.S., and Johnston, A.R., "A Seismotectonic Model for the 300-Kilometer-Long Eastern Tennessee Seismic Zone," *Science* 264:686-688, 1994.
363. Chapman, M.C., Munsey, J.W., Powell, C.A., Whisner, S.C., and Whisner, J., "The Eastern Tennessee Seismic Zone: Summary After 20 Years of Network Monitoring," *Seismological Research Letters* 73 (2):245, 2002.

-
364. Chapman, M.C., Powell, C.A., Vlahovic, G., and Sibol, M.S., "A Statistical Analysis of Earthquake Focal Mechanisms and Epicenter Locations in the Eastern Tennessee Seismic Zone," *Bulletin of the Seismological Society of America* 87 (6):1,522-1,536, 1997.
365. Removed
366. Removed
367. Removed
368. Removed
369. Removed
370. Johnston, A.C., Coppersmith, K.J., Kanter, L.R., and Cornell, C.A., *The Earthquakes of Stable Continental Regions, Volume I: Assessment of Large Earthquake Potential - Final Report TR-102261-V1*, prepared for Electric Power Research Institute, 1994.
371. Chapman, M.C. and Krimgold, F., *Seismic Hazard Assessment for Virginia*, Virginia Tech Seismological Observatory report, Virginia Tech Department of Geological Sciences, 1994.
372. Removed
373. Wheeler, R.L. and Crone, A.J., "Known and Suggested Quaternary Faulting in the Mid-Continent United States," *Engineering Geology* 62:51-78, 2001.
374. Hough, S.E., Armbruster J.G., Seeber, L., and Hough, J.F., "On the Modified Mercalli Intensities and Magnitudes of the 1811-1812 New Madrid Earthquakes," *Journal of Geophysical Research* 105 (B10):23,839-23,864, 2000.
375. Johnston, A.C. and Schweig, G.D., "The Enigma of the New Madrid Earthquakes of 1811-1812," *Annual Review of Earth and Planetary Sciences* 24:339-384, 1996.
376. Van Arsdale, R.B., Kelson, K.I., and Lurnden, C.H., "Northern Extension of the Tennessee Reelfoot Scarp into Kentucky and Missouri," *Seismological Research Letters* 66 (5):57-62, 1995.
377. Kelson, K.I., Simpson, G.D., Van Arsdale, R.B., Harden, C.C., and Lettis, W.R., "Multiple Late Holocene Earthquakes Along the Reelfoot Fault, Central New Madrid Seismic Zone," *Journal of Geophysical Research* 101 (B3):6,151-6,170, 1996.

378. Van Arsdale, R.B., "Displacement History and Slip Rate on the Reelfoot Fault of the New Madrid Seismic Zone," *Engineering Geology* 55:219-226, 2000.
379. Tuttle, M.P., Schweig, E.G., Sims, J.D., Lafferty, R.H., Wolf, L.W., and Haynes, M.L., "The Earthquake Potential of the New Madrid Seismic Zone," *Bulletin of the Seismological Society of America* 92 (6):2,080-2,089, 2002.
380. Tuttle, M.P., Schweig, E.S., Campbell, J., Thomas, P.M., Sims, J.D., and Lafferty, R.H., *Evidence for New Madrid Earthquakes in A.D. 300 and 2350 B.C.*, *Seismological Research Letters* 76 (4):489-501, 2005.
381. Guccione, M.J., "Late Pleistocene and Holocene Paleoseismology of an Intraplate Seismic Zone in a Large Alluvial Valley, The New Madrid Seismic Zone, Central USA," *Tectonophysics* 408:237-264, 2005.
382. Bollinger, G.A. and Sibol, M.S., "Seismicity, Seismic Reflection Studies, Gravity and Geology of the Central Virginia Seismic Zone: Part I – Seismicity," *Geological Society of America Bulletin* 96:49-57, 1985.
383. Wheeler, R.L., and Johnston, A.C., "Geologic Implications of Earthquake Source Parameters in Central and Eastern North America," *Seismological Research Letters* 63 (4):491-505, 1992.
384. Coruh, C., Costain, J.K., Glover, L., III, Pratt, T., and Brennan, J., *Seismicity, Seismic Reflection, Gravity and Geology of the Central Virginia Seismic Zone: Part I, Reflection Seismology*, U.S. Nuclear Regulatory Commission Report NUREG/CR-5123, 1988.
385. Obermeier, S.F. and McNulty, W.E., "Paleoliquefaction Evidence for Seismic Quiescence in Central Virginia During the Late and Middle Holocene Time," *Eos Transactions of the American Geophysical Union* 79 (17):S342, 1998.
386. France, N.A. and Brown, H.S., "A Petrographic Study of Kings Mountain Belt Metaconglomerates," in *Geological Investigations of the Kings Mountain Belt and Adjacent Areas in the Carolinas*, Carolina Geological Society Field Trip Guidebook, 1981.
387. Hatcher, R.D., Jr. and Morgan, B.K., "Finite Strain and Regional Implications of the Deformed Draytonville Metaconglomerate Near Gaffney, South Carolina," in *Geological Investigations of the Kings Mountain Belt and adjacent areas in the Carolinas*, Carolina Geological Society Field Trip Guidebook, 1981.
388. McDougall, I. and Harrison, T.M., *Geochronology and Thermochronology by the $^{40}\text{Ar}/^{39}\text{Ar}$ method*, 2nd edition, Oxford University Press, New York, 1999.

389. Murphy, C.F. and Butler, J.R., "Geology of the Northern Half of the Kings Creek Quadrangle, South Carolina," in *Geological Investigations of the Kings Mountain Belt and Adjacent Areas in the Carolinas*, Carolina Geological Society Field Trip Guidebook, 1981.
390. Horton, J.W., Jr. and Butler, J.R., "Geology and Mining History of the Kings Mountain Belt in the Carolinas; a Summary and Status Report," in *Geological investigations of the Kings Mountain Belt and Adjacent Areas in the Carolinas*, Carolina Geological Society Field Trip Guidebook, 1981.
391. Nystrom Jr., P.G, *Geologic Map of the Blacksburg South 7.5 - Minute Quadrangle, Cherokee County, South Carolina [preliminary draft]*, South Carolina Department of Natural Resources Geological Survey, 1:24,000 scale, 1 sheet, 2004.
392. Schaffer, M.F., "Polyphase Folding in a Portion of the Kings Mountain Belt, North-Central South Carolina," in *Geological Investigations of the Kings Mountain Belt and Adjacent Areas in the Carolinas*, Carolina Geological Society Field Trip Guidebook, 1981.
393. Guidotti, C.V., "Micas in Metamorphic Rocks," in *Reviews in Mineralogy Volume 13*, ed. S.W. Bailey, Mineralogical Society of America, 1984.
394. Ramberg, H., "The Facies Classification of Rocks, a Clue to the Origin of Quartzo-Feldspathic Massifs and Veins," *Journal of Geology* 57 (1):18-54, 1949.
395. Bollinger, G.A., "Reinterpretation of the Intensity Data for the 1886 Charleston, South Carolina, Earthquake," in *Studies Related to the Charleston, South Carolina, Earthquake of 1886 - A Preliminary Report*, U.S. Geological Survey Professional Paper 1028:17-32, 1977.
396. Taber, S., "The South Carolina Earthquake of January 1, 1913," *Bulletin of the Seismological Society of America* 3:6-13, 1913.
397. Visvanathan, T.R., "Earthquakes in South Carolina, 1698-1975," *South Carolina Geological Survey Bulletin* 40, 1980.
398. U.S. Nuclear Regulatory Commission, *Safety Evaluation Report for an Early Site Permit (ESP) at the North Anna ESP Site*, U.S. Nuclear Regulatory Commission Report, NUREG-1835, September 2005.
399. Seeber, L., and Armbruster, J.G., "Seismicity Along the Atlantic Seaboard of the U.S.; Intraplate Neotectonics and Earthquake Hazard," in *The Atlantic Continental Margin: U.S., The Geology of North America*, vol. I-2, ed. R.E. Sheridan and J.A. Grow, Geological Society of America, Boulder, CO, 1988.

400. Van Schmus, W.R., Bickford, M.E., and Turek, A., "Proterozoic Geology of the East-Central Midcontinent Basin," in *Basement and Basins of Eastern North America*, ed. B.A. van der Pluijm and P. A. Catacosinos, Geological Society of America Special Paper 308, Boulder, CO, 1996.
401. Cherokee Nuclear Station Preliminary Safety Analysis Report (PSAR), prepared by Law Engineering Testing Company for Duke Power Company, Project 81, 1974.
402. Maybin, A.H., Mineral Resources Map of South Carolina, South Carolina Geological Survey, GGMS-3, 1:500,000-Scale, 1997.
403. Bream, B.R., 2002, The Southern Appalachian Inner Piedmont: New Perspectives Based on Recent Detailed Geologic Mapping, Nd Isotopic Evidence, and Zircon Geochronology, in Hatcher, R.D., Jr., and Bream, B.R., eds., *Inner Piedmont Geology in the South Mountains-Blue Ridge Foothills and the Southwestern Brushy Mountains, Central-Western North Carolina*: North Carolina Geological Survey, Carolina Geological Society Annual Field Trip Guidebook, p. 45-63.
404. Hatcher, R. D., Bream, B. R., and Mersch, A. J., 2007, Tectonic Map of the Southern and Central Appalachians: A Tale of Three Orogens and a Complete Wilson Cycle, in Hatcher, R. D., Carlson, M. P., McBride, J. H., and Martinez Catalan, J. R., eds., *4-D Framework of Continental Crust*: Geological Society of America Memoir 200, p. 595-632.
405. Dennis, A. J., 2007, Cat Square Basin, Catskill Clastic Wedge: Silurian-Devonian Orogenic Events in the Central Appalachians and the Crystalline Southern Appalachians: Geological Society of America Special Paper 433, p. 313-329.
406. Goldsmith, R, Milton, D. J., Horton, J. W., 1988, Geologic Map of the Charlotte 1x2 Degrees Quadrangle, North Carolina and South Carolina: USGS Miscellaneous Investigations Series Map I-1251-E; 1:250,000. Website <http://pubs.er.usgs.gov/usgspubs/i/i1251E> accessed February 6, 2009.
407. North Carolina Geological Survey (NCGS), Geology of North Carolina vector digital data onemap_prod.SDEADMIN.geo, Website <http://www.nconemap.com/Default.aspx?tabid=286>, accessed June 12, 2007, publication date 1998.
408. Milton, D. J., The northern termination of the Kings Mountain belt. In *Geological investigations of the Kings Mountain belt and adjacent areas in the Carolinas*, Carolina Geological Society Field Trip Guidebook 1982, p. 1-5, 1981.
409. McSween, H. Y. Jr., Speer, J. A., Fullagar, P. D., 1991, Chapter 7. Plutonic Rocks. *In*, *The Geology of the Carolinas*. Horton, J. W. Jr., Zullo, V. A. eds., University of Tennessee Press, p. 109-126.

-
410. Dallmeyer, R.D., Wright, J.E., Secor, D.T., Jr., and Snoke, A.W., Character of the Alleghanian Orogeny in the Southern Appalachians: Part II-Geochronological constraints on the tectonothermal evolutions of the Eastern Piedmont in South Carolina: Geological Society of America Bulletin. v. 97, p. 1,329-1,344, 1986.
411. Howard, C.S., Charleton, J.E., and McCarney, K.J., New geologic synthesis of the Dreher Shoals and Carolina Terranes, Lake Murray and Saluda Dam, Columbia, SC: Geological Society of America Abstracts with Programs, v. 37, no. 2, p. 36, 2005.
412. McCarney, K.J., Charleton, J.E., and Howard C.S., Brittle features mapped along a shear zone at Saluda Dam, central South Carolina: Geological Society of America Abstracts with Programs. v. 37. no. 2, p. 5. 2005.
413. Gohn, G.S., 1988, "Late Mesozoic and early Cenozoic geology of the Atlantic Coastal Plain: North Carolina to Florida," in *The Geology of North America vol. 1-2, The Atlantic Continental Margin*, The Geological Society of America.
414. Prowell, D.C. and Obermeier, S.F., 1991, "Evidence of Cenozoic Tectonism," in *The Geology of the Carolinas - Carolina Geological Society 50th Anniversary Volume*, University of Tennessee Press.
415. Giorgis, S. D., Mapes, R. W., Bream, B. R., The Walker Top Granite: Acadian granitoid or eastern Inner Piedmont basement, in Hatcher, R. D. and Bream, B. R., eds., Inner Piedmont geology in the South Mountains-Blue Ridge foothills and the southwestern Brushy Mountains, central-western North Carolina: North Carolina Geological Survey, Carolina Geological Society annual fieldtrip guidebook, p. 33-43, 2002.
416. Merschat, A. J., Kalbas, J. L., Geology of the southwestern Brushy Mountains, North Carolina Inner Piedmont: A summary and synthesis of recent studies, in Hatcher, R. D. and Bream, B. R., eds., Inner Piedmont geology in the South Mountains-Blue Ridge foothills and the southwestern Brushy Mountains, central-western North Carolina: North Carolina Geological Survey, Carolina Geological Society annual fieldtrip guidebook, p. 101-126, 2002.
417. Hibbard, J. P., Shell, G. S., Bradley, P. J., Samson, S. D., Wortman, G. L., 1998, The Hyco shear zone in North Carolina and southern Virginia: implications for the piedmont zone-Carolina zone boundary in the southern Appalachians: American Journal of Science, v. 298, p. 85-107.
418. Wortman, G. L., Samson, S. D., Hibbard, J. P., Precise timing constraints on the kinematic development of the Hyco shear zone: implications for the Central Piedmont shear zone, southern Appalachian orogen: American Journal of Science, v. 298, p. 108-130, 1998.

419. Davis, T. L., Geology of the Columbus promontory, western Piedmont, North Carolina, southern Appalachians, in Hatcher, R. D. and Davis, T. L., Studies of Inner Piedmont geology with a focus on the Columbus promontory: Carolina Geological Society Fieldtrip Guidebook, p. 17-39, 1993.
420. Garahan, J. M., Preddy, M. S., Ranson, W. A. (1993) Summary of Mid-Mesozoic Brittle Faulting in the Inner Piedmont and Nearby Charlotte Belt of the Carolinas. In Studies of Inner Piedmont Geology with a focus on the Columbus Promontory. Carolina Geological Society Field Trip Guidebook. p. 55-65.
421. Horton, J. W., Shear zone between the Inner Piedmont and Kings Mountain belts in the Carolinas: Geology, v. 9, p. 28-33, 1981.
422. Dennis, A. J., Wright, J. E., Mississippian (ca. 326-323 Ma) U-Pb crystallization for two granitoids in Spartanburg and union counties, South Carolina: Carolina Geological Society Guidebook, p. 43-47. 1995.
423. Griffin, V. S., The Lowndesville belt north of the South Carolina-Georgia border, in Horton, J. W., Butler, J. R., and Milton, D. J., eds. Geological investigations in the Kings Mountain belt and adjacent areas, Carolina Geological Society Fieldtrip Guidebook, p. 166-173, 1981.
424. Nelson, A. E., Polydeformed rocks of the Lowndesville shear zone in the Greenville 2 degree quadrangle, South Carolina and Georgia, in Horton, J. W., Butler, J. R., and Milton, D. J., eds. Geological investigations in the Kings Mountain belt and adjacent areas, Carolina Geological Society Fieldtrip Guidebook, p. 181-193, 1981.
425. Hibbard, J., Miller, B., Hames, W., Allen, J., and Standard, I., Carolina; definition and recent finding in central North Carolina: Geological Society of America, Southeastern Section Abstracts with Programs, v. 39, p. 11-12, 2007.
426. Hibbard, J., Pollock, J., Allen, J., and Brennan, M., The heart of Carolina: Stratigraphic and tectonic studies in the Carolina terrane of central North Carolina, Geological Society of America Southeast Section Fieldtrip Guidebook. 54 p., 2008.
427. Allen, J.S., Miller, B., Hibbard, J., and Boland, I., Significance of intrusive rocks along the Charlotte-Carolina terrane boundary: evidence for the timing of deformation in the Gold Hill fault zone near Waxhaw, NC: Geological Society of America Southeast Section Abstracts with Programs, v. 39, p. 12, 2007.
428. Hibbard, J. P., van Staal, C., Rankin, D. W., Comparative analysis of pre-Silurian crustal building blocks of the northern and the southern Appalachian orogen: American Journal of Science, v.307, p.23-45, 2007.

429. Hatcher, R. D. Jr., Tectonic synthesis of the U. S. Appalachians; in *The Geology of North America, The Appalachian-Ouachita Orogen in the United States, Volume F-2*, The Geological Society of America, p.511-535, 1989.
430. Hibbard, J. P., van Staal, C. R., Miller, B. V., Links among Carolina, Avalonia, and Ganderia in the Appalachian peri-Gondwanan realm, *Geological Society of America Special Paper 433*, p.291-311, 2007.
431. Nystrom, P.G. Jr., Late Cretaceous-Cenozoic Brittle Faulting Beneath the Western South Carolina Coastal Plain: Reactivation of the Eastern Piedmont Fault System, *Geological Society of America Abstracts with Programs, Southeastern Section 55th annual meeting*, 2006.
432. Nicolas, A., Poirier, J.P., *Crystalline Plasticity and Solid State Flow in Metamorphic Rocks*, John Wiley and Sons, 444p., 1976.
433. Duke Energy Submittal of Cherokee Nuclear Station Final Foundation Geologic Map Record, Fugro Consultants, Inc., *DUK-001-PR-01, Revision 2*, WLG2011.12-04, dated December 15, 2011 (ML12065A114).
434. Hodges, K.V., "Pressure-Temperature-Time Paths," *Annual Review of Earth and Planetary Science Letters*, v.19, p.207-236, 1991.
435. Evans, M.A., and Bartholomew, M.J., Crustal fluid evolution during deformation, uplift, and exhumation of the southeastern Piedmont of the southern Appalachians: Late Paleozoic through Mesozoic rifting, *in* Tollo, R.P., Bartholomew, M.J., Hibbard, J.P., Karabinos, P.M., eds., *From Rodinia to Pangea: The Lithotectonic Record of the Appalachian Region*; Geological Society of America Memoir 206, p.553-577, 2010.
436. Thompson, A.B., "PCO₂ in Low Grade Metamorphism: Zeolite, Carbonate, Clay Mineral, Prehnite Relations in the System CaO-Al₂O₃-SiO₂-CO₂-H₂O," *Contributions to Mineralogy and Petrology*, v.33, p.145-161, 1971.
437. American Society of Mechanical Engineers, ASME NQA-1 Part III, Subpart 3.3, Nonmandatory Appendix 3.1, "Guidance on Qualification of Existing Data," 2004.
438. Dennis, Allen J., Shervais, John W., LaPoint, Dennis, "Geology of the Ediacaran-Middle Cambrian Rocks of Western Carolina in South Carolina," *The Geological Society of America Field Guide 29*, p. 303-325, 2012.
439. Gallen, S.F., et al., "Miocene Rejuvenation of Topographic Relief in the Southern Appalachians," *GSA Today*, v 23, no. 2, p. 4-10, 2013.

-
440. Heidbach, O., Tingay, M., Barth, A., Reinecker, J., Kurfess, D., and Muller, B., "The World Stress Map Database Release 2008," Website http://dc-app3-14.gfz-potsdam.de/pub/stress_maps/stress_maps.html, accessed June 18, 2013, release date 2008.
441. NUREG-2115 "Central and Eastern United States Seismic Source Characterization for Nuclear Facilities," U.S. Nuclear Regulatory Commission NUREG-2115, Department of Energy DOE/NE-0140, and Electric Power Research Institute Report 1021097, 2012.
442. Davis, Brittany, A., "Tectonic Evolution of the Southern Appalachian Inner Piedmont: Identification and Interpretation of Crustal Features From Aeromagnetic Data and Detailed Geologic Mapping in Central Georgia," University of Tennessee-Knoxville Thesis, 2010.
443. Dura-Gomez, I., and Talwani, P., "Finding Faults in the Charleston Area, South Carolina, 1. Seismological Data," Seismological Research Letters, v. 80," no. 5, p. 883-900, 2009.
444. Talwani, P., and Dura-Gomez, I., "Finding Faults In The Charleston Area, South Carolina: 2. Complementary Data," Seismological Research Letters, v. 80, no. 5., p. 901-919, 2009.
445. Chapman, M. C., Beale, J. N., "Mesozoic and Cenozoic Faulting Imaged At The Epicent of the 1886 Charleston, South Carolina, Earthquake," Bulletin Of The Sesimological Society Of America, v. 98, p. 2533-2542, 2008.
446. Chapman, M. C., Beale, J. N., "On The Geologic Structure At The Epicenter Of The 1886 Charleston, South Carolina, Earthquake," Bulletin of the Seismological Society of America, v. 100, p. 1010-1030, 2010.
447. Obermeier, S. F., Weems, R. E., Jacobson, R. B., Gohn, G. S., "Liquefaction Evidence For Repeated Holocene Earthquakes in the Coastal Region of South Carolina," Annals of the New York Academy of Sciences, v. 558, p. 183-195, 1989.
448. Weems, R. E., Obermeier, S. F., "The 1886 Charleston Earthquake - An Overview Of Geological Studies: In Proceeding Of The US Nuclear Regulatory Commission Seventeenth Water Reactor Safety Information Meetings," NUREG/CP-0105, v. 2, p. 289-313, 1990.
449. Talwani, P., Dura-Gomez, I., Gassman, S., Hasek, M., and Chapman, A., "Studies Related to the Discovery of a Prehistoric Sandblow in the Epicentral Area Of The 1886 Charleston SC Earthquake: Trench and Geotechnical Investigations," Eastern Section of the Seismological Society of America Program and Abstracts, p. 50, 2008.

-
450. Marple, R. T. and Miller, A., "Association of the 1886 Charleston, South Carolina, Earthquake And Seismicity Near Summerville With A 12° Bend In The East Coast Fault System And Triple-Fault Junctions," *Southeastern Geology*, v. 44, p. 101-127, 2006.
451. Bartholomew, Mervin J. and Rich, F. R., "The Walls of Colonial Fort Dorchester: A Record of Structures Caused by the August 31, 1886 Charleston, South Carolina Earthquake and its Subsequent Earthquake History," *Southeastern Geology*, v 44, p. 147- 169, 2007.
452. Hu, K., Gassman, S. L., Talwani, P., "In-Situ Properties Of Soils at Paleoliquefaction Sites in the South Carolina Coastal Plain," *Seismological Research Letters*, v. 73, p. 962-978, 2002.
453. Hu, K., Gassman, S. L., Talwani, P., "Magnitudes of Prehistoric Earthquakes in the South Carolina Coastal Plain from Geotechnical Data," *Sesimological Research Letters*, v. 73, p. 979-991, 2002.
454. Leon, E., Gassman, S. L., Talwani, P., "Effect of Soil Aging on Assessing Magnitudes and Accelerations of Prehistoric Earthquakes," *Earthquake Spectra*, v. 21, p. 737-759, 2005.
455. Gassman, S., Talwani, P., Hasek, M., "Magnitudes of Charleston, South Carolina Earthquakes from Insitu Geotechnical Data," Presentation At CEUS Earthquake Hazards Program, USGS, October 28-29, Memphis, 2009.
456. Whisner, S. C., Hatcher, R. D., Munsey, J. W., "Disturbed Sediments In The East Tennessee Seismic Zone: Evidence Of Large Prehistoric Earthquakes in East Tennessee?" *Southeastern Geology*, v. 42, p. 67-82, 2003.
457. Hatcher, R. D., Vaughn, J. D., Obermeier S. F., "Large Earthquake Paleoseismology in the East Tennessee Seismic Zone: Results of an 18 Month Pilot Study," in Cox, R. T., Tuttle, M. P., Boyd, O. S., and Locat, J., eds., *Recent Advances in North American Paleoseismology and Neotectonics East of the Rockies: Geological Society of America Special Paper 493*, p. 111-142, 2012.
458. Holbrook, J., et al., "Stratigraphic Evidence for Millennial-Scale Temporal Clustering of Earthquakes on a Continental-Interior Fault: Holocene Mississippi River Floodplain Deposits, New Madrid Seismic Zone, USA," *Tectonophysics* 420, p.431-454, 2006.
459. Chapman, M. C., "On the Rupture Process of the 23 August 2011 Virginia Earthquake," *Bulletin of the Seismological Society of America*, v. 103, n. 2a, p. 613-628, 2013.

460. Li, Yong, "Post 23 August 2011 Mineral, Virginia Earthquake Investigations at North Anna Nuclear Power Plant," Seismological Research Letters, v. 84, p. 468-473, 2013.
461. Graizer, V., Munson, C. G., and Li, Y., "North Anna Nuclear Power Plant Strong-Motion Records of the Mineral, Virginia, Earthquake of 23 August 2011," Seismological Research Letters, v. 84, p. 551-557, 2013.
462. U.S. Geological Survey (USGS), "Earthquake Hazards Program, Preliminary Earthquake Report: Magnitude 5.8 - Virginia, 2011 August 23 17:51:04 UTC," Website:<http://earthquake.usgs.gov/earthquakes/recenteqsww/Quakes/se082311a.php#details> accessed 5/2/2012.

2.5.2 VIBRATORY GROUND MOTION

WLS COL 2.5-2 This section provides a detailed description of vibratory ground motion assessments, specifically the criteria and methodology for establishing the Ground Motion Response Spectra (GMRS) and Foundation Input Response Spectra (FIRS) for the Lee Nuclear Station Units 1 and 2. The section begins with a review of the approach in Regulatory Guide (RG) 1.208, *A Performance-Based Approach to Define The Site-Specific Earthquake Ground Motion*, which satisfies the requirements set forth in Section 100.23, "Geologic and Seismic Siting Criteria," of Title 10, Part 100, of the Code of Federal Regulations (10 CFR 100), "Reactor Site Criteria." The GMRS for the Lee Nuclear Station Site was developed by adopting methodology consistent with the approach recommended in RG 1.208.

Following this introductory section, the remainder of the Subsection is presented as follows:

- Seismicity ([Subsection 2.5.2.1](#))
- Geologic and Tectonic Characteristics of the Site and Region ([Subsection 2.5.2.2](#))
- Correlation of Earthquake Activity with Seismic Sources ([Subsection 2.5.2.3](#))
- Probabilistic Seismic Hazard Analysis (PSHA) and Controlling Earthquake ([Subsection 2.5.2.4](#))
- Seismic Wave Transmission Characteristics of the Site ([Subsection 2.5.2.5](#))
- Ground Motion Response Spectrum (GMRS) developed for Lee Nuclear Station Unit 2 ([Subsection 2.5.2.6](#))
- Development of FIRS for Units 1 and 2 ([Subsection 2.5.2.7](#))

RG 1.208 provides guidance on methods acceptable to the NRC to satisfy the requirements of the seismic and geologic regulation, 10 CFR 100.23, for assessing the appropriate Safe Shutdown Earthquake (SSE) ground motion levels for new nuclear power plants. RG 1.208 states that an acceptable starting point for this assessment at sites in the Central and Eastern United States (CEUS) is the PSHA conducted by the EPRI-SOG in the 1980s (References 201, 203, and 207). However, that has now been supplanted by the recent EPRI CEUS SSC model, detailed in NUREG 2115, which was created to provide a regionally consistent model of seismic hazard for nuclear facilities throughout the central and eastern United States (Reference 326). Subsection 2.5.2 takes this most recent CEUS SSC as the starting point for the Lee Nuclear site PSHA, but adding detail and updated data as necessary.

Subsection 2.5.2.4 describes the PSHA calculation for a base case rock seismic hazard. The GMRS and FIRS are developed using the graded, performance-based, risk-consistent method described in RG 1.208. The methodology for developing the GMRS is based on ASCE/SEI Standard 43-05, *Seismic Design Criteria for Structures, Systems, and Components in Nuclear Facilities* (Reference 295). The method specifies the level of conservatism and rigor in the seismic design process such that the performance of structures, systems, and components of the plant achieve a uniform seismic safety performance consistent with the NRC's safety goal policy statement (51 FR 28044 and 51 FR 30028, 10 CFR Part 50). The ASCE/SEI Standard 43-05 approach is designed to achieve a quantitative safety performance goal (PF). The method is based on the use of site-specific mean seismic hazard and assumes that the seismic design criteria and procedures contained in NUREG-0800 are applied in seismic source characterization (SSC) design.

The ASCE/SEI Standard 43-05 (Reference 295) approach aims conservatively to assure a seismic safety target, or performance goal of mean 10^{-5} per year for SDC-5 SSCs. ANSI/ANS Standard 2.26-2004 *Categorization of Nuclear Facility Structures, Systems, and Components for Seismic Design* (Reference 296) provides the criteria for selecting Seismic Design Category and Limit State that establishes the Seismic Design Basis for each SSC at a nuclear facility. The target mean annual performance goal for nuclear plants is achieved by coupling site-specific design response spectrum (DRS) with the deterministic Seismic Design Category and procedures specified by NUREG-0800. The ASCE/SEI Standard 43-05 criteria for deriving a site-specific DRS are based on the conservative assumption that the seismic design criteria specified by NUREG-0800 achieve less than a 1 percent chance of failure for a given DRS. The conservatism of this assumption is demonstrated by analyses described in McGuire et al. (Reference 274) that show plant level risk reduction factors ranging from about 20 to about 40 are attained by the NRC's seismic design criteria. The method is based on the use of mean hazard results consistent with the recommendation contained in McGuire et al. (Reference 274) and with the NRC's general policy on the use of seismic hazard in risk-informed regulation.

Subsections 2.5.2.1 through 2.5.2.4 document the review and update of the available EPRI CEUS seismicity, seismic source, and ground motion models.

Subsection 2.5.2.5 summarizes information about the seismic wave transmission characteristics of the Lee Nuclear Site with reference to more detailed discussion of all engineering aspects of the subsurface in **Subsection 2.5.4**.

Subsection 2.5.2.6 describes the development of the site-specific GMRS for the Lee Nuclear Site. Regulatory Guide 1.208 provides guidance for development of the GMRS. **Subsection 2.5.2.7** describes the development of the FIRS for Units 1 and 2, to evaluate potential site response effects attributed to existing fill concrete and structural concrete materials placed during construction of the existing Cherokee Nuclear Station as well as new fill concrete for Lee Nuclear Station placed above the existing Cherokee Nuclear Station concrete materials and within localized lower pump room areas. For Unit 2, sound, continuous rock meeting the hard rock definitions is located at the foundation level. Therefore, the calculated GMRS defines the input motion at Unit 2.

The information provided for the Lee Nuclear Station Units 1 and 2 is based on data from historic field explorations for the Cherokee Nuclear Station and the field explorations for the Lee Nuclear Station completed in 2006, 2007, and 2012.

2.5.2.1 Seismicity

The Lee Nuclear site region (**Figure 2.5.2-248**) is located within the CEUS SSC project study region (**Figure 2.5.2-249**). The CEUS SSC relied upon a complete, declustered earthquake catalog with uniform magnitude measures for each event to analyze historical seismicity in the CEUS and determine appropriate recurrence models for seismic source zones. The historical earthquake catalog used in the EPRI CEUS SSC analysis is complete through 2008 (**Reference 326**).

As described in **Subsection 2.5.4.8**, there is no potential for earthquake-induced liquefaction at the site. The stability of natural and manmade slopes where failure could adversely impact safety-related structures is discussed in **Subsection 2.5.5**.

2.5.2.1.1 Seismicity Catalog Used for 2012 CEUS SSC Project

The seismicity catalog used in the CEUS SSC (NUREG 2115) extends from the longitude of the Rocky Mountain foothills (105°W) in the west to 200 mi offshore of the Atlantic coastline to the east (**Reference 326**). The northern and southern boundaries extend a minimum of 200 mi into Canada or into the Gulf of Mexico (**Figure 2.5.2-249**). The CEUS catalog is assumed to be complete throughout the historical record to the time of the catalog compilation (December 31, 2008) in that all instrumental earthquakes and significant historical earthquakes are included. In addition, the catalog applies uniform size measure to each earthquake, moment magnitude **M** (see Section 3.3.2 of NUREG 2115 for conversion procedures) and only includes main events of earthquake clusters (i.e., the catalog is declustered).

RG 1.206 states that a COL applicant shall "provide a complete list of all historically reported earthquakes that could have reasonably affected the region surrounding the site, including all earthquakes of Modified Mercalli intensity greater than or equal to IV or of magnitude greater than or equal to 3.0 that have been reported within 200 miles of the site." The CEUS SSC catalog provides this information through 2008 for the Lee Nuclear site region (**Figure 2.5.2-248**).

2.5.2.1.2 Recent and Historical Seismicity

The CEUS SSC seismicity catalog described in [Subsection 2.5.2.1.1](#) is shown in [Figures 2.5.2-248, 2.5.2-249, and 2.5.1-210](#). Since the compilation of this catalog, the August 23, 2011 earthquake that occurred near Mineral, VA is arguably the most (or only) significant earthquake in the CEUS region since the completion of the CEUS SSC catalog. The epicenter was located approximately 280 mi. from the Lee Nuclear site. Although located outside the Lee Nuclear site region, this earthquake is discussed as part of the discussion of the Central Virginia seismic zone ([Subsection 2.5.1.1.3.2.4](#)) and in the source characterization below ([Subsection 2.5.2.2.5.2](#)).

The largest historical earthquake in the eastern U.S. occurred in Charleston, South Carolina on August 31, 1886. The earthquake produced modified Mercalli intensity (MMI) X shaking in the epicentral area near Charleston and was felt as far away as Chicago ([Reference 231](#)). Maximum MMI shaking intensity at the Lee Nuclear site from this event is estimated at approximately VI ([Figure 2.5.1-215](#)). Estimates of the magnitude of this earthquake are based on liquefaction data and isoseismal area regressions, and vary from the high-6 to mid-7 range, and the CEUS SSC catalog assigns it an E[M] of 6.90 ([Reference 326](#)).

Another significant historical earthquake located near the site was the January 1, 1913 E[M] 4.54 Union County, South Carolina earthquake, located just outside the site vicinity ([Figure 2.5.1-210](#)). This event was felt over an area of approximately 43,000 square mi, with an estimated Rossi-Forel shaking intensity VIII ([Reference 327](#)). Rossi Forel shaking from this event for the Lee Nuclear site is estimated at approximately VI ([Figure 2.5.1-232](#)). The epicenter of the Union County earthquake is poorly located and the fault on which this earthquake occurred has not been identified. The largest earthquake within 25 mi. of the Lee Nuclear Site included in the updated CEUS SSC earthquake catalog is the 1886 E[M] 4.13 Event.

2.5.2.1.3 Evaluation of the Potential for Reservoir-Induced Seismicity

This subsection presents information on the potential for Reservoir-Induced Seismicity (RIS) at the Lee Nuclear Station associated with the construction and operation of Make-Up Pond C ([Figure 1.1-202](#)). No documented RIS is associated with the impoundment of Make-Up Pond B, which was constructed as part of the former Cherokee Nuclear Station.

Evaluations to assess the potential for RIS associated with the Make-Up Pond C impoundment indicate a low potential for RIS and negligible risk to safe operations for Lee Nuclear Station Units 1 and 2. RIS has sometimes been observed at comparable-sized reservoirs and is usually confined to earthquake magnitudes of $M < 4$ for this depth of reservoir. Factors controlling the presence or absence of RIS are strongly dependent on local geologic properties, including reservoir rock type, fault and fracture characteristics, local and regional tectonics, and reservoir operation characteristics.

These evaluations consider RIS potential associated with the configuration and operating parameters for Make-Up Pond C and include an extensive review of RIS literature and scientific understanding of the potential for RIS based on crustal (e.g., underlying geologic and tectonic) properties and reservoir operations. The evaluations also include a review of past worldwide cases of RIS associated with reservoirs with similar or greater hydraulic heights to Make-Up Pond C, an analysis of seismicity associated with reservoirs operated in the Carolina Piedmont, and an analysis of U.S. Bureau of Reclamation dams and reservoirs located in metamorphic terranes with historic hydraulic height and operating configurations comparable to or exceeding Make-Up Pond C hydraulic height or hydraulic height variation operating parameters.

NUREG/CR-5503 (Reference 300) notes that almost all the largest magnitude RIS has occurred in areas where there is active Quaternary faulting. NUREG/CR-5503 makes several important distinctions. First, NUREG/CR-5503 distinguishes between a seismogenic fault, defined as being capable of producing a moderate to large earthquake ($M > 5$), and a nonseismogenic fault that is not capable of producing a moderate to large earthquake. Second, NUREG/CR-5503 defines a tectonic fault as produced by deep-seated crustal-scale processes acting at or below seismogenic depths and a nontectonic feature as a feature produced by shallow crustal or surficial processes acting above seismogenic depth (note seismogenic in this context refers to $M > 5$ earthquakes). These distinctions are important because they directly correspond to distinctions made between the most common form of RIS (nontectonic nonseismogenic shallow earthquakes with $M \leq 5$) and $M > 5$ triggered seismicity that occurs on tectonic seismogenic faults. The operation of Make-Up Pond C represents a surficial process. Based on NUREG/CR-5503, the lack of identified active seismogenic faults in the Make-Up Pond C reservoir area indicates that $M > 5$ triggered seismicity is unlikely.

The analysis considers reservoirs from regions of ongoing tectonic activity, such as California, as well as regions with low rates of tectonic deformation, such as the Carolina Piedmont.

Following NUREG/CR-5503, it is important to make a distinction between triggered seismicity in regions of active faulting that are characterized by $M > 5$ tectonic seismogenic earthquakes in the historical record, such as the region west of the Rocky Mountains, and RIS in regions that are not associated with ongoing seismic activity and generally lack $M > 4$ historical seismicity. Triggered seismicity implies that a tectonic seismogenic earthquake that was likely to occur at a later date is triggered and occurs earlier as a result of perturbations of elastic stresses and/or pressures associated with reservoir operations. The most significant example of triggered seismicity appears to be the 2008 M 7.9 Wenchuan, China earthquake (Klose (2008) (Reference 301)). This earthquake occurred in a tectonically active region of China on a large pre-existing active fault with a recurrence interval of large-magnitude ($M \sim 8$) surface-rupturing earthquakes in the late Holocene of ~1000-1200 yr (Lin et al. (2009) (Reference 302)). The reservoir did not influence the maximum size or the long-term likelihood that the earthquake would occur; it may have caused the earthquake to occur earlier than if the reservoir had not been impounded (Reference 301). The 2008 M 7.9

Wenchuan, China earthquake was inevitable in the geologic timeframe of seismic source characterization (Reference 302) and is the type of tectonic seismogenic source that would be accounted for in a probabilistic seismic hazard analysis and related ground motion analyses.

Analysis of documented cases of RIS for reservoirs located in metamorphic terranes, including reservoirs in the Carolina Piedmont, suggests that for low seismicity rate regions, maximum RIS magnitudes for reservoirs with hydraulic heights < 60 m are less than **M** 4. Considering all U.S. Bureau of Reclamation reservoirs located in metamorphic terranes and all earthquakes located within 30 km of the reservoirs, post-impoundment maximum magnitudes have been less than **M** 4 for reservoirs located in regions of low historical seismicity and have been less than or equal to **M** 5 for reservoirs located in regions where historical pre-impoundment maximum magnitudes were \geq **M** 5.5.

Consequently, available information indicates that any RIS that might be associated with Make-Up Pond C operating parameters would likely have a maximum RIS magnitude of **M** < 4 and is unlikely to have a maximum magnitude of **M** \geq 5. The current short-period design is controlled by a local **M** 6.0-6.2 as described in Subsection 2.5.2.4.2. There is no observed precedent for **M** > 5 RIS associated with reservoirs located in low seismicity rate metamorphic terranes.

In metamorphic terranes comparable to the Make-Up Pond C site, if through-going fault(s) and/or fractures that intersect the reservoir exist, increasing fluid pore pressure is likely to be the dominant mechanism that would induce earthquakes (Talwani et al. (2007) (Reference 303)). Talwani et al. (2007) shows that earthquakes are only induced over a specific range of fault and fracture hydraulic diffusivities. Outside the range of hydraulic diffusivity of 0.1 to 10 m²/s, induced seismicity rarely occurs and is mostly associated with injection-induced seismicity (Reference 303). The largest observed Carolina Piedmont RIS magnitude of **M** 4.3 occurred as a delayed response at Clark Hill (Strom Thurmond) Reservoir (Talwani (1976) (Reference 304) and Secor (1987) (Reference 305)). Assuming the Talwani et al. (2007) evaluation of hydraulic diffusivities is correct (Reference 303), it follows that steeply dipping faults and/or fractures with hydraulic diffusivity of 0.1 to 10 m²/s exist at Clark Hill (Strom Thurmond) Reservoir to produce the observed delayed RIS. The nearly universal observation of metamorphic RIS maximum magnitudes being less than **M** 4 documented in the Carolina Piedmont, the western United States, and the Brazilian craton strongly suggests that metamorphic terranes rarely contain steep faults and/or fractures with sufficient hydraulic diffusivities to allow pore pressure perturbations to propagate to sufficient depths to create enough fault area for maximum RIS magnitudes to exceed **M** > 4. Thus, metamorphic site RIS is typically caused by nontectonic nonseismogenic processes (NUREG/CR-5503) associated with initial elastic/pore pressure responses at shallow depths, such as observed at Monticello Reservoir (Chen and Talwani (2001a and 2001b) (References 306 and 307) and Secor et al. (1982) (Reference 310)), relatively tight faults/fractures that confine RIS to relatively shallow depths, or where more permeable faults/fractures exist, as observed at Jocassee Reservoir (Rajendran

(1995) (Reference 308)), Keowee Reservoir (Schaeffer (1991) (Reference 309)), and Clark Hill (Strom Thurmond) Reservoir (References 304 and 305).

By analogy, there is no documented RIS associated with Make-Up Pond B, located approximately 2.5 miles to the southeast and constructed over 30 years ago as part of the former Cherokee Nuclear Station project. It is likely that no significant steeply dipping faults or fractures exist beneath the Make-Up Pond C location that are oriented nearly orthogonal to the local direction of minimum compressive stress. Therefore, it would appear unlikely that RIS with maximum magnitudes exceeding $M > 4$ are probable at Make-Up Pond C, if at all. This is because of (1) the likely confinement of RIS responses to the top several km of the crust by low-effective hydraulic diffusivity and (2) the limited maximum magnitudes associated with coupled elastic/pore pressure initial loading and shallow confinement of fault/fracture-related RIS responses (Reference 307), and the nearly instantaneous poroelastic response (Reference 303).

Based on the review of the Carolina Reservoirs, it appears that five conditions are needed for RIS to occur:

- (1) Rock stressed close to failure conditions (a situation more likely to occur in felsic-crystalline rock rather than felsic to intermediate metavolcanic and metasedimentary crystalline rock underlying Make-Up Pond C),
- (2) Through-going fractures favorably oriented relative to the maximum horizontal stress direction,
- (3) Hydraulic diffusivity in the range of 0.1 to 10 m²/s as determined by Talwani et al. (2007) (Reference 303),
- (4) A maximum reservoir depth greater than 140 feet, and
- (5) A site dominated by medium to coarse grained felsic rocks.

RIS has been shown to not occur when one of these conditions does not exist. As an example, Bad Creek is a deep reservoir with primarily felsic rocks (condition 5), but the lack of RIS at Bad Creek shows that RIS does not occur when one of the first three conditions (condition 3 for Bad Creek) does not exist (References 309, 311, 312, and 313). The lack of RIS at most of the deepest Carolina Piedmont reservoirs is consistent with condition (5). The two deepest Carolina Piedmont Reservoirs lacking RIS with maximum depths > 200 ft (Murray and Badin Lake) share similarities with the Make-Up Pond C metavolcanic site geology, with Murray having metasedimentary rocks with locally interbedded intermediate to felsic fragmental metavolcanic rocks, and felsic to intermediate crystal-lapilli tuff with lenticular lenses of metasedimentary rocks, and Badin Lake having crystal and lithic tuffs of rhyolitic to rhyodacitic composition with minor ash flow tuffs and tuff breccias and siltstone and siltstone/mudstone; siltstone and argillite with minor tuff beds; graywacke, sandstone and minor siltstone; and mafic and intermediated metavolcanic rocks, primarily tuffs and flows with hypabyssal intrusives (References 317, 318, and 319). The three other non-RIS Carolina Piedmont

reservoirs with maximum depths greater than the Lake Keowee maximum depth are Hartwell, Richard Russell, and W. Scott Kerr, which also are comprised of more intermediate metamorphic rocks than the four felsic rock Carolina reservoirs with RIS (References 320, 321, and 322). Thus, while condition 5 is empirical, the occurrence of RIS at a dominantly fine-grained felsic metavolcanic site like Make-Up Pond C would be without precedent.

There is a NE-striking joint set at the William States Lee site that is optimally oriented to maximize seismic diffusivity. At Make-Up Pond B the dominant shears are oriented about 30° oblique to S_{Hmax} , with the dominant shear set at existing Make-Up Pond B striking N19°E and dipping 61° SE. Despite this, there have been no documented cases of RIS at Make-Up Pond B since it was impounded.

Geologic mapping demonstrates a more easterly structural orientation in the impoundment area of Make-Up Pond C. Dominant schistosity at Make-Up Pond C strikes N47°E and dips 55° SE (Reference 323). This mean orientation is subparallel to S_{Hmax} . Detailed shear orientation measurements have not been made in the vicinity of Make-Up Pond C but it is reasonable to expect that shears would be parallel the overall structural fabric (which is best indicated by the schistosity data). Thus, condition (2) is not met at Make-Up Pond C.

At Make-Up Pond B and possibly Make-Up Pond C, there are a small number of northwest-striking shears that dip 48°-62° NE that are reasonably oriented to accommodate shallow reverse-faulting consistent with condition (2). However, these dips are relatively steep in relation to the more optimally oriented shallow dipping shears observed at Monticello Reservoir (Reference 324). Thus, if RIS were to occur at Make-Up Pond C, it is most likely to be associated with $M < 3$ shallow reverse-faulting similar to that observed at Monticello Reservoir.

Review of the Lee Nuclear Station site conditions indicates that the Make-Up Pond C site properties are not conducive to satisfying conditions (1), (2), (3), (4) and (5). Thus $M > 3$ RIS is not expected to be associated with the Make-Up Pond C impoundment. Specifically, it is concluded that condition (1) is not met for depths greater than 0.5 km based on Carolina Piedmont in situ stress measurements (Reference 325), and that condition (2) is only partially satisfied at depths greater than 0.5-1.0 km because a 60° shear-plane dip is not optimal for predominant strike-slip faulting due to the rotation of the maximum principal stress toward vertical with increasing depth observed by Moos and Zoback (Reference 325). The conclusion that $M > 3$ RIS is not expected to be associated with the Make-Up Pond C impoundment is further supported by the fact that no known recorded RIS is associated with the Lee Nuclear Station Make-Up Pond B impoundment. Furthermore, there are no documented instances of RIS for reservoirs of similar maximum depth in rocks of similar lithologies (e.g., primarily felsic to intermediate mostly fine-grained metavolcanic and metasedimentary rock types).

In the event that RIS associated with Make-Up Pond C occurs, it is unlikely the induced magnitudes would exceed $M > 4$, a value well below the short-period controlling earthquake. Ground motions associated with RIS events ($M < 4$)

typically display high frequency and modest peak ground accelerations with low energy. The potential for RIS associated with the Make-Up Pond C impoundment is considered low with a negligible risk to safe operations for Lee Nuclear Station Units 1 and 2.

2.5.2.2 Geologic and Tectonic Characterizations of the Site and Region

This subsection describes the new SSC for the CEUS, and the sources within the CEUS-SSC model that are used in the PSHA for the Lee Nuclear Site. As described in [Subsection 2.5.1](#), a comprehensive review of available geological, seismological, and geophysical data has been performed for the Lee Nuclear Site region and adjoining areas. [Subsection 2.5.1.1.1](#) describes regional physiography, geomorphology, and stratigraphy. [Subsection 2.5.1.1.2](#) describes regional tectonic setting, including stress regimes and tectonic structures.

As discussed in RG 1.208, the seismic sources used in a PSHA study may be identified based on existing databases and models, with the provision that new information relevant to a seismic source must be evaluated and incorporated as appropriate ([Subsection 2.5.2.4](#)). The starting point for the Lee Nuclear Site PSHA is the regional seismic source model developed by the Central and Eastern United States CEUS SSC Project, which was published in 2012 ([Reference 326](#)). The CEUS SSC model is the most recent seismic source characterization specifically designed for PSHAs for nuclear facilities, replacing the EPRI SOG model ([Reference 201](#)) and the Lawrence Livermore National Laboratory model ([Reference 328](#)). The CEUS SSC model ([Reference 326](#)) also incorporates new data gathered during the most recent iteration of the National Seismic Hazard Mapping Project (NSHMP) ([Reference 329](#)).

The CEUS SSC model ([Reference 326](#)) was developed using SSHAC Study Level 3 methodology ([References 330, 331, and 332](#)), ensuring that uncertainty is represented in a manner consistent with NRC regulatory guidance. Toward this end, scientists involved in the development of the NSHMP, the most recent regional seismic source characterization at the time, were included in the evaluation process of the CEUS SSC model ([Reference 326](#)).

2.5.2.2.1 Overview of CEUS SSC

The CEUS SSC model was created to provide a regionally consistent model of seismic hazard for nuclear facilities throughout the central and eastern United States. The CEUS SSC model focuses on regionally significant elements, with the understanding that site-specific PSHAs would need to refine the CEUS SSC model with site-specific and updated data as necessary.

In the CEUS SSC model, the spatial and temporal distribution of future earthquakes is modeled by two types of seismic sources. The first type is a distributed seismicity source, which is based on observed seismicity. These sources cover the entire CEUS region. The second type is a RLME source, which is based on the paleo- and historical earthquake record, and requires evidence of previous earthquakes with $M \geq 6.5$. By definition, RLME sources are the locations of repeated (more than one) large-magnitude ($M \geq 6.5$) earthquakes in the

historical or paleoearthquake record. The RLME sources cover the much more localized phenomenon of repeated large magnitude earthquakes at specific locations. While notably considering distinct tectonic characteristics, the CEUS SSC model places less importance on specific discrete or localized tectonic features, which were emphasized in the older EPRI-SOG model.

Distributed seismicity sources are defined in the CEUS SSC model according to two conceptual approaches (Figure 2.5.2-250). The first approach smoothly varies seismicity rates throughout the entire CEUS; distributed seismicity sources are only differentiated by maximum magnitude (Mmax) potential. These sources are modeled as "Mmax Zones" (Subsection 2.5.2.2.2). Figure 2.5.2-249 shows the locations and extents of the Mmax zones and Figure 2.5.2-251 shows the logic tree for the Mmax zones. The second approach to distributed seismicity sources considers a wider array of seismotectonic properties in order to define distributed seismicity sources. These sources are modeled as "Seismotectonic Zones" (Subsection 2.5.2.2.3). Figures 2.5.2-252 and 2.5.2-253 show the location and extent of the seismotectonic zones and Figures 2.5.2-254a and 2.5.2-254b show the logic tree for the seismotectonic zones. In each model alternative, RLME sources are independently assessed and added to the hazard of the distributed seismicity sources (Subsections 2.5.2.2.2 and 2.5.2.2.3). Subsection 2.5.2.2.4 provides additional discussion of the RLME sources.

Table 2.5.2-227 lists all distributed seismic sources defined in the CEUS SSC model (Reference 326) (Figures 2.5.2-249, 2.5.2-252, and 2.5.2-253) and Table 2.5.2-228 provides a list of seismotectonic zones as they correspond (spatially) to the larger Mmax zones. Figure 2.5.2-255 shows the locations of all RLME sources in the CEUS SSC model (Reference 326).

2.5.2.2.1.1 CEUS SSC Methodology

The CEUS SSC model was created following SSHAC Level 3 guidelines (References 330, 331, and 332), ensuring that uncertainty is represented in a manner consistent with NRC regulatory guidance (RG 1.208). The SSHAC process calls for a Technical Integration (TI) Team, headed by a TI Lead, to evaluate and integrate all available data, models, and methods into the hazard model. These evaluation and integration steps are performed with the aid of the informed technical community, members of which serve as resource and proponent experts for the TI Team. Technical assessment and regulatory adherence is reviewed throughout the course of the project by the Participatory Peer Review Panel (PPRP). The intended result of the SSHAC process is to create a hazard model that represents the center, body, and range of technically defensible interpretations of the informed technical community.

As stated above, the CEUS SSC model accounts for the likely spatial and temporal distribution of future earthquakes using observed seismicity and the paleoearthquake record. Specifically, the model depends on the theory that the spatial pattern of small- to moderate-magnitude earthquakes is indicative of the future locations of moderate- to large-magnitude earthquakes. This idea is generally accepted by the scientific community, and thus forms the basis for the spatial model of distributed seismicity sources in the CEUS SSC model. Similarly,

the average rate and aperiodicity of future earthquakes is also governed by the temporal distribution of earthquakes in the instrumental and historical catalog.

2.5.2.2.1.2 CEUS SSC Earthquake Recurrence Rate

The earthquake recurrence rate within each distributed seismicity source is assessed by dividing each source into a number of $\frac{1}{4}^{\circ}$ to $\frac{1}{2}^{\circ}$ cells. The rate and b -value (recurrence parameter) in each cell is calculated using the likelihood function of the data in that cell (which addresses catalog completeness), along with penalty functions that smooth out large variations in rate and b -value between cells. Earthquakes associated with RLME sources are excluded from these calculations. The full earthquake recurrence calculation in each zone produces the following results:

- The recurrence rate of earthquakes of moment magnitude (M) $> m_0$ (where $m_0=2.9$ is the lowest magnitude considered in the recurrence analysis) per equatorial degree
- The b -value, expressed in log base-10 units
- The area of each cell in equatorial degrees

This is a simplified overview of the method for calculating and smoothing earthquake recurrence rates in distributed seismicity sources. A complete discussion of the smoothing approach is provided in the CEUS SSC report, Section 5.3.2 ([Reference 326](#)).

The calculation of earthquake recurrence rates in RLME sources is more straightforward, since RLME sources tend to have a more narrowly defined Mmax distribution and geographical extent. Earthquake occurrence rates for RLME sources are based on data in the paleo and historical earthquake record, and modeled using either a Poisson model or a renewal model. In the Poisson model, the time between RLME earthquakes is modeled by an exponential distribution with a standard deviation that equals the mean earthquake recurrence interval. This model is favored for RLME sources that exhibit a higher degree of aperiodic RLME occurrence. The renewal model is better suited to RLME sources in which RLME earthquakes appear to be more periodic. The time between RLME earthquakes in this model is based on the Brownian Passage Time (BPT) model, which represents the physical process of strain buildup and release ([References 238 and 239](#)). Full details related to the estimation of earthquake recurrence in RLME sources is provided in Section 5.3.3 of the CEUS SSC report ([Reference 326](#)).

2.5.2.2.1.3 CEUS SSC Maximum Magnitude

The maximum magnitude (Mmax) potential in the CEUS SSC distributed seismicity sources is assessed through two alternative approaches, a Bayesian approach and one from Kijko (2004) ([Reference 333](#)). In the Bayesian approach, a prior Mmax distribution (or, in some cases, two prior Mmax distributions) is

determined by comparison of each respective seismic source with analogous world-wide stable continental regions (SCR) (Reference 269). This prior distribution is then updated based on site-specific observations; the updated prior distribution is called a likelihood function. The prior distribution and the likelihood function are convolved to create a posterior Mmax distribution for use in the hazard analysis, truncated at **M5.5** and **M8.25**.

In the Kijko (Reference 333) approach, Mmax is based solely on the observed seismicity. The CEUS SSC model utilizes two weighted alternatives from Kijko (2004): the K-S estimator, which is a truncated exponential distribution, and the K-S-B estimator, which includes uncertainty in the *b*-value. Kijko (Reference 333) also includes a third estimator for Mmax. This third estimator, however, is not included in the CEUS SSC as a weighted alternative for the distributed seismicity sources since it is based on characteristic earthquake behavior. Earthquakes of this type are modeled by RLME sources in the CEUS SSC, as described below. Mmax distributions computed according to the Kijko (Reference 333) approach are truncated at **M5.5** and **M8.25**. A complete description of the process for assessing Mmax is provided in the CEUS SSC report, Section 5.2 (Reference 326).

Whereas the instrumental and historical record of small-to-moderate earthquakes is used to determine hazard in the distributed seismicity sources, historical and prehistorical data in some places point to the repeated occurrence of large-magnitude ($M \geq 6.5$) earthquakes. Where data are sufficient, these zones are modeled as RLME sources, and earthquakes associated with these zones are excluded from the calculation of Mmax in the host distributed seismicity source. The distribution of magnitudes used to model the characteristic earthquake size in RLME sources is narrower than that in the distributed seismicity sources, and is based on the amount and quality of data available for each RLME.

2.5.2.2.2 CEUS SSC Mmax Zones Included in the Lee Nuclear Site PSHA

In the CEUS SSC model, Mmax zones are sources of distributed seismicity defined solely by differences in potential maximum earthquake magnitude. Based on a statistical analysis of the global stable continental regions (SCR) database (References 269 and 334), alternative sets of Mmax zones are considered in the CEUS SSC. In the first alternative, which is given a slightly stronger weight, the eastern U.S. is divided into two zones of unique prior Mmax distributions, based upon areas that exhibit Mesozoic-and-younger extension (detailed in Subsection 2.5.2.2.2.1). In the second alternative, the seismic hazard of the entire CEUS region is modeled as a single Mmax zone with a single prior distribution, called Study Region (described in Subsection 2.5.2.2.2.3). In both alternatives, Mmax and recurrence are determined according to the methods described in Subsection 2.5.2.2.1.1. The full logic tree for the Mmax zones model alternative is shown in Figure 2.5.2-251.

All Mmax zones defined in the CEUS SSC model (Reference 326) are included in the hazard calculation for the Lee Nuclear site, truncated at a distance from the site of approximately 520 km (Figure 2.5.2-249, Figure 2.5.2-256). The maximum magnitude distributions for the Mmax zones are described in Table 2.5.2-229 and

the default characteristics for future earthquakes in the CEUS are described in [Table 2.5.2-230](#).

2.5.2.2.2.1 Mesozoic and Younger Extended Crust (MESE)

As discussed in [Subsection 2.5.1](#), rifting of the African and North American plates created a series of Mesozoic basins trending parallel to the Appalachian orogenic belt. Those portions of the CEUS exhibiting such Mesozoic-and-younger extension are included in the MESE Mmax zone ([Figures 2.5.2-249 and 2.5.2-256](#)).

Although Mesozoic basins are known to exist in the modern-day Piedmont, Blue Ridge, Coastal Plain, and Continental Shelf physiographic provinces, the western termination of Mesozoic extension is poorly constrained. To account for this uncertainty, two alternatives for the MESE Mmax zone are modeled: a "narrow" MESE (MESE-N), which only includes the portion of the CEUS that exhibits clear Mesozoic-and-younger extension, and a "wide" MESE (MESE-W) that extends further west to capture areas of more questionable Mesozoic-and-younger extension ([Figure 2.5.2-249](#)). The MESE-N zone is the more heavily weighted alternative due to the fact that evidence supporting this alternative is more technically defensible.

The largest historical earthquake in both the MESE-N and MESE-W zones that is not associated with an RLME source is the 1732 E[M] 6.25 St. Lawrence region earthquake ([Reference 326](#)). In the CEUS SSC, the term E[M] is defined as the uniform moment magnitude estimate for a given earthquake, as discussed in [Subsection 2.5.2.1.1](#). Modeled Mmax values and weights for the MESE-N and MESE-W zones are listed in [Table 2.5.2-229](#). A full description of the MESE-N and MESE-W zones is provided in the CEUS SSC report ([Reference 326](#)), Sections 6.2, 6.3, and 6.4.

2.5.2.2.2.2 Non-Mesozoic and Younger Extended Crust (NMESE)

The portion of the CEUS that is interpreted to have not experienced Mesozoic-and-younger extension (NMESE) is modeled by the NMESE Mmax zone. As is the case for the MESE, the NMESE is modeled by "narrow" and "wide" alternatives ([Figure 2.5.2-251](#)). These alternatives, however, are labeled according to their corresponding MESE zone. The result is that the NMESE-N zone is actually wider than the NMESE-W zone, since the "-N" and "-W" designators for the NMESE refer to the width of the MESE zone ([Figures 2.5.2-249 and 2.5.2-256](#)).

The largest historical earthquakes in the NMESE-N and NMESE-W zones that are not associated with an RLME source are, respectively, the 1897 E[M] 5.91 Giles County, Virginia earthquake and the 1909 E[M] 5.72 earthquake of eastern Montana ([Reference 326](#)). Modeled Mmax values and weights for the NMESE-N and NMESE-W zones are listed in [Table 2.5.2-229](#). A full description of the NMESE-N and NMESE-W zones is provided in the CEUS SSC report ([Reference 326](#)), Sections 6.2, 6.3, and 6.4.

2.5.2.2.2.3 Study Region

The statistical analysis conducted for the CEUS SSC model ([Reference 326](#)) concluded that there is only a marginally significant probability the MESE and NMESE could be characterized by unique prior distributions. As such, an alternative model in which the entire study region is treated as a single Mmax zone is labeled as the Study Region zone ([Figure 2.5.2-249](#)). This is indicated on the Mmax Zones logic tree as the "No" branch of the "Separation of Mesozoic Extended and Non-extended" node, which is assigned a weight of 0.4 ([Figure 2.5.2-251](#)).

The largest historical earthquake attributed to the Study Region Mmax zone that is not associated with an RLME source is the 1732 E[M] 6.25 St. Lawrence region earthquake ([Reference 326](#)). Modeled Mmax values and weights for the Study Region zone are listed in [Table 2.5.2-229](#).

2.5.2.2.3 CEUS SSC Seismotectonic Zones Included in the Lee Nuclear Site PSHA

In contrast to the Mmax zones, seismotectonic zones in the CEUS SSC model consider a number of factors, including regional differences in recurrence rates, Mmax, and probability of activity. Each seismotectonic zone is drawn to roughly follow the outline of a major tectonic domain in the CEUS and is characterized by a uniform and distinct value for one of the above-mentioned factors (with the exception of recurrence rates, which are smoothed as described in [Subsection 2.5.2.2.1.2](#)) ([Figures 2.5.2-252](#) and [2.5.2-253](#)). The uncertainty related to the location of zone boundaries is only considered for a few of the seismotectonic zones, with the assumption that site-specific studies will examine zone boundaries in more detail as necessary. In all seismotectonic zones, recurrence rate and Mmax are calculated according to the procedures detailed in [Subsections 2.5.2.2.1.2](#) and [2.5.2.2.1.3](#). The full logic tree for the seismotectonic zones model alternative is shown in [Figures 2.5.2-254a](#) and [2.5.2-254b](#).

The seismotectonic zones included in the hazard calculation for the Lee Nuclear site are the Atlantic Highly Extended Crust (AHEX), Extended Continental Crust-Atlantic Margin (ECC-AM), Extended Continental Crust-Gulf Coast (ECC-GC), Illinois Basin Extended Basement (IBEB), Paleozoic Extended Crust (PEZ), Midcontinent-Craton (MidC) seismotectonic zones (MidC-A through MidC-D), and Reelfoot Rift zone-Rough Creek graben (RR-RCG) zones. Each zone is truncated at a distance of 520 km from the site.

2.5.2.2.3.1 Atlantic Highly Extended Crust (AHEX)

Mesozoic extension associated with the breakup of Pangea and development of the Atlantic Ocean had a great impact on the mafic oceanic crust adjacent to the eastern edge of the North American continent; this thinned oceanic crust is represented as the AHEX seismotectonic zone. The greater degree of extension in this zone has produced crust that is 15-30 km thick, thinner than the 35-40 km thickness of the adjacent thinned continental crust, represented by the ECC-AM zone (discussed below). Although seismological data within the AHEX are too

sparse to directly assess seismogenic thickness, the observation of thinner crust is taken to indicate that seismogenic thickness is correspondingly thinner. This is expected to result in a significant difference in future earthquake rupture characteristics between the ECC-AM and AHEX zones (Table 2.5.2-231). In addition, the AHEX zone can be compositionally distinguished from the ECC-AM due to the introduction of large amounts of basalt during extension of the AHEX zone.

The AHEX zone lies entirely offshore (Figure 2.5.2-257), roughly paralleling the continental shelf. The boundary between the ECC-AM zone and the AHEX zone is the ECMA (Figure 2.5.2-258), which has been shown to be spatially correlated with the easternmost extent of continental crust using seismic reflection data (e.g., References 335 and 336).

The largest historical earthquake in the AHEX zone is the September 24, 1996 E[M] 2.89 earthquake (Reference 326). Due to the sparse seismicity of the AHEX zone, the Kijko (Reference 333) methods of Mmax calculation (which depend on observed seismicity) are not used in the calculation of Mmax. Modeled Mmax values and weights for the AHEX zone are listed in Table 2.5.2-232.

2.5.2.2.3.2 Extended Continental Crust-Atlantic Margin (ECC-AM)

The ECC-AM seismotectonic zone encompasses the portions of the Piedmont, Coastal Plain, and Continental Shelf physiographic provinces that have experienced Mesozoic-and-younger extension (Figure 2.5.2-257). The rationale for defining this zone is primarily based on the observation that all $M > 7$ earthquakes in SCR crust occur within Mesozoic-and-younger extended crust (Reference 269). In addition, the continental crust outside the ECC-AM is characterized by a different structural grain and reactivation history, suggesting a difference in future earthquake rupture characteristics. In the vicinity of the Lee Nuclear site, the boundaries of the ECC-AM zone are established with the Piedmont gravity anomaly to the west, the ECMA to the east, and the Brunswick magnetic anomaly to the south (Figure 2.5.2-258).

The primary structural feature of the ECC-AM zone is an east-dipping Paleozoic basal thrust that juxtaposes sheared Appalachian terranes against the underlying North American craton (Figure 2.5.1-207). No faults within the ECC-AM show direct evidence for Quaternary activity. Expected future earthquake characteristics within the ECC-AM zone are summarized in Table 2.5.2-231.

Seismicity within the ECC-AM zone is spatially variable. For example, near the Lee Nuclear site, notable clusters of earthquakes occur in Charleston, South Carolina (see Subsection 2.5.1.1.3.2.1) and central Virginia (Central Virginia seismic zone, see Subsection 2.5.1.1.3.2.4) (Figure 2.5.2-259). The largest non-RLME historical earthquake to have occurred within the ECC-AM zone is the 1755 E[M] 6.10 Cape Ann, Massachusetts earthquake. Given location uncertainty for this event; however the CEUS SSC report assigned a 60% probability of having occurred within the ECC-AM, leaving a 40% probability that the largest earthquake within the ECC-AM is instead the June 11, 1638 E[M] 5.32 earthquake (Reference 326). The recent 2011 E[M] 5.71 Mineral, Virginia earthquake

occurred after the development of the CEUS SSC earthquake catalog. This 2011 earthquake now represents the second largest earthquake in the ECC-AM that is not associated with an RLME source. Further discussion of this earthquake is included in [Subsection 2.5.2.1](#). Mmax values and weights for the ECC-AM zone as originally modeled by CEUS SSC ([Reference 326](#)) and used here are listed in [Table 2.5.2-232](#). The E[M] 5.71 earthquake is below the lower magnitude range defined for the ECC-AM in NUREG 2115 ([Reference 326](#)).

2.5.2.2.3.3 Extended Continental Crust-Gulf Coast zone (ECC-GC)

Like the ECC-AM, the ECC-GC represents continental crust that was thinned during the Mesozoic as Pangea broke up. Adjacent to the ECC-GC zone, both the Atlantic Ocean and the Gulf of Mexico were formed during this rifting. The crust here varied between 20 and 40 km thick, with the thickest crust being places of relatively high basement, and thin crust corresponding to basement lows. The northern boundary of this zone is the Brunswick magnetic anomaly ([Figure 2.5.2-258](#)). This zone is distinguished from the ECC-AM zone based on differences in expected future earthquake characteristics. In particular, the ECC-GC does not display a well-defined structural grain and the orientation of the structures that accommodated the opening of the Gulf of Mexico is both variable and uncertain ([Reference 326](#)). Expected future earthquake characteristics within the ECC-GC zone are summarized in [Table 2.5.2-231](#).

The largest historical earthquake in the ECC-GC zone is the October 22, 1882 E[M] 5.58 event, although the largest instrumentally recorded earthquake in the zone is the October 24, 1997 E[M] 4.88 earthquake. Due to the sparse seismicity of the ECC-GC zone, the Kijko ([Reference 333](#)) methods of Mmax calculation (which depend on observed seismicity) are not used in the calculation of Mmax. Modeled Mmax values and weights for the ECC-GC zone are listed in [Table 2.5.2-232](#).

2.5.2.2.3.4 Illinois Basin Extended Basement (IBEB)

The IBEB seismotectonic zone models seismicity associated with the Illinois basin, which is an area of structural complexity within the midcontinent ([Reference 337](#)). The primary rationale for defining this zone is the observation of an elevated rate of instrumental seismicity compared to the neighboring craton, as well as evidence for moderate-magnitude earthquakes in the paleoearthquake record. Additionally, the structural complexity of the IBEB zone suggests that its crust is distinct from the crust in neighboring zones.

The boundaries of the IBEB zone are based on the oval shape of the Illinois basin and the spatial distribution of underlying Precambrian basement structures. The extent of these basement structures, however, is poorly constrained. At its closest approach, the IBEB zone barely extends to within the 520 km limit of the Lee Nuclear site study area ([Figure 2.5.2-252](#)). This distant source only contributes 3 cells to the Lee Nuclear site gridded seismicity and does not make a significant contribution to the hazard (<1%), but was included for completeness.

Seismicity within the IBEB zone is concentrated at its southern end, adjacent to the Reelfoot Rift. Although McBride et al. (Reference 337) note that seismicity tends not to be clearly associated with mapped structures in the IBEB zone, the location of some moderate-magnitude earthquakes suggests that Precambrian basement faults and Paleozoic faults are being reactivated. The largest historical non-RLME event in the IBEB seismotectonic zone is the September 27, 1891 E[M]5.52 earthquake. Paleoliquefaction studies, however, suggest that the IBEB zone has experienced one approximately M6.3 event and three approximately M6.2 events (Reference 326). Modeled Mmax values for this seismotectonic zone are provided in Table 2.5.2-232.

2.5.2.2.3.5 Paleozoic Extended Crust (PEZ)

As described in Subsection 2.5.1, the African and North American plates experienced several phases of rifting and collision. The Mesozoic phase of rifting and associated continental extension discussed above partially overprinted structures formed during a more extensive phase of late Proterozoic to early Paleozoic rifting (during the opening of the Iapetus Ocean). The portion of the craton containing all known and inferred normal faulting associated with the opening of the Iapetus Ocean is the Iapetan rifted margin (IRM) (Reference 338). The western boundary of the IRM is poorly defined, since Paleozoic rift structures irregularly decrease in size and abundance to the west.

In the CEUS SSC model, the IRM is divided into three seismotectonic zones: the Northern Appalachian (NAP), St. Lawrence Rift (SLR), and PEZ zones (Figures 2.5.2-252 and 2.5.2-253). The PEZ zone is the portion of the IRM abutting against the ECC-AM zone. The boundary between the PEZ and ECC-AM zones is marked by the Piedmont gravity gradient (Figure 2.5.2-258). Due to the uncertainty associated with the western boundary of the IRM, two alternative geometries of the PEZ zone are modeled in the CEUS SSC. In the PEZ Narrow (PEZ-N) geometry, the western boundary of the zone is formed by the Birmingham basement fault system of Alabama and the New York-Alabama lineament. This zone geometry encompasses the most well-defined set of Iapetan faults and rift sediments in the North American craton, and is heavily favored in the CEUS SSC model. The PEZ Wide (PEZ-W) geometry includes more tentative evidence of Iapetan rifting, and extends to the Rome trough of Kentucky and West Virginia. Expected future earthquake characteristics for both zones are summarized in Table 2.5.2-231.

In the region of the Lee Nuclear site, concentrated zones of seismicity of the PEZ zones occur in the Eastern Tennessee seismic zone (Subsection 2.5.1.1.3.2.2) and in the Giles County, Virginia seismic zone (Subsection 2.5.1.1.3.2.3) (Figure 2.5.2-259). The Giles County seismic zone produced the 1897 Giles County earthquake (MMI = VIII, mb = 5.7, E[M] 5.91), the largest observed earthquake in the PEZ seismotectonic zones (Reference 326). Modeled Mmax values and weights for the PEZ-N and PEZ-W zones are listed in Table 2.5.2-232.

2.5.2.2.3.6 Midcontinent Craton (MidC) Sesimotectonic Zones

The portion of the CEUS SSC model that did not experience Mesozoic-and-younger extension is represented by the MidC seismotectonic zone (Figure 2.5.2-257). The seismotectonic character of this zone is instead shaped by Paleoproterozoic plate collisions that formed the core of the North American continent. These collisions resulted in deeply buried Precambrian crustal structures that overlie a thick, strong, and compositionally depleted lithosphere (i.e., lithosphere from which certain dense minerals have been extracted via partial melting, resulting in a relatively buoyant, thick, and anhydrous composition). The absence of Mesozoic-and-younger extension, as described by Johnston et al. (Reference 269) and in Subsection 2.5.2.2.2, is expected to lower the Mmax potential of the MidC seismotectonic zone. In addition, Mooney and Ritsema (Reference 339) show that high lithospheric S-wave velocities (which serve as a proxy for high lithospheric strength) are correlated with lower Mmax potential. The MidC is further differentiated from other midcontinental sources based on the expectation that neighboring zones will have different future earthquake rupture characteristics, in part due to differences in structural grain (Table 2.5.2-230 and Table 2.5.2-231).

The northern and western boundaries of the MidC zone terminate at the CEUS study region boundary (Figures 2.5.2-252 and 2.5.2-253). The location of the southern and eastern boundaries of the MidC zone, however, vary based on the alternative geometries of neighboring seismotectonic zones, which results in four alternative MidC zone geometries. These model alternatives are labeled MidC-A, MidC-B, MidC-C, and MidC-D (Figures 2.5.2-252 and 2.5.2-253). All four model alternatives are included in the baseline hazard calculation (Figure 2.5.2-257).

As is the case throughout the CEUS region, seismicity in the MidC seismotectonic zone is spatially variable. Although several concentrated areas of seismicity occur in the MidC zone (e.g., the Anna, Ohio seismic zone (Figure 2.5.2-259) and the Northeast Ohio seismic zone), there is not enough evidence to suggest that any of these areas produce RLMEs. The largest earthquake in this zone that is not associated with an RLME source is the 1909 E[M] 5.72 earthquake of eastern Montana (Reference 326). Modeled Mmax values and weights for all MidC seismotectonic zones are listed in Table 2.5.2-232.

2.5.2.2.3.7 Reelfoot Rift (RR)-Rough Creek Graben (RCG)

The RCG represents the eastward extension of extensional deformation related to formation of the intracontinental rift system during Precambrian to earliest Cambrian rifting of North America (References 340, 341, and 342) (Figures 2.5.2-252 and 2.5.2-253). Some suggest that this graben should be considered part of the Reelfoot Rift, which is characterized by Mesozoic reactivation of faults, higher rates of seismicity, the occurrence of multiple Quaternary active faults and identified RLME sources (Reference 326). Although there is some evidence for Mesozoic activity on faults in the Rough Creek graben, the lack of clearly associated alkaline igneous rocks of Mesozoic age in the RCG suggests that Mesozoic reactivation of deep-penetrating faults was limited, and seismicity rates are lower than the Reelfoot Rift. Hence, a lower weight of 0.33 is

applied to the inclusion of the Rough Creek graben in the Reelfoot Rift zone. At the extreme edge of the Lee Nuclear site study area, the Rough Creek graben (rather than the Reelfoot Rift proper), contributes 8 cells to the gridded seismicity for the Lee Nuclear site study region. The RR-RCG zone does not make a significant contribution to the hazard (<1%), but was included for completeness. Expected future earthquake characteristics within the RR-RCG zone are summarized in [Table 2.5.2-231](#).

The two largest historical earthquakes in the RR-RCG zone are the January 5, 1843 and October 31, 1895 events, both interpreted as E[M] 6.0 earthquakes. Modeled Mmax values and weights for the RR-RCG zone are listed in [Table 2.5.2-232](#).

2.5.2.2.4 CEUS SSC RLME Sources Included in the Lee Nuclear Site PSHA

In several places throughout the CEUS, historical and paleoearthquake records point to the repeated occurrence of large-magnitude ($M \geq 6.5$) earthquakes in specific locations ([Figure 2.5.2-255](#)). Due to the amount of strain accumulation needed to generate a large magnitude earthquake, these events are most often interpreted from the paleoearthquake record. This inherently results in a bias in the location of RLMEs throughout the model, as the spatial coverage of the paleoearthquake record is more limited than that of the historical record. This limitation is recognized in the CEUS SSC model, and is accounted for by allowing significant earthquake potential in the distributed seismicity sources.

The only RLME sources that contribute significantly to hazard at the Lee Nuclear site are Charleston and New Madrid RLME sources. The largest earthquake within 25 mi. of the Lee Nuclear Site included in the updated CEUS SSC earthquake catalog is the 1886 E[M] 4.13 Event.

2.5.2.2.4.1 Charleston

The largest historical earthquake in the eastern U.S. occurred in Charleston, South Carolina in 1886. Estimates of the magnitude of this earthquake are based on liquefaction data and isoseismal area regressions, and vary from the high-6 to mid-7 range ([Reference 326](#)). In addition, a number of geologic investigations have documented evidence for large pre-1886 earthquakes in the Charleston, South Carolina area based on sand blows and paleoliquefaction features (e.g., [References 220, 221, 222, 224, 343, and 344](#)). Based on the quality and quantity of the available data, Charleston is modeled as an RLME source in the CEUS SSC model. The Charleston RLME source is located within the Lee Nuclear Site region as near as 187 km away ([Figures 2.5.2-255, 2.5.2-259 and 2.5.2-260](#)).

No tectonic features have been conclusively correlated with the 1886 earthquake. In addition, although a number of faults have been postulated in the Charleston area, none have been shown to be tectonically active. In order to account for the spatial uncertainty associated with Charleston RLME source, three alternative geometries are modeled ([Figures 2.5.2-260 and 2.5.2-261a through 2.5.2-261d](#)). The Charleston Local geometry encompasses the area with the densest concentration of liquefaction associated with the 1886 earthquake and prehistoric

earthquakes, the meizoseismal area of the 1886 earthquake, and the majority of local tectonic features. This alternative is the most heavily weighted of the three. The Charleston Narrow geometry is based on the location and orientation of postulated faults and tectonic features in the Charleston area, resulting in a relatively narrow, north-northeast oriented source geometry. The Charleston Regional geometry encompasses the Local and Narrow zones, along with outlying paleoliquefaction sites and other tectonic features. In all cases, future earthquakes are modeled as occurring on pseudofaults with the properties listed in [Table 2.5.2-231](#).

Geologic and geomorphic studies have suggested that the seismic activity of the Charleston RLME source since the mid-Holocene may not be indicative of the long-term recurrence rate (e.g., [References 345](#) and [346](#)). Models of temporal clustering used to account for this uncertainty are discussed in detail in Section 5.1.2 of the CEUS SSC report and further uncertainties associated with the earthquake recurrence rate are discussed in the CEUS SSC report ([Reference 326](#)), Section 6.1.2.5.

The CEUS SSC model assigns $E[M]$ 6.90 to the 1886 Charleston earthquake. Geotechnical studies in the Charleston, South Carolina area suggest that prehistorical large earthquakes were in the high-5 to high-7 range (e.g., [References 347](#), [348](#), [349](#), and [350](#)). Based on the assumption that future earthquakes in the Charleston RLME source will be similar to previous large earthquakes in the Charleston area, the CEUS SSC model assigns M_{max} values of between $M6.7$ and $M7.5$ ([Table 2.5.2-233](#)).

2.5.2.2.4.2 New Madrid Fault System

The three largest historical earthquakes in the CEUS region all occurred in the New Madrid area. These earthquakes occurred on December 16, 1811, January 23, 1812, and February 7, 1812, and a great deal of uncertainty exists regarding their exact magnitudes. In addition, a number of paleoliquefaction studies document multiple major prehistorical earthquakes in the New Madrid area (e.g., [References 248](#), [351](#), [352](#), and [353](#)). Based on these observations, the CEUS SSC model defines the New Madrid fault system (NMFS) as an RLME to account for large prehistoric earthquakes and the three large events that occurred in 1811-1812. At its closest approach, this RLME is approximately 720 km from the Lee Nuclear site ([Figure 2.5.2-255](#)).

Modern seismic activity within the New Madrid area closely aligns with the three fault segments that constitute the NMFS (also referred to as "Reelfoot Rift Central Fault System" in CEUS SSC report ([Reference 326](#)) ([Figure 2.5.2-260](#)). These individual fault segments (New Madrid North, New Madrid South, Reelfoot Thrust) have been associated with the earthquakes of the 1811-1812 sequence (see discussion in the CEUS SSC report, Section 6.1.5 ([Reference 326](#)), and sources therein). Consequently, the geometry of the NMFS RLME source is narrowly defined, with alternative geometries for long and short interpretations of the New Madrid North fault and the Reelfoot thrust ([Figure 2.5.2-262](#)). Alternative geometries for the New Madrid South fault either combine the Blytheville arch with

the Bootheel lineament or the Blytheville fault zone (Figures 2.5.2-263a and 2.5.2-263b).

Seismic reflection data (e.g., References 354 and 355) and geomorphic observations (e.g., Reference 356) suggest that the Holocene Epoch represents a period of temporally clustered earthquake activity along the NMFS that is not representative of the long-term rate of activity. Additionally, geodetic studies suggest that the present rate of strain accumulation is much too small to account for the Holocene rate of paleoseismicity (References 357 and 358). To account for uncertainty in the future rate of earthquakes in the NMFS RLME, the CEUS SSC model allows for alternatives (at very low weights) in which some or all of the fault segments of the NMFS are inactive. A detailed discussion of the recurrence of large earthquakes in the NMFS RLME source is presented in Section 6.1.5.4 of NUREG 2115 (Reference 326).

The Mmax distribution for the NMFS RLME source is based on the estimated magnitudes of the earthquakes in the 1811-1812 sequence. The CEUS SSC model equally weights the estimates from Bakun and Hopper (Reference 232), Johnston (2004, personal communication, as cited in Reference 326), and Hough and Page (Reference 359), which are M7.2 to M7.8, M7.5 to M7.9, and M6.5 to M6.9, respectively. The resulting Mmax distribution for the NMFS RLME source in the CEUS SSC model ranges from M6.7 to M7.9 (Table 2.5.2-234).

All other uncertainties identified in the NMFS logic tree (Figures 2.5.2-263a and 2.5.2-263b) are included in the Lee Nuclear site hazard calculation exactly as detailed in the CEUS SSC report, with the exception of seismogenic depth, which is simplified from the distribution listed in Table 2.5.2-231 to a single value of 15 km. Given the distance of the NMFS RLME source to the Lee Nuclear site, this simplification is judged to be appropriate for the Lee Nuclear site PSHA.

2.5.2.2.5 Post-CEUS SSC Studies

This subsection describes geologic and seismic investigations of the site region and beyond that provide information that can be used to evaluate and potentially update the CEUS SSC model relevant to the Lee Nuclear site PSHA. Specifically, these studies include ongoing investigations of: (1) geologic investigations of the Eastern Tennessee seismic zone; and (2) the 2011 Mineral, Virginia earthquake that occurred in or near the Central Virginia seismic zone.

2.5.2.2.5.1 Geologic Investigations of the Eastern Tennessee Seismic Zone

Seismicity associated with the ETSZ is located within the Lee Nuclear site region (Figure 2.5.2-259) (Subsection 2.5.1.1.3.2.2). The ETSZ can be identified as a narrow trend of concentrated seismicity east of the New York-Alabama magnetic lineament (Reference 244). However, in spite of the high rate of seismic activity, the largest historical earthquake in the region is magnitude 4.6 (magnitude scale unspecified) (References 244 and 360).

The most recent geologic studies of the ETSZ either post-date the CEUS SSC model or were published during development of the CEUS SSC model. These studies suggest that the ETSZ may have produced large prehistoric earthquakes. Vaughn et al. (Reference 361) find evidence of minor surface faulting, fracturing, and disrupted features in terrace alluvium, along with minor paleoliquefaction, northeast of Knoxville, Tennessee. Similarly, Obermeier et al.'s (2010) study (Reference 360) of Douglas Reservoir documents fracture systems and sandy intrusions in terrace deposits that they interpret as paleoseismic in origin, although the significance of these features is unclear. Howard et al. (Reference 362) and Warrell et al. (Reference 363) document fractures, small faults, and displacements in Quaternary alluvium along Douglas Reservoir that they suggest resulted from earthquakes with magnitudes greater than 6.0 and 6.5 (magnitude scale unspecified).

These Douglas reservoir studies were continued by Hatcher et al (2012) (Reference 364), which coupled the geologic observations with preliminary optically stimulated luminescence age dating of Quaternary deposits. Hatcher et al (Reference 364) conclude that one or more "probable minimum" **M** 6.5 earthquakes could be associated with the ETSZ within the last 73 to approximately 200 ka. However, because of poor age limits on soils cut by fractures, the ages of the structures observed remain poorly defined and no recurrence intervals could be estimated (Reference 364).

While these recent studies strengthen the argument that the ETSZ has experienced at least one moderate-sized earthquake in the late Quaternary, they do not quantify parameters (e.g., recurrence interval, magnitude) necessary to demonstrate that the ETSZ produces repeating large-magnitude events as defined in NUREG 2115. As such, the ETSZ is modeled within the MESE Mmax zone and the PEZ seismotectonic zone using smooth seismicity. No RLME source is defined for the ETSZ.

2.5.2.2.5.2 Investigations of the 2011 Mineral, Virginia Earthquake

The Mineral earthquake occurred on August 23, 2011 at 17:51 UTC near Mineral, Louisa County, Virginia (Reference 365) (Figure 2.5.2-259) (Subsection 2.5.1.1.3.2.4). The epicentral region lies within the Appalachian Piedmont, about 130 km southwest of Washington, D.C., and within or near the Central Virginia seismic zone (Reference 365). The **M**5.8 main shock hypocenter originated at 6.0 ± 3.1 km depth (Reference 365), with an epicentral uncertainty of 2.3 km stemming from the sparse P-wave recordings (References 365 and 366). Chapman (Reference 366) notes that only four stations within 150 km recorded mainshock arrival times. The earthquake has been given various names and assigned magnitudes in the **M**5.7 to 5.8 range. Following the CEUS SSC methodology (Reference 326), this earthquake is assigned an expected moment magnitude of **E**[**M**]5.71 in the updated project catalog (Subsection 2.5.2.1). The Mineral earthquake was the largest historical event in the region and the largest instrumentally recorded earthquake in eastern North America since the 1988 **M**5.84 Saguenay earthquake (Reference 367).

A series of aftershocks highlighted the rupture plane of the Mineral earthquake, which was previously unrecognized at the surface or in the subsurface (Figure 2.5.2-264). Aftershocks ranged in depth from 1 to 7.5 km and included events up to M3.9 (References 368 and 369). Walsh et al. (Reference 370) suggest that aftershocks of the Mineral earthquake, as well as other intraplate earthquakes, could last up to 100 years, as opposed to only a few years in more tectonically active margins (e.g., Southern California). The majority of 2011 Mineral, Virginia earthquake aftershock hypocenters defined surface suggesting a plane oriented approximately north-northeast with a moderate dip of about 45°-51° to the southeast (References 366, 368, 371, 372, 373 and 374). Propagation of the rupture was complex, exhibiting three distinct slip events: a smaller and deeper initiation event, followed by two larger and shallower events (Reference 366). Focal mechanisms of the mainshock indicate a primarily reverse sense of slip (Reference 365).

The earthquake caused moderate damage in the epicentral region, although felt intensity at close distances (less than 100 km) was less than predicted by Atkinson and Wald relations (Reference 375) as noted by Assatourians and Atkinson (Reference 376). Ground motions at larger distances were in relatively close agreement with the Atkinson and Wald (2007) relations, and the earthquake was felt by more people than any other earthquake in U.S. history (Reference 377). At short periods (0.2 s), ground motions agreed well with eastern ground motion prediction equations, but were less than expected at longer periods (1.0 s) (Reference 367).

Geologic evidence of the 2011 Mineral, Virginia earthquake was sparse, although some coseismic features were observed. Rock falls were identified over a wide region covering most of mountainous Virginia and parts of Maryland and West Virginia (References 377, 378, and 379). Four sand boils (two definite, one likely, and one questionable) were observed in two locations that lie within the approximate vertical surface projection of the rupture plane (References 378, 379, and 380).

Despite targeted searches in the field, the Earthquake Engineering Research Institute (EERI) (Reference 378) and Geotechnical Extreme Events Reconnaissance (GEER) association (Reference 379), did not identify surface rupture associated with the 2011 Mineral, Virginia earthquake (Subsection 2.5.1.1.3.2.4). The consensus results of these investigations suggest that the Mineral earthquake occurred on a previously unrecognized structure, the dimensions of which are unknown and not observable at the ground surface.

The 2011 Mineral earthquake is not included as a new fault or RLME source in the Lee Nuclear site PSHA. Without slip-rate, recurrence, or Mmax constraints for the structure defined by the distribution of aftershock hypocenters that likely produced the Mineral earthquake, it is most appropriate to consider this earthquake as an event captured by the host zones (ECC-AM, MESE-N, MESE-W, and Study Region) in the CEUS SSC model framework. Because of the distance to the Lee Nuclear site (450 km), and the buffer between the Mineral earthquake magnitude and lower end of the Mmax magnitude distribution, no changes to the EPRI CEUS model were required due to this event.

2.5.2.3 Correlation of Earthquake Activity with Seismic Sources

The CEUS SSC earthquake catalog ([Reference 326](#)) includes earthquakes in the CEUS from 1568 through the end of 2008, and its development is discussed in [Subsection 2.5.2.1](#) ([Figure 2.5.2-248](#)). The complete CEUS SSC catalog comprises 10,984 earthquakes, including 3,298 events added during the update of the earthquake catalog ([Subsection 2.5.2.1](#)). The complete catalog and the updated events include dependent events and earthquakes with $E[M] \geq 2.2$. For rate calculations, the dependent and small events are removed, but patterns of seismicity are better illustrated when these events are included (e.g., as shown in [Figures 2.5.2-249](#), [2.5.2-256](#), [2.5.2-257](#), [2.5.2-259](#), and [2.5.2-260](#)). Over 80% of the independent earthquakes in the CEUS SSC catalog with $E[M] \geq 2.9$ are contained in the 2008 NSHMP earthquake catalog ([Reference 329](#)), with remaining events gathered from special studies, and local and regional catalogs ([Reference 326](#)).

The uncertainty in the horizontal location of earthquakes included in the CEUS SSC catalog is the result of a combination of standard errors for instrumentally recorded earthquakes from the various catalog sources and estimates based on accounts of shaking intensity ([Reference 326](#)). In general, location uncertainties have improved through time, with horizontal uncertainties up to 50 km for less well-documented events in the earliest part of the catalog, to as little as 1-2 km for well-recorded events in the most recent part of the catalog ([Appendix B of Reference 326](#)).

Earthquake depths are reported in the updated CEUS SSC catalog based on data from source catalogs, or depths documented in a variety of published sources ([Reference 326](#)). Many of the earthquake depths represent fixed crustal depths for either shallow or deep events. For example, the NEIC catalog uses fixed depths of 10 km for shallow events and 33 km for deep events ([Reference 326](#)). Additionally, many earthquakes in the CEUS SSC catalog are assigned a depth of 0 km when no data are available to provide a basis for an estimate. This is most common in earlier parts of the catalog. Alternative depth estimates are presented if more than one value was reported in source catalogs or published literature; however, depth uncertainties are not provided in the CEUS SSC catalog ([Reference 326](#)). Despite these horizontal and depth location uncertainties, gross regional patterns of seismicity are preserved and partially form the basis for defining some CEUS SSC seismic sources.

As described in [Subsection 2.5.2.2](#), the CEUS SSC source model defines three types of seismic sources: Mmax zones, zones of repeated large-magnitude earthquakes (RLMEs), and seismotectonic zones ([Reference 326](#)). Mmax zones are defined on expected differences in Mmax potential and are broad zones that are not defined on the basis of geologic structures or the spatial distribution of seismicity. The discussion of correlation of seismicity with seismic sources presented in this subsection is limited to seismotectonic zones and RLME sources significant to the Lee Nuclear site ([Subsections 2.5.2.2.3 and 2.5.2.2.4](#)).

The Charleston, South Carolina RLME source is within the 200-mile radius site region ([Figure 2.5.2-255](#)) and, as described in [Subsection 2.5.2.2](#), the more

distant New Madrid fault system (NMFS) RLME is also included in the site PSHA. At its nearest point, the Charleston RLME is located approximately 190 km southeast of the site. The NMFS RLME is located approximately 720 km west of the site. The correlation of seismicity with these two RLMEs is described in the following text:

Charleston. The Charleston RLME, as described in [Subsection 2.5.2.2.4.1](#), represents the Charleston seismic zone, the source for the largest recorded earthquake in the eastern U.S., the 1886 Charleston E[M] 6.90 earthquake ([Figure 2.5.2-260](#)). The Charleston seismic zone is characterized by sparse seismicity (in comparison to the Eastern Tennessee or New Madrid seismic zones) that is tightly concentrated, but lacking prominent linear trends. There is no evidence that indicates a correlation of well-documented prehistoric large earthquakes or historical earthquakes with a discrete structure. Therefore, three alternative zones are hypothesized for the Charleston RLME that are based on locations of posited fault sources, damage, felt intensity, and/or density of liquefaction features. Theorized fault sources, spaced about 10 km apart, are modeled throughout the zones. This approach accounts for uncertainty in the location, extent, and existence of faulting, reflecting the poor understanding of the correlation of earthquakes with structures in the Charleston seismic zone.

New Madrid Fault System (NMFS). The NMFS RLME lies within the broader New Madrid seismic zone and represents the source of the three largest historical earthquakes in the CEUS region, and several prehistoric large earthquakes in 1811 and 1812 (E[M] 7.60, 7.50, and 7.80) ([Figure 2.5.2-262](#)). A number of faults have been identified in the New Madrid seismic zone. The NMFS RLME comprises three main fault sources, each with two alternative geometries to reflect uncertainty in their extent and/or location. The spatial distribution of seismicity defines clear, highly concentrated trends of earthquakes along these faults as seen on [Figure 2.5.2-262](#). Seismicity also occurs away from these faults, defining a roughly 250 x 400 km concentration of earthquakes from the Marianna zone near the southern end, extending northeast along the Mississippi River to just south of northwest-trending basement structures in Illinois ([Figure 2.5.2-260](#)). Earthquakes within this broader concentration of seismicity are commonly associated with faults comprising the Reelfoot Rift system.

Atlantic Highly Extended Crust (AHEx). The AHEx seismotectonic zone represents the highly extended transition between extended and thick continental crust and thin oceanic crust. The zone is defined primarily on the basis of its shallow seismogenic thickness. Only five earthquakes from the updated CEUS SSC catalog lie within the AHEx, and seismicity is sparse throughout the zone ([Figure 2.5.2-257](#)). Therefore, trends in seismicity are not readily apparent, despite the presence of large faults inferred from geophysical data. The largest earthquake observed within the AHEx is the 1996 E[M] 2.89 earthquake located approximately 310 km off the coast of New Jersey.

Extended Continental Crust - Atlantic Margin (ECC-AM). As discussed in [Subsection 2.5.2.2](#), the ECC-AM seismotectonic zone is defined primarily on the basis of Mesozoic rift-related extension. Seismicity within the ECC-AM is spatially variable, ranging from very diffuse to spatially concentrated. As seen in

Figure 2.5.2-257, higher concentrations of seismicity are observed near the southern end of the ECC-AM in South Carolina, as well as along the Atlantic Coast from New Jersey northward. Additionally, the ECC-AM encompasses the CVSZ, an area with an elevated rate of generally small-magnitude seismicity (**Figure 2.5.2-259**). Seismicity is generally shallow within the CVSZ, and interpreted to occur on Paleozoic and Mesozoic faults that lie above the Appalachian detachment (**References 381 and 382**). An area of elevated concentration of seismicity with similar characteristics occurs in the New York-Philadelphia region. These areas lack evidence for repeated, large-magnitude earthquakes and discrete faults associated with seismicity are not mapped at the surface. Thus, these seismic zones do not meet the CEUS SSC criteria for inclusion as RLMEs. Outside of these more prominent zones of seismicity, earthquakes in the ECC-AM do not appear to correlate with known geologic structures or define linear trends.

The largest observed earthquake possibly within the ECC-AM seismotectonic zone is the 1755 Cape Ann, Massachusetts E[M] 6.10 earthquake. Due to the uncertainty associated with the horizontal location of the Cape Ann earthquake, it is assigned a 60% probability of having occurred within the ECC-AM and 40% probability of having occurred within the Northern Appalachian seismotectonic zone (NAP) (**Reference 326**). When the Cape Ann earthquake is considered to have occurred in the NAP, the 2011 Mineral, Virginia E[M] 5.71 earthquake is the largest event in the ECC-AM.

The 2011 Mineral, Virginia earthquake and associated aftershocks occurred within the ECC-AM on a previously unknown structure, oriented similar to many of the thrust faults in the region. As discussed in **Subsections 2.5.1.1.3.2.4 and 2.5.2.2**, the aftershocks defined a southeast-dipping, northeast-striking rupture plane that extends from about 7.5 to 1.0 km depth (**References 366 and 368**) (**Figure 2.5.2-264**). However, too little is known regarding the fault that produced the Mineral earthquake to justify the addition of an additional RLME or discrete fault source to the CEUS SSC model.

Extended Continental Crust - Gulf Coast Zone (ECC-GC). As discussed in **Subsection 2.5.2.2**, the ECC-GC seismotectonic zone is defined primarily on the basis of Mesozoic rift-related extension. Like AHX, ECC-GC has very sparse seismicity and trends in seismicity are not readily apparent. As described in NUREG 2115 (**Reference 326**), the largest earthquake in the ECC-GC is either the October 22, 1882 E[M] 5.58 earthquake, the October 24, 1997 E[M] 4.88 earthquake, or the potential paleoearthquake identified from the studies of Cox and others (see discussion in Section 7.3.9.5 of NUREG 2115) (**Reference 326**). The uncertainty in the location of the October 22, 1882 E[M] 5.58 earthquake allows for the possibility that this event occurred within the neighboring OKA seismotectonic zone (**Reference 326**).

Illinois Basin Extended Basement Zone (IBEB). The IBEZ zone encompasses faults within Precambrian basement and the Paleozoic Illinois Basin as well as a zone of liquefaction features thought to be associated with four moderate events (approximately M 6.20 to 6.30). The largest historical event to have occurred in the IBEZ zone was the 1891 E[M] 5.52 event in southern Illinois. Larger

earthquakes have occurred in the zone ($E[M] \geq 6.5$), but they are characterized by the Wabash Valley RLME. Seismicity is sparse in the northern part of the IBEB zone, increasing regularly to the south (Figure 2.5.2-248). Hypocentral depths range from shallow (less than 5 km) to deep (up to 27 km), with shallower earthquakes slightly more common. Earthquakes do not define linear trends or areas of concentrated seismicity. Seismicity is relatively evenly distributed and dense compared with surrounding regions not characterized as RLME sources. Several structures and processes have been posited as sources of earthquakes in the IBEB zone, but they remain poorly understood.

Midcontinent-Craton Zone (MidC). The MidC seismotectonic zone comprises crust that has not been significantly deformed by Phanerozoic orogens. Seismicity of the MidC zone is generally diffuse with a few areas of spatially concentrated seismicity including the Anna (Ohio), northeast Ohio, and Nemaha Ridge-Humboldt fault (Oklahoma, Kansas, and Nebraska) seismic zones (Figure 2.5.2-248). Seismicity within the Anna seismic zone is spatially concentrated and tenuously associated with basement faults that comprise the Fort Wayne rift. A paleoseismic investigation by Obermeier (Reference 383) indicates a lack of large-magnitude, repeated earthquakes for several thousand years in the Anna seismic zone. Seismicity within the northeast Ohio seismic zone is defined by a northeast-trending zone of earthquakes. A 1986 $E[M]$ 4.65 earthquake and aftershock sequence within the zone has been associated with northeast-trending geophysical anomalies (References 384 and 385). In a paleoseismic investigation, however, Obermeier (Reference 383) found a lack of evidence for large, repeated earthquakes in the zone. Seismicity within the Nemaha Ridge-Humboldt fault seismic zone is questionably associated with basement structures that are sub-parallel and west of the Proterozoic Midcontinent rift system (References 386 and 387). Outside of the seismic zones described above, spatially concentrated areas of seismicity within the MidC zone are observed in central Oklahoma and northern Alabama, and along the Nebraska-South Dakota border (Figure 2.5.2-248).

Paleozoic Extended Crust (PEZ). The PEZ seismotectonic zone represents the western portion of the IRM and includes narrow (PEZ-N) and wide (PEZ-W) alternative geometries as discussed in Subsection 2.5.2.2. Seismicity within the zone is spatially variable, ranging from diffuse to concentrated, occasionally defining trends. Relatively high concentrations of seismicity are observed between Lake Ontario and Lake Erie (PEZ-W only) and at the southern end of the PEZ zone in Alabama. Additionally, the PEZ encompasses several well-studied areas of elevated seismicity including the eastern Tennessee and Giles County, Virginia seismic zones (Figure 2.5.2-248). Earthquakes within the ETSZ are generally deep, spatially associated with or limited in extent by geophysical anomalies including the Alabama-New York lineament, and define several northeast-oriented linear trends. Several studies have posited a variety of possible structures and processes associated with earthquakes in the ETSZ, including reactivated basement faults (Reference 244), depositional anisotropies (Reference 388), and heterogeneity in crustal strength (Reference 389).

The GCVSZ (Figure 2.5.2-259) is similarly characterized by deep seismicity that defines a northeast-oriented, steeply southeast-dipping tabular zone. This zone of

seismicity lies beneath the Appalachian detachment in Precambrian basement (References 390 and 391) and, therefore, the deep seismicity is not reflected in the geology of overlying thrust sheets. Several small-displacement faults and folds have been identified at the ground surface in terrace sands within the GCVSZ (Reference 392). Whether this surface deformation is related to deep seismicity, or other processes such as karst development and collapse in underlying carbonate rocks, is unclear (References 393, 394, and 395). The GCVSZ hosted the largest earthquake observed in the PEZ, the 1897 Giles County, Virginia E[M] 5.91 earthquake.

Reelfoot Rift-Rough Creek Graben Zone (RR-RCG). The RR-RCG seismotectonic zone includes faults that developed during late Proterozoic-Cambrian Iapetan-phase rifting and were later reactivated in the late Paleozoic, and then the Mesozoic. Seismicity rates are lower in the portions of the RR-RCG that are within the Lee Nuclear site study region (radius of 520 km), relative to the rest of the RR or RR-RCG zones (Figure 2.5.2-265). Seismicity ranges from 13 to 17 km deep (Reference 326). The two largest earthquakes in the RR-RCG zone are the historical January 5, 1843 and October 31, 1895 events, both interpreted as E[M] 6.0 earthquakes. The 1811-1812 large magnitude earthquakes located within this zone are considered part of the NMFS RLME source.

2.5.2.4 Probabilistic Seismic Hazard Analysis and Controlling Earthquake

A PSHA on rock requires a set of seismic sources and their characteristics, and a set of earthquake ground motion models. For the PSHA for the Lee site, the seismic sources published in NUREG 2115 (Reference 326) were used. These seismic sources were derived for the central and eastern CEUS-SSC by considering a wide range of alternative interpretations, and the characteristics of earthquake occurrences in each source (activity rates, magnitude distributions, and maximum magnitudes) were derived by developing an updated earthquake catalog for the CEUS. Alternative models of earthquake sources and characteristics of earthquake occurrences were determined, with weights representing the relative credibility of each model. This model of earthquake sources has been accepted by the USNRC (Reference 326) as a valid model for use in PSHA for nuclear licensing applications in the CEUS.

Earthquake ground motion models were adopted from an EPRI 2013 study (Reference 396), which updated earlier models of earthquake ground motions (References 202 and 249). These ground motion models represent alternative methods of estimating earthquake shaking and include estimates of variability in ground motion amplitudes. Weights on alternatives represent the relative credibility of each model. This representation of earthquake ground motion has been accepted by the USNRC (Reference 397) as a valid model for use in PSHA for nuclear licensing applications in the CEUS.

Table 2.5.2-235 compares the results of a PSHA hazard analysis at the Chattanooga test site (Chattanooga) using LCI seismic hazard software compared to published results from the 2012 CEUS SSC Report (Reference 326). The total mean rock hazard at 0.2 g and 0.6 g is obtained using each methodology (LCI software and digitized CEUS data) for three spectral frequencies (1 Hz, 10 Hz,

and PGA) with % differences computed. A cumulative absolute velocity (CAV) filter was not applied in this calculation and no site amplification factors are used. All results are for hard rock conditions. The "% difference" row shows the percent difference of hazard calculated for the CEUS Chattanooga test site compared to LCI Chattanooga site. For this comparison the LCI hazard result is higher than those published from the 2012 CEUS EPRI study, except for the 10 Hz value at 0.2g which is 0.2% below the CEUS result.

The comparisons shown in [Table 2.5.2-235](#) are considered acceptable agreement, given that the comparison is made with the EPRI 2012 Chattanooga test site using independent software. Comparisons were made using mean annual frequencies of exceedance because these are the most important results used to derive seismic design spectra. The similarity of these results, verifies that the LCI software suite is calculating hazard correctly.

2.5.2.4.1 New Ground Motion Models

As indicated in [Subsection 2.5.2.4](#), updated ground motion models were published in 2013 by EPRI ([Reference 396](#)). These updated equations estimate median spectral acceleration and its uncertainty as a function of earthquake magnitude and distance. Epistemic uncertainty is modeled using multiple ground motion equations with weights, and multiple estimates of aleatory uncertainty, also with weights. Different sets of sources are recommended for seismic sources that represent rifted versus non-rifted regions of the earth's crust. Difference equations are also recommended for the mid-continent region of the CEUS and for the Gulf region. Equations are available for spectral frequencies at hard rock sites of 100 Hz (which is equivalent to peak ground acceleration, PGA), 25 Hz, 10 Hz, 5 Hz, 2.5 Hz, 1 Hz, and 0.5 Hz.

As part of the EPRI 2013 ([Reference 396](#)) project, aleatory variabilities were estimated for the ground motion models of the CEUS. To create a complete model, epistemic uncertainties in the aleatory variabilities were represented with alternative models, with weights.

In summary, the ground motion model used in the seismic hazard calculations consists of the median equations and uncertainties from NRC, EPRI, and DOE ([Reference 396](#)). The cumulative absolute velocity (CAV) filter which accounts for the damageability of small magnitude earthquake ground motions was not used, and a minimum magnitude of $E[M] 5.0$ was used for all earthquake sources.

2.5.2.4.2 Updated Probabilistic Seismic Hazard Analysis and Deaggregation

The seismic hazard at the Lee site is recalculated with the CEUS SSC model for the CEUS. This calculation is for hard rock conditions, which is consistent with the updated ground motion model.

A PSHA consists of calculating annual frequencies of exceeding various ground motion amplitudes for all possible earthquakes that are hypothesized in a region. The seismic sources specify the rates of occurrence of earthquakes as a function of magnitude and location, and the ground motion prediction model estimates the

distribution of ground motions at the site for each event. Multiple weighted hypotheses on seismic sources, earthquake rates of occurrence, and ground motions (characterized by the median ground motion amplitude and its uncertainty) result in multiple, weighted seismic hazard curves, and from these the mean and fractile seismic hazard can be determined.

Figures 2.5.2-223, 224, 225, 226, 227, 228, and 229 show mean and fractile (15th, median, and 85th) seismic hazard curves from this calculation for the 7 spectral frequencies that are available from the EPRI ground motion model.

Figure 2.5.2-266a shows high and low frequency mean spectra for 10^{-4} , 10^{-5} , and 10^{-6} annual frequencies of exceedance. The mean UHRS values are also documented in Table 2.5.2-217 for annual frequencies of exceedance of 10^{-4} , 10^{-5} , and 10^{-6} .

The seismic hazard is deaggregated following the guidelines of RG 1.208. Specifically, the mean contributions to seismic hazard for 1 Hz and 2.5 Hz are deaggregated by magnitude and distance for the mean 10^{-4} ground motions at 1 Hz and 2.5 Hz, and these deaggregations are combined. Figure 2.5.2-231 shows this combined deaggregation. Similar deaggregations of the mean hazard are performed for 5 and 10 Hz spectral accelerations (Figure 2.5.2-232). Figures 2.5.2-233 and 234 show deaggregations of the mean hazard for 10^{-5} ground motions, and Figures 2.5.2-235 and 236 show deaggregations of the mean hazard for 10^{-6} ground motions. RG 1.206 recommends deaggregation of the mean seismic hazard. Table 2.5.2-218 summarizes the mean magnitude and distance resulting from these deaggregations, for the mean 10^{-4} , 10^{-5} , and 10^{-6} ground motion amplitudes for all contributions to hazard and for contributions with distances exceeding 62 miles (100 km).

The deaggregation plots in Figures 2.5.2-231, 232, 233, 234, 235, and 236 indicate that the local background, Charleston and New Madrid seismic sources contribute to seismic hazard at the Lee site. Note that the 160 - 360 km bins represent hazard contribution from the Charleston RLME, and the 730 km bin represents hazard contribution from the New Madrid RLME. For 10^{-4} annual frequency of exceedance, the background and Charleston sources are the largest contributor to seismic hazard for both 1 and 2.5 Hz (Figure 2.5.2-231) and 5 and 10 Hz (Figure 2.5.2-232). For 10^{-5} annual frequency of exceedance, the background and Charleston sources are the largest contributor to seismic hazard for both 1 and 2.5 Hz (Figure 2.5.2-233) with the background source being the largest contributor to seismic hazard at 5 and 10 Hz (Figure 2.5.2-234). For 10^{-6} annual frequency of exceedance, the Charleston contribution is smaller at 1 and 2.5 Hz and is absent for 5 and 10 Hz (Figures 2.5.2-235 and 2.5.2-236). The local background sources representing seismicity out to a distance of 520 km dominate for all annual frequencies for 5 and 10 Hz.

As an update to Reference 326 in June, 2012 (Reference 398), the logic tree structures for the Charleston and New Madrid RLMEs were revised. For the Lee

site, these changes affect the seismogenic crustal thickness branch of the Charleston RLME source logic tree (Figures 2.5.2-261a through 2.5.2-261d). Seismogenic crustal thickness branch weights of the New Madrid RLME logic tree are also revised (Figures 2.5.2-263a and 2.5.2-263b); however, this branch is collapsed to its central value for expedience, and the central value is not affected.

A sensitivity study was conducted to determine the effect of these changes on the total mean rock hazard at the Lee site. The observed effect of including changes to the logic trees is a slight decrease in mean hazard between 0% and -1% for each analyzed combination of spectral frequency and amplitude. Thus, the results of the sensitivity study demonstrate that the revised Charleston RLME logic tree have no impact on the seismic hazard calculated at Lee.

Smooth UHRS are developed from the UHRS amplitudes in Table 2.5.2-217, using the hard rock spectral shapes for CEUS earthquake ground motions recommended in NUREG/CR-6728 (Reference 251). The UHRS for the 7 spectral frequencies at which hazard calculations were made (Table 2.5.2-217) were obtained by interpolation of hazard curves. In between the 7 spectral frequencies, interpolation is used adopting spectral shapes published in Reference 251. To apply these spectral shapes, the high-frequency magnitude and distance were used for 5 Hz and higher spectral frequencies, and the low-frequency magnitude and distance were used for 2.5 Hz and lower spectral frequencies. For spectral frequencies below 0.5 Hz but above 0.125 Hz, $1/T$ scaling is assumed (where T is spectral period). Below 0.125 Hz $1/T^2$ scaling is applied. This is the low frequency spectral shape recommended by Building Seismic Safety Council for seismic design (Reference 294).

Figure 2.5.2-266a shows the horizontal HF and LF spectra calculated in this way for 10^{-4} , 10^{-5} , and 10^{-6} annual frequencies of exceedance. Figure 2.5.2-266b shows the resultant mean rock UHRS for 10^{-4} , 10^{-5} , and 10^{-6} annual frequencies of exceedance. As mentioned previously, these spectra accurately reflect the UHRS amplitudes in Table 2.5.2-217 that are calculated for the seven spectral frequencies at which PSHA calculations are performed.

2.5.2.5 Seismic Wave Transmission Characteristics of the Site

The Lee Nuclear Site is a hard rock site located on igneous and metamorphic rocks of Paleozoic age. Subsection 2.5.1.2 describes the geology of the site area. Subsection 2.5.4 presents a detailed discussion of dynamic and static properties of the site foundation materials. The majority of shear wave velocity measurements at the site exceed 9,200 ft/sec, the hard rock definition used by CEUS attenuation relations (2.83 km/s, 9,282 ft/sec) (Reference 202). Some near-surface shear wave velocity measurements fall below 9,200 ft/sec. Variation in shear wave velocity measurements of several hundred ft/sec centered at the hard rock condition result in a negligible variation in site response calculations.

In summary, the Lee Nuclear Site is a hard rock site with a shear-wave velocity exceeding 9,200 ft/sec. Therefore the EPRI 2004, 2006 GMM Review Project (Reference 396) ground motion equations are used directly, without calculation of

site response. The recommended uniform hazard response spectrum reflects this hard rock condition.

2.5.2.6 Ground Motion Response Spectra (GMRS)

This subsection presents the performance goal-based approach used to develop the ground motion response spectrum GMRS for the Lee Nuclear Site, based on the PSHA methodology and results described in [Subsection 2.5.2.4](#). Specifically, the envelope of the 10^{-4} and 10^{-5} horizontal HF and LF spectra shown in [Figure 2.5.2-266a](#) is used to represent the 10^{-4} and 10^{-5} UHRS, and the horizontal GMRS is determined from the following equations:

$$A_R = SA(10^{-5})/SA(10^{-4}) \quad \text{Equation 2.5.2-1}$$

$$DF = 0.6 A_R^{0.8} \quad \text{Equation 2.5.2-2}$$

$$GMRS = \max([SA(10^{-4}) \times \max(1, DF)], 0.45 SA(10^{-5})) \quad \text{Equation 2.5.2-3}$$

where A_R is the ground motion slope ratio, DF is the design factor, and $SA(10^{-4})$ and $SA(10^{-5})$ are the horizontal envelope spectral amplitudes corresponding to UHRS annual frequencies of 10^{-4} and 10^{-5} , respectively.

[Figure 2.5.2-239](#) shows the horizontal Lee Nuclear Station GMRS calculated at the top of hard rock. [Table 2.5.2-219](#) documents the horizontal 10^{-4} , 10^{-5} , and 10^{-6} UHRS and the horizontal GMRS (Equation 2.5.2-3).

For the vertical GMRS ([Table 2.5.2-220](#)), a fully probabilistic approach is used to develop the vertical hazard curves along with UHRS and GMRS to maintain exceedance probabilities consistent with the horizontal UHRS ([Subsection 2.5.2.7.1.1](#)). The method employed, Approach 3 ([Subsection 2.5.2.7.1](#)), integrates the horizontal hazard curves with distributions of V/H ratios resulting in vertical hazard curves, which are intended to maintain the same exceedance probability as the horizontal hazard. For the V/H ratios, the stochastic point source model is used to compute both horizontal (normally incident SH-waves) and vertical (incident inclined P-SV waves) motions ([References 280 and 281](#)) using the hard rock crustal model ([Table 2.5.2-221](#)). For the hard rock profile, because the shear-wave velocities are high, a linear analysis is performed for the horizontal as well as vertical motions ([References 273 and 286](#)) ([Subsection 2.5.2.7.1.1](#)). [Table 2.5.2-221](#) lists the source distances and depths intended to cover the range in expected hard rock horizontal peak acceleration values at exceedance probabilities ranging from 10^{-2} to 10^{-7} yr^{-1} . Because V/H ratios typically vary with source distance ([Reference 292](#)), the range is also intended to cover the distance deaggregation. While the hard rock V/H ratios are largely independent of M ([Reference 251](#)), M 5.1 is selected as small magnitudes dominate the contribution at close distances and at high frequency ([Figures 2.5.2-231, 232, and 233](#)), where the V/H ratios typically reach maximum values ([References 251, 286, and 292](#)). The

median estimates of the computed V/H ratios are shown in [Figures 2.5.2-240a, 2.5.2-240b and 2.5.2-240c](#). Only a subset of the computed ratios are shown in [Figures 2.5.2-240a, 2.5.2-240b and 2.5.2-240c](#), as there is little change at distances beyond about 6 to 9 mi. (10 to 15 km), with an abrupt jump in the ratios within about 6 mi. (10 km). The ratios are largely independent of frequency with a peak near 60 Hz and range in amplitude from about 0.5 to about 1 as distance decreases. These values, at low frequency, are lower than empirical hard rock central and eastern North America (CENA) V/H ratios, which average about 0.8, decreasing from about 0.9 at 1 Hz to about 0.7 at 10 Hz ([References 297 and 298](#)). While these empirical V/H ratios are for Fourier amplitude spectra and not 5% damped response spectra and are dominated by small **M** earthquakes (\leq about 4) and large distances ($D \geq$ about 125 mi.), the results illustrate the large uncertainty in vertical hard rock hazard for CENA and suggest large distant ratios may be greater than model predictions at low frequency. To accommodate the large uncertainty, a minimum V/H ratio of 0.7, the average of the empirical and simulations, is adopted. To accommodate the change in source distance with both annual exceedance probability and structural frequency shown in the deaggregation plots ([Figures 2.5.2-231, 232, 233, 234, 235, and 236](#)), V/H ratios computed at a suite of distances are given relative weights ([Table 2.5.2-223](#)). The distances selected are 17 mi. (28 km), 4 mi. (7 km), and 0 mi. (0 km) to cover ratios reflecting distant, intermediate, and near source contributions.

[Table 2.5.2-220](#) lists the resulting vertical 10^{-4} , 10^{-5} , and 10^{-6} UHRS and GMRS, and [Figure 2.5.2-239](#) shows the horizontal and vertical GMRS.

2.5.2.7 Development of FIRS for Units 1 and 2

This subsection presents location-specific Lee Nuclear Station Unit 1 FIRS A1 with Unit 1 FIRS A5 and Unit 2 FIRS C4 representing sensitivity evaluations to assess localized foundation conditions described below. As previously stated, the Lee Nuclear Station Unit 1 foundation is supported on new and previously placed concrete materials positioned directly over continuous hard rock with shear wave velocity dominantly over 9,200 ft/sec. Localized portions of the Unit 1 nuclear island overlie legacy Cherokee lower rooms ([Figure 2.5.4-266](#)). The Lee Nuclear Station Unit 2 foundation is supported on continuous hard rock with shear wave velocity dominantly over 9,200 ft/sec with the exception of the eastern edge of the nuclear island which may be supported by up to 20 feet of new leveling fill concrete ([Figure 2.5.4-267](#)).

To address these configurations, location-specific FIRS analyses are conducted for the Unit 1 nuclear island, referred to as Unit 1 FIRS A1, the Unit 1 localized condition where the nuclear island overlies legacy CNS pump rooms, referred to as FIRS A5, and the eastern edge of the Unit 2 nuclear island, referred to as FIRS C4. [Subsection 2.5.4.7](#) describes the material dynamic properties and [Figures 2.5.4-252a, 2.5.4-252b and 2.5.4-252c](#) show the dynamic profile for Base Cases A1, A5, and C4 respectively that represent the Unit 1 FIRS A1, Unit 1 FIRS A5 and Unit 2 FIRS C4 configurations.

Unit 1 FIRS ([Figure 2.5.4-252a](#)) defines the Unit 1 nuclear island centerline foundation input motion and is based on the Lee Nuclear Station GMRS

developed at the top of a hypothetical outcrop (continuous rock) transferred up through previously placed Cherokee Nuclear Station concrete materials and newly placed Lee Nuclear Station concrete materials to the basemat foundation level at 553.5 ft (NAVD). Unit 1 FIRS as described in this subsection is calculated using the mean and fractiles hazard curves described in [Subsection 2.5.2.4.2](#).

The profile for the Lee Nuclear Station Unit 1 FIRS is shown in [Figure 2.5.4-252a](#) with approximately eight (8) feet of new fill concrete overlying an average of about 15 feet of existing fill concrete, structural basemat concrete and native rock from the former Cherokee foundation. The Unit 1 NI centerline Vs reflects shear wave velocities from about 7,500 feet per second (fps) (fill concrete) to about 9,600 fps (continuous rock) as shown in [Figure 2.5.4-252a](#), Base Case A1 - Unit 1 for basemat at 553.5 ft.

Unit 1 FIRS A5 defines the localized condition of the Lee Unit 1 nuclear island that will overlie legacy CNS pump rooms at approximately 527 ft (NAVD). As described in [Subsection 2.5.4.5.2](#) the horizontal slab concrete of these CNS pump rooms and existing waterproofing membrane will be removed during construction and the pump rooms will then be backfilled using fill concrete up to the basemat floor level at 553.5 ft (NAVD). FIRS A5 is based on the Lee Nuclear Station Ground Motion Response Spectra (GMRS) developed at the top of a hypothetical outcrop (continuous rock) fixed at 523 ft (NAVD) transferred up through previously placed Cherokee Nuclear Station concrete materials and newly placed Lee Nuclear Station concrete materials to the basemat foundation level at 553.5 ft (NAVD).

Unit 2 FIRS C4 defines the Unit 2 nuclear island eastern edge foundation input motion and is based on the Lee Nuclear Station GMRS developed at the top of a hypothetical outcrop (continuous rock) fixed at 509 ft (NAVD) transferred up through newly placed Lee Nuclear Station concrete materials to the basemat foundation level at 553.5 ft (NAVD).

2.5.2.7.1 Site Response Analysis

In calculating the probabilistic ground motions at the Lee Nuclear Site, the FIRS A1, FIRS A5, and FIRS C4 must be hazard consistent (i.e., the annual exceedance probability of the UHRS from which the FIRS is derived should be the same as the hard rock UHRS, referred to herein as the hypothetical rock outcrop UHRS). NUREG/CR-6728 ([Reference 251](#)), recommends several site response approaches to produce soil or rock motions consistent with the hypothetical outcrop UHRS. These approaches incorporate site-specific aleatory variabilities into the motions. NUREG/CR-6728 ([Reference 251](#)) identifies four basic approaches for determining the site response at the site, referred to as Approaches 1 through 4. The approaches range from performing a PSHA using ground motion attenuation relations developed for the specific site (profile) of interest (Approach 4) to scaling the hypothetical UHRS on the basis of a site response analysis using a broadband input (control, UHRS) motion (Approach 1). The probabilistic method, Approach 3, described in NUREG/CR-6728 is used to compute the location-specific foundation ground motion shaking hazard (FIRS) at the Lee Nuclear Station Unit 1.

The analysis methodology presented in this subsection is described in a supplemental technical report (Reference 299). The report describes, in detail, the analysis methodology used to develop horizontal and vertical site-specific FIRS that are hazard-consistent and incorporate both aleatory and epistemic variabilities in dynamic material properties at the Lee Nuclear Station Unit 1. The report addresses, in detail, the RVT approach to equivalent-linear site response, as well as the fully probabilistic method used to incorporate the effects of site-specific dynamic material properties and their variabilities into the hard rock UHRS.

Using Approach 3, the location-specific amplification is characterized by suites of frequency-dependent amplification factors. Approach 3 involves approximations to the hazard integration using suites of transfer functions that result in complete hazard curves at the foundation level for specific ground motion parameters (e.g., spectral accelerations) and a range of structural frequencies.

There are two ways to implement Approach 3: (1) by the integration method, or (2) by simply modifying the attenuation relation ground motion value during the hazard analysis with a suite (distribution) of transfer functions (Reference 275). Both approaches tend to double count site aleatory variability, once in the suite of transfer function realizations and again in the aleatory variability about each median attenuation relation. The full integration method tends to lessen any potential impacts of the large total site aleatory variability (Reference 278).

Potential conservatism introduced by double counting site aleatory variability may be reduced by removing the site-specific aleatory variability (sigma of the transfer functions) from the resulting hazard curves. This is accomplished using the analytical Approach 3 approximation given in References 278 and 202 and setting the slope of the transfer function to zero. The equation for amplitude becomes:

$$A_C = A_e^{\frac{-k\sigma^2}{2}} \quad \text{Equation 2.5.2-4}$$

where A_C is the corrected amplitude at a given annual probability of exceedance, k is the slope (log) of the hazard curve, and sigma is the standard deviation of the transfer function. For hazard curve slopes of about 3 and sigma in the 0.2 to 0.3 range, the correction (reduction) is about 10%. This correction can be applied to either implementations of Approach 3. Alternatively, in the implementation of Approach 3 wherein attenuation relations are modified, one can simply use the median transfer function rather than the full distribution, or remove the transfer function sigma from the attenuation relation aleatory variability and use the full distribution. Any of these corrections will approximately remove potential double counting of site aleatory variability.

A distinct advantage of Approach 3 is the proper incorporation of site epistemic variability. Using Approach 3, multiple hazard curves may be developed reflecting multiple site profiles (e.g., velocity profiles, G/G_{\max} , and hysteretic damping curves) that are then averaged over probability to develop mean, median, and

fractile estimates. Additionally, vertical hazard curves may be developed that are consistent with the horizontal hazard by integrating distributions of V/H ratios (transfer functions) with the resulting site-specific horizontal hazard curves.

2.5.2.7.1.1 Implementation of Approach 3

The Lee Nuclear Station Unit 1 FIRS site response analysis utilizes Approach 3 with the following main steps:

- Randomization of the base case site-dynamic velocity profiles (A1, A5, and C4) to produce suites of velocity profiles that incorporates site-specific randomness.
- Transfer functions (amplification for horizontal motions and V/H ratios for vertical motions) as characterized by distributions developed using the RVT based equivalent-linear site response method.
- Based on the deaggregation ([Subsection 2.5.2.4.2](#) describes deaggregation procedure), transfer functions are computed for **M** 5.1 using the omega-square source model and CEUS parameters ([Table 2.5.2-221](#)). Because the site-specific condition is quite stiff (concrete), linear site response analyses are used requiring a single (large or small **M**) earthquake.
- Full integration of the generic hard rock and location-specific mean hazard curves with transfer functions to arrive at a distribution of location-specific horizontal and vertical hazard curves reflecting location-specific site aleatory and epistemic variabilities.
- Computation of location-specific UHRS and FIRS.

2.5.2.7.1.1.1 Development of Transfer Functions

Transfer functions are spectral ratios (5% damping) of horizontal top of concrete foundation (firm rock) motions to hard rock ([Table 2.5.2-221](#)) as well as vertical-to-horizontal ratios (5% damping) computed for the location-specific profiles. Horizontal amplification factors reflect motions (5% damping response spectra) computed at the top of the profiles (concrete) divided by motions computed for a hypothetical (hard) rock outcrop (9,300 ft/sec, [Table 2.5.2-221](#)). Due to the profile stiffness, 7,500 ft/sec for concrete, linear analyses are performed.

For vertical motions, site-specific V/H ratios are developed using the point-source model to compute both horizontal (normally incident SH-waves) and vertical (incident inclined P- SV waves) ([References 280 and 281](#)) over a range in source distances and depths ([Table 2.5.2-221](#)).

Empirical western North America (WNA) V/H ratios are included in the development of vertical motions in addition to site-specific point-source simulations. The use of WNA empirical V/H ratios implicitly assumes similarity in shear- and compression-wave profiles and nonlinear dynamic material properties

between site conditions in WNA and location-specific soft rock columns (Figures 2.5.4-252a, 2.5.4-252b, and 2.5.4-252c). Whereas this may not be the case for the average WNA rock site profile (Reference 281), the range in site conditions sampled by the WNA empirical generic rock relations likely accommodates site-specific conditions. The relative weights listed in Table 2.5.2-223 reflect the assumed appropriateness of WNA soft rock empirical V/H ratios for Unit 1 and Unit 2. Additionally, because the model for vertical motions is not as thoroughly validated as the model for horizontal motions (References 277, 280, and 281), inclusion of empirical models is warranted. The additional epistemic variability introduced by inclusion of both analytical and empirical models also appropriately reflects the difficulty and lack of consensus regarding the modeling of site-specific vertical motions (Reference 282). In the implementation of Approach 3 to develop vertical hazard curves, the epistemic variability is properly accommodated in the vertical mean UHRS, reflecting a weighted average over multiple vertical hazard curves computed for the FIRS A1, FIRS A5, and FIRS C4 (Figures 2.5.4-252a, 2.5.4-252b, and 2.5.4-252c) models (empirical and numerical). The vertical FIRS (and UHRSs) then maintain the desired risk and hazard levels, consistent with the horizontal design response spectra (GMRS) and UHRSs.

2.5.2.7.1.1.1.1 Horizontal Amplification Factors

Horizontal amplification factors are developed using hard rock spectral shapes as control motions (Reference 251). Base Case Profiles A1, A5, and C4 were placed on top of the regional hard rock crustal model (Table 2.5.2-221, Reference 273). A hard rock kappa value of 0.006 sec (Table 2.5.2-221) is used, consistent with that incorporated in the hard rock attenuation relations (Reference 273). With a hysteretic damping in concrete between 0.5% and 1.0% any additional damping in the shallow concrete profile is neglected as its impacts will be beyond the fundamental shallow column resonance, well above 50 Hz.

While the site response analyses are linear and therefore strictly independent of control motion spectral shape for Fourier amplitude spectral ratios, at high frequency, 5% damped response spectral ratios may not be strictly independent of control motion spectral shape. This can occur because the width of the simple harmonic oscillator transfer function is constant in log frequency and increases directly with frequency, averaging over a wider range in frequencies as oscillator frequency increases. At very large distances, where crustal damping has depleted high frequencies (spectral shapes shift to lower frequencies, Reference 251) and the site resonance is not highly excited, response spectral ratios may depart from those computed using control motions relatively rich in high frequency energy (close distances). To accommodate the possibility of distance dependent transfer functions in a linear analysis, a suite of spectral shapes is used as control motions at distances of 0.6, 12, 62, 125, 250 mi (1, 20, 100, 200, and 400 km). Results are shown in Figures 2.5.2-241a, 2.5.2-241b, and 2.5.2-241c and reveal the shallow site resonance. The FIRS demonstrate median amplification of about 11%, 15% and 10% for A1, A5 and C4 respectively. This occurs near 60 Hz to 70 Hz for FIRS A1 and A5 and near 40 and 80 Hz for FIRS C4. All amplification factors show very slight differences only at 250 mi (400 km). The width of the resonance is broadened by the profile randomization with shear-wave velocities varying

$\pm 10\%$ about the concrete V_s value of 7,500 ft/sec along with depth to hard rock at 23.5 ft for FIRS A1, 30.5 ft for FIRS A5, and 20 ft for FIRS C4, randomly varied ± 3 ft.

2.5.2.7.1.1.2 Site Aleatory Variability

For the Lee Nuclear Station, the concrete profile is randomized between depths of 23.5 ± 3 ft for FIRS A1, 30.5 ± 3 ft for FIRS A5, and 20 ± 3 ft for FIRS C4, the range in depths to hard rock conditions [shear-wave velocity exceeding, on average, 9,300 ft/sec (2.83 km/sec)] (Reference 273). A uniform distribution is assumed for the depth randomization. For the shear-wave velocity randomization, a soft rock correlation model was used (References 277 and 280). Because concrete velocities show much less variability than firm rock, being a uniform and controlled emplacement material, variations in velocity were constrained to $\pm 10\%$ about the base case value of 7,500 ft/sec with a COV of 0.1.

To accommodate random fluctuations in compression-wave velocity when modeling vertical motions, Poisson ratio is held constant at the base-case values, and random compression-wave velocities are then generated based on shear-wave velocity realizations and base-case Poisson ratios. In reality, Poisson ratio will vary but is likely correlated with shear-wave velocity. As a result, varying Poisson ratio, when properly correlated with shear-wave velocity, will likely not result in a greater variation in compression-wave velocity than assumed here. Additionally, variation in compression-wave velocity has a much smaller effect on motions than shear-wave velocity as the wavelengths typically are 2 to 5 times greater.

2.5.2.7.2 Development of V/H Ratios

To model vertical motions, incident inclined P-SV waves are modeled from the source to the site using the plane-wave propagators of Silva et al. (1996) (Reference 288) assuming a shear-wave point-source spectrum (References 277, 280, and 281). The point source model is used to accommodate the effects of distance and source depth on V/H ratios (Table 2.5.2-221). For consistency, both the horizontal and vertical motions are modeled using the same parameters (Table 2.5.2-221). The horizontal motions are modeled as vertically propagating shear-waves. For the vertical motions, the angles of incidence are computed by two-point ray tracing through the crust and site-specific profile. To model site response, the near-surface V_P and V_S profiles (Figures 2.5.4-252a, 2.5.4-252b and 2.5.4-252c) are placed on top of the crustal structure (Table 2.5.2-221), the incident P-SV wavefield is propagated to the surface, and the vertical motions are computed.

In the implementation of the equivalent-linear approach to estimate V/H response spectral ratios for the Lee Nuclear Station FIRS A1, FIRS A5, and FIRS C4, the horizontal component analyses are performed for vertically propagating shear waves. To compute the vertical motions, a linear analysis is performed for incident inclined P-SV waves using low-strain V_P and V_S derived from the profiles FIRS A1, FIRS A5, and FIRS C4 (Subsection 2.5.4.7). The P-wave damping is set

equal to the low strain S-wave damping (Reference 289). The horizontal component and vertical component analyses are performed independently.

The approximations of linear analysis for the vertical component and uncoupled vertical and horizontal components are validated in two ways. Fully nonlinear modeling using a 3-D soil model shows that the assumption of largely independent horizontal and vertical motions for loading levels up to about 0.5g (soil surface, horizontal component) for moderately stiff profiles is appropriate (Reference 280). Additionally, validation exercises with recorded motions have been conducted at over 50 sites that recorded the 1989 M 6.9 Loma Prieta, California earthquake (Reference 273). These validations show the overall bias and variability is low but is higher than that for horizontal motions. The vertical model does not perform as well as the model for horizontal motions (References 280 and 281). An indirect validation is also performed by comparing V/H ratios from WNA empirical attenuation relations with model predictions (Reference 281) over a wide range in loading conditions (Reference 281). The results show a favorable comparison with the model exceeding the empirical V/H ratios at high frequency, particularly at high loading levels. In the V/H comparisons with empirical relations, the model also shows a small under prediction at low frequency (≤ 1 Hz) and at large distance (≥ 12 mi.).

For the vertical analyses, a hard rock kappa value of 0.003 sec, half that of the horizontal, is used. This factor of 50% is based on observations of kappa at strong motion sites (Reference 290), validation exercises (Reference 280), and the observation that the peak in the vertical spectral acceleration (5% damped) for WNA rock and soil sites is generally near 10 to 12 Hz compared to the horizontal motion peak that occurs at about 5 Hz, conditional on M 6.5 at a distance of about 6 to 20 mi. This difference of about 2 in peak frequency is directly attributable to differences in kappa of about 2. Similar trends are seen in CEUS hard rock spectra with the vertical component peaking at higher frequencies than the horizontal component (Reference 251).

For Lee Nuclear Station FIRS the site-specific V/H ratios, Figures 2.5.2-240a, 2.5.2-240b, and 2.5.2-240c for FIRS A1, FIRS A5 and FIRS C4 respectively show median estimates computed with the stochastic model for M 5.1. For M 5.1, the distances range from 50 to 0 mi. (80 to 0 km) (Table 2.5.2-221) with expected horizontal hard rock peak accelerations ranging from 0.01 to 0.50g. Figures 2.5.2-240a, 2.5.2-240b, and 2.5.2-240c all show that the V/H for the shallow concrete profile FIRS are nearly constant with frequency and increase rapidly as distance decreases, within about a 9 mi. source distance. For distances beyond 6 to 9 mi., the V/H ratio is about 0.5 and increases rapidly to about 0.9. The peaks near 60 Hz are likely due to the peak in the horizontal amplification factors (Figures 2.5.2-241a, 2.5.2-241b, and 2.5.2-241c). In Figures 2.5.2-240a, 2.5.2-240b, and 2.5.2-240c, the multiple peaks beginning near 1 Hz reflect deep crustal resonances (structure below 0.5 mi., Table 2.5.2-221) that would be smoothed if the crustal model were randomized and discrete layers replaced with steep velocity gradients to reflect lateral variability and a more realistic crustal structure. The M 5.1 distance ranges more than adequately accommodate the hazard deaggregation (Subsection 2.5.2.4.2).

As previously discussed ([Subsection 2.5.2.7.1.1.1](#)), the model predictions of V/H ratios at low frequency may be slightly unconservative and at high frequency they may be conservative. While it is important to include site-specific effects on the vertical hazard, potential model deficiencies can be compensated with inclusion of empirical V/H ratios computed from WNA generic rock and soil site attenuation relations. Additionally, empirical V/H ratios of Fourier amplitude spectra based on CENA recordings at hard rock sites have median values near about 0.8 and vary slowly with frequency. As with the development of the hard rock V/H ratios ([Subsection 2.5.2.6](#)), to adequately accommodate potential model deficiencies as well as the large uncertainty in hard and firm rock V/H ratios for CENA, a minimum value of 0.7 is adopted.

For the empirical V/H ratios, both Abrahamson and Silva ([Reference 290](#)) and Campbell and Bozorgnia ([Reference 292](#)) soft rock WNA relations are used with equal weights ([Table 2.5.2-222](#)). As an example, [Figure 2.5.2-242](#) shows the Campbell and Bozorgnia V/H ratios computed for **M** 5.1. Distance bins differ between the empirical and analytical V/H ratios because the empirical ratios use a generic suite of distances used on many projects while the analytical V/H ratios are region specific. For distances beyond 35 mi. (57 km), the empirical V/H ratios are nearly constant with increasing distance. Additionally, for the smaller **M** (**M** < 5.5), there are few strong motion data available at larger distances ([Reference 292](#)). Because the ratios vary slowly with distance, the differences in distances are not significant. The empirical WNA soft rock ratios show more distance (loading level) dependence than the firm rock analytical ratios ([Figure 2.5.2-242](#)), perhaps due to nonlinearity in the horizontal soft rock motion ([Reference 286](#)). [Figure 2.5.2-243](#) shows the empirical soft rock V/H ratios computed for **M** 8.0. Similar trends are seen with the **M** 5.1 V/H ratios, suggesting a **M** (loading level) sensitivity for soft rock that is much less than that for soil ([Reference 286](#)). These trends, with the **M** independence of V/H ratios, are expected for firm rock conditions. That is, as the profile becomes stiffer, nonlinearity decreases, and for distances within about 6 to 9 mi., distance becomes the dominant controlling factor in V/H ratios ([Reference 274](#)).

It is important to note the site-specific and generic V/H ratios peak at very different frequencies, about 60 Hz and about 10 to 20 Hz, respectively, with the site-specific having generally higher V/H ratios, particularly at close distances. Use of an empirical V/H ratio alone may underestimate the vertical hazard at high frequency, provided the model predictions are reasonably accurate.

In assigning the V/H ratios in the Approach 3 analysis, the source **M** and **D** change significantly with structural frequency as probability changes. To accommodate the deaggregation in (contributing sources) integrating the horizontal hazard with the distributions of V/H ratios, the **M** and **D** distribution used is listed in [Table 2.5.2-223](#). The magnitudes selected are intended to capture the dominant sources: **M** 5.1 for close-in sources and **M** 7.0 and **M** 8.0 for the Charleston, South Carolina, and New Madrid, Missouri sources, respectively, both at distances well beyond 60 mi. (100 km) ([Subsection 2.5.2.2.4](#)). The distances used for the V/H ratios ([Table 2.5.2-223](#)) reflect the distance sensitivity, or lack of sensitivity beyond about 6 to 9 mi. (10 to 15 km) for the site-specific ratios and beyond about 30 mi. (50 km) for the empirical ratios, considering the contributing

source distances (Subsection 2.5.2.2.4). The weights listed in Table 2.5.2-223 are intended to approximate the relative contributions of the three sources across structural frequency and exceedance probability. Because the V/H ratios vary slowly with distance, only a smooth approximation to the hazard deaggregation is necessary. To adequately capture the change in **M** and **D** with Annual Exceedance Probability (AEP), only a few distance bins are required: 3 and 35 mi. (5 and 57 km) for the empirical and 0, 4, and 17 mi. (0, 7, and 28 km) for the analytical (Table 2.5.2-223).

2.5.2.7.3 UHRS Interpolation and Extrapolation

Because the hard rock hazard is computed at only seven frequencies, namely 0.5, 1.0, 2.5, 5.0, 10.0, 25.0, and 100.0 Hz (taken as peak acceleration), the site-specific hazard has been both extrapolated to 0.1 Hz and interpolated to 100 points per decade from 0.1 to 100.0 Hz (about 300 points). At high frequency, hard rock hazard curves are interpolated at 34 and 50 Hz, as these are the critical frequencies to define the FIRS A1, FIRS A5, FIRS C4, and UHRS shapes beyond 25 Hz. This interpolation is performed by using the deterministic shapes (Reference 251) for the appropriate **M** to interpolate the hard rock UHRS at AEP of 10^{-4} , 10^{-5} , and 10^{-6} yr⁻¹, resulting in three points on 34 and 50 Hz hazard curves. The adjacent hazard curves at 25 and 100 Hz are then used as shapes to extrapolate to lower and higher exceedance probabilities, resulting in approximate hard rock hazard curves. Approach 3 is then applied to develop site-specific horizontal and vertical UHRS at the same exceedance probability as the 25 and 100 Hz hard rock hazard. For the vertical component, because the site specific V/H ratios peak at very high frequency (beyond 50 Hz), it is important to maintain the appropriate hazard levels between 25 and 50 Hz. Below 0.5 Hz, the extrapolation is performed in a similar way using the 0.5 Hz hazard curve as a shape taken through estimates of the 10^{-4} , 10^{-5} , and 10^{-6} yr⁻¹ hazard at frequencies below 0.5 Hz. Because the aleatory variability in attenuation relations increases with period (References 202, 290, 291, and 292), use of a median spectral shape (Reference 274) to extrapolate at low frequency may be inappropriate and result in potentially unconservative hazard or higher probability than desired. To address this uncertainty, a conservative approach is adopted by extrapolating the 0.5 Hz 10^{-4} , 10^{-5} , and 10^{-6} hard rock UHRSs, assuming a constant slope in spectral velocity (+1 slope in pseudo-absolute spectral acceleration) (Reference 294). The extrapolation is extended at low frequency to the earthquake source corner frequency, where the slope is increased to a constant spectral displacement. Since the source corner frequency, or transition from approximately constant spectral velocity to spectral displacement, depends on magnitude, an average representative magnitude of **M** 7.2, based on the deaggregations, is assumed to apply for frequencies below 0.5 Hz, based on the low-frequency deaggregation (Subsection 2.5.2.4.2). Application of the empirical relation

$$\text{Log } T = -1.25 + 0.3M$$

$$\text{Equation 2.5.2-5}$$

(Reference 294) results in a corner period (T) of approximately 8 sec (0.125 Hz). To accommodate this expected change in slope, the extrapolations are performed at 0.125 and 0.1 Hz, assuming constant spectral velocity from 0.5 to 0.125 Hz and constant spectral displacement for frequencies below 0.125 Hz.

2.5.2.7.4 Design Basis Response Spectra

Tables 2.5.2-224, 2.5.2-225, and 2.5.2-226 and Figures 2.5.2-244a, 2.5.2-244b, 2.5.2-244c, 2.5.2-245a, 2.5.2-245b, and 2.5.2-245c show horizontal and vertical FIRS A1, A5, and C4 developed compared to the horizontal and vertical GMRS developed for Unit 2. Figures 2.5.2-246a, 2.5.2-246b, and 2.5.2-246c show both the horizontal and vertical FIRS A1, A5, and C4, respectively. Figures 2.5.2-247a, 2.5.2-247b, and 2.5.2-247c show the horizontal and vertical UHRS at exceedance levels of 10^{-4} , 10^{-5} , and 10^{-6} yr⁻¹ for FIRS A1, A5, and C4, respectively. Through Approach 3, both the horizontal and vertical UHRS and FIRS are hazard- and performance-based consistent across structural frequency from 0.5 to 100 Hz, the frequency range over which the hard rock hazard is computed (Reference 273). For frequencies below 0.5 to 0.1 Hz, the extrapolation employed is intended to reflect conservatism, likely resulting in motions of lower probability. Tables 2.5.2-224, 2.5.2-225, and 2.5.2-226 list discrete FIRS and UHRS horizontal and vertical spectral acceleration values.

As illustrated in Figure 2.5.4-266, the conditions associated with FIRS A5 are only applicable to a small localized portion of the Unit 1 footprint, while FIRS A1 is applicable to the remainder. Since the nuclear island basemat will respond as a unit, the actual input to the nuclear island will be much closer to FIRS A1, and the contribution of FIRS A5 will not adversely impact the overall response of Unit 1. Similarly, FIRS C4 was developed as a sensitivity analysis of the potential effects of localized fill concrete beneath the eastern extents of Unit 2. The potential effects of FIRS C4 are bounded by FIRS A1 for Unit 1, and the GMRS presented in Subsection 2.5.2.6 defines the input motion at Unit 2. Section 3.7 compares the site-specific ground motions to the AP-1000 design ground motions.

2.5.2.8 References

201. Electric Power Research Institute (EPRI), *Seismic Hazard Methodology for the Central and Eastern United States, Tectonic Interpretations*, EPRI Report NP-4726, volumes 5-10, July 1986.
202. Electric Power Research Institute (EPRI), *CEUS Ground Motion Project Final Report*, EPRI Technical Report 1009684, December 2004.
203. Electric Power Research Institute (EPRI), *Probabilistic Seismic Hazard Evaluation at Nuclear Plant Sites in the Central and Eastern United States, Resolution of the Charleston Earthquake Issue*, EPRI Report 6395-D, April 1989.
204. Deleted.

- 205. Deleted.
- 206. Deleted.
- 207. Electric Power Research Institute (EPRI), *EQHAZARD Primer*, EPRI Special Report NP-6452-D, Prepared by Risk Engineering for Seismicity Owners Group and EPRI, June 1989.
- 208. Deleted.
- 209. Deleted.
- 210. Deleted.
- 211. Deleted.
- 212. Deleted.
- 213. Deleted.
- 214. Deleted.
- 215. Deleted.
- 216. Deleted.
- 217. Deleted.
- 218. Deleted.
- 219. Deleted.
- 220. Amick, D., Gelinas, R., Maurath, G., Cannon, R., Moore, D., Billington, E., and Kempainen, H., *Paleoliquefaction Features along the Atlantic Seaboard*, U.S. Nuclear Regulatory Commission Report, NUREG/CR-5613, 1990.
- 221. Amick, D., Maurath, G., and Gelinas, R., "Characteristics of Seismically Induced Liquefaction Sites and Features Located in the Vicinity of the 1886 Charleston, South Carolina Earthquake," *Seismological Research Letters* 61 (2):117-130, 1990.
- 222. Talwani, P. and Schaeffer, W.T., "Recurrence Rates of Large Earthquakes in the South Carolina Coastal Plain Based on Paleoliquefaction Data," *Journal of Geophysical Research* 106 (B4):6,621-6,642, 2001.
- 223. Deleted.

224. Obermeier, S.F., Weems, R.E., Jacobson, R.B., and Gohn, G.S., "Liquefaction Evidence for Repeated Holocene Earthquakes in the Coastal Region of South Carolina," in "Earthquake Hazards and the Design of Constructed Facilities in the Eastern United States," *Annals of the New York Academy of Sciences* 558:183-195, 1989.
225. Deleted.
226. Deleted.
227. Deleted.
228. Deleted.
229. Deleted.
230. Deleted.
231. Johnston, A.C., "Seismic Moment Assessment of Earthquakes in Stable Continental Regions - III. New Madrid 1811-1812, Charleston 1886 and Lisbon 1755," *Geophysical Journal International* 126:314-344, 1996.
232. Bakun, W.H. and Hopper, M.G., "Magnitudes and Locations of the 1811-1812 New Madrid, Missouri, and the 1886 Charleston, South Carolina, Earthquakes," *Bulletin of the Seismological Society of America* 94 (1):64-75, 2004.
233. Deleted.
234. Deleted.
235. Deleted.
236. Deleted.
237. Deleted.
238. Ellsworth, W.L., Matthews, M.V., Nadeau, R.M., Nishenko, S.P., Reasenber, P.A., and Simpson, R.W., *A Physically-Based Earthquake Recurrence Model for Estimation of Long-Term Earthquake Probabilities*, U.S. Geological Survey Open-File Report 99-522, 1999.
239. Matthews, M.V., Ellsworth, W.L., and Reasenber, P.A., "A Brownian Model for Recurrent Earthquakes," *Bulletin of the Seismological Society of America* 92:2,233-2,250, 2002.
240. Deleted.
241. Deleted.

242. Deleted.
243. Deleted.
244. Chapman, M.C., Munsey, J.W., Powell, C.A., Whisner, S.C., and Whisner J., "The Eastern Tennessee Seismic Zone - Summary after 20 Years of Network Monitoring," *Seismological Research Letters* 73 (2):245, 2002.
245. Deleted.
246. Deleted.
247. Deleted.
248. Tuttle, M.P., Schweig, E.G., Sims, J.D., Lafferty, R.H., Wolf, L.W., and Haynes, M.L., "The Earthquake Potential of the New Madrid Seismic Zone," *Bulletin of the Seismological Society of America* 92 (6):2,080-2,089, 2002.
249. Abrahamson, N.A., and Bommer, J., *Program on Technology Innovation: Truncation of the Lognormal Distribution and Value of the Standard Deviation for Ground Motion Models in the Central and Eastern United States*, Electric Power Research Institute (EPRI) Technical Report 1014381, August 2006.
250. Deleted.
251. McGuire, R.K., Silva, W.J., and Constantino, C.J. *Technical Basis for Revision of Regulatory Guidance on Design Ground Motions: Hazard and Risk-Consistent Ground Motions Spectra Guidelines*, U.S. Nuclear Regulatory Commission Report Prepared for Division of Engineering Technology, Washington, D.C., NUREG/CR-6728, 2001.
252. Deleted.
253. Deleted.
254. Deleted.
255. Deleted.
256. Deleted.
257. Deleted.
258. Deleted.
259. Deleted.
260. Deleted.

- 261. Deleted.
- 262. Deleted.
- 263. Deleted.
- 264. Deleted.
- 265. Deleted.
- 266. Deleted.
- 267. Deleted.
- 268. Deleted.
- 269. Johnston, A.C., Coppersmith, K.J., Kanter, L.R., and Cornell, C.A., *The Earthquakes of Stable Continental Regions, Volume I: Assessment of Large Earthquake Potential*, EPRI Final Report TR-102261-V1, 1994.
- 270. Deleted.
- 271. Deleted.
- 272. Deleted.
- 273. Electric Power Research Institute (EPRI), *Guidelines for Determining Design Basis Ground Motions, Volume 5- Quantification of Seismic Source Effects*, EPRI Report TR-102293, Project 3302, Final Report, November 1993.
- 274. McGuire, R.K., Silva, W.J., and Costantino, C.J., *Technical Basis for Revision of Regulatory Guidance on Design Ground Motions: Development of Hazard- and Risk-consistent Seismic Spectra for Two Sites*, U.S. Nuclear Regulatory Commission Report, NUREG/CR-6769, 2002.
- 275. Bazzurro, P. and Cornell, C.A., "Nonlinear Soil-Site Effects in Probabilistic Seismic-Hazard Analysis," *Bulletin of the Seismological Society of America* 94:2,110-2,123, 2004.
- 276. Deleted.
- 277. Lee, R., Maryak, M.E., and Kimball, J., "A Methodology to Estimate Site-Specific Seismic Hazard for Critical Facilities on Soil or Soft-Rock Sites," *Seismological Research Letters* 70:230, 1999.
- 278. Anderson, J.G. and Hough, S.E., "A Model for the Shape of the Fourier Amplitude Spectrum of Acceleration at High Frequencies," *Bulletin of the Seismological Society of America* 74 (5):1,969-1,993, 1984.

279. Deleted.
280. Electric Power Research Institute (EPRI), *Proceedings: Engineering Characterization of Small-Magnitude Earthquakes*, EPRI Project 2556-25 Final Report NP-6389, Section 1-6, 1989.
281. Silva, W.J., "Body Waves in a Layered Anelastic Solid," *Bulletin of the Seismological Society of America* 66:1,539-1,554, 1976.
282. Silva, W.J., Li, S., Darragh, B., and Gregor, N., "Surface Geology Based Strong Motion Amplification Factors for the San Francisco Bay and Los Angeles Areas," in *A PEARL Report to PG&E/CEC/Caltrans*, Award No. SA2120-59652, 1999.
283. Deleted.
284. Deleted.
285. Deleted.
286. Silva, W.J., "Characteristics of Vertical Strong Ground Motions for Applications to Engineering Design," in *Proceedings of the FHWA/NCEER Workshop on the National Representation of Seismic Ground Motion for New and Existing Highway Facilities*, ed. I.M. Friedland, M.S Power and R. L. Mayes, Technical Report NCEER-97-0010, 1997.
287. Deleted.
288. Silva, W.J., Abrahamson, N., Toro, G., and Costantino, C., *Description and Validation of the Stochastic Ground Motion Model*, unpub. report prepared by Pacific Engineering and Analysis for Brookhaven National Laboratory, 1996.
289. Johnson, L.R. and Silva W.J., "The Effects of Unconsolidated Sediments Upon the Ground Motion During Local Earthquakes," *Bulletin of the Seismological Society of America* 71:127-142, 1981.
290. Abrahamson, N.A. and Silva, W.J, "Empirical Response Spectral Attenuation Relations for Shallow Crustal Earthquakes," *Seismological Research Letters* 68 (1):94-127, 1997.
291. Campbell, K.W., "Empirical Near Source Attenuation Relationships for Horizontal and Vertical Components of Peak Ground Acceleration, Peak Ground Velocity, and Pseudo Absolute Acceleration Response Spectra," *Seismological Research Letters* 68 (1):154-176, 1997.
292. Campbell, K.W. and Bozorgnia, Y., "Updated Near-Source Ground Motion (Attenuation) Relations for the Horizontal and Vertical Components of Peak Ground Acceleration and Acceleration Response Spectra," *Bulletin of the Seismological Society of America* 93 (1):314-331, 2003.

293. Deleted.
294. Building Seismic Safety Council (BSSC), *National Earthquake Hazards Reduction Program (NEHRP), Recommended Provisions for Seismic Regulations for New Buildings and Other Structures (FEMA 450)*, Report prepared for the Federal Emergency Management Agency (FEMA), 2004.
295. American Society of Civil Engineers (ASCE)/Structural Engineering Institute (SEI), *Seismic Design Criteria for Structures, Systems, and Components in Nuclear Facilities*, ASCE/SEI 43-05, 2005.
296. American National Standards Institute (ANSI)/American Nuclear Society (ANS), *Categorization of Nuclear Facility Structures, Systems, and Components for Seismic Design*, ANSI/ANS-2.26-2004, 2004.
297. Atkinson, G.M., "Empirical Attenuation of Ground Motion Spectral Amplitudes in Southeastern Canada and the Northeastern United States," *Bulletin of the Seismological Society of America* 94 (3): 1079-1095, 2004
298. Atkinson, G.M., "Notes on Ground Motion Parameters for Eastern North America: Duration and H/V Ratio," *Bulletin of the Seismological Society of America* 83 (2): 587-596, 1993.
299. Bryan J. Dolan to Document Control Desk, U.S. Nuclear Regulatory Commission, Development of Horizontal and Vertical Site-Specific Hazard Consistent Uniform Hazard Response Spectra at the Lee Nuclear Station Unit 1, dated April 30, 2008 (ML081230546).
300. NUREG/CR-5503, *Techniques for Identifying Faults and Determining their Origins*, authored by K. L. Hansen, K. I. Kelson, M. A. Angell, and W. R. Lettis, Office of Nuclear Regulatory Research, U.S. Nuclear Regulatory Commission, Washington, DC, 1999.
301. Klose, C.D., *The 2008 M7.9 Wenchuan Earthquake - Result of Local and Abnormal Mass Imbalances?*, *Eos Transactions. AGU*, 89(53), Fall Meeting Supplement, Abstract U21C-08, 2008.
302. Lin, A., Ren, Z., Jia, D., and X. Wu, *Co-Seismic Thrusting Rupture and Slip Distribution Produced by the 2008 Mw 7.9 Wenchuan Earthquake, China*, *Tectonophysics*, Vol. 471, p. 203–215., 2009.
303. Talwani, P., L. Chen, and K. Gahalaut, *Seismogenic Permeability*, *Journal of Geophysical Research*, v. 112, B07309, doi:10.1029/2006JB004665, 2007.
304. Talwani, P., *Earthquakes Associated with the Clark Hill Reservoir, South Carolina—A Case of Induced Seismicity*, *Engineering. Geology.*, 10, 239-253, 1976.

-
305. Secor, D.T., Jr., Regional Overview, p. 1-18, in, Secor, D.T., Jr., ed., Anatomy of the Alleghanian Orogeny as seen from the Piedmont of South Carolina and Georgia: Carolina Geological Society Field Trip Guidebook, November 14-15, 1987, 97p, 1987.
306. Chen, L., and P. Talwani, Renewed Seismicity near Monticello Reservoir, South Carolina, 1996–1999, Bulletin of the Seismological Society of America, 91, 94-101, 2001a.
307. Chen, L., and P. Talwani, Mechanism of Initial Seismicity Following Impoundment of the Monticello Reservoir, South Carolina, Bulletin of the Seismological Society of America, 91, 1582–1594., 2001b.
308. Rajendran, K., Sensitivity of a Seismically Active Reservoir to Low-Amplitude Fluctuations: Observations from Lake Jocassee, S. Carolina, Pure and Applied Geophysics, v. 145, 87-95, 1995.
309. Schaeffer, M.F., A Relationship between Joint Intensity and Induced Seismicity at Lake Keowee, Northwestern South Carolina, Bulletin of the Association of Engineering Geologists, v. 28, no. 1, p. 7-30, 1991.
310. Secor, D.T., Jr., L.S. Peck, D.M. Pitcher, D.C. Prowell, D.H. Simpson, W.A. Smith, and A.W. Snoke, Geology of the Area of Induced Seismicity Activity at Monticello Reservoir, South Carolina: Journal of Geophysical Research, vol. 87, no. B8, p. 6945-6957, 1982.
311. Talwani, P., A Onwby, K. Rajendran, and M. F. Schaeffer, A Field Study of Reservoir Induced Seismicity at Bad Creek, South Carolina; the Preimpoundment Phase, Seismological Research Letters, v. 61, No. 3-4, p. 162, 1990a.
312. Talwani, P., A Onwby, K. Rajendran, and M. F. Schaeffer, Bad Creek Project: A Progress Report, EOS, Transactions, American Geophysical Union, v. 71, No. 43, p. 1453, 1990b.
313. Widdowson, M.A., Meadows, M.E., Dickerson, J.R., Talwani, P., Schaffer, M., Orne, W.H., Hydrologic Impact of Reservoir Filling on a Fractured Crystalline Rock Aquifer, Proc. of the 1991 National Conf. on Irrigation and Drainage Engineering, Ed. Ritter, W.F., American Society of Civil Engineers, New York, pp.161-167, 1991.
314. Deleted.
315. Deleted.
316. Deleted.

317. Secor, D.T., Jr., and Snoke, A.W., Stratigraphy, structure and plutonism in the central South Carolina Piedmont, p. 65-123, in, Snoke, A.W., ed., Geological investigations of the eastern Piedmont, southern Appalachians (with a field trip guide on the bedrock geology of central South Carolina): Carolina Geological Society Field Trip Guidebook, 123 p., October 7-8, 1978.
318. Secor, D.T., Jr., Geology of the eastern Piedmont in South Carolina, p. 204-225, in, Secor, D.T., Jr., ed., Southeastern Geological Excursions – Guidebook for Geological Excursions: Geological Society of America Southeastern Section Annual Meeting, Columbia, South Carolina, 350 p. April 4-10, 1988.
319. Goldsmith, R., Milton, D.J. and Horton, J.W., Jr., Geologic map of the Charlotte 1° x 2° Quadrangle, North Carolina and South Carolina: United States Geological Survey, Miscellaneous Investigations Series, Map I-2175, 1:250,000, 1988.
320. Nelson, A.E., Horton, J.W., Jr., and Clarke, J.W., Geologic map of the Greenville 1° x 2° Quadrangle, Georgia, South Carolina, and North Carolina and South Carolina: United States Geological Survey, Miscellaneous Investigations Series, Map I-1251-E, 1:250,000, 1998.
321. Bryant, B. and Reed, J.C., Jr., Geology of the Grandfather Mountain Window and vicinity, North Carolina and Tennessee: United States Geological Survey Professional Paper 615, 190 p., 1:62,500, 1970.
322. North Carolina Geological Survey, Geologic map of North Carolina: Department of Natural Resources and Community Development, Division of Land Resources, North Carolina Geological Survey, 1:500,000, 1985.
323. Nystrom, P., Jr., 2008, Geologic map of the Blacksburg South quadrangle, Cherokee County, South Carolina (draft): South Carolina Department of Natural Resources, S.C. Geological Survey, Map GQM-XX.
324. Zoback, M.D., and Hickman, S., In situ study of the physical mechanisms controlling induced seismicity at Monticello Reservoir, South Carolina, Journal of Geophysical Research, vol. 87, p. 6959-6974, 1982.
325. Moos, D., and Zoback M.D., Near surface, "Thin Skin" reverse faulting stresses in the Southeastern United States, International Journal of Rock Mechanics and Mining Science & Geomechanics Abstracts, vol.30, No.7, p. 965-971, 1993.
326. NUREG 2115, Central and Eastern United States Seismic Source Characterization for Nuclear Facilities, U.S. Nuclear Regulatory Commission NUREG-2115, Department of Energy DOE/NE-0140, and Electric Power Research Institute Report 1021097, 2012.

327. Visvanathan, T.R., "Earthquakes in South Carolina, 1698-1975," South Carolina Geological Survey Bulletin 40, 1980.
328. Bernreuter, D.L., Savy, J.B., Mensing, R.W., Chen, J.C., and Davis, B.C., Seismic Hazard Characterization of 69 Nuclear Plant Sites East of the Rocky Mountains: U.S. Nuclear Regulatory Commission, NUREG/CR-5250, Volumes 1-8, 1989.
329. Petersen, M.D., Frankel, A.D., Harmsen, S.C., Mueller, C.S., Haller, K.M., Wheeler, R.L., Wesson, R.L., Oliver, Y.Z, Boyd, S., Perkins, D.M., Luco, N., Field, E.H., Wills, C.J., and Rukstales, K.S., Documentation for the 2008 Update of the United States National Seismic Hazard Maps: USGS Open-File Report 2008-1128, 128 p., 2008.
330. Senior Seismic Hazard Analysis Committee (SSHAC), Recommendations for Probabilistic Seismic Hazard Analysis - Guidance on Uncertainty and Use of Experts: Prepared by SSHAC, NUREG/CR-6372, 256 p., 1997.
331. Hanks, T.C., Abrahamson, N.A., Boore, D.M., Coppersmith, K.J, and Knepprath, N.E., Implementation of the SSHAC Guidelines for Level 3 and 4 PSHAs-Experience Gained from Actual Applications: U.S. Geological Survey Open-File Report 2009-1093, 66 p., 2009.
332. Kammerer, A.M. and Ake, J.P., Practical Implementation Guidelines for SSHAC Level 3 and 4 Hazard Studies: U.S. Nuclear Regulatory Commission NUREG-2117, Rev 1, 235 p., 2012.
333. Kijko, A., Estimation of the Maximum Earthquake Magnitude, Mmax: Pure and Applied Geophysics, v. 161, pp. 1-27, 2004.
334. Schulte, S.M., and Mooney, W.D., An Updated Global Earthquake Catalog for Stable Continental Regions: Reassessing the Correlation with Ancient Rifts, Geophysical Journal International, v. 161, pp. 707-721, 2005.
335. LASE Study Group, Deep structure of the US East Coast passive margin from large aperture seismic experiments, Marine and Petroleum Geology, v. 3, pp. 234-242, 1986.
336. Austin, J.A., Jr., Stoffa, P.L., Phillips, J.D., Oh, J., Sawyer, D.S., Purdy, G.M., Reiter, E., and Makris, J., Crustal structure of the Southeast Georgia embayment-Carolina trough: Preliminary results of a composite seismic image of a continental suture(?) and a volcanic passive margin, Geology, v.18, pp. 1023-1027, 1990.
337. McBride, J.H., Leetaru, H.E., Bauer, R.A., Tingey, B.E., and Schmidt, S.E.A., Deep faulting and structural reactivation beneath the southern Illinois basin: Precambrian Research, v. 157, pp. 289-313, doi:10.1016/j.precamres.2007.02.020, 2007.

-
338. Wheeler, R.L., Earthquakes and the Cratonward Limit of Lapetan faulting in eastern North America: *Geology*, v. 23, no. 2, pp. 105-108, 1995.
339. Mooney, W.D., and Ritsema, J., Mmax and Lithospheric Structure in Central and Eastern North America [abstract]: *Proceedings, Meeting of Central and Eastern U.S. (CEUS) Earthquake Hazards Program*, October 28-29, 2009, Memphis, TN, U.S. Geological Survey Memphis, TN, office, p. 25, 2009.
340. Braile, L.W., Keller, G.R., Hinze, W.J., and Lidiak, E.G., An ancient rift complex and its relation to contemporary seismicity in the New Madrid seismic zone: *Tectonics*, v. 1, pp. 225-237, 1982.
341. Braile, L.W., Hinze, W.J., Keller, G.R., Lidiak, E.G., and Sexton, J.L., Tectonic development of the New Madrid Rift Complex, Mississippi Embayment, North America: *Tectonophysics*, v. 131, pp. 1-21, 1986.
342. Kolata, D.R., and Nelson, W.J., 1991 Tectonic history of the Illinois Basin: in Leighton, M.W., Kolata, D.R., Oltz, D.F., and Eidel, J.J. (editors), *Interior Cratonic Basins*, AAPG Memoir 51, Chapter 18, pp. 263-285.
343. Weems, R.E., and Obermeier, S.F., The 1886 Charleston earthquake-An Overview of Geological Studies: in *Proceedings of the U.S. Nuclear Regulatory Commission Seventeenth Water Reactor Safety Information Meeting*, NUREG/CP-0105, v. 2, pp. 289-313, 1990.
344. Talwani, P., Dura-Gomez, I., Gassman, S., Hasek, M., and Chapman, A., Studies related to the Discovery of a Prehistoric Sandblow in the Epicentral Area of the 1886 Charleston SC Earthquake: *Trenching and Geotechnical Investigations: Program and Abstracts*, Eastern Section of the Seismological Society of America, p. 50, 2008.
345. Chapman, M. C., Beale, J. N., Mesozoic and Cenozoic faulting imaged at the epicenter of the 1886 Charleston, South Carolina, Earthquake, *bulletin of the Sesimological Society of America*, v. 98, p. 2533-2542, 2008.
346. Chapman, M. C., Beale, J. N., On the geologic structure at the epicenter of the 1886 Charleston, South Carolina, earthquake, *Bulletin of the Seismological Society of America*, v. 100, p. 1010-1030, 2010
347. Hu, K., Gassman, S. L., Talwani, P., In-situ properties of soils at paleoliquefaction sites in the South Carolina coastal plain: *Seismological Research Letters*, v. 73, p. 962-978, 2002.
348. Hu, K., Gassman, S. L., Talwani, P., Magnitudes of Prehistoric earthquakes in the South Carolina Coastal Plain from geotechnical data: *Sesimological Research Letters* v. 73, p. 979-991, 2002.

349. Leon, E., Gassman, S. L., Talwani, P., Effect of soil aging on assessing magnitudes and accelerations of prehistoric earthquakes: *Earthquake Spectra*, v. 21, p. 737-759, 2005
350. Gassman, S., Talwani, P., Hasek, M., Magnitudes of Charleston, South Carolina Earthquakes from in-situ geotechnical data: presentation at CEUS Earthquake Hazards Program, USGS, October 28-29, Memphis, 2009.
351. Saucier, R., Geoarchaeological Evidence of Strong Prehistoric Earthquakes in the New Madrid (Missouri) Seismic Zone: *Geology*, v. 19, pp. 296-298, 1991.
352. Tuttle, M.P., and Schweig, E.S., Towards a Paleoearthquake Chronology of the New Madrid Seismic Zone: U.S. Geological Survey, Earthquake Hazards Program, Progress Report (99HQGR0022), 28 p., 2001.
353. Tuttle, M.P., Schweig, E., III, Campbell, J., Thomas, P.M., Sims, J.D., and Lafferty, R.H., III, Evidence for New Madrid earthquakes in A.D. 300 and 2350 B.C.: *Seismological Research Letters*, v. 76, no. 4, pp. 489-501, 2005.
354. Schweig, E.S., and Ellis, M.A., Reconciling Short Recurrence Intervals with Minor Deformation in the New Madrid Seismic Zone: *Science*, v. 264, pp. 1308-1311, 1994.
355. Van Arsdale, R.B., Displacement History and Slip Rate on the Reelfoot Fault of the New Madrid Seismic Zone: *Engineering Geology*, v. 55, no. 4, pp. 219-226, 2000.
356. Holbrook, J., Autin, W.J., Rittenour, T.M., Marshak, S., and Goble, R.J., Stratigraphic Evidence for Millennial-Scale Temporal Clustering of Earthquakes on a Continental-Interior Fault: Holocene Mississippi River Floodplain Deposits, New Madrid Seismic Zone, USA: *Tectonophysics*, v. 420, pp. 431-454, 2006.
357. Calais, E., Mattioli, G., DeMets, C., Nocquet, J.M., Stein, S., Newman, A., and Rydelek, P., Tectonic Strain in the Interior of the North American Plate, *Nature*, v. 438, doi: 10.1038/nature04428, 2005.
358. Smalley, R., Jr., Ellis, M.A., Paul, J., and VanArsdale, R.B., Space Geodetic Evidence for Rapid Strain Rates in the New Madrid Seismic Zone of the Central USA: *Nature*, v. 435, pp.1088-1090, doi:10.1038/nature03642, 2005.
359. Hough, S.E., and Page, M., Toward a Consistent Model for Strain Accrual and Release for the New Madrid, Central United States: *Journal of Geophysical Research*, v. 116, no. B03311, doi:10.1029/2010JB007783, 2011.

-
360. Obermeier, S.F., Vaughn, J.D., and Hatcher, R.D., Field Trip Guide: Paleoseismic Features in and near Douglas Reservoir, East Tennessee Seismic Zone, Northeastern Tennessee, 25 p., 2010.
361. Vaughn, J. D., Obermeier, S. F., Hatcher, R. D., Howard, C. W., Mills, H. H., and Whisner, S. C., Evidence for One or More Major Late-Quaternary Earthquakes and Surface Faulting in the East Tennessee Seismic Zone, *Seismological Research Letters*, v. 81, no. 2, p. 323, 2010.
362. Howard, C.W., Derryberry, P.M., Hatcher, R.D. Jr., Vaughn, J.D., and Obermeier, S.F., Detailed geologic maps of two sites south of Dandridge, Tennessee, record evidence of polyphase paleoseismic activity in the East Tennessee seismic zone: Abstract from the 60th Annual Meeting of the Southeastern Section of the Geological Society of America, p. 16-1, 2011.
363. Warrell, K.F., Hatcher, R.D. Jr., Blankenship, S.A., Howard, C.W., Derryberry, P.M., Wunderlich, A.L., Obermeier, S.O., Counts, R.C., and Vaughn, J.D., Detailed geologic mapping of paleoseismic features: an added tool for seismic hazard assessment in the East Tennessee seismic zone, Abstract from the 61st Annual Meeting of the Southeastern Section of the Geological Society of America, p. 8-3, 2012.
364. Hatcher, R.D., Vaughn, J.D., and Obermeier, S.F., Large earthquake paleoseismology in the East Tennessee seismic zone: Results of an 18-month pilot study, *The Geological Society of America, Special Paper* 493, 2012.
365. U.S. Geological Survey (USGS), Earthquake Hazards Program, Preliminary Earthquake Report: Magnitude 5.8 - Virginia, 2011 August 23 17:51:04 UTC, website <http://earthquake.usgs.gov/earthquakes/recenteqsww/Quakes/se082311a.php#details> accessed 5/2/2012.
366. Chapman, M., The Rupture Process of the August 23, 2011 Louisa County, Virginia Earthquake, *Seismological Research Letters*, v. 83, no. 2, p. 403, 2012.
367. Cramer, C.H., Kutliroff, J.R., and Dangkua, D.T., The 2011 M5.7 Mineral, VA and M5.6 Sparks, OK earthquake ground motions and stress drops: An important contribution to the NGA East ground motion database, *Seismological Research Letters*, v. 83, no. 2, p. 420, 2012.
368. Horton, J.W., Chapman, M.C., Carter, A.M., Carter, M.W., Harrison, R.W., Herrmann, R.B., and Snyder, S.L., Faults Delineated by Aftershocks Associated with the 2011 Central Virginia Earthquake and their Tectonic Setting, *Geological Society of America, Abstracts with Programs*, v. 44, no. 4, p. 14, 2012.
369. Virginia Tech Seismological Observatory (VTSO), Louisa County Earthquake: August 23, 2011, website <http://www.geol.vt.edu/outreach/vtso/2011/0823-louisa> accessed 2/16/2012.

-
370. Walsh, L.S., Montesi, L.G., Sauber, J.M., Watters, T.R., Kim, W., Martin, A.J., and Anderson, R., Comparing the stress change characteristics and aftershock decay rate of the 2011 Mineral, VA earthquake with similar earthquakes from a variety of tectonic settings, Abstract S11B-2241 presented at 2011 Fall Meeting, AGU, San Francisco, Calif., 5-9 Dec, 2011.
371. Ellsworth, W.L., Imanishi, K., Aist, T., Luetgert, J.H., and Pratt, T.L., The Mw5.8 Virginia earthquake of August 23, 2011: A high stress drop event in a critically stressed crust, 83rd Annual Meeting of the Eastern Section of the Seismological Society of America, October 16-18, Little Rock, Arkansas, 2011.
372. Saint Louis University (SLU) Earthquake Center, Aftershock monitoring (for the 2011 Virginia Earthquake), St. Louis University Earthquake Center, website http://www.eas.slu.edu/eqc_significant/2011_Virginia/aftershock.html, date accessed 5/8/2012, 2012.
373. Chapman, M. C., On the rupture process of the 23 August 2011 Virginia Earthquake, Bulletin of the Seismological Society of America, v. 103, n. 2a, p. 613-628, 2013.
374. Saint Louis University, Earthquake Center, August 23, 2011 Virginia http://www.eas.slu.edu/eqc/eqcsignificant/2011_Virginia/aftershock.html, date accessed 12/16/2013.
375. Atkinson, G.M., and Wald, D.J., "Did You Feel It?" intensity data-A surprisingly good measure of earthquake ground motion: Seismological Research Letters, v. 78, no. 3, p. 362-368, 2007.
376. Assatourians, K., and Atkinson, G.M., Ground motion characteristics of the 2011 Virginia and 1988 Quebec M5.8 earthquakes, Abstract S14B-04 presented at 2011 Fall Meeting, AGU, San Francisco, Calif., 5-9 Dec, 2011.
377. Carter, M.W., Blabpied, M.L., Leeds, A.L., Harp, E.L., McNamara, D.E., Harrison, R.W., and Schindler, J.S., USGS response to the Mineral, Virginia MW 5.8 earthquake of 23 August 2011, Geological Society of America, Abstracts with Programs, v. 44, no. 4, p. 13, 2012.
378. Earthquake Engineering Research Institute (EERI), The Mw 5.8 Virginia earthquake of August 23, 2011, EERI Special Earthquake Report, December 2011.
379. Geotechnical Extreme Events Reconnaissance (GEER), Geotechnical quick report on the affected region of the 23 August 2011 M5.8 Central Virginia earthquake near Mineral, Virginia, GEER Association Report No. GEER-026, 2011.

-
380. Green, R.A., and Lasley, S., Liquefaction resulting from the 2011 Central Virginia earthquake, Geological Society of America, Abstracts with Programs, v. 44, no. 4, p. 14, 2012.
381. Keller, M.R., Robinson, E.S., and Glover III, L., 1985, Seismicity, seismic reflection, gravity, and geology of the central Virginia seismic zone: Part 3. Gravity: Geological Society of America Bulletin, v. 96, pp. 1,580-1,584.
382. de Witt, W., and Bayer, K.C., 1986, Seismicity, seismic reflection, gravity, and geology of the Central Virginia Seismic Zone: Part 3. Gravity: Discussion and reply: Geological Society of America Bulletin, v. 97, Discussion, pp. 1285-1286.
383. Obermeier, S.F., 1995, Paleoseismic liquefaction studies-Central U.S. and Pacific Northwestern U.S.: in Jacobsen, M.L. (compiler), National Earthquake Hazards Reduction Program Annual Project Summaries: XXXVI, Volume II, U.S. Geological Survey Open-File Report 95-210, pp. 606-609.
384. Seeber, L., and Armbruster, J.G., 1993, Natural and induced seismicity in the Lake Erie-Lake Ontario region: Reactivation of ancient faults with little neotectonic displacement: Géographie physique et Quaternaire, v. 47, no. 3, pp. 363-378.
385. Dineva, S., Eaton, D., and Mereu, R., Seismicity of the southern Great Lakes: Revised earthquake hypocenters and possible tectonic controls: Bulletin of the Seismological Society of America, v. 94, no. 5, pp. 1902-1918, 2004.
386. Wheeler, R.L., and Crone, A.J., 2001, Known and suggested Quaternary faulting in the midcontinent United States: Engineering Geology, v. 62, pp. 51-78.
387. Niemi, T.M., Ferris, A.N., and Abers, G.A., 2004, Investigation of microearthquakes, macroseismic data, and liquefaction associated with the 1867 Wamego earthquake in eastern Kansas: Bulletin of the Seismological Society of America, v. 94, no. 6, pp. 2317-2329.
388. Steltenpohl, M.G., Zietz, I., Horton, J.W., Jr., and Daniels, D.L., 2010, New York-Alabama lineament: A buried right-slip fault bordering the Appalachians and mid-continent North America: Geology, v. 38, no. 6, pp. 571-574.
389. Chapman, M.C., Powell, C.A., Vlahovic, G., and Sibol, M.S., A statistical analysis of earthquake focal mechanisms and epicenter locations in the eastern Tennessee seismic zone: Bulletin of the Seismological Society of America, v. 87, no. 6, pp. 1522-1536, 1997.
390. Bollinger, G.A., and Wheeler, R.L., 1983, The Giles County seismic zone: Science, v. 219, pp. 1063-1065.

391. Bollinger, G.A., and Wheeler, R.L., 1988, The Giles County, Virginia, Seismogenic Zone-Seismological Results and Geological Interpretations: U.S. Geological Survey Professional Paper 1355, 85 pp.
392. Law, R.D., Pope, M.C., Wirgart, R.H., Eriksson, K.A., Carpenter, D., Robinson, E.S., and Bollinger, G.A., 1993, Geologically recent near-surface folding and faulting in the Valley and Ridge Province: New exposures of extensional faults in alluvial sediments, Giles County, SW Virginia [abstract]: Eos, Transactions of the American Geophysical Union, v. 74, no. 16, p. 282.
393. Chapman, M.C., and Krimgold, F., 1994, Seismic Hazard Assessment for Virginia: report prepared for the Virginia Department of Emergency Services and the Federal Emergency Management Agency, Virginia Tech Seismological Observatory, Blacksburg, Va., 62 pp.
394. Law, R.D., Pope, M.C., Wirgart, R.H., Eriksson, K.A., Robinson, E.S., Sayer, S., Phinney, E.J., and Bollinger, G.A., 1994, Geologically recent near-surface faulting and folding in Giles County, southwest Virginia: New exposures of extensional and apparent reverse faults in alluvial sediments between Pembroke and Pearisburg: Proceedings of the U.S. Nuclear Regulatory Commission for 1994, Twenty-First Water Reactor Safety Information Meeting, October 25-27, 1993, Bethesda, Maryland, NUREG/CP-0133, v. 3, pp. 415-432.
395. Law, R.D., Robinson, E.S., Cyrnak, J.S., Sayer, S., Williams, R.T., Callis, J., and Pope, M., 1997, Geologically-recent faulting and folding of alluvial sediments near Pearisburg, Giles County, Virginia-Tectonic faulting or karst subsidence in origin? [abstract]: Eos, Transactions of the American Geophysical Union, v. 78, no. 17 (supplement), p. S316.
396. EPRI, 2013, EPRI (2004, 2006) Ground-Motion Model (GMM) Review Project, Elec. Power Res. Inst, Palo Alto, CA, Rept. 3002000717, June 2.
397. NRC, 2013, Approval of Electrical Power Research Institute Ground Motion Model Review Project for Use by Central and Eastern United States Nuclear Power Plants, ML13233A102, August 28, 2013.
398. NRC, EPRI, DOE (2012). Central and Eastern United States Seismic Source Characterization for Nuclear Facilities, Corrected tables and figures, Download Updates (06/27/2012), CEUS-SSC website (<http://www.ceus-ssc.com>).

2.5.3 SURFACE FAULTING

WLS COL 2.5-4 NRC Regulatory Guide 1.208 defines a capable tectonic source as a tectonic structure that can generate both vibratory ground motion and tectonic surface deformation, such as faulting or folding at or near the earth's surface, in the

present seismotectonic regime. This section evaluates the potential for tectonic surface deformation and non-tectonic surface deformation at the William States Lee III Nuclear Station Site (Lee Nuclear Site). Information contained in [Subsection 2.5.3](#) was developed in accordance with Regulatory Guide (RG) 1.208 and is intended to satisfy 10 CFR 100.23, *Geologic and Seismic Siting Criteria*.

There are no capable tectonic sources within the Lee Nuclear Site vicinity (25 mi. radius), and there is negligible potential for tectonic fault rupture at the site and within the site vicinity. There is also negligible potential for non-tectonic surface deformation at the site and within the site area (5 mi. radius). The following subsections provide the data, observations, and references to support these conclusions.

2.5.3.1 Geological, Seismological, and Geophysical Investigations

The following investigations were performed to assess the potential for tectonic and non-tectonic deformation within the Lee Nuclear Site vicinity and area:

- Compilation and review of existing data and literature.
- Interpretation of aerial photography and satellite imagery.
- Field and aerial reconnaissance.
- Review of historical and recorded seismicity.
- Discussions with current researchers in the area.

An extensive body of information is available for the Lee Nuclear Site. This information is contained in four main sources:

- Previous investigations performed for the former Duke Cherokee nuclear site, presented in the Preliminary Safety Analysis Report (PSAR) and supporting basis documents ([References 201](#), [202](#), and [203](#)).
- Geologic mapping published by the U.S. Geological Survey (USGS), the South Carolina Department of Natural Resources, and other researchers.
- Articles published in peer-reviewed journals by various researchers and field trip guidebooks published primarily by the Carolina Geological Society.
- Seismicity data compiled and analyzed in published journal articles and the CEUS SSC ([Reference 244](#)).

This existing information is supplemented by aerial and field reconnaissance performed within and beyond the site vicinity, and by interpretation of aerial photography and satellite imagery within and beyond the site area.

2.5.3.1.1 Previous Lee Nuclear Site Investigations

The results of previous site investigations are presented in the PSAR (References 201, 202, and 203). This previous work does not identify the existence of tectonic faulting within the site area.

Detailed geologic mapping and inspection of excavations during construction for Units 1, 2, and 3 of the former Duke Cherokee nuclear site reveal no evidence of active or geologically recent faulting within the site area (Subsection 2.5.1.2.5.4 provides detailed discussion of site area geology and recorded deformation events). These excavations did expose minor bedrock shears that are related to mafic intrusions (e.g., meta-diorite and amphibolite rock units) in the meta-granodiorite pluton (e.g., meta-granodiorite to meta-quartz diorite rock units). Most of this minor deformation is associated with the contact between the mafic intrusions and the meta-granodiorite pluton (Figure 2.5.1-229). A more detailed discussion of the minor bedrock features is provided in Subsections 2.5.1.2 and 2.5.4.1.

2.5.3.1.2 Published Geologic Mapping

This subsection describes the geologic mapping completed, at a variety of scales, by the USGS, South Carolina Geological Survey, and other researchers in the site vicinity. This mapping suggests no evidence of geologically recent or active faulting within the site area.

Regional geologic mapping compilations assembled by experts in the geology of the Carolinas that cover the Lee Nuclear Site are incorporated into geologic maps of the site region, vicinity, and area (Figures 2.5.1-203a, 203b, 204a, 204b, 218a, 218b, 219a, and 219b). Hibbard et al.'s (2006, Reference 210) 1:1,500,000-scale lithotectonic map of the Appalachian Orogen is a compilation of geologic and structural mapping that spans eastern North America from Alabama to Lake Ontario. This map presents integrated data and interpretations from a variety of pre-existing sources (see references in Hibbard et al. 2006) (Figure 2.5.1-204a). Horton and Dicken (2001, Reference 209) compile geologic mapping of the Piedmont and Blue Ridge of South Carolina at 1:500,000-scale. This map presents integrated data and interpretations from a variety of pre-existing sources (see references in Horton and Dicken 2001). Horton and Dicken's (Reference 209) geologic mapping supplements those areas not covered by more-detailed, 1:24,000-scale mapping (Figures 2.5.1-218a, 218b, 219a and 219b).

The South Carolina Geological Survey's 1:24,000-scale maps present the most-detailed published geologic mapping in the site area. Nystrom's (2004, Reference 205) geologic map of the Blacksburg South 7.5-minute quadrangle covers the Lee Nuclear Site (Figures 2.5.1-219a and 219b). Howard (2004, Reference 206) and Nystrom (2003, Reference 207) presents geologic mapping of the two adjacent 7.5-minute quadrangles to the east (Kings Creek and Filbert). Portions of the Kings Creek quadrangle provide 1:24,000-scale mapping within the Lee Nuclear Site area (Figure 2.5.1-218a and 218b).

The USGS has also published 1:24,000-scale geologic maps that cover portions of the site vicinity. The coverage area of Horton's (2006, [Reference 208](#)) geologic mapping of the Kings Mountain and Grover 7.5-minute quadrangles, South Carolina and North Carolina is beyond the site area, but entirely within the site vicinity ([Figures 2.5.1-218a](#) and [218b](#)).

The most detailed mapping of the Duke Lee Nuclear Site is the unpublished mapping developed by Duke Power geologists performed as part of the Cherokee nuclear site construction. This detailed mapping at both the 1:24,000 scale for the site area and more detailed mapping of the top of rock and foundation grade exposures at 1:120 and 1:240 scales was performed for investigations of the former Duke Cherokee nuclear site. The 1:24,000-scale mapping of the Blacksburg South quadrangle, which includes the Duke Lee Nuclear Site, is nearly identical to the 2004 preliminary geologic map of the same quadrangle by Nystrom ([Reference 205](#)).

In addition to the geologic mapping discussed above, the USGS has published a compilation of all known or suggested Quaternary faults, liquefaction features, and possible tectonic features in the central and eastern United States ([Reference 211](#), updated in [Reference 212](#)) ([Figure 2.5.1-213](#)). Only one such feature identified by these authors is potentially located within the Lee Nuclear Site area radius. The Fall Lines of Weems (1998, [Reference 213](#)) are alignments of rapids or anomalously steep sections of rivers draining the Piedmont and Blue Ridge Provinces of North Carolina and Virginia. Weems's (1998, [Reference 213](#)) delineation of these fall zones is crude, but, as presented in his Figure 8, the Western Piedmont Fall Line appears to be located within or close to the Lee Nuclear Site area at its nearest point ([Figure 2.5.1-213](#)). Wheeler (2005, [Reference 212](#)) classifies the Fall Lines of Weems (1998, [Reference 213](#)) as a Class C feature ([Table 2.5.1-201](#)) because: (1) identification of the fall zones is subjective and the criteria for recognizing them are not stated clearly enough to make the results reproducible, and (2) a tectonic faulting origin is not demonstrated for the fall zones ([Subsection 2.5.1.1.2.4.5](#) presents a more detailed discussion of the Fall Lines). Based on review of published literature, field reconnaissance, and work performed as part of the North Anna ESP application ([Reference 214](#)), the Fall Lines of Weems (1998, [Reference 213](#)) are interpreted as erosional features related to contrasting erosional resistances of adjacent rock types, and are not tectonic in origin.

No other Crone and Wheeler ([Reference 211](#)) or Wheeler ([Reference 212](#)) suspected Quaternary features are located within the Lee Nuclear Site vicinity. In addition, reviews of literature and consultations with experts for this project found no additional tectonic features.

2.5.3.1.3 Current Geologic Mapping

The existing geologic maps discussed in the preceding [Subsection 2.5.3.1.2](#) form the basis for the geologic maps presented in [Subsection 2.5.1](#). Field reconnaissance of the site (0.6 mile radius), site area (5 mile radius), and site vicinity (25 mile radius) included field checks of existing mapping and, where necessary, refinement of previous geologic maps.

A very linear geologic contact at the Lee Nuclear Site was investigated in detail to preclude the presence of a fault. Nystrom (2004, [Reference 205](#)) maps at 1:24,000-scale the western margin of a meta-granodiorite pluton at the Lee Nuclear Site as a linear, north-northwest-trending contact ([Figures 2.5.1-219a, 2.5.1-219b, and 2.5.1-226](#)). The nature of this contact between the meta-granodiorite pluton and metavolcanic country rock was investigated by means of detailed geologic mapping, compilation and review of borehole information, and geologic logging of six test pits. The results of this investigation demonstrate that this contact is more irregular than mapped by Nystrom (2004, [Reference 205](#)), and confirm the intrusive nature of the contact. The more irregular map pattern ([Figures 2.5.1-220 and 2.5.1-226](#)) and the intrusive nature of the contact preclude a fault interpretation for the western margin of the pluton.

Refinements were made to existing geologic maps at the site vicinity, site area and site scale as well as at the scale of the existing excavation to develop the geologic maps as described in [Subsection 2.5.1.2.5.5](#) and presented in [Figures 2.5.1-218a, 2.5.1-218b, 2.5.1-219a, 2.5.1-219b, 2.5.1-220, 2.5.1-226 and 2.5.1-229](#). These modifications reflect new geologic mapping performed as part of this project, as well as efforts to reconcile previous geologic and structural mapping from various sources conducted at varying scales.

The geologic map of the site vicinity ([Figures 2.5.1-218a and 2.5.1-218b](#)) comprises 1:500,000-scale mapping of South Carolina by Horton and Dicken (2001, [Reference 209](#)) and 1:500,000-scale mapping of North Carolina by the North Carolina Geological Survey (1998, [Reference 243](#)). Geologic contacts and descriptions from these two sources are presented in [Figures 2.5.1-218a and 2.5.1-218b](#) without modification, but unit colors have been altered for consistency across the South Carolina-North Carolina state border. Fault locations shown on [Figure 2.5.1-218a](#) are slightly modified after 1:1,500,000-scale mapping by Hibbard et al. (2006, [Reference 210](#)), such that the faults "snap" to geologic contacts.

The site area geologic maps ([Figures 2.5.1-219a and 2.5.1-219b](#)) are modified after 1:24,000-scale geologic mapping by Nystrom (2004, [Reference 205](#)) and Howard (2004, [Reference 206](#)), as well as 1:500,000-scale mapping by Horton and Dicken (2001, [Reference 209](#)). This geologic mapping is supplemented on [Figure 2.5.1-219a](#) with fold axes from Butler (1981, [Reference 235](#)) and fault locations slightly modified after 1:1,500,000-scale mapping by Hibbard et al. (2006, [Reference 210](#)), such that the faults "snap" to geologic contacts.

The site geologic map ([Figure 2.5.1-220](#)) is modified after 1:24,000-scale geologic mapping by Nystrom (2004, [Reference 205](#)) and Howard (2004, [Reference 206](#)), and represents the only geologic map that incorporates significant revisions to previously published data. As described above, Nystrom (2004, [Reference 205](#)) maps a metatonalite (herein referred to as meta-granodiorite) pluton that underlies much of the site. Nystrom (2004, [Reference 205](#)) maps a relatively straight western boundary of this pluton ([Figure 2.5.1-219a](#)). The nature of this western pluton boundary was investigated in detail and remapped as part of this project. [Figure 2.5.1-226](#) and [Subsection 2.5.4.2](#) present the details of this remapping,

and the refined mapping of the western pluton boundary is incorporated into the site geologic map ([Figure 2.5.1-220](#)).

Of particular interest at the site scale is the western boundary of the pluton (Nystrom 2004, [Reference 205](#)), which is the foundation bearing unit as shown on [Figure 2.5.1-219a](#). Nystrom (2004, [Reference 205](#)) maps the western margin of the pluton (noted as Zto) as a pronounced linear feature. Field reconnaissance indicated that this boundary is not constrained by actual observation or data although it is shown as a solid line contact on Nystrom (2004, [Reference 205](#)).

To improve the control on the western margin of the pluton, borings from the Cherokee Nuclear Station as well as this investigation were evaluated. Previous mapping performed during the original site construction for a cooling water corridor had previously exposed the contact between the pluton and country rock outside of the north western corner of the excavation for Unit 1 as shown on [Figure 2.5.1-226](#). A series of geologic trenches were located along the western margin to confirm this contact.

As shown on [Figure 2.5.1-226](#), existing boring and test pits were evaluated to refine the western pluton contact with the metavolcanic country rock. Also, two geologic trenches were excavated to investigate the margin location and nature of the rock lithologies to correlate with the boring log descriptions. The exposed rock in the first trench indicated saprolitic and partially weathered rock indicative of plutonic rock and a second trench was opened about 300 feet to the west. The second trench indicated that the western saprolite lithology was not typical of saprolites of plutonic origin and that the fabric was foliated thus suggesting a metamorphic lithology more representative of the metavolcanic country rocks of the region. The borings, geologic trenches, and field reconnaissance as shown on [Figure 2.5.1-226](#) were thus used to refine the geologic map presented as [Figure 2.5.1-220](#).

At the scale of the excavation, because extensive mapping during the original construction had been performed but was not completed or verified, mapping of the existing exposure was completed. Specifically, the noted rock lithologies were cataloged for correlation with more general nomenclature established during Cherokee Nuclear Station evaluations. The exposed limits of the excavation were mapped to document the spatial relationship of major lithologic units and structural features observed in the excavation area. [Figure 2.5.1-229](#) shows the major lithologic units and structural features within the former Cherokee Nuclear Station Unit 2 and 3 areas and limited areas bordering the former Cherokee Nuclear Station Unit 1 area. Also shown on this map are the limits of available exposure for mapping.

2.5.3.1.4 Previous Seismicity Data

The highest recorded ground shaking intensities at the Lee Nuclear Site are the result of earthquakes located beyond the site vicinity. The largest earthquake within 25 mi. of the Lee Nuclear Site included in the updated CEUS SSC earthquake catalog is the 1886 E[M] 4.13 event. Located just outside the 25 mi site radius was the 1913 E[M] 4.54 Union County, South Carolina earthquake,

located approximately 25 mi. southwest of the Lee Nuclear Station (Figure 2.5.1-210) (Reference 244).

The Union County earthquake was felt over an area of approximately 43,000 square miles, with an estimated Rossi-Forel shaking intensity VIII (Reference 215, as reported in Reference 216) (Figure 2.5.1-232). Rossi-Forel shaking intensity at the Lee Nuclear Site is estimated at VI (Reference 215, as reported in Reference 216). The epicenter of the Union County earthquake is poorly located and there is no known causative fault for this event.

The 1886 Charleston earthquake was likely located more than 150 mi. from the Lee Nuclear Site, and produced shaking intensity of about MMI VI at the site (Reference 217) (Figure 2.5.1-217). The fault on which this earthquake occurred remains unknown.

2.5.3.1.5 Current Seismicity Data

As described in Subsection 2.5.2.1, the CEUS SSC earthquake catalog of the central and eastern United States is updated to incorporate earthquakes that occurred between 1568 and 2008.

In 2006, four minor earthquakes occurred in northeast South Carolina. Two of these events that occurred in January were less than m_b 3.0, and two events that occurred in September were larger than m_b 3.0. None of these four events are included in the CEUS SSC earthquake catalog. In an unpublished online report, Talwani (2006a, Reference 218) describes the two January earthquakes located near Jonesville, South Carolina, approximately 20 mi. southwest of the Lee Nuclear Site. Talwani (2006a, Reference 218) suggests that the January 24, 2006 magnitude 2.5 and January 25, 2006 magnitude 1.5 (magnitude scale unspecified) earthquakes are associated with the western margin of the Baldrock granitic pluton. Talwani (2006a, Reference 218) does not provide estimates of location uncertainty for these two micro-earthquakes, but the epicentral locations are likely inaccurate due to the small magnitudes of these events.

The additional, minor earthquakes occurred in September 2006, in northeast South Carolina near the town of Bennettsville. In unpublished online reports, the USGS National Earthquake Information Center describes the September 22, 2006 m_b 3.5 and the September 25, 2006 m_b 3.7 earthquakes (References 219 and 220). The epicenters of these two earthquakes are not precisely located, but are more than 75 mi. east-southeast of the Lee Nuclear Site. Estimates of location uncertainty for the September 22, 2006 event are: ± 4.5 mi. horizontal, ± 7.9 mi. depth (± 7.3 km horizontal, ± 12.8 km depth) (Reference 219). Estimates of location uncertainty for the September 25, 2006 event are: ± 6.8 mi. horizontal, with depth fixed at 3.1 mi. by the location program (± 10.9 km horizontal, depth fixed at 5 km) (Reference 220). Due to the lack of nearby seismograph stations, focal mechanisms are not determined for these events. The September 2006 earthquakes are spatially associated with a small Mesozoic extensional basin mapped beneath the Coastal Plain by Benson (1992, Reference 221) (Figure 2.5.1-210). In an unpublished online report, Talwani (2006b,

Reference 222) suggests that these two earthquakes may be spatially related to the Eastern Piedmont fault system, a broad zone of faults interpreted by Hatcher et al. (1977, Reference 223) as a regional fault zone (Figure 2.5.1-209). At the latitude of the two September 2006 earthquakes, the Eastern Piedmont fault system is up to 40 mi. wide. Given the uncertainty associated with the locations of the two September 2006 earthquakes and the broad regional extent of the Eastern Piedmont fault system, these two minor events cannot be positively correlated with this fault system.

2.5.3.1.6 Current Aerial and Field Reconnaissance

Aerial photography, satellite imagery, and topographic maps of varying scales and vintages reveal no evidence of geomorphic features indicative of the potential for surface deformation (e.g., faulting or warping) within the site area. Imagery reviewed as part of this license application includes:

- 1:20,000-scale, black and white, stereo aerial photographs from the U.S. Department of Agriculture (1959) covering the entire site area and beyond.
- 1:40,000-scale, color-infrared, stereo aerial photographs from the USGS (1994) covering the majority of the site area.
- Landsat satellite imagery of varying color bands covering the site vicinity and beyond.
- Shaded relief topographic imagery with 100-foot (30-m) grid spacing covering the site vicinity and beyond.

Review of aerial photography reveals a linear topographic feature within the Lee Nuclear Site area that, because of its orientation parallel to the predominant regional structural grain and its proximity to the site, was investigated in detail to assess its origin. This approximately 4.5-mi.-long, linear feature is located approximately 2 mi. northwest of the site, and strikes approximately N55°E with a steeper slope facing to the northwest (shown as “Lineament No. 1” on Figure 2.5.1-221). London Creek flows northeastward along much of the length of the northwestern base of the ridge, before joining with the Broad River near the southernmost tip of Ninety-Nine Islands. The lineament, which is most easily recognized on the 1:40,000-scale USGS photography, terminates northeastward at the Broad River and is not expressed in the topography northeast of the river. Field reconnaissance and previous geologic mapping by Nystrom (2004, Reference 205) reveal that resistant, northeast-striking quartzite layers core this linear ridge. The linear topographic expression of this ridge is the result of erosion by London Creek (and the erosion resistance of the quartzite layers) and is assessed to be non-tectonic in origin.

Field and aerial reconnaissance inspections reveal no evidence for surface rupture, surface warping, or the offset of geomorphic features indicative of active faulting within the site area.

2.5.3.2 Geological Evidence, or Absence of Evidence, for Surface Deformation

As shown in [Figures 2.5.1-218a](#) and [218b](#) and discussed in [Subsection 2.5.1.1.2.4](#), six bedrock faults of Paleozoic age are mapped within the site vicinity. These six faults are:

- Kings Mountain shear zone, including the Blacksburg shear zone and the Kings Creek shear zone.
- Tinsley Bridge fault.
- Southwestern extension of the Boogertown shear zone.
- Brindle Creek thrust fault.
- Reedy River thrust fault.
- Unnamed fault north of Gaffney.

No deformation or geomorphic features suggestive of potential Quaternary activity are reported in the literature for these six faults. Aerial and field reconnaissance and interpretation of aerial photographs and satellite imagery show that no geomorphic features indicative of Quaternary activity exist along any of the mapped fault traces. These six features are discussed in [Subsection 2.5.1.1.2.4.2](#), summarized in [Table 2.5.3-201](#) and described below.

- Kings Mountain shear zone. The northeast-striking Kings Mountain shear zone ([Figure 2.5.1-210](#)) in the Lee Nuclear Site vicinity is a zone of mylonitic deformation ([References 224, 225, 226, 227, and 228](#)) and considered part of the Central Piedmont shear zone separating the Carolina and Piedmont Zones ([Figure 2.5.1-218a](#)) ([Reference 224](#)). The sense of motion on the Kings Mountain shear zone is uncertain, but structural data suggest that the zone is a steeply northwest-dipping reverse fault ([Reference 224](#)). Deformation of this mylonitic shear zone is overprinted by semi brittle cleavage. Pegmatitic dikes in North Carolina intruded parallel to the semi-brittle cleavage and some have been ductile deformed. Hence, the dikes are interpreted as syn- to post-kinematic and their Rb-Sr whole rock isochron age of 352 ± 10 Ma indicates that the late-stage semi-brittle deformation occurred in the Late Devonian ([Reference 224](#)). Furthermore, an unnamed granite with a 326 ± 3 Ma U-Pb upper-intercept age cuts and is undeformed by the central Piedmont shear zone in South Carolina south of the intersection of the Kings Mountain shear zone and the Tinsley Bridge faults ([Reference 236](#)).
- Tinsley Bridge fault. The Tinsley Bridge fault ([Figure 2.5.1-210](#)) is a zone of retrograde mylonite with apparent down-to-the-northwest sense of slip and is less than 20 mi. in length ([Reference 229](#)). Mineral assemblages in the mylonite indicate that deformation on the Tinsley Bridge fault occurred after peak metamorphic conditions ([Reference 229](#)). The fault is cut by the

undeformed Pacolet granite with a whole rock Rb/Sr age of 383 ± 5 Ma (Reference 229).

- Southwest extension of the Boogertown shear zone. The northeast-striking Boogertown shear zone (Figure 2.5.1-210) is sometimes interpreted as a terrane boundary (References 225 and 230). The northeastern end of the Boogertown shear zone is mapped terminating into an unsheared granitic pluton (References 237 and 210). This pluton is undated, but the youngest plutons within the Carolina Zone are generally 300–265 Ma (Reference 238). There is no evidence to suggest post-Paleozoic motion on the southwest extension of the Boogertown shear zone.
- Brindle Creek thrust fault. The Brindle Creek thrust was recognized in North Carolina as a low-angle fault with an extensive mylonite zone, but authors have indicated that the mapping of this structure in South Carolina is speculative (Reference 239). In North Carolina, a granite found only in the hanging-wall of the Brindle Creek fault (and hence older than movement on the structure) has zircons with a weighted $^{206}\text{Pb}/^{238}\text{U}$ ion microprobe age of 366 ± 3 Ma (Reference 240). These field relations were interpreted to indicate that the Brindle Creek fault was active after the intrusion of the granite, or is Devonian or younger in age. In North Carolina, migmatitic, high-temperature deformation is spatially associated with the Brindle Creek fault (Reference 240). Metamorphic rims on migmatitic rocks in the immediate footwall of the Brindle Creek fault yield ion-microprobe U-Pb ages of ~350 Ma, probably correlative with emplacement of the Brindle Creek hanging-wall (Reference 241).
- Reedy River thrust fault. The Reedy River thrust fault is a northeast-striking structure in the Inner Piedmont (References 208, 231, 232, and 233) (Figure 2.5.1-210). There is no evidence to suggest post-Paleozoic motion on the Reedy River thrust fault.
- Unnamed fault north of Gaffney. In their tectonostratigraphic compilation map of the Appalachians, Hibbard et al. (2006, Reference 210) suggest that this approximately 20-mi.-long, northerly striking fault records up-to-the-east displacement and Goldsmith et al. (1988, Reference 242) indicate it is a northwest-vergent thrust fault. Horton and Dicken (2001, Reference 209) do not include this fault in their compilation of South Carolina Piedmont and Blue Ridge geology. There is no evidence to suggest post-Paleozoic motion on the unnamed fault North of Gaffney.

There is direct geologic evidence to preclude the presence of northeast- or east-striking faults projecting through the Lee Nuclear Site. The predominant structural grain of the site area, vicinity, and region is oriented northeast. As mapped by Nystrom (2004, Reference 205) and confirmed by reconnaissance mapping, two elongated, north-striking quartzite bodies are located in the western portion of the site area (Figures 2.5.1-219a, 219b and 2.5.1-220). These unfaulted, continuous quartzite beds, oriented at a high angle to the regional

structural grain, demonstrate the absence of any northeasterly or easterly striking fault through the Lee Nuclear Site. In addition, the northerly striking western margin of the pluton provides an additional strain marker that precludes the presence of any northeasterly or easterly striking faults through the Lee Nuclear Site. The timing of emplacement of this pluton is uncertain, but according to Butler (1981, [Reference 235](#)), it is likely early Paleozoic or older in age.

2.5.3.3 Correlation of Earthquakes With Capable Tectonic Sources

Seismicity with the Lee Nuclear Site vicinity is shown in [Figure 2.5.1-210](#). As shown on this figure, there is no spatial correlation of earthquake epicenters with known or postulated faults or other tectonic features. No faults or geomorphic features within the site vicinity can be correlated with earthquakes. Based on review of existing literature, no reported historical earthquake epicenters have been associated with bedrock faults within the Lee Nuclear Site vicinity ([Figure 2.5.1-210](#)). None of these faults within the Lee Nuclear Site vicinity are classified as capable tectonic sources.

The CEUS SSC earthquake catalog does not include any earthquakes of $E[M] > 3.0$ within the site area. However, several small events have occurred within or just beyond the site vicinity ([Figure 2.5.1-210](#)) and are discussed above in [Subsections 2.5.3.1.4](#) and [2.5.3.1.5](#). The largest of these is the January 1, 1913 ($E[M]$ 4.54, ([Reference 244](#)) Union County, South Carolina earthquake, located approximately 25 mi. southwest of the Lee Nuclear Station ([Reference 216](#)). The fault on which this earthquake occurred has not been identified.

2.5.3.4 Ages of Most Recent Deformations

The six faults mapped in the Lee Nuclear Site vicinity (i.e., the Kings Mountain shear zone, the Tinsley Bridge fault, the southwest extension of the Boogertown shear zone, the Brindle Creek thrust, the Reedy River thrust fault, and the unnamed fault north of Gaffney) have not been active since Paleozoic time ([References 224](#) and [229](#)), although Garihan et al. (1993, [Reference 231](#)) suggest the possibility that the Kings Mountain shear zone may have experienced localized Mesozoic reactivation.

2.5.3.5 Relationships of Tectonic Structures in the Site Area to Regional Tectonic Structures

Of the five faults identified within the site area (i.e., the Kings Mountain shear zone, the Tinsley Bridge fault, the southwest extension of the Boogertown shear zone, the Reedy River thrust fault, and the unnamed fault north of Gaffney), at least four are considered part of a larger regional shear zone known as the Central Piedmont shear zone (the relationship between the unnamed fault and the Central Piedmont suture is unclear). The Central Piedmont shear zone extends northeastward from Georgia, through the Carolinas, and into Virginia. At the latitude of the Lee Nuclear Site, the Central Piedmont shear zone separates the Piedmont zone from the Charlotte terrane ([Reference 234](#)) ([Figure 2.5.1-202a](#)).

As described in [Subsection 2.5.3.6](#), none of the potential faults within the site area is considered a capable tectonic feature.

2.5.3.6 Characterization of Capable Tectonic Sources

Based on reviews of updated geologic, seismic, and geophysical data from published literature, interviews with expert earth scientists, and the COL investigations, no evidence for capable tectonic sources is identified within the Lee Nuclear Site vicinity. These data are presented in detail throughout [Subsection 2.5.1](#), and are summarized in [Subsection 2.5.3.2](#). This interpretation is consistent with investigations performed for the former Cherokee nuclear site. The Tinsley Bridge fault and the Kings Mountain shear zone are the nearest mapped faults to Lee Nuclear Site (located approximately 5 mi. away at their nearest points), and have not been active since Paleozoic time ([References 224 and 229](#)), although Garihan et al. (1993, [Reference 231](#)) suggest the possibility that the Kings Mountain shear zone may have experienced localized Mesozoic reactivation.

2.5.3.7 Designation of Zones of Quaternary Deformation in the Site Region

Based on reviews of updated geologic, seismic, and geophysical data from published literature, interviews with expert earth scientists, and the COL investigations, no evidence of Quaternary deformation is identified. These data are presented in detail throughout [Subsection 2.5.1](#). Based on this finding, no investigation is required.

2.5.3.8 Potential for Surface Tectonic Deformation at the Site

The potential for tectonic deformation at the site is negligible. Detailed geologic mapping and inspection of excavations during construction of the former Duke Cherokee nuclear site reveal no evidence of geologically recent or active faulting ([References 201, 202, and 203](#)). Based on reviews of updated geologic, seismic, and geophysical data from published literature, interviews with expert earth scientists, and the COL investigations, there are no Quaternary faults or capable tectonic sources within the site vicinity. The potential for non-tectonic surface deformation, including RIS, within the site area is negligible. There is no information suggesting the potential for non-tectonic surface deformation within the site area. Rocks within the site area are igneous and metamorphic crystalline rocks ([References 205 and 206](#)) that are neither susceptible to karst-type dissolution collapse nor to subsidence due to fluid withdrawal. Evaluations related to the potential of RIS associated with Make-Up Pond C are described in [Subsection 2.5.2.1.3](#).

2.5.3.9 References

201. Cherokee Nuclear Station Preliminary Safety Analysis Report (PSAR), vol. 4, Appendix 2C - Seismology, Attachment V - Seismic Refraction Data, prepared by Law Engineering Testing Company for Duke Power Company Project 81, June 1974a.
202. Cherokee Nuclear Station Preliminary Safety Analysis Report (PSAR), vol. 4, Appendix 2C - Geology, prepared by Law Engineering Testing Company for Duke Power Company Project 81, July 1974b.
203. Cherokee Nuclear Station Preliminary Safety Analysis Report (PSAR), vol. 4, Appendix 2E - Seismology, prepared by Law Engineering Testing Company for Duke Power Company Project 81, January 1974c.
204. Removed
205. Nystrom, P.G., *Geologic Map of the Blacksburg South 7.5-Minute Quadrangle, Cherokee and York Counties, South Carolina (Preliminary Draft)*, South Carolina Geological Survey, GQM-X, 1:24,000-scale, 2004.
206. Howard, C.S., *Geologic Map of the Kings Creek 7.5-Minute Quadrangle, York County, South Carolina*, South Carolina Geological Survey, GQM-6, 1:24,000-scale, 2004.
207. Nystrom, P.G., *Geologic Map of the Filbert 7.5-Minute Quadrangle, Cherokee and York Counties, South Carolina*, South Carolina Geological Survey, GQM-25, 1:24,000-scale, 2003.
208. Horton J.W. Jr., *Geologic map of the Kings Mountain and Grover Quadrangles, Cleveland and Gaston Counties, North Carolina, and Cherokee and York Counties, South Carolina*, U.S. Geological Survey Open-File Report 2006-1238, 2006.
209. Horton, J.W. Jr. and Dicken, C.L., *Preliminary Digital Geologic Map of the Appalachian Piedmont and Blue Ridge, South Carolina Segment*, U.S. Geological Survey Open-File Report 01-298, 1:500,000 scale, 2001.
210. Hibbard, J.P., van Staal, C.R., Rankin, D.W., Williams, H., *Lithotectonic Map of the Appalachian Orogen, Canada - United States of America*, Geological Society of Canada, map 2096A, 1:1,500,000 scale, 2006.
211. Crone, A.J. and Wheeler, R.L., *Data for Quaternary Faults, Liquefaction Features, and Possible Tectonic Features in the Central and Eastern United States, East of the Rocky Mountain Front*, U.S. Geological Survey Open-File Report 00-260, 2000.
212. Wheeler, R.L., *Known or Suggested Quaternary Tectonic Faulting, Central and Eastern United States- New and Updated Assessments for 2005*, U.S. Geological Survey Open-File Report 2005-1336, 37 pp., 2005.

213. Weems, R.E., *Newly Recognized En Echelon Fall Lines in the Piedmont and Blue Ridge Provinces of North Carolina and Virginia, With a Discussion of their Possible Ages and Origins*, U.S. Geological Survey Open-File Report 98-0374, 1998.
214. U.S. Nuclear Regulatory Commission, *Safety Evaluation Report for an Early Site Permit (ESP) at the North Anna ESP Site*, U.S. Nuclear Regulatory Commission Report, NUREG-1835, September 2005.
215. Taber, S., "The South Carolina Earthquake of January 1, 1913," *Bulletin of the Seismological Society of America* 3:6-13, 1913.
216. Visvanathan, T.R., "Earthquakes in South Carolina, 1698-1975," *South Carolina Geological Survey Bulletin* 40, 1980.
217. Bollinger, G.A., "Reinterpretation of the Intensity Data for the 1886 Charleston, South Carolina, Earthquake," in *Studies Related to the Charleston, South Carolina, Earthquake of 1886- A Preliminary Report*, ed. D.W. Rankin, U.S. Geological Survey Professional Paper 1028, 1977.
218. South Carolina Seismic Network, Website, Talwani, P., "The Jonesville Earthquake," <http://scsn.seis.sc.edu/images/jonesville.pdf>, accessed October 16, 2006a.
219. U.S. Geological Survey National Earthquake Information Center, Website, "Magnitude 3.7 Earthquake, South Carolina, Monday September 25, 2006 at 05:44:23 UTC," <http://earthquake.usgs.gov/eqcenter/recenteqs/Quakes/ustbaj.php>, accessed September 25, 2006.
220. U.S. Geological Survey National Earthquake Information Center, Website, "Magnitude 3.5 Earthquake, South Carolina, Friday September 22, 2006 at 11:22:01 UTC," <http://earthquake.usgs.gov/eqcenter/recenteqs/Quakes/semc0922a.php> accessed on September 25, 2006.
221. Benson, R.N., *Map of Exposed and Buried Early Mesozoic Rift Basins/ Synrift Rocks of the U.S. Middle Atlantic Continental Margin*, Delaware Geological Survey Miscellaneous map series no. 5, 1:1,000,000 scale, 1992.
222. South Carolina Seismic Network, Website, Talwani, P., "Two Felt Earthquakes Hit Northeast South Carolina," <http://scsn.seis.sc.edu/images/Sept2006earthquakes.pdf> accessed October 16, 2006b.
223. Hatcher R.D. Jr., Howell, D.E., and Talwani, P., "Eastern Piedmont Fault System - Speculations on its Extent," *Geology* 5:636-640, 1977.
224. Horton Jr., J.W., "Shear Zone Between the Inner Piedmont and Kings Mountain Belts in the Carolinas," *Geology* 9:28-33, 1981a.

-
225. Horton, J.W. Jr., "Geologic Map of the Kings Mountain Belt Between Gaffney, South Carolina and Lincolnton, North Carolina," in *Geological Investigations of the Kings Mountain Belt and Adjacent Areas in the Carolinas*, Carolina Geological Society Field Trip Guidebook, 1981b.
226. Dennis, A.J., "Is the Central Piedmont Suture a Low-Angle Normal Fault?" *Geology* 19:1081-1084, 1991.
227. Wilkins, J.K., Shell, G.S., and Hibbard, J.P., "Geologic Contrasts Across the Central Piedmont Suture in North-Central, North Carolina," in *Carolina Geological Society Guidebook for 1995 Annual Meeting*, South Carolina Geology 38:25-32, 1995.
228. West, T.E. Jr., "Structural Analysis of the Carolina-Inner Piedmont Terrane Boundary: Implications for the Age and Kinematics of the Central Piedmont Suture, a Terrane Boundary that Records Paleozoic Laurentia-Gondwana Interactions," *Tectonics* 17 (3):379-394, 1998.
229. Dennis, A.J., Rocks of the Carolina Terrane in the Spartanburg 30- x 60-Degree Quadrangle, prepared for the 1995 Carolina Geological Survey annual meeting, 1:100,000 scale, 1995.
230. Maybin, A.H. and Nystrom, P.G., *Geologic Map of South Carolina*, South Carolina Geological Survey GGMS-1, 1:1,00,000-scale, 1997.
231. Garihan, J.M., Preddy, M.S., and Ranson, W.A., "Summary of Mid-Mesozoic Brittle Faulting in the Inner Piedmont and Nearby Charlotte Belt of the Carolinas," in *Carolina Geological Society Field Trip Guidebook - Studies of Inner Piedmont Geology with a Focus on the Columbus Promontory*, Carolina Geological Society Field Trip Guidebook, 1993.
232. Nystrom, P.G., "Structure and Stratigraphy Across the Reedy River Thrust Fault, Inner Piedmont of South Carolina," *Geological Society of America Abstracts with Programs*, Southeastern Section 50th annual meeting, 2001.
233. Maybin, A.H. and Nystrom, P.G., *Geology of the Reedy River Thrust in the Vicinity of Southwest Spartanburg, South Carolina*, South Carolina Geological Survey Open-File Report 143, 2002.
234. Hibbard, J.P., Stoddard, E.F., Secor, D.T., and Dennis, A.J., "The Carolina Zone: Overview of Neoproterozoic to Early Paleozoic Peri-Gondwanan Terranes Along the Eastern Flank of the Southern Appalachians," *Earth Science Reviews* 57:299-339, 2002.
235. Butler, J.R., Geology of the Blacksburg South Quadrangle, South Carolina, in *Geological investigations of the Kings Mountain Belt and Adjacent Areas in the Carolinas*, Carolina Geological Society Field Trip Guidebook, 1981.

236. Dennis, A. J., Wright, J. E., 1995, Mississippian (ca. 326-323 Ma) U-Pb crystallization for two granitoids in Spartanburg and Union counties, South Carolina, in Dennis et al., eds., *Geology of the western part of the Carolina terrane in northwestern South Carolina*, CGS Fieldtrip Guidebook v. 37, p. 43-47.
237. Milton, D. J., 1981, The northern termination of the Kings Mountain belt, in Horton, J. W., Butler, J. R., Milton, D. M., eds., *Geological investigations of the Kings Mountain belt and adjacent areas in the Carolinas: Carolina Geological Society Field Trip Guidebook*, p. 1-5.
238. Hatcher, R. D., Bream, B. R., and Mersch, A. J., 2007, Tectonic map of the southern and central Appalachians: A tale of three orogens and a complete Wilson cycle, in Hatcher, R. D., Carlson, M. P., McBride, J. H., and Martinez Catalan, J. R., eds., *4-D Framework of Continental Crust: Geological Society of America Memoir 200*, p. 595-632.
239. Bream, B.R., 2002, The southern Appalachian Inner Piedmont: New perspectives based on recent detailed geologic mapping, Nd isotopic evidence, and zircon geochronology, in Hatcher, R.D., Jr., and Bream, B.R., eds., *Inner Piedmont geology in the South Mountains-Blue Ridge Foothills and the southwestern Brushy Mountains, central-western North Carolina: North Carolina Geological Survey, Carolina Geological Society annual field trip guidebook*, p. 45-63.
240. Giorgis, S. D., Mapes, R. W., Bream, B. R., 2002, The Walker Top Granite: Acadian granitoid or eastern Inner Piedmont basement? in Hatcher, R. D. and Bream, B. R., eds., *Inner Piedmont geology in the South Mountains-Blue Ridge foothills and the southwestern Brushy Mountains, central-western North Carolina: North Carolina Geological Survey, Carolina Geological Society annual fieldtrip guidebook*, p. 33-43.
241. Mersch, A. J., Kalbas, J. L., 2002, Geology of the southwestern Brushy Mountains, North Carolina Inner Piedmont: A summary and synthesis of recent studies, in Hatcher, R. D. and Bream, B. R., eds., *Inner Piedmont geology in the South Mountains-Blue Ridge foothills and the southwestern Brushy Mountains, central-western North Carolina: North Carolina Geological Survey, Carolina Geological Society annual fieldtrip guidebook*, p. 101-126.
242. Goldsmith, R., Milton, D. J., Horton, J. W., 1988, Geologic map of the Charlotte 1x2 degrees quadrangle, North Carolina and South Carolina: USGS Miscellaneous Investigations Series Map I-1251-E; 1:250,000. Website <http://pubs.er.usgs.gov/usgspubs/i/i/25/E>, accessed February 6, 2009.
243. North Carolina Geological Survey (NCGS), *Geology of North Carolina vector digital data onemap_prod.SDEADMIN.geo*, Website <http://www.nconemap.com/Default.aspx?tabid=286>, accessed June 12, 2007, publication date 1998.

244. NUREG-2115, Central and Eastern United States Seismic Source Characterization for Nuclear Facilities, U.S. Nuclear Regulatory Commission NUREG-2115, Department of Energy DOE/NE-0140, and Electric Power Research Institute Report 1021097, 2012.
-

2.5.4 STABILITY OF SUBSURFACE MATERIALS AND FOUNDATIONS

This Section presents information on the properties and stability of soils and rock that may affect the nuclear power plant facilities, under both static and dynamic conditions, including vibratory ground motions associated with the Ground Motion Response Spectrum (GMRS) and Foundation Input Response Spectra (FIRS) for seismic Category I structures at the Lee Nuclear Station Site. The discussion focuses on the stability of subsurface materials and foundations as they influence the safety of seismic Category I facilities and presents a comparison of the site conditions and geologic features to the DCD design criteria.

As specified in Regulatory Guide 1.206, pages C.III.1-44 to C.III.1-47, this Subsection is organized into the following Subsections. These include:

- Geologic Features (2.5.4.1)
- Properties of Subsurface Materials (2.5.4.2)
- Foundation Interfaces (2.5.4.3)
- Geophysical Surveys (2.5.4.4)
- Excavations and Backfill (2.5.4.5)
- Groundwater Conditions (2.5.4.6)
- Response of Soil, Granular Fill, and Rock to Dynamic Loading (2.5.4.7)
- Liquefaction Potential (2.5.4.8)
- Earthquake Site Characteristics (2.5.4.9)
- Static Stability (2.5.4.10)
- Design Criteria (2.5.4.11)
- Techniques to Improve Subsurface Conditions (2.5.4.12).

The information presented in this Subsection was developed on the basis of evaluations of historic field explorations performed for the Cherokee Nuclear Station (CNS) and field investigations for Lee Nuclear Station, Units 1 and 2 completed between early 2006 and mid-2007, and the 2012 field data (described below). Further information was gathered using geophysical investigations and

laboratory tests conducted on soil and rock samples obtained during the field exploration program for Lee Nuclear Station. Results from historic site investigations for Cherokee Nuclear Station are presented in the Preliminary Safety Analysis Report (PSAR) ([Reference 201](#)) and Final Safety Evaluation Report ([Reference 202](#)).

Additional field work consisting of borings and geophysical tests was performed in 2012 to obtain additional geotechnical data at the nuclear islands to confirm the applicability of the 2006-2007 data. The information provided for the Lee Nuclear Station Units 1 and 2 is based on data from historic field explorations for the Cherokee Nuclear Station, the field explorations for the Lee Nuclear Station completed in 2006 and 2007, and the 2012 field data.

2.5.4.1 Geologic Features

WLS COL 2.5-1 This Subsection evaluates non-tectonic processes and features that may cause
WLS COL 2.5-5 permanent ground deformation or foundation instability at the Lee Nuclear Station Site. Processes and features evaluated include areas of actual or potential surface or subsurface subsidence, solution activity, uplift or collapse, and causes of these conditions. This subsection also addresses zones of alteration, irregular weathering profiles, zones of structural weakness, the geologic history and unrelieved residual stresses in bedrock at the site, and of rocks or soils that may be unstable due to physical or chemical properties.

All of the data collected serve as the basis for evaluating excavation and backfill issues, construction excavation and dewatering, earth fill and granular fill requirements, groundwater, response of soil, granular fill, and rock to dynamic loading, liquefaction potential, static stability, techniques to improve subsurface conditions, and issues related to construction. The results of these evaluations, along with methods and results of field and laboratory programs, are summarized in the following Subsections.

- [Subsection 2.5.4.1.1](#), Geologic History and Stress Conditions, reviews aspects of geologic history that are relevant to the potential for uplift and residual stresses in the bedrock or soil. There is no evidence for uplift occurring at the present time, and there are no geologic or human-induced processes that are expected to lead to uplift at the site.
- [Subsection 2.5.4.1.2](#), Stratigraphy, Lithology, and Soil and Rock Characteristics, presents information on the physical and chemical properties of the rock and soil, and an evaluation of erosion, zones of alteration, and zones of potential weakness. There are no rocks which may be unstable because of their erosive potential, mineralogy, lack of consolidation, water content, or potentially undesirable response to seismic or other events.

- **Subsection 2.5.4.1.3**, Groundwater, discusses groundwater conditions at the site and how they may affect weathering and stability of the rock and soil.
- **Subsection 2.5.4.1.4**, Effects of Human Activities, evaluates the effects of human activities such as mineral, oil, water, oil, and gas extraction on the potential for subsidence and collapse at the Lee Nuclear Station Site. These activities are found to have not affected the site. The potential for RIS associated with Make-Up Pond C is also evaluated. This activity is not expected to affect the site.
- **Subsection 2.5.4.1.5**, Summary of Geologic Hazards, summarizes the conclusions of the preceding four Subsections regarding the potential for non-tectonic deformation beneath the Units 1 and 2 nuclear islands.

As background for this subsection, descriptions, maps, and profiles of regional and site geology are described in detail in **Subsections 2.5.1** and **2.5.2**. Detailed descriptions of site and geotechnical conditions encountered during the field investigations at the Lee Nuclear Station Site are presented in **Subsections 2.5.4.2**, **2.5.4.3** and **2.5.4.4**.

The Lee Nuclear Station Units 1 and 2 power block excavation area is defined by a rectangular boundary with an approximate dimension of 2000 feet by 1200 feet. Exploration was focused within the power block excavation and adjacent area, with an appropriately focused exploration effort to characterize the surrounding site area. **Figure 2.5.4-201** shows site features at the Lee Nuclear Station Site. Relative topographic site change between the pre-Cherokee Nuclear Station and Lee Nuclear Station ground elevations is shown on **Figure 2.5.4-202**.

2.5.4.1.1 Geologic History and Stress Conditions

This Subsection describes aspects of geologic history that are relevant to the potential for uplift and unrelieved residual stresses in the bedrock. Information on the site geologic history is summarized from **Subsection 2.5.1.2**.

The Lee Nuclear Station Site lies within the northeast-southwest trending Appalachian orogenic belt. This orogenic belt formed during the Paleozoic Era and has undergone multiple orogenic events related to the opening and closing of the proto-Atlantic along the eastern margin of ancestral North America.

The most recent and significant major tectonic event to affect the Appalachian orogenic belt was the late Paleozoic Alleghanian orogeny. At the latitude of the Lee Nuclear Station Site region, the Alleghanian collision telescoped and drove previously accreted Taconic terranes westward up and across the Laurentian basement, folding the passive margin sequence before them and creating the Valley and Ridge fold-and-thrust belt. The collisional process also thrust a fragment from the underlying Laurentian basement eastward over the passive margin sequence, forming the western Blue Ridge. Significant strike-slip faulting and lateral transport of terranes are interpreted to have occurred during the Alleghanian orogeny (**Reference 203**).

Since the 1980's, researchers have assessed and compiled available stress data for the central and eastern United States, including well-bore breakouts, results of hydraulic fracturing studies, in situ stress measurements and earthquake focal mechanisms ([References 241, 242, 243, 244](#)). The most recent compilations as part of the CEUS SSC project confirm previous work that indicates the prevailing stress field in the midcontinent is east-northeast to northeast maximum horizontal stress direction, with no strong evidence for stress subprovinces ([Reference 245](#)). This is consistent with the theoretical trend of compressive forces acting on the North American plate from the mid-Atlantic Ridge as shown in [Figure 2.5.1-245](#).

Unrelieved stress in bedrock could potentially result from thermally induced stresses, unloading due to removal of overburden by erosion or excavation, and tectonic stresses imposed during past deformation. Thermally induced stresses result from differences of cooling-related contraction along adjacent mineral grains of different composition. Residual stresses are typically small and tend to be relieved as the rocks are exposed by erosion or excavation. The relief of such residual stresses is time dependent and depends on the rate at which the ambient stress conditions of the rock change.

Thermally induced stresses are unlikely to be present. At a shallow depth of burial, the bedrock has equilibrated to surficial temperatures and any intergranular stress has had considerable time to be relieved. Likewise, stresses resulting from the removal of overburden are likely to be largely relieved due to the long period of the time when the rocks were near the surface with relatively low overburden pressures. Relief of those residual stresses and CNS blasting and excavation methods account for the relatively increased frequency of subhorizontal fractures observed at shallow depths in borehole televiewer logs, refer to [Subsection 2.5.4.3](#). The long-term residence of the bedrock near the surface provided ample time for the relief of residual stresses due to the release of overburden pressure.

Intragranular stresses may be preserved from deformation dating from Precambrian and Paleozoic tectonic events. However, thermal annealing of strained minerals coincident with late Paleozoic metamorphism and Mesozoic intrusions of mafic igneous rocks may have relieved much if not all of the elastic strain energy stored in older, strained mineral grains. Additionally, long residence near the surface and the presence of multiple fractures provides ample means to relieve any residual stresses and the likelihood that residual stresses from past tectonic events are preserved at the magnitude that result in creep or rebound is unlikely.

2.5.4.1.2 Stratigraphy, Lithology, and Soil and Rock Characteristics

This Subsection summarizes bedrock and stratigraphic information collected from previous studies and the Lee Nuclear Site exploration program. Following this, information relating to the characteristics of soil and rock at the Lee Nuclear Station Site, the physical and chemical properties of the rock and soil, and an evaluation of zones of alteration and zones of potential weakness are presented. This data is primarily derived from the compilation and analysis of borehole and other site-specific information presented in Cherokee Nuclear Station PSAR

(Reference 205), Cherokee Nuclear Station construction documents and the Lee Nuclear Site investigation collected during the 2006 - 2007 field exploration.

2.5.4.1.2.1 Site Area Stratigraphy and Lithology

Locally, the Lee Nuclear Station Site is underlain by a complexly deformed and metamorphosed plutonic-volcanic sequence that is mantled in most places by thick residual soils and saprolites. These soils and saprolites are evidence of a long weathering history. The relatively flat rolling plains and limited outcrop exposure are also evidence of the prolonged period of weathering. Local relief is caused by differences in the weathering resistance of bedrock and stream incision.

Rock units in the site area belong to the Battleground Formation, with the exception of later Mesozoic diabase dikes (References 206 and 207). The Battleground Formation is comprised primarily of felsic metavolcanic rocks, intermediate to mafic metavolcanic rocks, and quartz-rich metasedimentary rocks of Neoproterozoic age (Reference 226). Based on textures and the similarity of composition of the plutonic and volcanoclastic units, the entire sequence is considered to be a volcanoclastic pile that has been intruded by its own parent magmas (Reference 206). The occurrence of carbonate in the metasedimentary component is indicative of a marine environment, and reworking of the pile has resulted in both clastic and chemical deposition. Locally the composition of the volcanoclastics has been altered to various degrees by hydrothermal leaching due to large-scale circulation of seawater interacting with hot volcanic rocks.

The Lee Nuclear Station site itself is underlain by a metamorphosed pluton variously ascribed to intrusion of the Battleground Formation by the parent magmas of the Battleground volcanoclastics (Reference 207), intrusive metatonalite containing angular xenoliths of the Battleground Formation (Reference 226), and intrusive metatonalite and volcanoclastic rocks (Reference 227). This plutonic unit is generally composed of metatonalite that exhibits spatially variable composition. Within the plutonic unit exposed by excavation at the site, meta-granodiorite is the most abundant rock type based on petrographic analyses (Reference 205). This pluton is assessed to be separate from, and younger than (or possibly coeval with), the Battleground Formation (Reference 207).

Due to intense deformation, few primary features survive with which to determine stratigraphic order. Tentative inferences (References 206, 207, and 208) consider the South Fork antiform to be an upright feature and the Battleground Formation to be a homocline that “yongs” to the northwest (Reference 206). This inference is supported by the occurrence of the metasedimentary component primarily to the northwest, the expected stratigraphic relationships for deposition of marine-dominated clastic and chemical precipitate rocks at the later stages of the volcanic pile accumulation. Stratigraphic relationships of the various units are shown schematically in Figure 2.5.1-224.

2.5.4.1.2.2 Soil and Rock Characteristics

Borehole data show that the bedrock at the Lee Nuclear Station Site is overlain by residual soil comprised of silt and fine sand, 0 to greater than 100 feet, typically 40 to 80, feet thick, derived from in situ weathering of intact rock material. In some areas, this saprolite has developed a 'B' soil horizon. In many places the silts and sands preserve relict bedrock structures such as rock fabric and mineral foliation. The transition from saprolite to intact rock material can be gradual or abrupt.

Rock core and hand specimen samples collected from the Cherokee Nuclear Station and Lee Nuclear Station Sites have been logged using various classification systems. Historically, bedrock units at Cherokee Nuclear Station were described and grouped as either felsic (light color) gneiss or mafic (dark color) gneiss. Rocks described during the Lee Nuclear Station exploration program, were systematically classified into the following primary groups based on estimated mineral composition and texture: meta-diorite, meta-granodiorite, and meta-quartz diorite. Representative rock samples recovered core Lee Nuclear Station borings were sent for petrologic analysis to more precisely identify the mineralogy and rock types. [Table 2.5.4-201](#) presents the petrographic analysis results. For purposes of consistency, rock descriptions described in [Section 2.5](#) use the rock classification system developed for the Lee Nuclear Station Site unless indicated otherwise.

Petrologic examination of thin sections obtained from the site revealed the following rock types: mica schist, meta-quartz diorite, meta-dacite porphyry, and meta-basalt. These rock types are generally consistent with the rock types categorized as Felsic Gneiss and Mafic Gneiss rock groups described for the Cherokee Nuclear Station site ([Reference 205](#), PSAR, Appendix 2C, Table 2C-2). The mineralogical characterizations of these rock types including description of rock name, estimated modal mineralogy, primary and secondary textures and structures, and alteration and metamorphism features are described in the following paragraphs.

Meta-quartz diorite at the site probably formed by hydrothermal alteration and regional dynamo-thermal metamorphism of quartz diorite intrusions. This rock type composes the bulk of the bedrock at the Lee Nuclear Station Site. Samples examined contain 38% to 55% plagioclase, 18% and 26% quartz, 5% to 20% biotite, 5% to 18% sericite, up to 9% actinolite, 3% to 10% ferroan calcite, and traces of chlorite, clinozoisite, apatite, FeOH, zircon, and opaques. Texturally, the meta-quartz diorite is phaneritic, holocrystalline, equigranular, fine to medium grained with a non- to weakly directed fabric. [Figure 2.5.4-203](#) shows a representative hand sample photograph and photomicrograph of typical meta-quartz diorite.

Mica schist found on the site probably formed by hydrothermal alteration and regional dynamo-thermal metamorphism of fine grained siliciclastic or feldspathic sedimentary protoliths. These samples are composed of 25% to 68% quartz, 8% to 40% biotite, 10% to 35% sericite, up to 10% plagioclase, 3% to 10% ferroan calcite and traces of chlorite, clinozoisite, and opaques. Texturally the mica schist is phaneritic, holocrystalline, porphyroblastic to granoblastic, fine grained, and has

a non-directed to moderately directed fabric. [Figure 2.5.4-204](#) shows a representative hand sample photograph and photomicrograph of typical mica schist.

Meta-dacite porphyry rock on the site probably formed by hydrothermal alteration of dacite porphyry shallow intrusions. These samples are composed of 45% to 65% plagioclase, 18% to 25% biotite, 8% to 15% quartz, up to 18% actinolite and traces of ferroan calcite, chlorite, apatite, garnet, and opaques. Texturally these samples are phaneritic, holocrystalline, porphyritic, fine to coarse grained and have a non-directed fabric. [Figure 2.5.4-205](#) shows a representative hand sample photograph and photomicrograph of typical meta-dacite.

Meta-basalt at the site probably formed by hydrothermal alteration of an aphanitic basalt protolith. These samples are composed of 36% to 41% plagioclase, 25% to 30% actinolite, up to 10% quartz, 5% to 10% clinozoisite / epidote, up to 9% biotite, 3% to 7% ferroan calcite and traces of K-feldspar, and opaques. Texturally these samples are phaneritic, holocrystalline, aphyric, equigranular, fine grained and have non-directed to moderately directed fabrics. [Figure 2.5.4-206](#) shows a representative hand sample photograph and photomicrograph of typical meta-basalt.

Numerous alteration features were noted in the examination of the thin-sections. Many of the samples had fine intrusive veins containing some or all of: quartz, ferroan calcite, sericite, biotite, and K-feldspar. Cataclastic and ductile metamorphism features were also noted. Some biotite has altered to chlorite and opaque minerals. Some plagioclase has weakly to moderately altered to sericite, ferroan calcite, chlorite, clinozoisite, and/or K-feldspar. Some actinolite has weakly altered to ferroan calcite.

Foliation joints, typically at high angles, are the most common type of discontinuities found within the partially weathered and slightly weathered bedrock. Foliation features were observed in both outcrop exposures, hand sample sized specimens and in petrologic examination of thin sections. Foliation planes represent zones of weakness within the rock and when additional stresses act on the rock (e.g., diamond coring), it is these zones that preferentially fracture. It is important to note that the more highly fractured rock, classified as partially weathered rock, was excavated and removed during construction of the Cherokee Nuclear Station Unit 1, excavated and removed on Unit 2 and partially excavated on Unit 3. The exposed slightly weathered bedrock has very few discontinuities, and these do not represent significant zones of weakness.

Rock at the Lee Nuclear Station Site is not soluble in groundwater. While some are composed of up to 10% ferroan calcite, this mineral is broadly distributed within the rock mass. If it were to completely weather out, which is highly unlikely, it would not leave voids of large size to endanger safety-related structures, or sufficiently interconnected to serve as a significant groundwater flow path.

2.5.4.1.3 Groundwater

The primary drainage in the site area is the Broad River and associated tributary drainages. Typical of most first order Piedmont streams, the Broad River flows southeast directly across the regional trend of most geologic contacts and structure. The streambed is at about 500 ft msl and has incised into the Piedmont surface about 200 ft below the drainage divides. The Broad River lacks a well-developed flood plain in the Lee Nuclear Station Site area.

The high historic groundwater level in the plant area is at Elevation 579 ft. msl. This elevation value is based on the existing well delineated high water mark along the exterior of the Cherokee Nuclear Station (CNS) Unit 1 reactor building. The existing excavations flooded naturally after cessation of dewatering operations when the plant construction was halted in the early 1980's. The water level in the excavations rose to, or near, the typical (static) groundwater table and remained in this state for over 20 years prior to dewatering for the Lee Nuclear Station project. Long-term standing water in the vacated CNS excavation left a high water mark on the partially constructed CNS Unit 1 reactor building structure that was surveyed at an elevation of 579 ft. msl. The design groundwater level for Lee Nuclear Station is Elevation 579±5 ft. msl, allowing for a 5-foot seasonal variation over the high water mark level. Numerical analysis confirmed that the maximum post-construction groundwater level anticipated at Lee Nuclear Station is bounded by elevation 584 ft. msl (see [Subsection 2.4.12.2.3.1](#) and [Table 2.0-201](#)).

2.5.4.1.4 Effects of Human Activities

Human activities such as mining or groundwater withdrawal have the potential to cause surface deformation. There are no mining operations with the potential to impact the Lee Nuclear Station Site. There is no excessive extraction or injection of groundwater, or impoundment of water occurring within the site area that can affect geologic conditions. One active sand mine, hydraulic dredge and wash operation, is located along the Broad River approximately one mile north of the Site. This mining operation does not present a potential hazard to the Lee Nuclear Station Site.

RIS associated with the filling and operation of Make-Up Pond C is considered negligible, and it is unlikely the induced magnitudes would exceed $M > 4$, a value well below the short-period controlling earthquake. Evaluations related to the potential of RIS associated with Make-Up Pond C are described in [Subsection 2.5.2.1.3](#).

2.5.4.1.5 Summary of Geologic Hazards

The Lee Nuclear Station Site investigation did not encounter adverse geologic conditions in the safety-related explorations that pose a stability or surface hazard. Major safety related structures can be founded on fresh, hard bedrock or on engineered fill placed over fresh, hard bedrock.

There are no significant unrelieved stresses in the bedrock that could cause creep or rebound. Erosion rates are slow. These conditions are not conducive to "locked-in" residual stresses.

No zones of alteration or structural weakness are present. Bedrock contains foliation joints and foliated zones, which do not significantly reduce rock strength.

There are no human activities, such as mining or groundwater extraction, which could cause subsidence or collapse.

As noted in [Subsection 2.5.3](#), earthquake activity with its resulting ground motion effects is judged to be the primary geologic hazard to the Lee Nuclear Station Site. The potential for tectonic surface deformation within the site area is judged to be negligible. The potential for non-tectonic surface deformation within the site area, including surface deformation associated with potential Make-Up Pond C RIS, is negligible. A detailed discussion of vibratory ground motion and potential for surface faulting at the Lee Nuclear Station Site is presented in [Subsections 2.5.2](#) and [2.5.3](#), respectively.

2.5.4.2 Properties of Subsurface Materials

WLS COL 2.5-6 This subsection presents a summary of the field investigation and subsurface material properties at the Lee Nuclear Station Site. The laboratory testing and sample control procedures are discussed as well. Refer to [Subsection 2.5.4.3](#) for drawings showing the boring and other field investigation locations and for sections of the subsurface conditions. Soil, granular fill, and rock dynamic material properties are presented in [Subsection 2.5.4.7](#).

The procedures used to perform field investigations for determining the engineering properties of soil and rock materials conform to Regulatory Guide 1.132, "Site Investigations for Foundations of Nuclear Power Plants." The field exploration and laboratory testing program conform with this regulatory standard.

Information from literature, regional and local maps, and historical information from exploration activities completed for the Cherokee Nuclear Station were all used as additional guidance for planning the field exploration program. The exploration program included multiple methods of exploration and utilized both traditional and state-of-the-practice methods of subsurface exploration and in situ testing. Soil and rock sampling was planned to meet the requirements for spacing, depth, and sample frequency provided in the regulatory guide. Borings in the nuclear island foundation areas were generally extended at least 20 feet into sound rock materials in accordance with the guidance from Regulatory Guide 1.132. Geophysical testing was included in the exploration program and included both surface and borehole geophysical methods. Samples of site materials obtained during the exploration work were documented and logged by geologists and engineers and preserved in the field for further analysis and laboratory testing. Further details regarding the field exploration program are

provided in [Subsections 2.5.4.2.1](#) and [2.5.4.2.2](#). The field exploration and laboratory testing plan provide detailed coverage of the safety-related structures and other site areas. This information was integrated with available historic site data and published information to develop a comprehensive characterization and evaluation of the subsurface materials.

The laboratory testing program was planned and conducted using the guidance provided by Regulatory Guide 1.138. Information from the historic field exploration program, literature, and information from the historic laboratory testing completed for the Cherokee Nuclear Station were all used as additional guidance for planning the laboratory testing program for Lee Nuclear Station. The laboratory testing program for soil included samples obtained using disturbed and undisturbed sampling methods. The testing program included a variety of tests on the significant soil and rock materials encountered during the field exploration program. Static and dynamic laboratory test methods were performed. Further details regarding the laboratory testing program are provided in [Subsections 2.5.4.2.3](#) and [2.5.4.2.4](#). Liquefaction potential of the foundation materials is discussed in [Subsection 2.5.4.8](#).

2.5.4.2.1 Site Explorations

WLS COL 2.5-6 Site subsurface exploration described in this subsection includes soil and rock borings, installation of groundwater monitoring wells and performing packer tests, surface geophysical surveys, cone penetration testing (standard and seismic), geotechnical test pit and geologic trench excavations, and borehole and geophysical in situ testing methods. These explorations (referred to as exploration points) were performed specifically for the Lee Nuclear Station Unit 1 and Unit 2. Geophysical explorations are described in [Subsection 2.5.4.4](#). The number and type of explorations performed for the Lee Nuclear Station investigations are summarized in the following tables.

- [Table 2.5.4-202](#) Summary of Lee Nuclear Station Geotechnical Exploration
- [Table 2.5.4-203](#) Summary of Completed Exploration Borings and Field Tests
- [Table 2.5.4-204](#) Summary of Geotechnical Borings for Completed Monitoring Wells
- [Table 2.5.4-205](#) Summary of Completed Cone Penetrometer Test Soundings
- [Table 2.5.4-206](#) Summary of Completed Geotechnical Test Pit and Geologic Trench Locations

- **Table 2.5.4-207** Summary of Completed Surface Geophysical Test Locations

The exploration map explanation is provided in **Figure 2.5.4-207**. The site exploration points for the complete site geotechnical exploration are shown on **Figure 2.5.4-208**. The exploration points for the Lee Nuclear Station power blocks and adjacent areas are shown on **Figure 2.5.4-209**.

The as-built site explorations were recorded by horizontal and vertical survey of the locations. Horizontal and vertical surveys were completed to third order accuracy standards. The surveyed horizontal and vertical coordinate values are provided on the individual test results (logs, records, etc.) for surface exploration points.

Site explorations were also performed at this site location prior to construction of the Cherokee Nuclear Station. The historic exploration results from the Cherokee Nuclear Station work are published in the Cherokee Nuclear Station Preliminary Safety Analysis Report (**Reference 201**) and additionally, more historic explorations were conducted during construction of the Cherokee Nuclear Station. These historic explorations from the Cherokee Nuclear Station were used to guide the planning of additional explorations made during the Lee Nuclear Station exploration. Portions of the historic Cherokee Nuclear Station exploratory work are used to supplement the information obtained specifically for Lee Nuclear Station. These Cherokee Nuclear Station results, where mentioned in the following text, are identified as historic results.

2.5.4.2.1.1 Soil, Rock, and Concrete Borings

Subsurface explorations were performed using geotechnical drill rigs mounted on trucks or tracked vehicles. Specific equipment used at each borehole is recorded on the boring logs. Field boring logs and other field records were maintained by a rig geologist (geologist or geotechnical engineer). A rig geologist was assigned to each drill rig and was responsible for maintaining the field records associated with activities conducted at a specific exploration point.

Borings for geotechnical purposes were advanced in soil using solid or hollow stem auger and/or mud rotary (wash) drilling techniques until refusal (defined as the physical inability to advance the hole using soil drilling procedures) was encountered. In geotechnical borings the drilling method for depths greater than 15 ft was generally mud rotary (wash) drilling. Standard Penetration Test (SPT) samples were typically obtained on 5-foot intervals, beginning 3.5 ft. below ground surface, in soil materials. Additional details concerning sampling are provided in **Subsection 2.5.4.2.2.1**.

The Cherokee Nuclear Station Unit 1 structure had to be penetrated with geotechnical borings to explore the underlying materials for the Lee Nuclear Station geotechnical investigation.

Structural concrete from the Cherokee Nuclear Station Unit 1 structure was pre-cored using a thin-walled concrete coring machine. The 6-inch diameter

thin-walled bit was advanced through the upper and lower level rebar within the structural slab. Coring continued to depths of approximately 4 to 6 ft. or approximately 6 to 12 inches beyond the lower level rebar. The concrete plug was removed and geotechnical core drills were used to continue coring to the final depth.

Once refusal was encountered, and if rock coring was required, a steel or PVC casing was set if soil was present. The holes were advanced using wire-line rock coring equipment and procedures, ASTM D 2113-99. A five-foot or ten-foot long NQ or HQ size core barrel was used for all rock coring. Additional details concerning coring are provided in [Subsection 2.5.4.2.2.2](#).

Permanent PVC casing was installed and grouted in place extending a short distance above the soil or rock surface in several locations where downhole geophysics was assigned. PVC casing for this purpose was 4-inch diameter riser pipe grouted in place using a cement bentonite grout mix to provide a consistent seal between the casing and the surrounding soil and rock.

The boreholes, including the grouted-in PVC casings for geophysical tests, were filled using a cement-bentonite grout prior to demobilizing from the site. The grout was placed by pumping through a tremie pipe.

Copies of Lee Nuclear Station exploration records including boring logs and monitoring well construction diagrams, SPT energy measurements, geotechnical test pit and geologic trench logs, and packer test results are provided in [Appendix 2AA](#). This appendix is comprised of five attachments as described below.

- [Appendix 2AA](#), Attachment 1, Lee Nuclear Station Geotechnical Borings Logs and Groundwater Monitoring Well Construction Logs
- [Appendix 2AA](#), Attachment 2, Lee Nuclear Station SPT Energy Measurements
- [Appendix 2AA](#), Attachment 3, Lee Nuclear Station Geotechnical Test Pit and Geologic Trench Logs
- [Appendix 2AA](#), Attachment 4, Lee Nuclear Station Packer Test Results
- [Appendix 2AA](#), Attachment 5, Lee Nuclear Station Cone Penetration Testing Logs.
- [Appendix 2AA](#), Attachment 6, Lee Nuclear Station Geotechnical Boring Logs, 2012 Exploration.

Copies of Cherokee Nuclear Station historic geotechnical boring logs are provided in [Appendix 2BB](#). These borings logs represent historic records that were developed during various stages of field exploration for the Cherokee Nuclear Station.

2.5.4.2.1.2 Groundwater Monitoring Wells

Geotechnical exploratory borings for Monitoring Well (MW) locations were generally drilled using hollow stem augers through which a Central Mine Equipment Company (CME) type continuous soil sampler was used. In some instances, a geoprobe continuous sampler was used. Continuous samples were obtained in 5-foot segments beginning 3.5 feet below the initial ground surface. The CME sampling continued to refusal after which NQ rock coring was utilized to reach the required borehole depth. Occasionally refusal of the CME sampler was reached prior to reaching material suitable for rock coring. When this occurred, rotary drilling using wash water without bentonite was used to advance the borehole combined with Standard Penetration Test sampling to obtain samples until material suitable for NQ coring was reached.

Observation wells were installed in hollow stem auger or air rotary drilled holes of appropriate diameter (at least 6 inches). The wells consist of 2-inch diameter PVC screen and riser pipe, sand filter pack, bentonite chips or pellets, and cement bentonite grout. Protective steel well covers and concrete pads were placed at the surface. One 6-inch diameter well of similar construction was installed to use as a pumping well for permeability testing. The location of groundwater monitoring wells constructed as part of the Lee Nuclear Station exploration is shown on [Figure 2.5.4-210](#).

WLS SUP 2.5-2 The exploratory boreholes for monitoring well locations were backfilled as
WLS SUP 2.5-3 described above. PVC monitoring well locations were not grouted, but were left open for continued monitoring.

Additional information regarding the groundwater monitoring wells is included in [Subsection 2.4.12](#).

2.5.4.2.1.3 Surface Geophysical Testing

Surface geophysical testing was performed using the Spectral Analysis of Surface Waves (SASW) technique. Fifteen SASW surveys were performed during site investigation activities at the Lee Nuclear Station Site. Survey depths ranged from tens of feet up to approximately 150 feet below ground surface, depending on material attenuation conditions and length of survey lines. [Figure 2.5.4-211](#) shows the locations of SASW survey lines at the Lee Nuclear Station Site. Discussion of SASW survey testing methodology and results is located in [Subsection 2.5.4.4.1](#).

2.5.4.2.1.4 Cone Penetration Testing

Cone Penetration Testing (CPT) was performed at twenty-nine locations using a 20 ton self-contained rig mounted on a tracked all-terrain vehicle. CPT locations were advanced to an assigned depth or to the depth of refusal of the CPT probe. The CPT testing was performed using an electronic cone system. CPT measurements were performed using procedures described in ASTM D 5778-95.

Seismic Cone Penetration Testing (SCPT) was completed in ten of the CPT locations at intervals of one meter. Of these tests, nine provided useful data. Pore

pressure dissipation tests were performed in twelve of the CPT locations at depths selected during performance of the CPT.

Figure 2.5.4-212 shows the CPT and SCPT test locations performed as part of the Lee Nuclear Station exploration. Discussion of the SCPT testing methodology and results is described in Subsection 2.5.4.4.2.

2.5.4.2.1.5 Geotechnical Test Pits and Geologic Trenches

Both geotechnical test pits and geologic trenches were excavated during Lee Nuclear Station Site investigations. Geotechnical test pits were designed to collect bulk samples for laboratory testing, and the geologic trenches were designed to examine large-scale subsurface geologic features.

Geotechnical test pits and geologic trenches were excavated at fourteen locations, to depths ranging from approximately 4 feet up to 20 feet. A track-mounted backhoe was used to excavate and then later to backfill the test pits. A rig geologist selected the materials to be sampled and collected the bulk samples. At each test pit, portions of soil from the upper 3 feet were collected and combined to form a single representative bulk sample of surface material at that particular location. Sampling of geotechnical test pits is described in Subsection 2.5.4.2.2.4.

The four corners of the geotechnical test pit or geologic trench were marked and are documented in the survey record. The survey coordinates for the northernmost corner of the geotechnical test pits and geologic trenches are summarized in Table 2.5.4-206. The locations of test pits and trenches excavated as part of the Lee Nuclear Station exploration is shown on Figure 2.5.4-213.

2.5.4.2.1.6 In Situ Testing

In situ testing was performed to estimate elastic compressibility properties of rock materials using the Goodman Jack and borehole pressuremeter. In situ testing was also performed in rock materials using downhole geophysical techniques including optical televiewer, acoustic televiewer, P-S suspension logging, and downhole velocity logging. Some P-S suspension logging was also performed in soil materials. In situ testing to estimate the permeability of rock materials was performed using the borehole packer test.

2.5.4.2.1.6.1 Goodman Jack Testing

Fourteen Goodman Jack tests were performed in two boreholes at multiple depth intervals to measure elastic modulus in situ using procedures described in ASTM D 4971-02. The Goodman Jack is a borehole probe used for the measurement of wall deformation as a function of applied load. Data obtained from the load-deformation measurements gives the elastic modulus of rock directly. Hydraulic pressure is transmitted to the rock through the movable plates.

2.5.4.2.1.6.2 Borehole Pressuremeter Testing

Twenty-four pressuremeter tests were performed in two boreholes at multiple depth intervals to measure elastic modulus in situ using procedures described in ASTM D 4719-00. Of these tests, twenty-two provided useful data. The pressuremeter test is an in situ stress-strain test performed on the wall of a borehole using a cylindrical probe that is expanded radially.

The Goodman Jack and borehole pressuremeter test locations performed as part of the Lee Nuclear Station exploration are shown on [Figure 2.5.4-214](#). [Tables 2.5.4-208](#) and [2.5.4-209](#) present the results of Goodman Jack and borehole pressuremeter tests, respectively.

2.5.4.2.1.6.3 Borehole Geophysical Testing

Geophysical testing using multiple test methods was performed in fifteen borings. Geophysical logging performed included P-S suspension logging in thirteen borings with comparative downhole velocity profiles in four selected borings, and borehole televiewer logging in thirteen borings using optical and/or acoustic methods. Test procedures and results of the downhole geophysical testing are presented in [Subsection 2.5.4.4](#). The borehole geophysical test locations performed as part of the Lee Nuclear Station 2006-2007 exploration and 2012 exploration are shown on [Figure 2.5.4-215](#).

2.5.4.2.1.6.4 Packer Testing

Field permeability testing by the packer method was conducted in selected borings using test procedures described in ASTM D 4630-96 (2002), modified to use a manually-read flow meter rather than a digitally recorded one. The packer testing method involved establishing and maintaining a constant pressure in the packer test interval or test length, measured by a gauge at the surface, and determining the rate of inflow associated with maintaining the pressure. The test method is thus known as the “constant head injection test.” Three or more pressure values were generally used in each assigned test interval. The purpose of the packer testing was to establish the coefficient of permeability (also called hydraulic conductivity) of the rock within the packer test length. The packer test locations performed as part of the Lee Nuclear Station exploration are shown on [Figure 2.5.4-210](#).

2.5.4.2.1.7 Petrographic Testing

Petrographic testing was performed on fifteen rock core samples collected from nine borings. Selected rock core samples were prepared into standard 27 x 46 mm covered thin sections stained for K-feldspar and calcite/ferroan carbonate. Petrographic analyses and photomicrography of thin sections was performed using a petrographic microscope at magnifications ranging from 25X to 500X. The petrographic test locations performed as part of the Lee Nuclear Station exploration are shown on [Figure 2.5.4-216](#).

2.5.4.2.2 Soil and Rock Sampling

2.5.4.2.2.1 Standard Penetration Test Sampling

Soil sampling in the geotechnical borings using the SPT was generally conducted at intervals of 5 feet using equipment and methods described in ASTM D 1586-99. Sampling generally started at 3.5 feet below the ground surface. Automatic hammers were used to perform the SPT tests. The sampler was typically driven 18 inches in soil with blows recorded for each six-inch interval of penetration. In very hard soils and weathered rock, driving was terminated at 50 blows and the actual penetration recorded for the penetrated interval (e.g., 50 blows / 3 inches).

Fill soils in place at the site at the time of the Lee Nuclear Station explorations in 2006 and 2007 were explored in detail to assist in characterizing the backfill that was initially planned to be used around the Lee Nuclear Station Unit 1 and Unit 2 nuclear island areas. These fill soils were in-place at the time of the Lee Nuclear Station exploration in 2006 and 2007 and had been placed and compacted during site preparation work for the Cherokee Nuclear Station. These areas where fill materials were explored were designated "test fill" areas. In several borings drilled in the "test fill" areas, SPT sampling was conducted at intervals of 2 feet. For these locations a 30-inch sampler was used and was driven 24 inches with blows recorded for each six-inch interval of penetration. Sampling at these "test fill" locations started at the ground surface. Subsequent to the exploration of the "test fill" areas, a decision was made that granular fill materials instead of fill soils will be used as backfill around the Lee Nuclear Station Unit 1 and Unit 2 nuclear island areas. Therefore, the "test fill" areas have no special significance subsequent to the decision to use granular fill.

In the geotechnical borings for the Lee Nuclear Station exploration in 2006 and 2007, the split tube sampler was opened at the drill site and the recovered materials were visually described and classified by the rig geologist. A selected portion of the sample was placed in a glass sample jar with a moisture-proof lid. Sample jars were labeled, placed in cardboard boxes, and transported to the on-site storage area.

Energy measurements were made on the drill rigs that performed SPT testing for the Lee Nuclear Station exploration. Energy measurements were recorded during sampling at several different depth intervals. The energy measurement work was done in general accordance with ASTM D 4633-05. The ratio of the average measured energy to the theoretical potential energy of the SPT system (140-pound weight with the specified 30-inch fall) is the energy transfer ratio (ETR).

The ETR range of the automatic hammers used at the Lee Nuclear Station Site is 76.8% to 82.8% of the theoretical potential energy. These ETR values are within the range of typical values for automatic hammers.

2.5.4.2.2.2 Coring

For the borings of the Lee Nuclear Station exploration in 2006-2007 and 2012, rock coring was performed, when assigned, for those materials that could not be penetrated with soil drilling methods. For purposes of determining the depth at which to begin rock coring procedures, refusal to soil drilling was defined as the physical inability to advance the hole using soil drilling procedures. Rock coring was performed in accordance with ASTM D 2113-99. Rock recovered by the coring process was carefully removed from the inner barrel and placed in wooden core boxes with wooden blocks used to mark ends of runs. Wood spacers were placed in the core box when needed to stabilize the core laterally. Filled core boxes were taken to the on-site sample storage facility. Photographs of the cores were taken in the field.

The rig geologist visually described the rock core and noted the presence of joints and fractures, distinguishing mechanical breaks from natural breaks where possible. The rig geologist also calculated percent recovery and Rock Quality Designation (RQD) prior to moving the core from the drill site. Field boring logs and photographs were used to document the drilling operations and recovered materials. The construction of casing for completion of drilling was recorded on a casing installation field log. In borings to be geophysically logged, PVC casing was grouted in place in lieu of the temporary casing. The grouting process was recorded on grouting field logs.

2.5.4.2.2.3 Undisturbed Sampling

For the Lee Nuclear Station exploration in 2006 and 2007, undisturbed samples were taken in separately drilled boreholes located adjacent to geotechnical boring locations. Undisturbed soil samples were taken using a 3-inch diameter thin-walled tube sampler in accordance with ASTM D 1587-00. Depth intervals for undisturbed samples were assigned based on a review of the field log from the geotechnical boring.

When subsurface material was too dense or hard to allow satisfactory samples to be recovered by pressing the tube sampler into the material, a Pitcher sampler was used. The Pitcher is a rotary sampler which drills the 3-inch tube into the subsurface material. Pitcher samplers were generally used when SPT blow counts from the adjacent borehole were greater than 30 blows per foot at the desired sample depth. Undisturbed samples were sealed at the top and bottom against moisture loss, labeled, kept in an upright condition, and transported to the climate-controlled on-site storage area in accordance with ASTM D 4220-95 (2000).

2.5.4.2.2.4 Bulk Sampling (Test Pits)

For the Lee Nuclear Station exploration in 2006 and 2007, a track mounted backhoe was used to excavate and backfill the test pits for soil sampling purposes. Bulk samples were obtained from the materials excavated from the test pit. A rig geologist selected the materials to be sampled and collected the bulk samples. Bulk samples were placed in new 5-gallon plastic buckets with lids and

handles for carrying. Glass jar samples were obtained and sealed for moisture retention. The buckets and jar samples were labeled and transported to the on-site storage area. The rig geologist prepared a Geotechnical Test Pit Log based on visual description of the excavated materials according to ASTM D 2488-00. The backhoe was used to backfill the test pit excavation using the excavated materials. The backfilled materials were tamped in-place using the backhoe bucket.

The bulk sampling of the geotechnical test pits was for testing to characterize soils for use in constructing Group I fill. Group I fill is a term specific to the former Cherokee Nuclear Station construction documents. Group I fill is a conventional quality fill of selected soil types compacted to 95 percent of the standard Proctor (ASTM D 698-00) maximum dry density. Group I fill performs no safety function for the Lee Nuclear Station because select granular fill materials surround the nuclear islands and support the structures adjacent to the nuclear islands. No further reference to the Group I fill testing or results is contained herein. Group I fill is illustrated on selected figures to convey the backfill relationship of select granular fill and Group I fill within the existing excavation.

2.5.4.2.2.5 Sample Control and Preservation

An on-site sample storage facility was established for the Lee Nuclear Station exploration in 2006-2007 and 2012 in a warehouse building that remained on-site from Cherokee Nuclear Station Site construction activities. Electrical power, overhead lighting, and a ventilation fan were installed in the warehouse building. A travel trailer was brought to the site to serve as the field office during site exploration. The field office trailer was located inside the sample storage facility and housed the on-site temporary file storage system and provided office space for the field geologists and engineers. The warehouse building was not climate controlled; however, the field office trailer was capable of providing a climate controlled environment when necessary, such as for storage of undisturbed samples. The warehouse building served as the sample storage facility, supply storage building, sample examination area, and field exploration project headquarters.

Soil samples were obtained from split spoon sampler or undisturbed tube samples as part of the geotechnical exploration process for the Lee Nuclear Station exploration in 2006 and 2007. Split spoon samples were placed in glass jars and sealed with a moisture-tight lid. Undisturbed tube samples were sealed on both ends in the field using beeswax, covered with plastic caps, and sealed with duct tape. All samples were labeled with identifying information and transferred to the on-site lockable temporary storage area.

Samples were transported daily from the field to the sample storage warehouse by the rig geologists. SPT samples were transported as Group B samples in their compartmentalized cardboard boxes, each labeled to show the contents. The CME soil core samples and rock cores were transported in wooden core boxes, kept horizontal, and labeled to show the contents. The undisturbed tube samples were transported according to ASTM D 4220-95 (2000), Group C samples. Undisturbed samples were stored inside the field office trailer which provided a

climate-controlled environment until the samples could be transported to the laboratory. Rock and concrete cores were transported according to ASTM D 5079-02 (2006).

A portion of the warehouse was designated as the sample storage area. Rock core boxes were placed on wooden pallets located within the sample storage area of the warehouse and were grouped by boring. SPT sample boxes were placed with the core boxes for borings having both SPT sampling and coring. For borings with SPT sampling only, SPT samples were placed on wood tables inside the sample storage area of the warehouse. Test pit sample buckets were also placed within the sample storage area.

Boring field records were reviewed and samples were identified for possible laboratory testing. Work instructions were issued listing samples to be removed from the site storage and shipped to the laboratories. Following the work instructions, samples were removed from the site storage area and prepared for shipping.

Soil samples were handled and transported or shipped to the appropriate laboratory in accordance with ASTM D 4220. Samples for index testing were handled as Group B samples, while undisturbed tube samples were handled as Group C samples. The undisturbed samples were transported by MACTEC or WLA personnel in personal, company, or rented passenger vehicles. All samples were shipped under chain of custody, and the receiving laboratory signed for them upon receipt. At the laboratory, prior to testing, the undisturbed samples were stored in the controlled laboratory environment in a secure location. Work instructions were prepared by MACTEC engineers and provided to the laboratories.

For soil samples which were selected for chemical testing, a portion of the total sample received was prepared by MACTEC laboratory personnel, as directed in a work instruction, and placed in jars with moisture-tight lids before being shipped under chain of custody to the chemical testing laboratory.

Representative portions of jar and undisturbed tube samples were taken to complete the assigned tests. In many cases, the entire sample was used for testing. Some unused portions of the jar or undisturbed tube sample were returned to the sample storage facility if the portion was of reasonable size.

2.5.4.2.3 Laboratory Testing

For the Lee Nuclear Station exploration in 2006 and 2007, laboratory testing was performed on disturbed, undisturbed, and bulk soil samples, and on rock cores obtained during the subsurface investigation. Testing was performed in accordance with ASTM standards or other standards where applicable. Other standards used for laboratory testing included Environmental Protection Agency methods for chemical analysis of soils. No additional laboratory tests were performed in 2012.

The quantity of each test completed on each sample type is identified in [Table 2.5.4-210](#). Test standards used for laboratory testing are listed in this subsection. Laboratory testing was in accordance with the standard method or procedure. Additional descriptions for selected test methods are provided in [Subsections 2.5.4.2.3.1](#) through [2.5.4.2.3.12](#).

- Moisture content, ASTM D 2216-05
- Atterberg limits, ASTM D 4318-05
- Grain size testing (sieve + hydrometer and sieve), ASTM D 422-63 (2002) and ASTM D 6913-04
- Specific gravity, ASTM D 854-06
- Chemical analysis,
 - pH, ASTM G 51-95 (2005)
 - Resistivity, ASTM G 57-95a (2001)
 - Chloride, EPA SW-846 9056/300.0,
 - Sulfate, EPA SW-846 8056/300.0
- Unit weight of soil, ASTM D 5084-03 (Sections 5.7 – 5.9, 8.1, 11.3.2)
- Consolidated-undrained triaxial shear, ASTM D 4767-04
- Specimen preparation – rock cores, ASTM D 4543-04
- Compressive strength and elastic moduli – rock cores, ASTM D 7012-04
- Consolidation tests, ASTM D 2435-04

Petrographic analysis of selected rock samples was also performed. The descriptions and results of petrographic analyses are provided in [Subsection 2.5.4.1](#) and [Table 2.5.4-201](#).

2.5.4.2.3.1 Particle Size Analysis, ASTM D 422-63 (2002) and ASTM D 6913-04

Sieve Analysis – The dried soil sample is separated into a series of fractions using a standard set of nested sieves. The sieving operation is conducted by means of a lateral and vertical motion of the nest of sieves, accompanied by jarring action to keep the sample moving continuously over the surface of the sieves. The weights retained on each of the set of nested sieves are used to calculate the percent of the sample passing each sieve size.

Hydrometer Analysis – The portion of the soil sample passing the No. 200 (75 micrometers) sieve is soaked in water and dispersed using a dispersing agent. The solution is placed in a cylinder and stirred, and the density of the solution is monitored over time with a hydrometer to observe the settling out of suspended soil particles. Diameters corresponding to the readings of the hydrometer are then calculated using Stoke's law.

At the time of laboratory testing ASTM D 6913-04 was the current specification for grain size analysis, but it did not include hydrometer testing. Where hydrometer testing was required, Section 1.4 of the specification allows that ASTM D 422 – 63 (2002) be used.

Section 5.1.1 of ASTM D 422 – 63 (2002) and Table 1 of ASTM D 6913 – 04 give minimum sample mass requirements (the minimum depends on the maximum particle size present) for each test. In cases where there was not enough sample to meet the appropriate recommended mass, the test was completed using the available sample and it was noted in the Remarks section of the Particle Size Distribution Report.

2.5.4.2.3.2 Chemical Analysis (pH, Resistivity), ASTM G 51-95 (2005), ASTM G 57-95a (2001)

For purposes of corrosion testing, soil pH measurements in the laboratory are made within 24 hours from the time of sampling. Measurements are made at the soil's natural moisture content using a pH-sensitive electrode system, and reported to the nearest 0.1 pH units. Soil resistivity measurements indicate the ability of soil to resist electrical currents, and are the reciprocal of electrical conductivity. Resistivity was reported in units of Ohm-cm at the natural ("as received") moisture content and saturated.

2.5.4.2.3.3 Chemical Analysis (Chloride, Sulfate), EPA SW-846 9056/300.0, EPA SW-846 8056/300.0

A small quantity of soil was split from the original sample, placed in a separate clean jar, and sent to the laboratory for analysis of chloride ion and sulfate ion concentration. The concentrations are measured using an ion chromatograph with results reported in units of milligrams per kilogram. In many cases the measured concentrations were below the reporting limit of the test equipment, and were noted as estimated results less than the reporting limit in the report.

2.5.4.2.3.4 Unit Weight of Soil, ASTM D 5084-03 (Sections 5.7 – 5.9. 8.1, 11.3.2)

Sections of the undisturbed samples were extruded from the sampling tubes and trimmed to remove any surface irregularities. Dimensions of the sample were measured and recorded and the weight is determined. Unit weight is calculated by dividing the sample weight by volume. If the moisture content is known, dry unit weight can be calculated by dividing the wet sample unit weight by the quantity (1 + moisture content, in decimal format).

2.5.4.2.3.5 Deleted

2.5.4.2.3.6 Deleted

2.5.4.2.3.7 Consolidated – Undrained Triaxial Shear Testing,
ASTM D 4767-04

Consolidated – undrained (CU) testing was performed on undisturbed test specimens. Undisturbed specimens were extruded from sampling tubes and trimmed to appropriate dimensions. The specimens, encased in the rubber membranes, were then saturated by back-pressure prior to shearing. Drainage was allowed from the specimen during the consolidation phase, thus allowing equilibrium under the confining stress, but no drainage was allowed during the loading phase. For undisturbed specimens failure was defined at the point of maximum pore pressure. The maximum pore pressure failure criterion was investigated to compare with historic triaxial tests performed for construction of the former Cherokee Nuclear Station. Information contained in Brandon, et al. (2006) confirms the conclusion that peak pore pressure is a conservative method for assigning the failure criterion for the CU triaxial tests ([Reference 210](#)).

Vertical load, vertical displacement, chamber pressure, and pore pressures generated during the loading phase were measured. The test is termed consolidated-undrained and total stresses result if no pore pressure corrections are included. When the pore pressures generated during the loading phase are subtracted from the total stresses, effective stresses result.

Section 8.2.3.1 of the ASTM standard describes how to determine when the specimen is saturated. Specifically, it states that a sample is considered saturated if the B-parameter is equal to 0.95 or greater, or if B remains unchanged with additional increments of back-pressure.

2.5.4.2.3.8 Deleted

2.5.4.2.3.9 Deleted

2.5.4.2.3.10 Specimen Preparation – Rock Cores, ASTM D 4543-04

This procedure specifies the methods for laboratory specimen preparation and determination of the length and diameter of rock core specimens and the conformance of the dimensions with established standards. Because the dimensional, shape, and surface tolerances of rock core specimens are important for determining rock properties of intact specimens, great care must be exercised when preparing core samples for strength testing. The prepared cores are measured to determine the straightness of elements on the cylindrical surface, flatness of the specimen ends, parallelism of the specimen ends, and perpendicularity of end surfaces to the specimen axis.

Possible deviations to core preparation include side straightness, end flatness, parallelism, and perpendicularity. Deviations to the specimen preparation criteria

were unavoidable for several cores. Where deviations occurred they were reported on the individual test reports.

2.5.4.2.3.11 Compressive Strength and Elastic Moduli – Rock Cores, ASTM D 7012-04

This procedure specifies the manner in which to determine the strength of rock, in this case the uniaxial or unconfined compressive strength. This method also specifies the apparatus, instrumentation, and procedures for determining the stress-axial strain and the stress-lateral strain curves, as well as Young's modulus and Poisson's ratio.

The prepared specimen is placed in a loading frame and axial load is increased continuously on the specimen until peak load or failure of the specimen is obtained. To determine the elastic moduli, the specimen is instrumented with four strain gauges (two mounted axially, two mounted laterally) prior to placement in the loading frame. Axial strain gauges were 2 inches in length and lateral strain gauges were 1 inch in length. Axial load and deformation (axial and lateral) readings are obtained as the load is applied to the specimen. Unconfined compressive strength is determined based on the cross-sectional area and the maximum recorded load applied to the specimen. Young's modulus (the slope of the stress-axial strain curve) and Poisson's ratio (ratio of lateral strain to axial strain) are calculated using the strain gauge data from a portion of the data range generally between 40 and 60% of maximum strain. The specific data range for each core was individually selected based on review of the data. The selection utilized the average slope method over a range where both the axial and lateral stress-strain curves appeared most linear.

Two-inch axial strain gauges were used for all cores. Two-inch gauges were used to comply with the minimum axial strain gauge length of 10 mineral grain diameters specified in the test standard.

2.5.4.2.3.12 Consolidation Tests, ASTM D 2435-04

Sections of the undisturbed samples were extruded from the sampling tube for consolidation testing. The specimen was then trimmed into a disc 2.5 inches in diameter and 1-inch thick. The disc was confined in a stainless steel ring and sandwiched between porous plates. No saturation of the samples was performed, but the samples were carefully covered to prevent loss of moisture to evaporation during the test. The specimen was then subjected to incrementally increasing vertical loads and the resulting changes in specimen height with respect to time were measured with a linear variable differential transformer. The load increments were typically doubled with each loading phase, and deformation (consolidation) under each load increment was considered complete when the deformations versus time plot was analyzed using the log-time method.

The vertical load on the sample and number of loading increments varied slightly among the samples.

2.5.4.2.3.13 Deleted

2.5.4.2.3.14 Deleted

2.5.4.2.4 Material Properties

2.5.4.2.4.1 Geotechnical Model

A geotechnical model of the site was developed in the Cherokee Nuclear Station Preliminary Safety Analysis Report document prepared in the early to mid-1970s. This model has been adopted for use at the Lee Nuclear Station Site to maintain consistency with the work completed during Cherokee Nuclear Station construction activities. The conditions at the site are amenable to being classified into a geotechnical model that consists of existing engineered fill soils, alluvial soils, residual soils, saprolite, partially weathered rock (PWR), existing concrete, and rock. Also added to the model is the granular backfill material placed around the nuclear islands and beneath Seismic Category II structure adjacent to the nuclear islands. The explorations in 2012 encountered only rock and the pre-existing concrete; these materials are already included in the geotechnical model.

2.5.4.2.4.1.1 Pre-existing Engineered Fill Soils

The pre-existing site fill soils at the time of the Lee Nuclear Station geotechnical exploration in 2006-2007 were placed during the site grading activities for the Cherokee Nuclear Station project beginning in the mid 1970's and continuing until abandonment of the Cherokee Nuclear Station project in 1983. The fill soils characterized in this Subsection were constructed as Group 1 or Group 2 fills as defined in the Cherokee Nuclear Station Preliminary Safety Analysis Report. These fill soils were derived from the materials excavated from cut areas, and therefore their composition is made of the same soil types (predominantly ML and SM and relatively minor amounts of MH and CL) as the residual soil, saprolite, and partially weathered rock zones. None of these engineered fill soils will be adjacent to the walls of the nuclear islands or beneath the structures adjacent to the nuclear islands.

2.5.4.2.4.1.2 Alluvial Soils

In drainage channels and along the Broad River, residual soils washed from higher ground have settled to form alluvial deposits. During the Cherokee Nuclear Station construction, these alluvial soils were removed from beneath former safety-related man-made fills and structures such as the dam that now serves as the Lee Nuclear Station Make-Up Pond B Dam. Significant amounts of alluvial soil are not expected to remain anywhere within the areas explored for Lee Nuclear Station. Minor amounts of alluvial soil were encountered in borings B-1028, B-1052, MW-1205, and MW-1209 of the Lee Nuclear Station Site exploration.

2.5.4.2.4.1.3 Residual Soils

The residual soils are the near-surface zone of the pre-construction undisturbed profile. The residual soils have undergone relatively complete weathering, and

lack the relict features found in the saprolite zone. These are called the “B-horizon” soils in the Cherokee Nuclear Station Preliminary Safety Analysis Report. Most of the “B-horizon” soils at the site were utilized in the central core area of the former Cherokee Nuclear Station Nuclear Service Water Dam, now known as Lee Nuclear Station Make-Up Pond B Dam, so relatively minor amounts were encountered in the borings for the Lee Nuclear Station.

2.5.4.2.4.1.4 Saprolite Soils

Saprolite soils are the natural soils of the undisturbed weathering profile that retain relict features from the parent bedrock from which they were formed. The borings for Lee Nuclear Station found soil types consistent with data in the Cherokee Nuclear Station Preliminary Safety Analysis Report which indicates these saprolitic soils are comprised of about 2/3 of the samples being ML (silt of low plasticity), and about 1/3 being SM (silty sand).

2.5.4.2.4.1.5 Partially Weathered Rock

Partially Weathered Rock, termed PWR, is a transitional weathering zone between the saprolite and the less weathered bedrock. Texturally, the partially weathered rock materials are similar to the SM and ML soils in the overlying saprolite zone, but include more pieces of less weathered rock. As a practical matter and consistent with the Cherokee Nuclear Station Preliminary Safety Analysis Report, the PWR zone is usually associated with SPT values of 100 blows per foot or higher.

2.5.4.2.4.1.6 Pre-existing Concrete

Pre-existing reinforced concrete mat foundations and unreinforced fill concrete are present from the Cherokee Nuclear Station construction. The fill concrete was used to extend from the bottom of the Cherokee Nuclear Station foundation mats down to the rock foundation support. At the time of the Lee Nuclear Station exploration program in 2006, 2007, and 2012, the pre-existing concrete was encountered in the Cherokee Nuclear Station Unit 1 construction area. The Cherokee Nuclear Station concrete remains under portions of the Lee Nuclear Station Unit 1 structure, as described in [Subsection 2.5.4.5](#).

2.5.4.2.4.1.7 Rock

The parent bedrock materials underlie the residual soil, saprolite, and partially weathered rock throughout the site. The Cherokee Nuclear Station Preliminary Safety Analysis Report describes the rock as felsic and mafic gneiss, a metamorphic crystalline rock that is often closely banded and jointed. The Lee Nuclear Station Site exploration identifies rock as being made up of predominant rock types as described in [Subsection 2.5.4.1.2.2](#). The rock is fine to medium grained. Moderately dipping joints are healed with quartz and very thinly healed joints with calcite and epidote. The rock surface is uneven due to the differential depth to which weathering has advanced into the mass. The rock forms the foundation support for the Unit 1 and Unit 2 nuclear islands at the Lee Nuclear Station.

2.5.4.2.4.1.8 Granular Backfill

No safety-related structures will be placed on granular fill. Granular fill composed of select materials from a quarry rock crushing product will be placed and compacted around the walls of the nuclear islands and extending outward to form the support for the structures adjacent to the nuclear islands. These select granular materials will be compacted to a minimum relative compaction of 96 percent of the modified Proctor (ASTM D 1557-02) maximum dry density. [FSAR Subsection 3.7.2.8.4](#) describes the material property characteristics of the granular fill used to support Seismic Category II structures adjacent to the nuclear island.

2.5.4.2.4.2 Static Properties of Geotechnical Materials

Static geotechnical properties were compiled for the materials which comprise the Geotechnical Model, as described in [Subsection 2.5.4.2.4.1](#). Material properties for alluvial soils are not included due to the limited presence of these materials at the site.

Static geotechnical properties for the soil materials described in the Geotechnical Model are provided in [Table 2.5.4-211](#). [Table 2.5.4-211](#) lists soil properties used to support non-safety related structures as no safety related structures are supported on soil. No table values are listed for remolded fill soil samples as these materials are not used in the vicinity of the nuclear islands or beneath the structures adjacent to the nuclear islands. Only granular backfill materials are placed around the nuclear islands. The properties of the granular materials are used as input for calculation of the static and dynamic lateral earth pressure against the nuclear island walls. Corrosion test results (pH, resistivity, chlorides, and sulfates) for soil fill are provided in [Table 2.5.4-212](#). Static geotechnical properties for the granular backfill materials are provided in [Table 2.5.4-211](#). Table values listed for granular backfill materials are for typical granular materials and will be verified by laboratory testing when the source of and specific materials to be used are known, as outlined in [Table 2.5.4-222](#). Static geotechnical properties for the rock materials described in the Geotechnical Model are provided in [Table 2.5.4-213](#). The properties reported in these tables are average properties based on the laboratory results from samples obtained during the Lee Nuclear Station Site exploration in 2006 and 2007. Standard deviations are reported when the amount of data was sufficient to allow calculation of this value. Data from the Cherokee Nuclear Station Preliminary Safety Analysis Report was used, only where indicated in the table, to supplement the information obtained during the Lee Nuclear Station Site exploration for soils where limited data was available, such as the partially weathered rock.

Portions of the Cherokee Nuclear Station concrete that will remain under Lee Nuclear Station Unit 1 are described in [Subsection 2.5.4.5](#). The existing Cherokee Nuclear Station concrete meets the strength requirements for concrete in [DCD Subsection 2.5.4.1.3](#).

Dynamic geotechnical properties for the soil, granular fill, and rock materials described in the Geotechnical Model are described in [Subsection 2.5.4.7](#).

2.5.4.3 Foundation Interfaces

WLS COL 2.5-1 This Subsection provides graphically the relationship between site exploration, subsurface materials, and the foundations of seismic Category I facilities. The information was developed on the basis of field explorations performed at the Lee Nuclear Station Units 1 and 2 and on laboratory tests performed on soil and rock samples obtained during the field exploration program which took place in 2006-2007. Field investigations performed at the Cherokee Nuclear Station in the late 1970s and early 1980s ([Reference 201](#)), shown on [Figure 2.5.4-209](#), were also considered in this assessment, as these historic exploration points are co-located within the Lee Nuclear Station facility footprints.

The Lee Nuclear Station Site investigation program was conducted in 2006, 2007, and 2012. Geotechnical data collected during the field and laboratory exploration program were analyzed and evaluated. The analysis included preparing tables and figures that represent interpretations of the subsurface geotechnical conditions beneath and adjacent to safety-related structures.

2.5.4.3.1 Power Block Exploration

A comprehensive exploration program of surface geophysics, in situ testing, and subsurface drilling and sampling was conducted in 2006-2007 as shown in a site view on [Figure 2.5.4-208](#) and Power Block and Adjacent Areas on [Figure 2.5.4-209](#). These figures show the principal and secondary exploration borings and other field explorations performed. The historic boring locations on this figure are identified to distinguish them from the 2006-2007 boring and test locations. The locations of groundwater monitoring wells constructed and packer test performed as part of the Lee Nuclear Station exploration are shown on [Figure 2.5.4-210](#). [Figure 2.5.4-211](#) shows the location of SASW survey lines at the Lee Nuclear Station Site. The location of CPT tests performed as part of the Lee Nuclear Station exploration is shown on [Figure 2.5.4-212](#). The location of test pits and trenches excavated as part of the Lee Nuclear Station exploration is shown on [Figure 2.5.4-213](#). The Goodman Jack and borehole pressuremeter test locations performed as part of the Lee Nuclear Station exploration are shown on [Figure 2.5.4-214](#). The borehole geophysical test locations performed as part of the Lee Nuclear Station 2006-2007 exploration and 2012 exploration are shown on [Figure 2.5.4-215](#). The petrographic test locations performed as part of the Lee Nuclear Station exploration are shown on [Figure 2.5.4-216](#).

The geotechnical field exploration program in 2012 consisted of additional borings, some with borehole geophysical tests consisting of P-S velocity measurements and/or acoustic televiewer logging. The locations of the borings made in 2012 are shown on [Figure 2.5.4-209](#) in addition to those made in 2006-2007. The locations of the borings with borehole geophysical tests in 2012 are shown on [Figure 2.5.4-215](#) in addition to those made in 2006-2007.

2.5.4.3.2 Surrounding and Adjacent Structures Exploration

Exploration of facilities beyond the power block was conducted to support an understanding of the distribution of geological features (e.g. rock, soil, extent of weathering, etc.) at the site and to characterize site condition and material properties of non-safety related site features such as cooling towers, switchyard, pipelines, and general facilities. These explorations included profile borings for characterization and siting of monitoring wells, cooling towers, switchyard, pipelines, and general facilities, and confirm previous explorations. Several test pits and trenches were also excavated. The exploration locations made in 2006-2007 are shown on [Figure 2.5.4-208](#). The locations of the borings made in 2012 are shown on [Figure 2.5.4-209](#) in addition to those made in 2006-2007.

2.5.4.3.3 Geotechnical Data Logs and Records

WLS COL 2.5-2 Contemporary and historic geotechnical data sets were used to compile the
WLS COL 2.5-3 geotechnical figures contained in this Subsection. The Lee Nuclear Station field exploration records are presented in [Appendix 2AA](#), Attachments 1 through 5. The boring logs for the geotechnical borings made in 2012 are contained in [Appendix 2AA](#), Attachment 6. The Cherokee Nuclear Station field exploration records are presented in [Appendix 2BB](#).

WLS COL 2.5-1 As-built survey data and topographic surveys were used to prepare maps of the final geotechnical data exploration program as presented in [Figures 2.5.4-208](#) (2006-2007 explorations only) and [2.5.4-209](#) (2012 explorations in addition to 2006-2007 explorations). The locations of exploratory borings, monitoring wells, test pits, and surface geophysical lines were recorded in digital format. These data were uploaded into a geographic information system (GIS). The GIS was used to prepare plan view maps and profile drawings that were used to develop geologic interpretations.

Geotechnical borings, surface geophysical testing, CPT soundings, borehole in situ testing, including Goodman Jack and pressuremeter testing, and borehole geophysical testing, including P-S Suspension logging, downhole velocity, televiwer surveys were integrated to interpret the geologic and geotechnical properties presented in the geotechnical profiles, as discussed below in [Subsection 2.5.4.3.5](#).

In addition, in situ and laboratory test results of rock strength and petrographic test locations are provided on the borehole summary sheets described below.

2.5.4.3.4 Borehole Summaries

The compilation of the geologic and geotechnical data collected from the field program is essential to interpret the subsurface conditions. Data including lithology, laboratory strength, borehole and surface geophysical results, in situ test results, Standard Penetration Test (SPT), Rock Quality Designation (RQD), and percent recovery were used to compile borehole summaries of power block and other important borings. An explanatory figure showing these data sources is included as [Figure 2.5.4-218](#), followed by 21 Borehole Summaries, [Figures 2.5.4-219 through 2.5.4-232](#) and [Figures 2.5.4-233a through 2.5.4-233g](#). These summaries convey the integrated field, laboratory, and geologic framework essential for creating profiles across the nuclear islands as discussed in [Subsection 2.5.4.3.5](#).

2.5.4.3.5 Geotechnical Profiles

WLS COL 2.5-1 The borehole summaries are evaluated in the geologic context described in more
WLS COL 2.5-5 detail in [Subsections 2.5.1 and 2.5.4.1](#) to construct geotechnical profiles. Seven geologic cross sections intersecting the Lee Nuclear Station Unit 1 and 2 nuclear islands and adjacent areas are presented; the locations of these cross sections are shown on [Figure 2.5.4-209](#). Geologic Cross Sections BB-BB', CC-CC', EE-EE', F-F', FF-FF', UU-UU', and ZZ-ZZ' are shown on [Figures 2.5.4-234 through 2.5.4-240](#).

Key cross sections in this evaluation include the following:

- [Figure 2.5.4-234](#), Cross Section BB-BB', west-east profile through Unit 1 and Unit 2 centerline
- [Figure 2.5.4-235](#), Cross Section CC-CC', west-east profile through the south ends of Unit 1 and Unit 2 turbine buildings
- [Figure 2.5.4-239](#), Cross Section UU-UU', west-east profile through the north end of the Units 1 and 2 nuclear island
- [Figure 2.5.4-240](#), Cross Section ZZ-ZZ', west-east profile through the south end of Units 1 and 2 nuclear island
- [Figure 2.5.4-236](#), Cross Section EE-EE', north-south profile through the Unit 1 centerline
- [Figure 2.5.4-237](#), Cross Section F-F', north-south profile through the Unit 2 centerline
- [Figure 2.5.4-238](#), Cross Section FF-FF', north-south profile through the east side of Unit 2 nuclear island

These profiles depict former and existing ground surface, plant and yard grade representations including nuclear island foundation and other important power block foundation features and relevant boring and geophysical test data.

A detailed description of the site geology is presented in [Subsections 2.5.1 and 2.5.4.1](#). Material properties are discussed in [Subsection 2.5.4.2](#). Groundwater is discussed in [Subsection 2.5.4.6](#). Continuous rock is discussed in [Subsections 2.5.4.7.3 and 2.5.4.7.4](#).

2.5.4.3.6 Extent of Granular Fill

WLS COL 2.5-6 To indicate the extent of the granular fill to be placed around the nuclear islands
WLS COL 2.5-7 and extending out to form the supporting materials for the adjacent buildings (radwaste, annex, and turbine buildings), seven geologic cross sections intersecting the Lee Nuclear Station Unit 1 and 2 nuclear islands and adjacent areas are presented. The locations of these cross sections are shown on [Figure 2.5.4-209](#). Cross Sections BB-BB', CC-CC', EE-EE', F-F', FF-FF', UU-UU', and ZZ-ZZ' are shown on [Figures 2.5.4-245 and 2.5.4-260 through 2.5.4-265](#). All of these planned excavation geologic cross sections correspond to the geotechnical profiles presented in [Subsection 2.5.4.3.5](#).

Geologic cross sections depicting the granular fill are the following:

- [Figure 2.5.4-260](#), Planned Excavation Profile, Cross Section BB-BB', west-east profile through Unit 1 and Unit 2 centerline
- [Figure 2.5.4-261](#), Planned Excavation Profile, Cross Section CC-CC', west-east profile through the south end of Units 1 and 2 turbine building
- [Figure 2.5.4-245](#), Planned Excavation Profile, Cross Section UU-UU', west-east profile through the north end of the Unit 1 and Unit 2 nuclear islands
- [Figure 2.5.4-262](#), Planned Excavation Profile, Cross Section EE-EE', north-south profile through the Unit 1 centerline
- [Figure 2.5.4-263](#), Planned Excavation Profile, Cross Section F-F', north-south profile through the Unit 2 centerline
- [Figure 2.5.4-264](#), Planned Excavation Profile, Cross Section FF-FF', north-south profile along the east side of the Unit 2 nuclear island
- [Figure 2.5.4-265](#), Planned Excavation Profile, Cross Section ZZ-ZZ', west-east profile through the south end of the Unit 1 and Unit 2 nuclear islands

These profiles depict the original and existing ground surface, extent of granular fill, plant and yard grade representations, nuclear island foundation and other important power block foundation features, and the location of borings and geophysical tests in the vicinity of each profile. The granular fill depicted on these cross sections will extend horizontally outward from the walls of the nuclear island a distance of 100 feet or as necessary to form the foundation support zone of the seismic category II portion of the annex building and the turbine building (including the seismic category II first bay), whichever is the greater distance.

2.5.4.4 Geophysical Surveys

WLS COL 2.5-6 Surface and borehole geophysical surveys were conducted on the Lee Nuclear Station Site in 2006-2007 and 2012 to characterize the subsurface conditions of the soil and bedrock including dynamic properties and geologic features. Information obtained from these surveys was utilized in the analysis of and discussions pertaining to the site geology in [Subsection 2.5.1.2](#), surface faulting potential presented in [Subsection 2.5.3](#), and characterization of geologic features as presented in [Subsection 2.5.4.1](#).

The investigations were conducted using methods described in Subsection 4.4, Geophysical Investigations, of Regulatory Guide 1.132. Planning and exploration layout and data collection was coordinated by project engineering geologists and geotechnical engineers. All geophysical survey activities were performed in accordance with approved procedures.

Four geophysical survey methods were performed in 2006-2007 at the Lee Nuclear Station Site:

- Spectral Analysis of Surface Waves (SASW) performed by the University of Texas – Austin;
- Seismic cone wave velocity measurements in overburden soils by Gregg In Situ Inc.;
- Suspension and downhole velocity logging tests by GEOVision; and
- Televiwer (acoustic and optical) boring wall logging by GEOVision.

2.5.4.4.1 Spectral Analysis of Surface Waves (SASW) Surveys

SASW surveys were conducted at 15 locations on the Lee Nuclear Station Site, as discussed in [Subsection 2.5.4.2.1.3](#). The goal of conducting these tests was to characterize the shear wave velocity of native soil, undisturbed existing fill, and rock underlying the Lee Nuclear Station Site. The SASW surveys of the Lee Nuclear Station Site were conducted by Dr. K.H. Stokoe II of the Geotechnical Engineering Center at the University of Texas at Austin under the supervision of

project personnel. Survey depths ranged from tens of feet to approximately 100 feet below ground surface, depending on site survey conditions, material attenuation properties, and the length of survey line. Collection and processing of SASW survey data was performed pursuant to a proprietary protocol authored by Dr. Stokoe.

2.5.4.4.1.1 Survey Method

The SASW surveys determined shear wave (Vs) by measuring dispersion of surface seismic waves as they propagated through subsurface materials. Rayleigh-type surface waves were generated using truck-mounted vibroseis equipment and motions perpendicular to the ground surface were measured at points arranged on a single radial path from the source. Each array consisted of a source and three receivers with variable spacing dependent on a particular survey goal and location. Testing was conducted using Mark Products Model L-4C vertical velocity transducers with natural frequencies of 1 Hz. Data were recorded using a four-channel Agilent 35670A Dynamic Signal Analyzer. Field data were transferred to a desktop computer for analysis using WinSASW software. Data were converted into composite dispersion curves and iterative forward modeling was used to create layer stiffness models with synthetic dispersion curves that most closely matched the experimental curves. The SASW survey locations conducted at Lee Nuclear Station Site are shown on [Figure 2.5.4-211](#). The SASW results are tabulated in [Table 2.5.4-214](#).

2.5.4.4.1.2 Survey Results

Taking into account that the SASW technique yields average Vs values from across the length of each survey line, results of the SASW surveys compare very favorably when compared to adjacent borehole P-S suspension and downhole velocity logs. The results of SASW and borehole Vs measurements are presented on the Boring Summary Sheets, [Figures 2.5.4-219 through 2.5.4-232](#) and [Figures 2.5.4-233a through 2.5.4-233g](#).

2.5.4.4.2 Seismic Cone Penetration Tests

CPT seismic shear wave velocity tests were performed at nine CPT locations, as discussed in [Subsection 2.5.4.2.1.4](#). The SCPT test locations are shown on [Figure 2.5.4-212](#). Each of the CPT seismic shear wave velocity tests was performed in residuum, saprolite, or pre-existing fill soils above bedrock.

2.5.4.4.2.1 Seismic CPT Methods

A modified CPT cone containing a built-in seismometer was used to measure compression and shear wave velocities in addition to the standard piezocone parameters. Seismic tests were usually performed at 3-foot (1-meter) intervals. Shear waves (S-waves) were generated by a sledgehammer striking a traction beam coupled to the ground surface by a hydraulic cylinder under the CPT rig. The sledgehammer used also acted as a trigger, initiating the recording of the seismic wave trace. Before measurements were taken, the rods were decoupled from the CPT rig to prevent energy transmission down the rods.

Geophones in the body of the piezocone measured the arriving waves generated at the ground surface. Any waves received by the geophones on the cone penetrometer were transmitted via a cable back up to the truck to be displayed on an oscilloscope and stored on a computer. On site software then used wave amplitude versus time to calculate the point wave velocity. At least two waves were recorded for each test depth so the operator could check consistency of the waveforms.

The shear wave velocity provides information about small-strain stiffness. From point shear wave velocity and the mass density of a soil layer, the dynamic shear modulus of the soil was calculated at the specific point location. The dynamic shear modulus is a key parameter for the analysis of soil behavior in response to dynamic loading such as from earthquakes.

The CPT seismic test results summarized in [Table 2.5.4-215](#) indicate that the shear wave velocity of the overburden soils at the Lee Nuclear Station Site ranges from 616 to 2990 feet per second (fps).

2.5.4.4.3 Suspension and Downhole Velocity Logging

A total of 16 borehole velocity surveys were performed at the Lee Nuclear Station site. The borehole velocity surveys consisted of 13 P-S suspension logging tests with four companion downhole velocity tests in 2006-2007, and three P-S suspension logging tests in 2012. The surveys were performed within uncased and cased boreholes. Downhole surveys were performed in four boreholes with P-S suspension surveys as a means to compare and validate P-S suspension results. Comparison of downhole velocity measurements to the companion P-S suspension measurements indicated good correlation of velocity values. [Table 2.5.4-216](#) provides a summary of the borehole geophysical testing performed in 2006-2007 and 2012. [Figure 2.5.4-215](#) shows the locations of the borehole surveys. The objective of the suspension and downhole logging tests was to obtain shear wave (V_s) and compressional wave (V_p) velocity measurements as a function of depth within each borehole. The V_s velocity values were used to determine whether the unweathered rock met the hard rock requirements for the site response analyses and development of the GMRS as discussed in [Subsection 2.5.2](#). The seismic hazard model defines hard rock as having a minimum V_s of 9200 fps.

2.5.4.4.3.1 P-S Velocity Logging Methods

The suspension logging tests were performed using an OYO Model 170 Suspension Logging Recorder and Probe. In this OYO downhole configuration, the seismic source is mounted near the base of the probe, and a pair of receivers is mounted approximately 3 feet (0.91 meters) apart from one another, centered approximately 12 feet (3.7 meters) above the source. The source generates a V_p wave in the pore fluid near the base of the probe, which was converted to a V_s wave and separate V_p wave at the borehole wall. The shear wave travels up along the wall, and the resulting wave is measured by the receiver pair. The S-wave and P-wave velocities for the interval between the receivers were calculated based on the difference in wave arrival times.

2.5.4.4.3.2 Downhole Velocity Logging Methods

The downhole velocity measurements were performed using a Geostuff BHG-3, 3-component geophone ("probe"). The probe consists of a horizontal and vertical geophone mounted on a rotatable structure with a fluxgate compass sensor. This probe was lowered down the hole with the orientation of the geophone components held parallel to the axis of excitation at the surface. Seismic energy was produced by hitting a steel capped traction plank or a welded steel box bolted to the rock surface using a 20-pound sledgehammer. For Vs energy, the side of the steel plate was hit; for Vp wave energy, the top of the steel plate was hit.

The probe was lowered down the holes in 3.28-foot intervals and locked in place using an inflatable air bladder before each test was conducted. Multiple blows were used to stack the data and improve the signal-to-noise ratio. Signals from the probe were recorded using a Geometrics Strataview seismograph. The Vs and Vp wave velocity for the interval between the receivers was then calculated based on the difference in wave arrival times.

2.5.4.4.3.3 Velocity Logging Results

The travel-time data from the P-S suspension logging and the downhole tests were used to create velocity layer models. The resultant velocity layers are presented on the Lee Nuclear Station boring summary sheets [Figures 2.5.4-218 through 2.5.4-232](#) and [Figures 2.5.4-233a through 2.5.4-233g](#). The interpreted P-S Suspension and Downhole velocity layer models are presented in [Tables 2.5.4-217 and 2.5.4-218](#), respectively for 2006-2007 borehole tests. The interpreted P-S Suspension velocity layer models for the 2012 borehole tests are also presented in [Table 2.5.4-217](#).

2.5.4.4.4 Acoustic and Optical Televierer Logging

Acoustic televierer logging was conducted in seventeen boreholes and optical televierer logging was conducted in nine boreholes on the Lee Nuclear Station Site. The goals of these tests included: (1) correction of soil, rock and geophysical log depths to true depths where needed, (2) acoustic imaging of the boring wall to identify fractures, and determine the dip and azimuth of these features, and (3) perform borehole deviation surveys. The fracture orientation data was used to estimate the Rock Mass Rating for the various layers and to evaluate observed discontinuity characteristics.

The acoustic and optic televierer logging was collected using a High Resolution Acoustic Televierer (HiRAT) manufactured by Robertson Geologging, Inc. that was lowered down the borings via connection to an armored conductor cable that also acted as a conduit for the data to travel to the Robertson Micrologger II at the surface. The probe is 7.58 feet long, 1.9 inches in diameter and is fitted with upper and lower four-band centralizers. The acoustic sensors produce images of the boring wall based on the amplitude and travel time of an ultrasonic beam reflected from the formation wall. The borings are kept filled with water during this testing

because the contact between clear water and the rock formation provide a high contrast. The data were stored on hard disk for later processing.

2.5.4.5 Excavations and Backfill

WLS COL 2.5-5 The Lee Nuclear Station utilizes a combination of excavation slopes and temporary retaining structures to facilitate construction of below grade portions of the nuclear island. The excavation remaining from Cherokee Nuclear Station construction activities is utilized and enlarged or reconfigured, as needed, to support Lee Nuclear Station construction. Backfill is placed within the excavation against the below grade nuclear island walls to create the ground surface surrounding the nuclear island structure. The ground surface surrounding the nuclear island is generally at about Elevation 589 feet which is 4.0 feet below the building floor slab elevation 593 ft (AP1000 Grade El. 100'-00"). The yard grade adjacent to the buildings is at Elevation 592 ft (AP1000 Grade El. 99'-00").

The seismic Category I structures consist of the Unit 1 and Unit 2 nuclear islands. Other structures within the power block are not seismic Category I structures and are not safety related. The location of the nuclear island structures is shown on [Figures 2.5.4-201](#) and [2.5.4-208](#). The Lee Nuclear Station nuclear island is constructed with a building floor slab elevation of 593 feet (AP1000 Grade El. 100'-00"). Below grade portions of the nuclear island extend 39.5 feet below building slab elevation, to Elevation 553.5 feet (AP1000 Grade El. 60'-6"). Foundation materials, consisting of continuous rock or concrete, are located at this elevation or below for support of the nuclear island. Fill concrete is used in areas where continuous rock or Cherokee Nuclear Station concrete is below Elevation 553.5 feet (AP1000 Grade El. 60'-6") to bring that surface up to the Lee Nuclear Station base of foundation elevation.

2.5.4.5.1 Sources and Quantities

WLS COL 2.5-6 The Lee Nuclear Station Site requires granular backfill material described in
WLS COL 2.5-7 [Subsection 2.5.4.5.3.5](#) to fill the area around the below-grade nuclear island walls out to the extents shown on [Figures 2.5.4-245](#) and [2.5.4-260](#) through [2.5.4-265](#). This backfill also forms the yard elevation and supporting materials for the power block structures outside but adjacent to the nuclear island.

The source for the granular fill is not identified. At a rock quarry, material is crushed to form granular product consisting of a mixture of gravel, sand, and some fines. The granular fill material will likely be obtained from an off-site source such as an operating rock quarry. Imported granular fill intended to be placed adjacent to seismic Category I structures or beneath other important adjacent facilities will be verified as compatible with Lee Nuclear Station site response calculations. [FSAR Subsection 3.7.2.8.4](#) describes the material property

characteristics of the granular fill used to support Seismic Category II structures adjacent to the nuclear island.

2.5.4.5.2 Extent of Excavation

WLS COL 2.5-6

WLS COL 2.5-7

A large excavation was constructed during site preparation work for Cherokee Nuclear Station construction. This excavation is utilized as the initial excavation for the Lee Nuclear Station. Additional excavation for Lee Nuclear Station extends about 10 feet laterally into the fill and natural soil materials comprising the Cherokee Nuclear Station construction slope or as necessary to remove softened, sloughed, or other loose soil and rock materials. This excavation extends only a sufficient distance into the slope to reach materials that are relatively undisturbed by erosion or shallow sloughing during the time the excavation remained open following Cherokee Nuclear Station construction.

In addition to the slope trimming described above, additional excavation of the soil and partially weathered rock slope that formed the Cherokee Nuclear Station excavation limits is necessary to provide relatively uniform thickness of fill for support conditions beneath the Lee Nuclear Station power block structures adjacent to the nuclear island. Excavation to a reasonably uniform subgrade elevation is performed within the limits of the adjacent non safety-related power block structures and outside the structure limits to a point defined by a line extended at 1 horizontal to 1 vertical or flatter from the base edge of the structure foundations. This geometry defines the foundation support zone for the non-safety annex, turbine and radwaste buildings. For the nuclear island foundation, the line is 0.5 horizontal to 1 vertical or flatter and the line begins at a point located 6 feet or more horizontally from the perimeter of the nuclear island foundation limits. This geometry defines the foundation support zone for the nuclear island. These nuclear island area excavation limits, as estimated prior to construction of Lee Nuclear Station, are shown on [Figure 2.5.4-243](#). Excavation to a uniform subgrade elevation for adjacent non-safety and non-seismic structures exposes fill concrete, rock, partially weathered rock, or saprolite. The adjacent non-safety related structures include two areas designated as Seismic Category II (SC-II) structures because of their characteristics and proximity to the nuclear island. These are the annex building area outlined by columns E-I.1 and 2-13 and the turbine building, first bay adjacent to the nuclear island as outlined by columns I.1 to R and 11.05 to 11.2. Excavations within the support zone of these SC-II structures expose concrete or rock.

Excavation to a subgrade elevation for the seismic category II portions of the adjacent non-safety structures exposes concrete or rock. The foundation support zone for the Unit 1 annex building (SC-II) may expose a relatively small area of partially weathered rock to fractured rock in the northwest corner, but the majority of the foundation support zone for this structure will encounter rock or concrete overlying rock. Within the foundation support zone these SC-II structures, in areas where the pre-existing concrete and/or rock are at a lower elevation than the base of the nuclear island, fill concrete will be used to build up the base level of the nuclear island. If rock within the support zones of the SC-II structures is higher than the base of the nuclear island, the rock will be removed to the elevation of the base of the nuclear island.

Outside the Unit 1 and Unit 2 foundation subgrade excavation limits the construction excavation slope or backfill slope is constructed up to the ground surface elevation. The limit of this slope projected to the ground surface, as estimated prior to construction of Lee Nuclear Station, is shown on [Figure 2.5.4-243](#). The construction excavation slope exists until backfill is placed to gain access to the nuclear island structure with construction cranes operating from yard level.

Soil excavation slopes for Lee Nuclear Station are constructed with a maximum slope of 1.5 horizontal to 1.0 vertical or flatter and a maximum height of 40 feet. Soil excavation slopes requiring heights greater than 40 feet are constructed using benches to maintain adequate safety factors for stability. Excavation slopes are backfilled to yard grade during placement of fill materials around the below-grade nuclear island structures.

2.5.4.5.2.1 Unit 1 Excavation Conditions

Excavation to a uniform foundation subgrade elevation of approximately 540 to 545 feet was required for Lee Nuclear Station due to the depth of the pre-existing Cherokee Nuclear Station excavation and the elevation of the Cherokee Nuclear Station structural elements that remained beneath the Lee Nuclear Station foundations. Excavation within the foundation support zone of the nuclear island extends to pre-existing concrete, pre-existing fill concrete, or to continuous rock where no pre-existing concrete exists. Fill concrete is utilized to bring the subgrade elevation up to the nuclear island foundation elevation within the foundation support zone of the nuclear island for the Lee Nuclear Station.

Excavation to the foundation subgrade elevation includes removal of the Cherokee Nuclear Station reactor building superstructure and portions of the Cherokee Nuclear Station auxiliary building mat foundations within the nuclear island foundation support zone. The Cherokee Nuclear Station reactor building foundation mat and some of the Cherokee auxiliary building basemat are left in place. To avoid damage to the reactor building mat, 3 to 6 inches of the vertical walls may remain above the mat surface after the walls are removed. In areas where the Cherokee auxiliary building basemat is within the foundation support zone for the Lee Nuclear Station Unit 1 nuclear island, the isolation joint surrounding the Cherokee Nuclear Station reactor building mat is also removed to reduce the discontinuity between reactor building basemat and new fill concrete. Removal of the Cherokee Nuclear Station foundation mats exposes underlying fill concrete or continuous rock. The Lee Nuclear Station nuclear island for Unit 1 is positioned so that additional excavation beyond the Cherokee Nuclear Station concrete edges is not necessary. The foundation support zone for the Lee Nuclear Station Unit 1 nuclear island is entirely underlain by the existing concrete of Cherokee Nuclear Station Unit 1 which is underlain by continuous rock.

Construction procedures for Cherokee Nuclear Station required removal of soil and weathered rock materials prior to placement of foundation concrete and fill concrete. Cherokee Nuclear Station foundation concrete was placed on material described as continuous rock, or on fill concrete that was used as a leveling pad above continuous rock. This same procedure is followed for the Lee Nuclear

Station. Therefore concrete placed during Cherokee Nuclear Station construction and Lee Nuclear Station construction are supported on the same quality rock materials.

The Cherokee Nuclear Station foundation mat for the reactor building and auxiliary building was underlain by a groundwater drainage system. When this drainage system is exposed by excavation for the Lee Nuclear Station nuclear island foundation it is sealed with fill concrete material as illustrated by [Figures 2.5.4-244a](#) through [2.5.4-244e](#). Exposure of this drainage system is most likely to occur at the perimeter of the Cherokee Nuclear Station reactor building mat where a portion of the Cherokee Nuclear Station auxiliary building basemat is removed to take out the existing isolation joint ([Figures 2.5.4-244b](#) and [2.5.4-244c](#)) or in the southern end of the Lee Nuclear Station nuclear island where the Cherokee Nuclear Station auxiliary building basemat must be removed because it is above the bottom of the nuclear island ([Figure 2.5.4-244d](#)).

The existing Cherokee Nuclear Station concrete foundation has several local pits (referred to as pump rooms) that were to serve various purposes ([Figure 2.5.4-266](#)). These local pits were typically to be provided with horizontal and vertical waterproofing membranes. The horizontal membrane was to be installed on a fill concrete layer resting on the continuous rock and then covered by a fill concrete mudmat approximately 3.5 inches thick. The vertical membrane was to be secured to the outside face of the vertical structural walls and covered by a protective sheathing. The space between the surrounding rock and the vertical pit walls with their protective sheathing and vertical membrane was then backfilled with fill concrete. In pits having the horizontal and vertical waterproofing membranes, these features will be removed down to the top of the fill concrete layer resting on the continuous rock and outward to the surrounding rock and replaced with new fill concrete as depicted on [Figure 2.5.4-244e](#). The width of the pits, thus excavated, will be increased by an estimated 13 feet which is equal to the combined width of the structural pit walls (estimated to be 3.5 feet for each typical wall) plus the combined widths of the concrete fill behind the structural pit walls (having an estimated typical width of 3 feet from the back of each structural pit wall). The depth of the pits, thus excavated, will be increased by an estimated 4.3 feet, which is equal to the thickness of the structural basemat (estimated to be typically 4 feet) plus the horizontal membrane and the 3.5 inch thick mudmat. The pits, thus excavated and backfilled with new fill concrete, will continue to be localized areas of deeper fill concrete below the nuclear island of Unit 1.

The foundation support zone for the Lee Nuclear Station nuclear island is entirely underlain by the footprint of the existing concrete foundation of Cherokee Nuclear Station Unit 1 which is underlain by continuous rock.

2.5.4.5.2.2 Unit 2 Excavation Conditions

Excavation to a uniform foundation subgrade elevation of approximately 553.5 feet is possible for Lee Nuclear Station because some of the Cherokee Nuclear Station excavation in this area remained above this elevation.

During the site exploration for Lee Nuclear Station in 2006 and 2007, the base of the Cherokee Nuclear Station excavation generally consisted of exposed rock beneath the location of the Lee Nuclear Station Unit 2 nuclear island. The same is true for the Lee Nuclear Station Unit 2 nuclear island in the 2012 exploration, but to a somewhat lesser extent because of the raised plant elevation. At 2012 boring B-2006 near the northeast corner of the Unit 2 nuclear island the continuous rock level is 2 feet above the foundation elevation 553.5 feet. In much of the Lee Nuclear Station Unit 2 nuclear island foundation area the elevation of the rock was higher than the Lee Nuclear Station foundation elevation. Excavation into soil, partially weathered rock, weathered or loose rock, and continuous rock is required to reach the Lee Nuclear Station Unit 2 nuclear island foundation elevation. These materials are excavated and removed down to the Unit 2 nuclear island foundation elevation. Below this elevation soil, partially weathered rock, and weathered or loose rock materials are excavated until continuous rock is reached.

Backfill material is required where the rock surface elevation is below the Lee Nuclear Station foundation elevation or where additional rock removal is required to reach continuous rock due to localized weathering conditions. One area where the rock surface was already below the Lee Nuclear Station Unit 2 nuclear island foundation elevation is the east side of the nuclear island near the boring locations B-1014 and B-1018. At 2012 boring B-2005 near the southeast corner of the Unit 2 nuclear island, the continuous rock is 8 feet below the foundation elevation 553.5 feet. Fill concrete is used in this and any other area to bring the bearing surface back up to the Unit 2 nuclear island foundation elevation (Figure 2.5.4-267).

2.5.4.5.3 Specifications and Control

2.5.4.5.3.1 Nuclear Island Foundation Materials

WLS COL 2.5-6
WLS COL 2.5-7

Properties of the nuclear island foundation materials are discussed in Subsection 2.5.4.2. This Subsection describes methods and procedures used for verification and quality control of the nuclear island foundation materials.

Quality control will verify foundation quality materials are reached prior to placement of fill materials. This applies to continuous rock as well as to fill concrete or structural concrete within the Lee Nuclear Station nuclear island foundation limits that remains from Cherokee Nuclear Station construction. The foundation quality rock and fill concrete provide very high safety margins against bearing capacity failure under both static and seismic loading of the nuclear island, and only nominal settlements occur. Quality Control testing requirements for continuous rock and remaining Cherokee Nuclear Station concrete foundation material is provided in Table 2.5.4-219. The procedure for verification of foundation conditions consists of geologic mapping of the final exposed excavation surface prior to placement of foundation concrete or fill concrete materials.

Geologic mapping of the final exposed excavation rock surface beneath the nuclear island, and any required extension due to depth of suitable continuous

rock material, is performed at a scale of 1 inch equals 10 feet. Geologic mapping is performed at a scale of 1 inch equals 5 feet for local areas where further detail is needed to document significant features. The geologic mapping program includes photographic documentation of the exposed surface and laboratory testing and documentation for significant features.

Lee Unit 1 is entirely underlain by Cherokee concrete over previously-mapped rock. Because of different footprints of legacy Cherokee structures, some additional excavation will be required, and may expose previously-mapped foundation rock. Exposed rock at Lee Unit 1 will be mapped and compared to the previous Cherokee mapping to confirm interpretations discussed in [Subsection 2.5.1.2.5.5](#).

2.5.4.5.3.2 Fill Concrete beneath the Nuclear Island Foundation Limits

The following requirements are also applicable to the fill concrete that is used to build up the rock surface exposed by excavation to the same level as the bottom of the nuclear island foundation in the foundation support zones of the SC-II building areas (annex building and turbine building first bay).

Quality control of backfill materials will be conducted during fill concrete placement below the nuclear island foundation areas of Lee Nuclear Station. Fill concrete mix designs are in accordance with ACI 318-02 ([DCD Chapter 2 Reference 1](#)). Field observation is provided to verify that the approved mixes are used and to obtain test specimens that are used to verify required compressive strengths. Test specimens are also prepared to verify that the average design shear wave velocity of 7500 ft/sec are obtained for compatibility with Lee Nuclear Station site response calculations. Quality control sampling and testing requirements for these materials are provided in [Table 2.5.4-220](#).

Fill concrete to build up the nuclear island foundation support area is required in varying thicknesses beneath the nuclear island. This fill concrete is placed in layers, and lower layers are hardened by curing before the succeeding layers are placed. At Unit 1, fill concrete is placed on top of the Cherokee Nuclear Station Unit 1 reactor building and auxiliary building basemat, or on Cherokee Nuclear Station fill concrete or underlying rock exposed by removal of the Cherokee Nuclear Station auxiliary building basemat.

The former reactor building for Cherokee Nuclear Station Unit 1 is completely removed down to the top of the basemat as described in [Subsection 2.5.4.5.2.1](#). The pits in the Cherokee Nuclear Station Unit 1 basemat, such as the pipe chases and sump pits, are backfilled with fill concrete level with the top of the basemat during Lee Nuclear Station Construction. The top of the reactor building basemat for Cherokee Nuclear Station Unit 1 is nominally level at an approximate elevation of 545 feet after removal of the structural components and filling the pits in the Cherokee Nuclear Station basemat. The resulting surface is then intentionally roughened approximately one-quarter inch using the guidance in ACI 349, Part 4 – Construction Requirements, Section 11.7.9 ([Reference 209](#)), which reads “when concrete is placed against previously hardened concrete, the interface for

shear transfer shall be clean and free of laitance. If μ is assumed equal to 1.0, interface shall be roughened to a full amplitude approximately $\frac{1}{4}$ inch."

The roughening criterion described above is also applied to other hardened concrete layers on which additional fill concrete is placed. This includes the top layer of fill concrete against which the waterproofing membrane layer or the structural mat concrete is placed. Use of wet sandblasting, chipping hammers, or other similar methods are acceptable procedures for roughening the surface. The top of the concrete mass is considered roughened when about one-quarter inch of the surface had been removed to expose the aggregate in the concrete.

2.5.4.5.3.3 Foundation Materials Outside the Nuclear Island

Outside the limits of the nuclear island support zone, steps are used to determine the presence of suitable foundation materials prior to placement of granular backfill materials within the foundation support zones beneath the non safety-related structures. For the structures not designated as SC-II, or for areas to be supported only on granular fill, this applies to continuous rock, existing concrete remaining from Cherokee Nuclear Station construction, weathered rock, partially weathered rock, or saprolite that remains in place below the non safety-related power block structures adjacent to the SC-II structures or the nuclear island. This also applies to areas to support only the granular fill. For the structures designated as SC-II (part of the annex building and the turbine building first bay as described in [Subsection 2.5.4.5.3](#)) the acceptable subgrade exposes concrete, rock, or the limited area of partially weathered rock in the northwest corner of the foundation support zone for the Unit 1 annex building. Steps for verification of proper foundation conditions consist of:

- Removing loose soil, rock, and any organic materials.
- Determine if the base of excavation consists of saprolite having N_{60} values, equal to or greater than 15 blows per foot, measured at a depth of 3 feet below the base of the excavation. Partially weathered rock, weathered rock, or rock would also be suitable in these areas provided it meets or exceeds the minimum criteria stated for saprolite and any loose material or soft zones are removed. For the SC-II building areas, rock is the acceptable support material, with limited areas of partially weathered rock such as in the northwest corner of the foundation support zone for the Unit 1 annex building. For the SC-II building areas, if rock within the foundation support zone is higher than the elevation of the bottom of the nuclear island, remove the rock to the elevation of the bottom of the nuclear island to be replaced with granular fill materials.
- For the SC-II building areas, fill any depressions in the surface of the subgrade rock with fill concrete, then use fill concrete to backfill to the elevation level with that of the nuclear island (elevation 553.5 ft). This forms a uniform surface grade for the placement of granular backfill to support the SC-II building areas. If the rock in the foundation support zone of the SC-II buildings is above the elevation of the bottom of the nuclear

island, the rock will be excavated to the elevation of the nuclear island bottom and replaced with granular fill materials.

- For the structures not designated as SC-II or for areas that support only granular fill, fill any depressions or cavities in the surface of the foundation soil or rock with fill concrete or properly compacted granular fill materials. This forms a uniform surface grade for the placement of additional granular fill, to support the non SC-II buildings or to complete the area of granular fill.
- Continue placing granular fill materials in layers according to the procedures described in [Subsection 2.5.4.5.3.5](#).

2.5.4.5.3.4 Fill Concrete Outside the Nuclear Island Foundation Limits

For fill concrete used within the foundation support zone of the SC-II building areas adjacent to the nuclear island, see [Subsection 2.5.4.5.3.2](#).

Fill concrete mix design is approved in advance. Field observation verifies that the approved mixes are used and obtains test specimens that verify the required design parameters are reached. A quality control sampling and testing program is developed that verifies the fill concrete material properties are consistent with the design parameters.

2.5.4.5.3.5 Granular Backfill Outside the Nuclear Island

Outside the below grade nuclear island walls (Units 1 and 2), a granular backfill will be placed up to approximately the yard elevation or to the underside of the adjacent buildings. The backfill adjacent to the nuclear island walls and extending outward to form the foundation support of the adjacent buildings (radwaste, annex, and turbine buildings) will be an engineered granular backfill. Outside the limits of the granular fill, soil backfill will be used. This subsection describes the specifications and controls of granular fill materials. The soil backfill placed beyond the granular fill limits is non safety-related and the placement specifications will be developed as part of construction.

Static properties of typical granular backfill materials are discussed in [Subsection 2.5.4.2](#). Dynamic properties of typical granular backfill materials are discussed in [Subsection 2.5.4.7](#).

Quality control for granular backfill includes verification that the material was obtained from an approved source (e.g., an approved quarry). The maximum dry density and optimum moisture content are determined according to the modified Proctor (ASTM D 1557) method. For gradation and moisture content testing, the test samples are obtained after placing the material but before compaction. Measurement of in-place dry density of each lift after compaction is performed using the sand cone (ASTM D 1556) or rubber balloon (ASTM D 2167) method. The nuclear gauge (ASTM D 6938) method is used to augment (but not completely replace) the other methods.

A quality control sampling and testing program for the granular backfill inclusive of the items provided by [Table 2.5.4-222](#) is implemented during construction of the granular backfill. This quality control sampling and testing program verifies that the granular backfill is constructed in accordance with the parameters described in this subsection. To ensure that the engineering properties of the backfill meet the values used to calculate the static and dynamic lateral earth pressures, and the values used to establish seismic requirements for the Category II structures (annex building and turbine building Bay 1), the backfill will be tested in the laboratory. Testing to be performed on granular backfill before construction begins is also provided by [Table 2.5.4-222](#). Prior to constructing the backfill around the nuclear island structures, a “test fill” pad will be constructed on-site using the equipment and granular fill materials to be used in the backfill. Before the production backfill commences, an engineering report will exist that concludes that the equipment and methods used to construct the “test fill” are capable of producing acceptable and consistent results.

Compactors equivalent to those used in the test fill may be utilized in the production backfill provided that results of in situ tests of the backfill compacted using the equivalent compactors are capable of producing acceptable and consistent results.

The non safety-related structures adjacent to the nuclear island (radwaste, annex, and turbine buildings) will be supported on the granular fill. The following criteria are required for granular backfill placed adjacent to the nuclear island walls and extending outward to form the supporting material for the adjacent structures:

- The granular fill is obtained from a quarry and will conform to SCDOT gradation limits ([Reference 224](#), SCDOT, 2007). Anticipated material types are Macadam Base Course and Washed Screenings.
- The material is from an approved source (e.g., a quarry) and meets the assigned gradation requirements after the material is hauled and placed (before compaction).
- The coarse particles (materials retained on and above the No. 4 sieve) have an abrasion loss no more than 65 percent ([Reference 224](#)) when subjected to the Los Angeles Abrasion Test (ASTM C 131) and has an apparent specific gravity (ASTM C 127) that is greater than or equal to approximately 2.65.
- The material has a defined moisture-density relationship to allow a maximum dry density to be determined in accordance with ASTM D 1557 (modified Proctor) for compaction control.
- Care is taken to prevent segregation of the materials during handling and placement.
- The lift thickness is appropriate for the type of compaction equipment, but generally does not exceed about 8 inches (compacted thickness) for mechanized equipment nor about 4 to 6 inches for hand-guided

compactors. Lift thicknesses may vary from the above values depending on the capability of the equipment being used as demonstrated by the test fill and in situ tests in the production fill.

- Within confined areas, or within close proximity of the nuclear island walls, appropriate compactors are used to prevent excessive lateral pressures against the walls from the residual soil stress caused by heavy compactors. The compactors have sufficient weight and striking power to produce the same degree of compaction that is obtained on the other portions of the fill by the rolling equipment, as specified.
- The granular fill is compacted to a minimum of 96 percent of the maximum dry density determined in accordance with the modified Proctor test method (ASTM D 1557) with a moisture content that is generally within 3 percentage points above or below the optimum moisture content. If the compacted density meets the requirements, moisture present during compaction is controlled only for compaction efficiency and not as an engineering requirement. Nonconformance to recommended compaction moisture content does not alter the engineering properties of the cohesionless fill and should not form the basis for rejection of the constructed material. This relative compaction is selected to produce a granular fill equivalent to a relative density of 80 percent (Reference 225), and thus highly resistant to liquefaction.

Lateral pressures applied against the below grade nuclear island walls are evaluated and discussed in [Subsection 2.5.4.10.3](#). Evaluation and discussion of liquefaction issues related to the backfill materials is provided in [Subsection 2.5.4.8](#).

2.5.4.5.4 Groundwater Control

WLS COL 2.5-8 Dewatering of the nuclear island areas was successfully performed on several occasions in the history of the site. Dewatering during Cherokee Nuclear Station construction was performed using a dewatering well system outside the excavated area combined with local sump areas and pumps within the excavated area. Dewatering of the nuclear island area during Lee Nuclear Station Site exploration activities in 2006-2007 was performed using a sump pit and pump system within the excavation. Existing low areas of the site acted as the sump pits and a series of pump systems were maintained to periodically pump accumulated water from these pits to the nearby Make-Up Pond B.

Dewatering during Lee Nuclear Station construction is performed using a series of dewatering wells located outside the existing excavation limits. Localized sump and pump systems are utilized to supplement the dewatering wells in areas of the site where water accumulates. This is the same combination of dewatering methods used for the Cherokee Nuclear Station construction.

The construction dewatering system maintains the groundwater elevation below the elevation of construction activities during foundation construction and during placement and compaction of engineered backfill materials outside the nuclear island. Following completion of engineered backfill placement and compaction activities, the groundwater is allowed to return to static levels.

Additional discussion of groundwater and site dewatering activities is provided in [Subsection 2.5.4.6](#).

2.5.4.6 Groundwater Conditions

The nuclear island structure extends below grade to Elevation 553.5 feet. This elevation is below the long term static groundwater elevation. Construction dewatering is required during construction of the below grade nuclear island walls and placement of backfill materials. Dewatering beyond construction is not required as the foundation basemat and below grade walls are waterproofed during construction and designed for hydrostatic pressure.

2.5.4.6.1 Groundwater Occurrence

Groundwater at the location of the nuclear island is present as a result of infiltration of precipitation upgradient of the nuclear island. Groundwater flow occurs primarily in the fractured portions of the bedrock and in the relict fracturing in the weathered rock and saprolite material above the bedrock. Additional discussion regarding the occurrence and movement of groundwater at the Lee Nuclear Station Site is provided in [Subsection 2.4.12.1](#).

Immediately following construction the groundwater elevation remains artificially depressed as a result of dewatering activities required to support construction. After construction of the nuclear island and the backfill surrounding the nuclear island is placed, dewatering activities cease and the groundwater is allowed to return to static levels. The long term groundwater elevation at the Unit 1 and Unit 2 nuclear island structures is expected to fluctuate over time between Elevation 584 feet and 574 feet. The upper end of this groundwater elevation range is below the design groundwater elevation of 591 feet (standard plant Elevation 98 feet) used in the [DCD Table 2-1](#). Additional discussion of groundwater elevations and fluctuations at the site is provided in [Subsection 2.4.12](#).

2.5.4.6.2 Permeability Testing

Field and laboratory permeability testing was initially performed at the site during the Cherokee Nuclear Plant Site exploration. Additional testing including in situ permeability from packer tests and slug tests and laboratory hydraulic conductivity is performed during the Lee Nuclear Station Site exploration. Results of in situ permeability testing performed at the site are presented in [Subsection 2.4.12.2.4](#). Results of laboratory permeability testing performed on remolded samples obtained from Lee Nuclear Station borrow areas are discussed in [Subsection 2.5.4.2](#).

2.5.4.6.3 Construction Dewatering

Dewatering during construction is accomplished by a combination of pumping from sumps within the construction excavation and groundwater pumping wells located outside the construction excavation limits. Experience during Cherokee Nuclear Station construction and Lee Nuclear Station Site exploration indicated the foundation excavation area could be dewatered using internal sumps only. However, construction experience during Cherokee Nuclear Station suggested that a combination of external dewatering wells and internal sumps was more practical for construction activities.

Open pumping locations inside the excavation are established where needed based on observed conditions. The open pumping locations are operated while the backfill is being placed by incrementally extending suitable diameter casing pipe vertically above the pumping location to provide for the pump and discharge lines. A granular filter is placed on the excavation floor around the casing pipe to prevent erosion of the backfill into the open pumping location. After the backfill is completed, the pumping from the wells and open pumping locations ceases.

The location of casing for the open pumping locations is selected to avoid creating a “hard spot” affecting foundation support for the structures supported on the backfill adjacent to the nuclear islands.

The casing for the open pumping locations are left in place and backfilled with concrete or cement grout having a compressive strength of at least 2,500 psi. Following the completion of construction activities, the pumping wells to be abandoned are grouted as required by South Carolina Department of Health & Environmental Control (SCDHEC) regulations.

2.5.4.6.4 Groundwater Impacts on Foundation Stability

WLS COL 2.5-8 A history of groundwater elevation measurements at the Lee Nuclear Station Site is provided in [Subsection 2.4.12](#). Groundwater measurements prior to construction of Lee Nuclear Station were influenced by site dewatering activities. Monitoring of groundwater elevations following cessation of site dewatering to confirm long term site groundwater elevations is not needed because the design groundwater level per the DCD (elevation 591-feet [AP1000 Grade El. 98'-00"]) exceeds the upper bound of the expected groundwater elevation range (elevation 584-feet) (see [Table 2.0-201](#)).

The Lee Nuclear Station Unit 1 and Unit 2 nuclear island foundations are supported on continuous crystalline rock or on fill concrete supported on the continuous rock. Rock materials are described in [Subsections 2.5.1.2](#) and [2.5.4.1](#). The continuous crystalline rock and concrete materials below the nuclear island foundation are not susceptible to softening or solution due to long term

groundwater movements at the site. These materials are also not susceptible to piping or disturbance from groundwater movement.

Groundwater conditions required to facilitate placement and compaction of soil backfill adjacent to the nuclear island structures are discussed in [Subsections 2.5.4.5.4](#) and [2.5.4.6.3](#). The effects of groundwater related to lateral pressures on the below grade nuclear island walls are discussed in [Subsection 2.5.4.10.3](#).

2.5.4.7 Response of Soil, Granular Fill, and Rock to Dynamic Loading

WLS COL 2.5-6 This subsection provides a description of the response of soil, granular fill, and rock to dynamic loading including the following:

- Investigations of the effects of historic earthquakes on soil and rock such as paleoliquefaction ([Subsection 2.5.4.7.1](#)).
- Compressional and shear (P and S) wave velocity profiles from surface or borehole geophysical surveys, including data and interpretation ([Subsection 2.5.4.7.2](#)).
- Foundation conditions and uniformity ([Subsection 2.5.4.7.4](#)).
- Presentation of dynamic profiles ([Subsection 2.5.4.7.5](#)).

The dynamic properties for the site (seismic wave velocity, shear modulus, and damping) were developed from extensive field measurements of rock. These data are compiled and statistically analyzed to develop a suite of dynamic velocity profiles to evaluate epistemic variability (uncertainty in the mean) in rock properties for general classification of the site (e.g., hard rock, [DCD Subsection 2.5.4.5](#)), develop the site GMRS ([Subsection 2.5.2.6](#)) and the Lee Nuclear Station Unit 1 FIRS ([Subsection 2.5.2.7](#)), and for comparison to the Certified Seismic Design Response Spectra (CSDRS) as presented in [DCD Subsection 2.5.2.1](#). The GMRS and Unit 1 FIRS analysis, and comparison to the CSDRS are described in [Subsections 2.5.2.6](#) and [2.5.2.7](#), and [Section 3.7](#), respectively.

Granular backfill material obtained from an off-site source will be placed adjacent to the nuclear islands and beneath adjacent structures. Samples of this granular backfill material will be laboratory tested to determine its dynamic properties once the off-site source has been identified. Dynamic properties, modulus, Poisson's ratio, V_p and V_s wave velocities developed for granular fill are estimates based on Menq (2003) ([Reference 223](#)). The lower range and upper range of the shear modulus values ($G_{max} \times 1.5$ and $G_{max} / 1.5$) are considered for analysis (ASCE 4-98) ([Reference 220](#)).

2.5.4.7.1 Prior Earthquake Effects and Geologic Stability

As discussed in [Subsections 2.5.1](#) and [2.5.3](#), no active or potentially active faults or seismic deformation zones occur at the Lee Nuclear Station. Geologic mapping and subsurface explorations discussed in [Subsection 2.5.4.1](#), and presented in the Cherokee Nuclear Station PSAR ([Reference 201](#)), confirm that rock and soil materials at Lee Nuclear Station Units 1 and 2 nuclear island structures have not experienced seismically-induced ground failure (e.g., slope failure, liquefaction, lurching, subsidence) from historic or paleoearthquakes. The Lee Nuclear Station site investigation included geologic mapping of exposed rock surfaces within the existing Cherokee Nuclear Station excavation, and review of detailed historic construction records that include foundation level excavation mapping and rock structure zone report assessments developed during construction of the Cherokee Nuclear Station.

As described in [Subsection 2.5.4.1](#), bedrock underlying the Lee Nuclear Station Units 1 and 2 nuclear island structures is Middle Proterozoic to Permian (1,100 to 265 Ma) meta-granodiorite to meta-quartz diorite intruded by mafic dikes. These dense rock units are competent and not vulnerable to liquefaction or earthquake-induced ground failure. Continuity of bedrock below, between, and adjacent to the Lee Nuclear Station Units 1 and 2 nuclear islands is confirmed in the subsurface by a dense network of continuously-logged vertical and inclined rock core borings (to a maximum depth of 255 feet) as shown in [Figures 2.5.4-234](#) to [2.5.4-240](#).

Surficial geologic materials consist predominantly of medium dense to dense silty sand (SM) residual soils and saprolite developed over the igneous and metamorphic bedrock, and typically ranging in thickness between about 15 to 50 feet beyond the perimeter of the existing Cherokee Nuclear Station excavation. During construction of the Cherokee Nuclear Station unconsolidated materials were stripped off the bedrock in the former Units 1 and 2 and portions of Unit 3 excavations. Exposed non-weathered bedrock surfaces within the Cherokee Nuclear Station Units 2 and 3 excavations were evaluated during the Lee Nuclear Station investigation.

The maximum groundwater elevation is estimated to be at 579±5 ft msl and is described in [Subsection 2.5.4.6](#).

2.5.4.7.2 Field Dynamic Measurements

The following techniques were used to measure field dynamic properties in 2006-2007:

- Borehole P-S seismic velocity suspension logging surveys in 13 borings ranging in depth between about 95 to 255 feet and including rock and soil;
- Borehole downhole seismic velocity surveys in four borings (boring B-1000, B-1011, B-1024, and B-1037A) ranging in depth between about 84 to 215 feet that also were surveyed with P-S suspension logging for independent comparison of velocities measured in rock and soil;

- SASW surveys consisting of 15 linear arrays ranging in length from about 30 to 300 feet and including measurements in rock and soil;
- Seismic CPT seismic velocity surveys made in ten soundings ranging in depth between 32 to 84 feet and include measurements in soil.

In 2006-2007 and 2012, borehole P-S suspension log seismic velocity surveys were performed in the nuclear island footprint areas for both Lee Nuclear Station Unit 1 and 2, and between the two plant footprints, as shown on [Figure 2.5.4-215](#). The distribution of velocity measurements allowed confirmation of uniform seismic response under the Lee Nuclear Station nuclear island structures, evaluation of the local lower velocities at the Lee Nuclear Station Unit 1 northwest corner, and also within selected existing engineered fills. Each individual borehole velocity profile was evaluated and compared against the stratigraphic logging and laboratory test data of borehole samples to correlate velocities with rock type and structure (e.g., comparison of host and dike rock velocity) by elevation and corresponding depth below ground surface. After each individual borehole velocity data set was evaluated, borehole profiles were grouped based on site-specific location and were compiled using a common reference point (elevation or depth below ground surface).

In 2006-2007, four downhole seismic surveys were completed in boreholes that also were surveyed using P-S Suspension logging methods to provide an independent verification of rock velocity. The two methods produced velocity profiles that are very similar, as shown in [Figure 2.5.4-219](#), [Figure 2.5.4-222](#), [Figure 2.5.4-226](#), and [Figure 2.5.4-227](#). Data from both borehole survey techniques were integrated for development of the site velocity profiles. The comparative P-S suspension and downhole methods show quite consistent Vs values in the continuous rock throughout the 255 foot maximum velocity survey depth range with most borehole-average shear wave velocities generally centered at about 9,500 to 10,000 feet per second indicating uniform hard rock conditions. The P-S and downhole surveys show a good match, providing an independent check of the accuracy of measured velocities. The P-S velocity profiles show discrete velocity "spikes" or zones that range from about 1-foot to several tens of feet thick that are not observed by the "averaging" method inherent in the downhole surveys. These velocity differences are attributed to differing sample measurement intervals and methods between P-S suspension and downhole techniques. Additionally, the P-S velocity spikes may also correlate to variations in rock type, structure (e.g., jointing intensity), and intrusional dikes, but in other cases appear to represent limited randomness in velocity or possible survey-induced fluctuations, as measurement intervals using the P-S method are more closely spaced (3.3-foot intervals) than the downhole method (10-foot intervals). Even though the profiles are jagged with these localized vertical variations, the ranges in velocity fall within a tight range for the composite of all surveys.

In 2006-2007, a third geophysical method, Spectral Analysis of Surface Waves (SASW) described in [Subsection 2.5.4.4](#) was performed in the Lee Nuclear Station Unit 2 footprint area in the floor of the excavation and in existing fill materials located in both Unit 1 and Unit 2 Cooling Tower Pads. The SASW is a

surface method, and penetration into the hard bedrock exposed in the Cherokee Nuclear Station excavation floor was limited using the attempted wave generation sources. Therefore, a complete velocity profile for comparison against the borehole surveys was not possible. However, the shear wave velocities measured at the rock surface in the excavation floor by the SASW technique generally agree with the borehole survey measurements as shown on [Figure 2.5.4-224](#) and [Figure 2.5.4-225](#).

In 2006-2007, a fourth geophysical method, SCPT surveys, was performed in soil.

2.5.4.7.3 Deleted

2.5.4.7.4 Foundation Conditions and Uniformity

[Figure 2.5.4-241](#) shows the Lee Nuclear Station Units 1 and 2 footprints superimposed on a contour map showing the surface of continuous rock (rock defined with an RQD of at least 65 percent). The contours illustrated on this figure represent the top of continuous rock surface, defined as continuous rock displaying fresh to moderate weathering with an RQD of at least 65 percent, developed using borehole data from historic field explorations for the Cherokee Nuclear Station and the field explorations for the Lee Nuclear Station completed in 2006 and 2007. [Figure 2.5.4-241](#) also shows the extent of the partially constructed Cherokee Nuclear Station Unit 1 structures and the position of the Lee Nuclear Station Units 1 and 2 power block structures relative to the Cherokee Nuclear Station excavation.

2.5.4.7.4.1 Lee Nuclear Station, Unit 1 Nuclear Island

The foundation rock consists primarily of slightly weathered to fresh meta-granodiorite and meta-quartz diorite that exhibits high average seismic wave velocity (e.g., typical shear wave velocity range of about 9,000 to 10,000 feet per second). Northeast-trending meta-diorite dikes are present in the meta-granodiorite and meta-quartz diorite host rock. Rock in these dikes is similar in strength to the host rock, and contact margins typically are tight or minor local narrow altered/weathered zones. Borehole P-S and downhole seismic velocities measured in the intrusive dikes are similar to the host rock, and the dikes do not form significant zones of varied velocity. Therefore these intrusive bodies do not significantly influence the dynamic response of the rock mass. Relative variability in rock properties between the host rocks and dikes/intrusions are not deemed significant as their high strength and moduli are well above requirements for foundation bearing capacity, settlement, etc. and therefore do not represent a potential for differential site velocity or foundation performance.

Within the influence zone of the nuclear island foundation, the Lee Nuclear Station Unit 1 nuclear island footprint is entirely underlain by sound concrete that was placed over continuous rock during construction of the Cherokee Nuclear Station Unit 1 as shown on [Figure 2.5.4-241](#). The Cherokee Nuclear Station concrete was placed over a prepared rock surface of sound, continuous rock that met the [DCD Subsection 2.5.4.5](#) Subsurface Uniformity criteria. In some places, new fill concrete is placed over a sound prepared rock surface, or a cleaned and

roughened Cherokee Nuclear Station concrete surface, to develop the level basemat grade as part of the Lee Nuclear Station Unit 1 foundation construction. The thicknesses of the composite concrete, defined as Lee Nuclear Station and Cherokee Nuclear Station Unit 1 fill and structural concretes, under Lee Nuclear Station Unit 1 nuclear island basemat generally ranges between several feet to about 25 feet thick and contains localized areas underlain by CNS pump room that will be backfilled with approximately 22 ft of new fill concrete. The localized condition associated with the CNS pump rooms is limited to a small portion of the Unit 1 nuclear island footprint as depicted in [Figure 2.5.4-266](#). For development of the Lee Nuclear Station dynamic velocity model, the Unit 1 concrete materials are assumed to be of similar composition, strength, quality, and dynamic properties. Assumed dynamic properties for Cherokee Nuclear Station fill and structural concrete materials are estimated using static and dynamic field and laboratory correlations developed by Boone (2005) ([Reference 211](#)). The composite sound rock and fill concrete underlying the Lee Nuclear Station Unit 1 nuclear island basemat comply with the subsurface uniformity criteria as described in [DCD Subsection 2.5.4.5](#).

The foundation support zone for the Lee Nuclear Station nuclear island is entirely underlain by the footprint of the existing concrete foundation of Cherokee Nuclear Station Unit 1 which is underlain by continuous rock.

The nuclear island foundation rock is characterized as sound, massive meta-granodioritic to meta-quartz dioritic rock, no dipping layers exist and the rock supporting the nuclear island foundation meet DCD case 1 criteria.

2.5.4.7.4.2 Lee Nuclear Station, Unit 2 Nuclear Island

The Lee Nuclear Station Unit 2 nuclear island basemat at subgrade elevation is underlain by sound, massive meta-granodiorite and meta-quartz diorite bedrock with meta-diorite dikes. Rock in these intrusions is strong and similar in strength to the host rock, and contact margins are tight with minor local narrow altered/ weathered zones. The rock underlying the Lee Nuclear Station Unit 2 nuclear island complies with the subsurface uniformity criteria as described in [DCD Subsection 2.5.4.5](#). Minor localized areas of rock excavation or infilling with fill concrete is required under portions of the Lee Nuclear Station Unit 2 nuclear island footprint to develop a level bearing surface. Low areas will be backfilled with fill concrete to achieve basemat subgrade of similar composition and quality as that described above for Lee Nuclear Station Unit 1 nuclear island concrete fill to provide a dense, coupled interface with sound rock. The maximum thickness of fill concrete is about 20 feet beneath the east portion of the nuclear island, but generally will be less than about 1 to 2 feet. Unit 2 excavation conditions will require about 20 ft. of fill concrete between the bottom of the nuclear island and the top of continuous rock along the eastern edge of the nuclear island, [Subsection 2.5.4.2.2](#). This relatively small area of concrete fill required to build up the eastern edge of the Unit 2 nuclear island basemat will not result in localized adverse conditions due to the relatively small difference in shear wave velocity of fill concrete (7,500 ft/sec) and rock (8391 to 8983 ft/sec) in this area. The fill concrete conditions described for the Lee Nuclear Station Unit 2 nuclear island eastern portion have no practical significance on differential shear wave velocity,

site amplification or foundation performance. The nuclear island foundation rock is characterized as sound, massive meta-granodioritic to meta-quartz dioritic rock, no dipping layers exist and the rock supporting the nuclear island foundation meet DCD case 1 criteria.

2.5.4.7.5 Dynamic Profiles

This subsection presents the methodology and approach to develop site-specific dynamic velocity profiles at the Lee Nuclear Station site. Dynamic velocity profiles were compiled and applied at two locations for evaluation of site ground motion characteristics of Class I safety-related plant facilities with a third profile developed to evaluate generic engineered granular fill properties. These profiles are defined below.

- Smoothed Dynamic Profile A, Unit 1 nuclear island centerline
- Smoothed Dynamic Profile C, Unit 2 nuclear island centerline
- Best Estimate Layer Velocity Profile G, Generic engineered granular fill

Figure 2.5.4-247 shows the locations of the dynamic profiles (Profiles A and C) developed for the Duke Lee Nuclear Station. Smoothed dynamic profiles, Dynamic Profiles A and C, are shown on Figures 2.5.4-248 and 2.5.4-250, respectively. The site GMRS, discussed below and in Subsection 2.5.2, is represented by Profile A. Dynamic Profile C is used to evaluate possible differences in site response between Lee Nuclear Station Units 1 (Profile A) and 2 (Profile C) as a result of the spatial separation and possible lateral variability in the rock properties.

A third, artificial generic engineered granular fill profile, identified as Best Estimate Layer Velocity Profile G, was developed to represent engineered granular fill placed over the bedrock and around the plant nuclear islands to develop the plant grade. It represents a reasonable range of granular engineered fill materials, well-graded gravel (GW) (Figure 2.5.4-251a), poorly-graded gravel (GP) (Figure 2.5.4-251b), and well graded sand (SW) (Figure 2.5.4-251c) that may be placed adjacent to the AP1000 nuclear islands. These generic engineered granular fill seismic velocity profiles were constructed by estimating the maximum shear wave velocities, the elastic modulus values and the corresponding Poisson's ratio, and compression wave velocities for granular fill materials, well-graded gravel (GW) (Table 2.5.4-224A), poorly-graded gravel (GP) (Table 2.5.4-224B), and well graded sand (SW) (Table 2.5.4-224C) that may be typical of that to be placed at the site. The modulus ratio and damping ratio at various values of shear strain for generic granular fill materials, well-graded gravel (GW), poorly-graded gravel (GP), and well-graded sand (SW) are summarized in Tables 2.5.4-224D, 2.5.4-224E, and 2.5.4-224F. Shear modulus and damping ratio plots of these data are illustrated in Figures 2.5.4-253a, 2.5.4-253b, and 2.5.4-253c. During site preparation, the area forming the foundation support zone, as defined in Subsection 2.5.4.5.2 of the DCD, of the SC-II areas of the annex building and the turbine building first bay will be excavated to pre-existing concrete or to rock and built up to the level of the bottom of the nuclear island

foundation with fill concrete. If the rock in the foundation support zones of the SC-II buildings is above the elevation of the bottom of the nuclear island, the rock will be excavated to the elevation of the nuclear island bottom and replaced with granular fill materials. Generic granular fill Profile G extends to a depth that is consistent with this condition. The generic granular fill is described in [Subsection 2.5.4.5.3.5](#).

The shear wave velocities of granular fill in [Tables 2.5.4-224A](#), [2.5.4-224B](#) and [2.5.4-224C](#) are estimated based on the ground surface (yard elevation) at Elevation 592 feet. The modulus ratio and damping ratio results for the granular fill are in [Tables 2.5.4-224D](#), [2.5.4-224E](#) and [2.5.4-224F](#). In these tables, the depth reference is the ground surface.

Following the development of the dynamic profiles, two base case dynamic velocity profiles were developed for the Lee Nuclear Station Unit 1 centerline and one base case dynamic profile was developed for Lee Nuclear Station Unit 2. The base case models the Lee Units 1 and 2 nuclear island configuration and are described below.

- Base Case A1, Unit 1 Nuclear Island Centerline

Defines the GMRS and the typical relationship of the Lee Nuclear Station fill concrete (8.5 feet) overlying Cherokee Nuclear Station structural and fill concrete (composite 23.5 feet) above continuous rock.

- Base Case A5, Unit 1 CNS Pump Rooms

Defines the GMRS and localized condition of the Lee Unit 1 nuclear island that will overlie legacy CNS pump rooms at approximately 527 ft (NAVD). Base Case Profile A5 is based on the Lee Nuclear Station GMRS developed at the top of a hypothetical outcrop fixed at 523 ft (NAVD) transferred up through previously placed Cherokee Nuclear Station concrete materials and newly placed Lee Nuclear Station concrete materials to the basemat foundation level at 553.5 ft (NAVD). Base Case Profile A5 models the localized as-built areas of the Lee Unit 1 nuclear island that will overlie legacy CNS pump rooms ([Figure 2.5.4-266](#)). As depicted in [Figure 2.5.4-244e](#), the horizontal slab concrete of these pump rooms and existing waterproofing membrane will be removed during Lee construction and the pump rooms will then be backfilled using approximately 22 feet of fill concrete up to CNS basemat elevation 545 feet MSL with an additional 8.5 feet of fill concrete placed up to the basemat floor elevation (553.5 feet MSL) ([Reference 239](#)).

- Base Case C4, Unit 2 Nuclear Island Eastern Edge

Defines the GMRS and the typical relationship of proposed new leveling fill concrete above continuous rock. The location of Lee Unit 2 will require the emplacement of between 8 and 20 feet of new leveling fill concrete beneath the eastern extents of the Lee Unit 2 nuclear island as depicted in

Figure 2.5.4-267. Base Case C4 defines the GMRS and the maximum concrete thickness along the eastern extents of Lee Nuclear Station Unit 2.

The model representing Dynamic Profile Base Case A1, Unit 1 Centerline is shown on **Figure 2.5.4-252a**. Base Case A1 defined for the Lee Nuclear Station Unit 1 considers variability of site conditions such as material thickness and lateral variability within foundation rock, including Cherokee and Lee Nuclear Station concrete materials based on an average shear wave velocity of 7500 ft/sec. Assumed typical index properties for Cherokee Nuclear Station and Lee Nuclear Station concrete materials are summarized in **Table 2.5.4-223**. The site GMRS and Unit 1 FIRS (Base case profile A1) analysis are described in **Subsections 2.5.2.6** and **2.5.2.7**, respectively.

The model representing Dynamic Profile Base Case A5, Unit 1 CNS Pump Rooms is shown on **Figure 2.5.4-252b**. Base Case A5 defined for the localized as-built areas of the Lee Unit 1 nuclear island that will overlie legacy CNS pump rooms considers variability of site conditions such as as-built Lee constructed condition, material thickness and lateral variability within foundation rock, including Cherokee and Lee Nuclear Station concrete materials based on an average shear wave velocity of 7500 ft/sec. The additional thickness of fill concrete amounts to a 30% increase in the fill concrete profile is applicable for this small portion of the nuclear island foundation. Considering the limited area beneath the Unit 1 nuclear island represented by Base Case Profile A5, the increased fill concrete thickness will have no practical significance on differential shear wave velocity, site amplification or foundation performance and comply with the subsurface uniformity criteria as described in **DCD Subsection 2.5.4.5**. Base Case Profile FIRS A1 represents the dominant dynamic profile for Lee Nuclear Station Unit 1.

The model representing Dynamic Profile Base Case C4, Unit 2 Nuclear Island Eastern Edge is shown on **Figure 2.5.4-252c**. Base Case C4 defined for the location-specific as-built conditions beneath the eastern edge of the Unit 2 nuclear island considers variability of site conditions such as as-built Lee constructed condition, material thickness and lateral variability within foundation rock, including Lee Nuclear Station concrete materials based on an average shear wave velocity of 7500 ft/sec. The concrete profile represented in Base Case C4 is very similar to Base Case A1 (**Figure 2.5.4-252a**). The placement of up to about 20 ft of new fill concrete along the eastern edge of the Unit 2 nuclear island represents a minor difference in the base case profile and will have no practical significance on differential shear wave velocity, site amplification or foundation performance and comply with the subsurface uniformity criteria as described in **DCD Subsection 2.5.4.5**.

Assumed typical index properties for Cherokee Nuclear Station and Lee Nuclear Station concrete materials are summarized in **Table 2.5.4-223**. The site GMRS, Unit 1 FIRS (Base Case Profiles A1 and A5) and Unit 2 FIRS (Base Case

Profile C4) analysis are described in [Subsections 2.5.2.6](#) and [2.5.2.7](#), respectively.

2.5.4.8 Liquefaction Potential

WLS COL 2.5-1 In meeting the requirements of 10 CFR Parts 50 and 100, if the foundation
WLS COL 2.5-9 materials at the site adjacent to and under Category I structures and facilities are saturated soils and the water table is above bedrock, then an analysis of the liquefaction potential at the site is required. The need for a detailed analysis is determined by a study on a case-by-case basis of the site stratigraphy, critical soil parameters, and the location of safety-related foundations.

All seismic Category I safety-related plant foundations for Lee Nuclear Station Units 1 and 2 will bear on rock, or fill concrete over rock. Neither fill concrete nor rock is susceptible to liquefaction. Plan maps, cross sections, and summary boring logs presented in [Subsection 2.5.4.3](#) show the locations and rock foundation conditions of the Category I nuclear island structures that have a design subgrade elevation of 553.5 feet (AP1000 El. 60'-6"). The design basemat subgrade places the foundation for the Lee Nuclear Station Unit 1 nuclear island on existing concrete that was placed over a sound and cleaned rock surface remaining from the Cherokee Nuclear Station Unit 1, and directly on a newly-excavated and cleaned sound rock surface for the Lee Nuclear Station Unit 2 nuclear island. Therefore, a liquefaction hazard does not exist that could affect the Category I plant structures and facilities.

Outside the nuclear islands, compacted engineered granular fill is placed adjacent to seismic Category I structures over the exposed rock/fill concrete surfaces to the extent of 100 ft from the nuclear island walls or as necessary to form the foundation support zone of the seismic category II portion of the annex building and the turbine building (including the seismic category II first bay), whichever is the greater distance, as shown on [Figures 2.5.4-245](#) and [2.5.4-260](#) through [2.5.4-265](#). This granular backfill forms the supporting materials for the power block structures outside but adjacent to the nuclear islands. The typical thickness of granular fill is about 40 feet with a maximum thickness of about 55 feet under the radwaste building where fill concrete is not used to build up to the bottom of the nuclear island foundation. Beyond the perimeter of the granular fill as described above, Group I engineered fill is placed as necessary to completely backfill the Cherokee Nuclear Station excavation, encompassing the granular backfill around the Lee Nuclear Station nuclear island structures up to yard grade. As discussed in [Subsection 2.5.4.6](#), groundwater will rise above the bedrock surface within the engineered granular fill to elevations between about 574 feet to 584 feet msl.

Shallow foundations for non-Category I plant facilities adjacent to the nuclear island (i.e., seismic Category II part of the annex building, non-seismic radwaste building, and seismic Category II part of the turbine building), as well as the

foundations for the non-seismic part of the turbine building, are completely founded on or over compacted engineered granular fill over partially weathered rock/continuous rock, or compacted engineered granular fill over concrete and partially weathered rock/continuous rock. The non-seismic part of the annex building for Unit 1 is underlain at depth by continuous rock or by concrete over continuous rock. The northern part of the non-seismic part of the annex building for Unit 2 is underlain at depth by partially weathered rock, continuous rock, or fill concrete. The southern part of the non-seismic part of the Unit 2 annex building is underlain at depth by saprolite soils overlying partially weathered rock/continuous rock.

Subsection 2.5.4.5.1 describes the sources and extents of granular fill. The granular fill will likely have Unified Soil Classification System (USCS) classification symbol GW to GP (well-graded gravel to poorly-graded gravel) or SW (well-graded sand). **Subsection 2.5.4.5** describes material specifications and compaction for engineered granular fill. Granular fill will be compacted to 96 percent modified Proctor (ASTM D 1557) maximum dry density. Using an empirical relationship from **Reference 225** (Lee and Singh, 1971), the relative density of the granular fill compacted to 96 percent of the modified Proctor maximum dry density is 80 percent. According to an empirical correlation from **Reference 232** (Rollins, et al., 1998), gravel having 80 percent relative density would have a corresponding $(N_1)_{60}$ blow count of 45 blows per foot. According to **Reference 230** (Idriss and Boulanger, 2008), sand having 80 percent relative density would have a corresponding $(N_1)_{60}$ blow count of 29-30 blows per foot. These $(N_1)_{60}$ values may be considered as $(N_1)_{60cs}$ values owing to the low fines contents of the typical granular fill materials. Granular soils having $(N_1)_{60cs}$ blow counts of 29-30 or higher are classified as non-liquefiable according to Figure 2 of **Reference 231** (Youd, et al., 2001). Therefore the granular fill compacted to 96 percent modified Proctor relative compaction is not subject to liquefaction. Additionally, the floor of the excavation is relatively flat, and potential sloping basal surfaces do not exist adjacent to or below the granular fill that could present a potential lateral spread condition.

Subsection 2.5.4.5.3.3 describes the criteria and steps for verification of proper foundation support conditions below the base of the granular fill. **Figures 2.5.4-245** and **2.5.4-260** through **2.5.4-265** depict the conditions below the base of the granular fill. No saprolite underlies the granular fill supporting the seismic Category II parts of the annex and turbine buildings for Unit 1 and Unit 2, or the non-seismic parts of the turbine buildings for Unit 1 and Unit 2, or the non-seismic radwaste buildings for Unit 1 and Unit 2. The same is true for the non-seismic part of the annex building for Unit 1 and the northern portion of the non-seismic part of the annex building for Unit 2. Some saprolite may underlie the granular fill supporting the southernmost area of the non-seismic part of the Unit 2 annex building.

Saprolite to support the granular fill has N_{60} values greater than or equal to 15 blows per foot, measured at a depth of 3 feet below the base of the open excavation. **Table 2.5.4-211** indicates the saprolite soils have mean fines content of 46 percent with a standard deviation of 15 percent. The mean minus one

standard deviation fines content is thus 31 percent. For a fines content conservatively assumed as on the order of 15 percent, saprolite with N_{60} equal to 15 blows per foot at a depth of 3 feet below the base of the open excavation has $(N_1)_{60cs}$ values equal to 26-27 blows per foot, and thus may be considered as highly resistant to liquefaction per Figure 2 of [Reference 231](#) (Youd, et al., 2001).

The preceding analysis determines that no liquefaction hazard exists to seismic Category I safety-related plant structures and facilities, supported on sound rock or concrete over rock. As described above, neither fill concrete nor rock are susceptible to liquefaction. The analysis also determines that no liquefaction hazard exists for adjacent seismic Category II structures and facilities supported on compacted engineered granular fill over partially weathered rock/continuous rock, or compacted engineered granular fill over fill concrete and partially weathered rock/continuous rock. The compacted engineered granular fill and partially weathered rock will exhibit neither potential for liquefaction and related deformation, nor potential for adverse effects attributed to cyclic strain-softening or pore pressure build-up. Thus, any structure that could affect the Lee Nuclear Station Unit 1 and Unit 2 nuclear islands (including the seismic Category II portions of both the annex buildings and the turbine buildings, the non-seismic radwaste buildings), and also the non-seismic turbine buildings is on compacted engineered granular fill over partially weathered rock/continuous rock or compacted engineered granular fill over fill concrete over partially weathered rock/continuous rock, and is not subject to liquefaction.

Some saprolite may underlie the fill supporting the southernmost area of the non-seismic part of the annex building for Unit 2. This area will be highly resistant to liquefaction per Figure 2 of [Reference 231](#), and will exhibit low to nil potential for liquefaction and related deformation, and low potential for adverse effects attributed to cyclic strain-softening or pore pressure build-up. This location is also remote from the nuclear island and thus has no potential for affecting the nuclear island.

2.5.4.9 Earthquake Site Characteristics

WLS COL 2.5-6 A performance-based site-specific GMRS and FIRS was developed in accordance with the methodology provided in Regulatory Guide 1.208. This methodology and the development of the Unit 2 location-specific GMRS and Unit 1 location-specific FIRS are described in [Subsections 2.5.2.6](#) and [2.5.2.7](#), respectively. The GMRS and FIRS satisfies the requirements of 10 CFR 100.23 for development of a site-specific Safe Shutdown Earthquake (SSE) ground motion.

As recommended in RG 1.208, the following general steps were undertaken:

- Review the 2012 CEUS seismic source characterization (CEUS SSC) model, detailed in NUREG-2115, which was created to provide a regionally consistent model of seismic hazard for facilities throughout the central and eastern United States (Reference 245). Subsection 2.5.2 uses this most recent CEUS SSC as the starting point for the Lee Nuclear site PSHA for the site region (200-mile radius).
- Review the 2013 EPRI (2004, 2006) Ground-Motion Model (GMM) Review Project ground motion prediction equations (Reference 246).
- Perform sensitivity studies and an updated Probabilistic Seismic Hazard Analysis (PSHA) to develop rock hazard spectra and define the controlling earthquakes.
- Derive performance-based GMRS for Unit 2 and FIRS for Unit 1 from the updated PSHA at a free field hypothetical outcrop of the top of competent material beneath the proposed nuclear island.

The dynamic properties of soil, granular fill, concrete, and rock at the site were determined through a program of field exploration, laboratory testing, and analysis as described in Subsections 2.5.4.2, 2.5.4.4, and 2.5.4.7. The Lee Nuclear Station site is considered a hard rock site with rock having a shear wave velocity generally greater than 8000 fps. Results of site response analysis are described in Subsection 2.5.2, and a comparison to DCD design parameters is presented in Table 2.0-201.

2.5.4.10 Static Stability

WLS COL 2.5-6 The static stability of the Lee Nuclear Station nuclear island is evaluated for foundation bearing capacity, foundation settlement, and lateral pressures against below-grade walls. Evaluation of static stability includes the safety-related nuclear island facilities and the non-safety related structures adjacent to the nuclear island facilities. A discussion of bearing capacity, settlement, and lateral pressure evaluations is provided in Subsections 2.5.4.10.1 through 2.5.4.10.3. Foundation materials at the location of Lee Nuclear Station Unit 1 and Unit 2 nuclear islands consist of continuous rock and fill concrete placed on top of continuous rock. The fill concrete is used where the elevation of continuous rock is below the elevation of the nuclear island foundation.

Shallow foundations for non-Category I plant facilities adjacent to the nuclear island (i.e., seismic Category II part of the annex building, non-seismic radwaste building, and seismic Category II part of the turbine building) are completely founded on or over compacted engineered granular fill over partially weathered rock/continuous rock, or compacted engineered granular fill over fill concrete and partially weathered rock/continuous rock. The non-seismic part of the annex building and non-seismic part of the turbine building are founded on or over

compacted engineered granular fill over partially weathered rock/continuous rock, compacted engineered granular fill over fill concrete and partially weathered rock/continuous rock, or compacted engineered granular fill over saprolite soils overlying partially weathered rock/continuous rock.

WLS COL 2.5-13 The Unit 1 and Unit 2 nuclear island foundations are supported directly on continuous rock or fill concrete placed on top of continuous rock. Bearing capacity and settlement estimates of foundations supported on these materials are well within the limits provided in the DCD Subsections 2.5.4.2 and 2.5.4.3 as discussed in Subsections 2.5.4.10.1 and 2.5.4.10.2. Subsurface improvement of foundation materials is performed when necessary as described in Subsection 2.5.4.12. Cleaning and preparation of the continuous rock and fill concrete surfaces is also completed as described in Subsection 2.5.4.12 prior to placement of nuclear island foundation concrete. Instrumentation to monitor performance of the nuclear island foundations supported on the properly prepared continuous rock and on fill concrete materials supported on continuous rock is not necessary. As discussed in Subsection 2.5.4.6.1, the generic design groundwater elevation is 591 feet (AP1000 Elevation 98'-00") per the DCD. The basemat and below-grade walls are waterproofed to accommodate hydrostatic pressure due to groundwater. Groundwater loads are depicted in Figures 2.5.4-255a, 2.5.4-255b, and 2.5.4-255c.

2.5.4.10.1 Bearing Capacity

2.5.4.10.1.1 Bearing Capacity of Nuclear Islands

WLS COL 2.5-10 The bearing capacity of the Unit 1 and Unit 2 nuclear island foundation is evaluated separately for each unit. Two independent methods are used to determine the bearing capacity of the foundation materials. These methods are:

- Peck, Hanson and Thornburn (Reference 213) for allowable bearing pressure based on RQD of the rock as recorded at individual boring locations, and
- Ultimate Bearing Capacity based on the strength of the rock mass.

The Peck, Hanson, and Thornburn method utilizes an empirical relationship between allowable bearing pressure and average Rock Quality Designation. The allowable bearing pressure determined from this empirical relationship is compared to the required allowable bearing capacity provided in the DCD Subsection 2.5.4.2. The FSAR specifically considers 2006-2007 data, 2012 data, and historic boring data relevant to the positions of the nuclear islands. Calculations using this method estimate a minimum allowable bearing pressure of 190,000 lb/ft² at Unit 1 and 242,000 lb/ft² at Unit 2. These allowable bearing pressures exceed the bearing requirements of 8,900 lb/ft² static and 35,000 lb/ft²

combined (static plus seismic) loading provided in the [DCD Subsection 2.5.4.2](#) and [DCD Table 2-1](#).

The Ultimate Bearing Capacity method utilizes Hoek-Brown parameters of the rock mass to establish the Mohr-Coulomb parameters of friction angle and cohesion for the rock. The bearing capacity factors, as developed in EM 1110-1-2908 ([Reference 214](#)) and in Sowers ([Reference 215](#)), are determined based on the established Mohr-Coulomb parameters. Shape, size, and eccentricity correction factors are applied to the foundation conditions based on the size and shape of the nuclear island. The ultimate bearing capacity is then calculated using these parameters and factors. Bearing capacity calculations using these methods estimate an ultimate bearing capacity of at least 2,539,000 lb/ft² under static conditions and 2,444,000 lb/ft² under combined (static plus seismic) loading conditions.

The ultimate static bearing capacity of the foundation materials at the Lee Nuclear Station Site exceeds the [DCD Subsection 2.5.4.2](#) and [DCD Table 2-1](#) average static bearing reaction requirement of 8,900 lb/ft² by a factor of safety of at least 3.0. The ultimate bearing capacity of the foundation materials also exceeds the [DCD Subsection 2.5.4.2](#) and [DCD Table 2-1](#) required amount of 35,000 lb/ft² under all combined loads by a factor of safety of at least 1.5.

As described in [FSAR Subsection 3.8.5.5.1](#), the site-specific maximum bearing pressure is approximately 23,030 lb/ft², which is less than the AP1000 DCD requirement of 35,000 lb/ft², and significantly less than the site capacity described above.

2.5.4.10.1.2 Bearing Capacity of Adjacent Structures

The bearing capacity of the non-safety related structures adjacent to the nuclear islands [radwaste buildings, annex buildings (both non-seismic and Category II portions), and turbine buildings] is evaluated and the results are applicable to each unit. The methods used are:

- Peck, Hanson and Thornburn ([Reference 213](#)) for allowable bearing pressure on the granular backfill to limit settlement, and
- Ultimate Bearing Capacity based on the strength of the granular fill divided by a factor of safety equal to 3 to determine the safe bearing capacity.

The method of Peck, Hanson and Thornburn ([Reference 213](#)) is used to estimate the allowable bearing pressure to limit settlement based on SPT blow count of the granular fill. The Peck, Hanson and Thornburn ([Reference 213](#)) method determines the allowable foundation loading which, if not exceeded, will result in settlements not to exceed 1 inch for smaller footings and not to exceed 2 inches for larger foundation areas (e.g., mat foundations). However, Peck, Hanson and Thornburn ([Reference 213](#)) recommend that the ultimate bearing capacity also be calculated to verify that foundations that would appear not to undergo the limiting

settlement also have an acceptable margin of safety against a bearing capacity failure.

The $(N_1)_{60cs}$ values for the granular fill mentioned in Subsection 2.5.4.8 are used as the SPT $(N_1)_{60}$ blow counts of the potential granular fill.

Peck, Hanson and Thornburn (Reference 213) published a convenient chart for proportioning shallow foundations bearing on granular soil, shown on their Figure 19.3. In the Peck, Hanson and Thornburn (Reference 213) Figure 19.3, the allowable bearing pressure is plotted on the y-axis and foundation width is plotted on the x-axis. For a given N value, the allowable bearing pressure increases as the foundation width increases until a maximum value is reached at a particular foundation width; beyond this point, allowable bearing pressure is constant, independent of foundation width. The sloping lines rising up from the origin as the width of footing increases represent the region where the safe bearing capacity governs. The horizontal lines for various N values represent the region where the allowable settlement governs.

Peck, Hanson and Thornburn (Reference 213) state that footing foundations proportioned in accordance with the chart on their Figure 19.3 will, on the basis of experience, not settle more than 1 inch total, and the differential settlements between individual foundations will not exceed tolerable limits.

For large mat foundations (such as those that support the project structures), Peck, Hanson, and Thornburn (Reference 213) indicate that, based on geotechnical experience, if total foundation settlement is limited to 2 inches, differential settlement will be limited to 0.75 inch, and the performance of the structure should not be impacted.

Peck, Hanson, and Thornburn (Reference 213) thus determines the allowable foundation loading which, if not exceeded, will result in settlements not to exceed 1 inch for smaller footings and not to exceed 2 inches for larger foundation areas (e.g., mat foundations). If the safety factor against exceeding the ultimate bearing capacity as calculated earlier herein is adequate, the maximum applied bearing pressure to cause settlement not to exceed 1 or 2 inches according to Peck, Hanson, and Thornburn (Reference 213) is:

$$q_{\text{allowable_1 inch}} = 0.11 (N_1)_{60} \times C_w \text{ (tsf), and}$$

$$q_{\text{allowable_2 inches}} = 0.22 (N_1)_{60} \times C_w \text{ (tsf)}$$

where C_w is the effect of the water table, as discussed below.

The chart on Peck, Hanson, and Thornburn (Reference 213) Figure 19.3 is for the conditions where the supporting granular material remains above the water table. If the depth of the groundwater table (D_w) will be less than the sum of the foundation depth (D_f) and the width (B), then the allowable bearing pressure to

limit total settlement is adjusted for water table depth using the water table correction factor (C_w):

$$C_w = 0.5 + \frac{0.5D_w}{D_f + B}$$

where:

D_w = depth to groundwater measured from the ground surface surrounding the foundation; and

C_w = adjustment factor for depth of the groundwater table (D_w) if less than the sum of the foundation depth below the ground surface (D_f) and smallest foundation dimension (B); the minimum value is 0.5; the maximum value is 1.0.

Note: If $D_w \leq D_f$, $C_w = 0.5$.

Due to the yard surface not being level, the operative values of D_f shown in [Table 2.5.4-230](#) are used for computing C_w . The future water table may be as high as an elevation of 584 ft, which would be about 8 ft below the yard surface at the perimeter of the buildings. The yard surface slopes down away from the buildings and therefore is not level; the datum for measuring D_w is the average yard surface. For example, for an average depth to the bottom of the mat equal to 3.0 ft, below the average sloping yard level this would place the future water table at a depth of 7.5 ft below the average yard level for computing C_w . This depth of water table, about 7.5 ft, is reasonable to apply to the foundations for the radwaste and annex buildings. The foundation bearing levels in the turbine building are at generally differing elevations than those of the radwaste and annex buildings, and D_f and D_w are appropriately assigned.

The ultimate bearing capacity calculation utilizes the unit weight and shear strength parameters of the potential granular fill materials found in [Table 2.5.4-211](#) in conjunction with the bearing capacity equations by Hanson as found in Bowles (5th ed., [Reference 216](#)).

The radwaste buildings, annex buildings (Category II portion), and turbine buildings have mat foundations that occupy the entire building area. Therefore, the case for limiting settlement equal to 2 inches is applicable for these buildings. The annex building (non-Category II portion) may have individual spread footing foundations.

Building dimensions in [Table 2.5.4-230](#) are based on [Reference 235](#); the foundation base elevations in [Table 2.5.4-230](#) are based on [Reference 237](#); the best estimates of loading of the building foundations in [Table 2.5.4-230](#) are based on [Reference 236](#). The calculated allowable bearing pressures (with a factor of safety of 3 against the ultimate bearing capacity) on the granular fill are shown in

Table 2.5.4-228. The calculated allowable bearing pressures for settlements not to exceed 2 inches for mats are shown in **Table 2.5.4-229**. The results show the maximum safe bearing pressures based on the factor of safety are significantly greater than the applied pressures (**Table 2.5.4-230**). The allowable pressures to limit settlement are also greater than the applied pressures.

The bearing capacity calculations indicate the mat foundations of the radwaste buildings, annex buildings (Category II portion), and turbine buildings will perform as intended. This is consistent with the expected performance of foundations supported on dense granular fill. The calculations demonstrate that the allowable safe bearing pressure with a factor of safety of 3 against exceeding the ultimate bearing capacity will not govern foundation performance for the mat foundations. The allowable bearing pressure for settlements not to exceed 2 inches for mat foundations will exceed the applied pressures on the foundations. The granular fill will provide acceptable support for the buildings to be placed on it (radwaste, annex (Category II portion), and turbine buildings) and anticipated settlement of these foundations are less than the published limit of 2 inches.

2.5.4.10.2 Settlement

WLS COL 2.5-12 2.5.4.10.2.1 Settlement of Nuclear Islands

Estimates of post-construction settlement are calculated separately for Unit 1 and Unit 2 based on the theory of elasticity. Three settlement methods (equations) are employed for estimation of settlement beneath the nuclear island using this approach. The three methods used are:

- The Steinbrenner equation (**Reference 216**).
- The Corps of Engineers equation (**Reference 214**).
- The Boussinesq equation (**Reference 217**).

The calculations estimate settlement resulting from static loading of the nuclear island foundation bearing directly on rock or bearing on a depth of fill concrete in turn resting on rock. An equivalent area approach is used to model the nuclear island as one or more rectangular areas for purposes of estimating settlement.

The theory of elasticity based on the elastic modulus (Young's modulus) and Poisson's ratio is used to develop a subsurface model of the fill concrete and rock layers below the foundation. Poisson's ratio measurements from P-S suspension logging (as described in **Subsection 2.5.4.2**) are used along with Young's modulus values measured from laboratory tests on intact cores and from P-S suspension logging measurements. Young's modulus values based on laboratory core measurements are reduced to account for Rock Quality Designation based on a relationship by Zhang and Einstein (**Reference 218**) to develop a representative

in situ rock mass modulus. Young's modulus values based on P-S suspension logging measurements were reduced by 50 percent to develop a representation of in situ rock mass modulus independent of the Rock Quality Designation.

Young's modulus values for continuous rock are used even where rock of lesser Rock Quality Designation is removed and replaced with fill concrete. This is because modulus values of the in situ foundation quality rock are lower than that of the fill concrete. This results in additional conservatism for the settlement estimate because the rock modulus values are used in place of fill concrete modulus values.

An estimate of settlement is also performed using the results of the empirical approach described by Peck, Hanson, and Thornburn ([Reference 213](#)) which is based on the Rock Quality Designation of the rock below the foundation. The allowable bearing pressure determined using this method assumes that the foundation settlement is limited to one-half inch. The settlement is assumed to be proportional to the ratio of allowable bearing pressure (as described in [Subsection 2.5.4.10.1](#)) versus the required allowable average bearing pressure (as developed in [DCD Table 2-1](#)).

Lee Nuclear Station nuclear island structures are founded on rock and fill concrete which does not incur sufficient settlement to disrupt the operation of the structure. The FSAR considers the 2006-2007 data, 2012 data, and historic CNS data. Settlement of Lee Nuclear Station Unit 1 and Unit 2 nuclear island structures founded on rock or fill concrete is calculated to be less than 1/10 of an inch. The maximum estimated settlement is 0.047 inches beneath Unit 1 and 0.048 inches beneath Unit 2 using the elastic modulus methods. The maximum estimated settlement is 0.071 inches beneath Unit 1 and 0.055 inches beneath Unit 2 using the empirical Rock Quality Designation based method. Differential settlement, even if equivalent to the estimated maximum total settlement, is within the limits allowed by [DCD Subsection 2.5.4.3](#) (0.5 inch in 50 ft allowable).

The settlement calculations assumed the foundation load is applied while the water table is maintained at the bottom elevation of the nuclear island. Some of the settlement is recovered as heave (also called rebound) when the water table is allowed to rise and thus apply buoyant unloading to the nuclear island. This is of no practical significance because the settlements calculated are small and therefore the portion of settlement recovered as heave (rebound) is small and insignificant.

2.5.4.10.2.2 Settlement of Adjacent Structures

Settlement of the structures adjacent to the nuclear islands is discussed in [Subsection 2.5.4.10.1.2](#) as part of the evaluation of bearing capacity of the granular fill. These results indicate the mat foundations of the radwaste buildings, annex buildings (Category II portion), and turbine buildings will settle less than 2 inches. The foundation performance of these buildings supported on the

granular fill will meet the [DCD Subsection 2.5.4.3](#) criterion of 3-inch differential settlement relative to the settlement of the nuclear islands.

2.5.4.10.3 Lateral Pressures

WLS COL 2.5-11 The highest water table (Elevation 584 feet) is below the design water table from the DCD (AP1000 Elevation 98'-00", corresponding to Lee Nuclear Station Elevation 591 ft).

Lateral pressures are developed against the below-grade nuclear island wall resulting from the placement and compaction of granular backfill materials. Earth pressure envelopes are calculated for active, at-rest, and passive pressure conditions as developed in [Figures 2.5.4-255a](#), [2.5.4-255b](#), and [2.5.4-255c](#). Lateral earth pressure values based on the maximum groundwater elevation are provided in [Tables 2.5.4-225A](#), [2.5.4-225B](#), and [2.5.4-225C](#). Potential compaction-induced earth pressures are presented in [Figure 2.5.4-256a](#). Numerical values of compaction-induced earth pressure are given in [Table 2.5.4-226A](#). The compaction-induced earth pressures in [Table 2.5.4-226A](#) do not result in excessive lateral pressures on the nuclear island walls ([Reference 247](#)). [Table 2.5.4-226B](#) provides some generic combinations of soil compaction equipment and closest distance from the nuclear island wall the compaction equipment can be operated without exceeding the envelope of residual + at-rest pressure values adjacent to the nuclear island wall in [Table 2.5.4-226A](#). Assumptions or references used to develop the active, at-rest, passive, and compaction-induced earth pressure envelopes are described in the following list.

Earth Pressure Assumptions:

- The granular fill used to backfill around the nuclear islands will likely come from an off-site borrow source such as an operating quarry, as described in [Subsection 2.5.4.5](#). The granular fill will likely be USCS group symbol GW to GP (well-graded gravel to poorly-graded gravel) or SW (well-graded sand) and have material properties as described in [Subsection 2.5.4.2](#).
- Granular backfill is compacted to 96 percent of the maximum dry density determined from the modified Proctor laboratory test performed in accordance with ASTM D 1557.
- Appropriate compaction equipment is used to compact the granular fill within close proximity of the nuclear island walls. Heavier compaction equipment may be used at greater distances from the walls. The use of appropriate compaction equipment near the wall avoids excessive compaction-induced stresses against the wall.

- The potential compaction-induced earth pressures for vibratory roller compactors are computed using the method in Peck and Mesri, 1987 (Reference 229). The potential compaction-induced earth pressures for vibratory plate compactors are computed using information in Duncan, et al., 1991 (Reference 238).
- The groundwater table elevation may vary over time between elevations 584 and 574 feet. The design water table elevation from the Design Control Document is up to elevation 591 feet (AP1000 Elevation 98'-00").
- The nuclear island walls do not yield due to the lateral earth pressure applied to them. The at-rest pressure is the appropriate earth pressure to assume for design of the walls.

The Rankine earth pressure theory is used to compute the active and passive (ultimate) earth pressure.

The dynamic lateral earth pressure in Table 2.5.4-227 and plotted on Figure 2.5.4-256b is calculated in accordance with Reference 220 - ASCE 4-98, Section 3.5.3, Figure 3.5-1, "Variation of Normal Dynamic Soil Pressures for the Elastic Solution." Backfill properties for granular fill adjacent to the vertical surface of the nuclear island exterior walls and basemat for dynamic earth pressure calculation are as follows:

- Saturated unit weight of backfill (γ) = 150 lb/ft³ (GW)
= 142 lb/ft³ (GP)
= 136 lb/ft³ (SW)
(from Table 2.5.4-211)
- Poisson's ratio (ν) = 0.5 (see discussion below)

The Poisson's ratio, $\nu = 0.5$, is used because the granular fill is predominantly below the design groundwater table.

The seismic acceleration used, $(a) = 0.352g$, is applied as a uniform seismic acceleration to the granular backfill along the height of the nuclear island wall.

Westinghouse has evaluated the Lee Nuclear Station site-specific lateral earth pressures and has determined that they are bounded by the standard AP1000 design pressures (Reference 247). FSAR Subsection 3.8.4.4.4 describes the evaluation of those site-specific lateral earth pressures.

The lateral earth pressure is calculated for a ground surface associated with the presence of the adjacent buildings; this is not affected by changes to the ground surface contour elevations beyond the outside walls of these buildings.

2.5.4.11 Design Criteria

Table 2.0-201 compares the DCD site parameter criteria and the site characteristics, including the following items:

- Average Allowable Static Bearing Capacity
- Maximum Allowable Dynamic Bearing Capacity for Normal Plus SSE
- Shear Wave Velocity
- Site and Structures Conditions and Geologic Features
- Properties of the Underlying and Adjacent Subsurface Materials and Geologic Features
- Lateral Variability of Foundation Bearing Material Stiffness
- Liquefaction Potential

Design of safety-related foundations is based on the nuclear island foundation mat being supported by continuous rock or by fill concrete supported on continuous rock. Continuous rock is defined, for this purpose, as rock that is fresh to moderately weathered and has a Rock Quality Designation of at least 65%, based on the boring logs. Soil and rock not meeting this definition of continuous rock is removed down to the level of continuous rock. Where the elevation of continuous rock is below the elevation of the base of the foundation mat, fill concrete is placed between the continuous rock and the foundation mat. Fill concrete material meets the requirements for structural plain concrete as defined in Section 2.1 of ACI 318-02 (**Reference 233**).

Discussions of design criteria, assumptions, and conservatism used in analysis of soil and rock response to dynamic loading are included in **Subsection 2.5.4.7**.

Discussions of design criteria, assumptions, and conservatism in liquefaction analysis are included in **Subsection 2.5.4.8**.

The design criteria used for static stability analyses are identified in **Subsection 2.5.4.10**. Factors of safety estimates are applicable to the calculation of bearing capacity only and are discussed in **Subsection 2.5.4.10.1**. Discussion of assumptions and conservatism in static stability analyses are included in **Subsection 2.5.4.10**.

2.5.4.12 Techniques to Improve Subsurface Conditions

For Unit 1 and Unit 2, the nuclear island foundation mat is supported by continuous rock, or by fill concrete that is supported on continuous rock. Soil, rock, and concrete material above the design foundation subgrade elevation in the nuclear island area is removed by mechanical excavators or by controlled blasting. Poor quality rock, if present, is excavated and removed down to

continuous rock. Continuous rock is based on criteria of fresh to moderate weathering and RQD of at least 65%, based on the boring logs. Relatively minor zones of lower RQD rock are allowed to remain. The verification program to monitor the effectiveness of this foundation improvement is described as follows. The final excavation surface is observed and geologically mapped to document the presence of suitable materials prior to placement of fill concrete or foundation concrete. Mapping of the final excavation surface is completed as described in [Subsection 2.5.4.5](#) prior to foundation treatment or placement of any fill materials.

When suitable continuous rock or concrete at or below the foundation elevation is reached, the rock or concrete surface is cleaned and prepared to receive fill concrete or foundation concrete. Cleaning and preparation of foundation materials consists of the following:

- Removing loose soil, rock, or other materials from the foundation surface.
- Removing protrusions and overhangs within the rock or concrete.
- Washing the exposed rock or concrete surface with air and/or water.
- Treating isolated depressions or cracks in the rock or concrete surface with fill concrete.
- Roughening exposed concrete surfaces as described in [Subsection 2.5.4.5.3.2](#).

The cleaning and preparation of the rock foundation surface, to support the nuclear islands and fill concrete, extends to expose continuous rock for a distance of at least 6 feet beyond the nuclear island foundation limits. Beyond the 6-foot distance, the excavations extend to expose continuous rock for supporting fill concrete within the 0.5 horizontal to 1 vertical distance needed for lateral extension due to depth of suitable materials below the fill concrete surface.

Beneath the nuclear island footprints and within the 6-foot zone around the nuclear island foundation footprint, or beneath the slope of fill concrete associated with the nuclear island, isolated weathered rock or joints in the rock surface that were filled with soil-like material are excavated and treated with fill concrete. This generally applies to relatively steeply dipping linear features less than five feet in horizontal width as shown in [Figure 2.5.4-257](#). Steeply dipping linear features less than three feet in horizontal width remain as their presence does not adversely affect the stresses in the thick, heavily reinforced structural basemat of the nuclear island. The soil or weathered rock material filling the joint is excavated to a depth equal to at least twice the width of the joint and the excavated area replaced with fill concrete. If a feature is found to be more shallowly dipping, it is similarly treated to remove the soil, facilitate cleaning, and allow placement of fill concrete as shown in [Figure 2.5.4-258](#). The presence of other intersecting joints and fractures within the rock surface, if present, requires the removal of overhanging rock surfaces as shown in [Figure 2.5.4-259](#).

The Cherokee Nuclear Station Unit 1 circular reactor building and the structures adjacent to it were designed for the dewatered condition and were constructed with an under slab drainage system. This drainage system consists of a network of channels located below the Cherokee Nuclear Station foundation slabs. The under slab drainage network is contained within the footprint of the Cherokee Nuclear Station structures and was sealed at the Cherokee foundation perimeter. Removal of the isolation joint surrounding the Cherokee Nuclear Station circular reactor building exposes portions of this existing drainage network within the foundation support zone of the nuclear island. Removal of the Cherokee Nuclear Station auxiliary building basemat because of its high elevation in the southern end of the Lee Nuclear Station nuclear island basemat exposed portions of this existing drainage network. Where the Cherokee Nuclear Station drainage system is exposed by Lee Nuclear Station construction it is sealed off to keep the Lee Nuclear Station fill materials from eroding into the Cherokee Nuclear Station drainage channels. The sealing of these drainage channels is not an issue where the Cherokee Nuclear Station foundation structures are not removed; the drainage channels do not extend to the edges of the Lee Nuclear Station basemats and thus pose no risk that the Lee Nuclear Station fill materials can erode into the drainage channels. The Cherokee Nuclear Station foundation basemat drainage system and an outline of the Lee Nuclear Station nuclear island foundation limits are shown on [Figures 2.5.4-244a](#) through [2.5.4-244e](#).

2.5.4.13 References

201. Duke Power Company, Project 81, Cherokee Nuclear Station Preliminary Safety Analysis Report, 1974.
202. NUREG-0189, "Final Safety Evaluation Report, Cherokee Nuclear Station, Units 1, 2, and 3, Duke Power Company," Office of Nuclear Reactor Regulation, Docket Nos. STN 50-491, 50-492, and 50-493, pp 2-20-2-25.
203. Horton, J.W., Drake, A.A., and Rankin, D.W., "Tectonstratigraphic terranes and their Paleozoic boundaries in the central and southern Appalachians," Geological Society of America, Special Paper 230, p. 213-245, 1989.
204. Removed
205. Duke Power Company, Project 81, "Preliminary Safety Analysis Report (PSAR), vol. 4, Appendix 2C – Geology," Prepared by Law Engineering Testing Company – Cherokee Nuclear Station, 270p., July 1974.
206. Horton, J.W. Jr., "Geologic Map of the Kings Mountain Belt Between Gaffney, South Carolina and Lincolnton, North Carolina," in *Geological Investigations of the Kings Mountain Belt and Adjacent Areas in the Carolinas*, Carolina Geological Society field trip guidebook, 1981.
207. Murphy, C.F. and Butler, J.R., "Geology of the Northern Half of the Kings Creek Quadrangle, South Carolina," in *Geological Investigations of the Kings Mountain Belt and Adjacent Areas in the Carolinas*, Carolina Geological Society field trip guidebook, 1981.

208. Horton, J.W., Jr. and Butler, J.R., "Geology and Mining History of the Kings Mountain Belt in the Carolinas; a Summary and Status Report," in *Geological Investigations of the Kings Mountain Belt and Adjacent Areas in the Carolinas*, Carolina Geological Society field trip guidebook, 1981.
209. American Concrete Institute (ACI), "Code Requirements for Nuclear Safety Related Concrete Structures," ACI 349-02, Chapter 11.7.
210. Brandon, Thomas M., Rose, Andrew T., and Duncan, J. Michael, (2006), "Drained and Undrained Strength Interpretations for Low-Plasticity Silts," *Journal of Geotechnical and Geoenvironmental Engineering*, ASCE Volume 132, No. 2, February, 2006, pages 250-257.
211. Boone, S.D., 2005, "A Comparison Between the Compressive Strength and the Dynamic Properties of Concrete as a Function of Time" MS Thesis, University of Tennessee, Knoxville, May 2005.
212. Removed
213. Peck, Ralph B., Hanson, Walter E., and Thornburn, Thomas H., *Foundation Engineering*, 2nd Edition, John Wiley and Sons, NY, pp. 362, 1974.
214. US Army Corps of Engineers, 1994, "EM 1110-1-2908, Engineering and Design – Rock Foundations," Chapter 6.
215. Sowers, George F., "Introductory Soil Mechanics and Foundations: Geotechnical Engineering," 4th Edition, McMillian, NY, Chapter 10, 1979.
216. Bowles, Joseph E., "Foundation Analysis and Design," 5th Edition pp. 303-310, 4th Edition pp. 256-261, 443-447, McGraw-Hill, Inc., 1996, 1988.
217. Li, K. S. (1995). "Discussion of Foundation Uniform Pressure and Soil-structure Interaction," *ASCE Journal of Geotechnical Engineering*, December 1995, page 912.
218. Zhang, Lianyang and Einstein, H.H., 2004, "Using RQD to estimate the deformation modulus of rock masses," *Intl. Journal of Rock Mechanics & Mining Sciences* 41, pp. 337-341.
219. Removed
220. ASCE Standard 4-98, *Seismic Analysis of Safety-Related Nuclear Structures and Commentary*, American Society of Civil Engineers, 2000.
221. Not used.
222. Deleted.

-
223. Menq, F.Y. 2003. Dynamic Properties of Sandy and Gravelly Soils, Ph.D. Dissertation, University of Texas at Austin, 364 pages.
224. South Carolina Department of Transportation (SCDOT), 2007. Standard Specifications for Highway Construction, Subsection 305.2.5.5 (Macadam Base Course) and Subsection 408.2.2 (Washed Screenings).
225. Lee, K.L., and Singh, A., 1971. Relative Density and Relative Compaction, Journal of the Soil Mechanics and Foundation Division, Proc. of the American Society of Civil Engineers, Vol. 97, No. SM7, July, pp. 1049 – 1052.
226. Horton, J.W. Jr., and Dicken, C.L., Preliminary Digital Geologic Map of the Appalachian Piedmont and Blue Ridge, South Carolina Segment, U.S. Geological Survey Open-File Report 01-298, 1:500,000 scale, 2001.
227. Nystrom Jr., P.G. Geologic Map of the Blacksburg South 7.5 Minute Quadrangle, Cherokee County, South Carolina [preliminary draft], South Carolina Department of Natural Resources Geological Survey, 1:24,000 scale, 1 sheet, 2004.
228. NAVFAC, 1986. Soil Mechanics, Design Manuals 7.01 and 7.02, Naval Facilities Engineering Command, Alexandria, VA.
229. Peck, R. B., and Mesri, G., 1987. "Discussion of Compaction - Induced Earth Pressure under K_0 Conditions," Journal of Geotechnical Engineering, ASCE, 113 (11), pp. 1406-1408.
230. Idriss, I. M., and Boulanger, R. W., 2008. Soil Liquefaction during Earthquakes, Monograph MNO 12, Earthquake Engineering Research Institute, Oakland, CA, Equation (37), page 87.
231. Youd, T. L., Idriss, I. M., Andrus, R. D., Arango, I., Castro, G., Christian, J. T., Dobry, R., Finn, W. D., Harder Jr., L. F., Hynes, M. E., Ishihara, K., Koester, J. P., Liao, S. C., Marcuson III, W. F., Martin, G. R., Mitchell, J. K., Moriwaki, Y., Power, M. S., Robertson, P. K., Seed, R. B., and K. H. Stokoe II, 2001. Liquefaction Resistance of Soils: Summary Report from the 1996 NCEER and 1998 NCEER/NSF Workshops on Evaluation of Liquefaction Resistance of Soils, Journal of Geotechnical and Geoenvironmental Engineering, Vol. 127, No. 10, American Society of Civil Engineers, October, 2001, pages 817 to 833. Also, see Errata in Closure to "Liquefaction Resistance of Soils: Summary Report from the 1996 NCEER and 1998 NCEER/NSF Workshops on Evaluation of Liquefaction Resistance of Soils", Journal of Geotechnical and Geoenvironmental Engineering, Vol. 129, No. 3, American Society of Civil Engineers, March, 2003, pages 284 to 286.

232. Rollins, K. M., Evans, M., Diehl, N. and Daily, W., 1998. "Shear Modulus and Damping Relationships for Gravels," Journal of Geotechnical and Geoenvironmental Engineering, ASCE, Vol. 124, No. 5, pp. 396 – 405, Equation (7), page 397.
233. American Concrete Institute (ACI), "Building Code Requirements for Structural Concrete," ACI 318-02, Chapter 2.1, 2002.
234. Not used.
235. Westinghouse Electric Company LLC. AP1000 Plant Grid Coordinates and Column Line Identification Plan, Drawing APP-0030-X4-001, Revision C.
236. Westinghouse Electric Company LLC, 2012. APC/WLG000108, Letter to Mr. John McConaghy, Duke Energy, Subject: "Transmittal of Table 5 - Surcharge Pressure from APP-1000-CCC-005, Revision 4", dated June 19.
237. Westinghouse Electric Company LLC, AP1000 Plant Grid Coordinates and Column Line Identification Plan, Drawing APP-0000-X4-901, Revision A.
238. Duncan, J. M., Williams, G. W., Sehn, A. L., and Seed, R. B., 1991. Estimation Earth Pressures Due to Compaction, Journal of Geotechnical Engineering, Vol. 117, No. 12.
239. Shaw, 2011, Constructability Study: Methodology and Sequence for Final Demolition Activities for the Removal of Cherokee Legacy Waterproofing Membrane and Sheathing of Steel-lined Collection Puts, Pump Rooms and Other Localized Sumps and Pits, Rev. 0, December 20, 2011.
240. Removed
241. Zoback, M.L. and Zoback, M.D., "Tectonic Stress Field of the Continental United States," in Geophysical Framework of the Continental United States, Geological Society of America Memoir 172:523-539, 1989.
242. Zoback, M.L., Zoback, M.D., Adams, J., Assumpcao, M., Bell, S., Bergman, E.A., Bluemling, P., Brereton, N.R., Denham, D., Ding, J., Fuchs, K., Gay, N., Gregersen, S., Gupta, H.K., Gvishiani, A., Jacob, K., Klein, R., Knoll, P., Magee, M., Mercier, J.L., Mueller, B.C., Paquin, C., Rajendran, K., Stephansson, O., Suarez, G., Suter, M., Udias, A., Xu, Z.H., and Zhizin, M., "Global Patterns of Tectonic Stress," Nature 341 (6240):291-298, 1989.
243. Zoback, M.L., "Stress Field Constraints on Intraplate Seismicity in Eastern North America," Journal of Geophysical Research 97 (B8):11,761-11,782, 1992.

244. Heidbach, O., Tingay, M., Barth, A., Reinecker, J., Kurfess, D., and Muller, B., The World Stress Map database release 2008, doi:10.1594/GFZ.WSM.Rel2008.
245. U.S. NRC, 2012, NUREG-2115, Technical Report: Central and Eastern United States Seismic Source Characterization for Nuclear Facilities. EPRI, Palo Alto, CA, U.S. DOE, and U.S. NRC: January, 2012.
246. EPRI (2013). EPRI (2004, 2006) Ground-Motion Model (GMM) Review Project, Elec. Power Res. Inst, Palo Alto, CA, Rept. 3002000717, June 2013.
247. Westinghouse Electric Company LLC, 2013. "William S. Lee Site-Specific Assessment of Lateral Earth Pressure Loads Due to 2012/2013 CEUS Ground Motion Seismic Input," Document No.WLG-1000-S2R-806, Rev. 2, November, 2013.

2.5.5 STABILITY OF SLOPES

WLS COL 2.5-14 This section provides an evaluation of the stability of earth and rock slopes, both natural and manmade, failure of which could adversely affect the safety of the seismic Category I plant components. The plant design for Lee Nuclear Station Units 1 and 2 does not require external safety cooling, ultimate heat sink, or related embankments. No safety related retaining walls, bulkheads, or jetties are constructed at the site.

WLS COL 2.5-15 No manmade earth or rock dams are present on the site that could adversely affect the safety of the nuclear power plant facilities. Potential dam failure is addressed in [Subsection 2.4.4](#).

WLS COL 2.5-14 The plants are centrally sited within a backfilled excavation forming a broad, relatively level yard grade at approximate elevation 592 feet for a distance of approximately 1000 feet from the nuclear island. No natural or manmade slopes exist in proximity to the safety related nuclear island structures that pose a potential slope stability hazard to the safe operation of the plant. Additionally, no natural descending slopes, such as river banks or ridge slopes, exist around the perimeter of the Lee Nuclear Station plant yard area that pose a potential encroachment or undermining hazard. Site investigations, subsurface geotechnical characterizations, and excavation and backfill profiles used for the slope stability evaluation are presented in [Subsections 2.5.4.1, 2.5.4.2, 2.5.4.3, and 2.5.4.5](#).

2.5.5.1 Slope Characteristics

2.5.5.1.1 General Discussion

Permanent slopes within a one-quarter mile distance of the Lee Nuclear Station Units 1 and 2 nuclear island structures were evaluated to determine the potential hazard to the safety-related structures. The locations of permanent slopes within this search area are identified on [Figure 2.5.5-201](#) and include both natural slopes and cut slopes in native soil and rock materials, and engineered fill slopes. The permanent slope conditions, including features such as slope number, constructed condition, slope height and inclination, and approximate distances from the Units 1 and 2 nuclear islands, are summarized in [Table 2.5.5-201](#). Additional descriptions for two of these slopes nearest to the nuclear island structures are provided below.

The permanent slopes are either natural slopes that have existed for a long period of time (through most or all of the Holocene; natural slopes), or cut and fill slopes developed as part of the Cherokee Nuclear Station construction in the early 1980's. These slopes exhibit acceptable stability without visual evidence of groundwater seepage, past failure, incipient movement, or major creep.

Liquefaction potential, as discussed in [Subsection 2.5.4.8](#), indicates that the native soils and engineered fill are not prone to liquefaction. Therefore, a potential liquefaction-induced slope stability hazard does not exist under static or dynamic conditions that could adversely affect the seismic Category I plant components.

The nearest permanent slope that ascends above the Lee Nuclear Station nuclear island area is a natural hill slope located southwest of the Unit 1 (Slope 5). This slope is also the highest slope within the one-quarter mile search area. This hill slope may be trimmed during plant grading.

This hill rises approximately 80 feet above the yard elevation. The hill has a slope of approximately 2.5 horizontal to 1 vertical and is located about 1000 feet from the Unit 1 nuclear island. The closest distance to the toe of the slope is more than 9 times the height of the slope. No credible mechanism of slope failure would predict movement of the slope failure material over such a large distance. Based on the past stable history, slope height and inclination, and the distance from the nuclear island, this hill does not pose a hazard to safety related structures. Excavation of this hill for borrow source material may reduce the slope height, and the toe of slope may be relocated in a southerly direction away from the plant area, further reducing the already negligible potential hazard.

The nearest permanent slope that descends below the plant yard grade and the nuclear island area is an engineered slope located north of Unit 2 (Slope 7). The top of this slope is about 1200 feet from the nuclear island. This slope descends 55 feet below the yard elevation to the surface of a pond adjacent to the Broad River. The slope is inclined approximately 2 horizontal to 1 vertical. There is no credible mechanism whereby failure of a descending slope 55 feet high and 1200 feet away could affect the nuclear island. Based on the distance, height, and

inclination of this slope from the nuclear island, it does not pose a hazard to the safety related structures.

2.5.5.1.2 Exploration Program

Site investigations and subsurface geotechnical characterization used for the slope stability evaluation are presented in [Subsections 2.5.4.1](#), [2.5.4.2](#), and [2.5.4.3](#). The geological interpretation and geotechnical material properties presented in these sections were considered in this stability assessment of permanent slopes. The site exploration and testing data provide information regarding the stratigraphy, and engineering properties of rock, soil, and engineered fill that form the permanent slopes.

2.5.5.1.3 Groundwater and Seepage

A detailed discussion of groundwater conditions and characterization, including water levels and in situ rock mass and soil hydraulic conductivity, is provided in [Subsections 2.4.12](#) and [2.5.4.6](#). Groundwater characterization included installation of monitoring wells and pump test wells adjacent to the Lee Nuclear Station Units 1 and 2 power block excavation area, and an evaluation of existing information from the Duke Power Company Project 81 Preliminary Safety Analysis Report Amendment 31 ([Reference 201](#)). As discussed in [Subsection 2.5.4.6](#), the maximum groundwater elevation is estimated to be at 579±5 feet mean sea level. This 579 foot elevation value was based on the water mark along the exterior of the Cherokee Nuclear Station Unit 1 reactor building. At the time of this measurement in 2006, the Cherokee Nuclear Station excavation was being dewatered using a series of automated pumps that conveyed discharge water to the nearby Make-Up Pond B.

Groundwater seepage in natural and manmade slopes is not considered a hazard as no natural or manmade slopes exist in close proximity to the safety-related structures.

2.5.5.1.4 Slope Materials and Properties

Permanent slopes include slopes comprised of existing engineered fill and native residual and saprolitic soil and the material properties are described in [Subsection 2.5.4.2](#). Geologic maps and cross sections presented in [Subsection 2.5.4.3](#) show the distribution of geologic materials with respect to the locations of permanent slopes. Permanent slopes will not affect seismic Category I structures, and therefore the selection of material properties is not necessary.

The stability assessment consisted of an evaluation of the slope locations, geometries, inclinations, past stability, distance from the Units 1 and 2 nuclear island structures, and observed long-term slope performance. Slope materials and properties were used in a general sense to help guide engineering judgment regarding set back distances between the slopes and safety-related structures, including consideration of reasonable angle of friction values for various site slope materials in the event of a large slope failure.

Existing permanent slope inclinations are inclined at about 2 horizontal to 1 vertical (about 26.5 degrees) or less. Angles of friction for materials comprising the slopes are higher than this angle of slope inclination. Because the permanent slope inclinations are less than the material angles of friction, the evaluated slopes are determined to be inherently stable even when ignoring the cohesive component of the shear strength of the material. Consideration of the cohesive component considerably increases the perceived inherent stability of the slopes. In the unlikely event of slope failure induced by groundwater rise, seepage, or dynamic loading, any mobilized materials will not travel significantly from the toe of slope. In a similar sense, potential headscarp inclinations related to failure of descending slopes likely would be steeply inclined due to the cohesive strength component of the slope materials. In any event, the long-term static stability of permanent slopes located within the one-quarter mile evaluation distance does not pose a hazard to the safety related structures.

As discussed in [Subsection 2.5.4.1](#), no continuous, adversely-oriented weak clay or mylotinized zones, or planes of past slope failure were observed, or are expected, in the bedrock underlying the Lee Nuclear Station Units 1 and 2 power block area that could affect stability of the plant. As described in [Subsection 2.5.4.8](#), the native residual soils, and engineered fill composed of native residual soils are not prone to liquefaction. Therefore, a potential slope stability hazard does not exist under static or dynamic conditions that could adversely affect the seismic Category I plant components.

2.5.5.2 Design Criteria and Analyses

Analyses of permanent slope conditions were limited to a review of permanent slopes within a one-quarter mile distance from the Units 1 and 2 nuclear island structures. This conservative evaluation is based on past performance, height, slope angle, and distance from the safety related structures. The nearest permanent slopes are 1000 feet or more away from the Units 1 and 2 nuclear island structures. These permanent slopes do not require further analysis, including quantitative pseudostatic analysis, to calculate a safety factor because there is no failure mechanism that would create a hazard to the safety related structures.

No permanent slopes were identified in which failure would pose a hazard to the Lee Nuclear Station Units 1 and 2 safety-related structures.

2.5.5.3 Logs of Borings

No borings, test pits, or trenches were used for stability analyses of permanent slope conditions surrounding the Lee Nuclear Station Units 1 and 2 safety-related nuclear island structures. Boring logs for general site conditions are discussed in [Subsection 2.5.4.3](#).

2.5.5.3.1 Soil Borings

No logs of soil borings were used for stability analyses of permanent slope conditions because there were no slopes determined to be a hazard to safety related structures.

2.5.5.3.2 Rock Borings

No logs of rock borings were used for stability analyses of permanent slope conditions because there were no slopes determined to be a hazard to safety related structures.

2.5.5.3.3 Test Pits and Trenches

No logs of test pits or trenches were used for stability analyses of permanent slope conditions because there were no slopes determined to be a hazard to safety related structures.

2.5.5.4 Compacted Fill

There are no safety-related permanent dams, dikes, or embankments constructed at the Lee Nuclear Station site. Therefore, design/performance criteria for compacted fills are not described.

2.5.5.5 References

201. Duke Power Company, Project 81, *Preliminary Safety Analysis Report, Amendment 31*.

STD DEP 1.1-1 2.5.6 COMBINED LICENSE INFORMATION

2.5.6.1 Basic Geologic and Seismic Information

WLS COL 2.5-1 This COL item is addressed in [Subsections 2.5.1, 2.5.4.1, 2.5.4.3, 2.5.4.3.3, 2.5.4.3.5, 2.5.4.8, Appendix 2AA, and Appendix 2BB](#).

2.5.6.2 Site Seismic and Tectonic Characteristics Information

WLS COL 2.5-2 This COL item is addressed in [Section 2.5](#) and [Subsections 2.5.2 and 2.5.4.3.3](#).

2.5.6.3 Geoscience Parameters

WLS COL 2.5-3 This COL item is addressed in [Subsection 2.5.4.3.3](#).

2.5.6.4 Surface Faulting

WLS COL 2.5-4 This COL item is addressed in [Subsection 2.5.3](#).

2.5.6.5 Site and Structures

WLS COL 2.5-5 This COL item is addressed in [Subsections 2.5.4.1](#), [2.5.4.3.5](#), and [2.5.4.5](#).

2.5.6.6 Properties of Underlying Materials

WLS COL 2.5-6 This COL item is addressed in [Subsections 2.5.4.2](#), [2.5.4.2.1](#), [2.5.4.3.6](#), [2.5.4.4](#), [2.5.4.5.1](#), [2.5.4.5.2](#), [2.5.4.5.3](#), [2.5.4.7](#), [2.5.4.9](#), and [2.5.4.10](#).

2.5.6.7 Excavation and Backfill

WLS COL 2.5-7 This COL item is addressed in [Subsections 2.5.4.3.6](#), [2.5.4.5.1](#), [2.5.4.5.2](#), and [2.5.4.5.3](#).

2.5.6.8 Groundwater Conditions

WLS COL 2.5-8 This COL item is addressed in [Subsections 2.5.4.5.4](#) and [2.5.4.6.4](#).

2.5.6.9 Liquefaction Potential

WLS COL 2.5-9 This COL item is addressed in [Subsection 2.5.4.8](#).

2.5.6.10 Bearing Capacity

WLS COL 2.5-10 This COL item is addressed in [Subsection 2.5.4.10.1](#).

2.5.6.11 Earth Pressures

WLS COL 2.5-11 This COL item is addressed in [Subsection 2.5.4.10.3](#).

2.5.6.12 Static and Dynamic Stability of Facilities

WLS COL 2.5-12 This COL item is addressed in [Subsection 2.5.4.10.2](#).

2.5.6.13 Subsurface Instrumentation

WLS COL 2.5-13 This COL item is addressed in [Subsection 2.5.4.10](#).

2.5.6.14 Stability of Slopes

WLS COL 2.5-14 This COL item is addressed in [Subsection 2.5.5](#).

2.5.6.15 Embankments and Dams

WLS COL 2.5-15 This COL item is addressed in [Subsection 2.5.5](#).

2.5.6.16 Settlement of Nuclear Island

WLS COL 2.5-16 This COL item is not addressed because it relates only to soil sites. Lee Nuclear Station is a rock site.

2.5.6.17 Waterproofing Systems

WLS COL 2.5-17 This COL item is addressed in [Subsection 14.3.3.1](#).

TABLE 2.5.1-201
DEFINITIONS OF CLASSES USED IN THE COMPILATION OF
QUATERNARY FAULTS, LIQUEFACTION FEATURES, AND
DEFORMATION IN THE CENTRAL AND EASTERN UNITED
STATES

	Class Category	Definition
WLS COL 2.5-1	Class A	Geologic evidence demonstrates the existence of a Quaternary fault of tectonic origin, whether the fault is exposed for mapping or inferred from liquefaction to other deformational features.
	Class B	Geologic evidence demonstrates the existence of a fault or suggests Quaternary deformation, but either (1) the fault might not extend deeply enough to be a potential source of significant earthquakes, or (2) the currently available geologic evidence is too strong to confidently assign the feature to Class C but not strong enough to assign it to Class A.
	Class C	Geologic evidence is insufficient to demonstrate (1) the existence of tectonic fault, or (2) Quaternary slip or deformation associated with the feature.
	Class D	Geologic evidence demonstrates that the feature is not a tectonic fault or feature; this category includes features such as demonstrated joints or joint zones, landslides, erosional or fluvial scarps, or landforms resembling fault scarps, but of demonstrable non-tectonic origin.

Source: Crone and Wheeler (2000) ([Reference 310](#)); Wheeler (2005) ([Reference 311](#))

TABLE 2.5.1-202
RADIOMETRIC AGE DETERMINATIONS FROM UNDISTURBED SITE ROCKS

Rubidium-Strontium Analyses

	Sample ID	Sample Material	Rb (ppm)	Sr (ppm)	Rb/Sr	Rb ⁸⁷ /Sr ⁸⁶	Apparent Age (millions of yrs.)
WLS COL 2.5-1	B-51, 76 ft	Biotite from undisturbed felsic gneiss behind slickenside	247.6	43.68	5.669	16.52	291 ± 10
	B-64, 120 ft	Biotite from felsic gneiss	184.4	40.92	4.516	13.14	277 ± 10

Potassium-Argon Analyses

	Sample ID	Sample Material	K (weight %)	Sample weight (g)	% radiogenic Ar	Apparent Age (millions of yrs.)
	BP-7, 59 ft	Biotite from undisturbed felsic gneiss behind slickenside	6.74	0.0433	95.4	296 ± 7
	B-28, 106 ft	Hornblende from undisturbed mafic gneiss behind slickenside	0.248	0.4345	84.8	290 ± 9
	B-37, 70.5 ft	Whole rock very fine-grained felsic gneiss (metagraywacke?)	1.054	0.8759	88.2	322 ± 2
	B-53, 69 ft	Whole rock felsic gneiss	1.371	0.2697	35.5	362 ± 7
	B-58, 33 ft	Whole rock felsic gneiss	0.931	1.0103	87.9	288 ± 1
	B-236, 72 ft	Whole rock felsic gneiss	4.975	0.5395	92.6	234 ± 1
	GTP-7, Sta. 18	Potassium feldspar and quartz from undisturbed pegmatitic quartz vein crossing a shear zone	8.946	0.1984	87.8	219 ± 1

Source: Duke PSAR Table 2C-3B (Reference 401).

TABLE 2.5.1-203 (Sheet 1 of 2)
DEFORMATION PHASES AND STRUCTURAL ELEMENTS IN THE STUDY AREA

Deformation Phase	D ₁	D ₂	D ₃	D ₄	D ₅
Folds	F ₁ , isoclinal, upright	F ₂ , isoclinal to tight, upright	F ₃ open, upright (crenulations)	F ₄ , close to tight	F ₅ , gentle to open warp, kink folds
WLS COL 2.5-1 Surface Folded	S ₀ , bedding and/or compositional layering	S ₀ and S ₁ foliation	S ₀ , S ₁ , S ₂	S ₀ , S ₁ , S ₂ , S ₃	S ₀ , S ₁ , S ₂ , S ₃ , S ₄
Planar Structures	S ₁ , generally present only in hinge area of F ₂ folds, transposed by later D ₂ deformation, axial planar to F ₁	S ₂ , dominant metamorphic schistosity, axial planar to F ₂	S ₃ , crenulation cleavage, axial planar to F ₃	S ₄ , crenulation (weak)	S ₅ , kink planes
Linear Structures	L ₁ , locally intersection of S ₀ with S ₁	L ₂ , intersection of S ₁ and S ₂ , boudinage of thin biotite schist layers and quartz veins, mineral elongation lineation	L ₃ , crenulation axes, intersection S ₃ with S ₂	L ₄ , crenulation axes (?), intersection S ₄ with S ₂	L ₅ , axes of kink folds, intersection of S ₅ with S ₂
Attitude	F ₁ -NE to SE axes rotated in plane of S ₂ , S ₁ dips to SE	F ₂ -N to NE axes, S to SW axes, S ₂ predominantly dips steeply SE, in areas dips NW	F ₃ -NE axes, S ₃ strikes NE, dips steeply NW	F ₄ -NE axes, plunge at low angles, axial planar S ₄ cleavage subhorizontal	F ₅ -NE and SE axes, axial planes and kink planes sub-vertical, strike NE and NW, intersection of S ₅ and S ₂ plunges steeply down dip on S ₂
Shearing and Faulting	Ductile, N to NE strike, parallel to limbs of F ₂ folds, possibly due to the attenuation of limbs during F ₂ fold event		Brittle, brecciation, NE and NW strikes reactivation of earlier ductile shear zones		

TABLE 2.5.1-203 (Sheet 2 of 2)
DEFORMATION PHASES AND STRUCTURAL ELEMENTS IN THE STUDY AREA

Deformation Phase	D ₁	D ₂	D ₃	D ₄	D ₅
Metamorphism	M ₁ , progressive regional metamorphism to amphibolite grade, central portion of belt to upper greenschist grade, M ₁ , D ₁ , and D ₂ closely related in time, thermal peak of regional metamorphism after major D ₁ deformation and during or after D ₂ deformation		Lower greenschist conditions present, shear and breccia zones healed by quartz, epidote, mica, and K-feldspar, near end M ₁		M ₂ , hydrothermal zeolite event, probably occurs after D ₅

Source: Schaeffer (1981) ([Reference 392](#))

TABLE 2.5.1-204
DEFORMATION EVENTS RECORDED AT THE SITE LOCATION

WLS COL 2.5-1

Site Deformation Event	Structural Expression	Correlation to Site Area Deformational Events	Age Constraint
d ₁	Ductile fabric in shear - breccia zones	Possibly D ₂ but may be D ₃ or D ₄	Pre-300 Ma greenschist facies overprint
d ₂	Brittle overprint of ductile fabric in shear - breccia zones	Possibly D ₃ but may be D ₄ or D ₅	Pre-300 Ma greenschist facies overprint
d ₃	Dilation fractures	Possibly D ₃ but may be D ₄ or D ₅	Pre-300 Ma greenschist facies overprint
d ₄	Joints and joints with slickensides on surfaces associated with calcite and chlorite	Possibly D ₃ but may be D ₄ or D ₅	Pre-300 Ma greenschist facies overprint
d ₅	Joints and joints with slickensides	Mesozoic extension	Mesozoic
d ₆	Slickensides in saprolite	weathering	soil development

TABLE 2.5.2-201
DELETED

TABLE 2.5.2-202
DELETED

TABLE 2.5.2-203
DELETED

TABLE 2.5.2-204
DELETED

TABLE 2.5.2-205
DELETED

TABLE 2.5.2-206
DELETED

TABLE 2.5.2-207
DELETED

TABLE 2.5.2-208
DELETED

TABLE 2.5.2-209
DELETED

TABLE 2.5.2-210
DELETED

TABLE 2.5.2-211
DELETED

TABLE 2.5.2-212
DELETED

TABLE 2.5.2-213
DELETED

TABLE 2.5.2-214
DELETED

TABLE 2.5.2-215
DELETED

TABLE 2.5.2-216
DELETED

WLS COL 2.5-2

TABLE 2.5.2-217
UHRs AMPLITUDES FOR 10^{-4} , 10^{-5} , AND 10^{-6}

UHRs results, g			
ground motion frequency	mean 10^{-4}	mean 10^{-5}	mean 10^{-6}
PGA	0.228	0.724	1.79
25 Hz	0.468	1.51	3.83
10 Hz	0.379	1.14	2.82
5.0 Hz	0.245	0.688	1.69
2.5 Hz	0.145	0.372	0.926
1.0 Hz	0.0694	0.163	0.390
0.5 Hz	0.0436	0.101	0.230

WLS COL 2.5-2

TABLE 2.5.2-218
CONTROLLING EARTHQUAKES FROM DEAGGREGATION

	mean 10^{-4}	mean 10^{-5}	mean 10^{-6}
Low Frequency M ^(a)	7.2	7.3	7.4
Low Frequency R ^(a) (km)	250	230	190
High Frequency M	6.1	6.0	6.2
High Frequency R (km)	35	16	12

a) M and R calculated for R>100 km.

WLS COL 2.5-2

TABLE 2.5.2-219 (Sheet 1 of 2)
HORIZONTAL UHRS AND GMRS AMPLITUDES

Frequency Hz	10^{-4} Horizontal UHRS, g	10^{-5} Horizontal UHRS, g	10^{-6} Horizontal UHRS, g	Horizontal GMRS, g
100	2.28E-01	7.24E-01	1.79E+00	3.45E-01
90	2.46E-01	7.83E-01	1.94E+00	3.73E-01
80	2.79E-01	8.87E-01	2.20E+00	4.22E-01
70	3.28E-01	1.05E+00	2.60E+00	4.97E-01
60	3.89E-01	1.24E+00	3.10E+00	5.91E-01
50	4.44E-01	1.42E+00	3.56E+00	6.76E-01
40	4.76E-01	1.53E+00	3.84E+00	7.27E-01
35	4.82E-01	1.55E+00	3.90E+00	7.36E-01
30	4.79E-01	1.54E+00	3.90E+00	7.33E-01
25	4.68E-01	1.51E+00	3.83E+00	7.17E-01
20	4.62E-01	1.47E+00	3.70E+00	6.99E-01
15	4.38E-01	1.36E+00	3.40E+00	6.51E-01
12.5	4.14E-01	1.27E+00	3.15E+00	6.09E-01
10	3.79E-01	1.14E+00	2.82E+00	5.49E-01
9	3.57E-01	1.06E+00	2.63E+00	5.13E-01
8	3.33E-01	9.81E-01	2.42E+00	4.74E-01
7	3.07E-01	8.90E-01	2.19E+00	4.32E-01
6	2.77E-01	7.93E-01	1.95E+00	3.86E-01
5	2.45E-01	6.88E-01	1.69E+00	3.36E-01
4	2.10E-01	5.73E-01	1.41E+00	2.81E-01
3.5	1.91E-01	5.11E-01	1.26E+00	2.52E-01
3	1.69E-01	4.45E-01	1.10E+00	2.20E-01
2.5	1.45E-01	3.72E-01	9.26E-01	1.85E-01

WLS COL 2.5-2

TABLE 2.5.2-219 (Sheet 2 of 2)
HORIZONTAL UHRS AND GMRS AMPLITUDES

Frequency Hz	10^{-4} Horizontal UHRS, g	10^{-5} Horizontal UHRS, g	10^{-6} Horizontal UHRS, g	Horizontal GMRS, g
2	1.27E-01	3.19E-01	7.84E-01	1.59E-01
1.5	1.03E-01	2.51E-01	6.09E-01	1.26E-01
1.25	8.72E-02	2.09E-01	5.05E-01	1.05E-01
1	6.94E-02	1.63E-01	3.90E-01	8.24E-02
0.9	6.58E-02	1.54E-01	3.65E-01	7.80E-02
0.8	6.13E-02	1.43E-01	3.37E-01	7.26E-02
0.7	5.62E-02	1.31E-01	3.05E-01	6.63E-02
0.6	5.03E-02	1.17E-01	2.69E-01	5.92E-02
0.5	4.36E-02	1.01E-01	2.30E-01	5.12E-02
0.4	3.49E-02	8.08E-02	1.84E-01	4.10E-02
0.35	3.05E-02	7.07E-02	1.61E-01	3.59E-02
0.3	2.62E-02	6.06E-02	1.38E-01	3.07E-02
0.25	2.18E-02	5.05E-02	1.15E-01	2.56E-02
0.2	1.74E-02	4.04E-02	9.20E-02	2.05E-02
0.15	1.31E-02	3.03E-02	6.90E-02	1.54E-02
0.125	1.09E-02	2.53E-02	5.75E-02	1.28E-02
0.1	6.98E-03	1.62E-02	3.68E-02	8.20E-03

WLS COL 2.5-2

TABLE 2.5.2-220 (Sheet 1 of 2)
VERTICAL UHRS AND GMRS AMPLITUDES

Frequency (Hz)	10^{-4} Vertical UHRS, g	10^{-5} Vertical UHRS, g	10^{-6} Vertical UHRS, g	Vertical GMRS, g
100	0.208	0.674	1.67	0.320
90	0.214	0.697	1.74	0.330
80	0.225	0.741	1.87	0.350
70	0.246	0.830	2.14	0.391
60	0.304	1.059	2.75	0.495
50	0.403	1.439	3.64	0.669
40	0.444	1.50	4.11	0.706
35	0.419	1.45	4.12	0.680
30	0.420	1.41	3.94	0.664
25	0.421	1.39	3.64	0.657
20	0.418	1.31	3.41	0.624
15	0.394	1.21	2.95	0.579
12.5	0.371	1.086	2.65	0.526
10	0.317	0.968	2.37	0.464
9	0.311	0.928	2.21	0.448
8	0.303	0.872	2.09	0.424
7	0.287	0.802	1.94	0.392
6	0.251	0.710	1.76	0.346
5	0.214	0.611	1.52	0.297
4	0.164	0.478	1.23	0.232
3.5	0.144	0.410	1.055	0.199
3	0.119	0.333	0.855	0.163
2.5	0.090	0.250	0.635	0.122

WLS COL 2.5-2

TABLE 2.5.2-220 (Sheet 2 of 2)
VERTICAL UHRS AND GMRS AMPLITUDES

Frequency (Hz)	10^{-4} Vertical UHRS, g	10^{-5} Vertical UHRS, g	10^{-6} Vertical UHRS, g	Vertical GMRS, g
2	0.081	0.217	0.539	0.107
1.5	0.0678	0.179	0.448	0.0883
1.25	0.0590	0.155	0.387	0.0767
1	0.0478	0.124	0.306	0.0616
0.9	0.0451	0.117	0.286	0.0581
0.8	0.0417	0.108	0.261	0.0535
0.7	0.0373	0.096	0.230	0.0478
0.6	0.0323	0.083	0.196	0.0412
0.5	0.0266	0.0681	0.160	0.0339
0.4	0.0213	0.0545	0.128	0.0271
0.35	0.0186	0.0477	0.112	0.0237
0.3	0.0160	0.0409	0.096	0.0203
0.25	0.0133	0.0341	0.0798	0.0169
0.2	0.0106	0.0272	0.0638	0.0135
0.15	0.0080	0.0204	0.0479	0.0102
0.125	0.00665	0.0170	0.0399	0.0085
0.1	0.00426	0.0109	0.0255	0.00542

WLS COL 2.5-2

TABLE 2.5.2-221
POINT SOURCE PARAMETERS**M 5.1, single-corner**

G(g)	Distance, mi. [km]	Depth, mi. [km]
1.50	0 [0]	1.25 [2]
1.25	0 [0]	1.25 [2]
1.00	0 [0]	2.5 [3]
0.75	0 [0]	2.5 [4]
0.50	0 [0]	3 [5]
0.40	0 [0]	4 [6]
0.30	0 [0]	5 [8]
0.20	4 [7]	5 [8]
0.10	10 [16]	5 [8]
0.05	17 [28]	5 [8]
0.01	50 [80]	5 [8]

Notes: Additional parameters used in each model are:

$$Q = 670 f^{0.33}$$

$$\Delta\sigma (1c) = 110 \text{ bars}$$

$$k = 0.006 \text{ sec, hard rock}$$

Hard Rock Crustal Model

Thickness, mi. [km]	Vs (km/sec)	Vp (km/sec)	ρ (cgs)
0.6 [1]	2.83	4.90	2.52
7 [11]	3.52	6.10	2.71
17 [28]	3.75	6.50	2.78
[infinite]	4.62	8.00	3.35

WLS COL 2.5-2

TABLE 2.5.2-222
WEIGHTING SCHEME TO DEVELOP V/H RATIOS

Profile	Weighting		Empirical Relation Weights		Site Condition Weights	
	Empirical	Model	A&S (1997)	C&B (2003)	Soft Rock	Soil
A1	0.2	0.8	0.5	0.5	1.0	0.0
A5	0.2	0.8	0.5	0.5	1.0	0.0
C4	0.2	0.8	0.5	0.5	1.0	0.0

Notes:

A&S (1997) = Abrahamson and Silva (1997) (Reference 296)

C&B (2003) = Campbell and Bozorgnia (2003) (Reference 298)

TABLE 2.5.2-223
MOMENT MAGNITUDE, DISTANCE RANGES, AND WEIGHTS
FOR V/H RATIOS

Empirical V/H Ratio Weights						
APE (yr ⁻¹)	High-Frequency ≥ 5.0 Hz			Low-Frequency ≤ 2.5 Hz		
	Magnitude (M)			Magnitude (M)		
	5.1	7.0	8.0	5.1	7.0	8.0
	weights			weights		
10 ⁻⁴	0.9	0.1	0.0	0.40	0.50	0.10
10 ⁻⁵	1.00	0.0	0.0	0.80	0.15	0.05
10 ⁻⁶	1.00	0.0	0.0	0.95	0.05	0.0

Empirical V/H Ratio Distances	
Magnitude (M)	Distance, mi. (km)
5.1	3 (5)
7.0	35 (57)
8.0	35 (57)

Model V/H Ratio Weights (M 5.1)						
APE (yr ⁻¹)	High-Frequency ≥ 5.0 Hz			Low-Frequency ≤ 2.5 Hz		
	Distance, mi. (km)			Distance, mi. (km)		
	17 (28)	4 (7)	0 (0)	17 (28)	4 (7)	0 (0)
	weights			weights		
10 ⁻⁴	0.1	0.45	0.45	0.6	0.2	0.2
10 ⁻⁵	0.0	0.55	0.45	0.2	0.4	0.4
10 ⁻⁶	0.0	0.6	0.4	0.05	0.6	0.35

WLS COL 2.5-2

TABLE 2.5.2-224 (Sheet 1 of 2)
FIRS AND UHRS FOR PROFILE A1

Frequency (Hz)	FIRS Horizontal SA (G)	FIRS Vertical SA (G)	UHRS(10 ⁻⁴) Horizontal SA (G)	UHRS(10 ⁻⁴) Vertical SA (G)	UHRS(10 ⁻⁵) Horizontal SA (G)	UHRS(10 ⁻⁵) Vertical SA (G)	UHRS(10 ⁻⁶) Horizontal SA (G)	UHRS(10 ⁻⁶) Vertical SA (G)
100	3.52E-01	3.01E-01	2.32E-01	1.98E-01	7.40E-01	6.34E-01	1.82E+00	1.59E+00
90	3.60E-01	3.07E-01	2.37E-01	2.02E-01	7.56E-01	6.46E-01	1.87E+00	1.64E+00
80	3.76E-01	3.20E-01	2.47E-01	2.11E-01	7.92E-01	6.71E-01	1.97E+00	1.75E+00
70	4.14E-01	3.48E-01	2.70E-01	2.32E-01	8.73E-01	7.29E-01	2.19E+00	1.97E+00
60	5.04E-01	4.16E-01	3.25E-01	2.81E-01	1.07E+00	8.68E-01	2.69E+00	2.46E+00
50	6.68E-01	5.46E-01	4.29E-01	3.68E-01	1.41E+00	1.14E+00	3.59E+00	3.27E+00
40	7.85E-01	6.55E-01	5.06E-01	4.28E-01	1.66E+00	1.38E+00	4.21E+00	3.74E+00
35	7.90E-01	6.67E-01	5.11E-01	4.34E-01	1.67E+00	1.41E+00	4.23E+00	3.69E+00
30	7.69E-01	6.56E-01	5.00E-01	4.27E-01	1.62E+00	1.38E+00	4.11E+00	3.52E+00
25	7.29E-01	6.33E-01	4.76E-01	4.13E-01	1.54E+00	1.33E+00	3.89E+00	3.26E+00
20	7.02E-01	6.04E-01	4.65E-01	4.02E-01	1.47E+00	1.27E+00	3.71E+00	3.06E+00
15	6.56E-01	5.57E-01	4.43E-01	3.74E-01	1.37E+00	1.16E+00	3.43E+00	2.78E+00
12.5	6.16E-01	4.96E-01	4.21E-01	3.42E-01	1.28E+00	1.03E+00	3.20E+00	2.58E+00
10	5.63E-01	4.58E-01	3.90E-01	3.16E-01	1.17E+00	9.52E-01	2.90E+00	2.32E+00
9	5.40E-01	4.35E-01	3.76E-01	3.20E-01	1.12E+00	8.90E-01	2.77E+00	2.25E+00
8	4.98E-01	3.84E-01	3.50E-01	2.96E-01	1.03E+00	7.76E-01	2.55E+00	2.04E+00
7	4.41E-01	3.48E-01	3.12E-01	2.49E-01	9.09E-01	7.16E-01	2.25E+00	1.77E+00
6	4.03E-01	2.76E-01	2.88E-01	2.03E-01	8.29E-01	5.64E-01	2.04E+00	1.70E+00
5	3.60E-01	2.57E-01	2.62E-01	1.87E-01	7.39E-01	5.28E-01	1.81E+00	1.30E+00
4	2.75E-01	2.02E-01	2.05E-01	1.52E-01	5.61E-01	4.12E-01	1.39E+00	1.15E+00
3.5	2.59E-01	1.78E-01	1.96E-01	1.38E-01	5.26E-01	3.60E-01	1.30E+00	1.02E+00

WLS COL 2.5-2

TABLE 2.5.2-224 (Sheet 2 of 2)
FIRS AND UHRS FOR PROFILE A1

Frequency (Hz)	FIRS Horizontal SA (G)	FIRS Vertical SA (G)	UHRS(10 ⁻⁴) Horizontal SA (G)	UHRS(10 ⁻⁴) Vertical SA (G)	UHRS(10 ⁻⁵) Horizontal SA (G)	UHRS(10 ⁻⁵) Vertical SA (G)	UHRS(10 ⁻⁶) Horizontal SA (G)	UHRS(10 ⁻⁶) Vertical SA (G)
3	1.99E-01	1.53E-01	1.53E-01	1.18E-01	4.02E-01	3.10E-01	1.00E+00	7.89E-01
2.5	1.64E-01	1.17E-01	1.29E-01	9.18E-02	3.29E-01	2.35E-01	8.25E-01	5.88E-01
2	1.59E-01	1.04E-01	1.29E-01	8.56E-02	3.19E-01	2.06E-01	7.83E-01	5.38E-01
1.5	1.16E-01	9.36E-02	9.56E-02	7.52E-02	2.29E-01	1.87E-01	5.49E-01	4.81E-01
1.25	9.97E-02	8.42E-02	8.36E-02	6.69E-02	1.97E-01	1.69E-01	4.70E-01	4.19E-01
1	8.81E-02	6.80E-02	7.35E-02	5.45E-02	1.75E-01	1.36E-01	4.16E-01	3.24E-01
0.9	8.81E-02	6.31E-02	7.29E-02	5.10E-02	1.75E-01	1.26E-01	4.13E-01	2.99E-01
0.8	8.57E-02	5.72E-02	7.10E-02	4.65E-02	1.70E-01	1.14E-01	3.98E-01	2.68E-01
0.7	7.95E-02	5.02E-02	6.63E-02	4.13E-02	1.57E-01	9.99E-02	3.64E-01	2.34E-01
0.6	6.90E-02	4.26E-02	5.80E-02	3.54E-02	1.36E-01	8.46E-02	3.12E-01	1.96E-01
0.5	5.56E-02	3.46E-02	4.72E-02	2.89E-02	1.10E-01	6.84E-02	2.47E-01	1.57E-01
0.4	4.44E-02	2.77E-02	3.77E-02	2.31E-02	8.77E-02	5.47E-02	1.98E-01	1.26E-01
0.35	3.89E-02	2.42E-02	3.30E-02	2.03E-02	7.67E-02	4.79E-02	1.73E-01	1.10E-01
0.3	3.33E-02	2.07E-02	2.83E-02	1.74E-02	6.58E-02	4.11E-02	1.48E-01	9.43E-02
0.25	2.78E-02	1.73E-02	2.36E-02	1.45E-02	5.48E-02	3.42E-02	1.24E-01	7.86E-02
0.2	2.22E-02	1.38E-02	1.89E-02	1.16E-02	4.38E-02	2.74E-02	9.89E-02	6.28E-02
0.15	1.67E-02	1.04E-02	1.42E-02	8.68E-03	3.29E-02	2.05E-02	7.41E-02	4.71E-02
0.125	1.39E-02	8.64E-03	1.18E-02	7.23E-03	2.74E-02	1.71E-02	6.18E-02	3.93E-02
0.1	8.89E-03	5.53E-03	7.55E-03	4.63E-03	1.75E-02	1.09E-02	3.95E-02	2.51E-02

WLS COL 2.5-2

TABLE 2.5.2-225 (Sheet 1 of 2)
FIRS AND UHRS FOR PROFILE A5

Frequency (Hz)	FIRS Horizontal SA (G)	FIRS Vertical SA (G)	UHRS(10 ⁻⁴) Horizontal SA (G)	UHRS(10 ⁻⁴) Vertical SA (G)	UHRS(10 ⁻⁵) Horizontal SA (G)	UHRS(10 ⁻⁵) Vertical SA (G)	UHRS(10 ⁻⁶) Horizontal SA (G)	UHRS(10 ⁻⁶) Vertical SA (G)
100	3.61E-01	3.05E-01	2.39E-01	2.01E-01	7.58E-01	6.41E-01	1.87E+00	1.61E+00
90	3.69E-01	3.11E-01	2.43E-01	2.05E-01	7.75E-01	6.54E-01	1.91E+00	1.66E+00
80	3.85E-01	3.24E-01	2.53E-01	2.15E-01	8.10E-01	6.81E-01	2.01E+00	1.77E+00
70	4.25E-01	3.54E-01	2.77E-01	2.37E-01	8.95E-01	7.41E-01	2.24E+00	2.00E+00
60	5.21E-01	4.26E-01	3.37E-01	2.89E-01	1.10E+00	8.88E-01	2.78E+00	2.50E+00
50	6.99E-01	5.60E-01	4.50E-01	3.79E-01	1.48E+00	1.17E+00	3.75E+00	3.32E+00
40	8.22E-01	6.68E-01	5.31E-01	4.38E-01	1.74E+00	1.41E+00	4.41E+00	3.78E+00
35	8.23E-01	6.77E-01	5.33E-01	4.43E-01	1.74E+00	1.43E+00	4.40E+00	3.72E+00
30	7.95E-01	6.64E-01	5.18E-01	4.33E-01	1.68E+00	1.40E+00	4.25E+00	3.53E+00
25	7.47E-01	6.39E-01	4.89E-01	4.17E-01	1.57E+00	1.35E+00	3.98E+00	3.26E+00
20	7.14E-01	6.08E-01	4.74E-01	4.04E-01	1.50E+00	1.28E+00	3.78E+00	3.07E+00
15	6.62E-01	5.59E-01	4.48E-01	3.76E-01	1.38E+00	1.17E+00	3.46E+00	2.78E+00
12.5	6.21E-01	4.98E-01	4.24E-01	3.44E-01	1.29E+00	1.03E+00	3.22E+00	2.59E+00
10	5.67E-01	4.59E-01	3.92E-01	3.17E-01	1.18E+00	9.54E-01	2.92E+00	2.33E+00
9	5.43E-01	4.36E-01	3.78E-01	3.21E-01	1.12E+00	8.92E-01	2.79E+00	2.24E+00
8	5.00E-01	3.85E-01	3.51E-01	2.97E-01	1.03E+00	7.78E-01	2.56E+00	2.05E+00
7	4.43E-01	3.49E-01	3.13E-01	2.50E-01	9.14E-01	7.18E-01	2.25E+00	1.77E+00
6	4.05E-01	2.77E-01	2.89E-01	2.03E-01	8.35E-01	5.67E-01	2.05E+00	1.70E+00
5	3.62E-01	2.58E-01	2.62E-01	1.86E-01	7.43E-01	5.29E-01	1.81E+00	1.30E+00
4	2.76E-01	2.03E-01	2.05E-01	1.52E-01	5.63E-01	4.13E-01	1.39E+00	1.15E+00
3.5	2.60E-01	1.78E-01	1.96E-01	1.38E-01	5.28E-01	3.60E-01	1.30E+00	1.02E+00

WLS COL 2.5-2

TABLE 2.5.2-225 (Sheet 2 of 2)
FIRS AND UHRS FOR PROFILE A5

Frequency (Hz)	FIRS Horizontal SA (G)	FIRS Vertical SA (G)	UHRS(10 ⁻⁴) Horizontal SA (G)	UHRS(10 ⁻⁴) Vertical SA (G)	UHRS(10 ⁻⁵) Horizontal SA (G)	UHRS(10 ⁻⁵) Vertical SA (G)	UHRS(10 ⁻⁶) Horizontal SA (G)	UHRS(10 ⁻⁶) Vertical SA (G)
3	2.00E-01	1.53E-01	1.54E-01	1.18E-01	4.04E-01	3.10E-01	1.01E+00	7.90E-01
2.5	1.64E-01	1.17E-01	1.29E-01	9.18E-02	3.29E-01	2.35E-01	8.25E-01	5.88E-01
2	1.60E-01	1.04E-01	1.29E-01	8.57E-02	3.19E-01	2.06E-01	7.85E-01	5.38E-01
1.5	1.16E-01	9.36E-02	9.58E-02	7.52E-02	2.30E-01	1.87E-01	5.50E-01	4.81E-01
1.25	9.98E-02	8.42E-02	8.36E-02	6.70E-02	1.98E-01	1.69E-01	4.70E-01	4.20E-01
1	8.81E-02	6.80E-02	7.35E-02	5.46E-02	1.75E-01	1.36E-01	4.16E-01	3.25E-01
0.9	8.81E-02	6.32E-02	7.29E-02	5.10E-02	1.75E-01	1.26E-01	4.13E-01	2.99E-01
0.8	8.57E-02	5.72E-02	7.09E-02	4.66E-02	1.70E-01	1.14E-01	3.98E-01	2.69E-01
0.7	7.95E-02	5.03E-02	6.63E-02	4.13E-02	1.57E-01	1.00E-01	3.65E-01	2.34E-01
0.6	6.90E-02	4.26E-02	5.80E-02	3.54E-02	1.36E-01	8.46E-02	3.12E-01	1.96E-01
0.5	5.56E-02	3.46E-02	4.72E-02	2.89E-02	1.10E-01	6.84E-02	2.47E-01	1.57E-01
0.4	4.44E-02	2.76E-02	3.77E-02	2.31E-02	8.77E-02	5.47E-02	1.98E-01	1.26E-01
0.35	3.89E-02	2.42E-02	3.30E-02	2.03E-02	7.67E-02	4.79E-02	1.73E-01	1.10E-01
0.3	3.33E-02	2.07E-02	2.83E-02	1.74E-02	6.58E-02	4.10E-02	1.48E-01	9.43E-02
0.25	2.78E-02	1.73E-02	2.36E-02	1.45E-02	5.48E-02	3.42E-02	1.24E-01	7.85E-02
0.2	2.22E-02	1.38E-02	1.89E-02	1.16E-02	4.38E-02	2.74E-02	9.89E-02	6.28E-02
0.15	1.67E-02	1.04E-02	1.42E-02	8.68E-03	3.29E-02	2.05E-02	7.41E-02	4.71E-02
0.125	1.39E-02	8.64E-03	1.18E-02	7.23E-03	2.74E-02	1.71E-02	6.18E-02	3.93E-02
0.1	8.89E-03	5.53E-03	7.55E-03	4.63E-03	1.75E-02	1.09E-02	3.95E-02	2.51E-02

WLS COL 2.5-2

TABLE 2.5.2-226 (Sheet 1 of 2)
FIRS AND UHRS FOR PROFILE C4

Frequency (Hz)	FIRS Horizontal SA (G)	FIRS Vertical SA (G)	UHRS(10 ⁻⁴) Horizontal SA (G)	UHRS(10 ⁻⁴) Vertical SA (G)	UHRS(10 ⁻⁵) Horizontal SA (G)	UHRS(10 ⁻⁵) Vertical SA (G)	UHRS(10 ⁻⁶) Horizontal SA (G)	UHRS(10 ⁻⁶) Vertical SA (G)
100	3.45E-01	2.85E-01	2.28E-01	1.88E-01	7.24E-01	5.99E-01	1.79E+00	1.51E+00
90	3.52E-01	2.90E-01	2.32E-01	1.92E-01	7.40E-01	6.10E-01	1.83E+00	1.56E+00
80	3.67E-01	3.02E-01	2.41E-01	2.00E-01	7.73E-01	6.33E-01	1.92E+00	1.66E+00
70	4.02E-01	3.28E-01	2.62E-01	2.19E-01	8.46E-01	6.86E-01	2.12E+00	1.87E+00
60	4.84E-01	3.91E-01	3.12E-01	2.65E-01	1.02E+00	8.15E-01	2.59E+00	2.35E+00
50	6.38E-01	5.14E-01	4.10E-01	3.50E-01	1.35E+00	1.07E+00	3.43E+00	3.13E+00
40	7.56E-01	6.17E-01	4.88E-01	4.15E-01	1.60E+00	1.29E+00	4.07E+00	3.59E+00
35	7.66E-01	6.31E-01	4.96E-01	4.21E-01	1.62E+00	1.32E+00	4.12E+00	3.55E+00
30	7.51E-01	6.25E-01	4.88E-01	4.12E-01	1.59E+00	1.31E+00	4.04E+00	3.39E+00
25	7.17E-01	6.01E-01	4.68E-01	3.92E-01	1.51E+00	1.27E+00	3.85E+00	3.14E+00
20	6.95E-01	5.73E-01	4.60E-01	3.76E-01	1.46E+00	1.21E+00	3.69E+00	2.94E+00
15	6.51E-01	5.26E-01	4.39E-01	3.49E-01	1.36E+00	1.10E+00	3.41E+00	2.66E+00
12.5	6.12E-01	5.05E-01	4.18E-01	3.45E-01	1.28E+00	1.05E+00	3.18E+00	2.47E+00
10	5.63E-01	4.38E-01	3.90E-01	3.03E-01	1.17E+00	9.09E-01	2.90E+00	2.21E+00
9	5.39E-01	4.19E-01	3.76E-01	2.72E-01	1.12E+00	8.85E-01	2.77E+00	2.04E+00
8	4.95E-01	3.86E-01	3.48E-01	2.80E-01	1.02E+00	7.93E-01	2.53E+00	1.82E+00
7	4.40E-01	3.55E-01	3.12E-01	2.56E-01	9.08E-01	7.29E-01	2.24E+00	1.74E+00
6	4.05E-01	2.89E-01	2.90E-01	2.27E-01	8.33E-01	5.81E-01	2.05E+00	1.47E+00
5	3.60E-01	2.48E-01	2.62E-01	1.80E-01	7.37E-01	5.10E-01	1.80E+00	1.25E+00
4	2.75E-01	1.90E-01	2.05E-01	1.47E-01	5.59E-01	3.83E-01	1.38E+00	1.07E+00
3.5	2.60E-01	1.75E-01	1.97E-01	1.37E-01	5.27E-01	3.53E-01	1.30E+00	8.94E-01

WLS COL 2.5-2

TABLE 2.5.2-226 (Sheet 2 of 2)
FIRS AND UHRS FOR PROFILE C4

Frequency (Hz)	FIRS Horizontal SA (G)	FIRS Vertical SA (G)	UHRS(10 ⁻⁴) Horizontal SA (G)	UHRS(10 ⁻⁴) Vertical SA (G)	UHRS(10 ⁻⁵) Horizontal SA (G)	UHRS(10 ⁻⁵) Vertical SA (G)	UHRS(10 ⁻⁶) Horizontal SA (G)	UHRS(10 ⁻⁶) Vertical SA (G)
3	2.00E-01	1.52E-01	1.54E-01	1.15E-01	4.05E-01	3.07E-01	1.00E+00	7.15E-01
2.5	1.64E-01	1.13E-01	1.29E-01	8.90E-02	3.29E-01	2.28E-01	8.19E-01	5.67E-01
2	1.60E-01	9.94E-02	1.29E-01	8.22E-02	3.21E-01	1.97E-01	7.84E-01	5.29E-01
1.5	1.16E-01	8.78E-02	9.61E-02	7.13E-02	2.31E-01	1.75E-01	5.50E-01	4.52E-01
1.25	9.99E-02	7.77E-02	8.37E-02	6.23E-02	1.98E-01	1.56E-01	4.70E-01	3.84E-01
1	8.81E-02	6.23E-02	7.35E-02	4.96E-02	1.75E-01	1.25E-01	4.16E-01	2.98E-01
0.9	8.81E-02	5.85E-02	7.29E-02	4.69E-02	1.75E-01	1.17E-01	4.15E-01	2.76E-01
0.8	8.57E-02	5.35E-02	7.10E-02	4.33E-02	1.70E-01	1.07E-01	4.02E-01	2.52E-01
0.7	7.95E-02	4.75E-02	6.63E-02	3.89E-02	1.58E-01	9.46E-02	3.70E-01	2.23E-01
0.6	6.90E-02	4.07E-02	5.81E-02	3.37E-02	1.37E-01	8.08E-02	3.19E-01	1.91E-01
0.5	5.56E-02	3.33E-02	4.72E-02	2.80E-02	1.10E-01	6.59E-02	2.54E-01	1.55E-01
0.4	4.44E-02	2.67E-02	3.77E-02	2.24E-02	8.77E-02	5.27E-02	2.03E-01	1.24E-01
0.35	3.89E-02	2.33E-02	3.30E-02	1.96E-02	7.67E-02	4.61E-02	1.78E-01	1.09E-01
0.3	3.33E-02	2.00E-02	2.83E-02	1.68E-02	6.58E-02	3.96E-02	1.52E-01	9.32E-02
0.25	2.78E-02	1.67E-02	2.36E-02	1.40E-02	5.48E-02	3.30E-02	1.27E-01	7.76E-02
0.2	2.22E-02	1.33E-02	1.89E-02	1.12E-02	4.38E-02	2.64E-02	1.02E-01	6.21E-02
0.15	1.67E-02	9.99E-03	1.42E-02	8.39E-03	3.29E-02	1.98E-02	7.62E-02	4.66E-02
0.125	1.39E-02	8.33E-03	1.18E-02	6.99E-03	2.74E-02	1.65E-02	6.35E-02	3.88E-02
0.1	8.89E-03	5.33E-03	7.55E-03	4.47E-03	1.75E-02	1.05E-02	4.06E-02	2.48E-02

TABLE 2.5.2-227
DISTRIBUTED SEISMICITY SOURCES

Zone Acronym	Zone Name	Comments
Mmax Zones		
MESE-N* and MESE-W*	Mesozoic and Younger Extended Crust, narrow and wide geometries	
NMESE-N* and NMESE-W*	Non-Mesozoic and Younger Extended Crust, narrow and wide geometries	NMESE-N is paired with MESE-N, and NMESE-W is paired with MESE-W
STUDY_R*	CEUS Study Region	Exclusive with MESE and NMESE
Seismotectonic Source Zones		
AHEX*	Atlantic Highly Extended Crust	
ECC-AM*	Extended Continental Crust–Atlantic Margin	
ECC-GC*	Extended Continental Crust–Gulf Coast	
GHEX	Gulf Coast Highly Extended Crust	
GMH	Great Meteor Hotspot	
IBEB*	Illinois Basin Extended Basement	
MidC-A*, B*, C*, D*	Midcontinent-Craton	Alternative geometries depend on PEZ and RR/RR-RCG
NAP	Northern Appalachian	
OKA	Oklahoma Aulacogen	
PEZ-N* and PEZ-W*	Paleozoic Extended Crust narrow and Paleozoic Extended Crust wide	PEZ-N is modeled either with MidC-A and RR, or MidC-B and RR-RCG. PEZ-W is modeled with MidC-C and RR, or MidC-D and RR-RCG
RR and RR-RCG*	Reelfoot Rift, Reelfoot Rift with Rough Creek graben	RR and RR-RCG are mutually exclusive
SLR	St. Lawrence Rift, including the Ottawa and Saguenay grabens	
*Source area within 520 km included in Lee Nuclear site hazard calculation.		

WLS COL 2.5-2

TABLE 2.5.2-228
ALTERNATIVE MMAX ZONATION MODELS^(a)

	Mesozoic Extended–Narrow Model		Mesozoic Extended–Wide Model	
Mmax Zone	MESE-N*	NMESE-N*	MESE-W*	NMESE-W*
Corresponding Seismotectonic Zones	AHEX*	MidC-A*, -B*	AHEX*	MidC-C*, -D*
	ECC-AM*	IBEB*	ECC-AM*	OKA
	ECC-GC*	OKA	ECC-GC*	
	GHEX		GHEX	
	RR		RR-RCG*	
	SLR		SLR	
	NAP		NAP	
	GMH		GMH	
	PEZ-N*		PEZ-W*	
			IBEB*	

a) NUREG-2115 ([Reference 326](#)) Table 6.2-1.

*Source area within 520 km included in Lee Nuclear site hazard calculation.

WLS COL 2.5-2

TABLE 2.5.2-229
ALTERNATIVE MMAX ZONATION MODEL WEIGHTS^(a)

Weight Assigned to Mmax	Study Region	Maximum Magnitude for:			
		MESE-N	MESE-W	NMESE-N	NMESE-W
0.101	6.5	6.4	6.4	6.5	5.7
0.244	6.9	6.8	6.8	6.9	6.1
0.310	7.2	7.2	7.1	7.3	6.6
0.244	7.7	7.7	7.5	7.7	7.2
0.101	8.1	8.1	8.0	8.1	7.9

a) NUREG-2115 ([Reference 326](#)) Table H-3-3.

TABLE 2.5.2-230
ASSESSMENT OF DEFAULT CHARACTERISTICS OF FUTURE
EARTHQUAKES IN THE CEUS^(a)

WLS COL 2.5-2

Tectonic Stress Regime	Compressional
Sense of Slip/Style of Faulting	Treat as aleatory (relative frequency): <ul style="list-style-type: none"> • 2:1 strike-slip:reverse
Strike and Dip of Ruptures	<p>Aleatory distribution:</p> <ul style="list-style-type: none"> • N50W (0.2) • N-S (0.2) • N35E (0.4) • N60E (0.1) • E-W (0.1) <p>Dip is a function of sense of slip:</p> <ul style="list-style-type: none"> • Strike-slip (90°-60°) (uniform) • Reverse (30°-60°) (uniform) • Either direction (50:50)
Seismogenic Crustal Thickness	<p>Epistemic distribution:</p> <ul style="list-style-type: none"> • 13 km (0.4) • 17 km (0.4) • 22 km (0.2)
Fault Rupture Area	<p>Function of magnitude;</p> <ul style="list-style-type: none"> • Use Somerville et al. relation for Eastern North America
Rupture Length-to-Width Aspect Ratio	<p>Function of rupture area:</p> <ul style="list-style-type: none"> • 1:1 for smaller ruptures • With progressively larger areas, when rupture width equals seismogenic crustal thickness, extend only the length
Relationship of Rupture to Source Zone Boundaries	<p>Epicenter is at center of rupture length (map view)</p> <p>All boundaries are "leaky"; rupture is allowed to extend beyond boundary. (Note: If boundary is "strict," rupture cannot extend beyond boundary, although epicenter can be near boundary)</p>

a) NUREG-2115 ([Reference 326](#)) Table 5.4-1.

TABLE 2.5.2-231 (Sheet 1 of 3)
CHARACTERISTICS OF FUTURE EARTHQUAKES FOR
INDIVIDUAL SEISMIC SOURCES^(a)

WLS COL 2.5-2

Source	Sense of Slip ^(b)	Rupture Strike ^(b)	Rupture Dip ^(b)	Source Boundaries	Seismogenic Crustal Thickness ^(c)
RLME Sources					
Charlevoix	Reverse	Uniform 0°-360°	Uniform 40°-60°	Leaky	25 km (0.8) 30 km (0.2)
Charleston Regional*	Strike-slip	NE parallel to long axis (0.8) NW parallel to short axis (0.2)	90°	Strict	13 km (0.4) 17 km (0.4) 22 km (0.2)
Charleston–Local*	Strike-slip	NE parallel to long axis	90°	Strict	13 km (0.4) 17 km (0.4) 22 km (0.2)
Charleston Narrow*	Strike-slip	NE parallel to long axis	90°	Leaky at ends	13 km (0.4) 17 km (0.4) 22 km (0.2)
Cheraw	Normal-oblique	On fault trace (NE)	50° NW (0.6) 65° NW (0.4)	Strict	13 km (0.4) 17 km (0.4) 22 km (0.2)
Commerce	Strike-slip	NE parallel to long axis of zone	90°	Leaky at ends	13 km (0.4) 15 km (0.4) 17 km (0.2)
ERM-N	Strike-slip	NE parallel to long axis of zone	90°	Leaky at ends	13 km (0.4) 15 km (0.4) 17 km (0.2)
ERM-S	Strike-slip	NE parallel to long axis of zone	90°	Leaky at ends	13 km (0.4) 15 km (0.4) 17 km (0.2)
Marianna	Strike-slip	NE 45° (0.5) NE 45° (0.5)	90°	Leaky at ends	13 km (0.4) 15 km (0.4) 17 km (0.2)
Meers–Fault	Strike-slip (0.5) Reverse (0.5)	On fault	Strike-slip 90° Reverse 40° SW	Strict	15 km (0.5) 20 km (0.5)
Meers–Random in OKA	Reverse oblique	Parallel to long axis of zone	Uniform 40°-90°	Strict	15 km (0.5) 20 km (0.5)
NMFS*	NMN,NMS: Strike-slip RMT: reverse	On fault	NMN, NMS: 90°RFT: 40° SW	Strict	13 km (0.4) 15 km (0.4) 17 km (0.2)

TABLE 2.5.2-231 (Sheet 2 of 3)
CHARACTERISTICS OF FUTURE EARTHQUAKES FOR
INDIVIDUAL SEISMIC SOURCES^(a)

WLS COL 2.5-2

Source	Sense of Slip ^(b)	Rupture Strike ^(b)	Rupture Dip ^(b)	Source Boundaries	Seismogenic Crustal Thickness ^(c)
Wabash Valley	2/3 Strike-slip 1/3 Reverse	Strike parallel to the long axis of the zone (0.8) N50W (0.1) N20W (0.1)	2/3 Strike-slip, 90° 1/3 Reverse, 40°-60° Strike-slip, 90° Reverse, 40°	Leaky	17 km (0.7) 22 km (0.3)
Seismotectonic Zones					
AHEX*	2/3 Strike-slip 1/3 Reverse	N50W (0.1) N-S (0.1) N25E (0.4) N60E (0.3) E-W (0.1)	Strike-slip (90°-60°) (uniform) Reverse (30°-60°) (uniform)	Leaky	8 km (0.5) 15 km (0.5)
ECC-AM*	2/3 Strike-slip 1/3 Reverse	N50W (0.2) N-S (0.2) N35E (0.4) N60E (0.1) E-W (0.1)	Strike-slip (90°-60°) (uniform) Reverse (30°-60°) (uniform)	Leaky	13 km (0.6) 17 km (0.3) 22 km (0.1)
ECC-GC*	2/3 Strike-slip 1/3 Reverse	Uniform 0° to 360°	Strike-slip (90°-60°) (uniform) Reverse (30°-60°) (uniform)	Leaky	13 km (0.6) 17 km (0.3) 22 km (0.1)
GHEX	2/3 Strike-slip 1/3 Reverse	Uniform 0° to 360°	Strike-slip (90°-60°) (uniform) Reverse (30°-60°) (uniform)	Leaky	8 km (0.5) 15 km (0.5)
GMH	4/5 Reverse 1/5 Strike-slip	N50W (0.4) N20W (0.4) E-W (0.2)	Strike-slip (90°-60°) (uniform) Reverse (30°-60°) (uniform)	Leaky	25 km (0.5) 30 km (0.5)
PEZ*	2/3 Strike-slip 1/3 Reverse	N50W (0.2) N-S (0.2) N35E (0.4) N60E (0.1) E-W (0.1)	Strike-slip (90°-60°) (uniform) Reverse (30°-60°) (uniform)	Leaky	13 km (0.4) 17 km (0.4) 22 km (0.2)
MidC*	2/3 Strike-slip 1/3 Reverse	N50W (0.2) N-S (0.2) N35E (0.4) N60E (0.1) E-W (0.1)	Strike-slip (90°-60°) (uniform) Reverse (30°-60°) (uniform)	Strict	13 km (0.4) 17 km (0.4) 22 km (0.2)

TABLE 2.5.2-231 (Sheet 3 of 3)
CHARACTERISTICS OF FUTURE EARTHQUAKES FOR
INDIVIDUAL SEISMIC SOURCES^(a)

WLS COL 2.5-2

Source	Sense of Slip ^(b)	Rupture Strike ^(b)	Rupture Dip ^(b)	Source Boundaries	Seismogenic Crustal Thickness ^(c)
NAP	1/3 <i>Strike-slip</i> 2/3 <i>Reverse</i>	N50W (0.2) N-S (0.2) N35E (0.4) N60E (0.1) E-W (0.1)	<i>Strike-slip (90°-60°) (uniform)</i> <i>Reverse (30°-60°) (uniform)</i>	Leaky	13 km (0.4) 17 km (0.4) 22 km (0.2)
OKA	Reverse Oblique	Parallel to long axis of zone	Uniform 45°-75°	<i>Leaky</i>	15 km (0.5) 20 km (0.5)
RR and RR-RCG*	SS (0.2) R (0.35) SS (0.5) SS (0.2) SS (0.2)	N50W (0.2) N10W(0.35) E-W (0.05) N30E (0.2) N55E (0.2)	90° 70° (0.5), 40° (0.5) 90° 90° 90°	Strict	13 km (0.4) 15 km (0.4) 17 km (0.2)
SLR	1/3 <i>Strike-slip</i> 2/3 <i>Reverse</i>	N25E (0.2) N40E (0.2) N70E (0.2) N50W (0.15) N70W (0.15) N-S (0.05) E-W (0.05)	<i>Strike-slip (90°-60°) (uniform)</i> <i>Reverse (30°-60°) (uniform)</i>	Leaky	25 km (0.5) 30 km (0.5)

a) NUREG-2115 ([Reference 326](#)) Table 5.4-2. Charleston source names, ECC-AM seismogenic thickness, and IBEB boundaries corrected from original.

b) Weights reflect aleatory uncertainty (natural randomness); weights are therefore relative frequencies.

c) Weights reflect epistemic uncertainty (scientific uncertainty); weights are therefore relative credibility that the given thickness is correct.

*Source area within 520 km included in Lee Nuclear site hazard calculation (or considered in the PSHA).

Note: Default characteristics (i.e., those listed in Table 5.4-2 of NUREG/CR-2115 for the entire CEUS region) are indicated in italics.

TABLE 2.5.2-232

WLS COL 2.5-2

MAXIMUM MAGNITUDE DISTRIBUTIONS FOR SEISMOTECTONIC DISTRIBUTED SEISMICITY SOURCES^(a)

Weight	AHEx*	ECC-AM*	ECC-GC*	GHEX	GMH	IBEB*	Maximum Magnitude for:			PEZ-N* and PEZ-W*	RR	RR-RCG*	SLR
							MidC-A*, MidC-B*, MidC-C*, and MidC-D*						
0.101	6.0	6.0	6.0	6.0	6.0	6.5	5.6	6.1	5.8	5.9	6.2	6.1	6.2
0.244	6.7	6.7	6.7	6.7	6.7	6.9	6.1	6.7	6.4	6.4	6.7	6.6	6.8
0.310	7.2	7.2	7.2	7.2	7.2	7.4	6.6	7.2	6.9	6.8	7.2	7.1	7.3
0.244	7.7	7.7	7.7	7.7	7.7	7.8	7.2	7.7	7.4	7.2	7.7	7.6	7.7
0.101	8.1	8.1	8.1	8.1	8.1	8.1	8.0	8.1	8.0	7.9	8.1	8.1	8.1

a) NUREG-2115 (Reference 326) Table H-4-4.

*Source area within 520 km included in Lee Nuclear site hazard calculation.

WLS COL 2.5-2

TABLE 2.5.2-233
MAXIMUM MAGNITUDE DISTRIBUTION
FOR CHARLESTON RLME SOURCE^(a)

Expected Charleston RLME Magnitude [M]	Weight
6.7	0.10
6.9	0.25
7.1	0.30
7.3	0.25
7.5	0.10

a) NUREG-2115 ([Reference 326](#)) Table H-5.2-1.

WLS COL 2.5-2

TABLE 2.5.2-234
MAXIMUM MAGNITUDE DISTRIBUTION
FOR NEW MADRID RLME SOURCE^(a)

Expected NMFS RLME Magnitude for:			Weight
NMS	RFT	NMN	
7.9	7.8	7.6	0.167
7.8	7.7	7.5	0.167
7.6	7.8	7.5	0.250
7.2	7.4	7.2	0.083
6.9	7.3	7.0	0.250
6.7	7.1	6.8	0.083

a) NUREG-2115 ([Reference 326](#)) Table H-5.5-1.

WLS COL 2.5-2

TABLE 2.5.2-235
MEAN ROCK HAZARD AND % DIFFERENCES BETWEEN
LCI PSHA SOFTWARE CALCULATIONS AND CEUS DATA FOR
CHATTANOOGA TEST SITE

	Total hazard for spectral acceleration at 1 HZ	
	0.2g	0.6g
CEUS	2.40E-05	1.31E-06
LCI	2.55E-05	1.38E-06
Difference	6.2%	5.4%
	Total hazard for spectral acceleration at 10 HZ	
	0.2g	0.6g
CEUS	6.36E-04	1.04E-04
LCI	6.34E-04	1.06E-04
Difference	-0.2%	2.2%
	Total hazard for spectral acceleration at PGA	
	0.2g	0.6g
CEUS	2.22E-04	3.40E-05
LCI	2.28E-04	3.62E-05
Difference	2.8%	6.4%

WLS COL 2.5-4

TABLE 2.5.3-201
SUMMARY OF BEDROCK FAULTS MAPPED WITHIN THE SITE
VICINITY

Feature Name	Distance from Site	Mapped Length	Strike Orientation	Reference(s)	Assigned Age	Evidence for Age
Kings Mountain shear zone	~5 mi.	>70 mi.	NE	Garihan et al. (1993) (Reference 231) Hibbard et al. (2006) (Reference 210) Horton (1981a, 1981b) (References 224 and 225) West et al. (1998) (Reference 228)	Paleozoic (possibly Mesozoic)	Syn- to post-kinematic dikes have Rb/Sr isochron age of 325 Ma; Cut by a 326 Ma granite
Tinsley Bridge fault	~6 mi.	~20 mi.	NE	Dennis (1995) (Reference 229) Hibbard et al. (2006) (Reference 210)	Paleozoic	Cut by 383 Ma granite
Brindle Creek thrust fault	~11 mi.	>100 mi.	NE, variable	Hibbard et al. (2006) (Reference 210) Hatcher et al. (2007) (Reference 238) Giorgis et al. (2002) (Reference 240)	Paleozoic	Cuts a 366 Ma granite; Fault-related migmatites have ~350 Ma age
SW extension of Boogertown shear zone	~8 mi.	~12 mi.	NE	Hibbard et al. (2006) (Reference 210) Horton (1981b) (Reference 225) Maybin and Nystrom (1997) (Reference 230)	Paleozoic	Cut by an undated pluton (Pluton mapped as Ordovician to Devonian)
Reedy River thrust fault	>10 mi.	>100 mi.	NE	Hibbard et al. (2006) (Reference 210) Horton and Dicken (2001) (Reference 209) Maybin and Nystrom (1997, 2002) (References 230 and 233) Nystrom (2001) (Reference 232)	Paleozoic	
Unnamed fault north of Gaffney	>12 mi.	20 mi.	N	Hibbard et al. (2006) (Reference 210) Goldsmith et al. (1988) (Reference 242)	Paleozoic	

TABLE 2.5.4-201
PETROGRAPHIC TEST RESULTS

	Sample Borehole	Depth of Sample (ft. b.g.s.)	Lee Nuclear Station Rock Type	Mineral Composition (Percent)					Petrographic Rock Name
				Quartz	Plagioclase	Potassium Feldspar	Micaceous Mineral	Other	
WLS COL 2.5-1	B1000	80.2-80.3	Meta-Quartz Diorite	20	40	---	25	15	Meta-Quartz Diorite
	B1000	129.6-129.8	Meta-Diorite	15	45	---	19	21	Meta-Dacite Porphyry
	B1004	23.3-23.4	Meta-Quartz Diorite	26	45	5	19	5	Meta-Quartz Diorite
	B1004	33.2-33.3	Meta-Quartz Diorite	25	38	6	26	5	Meta-Quartz Diorite
	B1004	44.4-44.5	Meta-Quartz Diorite	30	50	0	18	2	Meta-Quartz Diorite
	B1007	22.8-22.9	Meta-Diorite	8	65	---	25	2	Meta-Dacite Porphyry
	B1013	21.6-21.7	Meta-Quartz Diorite	25	50	5	16	4	Meta-Quartz Diorite
	B1014	7.3-7.4	Meta-Diorite	25	---	---	65	10	Mica Schist
	B1014	16.3-16.4	Meta-Quartz Diorite	25	50	2	14	9	Meta-Quartz Diorite
	B1015	29.5-29.6	Meta-Quartz Diorite	25	38	9	22	6	Meta-Quartz Diorite
	B1018	39.8-39.9	Meta-Diorite (Monzodiorite)	10	36	1	12	41	Meta-Basalt
	B1018	46.5-46.6	Meta-Diorite	10	41	---	---	49	Meta-Basalt
	B1025	48.5-49.0	Meta-Granodiorite	53	---	---	43	4	Mica Schist
	B1025	49.8-50.1	Meta-Diorite	68	10	---	15	7	Mica Schist
	B1050	65.2-65.4	Meta-Quartz Diorite	18	55	---	21	6	Meta-Quartz Diorite

b.g.s. = below ground surface

ft. = feet

TABLE 2.5.4-202
SUMMARY OF LEE NUCLEAR STATION GEOTECHNICAL
EXPLORATION

	Test Type	Number (2006-2007 Exploration)	Number (2012 Exploration)
WLS COL 2.5-1	Soil and Rock Borings/Geotechnical Monitoring Well Borings	124/24	7/0
	Monitoring Wells/Packer Tests	21/4	0/0
	Cone Penetrometer Test/SCPT	29/10	0/0
	Geotechnical Test Pits and Geologic Trenches	14	0/0
	Goodman Jack	14 (2 borings)	0
	Pressuremeter Testing	24 (2 borings)	0
	P-S Suspension Log	13	3
	Downhole Velocity	4	0
	Televiewer Survey	13	4
	Spectral Analysis of Surface Waves (SASW) Survey	15	0
	Petrographic Analysis	15	0

TABLE 2.5.4-203 (Sheet 1 of 6)
SUMMARY OF COMPLETED EXPLORATION BORINGS AND FIELD TESTS

Facility or Zone	Boring Number	Coordinates and Elevation			Boring Type					SPT Interval		Depth (ft bgs) ^(a)		Borehole Geophysical Testing			In-situ Testing	
		Northing	Easting	Elevation (ft MSL) ^(b)	Rock Coring		Soil Sampling Method			From	To	Proposed	Actual	P-S Velocity	Televiewer	Packer Test	Goodman Jack	Pressuremeter
					HQ	NQ	SPT	UD	CME									
<div>Power Block and Adjacent Structures</div> <div>Unit 1</div> <div>(Basemat elevation 553.5 ft.)</div> <div>WLS COL 2.5-1</div>	B-1000	1166072.097	1846189.261	581.537	X		X			0	60	150	151	X	X			
	B-1000-UD	1166063.067	1846192.595	581.519				X		--	--	--	23					
	B-1000-UDA	1166062.371	1846181.346	581.615				X		--	--	--	29.2					
	B-1000-UDB	1166107.231	1846117.365	588.931				X		--	--	--	48					
	B-1001	1166067.122	1846370.397	565.473	X					--	--	100	118.1		X			
	B-1001A	1166085.286	1846293.470	568.083		X				--	--	--	270.8 (length)					
	B-1002	1166061.781	1846444.433	565.338	X					--	--	150	170.3	X	X		X	
	B-1003	1165938.073	1846226.728	597.163	X					--	--	100	100					
	B-1004	1165831.988	1846407.915	558.997	X	X				--	--	175	175	X	X	X	X	
	B-1004A	1165831.298	1846430.369	558.997		X				--	--	--	284.7 (length)					
	B-1074	1166069.515	1846246.401	569.244	X	X	X			--	--	--	67.5					X
	B-1074A	1166067.457	1846252.141	569.233	X	X				--	--	--	121.9	X	X			X
	B-1075	1166030.303	1846255.956	569.667			X			--	--	--	23.7					
	B-1075A	1166035.846	1846256.754	569.535	X					--	--	--	150.4	X	X			
	B-2000	1166027.29	1846301.71	544.45	X					--	--	125	126	X	X			
	B-2001	1165894.29	1846423.34	544.47		X				--	--	100	100.5					
	B-2002	1165782.16	1846364.98	558.84		X				--	--	100	225.6	X	X			
	B-2003	1165773.77	1846448.63	559.03	X					--	--	225	54.6		X			
	B-2004	1165936.81	1846506.19	544.55		X				--	--	100	101					

TABLE 2.5.4-203 (Sheet 2 of 6)
SUMMARY OF COMPLETED EXPLORATION BORINGS AND FIELD TESTS

Facility or Zone	Boring Number	Coordinates and Elevation			Boring Type					SPT Interval		Depth (ft bgs) ^(a)		Borehole Geophysical Testing			In-situ Testing	
		Northing	Easting	Elevation (ft MSL) ^(b)	Rock Coring		Soil Sampling Method			From	To	Proposed	Actual	P-S Velocity	Televiewer	Packer Test	Goodman Jack	Pressuremeter
					HQ	NQ	SPT	UD	CME									
Adjacent Structures	B-1005	1165715.711	1846277.806	562.189		X				--	--	50	50					
	B-1006	1165456.872	1846165.621	589.158		X				--	--	50	30					
	B-1006A	1165453.953	1846160.471	589.622		X				--	--	--	90					
	B-1007	1165712.405	1846489.105	563.038		X				--	--	50	51.25					
	B-1008	1165623.375	1846335.376	563.175		X				--	--	50	51					
	B-1009	1165530.408	1846393.253	562.965						--	--	50	2.5					
	B-1009A	1165529.086	1846392.312	562.948		X				--	--	--	51					
	B-1010	1165551.531	1846525.693	563.107		X				--	--	75	51					
	B-1011	1165997.940	1846673.057	537.714	X					--	--	150	220	X	X			
Unit 2 (Basemat elevation 553.5 ft.)	B-1012	1166228.569	1847098.384	566.153	X					--	--	150	150.2	X	X		X	
	B-1013	1166266.998	1847167.699	558.699		X				--	--	50	52					
	B-1014	1166150.213	1847262.006	544.382	X	X				--	--	75	75.5		X		X	
	B-1015	1166134.365	1847192.566	560.052	X					--	--	400	250.3	X	X	X		
	B-1016	1166124.243	1847132.581	559.249		X	X			0	3	100	100					
	B-1017	1166004.443	1847155.562	560.724	X					--	--	175	175.6	X	X		X	
	B-1018	1166028.814	1847265.117	552.733		X				--	--	100	100.3					
	B-2005	1165972.37	1847267.57	550.28	X					--	--	225	225	X	X			
	B-2006	1166175.58	1847173.13	558.37		X				--	--	100	101					

TABLE 2.5.4-203 (Sheet 3 of 6)
SUMMARY OF COMPLETED EXPLORATION BORINGS AND FIELD TESTS

Facility or Zone	Boring Number	Coordinates and Elevation			Boring Type					SPT Interval		Depth (ft bgs) ^(a)		Borehole Geophysical Testing			In-situ Testing	
		Northing	Easting	Elevation (ft MSL) ^(b)	Rock Coring		Soil Sampling Method			From	To	Proposed	Actual	P-S Velocity	Televiewer	Packer Test	Goodman Jack	Pressuremeter
					HQ	NQ	SPT	UD	CME									
Adjacent Structures	B-1019	1166204.465	1847001.388	558.168		X	X			0	9	75	75					
	B-1020	1166389.650	1847104.154	589.996		X	X			0	13.5	75	75					
	B-1021	1165897.314	1847301.608	565.519		X	X			0	5	75	75.4					
	B-1022	1165733.403	1847334.894	571.450		X	X			0	40	75	76					
	B-1023	1165696.674	1847233.087	571.173		X	X			0	27	75	75					
	B-1024	1166077.813	1846927.534	539.369	X	X				--	--	150	220.2	X	X			
	B-1037	1166205.496	1847506.541	589.279			X			0	78.75	50	78.75					
	B-1037A	1166215.133	1847504.721	589.279	X					--	--	--	96.6	X	X			
	B-1037-UD	1166209.149	1847500.977	589.246				X		--	--	--	68					
	B-1038	1166165.152	1847350.980	546.544		X				--	--	50	50.2					
Pipelines (Non-Safety Related)	Unit 1	B-1050	1164915.459	1846053.459	596.956		X	X		--	--	50	73.4					
			1164991.018	1846392.558	587.676		X	X		--	--	50	71.5					
			1165181.111	1846736.893	587.367		X	X		--	--	50	70.7					
	Unit 2	B-1053	1165781.941	1847797.307	589.279			X		--	--	50	13.5					
		B-1053A	1165778.372	1847798.567	589.279			X		--	--	--	16					
		B-1053B	1165778.077	1847780.641	589.583					--	--	--	13.5					
		B-1053C	1165682.617	1847809.363	589.482		X	X		--	--	--	69.2					
		B-1053-UD	1165682.863	1847817.422	589.327				X	--	--	--	26.3					
		B-1054	1165836.297	1847569.662	590.947		X	X		--	--	50	83.5					
		B-1055	1166463.354	1847463.729	590.486		X	X		--	--	50	66					

TABLE 2.5.4-203 (Sheet 4 of 6)
SUMMARY OF COMPLETED EXPLORATION BORINGS AND FIELD TESTS

Facility or Zone	Boring Number	Coordinates and Elevation			Boring Type					SPT Interval		Depth (ft bgs) ^(a)		Borehole Geophysical Testing			In-situ Testing	
		Northing	Easting	Elevation (ft MSL) ^(b)	Rock Coring		Soil Sampling Method			From	To	Proposed	Actual	P-S Velocity	Televiewer	Packer Test	Goodman Jack	Pressuremeter
					HQ	NQ	SPT	UD	CME									
Cooling Tower Unit 1	B-1025	1165263.848	1845471.841	609.654		X	X			0	28.5	50	52					
	B-1025-UD	1165268.740	1845470.006	609.654				X		--	--	--	21					
	B-1026	1164883.450	1845089.201	610.168		X				0	99.9	50	99.9					
	B-1026-UD	1164870.682	1845091.797	609.875				X		--	--	--	47					
	B-1027	1165384.243	1845448.133	609.673		X	X			--	--	--	50					
Cooling Tower Unit 2	B-1028	1166140.124	1848027.639	609.765			X			0	103.55	80	103.55					
	B-1028-UD	1166150.119	1848024.643	609.875				X		--	--	--	94.6					
	B-1029	1165581.365	1848117.315	609.811			X			0	99.25	80	99.25					
	B-1030	1165963.148	1848403.477	609.697			X			0	98.8	80	98.8					
	B-1070	1165725.759	1848283.701	610.663			X			--	--	--	106	X				
	B-1070-UD	1165720.845	1848293.604	610.657				X		--	--	--	57.7					
	B-1071	1165707.327	1848320.308	610.545			X			--	--	--	100					
Switchyard (525 and 230 kV)	B-1031	1164731.622	1847445.498	603.991			X			0	38.8	50	38.8					
	B-1031-UD	1164740.021	1847445.261	603.991				X		--	--	--	16					
	B-1031-UDA	1164728.537	1847439.841	603.836				X		--	--	--	37					
	B-1032	1164553.105	1846696.598	603.938			X			0	40.2	40	40.2					
	B-1033	1164557.162	1847059.050	604.405			X			0	40.5	40	40.5					
	B-1033-UD	1164563.916	1847059.310	604.110				X		--	--	--	28					
	B-1034	1164327.544	1847522.550	603.997			X			0	39.3	40	29					

TABLE 2.5.4-203 (Sheet 5 of 6)
SUMMARY OF COMPLETED EXPLORATION BORINGS AND FIELD TESTS

Facility or Zone	Boring Number	Coordinates and Elevation			Boring Type					SPT Interval		Depth (ft bgs) ^(a)		Borehole Geophysical Testing			In-situ Testing	
		Northing	Easting	Elevation (ft MSL) ^(b)	Rock Coring		Soil Sampling Method			From	To	Proposed	Actual	P-S Velocity	Televiewer	Packer Test	Goodman Jack	Pressuremeter
					HQ	NQ	SPT	UD	CME									
	B-1035	1164164.327	1847146.518	604.562			X			--	--	--	40.1					
	B-1068	1164807.458	1847481.381	605.704			X			--	--	--	39	X				
	B-1068-UD	1164805.263	1847471.664	605.786				X		--	--	--	32					
	B-1069	1164802.003	1847447.979	604.878			X			--	--	--	40					
Make-Up Pond B Dam	B-1036	1166863.111	1844076.180	591.051			X			0	23.5	160	23.5					
General Site Coverage and Facilities	B-1044	1167711.138	1847455.765	587.987		X	X			0	13.6	--	43.6					
	B-1045	1167756.187	1847636.642	588.394		X	X			--	--	--	54					
	B-1045-UD	1167749.848	1847628.174	588.394				X		--	--	--	16					
	B-1046	1167815.000	1847834.473	588.315		X	X			--	--	--	93.3					
	B-1046-UD	1167822.860	1847835.327	588.046				X		--	--	--	54					
	B-1047	1167543.561	1847907.867	588.079		X	X			--	--	--	93.5					
	B-1047-UD	1167548.776	1847908.725	588.231				X		--	--	--	40					
	B-1048	1167477.305	1847718.329	587.526		X	X			--	--	--	84.5					
	B-1048-UD	1167471.096	1847715.977	587.526				X		--	--	--	26					
	B-1049	1167470.743	1847541.280	587.444		X	X			--	--	--	81					
Borrow Areas	B-1056	1163896.899	1846786.571	642.830			X			0	58.9	45	58.9					
	B-1057	1163743.790	1846819.978	639.064			X			0	54.8	50	54.8					
	B-1058	1163577.599	1846860.987	638.355			X			0	44.96	45	44.96					

TABLE 2.5.4-203 (Sheet 6 of 6)
SUMMARY OF COMPLETED EXPLORATION BORINGS AND FIELD TESTS

Facility or Zone	Boring Number	Coordinates and Elevation			Boring Type					SPT Interval		Depth (ft bgs) ^(a)		Borehole Geophysical Testing			In-situ Testing	
		Northing	Easting	Elevation (ft MSL) ^(b)	Rock Coring		Soil Sampling Method			From	To	Proposed	Actual	P-S Velocity	Televiewer	Packer Test	Goodman Jack	Pressuremeter
					HQ	NQ	SPT	UD	CME									
	B-1059	1164621.202	1845733.239	686.991			X			0	55	40	55					
	B-1060	1163796.990	1847079.841	634.499			X			0	54.4	40	54.4					
	B-1061	1164300.248	1845630.540	685.282			X			0	50	40	50					
	B-1062	1164027.320	1847313.772	621.610			X			0	40	30	40					
	B-1063	1165768.794	1845001.137	610.939			X			0	28.8	30	28.8					
	B-1064	1166042.294	1845355.995	609.393			X			0	20	30	20					
	B-1065	1165642.457	1845273.637	610.082			X			0	30	25	30					
	B-1066	1163965.942	1847564.670	632.799			X			0	35	25	35					
	B-1067	1163861.880	1847598.060	629.049			X			0	60	25	60					
	B-1072	1164001.659	1847171.959	630.173			X			--	--	--	45					
	B-1073	1163676.681	1847239.214	626.706		X	X			--	--	--	78.5					

a) ft bgs = feet below ground surface.

b) ft MSL = feet above mean sea level.

TABLE 2.5.4-204 (Sheet 1 of 2)
SUMMARY OF GEOTECHNICAL BORINGS FOR COMPLETED MONITORING WELLS

Facility or Zone	Well Number	Coordinates and Elevation			Depth (ft bgs)		Boring Type					Packer Test Performed	
							Rock Coring		Soil Sampling Method				
		Northing (ft)	Easting (ft)	Elevation (ft MSL)	Proposed Max.	Actual	HQ	NQ	SPT	UD	CME		
Power Block and Adjacent Structures <small>WLS COL 2.5-1</small>	Unit 1 - Adjacent Structure	MW-1211	1165196.276	1846389.259	589.318	150	65.5		X			X	
	Unit 2 - Adjacent Structure	MW-1210	1165324.031	1847451.588	589.438	150	38					X	
		MW-1210A	1165324.523	1847455.093	589.438	--	126.3		X	X			X
Cooling Tower	Unit 1	MW-1212	1165375.527	1845450.152	609.717	150	22.0					X	
		MW-1212A	1165371.506	1845450.693	609.291	--	89.2		X				
Unit 2		MW-1203	1166694.460	1847841.558	589.519	150	112.5		X			X	
		MW-1204	1166135.181	1848031.336	609.844	150	98.4					X	
		MW-1204A	1166132.228	1848026.567	609.861	--	135		X				
Switchyard (525 and 230 kV)		MW-1213	1164716.565	1847770.708	587.549	150	78.3		X			X	
		MW-1214	1164174.596	1847143.086	604.508	150	15.0					X	
		MW-1214A	1164175.677	1847147.851	604.508	--	96.0		X				
General Site Coverage and Facilities		MW-1200	1166347.301	1845577.653	591.514	150	8.5					X	
		MW-1200A	1166348.244	1845580.355	591.771	--	63.5		X				
		MW-1201	1166696.031	1846574.254	589.524	150	150.0		X			X	
		MW-1202	1167007.315	1847460.055	587.318	150	53.5					X	
		MW-1202A	1167013.537999999	1847466.675	587.550	--	115.6		X	X			
		MW-1205	1165628.988	1848312.858	609.588	150	150		X			X	
		MW-1206	1166650.035	1846689.096	589.559	150	93.0		X			X	

TABLE 2.5.4-204 (Sheet 2 of 2)
SUMMARY OF GEOTECHNICAL BORINGS FOR COMPLETED MONITORING WELLS

Facility or Zone	Well Number	Coordinates and Elevation			Depth (ft bgs)		Boring Type					Packer Test Performed
							Rock Coring		Soil Sampling Method			
		Northing (ft)	Easting (ft)	Elevation (ft MSL)	Proposed Max.	Actual	HQ	NQ	SPT	UD	CME	
	MW-1207	1166840.186	1846668.529	588.785	150	62.0					X	
	MW-1207A	1166836.619	1846666.697	588.785	--	133.5		X				
	MW-1208	1167184.041	1846588.623	587.071	150	139.3		X			X	
	MW-1209	1165080.624	1848078.551	586.612	150	125.5		X			X	
	MW-1215	1166710.545	1846624.819	589.687	--	101.5						

- Notes:
1. ft b.g.s. = feet below ground surface

2. ft MSL = feet above mean sea level

TABLE 2.5.4-205 (Sheet 1 of 2)
SUMMARY OF COMPLETED CONE PENETROMETER TEST SOUNDINGS

Facility or Zone	CPT Number	Coordinates and Elevation			Depth (ft)		Tests Performed	
		Northing (ft)	Easting (ft)	Elevation (ft MSL)	Proposed	Actual	SCPT	Dissipation Test Depth (ft bgs)
WLS COL 2.5-1	Pipelines (Non-Safety Related)							
	CPT-1314	1164932.132	1846220.577	589.951	50	6.1		
	CPT-1315	1165032.071	1846589.827	586.86	50	40		
	CPT-1316	1165442.267	1847364.975	589.604	50	57.6		
	CPT-1317	1165480.571	1847652.112	588.745	50	8.7		
	CPT-1317A	1165481.237	1847632.773	588.636	50	19.5		
	CPT-1317B	1165497.097	1847636.906	588.802	50	20.7		
	Cooling Tower							
	Unit 1							
	CPT-1300	1165285.875	1845003.070	609.238	30	30		18.5, 30.0
	CPT-1301	1164894.227	1845085.762	609.833	30	30		
	Unit 2							
	CPT-1302	1166124.625	1848040.223	609.27	80	80.1		34.9, 80.1
	CPT-1303	1165582.495	1848103.243	609.599	80	90.6		65.9, 80.2
	CPT-1304	1165892.587	1848181.888	609.838	80	74		74
	CPT-1323	1165679.210	1848305.418	610.468	100	84.2	X	81.0, 84.2
	CPT-1324	1165733.296	1848334.24	610.241	100	3.1		
	CPT-1324B	1165733.296	1848334.24	610.241	100	77.3	X	77.3
	CPT-1325	1165730.729	1848273.936	610.349	100	40.0	X	
	CPT-1325A	1165728.968	1848272.952	610.057	100	55.1	X	55.1
	Switchyard (525 and 230 kV)							
	CPT-1305	1164732.401	1847452.325	603.729	50	34.3		
	CPT-1306	1164174.233	1847132.668	604.291	50	18.9		
	CPT-1306A	1164172.987	1847128.893	604.336	50	21.2		
	CPT-1320	1164809.635	1847497.262	604.865	40	32.3	X	32.3

TABLE 2.5.4-205 (Sheet 2 of 2)
SUMMARY OF COMPLETED CONE PENETROMETER TEST SOUNDINGS

Facility or Zone	CPT Number	Coordinates and Elevation			Depth (ft)		Tests Performed	
		Northing (ft)	Easting (ft)	Elevation (ft MSL)	Proposed	Actual	SCPT	Dissipation Test Depth (ft bgs)
Make-Up Pond B Dam	CPT-1321	1164802.257	1847460.695	604.865	40	43.3	X	43.3
	CPT-1322	1164794.98	1847472.656	605.226	40	48.1	X	48.1
	CPT-1307	1166393.067	1847138.502	589.841	80	20.2		
	CPT-1308	1166994.841	1844214.370	538	60	8.0		
General Site Coverage and Facilities	CPT-1308A	1167001.502	1844206.906	538	60	41.2	X	41.2
	CPT-1308B	1167008.152	1844199.436	538	60	39.5	X	
	CPT-1309	1166860.560	1844074.210	591.001	160	85.1	X	60.0, 85.1
	CPT-1318	1167614.443	1847587.310	586.374	50	16.2		
	CPT-1319	1167695.014	1847778.705	587.888	50	47.6		

Notes:

1. ft b.g.s. = feet below ground surface
2. ft MSL = feet above mean sea level
3. CPT-1308A; SCPT attempted, no useful data recovered.

TABLE 2.5.4-206 (Sheet 1 of 2)
SUMMARY OF COMPLETED GEOTECHNICAL TEST PIT AND GEOLOGIC TRENCH LOCATIONS

	Facility or Zone	Test Pit Number	Coordinates and Elevation ⁽³⁾		
			Northing	Easting	Elevation (ft MSL)
WLS COL 2.5-1	Power Block and Adjacent Structures				
	Unit 1	T-1400A	1165454.547	1846181.692	589.426
		T-1400B	1165328.497	1845955.529	590.177
	Unit 2	T-1401	1166317.379	1846815.739	590.44
		T-1402	1166376.698	1846887.698	590.032
		T-1403	1166394.130	1847140.590	589.882
		T-1404	1166250.245	1846714.042	551.273
	Cooling Tower				
	Unit 1	T-1426	1166029.449	1845369.840	609.56
	General Site Coverage and Facilities				
		T-1421	1164323.917	1845632.897	685.464
	Proposed Borrow Area				
	(former Borrow Area '1')				
		T-1419	1163896.961	1846789.678	642.468
		T-1420	1163582.443	1846854.298	638.047
		T-1422	1163992.360	1847171.647	630.767
		T-1423	1163666.925	1847256.094	625.823

TABLE 2.5.4-206 (Sheet 2 of 2)
SUMMARY OF COMPLETED GEOTECHNICAL TEST PIT AND GEOLOGIC TRENCH LOCATIONS

Facility or Zone	Test Pit Number	Coordinates and Elevation ⁽³⁾		
		Northing	Easting	Elevation (ft MSL)
	T-1424	1164081.712	1847436.633	628.342
	T-1425	1163869.581	1847595.432	629.604

Notes:

1. ft b.g.s. = feet below ground surface
2. ft MSL = feet above mean sea level
3. Coordinates and elevation given for northernmost corner of test pit or northernmost end of test pit trench

TABLE 2.5.4-207
SUMMARY OF COMPLETED SURFACE GEOPHYSICAL TEST LOCATIONS

		Point A Coordinates (northern point)		Point B Coordinates (southern point)				Total Length (ft)	Point A Elevation (ft MSL)
Facility or Zone		Seismic Line Number	Northing	Easting	Northing	Easting	Bearing		
WLS COL 2.5-1	Power Block and Adjacent Structures								
	Unit 1	S-1505	1166231.515	1846134.432	1165997.350	1845947.172	S38.7°W	299.833	589.148
	Unit 2	S-1503A (Profiles 1 and 2)	1166294.705	1847205.937	1166173.432	1847172.201	S13.5°W	126.204	558.857
		S-1503B (Profile 3)	1166277.379	1847189.534	1166174.904	1847147.062	S22.6°W	110.953	560.357
		S-1504	1166219.947	1847229.069	1166202.741	1847218.988	S30.4°W	19.950	558.799
	Adjacent Structures	S-1506	1166518.953	1847248.339	1166468.130	1846952.787	S79.9°W	299.938	589.286
		S-1507	1166432.500	1847505.178	1166139.308	1847567.671	S12.1°E	299.782	589.653
	Cooling Tower								
	Unit 1	S-1500	1165271.782	1845003.690	1164967.172	1845070.314	S12.2°E	311.815	609.216
		S-1501	1165118.678	1845267.690	1165066.423	1845049.417	S76.5°W	224.443	609.789
		S-1502	1165210.841	1845229.408	1164913.862	1845270.135	S7.6°E	299.769	609.564
	Unit 2	S-1508	1165995.359	1848380.679	1165805.968	1848147.121	S50.6°W	300.746	610.085
		S-1509	1165824.517	1848410.455	1165685.278	1848233.625	S51.7°W	225.071	610.190
		S-1510	1166132.383	1848050.349	1166025.972	1848247.572	S61.7°E	224.099	609.670
Make-Up Pond B Dam									
	S-1513	1166936.563	1844002.862	1166749.091	1844236.750	S51.3°E	299.749	591.358	
General Site Coverage and Facilities									
	S-1511	1167786.501	1847736.262	1167714.948	1847445.373	S76.1°W	299.562	588.490	
	S-1512	1167874.136	1847914.115	1167622.486	1847750.398	S33.0°W	300.219	587.774	

Notes:

1. ft MSL = feet above mean sea level

TABLE 2.5.4-208
SUMMARY OF GOODMAN JACK TEST RESULTS

	Hole	Test Number	Test Interval (ft. b.g.s.)	E _{calc} (psi)	E _{true} (psi)
WLS COL 2.5-1	B1004	CKE-01	13.22 - 13.89	1,038,000	1,100,000
	B1004	CKE-02	12.22 - 12.89	1,345,000	1,800,000
	B1004	CKE-03	23.22 - 23.89	2,077,000	3,400,000
	B1004	CKE-04	22.22 - 22.89	1,554,000	2,100,000
	B1004	CKE-05	33.89 - 34.56	2,559,000	5,200,000
	B1004	CKE-06	32.89 - 33.56	2,376,000	4,500,000
	B1004	CKE-07	44.64 - 45.31	2,024,000	4,300,000
	B1004	CKE-08	43.64 - 44.53	1,934,000	3,200,000
	B1014	CKE-09	8.29 - 8.96	1,913,000	3,100,000
	B1014	CKE-10	6.29 - 6.96	184,000	184,000
	B1014	CKE-11	7.29 - 7.96	1,730,000	2,600,000
	B1014	CKE-12	16.49 - 17.16	2,176,000	3,700,000
	B1014	CKE-13	14.89 - 15.56	2,772,000	6,200,000
	B1014	CKE-14	24.89 - 25.56	1,986,000	3,200,000

ft. = feet

b.g.s. = below ground surface

E_{calc} = Calculated maximum Young's Modulus

E_{true} = True Young's Modulus

TABLE 2.5.4-209
SUMMARY OF PRESSUREMETER TEST RESULTS

	Borehole	Test Number	Bottom of Instrument (ft. b.g.s.)	Center of Membrane (ft. b.g.s.)	Initial Shear Modulus (G) (psi)	Unload-Reload Shear Modulus (G) (psi)
WLS COL 2.5-1	B1074	Lee2	44.1	42.7	14,000	90,000
	B1074	Lee1	45.6	44.4	10,000	65,000
	B1074	Lee4	49.5	48.2	12,000	76,000
	B1074	Lee3	51.0	49.2	39,000	225,000
	B1074	Lee6	54.5	52.8	130,000	450,000
	B1074	Lee5	56.0	54.8	310,000	1,000,000
	B1074	Lee7	59.5	58.3	52,000	220,000
	B1074	Lee9	64.0	62.8	120,000	450,000
	B1074	Lee8	65.5	64.3	180,000	560,000
	B1074A	Lee12	53.4	51.7	350,000	740,000
	B1074A	Lee11	54.9	53.2	220,000	700,000
	B1074A	Lee10	56.4	54.7	320,000	1,000,000
	B1074A	Lee14	62.0	60.8	No useful data	No useful data
	B1074A	Lee13	63.5	62.3	870,000	1,500,000
	B1074A	Lee17	66.5	65.3	350,000	1,000,000
	B1074A	Lee16	68.0	66.8	440,000	6,000,000
	B1074A	Lee15	69.5	68.3	160,000	2,000,000
	B1074A	Lee21	73.5	72.3	360,000	5,000,000
	B1074A	Lee20	75.0	73.8	250,000	6,000,000
	B1074A	Lee19	76.5	75.3	200,000	1,800,000
	B1074A	Lee18	77.0	75.8	40,000 ^(a)	220,000 ^(a)
	B1074A	Lee22	81.7	80.5	320,000	6,000,000
	B1074A	Lee24	82.9	81.7	140,000	6,000,000
	B1074A	Lee23	84.4	83.2	160,000	6,000,000

ft. = feet

b.g.s. = below ground surface

psi = pounds per square inch

a) indicates data that is anomalously low, not used in analysis

TABLE 2.5.4-210
LABORATORY TESTING QUANTITIES BY SAMPLE TYPE AND
TEST METHOD

WLS COL 2.5-6	Test Standard	Tests Per Sampling Method			
		Soil			Rock
		Bulk ^(a)	Jar	Undisturbed	Rock Cores
Moisture Content	ASTM D 2216 – 05	-	113	39	0
Atterberg Limits	ASTM D 4318 – 05	-	7	37	0
Grain Size - Wash #200	ASTM D 6913 – 04	-	53	23	0
Grain Size - Sieve + Hydrometer	ASTM D 422 – 63 (2002)	-	8	14	0
Specific Gravity	ASTM D 854 – 06	-	8	37	0
Chemical Analysis	ASTM G 51 – 95 (2005)				
	ASTM G 57 – 95a (2001)				
	EPA SW – 846 9056/300.0	-	0	1	0
	EPA SW – 846 8056/300.0				
Consolidated-Undrained Triaxial Shear	ASTM D 4767 – 04	-	0	20	0
Unconfined Compression (UC)	ASTM D 7012 – 04	-	0	0	30
UC with Stress-Strain Analysis	ASTM D 7012 – 04	-	0	0	11
Consolidation	ASTM D 2435 – 04	-	0	24	0

a) The test data on bulk samples are removed because the materials are not used in the vicinity of the nuclear islands or under structures adjacent to the nuclear islands where only granular backfill is used.

TABLE 2.5.4-211 (Sheet 1 of 2)
AVERAGE ENGINEERING PROPERTIES OF SOIL

(Reported Values are Mean ± One Standard Deviation, Except for Granular Fill)

		All Fill Samples ^(a)			Granular Fill			Residual Soil			Saprolite			PWR
WLS COL 2.5-6		N ₆₀ ≤ 10 (N ≤ 8) ^(b)	11 < N ₆₀ ≤ 30 (8 < N ≤ 23) ^(b)	31 < N ₆₀ ≤ 100 (23 < N ≤ 75) ^(b)	GW	GP	SW	N ₆₀ ≤ 10 (N ≤ 8) ^(b)	11 < N ₆₀ ≤ 30 (8 < N ≤ 23) ^(b)	31 < N ₆₀ ≤ 100 (23 < N ≤ 75) ^(b)	N ₆₀ ≤ 10 (N ≤ 8) ^(b)	11 < N ₆₀ ≤ 30 (8 < N ≤ 23) ^(b)	31 < N ₆₀ ≤ 100 (23 < N ≤ 75) ^(b)	N ₆₀ > 100 (N > 75) ^(b)
N ₆₀ -value ^(c)		21 ± 8 [75]			45 ^(d)	45 ^(d)	29-30 ^(d)	25 ± 26 [14]			28 ± 23 [64]			-
Corrected tip resistance, q _c	tsf	46.6 ± 31.4 [1,646]			-	-	-	62.5 ± 41.1 [330]			69.3 ± 61.2 [367]			-
Friction ratio, FR	ft/sec	5.4 ± 1.7 [1,646]			-	-	-	3.5 ± 1.5 [330]			4.0 ± 2.0 [367]			-
Percent gravel ^(e)	%	0 [1] ^(f)	4 ± 6 [36]	6 ± 8 [6]	40-70 ^(g)	40-70 ^(g)	0-10 ^(g)	0 [1]	0 [4]	0 [1]	3 ± 3 [8]	3 ± 7 [20]	1 ± 1 [11]	9 ± 14 [8]
Percent sand ^(e)	%	42 [1] ^(f)	34 ± 8 [36]	47 ± 19 [6]	18-60 ^(g)	18-60 ^(g)	86-100 ^(g)	57 ^(f) [1]	46 ± 15 [4]	40 ^(f) [1]	44 ± 11 [8]	52 ± 12 [20]	52 ± 13 [11]	55 ± 19 [8]
Percent fines (<#200 sieve) ^(e)	%	58[1] ^(f)	62 ± 11 [36]	47 ± 21 [6]	0-12 ^(g)	0-12 ^(g)	0-4 ^(g)	43 ^(f) [1]	54 ± 14 [4]	60 ^(f) [1]	54 ± 13 [8]	46 ± 15 [20]	47 ± 13 [11]	36 ± 22 [8]
Percent silt	%	-	41 ± 9 [13]	42 ^(f) [1]	-	-	-	-	55 ^(f) [1]	56 ^(f) [1]	53 ^(f) [2]	41 ± 10 [3]	34 ^(f) [1]	-
Percent clay (<5μm)	%	-	18 ± 9 [13]	19 ^(f) [1]	-	-	-	-	19 ^(f) [1]	4 ^(f) [1]	6 ^(f) [2]	5 ± 2 [3]	8 ^(f) [1]	-
Plasticity index, PI	%	-	NP [20]	NP [1]	≤6 ^(g)	≤6 ^(g)	NP ^(g)	-	NP [2]	-	NP [5]	NP [10]	NP [5]	NP [1]
Liquid limit, LL	%	-	NV [20]	NV [1]	≤25 ^(g)	≤25 ^(g)	NV ^(g)	-	NV [2]	-	NV [5]	NV [10]	NV [5]	NV [1]
Water content ^(e) , w	%	33 ^(f) [1]	23 ± 6 [59]	21 ± 10 [9]	-	-	-	22 ^(f) [1]	32 ± 6 [9]	28 ± 10 [3]	32 ± 6 [15]	30 ± 12 [27]	20 ± 6 [16]	14 ± 4 [9]
Initial void ratio, e _o		-	0.69 ± .17 [13]	-	0.18	0.29	0.39	-	0.94 ^(f) [2]	-	0.84 ± 0.23 [4]	0.84 ± 0.33 [8]	0.83 ^(f) [2]	-
Specific gravity, G _s		-	2.71 ± .06 [20]	2.68 ^(f) [1]	2.65 ^(g)	2.65 ^(g)	2.65 ^(g)	-	2.72 ^(f) [2]	2.70 ^(f) [1]	2.72 ± 0.04 [6]	2.71 ± .04 [11]	2.69 ± .04 [4]	-
Dry unit weight, γ _{dry}	pcf	-	101 ± 8 [13]	-	140	128	119	-	88 ^(f) [2]	-	93 ± 11 [4]	94 ± 15 [8]	93 ^(f) [2]	-
Wet unit weight, γ _t	pcf	-	122 ± 5 [13]	-	150	142	136	-	113 ^(f) [2]	-	116 ± 11 [4]	117 ± 7 [8]	114 ^(f) [2]	135 ^(h)
Saturated unit weight, γ _{sat}	pcf	-	125 ± 5 [13]	-	150	142	136	-	118 ^(f) [2]	-	121 ± 7 [4]	124 ± 7 [7]	121 ^(f) [2]	140 ^(h)
Overconsolidation ratio ⁽ⁱ⁾ , OCR		4.9 ± 2.8 ⁽ⁱ⁾ [11]			-	-	-	-	1.6 ^(f) [1]	-	4.2 ± 2.4 [3]	3.5 ± 2.0 [7]	2.4 ^(f) [2]	-
Preconsolidation pressure ⁽ⁱ⁾ , σ _p '	ksf	8.8 ± 1.6 ⁽ⁱ⁾ [11]			-	-	-		10.0 ^(f) [1]		10.0 ± 1.5 [3]	9.4 ± 2.0 [7]	8.9 ^(f) [2]	-
Compression index ⁽ⁱ⁾ , C _c		0.19 ± 0.09 ⁽ⁱ⁾ [11]			-	-	-	-	0.34 ^(f) [1]	-	0.29 ± 0.03 [3]	0.33 ± 0.22 [7]	0.19 ^(f) [2]	-
Re-compression index ⁽ⁱ⁾ , C _r		0.024 ± 0.015 ⁽ⁱ⁾ [11]			-	-	-	-	0.030 ^(f) [1]	-	0.024 ± 0.016 [3]	0.027 ± 0.012 [7]	0.026 ^(f) [2]	-
Consolidation coefficient ⁽ⁱ⁾ , C _v	ft ² /day	5.6 ± 2.2 ⁽ⁱ⁾ [11]			-	-	-	-	6 ^(f) [1]	-	6.3 ± 0.6 [3]	5.1 ± 2.3 [7]	7 ^(f) [2]	-
Total cohesion ⁽ⁱ⁾ , c	psf	1,887 ± 178 ⁽ⁱ⁾ [13]			-	-	-	224 ± 61 ^(k)	-1,243 ± 346 ^(k)	1,406 ^(k)	224 ± 61 [4]	1,243 ± 346 [6]	1,406 ^(f) [2]	1,000 ^(h)
Total friction angle ⁽ⁱ⁾ , φ	deg	20 ± 2 ⁽ⁱ⁾ [13]			-	-	-	27 ± 5 ^(k)	20 ± 5 ^(k)	19 ^(k)	27 ± 5 [4]	20 ± 5 [6]	19 ^(f) [2]	45 ^(h)

TABLE 2.5.4-211 (Sheet 2 of 2)

AVERAGE ENGINEERING PROPERTIES OF SOIL

(Reported Values are Mean ± One Standard Deviation, Except for Granular Fill)

		All Fill Samples ^(a)			Granular Fill			Residual Soil			Saprolite			PWR
WLS COL 2.5-6		N ₆₀ ≤ 10 (N ≤ 8) ^(b)	11 < N ₆₀ ≤ 30 (8 < N ≤ 23) ^(b)	31 < N ₆₀ ≤ 100 (23 < N ≤ 75) ^(b)	GW	GP	SW	N ₆₀ ≤ 10 (N ≤ 8) ^(b)	11 < N ₆₀ ≤ 30 (8 < N ≤ 23) ^(b)	31 < N ₆₀ ≤ 100 (23 < N ≤ 75) ^(b)	N ₆₀ ≤ 10 (N ≤ 8) ^(b)	11 < N ₆₀ ≤ 30 (8 < N ≤ 23) ^(b)	31 < N ₆₀ ≤ 100 (23 < N ≤ 75) ^(b)	N ₆₀ > 100 (N > 75) ^(b)
Effective cohesion ^{(i)(l)} , c'	psf	276 ± 49 ^(j) [14]			0	0	0	-	130 ^(f) [3]	-	0 [4]	439 ± 94 [6]	230 ^(f) [2]	1,000 ^(h)
Effective friction angle ^{(i)(l)} , ϕ'	deg	28 ± 4 ^(j) [14]			≥35	≥35	≥35	-	30 ^(f) [3]	-	31 ± 4 [4]	23 ± 5 [6]	28 ^(f) [2]	45 ^(h)
Hydraulic conductivity ^(m) , k	ft/year	-	-	-	<~5,173 to 51,730	<~5,173 to 77,598	~5,173 to 17,589	-	-	-	-	-	-	-
	cm/sec	-	-	-	<~5.0E-03 to 5.0E-02	<~5.0E-03 to ~7.5E-02	~5.0E-03 to ~1.7E-02	-	-	-	-	-	-	-

- a) All Fill includes samples classified as fill on boring logs.
- b) Field SPT-N values to correlate to N₆₀-values are computed using the average energy transfer ratio (ETR) of 80.0 percent. N=N₆₀(60/80.0).
- c) N₆₀- value is obtained from field values corrected to Energy Transfer Ratios of 60%. The values for granular fill are (N₁)₆₀, and are for typical materials (see footnote d).
- d) Reported value is for (N₁)₆₀. Value obtained using correlations in [Reference 230](#) (Idriss and Boulanger, 2008) for sand (SW) and [Reference 232](#) (Rollins et al., 1998) for gravel (GW and GP) for relative density = 80% corresponding to relative compaction = 96% (ASTM D 1557).
- e) Three samples of alluvium were tested for moisture content and two underwent grain size analysis; the results are not shown in this table.
- f) Insufficient data to determine standard deviation.
- g) Values listed are for typical granular fill materials and will be verified by laboratory testing when the source of and specific materials to be used are known. Unit weight, friction angle, and hydraulic conductivity values reported are obtained from [Reference 228](#) (NAVFAC, 1986). Grain sizes and PI, LL for typical granular fill materials are obtained from [Reference 224](#) (SCDOT, 2007). The specific gravity of granular fill material is assumed as 2.65, a typical value.
- h) These values are from PSAR, Table 2D-3 and Table 2A-1 ([Reference 201](#)).
- i) The design engineer (i.e., engineer that will use data for design) must give careful consideration to compressibility and strength parameters based on test data, and the values reported in this table are estimates.
- j) Samples tested were all in the 11 < N₆₀ ≤ 30 range. The resulting consolidation and shear parameters may be applied to existing fill regardless of N₆₀.
- k) Insufficient data to determine total strength parameters; strength parameters have been assigned same as for saprolite having similar N₆₀. Little residual soil remains.
- l) For consolidated-undrained triaxial tests on undisturbed specimens, failure was said to occur at peak pore pressure.
- m) 1 ft/year * 9.67 x 10⁻⁷ = 1 cm/sec.

Note: The number in brackets is the count, [Number]

TABLE 2.5.4-212
CORROSION TESTING OF SOIL FILL

WLS COL 2.5-6

Sample Type	pH	Resistivity (Ohm-cm)		Chlorides (mg/kg)	Sulfates (mg/kg)
		As Received	Saturated		
Undisturbed	3.9 [1]	2.43 E+05 [1]	2.92 E+05 [1]	2.5 [1]	5.6 [1]

Note: The number in the brackets is the count, [count]

TABLE 2.5.4-213
SUMMARY OF LABORATORY TEST RESULTS FOR INTACT
ROCK CORES

			Meta Granodiorite	Meta Quartz Diorite	Meta Diorite	All Rock Types
WLS COL 2.5-6	Unit Weight, γ	pcf	168 \pm 1 [19]	169 \pm 3 [14]	177 \pm 2 [8]	170 \pm 4 [41]
	Unconfined Compressive Strength	ksi	23 \pm 5 [19]	17 \pm 7 [14]	22 \pm 6 [8]	21 \pm 7 [41]
	Young's Modulus, E	$\times 10^6$ psi	7.8 \pm 0.3 [3]	7.1 \pm 1.0 [7]	8.1 [1]	7.4 \pm 0.9 [11]
	Poisson's Ratio, ν	-	0.29 \pm 0.06 [3]	0.27 \pm 0.05 [7]	0.23 [1]	0.27 \pm 0.05 [11]

1. The number in the brackets is the count, [Number].

TABLE 2.5.4-214 (Sheet 1 of 7)
SUMMARY OF SASW VELOCITY SURVEY

WLS COL 2.5-6	Survey Line Number	Layer No.	Thickness, (ft)	Depth to Top of Layer (ft)	Assumed Poisson's Ratio	S-Wave Velocity (ft/sec)	P-Wave Velocity (ft/sec)
S-1500		1	1.5	0	0.33	480	120
		2	3	1.5	0.33	630	120
		3	5	4.5	0.33	720	120
		4	2	9.5	0.33	550	120
		5	15	11.5	0.33	760	120
		6	40	27	0.33	860	120
		7	7	67	0.47	1100	125
		8(a)	43	74	0.47	1100	125
		9(a)	11	117	0.44	1600	125
		10(a)(b)	Half Space	128	0.44	1600	125
S-1501		1	2	0	0.33	470	120
		2	2.6	1.5	0.33	600	120
		3	5	4.6	0.33	680	120
		4	15	9.6	0.33	730	120
		5	42	24.6	0.33	760	120
		6	28	67	0.47	1200	125
		7(a)	27	95	0.47	1200	125
		8(a)(b)	Half Space	122	0.47	1200	125

TABLE 2.5.4-214 (Sheet 2 of 7)
SUMMARY OF SASW VELOCITY SURVEY

WLS COL 2.5-6	Survey Line Number	Layer No.	Thickness, (ft)	Depth to Top of Layer (ft)	Assumed Poisson's Ratio	S-Wave Velocity (ft/sec)	P-Wave Velocity (ft/sec)
	S-1502	1	1.7	0	0.33	430	120
		2	1	1.7	0.33	500	120
		3	1	2.7	0.33	580	120
		4	2.3	3.7	0.33	690	120
		5	32	6	0.33	820	120
		6	10	38	0.33	900	120
		7	19	48	0.33	2200	130
		8 ^(b)	Half Space	67	0.38	2200	130
	S-1503A, Profile 1	1	0.27	0	0.25	4300	7448
		2	0.5	0.27	0.25	7800	13510
		3	14.38	0.77	0.25	8500	14722
		4 ^(b)	Half Space	15.15	0.25	8500	14722
	S-1503A, Profile 2	1	0.3	0	0.25	4900	8487
		2	1.5	0.3	0.25	8500	14722
		3	13.35	1.8	0.25	9000	15589
		4 ^(b)	Half Space	15.15	0.25	9000	15589

TABLE 2.5.4-214 (Sheet 3 of 7)
SUMMARY OF SASW VELOCITY SURVEY

WLS COL 2.5-6	Survey Line Number	Layer No.	Thickness, (ft)	Depth to Top of Layer (ft)	Assumed Poisson's Ratio	S-Wave Velocity (ft/sec)	P-Wave Velocity (ft/sec)
	S-1503B, Profile 3	1	0.27	0	0.25	4000	6928
		2	0.5	0.27	0.25	6500	11258
		3	14.38	0.77	0.25	7000	12124
		4 ^(b)	Half Space	15.15	0.25	7000	12124
	S-1504	1	0.2	0	0.25	4500	7794
		2	0.5	0.2	0.25	5500	9526
		3	0.5	0.7	0.25	6500	11258
		4	1.2	1.2	0.25	7500	12990
		5	1.7	2.4	0.25	10500	18187
		6 ^(b)	Half Space	4.1	0.25	10500	18187
	S-1505	1	2.2	0	0.33	1000	1985
		2	7	2.2	0.33	600	1191
		3	10	9.2	0.33	750	1489
		4	10	19.2	0.33	850	1688
		5	20	29	0.48	1000	5000
		6	23	49	0.33	2500	5000
		7 ^(b)	Half Space	72	0.33	2500	5000

TABLE 2.5.4-214 (Sheet 4 of 7)
SUMMARY OF SASW VELOCITY SURVEY

WLS COL 2.5-6	Survey Line Number	Layer No.	Thickness, (ft)	Depth to Top of Layer (ft)	Assumed Poisson's Ratio	S-Wave Velocity (ft/sec)	P-Wave Velocity (ft/sec)
	S-1506	1	1	0	0.33	1500	2978
		2	1	1	0.33	600	1191
		3	5.5	2	0.33	500	993
		4	5	7.5	0.33	650	1290
		5	5	12.5	0.33	780	1549
		6	10	17.5	0.33	1000	1985
		7	10	28	0.45	1500	5000
		8	30	38	0.38	2200	5000
		9	23	68	0.30	2850	5332
		10 ^(b)	Half Space	91	0.30	2850	5332
	S-1507	1	1.8	0	0.33	880	1747
		2	0.9	1.8	0.33	780	1549
		3	5.2	2.7	0.33	680	1350
		4	13	7.9	0.33	590	1171
		5	12	20.9	0.33	700	1390
		6	10	33	0.49	700	5000
		7	15	43	0.48	950	5000
		8	10	58	0.46	1350	5000
		9	5	68	0.33	2500	5000
		10	84	73	0.30	3000	5613
		11 ^(b)	Half Space	157	0.30	3000	5613

TABLE 2.5.4-214 (Sheet 5 of 7)
SUMMARY OF SASW VELOCITY SURVEY

WLS COL 2.5-6	Survey Line Number	Layer No.	Thickness, (ft)	Depth to Top of Layer (ft)	Assumed Poisson's Ratio	S-Wave Velocity (ft/sec)	P-Wave Velocity (ft/sec)
S-1508		1	1.1	0	0.33	350	695
		2	2.4	1.1	0.33	580	1151
		3	3	3.5	0.33	670	1330
		4	5	6.5	0.33	700	1390
		5	10	11.5	0.33	760	1509
		6	20	22	0.33	890	1767
		7	30	42	0.48	890	5000
		8	36	72	0.48	1050	5000
		9 ^(a)	51	108	0.48	1050	5000
		10 ^(a)	28	159	0.48	1050	5000
		11 ^{(a)(b)}	Half Space	187	0.47	1200	5000
S-1509		1	2.5	0	0.33	630	1251
		2	4.5	2.5	0.33	590	1171
		3	17	7	0.33	735	1459
		4	23	24	0.33	860	1707
		5	19	47	0.49	830	5000
		6	23	66	0.48	1000	5000
		7	17	89	0.46	1300	5000
		8 ^(b)	Half Space	106	0.46	1300	5000

TABLE 2.5.4-214 (Sheet 6 of 7)
SUMMARY OF SASW VELOCITY SURVEY

WLS COL 2.5-6	Survey Line Number	Layer No.	Thickness, (ft)	Depth to Top of Layer (ft)	Assumed Poisson's Ratio	S-Wave Velocity (ft/sec)	P-Wave Velocity (ft/sec)
	S-1510	1	2	0	0.33	500	993
		2	6	2	0.33	600	1191
		3	7	8	0.33	700	1390
		4	20	15	0.33	760	1509
		5	5	35	0.33	900	1787
		6	35	40	0.48	900	5000
		7	29	75	0.48	1080	5000
		8 ^(a)	21	104	0.48	1080	5000
		9 ^(a)	13	125	0.45	1500	5000
		10 ^{(a)(b)}	Half Space	138	0.45	1500	5000
	S-1511	1	1.5	0	0.33	485	963
		2	3.5	1.5	0.33	630	1251
		3	8	5	0.33	900	1787
		4	5	13	0.33	1030	2045
		5	10	18	0.33	1370	2720
		6	8	28	0.30	2150	4022
		7	15	36	0.39	2150	5000
		8	15	51	0.30	3300	6174
		9	74	66	0.30	4500	8419
		10 ^(b)	Half Space	140	0.30	4500	8419

TABLE 2.5.4-214 (Sheet 7 of 7)
SUMMARY OF SASW VELOCITY SURVEY

WLS COL 2.5-6	Survey Line Number	Layer No.	Thickness, (ft)	Depth to Top of Layer (ft)	Assumed Poisson's Ratio	S-Wave Velocity (ft/sec)	P-Wave Velocity (ft/sec)
	S-1512	1	3.5	0	0.33	780	1549
		2	4	3.5	0.33	600	1191
		3	13	7.5	0.33	735	1459
		4	15	20.5	0.33	800	1588
		5	5	36	0.49	800	5000
		6	10	41	0.48	900	5000
		7	10	51	0.47	1200	5000
		8	26	61	0.35	2400	5000
		9 ^(b)	Half Space	87	0.35	2400	5000
	S-1513	1	2.8	0	0.33	700	1390
		2	1.6	2.8	0.33	450	893
		3	6.7	4.4	0.33	700	1390
		4	28	11.1	0.33	800	1588
		5	72	39	0.48	890	5000
		6 ^(b)	14	97	0.48	1050	5000

a) Based on Sparse Data

b) Layer below maximum depth of the V_s Profile

TABLE 2.5.4-215 (Sheet 1 of 7)
SUMMARY OF SEISMIC CPT SHEAR WAVE (VS) VELOCITY
RESULTS

WLS COL 2.5-1	Test Number	Test Depth (ft)	Geophone Depth (ft)	Point Shear Velocity (fps)	Point Depth (ft)
	CPT-1308A		No useful data recovered		
WLS COL 2.5-6	CPT-1308B	3.12	2.46	---	---
		6.07	5.41	---	3.93
		9.02	8.36	1533.6	6.89
		12.14	11.48	702.1	9.92
		15.09	14.43	875.1	12.96
		19.03	18.37	927.5	16.40
		21.16	20.50	940.6	19.44
		24.11	23.45	908.1	21.98
		27.23	26.57	886.6	25.01
		30.02	29.36	868.7	27.97
		33.14	32.48	853.7	30.92
		36.91	36.25	922.8	34.36

TABLE 2.5.4-215 (Sheet 2 of 7)
SUMMARY OF SEISMIC CPT SHEAR WAVE (VS) VELOCITY
RESULTS

WLS COL 2.5-1	Test Number	Test Depth (ft)	Geophone Depth (ft)	Point Shear Velocity (fps)	Point Depth (ft)
	CPT-1309	3.12	2.46	---	---
		6.07	5.41	1356.8	3.93
		9.02	8.36	1007.8	6.89
		12.14	11.48	845.1	9.92
		15.09	14.43	617.1	12.96
		18.04	17.38	1345.3	15.91
		21.16	20.50	718.9	18.94
		24.11	23.45	1184.5	21.98
		27.07	26.41	1086.6	24.93
		30.02	29.36	863.0	27.88
		33.14	32.48	1086.5	30.92
		36.09	35.43	770.4	33.95
		39.04	38.38	868.3	36.91
		42.16	41.50	949.3	39.94
		45.11	44.45	962.6	42.98
		48.06	47.40	919.2	45.93
		51.06	50.36	1261.8	48.88
		54.13	53.47	1040.4	51.92
		57.09	56.43	809.0	54.95
		60.04	59.38	1100.5	57.90
		63.32	62.66	1297.7	61.02
		66.11	65.45	1150.2	64.05
		69.06	68.40	914.2	66.93
		72.34	71.68	956.8	70.04
		75.13	74.47	1152.9	73.08
		78.08	77.42	1028.6	75.95
		81.04	80.38	1011.4	78.90
		84.15	83.49	1147.2	81.93

TABLE 2.5.4-215 (Sheet 3 of 7)
SUMMARY OF SEISMIC CPT SHEAR WAVE (VS) VELOCITY
RESULTS

WLS COL 2.5-1	Test Number	Test Depth (ft)	Geophone Depth (ft)	Point Shear Velocity (fps)	Point Depth (ft)
	CPT-1320	3.12	2.46	---	---
		6.07	5.41	744.1	3.93
		9.02	8.36	904.4	6.89
		12.14	11.48	661.4	9.92
		15.09	14.43	789.1	12.96
		18.04	17.38	730.3	15.91
		21.16	20.50	1019.6	18.94
		24.11	23.45	707.6	21.98
		27.07	26.41	738.9	24.93
		30.02	29.36	790.0	27.88
		32.32	31.66	879.7	30.51
	CPT-1321	3.12	2.46	---	---
		6.07	5.41	1098.4	3.93
		9.02	8.36	766.8	6.89
		12.14	11.48	861.0	9.92
		15.09	14.43	641.8	12.96
		18.04	17.38	866.5	15.91
		21.16	20.50	789.8	18.94
		24.11	23.45	746.4	21.98
		27.73	26.57	780.2	25.01
		30.02	29.36	757.0	27.97
		33.14	32.48	786.3	30.92
		36.09	35.43	791.8	33.95
		39.04	38.38	895.5	36.91
		42.16	41.50	855.7	39.94
		43.31	42.65	1319.9	42.07

TABLE 2.5.4-215 (Sheet 4 of 7)
SUMMARY OF SEISMIC CPT SHEAR WAVE (VS) VELOCITY
RESULTS

WLS COL 2.5-1	Test Number	Test Depth (ft)	Geophone Depth (ft)	Point Shear Velocity (fps)	Point Depth (ft)
	CPT-1322	3.12	2.46	---	---
		6.07	5.41	699.0	3.93
		9.02	8.36	860.3	6.89
		12.14	11.48	814.9	9.92
		15.09	14.43	752.1	12.96
		18.04	17.38	751.8	15.91
		21.16	20.50	950.5	18.94
		24.11	23.45	801.3	21.98
		27.07	26.41	759.1	24.93
		30.02	29.36	710.0	27.88
		33.14	32.48	776.1	30.92
		36.09	35.43	791.8	33.95
		39.21	38.55	657.6	36.99
		42.32	41.66	750.2	40.10
		45.11	44.45	909.2	43.06
		48.06	47.40	1868.1	45.93

TABLE 2.5.4-215 (Sheet 5 of 7)
SUMMARY OF SEISMIC CPT SHEAR WAVE (VS) VELOCITY
RESULTS

WLS COL 2.5-1	Test Number	Test Depth (ft)	Geophone Depth (ft)	Point Shear Velocity (fps)	Point Depth (ft)
	CPT-1323	3.12	2.46	---	---
		6.07	5.41	2562.9	3.93
		9.02	8.36	881.8	6.89
		12.14	11.48	773.5	9.92
		15.09	14.43	802.2	12.96
		18.04	17.38	866.5	15.91
		21.16	20.50	616.2	18.94
		24.11	23.45	656.5	21.98
		27.07	26.41	839.6	24.93
		30.02	29.36	919.5	27.88
		33.14	32.48	703.0	30.92
		36.09	35.43	950.1	33.95
		39.04	38.38	764.1	36.91
		42.32	41.66	969.0	40.02
		45.11	44.45	1212.2	43.06
		48.06	47.40	965.2	45.93
		51.02	50.36	983.8	48.88
		54.13	53.47	1023.1	51.92
		57.09	56.43	910.1	54.95
		60.04	59.38	1041.6	57.90
		63.48	62.82	841.2	61.10
		66.11	65.45	1039.3	64.14
		69.06	68.40	928.7	66.93
		72.01	71.35	1027.2	69.88
		75.13	74.47	1237.0	72.91
		78.08	77.42	1085.7	75.95
		81.04	80.38	1197.1	78.90
		84.15	83.49	1376.6	81.93

TABLE 2.5.4-215 (Sheet 6 of 7)
SUMMARY OF SEISMIC CPT SHEAR WAVE (VS) VELOCITY
RESULTS

WLS COL 2.5-1	Test Number	Test Depth (ft)	Geophone Depth (ft)	Point Shear Velocity (fps)	Point Depth (ft)
	CTP-1324B	3.12	2.46	---	---
		6.07	5.41	1537.7	3.93
		9.02	8.36	783.8	6.89
		12.14	11.48	845.1	9.92
		15.09	14.43	740.5	12.96
		18.04	17.38	1043.3	15.91
		21.16	20.50	737.9	18.94
		24.11	23.45	813.2	21.98
		27.07	26.41	923.6	24.93
		30.02	29.36	876.4	27.88
		33.14	32.48	866.0	30.92
		36.09	35.43	850.9	33.95
		39.37	38.71	1044.2	37.07
		42.16	41.50	1087.4	40.10
		45.11	44.45	946.8	42.98
		48.06	47.40	1034.1	45.93
		51.02	50.36	1018.3	48.88
		54.13	53.47	1006.3	51.92
		57.09	56.43	820.4	54.95
		60.04	59.38	1121.7	57.90
		63.16	62.50	963.1	61.10
		66.11	65.45	942.9	63.97
		69.06	68.40	1194.0	66.93
		72.01	71.35	992.4	69.88
		75.13	74.47	1212.7	72.91
		77.26	76.60	1176.1	75.54

TABLE 2.5.4-215 (Sheet 7 of 7)
SUMMARY OF SEISMIC CPT SHEAR WAVE (VS) VELOCITY
RESULTS

WLS COL 2.5-1	Test Number	Test Depth (ft)	Geophone Depth (ft)	Point Shear Velocity (fps)	Point Depth (ft)
	CPT-1325	3.12	2.46	---	---
		6.07	5.41	2989.8	3.93
		9.02	8.36	1146.4	6.89
		12.14	11.48	1007.4	9.92
		15.09	14.43	1027.4	12.96
		18.04	17.38	1012.6	15.91
		21.16	20.50	874.6	18.94
		24.11	23.45	892.2	21.98
		27.07	26.41	982.0	24.93
		30.02	29.36	1016.4	27.88
		33.30	32.64	910.0	31.00
		36.09	35.43	913.2	34.03
		40.03	39.37	1484.2	37.40
	CPT-1325A	43.14	42.48	---	---
		46.10	45.44	947.7	43.96
		49.05	48.39	1136.4	46.91
		51.34	50.68	806.5	49.54
		54.63	53.97	1133.9	52.33
		55.12	54.46	---	54.21

TABLE 2.5.4-216 (Sheet 1 of 4)
BOREHOLE GEOPHYSICAL TEST LOCATIONS – P-S SUSPENSION, DOWNHOLE, AND TELEVIEWER TESTS

	Borehole	Tool and Run Number	Depth Range (ft.)	Total Depth as Drilled (ft.)	Depth to Bottom of Casing (ft)	Sample Interval (ft)
	B1000	Suspension	6.6 - 142.7	151.0	60.0 PVC	1.6
	B1000	Downhole	3.0 - 150.0	151.0	60.0 PVC	3.0-10.0
WLS COL 2.5-1	B1000	Optical Televierer	60.0 - 153.2	151.0	60.0 PVC	0.008
WLS COL 2.5-6	B1000	Acoustic Televierer 1	60.0 - 153.2	151.0	60.0 PVC	0.008
	B1000	Acoustic Televierer 2	60.0 - 153.0	151.0	60.0 PVC	0.008
	B1001	Acoustic Televierer	29.3 - 120.6	120.0	29.3 PVC	0.008
	B1002	Suspension	24.6 - 157.5	170.0	24.5 PVC	1.6
	B1002	Acoustic Televierer	24.8 - 169.9	170.0	24.5 PVC	0.008
	B1004	Suspension	9.8- 162.4	175.0	---	1.6
	B1004	Optical Televierer	6.2 - 174.0	175.0	---	0.008
	B1004	Acoustic Televierer	9.8 - 174.6	175.0	---	0.008
	B1011	Suspension 1	8.2 - 211.6	220.5	---	1.6
	B1011	Suspension 2	6.6 - 196.9	220.5	---	1.6
	B1011	Downhole	3.0 - 217.0	220.5	---	20
	B1011	Optical Televierer	4.5 - 222.0	220.5	---	0.008
	B1011	Acoustic Televierer	1.6 - 160.8	220.5	---	0.008

TABLE 2.5.4-216 (Sheet 2 of 4)
BOREHOLE GEOPHYSICAL TEST LOCATIONS – P-S SUSPENSION, DOWNHOLE, AND TELEVIEWER TESTS

Borehole	Tool and Run Number	Depth Range (ft.)	Total Depth as Drilled (ft.)	Depth to Bottom of Casing (ft)	Sample Interval (ft)
B1012	Suspension	13.1 - 137.8	150.0	---	1.6
B1012	Optical Televierer	4.5 - 149.8	150.0	---	0.008
B1012	Acoustic Televierer	12.5 - 149.8	150.0	---	0.008
B1014	Optical Televierer	6.4 - 67.4	75.0	3.0 PVC	0.008
B1014	Acoustic Televierer	3.6 - 67.3	75.0	3.0 PVC	0.008
B1015	Suspension	6.6 - 241.1	255.0	5.0 PVC	1.6
B1015	Optical Televierer	5.0 - 255.0	255.0	5.0 PVC	0.008
B1015	Acoustic Televierer	5.5 - 254.7	255.0	5.0 PVC	0.008
B1017	Suspension	8.2 - 162.4	175.0	10.0 PVC	1.6
B1017	Optical Televierer	6.5 - 176.2	175.0	10.0 PVC	0.008
B1017	Acoustic Televierer	6.7 - 175.9	175.0	10.0 PVC	0.008
B1024	Suspension	18.0 - 208.3	220.2	4.0 STEEL	1.6
B1024	Downhole	5.0 - 210.0	Blocked at 210.0	4.0 STEEL	5.0-10.0
B1024	Optical Televierer	5.4 - 222.0	220.2	4.0 STEEL	0.05
B1024	Acoustic Televierer	15.5 - 115.0	220.2	4.0 STEEL	0.05

TABLE 2.5.4-216 (Sheet 3 of 4)
BOREHOLE GEOPHYSICAL TEST LOCATIONS – P-S SUSPENSION, DOWNHOLE, AND TELEVIEWER TESTS

Borehole	Tool and Run Number	Depth Range (ft.)	Total Depth as Drilled (ft.)	Depth to Bottom of Casing (ft)	Sample Interval (ft)
B1037A	Suspension	5.3 - 85.3	97.5	70.6 PVC	1.6
B1037A	Downhole	3.0 - 84.0	97.5	70.6 PVC	3
B1037A	Optical Televiwer	71.8 - 97.8	97.5	70.6 PVC	0.008
B1037A	Acoustic Televiwer	72.0 - 97.5	97.5	70.6 PVC	0.008
B1068	Suspension	1.6 - 25.3	38.0	---	0.82
B1070	Suspension	1.6 - 91.9	105.0	---	1.6
B1074A ^(a)	Acoustic Televiwer 1	28.0 - 40.2	121.9	29.4 STEEL	0.008
B1074A ^(a)	Acoustic Televiwer 2	28.0 - 108.2	121.9	29.4 STEEL	0.008
B1074A ^(a)	Acoustic Televiwer 2	108.2 - 28.0	121.9	29.4 STEEL	0.008
B1074A ^(a)	Suspension 1	27.9 - 95.1	121.9	29.4 STEEL	1.6
B1075A ^(a)	Acoustic Televiwer 1	18.0 - 28.0	150.4	18.5 STEEL	0.008
B1075A ^(a)	Acoustic Televiwer 2	27.7 - 18.0	150.4	18.5 STEEL	0.008
B1075A ^(a)	Acoustic Televiwer 3	18.0 - 149.7	150.4	18.5 STEEL	0.008
B1075A ^(a)	Acoustic Televiwer 4	149.7 - 23.0	150.4	18.5 STEEL	0.008
B1075A ^(a)	Suspension 1	26.3 - 136.2	150.4	18.5 STEEL	1.6

TABLE 2.5.4-216 (Sheet 4 of 4)
BOREHOLE GEOPHYSICAL TEST LOCATIONS – P-S SUSPENSION, DOWNHOLE, AND TELEVIEWER TESTS

Borehole	Tool and Run Number	Depth Range (ft.)	Total Depth as Drilled (ft.)	Depth to Bottom of Casing (ft)	Sample Interval (ft)
B-2000	Acoustic Televierer 1	4.7 - 124.1	126.0	---	0.04
B-2000	Acoustic Televierer 2	124.0 - 4.0	126.0	---	0.004
B-2000	Suspension 1	4.9 - 113.2	126.0	---	1.6
B-2000	Suspension 2	105.0 - 95.1	126.0	---	1.6
B-2002	Suspension 1	11.5 - 211.6	225.6	---	1.6
B-2002	Suspension 2	180.5 - 170.6	225.6	---	1.6
B-2002	Acoustic Televierer 1	11.5 - 224.3	225.6	---	0.04
B-2002	Acoustic Televierer 2	224.0 - 7.5	225.6	---	0.004
B-2003	Acoustic Televierer 1	13.0 - 53.9	54.6	---	0.04
B-2003	Acoustic Televierer 2	53.8 - 5.0	54.6	---	0.004
B-2005	Suspension 1	4.9 - 211.6	225.0	---	1.6
B-2005	Suspension 2	180.5 - 167.3	225.0	---	1.6
B-2005	Acoustic Televierer 1	3.6 - 223.4	225.0	---	0.04
B-2005	Acoustic Televierer 2	223.0 - 1.5	225.0	---	0.004

a) Borings B-1074A and B-1075A are not representative of Unit 1 nuclear island.

TABLE 2.5.4-217 (Sheet 1 of 4)
SUMMARY OF INTERPRETED P-S SUSPENSION VELOCITY LAYER MODELS

	Boring Number	Layer No.	Depth to Top (ft.)	Depth to Bottom (ft.)	Layer model V_s (ft./sec.)	Layer model V_p (ft./sec.)
WLS COL 2.5-6	B-1000	1	4.1	23.8	1069.47	--
		2	23.8	36.9	1741.59	5024.47
		3	36.9	46.8	2921.97	6270.22
		4	46.8	63.2	2138.64	6846.60
		5	63.2	97.6	3858.39	9498.04
		6	97.6	107.5	5163.41	12097.82
		7	107.5	120.6	9011.92	18208.60
		8	120.6	138.6	10960.66	21638.16
	B-1002	1	27.1	32.0	8248.31	14766.43
		2	32.0	104.2	9998.31	18750.08
		3	104.2	156.7	10240.85	19149.11
	B-1004	1	10.7	22.2	6099.08	11869.06
		2	22.2	50.0	8459.07	16006.10
		3	50.0	161.6	9891.54	18465.19
	B-1011	1	9.0	210.8	9835.41	17208.75
	B-1012	1	15.6	22.2	7424.31	15025.56
		2	22.2	137.0	9588.94	18728.29

TABLE 2.5.4-217 (Sheet 2 of 4)
SUMMARY OF INTERPRETED P-S SUSPENSION VELOCITY LAYER MODELS

Boring Number	Layer No.	Depth to Top (ft.)	Depth to Bottom (ft.)	Layer model V_s (ft./sec.)	Layer model V_p (ft./sec.)
B-1015	1	9.0	71.4	8435.61	17102.59
	2	71.4	174.7	9288.90	18530.31
	3	174.7	240.3	9889.88	18932.41
B-1017	1	10.7	59.9	8474.78	17928.08
	2	59.9	122.2	9582.69	18860.15
	3	122.2	161.6	10197.85	18191.23
B-1024	1	18.9	48.4	9440.02	17871.07
	2	48.4	207.5	10263.27	20293.93
B-1037A ^(a)	1	5.9	13.9	728.00	1228.23
	2	13.9	28.7	763.42	1780.00
	3	28.7	64.8	740.24	4853.70
	4	64.8	84.5	3971.86	9785.20
B-1068	1	2.0	7.7	676.51	1418.23
	2	7.7	24.9	796.06	1779.29

TABLE 2.5.4-217 (Sheet 3 of 4)
SUMMARY OF INTERPRETED P-S SUSPENSION VELOCITY LAYER MODELS

Boring Number	Layer No.	Depth to Top (ft.)	Depth to Bottom (ft.)	Layer model V_s (ft./sec.)	Layer model V_p (ft./sec.)
B-1070	1	2.5	5.7	601.80	1503.77
	2	5.7	36.9	812.54	1852.83
	3	36.9	77.9	1011.06	2321.05
	4	77.9	91.0	1262.00	2621.05
B-1074A	1	28.7	40.2	4600.92	11333.75
	2	40.2	59.9	4424.71	12588.16
	3	59.9	68.1	6209.01	16494.41
	4	68.1	94.3	8086.92	16969.15
B-1075A	1	27.1	32.0	3238.00	7888.55
	2	32.0	43.5	4578.38	10703.25
	3	43.5	61.5	6315.67	14688.74
	4	61.5	135.3	9242.34	17840.32
B-2000 ^(a)	1	5.7	9.0	8995.32	16635.48
	2	9.0	112.4	9943.75	18255.12
B-2002 ^(a)	1	12.3	15.6	4628.73	10239.46
	2	15.6	210.8	10002.68	18099.98

TABLE 2.5.4-217 (Sheet 4 of 4)
SUMMARY OF INTERPRETED P-S SUSPENSION VELOCITY LAYER MODELS

Boring Number	Layer No.	Depth to Top (ft.)	Depth to Bottom (ft.)	Layer model V_s (ft./sec.)	Layer model V_p (ft./sec.)
B-2005 ^(a)	1	5.7	9.0	8742.89	16876.74
	2	9.0	210.8	10156.19	18585.93

- a) As B-1037A, B-1074A, and B-1075A were not used to calculate the smoothed velocity profiles, this data was not used in the evaluations presented herein. The layers presented in this table were developed by GEOVision ([Subsection 2.5.4.4](#)).

TABLE 2.5.4-218
SUMMARY OF DOWNHOLE VELOCITY LAYER MODELS

Borehole	Layer Number	Layer Data			Layer Velocity	
		Top (ft. b.g.s.)	Bottom (ft. b.g.s.)	Thickness (ft.)	Vs (ft/s)	Vp (ft/s)
	B1000	1	0.0	6.0	525	1295
	B1000	2	6.0	27.0	995	1774
	B1000	3	27.0	49.5	2150	4257
WLS COL 2.5-1	B1000	4	49.5	58.5	1755	6397
WLS COL 2.5-6	B1000	5	58.5	110.0	4958	12018
	B1000	6	110.0	130.0	11269	20053
	B1011	1	0.0	217.0	9230	17456
	B1024	1	0.0	20.0	6022	14555
	B1024	2	0.0	0.0	0	0
	B1024	3	30.0	210.0	9317	18236
	B1037A	1	0.0	12.0	695	1577
	B1037A	2	12.0	33.0	792	1544
	B1037A	3	33.0	66.0	736	4384
	B1037A	4	66.0	93.0	4634	11246

TABLE 2.5.4-219
QUALITY CONTROL RECOMMENDATIONS FOR NUCLEAR
ISLAND FOUNDATION MATERIALS

WLS COL 2.5-6 WLS COL 2.5-7	Minimum Sampling and Testing Frequency		
	Material	Test	
	Rock or Existing Concrete	Visual Inspection	Visual inspection of final exposed rock and concrete surface to confirm materials are in general conformance with expected foundation materials based on boring logs. Visual inspection to confirm that cleaning and surface preparation are properly completed prior to placement of fill concrete or foundation materials.
		Geologic Mapping	Geologic mapping of final exposed excavation surface prior to placement of fill concrete or foundation materials. Mapping at a minimum scale of 1 inch equals 10 feet. More detail may be provided as necessary.

TABLE 2.5.4-220
QUALITY CONTROL RECOMMENDATIONS FOR NUCLEAR
ISLAND FILL CONCRETE

WLS COL 2.5-6 WLS COL 2.5-7	Material	Test	Minimum Sampling and Testing Frequency
	Fill Concrete	Compressive Strength	One set of 4 cylinders for every 500 cubic yards placed. Minimum of one set each day material is placed. (Verify strength complies with mix design ^(a) and minimum strength of 2,500 psi)

-
- a) Note: The compressive strength as determined from the preconstruction mix design and testing program will ensure that the fill concrete will exhibit an average shear wave velocity greater than or equal to 7,500 ft/sec. This may result in compressive strength greater than the minimum of 2,500 psi.

TABLE 2.5.4-221
DELETED

TABLE 2.5.4-222 (Sheet 1 of 4)
 QUALITY CONTROL RECOMMENDATIONS FOR GENERIC
 ENGINEERED GRANULAR BACKFILL

WLS COL 2.5-6 WLS COL 2.5-7	Material	Test	Minimum Sampling and Testing Frequency
	Granular Backfill	Field Density	<p>Minimum 1 sample per lift per 10,000 square feet or per 250 cubic yards, whichever is smallest volume in cubic yards. One test for every 2,500 square feet per lift or per 250 cubic yards, whichever is smallest volume in cubic yards when manually operated compactors are used.</p> <p>Use sand cone (ASTM D 1556) or rubber balloon (ASTM D 2167) for at least 10% of field density measurements. Nuclear gauge (ASTM D 6938) may be used for 90% of measurements. The sand cone or rubber balloon test shall be performed at the location of at least two of the nuclear gauge tests (if used) for each day's work.</p>
		Moisture	One test for each sand cone or rubber balloon test. (ASTM D 2216)
		Moisture-Density Relationship (Modified Proctor)	One test for every borrow source and material type and any time material type changes. Additional test for every 40 Field Density tests, or as directed by geotechnical engineer in responsible charge. (ASTM D 1557)
		Gradation	One test for each Moisture-Density test. (ASTM D 422 and D 1140)
		Atterberg Limits	One test for each Moisture-Density test. (ASTM D 4318)
		Material Type	Granular fill must come from an approved borrow source (e.g. a quarry) and be the approved material for the project.

TABLE 2.5.4-222 (Sheet 2 of 4)
 QUALITY CONTROL RECOMMENDATIONS FOR GENERIC
 ENGINEERED GRANULAR BACKFILL

The following laboratory tests will be performed on samples of the proposed granular fill materials before they are approved for use.

Test	Minimum No. of Tests	Criterion for Acceptance Unless Approved by Engineer of Record
All below		An engineering report exists that concludes the granular fill material will produce a backfill having acceptable engineering properties.
Grain Size ASTM D 6913	1 per material type per source as-is, and 1 per material type per source scalped if necessary	Complies with SCDOT Specifications for Material Type (Reference 224) (may differ on some sieve sizes with approval of Engineer of Record). Anticipated material types are Macadam Base Course and Washed Screenings.
Atterberg Limits ASTM D 4318	1 per material type per source	Complies with SCDOT Specifications for Material Type (Reference 224).
Specific Gravity ASTM D 854	1 per material type per source	
Modified Proctor ASTM D 1557 and ASTM D 4718	1 per material type per source	Maximum Dry Density $\geq 124 \text{ lb/ft}^3$.
Constant Head Permeability ASTM D 2434	1 per material type per source	
pH ASTM G 51	1 per material type per source	
Chloride Content EPA SW-846 9056/300.0	1 per material type per source	
Sulfate Content EPA SW-846 8056/300.0	1 per material type per source	

TABLE 2.5.4-222 (Sheet 3 of 4)
 QUALITY CONTROL RECOMMENDATIONS FOR GENERIC
 ENGINEERED GRANULAR BACKFILL

Test	Minimum No. of Tests	Criterion for Acceptance Unless Approved by Engineer of Record
Resistivity ASTM G 57	1 per material type per source	
Consolidated Drained Triaxial Shear USACE EM-1110-2-1906 Appendix X (30 Nov. 70)	1 per material type per source (scalped) (minimum 2 confining pressures per material type)	$\phi' \geq 35^\circ$
Consolidation ASTM D 2435	1 per material type per source (up to 50 kip/ft ² effective vertical stress)	
Resonant Column Torsional Shear University of Texas Procedure PBRCTS-1	1 per material type per source (scalped) Test at 4 to 6 isotropic confining stress values	Maximum shear modulus, modulus ratio, and damping ratio consistent with upper range and lower range values used for site response calculation to determine compatibility with site response for Category II structures (Annex Building and Turbine Building Bay 1).
Free-Free Resonant Column Test University of Texas Procedure Fr-Fr-1	1 per material type per source (scalped) Test free-free resonance and direct travel time tests	

TABLE 2.5.4-222 (Sheet 4 of 4)
 QUALITY CONTROL RECOMMENDATIONS FOR GENERIC
 ENGINEERED GRANULAR BACKFILL

In addition to other tests performed during construction, the following field measurements of shear wave velocity of the in-place fill will be performed.

Test	Minimum No. of Tests	Criterion for Acceptance Unless Approved by Engineer of Record
Spectral Analysis of Surface Waves (SASW) University of Texas Procedure GR-07	When approximately 1/3, 2/3 and approximately full height of granular backfill is in-place	Maximum shear modulus consistent with values used for site response calculations for Category II structures.
Crosshole Seismic Testing (ASTM D 4428), Downhole Seismic Testing (ASTM D 7400) or PS Suspension Seismic Velocity Logging (GeoVision Procedure for OYO P-S Suspension Seismic Velocity Logging)	When approximately full height of granular backfill is in-place	

TABLE 2.5.4-223
ASSUMED MATERIAL PROPERTIES FOR CONCRETE
MATERIALS

	Concrete Source	Unit Weight (pcf)	Compressive Strength (f' _c) (psi)	Young's Modulus (E) (psi x 10 ⁶)	Poisson's Ratio (ν)
WLS COL 2.5-6	Pre-Existing Fill Concrete	145	3,000	3.16	0.17
	Pre-Existing Foundation Concrete	145	3,000	3.16	0.17
	Lee Nuclear Station Fill Concrete	145	3,000	3.16	0.17

Note: Unit weight and compressive strength are assumed. E and ν are from ASCE Standard 4-98.

TABLE 2.5.4-224
DELETED

TABLE 2.5.4-224A (Sheet 1 of 3)
 BEST ESTIMATE LAYERING, VELOCITIES, MODULI, AND RANGES OF GRANULAR FILL (GW OR
 MACADAM BASE COURSE) FOR YARD EL. 592 FT

Layer Name	Depth Below 592.0 MSL (ft)	Water Table Elev. (ft)	Unit Weight ^(a) (pcf)	Best Estimates					G _{max} ^(b) Lower Range (ksf)	G _{max} ^(b) Upper Range (ksf)
				V _p ^(b) (ft/sec)	V _s ^(b) (ft/sec)	Poisson's Ratio, v	G _{max} ^(b) (ksf)	E _{max} ^(b) (ksf)		
Fill	0-8	-	150	1375	794	0.25	2936	7341	1957	4404
	8-10.5	584 ^(c)	150	1587 [5000] ^(d)	916	0.25 [0.5] ^(d)	3910	9775 [11729] ^(d)	2606	5865
Fill	10.5-18	-	150	1676 [5000] ^(d)	968	0.25 [0.5] ^(d)	4363	10909 [13089] ^(d)	2909	6545
	18-20	-	150	1765 [5000] ^(d)	1019	0.25 [0.5] ^(d)	4839	12096 [14516] ^(d)	3226	7258
Fill	20-30	-	150	1910 [5000] ^(d)	1103	0.25 [0.5] ^(d)	5667	14167 [17000] ^(d)	3778	8500
Fill	30-40	-	150	2116 [5000] ^(d)	1222	0.25 [0.5] ^(d)	6955	17387 [20865] ^(d)	4637	10432
Fill	40-50	-	150	2292 [5000] ^(d)	1323	0.25 [0.5] ^(d)	8159	20396 [24476] ^(d)	5439	12238
Fill	50-60	-	150	2447 [5000] ^(d)	1413	0.25 [0.5] ^(d)	9299	23246 [27896] ^(d)	6199	13948
Fill	60-70	-	150	2586 [5000] ^(d)	1493	0.25 [0.5] ^(d)	10388	25970 [31164] ^(d)	6925	15582

TABLE 2.5.4-224A (Sheet 2 of 3)
 BEST ESTIMATE LAYERING, VELOCITIES, MODULI, AND RANGES OF GRANULAR FILL (GW OR
 MACADAM BASE COURSE) FOR YARD EL. 592 FT

Layer Name	Depth Below 592.0 MSL (ft)	Water Table Elev. (ft)	Unit Weight ^(a) (pcf)	Best Estimates					$G_{\max}^{(b)}$ Lower Range (ksf)	$G_{\max}^{(b)}$ Upper Range (ksf)
				$V_p^{(b)}$ (ft/sec)	$V_s^{(b)}$ (ft/sec)	Poisson's Ratio, ν	$G_{\max}^{(b)}$ (ksf)	$E_{\max}^{(b)}$ (ksf)		
Fill	70-80	-	150	2714 [5000] ^(d)	1567	0.25 [0.5] ^(d)	11436	28590 [34308] ^(d)	7624	17154
Fill	80-90	-	150	2831 [5000] ^(d)	1635	0.25 [0.5] ^(d)	12449	31123 [37347] ^(d)	8299	18674
Fill	90-100	-	150	2941 [5000] ^(d)	1698	0.25 [0.5] ^(d)	13432	33580 [40296] ^(d)	8955	20148
Fill	0-8	-	150	1375	794	0.25	2936	7340	1957	4404
	8-10.5	-	150	1614	932	0.25	4046	10115	2697	6069
Fill	10.5-18	-	150	1795	1036	0.25	5005	12511	3336	7507
	18-20	574 ^(e)	150	1935 [5000] ^(d)	1117	0.25 [0.5] ^(d)	5817	14541 [17450] ^(d)	3878	8725
Fill	20-30	-	150	2061 [5000] ^(d)	1190	0.25 [0.5] ^(d)	6594	16486 [19783] ^(d)	4396	9891
Fill	30-40	-	150	2244 [5000] ^(d)	1296	0.25 [0.5] ^(d)	7820	19549 [23459] ^(d)	5213	11729
Fill	40-50	-	150	2404 [5000] ^(d)	1388	0.25 [0.5] ^(d)	8976	22441 [26929] ^(d)	5984	13464

TABLE 2.5.4-224A (Sheet 3 of 3)
BEST ESTIMATE LAYERING, VELOCITIES, MODULI, AND RANGES OF GRANULAR FILL (GW OR
MACADAM BASE COURSE) FOR YARD EL. 592 FT

Layer Name	Depth Below 592.0 MSL (ft)	Water Table Elev. (ft)	Unit Weight ^(a) (pcf)	Best Estimates					$G_{\max}^{(b)}$ Lower Range (ksf)	$G_{\max}^{(b)}$ Upper Range (ksf)
				$V_p^{(b)}$ (ft/sec)	$V_s^{(b)}$ (ft/sec)	Poisson's Ratio, ν	$G_{\max}^{(b)}$ (ksf)	$E_{\max}^{(b)}$ (ksf)		
Fill	50-60	-	150	2548 [5000] ^(d)	1471	0.25 [0.5] ^(d)	10079	25198 [30238] ^(d)	6720	15119
Fill	60-70	-	150	2678 [5000] ^(d)	1546	0.25 [0.5] ^(d)	11138	27846 [33415] ^(d)	7426	16708
Fill	70-80	-	150	2799 [5000] ^(d)	1616	0.25 [0.5] ^(d)	12161	30402 [36483] ^(d)	8107	18241
Fill	80-90	-	150	2910 [5000] ^(d)	1680	0.25 [0.5] ^(d)	13152	32880 [39456] ^(d)	8768	19728
Fill	90-100	-	150	3015 [5000] ^(d)	1741	0.25 [0.5] ^(d)	14116	35289 [42347] ^(d)	9410	21174

- a) Moisture unit weight above water table = saturated unit weight below water table.
- b) Free field condition, confining stress of building foundation not considered. G_{\max} lower range = $G_{\max}/1.5$; G_{\max} upper range = $1.5 \times G_{\max}$ (ASCE 4-98) ([Reference 220](#)).
- c) Upper range of water table.
- d) Below the water table, V_p will be 5000 ft/sec, Poisson's ratio of soil-water system will be 0.5, and $E_{\max} = 3 \times G_{\max}$, as shown in brackets [].
- e) Lower range of water table.

TABLE 2.5.4-224B (Sheet 1 of 3)
 BEST ESTIMATE LAYERING, VELOCITIES, MODULI, AND RANGES OF GRANULAR FILL (GP OR
 MACADAM BASE COURSE) FOR YARD EL. 592 FT

Layer Name	Depth Below 592.0 MSL (ft)	Water Table Elev. (ft)	Unit Weight ^(a) (pcf)	Best Estimates					$G_{\max}^{(b)}$ Lower Range (ksf)	$G_{\max}^{(b)}$ Upper Range (ksf)
				$V_p^{(b)}$ (ft/sec)	$V_s^{(b)}$ (ft/sec)	Poisson's Ratio, ν	$G_{\max}^{(b)}$ (ksf)	$E_{\max}^{(b)}$ (ksf)		
Fill	0-8	-	142	1217	703	0.25	2177	5442	1451	3265
	8-10.5	584 ^(c)	142	1365 [5000] ^(d)	788	0.25 [0.5] ^(d)	2740	6849 [8219] ^(d)	1826	4110
Fill	10.5-18	-	142	1423 [5000] ^(d)	822	0.25 [0.5] ^(d)	2978	7446 [8935] ^(d)	1986	4467
	18-20	-	142	1480 [5000] ^(d)	855	0.25 [0.5] ^(d)	3221	8052 [9662] ^(d)	2147	4831
Fill	20-30	-	142	1576 [5000] ^(d)	910	0.25 [0.5] ^(d)	3652	9131 [10957] ^(d)	2435	5479
Fill	30-40	-	142	1711 [5000] ^(d)	988	0.25 [0.5] ^(d)	4303	10757 [12908] ^(d)	2868	6454
Fill	40-50	-	142	1824 [5000] ^(d)	1053	0.25 [0.5] ^(d)	4891	12227 [14673] ^(d)	3261	7336
Fill	50-60	-	142	1923 [5000] ^(d)	1110	0.25 [0.5] ^(d)	5434	13584 [16301] ^(d)	3622	8150
Fill	60-70	-	142	2010 [5000] ^(d)	1161	0.25 [0.5] ^(d)	5941	14852 [17823] ^(d)	3961	8911

TABLE 2.5.4-224B (Sheet 2 of 3)
 BEST ESTIMATE LAYERING, VELOCITIES, MODULI, AND RANGES OF GRANULAR FILL (GP OR
 MACADAM BASE COURSE) FOR YARD EL. 592 FT

Layer Name	Depth Below 592.0 MSL (ft)	Water Table Elev. (ft)	Unit Weight ^(a) (pcf)	Best Estimates					$G_{\max}^{(b)}$ Lower Range (ksf)	$G_{\max}^{(b)}$ Upper Range (ksf)
				$V_p^{(b)}$ (ft/sec)	$V_s^{(b)}$ (ft/sec)	Poisson's Ratio, ν	$G_{\max}^{(b)}$ (ksf)	$E_{\max}^{(b)}$ (ksf)		
Fill	70-80	-	142	2090 [5000] ^(d)	1207	0.25 [0.5] ^(d)	6420	16050 [19260] ^(d)	4280	9630
Fill	80-90	-	142	2163 [5000] ^(d)	1249	0.25 [0.5] ^(d)	6875	17188 [20626] ^(d)	4584	10313
Fill	90-100	-	142	2230 [5000] ^(d)	1288	0.25 [0.5] ^(d)	7311	18276 [21932] ^(d)	4874	10966
Fill	0-8	-	142	1217	703	0.25	2177	5442	1451	3265
	8-10.5	-	142	1385	800	0.25	2821	7053	1881	4232
Fill	10.5-18	-	142	1510	872	0.25	3352	8379	2234	5027
	18-20	574 ^(e)	142	1603 [5000] ^(d)	926	0.25 [0.5] ^(d)	3778	9444 [11333] ^(d)	2519	5667
Fill	20-30	-	142	1684 [5000] ^(d)	972	0.25 [0.5] ^(d)	4168	10421 [12505] ^(d)	2779	6252
Fill	30-40	-	142	1801 [5000] ^(d)	1040	0.25 [0.5] ^(d)	4768	11920 [14304] ^(d)	3179	7152
Fill	40-50	-	142	1902 [5000] ^(d)	1098	0.25 [0.5] ^(d)	5320	13299 [15959] ^(d)	3546	7979

TABLE 2.5.4-224B (Sheet 3 of 3)
 BEST ESTIMATE LAYERING, VELOCITIES, MODULI, AND RANGES OF GRANULAR FILL (GP OR
 MACADAM BASE COURSE) FOR YARD EL. 592 FT

Layer Name	Depth Below 592.0 MSL (ft)	Water Table Elev. (ft)	Unit Weight ^(a) (pcf)	Best Estimates					$G_{\max}^{(b)}$ Lower Range (ksf)	$G_{\max}^{(b)}$ Upper Range (ksf)
				$V_p^{(b)}$ (ft/sec)	$V_s^{(b)}$ (ft/sec)	Poisson's Ratio, ν	$G_{\max}^{(b)}$ (ksf)	$E_{\max}^{(b)}$ (ksf)		
Fill	50-60	-	142	1992 [5000] ^(d)	1150	0.25 [0.5] ^(d)	5834	14585 [17502] ^(d)	3889	8751
Fill	60-70	-	142	2073 [5000] ^(d)	1197	0.25 [0.5] ^(d)	6319	15796 [18956] ^(d)	4212	9478
Fill	70-80	-	142	2147 [5000] ^(d)	1240	0.25 [0.5] ^(d)	6779	16947 [20336] ^(d)	4519	10168
Fill	80-90	-	142	2216 [5000] ^(d)	1279	0.25 [0.5] ^(d)	7218	18045 [21654] ^(d)	4812	10827
Fill	90-100	-	142	2280 [5000] ^(d)	1316	0.25 [0.5] ^(d)	7640	19099 [22919] ^(d)	5093	11459

- a) Moisture unit weight above water table = saturated unit weight below water table.
- b) Free field condition, confining stress of building foundation not considered. G_{\max} lower range = $G_{\max}/1.5$; G_{\max} upper range = $1.5 \times G_{\max}$ (ASCE 4-98) ([Reference 220](#)).
- c) Upper range of water table.
- d) Below the water table, V_p will be 5000 ft/sec, Poisson's ratio of soil-water system will be 0.5, and $E_{\max} = 3 \times G_{\max}$, as shown in brackets [].
- e) Lower range of water table.

TABLE 2.5.4-224C (Sheet 1 of 3)
 BEST ESTIMATE LAYERING, VELOCITIES, MODULI, AND RANGES OF GRANULAR FILL (SW)
 FOR YARD EL. 592 FT

Layer Name	Depth Below 592.0 MSL (ft)	Water Table Elev. (ft)	Unit Weight ^(a) (pcf)	Best Estimates					$G_{\max}^{(b)}$ Lower Range (ksf)	$G_{\max}^{(b)}$ Upper Range (ksf)
				$V_p^{(b)}$ (ft/sec)	$V_s^{(b)}$ (ft/sec)	Poisson's Ratio, ν	$G_{\max}^{(b)}$ (ksf)	$E_{\max}^{(b)}$ (ksf)		
Fill	0-8	-	136	1003	579	0.25	1415	3538	943	2123
	8-10.5	584 ^(c)	136	1116 [5000] ^(d)	645	0.25 [0.5] ^(d)	1755	4386 [5264] ^(d)	1170	2632
Fill	10.5-18	-	136	1159 [5000] ^(d)	669	0.25 [0.5] ^(d)	1890	4724 [5669] ^(d)	1260	2835
	18-20	-	136	1200 [5000] ^(d)	693	0.25 [0.5] ^(d)	2028	5070 [6084] ^(d)	1352	3042
Fill	20-30	-	136	1272 [5000] ^(d)	734	0.25 [0.5] ^(d)	2278	5694 [6833] ^(d)	1518	3416
Fill	30-40	-	136	1372 [5000] ^(d)	792	0.25 [0.5] ^(d)	2651	6627 [7953] ^(d)	1767	3976
Fill	40-50	-	136	1456 [5000] ^(d)	841	0.25 [0.5] ^(d)	2986	7465 [8958] ^(d)	1991	4479
Fill	50-60	-	136	1529 [5000] ^(d)	883	0.25 [0.5] ^(d)	3293	8233 [9880] ^(d)	2196	4940
Fill	60-70	-	136	1594 [5000] ^(d)	921	0.25 [0.5] ^(d)	3579	8948 [10737] ^(d)	2386	5369

TABLE 2.5.4-224C (Sheet 2 of 3)
 BEST ESTIMATE LAYERING, VELOCITIES, MODULI, AND RANGES OF GRANULAR FILL (SW)
 FOR YARD EL. 592 FT

Layer Name	Depth Below 592.0 MSL (ft)	Water Table Elev. (ft)	Unit Weight ^(a) (pcf)	Best Estimates					$G_{\max}^{(b)}$ Lower Range (ksf)	$G_{\max}^{(b)}$ Upper Range (ksf)
				$V_p^{(b)}$ (ft/sec)	$V_s^{(b)}$ (ft/sec)	Poisson's Ratio, ν	$G_{\max}^{(b)}$ (ksf)	$E_{\max}^{(b)}$ (ksf)		
Fill	70-80	-	136	1653 [5000] ^(d)	954	0.25 [0.5] ^(d)	3848	9619 [11543] ^(d)	2565	5772
Fill	80-90	-	136	1707 [5000] ^(d)	986	0.25 [0.5] ^(d)	4102	10255 [12306] ^(d)	2735	6153
Fill	90-100	-	136	1757 [5000] ^(d)	1014	0.25 [0.5] ^(d)	4344	10861 [13033] ^(d)	2896	6516
Fill	0-8	-	136	1003	579	0.25	1415	3538	943	2123
	8-10.5	-	136	1133	654	0.25	1806	4515	1204	2709
Fill	10.5-18	-	136	1228	709	0.25	2123	5308	1415	3185
	18-20	574 ^(e)	136	1299 [5000] ^(d)	750	0.25 [0.5] ^(d)	2374	5936 [7123] ^(d)	1583	3562
Fill	20-30	-	136	1358 [5000] ^(d)	784	0.25 [0.5] ^(d)	2597	6492 [7791] ^(d)	1731	3895
Fill	30-40	-	136	1444 [5000] ^(d)	834	0.25 [0.5] ^(d)	2937	7342 [8811] ^(d)	1958	4405
Fill	40-50	-	136	1519 [5000] ^(d)	877	0.25 [0.5] ^(d)	3248	8120 [9744] ^(d)	2165	4872

TABLE 2.5.4-224C (Sheet 3 of 3)
 BEST ESTIMATE LAYERING, VELOCITIES, MODULI, AND RANGES OF GRANULAR FILL (SW)
 FOR YARD EL. 592 FT

Layer Name	Depth Below 592.0 MSL (ft)	Water Table Elev. (ft)	Unit Weight ^(a) (pcf)	Best Estimates					$G_{\max}^{(b)}$ Lower Range (ksf)	$G_{\max}^{(b)}$ Upper Range (ksf)
				$V_p^{(b)}$ (ft/sec)	$V_s^{(b)}$ (ft/sec)	Poisson's Ratio, ν	$G_{\max}^{(b)}$ (ksf)	$E_{\max}^{(b)}$ (ksf)		
Fill	50-60	-	136	1585 [5000] ^(d)	915	0.25 [0.5] ^(d)	3537	8842 [10611] ^(d)	2358	5305
Fill	60-70	-	136	1645 [5000] ^(d)	950	0.25 [0.5] ^(d)	3808	9520 [11424] ^(d)	2539	5712
Fill	70-80	-	136	1699 [5000] ^(d)	981	0.25 [0.5] ^(d)	4064	10160 [12193] ^(d)	2709	6096
Fill	80-90	-	136	1749 [5000] ^(d)	1010	0.25 [0.5] ^(d)	4308	10770 [12924] ^(d)	2872	6462
Fill	90-100	-	136	1796 [5000] ^(d)	1037	0.25 [0.5] ^(d)	4541	11354 [13624] ^(d)	3028	6812

- a) Moisture unit weight above water table = saturated unit weight below water table.
- b) Free field condition, confining stress of building foundation not considered. G_{\max} lower range = $G_{\max}/1.5$; G_{\max} upper range = $1.5 \times G_{\max}$ (ASCE 4-98) ([Reference 220](#)).
- c) Upper range of water table.
- d) Below the water table, V_p will be 5000 ft/sec, Poisson's ratio of soil-water system will be 0.5, and $E_{\max} = 3 \times G_{\max}$, as shown in brackets [].
- e) Lower range of water table.

TABLE 2.5.4-224D
MODULUS AND DAMPING RATIO OF GRANULAR FILL (GW OR
MACADAM BASE COURSE)

Granular Fill (GW or Macadam Base Course)						
Shear Strain γ (%)	Depth Range (up to 10.5 ft) ^(a)		Depth Range (10.5 - 50 ft) ^(a)		Depth Range (> 50 ft) ^(a)	
	Modulus Ratio, G/G_{\max}	Damping Ratio, D_s	Modulus Ratio, G/G_{\max}	Damping Ratio, D_s	Modulus Ratio, G/G_{\max}	Damping Ratio, D_s
0.00001	1.00	0.54	1.00	0.50	1.00	0.47
0.0001	0.97	0.72	0.98	0.66	0.98	0.61
0.0002	0.95	0.92	0.96	0.83	0.97	0.75
0.0003	0.93	1.12	0.94	1.00	0.95	0.89
0.0005	0.89	1.50	0.91	1.33	0.93	1.17
0.001	0.82	2.36	0.85	2.08	0.88	1.83
0.002	0.72	3.82	0.76	3.39	0.79	2.99
0.003	0.65	4.99	0.69	4.49	0.73	4.00
0.005	0.55	6.79	0.59	6.23	0.63	5.66
0.01	0.41	9.53	0.44	9.07	0.48	8.53
0.02	0.28	12.15	0.30	12.00	0.33	11.72
0.03	0.22	13.49	0.23	13.56	0.26	13.50
0.05	0.15	14.91	0.16	15.25	0.18	15.49
0.1	0.09	16.35	0.10	16.99	0.11	17.58
0.2	0.05	17.22	0.06	18.04	0.06	18.88
0.3	0.04	17.47	0.04	18.36	0.04	19.29
1	0.01	17.32	0.01	18.27	0.01	19.30

a) Depths are below elevation 589.5± ft.

TABLE 2.5.4-224E
MODULUS AND DAMPING RATIO OF GRANULAR FILL (GP OR
MACADAM BASE COURSE)

Granular Fill (GP or Macadam Base Course)						
Shear Strain $\gamma(\%)$	Depth Range (up to 10.5 ft) ^(a)		Depth Range (10.5 - 50 ft) ^(a)		Depth Range (> 50 ft) ^(a)	
	Modulus Ratio, G/G_{\max}	Damping Ratio, D_s	Modulus Ratio, G/G_{\max}	Damping Ratio, D_s	Modulus Ratio, G/G_{\max}	Damping Ratio, D_s
0.00001	1.00	0.49	1.00	0.46	1.00	0.44
0.0001	0.99	0.54	0.99	0.50	1.00	0.47
0.0002	0.98	0.60	0.99	0.55	0.99	0.50
0.0003	0.97	0.65	0.98	0.59	0.99	0.54
0.0005	0.96	0.76	0.97	0.68	0.98	0.60
0.001	0.93	1.03	0.95	0.89	0.96	0.77
0.002	0.89	1.54	0.91	1.30	0.93	1.10
0.003	0.85	2.02	0.88	1.69	0.91	1.41
0.005	0.78	2.88	0.82	2.41	0.86	2.01
0.01	0.67	4.63	0.72	3.95	0.77	3.32
0.02	0.53	7.05	0.59	6.22	0.64	5.39
0.03	0.45	8.65	0.50	7.84	0.56	6.96
0.05	0.35	10.67	0.39	10.03	0.44	9.21
0.1	0.23	13.12	0.26	12.87	0.30	12.39
0.2	0.15	15.06	0.16	15.24	0.19	15.22
0.3	0.11	15.94	0.12	16.33	0.14	16.58
1	0.04	17.39	0.05	18.22	0.05	19.04

a) Depths are below elevation 589.5± ft.

TABLE 2.5.4-224F
MODULUS AND DAMPING RATIO OF GRANULAR FILL (SW OR
MACADAM BASE COURSE)

Granular Fill (SW or Macadam Base Course)						
Shear Strain $\gamma(\%)$	Depth Range (up to 10.5 ft) ^(a)		Depth Range (10.5 - 50 ft) ^(a)		Depth Range (> 50 ft) ^(a)	
	Modulus Ratio, G/G_{\max}	Damping Ratio, D_s	Modulus Ratio, G/G_{\max}	Damping Ratio, D_s	Modulus Ratio, G/G_{\max}	Damping Ratio, D_s
0.00001	1.00	0.75	1.00	0.71	1.00	0.67
0.0001	0.99	0.79	0.99	0.74	1.00	0.69
0.0002	0.99	0.83	0.99	0.77	0.99	0.72
0.0003	0.98	0.87	0.99	0.80	0.99	0.74
0.0005	0.97	0.94	0.98	0.86	0.99	0.78
0.001	0.95	1.13	0.96	1.00	0.97	0.89
0.002	0.91	1.48	0.94	1.28	0.95	1.11
0.003	0.88	1.82	0.91	1.54	0.94	1.32
0.005	0.83	2.46	0.87	2.05	0.90	1.72
0.01	0.74	3.83	0.79	3.19	0.83	2.64
0.02	0.61	5.89	0.67	5.02	0.73	4.21
0.03	0.53	7.38	0.59	6.44	0.65	5.50
0.05	0.43	9.41	0.48	8.50	0.54	7.48
0.1	0.29	12.07	0.34	11.45	0.39	10.61
0.2	0.19	14.31	0.22	14.14	0.26	13.72
0.3	0.14	15.37	0.17	15.46	0.19	15.33
1	0.06	17.38	0.07	18.05	0.08	18.65

a) Depths are below elevation 589.5± ft.

TABLE 2.5.4-225
DELETED

TABLE 2.5.4-225A
ACTIVE EARTH PRESSURE FROM GRANULAR BACKFILL

Depth Below 592.0 ft MSL (ft)	Active earth pressure, WLS, for design water (d_w) table at 8.0 ft:		
	GW (psf)	GP (psf)	SW (psf)
0	0	0	0
8.0	325	308	295
13.0	444	416	395
18.0	563	524	494
33.0	919	847	793
38.5	1049	966	903

TABLE 2.5.4-225B
AT-REST EARTH PRESSURE FROM GRANULAR BACKFILL

Depth Below 592.0 ft MSL (ft)	At-rest earth pressure, WLS, for design water (d_w) table at 8.0 ft:		
	GW (psf)	GP (psf)	SW (psf)
0	0	0	0
8.0	512	484	464
13.0	698	654	621
18.0	885	824	778
33.0	1446	1333	1249
38.5	1651	1520	1421

TABLE 2.5.4-225C
PASSIVE EARTH PRESSURE FROM GRANULAR BACKFILL

Depth Below 592.0 ft MSL (ft)	Passive earth pressure, WLS, for design water (d_w) table at 8.0 ft:		
	GW (psf)	GP (psf)	SW (psf)
0	0	0	0
8.0	4428	4192	4015
13.0	6045	5661	5373
18.0	7661	7129	6731
33.0	12,510	11,535	10,805
38.5	14,288	13,151	12,229

TABLE 2.5.4-226
DELETED

TABLE 2.5.4-226A (Sheet 1 of 3)
 COMPACTION-INDUCED EARTH PRESSURE FROM
 GRANULAR BACKFILL MATERIAL

Depth	Hand-Guided Roller ^(a) Adjacent to NI Wall			Heavy Roller ^(b) 5 ft from NI Wall		
	At-Rest Pressure	Residual + At-Rest Pressure	Residual Pressure	Residual + At-Rest Pressure	Residual Pressure	
	(lb/ft ²)	(lb/ft ²)	(lb/ft ²)	(lb/ft ²)	(lb/ft ²)	(lb/ft ²)
0.0	0	0	0	0	0	0
0.5	32	277	245	36	4	4
1.0	64	416	352	105	41	41
1.5	96	432	336	169	73	73
2.0	128	448	320	225	97	97
2.5	160	463	304	274	114	114
3.0	192	479	287	316	124	124
3.5	224	495	271	352	128	128
4.0	256	511	255	383	128	128
4.5	288	527	239	412	124	124
5.0	320	542	222	438	118	118
5.5	352	558	206	463	111	111
6.0	384	574	190	487	104	104
6.5	416	590	174	512	96	96
7.0	448	605	158	536	88	88
7.5	480	621	141	560	80	80
8.0	512	637	125	585	73	73
8.5	544	653	109	610	66	66
9.0	576	668	93	636	60	60
9.5	608	684	77	662	54	54

TABLE 2.5.4-226A (Sheet 2 of 3)
COMPACTION-INDUCED EARTH PRESSURE FROM
GRANULAR BACKFILL MATERIAL

Depth	Hand-Guided Roller ^(a) Adjacent to NI Wall			Heavy Roller ^(b) 5 ft from NI Wall		
	At-Rest Pressure	Residual + At-Rest Pressure	Residual Pressure	Residual + At-Rest Pressure	Residual Pressure	
	(lb/ft ²)	(lb/ft ²)	(lb/ft ²)	(lb/ft ²)	(lb/ft ²)	(lb/ft ²)
10.0	640	700	60	689	49	
10.5	672	716	44	716	44	
11.0	704	732	28	744	40	
11.5	736	747	12	772	36	
12.0	768	768	0	800	33	
12.5	800	800	0	829	30	
13.0	832	832	0	858	27	
13.5	864	864	0	888	24	
14.0	895	895	0	917	22	
14.5	927	927	0	947	20	
15.0	959	959	0	977	18	
15.5	991	991	0	1008	16	
16.0	1023	1023	0	1038	15	
16.5	1055	1055	0	1069	13	
17.0	1087	1087	0	1100	12	
17.5	1119	1119	0	1131	11	
18.0	1151	1151	0	1162	10	
18.5	1183	1183	0	1193	9	
19.0	1215	1215	0	1224	8	
19.5	1247	1247	0	1255	8	

TABLE 2.5.4-226A (Sheet 3 of 3)
 COMPACTION-INDUCED EARTH PRESSURE FROM
 GRANULAR BACKFILL MATERIAL

Depth	Hand-Guided Roller ^(a) Adjacent to NI Wall			Heavy Roller ^(b) 5 ft from NI Wall	
	At-Rest Pressure	Residual + At-Rest Pressure	Residual Pressure	Residual + At-Rest Pressure	Residual Pressure
	(lb/ft ²)	(lb/ft ²)	(lb/ft ²)	(lb/ft ²)	(lb/ft ²)
20.0	1279	1279	0	1286	7

a) Steel drum, $p = 190$ lb/in, roller width = 21.6 in.

b) Steel drum, $p = 800$ lb/in, roller width = 84 in.

TABLE 2.5.4-226B (Sheet 1 of 2)
CRITERIA FOR SOIL COMPACTORS OPERATED IN
CLOSE PROXIMITY OF NUCLEAR ISLAND FOUNDATION
WALL

Compactor Type	Criteria
Vibratory Drum ^(a)	<ul style="list-style-type: none">• Drum width and operating weight that are within $\pm 25\%$ of the values applicable for the particular models used during the test fill program;• [Static weight at drum + maximum centrifugal force applied by drum] \div width of drum that is within $\pm 25\%$ of the values applicable for the particular models used during the test fill program, but with the following limitations^(b):<ul style="list-style-type: none">◦ not to exceed 190 lbs/inch on drum width = 21.6 inches for compactors operated immediately adjacent to the nuclear island foundation wall;◦ not to exceed 500 lbs/inch on drum width = 24 inches for compactors operated as close as 1.2 feet to the nuclear island foundation wall;◦ not to exceed 600 lbs/inch on drum width = 66 inches for compactors operated as close as 1.75 feet to the nuclear island foundation wall;◦ not to exceed 800 lbs/inch for compactors on drum width = 84 inches operated as close as 2.5 feet to the nuclear island foundation wall;◦ not to exceed 1,000 lbs/inch on drum width = 84 inches for compactors operated as close as 3.0 feet to the nuclear island foundation wall.

TABLE 2.5.4-226B (Sheet 2 of 2)
 CRITERIA FOR SOIL COMPACTORS OPERATED IN
 CLOSE PROXIMITY OF NUCLEAR ISLAND FOUNDATION
 WALL

Compactor Type	Criteria
Hand-Guided Vibratory Plate	<ul style="list-style-type: none"> • Operating weight and plate dimensions (area) that are within $\pm 25\%$ of the values applicable for the particular models used during the test fill program; • [Static weight of compactor + maximum centrifugal force applied] \div area of plate that is within $\pm 25\%$ of the values applicable for the particular models used during the test fill program, but with the following limitations^(b): <ul style="list-style-type: none"> ◦ not to exceed 20 lbs/inch² for compactors with plate area up to 910 inch² on lift thickness 6 inches operated immediately adjacent to the nuclear island foundation wall; ◦ not to exceed 18.5 lbs/inch² for compactors with plate area = 1088 inch² on lift thickness 6 inches operated immediately adjacent to the nuclear island foundation wall; ◦ not to exceed 20 lbs/inch² for compactors with plate area = 1088 inch² on lift thickness 6 inches operated as close as 0.25 feet to the nuclear island foundation wall.

a) Drum roller compactor is operated rolling parallel to the wall.

b) Limitations are combinations that produce stresses that do not exceed the envelope of residual + at-rest pressure in **FSAR Table 2.5.4-226A**.

TABLE 2.5.4-227
DYNAMIC EARTH PRESSURE FROM GRANULAR BACKFILL
MATERIAL

Site-Specific WLS Backfill Dynamic Earth Pressure by Typical Backfill Group Symbol ^(a)			
AP1000 Plant Grade Elevation 100 ft.	GW $\gamma = 150 \text{ lb/ft}^3$	GP $\gamma = 142 \text{ lb/ft}^3$	SW $\gamma = 136 \text{ lb/ft}^3$
99.0 (=592.0 WLS)	2187	2071	1983
97.075	2460	2329	2230
95.150	2608	2469	2365
91.300	2744	2598	2488
87.450	2777	2629	2518
83.600	2726	2581	2472
79.750	2608	2469	2365
75.900	2427	2298	2201
75.515	2409	2280	2184
72.050	2195	2078	1991
68.200	1897	1795	1720
66.275	1722	1630	1561
64.350	1529	1447	1386
60.500	1108	1049	1004

- a) Per [Reference 220](#), ASCE 4-98, Section 3.5.3, Figure 3.5-1, "Variation of Normal Dynamic Soil Pressures for the Elastic Solution."

Soil Properties:

γ = unit weight as shown

$\nu = 0.5$

Acceleration:

$a = 0.352g$, applied uniform along the height of the wall.

TABLE 2.5.4-228
ALLOWABLE BEARING PRESSURE BASED ON FACTOR OF
SAFETY

Structure	Subsurface	B x L (ft)	Bearing Pressure (k/ft ²)		q _{applied} (k/ft ²)	q _{safe} > q _{applied}
			q _{ult} ^(a)	q _{safe} ^(b)		
SW Sand Granular Fill						
Annex Building	Granular Fill - SW	70 x 289	86.92	28.97	2.43	Yes
Turbine Building	Granular Fill - SW	127 x 312	115.46	38.49	3.51	Yes
Radwaste Building	Granular Fill - SW	69 x 178	78.79	26.26	1.31	Yes
GP Gravel Granular Fill						
Annex Building	Granular Fill - GP	70 x 289	92.81	30.94	2.43	Yes
Turbine Building	Granular Fill - GP	127 x 312	123.88	41.29	3.51	Yes
Radwaste Building	Granular Fill - GP	69 x 178	84.16	28.05	1.31	Yes
GW Gravel Granular Fill						
Annex Building	Granular Fill - GW	70 x 289	100.66	33.55	2.43	Yes
Turbine Building	Granular Fill - GW	127 x 312	135.09	45.03	3.51	Yes
Radwaste Building	Granular Fill - GW	69 x 178	91.31	30.44	1.31	Yes

a) Groundwater level is assumed to be at elevation 584 ft.

b) Factor of safety of 3 is used in the analyses.

TABLE 2.5.4-229
ALLOWABLE BEARING PRESSURE BASED ON LIMITING
SETTLEMENT

Structure	Subsurface	$q_{allow}^{(a)}$ (k/ft ²)	$q_{applied}$ (k/ft ²)	$q_{allow} >$ $q_{applied}$	Anticipated Settlement (inches)
SW Sand Granular Backfill					
Annex Building	Granular Fill - SW	7.29	2.43	Yes	< 2
Turbine Building	Granular Fill - SW	6.96	3.51	Yes	< 2
Radwaste Building	Granular Fill - SW	7.24	1.31	Yes	< 2
GP Gravel Granular Backfill					
Annex Building	Granular Fill - GP	10.93	2.43	Yes	< 2
Turbine Building	Granular Fill - GP	10.44	3.51	Yes	< 2
Radwaste Building	Granular Fill - GP	10.86	1.31	Yes	< 2
GW Gravel Granular Backfill					
Annex Building	Granular Fill - GW	10.93	2.43	Yes	< 2
Turbine Building	Granular Fill - GW	10.44	3.51	Yes	< 2
Radwaste Building	Granular Fill - GW	10.86	1.31	Yes	< 2

a) For limiting settlement to 2 inches.

TABLE 2.5.4-230
STRUCTURE SIZES

Structure	Seismic Category	Elevation of Base of Foundation ^(a) (ft)	Depth of Foundation D_f (ft)	Width ^(b) B (ft)	Length L (ft)	$q_{\text{applied}}^{(c)}$ (k/ft ²)
Annex Building	II	588.5	3.1	70	289	2.43
Turbine Building	II and Non-seismic	589 - 572 ^(d)	2.1	127	312	3.51
Radwaste Building	Non-seismic	588.5	2.4	69	178	1.31

a) See [Reference 237](#), raised 3 ft per [Reference 247](#).

b) Smallest width of building shown; [Reference 235](#).

c) See [Reference 236](#).

d) Higher elevation used.

WLS COL 2.5-14

TABLE 2.5.5-201
PERMANENT SLOPES WITHIN ONE-QUARTER MILE OF UNIT 1 AND 2 NUCLEAR ISLAND STRUCTURES

Slope (Number)	Constructed Condition	Approximate Distance to Toe	Approximate Distance to Crest	Approximate Slope Height	Approximate Slope Inclination (Horizontal to Vertical)
		(feet)	(feet)	(feet)	
Hill Southwest of Unit 1 (5)	Natural Slope – cut	1000	-	80	2.5:1.0
Pond North of Units (7)	Engineered Fill	-	1200	55	2.0:1.0

APPENDIX 2AA

LEE NUCLEAR STATION FIELD EXPLORATION DATA

- WLS COL 2.5-1 This **Appendix** contains geotechnical boring logs, test pit logs, SPT energy measurements, and Packer Test results that are the basis for discussion in relevant sections of 2.5. The logs and tests represent a record of subsurface conditions at the William States Lee III Nuclear Station site. Attachment 1 contains geotechnical boring logs (124 borings in total) and monitoring well construction logs (24 in total) resulting from the COL investigation as well as a key to symbols and descriptions. Attachment 2 contains the results of SPT energy measurement testing performed on the Lee Nuclear Station site. Attachment 3 contains test pit logs resulting from the COL investigation, 14 logs in total. Attachment 4 contains Packer Test results from four locations on the Lee site. Attachment 5 contains the Cone Penetrometer Test, Seismic Cone Penetrometer Test, and Pore Pressure Dissipation Test results performed on the Lee Nuclear Station site. Attachment 6 contains seven geotechnical boring logs for Lee Units 1 and 2, which supplement the boring logs presented in Attachment 1.

APPENDIX 2BB

CHEROKEE NUCLEAR STATION GEOTECHNICAL BORING LOGS

WLS COL 2.5-1 This **Appendix** contains historic geotechnical boring logs developed as part of the Cherokee Nuclear Station Project investigation, and a list of the included borings (189 in total).

APPENDIX 2CC

WLS COL 2.3-1 EVALUATION OF METEOROLOGICAL DATA

This **Appendix** demonstrates the consistency of the Lee meteorological data between years. In addition, comparisons are provided between the onsite data and the National Weather Service station (Greenville-Spartanburg (GSP)) for selected data.

APPENDIX 2DD
COOLING TOWER PLUME ANALYSES

This **Appendix** provides an evaluation of the meteorological data used in the cooling tower plume analyses.